

Contaminant Hydrogeology

Third Edition

C. W. Fetter
Thomas Boving
David Kreamer

Contaminant Hydrogeology

Third Edition

C. W. Fetter

late of University of Wisconsin—Oshkosh

Thomas Boving

University of Rhode Island

David Kreamer

University of Nevada, Las Vegas



Long Grove, Illinois

For information about this book, contact:

Waveland Press, Inc.
4180 IL Route 83, Suite 101
Long Grove, IL 60047-9580
(847) 634-0081
info@waveland.com
www.waveland.com

Copyright © 2018 by Nancy Fetter, Thomas Boving, and David Kreamer

10-digit ISBN 1-4786-3279-8

13-digit ISBN 978-1-4786-3279-5

All rights reserved. No part of this book may be reproduced, stored in a retrieval system, or transmitted in any form or by any means without permission in writing from the publisher.

Printed in the United States of America

7 6 5 4 3 2 1

Contents

Acknowledgements and Dedication	xii
Preface	xiii
1 Introduction	1
1.1 Groundwater as a Resource	1
1.2 Types of Groundwater Contaminants	3
1.3 Drinking-Water Standards	16
1.4 Risk and Drinking Water	17
1.5 Sources of Groundwater Contamination	24
1.5.1 Category I: Sources Designed to Discharge Substances	24
1.5.2 Category II: Sources Designed to Store, Treat and/or Dispose of Substances	28
1.5.3 Category III: Sources Designed to Retain Substances During Transport	35
1.5.4 Category IV: Sources Discharging Substances as a Consequence of Other Planned Activities	35
1.5.5 Category V: Sources Providing a Conduit for Contaminated Water to Enter Aquifers	38
1.5.6 Category VI: Naturally Occurring Sources Whose Discharge is Created and/or Exacerbated by Human Activity	39
1.6 Relative Ranking of Groundwater-Contamination Sources and Substances	40
1.7 Groundwater Contamination as a Long-Term Problem	42
1.8 Review of Mathematics and the Flow Equation	44
1.8.1 Derivatives	44
1.8.2 Darcy's Law	46
1.8.3 Scalar, Vector, and Tensor Properties of Hydraulic Head and Hydraulic Conductivity	47
1.8.4 Derivation of the Flow Equation in a Deforming Medium	49
1.8.5 Mathematical Notation	51
References	52
Problems	55

2 Mass Transport in Saturated Media	56
2.1 Introduction	56
2.2 Transport by Concentration Gradients	56
2.3 Transport by Advection	61
2.4 Mechanical Dispersion	63
2.5 Hydrodynamic Dispersion	65
2.6 Derivation of the Advection-Dispersion Equation for Solute Transport	66
2.7 Diffusion versus Dispersion	68
2.8 Moment Analysis	70
2.9 Analytical Solutions of the Advection-Dispersion Equation	75
2.9.1 Methods of Solution	75
2.9.2 Boundary and Initial Conditions	76
2.9.3 One-Dimensional Step Change in Concentration (First-Type Boundary)	77
2.9.4 One-Dimensional Continuous Injection into a Flow Field (Second-Type Boundary)	78
2.9.5 Third-Type Boundary Condition	82
2.9.6 One-Dimensional Slug Injection into a Flow Field	82
2.9.7 Continuous Injection into a Uniform Two-Dimensional Flow Field	83
2.9.8 Slug Injection into a Uniform Two-Dimensional Flow Field	88
2.10 Effects of Transverse Dispersion	92
2.11 Tests to Determine Dispersivity Values	93
2.11.1 Laboratory Tests	93
2.11.2 Quantifying Dispersivity in the Field	96
2.11.3 Single-Well Tracer Test	97
2.12 Scale Effect of Dispersion	98
2.13 Stochastic Models of Solute Transport	103
2.13.1 Introduction	103
2.13.2 Stochastic Descriptions of Heterogeneity	104
2.13.3 Stochastic Approach to Solute Transport	106
2.14 Regression Analysis of Relationship between Apparent Longitudinal Dispersivity and Field Scale	107
2.15 Deterministic Models of Solute Transport	109
2.16 Transport in Fractured Media	117
2.17 Summary	124
Chapter Notation	124
References	126
Problems	131
3 Transformation, Retardation, and Attenuation of Solutes	133
3.1 Introduction	133
3.2 Classification of Chemical Reactions	134

3.3	Sorption Processes	134
3.4	Equilibrium Surface Reactions	135
3.4.1	Linear Sorption Isotherm	135
3.4.2	Freundlich Sorption Isotherm	138
3.4.3	Langmuir Sorption Isotherm	140
3.4.4	BET Sorption	142
3.4.5	Polanyi–Dubinin–Manes (PDM) Sorption Isotherm	143
3.4.6	Effect of Equilibrium Retardation on Solute Transport	144
3.5	Nonequilibrium (Kinetic) Sorption Models	148
3.6	Sorption of Hydrophobic (Organic) Compounds	153
3.6.1	Introduction	153
3.6.2	Partitioning onto Soil or Aquifer Organic Carbon	154
3.6.3	Estimating K_{oc} from K_{ow} Data	155
3.6.4	Estimating K_{oc} from Solubility Data	156
3.6.5	Estimating K_{oc} from Molecular Structure	161
3.6.6	Quantitative Structure-Property Relationships	163
3.6.7	Multiple Solute Effects	165
3.7	Homogeneous Reactions	168
3.7.1	Introduction	168
3.7.2	Chemical Equilibrium	168
3.7.3	Chemical Kinetics	168
3.8	Radioactive Decay	170
3.9	Biodegradation	171
3.10	Colloidal Transport	176
3.10.1	Colloid Attachment/Detachment and Straining Theory	179
3.11	Summary	187
	Chapter Notation	187
	References	189
	Problems	195
4	Flow and Mass Transport in the Vadose Zone	198
4.1	Introduction	198
4.2	Soil as a Porous Medium	199
4.3	Soil Colloids	200
4.4	The Electrostatic Double Layer	200
4.5	Salinity Effects on Hydraulic Conductivity of Soils	202
4.6	Flow of Water in the Unsaturated Zone	203
4.6.1	Soil-Water Potential	204
4.6.2	Soil-Water Characteristic Curves	204
4.6.3	Hysteresis	210
4.6.4	Construction of a Soil-Water-Retention Curve	211
4.6.5	Measurement of Soil-Water Potential	213
4.6.6	Unsaturated Hydraulic Conductivity	214
4.6.7	Buckingham Flux Law	218
4.6.8	Richards Equation	219

4.7	Liquid Mass Transport in the Unsaturated Zone	220
4.8	Equilibrium Models of Mass Transport	221
4.9	Nonequilibrium Models of Mass Transport	224
4.10	Anion Exclusion	225
4.11	Preferential Flowpaths in the Vadose Zone	229
4.12	Vapor Phase Transport	233
4.12.1	Gaseous Diffusion	233
4.12.2	Gaseous Advection	238
4.12.3	Effusion (Knudsen flow)	239
4.12.4	Combinations of Vapor Transport Processes	239
4.12.5	Other Environmental Factors	239
4.13	Summary	241
	Chapter Notation	241
	References	243
	Problems	246
5	Multiphase Flow	247
5.1	Introduction	247
5.2	Basic Concepts	248
5.2.1	Saturation Ratio	248
5.2.2	Interfacial Tension and Wettability	249
5.2.3	Capillary Pressure	250
5.2.4	Relative Permeability	253
5.2.5	Darcy's Law For Two-Phase Flow	257
5.2.6	Fluid Potential and Head	258
5.3	Migration of Light Nonaqueous Phase Liquids (LNAPLs)	262
5.4	Capillary and Bond Numbers	267
5.5	Partitioning Interwell Tracer Tests	269
5.6	Volatilization of NAPLs	271
5.7	Vapor Density	277
5.8	Measurement of the Thickness of a Floating Product	278
5.9	Effect of the Rise and Fall of the Water Table on the Distribution of LNAPLs	287
5.10	Migration of Dense Nonaqueous Phase Liquids (DNAPLs)	290
5.10.1	Relative Mobility	290
5.10.2	Vadose Zone Migration	292
5.10.3	Vertical Movement in the Saturated Zone	294
5.10.4	Horizontal Movement in the Saturated Zone	296
5.10.5	DNAPL Flow in Fracture Systems	301
5.10.6	Dissolution of DNAPL	303
5.11	Monitoring for LNAPLs and DNAPLs	305
5.12	Summary	308
	Chapter Notation	309
	References	310
	Problems	315

6 Inorganic Chemicals in Groundwater	316
6.1 Introduction	316
6.2 Units of Measurement and Concentration	316
6.3 Chemical Equilibrium and the Law of Mass Action	317
6.4 Oxidation-Reduction Reactions	320
6.5 Relationship between pH and Eh	323
6.5.1 pH	323
6.5.2 Relationship of Eh and pH	325
6.5.3 Eh-pH Diagrams	326
6.5.4 Calculating Eh-pH Stability Fields	328
6.6 Metal Complexes and Facilitated Particle Transport	338
6.6.1 Hydration of Cations	338
6.6.2 Complexation	339
6.6.3 Organic Complexing Agents	341
6.6.4 Facilitated Particle Transport	341
6.7 Chemistry of Nonmetallic Inorganic Contaminants	343
6.7.1 Fluoride	343
6.7.2 Chlorine and Bromine	344
6.7.3 Sulfur	344
6.7.4 Nitrogen	346
6.7.5 Arsenic	347
6.7.6 Selenium	348
6.7.7 Phosphorus	350
6.8 Chemistry of Metals	350
6.8.1 Beryllium	350
6.8.2 Strontium	350
6.8.3 Barium	351
6.8.4 Vanadium	351
6.8.5 Chromium	351
6.8.6 Cobalt	353
6.8.7 Nickel	353
6.8.8 Molybdenum	353
6.8.9 Copper	354
6.8.10 Silver	354
6.8.11 Zinc	354
6.8.12 Cadmium	354
6.8.13 Mercury	356
6.8.14 Lead	356
6.8.15 Rare Earth Elements	358
6.9 Radioactive Isotopes	358
6.9.1 Introduction	358
6.9.2 Adsorption of Cationic Radionuclides	359
6.9.3 Uranium	360
6.9.4 Thorium	363
6.9.5 Radium	364

viii Contents

6.9.6	Radon	367
6.9.7	Tritium	368
6.10	Geochemical Zonation	368
6.11	Summary	371
	Chapter Notation	372
	References	372
	Problems	375
7	Organic Compounds in Groundwater	376
7.1	Introduction	376
7.2	Physical Properties of Organic Compounds	376
7.3	Organic Structure and Nomenclature	378
7.3.1	Hydrocarbon Classes	378
7.3.2	Aromatic Hydrocarbons	382
7.4	Petroleum and Coal Tar	383
7.4.1	Petroleum Distillates	383
7.4.2	Coal Tar	389
7.4.3	Groundwater contamination associated with petroleum products and coal tar	390
7.5	Functional Groups	395
7.5.1	Organic Halides	395
7.5.2	Alcohols	395
7.5.3	Ethers	395
7.5.4	Aldehydes and Ketones	399
7.5.5	Carboxylic and Sulfonic Acids	400
7.5.6	Esters	402
7.5.7	Phenols	404
7.5.8	Organic Compounds Containing Nitrogen	405
7.5.9	Organic Compounds Containing Sulfur and Phosphorus	408
7.5.10	Emerging Contaminants	410
7.6	Degradation of Organic Compounds	415
7.6.1	Introduction	415
7.6.2	Degradation of Hydrocarbons	415
7.6.3	Degradation of Chlorinated Hydrocarbons	418
7.6.4	Degradation of Organic Pesticides	425
7.6.5	Degradation of Gasoline Compounds	427
7.7	Field Studies of Biological Degradation of Organic Molecules	428
7.8	Analysis of Organic Compounds in Groundwater	428
7.9	Fingerprinting Petroleum Distillates and Coal Tar	434
7.10	Summary	442
	References	442
	Problems	447

8 Site Characterization—Groundwater and Soil Monitoring	450
8.1 Introduction	450
8.2 Noninvasive Measures	452
8.2.1 Interpretation of Aerial Photography and Remote Sensing	452
8.2.2 The Use of Surface Geophysical Techniques for Site Characterization	453
8.2.3 Rapid Noninvasive Field Surveys and Screening	455
8.3 Minimally Invasive Soil Monitoring	456
8.3.1 Soil Vapor Monitoring—Introduction	456
8.3.2 Methods of Soil Gas Monitoring	457
8.3.3 Soil Water Sampling—Introduction	458
8.3.4 Suction Lysimeters	458
8.3.5 Installation of Suction Lysimeters	460
8.3.6 Phyto-screening	461
8.4 Invasive Methods - Monitoring Well Design	462
8.4.1 General Information	462
8.4.2 Monitoring Well Casing	464
8.4.3 Monitoring Well Screens	472
8.4.4 Naturally Developed and Filter-Packed Wells	473
8.4.5 Annular Seal	474
8.4.6 Protective Casing	475
8.4.7 Screen Length and Setting	476
8.4.8 Summary of Monitoring Design for Single Screened Wells	479
8.4.9 Multiple-level Wells and Multilevel Devices for Groundwater Monitoring	479
8.5 Installation of Monitoring Wells	485
8.5.1 Decontamination Procedures	485
8.5.2 Methods of Drilling	486
8.5.3 Drilling in Contaminated Soil	494
8.5.4 Sample Collection of Solid Material During Drilling	494
8.5.5 Installation of Monitoring Wells	498
8.5.6 Monitoring Well Development	503
8.5.7 Record Keeping During Monitoring Well Construction	507
8.5.8 Monitoring Well and Borehole Abandonment	507
8.6 Well Sampling	509
8.6.1 Introduction	509
8.6.2 Fluid Level and Pressure Measurement	509
8.6.3 Well Purging	510
8.6.4 Well-Sampling Devices	510
8.6.5 Methods of Collecting a Groundwater Sample Without Drilling a Well	514
8.6.6 Low-Flow Purging of Monitoring Wells	516
8.6.7 Sampling Frequency	518

8.7	Other Site Characterization Methods and Groundwater Contamination Forensics	519
8.7.1	Introduction	519
8.7.2	Borehole Geophysics and Downhole Techniques	520
8.7.3	Water Quality Indicators of Groundwater Provenance and Movement—Tracers	522
8.7.4	Water Quality Indicators of Groundwater Provenance and Movement—Groundwater Composition, Compound Ratios, Daughter Products, Degradation Indicators, and Other Indicator Compounds	526
8.7.5	Water Quality Indicators of Groundwater Provenance and Movement—Isotopic Identification of Pollution Sources and Groundwater Pathways	529
8.7.6	Water Quality Indicators of Groundwater Condition—Microbial testing and Genome Sequencing	532
8.8	Summary	534
	References	535
	Problem	542

9 Site Remediation 543

9.1	Introduction	543
9.2	Source-Control Measures	545
9.2.1	Solid Waste	545
9.2.2	Removal and Disposal	546
9.2.3	Containment	547
9.2.4	Hydrodynamic Isolation	552
9.3	Pump-and-Treat Systems	555
9.3.1	Overview	555
9.3.2	Capture Zones	562
9.3.3	Computation of Capture Zones	563
9.3.4	Optimizing Withdrawal-Injection Systems	563
9.3.5	Permanent Plume Stabilization	566
9.4	Treatment of Extracted Groundwater	568
9.4.1	Overview	568
9.4.2	Treatment of Inorganic Contaminants	569
9.4.3	Treatment of Dissolved Organic Contaminants	570
9.5	Recovery of Nonaqueous Phase Liquids	572
9.6	Removal of Leaking Underground Storage Tanks	576
9.7	Soil Vapor Extraction (SVE)	578
9.8	Air Sparging and Bioslurping	583
9.9	Combination Methods	584
9.10	Bioremediation	589
9.10.1	Introduction	589
9.10.2	Monitored Natural Attenuation	590
9.10.3	Enhanced Bioremediation	592

9.11	Conceptual Site Models	598
9.12	Permeable Reactive Barriers	599
9.13	Chemically-Enhanced <i>In Situ</i> Flushing	606
9.13.1	Surfactant Enhanced <i>In Situ</i> Flushing	607
9.13.2	Cosolvent Enhanced <i>In Situ</i> Flushing	609
9.13.3	Complexing Agent Enhanced <i>In Situ</i> Flushing	610
9.14	<i>In Situ</i> Thermal Treatment (ISTT)	612
9.15	<i>In situ</i> Chemical Oxidation (ISCO)	614
9.16	Phytoremediation	616
9.17	Summary	618
	Chapter Notation	620
	References	620
Appendix A Error Function Values		629
Appendix B Bessel Functions		630
Appendix C $W(t_D, B)$ Values		633
Appendix D Exponential Integral		635
Appendix E Unit Abbreviations		636
Index		637
About the Authors		647

Acknowledgements and Dedication

This edition is dedicated to C.W. “Bill” Fetter, Jr., who died on September 10, 2011. Bill had an illustrious career for 25 years as a professor at the University of Wisconsin-Oshkosh, including 16 years as Department Chairman. He was a valued mentor, well-known consultant and groundwater professional, served as an expert witness in more than 200 cases concerning groundwater and contamination, and authored the first two editions of this book. Having worked with Bill personally, a coauthor of the Third Edition always found him to be a warm, personable, and thoughtful man, in addition to being a superb groundwater professional and practitioner. He is greatly missed.

The authors would also like to acknowledge the support of family and friends, and the assistance of many professionals and colleagues who helped review and inform this edition, and our students who give continuing motivation for our work. The authors would particularly like to recognize the suggestions, insights, inspiration, and efforts of our mentors and colleagues (past and present) including: Jean M. Bahr, Stanley N. Davis, Herman Bouwer, David A. Sabatini, Glenn M. Thompson, Simon Ince, Lorne G. Everett, Eugene S. Simpson, Roger DeWiest, Franklin W. Schwartz, Patrick A. Domenico, Charles J. Newell, David M. Nielsen, Beth L. Parker, Michael E. Campana, Lorne Graham “Gray” Wilson, Peter Grathwohl, William “Bill” Blanford, Craig Devine, John McCray, Geoff Tick, KC Carrol, Mark Brusseau, Dakota West, and Don Rosso.

We would also like to recognize R. Allan Freeze and John A. Cherry, who, from the very front cover of their textbook to their inspiring work in the field, have shown us that looking at things from a different angle is not a bad thing.

It is impossible for the authors to acknowledge all those who contributed either directly or indirectly to this edition, and to all those unmentioned colleagues who we might have missed, our apologies.

Preface

Dr. C. W. Fetter, Jr., was an internationally recognized expert in hydrogeology and Emeritus Professor of Geology, University of Wisconsin Oshkosh. He passed away in September 2011. His legacy encompasses textbooks on the subject of applied hydrogeology, including the standard textbook on contaminant fate and transport in soil and groundwater, titled *Contaminant Hydrogeology*. Last updated in 1998 (the second edition), the *Contaminant Hydrogeology* textbook has been the go-to reference for generations of students in geology, civil and environmental engineering, environmental sciences, and agricultural engineering. The book is also found on the shelves of many professionals working in the field of contaminant site investigation and remediation as well as in the offices of the regulating agencies overseeing environmental clean-up and restoration.

Since Dr. Fetter authored the previous editions of *Contaminant Hydrogeology*, the interest in and importance of contaminant hydrogeology has been greater than ever, particularly in regions around the world where the extent of pollution of soil and groundwater is being recognized only very recently. Unprecedented advances in remediation technology and new concepts for dealing with soil and groundwater contamination problems made it necessary to take a critical look at the models and practices introduced by Fetter two decades earlier. When our publisher first approached us with the proposal to bring the *Contaminant Hydrogeology* textbook into the twenty-first century, we were both honored and humbled to build on Fetter's prior work. Our goal was to not entirely rewrite the book, but to revise, update, and expand on the materials originally developed. In particular, we recognized that a great deal of the most exciting research into the fate and transport of contaminants is now happening outside the United States, which in the past has been the driving force behind much of environmental innovation. Regions like Europe or East Asia are now important centers of environmental research and many of today's most pressing soil and groundwater pollution problems are found outside the United States. We intended to highlight this development by including examples and references from around the globe.

Major changes have been made to all chapters. In Chapter 1, we have expanded the discussion of contaminants, including an introduction to "emerging contaminants" whose risk to health and the environment is not completely understood, and new discussion of potential contaminant sources which are receiving increasing attention, such as deep well injection, fracking fluids, and newer mining methods, such as *in situ* leach mining. In Chapter 2's presentation of mass transport in the saturated zone,

we added a section on statistical tools (Moment analysis) and expanded the discussion of deterministic models of solute transport, including in fractured matrices, while cutting the discussion of the fractal mathematics, geometry, and scaling of transport parameters. In Chapter 3, which focuses on transformation, retardation, and attenuation of solutes, we added sections covering BET and Polanyi adsorption potential theory, expanded on kinetic models, quantitative structure-property relationships, and colloid-facilitated contaminant transport. Chapter 4's discussion of vadose zone contaminant migration includes a new section on vapor transport theory, among other additions. Major changes to Chapter 5 (multi-phase flow) include the introduction of the Capillary and Bond Numbers and the partitioning interwell tracer testing technique for investigating NAPL sites. Chapter 6 expands the description of distribution, movement, and impact of inorganic contaminants and radionuclides. On the topic of organic compounds, additions to Chapter 7 include a more detailed discussion of chemical structures and functional groups, as well as adapting the line form for showing the chemical structure of organic compounds. We also expanded or replaced the list of chemical compounds typically found in contaminated soil and groundwater, including a discussion of emerging contaminant characteristics and updated pollutant transformation pathways. Chapter 8 focuses on site assessment and has major additions and reorganization, proceeding from basic principles and general approaches, to noninvasive techniques, rapid field screening, invasive techniques, and monitoring well construction, to forensic techniques. New sections of this chapter include: aerial photographic interpretation, geophysics, immunological surveys, high resolution vertical sampling, flexible liner systems, directional drilling, sampling frequency considerations, groundwater tracers, isotopic identification of groundwater pollution and groundwater pathways, and genome sequencing of subsurface microbes. Finally, the substantial additions to Chapter 9 reflect the immense progress that has been made in the field of remediation technologies.

Similar to the prior editions, the third edition of *Contaminant Hydrogeology* is intended as a textbook in a graduate level course in mass transport and contaminant hydrogeology. We assumed that our readers have some basic course work in hydrogeology, mathematics and statistics, chemistry and physics, and are comfortable with spreadsheet software, like Excel.

Tom Boving and Dave Kreamer
September 2017

Introduction

■ 1.1 Groundwater as a Resource

Groundwater is the source of drinking water for many people around the world, especially in arid regions, rural areas, and increasingly in urban and suburban environments. It is the most abundant, available source of freshwater and most extracted raw material on earth, representing about 97% of nonfrozen fresh water with withdrawal rates near 982 km³/yr. Worldwide, groundwater accounts for approximately 35% of all water withdrawals by human populations. Groundwater supplies an estimated 38–42% of the global water used for irrigation, approximately 36% of the water resources needed for households, and roughly 27% of the water needed for industry and manufacturing (Döll et al. 2012; Siebert et al. 2010; Margat and van der Gun 2013; National Ground Water Association 2015). Excessive groundwater abstraction, where withdrawals exceed recharge over time, can have many negative consequences, and about 1.7 billion people live in areas where groundwater resources are under threat. Exploitation of limited groundwater can stress aquifers used for water supply, produce ground subsidence, increase saline water intrusion in coastal regions, contribute to sea-level rise, and reduce water supply to groundwater-dependent ecosystems surrounding springs, rivers, estuaries, and wetlands. (Gleeson et al. 2012; Konikow 2011; Wada et al. 2010). Tables 1.1 and 1.2 show the percentage portion of the world population and total population estimates respectively for those obtaining drinking water from dug holes and boreholes in 1990 and 2010.

In the United States, groundwater accounts for nearly 25% of all freshwater withdrawals and 43% of the water used for agriculture. Virtually all the homes that supply their

TABLE 1.1 Proportion of the population obtaining drinking water from boreholes and dug wells, urban and rural, 1990 and 2010 (percent).

	Urban Percent		Rural Percent		Total Percent	
	1990	2010	1990	2010	1990	2010
Boreholes	6	8	29	30	19	18
Dug Wells	5	4	27	19	18	12
Total	11	12	56	49	37	30

Source: UNICEF 2012.

TABLE 1.2 World population obtaining drinking water from boreholes and dug wells, 1990 and 2010 (population in millions).

	Urban			Rural			Total		
	1990	2010	Percent change	1990	2010	Percent change	1990	2010	Percent change
Boreholes	138	255	+84.8	878	996	+13.4	1,016	1,251	+23.1
Dug Wells	111	151	+36.0	843	656	-22.2	954	807	-15.4
Total	249	406	+63.1	1,721	1,652	-4.0	1,970	2,058	+4.5

Source: UNICEF 2012.

own water have wells (98%) and use groundwater. Approximately 115 million people rely on groundwater for drinking water, 43 million from private wells. There are more than 15.9 million water wells in the United States, and approximately 500,000 new residential wells are added each year (Maupin et al. 2014; National Ground Water Association 2015). Figure 1.1 shows groundwater withdrawals in the United States in 2010.

Inasmuch as groundwater provides drinking water to so many people, the quality of groundwater is of paramount importance. Public water suppliers in the United States are obligated by the Safe Drinking Water Act of 1986 to furnish water that meets specific drinking-water standards to their consumers. If the water does not meet the standards when it is withdrawn from its source, it must be treated. Groundwater may not meet the standards because it contains dissolved constituents coming from natural sources. Common examples of constituents coming from natural sources are total dissolved solids, sulfate, and chloride. Groundwater also may not meet the standards because it contains organic liquids, dissolved organic and inorganic constituents, excessive nutrients, or pathogens that came from an anthropogenic source. In such cases the groundwater has been contaminated by the acts of humans.

In the case of self-supplied systems, a source of uncontaminated water is of even greater importance. Such systems are typically tested initially for only a very limited range of constituents, such as coliform bacteria, nitrate, chloride, and iron. Most times groundwater contamination cannot be tasted, so that with such limited testing it is possible for a user to have a contaminated source and not be aware of it. In one example, the lack of complete water quality testing of groundwater in India and Bangladesh in the 1970s and 1980s led to the drilling of tens of thousands of shallow tube wells which were later found to be contaminated with arsenic, poisoning huge numbers of people. A 2007 study indicated that over 137 million people in more than 60 countries are likely affected by arsenic contamination of their drinking water (Ravenscroft et al. 2009). Self-supplied systems rarely undergo treatment other than softening and perhaps iron removal. There are limited options available for the homeowner who wishes to treat contaminated groundwater so that it can be consumed.

In addition to providing for the sustenance of human life, groundwater has important ecological functions. Many freshwater habitats are supplied by the discharge of springs. Springs can supply water to many sorts of ecological environments, including the gaining reaches of rivers, estuaries, and wetlands. If the groundwater supplying these springs is diminished in flow or contaminated, the ecological function of the

FIGURE 1.1 Groundwater withdrawals in the United States, 2010.

Source: Maupin et al. 2014.

freshwater habitat can be impaired with negative consequences to species diversity and sustainability (Kreamer et al. 2015).

■ 1.2 Types of Groundwater Contaminants

A wide variety of materials have been identified as contaminants found in groundwater. These include synthetic organic chemicals, hydrocarbons, inorganic cations, inorganic anions, pathogens, and radionuclides. Table 1.3 contains an extensive listing of these compounds. Most of these materials will dissolve in water to varying degrees. Some of the organic compounds are only slightly soluble and will exist in both a dissolved form and as an insoluble nonaqueous phase, which can also migrate through the ground. Examples of the uses of these materials are also given on Table 1.3. These uses may provide help in locating the source of a compound if it is found in groundwater. The inorganic cations and anions occur in nature and may come from natural as well as anthropogenic sources. Some of the radionuclides are naturally occurring and can come from natural sources as well as mining, milling, and processing ore, industrial uses, and disposal of radioactive waste. Other radionuclides are man-made and come from nuclear weapons production and testing. There is increasing public concern over the development of new chemicals and industrial processes which have the potential to pollute groundwater. For example, current challenges include the subsurface injection of liquid wastes, circulation of geothermal energy fluids, and the use of newly developed fracking fluids for enhanced extraction of hydrocarbon fuels, combined with increasing utilization of groundwater in stressed locales.

4 Chapter One

TABLE 1.3 Substances known to occur in groundwater.

Contaminant	Examples of uses
Aromatic hydrocarbons	
Acenaphthene	Coal tar by-product
Acenaphthylene	Coal tar by-product
Acetanilide	Intermediate manufacturing, pharmaceuticals, dyestuffs
Alkyl benzene sulfonates	Detergents
Aniline	Dyestuffs, intermediate, photographic chemicals, pharmaceuticals, herbicides, fungicides, petroleum refining, explosives
Anthracene	Dyestuffs, intermediate, semiconductor research, coal tar by-product
Benzene	Detergents, intermediate, solvents, gasoline, coal tar by-product
Benzidine	Dyestuffs, reagent, stiffening agent in rubber compounding
Benzo[a]anthracene	Coal tar by-product
Benzo[a]pyrene	Coal tar by-product
Benzo[b]fluroanthene	Coal tar by-product
Benzo[g,h,i]perylene	Coal tar by-product
Benzo[k]fluoranthene	Coal tar by-product
Benzyl alcohol	Solvent, perfumes and flavors, photographic developer inks, dye-stuffs, intermediate
Butoxymethylbenzene	NA
Chrysene	Organic synthesis, coal tar by-product
Creosote mixture	Wood preservatives, disinfectants
Dibenz[a,h]anthracene	NA
Di-butyl-p-benzoquinone	NA
Dihydrotrimethylquinoline	Rubber antioxidant
4,4-Dinitrosodiphenylamine	NA
Ethylbenzene	Intermediate, solvent, gasoline, coal tar by-product
Fluoranthene	Coal tar by-product
Fluorene	Resinous products, dyestuffs, insecticides, coal tar by-product
Fluorescein	Dyestuffs
Isopropyl benzene	Solvent, chemical manufacturing
4,4-methylene-bis-2-chloroaniline (MOCA)	Curing agent for polyurethanes and epoxy resins

(Cont'd)

TABLE 1.3 Cont'd

Contaminant	Examples of uses
Methylnaphthalene	Coal tar by product, diesel fuel
Methylthiobenzothiazole	NA
Naphthalene	Solvent, lubricant, explosives, preservatives, intermediate, fungicide, moth repellent, coal tar by product, gasoline
<i>o</i> -Nitroaniline	Dyestuffs, intermediate, interior paint pigments, chemical manufacturing
Nitrobenzene	Solvent, polishes, chemical manufacturing
4-Nitrophenol	Chemical manufacturing
<i>n</i> -Nitrosodiphenylamine	Pesticides, retarder of vulcanization of rubber
Phenanthrene	Dyestuffs, explosives, synthesis of drugs, biochemical research
<i>n</i> -Propylbenzene	Dyestuffs, solvent
Pyrene	Biochemical research, coal tar by-product
Styrene (vinyl benzene)	Plastics, resins, protective coatings, intermediate, gasoline
Toluene	Adhesive solvent in plastics, solvent, aviation and high-octane blending stock, dilutent and thinner, chemicals, explosives, detergents, gasoline, coal tar by-product
1,2,4-Trimethylbenzene	Manufacture of dyestuffs, pharmaceuticals, chemical manufacturing, gasoline
Xylenes (<i>m, o, p</i>)	Aviation gasoline, protective coatings, solvent, synthesis of organic chemicals, gasoline, coal tar by-product
Oxygenated hydrocarbons	
Acetic acid	Food additives, plastics, dyestuffs, pharmaceuticals, photographic chemicals, insecticides
Acetone	Dyestuffs, solvent, chemical manufacturing, cleaning and drying of precision equipment
Benzophenone	Organic synthesis, odor fixative, flavoring, pharmaceuticals
Butyl acetate	Solvent
<i>n</i> -Butyl-benzylphthalate	Plastics, intermediate
Di- <i>n</i> -butyl phthalate	Plasticizer, solvent, adhesives, insecticides, safety glass, inks, paper coatings
Diethyl ether	Chemical manufacturing, solvent, analytical chemistry, anesthetic, perfumes
Diethyl phthalate	Plastics, explosives, solvent, insecticides, perfumes
Diisopropyl ether	Solvent, rubber cements, paint and varnish removers
2,4-Dimethyl-3-hexanol	Intermediate, solvent, lubricant

(Cont'd)

TABLE 1.3 *Cont'd*

Contaminant	Examples of uses
2,4-Dimethyl phenol	Pharmaceuticals, plastics, disinfectants, solvent, dyestuffs, insecticides, fungicides, additives to lubricants and gasolines
Di- <i>n</i> -octyl phthalate	Plasticizer for polyvinyl chloride and other vinyls
1,4-Dioxane	Solvent, lacquers, paints, varnishes, cleaning and detergent preparations, fumigants, paint and varnish removers, wetting agent, cosmetics
Ethyl acrylate	Polymers, acrylic paints, intermediate
Formic acid	Dyeing and finishing, chemicals, manufacture of fumigants, insecticides, solvents, plastics, refrigerants
Methanol (methyl alcohol)	Chemical manufacturing, solvents, automotive antifreeze, fuels
Methylcyclohexanone	Solvent, lacquers
Methyl ethyl ketone (2-Butanone)	Solvent, paint removers, cements and adhesives, cleaning fluids, printing, acrylic coatings
Methylphenyl acetamide	NA
Phenols (e.g., p- <i>tert</i> -butylphenol)	Resins, solvent, pharmaceuticals, reagent, dyestuffs and indicators, germicidal paints
Phthalic acid	Dyestuffs, medicine, perfumes, reagent
2-Propanol	Chemical manufacturing, solvent, deicing agent, pharmaceuticals, perfumes, lacquers, dehydrating agent, preservatives
2-Propyl-1-heptanol	Solvent
Methyl <i>tert</i> -butyl ether (MTBE)	Gasoline additive
Tetrahydrofuran	Solvent
Varsol	Paint and varnish thinner
Hydrocarbons with specific elements (e.g., with N, P, S, Cl, Br, I, F)	
Acetyl chloride	Dyestuffs, pharmaceuticals, organic preparations
Alachlor (Lasso)	Herbicides
Aldicarb (sulfoxide and sulfone; Temik)	Insecticide, nematocide
Aldrin	Insecticides
Atrazine	Herbicides, plant growth regulator, weed-control agent
Benzoyl chloride	Medicine, intermediate
Bromacil	Herbicides
Bromobenzene	Solvent, motor oils, organic synthesis
Bromochloromethane	Fire extinguishers, organic synthesis

(Cont'd)

TABLE 1.3 Cont'd

Contaminant	Examples of uses
Bromodichloromethane	Solvent, fire extinguisher fluid, mineral and salt separations
Bromoform	Solvent, intermediate
Carbofuran	Insecticide, nematocide
Carbon tetrachloride	Degreasers, refrigerants and propellants, fumigants, chemical manufacturing
Chlordane	Insecticides, oil emulsions
Chlorobenzene	Solvent, pesticides, chemical manufacturing
Chloroform	Plastics, fumigants, insecticides, refrigerants and propellants
Chlorohexane	NA
Chloromethane (methyl chloride)	Refrigerants, medicine, propellants, herbicide, organic synthesis
Chloromethyl sulfide	NA
2-Chloronaphthalene	Plasticizer, solvent for dyestuffs, varnish gums and resins, waxes; moisture-, flame-, acid-, and insect-proofing of fibrous materials; moisture- and flame-proofing of electrical cable
Chlorpyrifos	NA
Chlorthal-methyl (DCPA, or Dacthal)	Herbicide
p-Chlorophenyl methylsulfone	Herbicide manufacture
Chlorophenylmethyl sulfide	Herbicide manufacture
Chlorophenylmethyl sulfoxide	Herbicide manufacture
<i>o</i> -Chlorotoluene	Solvent, intermediate
<i>p</i> -Chlorotoluene	Solvent, intermediate
Cyclopentadiene	Insecticide manufacture
Dibromochloromethane	Organic synthesis
Dibromochloropropane (DBCP)	Fumigant, nematocide
Dibromodichloroethylene	NA
Dibromoethane (ethylene dibromide, EDB)	Fumigant, nematocide, solvent, waterproofing preparations, organic synthesis, gasoline additive
Dibromomethane	Organic synthesis, solvent
Dichlofenthion (DCFT)	Pesticides
<i>o</i> -Dichlorobenzene	Solvent, fumigants, dyestuffs, insecticides, degreasers, polishes, industrial odor control

(Cont'd)

TABLE 1.3 *Cont'd*

Contaminant	Examples of uses
<i>p</i> -Dichlorobenzene	Insecticides, moth repellent, germicide, space odorant, intermediate, fumigants
Dichlorobenzidine	Intermediate, curing agent for resins
Dichlorocyclooctadiene	Pesticides
Dichlorodiphenyldichloroethane (DDD, TDE)	Insecticides
Dichlorodiphenyldichloroethylene (DDE)	Degradation product of DDT, found as an impurity in DDT residues
Dichlorodiphenyltrichloroethane (DDT)	Pesticides
1,1-Dichloroethane	Solvent, fumigants, medicine
1,2-Dichloroethane	Solvent, degreasers, soaps and scouring compounds, organic synthesis, additive in antiknock gasoline, paint and finish removers
1,1-Dichloroethylene (vinylidene chloride)	Saran (used in screens, upholstery, fabrics, carpets, etc.). adhesives, synthetic fibers
1,2-Dichloroethylene (cis and trans)	Solvent, perfumes, lacquers, thermoplastics, dye extraction organic synthesis, medicine
Dichloroethyl ether	Solvent, organic synthesis, paints, varnishes, lacquers, finish removers, dry cleaning, fumigants
Dichloroiodomethane	NA
Dichloroisopropylether (bis-2-chloroisopropylether)	Solvent, paint and varnish removers, cleaning solutions
Dichloromethane (methylene chloride)	Solvent, plastics, paint removers, propellants, blowing agent in foams
Dichloropentadiene	NA
2,4-Dichlorophenol	Organic synthesis
2,4-Dichlorophenoxyacetic acid (2,4-D)	Herbicides
1,2-Dichloropropane	Solvent, intermediate, scouring compounds, fumigant, nematocide, additive for antiknock fluids
Dicyclopentadiene (DCPD)	Insecticide manufacture
Dieldrin	Insecticides
Diiodomethane	Organic synthesis
Diisopropylmethyl phosphonate (DIMP)	Nerve gas manufacture
Dimethyl disulfide	NA
Dimethylformamide	Solvent, organic synthesis
2,4-Dinotrophenol (Dinoseb, DNBP)	Herbicides

(Cont'd)

TABLE 1.3 *Cont'd*

Contaminant	Examples of uses
Dithiane	Mustard gas manufacture
Dioxins (e.g., TCDD)	Impurity in the herbicide 2,4,5-T
Dodecyl mercaptan (lauryl mercaptan)	Manufacture of synthetic rubber and plastics, pharmaceuticals, insecticides, fungicides
Endosulfan	Insecticides
Endrin	Insecticides
Ethyl chloride	Chemical manufacturing, anesthetic, solvent, refrigerants, insecticides
Bis-2-ethylhexylphthalate	Plastics
Di-2-ethylhexylphthalate	Plasticizers
Fluorobenzene	Insecticide and larvicide intermediate
Fluoroform	Refrigerants, intermediate, blowing agent for foams
Heptachlor	Insecticides
Heptachlorepoxyde	Degradation product of heptachlor, also acts as an insecticide
Hexachlorobicycloheptadiene	NA
Hexachlorobutadiene	Solvent, transformer and hydraulic fluid, heat-transfer liquid
α -Hexachlorocyclohexane (Benzenehexachloride, or α -BHC)	Insecticides
β -Hexachlorocyclohexane (β -BHC)	Insecticides
γ -Hexachlorocyclohexane (γ -BHC, or Lindane)	Insecticides
Hexachlorocyclopentadiene	Intermediate for resins, dyestuffs, pesticides, fungicides, pharmaceuticals
Hexachloroethane	Solvent, pyrotechnics and smoke devices, explosives, organic synthesis
Hexachloronorbornadiene	NA
Isodrin	Intermediate compound in manufacture of Endrin
Kepone	Pesticides
Malathion	Insecticides
Methoxychlor	Insecticides
Methyl bromide	Fumigants, pesticides, organic synthesis
Methyl parathion	Insecticides
Oxathine	Mustard gas manufacture

(Cont'd)

TABLE 1.3 *Cont'd*

Contaminant	Examples of uses
Parathion	Insecticides
Pentachlorophenol (PCP)	Insecticides, fungicides, bactericides, algicides, herbicides, wood preservative
Phorate (Disulfoton)	Insecticides
Polybrominated biphenyls (PBBs)	Flame retardant for plastics, paper, and textiles
Polychlorinated biphenyls (PCBs)	Heat-exchange and insulating fluids in closed Systems
Prometon	Herbicides
RDX (Cyclonite)	Explosives
Simazine	Herbicides
Tetrachlorobenzene	NA ^a
Tetrachloroethanes (1,1,1,2 and 1,1,2,2)	Degreasers, paint removers, varnishes, lacquers, photographic film, organic synthesis, solvent, insecticides, fumigants, weed killer
Tetrachloroethylene (or perchloroethylene, PCE)	Degreasers, drycleaning, solvent, drying agent, chemical manufacturing, heat-transfer medium, vermicide
Toxaphene	Insecticides
Triazine	Herbicides
1,2,4-Trichlorobenzene	Solvent, dyestuffs, insecticides, lubricants, heattransfer medium (e.g., coolant)
Trichloroethanes (1,1,1 and 1,1,2)	Pesticides, degreasers, solvent
1,1,2-Trichloroethylene (TCE)	Degreasers, paints, drycleaning, dyestuffs, textiles, solvent, refrigerant and heat exchange liquid, fumigant, intermediate, aerospace operations
Tricholorfluoromethane (Freon)	Solvent, refrigerants, fire extinguishers, intermediate
2,4,6-Trichlorophenol	Fungicides, herbicides, defoliant
2,4,5-Trichlorophenoxyacetic acid (2,4,5-T)	Herbicides, defoliant
2,4,5-Trichlorophenoxypropionic acid (2,4,5-TP or Silvex)	Herbicides and plant growth regulator
Trichlorotrifluoroethane	Dry-cleaning, fire extinguishers, refrigerants, intermediate, drying agent
Trinitrotoluene (TNT)	Explosives, intermediate in dyestuffs and photographic chemicals
Tris-(2,3-dibromopropyl) phosphate	Flame retardant
Vinyl chloride	Organic synthesis, polyvinyl chloride and copolymers, adhesives

(Cont'd)

TABLE 1.3 *Cont'd*

Contaminant	Examples of uses
Other hydrocarbons	
Alkyl sulfonates	Detergents
Cyclohexane	Organic synthesis, solvent, oil extraction
1,3,5,7-Cyclooctatetraene	Organic research
Dicyclopentadiene (DCPD)	Intermediate for insecticides, paints and varnishes, flame retardants
2,3-Dimethylhexane	NA
Fuel oil	Fuel, heating
Gasoline	Fuel
Jet fuels	Fuel
Kerosene	Fuel, heating solvent, insecticides
Lignin	Newsprint, ceramic binder, dyestuffs, drilling fuel additive, plastics
Methylene blue activated substances (MBAS)	Dyestuffs, analytical chemistry
Propane	Fuel, solvent, refrigerants, propellants, organic synthesis
Tannin	Chemical manufacturing, tanning, textiles, electroplating, inks, pharmaceuticals, photography, paper
4,6,8-Trimethyl-1-nonene	NA
Undecane	Petroleum research, organic synthesis
Metals and cations	
Aluminum	Alloys, foundry, paints, protective coatings, electrical industry, packaging, building and construction, machinery and equipment
Antimony	Hardening alloys, solders, sheet and pipe, pyrotechnics
Arsenic	Alloys, dyestuffs, medicine, solders, electronic devices, insecticides, rodenticides, herbicide, preservative
Barium	Alloys, lubricant
Beryllium	Structural material in space technology, inertial guidance systems, additive to rocket fuels, moderator and reflector of neutrons in nuclear reactors
Cadmium	Alloys, coatings, batteries, electrical equipment, fire-protection systems, paints, fungicides, photography
Calcium	Alloys, fertilizers, reducing agent
Chromium	Alloys, protective coatings, paints, nuclear and high-temperature research

(Cont'd)

TABLE 1.3 *Cont'd*

Contaminant	Examples of uses
Cobalt	Alloys, ceramics, drugs, paints, glass, printing, catalyst, electroplating, lamp filaments
Copper	Alloys, paints, electrical wiring, machinery, construction materials, electroplating, piping, insecticides
Iron	Alloys, machinery, magnets
Lead	Alloys, batteries, gasoline additive, sheet and pipe, paints, radiation shielding
Lithium	Alloys, pharmaceuticals, coolant, batteries, solders, propellants
Magnesium	Alloys, batteries, pyrotechnics, precision instruments, optical mirrors
Manganese	Alloys, purifying agent
Mercury	Alloys, electrical apparatus, instruments, fungicides, bactericides, mildew proofing, paper, pharmaceuticals
Molybdenum	Alloys, pigments, lubricant
Nickel	Alloys, ceramics, batteries, electroplating, catalyst
Palladium	Alloys, catalyst, jewelry, protective coatings, electrical equipment
Potassium	Alloys, catalyst
Selenium	Alloys, electronics, ceramics, catalyst
Silver	Alloys, photography, chemical manufacturing, mirrors, electronic equipment, jewelry, equipment, catalyst, pharmaceuticals
Sodium	Chemical manufacturing, catalyst, coolant, nonglare lighting for highways, laboratory reagent
Thallium	Alloys, glass, pesticides, photoelectric applications
Titanium	Alloys, structural materials, abrasives, coatings
Vanadium	Alloys, catalysts, target material for x-rays
Zinc	Alloys, electroplating, electronics, automotive parts, fungicides, roofing, cable wrappings, nutrition
Nonmetals and anions	
Ammonia	Fertilizers, chemical manufacturing, refrigerants, synthetic fibers, fuels, dyestuffs
Boron	Alloys, fibers and filaments, semiconductors, propellants
Chlorides	Chemical manufacturing, water purification, shrink-proofing, flame retardants, food processing

(Cont'd)

TABLE 1.3 *Cont'd*

Contaminant	Examples of uses
Cyanides	Polymer production (heavy duty tires), coatings, metallurgy, pesticides
Fluorides	Toothpastes and other dentrifrices, additive to drinking water, aluminum smelting
Nitrates	Fertilizers, food preservatives
Nitrites	Fertilizers, food preservatives
Phosphates	Detergents, fertilizers, food additives
Sulfates	Fertilizers, pesticides
Sulfites	Pulp production and processing, food preservatives
Microorganisms	
Bacteria (coliform)	
Giardia	
Viruses	
Radionuclides	
Cesium 137	Gamma radiation source for certain foods
Chromium 51	Diagnosis of blood volume, blood cell life, cardiac output, etc.
Cobalt 60	Radiation therapy, irradiation, radiographic testing, research
Iodine 131	Medical diagnosis, therapy, leak detection, tracers (e.g., to study efficiency of mixing pulp fibers, chemical reactions, and thermal stability of additives to food products), measuring film thicknesses
Iron 59	Medicine, tracer
Lead 210	NA
Phosphorus 32	Tracer, medical treatment, industrial measurements (e.g., tire-tread wear and thickness of films and ink)
Plutonium 238, 243	Energy source, weaponry
Radium 226	Medical treatment, radiography
Radium 228	Naturally occurring
Radon 222	Medicine, leak detection, radiography, flow rate measurement
Ruthenium 106	Catalyst
Scandium 46	Tracer studies, leak detection, semiconductors
Strontium 90	Medicine, industrial applications (e.g., measuring thicknesses, density control)

(Cont'd)

TABLE 1.3 *Cont'd*

Contaminant	Examples of uses
Thorium 232	Naturally occurring
Tritium	Tracer, luminous instrument dials
Uranium 238	Nuclear reactors, mining operations
Zinc 65	Industrial tracers (e.g., to study wear in alloys, galvanizing, body metabolism, function of oil additives in lubricating oils)
Zirconium 95	NA

^aNA: No information in Standard sources.

Source: Office of Technology Assessment 1984, with additions.

It should be noted that many compounds can have multiple names, making identification of compounds difficult for the environmental practitioner. In one example from Table 1.3, the compound butoxymethylbenzene can also be known by at least 26 other names or numerical distinctions (Chemspider 2015). Nomenclature can be further confused, as there are other names given for the same compound by different suppliers and vendors. Using the same example of butoxymethylbenzene above, a selective list of vendors in 2015 and their designations for the compound would include at least 14 different additional names or numerical distinctions (Zincdocking 2015). This multiple nomenclature for the same compound can be even more confused with the manufacture and use of mixtures of potential groundwater pollutants, some containing unspecified impurities. There are many types of industrial chemical mixtures in use or being developed, with multiple names and descriptions, including tens of thousands of pesticide products. Also, in recent years there has been increased concern over “emerging” organic contaminants, which were previously not yet industrially developed, not yet discovered in the environment often due to analytical limitations, or alternatively, not yet recognized as potential pollutants. These compounds include pharmaceuticals, personal care products, industrial chemicals, and hormones. Table 1.4 lists some of these compounds and their uses.

The occurrence of the substances found on Tables 1.3 and 1.4 can be detected only if a groundwater sample has been collected and analyzed. In low concentrations most of these substances are colorless, tasteless, and odorless. Specific analytical techniques must be employed to detect the presence and concentration of each substance. Some methods can be employed to analyze a sample for all of the compounds of a particular class. For example, certain organic compounds fall into a class called volatile organic compounds. There are analytical methods that could target all compounds of this class. Likewise, there are methods available to analyze for many of the metals in a single sample. However, other compounds require a specific test. With so many potential contaminants, it is possible that a sample could be collected and tested and a specific contaminant still not be found because no analysis was done for that compound or element.

TABLE 1.4 Frequently reported emerging organic contaminants and degrates found in groundwater.

Contaminant	Primary Use
Pharmaceuticals	
Carbamazepine	Antiepileptic
Sulfamethoxazole	Antibiotic
Ibuprofen (known or potential endocrine disrupting compound)	Anti-inflammatory (also an analgesic)
Diclofenac	Anti-inflammatory
Clofibric acid (known or potential endocrine disrupting compound)	Lipid regulator
Paracetamol (known or potential endocrine disrupting compound)	Analgesic
Ketoprofen	Anti-inflammatory
Triclosan	Antibiotic
Iopamidol	X-ray contrast media
Lincomycin	Antibiotic
Propyphenazone	Analgesic
Sulfamethazine	Veterinary medicine
DEET (N,N-diethyl-meta-toluamide)	Insect repellent
Phenazone	Analgesic
Primidone	Barbiturate
Salicylic acid (known or potential endocrine disrupting compound)	Analgesic
Personal Care Products	
Caffeine	Diuretic
Cotinine (degradeate— nicotine metabolite)	Stimulant
Industrials	
Bisphenol A (known or potential endocrine disrupting compound)	Plasticiser
Nonylphenol (known or potential endocrine disrupting compound)	Detergent
Galoxalide (known or potential endocrine disrupting compound)	Fragrance
4-octylphenol monoethoxylate	Detergent metabolite
TCEP (Tris(2-Chloroethyl) phosphate)	Fire retardant
Hormones	
Estrone (known or potential endocrine disrupting compound)	Estrogenic hormone
17b-Estradiol (known or potential endocrine disrupting compound)	Estrogenic hormone

Source: Lapworth et al. 2012; Barnes et al 2008.

A great deal of expense is involved with a water-quality analysis; costs can vary for the same analysis performed at different laboratories, and can vary depending on the number of chemical parameters being tested. In some cases the form of the compound being analyzed can also vary the price of analysis (e.g., there is a price variance for cyanide analysis depending on whether one desires to know the total cyanide, free cyanide, cyanide amenable to chlorination, or cyanide available by flow injection, ligand exchange, and amperometry). Table 1.5 lists the approximate cost ranges of an extensive laboratory analysis. This table does not include the cost of collection and preservation of the sample to be analyzed.

The cost of analysis increases as the **detection limit**, the lowest concentration that can be reliably detected, decreases. Groundwater contaminants can be routinely detected at the parts-per-billion level, and with care some compounds can be quantified at the parts-per-trillion level. To put that concentration in perspective, 0.4 mm is one trillionth of the distance to the moon.

■ 1.3 Drinking-Water Standards

When measured at the parts-per-trillion level, even carefully prepared, triple-distilled, deionized water will be seen to contain some dissolved constituents. What does this mean? We must consider the quality of water with respect to the use to which it will be placed. Water for many industrial purposes need not be as pure as water used for drinking. Worldwide, the definition of groundwater pollution varies. Many definitions are rooted in common law and the history of individual judicial

TABLE 1.5 Cost of analysis of a single groundwater sample (2015 USD Approximate Price Ranges*).

Volatile Organic Compounds by Method 624	\$	65–150
Base/Neutral organics by Method 625	\$	230–390
Pesticides and PCBs by Method 608	\$	120–200
Phenols by Method 625	\$	120–275
Twenty three metals	\$	85–200
Radiological compounds	\$	80–385
Bacterial analysis (E.coli and Total Coliform)	\$	15–40
Cyanide	\$	18–90
Chloride	\$	10–15
Fluoride	\$	10–20
Nitrate and nitrite	\$	15–35
Sulfate	\$	10–15
pH	\$	5–10
Total	\$	783–1725

* Prices can vary greatly

decisions, whereas others are based on pollution regulations, directives, and statutes enacted by legislative bodies. Some legal precedents and legislative actions have sought to establish liability for past pollution, and others were initiated to head off future groundwater degradation, control potential sources, and/or to maintain an acceptable level of ambient groundwater quality. Groundwater pollution can be controlled by effective, overriding regulations and standards for activities potentially injurious to groundwater quality. It can also be controlled by individual mechanisms including permitting, constraints on land-use, construction and design practices, and injection and discharge limits. Importantly, it is recognized that in many instances there can be strong interactions between groundwater and surface water, meaning that groundwater protection can have benefits to surface water quality as well.

Groundwater protection takes many forms throughout the world. In Europe, Directive 2006/118/EC of the European Parliament and Council (12 December 2006) set out standards and procedures concerning the protection of groundwater against pollution and deterioration and is continually updated and amended (e.g., the modifying Commission Directive 2014/80/EU, 20 June 2014). In the United States there are many regulations that contribute to the preservation of high quality groundwater. Notably, the Safe Drinking Water Act and its amendments direct the Environmental Protection Agency (EPA) to establish maximum contaminant-level goals (MCLGs) and maximum contaminant levels (MCLs) for drinking water supplied by public water agencies. A maximum contaminant-level goal is a nonenforceable goal set at a level to prevent known or anticipated adverse health effects with a wide margin of safety. The MCLG for a carcinogen is zero, whereas for chronically toxic compounds it is based on an acceptable daily intake that takes into account exposure from air, food, and drinking water. Maximum contaminant levels are enforceable standards that are set as close as feasible to the MCLGs, taking into account water-treatment technologies and cost. Primary MCLs are based on health risk, and secondary MCLs are based on aesthetics. Table 1.6 contains the drinking-water standards promulgated by the U.S. Environmental Protection Agency.

■ 1.4 Risk and Drinking Water

Cancer-risk levels for varying exposures to chemicals have been established by toxicologists using extremely conservative methods. Rodents are fed a diet containing large amounts of synthetic chemicals at what is called the maximum tolerated dose. If such a diet increases the cancer rate in the rodents, the results are linearly extrapolated to low doses to which humans might be exposed. This methodology has been challenged as being scientifically unsound (Ames, Gold, and Willett 1995). Moreover, it has been assumed that if a chemical is carcinogenic at a high dose, it is carcinogenic to some degree at any level of exposure. This assumption has also been challenged as scientifically unsound (Goldman, 1996). As a result of this assumption the MCLG for any compound that has been shown to be a rodent carcinogen is set by the U.S. EPA as zero.

The U.S. EPA uses a risk assessment approach in determining the required clean-up level for groundwater and soil at contaminated sites that are under federal supervision, primarily Superfund sites under the Comprehensive Environmental Response,

TABLE 1.6 U.S. EPA drinking-water standards and health goals.

Microorganisms		
Contaminant	MCLG¹(mg/L)²	MCL or TT¹(mg/L)²
Cryptosporidium	zero	TT ³
Giardia lamblia	zero	TT ³
Heterotrophic plate count (HPC)	n/a	TT ³
Legionella	zero	TT ³
Total Coliforms (including fecal coliform and E. Coli)	zero	5.0% ⁴
Turbidity	n/a	TT ³
Viruses (enteric)	zero	TT ³

Disinfection Byproducts		
Contaminant	MCLG¹(mg/L)²	MCL or TT¹(mg/L)²
Bromate	zero	0.010
Chlorite	0.8	1.0
Haloacetic acids (HAA5)	n/a ⁶	0.060 ⁷
Total Trihalomethanes (TTHMs)	→ n/a ⁶	→ 0.080 ⁷

Disinfectants		
Contaminant	MCLG¹(mg/L)²	MCL or TT¹(mg/L)²
Chloramines (as Cl ₂)	MRDLG = 4 ¹	MRDL = 4.0 ¹
Chlorine (as Cl ₂)	MRDLG = 4 ¹	MRDL = 4.0 ¹
Chlorine dioxide (as ClO ₂)	MRDLG = 0.8 ¹	MRDL = 0.8 ¹

Source: U.S. EPA 2016.

Inorganic Chemicals		
Contaminant	MCLG¹(mg/L)²	MCL or TT¹(mg/L)²
Antimony	0.006	0.006
Arsenic	0	0.010 as of 01/23/06
Asbestos (fiber > 10 micrometers)	7 million fibers per liter (MFL)	7 MFL
Barium	2	2
Beryllium	0.004	0.004
Cadmium	0.005	0.005
Chromium (total)	0.1	0.1
Copper	1.3	TT ⁷ ; Action Level = 1.3
Cyanide (as free cyanide)	0.2	0.2

(Cont'd)

TABLE 1.6 *Cont'd*

Inorganic Chemicals		
Contaminant	MCLG¹(mg/L)²	MCL or TT¹(mg/L)²
Fluoride	4.0	4.0
Lead	zero	TT ⁷ ; Action Level = 0.015
Mercury (inorganic)	0.002	0.002
Nitrate (measured as Nitrogen)	10	10
Nitrite (measured as Nitrogen)	1	1
Selenium	0.05	0.05
Thallium	0.0005	0.002

Organic Chemicals		
Contaminant	MCLG¹(mg/L)²	MCL or TT¹(mg/L)²
Acrylamide	zero	TT ⁸
Alachlor	zero	0.002
Atrazine	0.003	0.003
Benzene	zero	0.005
Benzo(a)pyrene (PAHs)	zero	0.0002
Carbofuran	0.04	0.04
Carbon tetrachloride	zero	0.005
Chlordane	zero	0.002
Chlorobenzene	0.1	0.1
2,4-D	0.07	0.07
Dalapon	0.2	0.2
1,2-Dibromo-3-chloropropane (DBCP)	zero	0.0002
o-Dichlorobenzene	0.6	0.6
p-Dichlorobenzene	0.075	0.075
1,2-Dichloroethane	zero	0.005
1,1-Dichloroethylene	0.007	0.007
cis-1,2-Dichloroethylene	0.07	0.07
trans-1,2-Dichloroethylene	0.1	0.1
Dichloromethane	zero	0.005
1,2-Dichloropropane	zero	0.005
Di(2-ethylhexyl) adipate	0.4	0.4
Di(2-ethylhexyl) phthalate	zero	0.006
Dinoseb	0.007	0.007

(Cont'd)

TABLE 1.6 *Cont'd*

Contaminant	Organic Chemicals	
	MCLG¹(mg/L)²	MCL or TT¹(mg/L)²
Dioxin (2,3,7,8-TCDD)	zero	0.00000003
Diquat	0.02	0.02
Endothall	0.1	0.1
Endrin	0.002	0.002
Epichlorohydrin	zero	TT ⁸
Ethylbenzene	0.7	0.7
Ethylene dibromide	zero	0.00005
Glyphosate	0.7	0.7
Heptachlor	zero	0.0004
Heptachlor epoxide	zero	0.0002
Hexachlorobenzene	zero	0.001
Hexachlorocyclopentadiene	0.05	0.05
Lindane	0.0002	0.0002
Methoxychlor	0.04	0.04
Oxamyl (Vydate)	0.2	0.2
Polychlorinated biphenyls (PCBs)	zero	0.0005
Pentachlorophenol	zero	0.001
Picloram	0.5	0.5
Simazine	0.004	0.004
Styrene	0.1	0.1
Tetrachloroethylene	zero	0.005
Toluene	1	1
Toxaphene	zero	0.003
2,4,5-TP (<i>Silvex</i>)	0.05	0.05
1,2,4-Trichlorobenzene	0.07	0.07
1,1,1-Trichloroethane	0.20	0.2
1,1,2-Trichloroethane	0.003	0.005
Trichloroethylene	zero	0.005
Vinyl chloride	zero	0.002
Xylenes (total)	10	10

(Cont'd)

TABLE 1.6 Cont'd

Contaminant	Radionuclides	
	MCLG ¹ (mg/L) ²	MCL or TT ¹ (mg/L) ²
Alpha particles	none ⁷ ----- zero	15 picocuries per Liter (pCi/L)
Beta particles and photon emitters	none ⁷ ----- zero	4 millirems per year
Radium 226 and Radium 228 (combined)	none ⁷ ----- zero	5 pCi/L
Uranium	zero	30 µg/L as of 12/08/03

Source: <http://water.epa.gov/drink/contaminants/index.cfm#List>

¹Definitions:

- Maximum Contaminant Level Goal (MCLG): The level of a contaminant in drinking water below which there is no known or expected risk to health. MCLGs allow for a margin of safety and are nonenforceable public health goals.
- Maximum Contaminant Level (MCL): The highest level of a contaminant that is allowed in drinking water. MCLs are set as close to MCLGs as feasible using the best available treatment technology and taking cost into consideration. MCLs are enforceable standards.
- Maximum Residual Disinfectant Level Goal (MRDLG): The level of a drinking water disinfectant below which there is no known or expected risk to health. MRDLGs do not reflect the benefits of the use of disinfectants to control microbial contaminants.)
- Treatment Technique (TT): A required process intended to reduce the level of a contaminant in drinking water.
- Maximum Residual Disinfectant Level (MRDL): The highest level of a disinfectant allowed in drinking water. There is convincing evidence that addition of a disinfectant is necessary for control of microbial contaminants.

²Units are in milligrams per liter (mg/L) unless otherwise noted. Milligrams per liter are equivalent to parts per million (PPM).

³EPA's surface water treatment rules require systems using surface water or groundwater under the direct influence of surface water to

- disinfect their water, and
- filter their water, or
- meet criteria for avoiding filtration so that the following contaminants are controlled at the following levels:
 - * Cryptosporidium: Unfiltered systems are required to include Cryptosporidium in their existing watershed control provisions.
 - * Giardia lamblia: 99.9% removal/inactivation.
 - * Viruses: 99.99% removal/inactivation.
 - * Legionella: No limit, but EPA believes that if Giardia and viruses are removed/inactivated, according to the treatment techniques in the Surface Water Treatment Rule, Legionella will also be controlled.
 - * Turbidity: For systems that use conventional or direct filtration, at no time can turbidity (cloudiness of water) go higher than 1 Nephelometric Turbidity Unit (NTU), and samples for turbidity must be less than or equal to 0.3 NTUs in at least 95 percent of the samples in any month. Systems that use filtration other than the conventional or direct filtration must follow state limits, which must include turbidity at no time exceeding 5 NTUs.
 - * Heterotrophic Plate Count (HPC): No more than 500 bacterial colonies per milliliter.
 - * Long Term 1 Enhanced Surface Water Treatment: Surface water systems or groundwater under the direct influence (GWUDI) systems serving fewer than 10,000 people must comply with the applicable Long Term 1 Enhanced Surface Water Treatment Rule provisions (such as turbidity standards, individual filter monitoring, Cryptosporidium removal requirements, updated watershed control requirements for unfiltered systems).
 - * Long Term 2 Enhanced Surface Water Treatment Rule: This rule applies to all surface water systems or groundwater systems under the direct influence of surface water. The rule targets additional Cryptosporidium treatment requirements for higher risk systems and includes provisions to reduce risks from uncovered finished water storage facilities and to ensure that the systems maintain microbial protection as they take steps to reduce the formation of disinfection byproducts.

(Cont'd)

TABLE 1.6 Cont'd

* Filter Backwash Recycling: The Filter Backwash Recycling Rule requires systems that recycle to return specific recycle flows through all processes of the system's existing conventional or direct filtration system or at an alternate location approved by the state.

⁴No more than 5.0% samples total coliform-positive (TC-POSITIVE) in a month. (For water systems that collect fewer than 40 routine samples per month, no more than one sample can be total coliform-positive per month.) Every sample that has total coliform must be analyzed for either fecal coliforms or E. coli if two consecutive TC-POSITIVE samples, and one is also positive for E.coli fecal coliforms, system has an acute MCL violation.

⁵Fecal coliform and E. coli are bacteria whose presence indicates that the water may be contaminated with human or animal wastes. Disease-causing microbes (pathogens) in these wastes can cause diarrhea, cramps, nausea, headaches, or other symptoms. These pathogens may pose a special health risk for infants, young children, and people with severely compromised immune systems.

⁶Although there is no collective MCLG for this contaminant group, there are individual MCLGs for some of the individual contaminants:

- Trihalomethanes: bromodichloromethane (zero); bromoform (zero); dibromochloromethane (0.06 mg/L); chloroform (0.07 mg/L).
- Haloacetic acids: dichloroacetic acid (zero); trichloroacetic acid (0.02 mg/L); monochloroacetic acid (0.07mg/L). Bromoacetic acid and dibromoacetic acid are regulated with this group but have no MCLGs.

⁷Lead and copper are regulated by a treatment technique that requires systems to control the corrosiveness of their water. If more than 10% of tap water samples exceed the action level, water systems must take additional steps. For copper, the action level is 1.3 mg/L, and for lead is 0.015 mg/L.

⁸Each water system must certify, in writing, to the state (using third-party or manufacturer's certification) that when acrylamide and epichlorohydrin are used to treat water, the combination (or product) of dose and monomer level does not exceed the levels specified, as follows:

- Acrylamide = 0.05% dosed at 1 mg/L (or equivalent)
- Epichlorohydrin = 0.01% dosed at 20 mg/L (or equivalent)

Compensation, and Liability Act of 1980 (CERCLA). Cancer risk levels are expressed in terms of the chance that an individual will develop cancer due to a thirty-year exposure within a seventy year lifetime. For example, for drinking water it is assumed that the individual would drink two liters of water per day from the same source for the thirty year period. If one individual out of a million would develop cancer from that exposure alone, the risk is 10^{-6} . If 100 people out of one million would develop cancer from that exposure alone, the risk is 10^{-4} . The official EPA position in determining site remediation is that if the risk is 10^{-6} or less, then no cleanup would be required. If the risk is between 10^{-4} and 10^{-6} , then state officials could decide if cleanup is required and if the risk is greater than 10^{-4} , then cleanup is mandated. When assessing the risk, the EPA always uses upper bound estimates (95th percentile) of the various factors in the risk assessment. As a result, the calculated risk is about 100 times greater than it would be if average values of the risk factors were used. As a result the real cancer risks that form the basis from cleanup are in the 10^{-6} to 10^{-8} range (Viscusi and Hamilton 1996). This results in very expensive remediations being driven by very low risks.

Case Study

One of the ways that the risk calculation is inflated is the use of the highest concentration of a chemical found at a site. For example, in the case of groundwater, the risk calculation is done on the basis of the highest concentration of compounds found at the site, not the concentrations to which populations would most likely be exposed. For example, an old

municipal landfill in rural Wisconsin received waste for a four year period from 1970 to 1974. In 1975 it was closed by covering with a one foot thick layer of clay. Ten years later monitoring wells placed next to the edge of the landfill were found to have synthetic organic compounds present. During a remedial investigation done in 1991 these wells were found to have benzene and vinyl chloride in amounts greater than their MCLs. However, in this study done 15 years after the close of the landfill, it was found that the plume of contaminated groundwater had not reached the edge of the property on which the landfill was located. A private well located 100 feet from the edge of the waste disposal area was not impacted. However, the risk assessment for future risk was based on the assumption that the landfill site would be converted to residential use with private wells and that the water from those wells would be of the same quality as the water from the monitoring well located next to the waste mass. It was also assumed that the residence located 100 feet from the edge of the plume would eventually be impacted. This assessment did not include a recognition of the fact that as the landfill ages, it will produce less leachate and the groundwater quality will improve.

The assumption of future on site residential use of the landfill site required people to buy lots on a Superfund site in a county with a declining population and in an area surrounded by woods on one side and farmland on the other. After the saga of Love Canal in Niagara Falls, New York, who in the United States is going to buy a lot on a Superfund site? The selected remedy for this site was to cap the landfill with a new cover, to install trenches to capture and remove leachate, and to install a gas collection system. The cost of remediation of this small landfill was about \$7,500,000 for investigation and construction. The future costs for operation and maintenance for a 30-year period, including the cost of pumping and treating leachate, is estimated to be about \$1,700,000. (U.S. EPA, Record of Decision, Spickler Landfill, Spencer, Wisconsin)

The population in general appears to accept the high cost of clean drinking water, probably because according to estimates from the International Agency for Research on Cancer (IARC), there were 12.7 million new cancer cases in 2008 worldwide, and the corresponding estimates for total cancer deaths in 2008 were 7.6 million (about 21,000 cancer deaths a day). By 2030, the global burden is expected to grow annually to 21.4 million new cancer cases and 13.2 million cancer deaths (Ferlay et al., 2010). In the United States over 40% of the population will have a lifetime risk of being diagnosed with cancer (Howlader et al., 2015) and it caused about 582,780 deaths in the United States in 2014 (American Cancer Society 2015). However, very few of these deaths are the result of exposure to synthetic chemicals and pesticides. Principal causes of cancer are smoking, chronic inflammation and an unbalanced diet, i.e., one high in animal fat and low in fruits and vegetables (Ames, Gold, and Willett 1995).

There is an irreducible risk associated with drinking water. In order to protect against pathogenic disease, drinking water is usually chlorinated, especially if the water comes from a surface source, although groundwater is not invulnerable to pathogens. A study of groundwater systems in the United States and Canada from 1990 to 2013 found approximately 15% (316/2210) of groundwater samples to contain enteric pathogens (Hynds et al., 2014). The World Health Organization has reported waterborne and water-related illness to be the leading cause of death worldwide at an estimated 3.4 million people a year. Prior to chlorination of drinking water supplies, waterborne disease such as typhoid and cholera took many more lives. Between 1920 and 1950, a period when the percentage of the population served by safe drinking-water supplies

was increasing, there were 1050 deaths in the United States due to waterborne disease, including typhoid fever, gastroenteritis, shigellosis, and amebiasis (van der Leeden, Troise, and Todd 1990). Over a similar period from 1971 to 2002, but with a larger population and chlorination/disinfection of drinking water, there were only 79 documented deaths (Reynolds et al. 2008). Many forms of disinfection of water do have inherent risks, however. Chlorine reacts with naturally occurring organics in the water to produce trihalomethanes. The average chlorinated tap water in the United States is reported to contain 83 µg/L of chloroform (Ames, Magaw, and Gold 1987). Gold et al. (1992) used this as a base with which to compare other potential cancer risks. Table 1.7 contains cancer risks relative to drinking a liter of chlorinated tap water a day, with tap water having a risk of 1.0. The relative risks were determined as an index obtained by dividing the daily lifetime human exposure in milligrams per kilogram of body weight by the daily dose rate for rodents in milligrams per kilogram of body weight. The dose rate of rodents is the daily dose necessary to give cancer to half the rodents at the end of a standard lifetime. Examination of the table shows that there are numerous cancer risks associated with living and eating. Water from a contaminated well that was closed in Santa Clara County, California (Silicon Valley), had 2800 µg/L of trichloroethylene. Drinking 1L of this water per day has the same relative cancer risk as the risk from nitrosamines ingested when one has bacon for breakfast. The bacon carries additional risk because high dietary fat is thought to be a possible contributor to colon cancer (Ames, Gold, and Willett, 1995). Water with 2800 µg/L of trichloroethylene has a 10^{-3} cancer risk based on the EPA's Section 304(1)(1) criteria (Federal Register, November 28, 1983).

Table 1.7 clearly shows that the cancer risk from contaminated drinking water and pesticide residues on food is clearly less than that due to the natural pesticides found on fruits and vegetables. This does not mean that one should avoid eating vegetables, which are an important source of other natural chemicals that helps one to avoid getting cancer. While these data put the risks from contaminated water in perspective, one should still obviously avoid contaminated water if possible.

■ 1.5 Sources of Groundwater Contamination

In a 2015 report, *The Quality of the Nation's Groundwater*, the United States Geological Survey reported that on the basis of 6,600 wells sampled and 1.3 million chemical analyses, more than 1 in 5 samples (22%) from parts of aquifers used for drinking water contained a contaminant that exceeded a level for potential human-health concern. Some of the sources of groundwater contamination were identified as having a geologic origin, while others were determined to come from human sources. Although much attention has focused on waste materials as a source of groundwater contamination, there are numerous sources that are not associated with solid or liquid wastes. The following sections list and discuss sources of groundwater contamination. Figure 1.2 illustrates some of these contamination sources.

1.5.1 Category 1: Sources Designed to Discharge Substances

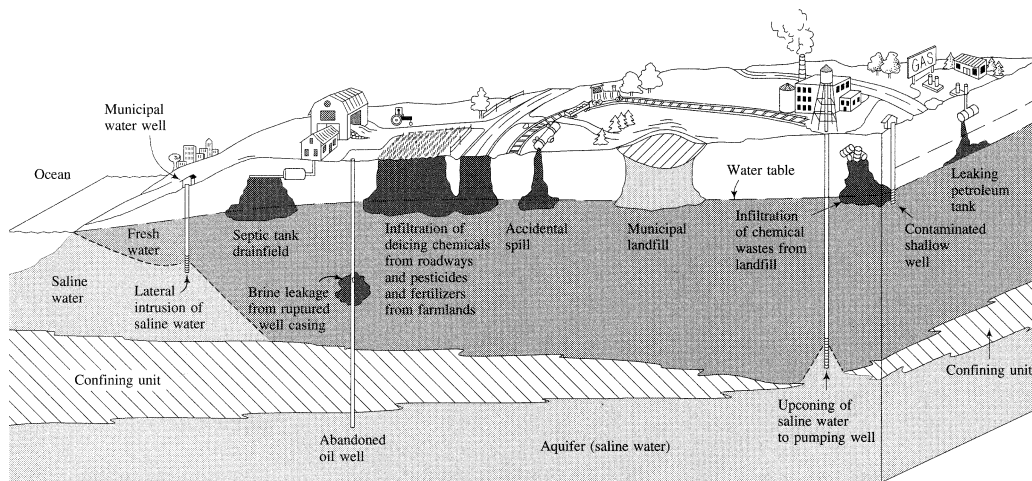
Septic tanks and cesspools Septic tanks and cesspools are designed to discharge domestic wastewater into the subsurface above the water table. In the absence of

TABLE 1.7 Risk of getting cancer relative to drinking chlorinated tap water.

Relative Risk	Source/Daily Human Exposure	Carcinogen
Risk Due to Synthetic Chemicals		
Respiratory Exposure		
1400	Mobile Home Air (14 hour/day)	Formaldehyde, 2.2 mg
400	Conventional Home air (14 hour/day)	Formaldehyde, 598 µg
8.0	Swimming pool (1 hour/day for a child)	Chloroform, 250 µg
Water		
6.0	Well water, Silicon Valley, CA, 1L	Trichloroethylene, 2,800 µg
1.0	Chlorinated tap water (US Average) 1L	Chloroform, 82 µg
0.6	Well Water, Woburn, MA, 1L	Trichloroethylene, 267 µg
0.3	Well Water, Woburn, MA, 1L	Tetrachloroethylene, 21 µg
Pesticide Residues on Food		
0.3	Carbaryl, daily average diet	Carbaryl, 2.6 µg
0.2	Toxaphene, daily average diet	Toxaphene, 595 ng
0.001	Lindane, daily average diet	Lindane, 32 ng
0.000006	Captan, daily average diet	Captan, 11.5 ng
Risk Due to Natural Chemicals Found in Food and Beverages		
4700	Wine (250 mL)	Ethyl alcohol, 30 mL
2800	Beer (12 ounces)	Ethyl alcohol, 18 mL
300	Lettuce, 1/8 head	Caffeic acid, 66.3 mg
100	Apple, 1 whole	Caffeic acid, 24.4 mg
100	Mushroom, 1 whole	Hydrazines
70	Mango, 1 whole	d-Limonene, 9.8 mg
40	Orange juice, 6 oz.	d-Limonene, 5.49 mg
30	Peanut butter, 1 sandwich	Aflatoxin, 64ng
30	Celery, 1 stalk	Caffeic acid, 5.4 mg
30	Carrot, 1 whole	Caffeic acid, 5.16 mg
20	Potato, 1 whole	Caffeic acid, 3.56 mg
6	Bacon, cooked (100 g)	Diethylnitrosomine, 0.1 µg
0.5	Salmon (3 oz. pan fried)	PhIP, 1.19 µg
0.5	Hamburger (3 oz. pan fried)	PhIP, 1.28 µg
0.03	Whole Wheat toast, 2 slices	Urethane, 540 ng

Source: Based on Table 2 from Gold et al. 1992.

sewage, water from toilets, sinks and showers, dishwashers, and washing machines passes from the home into a septic tank, where it undergoes settling and some anaerobic decomposition. It is then discharged to the soil via a drainage system. In the

FIGURE 1.2 Mechanisms of groundwater contamination.

European Union, discharge of septic waste into groundwater is regulated by Directive 2006/118/Ec of the European Parliament and Council (and its amendments) on the protection of groundwater against pollution and deterioration. The United Kingdom has instituted a registration system for septic tanks and requires an environmental permit for some. The U.S. Environmental Protection Agency estimates that one in four households in the United States uses a septic tank disposal system.

Septic systems discharge a variety of inorganic and organic compounds. Table 1.8 contains an analysis of septic-tank effluent. In addition to the domestic wastewater, septic-tank cleaners containing synthetic organic chemicals such as trichloroethylene, benzene, and methylene chloride were discharged to the subsurface. As far back as 1979, an estimated 400,000 gal of septic-tank cleaning fluids were used on Long Island, New York (Burmester and Harris 1982). Shallow groundwater on Long Island is known to be contaminated by these same chemicals (Eckhardt and Oaksford 1988).

Injection wells Injection wells are used to discharge liquid wastes and other liquids into subsurface zones below the water table. Liquids that are injected include (1) hazardous wastes, (2) brine from oil wells, (3) agricultural and urban runoff, (4) municipal sewage, (5) air-conditioning return water, (6) heat-pump return water, (7) liquids used for enhanced oil recovery from oil fields, (8) treated water intended for artificial aquifer recharge, and (9) fluids used in solution mining.

Injection wells can cause groundwater contamination if the fluid being injected accidentally or deliberately enters a drinking-water aquifer. This could happen because of poor well design, poor understanding of the geology, faulty well construction, or deteriorated well casing. Wastewater correctly injected into subsurface zones containing unusable water could still migrate to a usable aquifer by being forced through cracks in a confining layer under unnatural pressures or by flowing through the aquifer to a nearby well that was improperly constructed or abandoned. Injection wells are now regulated under the Underground Injection Control Program of the Safe Drinking

TABLE 1.8 Analysis of septic tank effluent from six different sources.

Site	Average Flow (g/da)	BOD (mg/L)	COD (mg/L) (unfiltered)	COD (mg/L) (filtered)	TSS (mg/L)	Fecal Coliforms (no./mL)	Fecal Strep (no./mL)	Total N (mg/L)	Ammonia N (mg/L)	Nitrate-Nitrogen (mg/L)	Total P (mg/L)	Ortho P (mg/L)
A	75	131	325	249	69	2907	2.7	50.5	34.1	0.68	12.3	10.8
B	125	176	361	323	44	4127	39.7	57.8	42.5	0.46	14.1	13.6
C	245	272	542	386	68	27,931	1387	76.3	45.6	0.60	31.4	14.0
D	315	127	291	217	52	11,113	184	40.2	33.2	0.35	11.0	10.1
E	860 ^b	120	294	245	51	2310	20.7	31.6	20.1	0.16	11.1	10.5
F	150	122	337	281	48	3246	25.3	56.7	38.3	0.83	11.6	10.5

Source: R. J. Otis, W. C. Boyle, and D. K. Sauer, Small-Scale Waste Management Program, University of Wisconsin—Madison, 1973.

^aAll values are means.

^bIncludes 340-g/da sewer flow and 520-g/da from foundation drain.

Water Act. The 1984 amendments to the Resource Conservation and Recovery Act prohibit the underground injection of certain hazardous wastes. The injection of waste fluids into the deep subsurface has increased particularly in localities with intensified oil and gas production. For example, over 23 km³ of water has been injected into the Western Canada Sedimentary Basin over the decades of the 1980s, 1990s, 2000s, and early 2010s, and even more subsurface injection has occurred in the State of Texas in the United States alone between 1998 and 2013 (Ferguson 2015). There is also concern that the underground injection of fluids can trigger earthquakes. The U.S. Geological Survey reports that the largest documented U.S. earthquake triggered by fluid injection was a 5.6 magnitude quake in central Oklahoma on November 6, 2011. There was a 5.3 magnitude in the Raton Basin, Colorado earlier that year, and magnitude 4.0 and 5.0 have been induced in Arkansas, Colorado, Kansas, Oklahoma, and Texas. Another important use of subsurface fluid injection is carbon sequestration, also called carbon capture and storage (CCS), which seeks to inject carbon dioxide (CO₂) or other forms of carbon below ground surface to counteract the build-up of CO₂ in the earth's atmosphere and to mitigate the effects of global warming and climate change.

Land application Treated or untreated municipal and industrial wastewater is applied to the land primarily via spray irrigation systems. Exposure to the elements, plants, and microorganisms in the soil can break down the natural organic matter in the wastewater.

Sludge from wastewater-treatment plants is often applied to the soil as a fertilizer, as is manure from farm animals and whey from cheese manufacturing. Oily wastes from refining operations have been applied to the soil so that they could be broken down by soil microbes. Nitrogen, phosphorous, heavy metals, and refractory organic

compounds are potential groundwater contaminants that can leach from soil used for land applications of wastes and wastewater.

1.5.2 Category II: Sources Designed to Store, Treat and/or Dispose of Substances

Landfills Landfills are, by definition, designed to minimize adverse effects of waste disposal (Miller, 1980). However, many were poorly designed and are leaking liquids, generically termed **leachate**, which are contaminating groundwater. Landfills can contain nonhazardous municipal waste, nonhazardous industrial waste, or hazardous waste as defined by the Resource Conservation and Recovery Act. Peterson (1983) reported that there were 12,991 landfills in the United States in the 1980s, including 2,395 open dumps. According to the EPA, by 2009 landfills were much larger, but there were only 1,908 solid waste municipal landfills reported. This does not include landfills for construction and demolition wastes, nonhazardous industrial waste landfills, or hazardous waste landfills. There are an unknown number of abandoned landfills.

Materials placed in landfills include such things as municipal garbage and trash, demolition debris, sludge from wastewater-treatment plants, incinerator ash, foundry sand and other foundry wastes, and toxic and hazardous materials. Although no longer permitted in the United States, liquid hazardous waste was disposed in landfills in the past. The U.S. Environmental Protection Agency (2015) estimated that in 2012 over 250 million tons of municipal waste was generated, which is over a three-fold increase in the last half century. The World Bank (2012) has estimated worldwide municipal waste generation at 1.3 billion tons per year with estimates of expected increase to 2.2 billion tons annually in 2025, and over 11 billion by 2100. Total solid waste generation (beyond just municipal waste) is considerably larger at an estimated 11.2 billion tons in 2011 (United Nations Environmental Programme). Interactive waste atlases have also been developed to summarize worldwide waste data (e.g., <http://www.atlas.d-waste.com/>).

Leachate is formed from the liquids found in the waste as well as by leaching of the solid waste by rainwater. Table 1.9 contains information on the chemical composition of leachate from municipal landfills. To minimize the amount of leachate generated, modern landfills are built in sections, with a low-permeability cover placed over the waste as soon as possible to limit the infiltration of rainwater. Modern landfills also have low-permeability liner systems and collection pipes to remove the leachate that forms so that it can be taken to a wastewater-treatment plant. A modern landfill that is properly sited with respect to the local geology and that has a properly designed and constructed liner, leachate collection system, and low-permeability cover has limited potential to contaminate groundwater. However, many landfills do not have liners and leachate collection systems. In the past, landfills tended to be placed in any convenient hole or low spot, such as a sand pit, quarry, or marsh. Groundwater contamination from such landfills is highly probable.

Municipal landfills are usually located near urban areas. The trend is toward large landfills that can handle many thousands of tons of waste per year. Hazardous-waste landfills are now regulated under the Resource Conservation and Recovery Act. There is frequently strong local opposition to the siting of either a municipal or a hazardous waste landfill. This is referred to as the NIMBY syndrome: Not In My Back Yard!

TABLE 1.9 Overall summary from the analysis of municipal solid-waste leachates in Wisconsin.

Parameter	Overall Range ^a	Typical Range (range of site medians) ^a	Number of Analyses
TDS	584–50,430	2180–25,873	172
Specific conductance	480–72,500	2840–15,485	1167
Total suspended solids	2–140,900	28–2835	2700
BOD	ND–195,000	101–29,200	2905
COD	6.6–97,900	1120–50,450	467
TOC	ND–30,500	427–5890	52
pH	5–8.9	5.4–7.2	1900
Total alkalinity (CaCO ₃)	ND–15,050	960–6845	328
Hardness (CaCO ₃)	52–225,000	1050–9380	404
Chloride	2–11,375	180–2651	303
Calcium	200–2500	200–2100	9
Sodium	12–6010	12–1630	192
Total Kjeldahl nitrogen	2–3320	47–1470	156
Iron	ND–1500	2.1–1400	416
Potassium	ND–2800	ND–1375	19
Magnesium	120–780	120–780	9
Ammonia-nitrogen	ND–1200	26–557	263
Sulfate	ND–1850	8.4–500	154
Aluminum	ND–85	ND–85	9
Zinc	ND–731	ND–54	158
Manganese	ND–31.1	0.03–25.9	67
Total phosphorus	ND–234	0.3–1.17	454
Boron	0.87–13	1.19–12.3	15
Barium	ND–12.5	ND–5	73
Nickel	ND–7.5	ND–1.65	133
Nitrate-nitrogen	ND–250	ND–1.4	88
Lead	ND–14.2	ND–1.11	142
Chromium	ND–5.6	ND–1.0	138
Antimony	ND–3.19	ND–0.56	76
Copper	ND–4.06	ND–0.32	138
Thallium	ND–0.78	ND–0.31	70
Cyanide	ND–6	ND–0.25	86

(Cont'd)

TABLE 1.9 Cont'd

Parameter	Overall Range ^a	Typical Range (range of site medians) ^a	Number of Analyses
Arsenic	ND–70.2	ND–0.225	112
Molybdenum	0.01–1.43	0.034–0.193	7
Tin	ND–0.16	0.16	3
Nitrite-nitrogen	ND–1.46	ND–0.11	20
Selenium	ND–1.85	ND–0.09	121
Cadmium	ND–0.4	ND–0.07	158
Silver	ND–1.96	ND–0.024	106
Beryllium	ND–0.36	ND–0.008	76
Mercury	ND–0.01	ND–0.001	111

^aAll concentrations in milligrams per liter except pH (standard units) and specific conductance ($\mu\text{mhos}/\text{cm}$). ND indicates not detected.

Source: Wisconsin Department of Natural Resources.

Open dumps Open dumps are typically unregulated. They receive waste mainly from households but are used for almost any type of waste. Waste is frequently burned, and the residue is only occasionally covered with fill. Such dumps do not have liners and leachate-collection systems and by their nature are highly likely to cause ground-water contamination. The use of open dumps in the United States is no longer possible due to 1991 EPA regulations issued under Subtitle D of the Resource Conservation and Recovery Act, which requires extensive groundwater monitoring at such facilities, requires the placement of daily cover, prohibits burning, and will require engineered liners for future expansions. Most operators of open dumps did not want the expense of such regulations and so closed the dumps.

Residential disposal Homeowners who are not served by a trash collection service must find alternative ways of disposing of their household waste. Included in the household waste are hazardous substances, such as used engine oil and anti-freeze, and leftover yard and garden chemicals, such as pesticides, unused paint, and used paint thinner. In the past these were often taken to the town dump. However, with the closing of most town dumps, the homeowner must find alternative means of disposal.

In the state of Wisconsin in the United States, virtually all town dumps were closed in 1989 and 1990. Most, but not all, counties offer waste disposal in a secure, engineered landfill. However, in large counties in the U.S. the county landfill may be 15 to 30 km from some parts of the county and a fee is charged, as opposed to the old town dump, which was close by and free. In some situations the residents must drive to a different county to find an open landfill. Unfortunately, this closing of town dumps has resulted in an increase in illegal dumping in state and national forests and a great increase in trash left at roadside rest areas and parks.

Homeowners may pour waste liquids into ditches or the sanitary sewer; combustibles may be burned in the backyard. These are undesirable practices that can easily result in environmental pollution, including groundwater contamination.

Surface impoundments Pits, ponds, and lagoons are used by industries, farmers, and municipalities for the storage and/or treatment of both liquid nonhazardous and hazardous waste and the discharge of nonhazardous waste. Prior to the passage of the Resource Conservation and Recovery Act, liquid hazardous wastes were also discharged into pits. These pits may be unlined or lined with natural material, such as clay, or artificial materials, such as plastic sheets, rubber membranes, or asphalt.

Impoundments are used to treat wastewater by such processes as settling of solids, biological oxidation, chemical coagulation and precipitation, and pH adjustment. They may also be used to store wastewater prior to treatment. Water from surface impoundments may be discharged to a receiving water course such as a stream or a lake. Unless a discharging impoundment is lined, it will also lose water by seepage into the subsurface. Nondischarging impoundments release water either by evaporation or seepage into the ground or a combination of both. Evaporation ponds are effective only in arid regions, where potential evapotranspiration far exceeds precipitation. Even evaporation ponds that were originally lined may leak and result in groundwater contamination if the liner deteriorates from contact with the pond's contents.

Impoundments are used for wastewater treatment by municipalities and industries such as paper manufacturing, petroleum refining, metals industry, mining, and chemical manufacturing. They are also used for treatment of agricultural waste, such as farm animal waste from feedlots. Power plants use surface impoundments as cooling ponds. Mining operations use surface ponds for the separation of tailings, which is waste rock from the processing of ore that occurs in a slurry mixture of liquid and solid.

Although it is now prohibited, until the 1970s lagoons were used for the disposal of untreated wastewater from manufacturing, ore processing, and other industrial uses into the groundwater. Brine pits were used for many years in the oil patch for the disposal of brines pumped up with the oil. Miller (1980) lists 57 cases of groundwater contamination caused by the leakage of wastewater from surface impoundments. In most of the reported cases water-supply wells had been affected; at the time when use of such impoundments was allowed, groundwater monitoring was not required; usually the only way that leakage was detected was by contamination of a supply well.

In one case in Illinois, up to 500,000 gals per day of mineralized wastewater, containing high total dissolved solids (TDS), which included chloride, sulfate, and calcium, from an ore-processing plant were discharged into waste-disposal ponds excavated in a glacial drift aquifer for a period of about 40 years. Concentrations of chloride, sulfate, TDS, and hardness were elevated in an underlying bedrock aquifer as much as a mile away from the site (U.S. Nuclear Regulatory Commission 1983).

Wastewater from the manufacturing of nerve gas and pesticides at the Rocky Mountain Arsenal at Denver was discharged into unlined evaporation ponds from 1942 until 1956. In 1956 a new pond lined with asphalt was constructed; ultimately that liner failed and the lined pond also leaked. Contamination of nearby farm wells was first detected in 1951 and was especially severe in the drought year of 1954, when irrigated crops died. Groundwater contamination extended at least 8 miles from the ponds and

was indicated by high chloride content. Ultimately the groundwater under and near the Rocky Mountain Arsenal was found to contain dozens of synthetic organic chemicals, including two that are especially mobile in the subsurface: diisopropylmethylphosphophosphate (DIMP), a by-product of the manufacture of nerve gas, and dicyclopentadiene (DCPD) a chemical used in the manufacture of pesticides (Konikow and Thompson 1984; Spanggord, Chou, and Mabey 1979). By 2010, after 23 years of active remediation the cleanup of contaminated soil and groundwater at the Rocky Mountain Arsenal, the cost has been \$2.1 billion dollars as parcels of the land are taken off the National Priorities list and tracts of land are converted to a National Wildlife Refuge.

There is very little information available on the number of surface impoundments worldwide, nor much up-to-date information from individual countries. Several decades ago the EPA performed a survey of the surface impoundments located in the United States (U.S. EPA 1983). They reported a total of 180,973 impoundments, including 37,185 municipal; 19,437 agricultural; 27,912 industrial; 25,038 mining; 65,688 brine pits for oil and gas; and 5,913 miscellaneous. A later U.S. EPA (2001) survey conducted in the 1990s estimated about 18,000 industrial impoundments. Energy related industrial surface impoundments are of particular concern, as these can hold many sorts of materials including coal combustion residues, water associated with *in situ* uranium leaching, and/or brines associated with deep oil and gas development. The large number of impoundments provides a significant threat to groundwater resources (OTA 1984).

Mine wastes Mining can produce spoils, or unneeded soil, sediment, and rock moved during the mining process, and tailings, or solid waste left over after the processing of ore. These wastes may be piled on the land surface, used to fill low areas, used to restore the land to pre-mining contours, or placed in engineered landfills with leachate collection systems. Mine wastes can generate leachate as rainwater passes through them. If sulfate or sulfide minerals are present, sulfuric acid can be generated, and the resulting drainage water can be acidic. This is likely to occur with coal-mining wastes, copper and gold ores, and ores from massive sulfide mineralization. Mine-waste leachate may also contain heavy metals and, in the case of uranium and thorium mines, radionuclides. Neutralization of the mine wastes can prevent the formation of acidic leachate and prevent the mobilization of many, but not all, metallic ions and radionuclides. The mine-waste disposal issue is a large one. In the United States, mining is estimated to produce waste material annually with a weight of nearly nine times that of refuse generated by all cities and towns (U.S. EPA 2003). The mining of many metals traditionally requires huge quantities of rock to be removed, for example, the production of a single ton of copper ore typically generates well over 100 times the tonnage of waste rock and about 200 times the tonnage of mined overburden, depending on the local geology. Leachate produced by unneutralized or uncontaminated mine wastes is a threat to surface and groundwater.

In some cases, *in situ* leach mining is used instead of physical removal of ore-containing rock. In these instances, a chemical mobilizing agent called a lixiviant is pumped down a well where it flows into an ore-bearing formation. After ore is dissolved, the pregnant solution circulating underground is removed using extraction wells. Problems can arise with *in situ* leach mining as the geologic structures associated with many ore

bodies are heterogeneous and anisotropic and contain secondary porosity, faults, and fractures. Roll front deposits mined for uranium fall into this category. These heterogeneities can complicate solution recovery, but perhaps just as importantly extend the time and areal extent needed to be investigated in order to successfully remediate the subsurface after mining is complete.

Material stockpiles Many bulk commodities, such as coal, road salt, ores, phosphate rock, and building stone, are stored in outdoor stockpiles. Rainwater percolating through the stockpile can produce leachate similar to that produced by the waste material that resulted from mining the commodities. For example, rainwater draining through a coal pile can become acidic from sulfide minerals contained in the coal. In the northern states road salt is usually stored indoors, although in the past outdoor storage piles were common. Leachate from the road-salt piles was a common source of groundwater contamination that has now been mostly eliminated.

Graveyards If bodies are buried without a casket or in a nonsealed casket, decomposition will release organic material. Areas of high rainfall with a shallow water table are most susceptible to groundwater contamination from graves. According to Bouwer (1978) contaminants can include high bacterial counts, ammonia, nitrate, and elevated chemical oxygen demand. Nash (1962) reported that hydrogen sulfide gas in a well was the result of a seventeenth-century graveyard for black plague victims. The well had apparently been unwittingly bored through the graveyard.

Animal burials Unless an animal is a famous Kentucky thoroughbred or a beloved family pet, it is likely to simply be buried in an open excavation. If large numbers of animals are buried in close proximity, groundwater contamination might occur from the decomposing carcasses. If the animals had died due to some type of toxic poisoning, then additional opportunities for groundwater contamination would exist if the toxic chemical were released as the animals decomposed.

Above-ground storage tanks Petroleum products, agricultural chemicals, and other chemicals are stored in aboveground tanks. Ruptures or leaks in the tanks can release chemicals, which then have the opportunity to seep into the ground. A serious case of groundwater contamination occurred in Shelbyville, Indiana, U.S.A. when one 55-gal tank of perchloroethylene was damaged by vandals and the contents leaked into the ground.

Underground storage tanks The Office of Technology Assessment estimated that in the United States there are some 569,000 underground storage tanks used to store fuel and other products (U.S. Environmental Protection Agency 2015). There are at least two tanks, and frequently more, at every gas station. Many homeowners and farmers have private underground tanks to store heating oil and fuel. Chemicals are also routinely stored in underground tanks at industrial facilities. Liquid hazardous wastes can also be stored in underground tanks. Leachate from landfills with leachate-collection systems may be stored in a tank while it awaits trucking to a treatment facility.

Underground tanks can leak through holes either in the tank itself or in any associated piping. The piping appears to be more vulnerable. Steel tanks are susceptible to corrosion and are being replaced by fiberglass tanks. However, even the fiberglass

tanks, the associated pipes can still leak. Fiberglass tanks do not have the strength of steel and may crack. A gas-station owner with a leaking tank can encounter tens of thousands of dollars in costs to remove a leaking tank and associated contaminated soil. Costs can be even higher if extensive groundwater contamination has occurred. In a 1-yr period a small consulting firm made 28 assessments of sites that contained underground fuel storage tanks. Even though none of the sites was known to have contamination prior to the assessments, 22 of the 28 sites (78%) were found to have leaking tanks (Gordon 1990). If one considered the sites being investigated because tanks were known to be leaking, the percentage of leaking tanks would be even higher.

Even the homeowner is at risk. One purchaser of an older home in the town of Black Wolf, Wisconsin, U.S.A. had the misfortune to discover an abandoned fuel-oil tank buried on his property. A total of forty-two 55-gal drums of a mixture of fuel oil and water were removed from the tank and had to be disposed of at considerable expense. Fortunately, as the tank was mostly below the water table, the water had leaked into the tank, rather than the fuel oil leaking out. Had the latter occurred, the costs to remove and dispose of contaminated soil would have been much higher.

Containers Many chemical and waste products are stored in drums and other containers. Should these leak, there is a potential for groundwater contamination.

Open incineration and detonation sites Incineration processes can reduce solid waste mass significantly, and these practices are popular in many countries, particularly in Europe and North America. Incineration of hazardous wastes (solids, liquids and sludges containing organic and inorganic wastes) is permitted in many countries, but with important restrictions. In the United States, sites for the open incineration of wastes are licensed under the Resource Conservation and Recovery Act (RCRA), with the number of facilities permitted to incinerate hazardous waste numbering 20 or slightly more. In 2015, three of the U.S. facilities had additional Toxic Substances Control Act (TCSA) permits and could incinerate polychlorinated biphenyl-contaminated materials. Materials not generally accepted for incineration include, some explosives, radioactive materials, dioxins, furans, infectious agents, shock-sensitive chemicals, and fluids under pressure. The U.S. Department of Defense operates specialized burning grounds and detonation sites for old ammunition. If not properly intercepted, chemicals released from incineration sites can leach into the ground with rainwater.

Radioactive-waste-disposal sites The disposal of civilian radioactive wastes and uranium mill tailings is licensed in the United States under the Nuclear Regulatory Commission. High-level radioactive wastes from nuclear power plants are currently in temporary storage but will eventually go into underground repositories excavated into rock. International consensus is that geologic burial of high-level waste is the preferred disposal method. Low-level radioactive wastes are buried in shallow landfills. Unless radioactive wastes are properly buried in engineered sites, there is a potential for radionuclides to migrate from the waste into groundwater, as happened at Oak Ridge, Tennessee; Hanford, Washington; Savannah River Facility, Georgia; and the Idaho National Engineering Lab.

1.5.3 Category III: Sources Designed to Retain Substances During Transport

Pipelines Included in Category III are sewers to transmit wastewater as well as pipelines for the transmission of natural gas, petroleum products, and other liquids such as anhydrous ammonia. Although the pipelines are designed to retain their contents, many leak to a greater or lesser extent. This is particularly true of sewers, especially older sections. Sewers usually have a friction joint that can leak if the pipe shifts position. If the sewer is above the water table, leaking sewage can contaminate the groundwater with bacteria, nitrogen, and chloride. Steel pipelines are subjected to corrosion and can also develop leaks. Such pipelines have been known to leak crude oil, gasoline, fuel oil, liquefied petroleum gas, natural gas liquids, jet fuel, diesel fuel, kerosene, and anhydrous ammonia (OTA 1984).

Material transport and transfer Material transport and transfer occurs by the movement of products and wastes via truck and train along transportation corridors and the associated use of loading facilities. Spills may result from accidents, and leaks can occur because of faulty equipment. A wide variety of materials can be released to the environment in this manner. Experienced and well-trained crews with the proper equipment are needed to clean up such spills. Improper actions can result in a spill becoming more severe as a result of a misguided cleanup effort.

1.5.4 Category IV: Sources Discharging Substances as a Consequence of Other Planned Activities

Irrigation When crops are irrigated, more water is applied to the field than is needed for evapotranspiration. The excess water, called **return flow**, percolates through the soil zone to the water table or overland to receiving streams, lakes, and wetlands. In doing so it can mobilize chemicals applied to the fields as fertilizers and pesticides. Soil salinity and salinity of the shallow groundwater can also increase, because the evaporation of water concentrates the natural salts carried in the irrigation water. Waterfowl and other animal are particularly sensitive to selenium. In the past, selenium has been concentrated in irrigation return water that has been discharged to the Kesterson Wildlife Refuge in California's Central Valley causing wildlife deaths.

Pesticide applications Chemicals are applied to crops to control weeds, insects, fungi, mites, nematodes, rats, rodents, algae in aqueous systems and other pests. In addition they are used for defoliation, desiccation, and growth regulation (OTA 1984). Worldwide estimates of pesticide use is over 5.2 billion pounds annually, with about 45% being used in Europe, 25% in the United States, and 30% in the rest of the world (De et al. 2014). Different pesticides and classes of pesticides can have widely varying environmental and health effects. For example, organochlorides can be long-lived in the environment, concentrated in the food chain (bioaccumulation), and resistant to degradation; organophosphates as a class are less persistent in the environment but generally more acutely toxic; phenoxyalkanoic acid derivatives have great variety including dioxins which can be teratogenic (birth defect producing); uptake of some

carbamate pesticides into plant roots can produce systemic contaminants; substituted ureas degrade readily as a class but can be a problem locally in the immediate area and period of application; and triazines can be persistent in anaerobic environments.

The use of pesticides has extensive potential for contaminating groundwater. Globally over 1.8 billion people produce agricultural crops and most use pesticides (Alavanja 2009). Pesticides applied to the soil may migrate through the soil to the water table. Pesticides in use today are usually biodegradable to some extent. However, their breakdown products (metabolites) can also be found in groundwater. The potential for contamination is higher at sites where pesticides are mixed and application equipment is loaded and then rinsed when its use is finished. Soils under such areas may receive a much greater loading of pesticides than the cropland to which the pesticides are applied. Application of pesticides by aerial spraying may result in uneven distribution. More than 65% of pesticides are applied by aerial spraying, and the cleanup of the planes and disposal of associated wastewater poses a special problem (OTA 1984).

Atrazine, a triazine, has been used extensively for pre-emergent weed control in corn cultivation. In 1985 alone, 3.3 million acres of Wisconsin, U.S.A. farmland planted with corn was treated with it. A survey of atrazine in Wisconsin groundwaters showed it occurred unevenly in areas where it was used on fields. Highest concentrations, up to 3.5 parts per billion, were associated with mixing sites and sandy river-bottom land (Wollenhaupt and Springman 1990).

Fertilizer application Farmers and homeowners alike apply fertilizers containing nitrogen, phosphorous, and potassium (potash). Phosphorous is not very mobile in soil and thus does not pose a significant threat to groundwater. The rate of potassium application is generally low and, although it is mobile, the literature does not indicate that potassium from fertilizers is a major factor in causing groundwater problems. However, nitrogen from fertilizers can be a major cause of groundwater contamination.

Farm animal wastes Farm animal wastes have the potential to contaminate groundwater with bacteria, viruses, nitrogen, and chloride. Animals that are kept on an open range disperse their wastes over a large area, and the potential for environmental contamination is low. Animals confined to a small area will concentrate their wastes in the barn, barnyard, or feedlot. Rainwater infiltrating these wastes can mobilize contaminants, which can be leached into the soil and eventually into groundwater. Manure from farms may be spread onto fields as a fertilizer, whereas large feedlot operations often have wastewater treatment plants. In northern climates manure spread on frozen fields can have a deleterious effect on both surface and groundwater during the spring melt. Many farms in northern areas now have concrete storage tanks for holding manure during the winter months.

Salt application for highway deicing Many states in the snowy regions have a dry-pavement policy that requires the use of highway deicing salts on city streets, rural highways, and interstate highways. The primary deicing salt is rock salt, consisting mainly of sodium chloride. Additives to improve the handling of the salt include ferric ferrocyanide and sodium ferrocyanide. Chromate and phosphate may be added to reduce the corrosiveness of the salt (OTA 1984). The salt and additives eventually are carried from the roadway in runoff and may either wash into surface streams or seep into groundwater.

Home water softeners In areas where the water supply has high calcium and magnesium content, home water softeners are used to reduce the hardness. Home water softeners are recharged with sodium chloride salt. Chlorides from the salt are contained in the backwash water. If the area is not served by sewers, the backwash water is disposed by subsurface drainage via septic tanks or separate drain fields. Chlorides from this source can enter the groundwater reservoir (Hoffman and Fetter 1978).

Urban runoff Precipitation over urban areas typically results in a greater proportion of runoff and less infiltration than that falling on nearby rural areas because of the greater amount of impervious land surface in the urban area. In addition, the urban runoff contains high amounts of dissolved and suspended solids from auto emissions, fluid leaks from vehicles, home use of fertilizers and pesticides, refuse, and pet feces, and in economically poor countries, raw sewage wastes. For the most part, the urban runoff is carried into surface receiving waters, but it may recharge the water table from leaking storm sewers. This can contribute to degradation of groundwater quality in urban areas.

Percolation of atmospheric pollutants Atmospheric pollutants reach the land either as dry deposition or as dissolved or particulate matter contained in precipitation. Sources include automobile emissions, power plant smokestacks, incinerators, foundries, and other industrial processes. Pollutants include hydrocarbons, synthetic organic chemicals, natural organic chemicals, heavy metals, sulfur, and nitrogen compounds. Infiltrating precipitation may carry these compounds into the soil and groundwater.

Mine drainage and excursions Surface and underground mining may disrupt natural groundwater flow patterns and expose rocks containing pyrite to oxygenated water. This can result in the production of acid water, which then drains from the mine. The acid mine drainage can result in surface- and groundwater contamination. In one very interesting case in Shullsburg, Wisconsin, a lead and zinc mine was active for 25 years. In order to work the mine, the groundwater table was lowered below the mine levels by pumping. Sulfide minerals in the rock were subjected to biologically mediated oxidation along fractures in the rock and mine workings. Contact of the resulting sulfuric acid with the dolomite host rock neutralized the sulfuric acid and produced highly soluble sulfate minerals. When the mining ceased due to economic factors, the dewatering pumps were shut down and the mine workings were flooded. Groundwater in the mine workings dissolved the sulfate minerals and resulted in high sulfate (up to 3500 mg/L), iron (up to 20 mg/L), and zinc (up to 18 mg/L) concentrations. As a result groundwater quality of a number of nearby water supply wells was adversely impacted (Hoffman 1984).

Oil and natural gas production has the potential to release and mobilize formerly sequestered hydrocarbons into the subsurface environment, although industry takes measures to minimize this risk. Traditional oil and natural gas extraction has been augmented by unconventional methods in shale, sandstone, carbonate and other tight formations, and these newer approaches are increasing hydrocarbon production worldwide, mainly as the result of newer horizontal drilling and hydraulic fracturing (i.e., “fracking” or “fracking”) techniques. Shale is a fine-grained sedimentary rock from a parent material of consolidated silts and clays, and “black shales” are rich in organic

material that can generate oil and gas and isolate those products in their pore spaces in the shale matrix. The newer, unconventional methods of shale oil extraction include pyrolysis (slow burning underground under low oxygen conditions), hydrogenation and or thermal dissolution. One method of natural gas production is coal bed methane production, also called coal seam gas, which produces a “sweet gas”, high in methane content from subsurface coal measures often located hundreds of meters to over a thousand meter depth. When surrounding hydraulic pressure is lowered near these coal bodies by pumping groundwater, this high quality natural methane degasses. The gas evolves from the pore spaces in coal layers, it is then collected in overlying recovery wells, and undergoes separation for any natural gas liquids and removal of oil and condensate, water, carbon dioxide, and sulfur. Notably, these methods for oil and gas production can produce significant amounts of poor-quality groundwater which must be disposed of properly.

Fracking fluids Fracking fluids are designed to open up formations around a well to increase the surrounding permeability and allow capture of oil or natural gas. These fluids are often injected at considerable distance below ground surface. Half a century ago, fracking fluids were basically water and sand with the mixtures pumped underground under great pressure to open up fractures. The sand was considered a propping agent which would enter fractures opened up by the overpressure, and keep them propped open. In the last decades fracking fluids have increased in complexity and chemical content, including chemicals such as guar gum, ammonium persulfate, acetic acid, ethanol, orange oil and other surfactants. Potentially toxic chemicals have been found in some fracking mixtures, including: petroleum distillates such as kerosene and diesel fuel (and their component organics including benzene, toluene, ethylbenzene, and xylenes), poly aromatic hydrocarbons (PAHs), sodium hydroxide, harmful alcohols like methanol, hydrochloric and other acids, ethylene glycol and glycol ethers, and formaldehyde.

1.5.5 Category V: Sources Providing a Conduit for Contaminated Water to Enter Aquifers

Production wells Wells are drilled for the production of oil, gas, geothermal energy, and water. Contaminants can be introduced into the ground during the drilling of production wells. Improperly constructed wells, corroded well casings, and improperly abandoned wells can provide a conduit for the flow of contaminated surface water into the ground or the movement of contaminated groundwater from one aquifer into another. Homeowners may route drainage water from their roof and basement drains into abandoned water-supply wells. Old dug wells may become receptacles for trash.

Monitoring wells and exploration borings Many thousands of monitoring wells are being installed in the United States each year. Exploration borings are installed for the purposes of mineral exploration or construction design. These wells and borings have the same potential for cross contamination of aquifers and introduction of contaminated surface water as production wells.

Infiltration galleries and dry wells Infiltration of some spills can be accelerated into the subsurface in the presence of infiltration galleries, dry wells and other facilities designed to remove standing water after storms in urban environments. Many communities have

set limits as to how long standing surface water pools and puddles can remain, and infiltration galleries and dry wells allow impounded water and runoff, potentially carrying pollutants, to be swiftly carried to subsurface leach fields or well screens. This removal of surface water is typically for short-term health, safety, and mosquito control purposes. The term “dry well” indicates the intent that these wells would only penetrate and leak water into the vadose zone, not below the water table. These wells would therefore be above the water table and dry, however, historically some “dry wells” were drilled deeper, allowing surface water and pollutants to be directly and quickly introduced into unconfined aquifers. Urban surface depressions with associated infiltration galleries can be constructed purposely for storm-water capture and diminution, or other purposes. For example, loading docks for trucks often have a depressed pavement surface next to the loading dock (which is also an area of possible spills) to assist transfer of cargo. Potentially contaminated water can be swiftly moved underground with these urban structures.

Construction excavation Construction activities can strip the soil from bedrock, thus removing much of the natural protection of bedrock aquifers from groundwater contamination. Urban runoff water can collect in open foundation excavations, which then provide a conduit to aquifers.

1.5.6 Category VI: Naturally Occurring Sources Whose Discharge is Created and/or Exacerbated by Human Activity

Groundwater-surface-water interactions Some aquifers are recharged naturally from surface water if the stream stage is higher than the water table (Fetter 1994). If the surface-water body becomes contaminated, then the aquifer being recharged by that water could also become contaminated. An exception to this might occur if the surface-water contamination is by a material that could be adsorbed or removed by filtration when it passes through the alluvium under the stream. Wells located near a stream can induce infiltration from the stream into the groundwater reservoir by development of a cone of depression. Contaminated surface water can thereby be drawn into an aquifer.

Natural leaching Dissolved minerals occur in groundwater due to natural leaching from rocks and soil. Naturally occurring groundwater may have total dissolved solids in excess of 10,000 to 100,000 mg/L and may contain undesirable concentrations of various anions and cations. Human activity that results in acid rain may enhance the ability of infiltrating rainwater to leach naturally occurring substances from rock and soil.

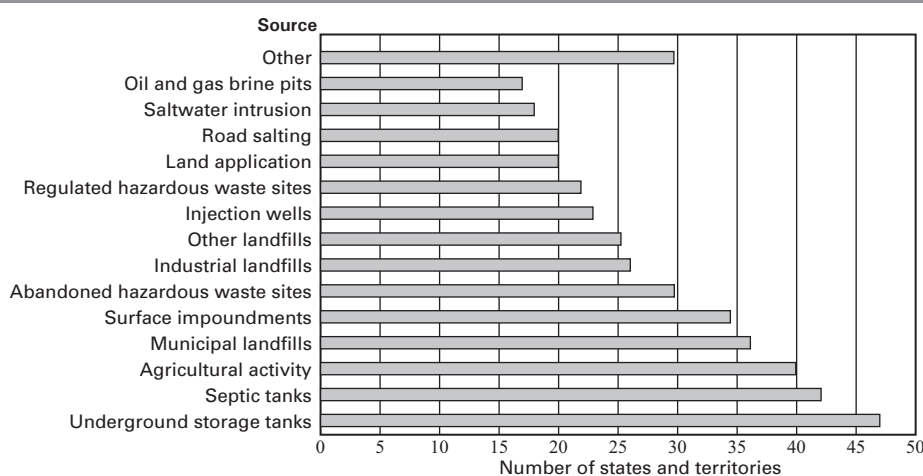
Saltwater intrusion Development of freshwater supplies from coastal aquifers may lower the water table and induce saline groundwater that occurs naturally beneath the oceans to move landward into formerly freshwater aquifers. Upconing of the saltwater-freshwater interface may also occur if the well field overlies an aquifer containing saline water (Fetter 1994). Groundwater development in areas susceptible to saltwater intrusion should be undertaken with a clear plan that is designed to maximize the amount of fresh water that can be developed while minimizing the amount of saltwater intrusion and other undesirable effects that can occur (Fetter 1972).

■ 1.6 Relative Ranking of Groundwater-Contamination Sources and Substances

Every site of groundwater contamination is unique in its geology, contaminant mixtures, surrounding human-made structures, and pollutant sources. Therefore the risks associated with different localities and their contaminants can vary greatly, and the approaches for site characterization and remediation are typically tailored to each individual site. Although there are many potential sources of groundwater contamination, some pose much more of a threat to groundwater than others. Section 305(b) of the Federal Clean Water Act requires individual States in the U.S. to submit reports to the Environmental Protection Agency on the sources of groundwater contamination in the state and the type of contaminants observed. The data submitted were used to compile *National Water Quality Inventory—1988 Report to Congress* (U.S. EPA 1990).

The states indicated all the groundwater-contamination sources that they considered to be major threats to groundwater in their state. Figure 1.3 shows that more than half the states and territories listed underground storage tanks, septic tanks, agricultural activities, municipal landfills, and abandoned hazardous-waste sites as major threats to groundwater. Other frequently listed sources include industrial landfills, other landfills, injection wells, regulated hazardous-waste sites, land application, road salt, saltwater intrusion, and brine pits from oil and gas wells.

FIGURE 1.3 Frequency of various contamination sources considered by states and territories of the United States to be major threats to groundwater quality.



Source: UNICEF 2012.

Additionally, every two years the Agency for Toxic Substance and Disease Registry (ATSDR) and the Environmental Protection Agency in the United States prepare a list of hazardous substances most commonly found at facilities on the National Priorities List (NPL), also called the “Superfund” program. The list is a prioritization of harmful substances based on a combination of their frequency of occurrence, their toxicity, and

the potential for human exposure at NPL sites. This prioritization is required by the Comprehensive Environmental Response, Compensation and Liability Act (CERCLA) section 104(i), as amended by the Superfund Amendments and Reauthorization Act (SARA). Table 1.10 below lists the first fifty substances listed of the 2013 ATSDR Substance Priority List. The disadvantage of this list is it is based on large hazardous waste sites, and harmful substances in regions of the country with naturally occurring geologic contaminants, such as radon, are not as highly ranked as their overall potential risk to the public.

TABLE 1.10 The highest ranked fifty substances (out of a total of 275 substances) on the Agency for Toxic Substance and Disease Registry 2015 Substance Priority List. Substances were assigned the same rank when two (or more) substances received equivalent total point scores.

2015 RANK	SUBSTANCE NAME	TOTAL POINTS	2013 RANK	CAS RN
1	ARSENIC	1671.6	1	007440-38-2
2	LEAD	1529.4	2	007439-92-1
3	MERCURY	1458.6	3	007439-97-6
4	VINYL CHLORIDE	1358.9	4	000075-01-4
5	POLYCHLORINATED BIPHENYLS	1345.1	5	001336-36-3
6	BENZENE	1327.6	6	000071-43-2
7	CADMIUM	1318.8	7	007440-43-9
8	BENZO(A)PYRENE	1304.4	8	000050-32-8
9	POLYCYCLIC AROMATIC HYDROCARBONS	1279.1	9	130498-29-2
10	BENZO(B)FLUORANTHENE	1249.7	10	000205-99-2
11	CHLOROFORM	1202.4	11	000067-66-3
12	AROCLOR 1260	1190.0	12	011096-82-5
13	DDT, P,P'	1182.0	13	000050-29-3
14	AROCLOR 1254	1171.3	14	011097-69-1
15	DIBENZO(A,H)ANTHRACENE	1155.6	15	000053-70-3
16	TRICHLOROETHYLENE	1153.4	16	000079-01-6
17	CHROMIUM, HEXAVALENT	1146.8	17	018540-29-9
18	DIELDRIN	1142.9	18	000060-57-1
19	PHOSPHORUS, WHITE	1141.3	19	007723-14-0
20	HEXACHLOROBUTADIENE	1128.2	20	000087-68-3
21	DDE, P,P'	1125.9	21	000072-55-9
22	CHLORDANE	1125.6	22	000057-74-9
23	AROCLOR 1242	1124.7	24	053469-21-9

(Cont'd)

TABLE 1.10 *Cont'd*

2015 RANK	SUBSTANCE NAME	TOTAL POINTS	2013 RANK	CAS RN
24	COAL TAR CREOSOTE	1124.4	23	008001-58-9
25	ALDRIN	1114.6	25	000309-00-2
26	DDD, P,P'-	1113.1	26	000072-54-8
27	AROCLOR 1248	1104.5	27	012672-29-6
28	HEPTACHLOR	1100.6	28	000076-44-8
29	AROCLOR	1099.5	29	012767-79-2
30	BENZIDINE	1091.2	30	000092-87-5
31	ACROLEIN	1088.5	31	000107-02-8
32	TOXAPHENE	1087.8	32	008001-35-2
33	TETRACHLOROETHYLENE	1076.7	33	000127-18-4
34	HEXACHLOROCYCLOHEXANE, GAMMA-	1075.1	34	000058-89-9
35	CYANIDE	1069.8	35	000057-12-5
36	HEXACHLOROCYCLOHEXANE, BETA-	1053.4	36	000319-85-7
37	DISULFOTON	1047.2	38	000298-04-4
38	BENZO(A)ANTHRACENE	1046.0	38	000056-55-3
39	1,2-DIBROMOETHANE	1041.7	39	000106-93-4
40	ENDRIN	1037.6	40	000072-20-8
41	DIAZINON	1036.6	41	000333-41-5
42	HEXACHLOROCYCLOHEXANE, DELTA-	1034.8	42	000319-86-8
43	BERYLLIUM	1031.0	43	007440-41-7
44	ENDOSULFAN	1027.7	44	000115-29-7
45	AROCLOR 1221	1027.0	45	011104-28-2
46	1,2-DIBROMO-3-CHLOROPROPANE	1025.7	46	000096-12-8
47	HEPTACHLOR EPOXIDE	1020.7	47	001024-57-3
48	ENDOSULFAN, ALPHA	1018.0	48	000959-98-8
49	CIS-CHLORDANE	1015.6	49	005103-71-9
50	CARBON TETRACHLORIDE	1012.1	50	000056-23-5

Source: ATSDR 2015.

■ 1.7 Groundwater Contamination as a Long-Term Problem

One of the factors of groundwater contamination that makes it so serious is its long-term nature. Wastes buried long ago may cause groundwater contamination that takes decades to be discovered. Although many groundwater contamination sites are

small, some of the long-term sites are fairly extensive due to the long time period over which contamination has been migrating away from the source.

In the 1930s poison baits utilizing arsenic were used in the Midwestern United States to counter a grasshopper infestation. Apparently, leftover poison bait was buried when the infestations ended. In 1972 a water-supply well was drilled for a small business. In short order, 11 of 13 employees became ill with arsenic poisoning. Tests of the well showed it contained 21 mg/L of arsenic and soil at the site had 3000 to 12,000 mg/L of arsenic. This was apparently a mixing or burial site for arsenic-laden grasshopper bait (American Water Resources Association 1975).

Beginning in 1910 waste fuel oil and solvents from a railroad yard were discharged into the dry bed of the Mojave River near Barstow, California, USA. A study in 1972 showed that a zone of contaminated groundwater extended nearly 4.25 miles from the site and was 1800 ft wide (Hughes 1975).

Starting in 1936 a seepage lagoon was used for the disposal of treated domestic sewage at the Otis Air Force base, Cape Cod, Massachusetts, USA. Over a 50-year period about 2.5 billion gals of treated sewage was discharged into the rapid-infiltration ponds. The sewage percolated through the unsaturated zone and recharged a shallow sand and gravel aquifer. Because of the high rate of groundwater flow, about 1.0 to 1.5 ft per day, the plume has migrated more than 2 miles downgradient. The plume can be traced by elevated concentrations of chloride, boron, nitrate, detergents, and volatile organic compounds. The plume is narrow and thin due to limited transverse dispersion (Hess 1988).

A coal-tar distillation and wood-preserved plant was operated from 1918 to 1972 at St. Louis Park, Minnesota, USA. Coal tar, which is obtained by heating coal in the absence of air, is a complex mixture of hundreds of organic compounds, including polynuclear aromatic hydrocarbons (PAH). The coal tar was distilled to form creosote, which was then used as a wood preservative. Coal-tar chemicals and creosote entered the environment by spills and drippings at the wood-preserved facility as well as via plant-process discharge water, which went into ponds. Coal tar is denser and more viscous than water and is only slightly soluble. The coal-tar compounds migrated downward into the underlying glacial drift aquifer. Several old, deep wells on the site had defective casings, which allowed coal tar to migrate downward into deep, bedrock aquifers. One 595-ft-deep well on the site was found to contain a column of coal tar 100 ft long. About 150 gal/min of contaminated water was entering this well from the glacial drift aquifer through a leak in the casing. This water then drained downward into the deep bedrock aquifers, carrying contamination with it. After 60 yr of leakage the contamination had spread more than 2 miles from the plant site in several directions. Water supply wells located outside of the area of contamination have drawn contaminated water into the bedrock aquifers up-gradient of the site in terms of the regional groundwater-flow direction (Hult and Stark 1988).

Starting in about 1850 and extending until the 1950's combustible gas was manufactured in the United States from coal, coke and oil in order to supply homes and business. It has been estimated that there were between 1000 and 2000 manufactured gas plants active sometime within this time span. The widespread availability of natural gas made manufactured gas uneconomical and the plants were all closed. One of the by-products of gas manufacture was tar. The tar was a complex mixture of organic

compounds that was denser than water and had limited solubility in water. Large volumes of tar were generated and due to routine leaks and spills, leaking tar storage tanks and deliberate disposal, tar was released into the environment. When some of the plants were decommissioned tanks containing tar were just buried in place. Today many of the former manufactured gas plant sites still have soil and groundwater contamination associated with the tar (Luthy et al. 1994).

■ 1.8 Review of Mathematics and the Flow Equation

1.8.1 Derivatives

Soil-moisture movement, groundwater flow, and solute transport may be described by means of partial differential equations. Thus, a brief review is in order.

If a bicyclist is traveling down a highway, we can measure the time that it takes the rider, who has a flying start, to go from a starting point ($S(t_1)$, or the location at the starting time, t_1), to a point somewhere down the highway ($S(t_2)$, or the location at elapsed time t_2). If we wish to know the average speed of the rider over this distance, we divide the distance from point $S(t_1)$ to point $S(t_2)$ by the elapsed time, $t_2 - t_1$.

$$\frac{\Delta S}{\Delta t} = \frac{S(t_2) - S(t_1)}{t_2 - t_1} \quad (1.1)$$

The rider will be going more slowly uphill and faster downhill. The average speed will thus include a lot of variation. If we were to measure the rider's speed over a shorter part of the course, there would be less variation in speed. As the length of time over which the distance traveled is measured becomes shorter and shorter, the variation in speed decreases. If the time becomes infinitesimally small—for example, the time that it takes the rider to travel a few microns—we obtain an instantaneous speed. This is known as the **first derivative of distance with respect to time** and is defined by

$$\frac{dS(t_1)}{dt} = \lim_{t \rightarrow t_1} \frac{S(t) - S(t_1)}{t - t_1} \quad (1.2)$$

where t is any arbitrary time. Figure 1.4 shows a graph of distance traveled by our bicyclist as a function of time. The slope of the line from time t_1 to time t_2 is the average speed over that part of the highway and is expressed as $\Delta S/\Delta t$. The *instantaneous speed at time t_1* is the slope of the tangent to the curve at that point, which is expressed as dS/dt .

Note that the slope of distance versus time on Figure 1.4 keeps changing. This reflects the changes in speed that occur as the rider goes up and down hills. As the rider goes over the crest of a hill, he or she will perhaps be going rather slowly. As the rider goes downhill, the velocity will increase. We can compare the crest-of-the-hill velocity with the bottom-of-the-hill velocity and see that it has increased. This is a measure of the acceleration that occurs as gravity and the leg muscles of the bicyclist combine to increase speed. Figure 1.5 shows the speed of the rider as he or she goes over a hill. At $t = 0$ the rider is coming over the crest of the hill and the speed is 10 mi/hr. At $t = 30$ sec, when the rider is near the bottom of the hill, the speed is 26 mi/hr. The average rate of change in speed is $(26 \text{ mi/hr} - 10 \text{ mi/hr})/(30 \text{ sec})$.

FIGURE 1.4 Graph of distance traveled versus time graphically showing speed, which is the first derivative of distance with respect to time.

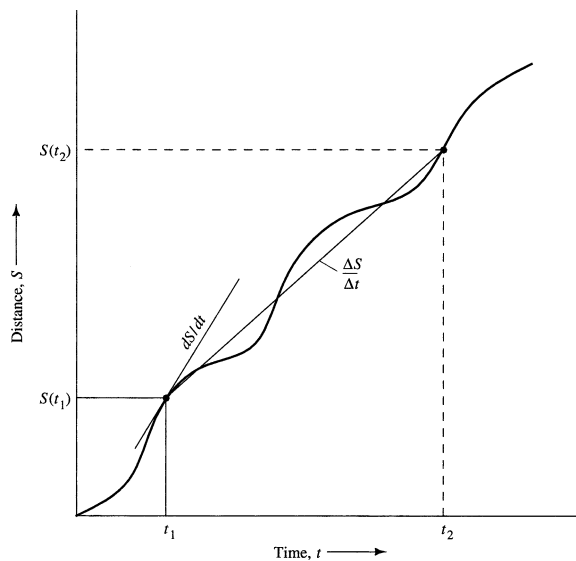
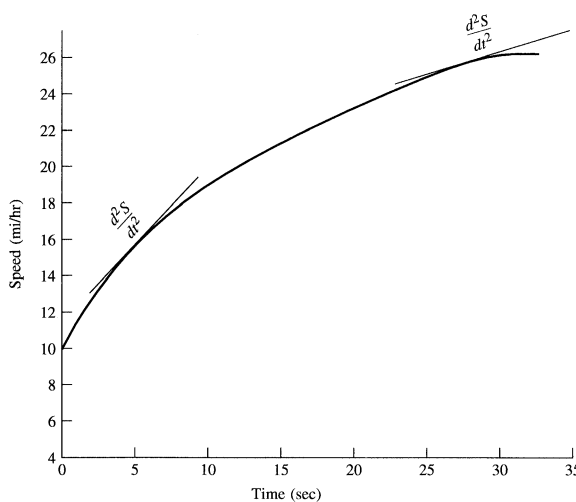


FIGURE 1.5 Graph of speed versus time graphically showing acceleration, which is the second derivative of distance with respect to time.



30 sec, or 0.53 mi/hr/sec. The rate of change is faster near the top of the hill where the slope is steeper and there is less wind resistance, since the rider is moving more slowly. From 0 to 5 sec the speed changes from 10 to 15 mi/hr, or 1.0 mi/hr/sec. Acceleration

is the rate of change of speed with time, which is a second derivative. It is the slope of a tangent to the curve at a given time. It can be expressed as

$$\frac{d\left(\frac{ds}{dt}\right)}{dt} \quad \text{or} \quad \frac{d^2s}{dt^2}$$

The tangent at 5 sec. can be seen to be steeper than the tangent at 30 sec, where the rate of change is less.

In hydrogeology we have many parameters that are a function of more than one independent variable. For example, hydraulic head is a function of the three space variables: $h = h(x, y, z)$. We frequently differentiate head with respect to one of the space variables while holding the other two variables constant. Such derivatives of a parameter with respect to a single variable are called **partial derivatives**. The second derivative of hydraulic head with respect to the space variables is

$$\frac{\partial^2 h}{\partial x^2} + \frac{\partial^2 h}{\partial y^2} + \frac{\partial^2 h}{\partial z^2}$$

1.8.2 Darcy's Law

The first experimental study of water movement through a porous medium was performed by Henry Darcy (Darcy 1856). He found that the one-dimensional flow of water through a pipe filled with sand was proportional to the cross-sectional area and the head loss along the pipe and inversely proportional to the flow length. Darcy's law can be expressed as

$$Q = -KA \frac{dh}{dl} \tag{1.3}$$

where

Q = volumetric discharge

K = proportionality constant known as hydraulic conductivity

A = cross-sectional area

dh/dl = gradient of hydraulic head

This equation can also be expressed in terms of **specific discharge**, or **Darcy flux**, q , which is the volumetric flow rate, Q , divided by the cross-sectional area, A .

$$q = -K \frac{dh}{dl} \tag{1.4}$$

Darcy's law was obtained for one-dimensional flow. However, as was previously stated, head is a function of all three dimensions: $h = h(x, y, z)$.

The hydraulic conductivity is the measure of the ability of the fractured or porous media to transmit water. It can have different values, depending upon the actual

direction that the water is flowing through the porous media. In such a case the medium is said to be **anisotropic**. The value of the hydraulic conductivity can be measured in three principle directions, K_x , K_y , and K_z . If the hydraulic conductivity is the same in all directions, then $K_x = K_y = K_z = K$ and the medium is said to be **isotropic**.

1.8.3 Scalar, Vector, and Tensor Properties of Hydraulic Head and Hydraulic Conductivity

We first need to define some terms relating to **tensors**. A zero-order tensor, also called a **scalar**, is a quantity characterized only by its size or magnitude. Examples in hydrogeology include hydraulic head, chemical concentration, and temperature. A first-order tensor, or **vector**, is a quantity that has both a magnitude and a direction. Vectors require three components, each having a magnitude and direction. Velocity, specific discharge, mass flux, and heat flux are examples. A second-order tensor—or, simply, **tensor**—acts like the product of two vectors, requiring nine components to account for all possible products of the three components of each vector. Examples in hydrogeology are intrinsic permeability, hydraulic conductivity, thermal conductivity, and hydrodynamic dispersion.

The hydraulic head is a scalar. However, the gradient of the head is a vector as it has both a magnitude and a direction. The gradient of h is designated as $\text{grad } h$:

$$\text{grad } h = i \frac{\partial h}{\partial x} + j \frac{\partial h}{\partial y} + k \frac{\partial h}{\partial z} \quad (1.5)$$

where **i**, **j**, and **k** are unit vectors in the x , y , and z directions. An equivalent notation is the use of the vector differential operator, **del**, which has the symbol ∇ . This operator is equivalent to

$$i \frac{\partial}{\partial x} + j \frac{\partial}{\partial y} + k \frac{\partial}{\partial z} \quad (1.6)$$

Another vector is the specific discharge, **q**. It has three components, q_x , q_y , and q_z , when measured along the Cartesian coordinate axes. Associated with any vector is a positive scalar with a value equal to the magnitude of the vector. If q is the magnitude of the vector **q**, this can be expressed as

$$q = |q| \quad (1.7)$$

A second-order tensor, such as **K**, hydraulic conductivity, can be described by nine components. In matrix form they are expressed as:

$$K = \begin{bmatrix} K_{xx} & K_{xy} & K_{xz} \\ K_{yx} & K_{yy} & K_{yz} \\ K_{zx} & K_{zy} & K_{zz} \end{bmatrix} \quad (1.8)$$

If the tensor is symmetric, $K_{ij} = K_{ji}$; then inspection of (1.8) shows that there are only six independent components of **K**.

If the coordinate system is oriented along the principal axes, the tensor becomes

$$K = \begin{bmatrix} K_{xx} & 0 & 0 \\ 0 & K_{yy} & 0 \\ 0 & 0 & K_{zz} \end{bmatrix} \quad (1.9)$$

For the special case of an isotropic media—that is, the value of \mathbf{K} does not depend upon the direction in which it is measured—the tensor becomes

$$K = \begin{bmatrix} K & 0 & 0 \\ 0 & K & 0 \\ 0 & 0 & K \end{bmatrix} \quad (1.10)$$

The three components of the specific discharge vector, \mathbf{q} , are

$$q_x = -K_{xx} \frac{\partial h}{\partial x} - K_{xy} \frac{\partial h}{\partial y} - K_{xz} \frac{\partial h}{\partial z}$$

$$q_y = -K_{yx} \frac{\partial h}{\partial x} - K_{yy} \frac{\partial h}{\partial y} - K_{yz} \frac{\partial h}{\partial z} \quad (1.11)$$

$$q_z = -K_{zx} \frac{\partial h}{\partial x} - K_{zy} \frac{\partial h}{\partial y} - K_{zz} \frac{\partial h}{\partial z}$$

For the special case where we orient the axes of the x , y , and z coordinate system with the three principal directions of anisotropy, \mathbf{K} is the matrix shown in (1.9) and the three components of the specific discharge vector are

$$q_x = -K_{xx} \frac{\partial h}{\partial x}$$

$$q_y = -K_{yy} \frac{\partial h}{\partial y} \quad (1.12)$$

$$q_z = -K_{zz} \frac{\partial h}{\partial z}$$

For an isotropic material, \mathbf{K} is represented by the matrix in (1.10) and

$$q = -K \frac{\partial h}{\partial x} - K \frac{\partial h}{\partial y} - K \frac{\partial h}{\partial z} \quad (1.13)$$

or

$$q = -K \operatorname{grad} h \quad (1.14)$$

If we multiply two vectors together and the result is a scalar, then the product is called a **dot product**, or **inner product**. For example, the del operator dotted into a vector

yields a scalar, called the **divergence**. Based on grad h , we can find a velocity vector \mathbf{v} such that the magnitude and direction vary throughout the porous media. If we apply the del operator to \mathbf{v} , we obtain the following:

$$\nabla \cdot \mathbf{v} = \text{div } \mathbf{v} = \frac{\partial v_x}{\partial x} + \frac{\partial v_y}{\partial y} + \frac{\partial v_z}{\partial z} \quad (1.15)$$

If we apply the del operator to grad h , the result is the second derivative of head:

$$\nabla \cdot \text{grad } h = \frac{\partial^2 h}{\partial x^2} + \frac{\partial^2 h}{\partial y^2} + \frac{\partial^2 h}{\partial z^2} \quad (1.16)$$

1.8.4 Derivation of the Flow Equation in a Deforming Medium

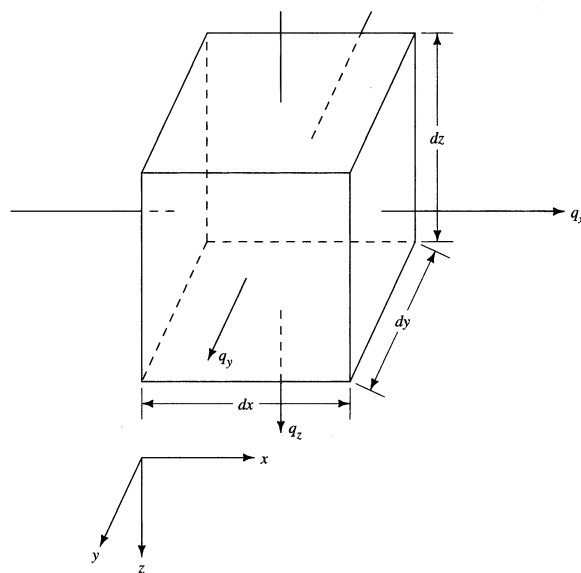
The **law of mass conservation** states that there can be no net change in the mass of fluid in a small representative elementary volume (REV) of a porous medium. In other words, the mass entering the REV less the mass leaving the REV is equal to the change in mass storage with time.

The representative elementary volume is shown on Figure 1.6. The three sides have length dx , dy , and dz , respectively. The area of the two faces normal to the x axis is $dy dz$, the area of the faces normal to the y axis is $dx dz$, and the area of the faces normal to the z axis is $dx dy$.

The component of mass flux into the REV parallel to the x axis is the fluid density times the flux rate:

$$\text{Mass influx along } x \text{ axis} = p_w q_x dy dz \quad (1.17)$$

FIGURE 1.6 Representative elementary volume for fluid flow.



where

p_w = fluid density (M/L^3)

q_x = specific discharge or volume of flow per cross-sectional area (L/T)

$dy dz$ = cross-sectional area (L^2)

The units of mass inflow are mass per unit time (M/T).*

The mass outflow rate will be different than the inflow rate and can be given as:

$$\text{Mass outflow rate parallel to } x \text{ axis} = \left[p_w q_x + \frac{\partial(p_w q_x) dx}{\partial x} \right] dy dz \quad (1.18)$$

The net mass accumulation within the control volume due to the flow component parallel to the x axis is the mass inflow minus the mass outflow, or

$$\frac{-\partial(p_w q_x) dx dy dz}{\partial x}$$

Similar terms exist for the net mass accumulation due to flow components parallel to the y and z axes:

$$\frac{-\partial(p_w q_y) dy dx dz}{\partial y}$$

$$\frac{-\partial(p_w q_z) dz dx dy}{\partial z}$$

These three terms can be summed to find the total net mass accumulation within the control volume.

$$-\left[\left(\frac{\partial}{\partial x}(p_w q_x) + \frac{\partial}{\partial y}(p_w q_y) + \frac{\partial}{\partial z}(p_w q_z) \right) \right] dx dy dz \quad (1.19)$$

The mass of water in the REV, M , is the density of water, p_w , times the porosity, n , times the volume, $dx dy dz$. The change in mass with respect to time is

$$\frac{\partial M}{\partial t} = \frac{\partial}{\partial t}(p_w n dx dy dz) \quad (1.20)$$

From the law of conservation of mass, Equation 1.19 must equal Equation 1.20.

$$-\left[\frac{\partial}{\partial x}(p_w q_x) + \frac{\partial}{\partial y}(p_w q_y) + \frac{\partial}{\partial z}(p_w q_z) \right] dx dy dz = \frac{\partial}{\partial t}(p_w n) dx dy dz \quad (1.21)$$

* The units of a variable can be expressed in terms of their fundamental dimensions. These are length, L, mass, M, and time, T. The fundamental dimensions for density are mass per unit volume. Volume is length cubed, so the shorthand expression for the fundamental dimensions of density is M/L^3 . Specific discharge has the dimensions of velocity, so the fundamental dimensions are L/T , and area has fundamental dimensions of L^2 .

We can assume that although density of the fluid may change with time, at any given time it will be the same everywhere in the REV. Under this assumption Equation 1.21 can be simplified to

$$-\left[\frac{\partial q_x}{\partial x} + \frac{\partial q_y}{\partial y} + \frac{\partial q_z}{\partial z} \right] = \frac{1}{p_w} \frac{\partial}{\partial t} (p_w n) \quad (1.22)$$

We may substitute Darcy's law for the specific discharge components given on the left side. If the xyz coordinate system is aligned with the principal axes of anisotropy, then Equation 1.12 may be used, and the left side of Equation 1.22 becomes

$$\frac{\partial}{\partial x} \left(K_{xx} \frac{\partial h}{\partial x} \right) + \frac{\partial}{\partial y} \left(K_{yy} \frac{\partial h}{\partial y} \right) + \frac{\partial}{\partial z} \left(K_{zz} \frac{\partial h}{\partial z} \right) \quad (1.23)$$

The change in mass within the REV is due to changes in the porosity and the density of water as the head changes with time. Thus the change in the volume of water in storage is proportional to the change in head with time. The right side of Equation 1.22 can be expressed as a proportionality constant, S_s , the specific storage, times the change in head with time.

$$\frac{1}{p_w} \frac{\partial}{\partial t} (p_w n) = S_s \frac{\partial h}{\partial t} \quad (1.24)$$

Combining Equations 1.22, 1.23, and 1.24 we obtain the main equation for transient flow in an anisotropic medium when the coordinate system is oriented along the principal axes of anisotropy:

$$\frac{\partial}{\partial x} \left(K_{xx} \frac{\partial h}{\partial x} \right) + \frac{\partial}{\partial y} \left(K_{yy} \frac{\partial h}{\partial y} \right) + \frac{\partial}{\partial z} \left(K_{zz} \frac{\partial h}{\partial z} \right) = S_s \frac{\partial h}{\partial t} \quad (1.25)$$

1.8.5 Mathematical Notation

In del and tensor notation Equation 1.25 becomes

$$\nabla \cdot K \cdot \nabla h = S_s \frac{\partial h}{\partial t} \quad (1.26)$$

Another form of expression is called Einstein's summation notation. For example, Darcy's law in the familiar, one-dimensional form is

$$q = -K \frac{dh}{dl} \quad (1.27)$$

It is implied in the preceding equation that the specific discharge is parallel to the direction of dh/dl and that the medium is isotropic. In a more general form, specific discharge, \mathbf{q} , is a vector with components q_1 , q_2 , and q_3 . Grad h is a vector that we will call \mathbf{h} . This vector also has components h_1 , h_2 , and h_3 . Hydraulic conductivity, \mathbf{K} , is a

tensor with nine components. To describe Darcy's law in the most general form, we need three equations.

$$q_1 = K_{11}h_1 + K_{12}h_2 + K_{13}h_3 \quad (1.28a)$$

$$q_2 = K_{21}h_1 + K_{22}h_2 + K_{23}h_3 \quad (1.28b)$$

$$q_3 = K_{31}h_1 + K_{32}h_2 + K_{33}h_3 \quad (1.28c)$$

The inner product can be expressed in index notation as

$$q_i = \sum_j K_{ij}h_i \quad (i, j = 1, 2, 3) \quad (1.29)$$

In Einstein's summation notation, the Σ is dropped with the understanding that the summation is over the repeated indices:

$$q_i = K_{ij}h_j \quad (i, j = 1, 2, 3) \quad (1.30)$$

In vector notation this can be expressed as either

$$\mathbf{q} = \mathbf{K} \cdot \nabla h \quad (1.31)$$

$$\mathbf{q} = \mathbf{K} \cdot \mathbf{h} \quad (1.32)$$

In del notation this is

$$\mathbf{q} = \mathbf{K} \cdot \nabla h \quad (1.33)$$

In general, we will use the standard form of differential equations rather than any of the shorthand notation. However, the literature cited in this text often uses the compact forms and the reader should be aware of them.

References

- Agency for Toxic Substances and Disease Registry (ATSDR). 2015) Priority List of Hazardous Substances. Available from https://www.atsdr.cdc.gov/spl/#modalIdString_myTable2015
- Alavanja, M. C. R. 2009. Pesticides use and exposure extensive worldwide. *Reviews on Environmental Health* 24:303–309.
- American Cancer Society. 2015. Cancer Facts & Figures 2014. Accessed August 21, 2015 from <http://water.epa.gov/drink/contaminants/index.cfm#List>
- American Water Resources Association. 1975. Status of water borne diseases in the U.S. and Canada. *Journal of American Water Works Association* 67:95–98.
- Ames, B. N., L. S. Gold, and W. C. Willett. 1995. The causes and prevention of cancer. *Proceedings of the National Academy of Science* 92:5258–5265.

- Ames, B. N., R. Magaw, and L. S. Gold. 1987. Ranking possible carcinogenic hazards. *Science* 236:271–277.
- Barnes, K. K., D. W. Kolpin, M. J. Focazio, E. T. Furlong, M. T. Meyer, S. D. Zaugg, S. K. Haack, L. B. Barber, and E. M. Thurman. 2008. *Water-quality data for pharmaceuticals and other organic wastewater contaminants in ground water and in untreated drinking water sources in the United States, 2000-01*. Available from <https://pubs.usgs.gov/of/2008/1293/pdf/OFR2008-1293.pdf>
- Bouwer, H. 1978. *Groundwater Hydrology*. New York: McGraw-Hill Book Company, pp. 423–424.
- Burmaster, D. R., and R. H. Harris. 1982. Groundwater contamination, an emerging threat. *Technology Review* 85:50–62.
- Chemspider. 2015. Benzyl Butyl Ether. Royal Society of Chemistry. <http://www.chemspider.com/Chemical-Structure.55081.html>, Accessed August 3, 2015.
- Darcy, H. 1856. *Les fontaines publiques de la ville de Dijon*. Paris: Victor Dalmont, 647 pp.
- De, A., R. Bose, A. Kumar, and S. Mozumdar. 2014. Targeted delivery of pesticides using biodegradable polymeric nanoparticles. *SpringerBriefs in Molecular Science*, DOI: 10.1007/978-81-322-1689-6_2.
- Döll, P., H. Hoffmann-Dobrev, F. T. Portmann, S. Siebert, A. Eicker, M. Rodell, G. Strassberg, and B. R. Scanlon. 2012. Impact of water withdrawals from groundwater and surface water on continental water storage variations. *Journal of Geodynamics* 59–60:143–156.
- Eckhardt, D. A., and E. T. Oaksford. 1988. “Relation of land use to groundwater quality in the upper glacial aquifer, Long Island, New York.” In *National Water Summary 1986—Hydrologic Events and Groundwater Quality*, eds. D. W. Moody, J. E. Carr, E. B. Chase, and R. W. Paulson, 115–121. U.S. Geological Survey Water Supply Paper 2325.
- Ferguson, G. 2015. Deep Injection of Waste Water in the Western Canada Sedimentary Basin. *Groundwater* 53:187–194.
- Forlay, J., H. R. Shin, F. Bray, D. Forman, C. D. Mathers, and D. Parkin. 2010. GLOBOCAN 2008, Cancer Incidence and Mortality Worldwide. Accessed August 21, 2015 from <https://www.iarc.fr/en/media-centre/iarcnews/2010/globocan2008.php>
- Fetter, C. W. 1972. The concept of safe groundwater yield in coastal aquifers. *Water Resources Bulletin* 8:1173–1176.
- . 1994. *Applied Hydrogeology, Second Edition*. Englewood Cliffs, NJ: Prentice Hall, 691 p.
- Gleeson, T., Y. Wada, M. F. P. Bierkens, and L. P. H. van Beek. 2012. Water balance of global aquifers revealed by groundwater footprint. *Nature* 488:97–200.
- Gold, L. S., T. H. Stone, B. R. Stern, N. B. Manley, and B. N. Ames. 1992. Rodent carcinogens: Setting priorities. *Science* 258:261–265.
- Goldman, M. 1996. Cancer risk at low-level exposure. *Science* 271:1821–1822.
- Gordon, J. 1990. OMNI Engineers, personal communication.
- Hanmer, R. 1989. Environmental Protection Agency, Testimony in a hearing on the seriousness and extent of ground-water contamination before the Senate Subcommittee on Superfund, Ocean and Water Protection of the Committee of Environment and Public Works, August 1, 1989.
- Hess, K. M. 1988. “Sewage plume in a sand and gravel aquifer, Cape Cod, Massachusetts.” In *National Water Summary, 1986*, eds. D. W. Moody, J. E. Carr, E. B. Chase, and R. W. Paulson, 87–92. U.S. Geological Survey Water Supply Paper 2325.
- Hoffman, J. I. 1984. “Geochemistry of acid mine drainage on the aquifers of southeastern Wisconsin and regulatory implications.” In *Proceedings of the National Water Well Association Conference on the Impact of Mining on Groundwater*, 146–161. August 24–27, 1984, Denver, Colorado, National Water Well Association, Dublin, Ohio.
- Hoffman, J. I., and C. W. Fetter. 1978. Water softener salt: A major source of groundwater contamination. *Geological Society of America, Abstracts with Programs* 10:423.
- Howlader, N., A. M. Noone, M. Krapcho, J. Garshell, D. Miller, S. F. Altekruse, C. L. Kosary, M. Yu, J. Ruhl, Z. Tatalovich, A. Mariotto, D. R. Lewis, H. S. Chen, E. J. Feuer, and K. A. Cronin (eds). 2015. SEER Cancer Statistics Review, 1975–2011, National Cancer Institute, Bethesda, MD, based on November 2013 SEER data submission, posted to the SEER website, April 2014. Accessed August 21, 2015 from http://seer.cancer.gov/archive/csr/1975_2011/results_merged/topic_lifetime_risk_diagnosis.pdf
- Hughes, J. L. 1975. Evaluation of groundwater degradation resulting from waste disposal to alluvium near Barstow, California. U.S. Geological Survey Professional Paper 878. Available at <https://pubs.usgs.gov/pp/0878/report.pdf>

- Hult, M. F., and J. R. Stark. 1988. Coal-tar derivatives in the Prairie du Chien–Jordan Aquifer, St. Louis Park, Minnesota. In *National Water Summary, 1986*, eds. D. W. Moody, J. E. Carr, E. B. Chase, and R. W. Paulson, 87–92. U.S. Geological Survey Water Supply Paper 2325.
- Hynds, P. D., M. K. Thomas, and K. D. M. Pintar. 2014. Contamination of groundwater systems in the US and Canada by enteric pathogens, 1990–2013: A review and pooled-analysis. *PLOS ONE* 9:e93301.
- Konikow, L. F. (2011). Contribution of global groundwater depletion since 1900 to sea-level rise. *Geophysical Research Letters* 38:L17401.
- Konikow, L. F., and D. W. Thompson. 1984. Groundwater contamination and aquifer reclamation at the Rocky Mountain Arsenal, Colorado. In *Groundwater Contamination*, 93–103. Washington, DC: National Academy Press.
- Kreamer, D. K., L. E. Stevens, and J. D. Ledbetter. 2015. “Groundwater Dependent Ecosystems—Science, Challenges, and Policy Directions.” In *Groundwater, Hydrochemistry, Environmental Impacts and Management Impacts*, ed. S. M. Adelana, 205–230. Hauppauge, NY: Nova Science Publishers.
- Lapworth, D. J., N. Baran, M. E. Stuart, and R. S. Ward. 2012. Emerging organic contaminants in groundwater: A review of sources, fate and occurrence. *Environmental Pollution* 163:287–303.
- Luthy, R. G., D. A. Dzombak, C. R. Peters, S. B. Roy, A. Ramaswami, D. V. Nakles, and B. R. Nott. 1994. Remediating Tar-contaminated soils at manufactured gas plant sites. *Environmental Science and Technology* 28:266A–276A.
- Margat, J., and J. van der Gun. 2013. *Groundwater around the World*. Lieden, Netherlands: CRC Press/Balkema.
- Maupin, M. A., J. F. Kenny, S. S. Hutson, J. K. Lovelace, N. L. Barber, and K. S. Linsey. 2014. Estimated use of water in the United States in 2010: U.S. Geological Survey Circular 1405, 56 p.
- Miller, D. 1980. *Waste disposal effects on groundwater*. Berkley, CA: Premier Press, 512 pp.
- Nash, G. J. C. 1962. Discussion of a paper by E. C. Wood. *Proceedings of the Society of Water Treatment and Examination* 11:33.
- National Ground Water Association. 2015. Facts about Global Groundwater Usage. Accessed July 28, 2015 from <http://www.ngwa.org/Fundamentals/use/Documents/global-groundwater-use-fact-sheet.pdf>
- Office of Technology Assessment. 1984. *Protecting the Nation's Groundwater from Contamination*. Washington, DC: U.S. Congress.
- Peterson, N. M. 1983. 1983 survey of landfills. *Waste Age* (March 1983):37–40.
- Ravenscroft, P., H. Brammer, and K. Richards. 2009. *Arsenic Pollution: A Global Synthesis*. West Sussex, UK: Wiley-Blackwell.
- Reynolds, K. A., K. D. Mena, and C. P. Gerba. 2008. Risk of waterborne illness via drinking water in the United States. *Reviews of Environmental Contamination and Toxicology* 192:117–158.
- Siebert, S., J. Burke, J. M. Faures, K. Frenken, J. Hoogeveen, P. Döll, and F. T. Portman. 2010. Groundwater use for irrigation—A global inventory. *Hydrology and Earth Systems Science* 14:1863–1880.
- Solley, W. B., R. R. Pierce, and H. A. Perlman. 1993. *Estimated use of water in the United States in 1990*. U.S. Geological Survey Circular 1081, 76 pp.
- Spanggord, R. J., T.-W. Chou, and W. P., Mabey. 1979. *Studies of environmental fates of DIMP and DCPD*. Contract report by SRI International, Menlo Park, CA, for U.S. Army Medical Research and Development Command, Fort Detrick, Fredrick, Md.
- UNICEF. 2012. *Progress on Drinking Water and Sanitation, 2012 Update*. United Nations International Children’s Emergency Fund, World Health Organization, p. 10.
- U.S. Department of Energy. 1988. *Site characterization plan overview, Yucca Mountain Site, Nevada Research and Development Area*. Washington, DC: Office of Civilian Radioactive Waste Management, 164 pp.
- U.S. Environmental Protection Agency. 1983. “Surface Impoundment Assessment National Report.” Office of Drinking Water. Washington, DC: U.S. EPA.
- . 1990. *National Water Quality Inventory*. 1988 Report to Congress, EPA-440-4-90-003, 187 pp.
- . 2003. *Resource Conservation and Recovery Act (RCRA)—Orientation Manual* U.S. EPA Report EPA-530-R-02-016 (Washington, DC).
- . 2015. *Underground Storage Tanks (USTs)*. Available from <http://www2.epa.gov/ust>
- . 2016. *Table of Regulated Drinking Water Contaminants*. Available from <https://www.epa.gov/ground-water-and-drinking-water/table-regulated-drinking-water-contaminants>
- U.S. Nuclear Regulatory Commission. 1983. *Final environmental statement related to the decommissioning*

- of the Rare Earths Facility, West Chicago, Illinois. NUREG-0904.
- van der Leeden, F., F. L. Troise, and D. K. Todd. 1990. *The Water Encyclopedia*. Chelsea, MI: Lewis Publishers.
- Viscusi, W. K., and J. T. Hamilton. 1996. Cleaning up superfund. *The Public Interest* 124:52–60.
- Wada, Y., L. P. H. van Beek, C. M. van Kempen, J. W. T. M. Reckman, S. Vasak, and M. F. P. Bierkens. 2010. Global depletion of groundwater resources. *Geophysical Research Letters* 37:L20402.
- Wilson, R., and E. A. C. Crouch. 1987. Risk assessment and comparisons: An introduction. *Science* 236:267–270.
- Wollenhaupt, N. C., and R. E. Springman. 1990. Atrazine in groundwater: A current perspective. University of Wisconsin-Extension, Agricultural Bulletin G3525, 17 pp.
- Wright, A. G. 1995. Looking for a cleanup strategy at Rocky Mountain Arsenal. *Engineering News Record* 234:42.
- Zinc docking. 2015. ZINC01586770, Benzyl Butyl Ether. Available from <http://zinc.docking.org/substance/1586770>

Problems

- 1.1 Look up the home page for the U.S. Environmental Protection Agency (www.epa.gov). Find the page for the Superfund program and then the National Priority List of Superfund sites either within your home state, the state where you are attending college, or a state in the U.S. that you have read about and would like to learn more about. Find the three sites that are closest to your hometown or city of interest and print out the NPL summary page.
- 1.2 Use the home page for the U.S. Environmental Protection Agency to find the latest listing of drinking water standards, which are at 40 CFR part 141. (CFR stands for Code of Federal Regulations.)

Mass Transport in Saturated Media

■ 2.1 Introduction

In this chapter we will consider the transport of solutes dissolved in groundwater. This is known as **mass** or **solute transport**. The methods presented in this chapter are based on partial differential equations for dispersion that have been developed for homogeneous media (Ogata and Banks 1961; Ogata 1970; Bear 1972; Bear and Verruijt 1987). These equations are similar in form to the familiar partial differential equations for fluid flow. Since those pioneering developments, much work has been done on the theories of mass transport in response to the great interest in problems of groundwater contamination (e.g., Bedient et al. 1994; Zhang and Bennett 1997; Grathwohl 1998; Domenico and Schwartz 1998; Yoram 2003; Yeh et al. 2015; Essaid et al. 2015). One of the outcomes has been the development of what is essentially a new branch of subsurface hydrology, where the flow of fluid and solutes is treated by statistical models; these models can account for the role of varying hydraulic conductivity and other spatially variable hydraulic parameters that accompany aquifer heterogeneity.

Many of the contaminant transport and fate concepts discussed in this chapter were developed based on tracer tests conducted in the field and at the laboratory scale. While a discussion of how tracer tests should be conducted and how the data can be interpreted is beyond the scope of this book, there are ample references and textbooks devoted to this topic (e.g., Davis et al. 1980; U.S. EPA 1985; Payne et al. 2008; Leibundgut et al. 2009; Suthersan et al. 2014).

■ 2.2 Transport by Concentration Gradients

A solute in water will move from an area of greater concentration toward an area where it is less concentrated. This process is known as **molecular diffusion**, or **diffusion**. Diffusion will occur as long as a concentration gradient exists, even if the fluid is not moving. The mass of fluid diffusing is proportional to the concentration gradient, which can be expressed as **Fick's first law**; in one dimension, Fick's first law is

$$F = -D_d (dC / dx) \quad (2.1)$$

where

F = mass flux of solute (M/L^2T) per unit area per unit time

D_d = diffusion coefficient (L^2/T)

TABLE 2.1 Diffusion coefficients in water.

Cations		
H ⁺	9.31×10^{-9} m ² /sec	1.00×10^{-7} ft ² /sec
Na ⁺	1.33×10^{-9} m ² /sec	1.43×10^{-8} ft ² /sec
K ⁺	1.96×10^{-9} m ² /sec	2.11×10^{-8} ft ² /sec
Rb ⁺	2.06×10^{-9} m ² /sec	2.22×10^{-8} ft ² /sec
Cs ⁺	2.07×10^{-9} m ² /sec	2.23×10^{-8} ft ² /sec
Mg ²⁺	7.05×10^{-10} m ² /sec	7.59×10^{-9} ft ² /sec
Ca ²⁺	7.93×10^{-10} m ² /sec	8.54×10^{-9} ft ² /sec
Sr ²⁺	7.94×10^{-10} m ² /sec	8.55×10^{-9} ft ² /sec
Ba ²⁺	8.48×10^{-10} m ² /sec	9.13×10^{-9} ft ² /sec
Ra ²⁺	8.89×10^{-10} m ² /sec	9.57×10^{-9} ft ² /sec
Mn ²⁺	6.88×10^{-10} m ² /sec	7.41×10^{-9} ft ² /sec
Fe ²⁺	7.19×10^{-10} m ² /sec	7.74×10^{-9} ft ² /sec
Cr ³⁺	5.94×10^{-10} m ² /sec	6.39×10^{-9} ft ² /sec
Fe ³⁺	6.07×10^{-10} m ² /sec	6.53×10^{-9} ft ² /sec
Anions		
OH ⁻	5.27×10^{-9} m ² /sec	5.67×10^{-8} ft ² /sec
F ⁻	1.46×10^{-9} m ² /sec	1.57×10^{-8} ft ² /sec
Cl ⁻	2.03×10^{-9} m ² /sec	2.19×10^{-8} ft ² /sec
Br ⁻	2.01×10^{-9} m ² /sec	2.16×10^{-8} ft ² /sec
HS ⁻	1.73×10^{-9} m ² /sec	1.86×10^{-8} ft ² /sec
HCO ₃ ⁻	1.18×10^{-9} m ² /sec	1.27×10^{-8} ft ² /sec
SO ₄ ²⁻	1.07×10^{-9} m ² /sec	1.15×10^{-8} ft ² /sec
CO ₃ ²⁻	9.55×10^{-10} m ² /sec	1.03×10^{-8} ft ² /sec
Organic Compounds		
Tetrachloroethylene (PCE)*	7.5×10^{-10} m ² /sec	8.07×10^{-9} ft ² /sec
Trichloroethene (TCE)*	8.3×10^{-10} m ² /sec	8.93×10^{-9} ft ² /sec
1,1,1-Trichloroethane (TCA)*	8.0×10^{-10} m ² /sec	8.61×10^{-9} ft ² /sec
Benzene**	9.0×10^{-10} m ² /sec	9.69×10^{-9} ft ² /sec
Toluene**	8.0×10^{-10} m ² /sec	8.61×10^{-9} ft ² /sec
Ethylbenzene**	7.2×10^{-10} m ² /sec	7.75×10^{-9} ft ² /sec
1,4-Dioxane***	1.6×10^{-9} m ² /sec	1.72×10^{-8} ft ² /sec

Source: Y.-H. Li and S. Gregory, 1974. Diffusion of ions in sea water and in deep-sea sediments. *Geochemica et Cosmochimica Acta*, Vol. 38. © 1974, with the kind permission of Elsevier Science. *Cohen and Mercer, 1993;

U.S.EPA, 2015; *Mohr 2010. Diffusion coefficients of ions at 25°C; organic compounds are in pure water at 20°C.

$$C = \text{solute concentration (M/L}^3\text{)}$$

$$dC/dx = \text{concentration gradient (M/L}^3/\text{L)}$$

The negative sign indicates that the movement is from areas of greater concentration to those of lesser concentration. Values of D_d for ions and select organic compounds in water at 25°C can be found in Table 2-1. They do not vary much with concentration, but they are somewhat temperature-dependent, being about 50% less at 5°C (Robinson and Stokes 2002). The values of D_d are only applicable when studying diffusion in aqueous systems. For systems where the concentrations are changing with time, **Fick's second law** applies. In one dimension this is

$$\partial C / \partial t = D_d \partial^2 C / \partial x^2 \quad (2.2)$$

where $\partial C / \partial t$ = change in concentration with time ($M/L^3/T$).

In porous media, diffusion cannot proceed as fast as it can in water because the ions must follow longer pathways as they travel around mineral grains. To account for this, an effective diffusion coefficient, D^* , must be used.

$$D^* = \omega D_d \quad (2.3)$$

where ω is a coefficient that is related to the tortuosity (Bear 1972). **Tortuosity** is a measure of the effect of the shape of the flowpath followed by water molecules in a porous media. If L is the straight-line distance between the ends of a tortuous flowpath of length L_e , the tortuosity, T , can be defined as $T = L_e/L$. Tortuosity in a porous media is always greater than 1, because the flowpaths that water molecules take must diverge around solid particles. Flowpaths across a representative sample of a well-sorted sediment would tend to be shorter than those across a poorly sorted sediment in which the smaller grains were filling the voids between the larger grains. Thus the well-sorted sediment would tend to have a lower value for tortuosity than the poorly sorted sediment. (Tortuosity has also been defined as $(L/L_e)^2$ (Carman 1997; Bear 1972). With this definition, tortuosity always has a value less than 1. This definition will not be used in this text.)

The value of ω , which is always less than 1, can be found from diffusion experiments in which a solute is allowed to diffuse across a volume of a porous medium. Perkins and Johnson (1963) found that ω was equal to 0.7 for sand column studies using a uniform sand. For laboratory studies using limestone and sandstone cores, Boving and Grathwohl (2001) found that ω ranges from 0.35 to 0.098 and that ω is related to the porosity, n , of these rocks by:

$$\omega = n^{-1.2}$$

Diffusion will cause a solute to spread away from the place where it is introduced into a porous medium, even in the absence of groundwater advective flow. Figure 2.1 shows the distribution of a solute introduced at concentration C_0 , at time t_0 , over an interval $(x - a)$ to $(x + a)$. At succeeding times t_1 and t_2 , the solute has spread out, resulting in a lower concentration over the interval $(x - a)$ to $(x + a)$ but increasing concentrations outside of this interval.

The solute concentration follows a normal, or Gaussian, distribution and can be described by two statistical properties, the mean, C and variance, σ_c^2 , which are defined in Section 2.12.2.

The effective diffusion coefficient, D^* , can be defined as (De Josselin and De Jong 1958)

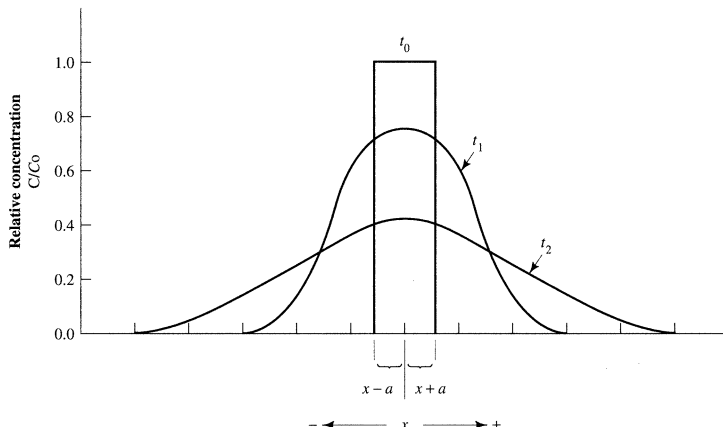
$$D^* = \frac{\sigma_c^2}{2t} \quad (2.4)$$

This is an alternative definition of effective diffusion coefficient to the one given in Equation 2.3.

The process of diffusion is complicated by the fact that the ions must maintain electrical neutrality as they diffuse. If we have a solution of NaCl, the Na^+ cannot diffuse faster than the Cl^- unless there is some other negative ion in the region into which

the Na^+ is diffusing. If the solute is adsorbed onto the mineral surfaces of the porous medium, the net rate of diffusion will be obviously less than for a nonadsorbed species.

Figure 2.1 Spreading of a solute slug with time due to diffusion. A slug of solute was injected into the aquifer at time t_0 with a resulting initial concentration of C_0 .



Diffusion can occur when the concentration of a chemical species is greater in one stratum than in an adjacent stratum. For example, solid waste containing a high concentration of chloride ion may be placed directly on the clay liner of a landfill. The concentration of chloride in the leachate contained in the solid waste is so much greater than the concentration of chloride in the pore water of the clay liner that the latter may be considered to be zero as a simplifying assumption in determining a conservative estimate of the maximum diffusion rate. If the solid waste and the clay are both saturated, the chloride ion will diffuse from the solid waste, where its concentration is greater, into the clay liner, even if there is no fluid flow. The concentration of chloride in the solid waste, C_0 , will be assumed to be a constant with time, as it can be replaced by dissolution of additional chloride. The concentration of chloride in the clay liner, $C_i(x, t)$, at some distance x from the solid waste interface and sometime t after the waste was placed, can be determined from Equation 2.5 (Crank 1956). This is a solution to Equation 2.2 for the appropriate boundary and initial conditions.

$$C_i(x, t) = C_0 \operatorname{erfc} \frac{x}{2(D^* t)^{0.5}} \quad (2.5)$$

where

C_i = the concentration at distance x from the source at time t since diffusion began

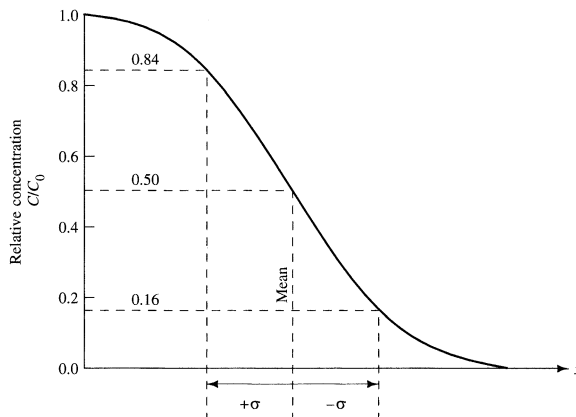
C_0 = the original concentration, which remains a constant

erfc = the complementary error function (Appendix A)

The complementary error function, erfc , is a mathematical function that is related to the normal, or Gaussian, distribution. This means that the solution described by Equation 2.5 is normally distributed, as is expected for a diffusional process. Figure 2.2

shows the profile of relative concentration for a solute diffusing from a region where the concentration is C_0 to a region where it was initially zero. Because the profile is normally distributed, 84% of the values will be less than the value that is one standard deviation more than the mean and 16% of the values will be less than the value that is one standard deviation less than the mean. The standard deviation is the square root of the variance.

Figure 2.2 The profile of a diffusing front as predicted by the complementary error function.



The complementary error function is tabulated in Appendix A or it can be calculated in the spreadsheet program Excel using the syntax: ERFC(x). It is related to the error function, erf, by

$$\text{erfc}(B) = 1 - \text{erf}(B)$$

The value of $\text{erfc}(B)$ is 0 for all positive values of B greater than 3.0 and 1.0 for a B of 0. For some applications it may be necessary to find erfc of a negative number. Appendix A does not give values for $\text{erfc}(B)$ for negative values of B . These must be computed from the relationship

$$\text{erfc}(-B) = 1 + \text{erf } B$$

The error function, $\text{erf}(B)$ is defined as:

$$\text{erf}(B) = \frac{2}{\sqrt{\pi}} \int_0^B e^{-t^2} dt$$

The above equation cannot be solved analytically. However, it is tabulated in Appendix A. It can also be approximated by the analytical expression:

$$\text{erf}(B) = \sqrt{1 - \exp\left(\frac{-4B^2}{\pi}\right)}$$

Thus values of $\text{erfc}(B)$ range from 0 to +2, since the maximum value of $\text{erf}(B)$ is 1.0 for 3.0 and all greater numbers.

EXAMPLE PROBLEM

Assume a D of 1×10^{-9} m 2 /sec and an ω of 0.5, to give a D^* of 5×10^{-10} m 2 /sec. Find the value of the concentration ratio, C_i/C_0 , at a distance of 5m after 100 yr of diffusion.

1. Convert 100 yr to seconds:

$$100 \text{ yr} \times 365 \text{ da/yr} \times 1440 \text{ min/da} \times 60 \text{ sec/min} = 3.15 \times 10^9 \text{ sec}$$

2. Insert values into Equation 2.5:

$$\frac{C_i}{C_0} = \operatorname{erfc} \frac{5}{2(5 \times 10^{-10} \text{ m}^2/\text{sec} \times 3.15 \times 10^9 \text{ sec})^{0.5}}$$

3. Solve:

$$\frac{C_i}{C_0} = \operatorname{erfc} \left(\frac{5}{2.51} \right) = \operatorname{erfc} 1.99 = 0.005$$

In 100 yr, diffusion over a 5-m distance would yield a concentration that is 0.5% of the original.

From the preceding example problem it is obvious that diffusion is not a particularly rapid means of transporting dissolved solutes. Diffusion is the predominant mechanism of transport only in low-permeability hydrogeologic regimes. However, it is possible for solutes to move through a porous or a fractured medium by diffusion even if the groundwater is not flowing.

■ 2.3 Transport by Advection

Dissolved solids are carried along with the flowing groundwater. This process is called **advective transport**, or **advection**. The amount of solute that is being transported is a function of its concentration in the groundwater and the quantity of the groundwater flowing. For one-dimensional flow normal to a unit cross-sectional area of the porous media, the quantity of water flowing is equal to the *average linear velocity* times *the effective porosity*. **Average linear velocity**, v_x , is the rate at which the flux of water across the unit cross-sectional area of pore space occurs. It is not the average rate at which the water molecules are moving along individual flowpaths, which is greater than the average linear velocity due to tortuosity. The **effective porosity**, n_e , is the porosity through which flow can occur. Noninterconnected and dead-end pores are not included in the effective porosity, so that $n_e < n$.

$$v_x = \frac{K}{n_e} \frac{dh}{dl} \quad (2.6)$$

where

v_x = average linear velocity (L/T)

K = hydraulic conductivity (L/T)

$$\begin{aligned} n_e &= \text{effective porosity} \\ dh/dl &= \text{hydraulic gradient (L/L)} \end{aligned}$$

Note that the abbreviation n is used in the context of flow and transport under saturated conditions. When discussing unsaturated flow, θ is preferred because it refers to the water content of the porous matrix, as defined in Chapter 4. When the matrix is fully saturated n equals θ . The one-dimensional mass flux, F_x , due to advection is equal to the quantity of water flowing times the concentration of dissolved solids and is given by Equation 2.7:

$$F_x = v_x n_e C \quad (2.7)$$

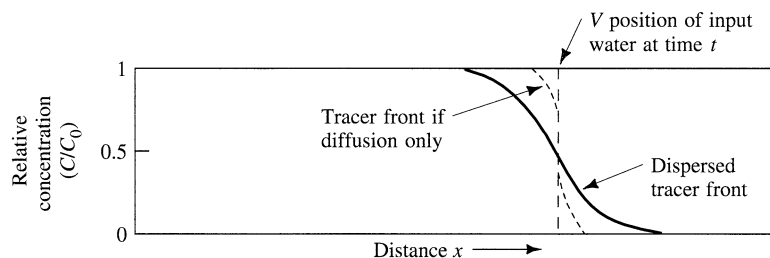
The one-dimensional advective transport equation is

$$\frac{\partial C}{\partial t} = -v_x \frac{\partial C}{\partial x} \quad (2.8)$$

(The derivation of this equation is given in Section 2.6.)

Solution of the advective transport equation yields a sharp concentration front. On the advancing side of the front, the concentration is equal to that of the invading groundwater, whereas on the other side of the front it is unchanged from the background value. This is known as **plug flow**, with all the pore fluid being replaced by the invading solute front. The sharp interface that results from plug flow is shown in Figure 2.3. The vertical dashed line at V represents an advancing solute front due to advection alone.

Figure 2.3 Advective transport and the influence of longitudinal dispersion and diffusion on the transport of a solute in one-dimensional flow.



Source: C.W. Fetter. 1994. *Applied Hydrogeology*, 3rd ed. Upper Saddle River, New Jersey: Prentice-Hall, Inc.

Due to the heterogeneity of geologic materials, advective transport in different strata can result in solute fronts spreading at different rates in each stratum. If one obtains a sample of water for purposes of monitoring the spread of a dissolved contaminant from a borehole that penetrates several strata, the water sample will be a composite of the water from each stratum. Due to the fact that advection will transport solutes at different rates in each stratum, the composite sample may be a mixture of water containing the transported solute coming from one stratum and uncontaminated groundwater coming

from a different stratum where the average linear velocity is lower. The concentration of the contaminant in the composite sample would thus be less than in the source.

EXAMPLE PROBLEM

Dissolved nitrate in a concentration of 18.0 mg/L is being advected with flowing groundwater at a velocity of 0.331 m/day in an aquifer with a porosity of 0.225. Groundwater from the aquifer discharges into a stream. What is the mass flux of nitrate into the stream if the aquifer is 1.80 m thick and 123 m wide where it discharges into the stream?

From Equation 2.7 the one dimensional mass flux is

$$F_x = v_x n_e C$$

$$\text{Given: } v_x = 0.331 \text{ m/da}$$

$$n_e = 0.225$$

$$C = 18.0 \text{ mg/L}$$

For consistent units the concentration should be in gm/m³.

$$C = 18.0 \text{ mg/L} \times 1/1000 \text{ gm/mg} \times 1000 \text{ L/m}^3$$

$$C = 18.0 \text{ gm/m}^3$$

The one dimensional mass flux is:

$$F_x = 0.331 \text{ m/da} \times 0.225 \times 18.0 \text{ gm/m}^3$$

$$F_x = 1.34 \text{ gm/da-m}^2$$

The flux into the stream is the one dimensional mass flux times the cross sectional area where the aquifer discharges into the stream.

$$\text{Total flux} = 1.34 \text{ gm/da-m}^2 \times 123 \text{ m} \times 1.80 \text{ m}$$

$$\text{Total flux} = 297 \text{ gm/da}$$

■ 2.4 Mechanical Dispersion

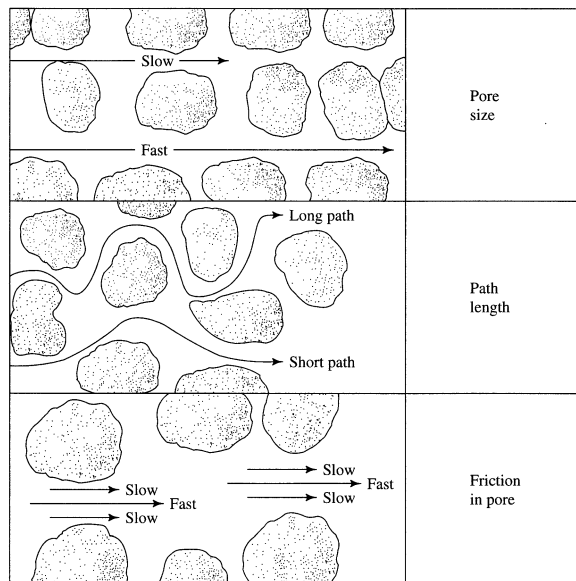
Groundwater is moving at rates that are both greater and less than the average linear velocity. At the macroscopic scale—that is, over a domain including a sufficient volume that the effects of individual pores are averaged (Bear 1972)—there are three basic causes of this phenomenon: (1) As fluid moves through the pores, it will move faster in the center of the pores than along the edges. (2) Some of the fluid particles will travel along longer flow paths in the porous media than other particles to go the same linear distance. (3) Some pores are larger than others, which allows the fluid flowing through these pores to move faster. These factors are illustrated in Figure 2.4.

If all groundwater containing a solute were to travel at exactly the same rate, it would displace water that does not contain the solute and create an abrupt interface between the two waters. However, because the invading solute-containing water is not all traveling at the same velocity, mixing occurs along the flowpath. This mixing is called **mechanical dispersion**, and it results in a dilution of the solute at the advancing edge of flow. The mixing that occurs along the direction of the flowpath is called **longitudinal dispersion**.

An advancing solute front will also tend to spread in directions normal to the direction of flow because at the pore scale the flowpaths can diverge, as shown in Figure 2.5. The result of this is mixing in directions normal to the flow path called **transverse dispersion**.

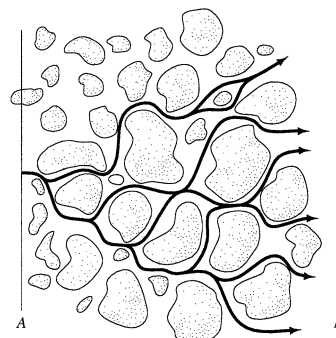
If we assume that mechanical dispersion can be described by Fick's law for diffusion (Equations 2.1 and 2.2) and that the amount of mechanical dispersion is a function of the average linear velocity, then we can introduce a coefficient of mechanical dispersion. This is equal to a property of the medium called *dynamic dispersivity*, or

FIGURE 2.4 Factors causing longitudinal dispersion at the scale of individual pores.



Source: C.W. Fetter. 1994. *Applied Hydrogeology*, 3d ed. Upper Saddle River, New Jersey: Prentice-Hall, Inc.

FIGURE 2.5 Flowpaths in a porous medium that cause lateral (transverse) hydrodynamic dispersion.



Source: C.W. Fetter. 1994. *Applied Hydrogeology*, Third Edition. Upper Saddle River, New Jersey: Prentice-Hall, Inc.

simply *dispersivity*, α , times the average linear velocity. If i is the principle direction of flow, the following definitions apply:

$$\text{Coefficient of longitudinal mechanical dispersion} = \alpha_i v_i \quad (2.9)$$

where

v_i = the average linear velocity in the i direction (L/T)

α_i = the dynamic dispersivity in the i direction (L)

and

$$\text{Coefficient of transverse mechanical dispersion} = \alpha_j v_i \quad (2.10)$$

where

v_i = the average linear velocity in the i direction (L/T)

α_j = the dynamic dispersivity in the j direction (L)

■ 2.5 Hydrodynamic Dispersion

The process of molecular diffusion cannot be separated from mechanical dispersion in flowing groundwater. The two are combined to define a parameter called the **hydrodynamic dispersion coefficient**, D . It is represented by the following formulas:

$$D_L = \alpha_L v_i + D^* \quad (2.11a)$$

$$D_T = \alpha_T v_i + D^* \quad (2.11b)$$

where

D_L = hydrodynamic dispersion coefficient parallel to the principal direction of flow (longitudinal)

D_T = hydrodynamic dispersion coefficient perpendicular to the principal direction of flow (transverse)

α_L = longitudinal dynamic dispersivity

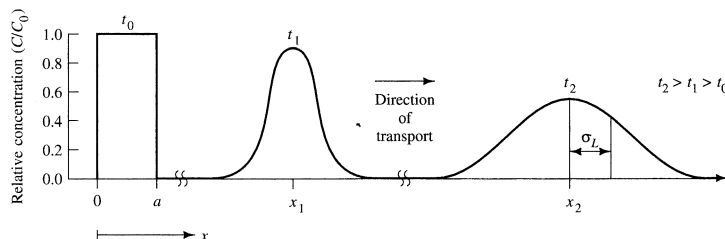
α_T = transverse dynamic dispersivity

Figure 2.3 shows the effect of diffusion and mechanical dispersion on the relative concentration (C/C_0) of a solute acting as a tracer that has been injected into a porous medium under one-dimensional flow conditions. The vertical line at V represents the advective transport without dispersion. Effects of diffusion and mechanical dispersion are shown.

The process of hydrodynamic dispersion can be illustrated by Figure 2.6. A mass of solute is instantaneously introduced into the aquifer at time t_0 over the interval $x = 0 + a$. The resulting initial concentration is C_0 . The advecting groundwater carries the mass of solute with it. In the process the solute slug spreads out, so that the maximum concentration decreases with time, as shown for times t_1 and t_2 . The diffusional model of hydrodynamic dispersion predicts that the concentration curves will have a Gaussian distribution that is described by the mean and the variance. With this distribution the coefficients of longitudinal and transverse hydrodynamic dispersion can be defined as

$$D_L = \frac{\sigma_L^2}{2t} \quad (2.12a)$$

FIGURE 2.6 Transport and spreading of a solute slug with time due to advection and dispersion. A slug of solute was injected at $x = 0 + a$ at time t_0 with a resulting concentration of C_0 . The groundwater flow is to the right.



$$D_T = \frac{\sigma_T^2}{2t} \quad (2.12b)$$

where

t = time

σ_T^2 = variance of the transverse spreading of the plume

σ_L^2 = variance of the longitudinal spreading of the plume

■ 2.6 Derivation of the Advection-Dispersion Equation for Solute Transport

This derivation of the advection-dispersion equation is based on work by Freeze and Cherry (1979), Bear (1972), and Ogata (1970). Working assumptions are that the porous medium is homogeneous, isotropic, and saturated with fluid and that flow conditions are such that Darcy's law is valid.

The derivation is based on the conservation of mass of solute flux into and out of a small representative elementary volume (REV) of the porous media. The REV is the smallest volume that is representative for the entirety of whole medium. A measurement made at the REV scale will yield a value typically of the whole (Hill 1963). The REV concept serves as a cornerstone in the continuum modeling of transport phenomena in porous media (Bachmat and Bear 1987). The flow is at a macroscopic scale, which means that it accounts for the differences in flow from pore to pore. A representative elementary volume is illustrated in Figure 1.6.

The average linear velocity, v , has components v_x , v_y , and v_z . The concentration of solute, C , is mass per unit volume of solution. Mass of solute per unit volume of aquifer is the product of the effective porosity, n_e , and C . Porosity is considered to be a constant because the aquifer is homogeneous.

The solute will be transported by advection and hydrodynamic dispersion. In the i direction the solute transport is given by

$$\text{Advection transport} = v_i n_e C dA \quad (2.13)$$

$$\text{Dispersive transport} = n_e D_i \frac{\partial C}{\partial i} dA \quad (2.14)$$

where dA is the cross-sectional area of the element and the i direction is normal to that cross-sectional face.

The total mass of solute per unit cross-sectional area transported in the i direction per unit time, F_i , is the sum of the advective and the dispersive transport and is given by

$$F_i = v_i n_e C - n_e D_i \frac{\partial C}{\partial i} \quad (2.15)$$

The negative sign indicates that the dispersive flux is from areas of greater to areas of lesser concentration.

The total amount of solute entering the representative elementary volume is

$$F_x dz dy + F_y dz dx + F_z dx dy$$

The total amount of solute leaving the representative elementary volume is

$$\left(F_x + \frac{\partial F_x}{\partial x} dx \right) dz dy + \left(F_y + \frac{\partial F_y}{\partial y} dy \right) dz dx + \left(F_z + \frac{\partial F_z}{\partial z} dz \right) dx dy$$

The difference between the mass of the solute entering the representative elementary volume and the amount leaving it is

$$-\left(\frac{\partial F_x}{\partial x} + \frac{\partial F_y}{\partial y} + \frac{\partial F_z}{\partial z} \right) dx dy dz$$

The rate of mass change in the representative elementary volume is

$$n_e \frac{\partial C}{\partial t} dx dy dz$$

By the law of mass conservation, the rate of mass change in the representative elementary volume must be equal to the difference in the mass of the solute entering and the mass leaving.

$$\frac{\partial F_x}{\partial x} + \frac{\partial F_y}{\partial y} + \frac{\partial F_z}{\partial z} = -n_e \frac{\partial C}{\partial t} \quad (2.16)$$

Equation 2.15 can be used to find the values of F_x , F_y , and F_z . These are substituted in Equation 2.16, which becomes, after cancellation of n_e from both sides,

$$\left[\frac{\partial}{\partial x} \left(D_x \frac{\partial C}{\partial x} \right) + \frac{\partial}{\partial y} \left(D_y \frac{\partial C}{\partial y} \right) + \frac{\partial}{\partial z} \left(D_z \frac{\partial C}{\partial z} \right) \right] \quad (2.17)$$

$$- \left[\frac{\partial}{\partial x} (v_x C) + \frac{\partial}{\partial y} (v_y C) + \frac{\partial}{\partial z} (v_z C) \right] = \frac{\partial C}{\partial t}$$

Equation 2.17 is the three-dimensional equation of mass transport for a *conservative* solute—that is, one that does not interact with the porous media or undergo biological or radioactive decay.

In a homogeneous medium, D_x , D_y , and D_z do not vary in space. However, because the coefficient of hydrodynamic dispersion is a function of the flow direction, even in an isotropic, homogeneous medium, $D_x \neq D_y \neq D_z$. For those domains where the

average linear velocity, v_x , is uniform in space, Equation 2.17 for one-dimensional flow in a homogeneous, isotropic porous media is

$$D_L \frac{\partial^2 C}{\partial x^2} - v_x \frac{\partial C}{\partial x} = \frac{\partial C}{\partial t} \quad (2.18)$$

In a homogeneous medium with a uniform velocity field, Equation 2.17 for two-dimensional flow with the direction of flow parallel to the x axis is

$$D_L \frac{\partial^2 C}{\partial x^2} + D_T \frac{\partial^2 C}{\partial y^2} - v_x \frac{\partial C}{\partial x} = \frac{\partial C}{\partial t} \quad (2.19)$$

where

D_L = the longitudinal hydrodynamic dispersion (L^2/T)

D_T = the transverse hydrodynamic dispersion (L^2/T)

Equation 2.17 for radial flow from a well can be written in polar coordinates (Ogata 1970) as

$$\frac{\partial}{\partial r} \left(D \frac{\partial C}{\partial r} \right) + \frac{D}{r} \frac{\partial C}{\partial r} - u \frac{\partial C}{\partial r} = \frac{\partial C}{\partial t} \quad (2.20)$$

where

r = radial distance to the well

u = average pore velocity of injection, which is found from

$$u = \frac{Q}{2 \pi n_e R r^2}$$

where

Q = the rate of injection into the well

n_e = effective porosity

R = length of well screen or open bore hole

2.7 Diffusion versus Dispersion

In the previous section the mass transport equation was derived on the basis of hydrodynamic dispersion, which is the sum of mechanical dispersion and diffusion. It would have been possible to separate the hydrodynamic dispersion term into the two components and have separate terms in the equation for them. However, as a practical matter, under most conditions of groundwater flow, diffusion is insignificant and is neglected.

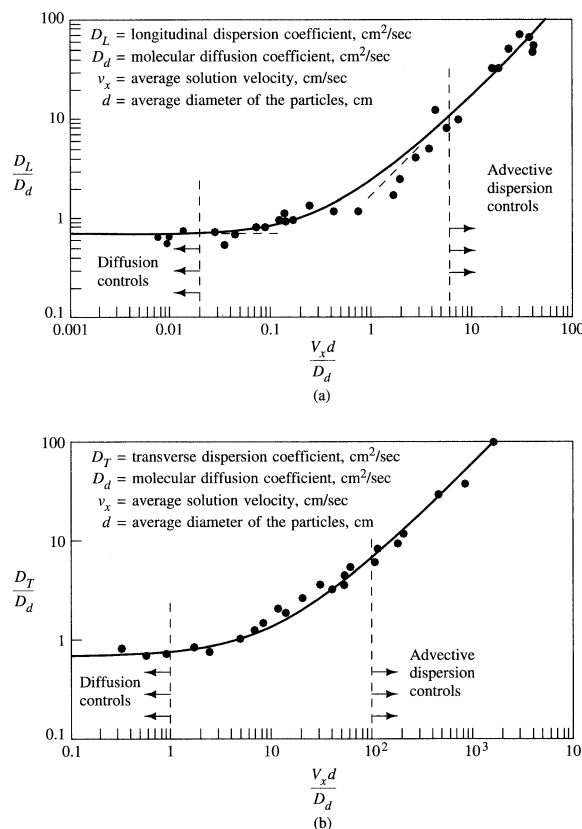
It is possible to evaluate the relative contribution of mechanical dispersion and diffusion to solute transport. A **Peclet number**, P_e , is a dimensionless number that can relate the effectiveness of mass transport by advection to the effectiveness of mass transport by either dispersion or diffusion. Peclet numbers have the general form of $v_x d / D_d$ or $v_x L / D_L$, where v_x is the advective velocity, d and L are characteristic flow lengths, D_d is the coefficient of molecular diffusion, and D_L is the longitudinal hydrodynamic dispersion coefficient. The column Peclet number, which defines the ratio of transport

by advection to the rate of transport by molecular diffusion in column studies, is a dimensionless parameter defined as $v_x d / D_d$, where d is the average grain diameter and D_d is the coefficient of molecular diffusion. A plot of the ratio of D_L / D_d versus the Peclet number is given in Figure 2.7a. Shown on this figure are the results of a number of experimental measurements using sand columns and tracers as well as some experimental curves from several investigators (Perkins and Johnson 1963). Delgado (2007) presents empirical correlations for the prediction of the dispersion coefficients (D_T and D_L) based Peclet number and Schmidt number (S_c). The dimensionless Schmidt number relates the viscous diffusion rate to the molecular diffusion rate. S_c is defined as:

$$S_c = \frac{\mu}{\rho D}$$

where μ and ρ are the dynamic viscosity (M/LT) and density of the fluid, respectively. D is the diffusion coefficient.

FIGURE 2.7 Graph of dimensionless dispersion coefficients versus Peclet number, $P_e = v_x d / D_d$: (a) D_L / D_d versus P_e and (b) D_T / D_d versus P_e .



Source: T. K. Perkins and O. C. Johnson. 1963. Society of Petroleum Engineers Journal 3:70–84. Society of Petroleum Engineers.

At zero flow velocity D_L is equal to D^* , since $D_L = a_L v_x + D^*$. In this manner the value of ω , the tortuosity factor, can be experimentally determined as $D^* = \omega D_d$. At very low velocities, the ratio of D_L/D_d is a constant with a value of about 0.7, which is the experimentally determined value of ω for uniform sand. This shows up on the left side of Figure 2.7(a) as a horizontal line. In this zone diffusion is the predominant force, and dispersion can be neglected. Between a Peclet number of about 0.4 to 6 there is a transition zone, where the effects of diffusion and longitudinal mechanical dispersion are more or less equal.

Figure 2.7(b) shows the plot of D_T/D_d as a function of Peclet number. Although the curve has the same shape as in (a), it occurs at Peclet numbers roughly 100 times greater. This means that diffusion has more control over transverse dispersion at higher Peclet numbers than it does for longitudinal dispersion. Higher Peclet numbers occur with higher velocities and/or longer flow paths. At higher Peclet numbers mechanical dispersion is the predominant cause of mixing of the contaminant plume (Perkins and Johnson 1963; Bear 1972; Bear and Verruijt 1987) and the effects of diffusion can be ignored. Under these conditions D_i can be replaced with $a_i v_i$ in the advection-dispersion equations.

■ 2.8 Moment Analysis

Contaminant hydrogeologists, like other scientists, have to work with a lot of data, such as periodic measurements of pollutant concentrations in monitoring wells or hydraulic values that determine the flow and transport of these pollutants. If writing a report or publishing data in peer reviewed manuscripts, one is expected to back up the significance of the data with a proper statistical analysis. A review of statistical concepts and methods is not the focus of this book, but excellent introductions into groundwater statistics are provided by Helsel and Hirsch (2002) or Interstate Technology and Regulatory Council (2013).

One statistical method, however, that is quite useful for the analysis of contaminant fate and transport data, especially results from laboratory or field-scale tracer tests, warrants a more detailed discussion. The method is known as moment analysis. This method can be an important tool for calculating mass recoveries in tracer experiments, travel velocities of a plume, and the description of the shape of the plume in terms of dispersivity, skewness, and kurtosis. Both temporal and spatial data can be used for this analysis. The relationship between the spatial and temporal moments and the properties of an evolving solute plume are based on work by Aris (1956) and subsequent modifications by Goltz and Roberts (1987), who developed moment concepts for the analysis of three-dimensional solute transport data. The spatial moment technique was utilized by Marle et al. (1967), Ghüven et al. (1984) and Valocchi (1989) to study solute transport in steady horizontal flow in a perfectly stratified aquifer. Valocchi (1990) provides an overview of the usefulness of temporal moment analysis for studying reactive solute transport in aggregated porous media.

The method of moment was employed for the analysis of many natural gradient field tracer tests. For instance, the spatial moments of the bromide tracer distribution were used to calculate the tracer mass, velocity, and dispersivity during the large-scale tracer test at the Canadian Air Force Base (CFB) in Borden, Ontario (Freyberg 1986; Farrell and Woodbury 1994) or the transport of nonreactive and reactive tracers in a sand and gravel aquifer on Cape Cod, Massachusetts (Leblanc et al. 1991; Garabedian et al. 1991) or at the Twin Lake aquifer test site within the property of the Chalk River

Nuclear Laboratories, where in 1982 and 1983 a pulse of groundwater labeled with ^{131}I odine was injected (Moltyaner and Killey 1988; Moltyaner and Wills 1991).

The analysis of moments ordinarily is accomplished by numerically solving one or more triple integrals of tracer concentration in the three-dimensional space of the test domain (Freyberg 1986; Glotz and Roberts 1987; Valochhi 1989; Garabedian et al. 1991). The absolute moments (M) in three dimensions are defined as follows:

$$M_{j k n} = \iiint_{-\infty}^{\infty} C x^j y^k z^n dx dy dz$$

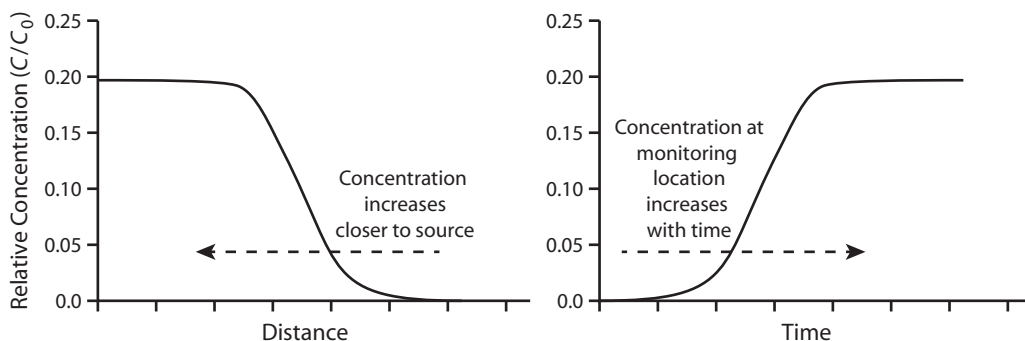
where C is the solute concentration at the spatial coordinates x , y , and z . For one-dimensional data sets, the moment analysis can be simplified to the temporal and spatial forms summarized in Table 2.2.

Temporal moments can be interpreted with the help of breakthrough curves (BTC) (Figure 2.8). A BTC is a graph of concentration versus time. This format of depiction is appropriate when the position of the observer is fixed (Eulerian approach). A BTC

TABLE 2.2 One-dimensional moments.

Moment	Temporal Moments	Spatial Moments
Zeroth Absolute Moment	$M_t^0 = \int_0^{\infty} C dt$	$M_s^0 = \int_0^{\infty} C dx$
First Normalized Moment	$M_t^1 = \frac{\int_0^{\infty} Ct dt}{\int_0^{\infty} C dt} = \frac{\int_0^{\infty} Ct dt}{M_t^0}$	$M_s^1 = \frac{\int_0^{\infty} Cx dx}{\int_0^{\infty} C dx} = \frac{\int_0^{\infty} Cx dx}{M_x^0}$
Adjusted First Temporal Moment	$M_{adj}^1 = \frac{\int_0^x Ct dt}{M_t^0} - \frac{1}{2} T_0$	Not defined
Second Central Moment	$M_t^2 = \frac{\int_0^{\infty} (t - M_t^1)^2 C dt}{M_t^0}$	$M_s^2 = \frac{\int_0^{\infty} (x - M_s^1)^2 C dx}{M_s^0}$
Third Central Moment	$M_t^3 = \frac{\int_0^{\infty} (t - M_t^1)^3 C dt}{M_t^0}$	$M_s^3 = \frac{\int_0^{\infty} (x - M_s^1)^3 C dx}{M_s^0}$
Fourth Central Moment	$M_t^4 = \frac{\int_0^{\infty} (t - M_t^1)^4 C dt}{M_t^0}$	$M_s^4 = \frac{\int_0^{\infty} (x - M_s^1)^4 C dx}{M_s^0}$

FIGURE 2.8 Representation of concentration data resulting from a continuous contaminant release scenario: (a) concentration versus distance and (b) concentration versus time. The concentration-time graph is called a breakthrough curve (BTC).



is typically used to report solute concentrations in column effluent during of tracer experiment or at the location of a specific monitoring well. In contrast, a graph of concentration versus distance is not a BTC. It represents a snapshot of concentration data collected more or less simultaneously at various locations within the test domain (Lagrangian approach). Such a graph is useful, for example, for reporting the tracer concentration in groundwater samples collected along the principal axis of a contaminant plume.

It is convenient to normalize the higher order temporal and spatial moments by scaling them to the zeroth temporal moment (M_t^0) or zeroth spatial moment (M_s^0), respectively. Higher moments are centralized by subtracting the first normalized temporal or spatial moment ($M_{t,s}^1$) from the elapsed time (t) or distance (x), respectively, since the start of the measurements.

The significance of M_t^0 is that it integrates the area under the concentration versus distance curve (Figure 2.8) and thus presents the mass of solute and a measure for calculating the solute mass recovery and mass balance. The M_s^0 aides in determining the amount of mass passing by a sampling point (i.e., monitoring well). A constant value of M_s^0 at different distances from the origin indicates that no mass loss occurred and therefore suggests a recalcitrance of a compound to sorption or degradation processes. The M_s^1 calculates the mean, i.e., the location of the center of mass of a plume and thus aides in calculating the plume travel velocity. M_t^1 describes the travel time of a dissolved compound (Figure 2.9). While not defined for spatial coordinate data, the adjusted first temporal moment, M_{adj}^1 , is:

$$M_{adj}^1 = \frac{\int_0^x C t \, dt}{M^0} - \frac{1}{2} T_0$$

where T_0 is the pulse length, i.e., the duration of the tracer slug injection. M_{adj}^1 permits the calculation of the tracer front travel time (Figure 2.11) and therefore M_{adj}^1 can be used to calculate the retardation factor from the inflection point of the BTC, i.e., where $C/C_{max} = 0.5$. The parameter C_{max} is the maximum concentration measured during the tracer test (Figure 2.9).

FIGURE 2.9 Ideal breakthrough curve (BTC). The arrival time is the time for the center of mass to arrive at the monitoring location. The travel time is the breakthrough time of the tracer front.

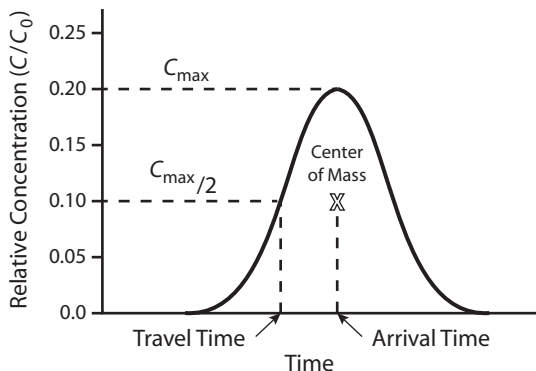
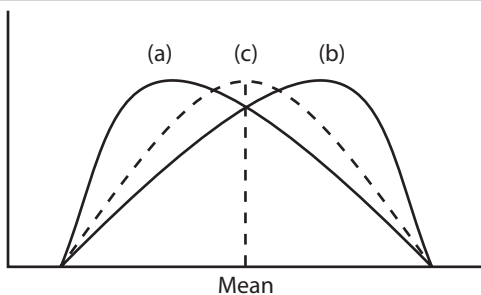


FIGURE 2.10 Skewness: (a) positive, (b) negative and (c) not skewed around the mean ($M^3 = 0$).



The second temporal moment (M_t^2) is the variance (σ^2) and provides a measure for the spread of a plume about the location of the center of mass. The analysis of the second spatial moment (M_s^2) can be used to determine the longitudinal dispersion coefficient, D_L , in either temporal or spatial coordinates:

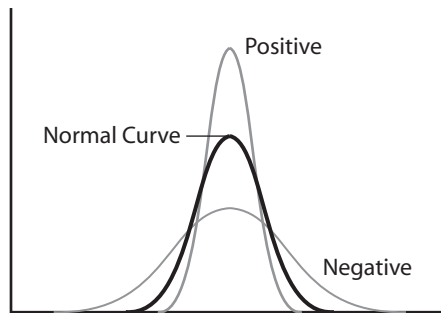
$$D_L = \frac{\sigma_L^2}{2t}$$

$$D_L = \frac{\sigma_L^2 v}{2x}$$

where σ_L^2 is the variance, t is time since the start of the tracer test and v is the linear flow velocity (constant).

The skewness of a curve is described by the third moment (M^3). A positive value indicates that the graph is skewed to the right, whereas a negative value means skewness to the left (Figure 2.10). A value of approximately zero suggests that the data is normally distributed. The fourth moment (M^4) is a measure of kurtosis (Figure 2.11). For a conservative tracer, both M^3 and M^4 should be approximately zero. Deviations

FIGURE 2.11 Negative and positive kurtosis. The M^4 is zero for when the tracer concentration data is normally distributed.



from that value indicate non-ideal transport conditions. Other applications of moment analysis are discussed in Suthersan et al. 2017.

EXAMPLE

A tracer test was conducted and concentration measurements have been collected downgradient from the injection location and at three different times ($t_1 = 30\text{ d}$, $t_2 = 60\text{ d}$, and $t_3 = 90\text{ d}$). Figure 2.12 shows the concentration versus distance data in terms of dimensionless concentration (C/C_0) at three observation points.

In this example, the tracer is nonreactive because the area under the curves (M^0) remains the same for all three data sets. Had the value of M^0 decreased however, it

FIGURE 2.12 The spatial position of the tracer concentrations profiles at times t_1 , t_2 , and t_3 .

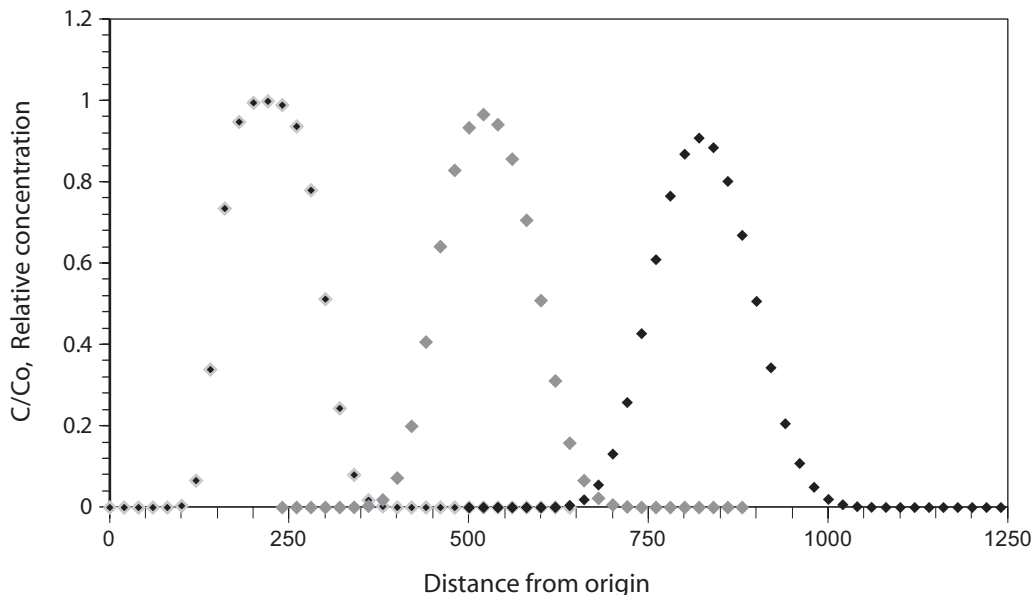
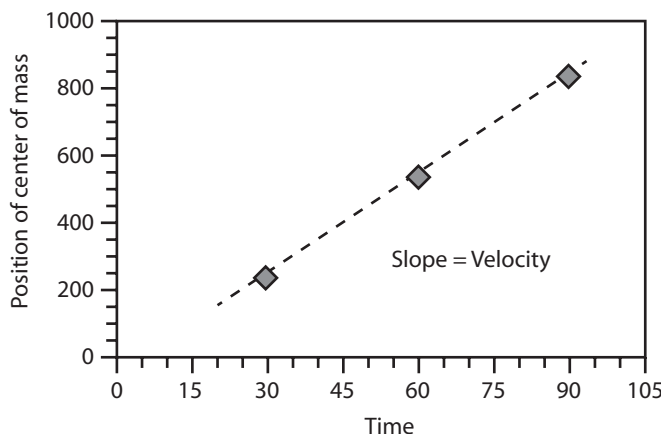


FIGURE 2.13 The velocity of a migrating plume can be estimated from the location of the center of mass (First spatial moment).



would have indicated that a fraction of the tracer was lost during the experiment. In that case, a plot of M^0 versus distance would reveal if the rate of loss is linear or nonlinear.

The velocity of a migrating plume was estimated from the location of the center of mass (M^1) at different times (Figure 2.12). In this example, the velocity remained constant throughout the experiment, which is expected for a nonreactive tracer. If the flow velocity is identical to the groundwater flow velocity, the tracer can be considered “conservative,” i.e., its flow is not retarded. By comparing the M^1 of a conservative tracer with that of other tracers that might have been co-injected at the start of the tracer test, one can calculate the relative travel times or relative travel distances and thus the retardation factors for each tracer.

When plotting M^2 for each of the three data sets against the time of measurement, the slope of the regression line is equal to $2D_L$. The M^3 and M^4 values indicate that the three data sets are not skewed and that they do not show kurtosis; once again indicating that the tracer was nonreactive.

■ 2.9 Analytical Solutions of the Advection-Dispersion Equation

2.9.1 Methods of Solution

The advection-dispersion equations can be solved by either numerical or analytical methods. Analytical methods involve the solution of the partial differential equations using calculus based on the initial and boundary value conditions. They are limited to simple geometry and in general require that the aquifer be homogeneous. A number of analytical solutions are presented in this chapter. They are useful in that they can be solved with spreadsheet, like EXCEL, or even a pencil and paper, if one is so inclined.

Numerical methods involve the solution of the partial differential equation by numerical methods of analysis. They are more powerful than analytical solutions in the sense that aquifers of any geometry can be analyzed and aquifer heterogeneities can be accommodated. However, there can be other problems with numerical models, such as numerical errors, which can cause solutions to show excess spreading of solute fronts or plumes that are not related to the dispersion of the tracer that is the subject of the modeling. Bear and Verruijt (1987) present a good introduction to the use of numerical models to solve mass transport equations. These solutions are normally found by methods of computer modeling, a topic beyond the scope of this text. Instead, the reader is referred to Bear and Cheng (2010), who offer an overview about the methodology and procedures for constructing conceptual and mathematical models for groundwater flow and the fate and transport of contaminants in both saturated and unsaturated zones. Also, Kuzmin (2010) provides a guide to numerical methods for solving transport equations with particular focus on finite element models.

2.9.2 Boundary and Initial Conditions

In order to obtain a unique solution to a differential equation it is necessary to specify the initial and the boundary conditions that apply. The **initial conditions** describe the values of the variable under consideration, in this case concentration, at some initial time equal to 0. The **boundary conditions** specify the interaction between the area under investigation and its external environment.

There are three types of boundary conditions for mass transport. The boundary condition of the first type is a **fixed concentration**. The boundary condition of the second type is a **fixed gradient**. A **variable flux** boundary constitutes the boundary condition of the third type.

Boundary and initial conditions are shown in a shorthand form. For one-dimensional flow we need to specify the conditions relative to the location, x , and the time, t . By convention this is shown in the form

$$C(x, t) = C(t)$$

where $C(t)$ is some known function.

For example, we can write

$$\begin{aligned} C(0, t) &= C_0, & t \geq 0 \\ C(x, 0) &= 0, & x \geq 0 \\ C(\infty, t) &= 0, & t \geq 0 \end{aligned}$$

The first statement says that for all time t equal to or greater than zero, at $x = 0$ the concentration is maintained at C_0 . This is a fixed-concentration boundary condition located at $x = 0$ (first-type boundary). The second statement is an initial condition that says at time $t = 0$, the concentration is zero everywhere within the flow domain, that is, where x is greater than or equal zero. As soon as flow starts, solute at a concentration of C_0 will cross the $x = 0$ boundary.

The third condition shows that the flow system is infinitely long and that no matter how large time gets, the concentration will still be zero at the end of the system (first-type boundary condition at $x = \infty$).

We could also have specified an initial condition that within the domain the initial solute concentration was C_i . This would be written as

$$C(x, 0) = C_i, \quad x \geq 0$$

Other examples of concentration (first-type) boundary conditions are exponential decay of the source term and pulse loading at a constant concentration for a period of time followed by another period of time with a different constant concentration.

Exponential decay for the source term can be expressed as

$$C(0, t) = C_0 e^{-it}$$

where i = a decay constant.

Pulse loading where the concentration is C_0 for times from 0 to t_0 and then is 0 for all time more than t_0 is expressed as

$$C(0, t) = C_0 \quad 0 < t \leq t_0$$

$$C(0, t) = 0 \quad t > t_0$$

Fixed-gradient boundaries are expressed as

$$\left. \frac{dC}{dx} \right|_{x=0} = f(t) \quad \text{or} \quad \left. \frac{dC}{dx} \right|_{x=\infty} = f(t)$$

where $f(t)$ is some known function. A common fixed-gradient condition is $dC/dx = 0$, or a no-gradient boundary.

The variable-flux boundary, a third type, is given as

$$-D \frac{\partial C}{\partial x} + v_x C = v_x C(t)$$

where $C(t)$ is a known concentration function. A common variable-flux boundary is a constant flux with a constant input concentration, expressed as

$$\left. \left(-D \frac{dC}{dx} + vC \right) \right|_{x=0} = C_0$$

2.9.3 One-Dimensional Step Change in Concentration (First-Type Boundary)

Sand column experiments have been used to evaluate both the coefficients of diffusion and dispersion at the laboratory scale. A tube is filled with sand and then saturated with water. Water is made to flow through the tube at a steady rate, creating, in effect, a permeameter. A solution containing a tracer is then introduced into the sand column in place of the water. The initial concentration of the solute in the column is zero, and the concentration of the tracer solution is C_0 . The tracer in the water exiting the tube is analyzed, and the ratio of C , the tracer concentration at time t , over C_0 , the injected tracer concentration, is plotted as a function of time. This is called a **fixedstep function**.

The boundary and initial conditions are given by

$$C(x, 0) = 0 \quad x \geq 0 \quad \text{Initial condition}$$

$$\left. \begin{array}{l} C(0, t) = C_0 \\ C(\infty, t) = 0 \end{array} \right\} \quad \begin{array}{l} t \geq 0 \\ t \geq 0 \end{array} \quad \text{Boundary conditions}$$

The solution to Equation 2.18 for these conditions is (Ogata and Banks 1961)

$$C = \frac{C_0}{2} \left[\operatorname{erfc} \left(\frac{L - v_x t}{2\sqrt{D_L t}} \right) + \exp \left(\frac{v_x L}{D_L} \right) \operatorname{erfc} \left(\frac{L + v_x t}{2\sqrt{D_L t}} \right) \right] \quad (2.21)$$

This equation may be expressed in dimensionless form as

$$C_R(t_R, P_e) = 0.5 \left\{ \operatorname{erfc} \left[\left(\frac{P_e}{4t_R} \right)^{1/2} \times (1 - t_R) \right] + \exp(P_e) \operatorname{erfc} \left[\left(\frac{P_e}{4t_R} \right)^{1/2} (1 + t_R) \right] \right\} \quad (2.22)$$

where

$$t_R = v_x t / L$$

$$C_R = C / C_0$$

P_e = Peclet number when flow distance, L , is chosen as the reference length ($P_e = v_x L / D_L$)

erfc = complementary error function

Equation 2.21 can be solved in Microsoft Excel after installing the *Plume1D()* add-in (Renshaw 2015a).

2.9.4 One-Dimensional Continuous Injection into a Flow Field (Second-Type Boundary)

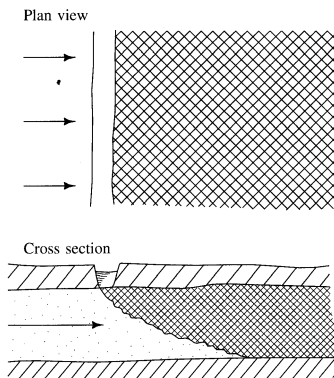
In nature there are not many situations where there would be a sudden change in the quality of the water entering an aquifer. A much more likely condition is that there would be leakage of contaminated water into the groundwater flowing in an aquifer. For the one-dimensional case, this might be a canal that is discharging contaminated water into an aquifer as a line source (Figure 2.14).

The rate of injection is considered to be constant, with the injected mass of the solute proportional to the duration of the injection. The initial concentration of the solute in the aquifer is zero, and the concentration of the solute being injected is C_0 . The solute is free to disperse both up-gradient and down-gradient.

The boundary and initial conditions are

$$C(x, 0) = 0 \quad -\infty < x < +\infty \quad \text{Initial condition}$$

$$\left. \begin{array}{l} \int_{-\infty}^{+\infty} n_e C(x, t) dx = C_0 n_e v_x t \\ C(\infty, t) = 0 \end{array} \right\} \quad \begin{array}{l} t > 0 \\ t \geq 0 \end{array} \quad \text{Boundary conditions}$$

FIGURE 2.14 Leakage from a canal as a line source for injection of a contaminant into an aquifer.

Source: J. P. Sauty. 1980. *Water Resources Research* 16:145–58. Copyright by the American Geophysical Union. Reproduced with permission.

The second boundary condition states that the injected mass of contaminant over the domain from $-\infty$ to $+\infty$ is proportional to the length of time of the injection.

The solution to this flow problem (Sauty 1980) is

$$C = \frac{C_0}{2} \left[\operatorname{erfc} \left(\frac{L - v_x t}{2\sqrt{D_L t}} \right) - \exp \left(\frac{v_x L}{D_L} \right) \operatorname{erfc} \left(\frac{L + v_x t}{2\sqrt{D_L t}} \right) \right] \quad (2.23)$$

In dimensionless form this is

$$C_R(t_R, P_e) = 0.5 \left\{ \operatorname{erfc} \left[\left(\frac{P_e}{4t_R} \right)^{1/2} (1 - t_R) \right] - \exp(P_e) \operatorname{erfc} \left[\left(\frac{P_e}{4t_R} \right)^{1/2} (1 + t_R) \right] \right\} \quad (2.24)$$

$$\left. -\exp(P_e) \operatorname{erfc} \left[\left(\frac{P_e}{4t_R} \right)^{1/2} (1 + t_R) \right] \right\}$$

It can be seen that Equations 2.21 and 2.23 are very similar, the only difference being that the second term is subtracted rather than added in 2.23.

Sauty (1980) gives an approximation for the one-dimensional dispersion equation as

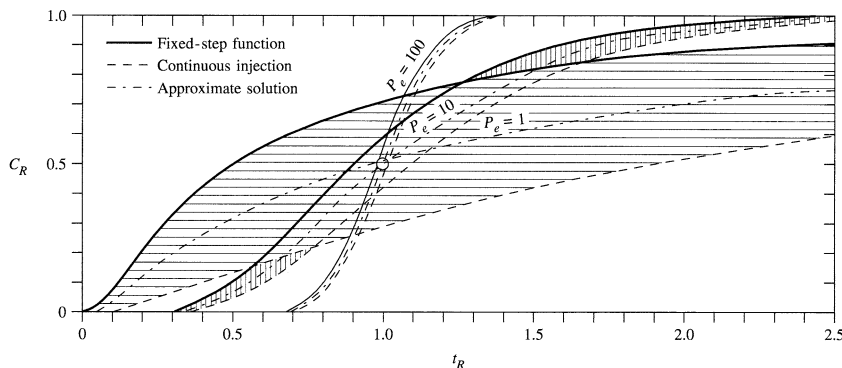
$$C = \frac{C_0}{2} \operatorname{erfc} \left(\frac{L - v_x t}{2\sqrt{D_L t}} \right) \quad (2.25)$$

In dimensionless form this is

$$C_R(t_R, P_e) = 0.5 \operatorname{erfc} \left[\left(\frac{P_e}{4t_R} \right)^{1/2} (1 - t_R) \right] \quad (2.26)$$

This approximation comes about because for large Peclet numbers, the second term of Equations 2.21 and 2.23 is much smaller than first term and can be neglected. Figure 2.15 demonstrates under what conditions this approximation is valid. In Figure 2.15 the dimensionless concentration, C_R , is plotted as a function of dimensionless time, t_R , for continuous tracer injection using the fixed-step function, Equation 2.22, the continuous-injection function, Equation 2.24, and the approximate solution, Equation 2.26. Curves are plotted for three Peclet numbers, 1, 10, and 100 (Section 2.7). The Peclet number defines the rate of transport by advection to the rate of transport by hydrodynamic dispersion. For Peclet number 1, the fixed-step function and the continuous-injection function give quite different results, whereas for Peclet number 100 they are almost identical. The approximate solution lies midway between the other two. This figure suggests that for Peclet numbers less than about 10, the exact solutions need to be considered, whereas for Peclet numbers greater than 10, the approximate solution is probably acceptable, especially as the Peclet number approaches 100. This Peclet number increases with flow-path length as advective transport becomes more dominant over dispersive transport. Thus for mass transport near the inlet boundary, it is important to use the correct equation, but as one goes away from the inlet boundary, it is less important that the correct form of the equation is employed.

FIGURE 2.15 Dimensionless-type curves for the continuous injection of a tracer into a one-dimensional flow field.



Source: J.P.Sauty, 1980. *Water Resources Research* 16:145–158. Copyright by the American Geophysical Union. Reproduced with permission.

EXAMPLE PROBLEM

Pickles are made in large wooden vats. At the Happy Gherkin Pickle Factory one of the vats has been leaking brine directly into the water table. The concentration of chloride in the brine is 1575 mg L^{-1} . The flow in the aquifer that receives the brine is essentially one-dimensional and has the following characteristics.

$$\text{Hydraulic conductivity} = 2.93 \times 10^{-4} \text{ ms}^{-1}$$

$$\text{Hydraulic gradient} = 0.00678$$

$$\text{Effective porosity} = 0.259$$

The estimated effective diffusion coefficient for chloride is $2 \times 10^{-9} \text{ m}^2\text{s}^{-1}$.

Calculate the concentration of chloride above any background value at a distance 125 m from the leaking vat 0.50 years after the leak began.

We will apply equation 2.25 to this problem. Note that this is an approximate solution as the second term of equation 2.23 has been dropped.

$$C = \frac{C_0}{2} \left[\operatorname{erfc} \left(\frac{L - v_x t}{2\sqrt{D_L t}} \right) \right]$$

1. Calculate v_x

$$v_x = \frac{K}{n_e} \frac{dh}{dl}$$

$$v_x = \frac{2.93 \times 10^{-4} \text{ ms}^{-1}}{0.259} \times 0.00678$$

$$v_x = 7.67 \times 10^{-6} \text{ ms}^{-1}$$

2. Find the value of the coefficient of longitudinal hydrodynamic dispersion, D_L . This can be found from equation 2.11a.

$$D_L = \alpha_L v_x + D^*$$

- a. The first step is to find the value of α_L . This can be estimated from equation 2.48, which will be introduced in a later section.

$$\alpha_L = 0.83(\log L)^{2.414}$$

$$\alpha_L = 0.83(\log 125)^{2.414} \text{ m}$$

$$\alpha_L = 4.96 \text{ m}$$

- b. The next step is to calculate D_L .

$$D_L = 4.96 \text{ m} \times 7.67 \times 10^{-6} \text{ ms}^{-1} + 2 \times 10^{-9} \text{ m}^2\text{s}^{-1}$$

$$D_L = 3.80 \times 10^{-5} \text{ m}^2\text{s}^{-1} + 2 \times 10^{-9} \text{ m}^2\text{s}^{-1}$$

The second term reflecting the effective diffusion coefficient can be neglected as it is so much smaller than the first term.

3. In order to have consistent units, the time must be expressed in seconds.

$$0.5 \text{ y} \times 365 \text{ d/y} \times 1440 \text{ min/d} \times 60 \text{ s/min} = 1.578 \times 10^7 \text{ s.}$$

4. The values of the variables are then substituted into Equation 2.25.

$$C_0 = 1575 \text{ mgL}^{-1}$$

$$v_x = 7.67 \times 10^{-6} \text{ ms}^{-1}$$

$$L = 125 \text{ m}$$

$$D_L = 3.80 \times 10^{-5} \text{ m}^2\text{s}^{-1}$$

$$t = 1.578 \times 10^7 \text{ s}$$

$$C = \frac{1575 \text{mgL}^{-1}}{2} \operatorname{erfc} \left(\frac{125\text{m} - (7.67 \times 10^{-6} \text{ms}^{-1} \times 1.578 \times 10^7 \text{s})}{2\sqrt{3.80 \times 10^{-5} \text{m}^2 \text{s}^{-1} \times 1.578 \times 10^7 \text{s}}} \right)$$

$$C = 787.5 \operatorname{erfc} \left(\frac{125\text{m} - 121.0\text{m}}{2\sqrt{5.99 \times 10^2 \text{m}^2}} \right) \text{mgL}^{-1}$$

$$C = 787.5 \operatorname{erfc} \left(\frac{4.0\text{m}}{2 \times 24.49\text{m}} \right) \text{mgL}^{-1}$$

$$C = 787.5 \operatorname{erfc}(0.0816) \text{ mg/L}$$

$$C = 787.5 \times 0.908 \text{mgL}^{-1} = 715 \text{mgL}^{-1}$$

2.9.5 Third-Type Boundary Condition

A solution for Equation 2.18 for the following boundary condition was given by van Genuchten (1981).

$$\begin{aligned} C(x, 0) &= 0 && \text{Initial condition} \\ \left. \left(-D \frac{\partial C}{\partial x} + \nu_x C \right) \right|_{x=0} &= \nu_x C_0 && \text{Boundary conditions} \\ \left. \frac{\partial C}{\partial x} \right|_{x \rightarrow \infty} &= (\text{finite}) \end{aligned}$$

The third condition specifies that as x approaches infinity, the concentration gradient will still be finite. Under these conditions the solution to Equation 2.18 is:

$$\begin{aligned} C &= \frac{C_0}{2} \left[\operatorname{erfc} \left(\frac{L - \nu_x t}{2\sqrt{D_L t}} \right) + \left(\frac{\nu_x^2 t}{\pi D_L} \right)^{1/2} \exp \left[-\frac{(L - \nu_x t)^2}{4D_L t} \right] \right. \\ &\quad \left. - \frac{1}{2} \left(1 + \frac{\nu_x L}{D_L} + \frac{\nu_x^2 t}{D_L} \right) \exp \left(\frac{\nu_x L}{D_L} \right) \operatorname{erfc} \left(\frac{L - \nu_x t}{2\sqrt{D_L t}} \right) \right] \end{aligned} \quad (2.27)$$

This equation also reduces to the approximate solution, Equation 2.25, as the flow length increases.

2.9.6 One-Dimensional Slug Injection into a Flow Field

If a slug of contamination is instantaneously injected into a uniform, one-dimensional flow field, it will pass through the aquifer as a pulse with a peak concentration, C_{\max} , at some time after injection, t_{\max} . The solution to Equation 2.18 under these conditions (Sauty 1980) is in dimensionless form:

$$C_R = (t_R, P_e) = \frac{E}{(t_R)^{1/2}} \exp \left(-\frac{P_e}{4t_R} (1 - t_R)^2 \right) \quad (2.28)$$

with

$$E = \left(t_{R\max} \right)^{1/2} \cdot \exp \left(-\frac{P_e}{4t_{R\max}} \left(1 - t_{R\max} \right)^2 \right) \quad (2.29)$$

where

$$t_{R\max} = (1 + P_e^{-2})^{1/2} - P_e^{-1} \text{ (dimensionless time at which peak concentration occurs)}$$

$$C_R = C/C_{\max}$$

In Figure 2.16, $C_R (C/C_{\max})$ for a slug injected into a uniform one-dimensional flow field is plotted against dimensionless time, t_R , for several Peclet numbers. It can be seen that the time for the peak concentration (C_{\max}) to occur increases with the Peclet number, up to a limit of $t_R = 1$. Breakthrough becomes more symmetric with increasing P_e .

2.9.7 Continuous Injection into a Uniform Two-Dimensional Flow Field

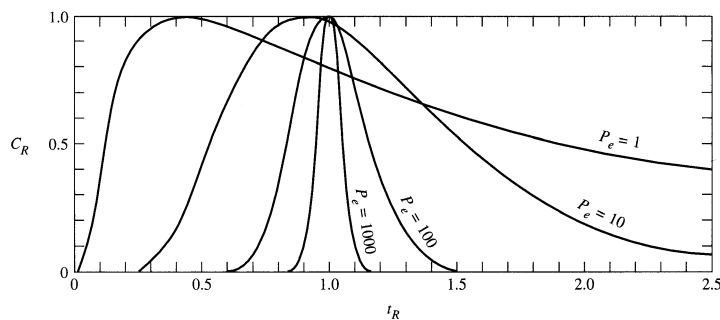
If a tracer is continuously injected into a uniform flow field from a single point that fully penetrates the aquifer, a two-dimensional plume will form that looks similar to Figure 2.16. It will spread along the axis of flow due to longitudinal dispersion and normal to the axis of flow due to transverse dispersion. This is the type of contamination that would spread from the use of an injection well, which would be a point source.

Flow is governed by Equation 2.19, the mass transport equation in two dimensions. The well is located at the origin ($x = 0, y = 0$), and there is a uniform flow velocity at a rate v_x parallel to the x axis. There is a continuous injection at the origin, of a solute with a concentration C_0 at a rate Q over the aquifer thickness, b .

The solution of Equation 2.19 can be found from a Green function (Bear 1972; Fried 1975) for the injection of a unit amount of a contaminant as:

$$C(x, y, t) = \frac{1}{4\pi t(D_L D_T)^{0.5}} \exp \left[-\frac{(x - v_x t)^2}{4D_L t} - \frac{y^2}{4D_T t} \right]$$

FIGURE 2.16 Dimensionless-type curve for the injection of a slug of a tracer into a one-dimensional flow field.



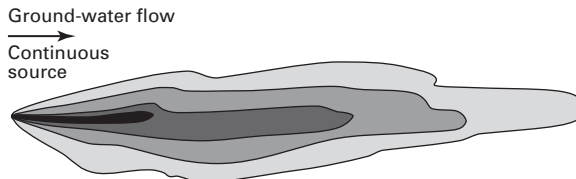
Source: J. P. Sauty. 1980. *Water Resources Research* 16:145–158. Copyright by the American Geophysical Union. Reproduced with permission.

Since the Green function is for a unit injection, and we have an injection rate that can be defined as $C_0(Q/b)$, the solution to the above is:

$$C(x, y, t) = \frac{C_0(Q/b)dt}{4\pi t(D_L D_T)^{0.5}} \exp\left[-\frac{(x - v_x t)^2}{4D_L t} - \frac{y^2}{4D_T t}\right]$$

If the injection rate, Q/b , is continuous then the solution at time t is:

FIGURE 2.17 Plume resulting from the continuous injection of a tracer into a two-dimensional flow field. (Source: C.W. Fetter. 1994. *Applied Hydrogeology, Third Edition*. Upper Saddle River, New Jersey: Prentice-Hall, Inc.)



$$C(x, y, t) = \frac{C_0(Q/b)}{4\pi(D_L D_T)^{0.5}} \int_{\theta=0}^{\theta=t} \exp\left[-\frac{(x - v_x \theta)^2}{4D_L \theta} - \frac{y^2}{4D_T \theta}\right] \frac{d\theta}{\theta} \quad (2.30)$$

Steady-state conditions are obtained when time approaches infinity. Therefore equation 2.30 is integrated from 0 to ∞ . The result is:

$$C(x, y) = \frac{C_0(Q/b)}{2\pi(D_L D_T)^{1/2}} \exp\left(\frac{v_x x}{2D_L}\right) K_0\left[\left(\frac{v_x^2}{4D_L} \left(\frac{x^2}{D_L} + \frac{y^2}{D_T}\right)\right)^{1/2}\right] \quad (2.30a)$$

where

K_0 = the modified Bessel function of the second kind and zero order
(values are tabulated in Appendix B)

Q = the rate that the contaminant is injected

b = the thickness of the aquifer over which the contaminant is injected

Equation 2.30a can be solved in EXCEL after installing the Plume2DSS() add-in (Renshaw 2015b).

EXAMPLE PROBLEM

A waste liquid containing fluoride at a concentration of 133 mg/L was pumped into a shallow disposal pit located above a thin, 1.75 m thick, (two-dimensional) aquifer at a rate of 3.66 m³/day for many years. The average linear velocity of the groundwater was 0.187 m/day. Assume that the transverse dispersion is 10% of the longitudinal dispersion. If the disposal pit is assumed to be at a location of $x_0 = 0$ and $y_0 = 0$, what would the concentration of fluoride be in a monitoring well located at $x = 123$ m and $y = 16$ m? Assume that the fluoride is non-reactive and non-adsorbed by the aquifer.

- First the value of α_L must be calculated using equation 2.48.

$$\alpha = 0.83(\log(L))^{2.414}$$

L is equal to $x - x_0$ or 123 m.

$$\alpha_L = 0.83(\log(123))^{2.414}$$

$$\alpha_L = 4.919 \text{ m}$$

- Next the value of D_L and D_T must be found.

$$D_L = v_x \alpha_L$$

$$D_L = 0.187 \text{ m/da} \times 4.919 \text{ m} = 0.920 \text{ m}^2/\text{da}$$

$$D_T = 0.10 D_L$$

$$D_T = 0.092 \text{ m}^2/\text{da}$$

The variables are then inserted into equation 2.30a.

$$C_0 = 133 \text{ mg/L}$$

$$Q = 3.66 \text{ m}^3/\text{da}$$

$$b = 1.75 \text{ m}$$

$$C = \frac{C_0(Q/b)}{2\pi(D_L D_T)^{1/2}} \exp\left(\frac{v_x x}{2D_L}\right) K_0\left[\left(\frac{v_x^2}{4D_L} \left(\frac{x^2}{D_L} - \frac{y^2}{D_T}\right)\right)^{1/2}\right]$$

$$C = \frac{133 \text{ mg/L} \times (3.66 \text{ m}^3/\text{da}/1.75 \text{ m})}{2 \times \pi \times (0.92 \text{ m}^2/\text{da} \times 0.092 \text{ m}^2/\text{da})^{1/2}} \times \exp\left(\frac{0.187 \text{ m/da} \times 123 \text{ m}}{2 \times 0.92 \text{ m}^2/\text{da}}\right)$$

$$K_0\left[\left(\frac{0.187^2 \text{ m}^2/\text{da}^2}{4 \times 0.92 \text{ m}^2/\text{da}} \left(\frac{123^2 \text{ m}^2}{0.92 \text{ m}^2/\text{da}} + \frac{16^2 \text{ m}^2}{0.092 \text{ m}^2/\text{da}}\right)\right)^{1/2}\right]$$

$$C = \frac{278.0 \text{ mg/L}}{1.828} \exp\left(\frac{23.0}{1.84}\right) K_0\left[\left[0.0095 \times (16445 + 2783)\right]^{1/2}\right]$$

$$C = 152.1 \exp(12.5) K_0(13.52) \text{ mg/L}$$

$$C = 152.1 \times 268337 \times 4.544 \times 10^{-7} \text{ mg/L}$$

Note: Although K_0 , a modified Bessel function of the zero order and second kind, can be obtained from Appendix B for a limited range of values, the table did not contain K_0 of 13.52. The value listed above, 4.54×10^{-7} was generated by a EXCEL function BESSELK(x,n).

According to Equation 2.30, as the value of D_L approaches zero, the concentration will approach infinity. As this is a physical impossibility, if the value of D_L is very small, then the one-dimensional equation, 2.23, should be used with a large value for time.

Equation 2.30 can also be solved for a specific value of time, so that the spread of a two-dimensional plume with time can be determined. In order to solve for time, Equation 2.30 can be written thusly:

$$C(x, y, t) = \frac{C_0(Q/b)}{4\pi(D_L D_T)^{1/2}} \exp\left(\frac{v_x x}{2D_L}\right) \int_{\theta=0}^{\theta=t} \exp\left[-\frac{\theta}{4D_L} - \left(\frac{x^2}{4D_L} + \frac{y^2}{4D_T}\right)\frac{1}{\theta}\right] \frac{d\theta}{\theta}$$

If we set $t_D = v_x^2/4 D_L$, then the above becomes:

$$C(x, y, t) = \frac{C_0(Q/b)}{4\pi(D_L D_T)^{1/2}} \exp\left(\frac{v_x x}{2D_L}\right) \int_{t_{D=0}}^{t_D=\infty} \exp\left[-t_D - \frac{B^2}{4t_D}\right] \frac{dt_D}{t_D}$$

with

$$B^2 = \frac{v_x^2 x^2}{4D_L^2} + \frac{v_x^2 y^2}{4D_L D_T}$$

The integral in the above equation was solved by Hantush (1956). This solution is

$$C(x, y, t) = \frac{C_0(Q/b)}{4\pi(D_L D_T)^{1/2}} \exp\left(\frac{v_x x}{2D_L}\right) [W(0, B) - W(t_D, B)] \quad (2.31)$$

with t_D and B as defined above.

It should be noted that in effect t_D is a dimensionless form of time. The values of $W[t_D, B]$ can be found in Hantush (1956) and a limited series is tabulated in Appendix C. It can also be determined in EXCEL after installing the Leaky() add-in (Renshaw 2015c). In well hydraulics this is known as the leaky well function, $W[u, r/b]$.

EXAMPLE PROBLEM

An underground tank which formerly held benzene but now holds water is leaking at a rate of $1.93\text{m}^3/\text{year}$. However, the water still contains some benzene at a concentration of $12,950\text{ }\mu\text{g/L}$. The groundwater which flows beneath the leaking tank goes directly north. A drinking water supply well is located at a spot that can be located by going 123.5m due north of the leaking tank and then 7.2m due east. Assume that the average linear velocity of the groundwater is 0.235 m/day and the longitudinal dispersivity is 12m and the lateral dispersivity is 1.2m and the aquifer thickness is 1.00m . What would the benzene concentration be after 2.00 years?

This is an example of a continuous leakage into a two dimensional flow field; equation 2-31.

1. The values of D_L and D_T must be calculated from equations 2-11a and 2-11b. We will ignore the effective diffusion coefficient as it is so much smaller than dispersivity.

$$D_L = \alpha_L v_X = 12\text{ m} \times 0.235\text{ m/day} = 2.82\text{ m}^2/\text{day}$$

$$D_T = \alpha_T v_X = 1.2\text{ m} \times 0.235\text{ m/day} = 0.282\text{ m}^2/\text{day}$$

2. The value of B must be calculated.

$$B = \left[\frac{(v_x x)^2}{4D_L^2} + \frac{(v_x y)^2}{4D_L D_T} \right]^{\frac{1}{2}}$$

$$B = \left[\frac{(0.235 \text{ m}/\text{da} \times 123.5 \text{ m})^2}{4 \times (2.8 \text{ m}^2/\text{da})^2} + \frac{(0.235/\text{da} \times 7.2 \text{ m})^2}{4 \times 2.8 \text{ m}^2/\text{da} \times 0.28 \text{ m}^2/\text{da}} \right]^{\frac{1}{2}}$$

$$B = \left[\frac{842 \text{ m}^4/\text{da}^2}{31.4 \text{ m}^4/\text{da}^2} + \frac{2.86 \text{ m}^4/\text{da}^2}{3.14 \text{ m}^4/\text{da}^2} \right]^{\frac{1}{2}}$$

$$B = \sqrt{26.8 + 0.91}$$

$$B = 5.26$$

3. The next step is to find t_D . Convert time in years to time in days by multiplying by 365 days per year.

$$t_D = \frac{v_x^2 t}{4D_L}$$

$$t_D = \frac{(0.235 \text{ m}/\text{da})^2 \times 730 \text{ da}}{4 \times 2.82 \text{ m}^2/\text{da}}$$

$$t_D = 3.57$$

4. One must now find $W[0, B]$ and $W[t_D, B]$ from Appendix C.

$$W[0, B] = W[0, 5.26] = 0.0098$$

$$W[t_D, B] = W[3.57, 5.26] = 0.0019$$

5. The values are then substituted into Equation 2.31. The rate of leakage, Q , is converted into cubic meters per day by dividing by 365. The aquifer thickness is 1.00m.

$$Q = 1.93 \text{ m}^3/\text{year} / 365 \text{ da/year} = 0.0053 \text{ m}^3/\text{da}$$

$$C(x, y, t) = \frac{C_0 Q / b}{4\pi(D_L D_T)^{1/2}} \exp\left(\frac{v_x x}{2D_L}\right) [W(0, B) - W(t_D, B)]$$

$$C(x, y, t) = \frac{12,950 \mu\text{g/L} \times 0.0053 \text{ m}^3/\text{da} / 1\text{m}}{4\pi(2.82 \text{ m}^2/\text{da} \times 0.28 \text{ m}^2/\text{da})^{1/2}} \exp\left(\frac{0.236 \text{ m}/\text{da} \times 123.5 \text{ m}}{2 \times 2.82 \text{ m}^2/\text{da}}\right) [0.0098 - 0.0019]$$

$$C(x, y, t) = 0.0061 \exp(5.16)[0.0079] \mu\text{g/L}$$

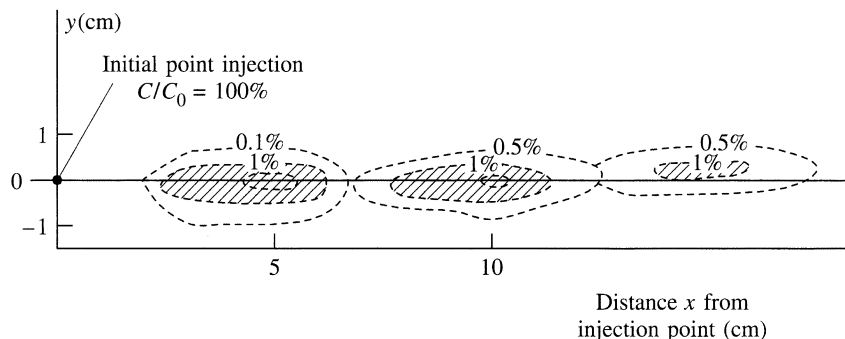
$$C(x, y, t) = 0.0061 \times 174 \times 0.0079 \mu\text{g/L}$$

$$C(x, y, t) = 0.0084 \mu\text{g/L}$$

2.9.8 Slug Injection into a Uniform Two-Dimensional Flow Field

If a slug of contamination is injected over the full thickness of a two-dimensional uniform flow field in a short period of time, it will move in the direction of flow and spread with time. This result is illustrated by Figure 2.18 and represents the pattern of contamination at three increments that result from a one-time spill. Figure 2.18 is based on the results of a laboratory experiment conducted by Bear (1961). Figure 2.19 shows the spread of a plume of chloride that was injected into an aquifer as a part of a large-scale field test (Mackay et al. 1986). The plume that resulted from the field test is more complex than the laboratory plume due to the heterogeneities encountered in the real world and the fact the plume may not be following the diffusional model of dispersion.

FIGURE 2.18 Injection of a slug of a tracer into a two-dimensional flow field shown at three time increments.



Experimental results from J. Bear. 1961. *Journal of Geophysical Research* 66:2455–2467. Copyright by the American Geophysical Union. Reproduced with permission.

De Josselin and De Jong (1958) derived a solution to this problem on the basis of a statistical treatment of lateral and transverse dispersivities. Bear (1961) later verified it experimentally. If a tracer with concentration C_0 is injected into a two-dimensional flow field over an area A at a point (x_0, y_0) , the concentration at a point (x, y) , at time t after the injection is

$$C(x, y, t) = \frac{C_0 A}{4\pi t(D_L D_T)^{1/2}} \exp \left[-\frac{((x - x_0) - v_x t)^2}{4D_L t} - \frac{(y - y_0)^2}{4D_T t} \right] \quad (2.32)$$

EXAMPLE PROBLEM

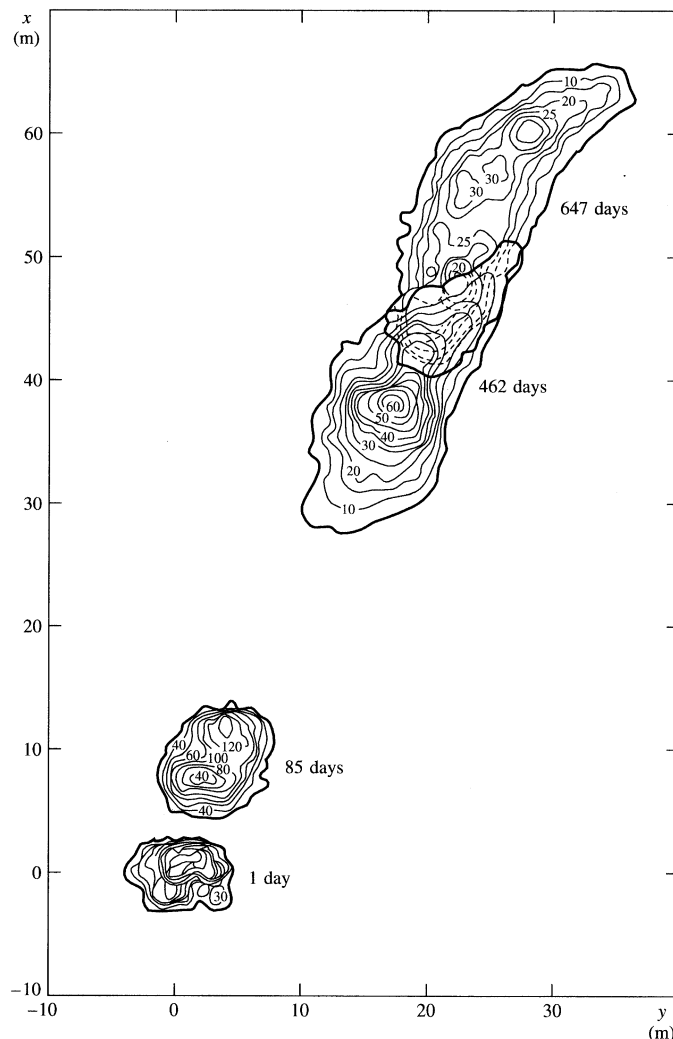
A tank truck, which is carrying water containing 1275 mg/L of dissolved benzene overturns and spills a volume of water sufficient to saturate a thin aquifer over an area of 5 m². The aquifer contains groundwater flowing with an average linear velocity of 0.45 m/day. Assume that the values of D_L and D_T are 2.1 m²/day and 0.21 m²/day respectively.

There is a nearby private well at a seasonal cottage. If the center of the spill is at location $x_0 = 0$ and $y_0 = 0$, then the location of the well is $x = 72$ m and $y = 5.5$ m. The owners of the private well are away for the season and will not return for another 200 days.

If there is no degradation or retardation of the benzene as it moves through the aquifer, what will the concentration of benzene be in the private well when the owner returns.

The correct equation to use is 2.32 for a slug injection of contamination into a two dimensional aquifer.

FIGURE 2.19 Vertically averaged chloride concentration at 1 day, 85 days, 462 days, and 647 days after the injection of a slug into a shallow aquifer.



Source: D.M. Mackay et al. 1986. *Water Resources Research* 22:2017–2029. Copyright by the American Geophysical Union. Reproduced with permission.

$$C = \frac{C_0 A}{4\pi \sqrt{D_L D_T}} \exp \left[-\frac{((x - x_0) - v_x t)^2}{4D_L t} - \frac{(y - y_0)^2}{4D_T t} \right]$$

$$C = \frac{1275 \text{ mgL}^{-1} \times 5 \text{ m}^2}{4 \times \pi \times 200 \text{ da} \times \sqrt{2.1 \text{ m}^2 \text{ da}^{-1} \times 0.21 \text{ m}^2 \text{ da}^{-1}}} \times$$

$$\exp \left[-\frac{((72 \text{ m} - 0) - (0.45 \text{ mda}^{-1} \times 200 \text{ da}))^2}{4 \times 2.1 \text{ m} \text{ da}^{-1} \times 200 \text{ da}} - \frac{(5.5 \text{ m})^2}{4 \times 0.21 \text{ m}^2 \text{ da}^{-1} \times 200 \text{ da}} \right]$$

$$C = \frac{6375 \text{ mgL}^{-1} \times \text{m}^2}{4 \times \pi \times 200 \text{ da} \times 0.664 \text{ m}^2 \text{ da}^{-1}} \exp \left[-\frac{(72 - 90)^2 \text{ m}^2}{1680 \text{ m}^2} - \frac{30.25 \text{ m}^2}{168 \text{ m}^2} \right]$$

$$C = 3.82 \text{ mgL}^{-1} \exp[-0.192 - 0.180]$$

$$C = 3.82 \exp(-0.372) = 3.82 \times 0.6892 = 2.63 \text{ mgL}^{-1}$$

The maximum concentration of a contaminant from a slug injection is found in the center of the plume, or the *center of mass*. If the flow is in the direction of the x axis, and the spill was at location $x_0 = 0$ and $y_0 = 0$, the center of mass of a conservative substance at any time t since the spill will be at a location where $x = v_x t$ and $y = 0$. If we substitute these values into equation 2-32, we obtain:

$$C_{max} = \frac{C_0 A}{4t\pi\sqrt{D_T D_L}} \exp \left[-\frac{((v_x t - 0) - v_x t)^2}{4D_L t} - \frac{(0 - 0)^2}{4D_T t} \right]$$

$$C_{max} = \frac{C_0 A}{4t\pi\sqrt{D_T D_L}} \exp(0)$$

$$C_{max} = \frac{C_0 A}{4t\pi\sqrt{D_T D_L}} \quad (2.32a)$$

The distribution of contamination in the plume will follow a normal or Gaussian distribution. From equations 2-12a and 2-12b the standard deviation of the distribution is given by:

$$\sigma_x = \sqrt{2D_L t} \qquad \sigma_y = \sqrt{2D_T t}$$

By definition, 99.7% of the mass of contamination will be contained within an area represented by three standard deviations away from the center of mass of the plume. Thus the plume can be defined by the location of the center of mass, $3\sigma_x$ and $3\sigma_y$.

EXAMPLE PROBLEM

A truck carrying dilute brine with 2130 mg/L chloride from the cleanup of a pond containing waste from a producing oil well overturns and spills the dilute brine over an area of 455 square feet. The underlying thin aquifer has an average linear ground-water velocity of 1.23 ft/day. Where would the center of mass of the plume be in

133 days, what would the maximum concentration be and how far beyond and to the side of the center of mass would the plume spread?

1. The plume would be advected by the flowing groundwater so that the center of mass would be at $x = v_x t$.

$$x = 1.23 \text{ ft/da} \times 133 \text{ da} = 164 \text{ feet.}$$

2. The maximum concentration at the center of mass can be found from equation 2.32a.

$$C_{max} = \frac{C_0 A}{4t\pi\sqrt{D_T D_L}}$$

- a. We need to find the values of D_L and D_T . This can be done using equations 2.11a and 2.11b; but, first we need to use equation 2.82 to estimate α_L .

$$\begin{aligned}\alpha_L &= 0.83(\log(L))^{2.414} \\ &= 5.66 \text{ ft}\end{aligned}$$

$$\begin{aligned}D_L &= \alpha_L v_x \\ &= 5.66 \text{ ft} \times 1.23 \text{ ft da}^{-1} \\ &= 6.96 \text{ ft}^2 \text{ da}^{-1}\end{aligned}$$

We can assume D_T to be 10% of D_L .

$$D_T = 0.696 \text{ ft}^2 \text{ da}^{-1}$$

The appropriate variables are substituted into equation 2.32.

$$C_{max} = \frac{2130 \text{ mgL}^{-1} \times 455 \text{ ft}^2}{4 \times \pi \times 133 \text{ da} \sqrt{6.96 \text{ ft}^2 \text{ da}^{-1} \times 0.696 \text{ ft}^2 \text{ da}^{-1}}}$$

$$C_{max} = 263 \text{ mgL}^{-1}$$

3. The size of the plume can be determined from the standard deviations.

$$\sigma_x = \sqrt{2D_L t}$$

$$\sigma_x = \sqrt{2 \times 6.96 \text{ ft}^2 \text{ da}^{-1} \times 133 \text{ da}}$$

$$\sigma_x = 43.0 \text{ ft}$$

$$\sigma_y = \sqrt{2D_T t}$$

$$\sigma_y = \sqrt{2 \times 6.96 \text{ ft}^2 \text{ da}^{-1} \times 133 \text{ da}}$$

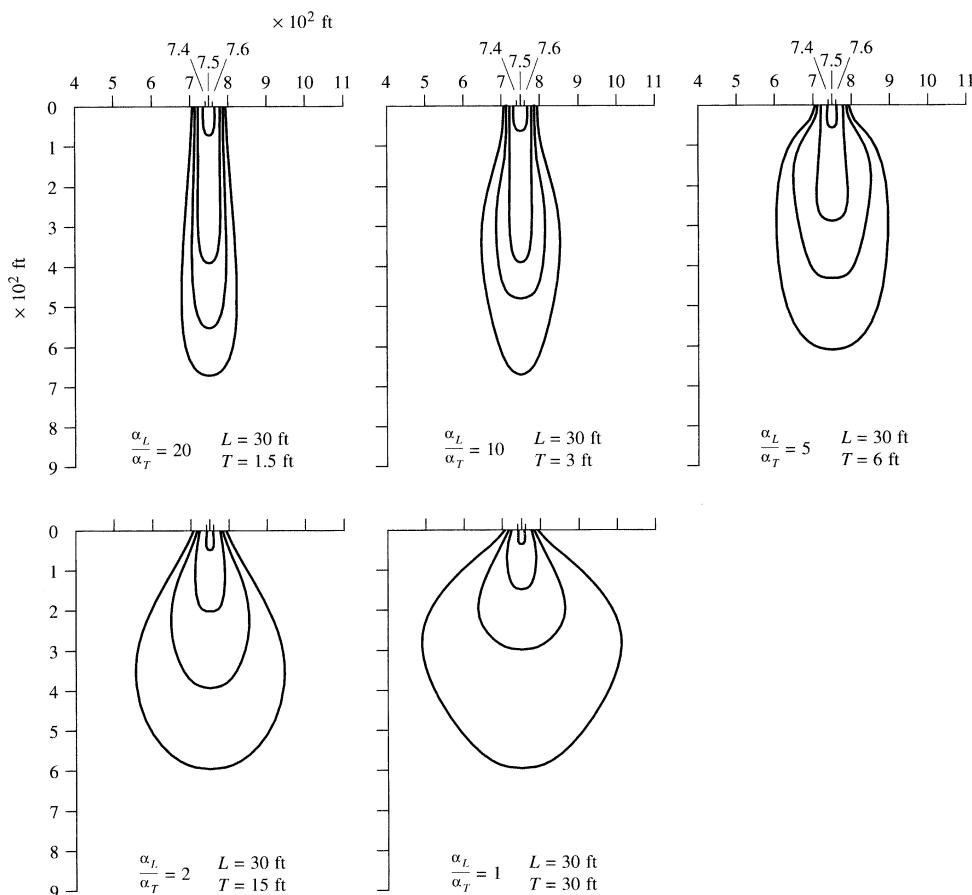
$$\sigma_y = 13.6 \text{ ft}$$

The leading edge of the plume is $3\sigma_x$ feet ahead of the center of mass or 129 feet and the plume had spread out $3\sigma_y$ feet on either side of the center of the mass or 40.8 feet.

■ 2.10 Effects of Transverse Dispersion

The ratio of longitudinal to transverse dispersivity (α_L/α_T) in an aquifer is an important control over the shape of a contaminant plume in two-dimensional mass transport. The lower the ratio, the broader the shape of the resulting plume will be. Figure 2.20 shows various two-dimensional shapes of a contaminant plume, where the only factor varied was the ratio of longitudinal to transverse dispersivity. This illustrates the fact that it is important to have some knowledge of the transverse dispersivity in addition to the longitudinal dispersivity. There is a paucity of data in the literature on the relationships of longitudinal to transverse dispersivities. From the few field studies available, α_L/α_T is in the range of 6 to 20 (Anderson 1979; Klotz et al. 1980). In addition, dispersivity ratios based on field studies are based on fitting the diffusional model of dispersion to cases where it might not be applicable.

FIGURE 2.20 The effect of changing dispersivity ratio on the spread of a contaminant plume from a continuous source.



■ 2.11 Tests to Determine Dispersivity Values

2.11.1 Laboratory Tests

Diffusion and dispersion values can be determined in the laboratory using columns packed with the porous media under investigation. The results of column studies are often reported in terms of pore volumes of fluid that are eluted. One pore volume is the cross-sectional area of the column times the length times the porosity (ALn), i.e., the column's capacity. The unit discharge rate from the column is the linear velocity times the porosity times the cross-sectional area ($v_x nA$). The total discharge over a period of time is the product of time and the discharge rate ($v_x nAt$).

The total number of pore volumes, PV is the total discharge divided by the volume of a single pore volume:

$$\begin{aligned} PV &= \frac{\text{Discharge}}{\text{Capacity}} \\ &= \frac{v_x nAt}{ALn} = \frac{Qt}{ALn} = \frac{v_x t}{L} = t_R \end{aligned} \quad (2.33)$$

It can be seen that the number of pore volumes is equivalent to a dimensionless time, t_R , which is referred to as the hydraulic residence time.

With this equivalency Equation 2.25, the approximate one-dimensional dispersion equation, can be rearranged to yield (Brigham 1974)

$$\frac{C}{C_0} = 0.5 \left[\operatorname{erfc} \left(\frac{1-PV}{2(PV D_L / v_x L)^{1/2}} \right) \right] \quad (2.34)$$

where

PV = the number of effluent pore volumes, where a pore volume is equal to the total column volume times the porosity

L = the length of the column

Equation 2.34 can, through appropriate substitution, be made equivalent to Equation 2.26.

The concentration of the tracer in the effluent, C , is measured for various values of PV , and then C/C_0 is plotted as a linear probability function of $[(PV - 1)/PV^{1/2}]$. If the data plot as a straight line, they are normally distributed, the diffusive form of the advection-dispersion equation is valid, and the slope of the line is related to the longitudinal hydrodynamic dispersion.

The value of D_L can be found from

$$D_L = \left(\frac{v_x L}{8} \right) (J_{0.84} - J_{0.16})^2 \quad (2.35)$$

where

$J_{0.84}$ = $[(PV - 1)/PV^{1/2}]$ when C/C_0 is 0.84

$J_{0.16}$ = $[(PV - 1)/PV^{1/2}]$ when C/C_0 is 0.16

Note that $J_{0.16}$ and $J_{0.84}$ correlate to one standard deviation. Since $D_L = a_L v_x + D^*$, then

$$\alpha_L = \frac{D_L - D^*}{v_x} \quad (2.36)$$

The average linear velocity in the column can be found from the quantity of water discharging per unit time divided by the product of the cross-sectional area and the porosity. The effective diffusion coefficient can either be measured in a column test or estimated (Grathwohl 1998).

EXAMPLE PROBLEM

Pickens and Grisak (1981) conducted a laboratory study of dispersion in sand columns with the following characteristics:

Tracer	Chloride
Column length	30 cm
Column diameter	4.45 cm
Mean grain size	0.20 mm
Uniformity coefficient of sand	2.3
Porosity	0.36
Flow rate	
Test R1	5.12×10^{-3} mL/sec
Test R2	1.40×10^{-2} mL/sec
Test R2	7.75×10^{-2} mL/sec
Average linear Velocity	
Test R1	9.26×10^{-4} cm/sec
Test R2	2.53×10^{-3} cm/sec
Test R3	8.60×10^{-3} cm/sec

Test R1 was run using chloride at 200 mg/L, followed by test R2, in which the saline solution was flushed out of the column using deionized water, and then test R3, where the 200-mg/L chloride solution was again introduced into the column.

The results of the three tests are plotted in Figure 2.21. The results of test R2 have a reverse slope as deionized water replaced the saline solution. It can be seen that the results form a straight line.

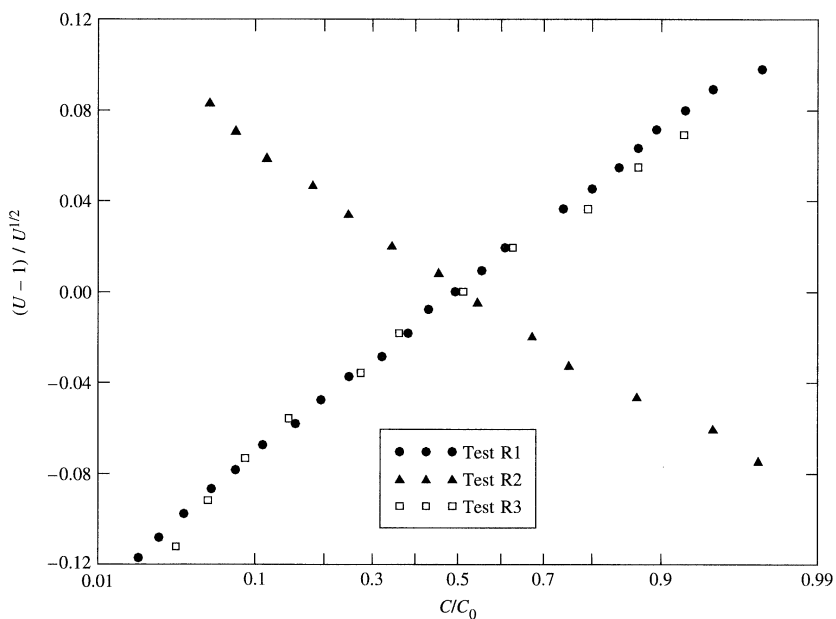
For chloride in water at 25°C, the molecular diffusion coefficient is 2.03×10^{-5} cm²/sec. Based on this, Pickens and Grisak estimated the effective diffusion coefficient to be 1.02×10^{-5} cm²/sec. The hydrodynamic dispersion coefficients are based on the slope of the straight lines. The following values were obtained for the three tests:

Test	Hydrodynamic Dispersion	Dispersivity
R1	$4.05 \times 10^{-5} \text{ cm}^2/\text{sec}$	0.033 cm
R2	$8.65 \times 10^{-5} \text{ cm}^2/\text{sec}$	0.030 cm
R3	$3.76 \times 10^{-4} \text{ cm}^2/\text{sec}$	0.043 cm

The replicate values are not equal because of experimental error.

The computation of the dispersion value for test R1 is illustrated here:

FIGURE 2.21 Probability plot of $(U - 1) / U^{1/2}$ versus C/C_0 for determination of dispersion in a laboratory sand column (note: $U = PV$).



Source: S. F. Pickens and G. E. Grisak. 1981. *Water Resources Research* 17:1191–1211. Copyright by the American Geophysical Union. Reproduced with permission.

$$\alpha_L = \frac{D_L - D^*}{v_x}$$

$$= \frac{(4.05 \times 10^{-5} \text{ cm}^2/\text{sec} - 1.02 \times 10^{-5} \text{ cm}^2/\text{sec})}{9.26 \times 10^{-4} \text{ cm/sec}} = 0.033 \text{ cm}$$

EXAMPLE PROBLEM

A soil column is 40 cm long. It is set up so that deionized water is flowing through at an average linear velocity of $1.35 \times 10^{-2} \text{ cm sec}^{-1}$. The fluid source is changed to one with a chloride concentration of 300 mg L^{-1} . After 500 seconds, t_1 , the concentration of

chloride was 48 mgL^{-1} and after 4000 seconds, t_2 , it was 252 mgL^{-1} . What is the dispersivity of the sand in the soil column?

The number of pore volumes at a given time can be calculated from Equation 2.33:

$$PV = v_x t / L$$

For the first measurement at t_1 :

$$PV = 1.35 \times 10^{-2} \text{ cms}^{-1} \times 500 \text{ s}/40 \text{ cm} = 0.17 \text{ pore volumes}$$

For the second measurement at t_2 :

$$PV = 1.35 \times 10^{-2} \text{ cms}^{-1} \times 4000 \text{ s}/40 \text{ cm} = 1.35 \text{ pore volumes}$$

At t_1 , C/C_0 is $48/300$, which equals 0.16. With a pore volume of 0.17

$$(PV - 1)/PV^{1/2} = (0.17 - 1)/(0.17)^{1/2} = -2.01$$

At t_2 , C/C_0 is $252/300$, which equals 0.84. With a pore volume of 1.32

$$(PV - 1)/PV^{1/2} = (1.32 - 1)/(1.32)^{1/2} = 0.28$$

Since C/C_0 at t_1 is conveniently equal to 0.16, then $(PV - 1)/PV^{1/2}$ for t_1 turns out to be $J_{0.16}$. Likewise C/C_0 at t_2 is 0.84 so that $(PV - 1)/PV^{1/2}$ for t_2 is $J_{0.84}$.

The value of D_L can be found from Equation 2.35:

$$D_L = \left(\frac{v_x L}{8} \right) (J_{0.84} - J_{0.16})^{1/2}$$

$$\begin{aligned} D_L &= (1/8) \times (1.35 \times 10^{-2} \text{ cms}^{-1} \times 40 \text{ cm}) \times (0.28 - -2.01)^{1/2} \\ &= 6.75 \times 10^{-2} \times 1.51 \text{ cm}^2 \text{s}^{-1} \\ &= 0.102 \text{ cm}^2 \text{s}^{-1} \end{aligned}$$

2.11.2 Quantifying Dispersivity in the Field

A value for dispersivity can be determined in the field by two means. If there is a contaminated aquifer, the plume of known contamination can be mapped and the advection-dispersion equation solved with dispersivity as the unknown. Pinder (1973) used this approach in a groundwater modeling study of a plume of dissolved chromium in a sand and gravel aquifer on Long Island, New York. He started with initial guesses of α_L and α_T and then varied them during successive model runs until the computer model yielded a reasonable reproduction of the observed contaminant plume. One of the difficulties of this approach is that the concentration and volume of the contaminant source are often not known.

A much more common approach is the use of a tracer that is injected into the ground via a well. There are a variety of variations to this approach. **Natural gradient tests** involve the injection of a tracer into an aquifer, followed by the measurement of the plume that developed under the prevailing water table gradient (e.g., Sudicky and Cherry 1979;

Gillham et al. 1984; Mackay et al. 1986; LeBlanc et al. 1991; Garabedian et al. 1991; Olsen and Tenbus 2004). The plume is measured by means of small amounts of water withdrawn from down-gradient observation wells and multilevel piezometers. Many of these field tests showed that thin plumes with less than expected transverse dispersivity often occur in field situations. This underlines a growing acceptance of the need for high resolution, vertically discrete, multilevel aquifer monitoring. Multilevel monitoring will be discussed in Chapter 8. One and two-well tests have also been used in which a tracer is pumped into the ground and then groundwater containing the tracer is pumped back out of the ground (e.g., Fried 1975; Grove and Beetem 1971; Sauty 1978; Pickens et al 1981; Pickens and Grisak, 1981). These so-called **forced hydraulic gradient tests** have the advantage that they can be completed in much shorter time relative to natural gradient tests. However, these tests require treatment if the pumped groundwater is contaminated. Also, the results of forced hydraulic gradient tests do not truly reflect the natural groundwater flow conditions. Ptak et al. (2004) reviewed the advantages and disadvantages of natural or forced hydraulic gradient tests for both nonreactive and reactive tracer compounds can be used.

2.11.3 Single-Well Tracer Test

A single-well tracer test involves the injection of water containing a conservative tracer into an aquifer via an injection well and then the subsequent pumping of that well to recover the injected fluid. The fluid velocities of the water being pumped and injected are much greater than the natural groundwater gradients.

Equation 2.20 can be written (Hoopes and Harleman 1967) as

$$\frac{\partial C}{\partial t} + u \frac{\partial C}{\partial r} = \alpha_L u \frac{\partial^2 C}{\partial r^2} + \frac{D^*}{r} \frac{\partial}{\partial r} \left(r \frac{\partial C}{\partial r} \right) \quad (2.37)$$

Gelhar and Collins (1971) derived a solution to Equation 2.37 for the withdrawal phase of an injection-withdrawal well test in which the diffusion term is neglected because it is very much smaller than the dispersion term. The relative concentration of the water being withdrawn from the injection well is

$$\frac{C}{C_0} = \frac{1}{2} \operatorname{erfc} \left(\frac{(U_p - U_i) - 1}{\sqrt{\frac{16}{3} (\alpha_L / R_f) [2 - (1 - U_p / U_i)]^{1/2} [1 - (U_p / U_i)]}} \right)^{1/2} \quad (2.38)$$

where

U_p = cumulative volume of water withdrawn during various times

U_i = total volume of water injected during the injection phase

R_f = average frontal position of the injected water at the end of the injection period, which is defined by

$$R_f = \left(\frac{Qt}{\pi b n} \right)^{1/2} \quad (2.39)$$

where

Q = rate of injection

t = total time of injection

b = aquifer thickness

n = porosity

EXAMPLE PROBLEM

Pickens and Grisak (1981) performed a single-well injection-withdrawal tracer test into a confined sand aquifer about 8.2 m thick with an average hydraulic conductivity of 1.4×10^{-2} cm/sec and a porosity of 0.38. The sediment tested in the column study described in the dispersivity example problem above came from this aquifer.

The injection well was 5.7 cm in diameter and the full thickness of the aquifer was screened. Clear water was injected at a constant rate for 24 hr prior to the start of the test to establish steady-state conditions. The tracer used during the tests was ^{131}I , a radioactive iodine isotope, which was added to the injected water. All measurements were corrected for the radioactive decay that occurred during the test.

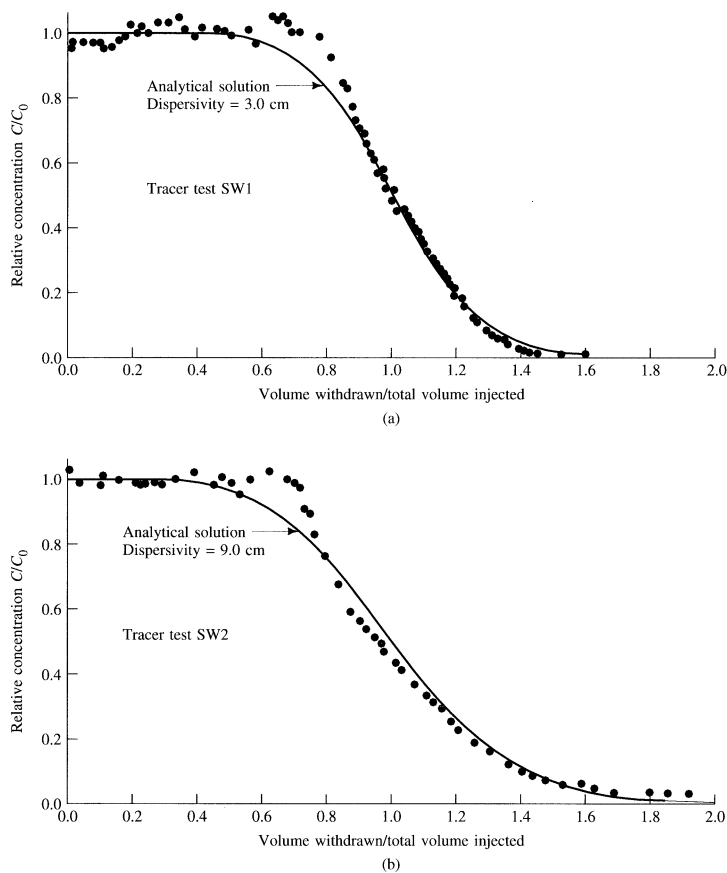
Two tests were performed on the well. The first test, SW1, had an injection rate of 0.886 L/sec and injection continued for 1.25 da. A total volume of 95.6 m^3 of water was injected, and the injection front reached an average radial distance away from the well of 3.13 m. Water was then pumped for 2.0 da at the same rate, so that a total of 153 m^3 of water was withdrawn. The second test, SW2, was longer. Water with the tracer was added at a rate of 0.719 L/sec for 3.93 da. A total of 244 m^3 of water was added, and the average position of the injection front reached to 4.99 m from the well. During the withdrawal phase a total of 886 m^3 of water was pumped over a period of 16.9 da at an average rate of 0.606 L/sec.

The results of the test are shown in Figure 2.22. Relative concentration, C/C_0 , is plotted against U_p / U_i . The dots represent field values and the solid lines are curves, which were computed using Equation 2.38. Various curves were computed for different values of α_L , and the curves with the best fit to the field data were plotted on the graphs. In Figure 2.22(a) the calculated curve was based on a longitudinal dispersivity of 3.0 cm, whereas for curve 2.22(b) the best-fit curve was based on a longitudinal dispersivity of 9.0 cm. This test illustrates the scale-dependent nature of dispersion. The second test, in which a larger volume of water was injected, tested a larger volume of the aquifer than the first test and yielded a higher dispersivity value.

■ 2.12 Scale Effect of Dispersion

The two example problems derived from Pickens and Grisak (1981) illustrate what has been called the **scale effect of dispersion** (Fried 1975). At the laboratory scale the mean value of α_L was determined to be 0.035 cm (0.014 in) when the flow length was 30 cm (12 in). With the single-well injection-withdrawal test, α_L was 3 cm (1.2 in) when the solute front traveled 3.1 m (10.2 ft) and 9 cm (3.5 in) when the solute front traveled 5.0 m (16.4 ft). In a two-well recirculating withdrawal-injection tracer test with wells located 8 m (26.2 ft) apart α_L was determined to be 50 cm (19.6 in). All these values were obtained from the same site. The greater the flow length, the larger the value of longitudinal dispersivity needed to fit the data to the advection-dispersion equation.

FIGURE 2.22 Comparison of measured C/C_0 values for a single-well injection-Withdrawal test versus an analytical solution.

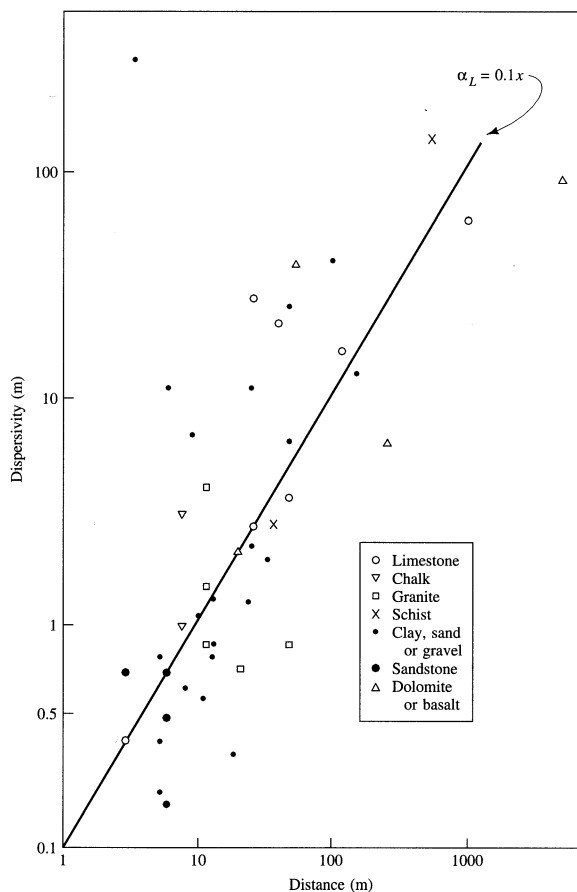


Source: S. F. Pickens and G. E. Grisak. 1981. *Water Resources Research* 17:1191–1211. Copyright by the American Geophysical Union. Reproduced with permission.

Lallemand-Barres and Peaudecerf (1978) published a graph on which dispersivity, as measured in the field, was plotted against flow length on log-log paper (Figure 2.23). This graph suggested that the longitudinal dispersivity could be estimated to be about 0.1 of the flow length. Gelhar (1986) published a similar graph (Figure 2.24), which contained more data points and was extended to flow lengths more than an order of magnitude greater than the Lallemand-Barres and Peaudecerf figure. The additional data on the Gelhar graph suggest that the relationship between α_L and flow length is more complex than a simple 1 to 10 ratio.

The dispersion that occurs at field-scale flow lengths can be called **macrodispersion**. In a flow domain that encompasses a few pore lengths, mechanical dispersion is caused by differences in the fluid velocities within a pore, between pores of slightly different size, and because different flow paths have slightly different lengths. However, at the field scale, even aquifers that are considered to be homogeneous will have layers

FIGURE 2.23 Field-measured values of longitudinal dispersivity as a function of the scale of measurement.



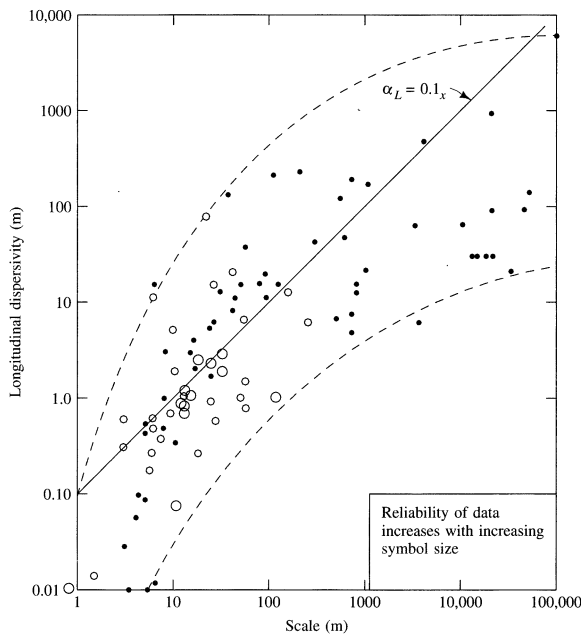
Source: P. Lallemand-Barres and P. Peauduc erf. 1978. *Bulletin, Bureau de Recherches Géologiques et Minières* 3/4: 277–284. Editions BRGM BP6009 45060 ORLEANS CEDEX 2.

and zones of somewhat different hydraulic conductivity. If mechanical dispersion can be caused by slight differences in the fluid velocity within a single pore, imagine the mechanical dispersion that will result as the fluid passes through regions of the aquifer with different conductivity values and corresponding different velocities.

Hydraulic conductivity is frequently determined on the basis of a pumping test, where water is removed from a large volume of the aquifer. As a result, the hydraulic conductivity that is obtained is an average value over the entire region of the aquifer contributing water to the well. This averaging will conceal real differences in hydraulic conductivity across the aquifer. These differences exist in both vertical and longitudinal sections.

Figure 2.25 shows profiles of the vertical variation in hydraulic conductivity based on permeameter tests of repacked core samples of sediment, from two borings located 1m apart (Sudicky 1986). Figure 2.21 shows the distribution of the log of hydraulic conductivity of a cross section in a stratified sandy outwash aquifer

FIGURE 2.24 Field-measured values of longitudinal dispersivity as a function of the scale of measurement. The largest circles represent the most reliable data.



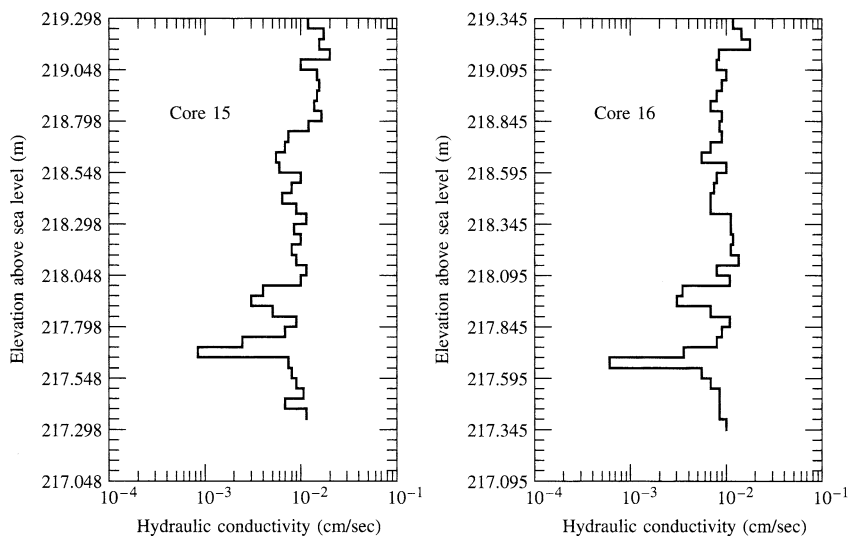
Source: L. W. Gelhar. 1986. Water Resources Research 22:135S–145S. Copyright by the American Geophysical Union. Reproduced with permission.

with layers of primarily medium-grained, fine-grained, and silty, fine-grained sand. The cross section is 1.75 m (5.75 ft) deep by 19 m (62 ft) long (Sudicky 1986).

Figures 2.25 and 2.26 illustrate the natural variation of both hydraulic conductivity and porosity. Even aquifers that are usually considered to be homogeneous still have variations in porosity and hydraulic conductivity. Hydraulic conductivity of geologic materials varies over a very wide range of values, over nine orders of magnitude. Porosity varies over a much, much smaller range: approximately from 1 to 60% or less than two orders of magnitude. From the standpoint of describing aquifers mathematically, it is sometimes useful to assume that hydraulic conductivity follows a lognormal distribution, which means that the logarithms of the conductivity values are normally distributed, whereas porosity is normally distributed (Freeze 1975). Since dispersion depends upon variations in the fluid velocity and from Darcy's law [$v = (K/n)(dh/dl)$], it is obvious that variations in both hydraulic conductivity and porosity play a role. However, since hydraulic conductivity varies over a much larger range, it is the more important.

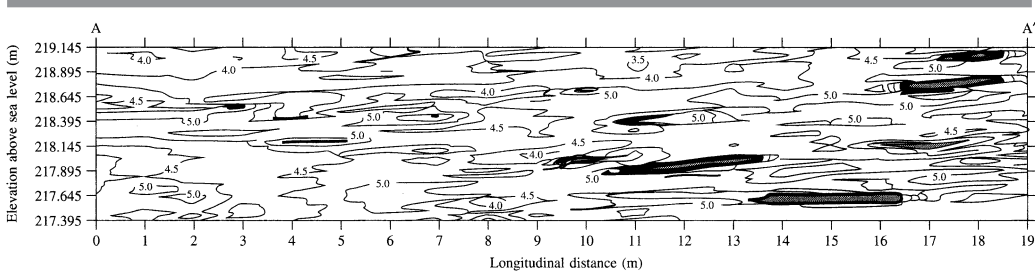
This leads us to an explanation for the scale factor. As the flow path gets longer, groundwater will have an opportunity to encounter greater and greater variations in hydraulic conductivity and porosity. Even if the average linear velocity remains the same, the deviations from the average will increase, and hence the mechanical dispersion will also increase. It is logical that the flow path will eventually become long enough that all possible variations in hydraulic conductivity will have been encountered

FIGURE 2.25 Hydraulic conductivity as determined by permeameter tests of remolded sediment samples from a glacial drift aquifer. The borings from which the cores were obtained are separated by one meter horizontally.



Source: E. A Sudicky, *Water Resources Research* 22, no. 13 (1986):2069–2082. Copyright by the American Geophysical Union. Reproduced with permission.

FIGURE 2.26 Distribution of the hydraulic conductivity along a cross section through a glacial drift aquifer. Hydraulic conductivity is expressed as a negative log value. (If $K = 5 \times 10^{-2}$ cm/sec, then -log K is 1.3.) Sample locations are every 5 cm vertically and every 1 m horizontally. Hydraulic conductivity was less than 10^{-3} cm/sec in the stippled zones.



Source: E. A Sudicky. 1986. *Water Resources Research* 22:2069–2082. Copyright by the American Geophysical Union. Reproduced with permission.

and that the value of mechanical dispersion will reach a maximum. If one assumes that the distribution of hydraulic conductivity has some definable distribution, such as normal or log-normal, and that transverse dispersion is occurring, it can be shown that apparent macrodispersion will approach an asymptotic limit at long travel distances and large travel times (Matheron and de Marsily 1980; Molz et al. 1983; Gelhar and Axness 1983; Dagan 1988). When the asymptotic limit is reached, the plume will continue to

spread. In this region the variance of the plume will grow proportionally to the time or mean travel distance, as it does at the laboratory column scale. The advective-dispersion model is based on the assumption that dispersion follows Fick's law. Some authors contend that dispersion follows Fick's law only at the laboratory scale, where it is caused by local mechanical dispersion, and for very long flow paths, where the effects of advection through heterogeneous materials and local transverse dispersion create macroscale dispersion that follows Fick's law (e.g., Gelhar 1986; Dagan 1988). The contention that macroscale dispersion becomes Fickian (i.e., follows Fick's law) at long travel times and distances is somewhat controversial, especially if the flow is through geological formations that are heterogeneous at different scales (Anderson 1990).

■ 2.13 Stochastic Models of Solute Transport

2.13.1 Introduction

The normal manner of determining a field-scale dispersion coefficient is to look for a natural tracer or inject a tracer into an aquifer and observe the resulting development of a plume. A solute-transport model is then constructed and the computed solute distribution is fitted to the observed field data by adjusting the dispersion coefficients. Dispersion coefficients obtained in this manner are fitted curve parameters and do not represent an intrinsic property of the aquifer. This is especially true when the aquifer is assumed to be homogeneous and is described by a single value for hydraulic conductivity and porosity. It is apparent that flow and transport modeling based on a single value for porosity and hydraulic conductivity is a gross simplification of the complexity of nature. For analytical solutions, we are constrained to use of a single value for average linear velocity, and for numerical models we often use a single value because that is all we have.

A **deterministic model** is one where a partial differential equation is solved, either numerically or analytically, for a given set of input values, aquifer parameters, and boundary conditions. The resulting output variable has a specific value at a given place in the aquifer. It is assumed that the distribution of aquifer parameters is known. The equations given earlier in this chapter are examples of deterministic models.

A **stochastic model** is a model in which there is a statistical uncertainty in the value of the output variables, such as solute distribution. The probabilistic nature of this outcome is due to the fact that there is uncertainty in the value and distribution of the underlying aquifer parameters, such as the distribution and value of hydraulic conductivity and porosity (Freeze 1975; Dagan 1988).

A widespread misconception about stochastic and deterministic models is that the latter use physical laws, while the stochastic models are largely empirical and based entirely on statistical data-analysis. In reality, any physically-based model becomes a stochastic model once its inputs, parameters, or outputs are treated as random (Bierkens and van Geer; 2014).

The idea behind stochastic modeling is very attractive. It is obvious that it takes a great effort to determine hydraulic conductivity and porosity at more than a few locations in an aquifer system. If we could determine the distribution of aquifer properties with a high degree of detail, then a numerical solution of a deterministic model would yield results with a high degree of reliability. However, with limited knowledge of aquifer

parameters, a deterministic model makes only a prediction of the value of an output variable at a given point and time in the aquifer. The stochastic model is based on a probabilistic distribution of aquifer parameters. At the outset it is recognized in the stochastic model that the result will be only some range of possible outcomes. The stochastic model thus recognizes the probabilistic nature of the answer, whereas the deterministic model suggests that there is only one “correct” answer. Of course, the experienced hydrogeologist recognizes the uncertainty even in the deterministic answer. There have been literally hundreds of papers written on various aspects of stochastic modeling of groundwater flow and solute transport. Textbooks like Zhang (2001), Rubin (2003), and Dagan and Neuman (2005) provide insights into analyzing and modeling subsurface heterogeneity using stochastics concepts and models for managing water resources, preserving subsurface water quality, storing energy and wastes, besides other applications.

2.13.2 Stochastic Descriptions of Heterogeneity

Stochastic hydrology is about combining deterministic model outcomes with a probability distribution of the errors, or alternatively, considering the hydrological variable as random and determining its probability distribution and some “best prediction” (Bierkens and van Geer 2014). The greatest uncertainty in the input parameters of a model is the value of hydraulic conductivity, because it varies over such a wide range for geologic materials. If we make a measurement of hydraulic conductivity at a given location, the only uncertainty in its value at that location is due to errors in measuring its value. However, at all locations where hydraulic conductivity is not measured, additional uncertainty exists. If we make a number of measurements of the value of hydraulic conductivity, we can estimate this uncertainty using certain statistical techniques.

Let us define Y as the log of the hydraulic conductivity, K , and assume that the log value Y is normally distributed. We will assume a one-dimensional series of Y values $\{Y_1, Y_2, Y_3, Y_4, \dots, Y_n\}$ (Freeze et al. 1990). Therefore,

$$Y_i = \log K_i \quad (2.40)$$

The population that consists of all of the values of Y has a mean value, μ_y , and a standard deviation, σ_y . The only way to obtain precise values of μ_y and σ_y would be to sample the aquifer everywhere, clearly an impossible task, but we can find estimates of their values based on the locations where we have actually measured K . If we have a series of Y values $\{Y_1, Y_2, Y_3, \dots, Y_n\}$, as in Figure 2.27(a), based on measured value of K , then our estimate of the population mean is obtained from the mean value of the sampled values, \bar{Y} , which can be found from

$$\bar{Y} = \frac{1}{n} \sum_{i=1}^n Y_i \quad (2.41)$$

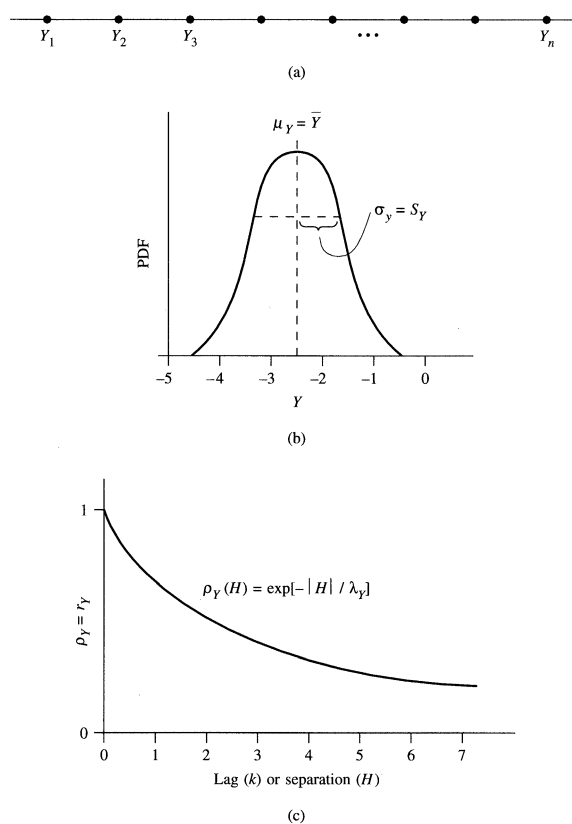
The estimate of the variance of the population is also obtained by the variance of the sampled values, S_y^2 , which is found from the following equation:

$$S_y^2 = \frac{1}{n} \sum_{i=1}^n (Y_i - \bar{Y})(Y_i - \bar{Y}) \quad (2.42)$$

For a normally distributed population, the probabilistic value is called a probability density function (PDF) and is described by the mean and the variance. The variance is a measure of the degree of heterogeneity of the aquifer. The greater the value, the more heterogeneous the aquifer. The PDF can be represented as a bell-shaped curve with the peak equal to the mean, as in Figure 2.27(b), and the spread of the bell can be defined by either the variance or the standard deviation, S_y , which is the square root of the variance.

If we have measured the value of Y_i at a number of locations and wish to estimate the value Y_j at some other location j that is not close to any of the measured values, how can we estimate the value of Y_j ? One approach is to say that the most likely estimate of Y_j is the mean of the measured values of Y_i , and the uncertainty in this value is normally distributed with a standard deviation equal to the standard deviation of the measured values, S_y . In doing so we have accepted the **ergodic hypothesis**. This means that there is a 16% chance that the value of Y_j is greater than $\bar{Y} - S_y$, a 50% chance that it is greater than \bar{Y} , and an 84% chance that it is greater than $\bar{Y} + S_y$. In broad terms ergodicity describes a dynamic system which has the same behavior averaged over time as averaged over space.

FIGURE 2.27(a) One-dimensional sequence of log hydraulic conductivity values, Y ; (b) probability distribution function for Y ; (c) autocorrelation function for Y .



Hydraulic conductivity values measured at locations close to each other are likely to be somewhat similar. The farther apart the measurements, the less likely that the values will be similar. This is due to the fact that as distances become greater, the chance that there will be a change in geologic formation increases. The function that describes this is the **autocorrelation function**, ρ_Y . The value of the autocorrelation function decreases with the distance between two measurements. An estimate of the autocorrelation function, r_Y , can be obtained from the measured sample values by the following equation:

$$r_Y(k) = \frac{1}{S_Y^2} \frac{1}{n} \sum_{i=1}^n (Y_i - \bar{Y})(Y_{i-k} - \bar{Y}) \quad (2.43)$$

with k , the **lag**, being a whole number representing a position in the sequence away from the i position. Figure 2.27(c) shows an autocorrelation function plotted against the lag. If the lag is zero, then Equation 2.43 reduces to $r_Y = S_Y^2 / S_Y^2 = 1$. This means that a Y value is perfectly correlated with itself.

The autocorrelation factor can be expressed in terms of either lag, ρ_{Yk} or distance, $\rho_Y(H)$. When a measurement of Y_i is made at position X_i and a measurement of Y_{i-k} is made at position X_{i-k} , the absolute value of $X_i - X_{i-k}$ is called the **separation**, H .

If the autocorrelation function has an exponential form, then it can be expressed as

$$\rho_Y(H) = \exp[-|H| / \lambda_Y] \quad (2.44)$$

where λ_Y , the **correlation length**, is representative of the length over which Y is correlated. It is the distance over which $\rho_Y(H)$ decays to a value of e^{-1} . The **integral scale**, ε_Y , is the area under the curve.

$$\varepsilon_Y = \int_0^\infty \rho_Y(H) dH \quad (2.45)$$

Integration of Equation 2.45 will show that $\varepsilon_Y = \lambda_Y$, so that the correlation structure can be described by either the correlation length or the integral scale.

The **autocovariance**, τ_{Yk} or $\tau_Y(H)$, is equal to the autocorrelation times the variance.

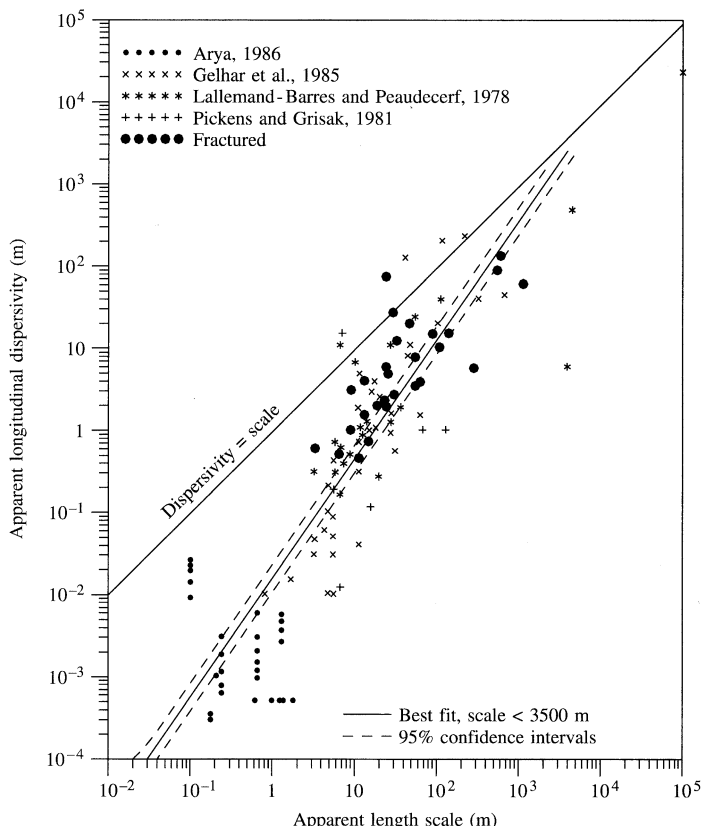
$$\tau_Y(H) = \sigma_Y^2 \rho_Y(H) \quad (2.46)$$

We can describe the distribution of heterogeneity of Y by the use of three stochastic functions, μ_Y , σ_Y (or σ_Y^2), and λ_Y . If a stochastic process is said to be stationary, the values of μ_Y , σ_Y (or σ_Y^2), and λ_Y do not vary in space in the region being studied. If the hydraulic conductivity of an aquifer can be described as a stationary stochastic process, the aquifer is uniformly heterogeneous.

2.13.3 Stochastic Approach to Solute Transport

If we accept the idea that we don't know the value of the hydraulic conductivity and the porosity everywhere, then we must accept the idea that it is not possible to predict the actual concentration of a solute that has undergone transport through an aquifer. The best estimate of the concentration is the **ensemble mean concentration**, $\langle C \rangle$, or the mean of all the means of an ensemble of all possible random but equivalent populations, and the associated variance. The movement of a solute body may be described by

FIGURE 2.28 Apparent longitudinal dispersivity from field and laboratory studies as a function of the scale of the study. Results from the calibration of numerical models are not included.



Source: S. Neuman. 1990. *Water Resources Research* 26:1749–1758. Copyright by the American Geophysical Union. Used with permission.

the motion of the center of mass of the body and the second-order spatial moment, or the moment of inertia (Dagan 1988). Hence, from the variance of the log transformed hydraulic conductivity distribution and the correlation length, a simple stochastic model allows predicting an asymptotic macrodispersivity value. However, it is important to note that the process of advective transport dominates macrodispersion. This means that whether one uses a deterministic model or a stochastic model, the large picture of solute transport will emerge, since both account primarily for advective transport, with the dispersion factor tending to smear the leading edge of the plume.

■ 2.14 Regression Analysis of Relationship between Apparent Longitudinal Dispersivity and Field Scale

Neuman (1990) plotted the apparent longitudinal dispersivity as measured in field and lab studies, α_m , as a function of the travel distance, L_s , or apparent length scale

(Figure 2.28). Dispersivities that are measured in the field were considered apparent dispersivities because they were obtained by calculations that depend upon the theory that the observer was using. Also, Neuman (1990) excluded for theoretical reasons all data with an apparent length scale greater than 3500 m (approximately 11,500 ft). Regression analysis showed that although the data are widely scattered, a best-fit line with narrow 95% confidence bands could be obtained. The equation for the line is

$$\alpha_m = 0.0175L_s^{1.46} \quad (2.47)$$

This line of best fit has a regression coefficient, r^2 , of 0.74, which means that it accounts for 74% of the variation about the mean. The other 26% may be due to experimental and interpretive errors or may represent deviation of the real system from that described by Equation 2.47. The 95% confidence intervals about the coefficient of 0.0175 are 0.0113 and 0.0272 and the 95% confidence intervals about the exponent of 1.46 are 1.30 and 1.61.

Equation 2.47 obtained by Neuman (1990) was based on data that he considered to be highly reliable. In doing so he discarded data that were less reliable, such as that obtained by the calibration of numerical models. Neuman recognized that as the flow path grew longer, the same equation relating apparent longitudinal dispersivity to field scale could not be used, so that he used two linear equations, one for flow distances less than 100m (328 ft) and one for flow distances greater than 100m (328 ft) (Equation 2.47). However, a discontinuity occurs in his method at 100m (328 ft); i.e., the two equations give different answers. Neuman and Di Federico (2003) demonstrated experimentally and theoretically that the scaling behavior of hydrogeologic variables is impacted strongly by their scale of spatial resolution.

Xu and Eckstein (1995) have overcome these problems by assigning different degrees of reliability to data: low, medium and high. They were then able to obtain a nonlinear relationship based on a regression analysis using all available data. The resulting equation had a correlation coefficient of 0.72, which is similar to that obtained by Neuman (1990) using only highly reliable data. Neuman (1990) also did not consider any data with a flow field longer than 3500m (~11,500 ft) because he did not consider it to be reliable, while Xu and Eckstein (1995) included these data.

The equation of Xu and Eckstein is:

$$\alpha_m = 0.83(\log L_s)^{2.414} \quad (2.48)$$

If one examines Figure 2.24, which includes data of low reliability, it appears that as the field scale increases, the rate of change of dispersion decreases. Being nonlinear as plotted on log-log paper, Equation 2.48 also has a decreasing rate of change of dispersion with increasing field scale. At a field scale of greater than a few thousand meters there is very little change in apparent dispersion with distance.

By analyzing jointly dispersivity values derived from models having variable scales of spatial resolution, Schulze-Makuch (2005) proposed a power law relationship that empirically best described the dispersivity data in regard to scale of measurement:

$$\alpha_L = cL^m$$

where c is a parameter characteristic for a geological medium, m is a scaling exponent, and L is the flow distance. The scaling exponent for consolidated and unconsolidated

geological media varied between 0.40 and 0.92, and 0.44 and 0.94, respectively. For example, an unconsolidated sandy aquifer: $c = 0.20$ and $m = 0.44$. For a distance of 100 m (328 ft), the longitudinal dispersivity value is $\alpha L = 1.6$ m. Similar equations exist for other types of aquifers. No upper bound on the relationships was apparent for a flow distance up to $\sim 10,000$ m (~ 6 miles) for all media except for granites where this relation currently can only be extended to a flow distance of 100 m (328 ft). However, the relationship proposed by Schulze-Makuch (2005) was criticized by Neuman (2006) for neglecting the spatial resolution scales of the models from which the dispersion data had been derived. A theoretical interpretation of the scaling behavior has been summarized in a nonmathematical way in the review paper of Neuman and Di Federico (2003).

■ 2.15 Deterministic Models of Solute Transport

Although workers in stochastic theory have asserted that the theoretical basis for the deterministic advective-dispersive solute transport equation is suspect except for long times and large distances (Anderson 1984), it has been used with a great deal of success in many field and model applications. Today, mathematical transport and fate modeling of contaminants in groundwater and soils has become an important tool for the interpretation of contaminated sites, the development of remedial strategies, and the human health risk assessment process.

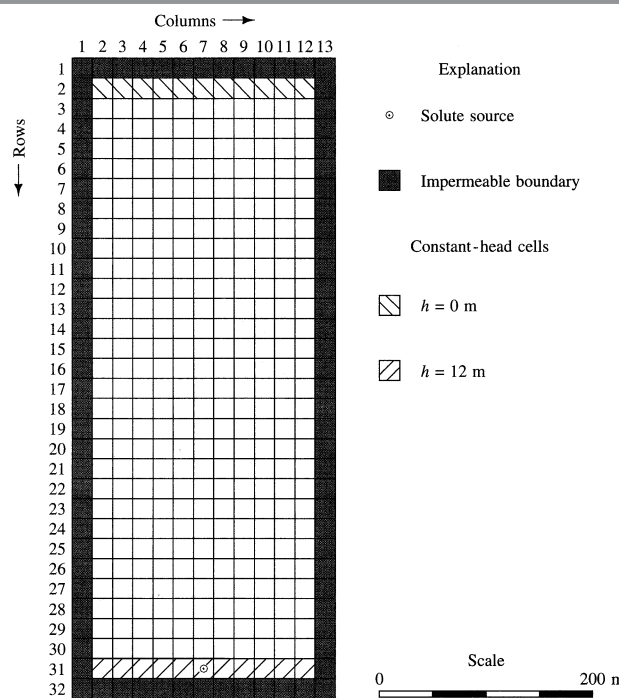
Over the past decades, many papers and textbooks have been written about deterministic models for contaminant transport modeling (e.g., Anderson and Woessner 1991; Zheng and Bennet 2002). In general, a deterministic mathematical model simulates groundwater flow and/or solute fate and transport indirectly by means of a set of governing equations, such as Darcy's law and law of mass conservation, thought to represent the physical processes that occur in the system (Anderson and Woessner 1991). The first step in the modeling process is to develop a conceptual model that is simpler than reality. Simplification can be achieved, for example, by combining strata with similar hydrogeologic properties into a single layer or aquifer. The next step requires translating the conceptual model into a mathematical model, which can then be solved in a computer simulation. A numerical mathematical model solves the underlying governing partial differential equations (PDEs) within a set of suitable boundary conditions, and if the transport problem is of transient nature, initial conditions. This step usually requires that additional simplifying assumptions have to be made to reduce the complexity of the mathematical model. For example, a coarser grid can be defined in parts of the flow domain where less accuracy is required, or fixed value boundaries (e.g., no-flux or constant head boundaries) can be defined, or the length of the simulation time steps can be manipulated to reduce the number of computations. These adjustments make the model amenable to either exact or numerical solution, but the modeler must weigh the risk of oversimplifying the flow domain against the problem of no longer reproducing the system adequately. A parsimonious model therefore is a model that accomplishes a desired level of explanation or prediction with the fewest predictor variables possible.

The flow and transport equations underlying the model are solved at discrete points within the flow domain. The two classical choices for the numerical solution of PDEs are the finite difference method (FDM) and the finite element method (FEM).

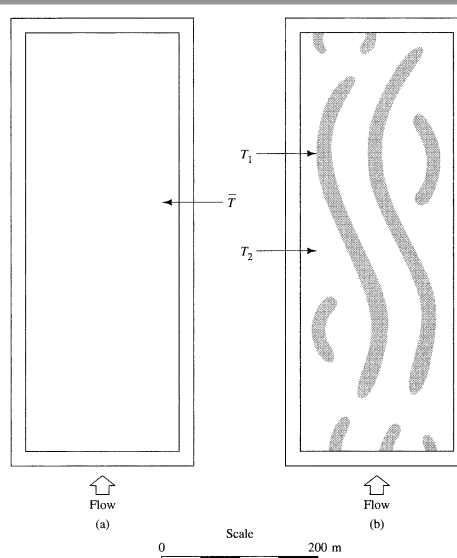
Other methods exists, such as the finite volume method (FVM) or the analytic element method (AEM), but models build around these numerical solution schemes are currently not used widely. A detailed discussion of numerical methods is beyond the scope of this textbook and the reader is referred to Peiro and Sherwin (2005).

The current standard FDM program is MODFLOW, which was developed by the U.S. Geological Survey (USGS) for three-dimensional flow modeling (McDonald and Harbaugh 1988). Over the years, many modules have been added to the MODFLOW program, including modules to simulate coupled groundwater/surface-water systems, solute transport, variable-density flow (including saltwater), aquifer-system compaction and land subsidence, parameter estimation, and groundwater management (USGS 2014). MODFLOW can be used in conjunction with MT3DMS, which is a 3D multi-species transport model (Zheng et al. 2010). MT3DMS solves the advection-dispersion-reaction equation based on the methods of characteristics, MOC (Konikow et al. 1994). The FDM model domain is subdivided or discretized into a grid of rectangular blocks or cells within which the physical properties of the domain are assumed to be homogeneous. The block structure of the FDM models often make them difficult to adopt to more complex modeling domains. Under those circumstances, FEM models provide greater flexibility in design because the modeling domain is discretized by triangular elements. Common FDM programs include SUTRA, a variable-density, variably-saturated flow, solute or energy transport model by the U.S. Geological Survey (2015a) or FEFLOW, a commercial modelling environment for subsurface flow, solute and heat transport processes. Another versatile commercial FVM model is HYDRUS 2D/3D, which also offers unsaturated flow modeling capabilities (Simunek et al. 1999; Simunek et al. 2006) and modeling of agricultural pollutants especially those from nonpoint source pollution stemming from plant and animal production (Simunek et al. 2013). There are many more noteworthy models available and many are in public domain. The U.S. Geological Survey maintains a website from which public domain software packages for the simulation of groundwater flow and transport can be downloaded (USGS 2015b).

A model study by Davis (1986) demonstrates that deterministic models can be developed that incorporate heterogeneities. He modeled two aquifers with identical boundary conditions (Figure 2.29). One was uniform (Figure 2.30(a)) and one had variable transmissivity in the form of more permeable channels (Figure 2.30b). The deterministic model, based on the two-dimensional solute-transport equation, was used with small values of α_L and a α_T , 0.0003 m (0.01 in), and 0.00009 m (0.003 in), respectively. The resulting solute plume in the uniform media is very long and narrow. See Figure 2.31(b). If larger values of α_L and α_T are used—3 m (10 ft) and 1 m (3 ft), respectively—then a much broader plume results. See Figure 2.31(a). However, if the heterogeneous aquifer is used with the small values of dispersivity, the resulting plume, shown in Figure 2.31(c) has a size very similar to that created in the uniform media by using large values of dispersivity. This demonstrates that if deterministic models include the aquifer heterogeneities, then it may be possible to use dispersivity values that are more on the order of lab-scale values. Davis (1986) used the advective-dispersion equation in a model with varying transmissivities and with a value of α_L of only 0.01 m (0.4 in) was able to reproduce a solute plume that extended over a flow length of about 500 m (1,640 ft). He found that a fine mesh for the finite-difference model grid was necessary for accurate results. Figure 2.32 compares the results of his model results with the field data.

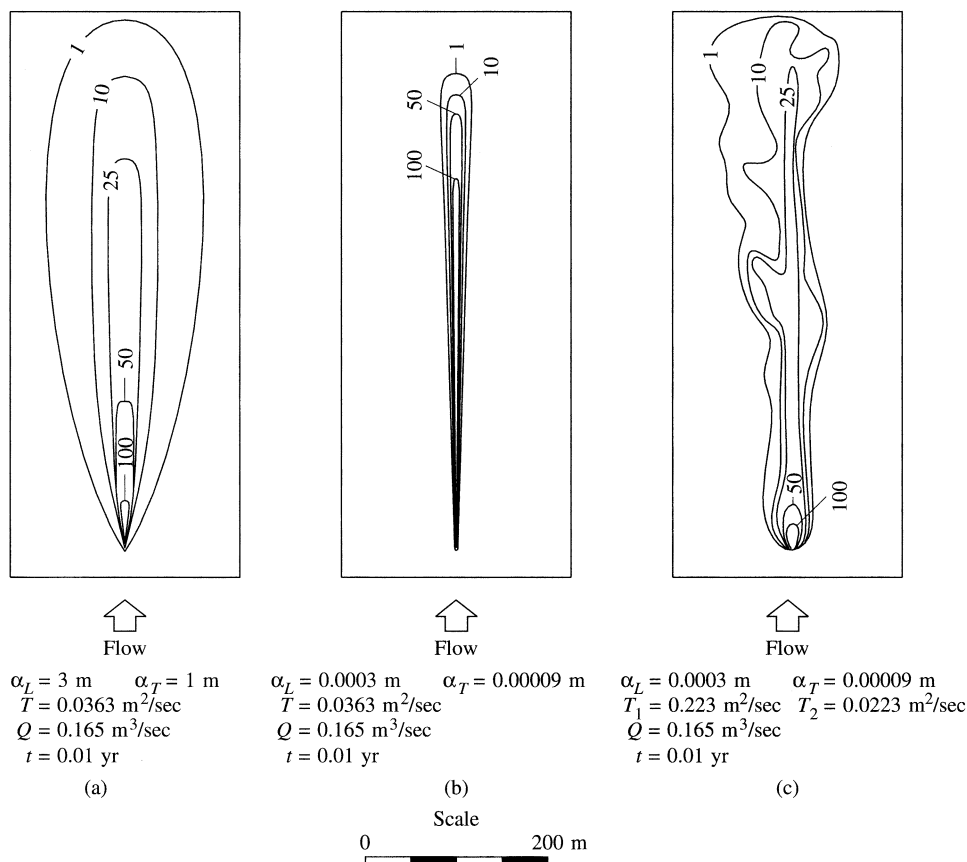
FIGURE 2.29 Finite-difference grid and boundary conditions for a deterministic model of solute transport.

Source: A. D. Davis. 1986. *Ground Water* 24:609–615. Used with permission. Copyright Ground Water Publishing Co.

FIGURE 2.30 Model areas for finite difference solute transport model with (a) uniform transmissivity and (b) with heterogeneous transmissivity.

Source: A. D. Davis. 1986. *Ground Water* 24:609–615. Used with permission. Copyright Ground Water Publishing Co.

FIGURE 2.31 Model results for finite-difference solute-transport model. (a) Uniform media with large dispersivity values, (b) uniform media with small dispersivity values, and (c) heterogeneous media with small dispersivity values.



Source: A. D. Davis. 1986. *Ground Water* 24:609–615. Used with permission. Copyright Ground Water Publishing Co.

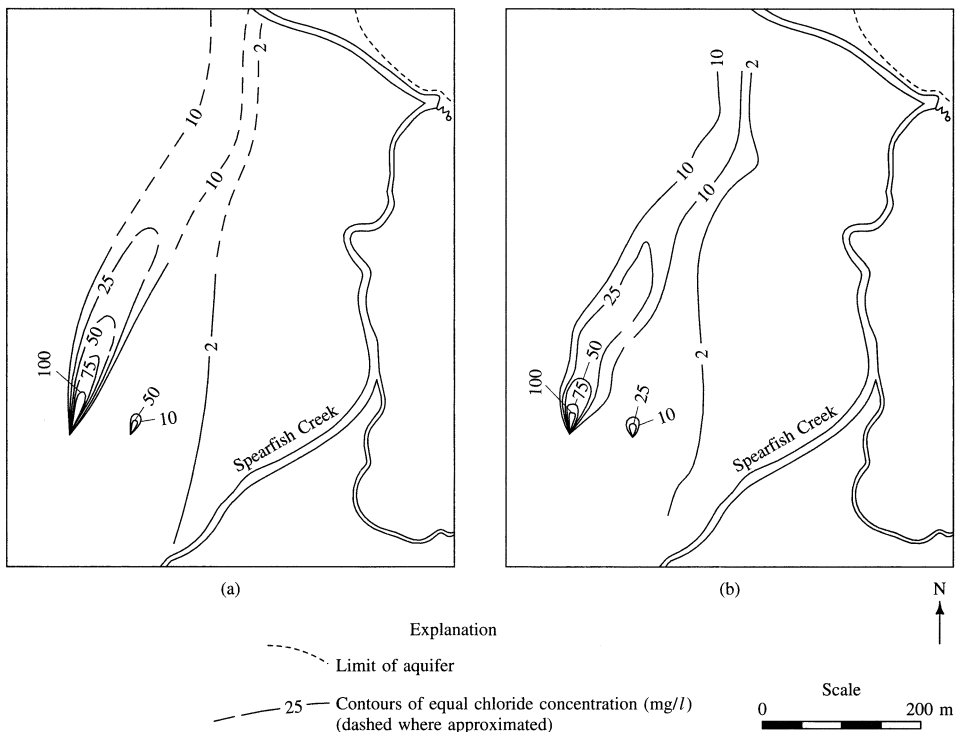
Case Study: Borden Landfill Plume

Probably the best known subsurface contaminant transport field test site is located on the Canadian Forces Base in Borden, Ontario (Sudicky and Illman 2011). An abandoned landfill in a shallow sand aquifer at Borden has been extensively studied (Cherry 1983; Macfarlane et al. 1983) and Frind and Hokkanen (1987) made a very interesting study of the plume based on a deterministic model.

The landfill was active from 1940 to 1976 and covers about 5.4 ha to a depth of 5 to 10 m (16 to 32 ft). Figure 2.33 shows the location of water table wells and multilevel sampling devices. The multilevel sampling devices are concentrated along the long axis of the plume of groundwater contamination. The vertical location of the sampling points along cross section A-A' are shown in Figure 2.34. The aquifer is about 20 m (65 ft) thick beneath the landfill and thins to about 9.5 m (31 ft) in the direction of groundwater flow. The aquifer consists of laminated fine to medium sand. An average hydraulic conductivity of $1.16 \times 10^{-2} \text{ cm/sec}$

horizontally and 5.8×10^{-4} cm/sec vertically was used in the model with a porosity of 0.38. In 1979 a very extensive study of the water quality of the plume was conducted. Figure 2.35 shows the plume of chloride contamination along cross section A-A'. In 1979 the plume extended about 750 m (2,460 ft) from the landfill and had sunk to the bottom of the aquifer and then moved laterally with the flowing groundwater. The sinking of the plume is believed to be caused by recharge concentrated in a sand pit to the north of the landfill, which is in the direction of flow.

FIGURE 2.32 Comparison of (a) field observations at solute plume in an aquifer and (b) solute plume as computed by finite-difference solute-transport model for a heterogeneous aquifer.



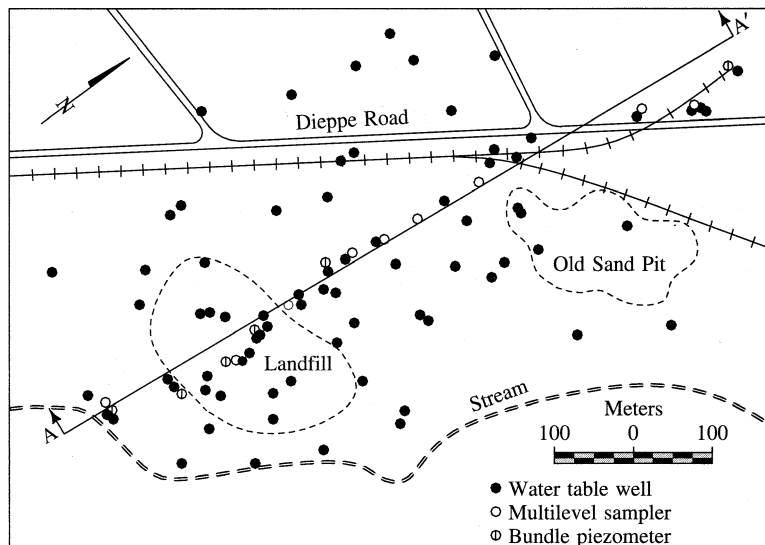
Source: A. D. Davis. 1986. *Ground Water* 24:609–615. Used with permission. Copyright Ground Water Publishing Co.

The finite-difference grid system for the cross-sectional model is shown in Figure 2.36. Equipotential lines for observed conditions were essentially vertical (Figure 2.37). The model was calibrated against the water-table contours for steady-state conditions.

Sensitivity analyses were performed to determine the impact of varying α_l and α_r . Field tests had indicated that the value of α_l at the site is on the order of 5 to 10 m (16 to 32 ft) (Sudicky et al. 1983). Figure 2.38 shows the sensitivity of the plume to the value of α_r . The value of α_l was kept at 10 m (32 ft) and α_r was varied from 0.005 m (0.02 in) to 1.0 m (3 ft). It can be seen that the shape of the plume is very sensitive to the value of α_r . With a high value of α_r , the plume spread through the entire vertical thickness of the aquifer, whereas with a low value it tended to sink toward the bottom. Figure 2.39 illustrates the fact that the

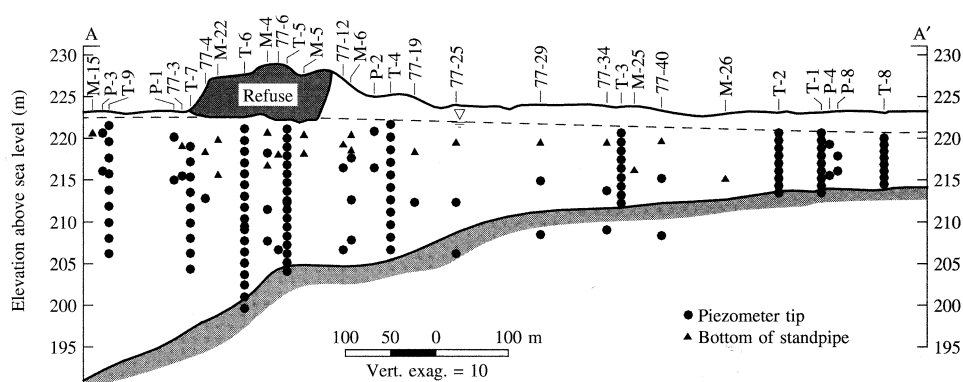
plume was not very sensitive to changes in the value of α_l over the range tested. The value of α_l was kept constant at 0.01 m (0.4 in), whereas α_v varied from 2.5 to 20 m (8 to 65 ft). This figure is slightly misleading in that there is a 10:1 vertical exaggeration, so that the vertical spreading is more obvious than the horizontal. Also, the value of α_v was varied by a factor of 200, whereas α_l was varied only by a factor of 8.

FIGURE 2.33 Location of landfill at Canadian Forces Base, Borden, Ontario, showing location of cross section and monitoring network.



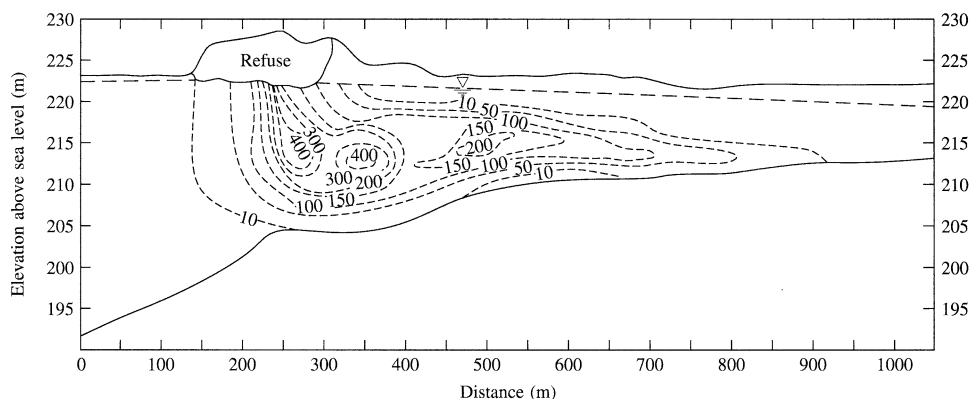
Source: E.O. Frind and G.E. Hokkanen. 1987. *Water Resources Research* 23:918–930. Copyright by the American Geophysical Union. Reproduced with permission.

FIGURE 2.34 Cross section of aquifer at the Border landfill showing the location of multilevel monitoring devices.



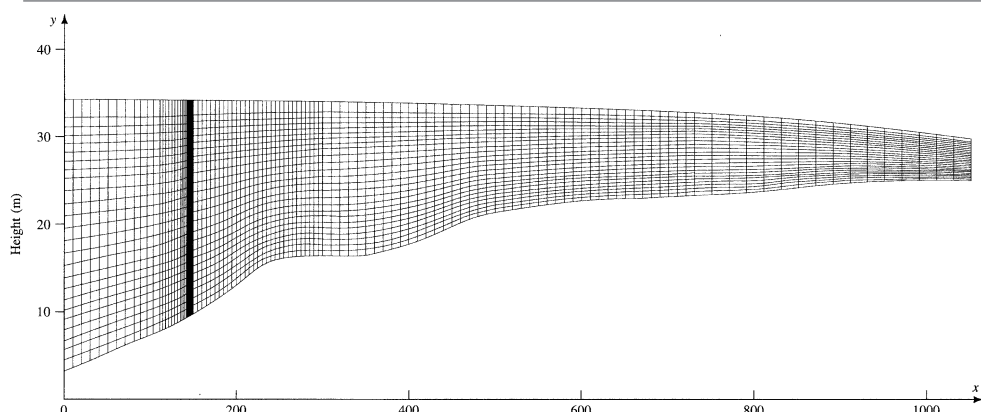
Source: E.O. Frind and G.E. Hokkanen. 1987. *Water Resources Research* 23:918–930. Copyright by the American Geophysical Union. Reproduced with permission.

FIGURE 2.35 Chloride plume along the Border landfill across section in 1979. Values are in milligrams per liter.



Source: E. O. Frind and G. E. Hokkanen. 1987. *Water Resources Research* 23:918–930. Copyright by the American Geophysical Union. Reproduced with permission.

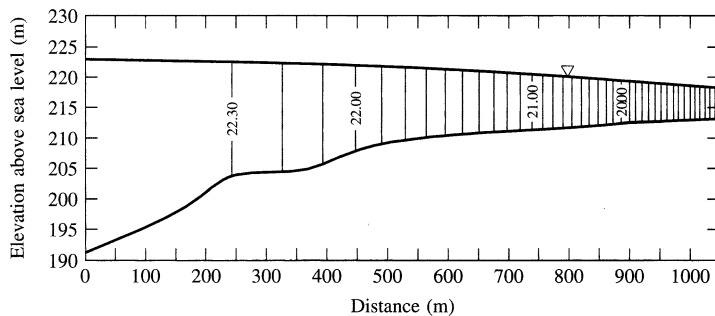
FIGURE 2.36 Finite-difference grid for Borden landfill solute transport model.



Source: E. O. Frind and G. E. Hokkanen. 1987. *Water Resources Research* 23:918–930. Copyright by the American Geophysical Union. Reproduced with permission.

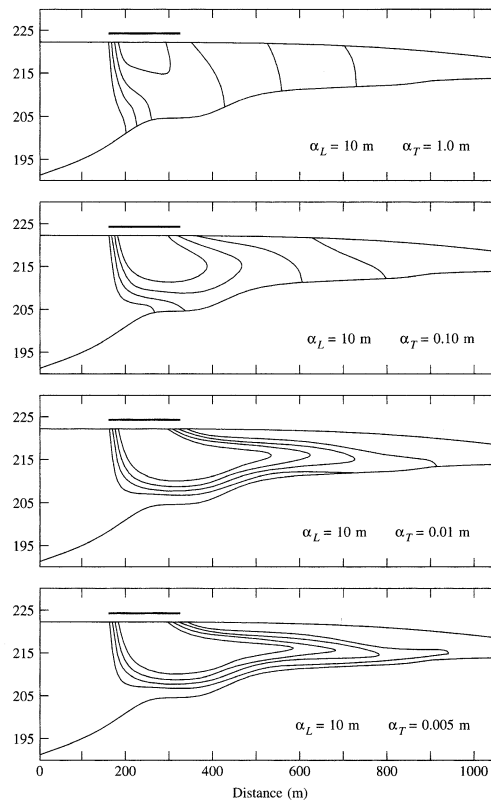
Additional sensitivity analyses were conducted with respect to the water table boundary conditions and the concentration, size, and growth pattern of the source. The authors found that in order to reproduce the observed distribution, a source history that included multiple periods of high concentration was needed. Figure 2.40(a) shows the shape of the observed plume, Figure 2.40(b) illustrates the shape of a plume generated by a source with a history in which the concentration gradually increased (smooth source concentration), and Figure 2.40(c) contains the computed plume with the best match to the observed plume. It was generated by a run of the model in which the source concentration had two different periods of peak concentration. Although the solution was not unique—that is, several different combinations of model inputs might yield the same output—the shape of the plume could be reproduced with good accuracy. This was especially true at the leading edge of the plume, which is the most important part from the standpoint of predicting the movement of the plume into uncontaminated areas of the aquifer.

FIGURE 2.37 Equipotential lines from the calibration of the Borden landfill solute-transport model; values in meters above datum.



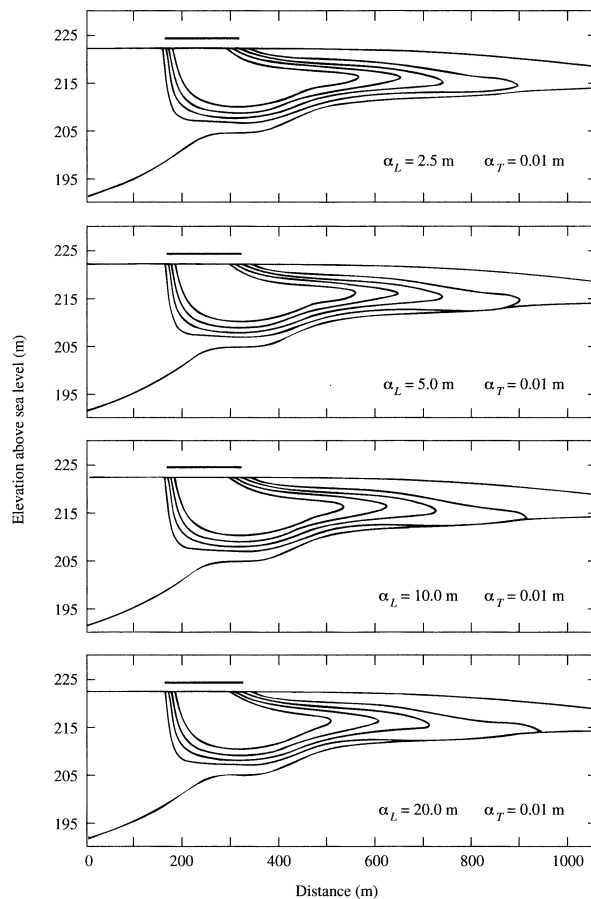
Source: E.O. Frind and G.E. Hokkanen. 1987. *Water Resources Research* 23:918–930. Copyright by the American Geophysical Union. Reproduced with permission.

FIGURE 2.38 Sensitivity analysis of the Borden landfill solute-transport model with respect to transverse dispersivity.



Source: E.O. Frind and G.E. Hokkanen. 1987. *Water Resources Research* 23:918–930. Copyright by the American Geophysical Union. Reproduced with permission.

FIGURE 2.39 Sensitivity analysis of the Borden landfill solute-transport model with respect to longitudinal dispersivity.



Source: E. O. Frind and G. E. Hokkanen. 1987. *Water Resources Research* 23:918–930. Copyright by the American Geophysical Union. Reproduced with permission.

■ 2.16 Transport in Fractured Media

Solute transport in fractured rock media is as important a process as transport in porous media. Understanding fluid flow and mass transport in fractured rocks is essential for assessing the groundwater resources of hard-rock aquifers and predicting the movement of hazardous chemicals if contamination occurs. Transport in fractured media is also important when assessing the suitability of underground sites for hazardous waste disposal, such as the heavily investigated former candidate site for a nuclear waste repository at Yucca Mountain in Nevada. However, less research has been done on this topic than on transport in porous media. One reason may be that existing theory of fluid flow through porous media is of limited usefulness when applied to fractured

rocks (USGS 2015c). The rock in which fractures exist is porous. Hence, fluid moves in the fractures as well as in the rock matrix. Solutes in the fractures can diffuse into the fluid contained in the rock matrix and vice versa (Neretnieks 1980; National Research Council 2015). The fractures themselves are not smooth channels but contain dead-end passages that hold nonmoving water into which solutes can diffuse (Raven et al. 1988).

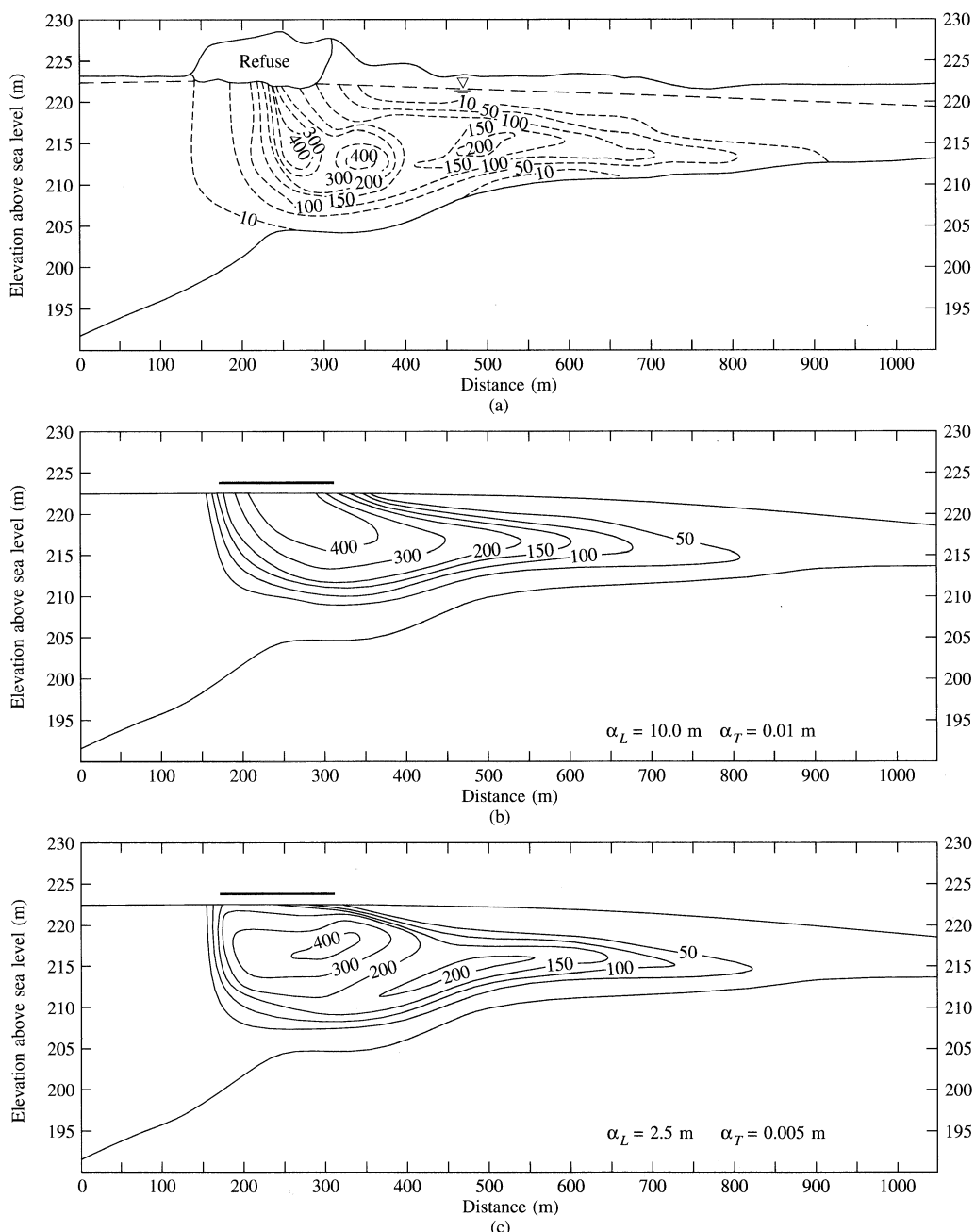
Berkowitz et al. (1988) suggested that solute transport in fractured media can be considered at a number of different scales. A very-near-field scale would be a single fracture near the source. A near-field scale would include a few fractures near the source. At a larger scale, the far field, the fracture network and the porous media matrix would have separate, discernible impacts on flow. At a very-far-field scale, which exists at considerable distance from the source, the entire flow domain can be considered as an equivalent porous medium in which the repeating fractures became large pores.

A number of different approaches to solute transport in fractured media have been attempted. These include analysis of transport in a single fracture in which effects of the transport in the fractures as well as interactions with a porous matrix are considered (e.g., Grisak and Pickens 1980; 1981; Tang et al. 1981; Rasmuson and Neretnieks 1981; Rasmussen 1984; Sudicky and Frind 1984). Sudicky and Frind (1982) and Barker (1982) examined transport in a media that consists of equally spaced fractures in a porous media. Endo and others (1984) made a deterministic study of flow in an irregular network of fractures contained in an impermeable host rock, whereas Schwartz et al. (1983) and Smith and Schwartz (1984) approached the same problem using a stochastic model. Berkowitz et al. (1988) and Schwartz and Smith (1988) examined the conditions under which the porous media matrix and the fractures can be considered to be a continuum that is representative of an equivalent porous media. Raven et al. (1988) made a field study of flow through a single fracture to test a model that incorporates the effects of nonflowing water in the fractures. Tsang et al. (1988) and Moreno et al. (1988) examine fracture flow on the basis of the assumption that most of the flow is concentrated in a few channels.

Dietrich et al. (2005) proposed a multi-continuum model in which separate, coupled hydraulic components in a heterogeneous aquifer are modeled. It is assumed that each component is distributed continuously in space and satisfies the condition of a porous medium (Bear and Bachmat 1990). For fracture matrix systems, this could be two fracture continua, such as a micro- and macro-fracture system, and a matrix continuum with appropriate equivalent parameters. The matrix and fractures are locally idealized as continua and the fractures are implemented discretely at their actual locations within the domain. It is obvious that the amount of data required to set up a discrete model of the actual domain is very large and to some extent not measureable. Consequently, the discrete model concept is preferentially used for relatively small domains and it is a suitable tool for principle studies of flow and transport processes (Dietrich et al. 2005).

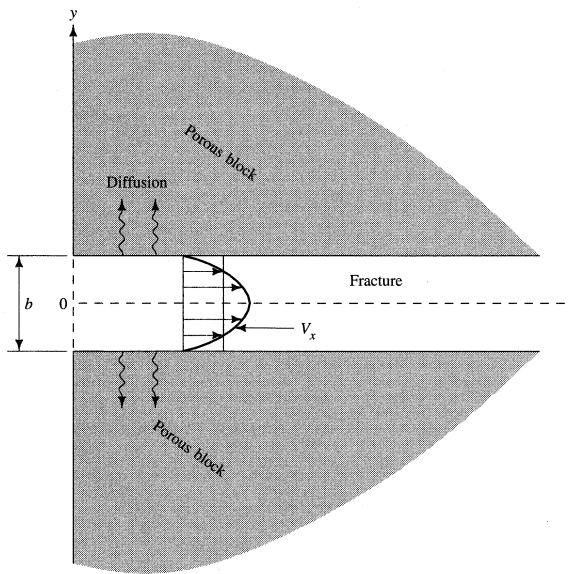
One of the first considerations in dealing with fracture flow is deciding how to treat flow in a single fracture. Some authors (e.g., Tang et al. 1981; Schwartz and Smith 1988) assume that the fluid in a fracture is all moving at a constant velocity. Conversely, Endo et al. (1984) treated flow in a fracture to be two-dimensional, with a parabolic velocity profile across the width of the fracture, as shown in Figure 2.41. Transport within a single fracture is due to advection, which occurs at different rates, depending upon the position between the parallel walls of the fracture, and molecular diffusion, both normal and parallel to the flow direction.

FIGURE 2.40 Comparison of (a) the observed chloride plume at the Borden landfill with (b) the chloride plume simulated by the solute transport model with a smooth source concentration and (c) the chloride plume simulated by the solute transport model with a doubly peaked source concentration.



Source: E.O. Frind and G.E. Hokkanen. 1987. *Water Resources Research* 23:918–930. Copyright by the American Geophysical Union. Reproduced with permission.

FIGURE 2.41 Horizontal distribution of flow in a vertical fracture and diffusion into the porous media matrix.



Hull et al. (1987) examined the conditions whereby diffusion within the fracture needs to be considered. In a fracture with parallel sides, the solute transport within the fracture is described by

$$\frac{\partial C}{\partial t} = D * \left(\frac{\partial^2 C}{\partial x^2} + \frac{\partial^2 C}{\partial y^2} \right) - 6V[(\tau) - (\tau)^2] \frac{\partial C}{\partial x} \quad (2.49)$$

where

V = average fluid velocity in a fracture

τ = fractional transverse position in a fracture

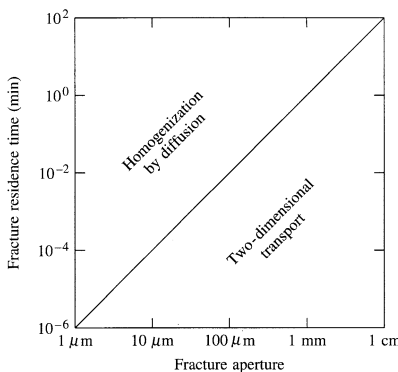
At high flow rates, advection will dominate and the concentration will follow the velocity profile of Figure 2.41. At low velocities, diffusion will be important, since the concentration gradient at the solute front will be high and the distance will be short. Under these conditions, diffusion will homogenize the solute across the width of the fracture.

If L is the length of the fracture between cross fractures and β is the aperture of the fracture, the fracture residence time is L/V . This can be compared with $(\beta/2)^2/D$ to determine if diffusion needs to be considered (Crank 1956). If diffusion induces a change in the tracer concentration of less than 2% over a distance of 10% of the width of the fracture, the diffusion can be considered negligible, and the residence time in the fracture will be

$$\frac{L}{V} < 0.003 \frac{(\beta/2)^2}{D} \quad (2.50)$$

If diffusion affects the tracer concentration to the extent that the tracer front is at 98% of the equilibrium value at all points across the fracture, the diffusion has homogenized the front, and the residence time in the fracture will be

FIGURE 2.42 Fracture residence time necessary for homogenization of the tracer across the fracture width by molecular diffusion.



Source: Modified from L.C. Hull, J.D. Miller, and T.M. Clemo. 1987. *Water Resources Research* 23:1505–1513. Copyright by the American Geophysical Union. Reproduced with permission.

$$\frac{L}{V} < 0.05 \frac{(\beta/2)^2}{D} \quad (2.51)$$

Figure 2.42 indicates the circumstances under which fracture flow can be considered to be one- or two-dimensional. Fracture residence time (L/V) is plotted against fracture aperture on this figure, which is based on a diffusion coefficient of $1.7 \times 10^{-9} \text{ m}^2/\text{sec}$ ($1.93 \times 10^{-8} \text{ ft}^2/\text{sec}$). The figure shows the conditions under which diffusion will homogenize the flow so that the transport within the fracture can be treated as one-dimensional (uniform conditions across the aperture). However, diffusion will still spread the tracer in advance of the advecting water. For even large fractures of 1mm aperture, this will occur with a residence time of 1min or more. This suggests that for most flow situations, one does not need to consider the velocity distribution across the fracture.

When the flow in a fracture is homogeneous, the mass transport can then be described by the one-dimensional advection-dispersion equation with the longitudinal dispersion coefficient equal to (Hull et al. 1987)

$$D_L = \frac{(V\beta)^2}{210D} \quad (2.52)$$

One approach to solute transport modeling is to determine the flux of water through the fractures and then use a numerical technique known as a random walk model to simulate diffusion of the solute (Hull et al. 1987). This ignores any diffusion into the porous media matrix. According to Witherspoon et al. (1980), flow through a fracture can be described by Darcy's law using an equivalent hydraulic conductivity for a fracture, K_f , given by

$$K_f = \frac{\rho g}{12\mu} \beta^2 \quad (2.53)$$

The quantity of flow, Q , can be found from the cubic law

$$Q = \frac{\rho g}{12\mu} I a \beta^3 \quad (2.54)$$

where

g = acceleration of gravity

I = hydraulic gradient along the fracture

a = width of the fracture—that is, the third dimension after length and aperture

μ = viscosity of fluid

If the velocity in the channel needs to be described in two dimensions, this can be done with three equations: one for the maximum velocity in the center of the fracture, one for the flow velocity profile across the aperture, and one for the vertical velocity profile in the fracture.

The maximum velocity can be found from (Hull et al. 1987):

$$V_x(\max) = \left[1.5 + 1.1664 \left(\frac{a}{\beta} \right)^{-1.0557} \right] V \quad (2.55)$$

The velocity profile across the aperture is given by.

$$V_x(y) = 4(\tau - \tau^2) \quad (2.56)$$

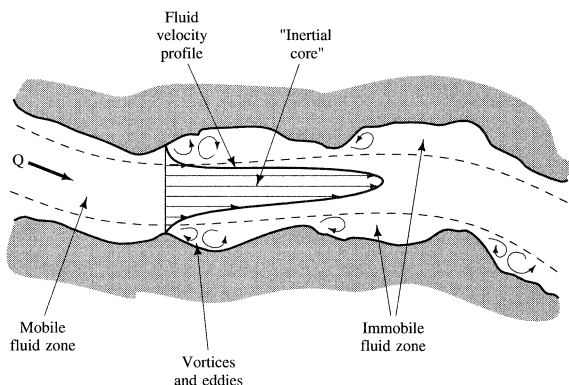
where τ = fractional transverse position in a fracture, y/β .

The vertical velocity profile is given by

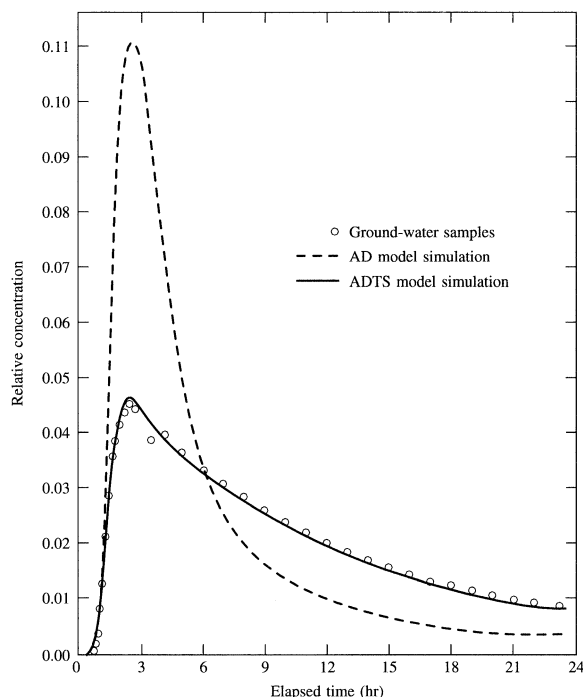
$$V_x(\zeta) = 15.56\zeta - 97.72\zeta^2 + 308\zeta^3 - 513\zeta^4 + 431\zeta^5 - 143.7\zeta^6 \quad (2.57)$$

where ζ = fractional vertical position in a fracture, z/a .

Raven et al. (1988) pointed out that the fractures through which flow occurs are not smooth, parallel plates but have irregular walls that promote the formation of zones along the edge of the fracture where the water is immobile (Figure 2.43). The fluid moves through the mobile zone, but the solutes can diffuse into the immobile fluid zones. The solute would be stored in the immobile fluid during the early part of solute transport and would be released from storage if the solute concentration in the mobile fluid would decrease—for example, as might happen during the latter part of a slug injection test. They derived an advection-dispersion equation for mass transport in the fracture with “transient solute storage in the immobile fluid zone (advection-dispersion transient storage model or ADTS). A field test was performed on the flow through a single fracture that had been isolated by packers in the borehole. Water was injected into one borehole and withdrawn from another. The water contained a tracer for the first few hours of the test, and then water without the tracer was again injected. Figure 2.44 contains circles representing the field data, in terms of relative concentration, plotted versus elapsed time. Also shown on this figure are the results of a conventional advection-dispersion (AD) model and an advection-dispersion transient storage (ADTS) model. Both models matched the observed data for the first few hours of the test. However, the ADTS model was far superior in matching the field data over the entire course of the test. The effect of transient storage was to reduce the peak concentration and to increase the concentrations above what would be produced by advection-dispersion alone during the later periods of the test.

FIGURE 2.43 Zones of mobile and immobile water in a fracture.

Source: K. G. Raven, K. S. Novakowski, and P. A. Lapcevic. 1988. *Water Resources Research* 24:2019–2032. Copyright by the American Geophysical Union. Reproduced with permission.

FIGURE 2.44 Comparison of field data from a tracer test in fractured rock with results of model simulation using an advection-diffusion (AD) model and an advection-diffusion transient storage (ADTS) model.

Source: K. G. Raven, K. S. Novakowski, and P. A. Lapcevic. 1988. *Water Resources Research* 24:2019–2032. Copyright by the American Geophysical Union. Reproduced with permission.

■ 2.17 Summary

Solutes dissolved in groundwater are transported in two ways. Diffusion will cause solutes to move in the direction of the concentration gradient—that is, from areas of higher to lower concentration. This transport can occur even if the groundwater is not flowing and may be the major factor in mass transport in geologic materials of very low permeability.

Solutes are also transported by the process of advection. This occurs as the flowing groundwater carries the dissolved solutes with it. At the scale of a few pore diameters, groundwater will move parallel to the flow path at different rates due to differences in pore size. This causes the solute plume to spread along the direction of the flow path, a process called longitudinal dispersion. The solute plume will also spread laterally as flow paths diverge around mineral grains, a process known as transverse dispersion. At the laboratory column scale, the movement of a contaminant through a uniform porous media can be described by the advection-dispersion equation, which accounts for advection, diffusion, and porescale dispersion.

In field-scale studies it has been found that the coefficient of longitudinal dispersion obtained from the advection-dispersion equation increases with the length of the flow path. This is due to the heterogeneous nature of aquifer materials. As the length of the flow path increases, the range of permeability values that affect the rate of groundwater flow also increases. This causes the resulting solute plume to spread out more and more. This can be called macrodispersion. An apparent diffusion coefficient can be statistically correlated with the length of the flow path by the expression $\alpha_m = 0.83(\log L_s)^{2 \times 414}$.

Stochastic methods of analysis have also been developed to analyze solute transport at the field scale. Stochastic methods are based on the variation in the hydraulic conductivity values because it is that variation that causes the solute plume to spread. The groundwater velocity depends upon the porosity as well as the hydraulic conductivity, but the hydraulic conductivity varies over a much greater range than porosity.

At the field scale the spreading due to hydraulic conductivity variation is much greater than that due to pore-scale dispersion. Both stochastic and advection-dispersion models demonstrate that the primary movement of the solute plume is due to advection. The stochastic model yields the movement of the center of mass of the solute plume from the average rate of movement of the groundwater. The variance of the solute concentration about the mean position, or the second spatial moment, is also obtained from stochastic models.

Chapter Notation

A	Cross-sectional area	$\langle C \rangle$	Ensemble mean concentration
a	Width of a fracture	c_o	Constant related to anisotropy
b	Aquifer thickness	d	Characteristic flow length for Peclet number, P
B	$[(v_x^2)/(2D_L)^2 + (v_y^2)/(4D_L D_T)]^{1/2}$	dh/dl	Hydraulic gradient
C	Solute concentration	D^*	Effective diffusion coefficient
C_i	Concentration at some point x and time t	D	Diffusion coefficient
C_0	Initial concentration, i.e. concentration at time 0	D_d	Molecular diffusion coefficient
C_R	Dimensionless solute concentration (C/C_0)	D_i	Coefficient of hydrodynamic dispersion in the i direction

D_L	Coefficient of longitudinal hydrodynamic dispersion	S_y^2	Variance of sampled values of Y
D_T	Coefficient of transverse hydrodynamic dispersion	t	Time
E	Euler number (0.577...)	t'	Dimensionless time (tU/ϵ_h)
E_i	Exponential integral	t_D	Dimensionless time $\left(\frac{V_x^2 t}{D_L}\right)$
f	Fractal dimension	t_R	Dimensionless time ($v_x t/L$)
F	Mass flux of solute per unit area per unit time	T	Tortuosity
g	Acceleration of gravity	T_f	Fractal tortuosity
G	Topological dimension	u	Average velocity of injection of water into a well
h	Hydraulic head	u	Fluctuation in the velocity vector
H	Separation of autocorrelation function	u_{ji}	Covariance
i	Decay constant	\bar{U}	$\langle V \rangle$ ensemble mean of velocity vectors
I	Hydraulic gradient along a fracture	U_i	Total volume of water injected into a well
J	Constant length	U_p	Cumulative volume of water withdrawn from a well
k	Lag in autocorrelation function	v_f	Velocity along a fractal flowpath
K	Hydraulic conductivity	v_x	Average linear velocity in the x direction
K_f	Equivalent hydraulic conductivity of a fracture	V	Average fluid velocity in a fracture
K_G	Geometric mean of hydraulic conductivity	\mathbf{V}	Velocity vector
K_0	Modified Bessel function of second kind and zero order	$\langle \mathbf{V} \rangle$	$\langle \mathbf{V} \rangle$ Ensemble mean of the velocity vectors
L	Straight-line distance between ends of a flowpath	$W[t, B]$	Hantush leaky well function
L_c	Length of a tortuous flowpath	x	Coordinate vector
L_f	Length of a fractal flowpath	x_f	Length of fractal flowpath
L_s	Straight-line length between ends of a fractal flowpath	(x_0, y_0)	Origin of an xy field
M	Total mass of solute	x_s	Straight-line distance
N	Number of units	\mathbf{X}'	Residual of the displacement of a particle
n	Porosity	$\langle \mathbf{X} \rangle$	$\langle \mathbf{X} \rangle$ Ensemble mean of the center of mass
n_e	Effective porosity	$X_j(t)$	Second spatial moment of the solute mass at time t and location j , l
P_e	Peclet number ($v_x L / D_L$)	\mathbf{X}_t	Total particle displacement
PV	Pore volume	\bar{Y}	Mean of sample values of Y
Q	Rate at which a tracer is being injected into an aquifer	Y_i	$\log K_i$
r	Radial distance to a well	Z_o	Constant related to a semivariogram
R	Length of well screen or open borehole	α	Dynamic dispersivity
R_f	Average frontal position of water injected into a well	α_L	Longitudinal dynamic dispersivity
r_Y	Autocorrelation of sampled values of Y	α_T	Transverse dynamic dispersivity
S_Y	Standard deviation of sampled values of Y	α_m	Apparent dispersivity
		β	Aperture of a fracture
		ϵ_h	Correlation length for horizontal hydraulic conductivity

ϵ_v	Correlation length for vertical hydraulic conductivity	ρ_Y	Autocorrelation of the population of Y
η	Fractal unit of measurement	σ_Y	Standard deviation of population of Y
η_c	Fractal cutoff limit	σ_Y^2	Variance of population of Y
γ_Y	Semivariogram of Y	τ	Fractional transverse position in a fracture
λ_Y	Correlation length of autocorrelation	τ_Y	Autocovariance
μ	Viscosity of a fluid	θ	Angle in polar coordinate system
\cdot_Y	Mean of population of Y	ξ	Fourier transform wave vector number
v	Hurst coefficient for fractal dimensions	ζ	Fractional vertical position in a fracture
ω	Coefficient related to tortuosity		
Ω	Anisotropy ratio (ϵ_v/ϵ_h)		
ρ	Density of a fluid		

References

- Anderson, M. P. 1979. Using models to simulate the movement of contaminants through groundwater flow systems. *Critical Reviews in Environmental Controls* 9:97–156.
- Anderson, M. P. 1984. “Movement of contaminants in groundwater: Groundwater transport—advection and dispersion.” In *Groundwater Contamination*, 37–45. Washington, DC: National Academy Press.
- Anderson, M. P. 1990. Aquifer heterogeneity—a geological perspective. *Proceedings, Fifth Canadian/American Conference on Hydrogeology*. National Water Well Association, pp. 3–22.
- Anderson, M. P., and W. W. Woessner. 1991. *Applied Groundwater Modeling: Simulation of Flow and Advective Transport*. San Diego, CA: Academic Press.
- Aris, R. 1956. On the dispersion of a solute in a fluid flowing through a tube. *Proceedings of The Royal Society of London* 235:67–77.
- Ayra, A. 1986. Dispersion and reservoir heterogeneity. Ph.D. Dissertation. University of Texas, Austin.
- Bachmat, Y., and J. Bear. 1987. On the concept and size of a representative elementary volume (REV). *Advances in Transport Phenomena in Porous Media* 128:3–20.
- Bakr, A. A. 1976. Effect of spatial variations of hydraulic conductivity on groundwater flow. Ph.D. Dissertation. New Mexico Institute of Mining and Technology, Socorro.
- Barker, J. A. 1982. Laplace transform solutions for solute transport in fissured aquifers. *Advances in Water Resources* 5:98–104.
- Bear, J. 1961. Some experiments on dispersion. *Journal of Geophysical Research* 66:2455–2467.
- Bear, J. 1972. *Dynamics of fluids in porous media*. New York: American Elsevier Publishing Company, 764 pp.
- Bear, J., and A. Verruijt. 1987. *Modeling Groundwater Flow and Pollution*. Dordrecht, Netherlands: D. Reidel Publishing Company, 414 pp.
- Bear, J., and A. H.-D. Cheng. 1990. “Modeling Groundwater Flow and Contaminant Transport.” In *Theory and Applications of Transport in Porous Media, Volume 23*. Reprint 2010. Springer, 396 pp.
- Bedient, P. B., H. S. Rifai, and C. J. Newell. 1994. *Ground Water Contamination: Transport and Remediation*. Englewood Cliffs, NJ: Prentice Hall.
- Berkowitz, B., J. Bear, and C. Braester. 1988. Continuum models for contaminant transport in fractured porous formations. *Water Resources Research* 24:1225–1236.
- Bierkens, M., and F. van Geer. 2014. Stochastic Hydrology. Lecture notes. Accessed October 3, 2015 at http://www.earthsurfacehydrology.nl/wp-content/uploads/2012/01/Syllabus_Stochastic-Hydrology.pdf
- Brigham, W. E. 1974. Mixing equations in short laboratory columns. *Society of Petroleum Engineers Journal* 14:91–99.
- Boving, T. B., and P. Grathwohl. 2001. Tracer diffusion coefficients in sedimentary rocks: Correlation to porosity and hydraulic conductivity. *Journal of Contaminant Hydrology* 53:85–100.
- Carman, P. C. 1997. Fluid flow through a granular bed. *Chemical Engineering Research and Design* 75: S32–S48.

- Cherry, J. A. 1983. Migration of contaminants in groundwater at a landfill: A case study. *Journal of Hydrology* 63:31–49.
- Crank, J. 1956. *The Mathematics of Diffusion*. New York: Oxford University Press.
- Cohen, R. M., and J. W. Mercer. 1993. *DNAPL site evaluation*. Boca Raton, FL: CRC Press, 384 pp.
- Dagan, G. 1988. Time-dependent macrodispersion for solute transport in anisotropic heterogeneous aquifers. *Water Resources Research* 24:1491–1500.
- Dagan, G., and S. P. Neuman. 2005. *Subsurface Flow and Transport: A Stochastic Approach*. New York: Cambridge University Press, 256 pp.
- Davis, S. N., G. M. Thompson, H. W. Bentley, and G. Stiles. 1980. Groundwater tracers—A short review. *Ground Water* 18:14–23.
- Davis, A. D. 1986. Deterministic modeling of dispersion in heterogeneous permeable media. *Ground Water* 24:609–615.
- De Josselin De Jong, G. 1958. Longitudinal and transverse diffusion in granular deposits. *American Geophysical Union* 39:67.
- Delgado, J. M. P. Q. 2007. Longitudinal and transverse dispersion in porous media. *Chemical Engineering Research and Design* 85:1245–1252.
- Dietrich, P., R. Helmig, M. Sauter, H. Hötzl, J. Köngeterand, and G. Teutsch. 2005. *Flow and Transport in Fractured Porous Media*. New York: Springer, 447 pp.
- Domenico, P. A., and F. W. Schwartz. 1998. *Physical and Chemical Hydrogeology, Second Edition*. Hoboken, NJ: Wiley & Sons, 506 pp.
- Endo, H. K., J. C. S. Long, C. R. Wilson, and P. A. Witherspoon. 1984. A model for investigating mechanical transport in fracture networks. *Water Resources Research* 20:1390–1400.
- Essaid, H. I., B. A. Bekins, and I. M. Cozzarelli. 2015. Organic contaminant transport and fate in the subsurface: Evolution of knowledge and understanding. Review Article. *Water Resources Research* 51:4861–4902.
- Farrell, D. A., and A. D. Woodbury. 1994. The 1978 Borden tracer experiment: Analysis of the spatial moments. *Water Resources Research* 30:3213–3223.
- Fetter, C. W., Jr. 1994. *Applied Hydrogeology, Third Edition*. New York: Prentice Hall.
- Freyberg, D. L. 1986. A natural gradient experiment on solute transport in a sand aquifer. II. Spatial moments and the advection and dispersion of nonreactive tracers. *Water Resources Research* 22:2031–2046.
- Freeze, R. A. 1975. A stochastic-conceptual analysis of one dimensional groundwater flow in a non-uniform homogeneous media. *Water Resources Research* 11:725–741.
- Freeze, R. A., and J. A. Cherry. 1979. *Groundwater*. Englewood Cliffs, NJ: Prentice Hall.
- Freeze, R., A. J. Massmann, L. Smith, T. Sperling, and B. James. 1990. Hydrogeological decision analysis: 1. A frame-work. *Ground Water* 28:738–766.
- Fried, J. J. 1975. *Groundwater Pollution*. Amsterdam: Elsevier Scientific Publishing Company.
- Frind, E. O., and G. E. Hokkanen. 1987. Simulation of the Borden plume using the alternating direction Galerkin technique. *Water Resources Research* 23:918–930.
- Garabedian, S. P., D. R. LeBlanc, L. W. Gelhar, and M. A. Celia. 1991. Large-scale natural gradient tracer test in sand and gravel, Cape Cod, Massachusetts, 2. Analysis of spatial moments for a nonreactive tracer. *Water Resources Research* 27:911–924.
- Gelhar, L. W. 1986. Stochastic subsurface hydrology from theory to applications. *Water Resources Research* 22:135S–145S.
- Gelhar, L. W., and C. L. Axness. 1983. Three-dimensional stochastic analysis of macrodispersion in aquifers. *Water Resources Research* 19:161–180.
- Gelhar, L. W., and M. A. Collins. 1971. General analysis of longitudinal dispersion in nonuniform flow. *Water Resources Research* 7:1511–1521.
- Ghüven, O., F. J. Molz, and J. G. Melville. 1984. An analysis of dispersion in a stratified aquifer, *Water Resources Research* 10:1337–1354.
- Gillham, R. W., E. A. Sudicky, J. A. Cherry, and E. O. Frind. 1984. An advection-diffusion concept for solute transport in heterogeneous unconsolidated geological deposits. *Water Resources Research* 20:369–378.
- Grisak, G. E., and Pickens, J. F. 1980. Solute transport through fractured media, 1. The effects of matrix diffusion. *Water Resources Research* 16:719–730.
- Grisak, G. E., and J. F. Pickens. 1981. An analytical solution for solute transport through fractured media with matrix diffusion. *Journal of Hydrology* 52:47–57.
- Grathwohl, P. 1998. *Diffusion in Natural Porous Media: Contaminant Transport, Sorption/Desorption and Dissolution Kinetics*. Boston, MA: Kluwer Academic Publishers.
- Goltz, M. N., and P. V. Roberts. 1987. Using the method of moments to analyze three-dimensional

- diffusion-limited solute transport from temporal and spatial perspectives. *Water Resources Research* 23:1575–1585.
- Grove, D. B., and W. A. Beetem. 1971. Porosity and dispersion constant calculations for a fractured carbonate aquifer using the two-well tracer method. *Water Resources Research* 7:128–134.
- Hill, R. 1963. Elastic properties of reinforced solids: Some theoretical principles. *Journal of Mechanics and Physics of Solids* 11:357–372.
- Hoopes, J. A., and D. R. F. Harleman. 1967. Dispersion in radial flow from a recharge well. *Journal of Geophysical Research* 72:3595–3607.
- Hull, L. C., J. D. Miller, and T. M. Clemo. 1987. Laboratory and simulation studies of solute transport in fracture networks. *Water Resources Research* 23, no. 8:1505–13.
- Klotz, D., K. P. Seiler, H. Moser, and F. Neumaier. 1980. Dispersivity and velocity relationship from laboratory and field relationships. *Journal of Hydrology* 45:169–184.
- Konikow, L. F., and D. W. Thompson. 1984. “Groundwater contamination and aquifer restoration at the Rocky Mountain Arsenal, Colorado.” In *Groundwater Contamination* 93–103. Washington, DC: National Academy Press.
- Konikow, L. F., G. E. Granato, and G. Z. Hornberger. 1994. *User’s Guide to Revised Method-of-Characteristics Solute-Transport Model (MOC-Version 3.1)*. U.S. Geological Survey Water Resources Investigations Report 94-4115, 63 p.
- Kuzmin, D. 2010. *A Guide to Numerical Methods for Transport Equations*. University Erlangen-Nuremberg. Accessed October 2, 2015 from <http://www.mathematik.uni-dortmund.de/~kuzmin/Transport.pdf>
- Lallemand-Barres, P., and P. Peaudcerf. 1978. Recherche des relations entre la valeur de la dispersivite macroscopique d’un milieu aquifere, ses autres caracteristiques et les conditions de mesure, etude bibliographique. *Bulletin, Bureau de Recherches Géologiques et Minières* 3/4:277–87.
- LeBlanc, D. R., S. P. Garabedian, K. M. Hess, L. W. Gelhard, R. D. Quadri, K. G. Stollenwerk, and W. W. Wood. 1991. Large-scale natural gradient tracer test in sand and gravel, Cape Cod, Massachusetts, 1. Experimental design and observed tracer movement. *Water Resources Research* 27:895–910.
- Leibundgut, C., P. Maloszewski, and C. Kulls. 2009. *Tracers in Hydrology*. West Sussex, UK: Wiley-Blackwell.
- MacFarlane, D. S., J. A. Cherry, R. W. Gillham, and E. A. Sudicky. 1983. Migration of contaminants in groundwater at a landfill: A case study, 1. Groundwater flow and plume definition. *Journal of Hydrology* 63:1–30.
- Mackay, D. M., D. L. Freyberg, P. V. Roberts, and J. A. Cherry. 1986. A natural gradient experiment on solute transport in a sand aquifer, 1. Approach and overview of plume movement. *Water Resources Research* 22:2017–2029.
- Marie, C., P. Simandoux, J. Pacsirsky, and C. Gaulier. 1967. Etude du Déplacement de fluides miscibles en milieu poreux statifié. *Revue de l’Institut Français du Pétrole* 22:272–294.
- Matheron, G., and G. de Marsily. 1980. Is transport in porous media always diffusive? A counterexample. *Water Resources Research* 16:901–917.
- McDonald, M. G., and A. W. Harbaugh. (1988). *A Modular Three-Dimensional Finite-Difference Groundwater Flow Model*. U.S. Geological Survey. Available from <https://pubs.usgs.gov/of/1983/0875/report.pdf>
- Mohr, T. K. G., J. A. Stickney, and W. H. DiGuiseppi. 2010. *Environmental Investigation and Remediation: 1,4-Dioxane and Other Solvent Stabilizers*. Boca Raton, FL: CRC Press.
- Moltyaner, G. L., and R. W. D. Killey. 1988. Twin Lake tracer test: Longitudinal Dispersion. *Water Resources Research* 24:1613–1627.
- Moltyaner, G. L., and R. W. D. Killey. 1991. Local- and plume-scale dispersion in the Twin Lake 40- and 260-m natural-gradient tracer tests. *Water Resources Research* 27:2007–2026.
- Molz, F. J., O. Guven, and J. G. Melville. 1983. An examination of scale-dependent dispersion coefficients. *Ground Water* 21:715–725.
- Moreno, L., Y. W. Tsang, C. F. Tsang, F. V. Hale, and I. Neretnieks. 1988. Flow and tracer transport in a single fracture: A stochastic model and its relation to some field observations. *Water Resources Research* 24:2033–2048.
- National Research Council. 2015. *Characterization, Modeling, Monitoring, and Remediation of Fractured Rock*. Washington, DC: National Academies of Sciences. Accessed October 5, 2015 from <http://www.nap.edu/21742>
- Neretnieks, I. 1980. Diffusion in the rock matrix: An important factor in radionuclide migration. *Journal of Geophysical Research* 85:4379–4397.
- Neuman, S. P. 1990. Universal scaling of hydraulic conductivities and dispersivities in geologic media. *Water Resources Research* 26:1749–1758.

- Neuman, S. P. 2006. Comment to Schulze-Makuch (2005) and reply. *Ground Water* 2:139–141.
- Neuman, S. P., and V. Di Federico. 2003. Multifaceted nature of hydrogeologic scaling and its interpretation. *Review of Geophysics* 41.
- Ogata, A. 1970. *Theory of dispersion in a granular medium*. U.S. Geological Survey Professional Paper 411-I.
- Ogata, A., and R. B. Banks. 1961. *A Solution of the Differential Equation of Longitudinal Dispersion in Porous Media*. U.S. Geological Survey Professional Paper 411-A.
- Olsen, L. D., and F. J. Tenbus. 2004. Design and analysis of a natural-gradient groundwater tracer test in a freshwater tidal wetland, West Branch Canal Creek, Aberdeen Proving Ground, Maryland. USGS Technical Report USGS-SIR-2004-5190.
- Perkins, T. K., and O. C. Johnson. 1963. A review of diffusion and dispersion in porous media. *Society of Petroleum Engineers Journal* 3:70–84.
- Pickens, J. F., R. E. Jackson, K. J. Inch, and W. F. Merritt. 1981. Measurement of distribution coefficients using a radial injection dual-tracer test. *Water Resources Research* 17:529–44.
- Pickens, J. F., and G. E. Grisak. 1981. Scale-dependent dispersion in a stratified granular aquifer. *Water Resources Research* 17:1191–1211.
- Pinder, G. 1973. A Galerkin-finite element simulation of groundwater contamination on Long Island, New York, *Water Resources Research* 9:1657–1669.
- Payne, F. C., J. A. Quinnan, and S. T. Potter. 2008. *Remediation Hydraulics*. Boca Raton, FL: CRC Press.
- Rasmussen, A. 1984. Migration of radionuclides in fissured rock: Analytical solutions for the case of constant source strength. *Water Resources Research* 20:1435–1442.
- Rasmussen, L., and I. Neretnieks. 1981. Migration of radionuclides in fissured rock: The influence of micropore diffusion and longitudinal dispersion. *Journal of Geophysical Research* 86:3749–3758.
- Raven, K. G., K. S. Novakowski, and P. A. Lapcevic. 1988. Interpretation of field tests of a single fracture using a transient solute storage model. *Water Resources Research* 24:2019–2032.
- Renshaw, C. 2015a. Plume1D(). Dartmouth College. Accessed October 2, 2015 from <http://www.dartmouth.edu/~renshaw/gwtools/functions/plume1d.html>
- Renshaw, C. 2015b. Plume2DSS(). Dartmouth College. Accessed October 2, 2015 <http://www.dartmouth.edu/~renshaw/gwtools/functions/plume2dss.html>
- Renshaw, C. 2015c. Leaky(). Dartmouth College. Accessed October 2, 2015 <http://www.dartmouth.edu/~renshaw/gwtools/functions/leaky.html>
- Robinson, R. A., and P. H. Stokes. 2002. *Electrolyte Solutions, Second Edition*. Mineola, NY: Dover Publications.
- Rubin, Y. 2003. *Applied Stochastic Hydrogeology*. New York: Oxford University Press.
- Sauty, J.-P. 1978. Identification des paramètres du transport hydrodispersif dans les aquifères par interprétation de tracages en écoulement cylindrique convergent ou divergent. *Journal of Hydrology* 39:69–103.
- Sauty, J.-P. 1980. An analysis of hydrodispersive transfer in aquifers. *Water Resources Research* 16:145–158.
- Schulze-Makuch, D. 2005. Longitudinal dispersivity data and implications for scaling behavior. *Ground Water* 3:443–456.
- Schwartz, F. W., and L. Smith. 1988. A continuum approach for modeling mass transport in fractured media. *Water Resources Research* 24:1360–1372.
- Schwartz, F. W., L. Smith, and A. S. Crowe. 1983. A stochastic analysis of macroscopic dispersion in fractured media. *Water Resources Research* 19:1253–1265.
- Simunek, J., M. Šejna, and M. Th. van Genuchten. 1999. The HYDRUS-2D software package for simulating two-dimensional movement of water, heat, and multiple solutes in variably saturated media. Version 2.0. U.S. Salinity Laboratory, Agricultural Research Service, U.S. Department Of Agriculture, Riverside, California. Available from http://www.pc-progress.com/downloads/pgm_hydrus2d/hydrus2d.pdf
- Simunek, J., M. Th. van Genuchten, and M. Šejna. 2006. The HYDRUS Software Package for Simulating Two- and Three-Dimensional Movement of Water, Heat, and Multiple Solutes in Variably-Saturated Media, Technical Manual, Version 1.0, PC Progress, Prague, Czech Republic.
- Simunek, J., D. Jacques, G. Langergraber, S. A. Bradford, M. Šejna, M. Th. van Genuchten. 2013. Numerical modeling of

- contaminant transport using HYDRUS and its specialized modules. *Journal of the Indian Institute of Science* 93:2.
- Smith, L., and F. W. Schwartz. 1984. An analysis of the influence of fracture geometry on mass transport in fractured media. *Water Resources Research* 20:1241–1252.
- Sudicky, E. A. 1986. A natural gradient experiment on solute transport in a sand aquifer: Spatial Variability of hydraulic conductivity and its role in the dispersion process. *Water Resources Research* 22:2069–2082.
- Sudicky, E. A., and J. A. Cherry. 1979. Field observations of tracer dispersion under natural flow conditions in an unconfined sandy aquifer. *Water Pollution Research, Canada* 14:1–17.
- Sudicky, E. A., J. K. Cherry, and E. O. Frind. 1983. Migration of contaminants in groundwater at a landfill: A case study, 4, A natural gradient dispersion test. *Journal of Hydrology* 63:81–108.
- Sudicky, E. K., and E. O. Frind. 1982. Contaminant transport in fractured porous media: Analytical solution for a system of parallel fractures. *Water Resources Research* 18:1634–1642.
- Sudicky, E. K., and E. O. Frind. 1984. Contaminant transport in fractured porous media: Analytical solution for a two-member decay chain in a single fracture. *Water Resources Research* 20:1021–1029.
- Sudicky, E. A., and W. A. Illman. 2011. Lessons learned from a suite of CFB Borden experiments (Review Paper). *Ground Water* 49:630–648.
- Suthersan, S., C. Divine, E. Cohen, K. Heinze. 2014. Tracer testing: Recommended best practice for design and optimization of in situ remediation systems. *Groundwater Monitoring and Remediation* 34:33–40.
- Tang, D. H., E. O. Frind, and E. A. Sudicky. 1981. Contaminant transport in fractured porous media: Analytical solution for a single fracture. *Water Resources Research* 17:555–564.
- Tsang, Y. W., C. F. Tsanf, I. Neretnieks, and L. Moreno. 1988. Flow and tracer transport in fractured media: A variable aperture channel model and its properties. *Water Resources Research* 24:2049–2060.
- U.S. EPA. 1985. An Introduction to groundwater tracers. EPA/600/205/022. 219 pp.
- U.S. EPA. 2015. On-line Tools for Site Assessment Calculation. Accessed October 3, 2015 from <http://www3.epa.gov/ceampubl/learn2model/part-two/onsite/>
- U.S. Geological Survey (USGS). 2014. MODFLOW and Related Programs. Accessed October 3, 2015 from <http://water.usgs.gov/ogw/modflow/index.html>
- U.S. Geological Survey (USGS). 2015a. SUTRA and related programs (Sutra Suite). Accessed October 3, 2015 from <http://water.usgs.gov/nrp/gwsoftware/sutra.html>
- U.S. Geological Survey (USGS). 2015b. Water Resources Groundwater Software. Accessed October 3, 2015 from <http://water.usgs.gov/software/lists/groundwater>
- U.S. Geological Survey (USGS). 2015c. Hydrology of fractured rocks. Accessed October 3, 2015 from <http://water.usgs.gov/nrp/proj.bib/hsieh.html>
- Valocchi, A. J. 1989. Spatial moment analysis of the transport of kinetically adsorbing solutes through stratified aquifers. *Water Resources Research* 25:273–270.
- Valocchi, A. J. 1990. Use of temporal moment analysis to study reactive solute transport in aggregated porous media. *Geoderma* 46:233–247.
- Van Genuchten, M. Th. 1981. Analytical solutions for chemical transport with simultaneous adsorption, zero-order production, and first-order decay. *Journal of Hydrology* 49:213–233.
- Witherspoon, P. A., J. S. Y. Yang, K. Iwai, and J. E. Gale. 1980. Validity of the cubic law for fluid flow in a deformable rock fracture. *Water Resources Research* 16:1016–1024.
- Xu, M., and Y. Eckstein. 1995. Use of weighted leastsquares method in evaluation of the relationship between dispersivity and field scale. *Ground Water* 33:905–908.
- Yeh, T.-C., R. Khaleel, and K. C. Carroll. 2015. *Flow through Heterogeneous Geologic Media*. New York: Cambridge University Press.
- Zhang, D. 2001. *Stochastic Methods for Flow in Porous Media: Coping with Uncertainties*. San Diego, CA: Academic Press.
- Zheng, C., and G. D. Bennet. 2002. *Applied Contaminant Transport Modeling, Second Edition*. Hoboken, NJ: Wiley-Interscience.
- Zheng, C., J. Weaver, and M. Tonkin. 2010. *MT3DMS - A Modular Three-dimensional Multispecies Transport Model User Guide to the Hydrocarbon Spill Source (HSS) Package*. Athens, GA: U.S. Environmental Protection Agency.

Problems

- 2.1 Assume that a solute has a D^* of $2.03 \times 10^{-9} \text{ m}^2/\text{sec}$ and that ω is equal to 0.5. If landfill leachate with a chloride concentration is next to a clay liner that is 2 m thick and the concentration of chloride is 2315 mg/L, what would be the chloride concentration at the outside of the liner after 50 years of diffusion. Ignore any effects of advection.
- 2.2 Assume that a solute has a D^* of $1.07 \times 10^{-9} \text{ m}^2\text{s}^{-1}$ and that ω is equal to 0.5. If landfill leachate with a sulfate concentration of 510 mg/L is next to a clay liner that is 1.35 m thick, what would be the sulfate concentration at the outside of the liner after 25 years of diffusion. Ignore any effects of advection.
- 2.3 An aquifer that is fed by infiltrating rainfall that falls on fertilized fields has 32.5 mg/L nitrate. The nitrate is being carried by flowing groundwater into a fish pond the farmer has constructed on the property. The average linear velocity of the flowing groundwater is 0.124 m/day and the aquifer porosity is 0.332. The aquifer has a saturated thickness of 3.1 m and the flow path into the pond is 123 m wide. What is the mass loading of nitrate into the pond?
- 2.4 An aquifer that is fed by infiltrating rainfall that falls on fertilized fields has 1.25 mg/L dissolved phosphate. The phosphate is being carried by flowing groundwater into a reach of a stream that contains trout. The average linear velocity of the flowing groundwater is 0.087 m/day and the aquifer porosity is 0.245. The aquifer has a saturated thickness of 2.55 m and the flow path into the stream is 87 m wide. What is the mass loading of nitrate into the stream?
- 2.5 A canal is leaking into an aquifer. The water in the canal is suddenly polluted by the new discharge of an industrial waste that contains a nondegradable organic compound called 1,4-dioxane in concentrations of 1.245 mg/L. The aquifer has an average linear groundwater velocity of 0.544 m/day. What is the concentration of 1,4-dioxane at a distance of 25 m from the canal at a time 45 days after the new discharge?
- 2.6 An industrial sewer pipe at a metal refining plant is leaking into an aquifer. The refining process is changed so that water in the sewer pipe begins to carry hexavalent chromium in concentrations of 235 mg/L. The aquifer has an average linear groundwater velocity of 0.023 m/day. What is the concentration of chromium at a distance of 34 m from the pipe at a time 5 years after the new discharge?
- 2.7 During the investigation of a contaminated site a large tank which was used to store water pumped from a contaminated aquifer leaks. The tank, which had been placed downgradient of the area of contamination where the underlying aquifer was not contaminated suddenly leaked all of the contents. The water in the tank had a concentration of 23.4 mg/L of trichloroethane. The tank was round with a diameter of 5m. The spill was located under the tank and saturated the aquifer. The aquifer had an average linear groundwater velocity of 0.033 m/day. Assume that the tank was centered on a grid at location $x = 0$ and $y = 0$. There is a monitoring well located downgradient at $x = 7.4$ m and $y = 1.1$ m. The transverse dispersivity is assumed to be 10% of the longitudinal

dispersivity. What will the concentration of TCA be in the monitoring well 120 days after the leak?

- 2.8** A train derails and a tank car leaks its contents onto the ground. The car is carrying phenol. When the phenol reaches the water table it has a concentration of 189 mg/L. There is a private well located 22 m directly downgradient from the location of the spill. The area of the spill is 115 m². The average linear groundwater velocity is 0.125 m/day. What would the concentration of phenol be in the private well after 255 days? Assume D_T is 10% of D_L .
- 2.9** With reference to the problem in 2.7, where would the center of mass be at the end of the 120 day period? How far would the leading edge of the plume have advanced beyond the center of mass? How wide would the plume be?
- 2.10** With reference to the problem in 2.8, where would the center of mass be at the end of the 255 day period? How far would the leading edge of the plume have advanced beyond the center of mass? How wide would the plume be?
- 2.11** A one-dimensional column test was conducted on a sediment sample. Deionized water was drained through the column until it came to a steady-state condition. A saline solution at a concentration of 200 mg/L was then passed through the column. The length of the column was 0.50 m. The seepage velocity was 0.0005m/sec. After 500 seconds the water eluting from the column had 2.0 mg/L of chloride, after 770 seconds it was 40 mg/L, after 1350 seconds it was 170 mg/L and after 1830 seconds it was 196 mg/L. Calculate the value of D_L and α_L for the soil in the column.
- 2.12** A metal plating company has been discharging plating waste which contains hexavalent chromium (Cr^{+6}) into an on-site dry well for many years. The waste solution has a chromium concentration of 35 mg/L and the amount being discharged amounts to 3.45 cubic meters per day. The groundwater velocity is 0.012 m/day. What is the concentration of chromium in a downgradient private well located in the same thin aquifer at location $x = 34.0$ m and $y = 6.23$ m? Assume a value for b .
- 2.13** A manufacturing facility that manufactures printed circuit boards puts wash water that was used to wash solvents from the circuit boards into a septic tank which discharges into groundwater. The wash water contains 7.34 mg/L of dissolved trichloroethylene (TCE). The daily rate of discharge is 13.6 m³/day. The underlying aquifer has an average linear groundwater velocity of 0.34 m/day. The discharge has been going on long enough so that steady state conditions have been reached. Assuming no degradation of the TCE, what is the concentration at a monitoring well located 22 meters downgradient of the septic tank discharge ($x = 22$ m, $y = 0$ m)? Assume a value for b .
- 2.14** A leaking underground tank contains water with 14,500 µg/L of 1, 1, 1-trichloroethane (TCA). The tank is leaking at a rate of 0.11 m³/day. The groundwater beneath the site is moving at an average linear velocity of 0.125 m/day through an aquifer that is 1.72 m thick. What would the concentration of TCA be in a monitoring well located at a position $x = 23.5$ m and $y = 1.56$ m after 125 days of leaking? Assume that α_T is 0.20 α_L .

Transformation, Retardation, and Attenuation of Solutes

■ 3.1 Introduction

Solutes dissolved in groundwater are subject to a number of different processes through which they can be transformed or removed from the groundwater. They can be sorbed onto the surfaces of the mineral grains of the aquifer, sorbed by organic carbon that might be present in the aquifer, undergo chemical precipitation, be subjected to abiotic as well as biodegradation, and participate in oxidation-reduction reactions. Furthermore, radioactive compounds can decay. As a result of sorption processes, some solutes will move much more slowly through the aquifer than the groundwater that is transporting them; this effect is called **retardation**. Biodegradation, radioactive decay, and precipitation will decrease the concentration of solute in the plume but may not necessarily slow the rate of plume movement.

Equation 2.18, the one-dimensional advection-dispersion equation, can be expanded to include sorption and decay. This can be conceptualized as (Miller and Weber 1984):

$$\frac{\partial C}{\partial t} = D_L \frac{\partial^2 C}{\partial x^2} - v_x \frac{\partial C}{\partial x} - \frac{\rho_b}{\theta} \frac{\partial C^*}{\partial t} + \left(\frac{\partial C}{\partial t} \right)_{rxn}$$

(dispersion) (advection) (sorption) (reaction) (3.1)

where

C = concentration of solute in liquid phase [M L⁻³]

t = time [T]

D_L = longitudinal dispersion coefficient [L² T]

v_x = average linear groundwater velocity [L T⁻¹]

ρ_b = bulk density of aquifer [M M⁻³]

θ = volumetric moisture content or porosity for saturated media [-]

C^* = amount of solute sorbed per unit weight of solid [M M⁻³]

rxn = subscript indicating a biological or chemical reaction of the solute
(other than sorption)

The first term on the right side of Equation 3.1 represents the dispersion of the solute, the second term is the advection of the solute, the third term is the transfer of the solute from the liquid phase to the solid particles by sorption, and the last term simply indicates that there may be a change in concentration of the solute with time due to biological or chemical reactions or radioactive decay.

■ 3.2 Classification of Chemical Reactions

Rubin (1983) listed six different classes of chemical reactions that can occur in solute transport. At the highest, or A, level, reactions are either (1) “sufficiently fast” and reversible or (2) “insufficiently fast” and/or irreversible. Sufficiently fast reactions are reversible reactions that are fast relative to groundwater flow rates and are faster than any other reactions that act to change solute concentration. With these reactions one can assume that locally the solute is in chemical equilibrium with the surroundings (local equilibrium assumption, or LEA system). If the reaction is not sufficiently fast for local equilibrium to develop or if it is irreversible, then it falls into the second major grouping.

At the second, or B, level reactions are either (1) homogeneous or (2) heterogeneous. Homogeneous reactions take place within a single phase, the dissolved phase, whereas heterogeneous reactions involve both the dissolved phase and the solid phase. Level C reactions, representing the greatest specification, apply only to heterogeneous reactions. These can be either (1) surface reactions, such as hydrophobic adsorption of neutral organic compounds and ion exchange of charged ions, or (2) classical chemical reactions such as precipitation and dissolution.

■ 3.3 Sorption Processes

Sorption processes include adsorption, chemisorption, absorption, and ion exchange. **Adsorption** includes the processes by which a solute clings to a solid surface. Cations may be attracted to the region close to a negatively charged clay-mineral surface and held there by electrostatic forces; this process is called **cation exchange**. Anion exchange can occur at positively charged sites on iron and aluminum oxides and the broken edges of clay minerals. **Chemisorption** occurs when the solute is incorporated on a sediment, soil, or rock surface by a chemical reaction. **Absorption** occurs when the aquifer particles are porous so that the solute can diffuse into the particle and be sorbed onto interior surfaces (Wood, Kramer, and Hem 1990).

In this chapter we will not attempt to separate these phenomena but will simply use the term *sorption* to indicate the overall result of the various processes. From a practical view the important aspect is the temporary or permanent removal of the solute from solution, irrespective of the process. The process by which a contaminant, which was originally in solution, becomes distributed between the solution and the solid phase is called **partitioning**.

Sorption is determined experimentally by measuring how much of a solute can be sorbed by a particular sediment, soil, or rock type. Aliquots of the solute in varying concentrations are well mixed with the solid, and the amount of solute removed is determined. The capacity of a solid to remove a solute is a function of the concentration of the solute. The results of the experiment are plotted on a graph called an

isotherm, which shows the solute concentration versus the amount sorbed onto the solid. If the sorptive process is rapid compared with the flow velocity, the solute will reach an equilibrium condition with the sorbed phase. This process can be described by an **equilibrium sorption isotherm**. It is an example of a sufficiently fast, heterogeneous surface reaction. If the sorptive process is slow compared with the rate of fluid flow in the porous media, the solute may not come to equilibrium with the sorbed phase, and a **kinetic sorption model** will be needed to describe the process. These are insufficiently fast, heterogeneous surface reactions. Limousin et al. (2007) or Matott et al. (2015) give comprehensive reviews of sorption isotherms and kinetic models.

■ 3.4 Equilibrium Surface Reactions

3.4.1 Linear Sorption Isotherm

If there is a direct, linear relationship between the amount of a solute sorbed onto solid, C^* , and the concentration of the solute, C , the adsorption isotherm of C as a function of C^* will plot as a straight line (Figure 3.1). The resulting linear sorption isotherm is described by the equation

$$C^* = K_d C \quad (3.2)$$

where

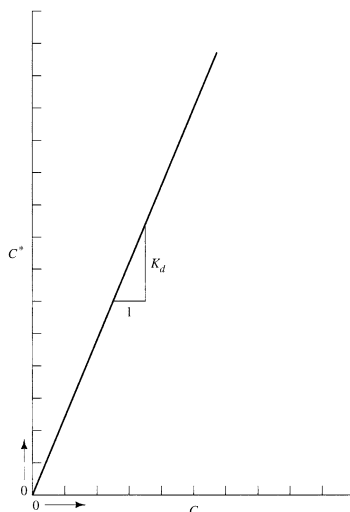
C^* = mass of solute sorbed per dry unit weight of solid (mg/kg)

C = concentration of solute in solution in equilibrium with the mass of solute sorbed onto the solid (mg/L)

K_d = coefficient (L/kg)

The coefficient K_d is known as the **distribution coefficient**. It is equal to the slope of the linear sorption isotherm.

FIGURE 3.1 Linear sorption isotherm with C^* versus C plotting as a straight line.



The linear sorption isotherm is very appealing from the standpoint of mathematical manipulation. If Equation 3.2 is substituted into Equation 3.1, the resulting advection-dispersion equation is

$$\frac{\partial C}{\partial t} = D_L \frac{\partial^2 C}{\partial x^2} - v_x \frac{\partial C}{\partial x} - \frac{\rho_b}{\theta} \frac{\partial (K_d C)}{\partial t} \quad (3.3)$$

This can be reorganized as

$$\frac{\partial C}{\partial t} \left(1 + \frac{\rho_b}{\theta} K_d \right) = D_L \frac{\partial^2 C}{\partial x^2} - v_x \frac{\partial C}{\partial x} \quad (3.4)$$

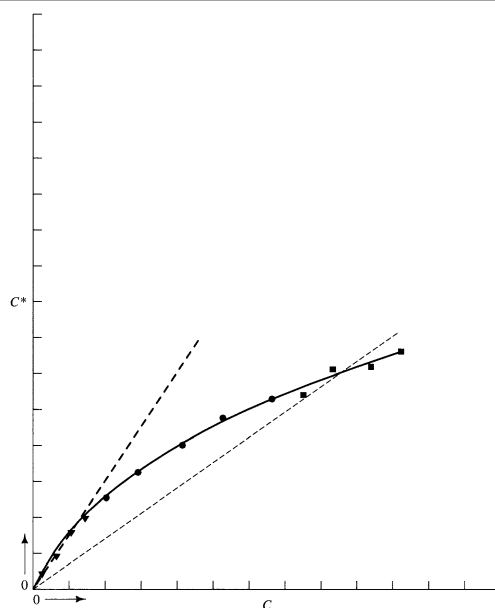
What has been termed the **retardation factor**, R is given by

$$1 + \frac{\rho_b}{\theta} K_d = R \quad (3.5)$$

If the average linear groundwater velocity is v_x , the average velocity of the solute front where the concentration is one-half of the original, v_c , is given by

$$v_c = \frac{v_x}{R} \quad (3.6)$$

FIGURE 3.2 Nonlinear sorption isotherms can be misinterpreted as linear sorption isotherms if a small data set is extrapolated out of its range. The subset of the data represented by triangles can be interpreted as a linear sorption isotherm, as can the data subset consisting of squares. However, if the complete data set, which includes the triangles, circles, and squares, is used, it can be seen that the isotherm is nonlinear. This example speaks to the necessity of carefully planning an isotherm sorption experiment, i.e., the number of data points must be sufficiently large and must cover the expected concentration range in the system under investigation.



Equations 3.3 through 3.6 are convenient to solve mathematically and have been used in a number of studies to predict the rate of movement of a solute front (e.g., Srinivasan and Mercer 1988; Boving 2014).

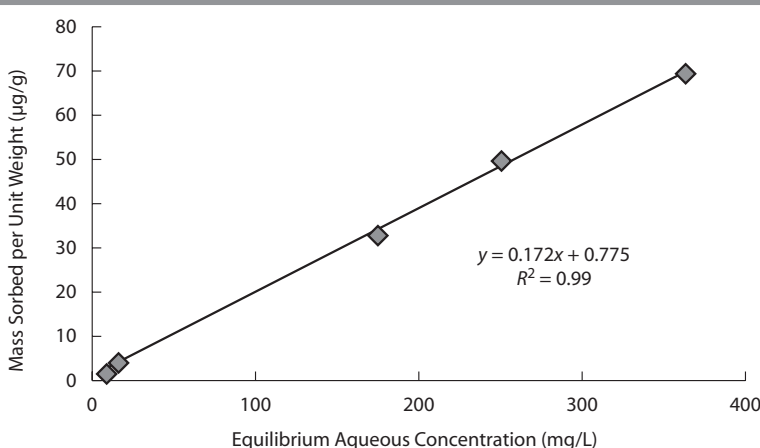
There are two limitations of the linear-sorption isotherm model. One is that it does not limit the amount of solute that can be sorbed onto the solid. This is clearly not the case; there must be an upper limit to the mass of solute that can be sorbed. In addition, if there are only a few data points, what is actually a curvilinear experimental plot of C versus C^* might be misinterpreted to be a linear relationship. Figure 3.2 illustrates how it is important never to extrapolate from a limited data set to a range outside the data set and assume that a linear relationship exists in that region. The subset of the sorption data on Figure 3.2 marked by triangles can be used with the origin to form a linear relationship. The subset of the sorption data marked with squares can also be used with the origin to create a different linear relationship. However, if all the data are included, one can see that the sorption isotherm is not linear at all.

EXAMPLE PROBLEM

A sorption study of Acenaphthene onto Red Cedar wood chips yielded the following results (Data from Kasaraneni et al. 2014):

Equilibrium Aqueous Acenaphthene Concentration ($\mu\text{g/L}$)	Equilibrium Mass of Acenaphthene Sorbed ($\mu\text{g/g}$)
7	2
15	4
174	33
249	50
362	70

FIGURE 3.3



What is the K_d ?

The data are plotted to create the isotherm (Figure 3.3). It can be seen that they form a straight line so that either the linear isotherm model or possibly the Freundlich isotherm can be used (Section 3.4.2). The slope of the straight line is $y = 0.192x + 0.775$ with $R^2 = 0.99$. This means that, for instance, at 100 µg/L, the equilibrium mass sorbed is 20.0 µg/g and $K_d = 20.0 \text{ µg/g}/100 \text{ µg/L}$, or 200 mL/g.

3.4.2 Freundlich Sorption Isotherm

A more general equilibrium isotherm is the **Freundlich sorption isotherm**. This is defined by the nonlinear relationship

$$C^* = KC^N \quad (3.7)$$

where K and N are constants.

If the sorption characteristics can be described by a Freundlich sorption isotherm, when C is plotted as a function of C^* the data will be curvilinear (Figure 3.4(a)). However, the data can be linearized by use of the following equation:

$$\log C^* = \log K_{Fr} + N \log C \quad (3.8)$$

If $\log C$ is plotted against $\log C^*$, the result will be linear with a slope of N and an intercept of $\log K_{Fr}$. This is illustrated in Figure 3.4(b).

If Equation 3.7 is substituted into Equation 3.1, the result is

$$\frac{\partial C}{\partial t} = D_L \frac{\partial^2 C}{\partial x^2} - v_x \frac{\partial C}{\partial x} - \frac{\rho_b}{\theta} \frac{\partial (KC^N)}{\partial t} \quad (3.9)$$

After differentiation and reorganization, Equation 3.9 becomes

$$\frac{\partial C}{\partial t} \left(1 + \frac{\rho_b KNC^{N-1}}{\theta} \right) = D_L \frac{\partial^2 C}{\partial x^2} - v_x \frac{\partial C}{\partial x} \quad (3.10)$$

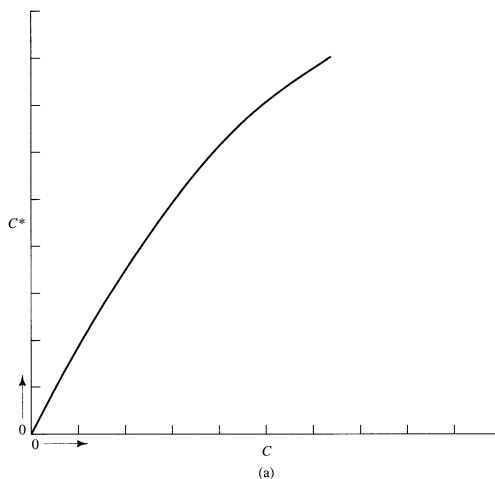
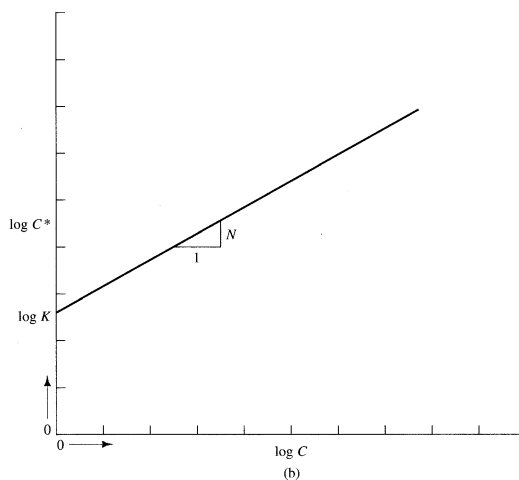
The retardation factor for a Freundlich sorption isotherm, R_F , is

$$1 + \frac{\rho_b KNC^{N-1}}{\theta} = R_F \quad (3.11)$$

If N is greater than 1, Equation 3.10 will lead to a spreading front, whereas if N is less than 1, the front will be self-sharpening. If N is equal to 1, the Freundlich sorption isotherm becomes the linear sorption isotherm.

The Freundlich sorption isotherm is one that has been widely applied to the sorption of various metals and organic compounds to a large number of sorbents, including soils (e.g., Carmo et al. 2000; Toll 2001) or biosorbents (e.g., Boving et al. 2004; Febrianto et al. 2009). Of particular interest is the sorption of contaminants to granular activated carbon (GAC), which is a widely used sorbent for treating water or air polluted with petroleum hydrocarbons, chlorinated solvents, heavy metals, pesticides, explosives, emerging contaminants (Speth and Miller 1990; Li et al. 2002; Faur-Brasquet et al. 2002; Morley and Fatem 2010; Hansen et al. 2010) and many other compounds.

The Freundlich sorption isotherm suffers from the same fundamental problem as the linear sorption isotherm; there is theoretically no upper limit to the amount of a solute that could be sorbed. One should be careful not to extrapolate the equation

FIGURE 3.4(a) Nonlinear Freundlich sorption isotherm with C^* versus C .**FIGURE 3.4(b)** The Freundlich sorption isotherm can be made linear by plotting $\log C^*$ versus C .

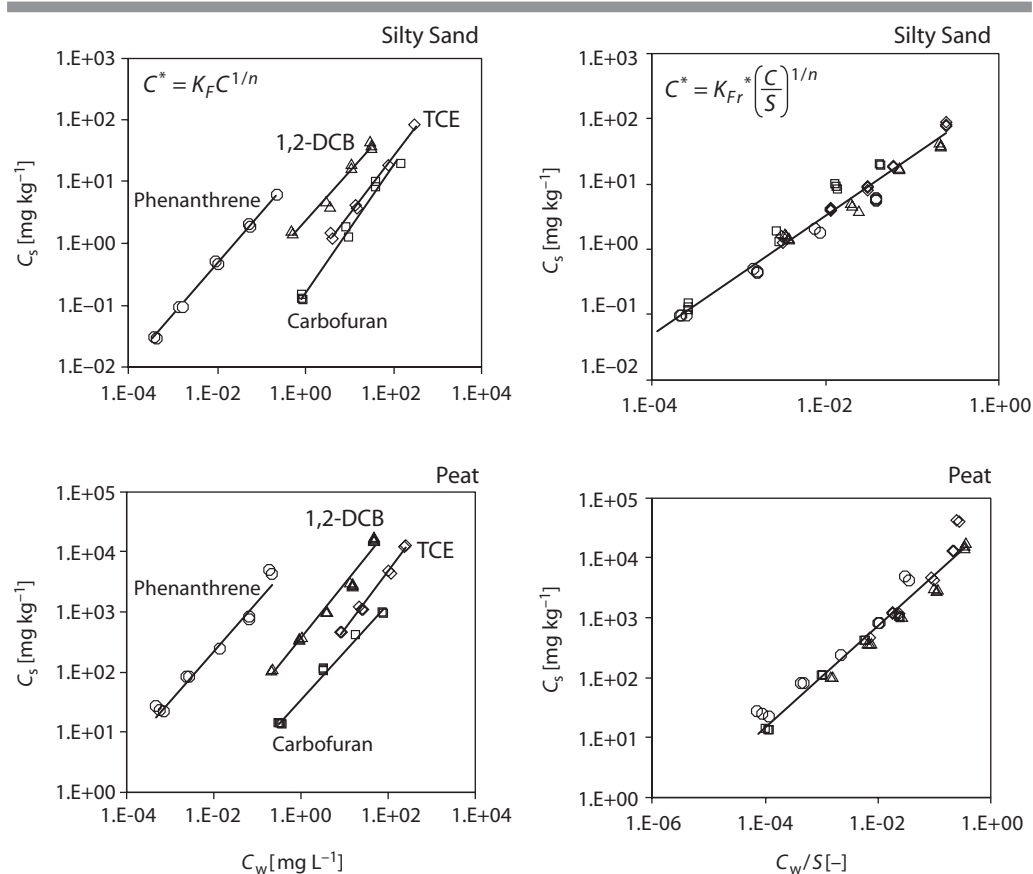
beyond the limits of the experimental data. The Freundlich sorption isotherm is usually obtained by an empirical fit to experimental data.

Because the total sorption of a compound is approximately the same for any given concentration relative to the compound's aqueous solubility (C_w/S), a solubility-normalized Freundlich sorption isotherm can be used to describe sorption for compounds with different solubilities (Equation 3.12):

$$C^* = K_{Fr} * \left(\frac{C}{S} \right)^{\frac{1}{n}} \quad (3.12)$$

where K_{Fr}^* is the Freundlich coefficient, which has the units of C^* and which is related to the usual Freundlich model by $K_{Fr}^* = K_{Fr} \times S^{1/n}$. Grathwohl and Rahman (2002) illustrates how normalization “collapses” the Freundlich isotherm data for four different compounds and two soil samples (Figure 3.5).

FIGURE 3.5 Example for “collapsing” sorption isotherms after the normalization to S (right). Lines denote Freundlich sorption isotherms.



Source: Modified after Grathwohl and Mokhlesur 2002.

3.4.3 Langmuir Sorption Isotherm

The **Langmuir sorption isotherm** was developed with the concept that a solid surface possesses a finite number of sorption sites. When all the sorption sites are filled, the surface will no longer sorb solute from solution. The form of the Langmuir sorption isotherm is

$$\frac{C}{C^*} = \frac{1}{\alpha\beta} + \frac{C}{\beta} \quad (3.13)$$

where

α = an adsorption constant related to the binding energy (L/mg)

β = the maximum amount of solute that can be absorbed by the solid (mg/kg)

The Langmuir sorption isotherm can also be expressed as

$$C^* = \frac{\alpha\beta C}{1 + \alpha C} \quad (3.14)$$

When Equation 3.14 is substituted into Equation 3.1, the following equation is obtained:

$$\frac{\partial C}{\partial t} = D_L \frac{\partial^2 C}{\partial x^2} - v_x \frac{\partial C}{\partial x} - \frac{\rho_b^\theta \left(\frac{\alpha\beta C}{1 + \alpha C} \right)}{\theta} \quad (3.15)$$

Differentiation and reorganization of Equation 3.15 yields

$$\frac{\partial C}{\partial t} \left[1 + \frac{\rho_b}{\theta} \left(\frac{\alpha\beta}{(1 + \alpha C)^2} \right) \right] = D_L \frac{\partial^2 C}{\partial x^2} - v_x \frac{\partial C}{\partial x} \quad (3.16)$$

The retardation factor for the Langmuir sorption isotherm, R_L , is

$$1 + \frac{\rho_b}{\theta} \left(\frac{\alpha\beta}{(1 + \alpha C)^2} \right) = R_L \quad (3.17)$$

If the sorption of a solute onto a solid surface follows a Langmuir sorption isotherm and the experimental data of C^* versus C are plotted on a graph, they will have a curved shape that reaches a maximum value (Figure 3.6a). If C/C^* is plotted versus C , the data will follow a straight line. The maximum ion sorption, β , is the reciprocal of the slope of the line, and the binding energy constant, α , is the slope of the line divided by the intercept (Figure 3.6b).

In studies of the sorption of phosphorous on soils, it has been found that a plot of C/C^* versus C will yield curves with two straight line segments (Fetter 1977; Munns and Fox 1976). This has been interpreted to mean that there are two types of sorption sites, which differ in their bonding energy. The **Langmuir two-surface sorption isotherm** is

$$\frac{C^*}{C} = \frac{\alpha_1 \beta_2}{1 + \alpha_1 C} + \frac{\alpha_2 \beta_2}{1 + \alpha_2 C} \quad (3.18)$$

where

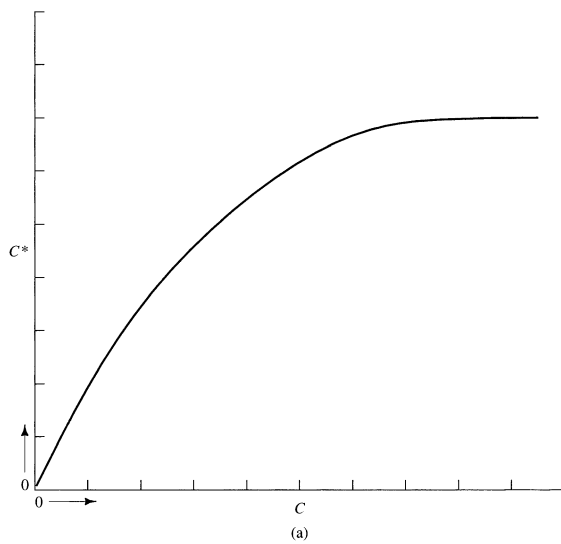
α_1 = the bonding strength at the type 1 sites

α_2 = the bonding strength at the type 2 sites

β_1 = the maximum amount of solute that can be sorbed at the type 1 sites

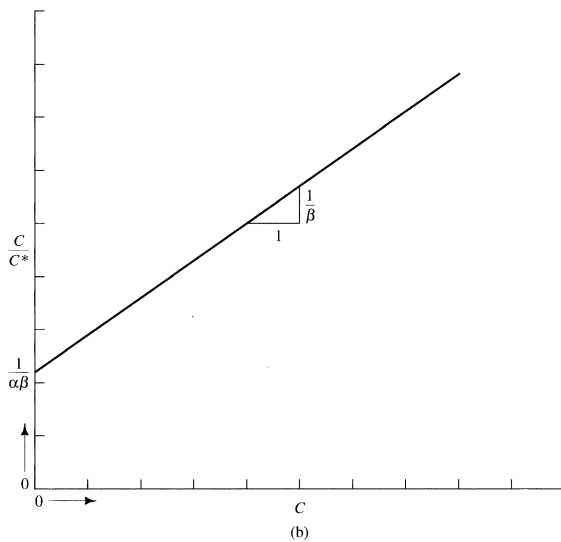
β_2 = the maximum amount of solute that can be sorbed at the type 2 sites

FIGURE 3.6(a) Nonlinear Langmuir sorption isotherm will reach a maximum sorption value when C^* is plotted versus C .



(a)

FIGURE 3.6(b) The Langmuir sorption isotherm can be made linear by plotting C/C^* versus C .



(b)

3.4.4 BET Sorption

Named for its inventors, Brunauer, Emmett, and Teller (Brunauer et al. 1938), the BET Isotherm is an extension of the Langmuir theory for situations where the adsorbate exceeds a monolayer. Originally developed for the sorption of noncorrosive gases, such as nitrogen, as adsorbates on solid surfaces, the BET is defined as:

$$C^* = \frac{K\beta C}{(C_{sat} - C) \left[\frac{1 + (K-1)C}{C_{sat}} \right]} \quad (3.19)$$

In equation 3.19, C_{sat} denotes the saturation concentration in vapor (or a compound's solubility in aqueous systems). β is the maximum sorbate concentration and is identical to that parameter in the Langmuir model.

Examples of sorption isotherms, including BET, are shown in Figure 3.7. The concept of the BET theory is based on three hypotheses: (1) gas molecules physically adsorb on a solid in multiple, infinite layers; (2) there is no interaction between each adsorption layer; and (3) the Langmuir theory can be applied to each layer. Figure 3.8 shows a conceptualization of surface layering for different isotherm models.

The principle of capillary condensation can be applied to assess the presence of pores, pore volume, and pore size distribution. In porous media, capillary condensation of the solute occurs in mesopores of 2 nm to 50 nm diameter. The BET theory is the basis of the International Standard Organization's ISO 9277:2010, which specifies the determination of the overall specific external and internal surface area of disperse or porous solids.

3.4.5 Polanyi–Dubinin–Manes (PDM) Sorption Isotherm

The adsorption potential theory proposed by Polanyi (1963) and further refined by Dubinin (1970) and Manes (1969) can be applied to both the sorption of gases and aqueous phase compounds. In case of gas sorption, the Polanyi–Dubinin–Manes (PDM) potential theory assumes that molecules near a surface at constant temperature

FIGURE 3.7 Examples of different sorption isotherms models.

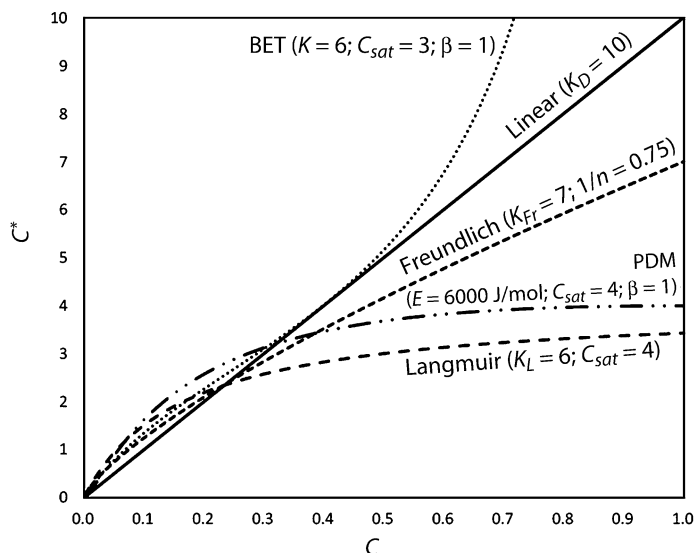
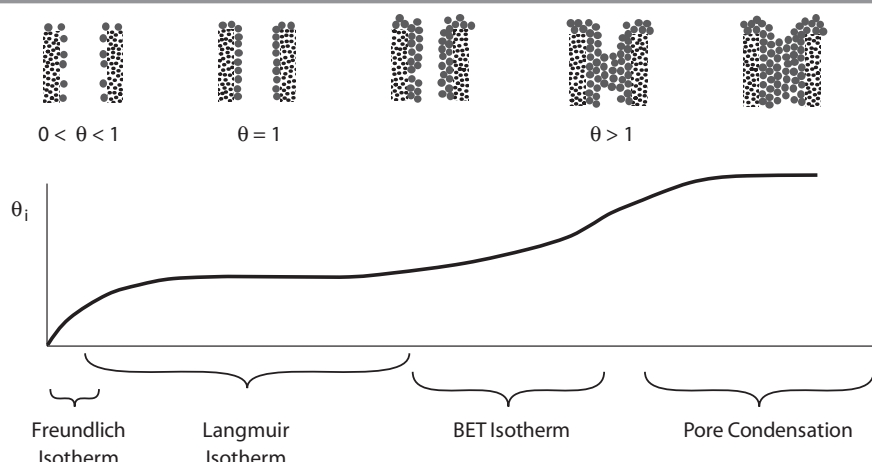


FIGURE 3.8 Conceptualization of surface layering for different isotherm models. θ denotes the fraction of sorbent surface sites occupied.



Source: Christmann 2012. Used with permission.

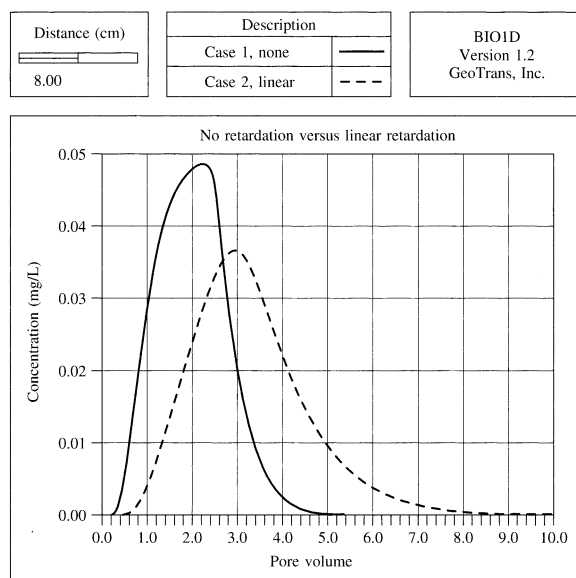
move according to a chemical potential. When the pressure is higher than the equilibrium vapor pressure, the molecules move closer to the sorbent surface and eventually condense into a liquid covering the micro pore surfaces of the sorbent (Figure 3.7). In aqueous systems, trace organic contaminants adsorb primarily as a result of nonspecific dispersive interactions (Li et al. 2005). The volume occupied by the adsorbed compound is a temperature-independent function of the adsorption potential. The adsorption potential can be measured through the equilibrium between the chemical potential of a molecule near the surface and the chemical potential of the molecule from a large distance away. According to Long et al. (2008), the adsorption isotherm at one temperature can also be developed by using the adsorption isotherm data at another temperature, or the adsorption potential curve of one adsorbate can be predicted from that of another adsorbate. The PDM potential theory has been used, for example, to predict the adsorption isotherms of aqueous organic contaminants, such as tetrachloroethene, on activated carbons (Li et al. 2005), or to model the adsorption equilibrium of PAHs on polymeric adsorbent (Long et al. 2008) and to describe the adsorptive properties of carbon nanotubes and carbon nanoparticles (Yang and Xing 2010).

3.4.6 Effect of Equilibrium Retardation on Solute Transport

The effects of equilibrium retardation can be illustrated through use of a commercial computer model, BIO1D. This model was developed by Srinivasan and Mercer (1988) and simulates both sorption processes and biodegradation in mass transport. Still widely used today, it is very flexible and can simulate linear, Freundlich, and Langmuir adsorption as well as aerobic and anaerobic biodegradation. The model is especially useful for analyzing laboratory data from column experiments.

The situation being modeled in the following figures is one-dimensional mass transport through a saturated porous medium that is in a column 16 cm (6.3 in) long.

FIGURE 3.9 Illustration of the effect of retardation by comparing the breakthrough curve of a solute which is not retarded with the breakthrough curve of a solute that undergoes linear-type retardation. Model simulation using BIO1D from Scientific Software Group.



The pore water velocity is 0.1 cm/sec (0.003 ft/sec), the dispersion coefficient is 0.1 cm²/sec (1×10^{-4} ft²/sec), and the porosity is 0.37. The initial solute concentration is 0.0 mg/L. For 2 min a solute with a concentration of 0.05 mg/L is injected into the top of the soil column and allowed to drain from the bottom. After 2 min the concentration of the solute in the water entering the column is set back to 0.00. The model yields the solute concentration in the water draining from the soil column as a function of the number of pore volumes that have been drained.

Figure 3.9 shows the general effect of retardation. One of the two curves, the solid one, is the solute breakthrough curve with no retardation (and no degradation). The dashed curve shows the breakthrough of a solute that is undergoing retardation, which follows a linear sorption isotherm, and has a k_d value of 0.476 µg/g. It can be seen that the retarded substance (dashed curve) has a lower peak value and that the peak comes later; i.e., it takes more pore volumes for it to occur than the unretarded peak (solid line).

Figure 3.10 illustrates the effect of different N values on the Freundlich sorption isotherm. The model is simulating exactly the same situation as before, except that there is Freundlich-type retardation. Figure 3.10 uses the same K_D values and compares breakthrough curves for cases where the N value is greater than 1.0 (dashed line) with one where the N value is less than 1.0 (solid line). The N value greater than 1.0 indicates a high sorption value, which results in a later arriving breakthrough curve (after more pore volumes) with a lower peak than the curve for the N value less than 1.0.

Caution should be used if experimental absorption studies indicate an N value greater than 1.0 for a Freundlich sorption isotherm. There is no theoretical reason why the exponential constant should be greater than the linear value of 1.0.

FIGURE 3.10 Illustration of the effect of the value of the constant N in the Freundlich sorption isotherm. The solid curve has an N less than 1, whereas the dashed curve has an N greater than 1. Model simulation using BIO1D from Scientific Software Group.

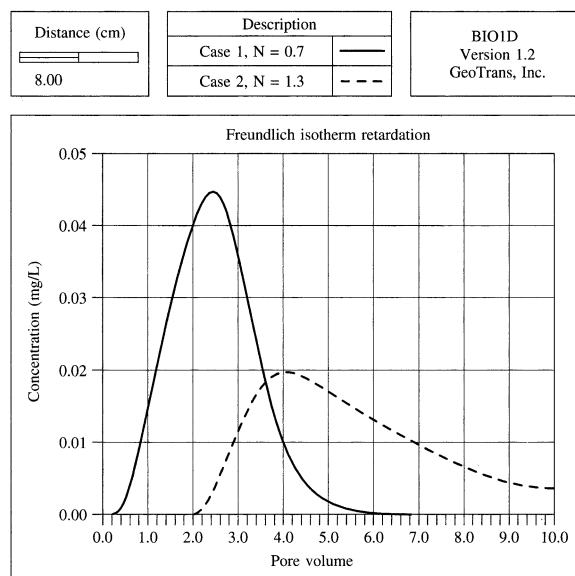
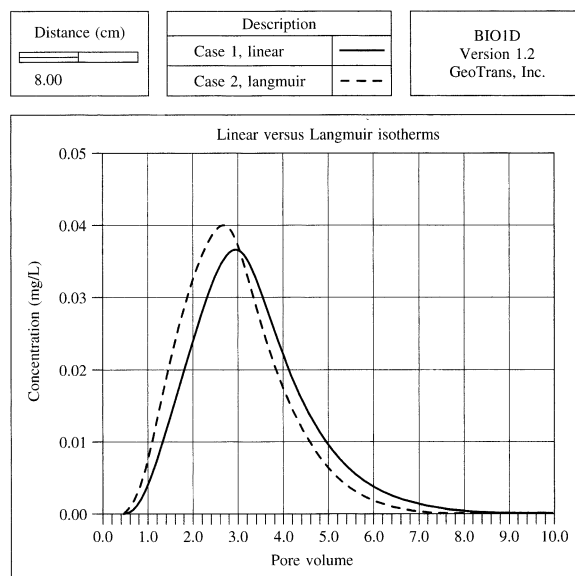


FIGURE 3.11 Illustration of the effect of different sorption isotherms in modeling solute transport. The solid curve is for a linear sorption isotherm while the dashed curve is for a Langmuir sorption isotherm. Model simulation using BIO1D from Scientific Software Group.



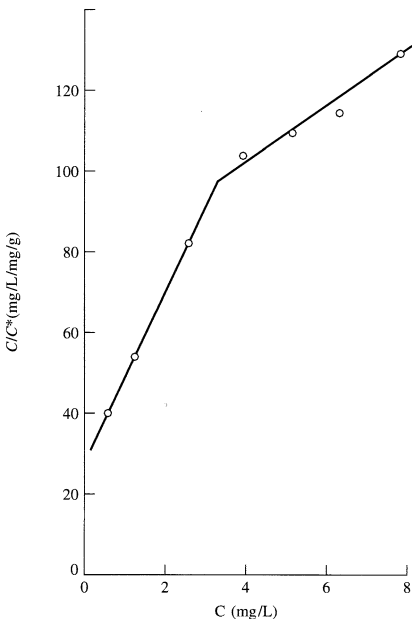
Some researchers believe that N values greater than 1.0 are a result of a combination of sorption and precipitation that is occurring because the experimental concentrations are exceeding the water solubility of the compound (Griffin 1991).

Figure 3.11 compares the linear sorption isotherm with a Langmuir sorption isotherm. The Langmuir sorption isotherm has a maximum binding energy of $0.345 \text{ }\mu\text{g/g}$ and a maximum sorption of $0.475 \text{ }\mu\text{g/g}$. The Langmuir sorption isotherm results in a higher peak value at breakthrough, which arrives at an earlier time than the linear sorption isotherm. In this particular case the Langmuir isotherm is not very different than the linear sorption isotherm.

EXAMPLE PROBLEM

Sorption of phosphorous by a calcareous glacial outwash was studied by means of a batch sorption test. The outwash was air-dried and then sieved to segregate the fraction that was finer than 2 mm (0.08 in). The coarser material was discarded. Ten-gram samples of the sediment were added to flasks containing 100 mL of 0.1 M NaCl and disodium phosphate in concentrations ranging from 0.53 to 12.1 mg/L . The flasks were shaken for 4 da on an autoshaker. The samples were then filtered and the filtrate analyzed for orthophosphate. The sediment was extracted with dilute HCl and the extract was analyzed to determine the amount of phosphorous sorbed to the sediment prior to the test. This amount was 0.016 mg/g .

FIGURE 3.12 Linear Langmuir two-surface sorption isotherm for the sorption of phosphate on calcareous glacial outwash.



Source: Fetter 1977.

The initial concentration of phosphorous in solution was known and the equilibrium concentration was determined by analysis. By knowing the volume of solution and the initial concentration, the mass of phosphorous could be computed. For example a 100-mL sample with a concentration of 3.85 mg/L has 0.385 mg of P. At equilibrium with the sediment, this aliquot had 2.45 mg/L of P, or 0.245 mg, still in solution. The amount sorbed was 0.14 mg (0.385 mg – 0.245 mg), or 0.014 mg/g of sediment. Prior to the sorption test the sediment had been extracted with dilute HCl and the extract tested for P. It was found to contain 0.016 mg/g of P. This amount already occupied some of the sorption sites and had to be added to the amount sorbed during the test. The following table lists the initial and equilibrium concentrations for P, the amount sorbed onto the soil, and the value of C/C^* . It is interesting to note that for the lowest initial concentration, the equilibrium concentration is greater than the initial concentration. This is due to P desorbing from the sediment.

Figure 3.12 shows the plot of C/C^* versus C. This is clearly a Langmuir two-surface sorption isotherm. The sorption maxima for low concentrations is 0.05 mg P per gram of sediment, and for the higher concentrations it is 0.16 mg P per gram of sediment.

Initial Concentration (mg/L)	Equilibrium Concentration C (mg/L)	Amount Sorbed per Gram during Test (mg/g)	Amount Sorbed in Test Plus 0.016 mg/g C* (mg/g)	C/C^* (mg/L) (mg/g)
0.53	0.55	-0.002	0.014	39
1.95	1.25	0.007	0.023	54.5
3.85	2.45	0.014	0.030	81
6.05	3.85	0.022	0.038	103
8.0	5.00	0.030	0.046	108.5
12.1	7.70	0.044	0.060	127.5

■ 3.5 Nonequilibrium (Kinetic) Sorption Models

All the equilibrium models assume that the rate of change in concentration due to sorption is much greater than the change due to any other cause and that the flow rate is low enough that equilibrium can be reached. If this is not the case and equilibrium is not attained, a kinetic model is more appropriate. In a kinetic model the solute transport equation is linked to an appropriate equation to describe the rate that the solute is sorbed onto the solid surface and desorbed from it.

The kinetic limitations of the solute transport to the surface of the sorbent are related to processes at the pore scale. Several physical models have been developed to describe these pore scale transport processes. In the aggregated media concept (Fig. 3.13a), advective-dispersive solute transport occurs in “mobile” regions, which is the network of macropores between soil aggregates through which the bulk of the aqueous phase travels.

A fraction of solute is transported from the mobile domain into and out of inter-aggregate pores. Solutes in these micropores are considered “immobile”. The solute transport in and out of micropores is governed by slow diffusive transport processes. In a related model, known as the stagnant film concept (Fig. 3.13b), solutes must diffuse from the mobile bulk aqueous phase through a film of stagnant, immobile soil-water that covers the surface of the sorbent. The diffusive transport in and out of the stagnant film can be described by Fick’s law of diffusion. A third model applies to fractured media where most of the solute transport takes place in discrete flow paths. In consolidated aquifer materials, e.g., bedrock aquifers, much of this preferential flow is restricted to fractures of different sizes. Solutes traveling through those fractures can diffuse into and out of the surrounding rock matrix (Fig. 3.13c). Models describing the physical nonequilibrium transport in fractured media are often referred to as dual permeability models (Gerke and van Genuchten 1993; Simunek et al. 2003; Dousset et al. 2007). All these conceptual models have in common that the solute transport is delayed before reaching the surface of the sorbent. The resulting nonequilibrium conditions require kinetic sorption models to adequately describe the delayed solute transport.

FIGURE 3.13 Conceptualization of physical transport processes in (a) aggregate media, (b) stagnant film concept, (c) fractured media.

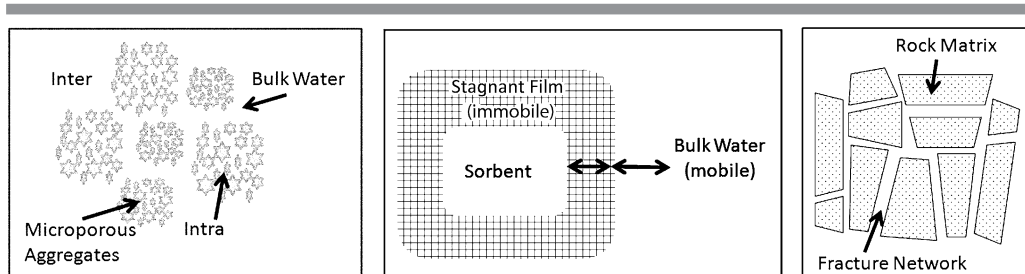


Figure 3.14 provides an overview of nonequilibrium transport model concepts. The most simple nonequilibrium condition is that the rate of sorption is a function of the concentration of the solute remaining in solution and that once sorbed onto the solid, the solute cannot be desorbed. This is an irreversible reaction and the process leads to attenuation of the solute (not retardation which by definition is reversible). The **irreversible first-order kinetic sorption model** that describes this consists of the following pair of equations:

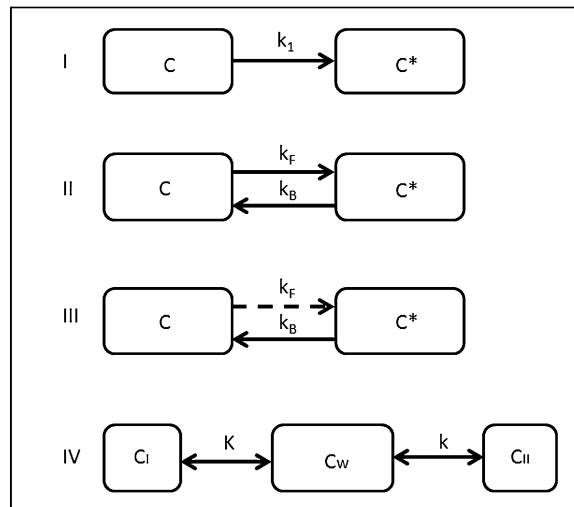
$$\frac{\partial C^*}{\partial t} = k_1 C \quad (3.20)$$

$$\frac{\partial C}{\partial t} = D_L \frac{\partial^2 C}{\partial x^2} - v_x \frac{\partial C}{\partial x} - \frac{\rho_b}{\theta} \frac{\partial C^*}{\partial t} \quad (3.21)$$

where k_1 = a first-order decay rate constant.

If the rate of solute sorption is related to the amount that has already been sorbed and the reaction is reversible, then the **reversible linear kinetic sorption model** can

FIGURE 3.14 Conceptualizations of nonequilibrium transport models. I: irreversible first-order kinetic sorption; II: reversible linear kinetic sorption. III: reversible nonlinear kinetic sorption, IV: "Two-Site" sorption.



be used. This consists of Equation 3.21 and the following expression for the rate of sorption:

$$\frac{\partial C^*}{\partial t} = k_2 C - k_3 C^* \quad (3.22)$$

where

k_2 = forward rate constant

k_3 = backward rate constant

If sufficient time is available for the system to reach equilibrium, then there is no further change in C^* with time and $dC^*/dt = 0$, so that $k_2 C = k_3 C^*$. This can be rearranged to $C^* = (k_2/k_3)C$, which is a linear equilibrium sorption isotherm.

Equation 3.22 is sometimes written in a slightly different form (Nielsen, van Genuchten, and Biggar 1986):

$$\frac{\partial C^*}{\partial t} = \gamma(k_4 C - C^*) \quad (3.23)$$

where

γ = a first-order rate coefficient

k_4 = a constant equivalent to K_d

Equation 3.23 describes a situation where reversible linear sorption is limited by a first-order diffusion process.

This model has been used to describe the sorption of pesticides (Leistra and Dekkers 1977; Hornsby and Davidson 1973) as well as some organics (Davidson and Chang 1972).

A third kinetic model is the **reversible nonlinear kinetic sorption model**. This couples Equation 3.21 with

$$\frac{\partial C^*}{\partial t} = k_5 C^N - k_6 C^* \quad (3.24)$$

where k_5 , k_6 and N are constants. This model describes a situation where the forward (sorption) reaction is nonlinear, whereas the backward (desorption) reaction is linear. This equation has been used, with a value of N less than 1, to describe the sorption of phosphorous (Fiskell et al. 1979) and herbicides (Enfield and Bledsoe 1975).

At the equilibrium condition for the reversible nonlinear model, $dC^*/dt = 0$ and $k_5 C^N = k_6 C^*$, which can be rearranged as $C^* = (k_5/k_6)C^N$, which is the Freundlich sorption isotherm.

The **bilinear adsorption model** is the kinetic version of the Langmuir sorption isotherm. This model has the form

$$\frac{\partial C^*}{\partial t} = k_7 C (\beta - C^*) - k_8 C^* \quad (3.25)$$

where

β = the maximum amount of solute that can be sorbed

k_7 = the forward rate constant

k_8 = the backward rate constant

“Two-Site” nonequilibrium sorption models are useful when simple one-site models (Equations 3.20, and 3.22–3.25) cannot adequately explain observed results from transport experiments involving reactive solutes (van Genuchten and Wagenet 1989). In these cases it may be necessary to define two types of sorption domains: **Type-I** sites are controlled by instantaneous sorption processes, whereas **Type-II** are nonequilibrium or kinetic sites. In this sorption model, the solute in the liquid phase that instantly partitions to the Type-I site is:

$$C_I = f K C \quad (3.26)$$

where C and C_I are liquid and instantaneously sorbed concentrations (mg/kg) and f is the fraction of sorption for which sorption is instantaneous. K is the distribution coefficient (L/kg) between the total sorbed concentration (S) and the liquid concentration ($K = S/C_w$). At equilibrium, K equals K_D . The total amount sorbed is the sum of the instantaneously (C_I) and kinetic (C_{II}) sorbed fraction. Then, assuming linear reversible kinetics for Type-II sites, the time-dependent sorption onto the Type-II site follows:

$$\frac{\partial C_{II}}{\partial t} = k_9 [(1-f)KC - C_{II}] \quad (3.27)$$

where C_{II} is the concentrations (mg/kg) associated with Type-II sites and k_9 is a first order rate constant (h^{-1}) (Brusseau et al. 1991; Lee et al. 2012). Combining Equations 3.26 and 3.27 yields:

$$\frac{\partial S}{\partial t} = \left[fK \frac{\partial C_w}{\partial t} \right] + \left[k_9 (1-f)KC_w - C_{II} \right] \quad (3.28)$$

“Two-region” or “bi-continuum” transport models have been found useful for modeling solute transport when the sorption rate is thought to be limited by the rate at which solutes are transported through a thin film of stagnant water sounding the sorbent (Fig. 3.13b). The bulk water is the “mobile” phase in which advective-dispersive flow dominates. The water near the solid surface of the sorbent is considered an “immobile” phase. Transfer of solutes across the immobile water to the solid surface occurs by diffusion and a **diffusion-controlled rate law** must be employed (Nkedi-Kizza et al. 1984; Brusseau et al. 1991; Brusseau and Rao 1990). The rate of solute transfer across the immobile water is assumed to be proportional to the difference in concentration between the two regions.

The equations that are given are applicable to both saturated and unsaturated flow. For unsaturated flow, θ is the volumetric water content and for saturated flow, θ is the porosity. The equations can account for a system where some of the solid is in direct contact with the mobile phase and some is in direct contact with the immobile phase. This is conceptually identical to the “Two-Site” sorption model (Fig. 3.14 IV), but unlike it, sorption to a fraction of the sorbent surface is controlled by diffusion processes. This system requires a pair of equations (Nkedi-Kizza et al. 1984):

$$\begin{aligned} \theta_m \frac{\partial C_m}{\partial t} = & \theta_m D_m \frac{\partial^2 C_m}{\partial z^2} - \theta_m v_m \frac{\partial C_m}{\partial z} - f \rho_b \frac{\partial C^*_m}{\partial t} \\ & - \theta_{im} \frac{\partial C_{im}}{\partial t} - (1-f) \rho_b \frac{\partial C^*_{im}}{\partial t} \end{aligned} \quad (3.29)$$

$$(1-f) \rho_b \frac{\partial C^*_{im}}{\partial t} = \gamma^* (C_m - C_{im}) - \theta_{im} \frac{\partial C_{im}}{\partial t} \quad (3.30)$$

where

- θ_m = porosity occupied by mobile phase
- θ_{im} = porosity occupied by immobile phase
- C_m = solute concentration in the mobile phase
- C_{im} = solute concentration in the immobile phase
- C^*_m = absorbed concentration in contact with the mobile phase
- C^*_{im} = absorbed concentration in contact with the immobile phase
- v_m = velocity of the mobile phase
- f = fraction of the solid surfaces in contact with the mobile phase
- D_m = apparent diffusion constant for mobile phase
- γ^* = first-order, mass-transfer coefficient
- ρ_b = bulk density

If the sorption of the solute is in equilibrium and reversible and follows a linear sorption isotherm, then

$$C^*_m = K_d C_m \text{ and } C^*_{im} = K_d C_{im} \quad (3.31)$$

The total sorption of solute from both the mobile and immobile regions is

$$C^* = fC_m^* + (1-f)C_{im}^* \quad (3.32)$$

With these sorption conditions, Equations 3.29 and 3.30 can be written as

$$\begin{aligned} (\theta_m + \rho_b f K_d) \frac{\partial C_m}{\partial t} &= \theta_m D_m \frac{\partial^2 C_m}{\partial z^2} - \theta_m v_m \frac{\partial C_m}{\partial z} \\ &\quad - [\theta_{im} + (1-f)\rho_b K_d] \frac{\partial C_{im}}{\partial t} \end{aligned} \quad (3.33)$$

$$\frac{\partial C_{im}}{\partial t} = \frac{\gamma^*(C_m - C_{im})}{[\theta_{im} + (1-f)\rho_b K_d]} \quad (3.34)$$

An analytical solution to Equations 3.33 and 3.34 is available (van Genuchten and Wierenga 1976).

There are a number of additional nonlinear sorption models described in the literature (e.g., Simunek et al. 2008). The sorption of solutes by solids is complex, and there does not appear to be a single universal model. The best approach is to conduct an experimental study of the sorptive capacity and rate of the particular solute and solid that is of concern. One can then search the literature for a model that conceptually describes the experimental results. Today, nonequilibrium sorption problems are commonly addressed by numerical models that can be applied more readily than analytical models to realistic laboratory and field problems (Simunek et al., 2003). One noteworthy software package is HYDRUS-1D, which includes provisions for transport equations for nonlinear nonequilibrium reactions between the solid and liquid phases (Simunek et al., 2008). Another widely used software package is MT3DMS (Zheng and Wang, 1999).

■ 3.6 Sorption of Hydrophobic (Organic) Compounds

3.6.1 Introduction

Many organic compounds dissolved in groundwater can be adsorbed onto solid surfaces by what is called the *hydrophobic effect* (Roy and Griffin 1985). These compounds exist as electrically-neutral species with differing degrees of polarity. The solubility of organic compounds in water is a function of the degree to which they are attracted by the polar water molecule. This attraction depends upon the polarity of the organic molecule itself. Hydrophobic compounds can be dissolved in many non-polar organic solvents but have a low solubility in water. When dissolved in water, these molecules tend to be attracted to surfaces that are less polar than water. There is a small but limited amount of adsorption of organics on pure mineral surfaces (Ciccioi et al. 1980; Rogers, McFarlane, and Cross 1980; Griffin and Chian 1980). However, the primary adsorptive surface is the fraction of organic solids in the soil or aquifer (Karickhoff et al. 1979; Schwarzenbach and Westall 1981; Dzombak and Luthy 1984). Also, it is now accepted that microporous organic particles (pore width <2 nm) occur in soils, sediments, and sedimentary rocks (Allen-King et al. 2002). These so-called carbonaceous geosorbent particles, like black carbon, coal, and

kerogen, (Goldberg 1985; Cornellisen et al. 2005; Lohman et al. 2005) can adsorb organic compounds by a pore-filling mechanism described by the Polanyi's theory of a variable adsorption potential (Polanyi 1963).

3.6.2 Partitioning onto Soil or Aquifer Organic Carbon

The partitioning of a solute onto mineral surface or organic carbon content of the soil or aquifer is almost exclusively onto the organic carbon fraction, f_{oc} , if it constitutes at least 1% of the soil or aquifer on a weight basis (Karickhoff et al. 1979). Under these circumstances a partition coefficient with respect to the organic fraction, K_{oc} , can be defined as

$$K_{oc} = \frac{K_d}{f_{oc}} \quad (3.35)$$

A partition coefficient based on soil or aquifer organic matter, K_{om} , is also used. Because the weight of the organic matter is greater than that of the organic carbon alone, K_{oc} will be larger than K_{om} . Based on lab studies K_{om} can be approximately related to K_{oc} by the equation (Olsen and Davis 1990)

$$K_{oc} = 1.724 K_{om} \quad (3.36)$$

If the organic fraction is less than 1% then it is not automatic that the soil or aquifer organic carbon will be the primary surface onto which the organic compounds will partition. There is some critical level of soil or aquifer organic carbon at which the sorption onto the organic matter is equal to the sorption onto the mineral matter. Below this critical level, f_{oc}^* , the organic molecules will be primarily sorbed onto the mineral surfaces. McCarty et al. (1981) have shown that this critical organic carbon level depends upon two variables, the surface area of the soil or aquifer, S_a , which is related to the clay content, and a property of the pure organic compound called the octanol-water partition coefficient.

The **octanol-water partition coefficient**, K_{ow} , is one measure of how hydrophobic a compound is. The organic compound is shaken with a mixture of *n*-octanol and water and the proportion dissolving into each phase is measured. The octanol-water partition coefficient is the ratio of the concentration in the octanol to the concentration in the water: $C_{\text{octanol}}/C_{\text{water}}$. It is usually expressed as a log value in reference books (e.g., Mackay 2006) or in online databases (e.g., National Research Council of Canada 2015).

According to McCarty et al. (1981), the value of f_{oc}^* , can be found from

$$f_{oc}^* = \frac{S_a}{200(K_{ow})^{0.84}} \quad (3.37)$$

This equation suggests that soils or aquifers with low organic carbon content would retain organic compounds with high K_{ow} values but might not retain those with low K_{ow} values. Assuming a surface area of 12 m²/g, which would be found with a typical kaolinite clay soil, Table 3.1 contains f_{oc}^* values and the corresponding minimum soil organic carbon content necessary before organic compounds with different K_{ow} values will sorb primarily on the organic carbon.

TABLE 3.1 Representative f_{oc} values for different organic compounds.

Chemical	K_{ow}	f_{oc}^*	Minimum Soil Organic Carbon (mg/kg)
Dichloroethane	62	0.002	2,000
Benzene	135	0.001	1,000
Trichloroethylene	195	0.0007	700
Perchloroethylene	760	0.0002	200
Naphthalene	2,350	0.00009	90
Pyrene	209,000	0.000002	2

3.6.3 Estimating K_{oc} from K_{ow} Data

A number of researchers have found that there is a relationship between the octanol-water partition coefficient and the K_{oc} value for various organic compounds. The use of such a relationship is predicated upon the following (Karickhoff 1984): (1) Sorption is primarily on the organic carbon in the soil or aquifer. (2) Sorption is primarily hydrophobic, as compared with polar group interactions, ionic bonding, or chemisorption. (3) There is a linear relationship between sorption and the concentration of the solute.

A number of different organic compounds have been studied, with the result that a number of different relationships have been developed. Olsen and Davis (1990) listed a total of nine different equations that have been developed. Karickhoff (1984) lists four equations that have published least squares regression correlation coefficients (r^2 values) that exceed 0.9. (A correlation coefficient of 1.00 would mean that there is a perfect correlation between K_{ow} and K_{oc} . A correlation coefficient of 0.9 means that 90% of the variation is accounted for by the equation.)

Table 3.2 lists a number of equations that relate K_{oc} to K_{ow} . Where known, correlation coefficients are listed below the equations.

The equations in Table 3.2 have been derived for many different organic compounds. Some have utilized related compounds, whereas others are based on a mixture of different organic molecules. The hydrogeologist or engineer who wishes to estimate a K_{oc} value is placed in the situation of deciding which equation to use. The best choice is an equation that was derived on the basis of chemicals similar to the one under study. The various equations tend to yield similar results for many compounds. Table 3.3 shows $\log K_{oc}$ values computed from the equations in Table 3.2 for several different organic compounds that cover a wide range of K_{ow} values.

Although there are a number of equations, most of the computed $\log K_{oc}$ values for the example chemicals fall close to or within one standard deviation of the geometric means. There are some data in the literature on actual measured values of $\log K_{oc}$. Table 3.4 gives some experimental K_{oc} values.

The values in Table 3.4 fall close to the means listed on Table 3.3. The equations that yield the maximum or minimum values for a particular compound may not be the most appropriate to use for that compound. It appears that there is no universal equation that relates K_{oc} to K_{ow} for all classes of organic compounds. In fact, from an analysis of the theory underlying the organic carbon/water partition coefficient and

TABLE 3.2 Equations for estimating K_{oc} from K_{ow} .

Equation Number	Equation	Chemicals Used	Reference
(T1)	$\log K_{om} = 0.52 \log K_{ow} + 0.62$	72 substituted benzene pesticides	Briggs, 1981
(T2)	$\log K_{oc} = 1.00 \log K_{ow} - 0.21$	10 polycyclic aromatic hydrocarbons	Karickhoff, Brown, and Scott 1979
(T3)	$K_{oc} = 0.63K_{ow}$	Miscellaneous organics	Karickhoff, Brown, and Scott 1979
(T4)	$\log K_{oc} = 0.544 \log K_{ow} + 1.377$	45 organics, mostly pesticides	Kenaga and Goring 1980
(T5)	$\log K_{oc} = 1.029 \log K_{ow} - 0.18$ $r^2 = 0.91; n = 13$	13 pesticides	Rao and Davidson 1980
(T6)	$\log K_{oc} = 0.94 \log K_{ow} + 0.22$	s-triazines and dinitroanilines	Rao and Davidson 1980
(T7)	$\log K_{oc} = 0.989 \log K_{ow} - 0.346$ $r^2 = 0.991; n = 5$	5 polycyclic aromatic hydrocarbons	Karickhoff 1981
(T8)	$\log K_{oc} = 0.937 \log K_{ow} - 0.006$	Aromatics, polycaromatics, -triazines	Lyman 1982
(T9)	$\ln K_{oc} = \ln K_{ow} - 0.7301$	DDT, tetrachlorobiphenyl, lindane, 2,4-D, and dichloropropane	McCall, Swann, and Laskowski 1983
(T10)	$\log K_{om} = 0.904 \log K_{ow} - 0.779$ $r^2 = 0.989; n = 12$	Benzene, chlorinated benzenes, PCBs	Chiou, Porter, and Schmedding 1983
(T11)	$\log K_{oc} = 0.72 \log K_{ow} + 0.49$ $r^2 = 0.95; n = 13$	Methylated and chlorinated benzenes	Schwarzenbach and Westall 1981
(T12)	$\log K_{oc} = 1.00 \log K_{ow} - 0.317$ $r^2 = 0.98; n = 22$	22 polynuclear aromatics	Hassett et al. 1980

an examination of existing data, Seth et al. (1999) suggested as a rule of thumb that K_{oc} is $0.35K_{ow}$ with variation by a factor of 2.5 in either direction (range 0.14 to 0.88) to account for differences in the nature of organic matter.

3.6.4 Estimating K_{oc} from Solubility Data

The value of K_{oc} can also be estimated from the solubility, S , of a particular compound. Several different equations describing this relationship have been published and are listed in Table 3.5.

Aqueous solubility can be expressed in several ways. The most common is a **mass per volume** unit, such as milligram per liter. Equation T13 in Table 3.5 uses the concept of **mole fraction**. This is the ratio of the moles of a substance to the total number of moles of solution. A **mole** of a substance is equal to its formula weight in grams. In Equation T17 (Table 3.5) solubility is in terms of moles of solute per liter of solution, a unit known as **molarity**. For dilute solutions, to convert molarity to mole fraction, divide the molarity by 55.6, the number of moles of water in a liter.

Table 3.6 contains $\log K_{oc}$ estimated from the solubility for the same compounds that are listed in Table 3.3. A comparison of the results of Table 3.6 with the experimentally derived values for K_{oc} found in Table 3.4 shows that all the equations yield an estimate that is within an order of magnitude of the experimental result.

TABLE 3.3 Estimated values of K_{oc} based on published K_{ow} values.

Equation Number^a	Dichloroethane Log K_{ow}	Benzene 2.13	Trichloroethene 2.29	Ethyl Benzene 3.14	Tetrachloroethene 3.40	Naphthalene 3.37	2,2'-Dichlorobiphenyl 4.80	Pyrene 5.32
[1]	1.55	1.73	1.81	2.25	2.34	2.37	3.17	3.39
[2]	1.58	1.92	2.08	2.93	3.19	3.16	4.59	5.11
[3]	1.59	1.93	2.09	2.94	3.20	3.17	4.60	5.12
[4]	2.35	2.54	2.62	3.09	3.23	3.21	3.99	4.27
[5]	1.66	2.01	2.18	3.05	3.32	3.29	4.76	5.29
[6]	1.90	2.22	2.37	3.17	3.42	3.39	4.73	5.22
[7]	1.42	1.76	1.92	2.76	3.02	2.99	4.40	4.92
[8]	1.67	1.99	2.14	2.94	3.18	3.15	4.49	4.98
[9]	1.47	1.81	1.97	2.82	3.08	3.05	4.48	5.00
[10]	1.08	1.39	1.53	2.30	2.53	2.51	3.80	4.27
[11]	1.78	2.02	2.14	2.75	2.94	2.92	3.95	4.32
[12]	1.47	1.81	1.97	2.82	3.08	3.05	4.48	5.00
Range	1.08–2.35	1.39–2.54	1.53–2.62	2.25–3.17	2.34–3.42	2.37–3.39	3.17–4.76	3.39–5.29
Mean	1.63	1.93	2.07	2.82	3.04	3.02	4.29	4.77
St. dev.	0.31	0.28	0.27	0.28	0.31	0.30	0.47	0.59
Coef. var.	0.19	0.15	0.13	0.10	0.10	0.10	0.11	0.12

TABLE 3.4 Experimentally derived K_{oc} values.

Compound	K_{oc}	Reference
Benzene	1.50	Chiou, Porter, and Schmedding 1983
	1.92	Karickhoff, Brown, and Scott 1979
	1.98	Rogers, McFarlane, and Cross 1980
Ethylbenzene	2.22	Chiou, Porter, and Schmedding 1983
2,2'-Dichlorobiphenyl	3.92	Chiou, Porter, and Schmedding 1983
Tetrachloroethene	2.32	Chiou, Peters, and Freed 1979
Naphthalene	3.11	Karickhoff, Brown, and Scott 1979
Pyrene	4.92	Karickhoff, Brown, and Scott 1979
	4.80	Means et al. 1980

TABLE 3.5 Empirical equations by which K_{oc} can be estimated from S .

Equation Number	Equation	Reference
(T13)	$\log K_{oc} = 0.44 - 0.54 \log S$ S in mole fraction, $r^2 = 0.94$	Karickhoff, Brown, and Scott 1979
(T14)	$\log K_{oc} = 3.64 - 0.55 \log S$ S in mg/L	Kenaga 1980
(T15)	$\log K_{oc} = 4.273 - 0.686 \log S$ S in mg/L	Means et al. 1980
(T16)	$\log K_{oc} = 3.95 - 0.62 \log S$ S in mg/L	Hassett et al. 1983
(T17)	$\log K_{oc} = 0.001 - 0.729 \log S$ S in moles/L, $r^2 = 0.996$	Chiou, Porter, and Schmedding 1983

Caution is in order with respect to published values for aqueous solubility of organic chemicals. There are published values for many of the organic compounds of environmental interest. Montgomery (2007) or Verschueren (1983) are excellent compendia. However, for a given compound there may well be several different published values at the same temperature.

The use of solubility data is complicated by temperature and ionic strength effects on solubility. Published solubility data sometimes do not indicate the temperature at which the measurement was made. For a number of reasons, such as the purity of the organic chemical, the ionic strength of the water, the temperature, and the experimental procedure, there can be a range in the reported solubility data in the literature.

For similar reasons there can be a range of octanol-water partition coefficient values reported for the same compound (Sabljić 1987). For instance, Pontolillo and Eganhousem (2001) reviewed some 700 publications from 1944 to 2001 and found up to 4 orders of magnitude variation in reported K_{ow} values for the insecticide DDT and its metabolite DDE with no convergence over time. Because of this, one should recognize that K_{oc} values obtained from K_{ow} or solubility data are truly estimates.

TABLE 3.6 K_{oc} values estimated from the aqueous solubility.

Compound:	Dichloroethane	Benzene	Trichloroethene	Ethyl Benzene	Tetrachloroethene	Naphthalene	2,2'-Dichlorobiphenyl	Pyrene
	Molecular weight:	98.96	78.12	131.38	Solubility (mg/l)			
Log S:	5500	1780	1100	140	106.18	128.18	223.10	202.26
	3.74	3.25	3.04	2.15	2.18	3.1 1.49	1.86 0.269	0.032 -1.50
Log S:	5.56×10^{-2}	2.28×10^{-2}	8.37×10^{-3}	8.44×10^{-4}	1.41×10^{-3}	2.42×10^{-4}	8.32×10^{-6}	1.58×10^{-7}
	-1.25	-1.64	-2.08	-3.07	-2.85	-3.62	-5.08	-6.80
Log S:	1.00×10^{-3}	4.10×10^{-4}	1.51×10^{-4}	1.52×10^{-5}	2.54×10^{-5}	4.35×10^{-6}	1.49×10^{-7}	2.84×10^{-9}
	-3.00	-3.39	-3.82	-4.82	-4.60	-5.36	-6.83	-8.55
Equation Number ^a								
Estimated log K_{oc}								
[T13]	2.06	2.27	2.50	3.04	2.87	3.33	4.13	5.06
[T14]	1.58	1.85	1.97	2.46	2.44	2.82	3.79	4.47
[T15]	1.67	2.01	2.15	2.76	2.74	3.21	4.46	5.27
[T16]	1.63	1.94	2.07	2.62	2.60	3.03	4.12	4.88
[T17]	1.15	1.43	1.75	2.47	2.31	2.88	3.93	5.19
Range	1.15-2.06	1.43-2.27	1.75-2.50	1.80-3.04	2.31-2.87	2.82-3.33	3.79-4.46	4.47-5.27
Mean	1.62	1.90	2.09	2.67	2.59	3.05	4.09	4.97
St. dev.	0.32	0.31	0.27	0.24	0.22	0.25	0.32	0.32
Coef. var.	0.08	0.07	0.06	0.05	0.04	0.05	0.05	0.08

EXAMPLE PROBLEM

Calculate the K_{oc} of o-xylene using equations T13, T14, and T17. The aqueous solubility of o-xylene is 152 mg/L at 20°C and the formula weight is 106.17.

Give the following equations:

$$\text{T13 } \log K_{oc} = 0.44 - 0.54 \log S \quad S \text{ in mole fraction}$$

$$\text{T14 } \log K_{oc} = 3.64 - 0.55 \log S \quad S \text{ in mg/L}$$

$$\text{T17 } \log K_{oc} = 0.001 - 0.729 \log S \quad S \text{ in moles/L}$$

- 1) To convert solubility to moles per liter, divide the solubility by the formula weight in grams. For the case of o-xylene this is:

$$S_{molarity} = 0.153 \text{ gm/L} / 106.17 \text{ gm/mole} = 0.00144 \text{ moles/L}$$

- 2) To convert moles per liter to mole fraction (for a dilute solution), divide by 55.6 (the number of moles of water in a liter). For the case of o-xylene this is:

$$S_{mole\ fraction} = 1.44 \times 10^{-3} \text{ mole/L} / 55.6 \text{ mole/L} = 2.59 \times 10^{-5}$$

- 3) Equation T13

$$\log K_{oc} = 0.44 - 0.54 \log S$$

$$\log K_{oc} = 0.44 - 0.54 \log (2.59 \times 10^{-5})$$

$$\log K_{oc} = 0.44 - 0.54 \times (-4.59)$$

$$\log K_{oc} = 0.44 - (-2.48) = 2.92$$

- 4) Equation T14

$$\log K_{oc} = 3.64 - 0.55 \log S$$

$$\log K_{oc} = 3.64 - 0.55 \log 152$$

$$\log K_{oc} = 3.64 - (0.55 \times 2.182)$$

$$\log K_{oc} = 3.64 - 1.200 = 2.44$$

- 5) Equation T17

$$\log K_{oc} = 0.001 - 0.729 \log S$$

$$\log K_{oc} = 0.001 - 0.729 \log 0.00144$$

$$\log K_{oc} = 0.001 - 0.729 \times (-2.82)$$

$$\log K_{oc} = 0.001 - (-2.0716) = 2.073$$

As a point of comparison, experimentally determined values of K_{oc} for o-xylene listed in Montgomery et al. (2007) range from 2.03 to 2.41.

3.6.5 Estimating K_{oc} from Molecular Structure

The applicability of using octanol-water partition coefficient and aqueous solubility data to estimate K_{oc} has been questioned because some organic compounds have similar aqueous solubility but very different octanol solubility (Ellgehausen et al. 1981; Mingelgrin and Gerstl 1983; Olsen and Davis 1990). A more fundamental approach has been suggested on the basis of molecular topology (Koch 1983; Sabljic 1984; 1987; Sabljic and Protic 1982).

Molecular topology refers to the shape of the organic molecule. The particular parameter of molecular structure that has been related to K_{oc} is the first order molecular connectivity index, $^1\chi$. The first-order molecular connectivity index is calculated on the basis of the nonhydrogen part of the molecule. Each nonhydrogen atom has an atomic δ value, which is the number of adjacent nonhydrogen atoms. A connectivity index is then calculated for the molecule by the following formula:

$$^1\chi = \sum (\delta_i \delta_j)^{-0.5} \quad (3.38)$$

where δ_i and δ_j are the delta values for a pair of adjacent nonhydrogen atoms and the summation takes place over all the bonds between nonhydrogen atoms.

Sabljic (1987) made a regression analysis between the molecular connectivity and observed K_{om} values for 72 organic molecules, including chlorobenzenes, polyaromatic hydrocarbons, alkylbenzenes, chlorinated alkanes and alkenes, chlorophenols, and heterocyclic and substituted polyaromatic hydrocarbons. The relationship between K_{om} and $^1\chi$, which had an r^2 value of 0.95, is given by Equation 3.39. In order to convert K_{om} to K_{oc} multiply by 1.724.

$$\log K_{om} = 0.53 ^1\chi + 0.54 \quad (3.39)$$

Equation 3.39 was derived on the basis of nonpolar organic compounds. Sabljic (1987) gave an empirical method of extending this equation to classes of polar and even ionic organic compounds. When Equation 3.39 is used for polar and ionic organic compounds, it predicts a K_{om} that is higher than observed values reported in the literature. The nonpolar organics from which Equation 3.39 was derived are more strongly sorbed to soil organic matter than polar organic compounds. Sabljic introduced a polarity correction value, P_f , for each of 17 different groups of polar organics (Table 3.7). Equation 3.40 can be used to predict the value of K_{om} for polar organics:

$$\log K_{om} = 0.53 ^1\chi + 0.54 - P_f \quad (3.40)$$

As these polarity correction factors are empirically determined, this method cannot be extended to other classes of polar organic compounds until additional experimental work is done. In addition, organic phosphates fall into two groups rather than one. However, this correction extends our ability to estimate K_{om} , and by extension K_{oc} ,

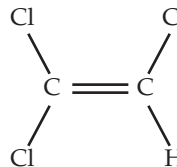
to a number of additional organic compounds. The molecular topology method has several advantages over the estimation of K_{ow} from octanol-water partition coefficients and aqueous solubility:

1. There is a theoretical basis to the molecular topology method for nonpolar organic compounds.
2. The literature contains a range of experimentally derived values for both the octanol-water partition coefficient and the aqueous solubility for a number of nonpolar organic compounds. One has no way of knowing which is the correct value.
3. Some compounds with similar aqueous solubility values have quite different octanol-water partition coefficients.
4. There are a number of competing equations that can be used for both the K_{ow} and solubility methods. One is never quite sure which to select.
5. The solubility and K_{ow} methods were devised strictly for nonpolar organic compounds. There is no way to extend them to polar organic compounds.

While considerable success has been achieved by calculating K_{ow} from the molecular structure, Montgomery (2007) states that any calculated $\log K_{ow}$ value above 7 should be regarded as suspect, and any experimental or calculated value above 8 should be treated with extreme caution. Also, the molecular topology method does not account for the ionic strength, pH, and temperature of the solution.

EXAMPLE PROBLEM

Compute the value of ${}^1\chi$ for trichloroethylene. The structure of trichloroethylene is as shown:



Trichloroethylene

There are four nonhydrogen pairs: Carbon 1 is bonded to two chlorine atoms and carbon 2. Carbon 2 is bonded to one chlorine atom. The following table shows the δ_i and δ_j values as well as the computed $(\delta_i \delta_j)^{-0.5}$ value for each pair.

Nonhydrogen pair	δ_i	δ_j	$(\delta_i \delta_j)^{-0.5}$
Cl-C(1)	1	3	0.577
Cl-C(1)	1	3	0.577
Cl-C(2)	3	2	0.408
C(2)-C(1)	2	1	0.707

$$2.269 = {}^1\chi$$

TABLE 3.7 Polarity correction factors for classes of polar organic compounds.

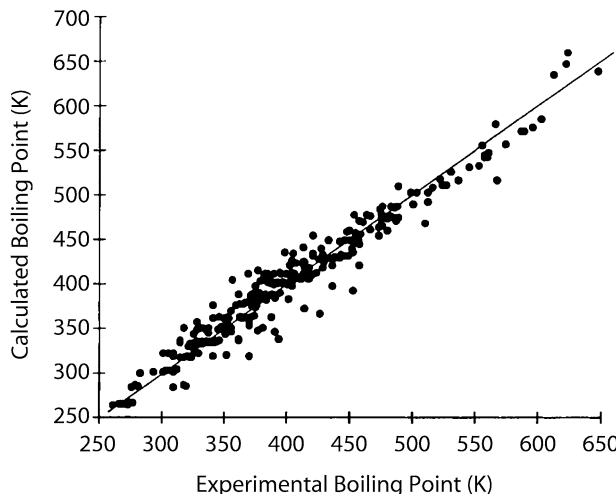
Class of Compounds	Polarity Correction Factor, P_f
Substituted benzenes and pyridines	1.00
Organic phosphates (group 1)	1.03
Carbamates	1.05
Anilines	1.08
Nitrobenzenes	1.16
Phenylureas	1.88
Triazines	1.88
Acetanilides	1.97
Uracils	1.99
Alkyl-N-phenylcarbamates	2.01
3-Phenyl-1-methylureas	2.07
3-Phenyl-1-methyl-1-methoxyureas	2.13
Dinitrobenzenes	2.28
3-Phenyl-1,1-dimethylureas	2.36
Organic acids	2.39
3-Phenyl-1-cycloalkylureas	2.76
Organic phosphates (group 2)	3.19

3.6.6 Quantitative Structure-Property Relationships

Quantitative structure-property relationships (QSPR) is a powerful analytical method for breaking down a molecule into a series of numerical values describing its relevant chemical and physical properties, such as partition coefficients, solubility, or reactivity. The QSPR concept is based on observations of linear free-energy relationships (Schwarzenbach et al. 2003) and usually takes the form of a plot or regression of the property of interest as a function of an appropriate molecular descriptor, which can be calculated using only a knowledge of molecular structure or a readily accessible molecular properties, such as molecular weight and volume, the number of specific atoms (e.g., carbon or chlorine), hydrophilic-lipophilic balance, or surface areas (Montgomery et al. 2006). Other parameters include, for example, steric and topological parameters, connectivities as well as quantum chemical parameters that can be calculated from molecular orbital calculations including charge and electron density. Figure 3.15 provides an example of a QSPR derived correlations for the calculated and measured boiling point of 298 organic compounds.

The use of descriptors calculated from a compound's molecular structure may eliminate the need for experimental determination of its physico-chemical properties and allows for the estimation of environmental properties even for molecules not yet synthesized (Le et al., 2012). For instance, Ghasemi and Saaidpour (2007) performed a QSPR study on 150 drug organic compounds. Modeling $\log K_{ow}$ of these compounds as a function of four theoretical molecular descriptors was established by multiple linear regression. The descriptors were molecular volume, hydrophilic-lipophilic balance, hydrogen bond forming ability and polar surface area. When tested against compounds with known K_{ow} , the square correlation coefficient (R^2)

FIGURE 3.15 QSPR model for boiling points of 298 organic compounds ($R^2 = 0.954$). The two descriptors for this QSPR model were the cubic root of the gravitational index and the hydrogen donor charged surface area.



Source: Reprinted with permission from Katritzky, Mu, Lobanov, and Karelson. 1996. The correlation of boiling points with molecular structure, Part I: A Training set of 298 diverse organics and a test of 9 simple inorganics. *Journal of Physical Chemistry* 100:10400–10407. American Chemical Society.

for the model was 0.99. Montgomery (2007) used the molar volume of a chemical compound at its normal boiling point as a major QSPR descriptor because it can be conveniently calculated by the Le Bas method (Reid et al. 1987; Mackay et al. 2006). The Le Bas method is based on a summation of atomic volumes with adjustment for the volume decrease arising from ring formation.

QSPR relationships have been applied to estimate the aqueous solubility, vapor pressure, octanol-water partition coefficient, Henry's law constant, bioconcentration factor, sorption coefficient, and environmental reaction rates and several other environmentally relevant partition coefficients, including the estimation of toxicological effects of chemical compounds. The applicability of QSPRs is limited by the quality of the experimental data, which typically is lower than the values of the molecular descriptors that can be calculated with relatively high precision (Montgomery 2007). Many environmentally relevant QSPRs are discussed in Montgomery et al. (2006) and QSPR tools and databases are available on the internet. For instance, the Estimation Programs Interface (EPISuite™) is a freely downloadable Windows-based group of physical/chemical property and environmental fate estimation programs developed by the United States Environmental Protection Agency (U.S. EPA 2012). The suite includes models that can predict physico-chemical properties such as $\log K_{ow}$ (KOWWIN), water solubility (WSKOW), Henry's law constant (HenryWin), etc. It also contains models that can predict the fate of organic substances in the environment, including bioaccumulation potential (BCFBAF), biodegradability (BioWin), and hydrolysis rate (HydroWin). Other online databases (e.g., National Institute of

Standards and Technology 2011 or CDS 2015) provide physic-chemical data, such as aqueous solubilities, vapor pressure, enthalpies or molecular structure information that might be useful for establishing QSPR of environmentally relevant compounds.

A related approach includes *quantitative structure–activity relationships (QSAR)* in which the physiochemical properties and/or structural properties of a compound are modeled as the response variable (Nantasesamat et al. 2009).

3.6.7 Multiple Solute Effects

Many hazardous waste sites contain more than one organic compound dissolved in groundwater. These may have come from several different sources, or from a single source, which is a mixture of organic liquids.

It has been shown that the solubility of structurally similar hydrophobic organic liquids in aqueous solutions is dependent upon the mixture of solutes present (Banerjee 1984). These liquids behave in a nearly ideal fashion, which is described by the following equation:

$$\frac{C_i}{S_i} = (x_i)_{org} \quad (3.41)$$

where

C_i = the equilibrium molar concentration of the i th component in the mixture

S_i = the water solubility of the component in its pure form

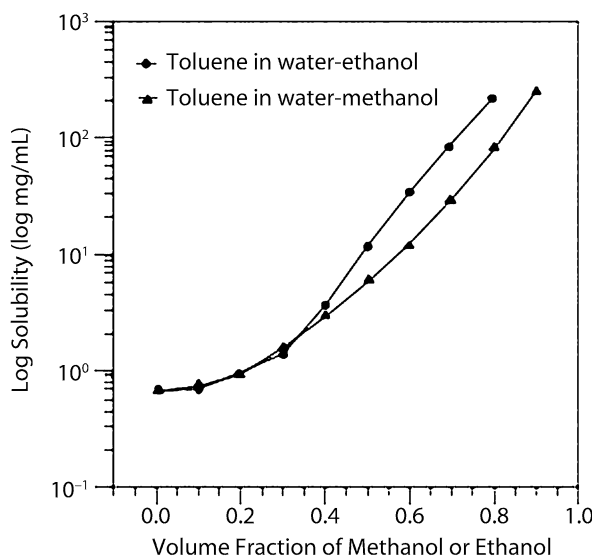
$(x_i)_{org}$ = the mole fraction of the i th compound in the organic phase

Equation 3.41 is a simplified version of Raoult's Law. It can be used to describe the water solubility of individual components of a nonaqueous phase liquid (NAPL) that is a mixture of several similar organic compounds. Such mixtures, which have been found in contact with groundwater include gasoline, diesel fuel, coal tar, creosote, and certain solvents that are a mixture of chlorinated ethanes and ethenes.

The concentration of a solute in a solution that is saturated with several structurally similar compounds is less than it would be in water alone. Mixtures of dissimilar liquids and of organic solids are more complex (Banerjee 1984). In addition to having mutual effects on solubility, organic mixtures will also compete for sorption sites.

In one study the presence of organic solvents, such as methanol, ethanol, 2-propanol, and butanol, in concentrations of 5 to 10%, reduced the soil-water partition coefficient for an organic molecule, kepone. This increased the rate at which kepone migrated through a soil column (Staples and Geiselmann 1988). This solubilization enhancing property of certain organic solvents is known as the **cosolvency effect** (Wood et al. 1990). Figure 3.16 illustrates the cosolvency effect of two alcohols, methanol and ethanol, on the solubility of a common petroleum hydrocarbon, toluene. The solubility of toluene increases with increasing volume fractions of the alcohols. This effect is being exploited for the enhanced remediation of soils polluted with hydrophobic compounds, such as polycyclic aromatic hydrocarbons (Birak et al. 2011). Chapter 9 will discuss this remediation approach in greater detail.

If a chemical analysis indicates that an aqueous sample contains a hydrophobic organic compound in amounts in excess of its solubility, it is likely that part of the

FIGURE 3.16 Solubility of toluene in water-ethanol and water-methanol mixtures.

Source: Yalkowski 1985.

compound is present as a nonaqueous phase liquid (NAPL). Under such conditions nonaqueous phase liquid transport theory must be considered (Hunt et al. 1988).

If a NAPL, such as creosote, is in contact with groundwater, Equation 3.41 means that the initial concentration of each of the individual organic compounds that makes up the creosote is a function of the mole fraction of that particular compound in the overall mixture as well as the aqueous solubility of the compound. Over time the more soluble constituents are leached from the NAPL and as their mole fraction of the NAPL decreases, the mole fraction of the compounds with lower solubility increases, as does their equilibrium concentration in water (Priddle and MacQuarrie 1994).

Case Study

Priddle and MacQuarrie (1994) studied the dissolution of creosote in water. Although the creosote was a mixture of many compounds, more than 50% was comprised of just 10 compounds of a class known as polynuclear aromatic hydrocarbons (PAH). Table 3.8 lists the hydrocarbons, their concentration in the creosote, their water solubility and their aqueous solubility as calculated by Raoult's law.

Priddle and MacQuarrie placed a small mass, 0.33 ml, of creosote in a glass column filled with uniform glass beads. Ultra-pure water was passed through the column with a mean residence time of the water in the column of 1.02 hour and a pore water velocity of 2.0 m/day. Seven of the ten compounds listed in Table 3.8 had effective solubilities greater than the detection limit of the analytical procedure being used. The other three compounds could not be detected. None of the seven compounds which were detected ever reached concentrations as great as their initial calculated effective solubilities. Over time, the observed concentrations of each compound decreased.

After 1 liter of water had contacted the 0.33 mL sample of creosote, the mass loss of the seven compounds was computed. The results are given in Table 3.9. It can be seen that most of the mass loss was due to dissolution of naphthalene, the most soluble of the compounds. The mass losses as well as the solubilities at the end of the test were in proportion to the initial effective solubilities.

TABLE 3.8 Calculated effective aqueous solubilities of major components of creosote.

Compound	Weight % in creosote	Formula weight	Aqueous solubility @ 20 to 25°C	Calculated Effective Solubility
Naphthalene	12.5	128.18	28 mg/L	16.4 mg/L
Acenaphthene	8.5	152.20	16.1 mg/L	1.97 mg/L
Fluorene	5.6	166.22	1.90 mg/L	0.65 mg/L
Phenanthrene	13.0	178.24	1.29 mg/L	0.54 mg/L
Anthracene	2.6	178.24	0.070 mg/L	0.17 mg/L
Fluoranthene	5.4	202.26	0.260 mg/L	0.081 mg/L
Pyrene	4.7	202.26	0.135 mg/L	0.10 mg/L
Benzo[a]anthracene	0.9	228.30	0.014 mg/L	0.0020 mg/L
Chrysene	0.8	228.30	0.002 mg/L	0.0022 mg/L
Benzo[a]pyrene	0.3	252.32	0.004 mg/L	0.00023 mg/L

Reprinted from Priddle and MacQuarrie (1994), with kind permission of Elsevier Science.

TABLE 3.9 Observed mean concentration of compounds in aqueous solution and mass loss from initial mass during contact with an amount of water equal to 330 times the initial mass of the creosote.

Compound	Calculated Effective Solubility (mg/L)	Observed mean concentration (mg/L)	Mean mass loss during leaching test in %
Naphthalene	16.4	5.10	4.5
Acenaphthene	1.97	0.94	0.83
Fluorene	0.65	0.41	0.34
Phenanthrene + Anthracene	0.71	0.45	0.40
Fluoranthene	0.081	0.025	0.022
Pyrene	0.10	0.013	0.011

EXAMPLE PROBLEM

A commercial solvent consists of 75% 1,1,1-trichloroethane (TCA) and 25% trichloroethene (TCE). What is the effective solubility of each compound if this solvent reaches groundwater? Use a formula weight of TCE of 139.39 and an aqueous solubility of 1,100 mg/L and a formula weight of TCA of 133.40 and an aqueous solubility of 730 mg/L.

Assume that the mixture is 750 grams of TCA to 250 grams of TCE. That is a ratio of 5.38 moles of TCA to 1.87 moles of TCE. The total number of moles is $5.38 + 1.87 = 7.25$. The mole fraction of TCA is $5.38/7.25 = 0.742$ and the mole fraction of TCE is $1.87/7.25 = 0.258$.

From Equation 3.36, the equilibrium concentration of TCA is

$$C = (x)_{TCA} S_{TCA}$$

$$C = 0.742 \times 1100 \text{ mg/L} = 816 \text{ mg/L}$$

The equilibrium concentration of TCE is

$$C = (x)_{TCE} S_{TCE}$$

$$C = 0.258 \times 730 \text{ mg/L} = 188 \text{ mg/L}$$

■ 3.7 Homogeneous Reactions

3.7.1 Introduction

According to the classification system of Rubin (1983) homogeneous reactions are ones that take place entirely within the liquid phase. If the reactions are reversible and proceed rapidly enough, the reaction can be described as being in local chemical equilibrium (Walsh et al. 1984). If the reaction either does not reach equilibrium or is nonreversible, then it is treated as a homogeneous, nonequilibrium reaction.

3.7.2 Chemical Equilibrium

If two compounds in solution, A and B, react to form product C, which can dissociate into A and B, then the reaction is reversible and is expressed as:



where a , b , and c represent the number of molecules of each compound that are needed to balance the reaction. When the reaction has progressed to the point that no further net production of C occurs, then it has reached equilibrium. The reaction continues, but the forward rate and the reverse rate have become equal. At that point, we can measure $[A]$, $[B]$, and $[C]$, the concentrations of the reactants and the product. The relationship between them is expressed as an equilibrium constant, K_{eq} .

$$K_{eq} = \frac{[C]^c}{[A]^a[B]^b} \quad (3.43)$$

The reaction must have sufficient time to proceed to the point of equilibrium before Equation 3.43 is valid.

3.7.3 Chemical Kinetics

If reaction 3.42 were to proceed so slowly that it would not have time to come to equilibrium in the framework of the groundwater flow system, then local equilibrium cannot be assumed and we must consider it in the framework of chemical kinetics. We can look at the reaction from the standpoint of either the disappearance of the reactants, A and B, or the appearance of the product, C. We have three rates to consider, two that describe the disappearance of the reactants and one that describes the production of the product:

$$R_A = -\frac{d[A]}{dt} = \kappa [A]^p [B]^q \quad (3.44)$$

$$R_B = -\frac{d[B]}{dt} = \kappa' [A]^p [B]^q \quad (3.45)$$

$$R_C = \frac{d[C]}{dt} = \kappa'' [C]^r \quad (3.46)$$

where

R_A and R_B = the reaction rates for the disappearance of A and B

R_C = the reaction rate for the appearance of C

$[A]$, $[B]$, $[C]$ = the measured concentrations of A, B, and C

κ , κ' , and κ'' = reaction rate constants

p , q , and r = reaction order with respect to the indicated reactant or product

If one of p , q , or r in Equations 3.44, 3.45, and 3.46 is equal to zero, then the reaction rate is not a function of that product or reactant and the reaction is said to be **zero order** with respect to that reactant or product.

If one of p , q , or r is equal to 1, then there is a linear relationship with respect to that product or reactant, and the reaction rate is said to be **first order**.

If neither p , q , or r is 0 or 1, then there is a more complex relationship with respect to that product or reactant. Such a reaction is more difficult to analyze mathematically than zero-or first-order kinetics.

If a compound is present in a system in great excess, then the reaction rate may well be independent of the concentration. If we consider the depletion of reactant A in such a system, it could be described by the zero-order equation

$$[A] = [A]_0 - \kappa t \quad (3.47)$$

where

κ = the reaction rate constant

$[A]_0$ = the initial concentration

$[A]$ = the concentration at some time t

In a first order system, the rate at which the reactant disappears is described by

$$\ln \frac{[A]}{[A]_0} = -\kappa t \quad (3.48)$$

or

$$[A] = [A]_0 e^{-\kappa t} \quad (3.49)$$

Reaction-rate constants and the order of the reactions must be determined experimentally. These are not equal to the equilibrium constant of the reaction.

■ 3.8 Radioactive Decay

If radionuclides enter the groundwater system, those which are cations, are possibly subjected to retardation on soil surfaces. In addition they will undergo radioactive decay, which will reduce the concentration of radionuclides in both the dissolved and sorbed phases. A factor for radioactive decay can be substituted for the last term of Equation 3.1 in the following form:

$$\left(\frac{\partial C}{\partial t} \right)_{\text{decay}} = -\frac{\ln 2}{\lambda} C \quad (3.50)$$

where λ is the half-life of the radionuclide.

Radioactive decay is a first order decay process and as such follows Equation 3.49. The reaction rate constant, K, is equal to $\ln 2 / \lambda$ so that Equation 3.49 becomes

$$[C] = [C_1] e^{-(\ln 2 / \lambda)t} \quad (3.51)$$

This term can be appended to any of the transport equations to calculate the effects of radioactive decay on top of the diffusion and dispersion accounted for by the transport equation. In essence, the C_1 of equation 3.51 is the concentration that would be present in the absence of any radioactive decay. As an example, Equation 2.25, the approximate solution for one-dimensional dispersion becomes:

$$C = \left\{ \frac{C_0}{2} \left[\operatorname{erfc} \left(\frac{L - v_x t}{2\sqrt{D_L t}} \right) \right] \right\} e^{-\frac{-\ln 2}{\lambda} t} \quad (3.52)$$

A slug injection into a one dimensional flow field can be expressed as

$$C = \frac{M / A}{\sqrt{4\pi D_L t}} \exp \left[-\frac{(L - v_x t)^2}{4D_L t} \right] \quad (3.53)$$

where M is the mass injected over aquifer cross sectional area A. When combined with the expression for radioactive decay this becomes:

$$C = \left\{ \frac{M / A}{\sqrt{4\pi D_L t}} \exp \left[-\frac{(L - v_x t)^2}{4D_L t} \right] \right\} e^{-\frac{-\ln 2}{\lambda} t} \quad (3.54)$$

EXAMPLE PROBLEM

A flask containing 0.55 kg of liquid radioactive cesium is spilled onto the ground. It soaks into a thin aquifer with a cross sectional area of 1.87 m². Groundwater is flowing at a rate of 0.22 m/d and the value of D_L is 3.88 m²/d. What is the concentration of Cesium, which has a half-life of 33 years, in the center of mass after 1 year?

The center of mass will move a distance, equal to $v_x t$. Therefore

$$L = v_x t = 0.22 \text{ m/d} \times 365 \text{ d} = 80.3 \text{ m}$$

Substituting into equation 3.54, we obtain:

$$C = \frac{0.55 \text{ kg} / 1.87 \text{ m}^2}{\sqrt{4 \times \pi \times 3.88 \text{ m}^2 / d \times 365 \text{ d}}} \exp \left[-\frac{(80.3 \text{ m} - 0.22 \text{ m/d} \times 365 \text{ d})^2}{4 \times 3.88 \text{ m}^2 / d \times 365 \text{ d}} \right] \exp \frac{-\ln 2}{33 \text{ yr}} \times 1 \text{ yr}$$

$$C = \frac{0.294 \text{ kg/m}^2}{133.4 \text{ m}} \times 1 \times \exp^{-0.021} = 0.0022 \text{ kg/m}^3$$

■ 3.9 Biodegradation

The degradation of dissolved organic molecules in groundwater is of great interest to practicing contaminant hydrogeologists. As was shown in Chapter 1, much of the groundwater contamination is due to organic chemicals, including hydrocarbons. The mechanism of biodegradation will be covered in detail in Chapter 7. In this section we will examine the transport and decay equations that can be used to describe the process. Although a wide range of organic molecules can be degraded, for the sake of this discussion we will refer to them simply as hydrocarbons. The hydrocarbons form a substrate for microbial growth—that is, they provide the energy source for the microbes which form a **biofilm** on the solid surfaces in the aquifer.

Anaerobic decomposition of hydrocarbons means that some microorganisms can degrade hydrocarbons in the absence of oxygen. These microbes use another electron acceptor, such as nitrate (Chapelle 1993). Anaerobic decomposition of hydrocarbons can be described by a variation of the Monod function (also known as Michaelis-Menten function), which describes two-step catalytic chemical reactions (Bouwer and McCarty 1984). This function is

$$\frac{dH}{dt} = -h_{ua} M_a \left(\frac{H}{K_a + H} \right) \quad (3.55)$$

where

H = hydrocarbon concentration in pore fluid (ML^{-3})

M_a = total mass of anaerobic microbes

h_{ua} = maximum hydrocarbon utilization rate per unit mass of anaerobic microbes

K_a = half-maximum rate concentration of the hydrocarbon for anaerobic decay

However, in some cases one would modify the Monod function to include an electron acceptor term similar to the term introduced later in this section when discussing the Monod function for aerobic conditions. Based on Eqn. 3.55, the solute transport and decay equation for anaerobic biodegradation in the aqueous phase is

$$\frac{\partial H}{\partial t} = \frac{1}{r_h} \left(D_L \frac{\partial^2 H}{\partial x^2} - v_x \frac{\partial H}{\partial x} \right) - \frac{h_{ua} M_a}{r_h} \left(\frac{H}{K_a + H} \right) \quad (3.56)$$

where r_h is the retardation factor for hydrocarbon.

If the concentration of the hydrocarbon, H , is much less than K_a , the half-maximum rate concentration, then Equation 3.55 can be simplified to a linear form by neglecting H in the denominator (Bouwer and McCarty 1984). This results in a first-order decay term:

$$\frac{dH}{dt} = -\left(\frac{h_{ua} M_a}{K_a}\right) H \quad (3.57)$$

Under these conditions the solute-transport equation with anaerobic biodegradation becomes

$$\frac{\partial H}{\partial t} = \frac{1}{r_h} \left(D_L \frac{\partial^2 H}{\partial x^2} - v_x \frac{\partial H}{\partial x} \right) - \left(\frac{h_{ua} M_a}{r_h K_a} \right) H \quad (3.58)$$

A single microbial growth substrate (that is, a hydrocarbon or other organic chemical that can serve as an energy source for the microbes) cannot be reduced for extended periods of time below the minimum concentration needed to maintain the microbial population. In other words, microbes cannot degrade a substance below the concentration that they need to continue to exist. This minimum concentration, H_{min} , is a function of the hydrocarbon, the electron acceptor, and the microorganism. It can be expressed as (Bouwer and McCarty 1984)

$$H_{min} = K_h \left(\frac{b}{Yh_u - b} \right) \quad (3.59)$$

where Y is the microbial yield coefficient (g cells/g hydrocarbon).

Although there is a minimum hydrocarbon concentration for each hydrocarbon that might be present, microbes may utilize more than one hydrocarbon as a growth substrate. As a result, if there is a mixture of hydrocarbons present, the microbes could degrade the separate hydrocarbons to concentrations that are lower than if the individual hydrocarbon were the only one present (McCarty, Reinhard, and Rittman 1981). The primary substrate that is supporting the microbes can be a single substance or a mixture of substances. Although the primary substrate is supporting the growth of the microbes, substances that are present in trace amounts can be consumed by the microbial population through a process known as **secondary utilization**. The decay of a hydrocarbon that is undergoing secondary utilization is described by Equation 3.57.

If the microbes require oxygen in their metabolism, then the process is called **aerobic biodegradation**. The removal of the hydrocarbons, the consumption of oxygen in the process, and the growth of the microbes in the aquifer, ignoring transport through the biofilm, can be described by the following equations, which is another modification of the **Monod function** (Borden and Bedient 1986):

$$\frac{dH}{dt} = -M_t h_u \left(\frac{H}{K_h + H} \right) \left(\frac{O}{K_0 + O} \right) \quad (3.60)$$

$$\frac{dO}{dt} = -M_t h_u G \left(\frac{H}{K_h + O} \right) \left(\frac{O}{K_0 + O} \right) \quad (3.61)$$

$$\frac{dM_t}{dt} = M_t h_u Y \left(\frac{H}{K_h + H} \right) \left(\frac{O}{K_o + O} \right) + K_c Y C_{oc} - b M_t \quad (3.62)$$

where

- O = oxygen concentration in pore fluid (ML^{-3})
- M_t = total aerobic microbial concentration (ML^{-3})
- h_u = maximum hydrocarbon utilization rate per unit mass of aerobic microorganisms (T^{-1})
- K_h = hydrocarbon half-saturation constant (ML^{-3})
- K_o = oxygen half-saturation constant (ML^{-3})
- k_c = first-order decay rate of natural organic carbon
- C_{oc} = natural organic carbon concentration (ML^{-3})
- b = microbial decay rate (T^{-1})
- G = ratio of oxygen to hydrocarbon consumed

In the case of aerobic microbial decay, there is some minimum oxygen concentration below which aerobic decay will not occur. The microorganisms will grow on both naturally occurring organic carbon as well as hydrocarbon contaminants. The microorganisms tend not to move in the aquifer because they generally adhere to aquifer materials (Harvey, Smith, and George 1984). Even if the microbes are free to move, the natural tendency of the aquifer matrix will be to filter them out. There will be some tendency for microbes to transfer between the solid surface and the solution. As a first approximation this can be considered to be a linear function of the total mass of microorganisms.

We can combine Equations 3.60, 3.61, and 3.62 individually with Equation 3.1 to obtain solute transport equations for hydrocarbon, oxygen and microorganisms. The hydrocarbon is assumed to sorb onto the solid surfaces following a linear sorption isotherm. The resulting equations are (Borden and Bedient 1986)

$$\frac{\partial H}{\partial t} = \frac{1}{r_h} \left(D_L \frac{\partial^2 H}{\partial x^2} - v_x \frac{\partial H}{\partial x} \right) - \frac{h_u M_t}{r_h} \left(\frac{H}{K_h + H} \right) \left(\frac{O}{K_o + O} \right) \quad (3.63)$$

$$\frac{\partial O}{\partial t} = D_L \frac{\partial^2 O}{\partial x^2} - v_x \frac{\partial O}{\partial x} - h_u M_t G \left(\frac{H}{K_h + H} \right) \left(\frac{O}{K_o + O} \right) \quad (3.64)$$

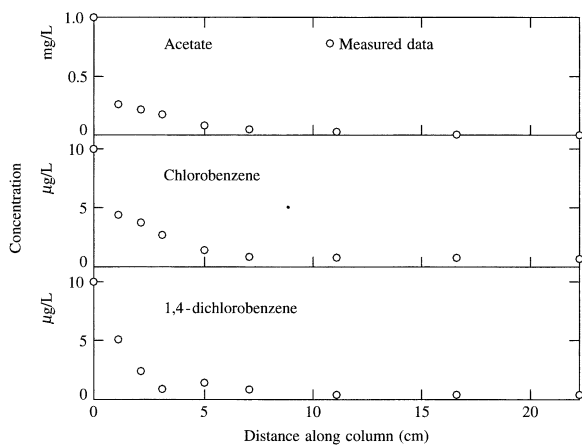
$$\begin{aligned} \frac{\partial M_s}{\partial t} &= \frac{1}{r_m} \left(D_L \frac{\partial^2 M_s}{\partial x^2} - v_x \frac{\partial M_s}{\partial x} \right) + h_u M_s Y \left(\frac{H}{K_h + H} \right) \left(\frac{O}{K_o + O} \right) \\ &\quad + \frac{K_c Y C_{oc}}{r_m} - b M_s \end{aligned} \quad (3.65)$$

where

- M_s = concentration of aerobic microbes in solution
- r_m = microbial retardation factor
- v_x = average linear groundwater velocity

Figure 3.17 shows the results of a laboratory experiment in microbial decay (Bouwer and McCarty 1984). An aerobic soil column was established with a

FIGURE 3.17 Measured steady-state profiles of the biodegradation of acetate, chlorobenzene and 1,4-dichlorobenzene in an aerobic biofilm reactor.



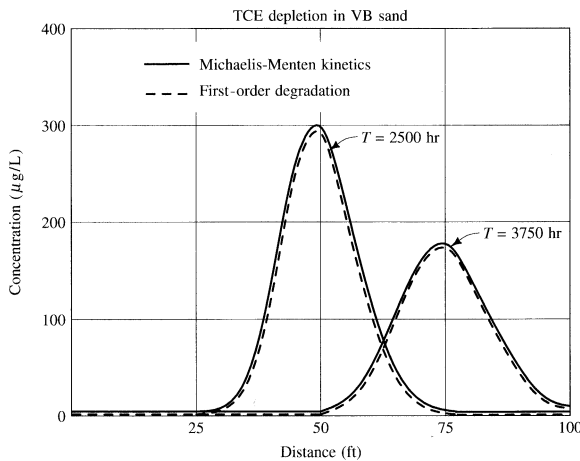
Source: Modified from Bouwer and McCarty. 1984. Modeling of trace organics biotransformation in the subsurface. *Groundwater* 22:433–440. Used with permission.

microbial population. A solution with 10 mg/L of acetate as the primary substrate along with 10 $\mu\text{g}/\text{L}$ of chlorobenzene and 10 $\mu\text{g}/\text{L}$ of 1,4-dichlorobenzene as secondary substrates was introduced into the soil column as a constant flow. The utilization of the primary and the secondary substrates occurred simultaneously in the first 7 cm (2.75 in) of the soil column. After that flow distance, all three compounds reached an irreducibly low concentration that would not support further microbial growth.

Srinivasan and Mercer (1988) developed a computer model, BIO1D, which simulates one-dimensional solute transport with biodegradation. In their model they relied upon the observations of Borden et al. (1986) that microbial growth reaches equilibrium rapidly with respect to the rate of groundwater flow and therefore the microbial population can be assumed to be constant. This means that Equation 3.65 is not needed, since $dM_s/dt = 0$. The model solves the equivalent of Equations 3.63 and 3.64 for aerobic biodegradation and Equation 3.56 for anaerobic decomposition. The computer code automatically switches from aerobic to anaerobic decomposition if the oxygen levels drop below the minimum to support aerobic decay.

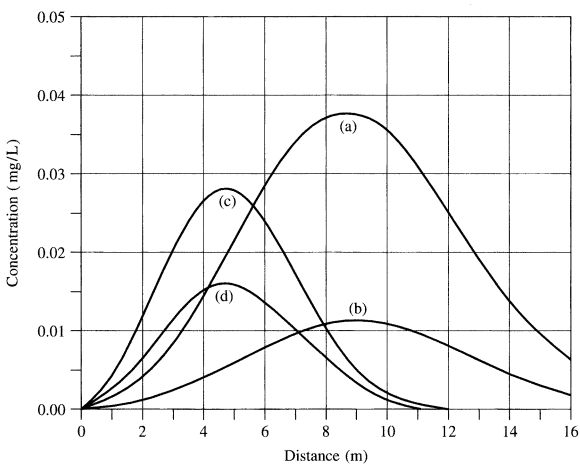
If the substrate concentration, H , is less than $0.25K_a$ and conditions are anaerobic, then the equation used is 3.58. If $H \ll K_a$, the Michaelis-Menten function and the first-order decay function will yield similar results. Figure 3.18 shows the modeling of the anaerobic biodegradation of trichloroethylene (Srinivasan and Mercer 1988). A pulse of contamination of 2780- $\mu\text{g}/\text{L}$ trichloroethylene (TCE) was injected into an aquifer for 150 hr, followed by continued injection of clean water. Figure 3.18 shows the concentration of TCE in the plume after 2500 hr and again after 3750 hr. Both Michaelis-Menten and first-order decay functions were used in the modeling, with very similar results. The reduction in the peak concentration of the TCE plume with travel time can also be seen on this figure.

FIGURE 3.18 Modeling of the movement and anaerobic biodegradation of a trichloroethylene plume in a sand aquifer using both Michaelis-Menten and first-order decay functions.



Source: Srinivasan and Mercer. 1988. Simulation of biodegradation and sorption processes in ground water. *Groundwater* 26:475–487. Used with permission.

FIGURE 3.19 BIO1D model showing the position of a solute plume with (a) no retardation and no decay, (b) no retardation but biodegradation, (c) retardation that follows a linear sorption isotherm but no decay, and (d) retardation that follows a linear sorption isotherm and biodegradation.



The BIO1D model can be used to illustrate the effects of retardation and biodegradation. Figure 3.19 shows the position of a solute plume with (a) no retardation and no decay, (b) no retardation but biodegradation, (c) retardation that follows a linear sorption isotherm but no decay and (d) retardation that follows a linear sorption isotherm and biodegradation. This model represents the movement of a slug of solute introduced into

an aquifer over a 160-da period. The position of the solute front is shown after 800 da of travel. Biodegradation is modeled as first-order decay with a half-life of 400 da. Retardation delays the advance of the solute front, whereas biodegradation reduces the peak value.

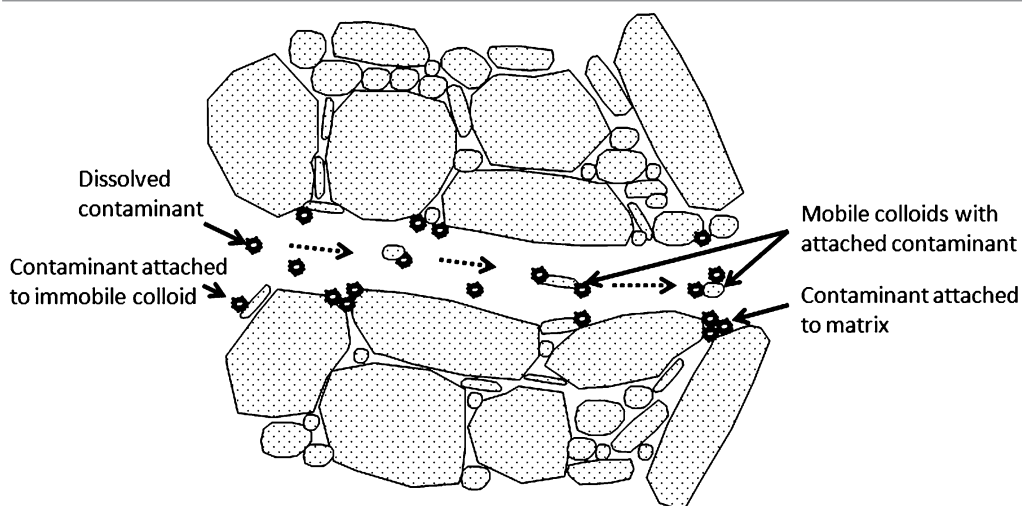
■ 3.10 Colloidal Transport

Colloids are particles with diameters approximately between 1 nm and 1 μm . Colloidal-size particles include dissolved organic macromolecules, such as humic substances, microorganisms, tiny droplets of insoluble organic liquids, and mineral matter (McCarthy and Zachara 1989; McCarthy and Degueldre 1993). Some colloids may be small enough to flow through the pores of an aquifer. If dissolved solutes partition onto a colloid, this can create a second mobile phase and a rapid transport pathway for a number of contaminants, including some heavy metals and hydrophobic organic pollutants (e.g., Boving and Brusseau 2000; Frimmel et al. 2007). The solute can then be found in three regions: dissolved in the aqueous phase, sorbed onto mobile colloids, and sorbed onto immobile surfaces, including immobile colloids (Figure 3.20). The study of colloids in groundwater is greatly complicated by the fact that the process of installing monitoring systems such as wells and piezometers may introduce colloids that were not originally present. Sampling processes may also create colloids, such as the precipitation of colloidal iron due to oxygenation of water and the dislocation of stable colloids due to too-rapid pumping.

Methods of collecting groundwater samples so that colloids are not drawn into the monitoring well will be discussed in Chapter 8.

In order for colloids to participate in contaminant transport, they must first be released to the groundwater. This can occur due to chemical precipitation, biological activity, or disaggregation of stable aggregates. They can also be carried into the aquifer by infiltrating water, especially through cracks and macropores.

FIGURE 3.20 Colloid facilitated transport affects the mobility of contaminants in porous media by providing a mobile phase to which the contaminant binds while flowing through the pores.



Colloids are mobile if their surface chemistry is such that the individual colloids are repulsed so that they remain disaggregated, rather than being attracted to form larger particles. In addition, the pore-size geometry must be such that the colloids are not filtered from the suspension.

There is ample evidence in the literature that colloids can migrate in aquifers. Keswick, Wang, and Gerba (1982) report that bacteria have migrated up to 900 m (2,950 ft) in an aquifer and viruses have migrated up to 920 m (~3,000 ft). In fact, Pang and Simunek (2006) suggest that biogenic cell materials may themselves convey the transport of metals and radionuclides. Layered silicate clays from surface soils have been found to travel up to several hundred meters to wells (Nightingale and Bianchi 1977). Asbestos fibers have been found in an aquifer recharged with surface water containing the mineral (Hayward 1984). Grolimund and Borkovec (2001) provide a model for the release and transport of colloidal particles in natural porous media.

Colloids have been implicated in the unexpected movement of plutonium and americium, radioactive elements that are normally believed to be relatively immobile in the soil due to a high distribution coefficient (McCarthy and Zachara 1989). For instance, Zavarin et al. (2013) concluded that colloids can potentially facilitate the transport of plutonium (IV) through fractured carbonate rock at the Yucca Mountain test site in Nevada.

Transport of contaminants as colloids can be affected by ionic strength and composition of the groundwater, its velocity, the quantity, size and nature of colloids, size and geometry of aquifer pores. Puls and Powell (1992) found that colloidal iron oxide could transport arsenic which was sorbed onto the iron oxide surface. They also found that under some conditions the iron oxide colloids could travel faster than tritiated water. This is a result of the size exclusion effect, which is discussed below.

An aqueous solution may contain dissolved organic macromolecules, such as humic acids. Hydrophobic organic solvents in aqueous mixtures may partition onto these macromolecules rather than soil organic carbon (Enfield 1985). When this happens the mobility of the organic solvent is greatly enhanced, especially if it has a low mobility (high K_{oc} value). In fine-grained soils or aquifers the macromolecules may even have a velocity greater than the average linear groundwater velocity (Enfield and Bengtsson 1988). This is due to the **size-exclusion effect**, which occurs when molecules or ions are so large that they cannot travel through the smaller pores. As a result, they are restricted to the larger pores, in which the groundwater velocity is greater than average. Thus these molecules will travel at a rate greater than the average linear groundwater velocity. This effect is more prevalent in fine-grained soils and aquifers with some pores small enough to exclude some molecules. Organic macromolecules are likely to be produced in municipal landfill leachate, which has a high amount of dissolved organic carbon. This is one reason co-disposal of toxic organic liquids and municipal refuse is not wise.

The colloid-facilitated contaminant transport in the presence of homogeneous colloids can be modeled by extending the advection-dispersion equation to include the three phases associated with colloid transport (Equation 3.66), i.e., $\sigma_s [M_c/M]$ is the chemical concentration sorbed to immobile surfaces of the porous matrix, $\sigma_c [M_c/M]$ is the chemical concentration sorbed to mobile colloids, and $\sigma_{cs} [M_c/M]$ is the chemical concentration sorbed to immobile colloids (M_c and M refer to the dimension for mass of contaminants and the mass of the sorbent, respectively) (Massoudieh and Ginn 2010).

$$\begin{aligned} \frac{\delta C}{\delta t} + \frac{\delta G_m \sigma_c}{\delta t} + \frac{\rho_b}{\theta} \frac{\delta \sigma_s}{\delta t} + \frac{\rho_b}{\theta} \frac{\delta G_s \sigma_{cs}}{\delta t} + v \frac{\delta C}{\delta z} + v_c \frac{\delta G_m \sigma_c}{\delta z} \\ = \frac{\delta}{\delta z} \left(D \frac{\delta C}{\delta z} + D_c \frac{\delta G_m \sigma_c}{\delta z} \right) \end{aligned} \quad (3.66)$$

where C [M_c/L^3] is the mass concentration of dissolved contaminants in the pore water; v [L/T] is the advective velocity for dissolved species, v_c [L/T] is the advective velocity for colloidal particles and D [L^2/T] and D_c [L^2/T] are the dispersion coefficients for dissolved and colloid-bound contaminants, respectively. G_m [M/L^3] is the mass concentration of mobile colloidal particles; G_s [M/M] is the immobilized (attached, filtered, trapped) colloid concentration. ρ_b [M/L^3] is the dry bulk density of the soil matrix; θ is the water content equal to the porosity in a saturated medium.

The concentration of the mobile colloids and those attached to the porous matrix can be expressed by a colloid equilibrium distribution coefficient:

$$K_s = \frac{G_s}{G_m} \quad (3.67)$$

Similarly, equilibrium distribution coefficients can be defined for the contaminant distribution between the bulk aqueous phase and mobile colloidal particles (K_{Dc}), the solid matrix (K_{Ds}), and the immobile colloidal particles (K_{Dsc}).

$$K_{Dc} = \frac{\sigma_c}{C} \quad (3.68)$$

$$K_{Ds} = \frac{\sigma_s}{C} \quad (3.69)$$

$$K_{Dsc} = \frac{\sigma_{sc}}{C} \quad (3.70)$$

Incorporating Equations 3.67 to 3.70 into Equation 3.71, and assuming that the advective velocities and dispersion coefficients are equal for colloidal particles and aqueous species, results in (Massoudieh and Ginn 2010)

$$\begin{aligned} \frac{\delta C}{\delta t} + K_{Dc} \frac{\delta G_m C}{\delta t} + \frac{\rho_b}{\theta} K_{Ds} \frac{\delta C}{\delta t} + \frac{\rho_b}{\theta} K_s K_{Dsc} \frac{\delta G_m C}{\delta t} + v \frac{\delta C}{\delta z} + v K_{Dc} \frac{\delta G_m C}{\delta z} \\ = \frac{\delta}{\delta z} \left(D \frac{\delta C}{\delta z} + D K_{Dc} \frac{\delta G_m C}{\delta z} \right) \end{aligned} \quad (3.71)$$

Equation 3.71 can be simplified by assuming that the total concentration of colloidal particles remains constant with time:

$$\begin{aligned} \left(1 + K_{Dc} G_m + \frac{\rho_b}{\theta} K_{Ds} + \frac{\rho_b}{\theta} K_s K_{Dsc} G_m \right) \frac{\delta C}{\delta t} + v \left(1 + K_{Dc} G_m \right) \frac{\delta C}{\delta z} \\ = \left(1 + K_{Dc} G_m \right) \frac{\delta}{\delta z} \left(D \frac{\delta C}{\delta z} \right) \end{aligned} \quad (3.72)$$

Massoudieh and Ginn (2007) point out that Equation 3.72 can be expressed either as a simple advection-dispersion equation with adjusted retardation factors (e.g., Magee et al. 1991), or with adjusted advective velocities and dispersion coefficients (Enfield and Bengtsson 1988).

3.10.1 Colloid Attachment/Detachment and Straining Theory

When moving with the aqueous phase, colloids occasionally collide with solid surfaces and become temporarily or permanently attached to them (Figure 3.20). If the colloid is only temporarily attached to the surface of a solid, it will eventually detach and re-enter the aqueous phase. The mass transfer of colloids to the solid-water interface occurs via diffusion, interception, and sedimentation (Yao et al. 1971). Clean bed filtration theory (CFT) is often used to characterize colloid attachment in porous media (e.g., Tufenkji and Elimelech 2004). Based on CFT, Bradford et al. (2002; 2003) developed a conceptual model for colloid transport that accounts for colloid attachment/detachment and straining. Colloid attachment and detachment, E_{att} , between the aqueous and solid phase is modeled using first-order rate expressions:

$$E_{att} = \frac{\delta(\rho_b S_{att})}{\delta t} = \theta_w k_{att} C - \rho_b k_{det} S_{att} \quad (3.73)$$

where ρ_b is the soil bulk density [$M\ L^{-3}$], S_{att} is the solid-phase concentration of attached colloids [$N\ M^{-1}$], k_{att} is the first-order colloid attachment coefficient [T^{-1}], k_{det} is the first-order colloid detachment coefficient [T^{-1}].

Equation 3.73 may include a dimensionless colloid attachment function φ_{att} when simulating colloid transport under conditions that do not adhere to clean-bed conditions (Bradford et al. 2003). Simunek et al. (2006) notes that the attachment and detachment coefficients are strongly dependent upon water content, with attachment significantly increasing as the water content decreases. The attachment coefficient is calculated using filtration theory (Logan et al. 1995), which is a quasi-empirical formulation in terms of the median grain diameter of the porous medium ("collector"), the pore-water velocity, and collector and collision ("sticking") efficiencies accounting for colloid removal due to diffusion, interception and gravitational sedimentation (Rajagopalan and Tien 1976; Logan et al. 1995).

Straining is the trapping of colloid particles in down gradient pore throats that are too small to allow particle passage (McDowell-Boyer et al. 1986). The magnitude of straining of colloids depends on the ratio of the colloid and pore size. In contrast to mechanical filtration, straining only occurs in a fraction of the soil pore space, and colloid transport can still occur in the larger portions of the continuous pore networks (Bradford et al. 2006). Colloid straining is described using an irreversible first-order straining term:

$$E_{str} = \frac{\delta(\rho_b S_{str})}{\delta t} = \theta_w k_{str} \varphi_{str} C \quad (3.74)$$

Where S_{str} is the solid-phase concentration of strained colloids [$N\ M^{-1}$], k_{str} is the first-order colloid straining coefficient [T^{-1}], and the value of k_{str} depends on the colloid and porous medium size (Bradford et al. 2003). The parameter φ_{str} is a dimensionless

colloid straining function and can be calculated from down gradient distance, z , from the porous medium inlet:

$$\varphi_{str} = \left(\frac{d_{50} + z}{d_{50}} \right)^{-\beta} \quad (3.75)$$

where β is a fitting parameter that controls the shape of the colloid spatial distribution. The parameter d_{50} is the mean pore diameter of the porous matrix.

Attachment/Detachment theory has been used to model not just the transport of colloids, but also the movement of pathogens through the unsaturated zone. For instance, Morales et al. (2014) used the attachment and detachment functions embedded in the HYDRUS 2D/3D model to simulate the transport of pathogen surrogates, *E. coli* and MS-2 coliphage, their fate in three types of soil under unsaturated conditions. It was shown that the rate of attachment of *E. coli* bacteria was approximately two to three orders of magnitude greater than the detachment rate. These findings suggest that bacteria prefer being attached to the solid material surface rather than returning into the aqueous phase. This has implications on the performance of soil based waste water treatment systems, such as septic tanks.

Case Study

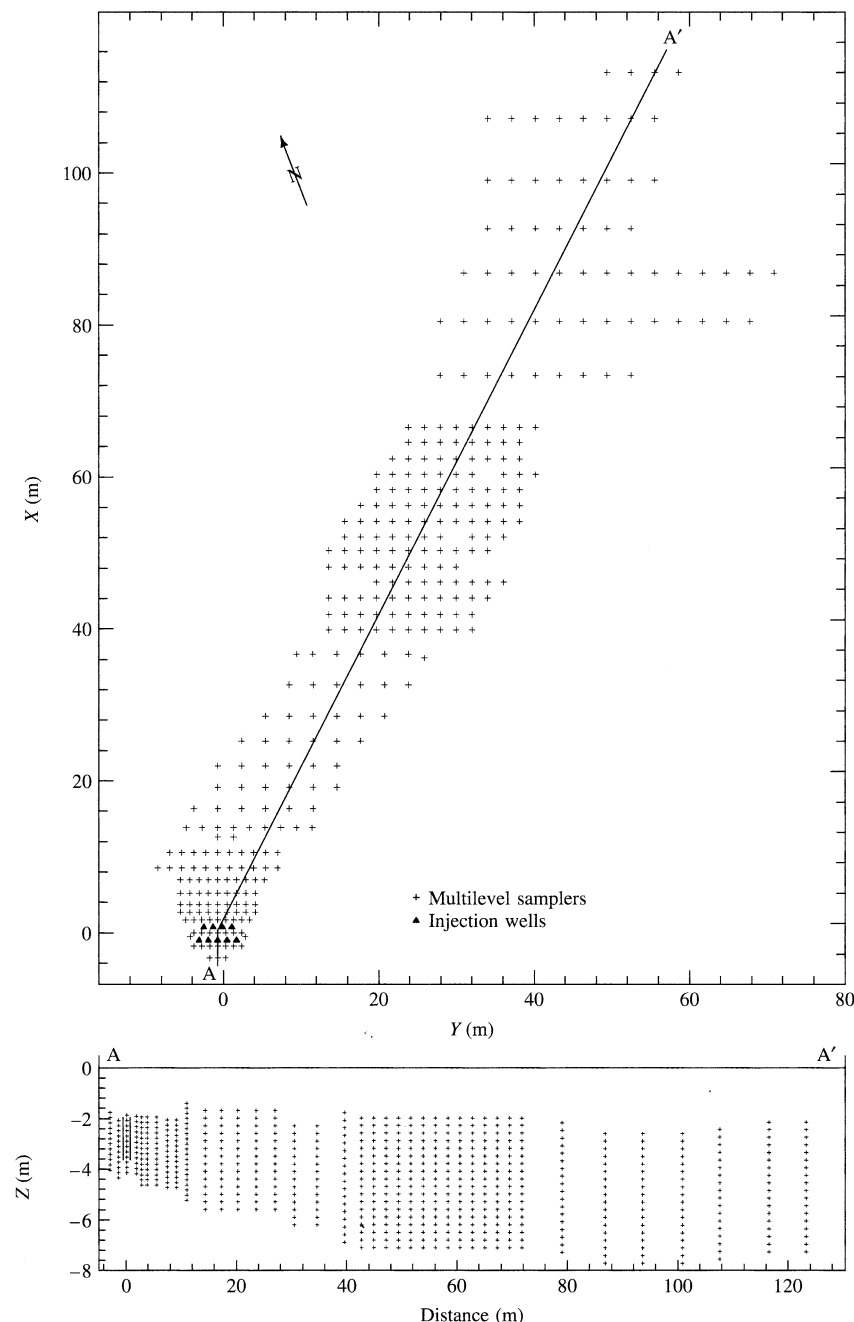
Large-Scale Field Experiment on the Transport of Reactive and Nonreactive Solutes in a Sand Aquifer Under Natural Groundwater Gradients-Borden, Ontario

The Canadian Forces Base (CFB) in Borden, Ontario was already introduced in Chapter 2 (Sudicky and Illman 2011). In August, 1982, an experiment was begun by injecting a slug of about 12 m^3 (3,170 gal) of a solution containing known masses of two inorganic tracers (chloride and bromide) and five halogenated organic chemicals in aqueous phase (bromoform, carbon tetrachloride, tetrachloroethylene, 1,2-dichlorobenzene, and hexachloroethane) into a sand aquifer. The tracer solution was allowed to advect and disperse under natural-gradient conditions. The aquifer was instrumented with 275 multilevel groundwater samplers (Mackay et al. 1986; Freyberg 1986; Roberts et al. 1986). Each multilevel sampler had from 14 to 18 sampling ports vertically separated by about 0.2 to 0.3 m (0.6 to 1 ft). Figure 3.14 shows the distribution of the sampling points. The average porosity of the sand is 0.33, the geometric mean of hydraulic conductivity is $7.2 \times 10^{-5} \text{ m/sec}$ (20.4 ft/da), and the mean annual horizontal gradient is 0.0043. The average linear groundwater velocity computed from these values is 29.6 m/yr (89 ft/yr). The direction of groundwater flow at the site is to the northeast in the direction indicated by line A-A' on Figure 3.21.

From August 24, 1982, to June 2, 1984, synoptic monitoring was accomplished as water was withdrawn from a large number of the monitoring devices and analyzed for the ionic tracers and organics on 18 different occasions. This was done in order to assess the overall movement of the plume. In addition, at selected points along the flowpath time-series monitoring was done by sampling on a much more frequent basis than the synoptic monitoring. In all, 14,465 samples were analyzed from over 5000 sampling points during this time period for the synoptic monitoring program, and 1246 samples were analyzed for the time-series monitoring.

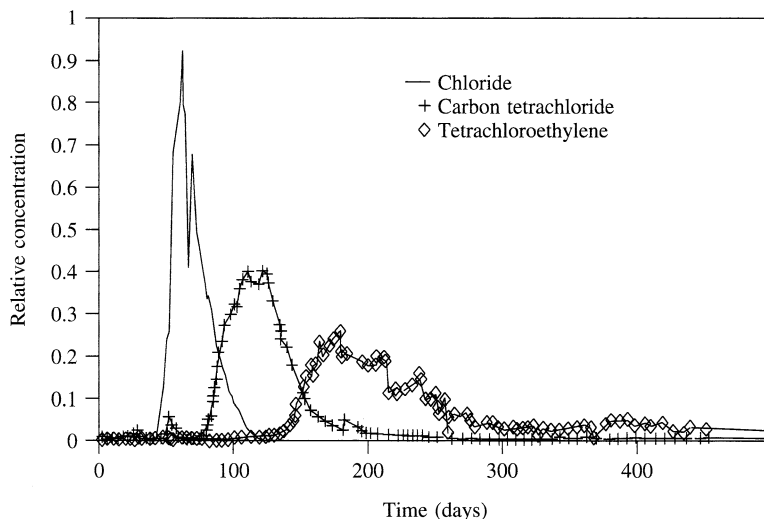
Figure 3.22 shows the breakthrough curves for chloride, carbon tetrachloride, and tetrachloroethylene at a monitoring point in the center of the plume located 5.0 m from the injection wells. Values are shown as relative concentration, which is the observed concentration

FIGURE 3.21 Location of multilevel sampling devices at the site of the Borden, Ontario, tracer test.



Source: Mackay et al. 1986. *Water Resources Research* 22:2017–2030. Copyright by the American Geophysical Union. Reproduced with permission.

FIGURE 3.22 Arrival times of chloride, carbon tetrachloride, and tetrachloroethylene at a measuring point 5.0 m downgradient from the injection well at Borden, Ontario.



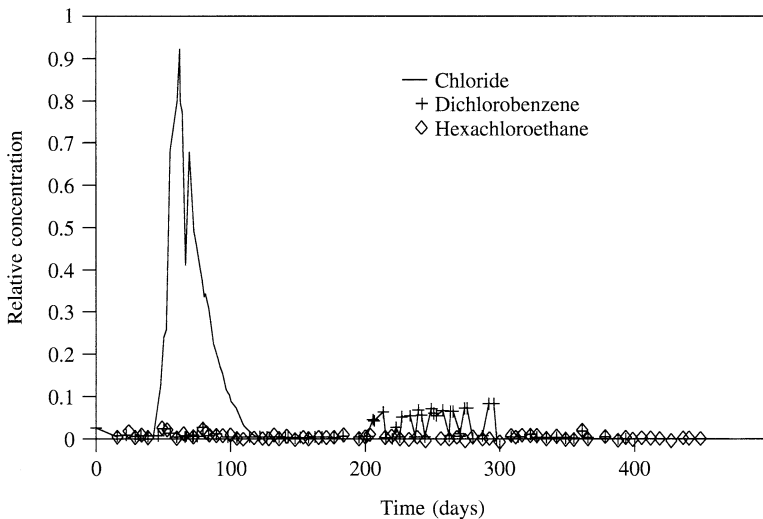
Source: Roberts, Goltz, and Mackay. 1986. *Water Resources Research* 22:2047–2059. Copyright by the American Geophysical Union. Reproduced with permission.

for a parameter divided by the injected concentration. At 100 da the chloride slug has just about passed the observation point, the carbon tetrachloride plume has just about reached a peak, and the tetrachloroethylene plume has yet to reach it. By 200 days both the carbon tetrachloride and the chloride plumes have passed the monitoring point, whereas the tetrachloroethylene is near its peak value. The behavior of bromoform was very close to that of carbon tetrachloride and is not shown. Figure 3.22 illustrates that the retardation of the organic solutes is generally in agreement with their hydrophobicity. The chloride ion is essentially unaffected by travel through the aquifer, whereas the carbon tetrachloride and the tetrachloroethylene are traveling at slower rates. The result is a separation of the components of the plume, a phenomenon known as the **chromatographic effect**.

Figure 3.23 shows the arrival at the monitoring point of chloride ion and two other organics, dichlorobenzene, and hexachloroethane. The occurrences of both of these compounds are sporadic, and they have relative concentrations much less than carbon tetrachloride and tetrachloroethylene. Freyberg (1986) examined the results from the tracer test through

Solute	Concentration (mg/L)	Mass (g)
Chloride ion	892	10,700
Bromide ion	324	3,870
Bromoform	0.032	0.38
Tetrachloroethylene	0.030	0.36
Carbon tetrachloride	0.031	0.37
1,2-dichlorobenzene	0.332	4.0
Hexachloroethane	0.020	0.23

FIGURE 3.23 Arrival times of chloride, dichlorobenzene, and hexachloroethane at a measuring point 5.0 m downgradient from the injection well at Borden, Ontario.



Source: Roberts, Goltz, and Mackay. 1986. *Water Resources Research* 22:2047–2059. Copyright by the American Geophysical Union. Reproduced with permission.

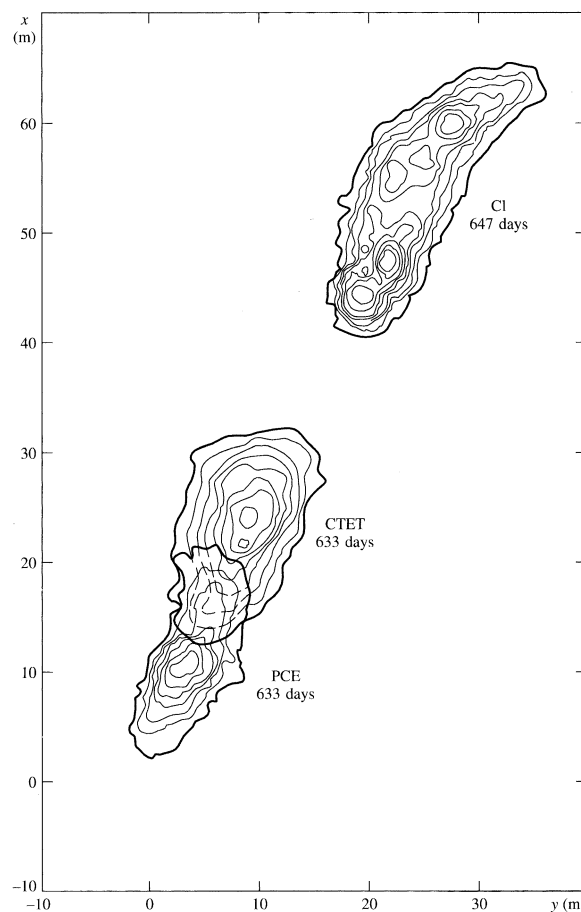
spatial moment analysis of the concentration data (Chapter 2). Analysis of the area under the time-concentration curves (zeroth-moment) shows that the relative areas of carbon tetrachloride, bromoform, and tetrachloroethylene are about the same size as the chloride curve. This indicates that the mass of these organics being measured is about the same as the mass that was introduced into the aquifer. However, for dichlorobenzene and hexachloroethane the relative areas are much less than that of chloride, indicating that the mass being measured is much less than the mass that was introduced. The missing mass was presumably removed by biodegradation or abiotic pathways such as hydrolysis (Chapter 7).

Similar results were obtained during the synoptic sampling. Figure 3.24 shows the plumes of chloride (Cl), carbon tetrachloride (CTET), and tetrachloroethylene (PCE) at the end of the experimental period (after 633 days for the organics and 647 days for the chloride). The chloride can be seen to have moved significantly beyond the organics and carbon tetrachloride has moved farther than tetrachloroethylene. Figure 3.25(a) shows the growth of the carbon tetrachloride plume and 3.25(b) shows the growth of the tetrachloroethylene plume.

The relative velocities of the various solutes are indicated by the positions of the centers of mass of the plumes at the end of the experiment (first-moment). The chloride plume was measured after 647 days of travel and the organic plumes were measured after 633 days. The distance from the center of the injection zone to the center of mass of the plume as well as the average velocities are given in the table below:

After 647 days of transport, the plume apparently encountered a relatively large-scale heterogeneity, leading to a distinct vertical layering, and slowing of the rate of advance of the center of mass of the plume (Sudicky and Illman 2011). Up to this time, the distances traveled by each of the compounds as a function of time are plotted in Figure 3.26. The distance traveled by the center of mass of the chloride plume is linear with time, indicating a constant advective rate. On the other hand, the organic solutes indicate decreasing velocities with increasing time.

FIGURE 3.24 Plumes of chloride, carbon tetrachloride, and tetrachloroethylene at the end of the experimental period. The plumes are based on depth-averaged values.



Source: Roberts, Goltz, and Mackay. 1986. *Water Resources Research* 22:2047–2059. Copyright by the American Geophysical Union. Reproduced with permission.

Closer examination of Figure 3.24 shows that the shape of the plume evolved over time. As Sudicky and Illman (2011) point out, the major principal axis of each plume, initially aligned roughly perpendicular to the hydraulic gradient, rotated smoothly over time until they nearly aligned with the mean solute velocity vector, as the plume itself elongates along the direction of movement. The authors conclude that because the growth of the covariance over time is non-linear, dispersion must have been “scale dependent.”

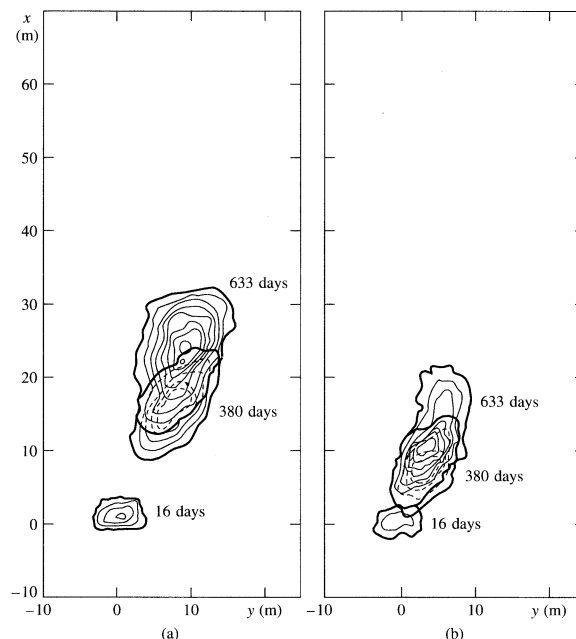
The organic compounds have aqueous solubilities provided in the table below, octanol-water partition coefficients, and first-order molecular connectivity indices.

This case history illustrates the problems with predicting the transport of organic compounds in groundwater. The organic carbon content of the aquifer is low (0.02%), so absorption is limited. The observed order of relative velocity from greatest to least was carbon tetrachloride, bromoform, tetrachloroethylene, and dichlorobenzene. The apparent

Compound	Distance to Center of Mass (m)	Distance to Center of Mass (ft)	Average Velocity (m/da)	ft/da
Chloride	58.21	191	0.0900	0.295
Carbon tetrachloride	24.82	81.2	0.0392	0.129
Bromoform	21.51	70.5	0.0340	0.112
Tetrachloroethylene	12.33	40.5	0.0195	0.640
Dichlorobenzene	8.09	26.5	0.0128	0.042
Hexachloroethane	None detected after 633 days			

retardation factor increased for all compounds over the duration of the experiment, by as much as 150%. In a forced-gradient tracer test at the same site as the natural gradient tracer test (Mackay et al., 1994) found spatially variable sorption for all solutes (iodide, carbon tetrachloride, trichloroethylene, tetrachloroethylene, and hexachloroethane). These non-ideal transport conditions can explain why the retardation of the tracer suites in the forced, as well as in the prior natural gradient tracer test increased over time. Thorbjarnarson and Mackay (1994) modeled the tracer test data and showed that first-order nonequilibrium sorption and rate-limited mass transfer between mobile and immobile water regions better explained this particular data set.

FIGURE 3.25 (a) Growth of carbon tetrachloride plume with time; (b) growth of tetrachloroethylene plume with time.



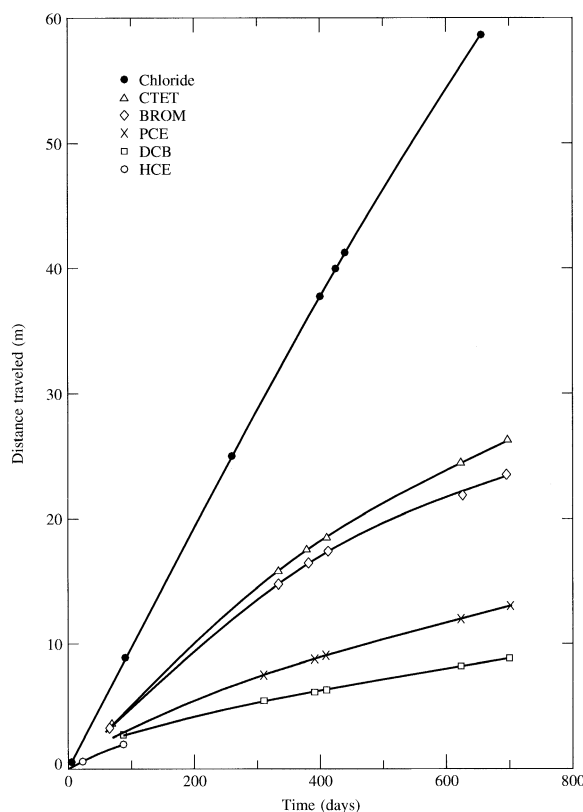
	Solubility	$\log K_{ow}^a$	$\log K_{ow}^b$	$^{1}\chi$
Bromoform	3190 mg /L at 30°C ^c		2.30	2.00
Carbon tetrachloride	805 mg/L at 20°C ^a	2.83	2.70	2.00
Tetrachloroethylene	1503 mg/L at 25°C ^a 150 mg/L at 25°C ^c	3.40	2.60	2.64
1,2-dichlorobenzene	156 mg /L at 25°C ^a	3.38	3.40	3.83
Hexachloroethane	50 mg /L at 22.3,C ^a	3.82	3.60	3.25

^aValue from P.H. Howard, *Fate and Exposure Data for Organic Chemicals* (Chelsea, Mich.: Lewis Publishers, 1990).

^bValue from Mackay et al. (1986).

^cValue from Karel Verschueren, *Handbook of Environmental Data on Organic Chemicals*, 2d ed. (New York: Van Nostrand Reinhold Co. 1983).

FIGURE 3.26 Distances traveled by the centers of mass of various plumes as a function of time since injection.



Source: Roberts, Goltz, and Mackay. 1986. *Water Resources Research* 22:2047–2059. Copyright by the American Geophysical Union. Reproduced with permission.

■ 3.11 Summary

The advection dispersion equation can be modified to reflect the effects of solutes that are removed from solution by sorption, chemical reaction, and biological and radioactive decay. Sorption may occur due to adsorption, chemisorption, ion exchange, and absorption. Sorption of inorganic solutes occurs primarily on mineral surfaces and is a function of the surface area available for sorption as well as the number of ion-exchange sites provided by clay and oxide minerals. The sorption of inorganic ions and organic chemical solutes can be quantified by experimentally derived adsorption isotherms.

Organic solutes may be sorbed on either soil mineral surfaces or by soil or aquifer organic matter. Nonpolar organic compounds are sorbed to a greater extent by soil organic matter than by general surfaces. The affinity of a particular organic molecule to be sorbed by soil or aquifer organic matter can be estimated from either the octanol-water partition coefficient, the aqueous solubility, or the molecular structure.

The advection-dispersion equation can also be modified to account for the disappearance of solutes or the appearance of a product due to other chemical reactions. Some of these reactions can be described by equilibrium reactions; others need to be dealt with on the basis of the kinetics of the reaction. A term to describe the disappearance of a solute due to radioactive decay can also be appended to the advection-dispersion equation. The biological degradation of organic compounds can occur under both aerobic and anaerobic conditions. Biodegradation terms can be joined to the advection-dispersion equation.

Chapter Notation

$[A]$	Concentration of ion in solution	D_{col}	Dispersion coefficients for colloid-bound contaminants
b	Microbial decay rate	D_m	Apparent diffusion constant for mobile phase
C	Concentration of solute in liquid phase	d_{50}	Mean pore diameter of the porous matrix
C^*	Amount of solute sorbed per unit weight of soil	E_{att}	First-order attachment term
C_i	Equilibrium molar concentration of the i th component	E_{str}	First-order straining term
C_{im}	Solute concentration in immobile phase	F_i	x -direction mass flux of a solute
C_m	Solute concentration in mobile phase	F^T	Total mass flux of chemical entity
C_{m^*}	Absorbed concentration in contact with mobile phase	f	Fraction of solid surfaces in contact with mobile phase
$C_{m^*}^*$	Absorbed concentration in contact with immobile phase	f_{inst}	Fraction of sorption for which sorption is instantaneous
C_{oc}	Natural organic carbon concentration	f_{oc}	Fraction of soil that consists of organic carbon
C_{max}	Maximum saturation concentration	f_{oc}^*	Critical level of soil organic carbon
C_{sat}	Saturation concentration in vapor	G	Ratio of oxygen to hydrocarbon consumed
D	Dispersion coefficients	G_m	Mass concentration of mobile colloidal particles
D_L	Longitudinal dispersion coefficient	G_s	Immobilized (attached, filtered, trapped) colloid concentration

H	Hydrocarbon concentration in pore fluid	k_6	Reversible nonlinear kinetic backward sorption model rate constant
H_{min}	Minimum hydrocarbon concentration to support microbial growth	k_7	Bilinear adsorption forward sorption model rate constant
h_u	Maximum hydrocarbon utilization rate by aerobic microbes	k_8	Bilinear adsorption backward sorption model rate constant
h_{ua}	Maximum hydrocarbon utilization rate by anaerobic microbes	k_9	"Two-Site" non-equilibrium sorption models rate constant
K_{Dc}	Distribution coefficient between the aqueous phase and mobile colloidal particles	L	Liter
K_{Ds}	Distribution coefficient between the aqueous phase and solid matrix	m^T	Global mass of chemical entity
K_{Dsc}	Distribution coefficient between the aqueous phase and immobile colloidal particles	M_a	Total mass of anaerobic microbes
K_{Fr}	Coefficient in Freundlich sorption isotherm	M_c	Mass of contaminants
K_{Fr}^*	Solubility normalized Freundlich isotherm coefficient	M_s	Concentration of aerobic microbes in solution
K_a	Half-maximum rate concentration for hydrocarbon for anaerobic decay	M_t	Total aerobic microbial mass
K_d	(linear) Distribution coefficient	N	Coefficient in Freundlich sorption isotherm
K_h	Hydrocarbon half-saturation ratio	O	Oxygen concentration in pore fluid
K_o	Oxygen half-saturation ratio	p_f	Polarity correction factor
K_{oc}	Distribution coefficient for soil organic carbon	Q	x-direction flux of water
K_{om}	Distribution coefficient for soil organic matter	q	Equal C^*
K_{ow}	Octanol-water partition coefficient	q_{max}	Equal C_{max}^*
k_{att}	First-order colloid attachment coefficient	R_A	Reaction rate for disappearance of A
k_c	First-order decay rate for natural organic carbon	R	Retardation factor for linear sorption isotherm
k_{det}	First-order colloid detachment coefficient	R_{Fr}	Retardation factor for Freundlich sorption isotherm
k_{str}	First-order colloid straining coefficient	R_L	Retardation factor for Langmuir sorption isotherm
k_i	Kinetic rate constants ($i = 1$ to 8)	r_h	Retardation factor for hydrocarbon
k_1	First-order decay rate constant.	R_m	Retardation factor for microbes
k_2	Forward rate constant	s	Solubility of chemical in water
k_3	Backward rate constant	S_a	Surface area of soil
k_4	Rate constant equivalent to K_d	S_i	Water solubility of i th compound
k_5	Reversible nonlinear kinetic forward sorption model rate constant	S^T	Source/sink term for chemical entity
		S_{att}	Solid-phase concentration of attached colloids
		S_{str}	Solid-phase concentration of strained colloids
		t	Time
		v_c	Average linear velocity of solute front
		v_{co}	Advection velocity for colloidal particles
		v_m	Groundwater velocity in mobile phase

v_x	Average linear groundwater velocity	γ	First-order rate coefficient
W	Linear operator defined in Equation 3.50	τ	First-order mass-transfer coefficient
$(x_i)_{\text{org}}$	Mole fraction of i th compound in organic phase	λ	Half-life of radionuclide
Y	Microbial yield coefficient	φ_{att}	Dimensionless colloid attachment function
α	Absorption constant for Langmuir sorption isotherm	φ_{str}	Dimensionless colloid straining function
β	Maximum solute sorption from Langmuir sorption isotherm	$\delta_{i,j}$	Number of adjacent nonhydrogen atoms in an organic molecule
ρ_b	Bulk density of soil	$^1\chi$	First-order molecular connectivity index
σ_{cs}	Chemical concentration sorbed to mobile colloids	θ	Volumetric moisture content
σ_s	Chemical concentration sorbed to immobile surfaces	θ_m	Porosity occupied by mobile phase
σ_{cs}	Chemical concentration sorbed to immobile colloids	θ_{im}	Porosity occupied by immobile phase
		$\kappa, \kappa', \kappa''$	Reaction-rate constants

References

- Allen-King, R., P. Grathwohl, and W. P. Ball. 2002. New Modeling Paradigms for the Sorption of Hydrophobic Organic Chemicals to Heterogeneous Carbonaceous Matter in Soils, Sediments, and Rocks. *Advances in Water Research* 25:985–1016.
- Banerjee, S. 1984. Solubility of organic mixtures in water. *Environmental Science and Technology* 18:587–591.
- Birak, P. S., A. P. Newman, S. D. Richardson, S. C. Hauswirth, J. A. Pedit, M. D. Aitken, and C. T. Miller. 2011. Cosolvent flushing for the remediation of PAHs from former manufactured gas plants. *Journal of Contaminant Hydrology* 126:72–84.
- Borden, R. C., and P. B. Bedient. 1986. Transport of dissolved hydrocarbons influenced by oxygen-limited biodegradation, 1. Theoretical development. *Water Resources Research* 22:1973–82.
- Borden, R. C., P. B. Bedient, M. D. Lee, C. H. Ward, and J. T. Wilson. 1986. Transport of dissolved hydrocarbons influenced by oxygen-limited biodegradation, 2. Field applications. *Water Resources Research* 22:1983–1990.
- Bouwer, E. J., and P. L. McCarty. 1984. Modeling of trace organics biotransformation in the subsurface. *Groundwater* 22:433–440.
- Boving, T. B., and M. L. Brusseau. 2000. Solubilization and removal of residual trichloroethene from porous media: Comparison of several solubilization agents. *Journal of Contaminant Hydrology* 42:51–67.
- Boving, T. B., and W. Zhang. 2004. Removal of aqueous phase polynuclear aromatic hydrocarbons using aspen wood fibers. *Chemosphere* 54:831–839.
- Boving, T. B. 2014. Forensic analysis of a MTBE contamination using basic hydrogeologic concepts. *Journal of Forensic Sciences* 59:967–973.
- Bradford, S. A., S. R. Yates, M. Bettahar, and J. Simunek. 2002. Physical factors affecting the transport and fate of colloids in saturated porous media. *Water Resources Research* 38:1327.
- Bradford, S. A., J. Simunek, M. Bettahar, M. Th. van Genuchten, and S. R. Yates. 2003. Modeling Colloid Attachment, Straining, and Exclusion in Saturated Porous Media. *Environmental Science and Technology* 37:2242–2250.
- Bradford, S. A., J. Simunek, M. Bettahar, M. Th. van Genuchten, and S. R. Yates. 2006. Significance of straining in colloid deposition: Evidence and implications. *Water Resources Research* 42:W12S12.
- Briggs, G. G. 1981. Theoretical and experimental relationships between soil adsorption, octanol-water partition coefficients, water solubilities, bioconcentration factors, and the parachor. *Journal of Agriculture and Food Chemistry* 29:1050–1059.
- Brunauer, S., P. H. Emmet, E. Teller. 1938. Adsorption of gases in multimolecular layers.

- layers. *Journal of the American Chemical Society* 60:309–319.
- Brusseau, M. L., and P. S. C. Rao. 1990. Modeling solute transport in structured soils: A review. *Geoderma* 46:169–192.
- Brusseau, M. L., R. E. Jessup, and P. S. C. Rao. 1991. Nonequilibrium sorption of organic chemicals: Elucidation of rate-limiting processes. *Environmental Science and Technology* 25:134–142.
- Carmo, A. M., S. H. Lakhwinder, and M. L. Thompson. 2000. Sorption of hydrophobic organic compounds by soil materials: Application of unit equivalent Freundlich coefficients. *Environmental Science and Technology* 34:4363–4369.
- CDS—National Chemical Database Service. 2015. Published by the Royal Society of Chemistry. Accessed October 3, 2015 from <http://cds.rsc.org>
- Christmann, K. 2012. *Thermodynamics and Kinetics of Adsorption*. IMPRS-Lecture Series, Institut für Chemie und Biochemie, Freie Universität Berlin. Available from http://w0.rz-berlin.mpg.de/imprs-cs/download/Vortrag_IMPRS_Schmoeckwitz_Mi_9-11_KChrist.pdf
- Ciccioli, P., W. T. Cooper, P. M. Hammer, and J. M. Hayes. 1980. Organic solute-mineral surface interactions: A new method for the determination of groundwater velocities. *Water Resources Research* 16:217–223.
- Chapelle, F. H. 1993. *Ground Water Microbiology and Geochemistry*. New York: John Wiley and Sons.
- Chiou, C. T., L. J. Peters, and V.H. Freed. 1979. A physical concept of soil-water equilibria for nonionic organic compounds. *Science* 206:831–832.
- Chiou, C. T., P. E. Porter, and D. W. Schmedding. 1983. Partition equilibrium of nonionic organic compounds between soil organic matter and water. *Environmental Science and Technology* 17:227–231.
- Cornelissen, G., O. Gustafsson, T. D. Bucheli, M. T. Jonker, A. A. Koelmans, and P. C. M. von Noort. 2005. Extensive Sorption of Organic Compounds to Black Carbon, Coal, and Kerogen in Sediments and Soils: Mechanisms and Consequences for Distribution, Bioaccumulation, and Biodegradation. *Environmental Science and Technology* 39:6881–6895.
- Davidson, J. M., and R. K. Chang. 1972. Transport of picloram in relation to soil-physical conditions and pore-water velocity. *Soil Science Society of America Proceedings* 36:257–301.
- Dousset, S., M. Thevenot, V. Pot, J. Simunek, and F. Andreux. 2007. Evaluating equilibrium and non-equilibrium transport of bromide and isoproturon in disturbed and undisturbed soil columns. *Journal of Contaminant Hydrology* 94:261–276.
- Dubinin, M. M., and V. A. Astakhov. 1970. Development of the Concepts of Volume Filling of Micropores in the Adsorption of Gases and Vapors by Microporous Adsorbents. *Bulletin of the Academy of Sciences of the USSR* 20:3–7.
- Dzombak, D. A., and R. G. Luthy. 1984. Estimating adsorption of polycyclic aromatic hydrocarbons on soils. *Soil Science* 137:292–308.
- Ellgehausen, H., C. D'Hondt, and R. Fuerer. 1981. Reversed phase chromatography as a general method for determining octanol/water partition coefficients. *Pesticide Science* 12:219–227.
- Enfield, C. G. 1985. Chemical transport facilitated by multiphase flow systems. *Water Science and Technology* 17:1–12.
- Enfield, C. G., and B. E. Bledsoe. 1975. Fate of wastewater phosphorus in soil. *Journal of Irrigation and Drainage Division, American Society of Civil Engineers* 101:145–55.
- Enfield, C. G., and G. Bengtsson. 1988. Macromolecular transport of hydrophobic contaminants in aqueous environments. *Groundwater* 26:64–70.
- Faur, C., C. Brasquet, K. Kadirvelu, and P. Le Cloirec. 2002. Removal of metal ions from aqueous solution by adsorption onto activated carbon cloths: Adsorption competition with organic matter. *Carbon* 40:2387–2392.
- Faust, C. R., and J. W. Mercer. 1980. Ground-water modeling: Recent developments. *Groundwater* 18:569–577.
- Febrianto, J., A. N. Kosasih, J. Sunarso, Y. H. Ju, N. Indraswati, and S. Ismadji. 2009. Equilibrium and kinetic studies in adsorption of heavy metals using biosorbent: A summary of recent studies (Review paper). *Journal of Hazardous Materials* 162:616–645.
- Fetter, C. W. 1977. Attenuation of waste water elutriated through glacial outwash. *Groundwater* 15:365–371.
- Fiskell, J. G. A., R. S. Mansell, H. M. Selim, and F. G. Martin. 1979. Kinetic behavior of phosphate sorption by acid, sandy soil. *Journal of Environmental Quality* 8:579–584.
- Freyberg, D. L. 1986. A natural gradient experiment on solute transport in a sand aquifer, 2. Spatial movements and the advection and dispersion of nonreactive tracers. *Water Resources Research* 22:2031–2047.

- Frimmel, F. H., F. von der Kammer, and H. C. Flemming (eds.). 2007. *Colloidal Transport in Porous Media*. New York: Springer.
- Gerke, H. H., and M. Th. van Genuchten. 1993. A dual-porosity model for simulating the preferential movement of water and solutes in structured porous media. *Water Resources Research* 29:305–319.
- Ghasemi, J., and S. Saaidpour. 2007. Quantitative structure–property relationship study of n-octanol–water partition coefficients of some of diverse drugs using multiple linear regression. *Analytica Chimica Acta* 60:99–106.
- Grathwohl, P., and M. D. Rahman. 2002. Partitioning and Pore-Filling: Solubility-Normalized Sorption Isotherms of Nonionic Organic Contaminants in Soils and Sediments. *Israel Journal of Chemistry* 42:67–75.
- Griffin, R. A. 1991. Personal communication.
- Griffin, R. A., and E. S. K. Chian. 1980. *Attenuation of Water-Soluble Polychlorinated Biphenyls by Earth Materials*. Cincinnati, OH: Municipal Environmental Research Laboratory.
- Grolimund, D., and M. Borkovec. 2001. Release and transport of colloidal particles in natural porous media. *Water Resources Research* 37:559–570.
- Goldberg E. D. 1985. *Black carbon in the environment*. New York: Wiley.
- Hansen, M., M. Borresen, M. Schlabach, and G. Cornelissen. 2010. Sorption of perfluorinated compounds from contaminated water to activated carbon. *Journal of Soils and Sediments* 10:179–185.
- Harvey, R. W., R. L. Smith, and L. George. 1984. Effect of organic contamination upon microbial distribution and heterotrophic uptake in a Cape Cod, Mass. aquifer. *Applied and Environmental Microbiology* 48:1197–1202.
- Hassett, J. J., J. C. Means, W. L. Banwart, and S. G. Wood. 1980. *Sorption properties of sediments and energy-related pollutants*. U.S. Environmental Protection Agency, EPA-600/3-80-041.
- Hassett, J. J., W. L. Banwart, and R. A. Griffin. 1983. Correlation of compound properties with sorption characteristics of nonpolar compounds by soils and sediments: Concepts and limitations. In *Environment and Solid Wastes: Characterization, Treatment and Disposal*, eds. C. W. Francis and S. I. Auerback, 161–178. Boston: Butterworth Publishers.
- Hayward, S. B. 1984. Field monitoring of chrysotile asbestos in California waters. *Journal of the American Water Works Association* 76:66–73.
- Hornsby, A. G., and J. M. Davidson. 1973. Solution and adsorbed fluometuron concentration distribution in a water-saturated soil: Experimental and predicted evaluation. *Soil Science Society of America Proceedings* 37:823–828.
- Hunt, J. R., N. Sitar, and K. S. Udell. 1988. Nonaqueous phase liquid transport and cleanup, 1. Analysis of mechanisms. *Water Resources Research* 24:1247–1258.
- Karickhoff, S. W., D. S. Brown, and T. A. Scott. 1979. Sorption of hydrophobic pollutants on natural sediments. *Water Research* 13:241–248.
- Karickhoff, S. W. 1981. Semi-empirical estimation of sorption of hydrophobic pollutants on natural sediments and soils. *Chemosphere* 10:833–846.
- Karickhoff, S. W. 1984. Organic pollutant sorption in aquatic systems. *Journal of Hydraulic Engineering* 110:707–735.
- Kasaraneni, V., L. A. Schifman, T. B. Boving, and V. Oyanedel-Craver. 2014. Enhancement of Surface Runoff Quality Using Nano-Modified Sorbents. *ACS Sustainable Chemistry & Engineering* 2:1609–1615.
- Katritzky, A. R., L. Mu, V. S. Lobanov, and M. Karelson. 1996. The correlation of boiling points with molecular structure, Part I: A Training set of 298 diverse organics and a test of 9 simple inorganics. *Journal of Physical Chemistry* 100:10400–10407.
- Kenaga, E. E., and C. A. I. Goring. 1980. “Relationship between water solubility, soil sorption, octanol-water partitioning and bioconcentration of chemicals in biota.” In *Aquatic Toxicology: Proceedings of the Third Annual Symposium on Aquatic Toxicology*, ed. J. G. Eaton. New Orleans: American Society for Testing and Materials.
- Kenaga, E. E. 1980. Predicted bioconcentration factors and soil sorption coefficients of pesticides and other chemicals. *Ecotoxicology and Environmental Safety* 4:26–38.
- Keswick, B. H., D. S. Wang, and C. P. Gerba. 1982. The use of microorganisms as ground-water tracers: A review. *Groundwater* 20:142–149.
- Koch, R. 1983. Molecular connectivity index for assessing ecotoxicological behavior of organic compounds. *Toxicological and Environmental Chemistry* 6:87–96.
- Le, T., V. C. Epa, F. R. Burden, and D. A. Winkler. 2012. Quantitative structure–property relationship modeling of diverse materials properties. *Chemical Reviews* 112:2889–2919.
- Lee, S., D. J. Kim, and J. W. Choi. 2012. Comparison of first-order sorption kinetics using concept

- of two-site sorption model. *Environmental Engineering Science* 29:1002–1007.
- Leistra, M., and W. A. Dekkers. 1977. Some models for the adsorption kinetics of pesticides in soils. *Journal of Environmental Science and Health* 12:85–103.
- Li, L., P. A. Quinlivan, and D. Knappe. 2002. Effects of activated carbon surface chemistry and pore structure on the adsorption of organic contaminants from aqueous solution. *Carbon* 40:2085–2100.
- Li, L., P. A. Quinlivan, and D. R. U. Knappe. 2005. Predicting Adsorption Isotherms for Aqueous Organic Micropollutants from Activated Carbon and Pollutant Properties. *Environmental Science & Technology* 39:3393–3400.
- Limousin, G., J. P. Gaudet, L. Charlet, S. Szenknect, V. Barthès, and M. Krimissa. 2007. Sorption isotherms: A review on physical bases, modeling and measurement. *Applied Geochemistry* 22:249–275.
- Logan, B. E., D. G. Jewett, R. G. Arnold, E. J. Bouwer, and C. R. O'Melia. 1995. Clarification of clean-bed filtration models, *Journal of Environmental Engineering* 121:869–873.
- Lohman, R., J. K. Macfarlane, and P. M. Gschwend. 2005. Importance of black carbon to sorption of native PAHs, PCBs, and PCDDs in Boston and New York harbor sediments. *Environmental Science and Technology* 39:141–148.
- Long, C., A. Li, D. Hu, F. Liu, and Q. X. Zhang. 2008. Description of adsorption equilibrium of PAHs on hypercrosslinked polymeric adsorbent using Polanyi potential theory. *Science in China Series B: Chemistry* 51:586–592.
- Lyman, W. J. 1982. "Adsorption coefficient for soils and sediment." In *Handbook of Chemical Property Estimation Methods*, ed. W. J. Lyman et al., 4.1–4–33. New York: McGraw-Hill.
- Mackay, D. M., D. L. Freyberg, P. V. Roberts, and J. A. Cherry. 1986. A natural gradient experiment on solute transport in a sand aquifer, 1. Approach and overview of plume movement. *Water Resources Research* 22:2017–2030.
- Mackay, D., W. Y. Shiu, K. C. Ma, and S. C. Lee. 2006. *Chemical properties and environmental fate for organic chemicals, Vol. 1: Introduction and Hydrocarbons, Second Edition*. Boca Raton, FL: CRC Press.
- Magee, B. R., L. W. Lion, and A. T. Lemley. 1991. Transport of dissolved organic macromolecules and their effect on the transport of phenanthrene in porous media. *Environmental Science and Technology* 25:323–331.
- Major, D. W., C. I. Mayfield, and J. F. Barker. 1988. Biotransformation of benzene by denitrification in aquifer sand. *Groundwater* 26:8–14.
- Manes, M., and L. J. E. Hofer. 1969. Application of the Polanyi adsorption potential theory to adsorption from solution on activated carbon. *Journal of Physical Chemistry* 73:584–590.
- Matott, L. S., J. Zhengzheng, A. J. Rabideau, and R. M. Allen-King. 2015. Isotherm ranking and selection using thirteen literature datasets involving hydrophobic organic compounds, *Journal of Contaminant Hydrology* 177–178:93–106.
- Massoudieh, A., and T. R. Ginn. 2007. Modeling colloid facilitated transport of multi-species contaminants in unsaturated porous media. *Journal of Contaminant Hydrology* 92:162–183.
- Massoudieh, A., and T. R. Ginn. 2010. Colloid-facilitated contaminant transport in unsaturated porous media. In *Modelling of Pollutants in Complex Environmental Systems, Volume II*, ed. G. Hanrahan. Glendale, AZ: ILM Publications.
- McCall, P. J., R. L. Swann, and D. A. Laskowski. 1983. Partition Models for Equilibrium Distribution of Chemicals in Environmental Compartments. In *Fate of Chemicals in the Environment*, ed. R. L. Swann and A. Eschenroder, 105–23. Washington, DC: American Chemical Society.
- McCarthy, J. F., and J. M. Zachara. 1989. Subsurface transport of contaminants. *Environmental Science and Technology* 23:496–502.
- McCarthy, J. F., and C. Degueldre. 1993. Sampling and characterization of colloids and particles in ground water for studying their role in contaminant transport. In *Environmental Particles, Volume II*, eds. I. Buffle and H. van Leeuwen. Boca Raton, FL: Lewis Publishers.
- McCarty, P. L., M. Reinhard, and B. E. Rittman. 1981. Trace organics in groundwater. *Environmental Science and Technology* 15:40–51.
- McDowell-Boyer, L. M., J. R. Hunt, and N. Sitar. 1986. Particle transport through porous media. *Water Resources Research* 22:1901–1921.
- Means, J. C., S. G. Wood, J. J. Hassett, and W. L. Banwart. 1980. Sorption of polynuclear aromatic hydrocarbons by sediments and soils. *Environmental Science and Technology* 14:1524–1528.
- Miller, C. T., and W. J. Weber, Jr. 1984. Modeling organic contamination partitioning in ground-water systems. *Groundwater* 22:584–592.

- Mingelgrin, U., and Z. Gerstl. 1983. Reevaluation of partitioning as a mechanism of nonionic chemicals adsorption in soils. *Journal of Environmental Quality* 12:1–11.
- Montgomery, J. M. 2007. *Groundwater Chemicals Desk Reference, Fourth Edition*. Boca Raton, FL: CRC Press.
- Morales, I., J. A. Atoyan, J. A. Amador, and T. Boving. 2014. Transport of pathogen surrogates in soil treatment units: Numerical modeling. *Water* 6:818–838.
- Morley, M., and M. Fatemi. 2010. Adsorption of RDX and its nitroso metabolites onto activated carbon. *Practice Periodical of Hazardous, Toxic, and Radioactive Waste Management* 14:90–97.
- Munns, D. N., and R. L. Fox. 1976. The slow reactions that continue after phosphate adsorption: Kinetics and equilibrium in tropical soils. *Soil Science Society of America Proceedings* 40:46–51.
- Nantasesamat C., C. Isarankura-Na-Ayudhya, T. Naenna, and V. Prachayasittikul. 2009. A practical overview of quantitative structure-activity relationship. *EXCLI Journal* 8:74–88.
- National Institute of Standards and Technology (NIST). 2012. Chemistry WebBook. Accessed October 3, 2015 from <http://webbook.nist.gov/chemistry/>
- National Research Council of Canada (NRCC). 2015. LogK_{ow} database. Accessed October 03, 2015 from <http://codata.ca/eng/resources/logkow.html>
- Nielsen, D. R., M. Th. van Genuchten and J. W. Biggar. 1986. Water flow and solute transport in the unsaturated zone. *Water Resources Research* 22:89S–108S.
- Nightingale, H. I., and W. C. Bianchi. 1977. Ground-water turbidity resulting from artificial recharge. *Groundwater* 15:146–152.
- Nkedi-Kizza, P., J. W. Biggar, H. M. Selim, M. Th. van Genuchten, P. J. Wierenga, J. M. Davidson, and D. R. Nielsen. 1984. On the equivalence of two conceptual models for describing ion exchange during transport through an aggregated oxisol. *Water Resources Research* 20:1123–1130.
- Olsen, R. L., and A. Davis. 1990. Predicting the Fate and Transport of Organic Compounds in Groundwater: Part 1. *Hazardous Materials Control* 3:38–64.
- Pang, L. P., and J. Simunek. 2006. Evaluation of bacteria-facilitated cadmium transport in gravel columns using the HYDRUS colloid-facilitated solute transport model. *Water Resources Research* 42:W12S10.
- Polanyi, M. 1963. The potential theory of adsorption. *Science* 141:1010–1013.
- Pontolillo, J., and R. P. Eganhouse. 2001. The search for reliable aqueous solubility (S_w) and octanol–water partition coefficient (K_{ow}) data for hydrophobic organic compounds: DDT and DDE as a case study. U.S. Geological Survey, Water-Resources Investigations Report 01-4201. Reston, VA: USGS.
- Priddle, M. W., and K. T. B. MacQuarrie. 1994. Dissolution of creosote in groundwater: An experimental and modeling investigation. *Journal of Contaminant Hydrogeology* 15:27–56.
- Puls, R. W., and R. M. Powell. 1992. Transport of inorganic colloids through natural aquifer material: Implications for contaminant transport. *Environmental Science and Technology* 26:614–621.
- Rajagopalan, R., and C. Tien. 1976. Trajectory analysis of deep-bed filtration with the sphere-in-cell porous media model. *American Institute of Chemical Engineers Journal* 22:523–533.
- Rao, P. S. C., and J. M. Davidson. 1980. Estimation of pesticide retention and transformation parameters required in nonpoint source pollution models. In *Environmental Impact of Nonpoint Source Pollution*, eds. M. R. Overcash and J. M. Davidson, 23–67. Ann Arbor, MI: Ann Arbor Science Publishers, Inc.
- Reid, R. C., J. M. Prausnitz, and B. E. Poling. 1987. *The Properties of Gases and Liquids*. New York: McGraw-Hill.
- Roberts, P. V., M. N. Goltz, and D. A. Mackay. 1986. A natural gradient experiment on solute transport in a sand aquifer, 3. Retardation estimates and mass balances for organic solutes. *Water Resources Research* 22:2047–2059.
- Rogers, R. D., J. C. McFarlane, and A. J. Cross. 1980. Adsorption and desorption of benzene in two soils and montmorillonite clay. *Environmental Science and Technology* 14:457–500.
- Roy, W. R., and R. A. Griffin. 1985. Mobility of organic solvents in water-saturated soil materials. *Environmental Geology and Water Sciences* 7:241–47.
- Rubin, J. 1983. Transport of reacting solutes in porous media: Relationship between mathematical nature of problem formation and chemical nature of reactions. *Water Resources Research* 19:1231–52.

- Sabljić, A., and M. Protic. 1982. Relationship between molecular connectivity indices and soil sorption coefficients of polycyclic aromatic hydrocarbons. *Bulletin of Environmental Contamination and Toxicology* 28:162–205.
- Sabljić, A. 1984. Predictions of the nature and strength of soil sorption of organic pollutants by molecular topology. *Journal of Agricultural and Food Chemistry* 32:243–246.
- Sabljić, A. 1987. On the prediction of soil sorption coefficients of organic pollutants from molecular structure: Application of molecular topology model. *Environmental Science and Technology* 21:358–405.
- Schwarzenbach, R. P., and J. Westall. 1981. Transport of nonpolar organic compounds from surface water to groundwater: Laboratory sorption studies. *Environmental Science and Technology* 15:1360–1367.
- Schwarzenbach, R. P., P. M. Gschwend, and D. M. Imboden. 2003. *Environmental Organic Chemistry, Second Edition*. Hoboken, NJ: Wiley-Interscience.
- Seth, R., D. Mackay, and J. Munthe. 1999. Estimation of organic carbon partition coefficient and its variability for hydrophobic chemicals. *Environmental Science and Technology* 33:2390–2394.
- Simunek, J., N. J. Jarvis, M. Th. van Genuchten, and A. Gärdenäs. 2003. Review and comparison of models for describing non-equilibrium and preferential flow and transport in the vadose zone. *Journal of Hydrology* 272:14–35.
- Simunek, J., M. Th. van Genuchten, and M. Šejna. 2006. *The HYDRUS software package for simulating two- and three-dimensional movement of water, heat, and multiple solutes in variably-saturated media, technical manual, version 1.0*. Prague, Czech Republic: PC Progress.
- Simunek, J., M. Th. van Genuchten, and M. Šejna. 2008. *The HYDRUS-ID software package for simulating the one-dimensional movement of water, heat, and multiple solutes in variably-saturated media, version 4.0*. HYDRUS Software Ser. 3. Department of Environmental Sciences, University of California, Riverside.
- Speth, T. F., and R. J. Miltner. 1990. Technical note: Adsorption capacity of GAC for synthetic organics. *Journal American Water Works Association* 82:72–75.
- Srinivasan, P., and J. W. Mercer. 1988. Simulation of biodegradation and sorption processes in ground water. *Groundwater* 26:475–487.
- Staples, C. A., and S. J. Geiselmann. 1988. Cosolvent influences on organic solute retardation factors. *Groundwater* 26:192–198.
- Sudicky, E. A., and W. A. Illman. 2011. Lessons Learned from a Suite of CFB Borden Experiments (Review Paper). *Groundwater* 49:630–648.
- Thorbjarnarson, K. W., and D. M. Mackay. 1994. A forced gradient experiment on solute transport in the Borden aquifer 3. Nonequilibrium transport of the sorbing organic compounds. *Water Resources Research* 30:401–419.
- Tolls, J. 2001. Sorption of Veterinary Pharmaceuticals in Soils: A Review. *Environmental Science and Technology* 35:3397–3406.
- Travis, C. C., and E. L. Etnier. 1981. A survey of sorption relationships for reactive solutes in soil. *Journal of Environmental Quality* 10:8–17.
- Tufenkji, N., and M. Elimelech. 2004. Correlation equation for predicting single-collector efficiency in physiochemical filtration in saturated porous media. *Environmental Science and Technology* 38:529–536.
- U.S. EPA. 2012. Estimation Program Interface (EPI) Suite. U.S. Environmental Protection Agency. Accessed October 3, 2015 from <http://www.epa.gov/opptintr/exposure/pubs/episuite.htm>
- Van Genuchten, M. Th., J. M. Davidson, and P. J. Wierenga. 1974. An evaluation of kinetic and equilibrium equations for the prediction of pesticide movement through porous media. *Soil Science Society of America Proceedings* 38:29–35.
- Van Genuchten, M. Th., and P. J. Wierenga. 1976. Mass-transfer studies in sorbing porous media, 1. Analytical solutions. *Soil Science Society of America Journal* 40:473–480.
- Van Genuchten, M. Th., and R. J. Wagenet. 1989. Two-site/two-region models for pesticide transport and degradation: Theoretical development and analytical solutions. *Soil Science Society of America Journal* 53:1303–1310.
- Verschueren, K. 1983. *Handbook of Environmental Data on Organic Chemicals, Second Edition*. New York: Van Nostrand Reinhold Company.
- Walsh, M. P., S. L. Bryant, R. S. Schechter, and L. W. Lake. 1984. Precipitation and dissolution of solids attending flow through porous media. *American Institute of Chemical Engineers Journal* 30:317–328.
- Wood, A. L., D. C. Bouchard, M. L. Brusseau, and P. S. Rao. 1990. Cosolvent effects on sorption and mobility of organic contaminants in soils. *Chemosphere* 21:575–587.

- Wood, W. W., T. P. Kramer, and P. P. Hem, Jr. 1990. Intergranular diffusion: An important mechanism influencing solute transport in elastic aquifers. *Science* 247:1569–1572.
- Yalkowski, S. H. 1985. Solubility of organic solutes in mixed aqueous solvent, Final Report to the R. S. Kerr Research Lab., U.S. EPA, contract CR811852-01-0, 1985; cited in C. T. Jafvert, 1996. Surfactants/Cosolvents. GWRTAC Technology Evaluation Report TE-96-02.
- Yang, K., and B. Xing. 2010. Adsorption of organic compounds by carbon nanomaterials in aqueous phase: Polanyi theory and its application. *Chemical Reviews* 110:5989–6008.
- Yao, K. M., M. T. Habibian, and C. R. O'Melia. 1971. Water and waste water filtration—Concepts and applications. *Environmental Science and Technology* 5:1105–1112.
- Zavarin M., S. K. Roberts, M. R. Johnson, Q. Hu, B. A. Powell, P. Zhao, A. B. Kersting, R. E. Lindvall, and R. J. Pletcher. 2013. Colloid-facilitated radionuclide transport in fractured carbonate rock from Yucca Flat, Nevada national security site. Report to the U. S. Department of Energy, National Nuclear Security Administration. LLNL-TR-619352
- Zheng, C., and P. P. Wang. 1999. MT3DMS A modular three-dimensional multispecies transport model for simulation of advection, dispersion and chemical reactions of contaminants in groundwater systems (Release DOD_3.50.A). U.S. Army Engineer Research and Development Center. Accessed October 3, 2015 from <http://hydro.geo.ua.edu/mt3d>

Problems

- 3.1** A sorption study of Cd²⁺ on a loamy sand gave the following results:

Equilibrium Concentration (mg/L)	Cd ²⁺ Sorbed (mg/gm)
0.045	10
0.10	19
0.13	27
0.20	38
0.24	47

What is the K_d ?

- 3.2** A sorption study of Cd²⁺ on a sandy loam gave the following results:

Equilibrium Concentration (mg/L)	Cd ²⁺ Sorbed (mg/gm)
0.045	7
0.10	15
0.14	21
0.20	30
0.24	37

What is the K_d ?

- 3.3 A sorption study of P on a sandy loam gave the following results:

Equilibrium Concentration (mg/L)	P Sorbed (mg/gm)	C/C*
0.55	0.0167	33
1.30	0.0217	60
1.88	0.0229	82
2.33	0.0240	97
3.45	0.0303	114
3.93	0.0322	122
4.32	0.0338	128
5.60	0.0389	144

What is the K_d ?

- 3.4 A sorption study of P on a sandy loam gave the following results:

Equilibrium Concentration (mg/L)	P Sorbed (mg/gm)	C/C*
0.40	0.00909	44
1.22	0.0174	70
1.78	0.0196	91
2.45	0.0225	109
3.55	0.0241	147
4.44	0.0267	166
4.95	0.0283	175
5.78	0.0306	189

What is the K_d ?

- 3.5 The log K_{ow} for 1,1,2-trichloroethane is 2.18 Using the equations found in Table 3.2, estimate the K_{oc} based on the K_{ow} .
- 3.6 The log K_{ow} for benzo(a)pyrene is 6.00. Using the equations found in Table 3.2, estimate the K_{oc} based on the K_{ow} .
- 3.7 The solubility of carbon disulfide in water is 2,200 mg/L at 22°C. Use Equations T14, T15 and T16 to estimate the value of K_{oc} .
- 3.8 The solubility of 1,1,2-trichlorotrifluoroethane in water is 170 mg/L at 25°C. Use Equations T14, T15 and T16 to estimate the value of K_{oc} .

- 3.9** A waste solvent tank contains by weight 25% 1,1,1-Trichloroethane, 37% benzene, 23% 1,2-Dichloroethane and 15 % perchloroethylene. The formula weights and aqueous solubility's of each are: TCA, $f_w = 133.4$, $S = 1,250 \text{ mg/L}$; BENZ, $f_w = 78.11$, $S = 1750 \text{ mg/L}$; DCA, $f_w = 98.96$, $S = 8300 \text{ mg/L}$; PCE, $f_w = 165.83$, $S = 240 \text{ mg/L}$. (Please note that there are a number of reported solubilities for these compounds in the literature and the values given in this problem are mid-range.) What are the equilibrium concentrations?
- 3.10** A waste solvent tank contains by weight 12% 1,1,1-Trichloroethane, 22 % benzene, 19% 1,2-Dichloroethane and 47 % perchloroethylene. The formula weights and aqueous solubility's of each are: TCA, $f_w = 133.4$, $S = 1,250 \text{ mg/L}$; BENZ, $f_w = 78.11$, $S = 1750 \text{ mg/L}$; DCA, $f_w = 98.96$, $S = 8300 \text{ mg/L}$; PCE, $f_w = 165.83$, $S = 240 \text{ mg/L}$. (Please note that there are a number of reported solubilities for these compounds in the literature and the values given in this problem are mid-range.) What are the equilibrium concentrations?
- 3.11** Discuss the relationship between the four curves shown in Figures 3.9 and 3.10.

Flow and Mass Transport in the Vadose Zone

■ 4.1 Introduction

Flow through the vadose zone is a topic that most hydrogeology texts tend to cover in a cursory manner. Classical hydrogeology is concerned primarily with obtaining water from wells. The **vadose**, or water-unsaturated zone, is seen as a somewhat mysterious realm through which recharge water must pass on the way to the water table—a watery purgatory. Soil scientists have been the primary force behind developing an understanding of unsaturated zone flow. Historically, soil scientists were concerned with such topics as the passage of water and solutes to roots of plants, water that flows primarily in the vadose zone. More recently soil scientists have studied the transport and fate of contaminants in the vadose zone. With the development of the science of contaminant hydrogeology, hydrogeologists have become much more interested in the mysteries of the vadose zone. Many releases of contaminants to the subsurface occur within or above the vadose zone. Contaminants are understood to include materials applied deliberately to the soil, such as fertilizers and pesticides, as well as those released accidentally. The hydrogeologist is suddenly faced with the daunting task of understanding the transport of dissolved contaminants through the vadose zone. To this end, much can be learned from the work of soil scientists. Transport in the vadose zone may also occur by flow of a pure nonaqueous phase liquid or gaseous phase.

In the last decades hydrogeologists and engineers have focused much more attention on the vadose zone, in addition to the continuing work of soil scientists. This has led to a number of new journals, agency guidance, numerous vadose zone models, and textbooks on vadose zone hydrology (Wilson et al. 1994; Tindall et al. 2009; Heinse and Link, 2013; UC Davis 2015). In karst systems, the vadose zone can exist as caves where often water and contaminants can move more swiftly, and be less subject to adsorption and retardation compared to flow through porous media where the surface area of soil particles can be great.

The vadose zone extends from the land surface to the water table. It includes the **capillary fringe**, where pores may actually be saturated. Areas of the vadose zone above the capillary fringe may temporarily be saturated due to surface ponding of water or because of the development of perched water tables above relatively low

permeability soil layers. The main distinguishing feature of the vadose zone is that the pore water pressures are generally negative.

■ 4.2 Soil as a Porous Medium

The vadose zone includes the soil layers at the Earth's surface. It may also include sediment and/or consolidated rock. However, the presence of soil complicates the study of vadose zone hydrology, also known as soil physics.

Soil is a complex material. In physical form it consists mostly of mineral grains of varying size as well as varying amounts of organic matter. The mineral grains are arranged in such a fashion that the soil has structure; that is, there is a specific orientation and arrangement of the individual grains. The individual grains usually form larger units called **aggregates**, or **peds**, which are bound by organic matter (e.g., Hillel 1980). Pedological classifications consider soil weathering, genesis, chemistry, profile thickness, and other factors. The porosity and permeability of the soil is a function of both soil texture and the soil structure. Soil texture refers to the relative content of various particle sizes, such as clay, silt, sand, and can include rock fragment modifiers such as gravel, cobbles, etc. One must be careful in classifying soil texture because there are various soil textural classification systems that differ, such as those of the International Association for Standardization 14688-1:2002, the United Kingdom ADAS system, U.S. Department of Agriculture classification system, the Australian and New Zealand soil classification systems, the Unified Soil Classification System (ASTM D2487-92), the Krumbein phi scale (modified Udden-Wentworth scale), the EMBRAPA (Empresa Brasileira de Pesquisa Agropecuária) system (Brazil), and the AASHTO classification system from the U.S. Bureau of Public Roads, to name a few. Soil structure is a function of the physical shape and size of the aggregates. Moreover, it may be vastly influenced by the soil chemistry, since soil minerals have an electrical charge on their surface. This surface charge, which is primarily due to the clay minerals, affects the stability of soil structural units. Soil contains mineral matter, organic matter, water containing dissolved solutes, and gases. The soil also has macropores, such as root casts and wormholes, and drying cracks in fine-textured soils. These form preferential channels for water movement.

The amount of moisture in a soil can be expressed as the gravimetric water content, w , which is the weight of the water as a ratio to the weight of the dry soil mass. The moisture state can also be expressed as the volumetric water content, θ , which is the volume of water as a ratio to the total volume of the soil mass. One must be careful in measuring volumetric water content, since in many soils (especially those with fine texture) the volume changes as water is imbibed or drained. This is due to the interactions between the charged soil particles and the polar water molecules.

It is important to mention here that symbols used historically in the literature for unsaturated fluid flow equations are not always the same as for saturated flow discussed earlier. For example, the letter "n" is often used to denote porosity in saturated flow equations, but is not as often used by soil and vadose zone scientists. Because many other volumetric qualities are considered in unsaturated fluid flow, both liquid and gaseous, volumetric notation historically has used the Greek symbol theta (θ) for volumes. Therefore, in vadose zone equations, θ represents the volumetric water content which is a variable, θ_T or θ_s typically represent porosity (total pore volume or saturated pore volume at atmospheric

pressure or greater, respectively), θ_D is the drained or air-filled porosity, θ_r describes the irreducible water content, θ_m is the mobile water content, θ_{im} the immobile water content, and θ_{ex} the exclusion zone volume. These terms will be more fully defined below.

■ 4.3 Soil Colloids

The clay fraction of the soil consists of mineral particles that are less than 2 μm in diameter (Hillel 1980) by most classification systems. Clay particles consist primarily of secondary minerals that have been formed by weathering. Clay minerals have an unbalanced negative electrical charge at the surface. Electrostatic attraction exists between the surface of the clay particles, the polar soil-water molecules, and solutes dissolved in the soil water. Finegrained materials with an electrostatic surface charge are called **colloids**.

Clay minerals have a definite crystal structure, consisting primarily of aluminum, silica, and oxygen. **Kaolinite** (e.g., $\text{Al}_4\text{Si}_4\text{O}_{10}(\text{OH})_8$) is a clay mineral with a low specific surface (surface area per unit mass); it ranges from 5 to 20 m^2/g . The low specific surface means that kaolinite is not particularly reactive. **Illite** (e.g., $\text{Al}_4\text{Si}_7\text{AlO}_{20}(\text{OH})_4\text{K}_{0.8}$, with the potassium occurring between layers) has a larger specific surface area, ranging from 80 to 120 m^2/g . **Montmorillonite** (e.g., $\text{Al}_{3.5}\text{Mg}_{0.5}\text{Si}_8\text{O}_{20}(\text{OH})_4$) is the most reactive clay with a specific surface area of 700 to 800 m^2/g . The reactive clays can absorb large amounts of water and ions between their sheet-like mineral grains. This property gives soils high in reactive clays the ability to swell as water is absorbed. It also means that they shrink and crack when dried. Montmorillonite has the largest shrink-swell behavior, and kaolinite has the least. **Chlorite** (e.g., $\text{Mg}_6\text{Si}_6\text{Al}_2\text{O}_{20}(\text{OH})_4$, with $\text{Mg}_6(\text{OH})_{12}$ occurring between the layers) is another common clay mineral with a behavior similar to illite.

Clay-size particles may also include **sesquioxides**, which are hydrated aluminum and iron oxides ($\text{Al}_2\text{O}_3 \cdot n\text{H}_2\text{O}$ and $\text{Fe}_2\text{O}_3 \cdot n\text{H}_2\text{O}$). Limonite, goethite, and gibbsite are examples. These substances are generally amorphous and have less electrostatic properties than the silicate clay minerals. Sesquioxides often act as cementing agents for soils.

Soil may also contain decomposed organic material, which is sometimes called **humus**. Humus is a complex mixture of organic molecules that are aggregated into colloidal-size particles. Humus particles are also negatively charged. Humus is found primarily in the A horizon of soils. The humus content of mineral soils can range from 0 to about 10% by weight. The organic content of organic soils, such as peat, can be up to 50% or more by weight.

■ 4.4 The Electrostatic Double Layer

The colloidal particles of the soil have an unbalanced, negative surface charge. This negative charge is balanced by positively charged cations that are attracted to the surface of the colloid. These cations exist as solutes in water. When the colloid is dry, the layer of water held to the surface will be thin, and the neutralizing cations will be closely held to the particle surface. As the colloid becomes more hydrated, the cations will dissociate from the surface and form a swarm of ions near the negatively charged surface layer. The cations have a more or less fixed position near the negatively charged particle surface. The particle surface and the cation swarm form what is known as an **electrostatic double layer**.

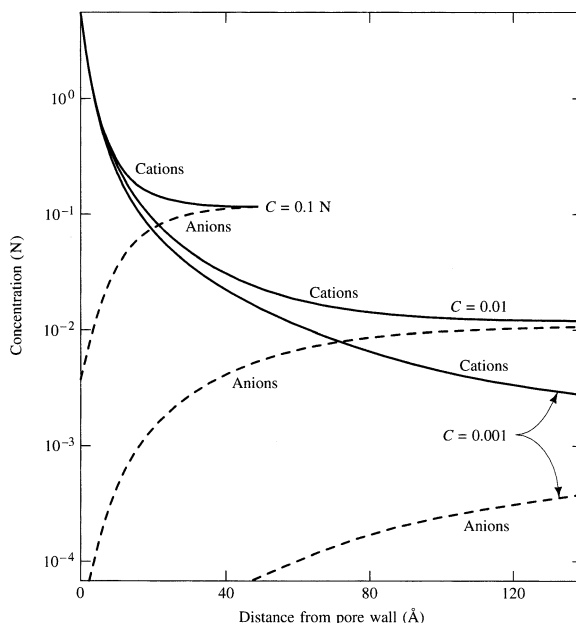
The negatively charged particle surface will tend to repel anions. Hence, the region near the particle surface will have an abundance of cations and relatively few anions. Figure 4.1 shows the distribution of monovalent cations and anions near the surface of a montmorillonite particle. The effects of the electrostatic double layer extend to the distance at which the number of cations in solution equals the number of anions. Figure 4.1 shows that the electrostatic double-layer effect is a function of the solute concentration and extends farther in more dilute solutions. The extent of the electrostatic double layer is less for divalent cations as opposed to monovalent cations. The thickness of the electrostatic double layer can be computed from:

$$z_0 = \frac{1}{eV} \sqrt{\frac{\epsilon k_B T}{8\pi n_0}} \quad (4.1)$$

where

- z_0 = the characteristic thickness of the double layer
- e = the elementary charge of an ion, 4.77×10^{-10} esu
- ϵ = the dielectric constant
- k_B = the Boltzmann constant (the ratio of the gas constant to Avagadro's number)
- V = the valence of the ions in solution
- n_0 = the concentration of ions in bulk solution (ions/cm³)
- T = temperature in Kelvins

FIGURE 4.1 Distribution of monovalent cations near the surface of a montmorillonite particle.

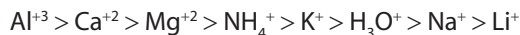


Source: Boersma et al. 1972.

The electrostatic double layer is very important in contaminant hydrogeology, because the cations associated with this layer can be replaced by other cations in solution. This replacement process is known as **cation exchange**. The total number of positive charges that can be exchanged in a soil is independent of the cation species and is expressed as the cation-exchange capacity. Cation exchange affects the transport of ions in solution. The type and concentration of cations involved in the exchange process can also affect the hydraulic conductivity of the soil.

Some colloids can also attract anions. Although the surface of clay particles carries a negative charge, the edges usually carry a net positive charge. Since the surface area far exceeds the edge area, the cation-exchange capacity for most soils far exceeds the anion-exchange capacity. Kaolinite and humus have the greater anion-exchange capacity.

Different cations are held with greater tenacity by the colloids. The smaller the ionic radius and the greater the valence charge, the more tightly the cation is held. The ionic radius of the cation is affected by hydration, because polar water molecules are attracted to the ion. It is the radius of the hydrated ion that is important. The normal order of preference for cation exchange is



However, if a soil is flooded with a solution containing a large concentration of one cation, the normal cation-exchange order can be reversed.

■ 4.5 Salinity Effects on Hydraulic Conductivity of Soils

The hydraulic conductivity of a soil can be affected by the strength and type of cations contained in the soil water (Nielsen, van Genuchten, and Biggar 1986). The impact of the solute increases with the amount of colloidal particles in the soil. Soil swelling caused by increased salinity can reduce hydraulic conductivity. As the electrostatic double layer grows thicker, the hydraulic conductivity decreases, because clay minerals tend to swell and expand into the pore space. Sodium is especially important in this process. The electrostatic double layer is thicker when it contains the monovalent sodium ions, and as such sodium tends to weaken the bonds between clay particles. The effect of swelling is reversible if the saline water is flushed from the pores. However, if smaller particles break loose from the soil structure, they can be transported by flowing water until they are carried into small pore throats, where they can lodge. This causes a more or less irreversible reduction in hydraulic conductivity (Dane and Klute 1977).

Examination of Equation 4.1 shows that the electrostatic double layer grows with decreasing concentration of cations in the soil water. It will also decrease with an increase in the ratio of the concentration of monovalent to divalent cations in the soil water. The principal cations in most natural waters are sodium, calcium, and magnesium. The sodium adsorption ratio (SAR) is a measure of the ratio of the concentration of monovalent sodium to divalent calcium and magnesium:

$$SAR = \frac{\text{Na}}{\sqrt{\frac{\text{Ca} + \text{Mg}}{2}}} \quad (4.2)$$

where

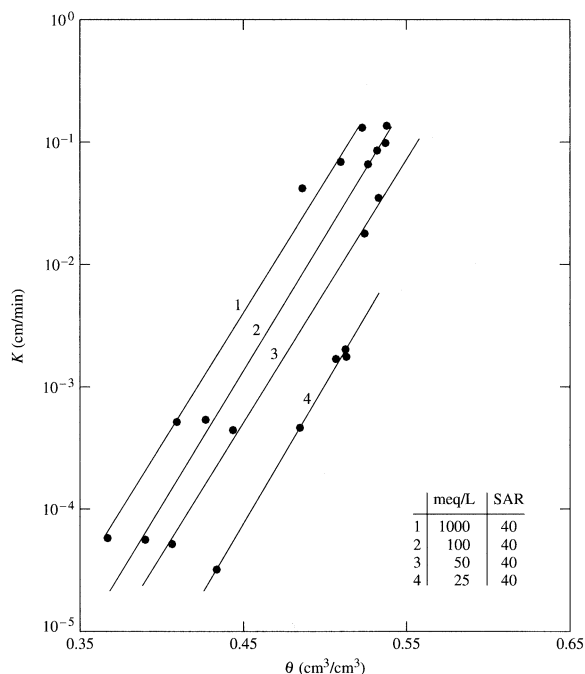
Na = concentration of sodium in milliequivalents per liter

Ca = concentration of calcium in milliequivalents per liter

Mg = concentration of magnesium in milliequivalents per liter

The greater the SAR of the soil water and the lower the total solute concentration, the lower the hydraulic conductivity of the soil, especially if it contains the expansive clays illite and montmorillonite. Figure 4.2 shows the effect for one soil of decreasing solute concentration on the unsaturated hydraulic conductivity of a soil. During these tests the SAR was kept at 40, so that the relative proportions of sodium, calcium, and magnesium did not change. An increase in the pH of soil water has also been demonstrated to result in a reduction of hydraulic conductivity for some soils (Suarez 1985).

FIGURE 4.2 Hydraulic conductivity as a function of volumetric water content for solutions of varying solute concentration but with a constant SAR value of 40.



Source: Dane and Klute 1977.

■ 4.6 Flow of Water in the Unsaturated Zone

Vadose zone hydrology is different from saturated zone hydrology because of the presence of air in the pore space. The relative proportion of air and water in the pores can vary, and with it can vary the hydraulic properties of the porous media.

4.6.1 Soil-Water Potential

In saturated flow the driving potential for groundwater flow is due to the pore-water pressure and elevation above a reference datum (Fetter 2001). However, in unsaturated flow the pore water is under a negative pressure caused by surface tension. Soil physicists call this the **capillary potential**, or **matric potential**, ψ ; it is a function of the volumetric water content of the soil, θ . The lower the water content, the lower—i.e., more negative—the value of the matric potential.

The total soil-moisture potential, ϕ , is the sum of the matric potential, ψ , a pressure potential, the gravitational potential, Z , an osmotic potential, and an electrochemical potential. However, we will assume that the osmotic potential and the electrochemical potential do not vary within the soil and that the pressure is equal to atmospheric. Since we will eventually want to find the gradient of the potential, we can neglect osmotic pressure and electrochemical potentials, because their gradient will be zero. Total soil moisture potential is therefore reduced to the sum of the matric and gravitational potentials:

$$\phi = \psi(\theta) + Z \quad (4.3)$$

Matric potential may be measured as a capillary pressure, P_c , which has the units of newtons per square meter, which are equivalent to joules per cubic meter or energy per unit volume ($ML^{-3}T^{-2}$). If the matric potential is measured on a pressure basis, then the gravitational potential, Z , is equal to $\rho_w g z$, where g is the acceleration of gravity, ρ_w is the density of water, and z is the elevation above a reference plane. The total soil moisture potential in terms of energy per unit volume can thus be found from

$$\phi_{EV} = P_c + \rho_w g z \quad (4.4)$$

If Equation 4.4 is divided by $\rho_w g$, the result is the soil moisture potential expressed as energy per unit weight, which also has units of length (L). This is equivalent to head in saturated flow. The matric potential is also expressed in units of length, typically centimeters of water:

$$\phi_{EW} = \frac{P_c}{\rho_w g} + z = h + z \quad (4.5)$$

where h , pressure potential, is the matric potential in units of length.

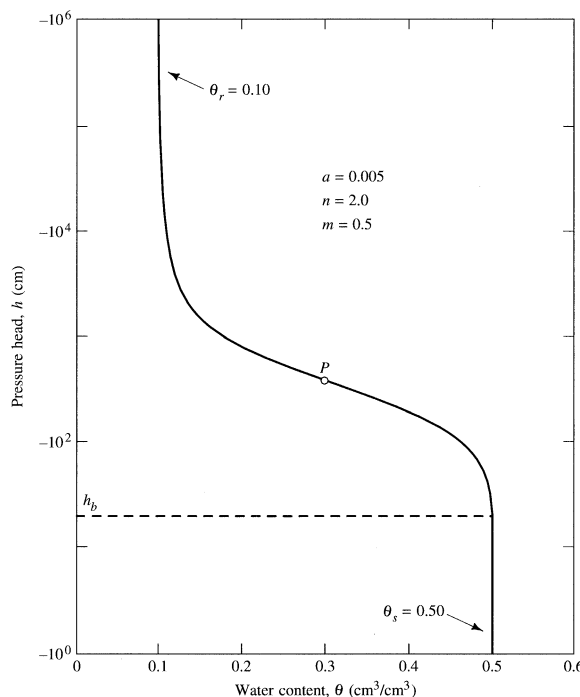
Dividing Equation 4.4 by ρ_w gives the soil-moisture potential expressed as energy per unit mass, with units of joules per kilogram (L^2T^{-2}):

$$\phi_{EM} = \frac{P_c}{\rho_w} + gz \quad (4.6)$$

Common units for total potential and pressure potential include atmospheres of pressure and centimeters of water. One atmosphere is equivalent to about 1000 cm of water. Also, 10^5 pascals of pressure is equal to about 1 atmosphere (atm).

4.6.2 Soil-Water Characteristic Curves

The relationship between matric potential or pressure head and volumetric water content for a particular soil is known as a **soil-water characteristic curve**, or a soil-water retention curve. Figure 4.3 shows an idealized soil-water characteristic curve.

FIGURE 4.3 Typical soil-water retention curve.

Source: van Genuchten 1980.

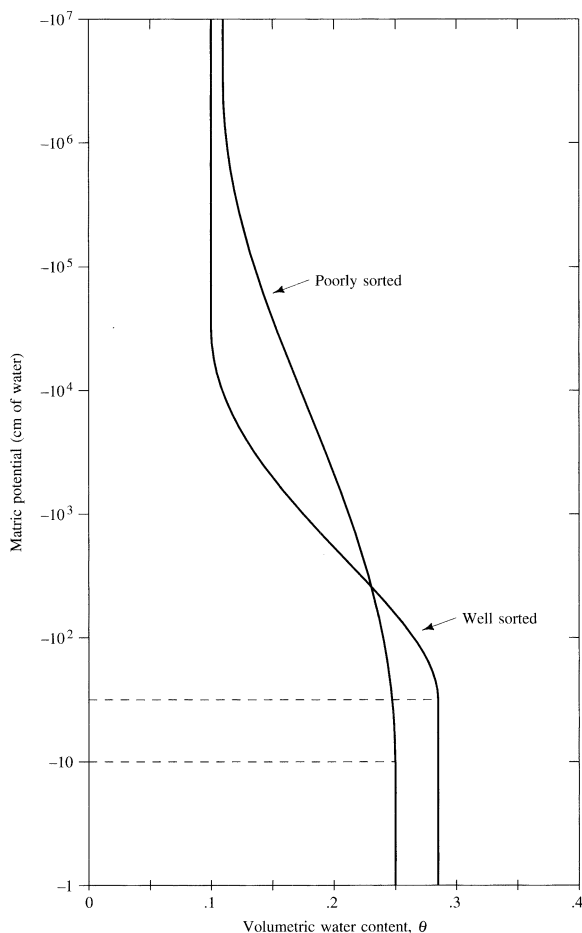
At atmospheric pressure the soil is saturated, with the water content equal to θ_s . The soil will remain saturated as the matric potential is gradually decreased. Eventually, the matric potential will become negative enough that water can begin to drain from the soil. This matric potential is known as the **bubbling pressure**. It is marked h_b on Figure 4.3. The moisture content will continue to decline as the matric pressure is lowered, until it reaches some irreducible minimum water content, θ_r . Should the matric potential be further reduced, the soil would not lose any additional moisture.

The soil-moisture characteristic curve also shows the pore-size distribution of the soil. Figure 4.4 shows idealized soil-moisture characteristic curves for two soils, one of which is well sorted and one of which is poorly sorted.

The well-sorted soil has a narrower range of matric potential over which the water content changes than the poorly sorted soil. In a well-sorted soil, most of the grains are in a narrow size range, and hence the pores also have a narrow size range. The poorly sorted soil has a wider size range for both grains and pores. The well-sorted soil has a higher bubbling pressure because it has larger pores. However, once the well-sorted soil begins to desaturate, it does so rapidly, again because most of the pores are large.

There are some simple empirical expressions that can be used to relate the water content of a soil to the matric potential. Brooks and Corey (1966) used the relationship

FIGURE 4.4 Typical soil-water retention curves showing the effect of grain-size sorting. The shape of the curves reflects the distribution of pore sizes in the soil.



$$\theta = \theta_r + (\theta_s - \theta_r) \left(\frac{\psi}{h_b} \right)^{-\lambda} \quad (4.7)$$

where

θ = volumetric water content

θ_s = volumetric water content at saturation

θ_r = irreducible minimum water content

ψ = matric potential

h_b = bubbling pressure

λ = experimentally derived parameter

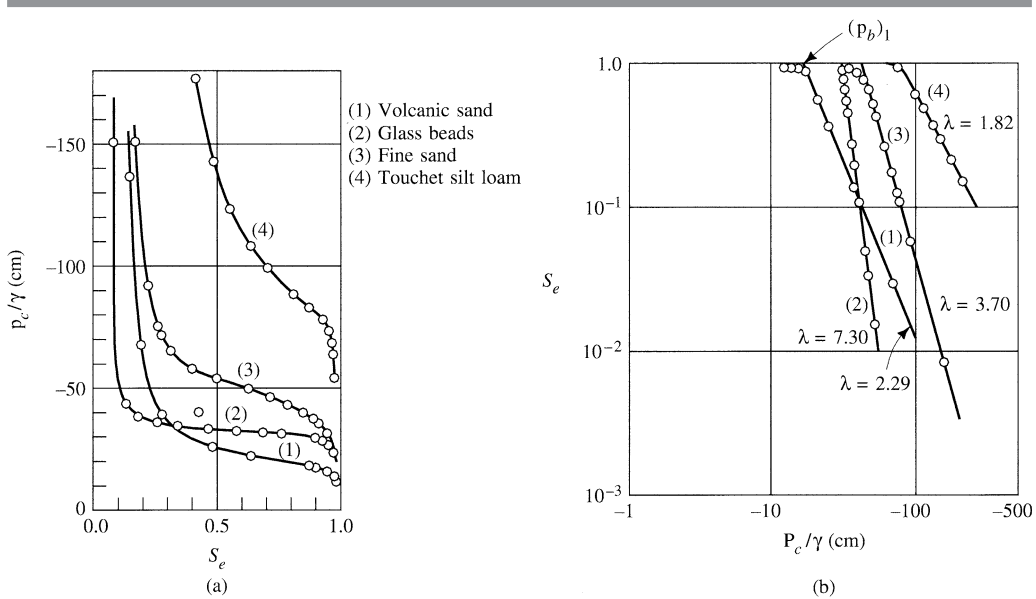
Brooks and Corey (1966) also defined an **effective saturation**, S_e , as

$$S_e = \left(\frac{S_w - \theta_r}{1 - \theta_r} \right) \quad (4.8)$$

where S_w = the saturation ratio, θ/θ_s .

A graph of capillary pressure divided by the specific weight (P_c/γ) of the fluid versus the effective saturation (S_e) is shown for water in four different porous media in Figure 4.5(a). Figure 4.5(b) shows P_c/γ plotted versus S_e on log-log paper for the same data sets. Note that on Figure 4.5(b) the data sets plot mainly as straight lines, except close to the point where S_e is equal to 1.0. (At $S_e = 1.0$, the saturation ratio, S_w , is equal to 1.0). The negative slope of the line is called λ , the Brooks-Corey pore-size distribution index, and is one of two constants that characterize the media. The other constant is the intercept of the extension of the straight line with the $S_e = 1.0$ axis. This constant h_b , the bubbling pressure, has already been defined. The capillary behavior of a porous medium can thus be defined on the basis of these two constants, λ and h_b . In Figure 4.5(b) curve 1 for volcanic sand has a λ value of 2.29 and an h_b of about 15 cm.

FIGURE 4.5 Capillary pressure head as a function of effective saturation for porous materials with various pore sizes. (a) Plotted on arithmetic paper and (b) plotted on log-log paper.



Source: Brooks and Corey 1966.

The volcanic sand, fine sand, and glass beads shown in Figure 4.5 have a fairly narrow grain-size distribution, which results in a narrow range of pore-size distribution. They are not representative of most natural soils. The calculated λ values for these soils are also higher than one finds in most natural soils. The Touchet silt loam is more representative of a normal soil than the other three.

Van Genuchten (1980) also derived an empirical relationship between matric potential and volumetric water content. He defined the relationship by the expression

$$\theta = \theta_r + \frac{\theta_s - \theta_r}{\left[1 + (\alpha |\psi|^n) \right]^m} \quad (4.9)$$

$$n = \frac{1}{1-m} \quad (4.10)$$

$$\alpha = \frac{1}{h_b} \left(2^{\frac{1}{m}} - 1 \right)^{1-m} \quad (4.11)$$

where m is a parameter estimated from the soil-water retention curve.

To find the van Genuchten soil parameters, a soil-water retention curve ranging from a matric potential of 0 to a matric potential of $-15,000$ cm is constructed. The value of θ_s is found at a matric potential of 0 and the value of θ_r is that corresponding to a matric potential of $-15,000$ cm. Figure 4.3 shows such a plot. The point P on the curve corresponds to a water content θ_p , which is found from

$$\theta_p = \frac{\theta_s + \theta_r}{2} \quad (4.12)$$

The slope, S , of the line at point P is determined graphically from the experimental soil-water retention curve. A dimensionless slope, S_p , is then found from the relationship:

$$S_p = \frac{S}{\theta_s - \theta_r} \quad (4.13)$$

The parameter m can then be determined from the value of S_p using one of these formulas:

$$m = \begin{cases} 1 - \exp(-0.8S_p) & (0 < S_p \leq 1) \\ 1 - \frac{0.5755}{S_p} + \frac{0.1}{S_p^2} + \frac{0.025}{S_p^3} & (S_p > 1) \end{cases} \quad (4.14)$$

We can find the values of m and α from Equations 4.14 and 4.11, respectively, by using the bubbling pressure obtained from the soil-water retention curve.

From Figure 4.3 the slope of the curve at P is about 0.34. The dimensionless slope determined from Equation 4.13 is about 0.85. From Equation 4.14 m is determined to be about 0.5 and from Equation 4.10, n is 2.0. To estimate α from Equation 4.11, we need the value of h_b , the bubbling pressure. From Figure 4.3 the value of h_b is about -35 so that the value of α is about -0.05 .

Carsel and Parrish (1988) have estimated the average van Genuchten soil parameters for various soil textural classes. These parameters can be used with Equations 4.9 and 4.10 to construct typical soil water retention curves with no actual experimental data. While such curves are useful when one has no data available, they should be used with caution. Table 4.1 contains these parameters.

EXAMPLE PROBLEM

Construct a soil water curve for a loamy sand using the values in Table 4.1. Equation 4.10 can be rearranged as:

$$m = 1 - \frac{1}{n}$$

The value of n for loamy sand is 2.28, so that

$$m = 1 - \frac{1}{2.28} = 0.56$$

Other values for the van Genuchten soil parameters are:

$$\alpha = 0.124$$

$$\theta_s = 0.41$$

$$\theta_r = 0.057$$

These values, plus m and n can be substituted into Equation 4.9 along with assumed values of the matric potential, ψ , in order to find the corresponding volumetric water content.

TABLE 4.1 Average values of the van Genuchten soil parameters obtained by experimental means.

Soil Texture	Porosity (ratio)	Residual Water Content (ratio)	Saturated Hydraulic Conductivity (cm/hour)	α Parameter (cm^{-1})	n Parameter (dimensionless)
Clay loam	0.41	0.095	0.26	0.019	1.31
Loam	0.43	0.078	1.04	0.036	1.56
Loamy sand	0.41	0.057	14.59	0.124	2.28
Silt	0.46	0.034	0.25	0.016	1.37
Silt loam	0.45	0.067	0.45	0.020	1.41
Silty clay	0.36	0.070	0.02	0.005	1.09
Silty clay loam	0.43	0.089	0.07	0.010	1.23
Sand	0.43	0.045	29.70	0.145	2.68
Sandy clay	0.38	0.100	0.12	0.027	1.23
Sandy clay loam	0.39	0.100	1.31	0.059	1.48
Sandy loam	0.41	0.065	4.42	0.075	1.89

Source: Carsel and Parrish. 1988. Developing joint probability distributions of soil water retention characteristics. *Water Resources Research* 24:755–769. Copyright by the American Geophysical Union. Reproduced with permission.

$$\theta = \theta_r + \frac{\theta_s - \theta_r}{\left[1 + (\alpha |\psi|)^n \right]^m}$$

$$\theta = 0.057 + \frac{0.41 - 0.057}{\left[1 + (0.124 \text{ cm}^{-1} |\psi|)^{2.28} \right]^{0.56}}$$

Assume values of ψ of 0 cm, -5 cm, -10 cm, -20 cm, -40 cm, -80 cm, -100 cm, -250 cm and -500 cm. The results are:

ψ	θ
0 cm	0.41
-5 cm	0.357
-10 cm	0.262
-20 cm	0.160
-40 cm	0.102
-80 cm	0.076
-100 cm	0.071
-250 cm	0.061
-500 cm	0.057

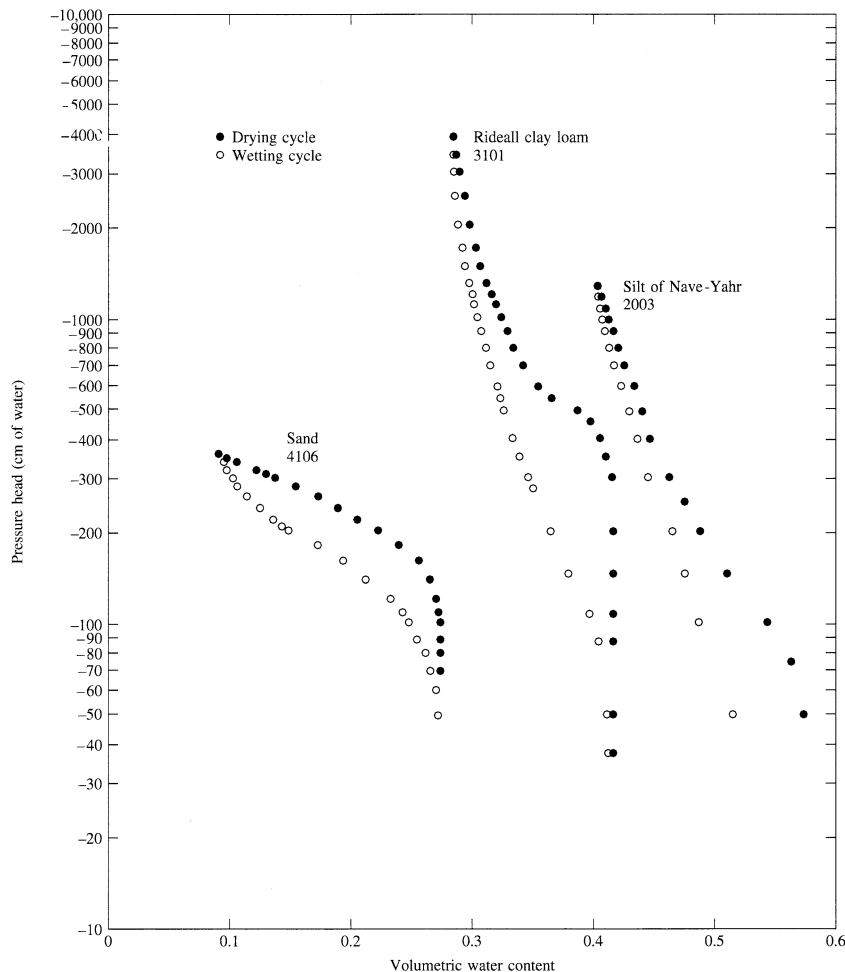
4.6.3 Hysteresis

If one constructs a soil-water retention curve by obtaining data from a sample that is initially saturated and then applying suction to desorb water, the curve is known as a **drying curve**. If the sample is then resaturated by decreasing the suction, it will follow a **wetting curve**. Figure 4.6 shows drying and wetting curves for three different soils. Typically, the drying curve and the wetting curve will not be the same. This phenomenon is called **hysteresis**. The causes of hysteresis include (Hillel 1980)

1. The geometric effects of the shape of single pores, which give rise to the so-called ink bottle effect. This effect is illustrated in Figure 4.7. The pore has a throat radius of r and a maximum radius of R . The matric potential when the air-water interface is at the pore throat, ψ_r , is equal to $2\sigma/r$, where σ is the interfacial tension between the pore water and the mineral surface (see Section 5.2.3). The pore will drain abruptly when ψ has a more negative pressure than ψ_r . The pore cannot then rewet until ψ falls below ψ_r . Since $R > r$, then $\psi_r > \psi_R$; that is, it takes a lower matric potential (more negative pressure) to drain a pore than to fill it.
2. The contact angle between the water and the mineral surface is greater during the period when a water front is advancing as opposed to when it is retreating. The advancing meniscus that forms during wetting will have a greater radius of curvature—and hence a lower matric potential—than that exhibited by a meniscus that forms during a drying cycle.
3. Air that is trapped in pores during a wetting cycle will reduce the water content of soil as it is being wetted. Eventually that trapped air will dissolve.

The hysteresis effect may be augmented by the shrinking and swelling of the clays as the soil wets and dries and may also be affected by the rates of wetting and drying (Davidson, Nielsen, and Biggar 1966). In near surface soil, the magnitude and nature of hysteresis can be modified by storm fluxes, vegetation dynamics, soil aggregate size, and soil wettability (Ivanov et al. 2010; Witkowska-Walczak 2006; Davis et al. 2009), and can be modeled in different ways (Kazimoglu et al. 2005).

If the soil is not dried to the maximum extent possible (greatest negative pressure head), when it is rewet, the soil will follow an intermediate curve known as a wetting (or drying) scanning curve. There are many wetting and drying scanning curves,

FIGURE 4.6 Soil-moisture-retention curves for three soils for both drying and wetting cycles.

Source: Yechezkel Mualem, Catalogue of Hydraulic Properties of Unsaturated Soils. Haifa, Israel: Technion, 1976.

depending upon the point on the main wetting or drying curve where the scanning curve starts.

4.6.4 Construction of a Soil-Water-Retention Curve

Laboratory measurements of matric potential as a function of water content are made to construct a soil-water-retention curve. In the wet-soil range -1 to -300 cm of water-pressure head, a tension plate assembly is used. A saturated soil sample of known water content is placed on a porous plate in a Buchner funnel. The porous plate is saturated and connected to a water column that ends in a burette (Figure 4.8). The position of the burette can be changed to decrease the pressure head. As the pressure

FIGURE 4.7 Pore geometry affects equilibrium height of capillary water during (a) drainage and (b) wetting.

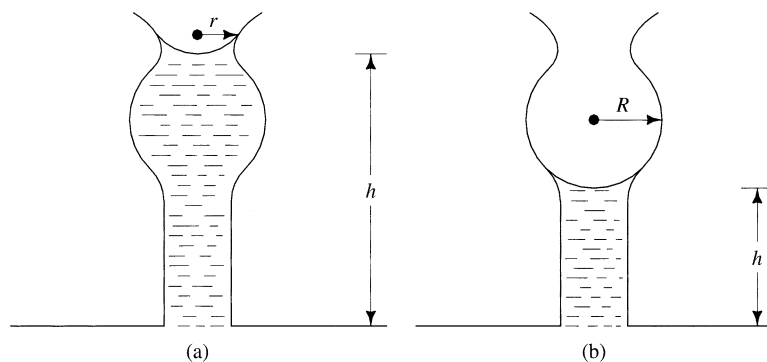
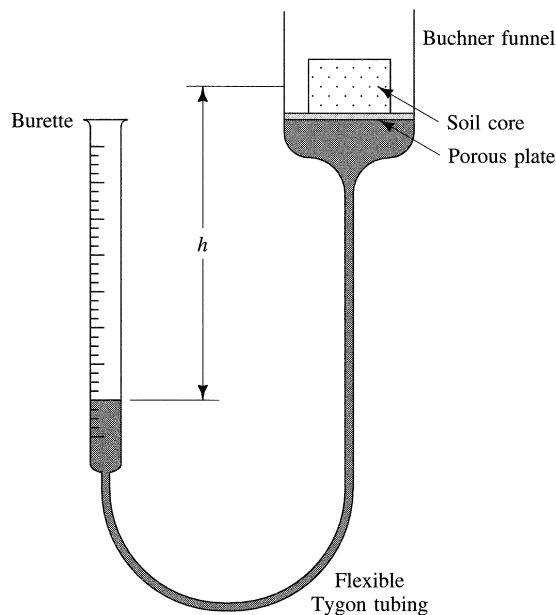


FIGURE 4.8 Equilibrating the water content of a soil sample with a known matric potential using a tension plate assembly.



head becomes more negative, water is drained from the soil sample and the amount is measured in the burette once equilibrium has been reached. Care must be taken to avoid evaporation of water from the soil sample and the burette. A number of measurements are made at progressively more negative pressure heads to determine the drying curve. Once the practical limit of the tension plate assembly is reached (-300 cm), the burette is raised in a number of steps to construct a wetting curve. This is a wetting scanning curve, as the soil is not fully drained at a pressure head of -300 cm of water.

For soils in the dry range (-300 to $-15,000$ cm of water), a pressure-plate assembly is used. The soil samples are placed on a saturated porous plate that is in a pressure chamber. The pressure below the porous plate is kept at atmospheric pressure and the pressure above the porous plate can be set between 0.3 atm (300 cm of water) and 15 atm ($15,000$ cm of water). The pressure across the soil sample and porous plate causes water to flow from the soil sample across the porous plate into a lower reservoir.

4.6.5 Measurement of Soil-Water Potential

Matric potential is measured in the field with a tensiometer. This apparatus consists of a porous ceramic cup attached to a tube, which is buried in the soil. The tube is filled with water and attached to a device such as a vacuum gauge, manometer, or pressure transducer, which can measure the tension. The matric potential of the soil tries to draw water from the water-filled porous cup, and the resulting tension is measured. Tensiometers can measure soil moisture tensions up to about 800 cm.

Figure 4.9 shows the operation of two tensiometers in determining the gradient of the matric potential. Tensiometer A has the porous ceramic cup at a depth of 100 cm, whereas tensiometer B is at a depth of 30 cm. The total potential measured for tensiometer A is -126 cm, whereas for tensiometer B it is -88 cm. Since total potential is the sum of pressure head and elevation head, one must subtract the elevation head from total head to get pressure head. Thus the pressure head measured in tensiometer A is -26 cm, whereas for tensiometer B it is -58 cm. However, the total potential gradient is downward, because the total head at A is more negative than that at B. The gradient is computed by finding the difference between the two total heads and dividing the difference by the distance between the two porous cups. In Figure 4.9 the gradient is

$$\frac{-126 - (-88)}{-70} = 0.54 \text{ (downward)}$$

EXAMPLE PROBLEM

The following data have been obtained for a soil sample using a tension-plate assembly. Construct a water-retention curve.

Volumetric Water Content

Pressure head (cm)	Wetting Cycle	Drying Cycle
0	0.447	0.448
-30	0.431	0.448
-60	0.411	0.443
-90	0.400	0.437
-120	0.392	0.424
-150	0.385	0.408
-180	0.379	0.391
-210	0.377	0.377

Wetting Scanning Curve

-120	0.411
-90	0.418
-60	0.423
-30	0.436
0	0.477

The data are plotted in Figure 4.10.

4.6.6 Unsaturated Hydraulic Conductivity

When a rock or sediment is saturated, all the pores are filled with water, and most of them transmit water. Only “dead-end” pores do not participate in the transmittal of water. Unsaturated soils have a lower hydraulic conductivity because some of the pore space is filled with air and thus can't transmit water. Soil moisture in the vadose zone travels through only the wetted cross section of pore space. As a saturated soil drains, the larger pores empty first, especially in soils that are structured. Because these have the greatest pore-level hydraulic conductivity, there is an immediate large drop in the ability of the soil to transmit water. The unsaturated hydraulic conductivity is a function of the water content of the soil: $K = K(\theta)$. Unsaturated hydraulic conductivity can also be considered to be a function of the matric potential: $K = K(\psi)$. Figure 4.11 is a graph of unsaturated hydraulic conductivity as a function of matric potential. It can be seen that this relationship also exhibits hysteresis.

The flow of soil moisture is influenced by temperature. Figure 4.12 shows the influence of water temperature on curves of unsaturated hydraulic conductivity versus water content. A change from 2°C to 25°C can cause unsaturated hydraulic conductivity to increase by as much as an order of magnitude. Constantz (1982) wrote the following expression for the relationship of unsaturated hydraulic conductivity to intrinsic permeability of the soil:

$$K(\theta) = \frac{k_r(\theta) k \rho_w g}{\mu_w} \quad (4.15)$$

where

$k_r(\theta)$ = the relative conductivity, which is a number from 0 to 1.0 that is the ratio of the unsaturated hydraulic conductivity at a given θ to the saturated hydraulic conductivity

k = the intrinsic permeability

ρ_w = the density of water at a given temperature

g = the acceleration of gravity

μ_w = the dynamic viscosity of soil water at a given temperature

Constantz (1982) reports that the effect of temperature on unsaturated hydraulic conductivity is primarily a function of the effect of temperature on dynamic viscosity.

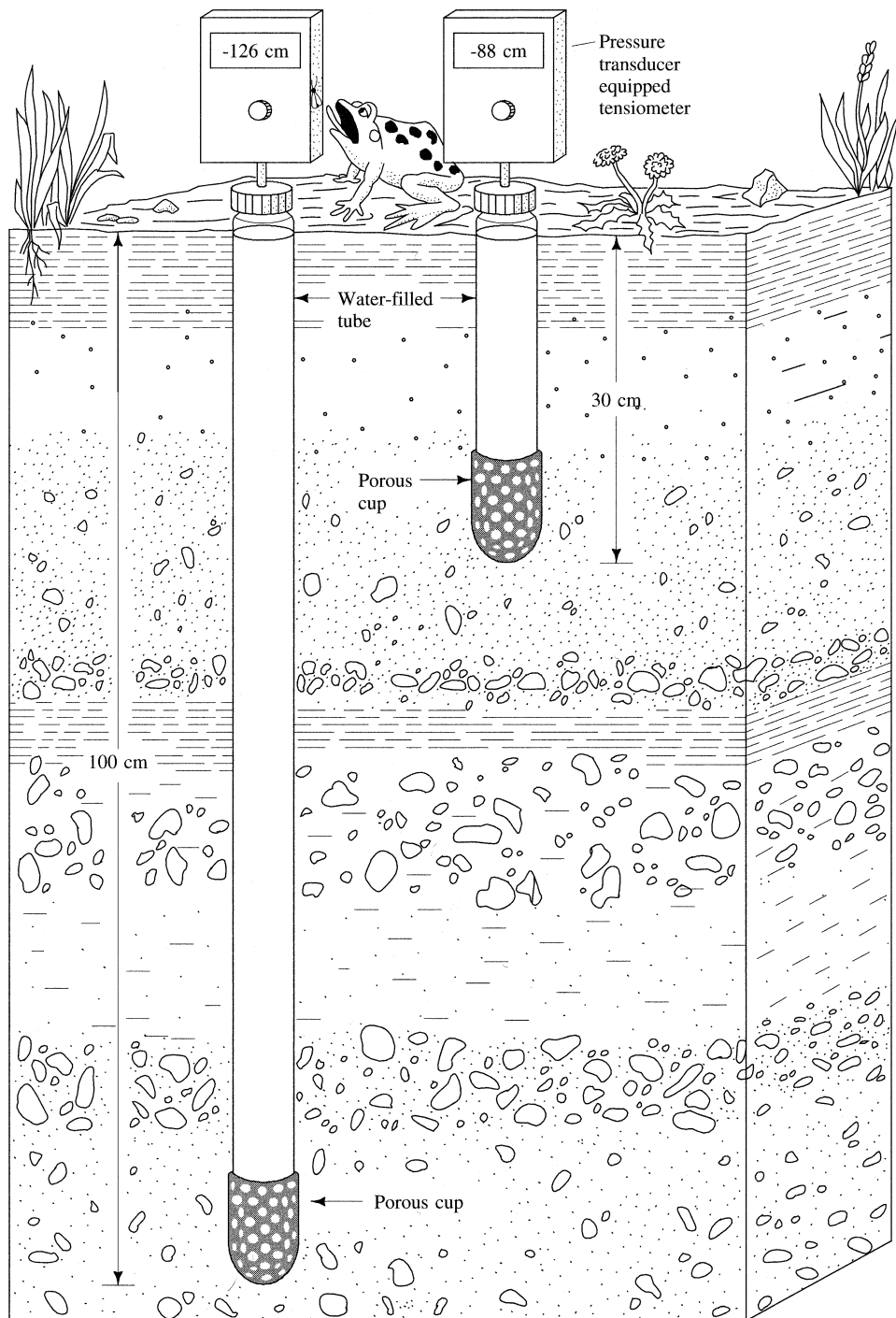
FIGURE 4.9 Tensiometer used to measure soil-water potential in the field.

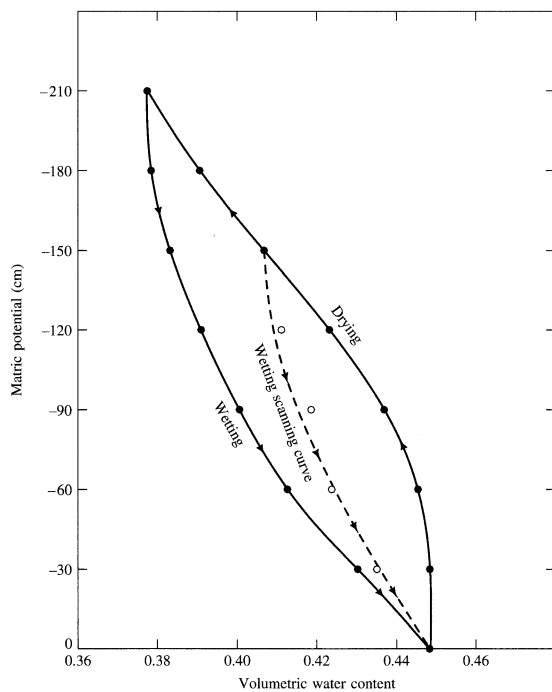
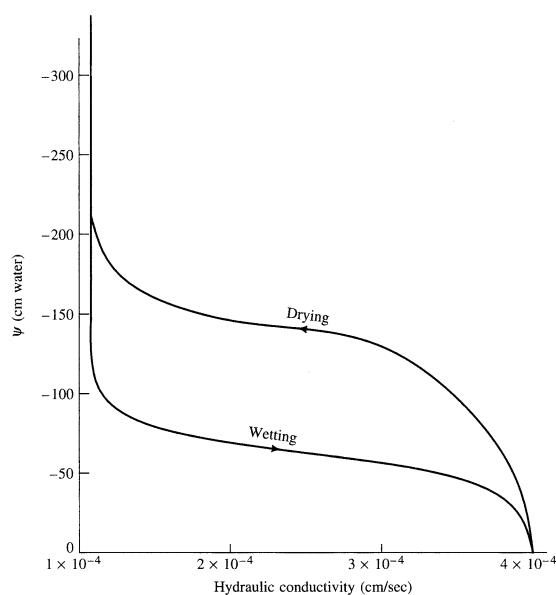
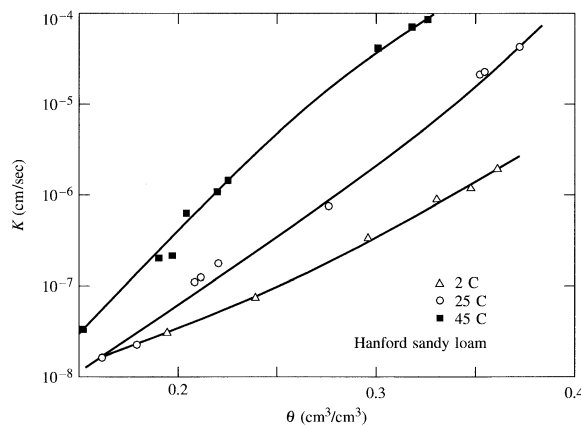
FIGURE 4.10 Matric potential as a function of volumetric water content for the example problem.**FIGURE 4.11** Relationship of hydraulic conductivity to matric potential for a wetting and drying cycle illustrating hysteresis.

FIGURE 4.12 Unsaturated hydraulic conductivity as a function of water content for three temperatures.

Source: Constantz 1982.

Unsaturated hydraulic conductivity can be determined by both field methods (Green, Ahuja, and Chong 1986) and laboratory techniques (Klute and Dirksen 1986). However, both field and laboratory methods are time consuming and tedious, with numerous practical limitations (van Genuchten 1988). As a result, unsaturated hydraulic conductivity is often estimated from soil parameters obtained from soil-water retention curves.

Van Genuchten (1980) derived expressions that relate the unsaturated hydraulic conductivity to both the water content and the pressure head. The relationship between the unsaturated hydraulic conductivity and the water content is

$$K(\theta) = K_s S_e^{\frac{1}{2}} \left[1 - \left(1 - S_e^{\frac{1}{m}} \right)^m \right]^2 \quad (4.16)$$

where

$$S_e = (\theta - \theta_r)/(\theta_s - \theta_r)$$

$K(\theta)$ = unsaturated hydraulic conductivity at water content θ

K_s = saturated hydraulic conductivity

m = van Genuchten soil parameter

The equivalent relationship between unsaturated hydraulic conductivity and pressure head is

$$K(h) = K_s \frac{\left\{ 1 - (\alpha h)^{n-1} [1 + (\alpha h)^n]^{-m} \right\}^2}{[1 + (\alpha h)^n]^{\frac{m}{2}}} \quad (4.17)$$

where

$K(h)$ = the unsaturated hydraulic conductivity at pressure head h

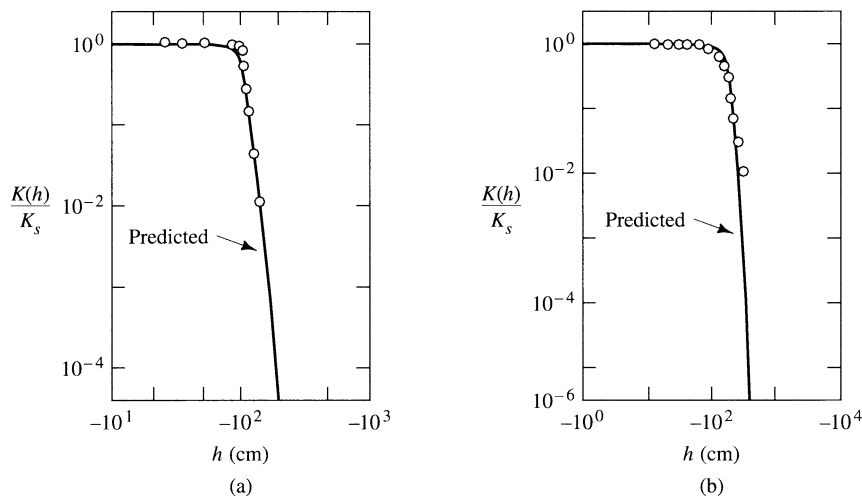
h = pressure head

n = van Genuchten soil parameter

α = van Genuchten soil parameter

Figure 4.13 shows observed values (open circles) and calculated curves (solid lines) based on Equation 4.17 for relative permeability ($K_r = K(h)/K_s$) as a function of pressure head for (a) a sandstone and (b) a silt loam. The predictive equation quite closely follows the observed values.

FIGURE 4.13 Observed values (open circles) and calculated curves (solid lines) for relative hydraulic conductivity of (a) Hygiene sandstone and (b) Touchet silt loam G.E.3.



Source: van Genuchten 1980.

4.6.7 Buckingham Flux Law

The first to recognize the basic laws for the flow of water in soil was Buckingham (1907). He recognized that the matric potential, ψ , of unsaturated soils was a function of the water content, θ , temperature, and bulk density of the soil. He also realized that the flow of water across a unit cross-sectional area was proportional to the gradient of the soil water matric potential. The proportionality constant, $K(\theta)$, was recognized to be a function of the water content. Buckingham, a physicist, appears to have had no knowledge of Darcy's work on saturated flow some half-century before (Sposito 1986).

What is now known as the Buckingham flux law was formalized by Richards (1928), who extended the concept of the potential gradient to include the total soil moisture potential, Φ . Written in vector notation, the Buckingham flux law is

$$\mathbf{q} = -K(\psi)\nabla(\phi) \quad (4.18)$$

where

- \mathbf{q} = the soil moisture flux ($L^3 L^{-2} T^{-1}$)
- $K(\psi)$ = the unsaturated hydraulic conductivity ($L T^{-1}$) at a given ψ
- $\nabla(\Phi)$ = the gradient of the total soil water potential, Φ , where

$$\Phi = \psi + Z (L L^{-1})$$

4.6.8 Richards Equation

The continuity equation for soil moisture through a representative elementary volume of the unsaturated zone can be stated as the change in total volumetric water content with time and is equal to the sum of any change in the flux of water into and out of the representative elemental volume. The continuity equation can be expressed as

$$\frac{\partial \theta}{\partial t} = - \left(\frac{\partial q_x}{\partial x} + \frac{\partial q_y}{\partial y} + \frac{\partial q_z}{\partial z} \right) \quad (4.19)$$

where q_x , q_y , and q_z are soil moisture fluxes.

In vector notation Equation 4.19 is

$$\frac{\partial \theta}{\partial t} = -\nabla \cdot \mathbf{q} \quad (4.20)$$

Combining Equations 4.20 with 4.18, we obtain the Richards equation (Richards 1931):

$$\frac{\partial \theta}{\partial t} = \nabla \cdot [K(\psi) \nabla \phi] \quad (4.21)$$

For vertical flow, the value of ∇z is 0 in the x and y directions and is 1 in the z direction. In addition, Φ is equal to $\psi + Z$. Therefore, if z is taken to be positive in a downward direction, Equation 4.21 can be rewritten as

$$\frac{\partial \theta}{\partial t} = \nabla \cdot [K(\psi) \nabla \phi] - \frac{\partial K(\psi)}{\partial z} \quad (4.22)$$

For one-dimensional flow, Equation 4.22 reduces to

$$\frac{\partial \theta}{\partial t} = \frac{\partial}{\partial z} \left(K(\psi) \frac{\partial \psi}{\partial z} \right) - \frac{\partial K(\psi)}{\partial z} \quad (4.23)$$

If the matric potential is much greater than the gravity gradient, then the last term of Equation 4.23 can be dropped; the resulting equation is

$$\frac{\partial \theta}{\partial t} = \frac{\partial}{\partial z} \left(K(\psi) \frac{\partial \psi}{\partial z} \right) \quad (4.24)$$

The preceding equations assume a constant temperature and air pressure, a non-deformable soil matrix, incompressible water, and that soil water density is independent of solute concentration and does not vary throughout the flow domain. Furthermore, these equations assume that the presence of air can be ignored, except as it affects the value of K . Equation 4.23 is nonlinear and difficult to solve by analytical

means. However, numerical methods of solution of this equation have been developed (Nielsen, van Genuchten, and Biggar 1986).

■ 4.7 Liquid Mass Transport in the Unsaturated Zone

The steady-state diffusion of a solute in soil moisture is given by (Hillel, 1980)

$$J = -D_s^*(\theta) dC / dz \quad (4.25)$$

where

J = the mass flux of solute per unit area per unit time

$D_s^*(\theta)$ = the soil diffusion coefficient, which is a function of the water content, the tortuosity of the soil, and other factors related to the electrostatic double layer

dC/dz = the concentration gradient in the soil moisture

The second-order diffusion equation for transient, one-dimensional diffusion of solutes, in a vertical direction in soil water is

$$\frac{\partial C}{\partial t} = \frac{\partial}{\partial z} \left[D_s^*(\theta) \frac{\partial C}{\partial z} \right] \quad (4.26)$$

Soil moisture traveling through the unsaturated zone moves at different velocities in different pores due to the fact that the saturated pores through which the moisture moves have different-sized pore throats. In addition, velocities within each saturated pore will vary across the width of the pore. As a result, soil water carrying a solute will mix with other soil moisture. This is analogous to the mechanical mixing of saturated flow. Mechanical mixing is found from the following equation (Nielsen, van Genuchten, and Biggar 1986):

$$\text{Mechanical mixing} = \zeta |\nu| \quad (4.27)$$

where

ζ = an empirical soil moisture dispersivity

ν = the average linear soil moisture velocity

The soil moisture dispersion coefficient, D_s is the sum of the diffusion and mechanical mixing:

$$D_s = D_s^* + \zeta |\lambda| \quad (4.28)$$

The total one-dimensional solute flux in the vadose zone is the result of advection, diffusion, and hydrodynamic dispersion. With diffusion and hydrodynamic dispersion combined as the soil-moisture dispersion coefficient, this result can be expressed as

$$J = \nu \theta C - D_s \theta dC / dz \quad (4.29)$$

where

J = the total mass of solute across a unit cross-sectional area in a unit time

ν = the average soil-moisture velocity

C = the solute concentration in the soil moisture

θ = the volumetric water content

dC/dz = the solute gradient

D_s = the soil moisture diffusion coefficient, which is a function of both θ and v

The continuity equation for a solute flux requires that the rate of change of the total solute mass present in a representative elemental volume be equal to the difference between the solute flux going into the REV and that leaving the REV. The total solute mass is the sum of the dissolved solute mass and the mass of any solute associated with the solid phase of the soil. The dissolved solute mass is equal to the product of θ and C . The solute mass bound to the soil is the product of the soil bulk density, ρ_b , and the concentration of the solute phase bound to the soil, C^* . The continuity equation for the solute is:

$$\frac{\partial(\rho_b C^*)}{\partial t} + \frac{\partial(\theta C)}{\partial t} = -\frac{\partial J}{\partial z} \quad (4.30)$$

By combining Equations 4.29 and 4.30, we obtain

$$\frac{\partial(\rho_b C^*)}{\partial t} + \frac{\partial(\theta C)}{\partial t} = \frac{\partial(v\theta C)}{\partial z} + \frac{\partial}{\partial z}\left(D_s \theta \frac{\partial C}{\partial z}\right) \quad (4.31)$$

The convective soil moisture flux, q , is the product of the volumetric water content, θ , and the average soil moisture velocity, v . There may also be sources and sinks of the solute not accounted for by the absorbed concentration, C^* . For example, plants may remove nutrients from solution and solutes might be created by biological decay as well as microbial and chemical transformation and precipitations. These can be added to Equation 4.31 by means of a term for the summation of γ_i , where γ represents other sources and sinks. With a slight rearrangement Equation 4.31 becomes the fundamental mass transport equation for the vadose zone:

$$\frac{\partial(\rho_b C^*)}{\partial t} + \frac{\partial(\theta C)}{\partial t} = \frac{\partial}{\partial z}\left(D_s \theta \frac{\partial C}{\partial z} - qC\right) + \sum_i Y_i \quad (4.32)$$

If ρ_b , D_s , θ , and q are assumed to be constant in time and space, Equation 4.32 reduces to Equation 3.1, the basic one-dimensional advection-dispersion equation.

■ 4.8 Equilibrium Models of Mass Transport

In order to account for a solute, which can be in either a dissolved form or absorbed by the soil, we need to know the relationship between the concentration in solution, C , and the absorbed concentration, C^* . If the solute reaches equilibrium rapidly between the dissolved and absorbed phase, then the relationship can be described by an absorption isotherm. Sorption isotherms are discussed more thoroughly in Chapter 3. For illustration in this chapter, we will use the linear isotherm

$$C^* = K_d C \quad (4.33)$$

where K_d , the distribution coefficient, is the slope of the plot of C^* as a function of C .

Under certain conditions the source and sink function, γ_i , may be approximated by zero- and first-order decay and production terms (Nielsen, van Genuchten, and Biggar 1986). If η_l and η_s are rate constants for first-order decay in the liquid and solid phases, respectively, and ξ_l and ξ_s are zero-order rate terms for production in the liquid and solid phases, then

$$\gamma_i = -\eta_l \theta C - \eta_s \rho_b C^* + \xi_l \theta + \xi_s \rho_b \quad (4.34)$$

By substitution of Equations 4.33 and 4.34 into 4.32 and simplification of terms, we can obtain the following equation:

$$R \frac{\partial C}{\partial t} = D_s \frac{\partial^2 C}{\partial z^2} - v \frac{\partial C}{\partial z} - \eta C + \xi \quad (4.35)$$

where R is the retardation factor, which is given by

$$R = 1 + \frac{\rho_b K_d}{\theta} \quad (4.36)$$

and η and ξ are consolidated rate factors, given by

$$\eta = \eta_l + \frac{\eta_s \rho_b K_d}{\theta} \quad (4.37)$$

$$\xi = \xi_l + \frac{\xi_s \rho_b}{\theta} \quad (4.38)$$

Equation 4.35 is based on steady-state flow, as the volumetric moisture content and the fluid velocity are taken to be constants.

Van Genuchten (1981) solved equation 4.35 for a number of different boundary conditions. In general, at time equals 0 and at some place in the soil column, z , the solute concentration is $C_i[C(z, 0) = C_i(z)]$. The concentration introduced into the top of the soil column where $z = 0$ at some time t is $C_0[C(0, t) = C_0(t)]$. The rate that solute is introduced into the top of the soil column by both advection and diffusion is equal to the pore water velocity, v , times C_0 . [The usual boundary condition adopted for this is $(-D_s dC/dz + vC) = vC_0$]

If a pulse of solute is introduced into the soil column for a time period of 0 to t_0 , during that time the rate is vC_0 . After time t_0 , the pulse is ended and the rate at which solute is introduced is 0. (For $0 < t < t_0$, $(-D_s dC/dz + vC) = vC_0$; for $t > t_0$, $(-D_s dC/dz + vC) = 0$). The soil column is infinitely long ($dC/dz(\infty, t) = 0$).

In this case the solution to Equation 4.35 for times when the pulse is being injected ($0 < t < t_0$) is

$$C(z, t) = \left(C_0 - \frac{\xi}{\eta} \right) A(z, t) + B(z, t) \quad (4.39)$$

For times greater than t_0 —that is, after injection of the pulse has stopped—the solution to Equation 4.35 is

$$C(z, t) = \left(C_0 - \frac{\xi}{\eta} \right) A(z, t) + B(z, t) - C_0 A(x, t - t_0) \quad (4.40)$$

In both Equations 4.39 and 4.40, the following arguments are used:

$$\begin{aligned} A(z, t) &= \frac{\nu}{(\nu + u)} \exp \left[\frac{(\nu - u)z}{2D_s} \right] \operatorname{erfc} \left[\frac{Rz - ut}{2(D_s R t)^{\frac{1}{2}}} \right] \\ &+ \frac{\nu}{(\nu - u)} \exp \left[\frac{(\nu + u)z}{2D_s} \right] \operatorname{erfc} \left[\frac{Rz + ut}{2(D_s R t)^{\frac{1}{2}}} \right] \\ &+ \frac{\nu^2}{2\eta D_s} \exp \left(\frac{\nu z}{D_s} - \frac{\eta t}{R} \right) \operatorname{erfc} \left[\frac{Rz + vt}{2(D_s R t)^{\frac{1}{2}}} \right] \end{aligned} \quad (4.41)$$

$$\begin{aligned} B(z, t) &= \left(\frac{\xi}{\eta} - C_i \right) \exp \left(-\frac{\eta t}{R} \right) \left\{ \frac{1}{2} \operatorname{erfc} \left[\frac{Rz - vt}{2(D_s R t)^{\frac{1}{2}}} \right] + \left(\frac{\nu^2 t}{\pi R D_s} \right)^{\frac{1}{2}} \right. \\ &\times \exp \left[-\frac{(Rz - vt)^2}{4D_s R t} \right] - \frac{1}{2} \left(1 + \frac{\nu z}{D_s} + \frac{\nu^2 t}{D_s R} \right) \exp \left(\frac{\nu z}{D_s} \right) \\ &\times \left. \operatorname{erfc} \left[\frac{Rz + vt}{2(D_s R t)^{\frac{1}{2}}} \right] \right\} + \frac{\xi}{\eta} + \left(C_i - \frac{\xi}{\eta} \right) \exp \left(-\frac{\eta t}{R} \right) \end{aligned} \quad (4.42)$$

and

$$u = \nu \left(1 + \frac{4\eta D_s}{\nu^2} \right)^{\frac{1}{2}} \quad (4.43)$$

For the steady-state case, Equation 4.35 may be written as

$$D_s \frac{\partial^2 C}{\partial z^2} - \nu \frac{\partial C}{\partial z} - \eta C + \xi = 0 \quad (4.44)$$

The solution to this is

$$C(z) = \frac{\xi}{\eta} + \left(C_0 - \frac{\xi}{\eta} \right) \left(\frac{2\nu}{\nu + u} \right) \exp \left[\frac{(\nu - u)z}{2D_s} \right] \quad (4.45)$$

where u is defined in Equation 4.43.

Equations 4.39, 4.40, and 4.45 are only some of the analytical solutions that van Genuchten (1981) has obtained for Equation 4.35. Solutions for other boundary and initial conditions include variable initial solute concentration in the soil column and an

exponentially decaying source term. The reader is directed to van Genuchten's original paper for additional solutions.

■ 4.9 Nonequilibrium Models of Mass Transport

The soil moisture may move at such a quick rate that a solute may not be able to reach an equilibrium position with respect to chemical reactions that are occurring. One nonequilibrium formulation arises when the adsorption process can be described by a first-order linear rate equation. Under this condition, assuming steady-state flow and ignoring the source/sink term; Equation 4.31 can be written as a coupled system (Nielsen, van Genuchten, and Biggar 1986) as follows:

$$\frac{\rho_b}{\theta} \frac{\partial C^*}{\partial t} + \frac{\partial C}{\partial t} = D_s \frac{\partial^2 C}{\partial z^2} - v \frac{\partial C}{\partial z} \quad (4.46a)$$

and

$$\frac{dC^*}{dt} = \zeta_r (K_d C - C^*) \quad (4.46b)$$

where ζ_r is a first-order rate coefficient. Equations 4.46a and b have been used by many to describe nonequilibrium transport in soils. As shown by van Genuchten, Davidson, and Wierenga (1974), the first-order rate model has not materially improved the description of nonequilibrium transport in soils. An alternative model of nonequilibrium transport arises when soil water is assumed to consist of a mobile phase and an immobile phase. The mobile phase occupies the center of saturated pores. Immobile water consists of thin coatings on soil particles, dead-end pores, and water trapped in small unsaturated pores (Coats and Smith 1964). Exchange of solute between the mobile and immobile phases occurs due to diffusion. In addition, solute in both the mobile and immobile phases can participate in adsorption-desorption reactions. For Freundlich-type linear equilibrium, this conceptualization can be described by the following equations (van Genuchten and Wierenga 1976):

$$\theta_m R_m \frac{\partial C_m}{\partial t} + \theta_{im} R_{im} \frac{\partial C_{im}}{\partial t} = \theta_m D_{sm} \frac{\partial^2 C_m}{\partial z^2} - \theta_m v_m \frac{\partial C_m}{\partial z} \quad (4.47a)$$

$$\theta_{im} R_{im} \frac{\partial C_{im}}{\partial t} = \beta (C_m - C_{im}) \quad (4.47b)$$

where

β = a mass transfer coefficient

R_m = a retardation factor for the mobile water

R_{im} = a retardation factor for the immobile water

C_m = solute concentration in the mobile water

C_{im} = solute concentration in the immobile water

θ_m = volumetric mobile water content

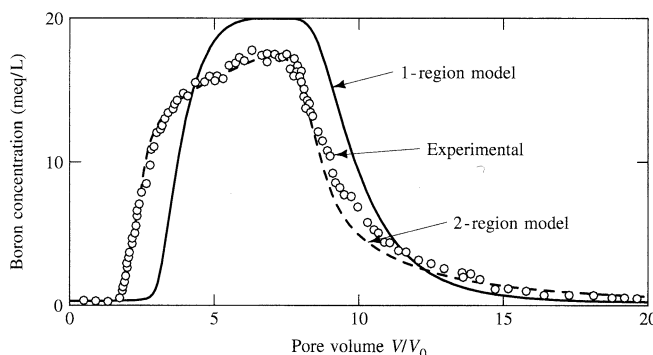
θ_{im} = volumetric immobile water content

D_{sm} = soil moisture dispersion coefficient for the mobile water

For saturated soils, the amount of immobile water is a function of the soil-water flux, the size of soil aggregates, and the concentration of the ionic solute. The mass transfer coefficient, β , is also a function of these same factors as well as the species being transferred (Nkedi-Kizza et al. 1983).

The preceding model with mobile and immobile water zones has been successfully used at the laboratory scale (Nkedi-Kizza, et. al. 1983; Nielsen, van Genuchten, and Biggar 1986). Figure 4.14 shows a breakthrough curve for a column study of the transport of a solution of boron in an aggregated clay loam soil. The curve labeled “1-region model” is based on Equation 4.35, and the curve labeled “2-region model” is based on Equations 4.47a and b. In this case the 2-region model does a better job of matching the experimental data.

FIGURE 4.14 Observed and calculated breakthrough curves for a solution of boron passing through a column filled with an aggregated clay loam soil.



Source: Nielsen, van Genuchten, and Biggar. 1980. *Water Resources Research* 16:145–158. Copyright by the American Geophysical Union. Reproduced with permission.

■ 4.10 Anion Exclusion

For a nonreactive solute, Equation 4.33 can be written as

$$\theta \frac{\partial C}{\partial t} = D_s \theta \frac{\partial^2 C}{\partial z^2} - q \frac{\partial C}{\partial z} \quad (4.48)$$

Many solutes are considered to be nonreactive in the sense that they do not sorb onto particle surfaces. Included in this category are anions such as chloride. However, chloride carries a negative charge, and if there are many clay particles in the porous medium, the electrostatic double layer will repel anions. Consequently, there is a region around each colloidal particle from which the anions are repelled, with the resulting distribution shown on Figure 4.1. As a first approximation we can assume there is a two-phase

distribution of the solute in the soil water. Within the exclusion volume the concentration is zero, with all of the solute thus being concentrated in the pore water outside of the exclusion volume (James and Rubin 1986). The volume of the exclusion zone is θ_{ex} .

The anion concentration in the pore water under conditions of anion exclusion is given by (Bresler 1973)

$$(\theta - \theta_{ex}) \frac{\partial C}{\partial t} = D_s \theta \frac{\partial^2 C}{\partial z^2} - q \frac{\partial C}{\partial z} \quad (4.49)$$

where C is the concentration of the solute in the bulk pore solution (that is, including the water in the exclusion zone).

The value of θ_{ex} can be found experimentally from a soil column test. Water with an initial concentration of a single anion of C_0 is introduced into a soil column that has a known water content. The water content is held constant, and sufficient solute of concentration C_0 is introduced so that the concentration of the water leaving the soil column, C_{out} , is equal to C_0 . The mass of the anion contained in the soil column is determined, and a concentration is calculated based on the total water content in the soil column, C_{calc} . This calculated concentration of anionic solution is less than C_{out} because water in the exclusion volume, which contains no anions, was used in the calculation. The value of the exclusion volume can be found from (Bond, Gardiner, and Smiles 1982):

$$\theta_{ex} = \theta \left[1 - \left(\frac{C_{calc}}{C_{out}} \right) \right] \quad (4.50)$$

In addition to decreasing the observed concentration of the anion in the soil column, anion exclusion causes the anions to travel faster than the average rate of moving pore water. The average rate of pore-water movement, v , is equal to the rate of the fluid flux, q , divided by the water content, θ . The anions cannot travel through the excluded part of the volumetric water content, which is close to the mineral surfaces and has a low or zero velocity. Therefore, they must move in the part of the pore water that is available to them—i.e., the center of the pores, where the fluid velocity is greater than average. As a result, excluded anions will travel further in a given period of time than they would in the absence of anion exclusion.

An approximate solution to Equation 4.49 for conditions of uniform water content and a steady flux of a dissolved anion of concentration C_0 into a semi-infinite soil column with an initial concentration of the dissolved anion, C_i is

$$\frac{C - C_i}{C_0 - C_i} = 0.5 \operatorname{erfc} \left\{ \frac{(\theta - \theta_{ex})z - qt}{2[(\theta - \theta_{ex})(D_s \theta t)]^{0.5}} \right\} \quad (4.51)$$

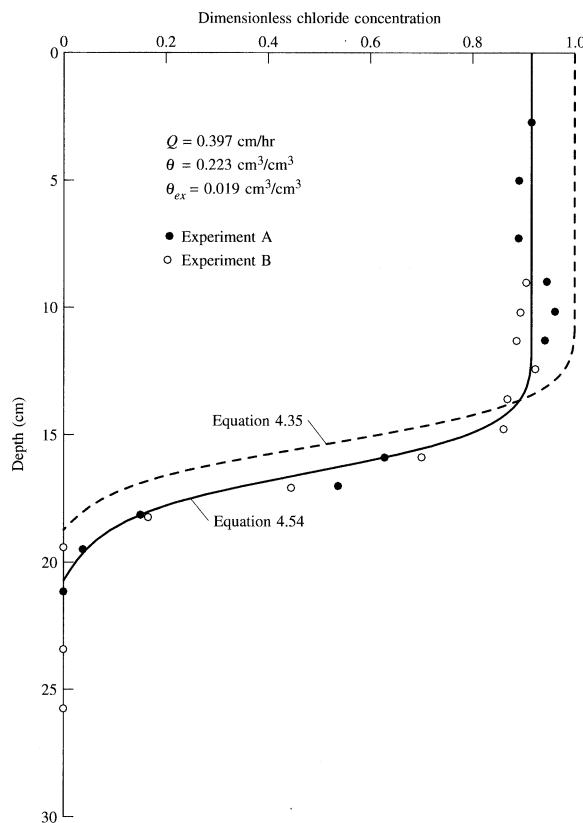
EXAMPLE PROBLEM

James and Rubin (1986) performed an experiment in which they measured the concentration profiles of chloride introduced into soil columns containing Delhi sand. The sand was 90% sand, 7% silt, and 3% clay by weight with a cation-exchange capacity of 0.05 mol/kg and an organic carbon content of 0.003 g of carbon per gram of soil. The soil column was constructed with a suction line on

the bottom to create a soil-water tension on the entire column. The soil columns were initially leached with a nitrate solution to remove any chloride. Water content (θ) was kept uniform throughout the soil column and the volumetric water flux (q) was numerically equal to the unsaturated hydraulic conductivity evaluated at θ . A solution containing chloride was introduced into the soil column at the same constant volumetric water flux established during the leaching phase. The soil columns were constructed as a series of sections either 1.14 cm or 2.28 cm long so that at the end of the injection phase they could be disassembled and the chloride mass and water content of each section could be measured.

Several experiments were conducted in which the water content ranged from 0.167 to 0.225 and the volumetric water fluxes ranged from 0.0393 cm/hr to 0.397 cm/hr. Figure 4.15 shows the results of experiments A and B, which had water contents of 0.221 and 0.225, respectively, while both had a water flux of 0.397 cm/hr. There are two curves on the figure, one computed using Equation 4.31 and one using Equation 4.51. Equation 4.32 is applied for a nonsorbing, nonreactive

FIGURE 4.15 Chloride concentration profiles in a soil column affected by anion exclusion.



Source: James and Rubin 1986.

solute. The chloride concentrations are shown as dimensionless chloride, that is C_{calc}/C_0 . No measured chloride values were equal to C_0 , illustrating the results of anion exclusion. The experimental results can be seen to follow closely the curve computed from Equation 4.51.

The excluded water content was computed from the experimental results at the top of the soil columns using Equation 4.50. It was found to be 0.019 for both saturated and unsaturated conditions. The dispersion coefficient was determined by solving Equation 4.49, with appropriate boundary conditions as

$$\operatorname{erfc}^{-1}\left[\frac{2(C - C_i)}{(C_0 - C_i)}\right] = \frac{(\theta - \theta_{\text{ex}})}{2\sqrt{(\theta - \theta_{\text{ex}})D_s t}} z - \frac{qt}{2\sqrt{(\theta - \theta_{\text{ex}})D_s \theta t}} \quad (4.52)$$

The left side of Equation 4.52 was plotted against the depth, z , and a straight line was determined by the method of least squares regression. The value of D_s was then calculated from the slope of the line. Inspection of Equation 4.52 shows that D_s is the only unknown. The curves on Figure 4.15 were calculated using the experimentally determined values of D_s .

Case Study: Relative Movement of Solute and Wetting Fronts

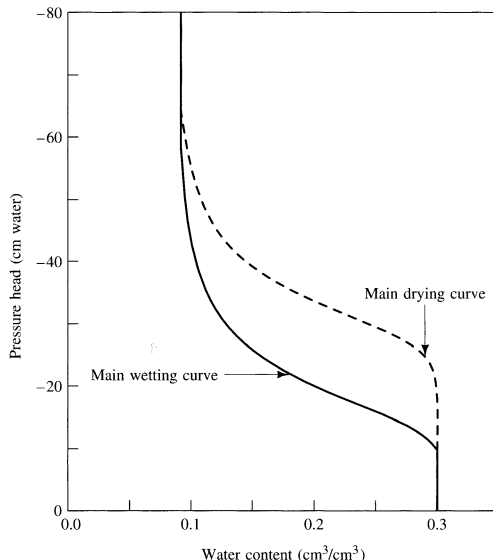
Pickens and Gillham (1980) studied the relative motion of the wetting front and the solute in an unsaturated soil column by use of a finite-element model. The model allows for the use of either nonhysteretic or hysteretic water-content-pressure-head relationships. Previous work (Gillham, Klute, and Heermann 1979) had shown that it was very important to include hysteresis in the model because the equation for computation of the pore-water velocity and the advection-dispersion equation contains a term for the water content.

The modeled soil column had a saturated hydraulic conductivity of 0.29 cm/min, a saturated water content of 0.301, and a longitudinal dispersivity of 0.5 cm. The initial soil moisture condition in the model had a linear pressure head variation between 0 at the bottom to -150 cm at the top of the soil column. The corresponding initial water-content values were obtained from a water-content-pressure-head hysteresis loop (Figure 4.16) and followed the main drainage curve, so that the model represented conditions that would develop if a saturated-soil column were drained. The soil column did not contain any solute prior to infiltration. A slug of water containing a solute at concentration C_0 was allowed to infiltrate at a rate of 0.17 cm/min for a 30-min period, resulting in a total depth of infiltration of 5 cm. The model computed the pressure head, water content, vertical pore-water velocity, relative solute concentration (C/C_0), and volumetric solute concentration ($\theta C/C_0$) after 30 min, 60 min, 300 min, and 5760 min. Figure 4.17 shows the results of the model study. At 5760 min the head distribution had returned to the pre-infiltration conditions, which indicates that equilibrium had been reached. Inspection of Figure 4.17 shows that although the water in the bottom of the soil column is above the irreducible water content at 5760 min, the solute has remained near the top of the soil column. This can occur because the water found at the bottom of the soil column was displaced downward from the top of the soil column by the infiltrating water containing the solute, which did not penetrate past the depth where $C/C_0 = 0$.

The model was run under three conditions. In the hysteretic mode the hysteretic relationship between water content and pressure head was used. As the slug of water infiltrated, the wetting relationships were used, followed by drying curves when the infiltrating slug

had passed. This model run is represented as a solid line on Figure 4.17. In the nonhysteretic wetting-curve mode, the pressure-head-water-content relation was based on the main wetting curve, and in the nonhysteretic drying-curve mode, it was based on the main drying curve. The results of these two modes are represented by circles and triangles, respectively. The importance of using the hysteretic mode appears to be greater for the pressure head and the water content than for the pore velocity and the solute front movement.

FIGURE 4.16 A water-content-pressure-head hysteresis loop used in a model study of solute infiltration in a soil column.



Source: Pickens and Gillham. 1980. Finite element analysis of solute transport under hysteretic unsaturated flow conditions. *Water Resources Research* 16:1071–1078. Copyright by the American Geophysical Union. Reproduced with permission.

Perhaps more importantly, tracking a wetting front does not necessarily directly correspond to the tracking rate at which solutes will migrate through the vadose zone as can be seen in Figure 4.17. This difference can become exacerbated when there are preferential flow paths and wetting front instabilities in non-homogeneous conditions.

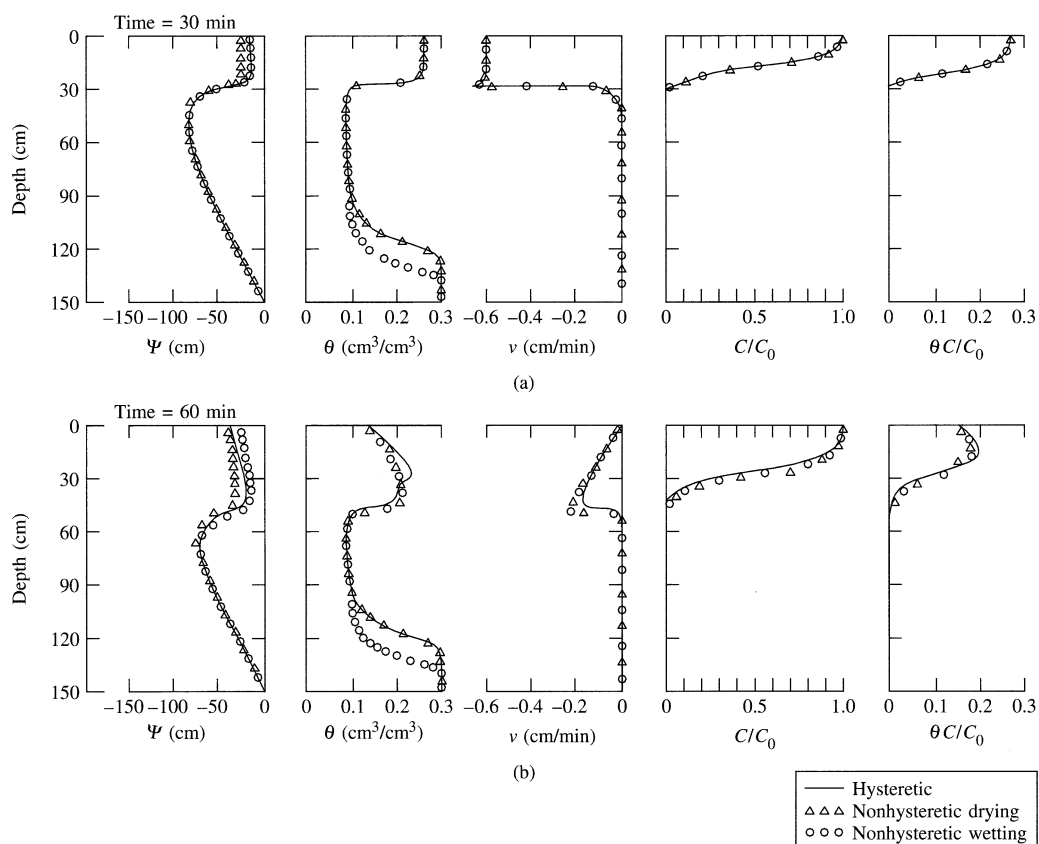
■ 4.11 Preferential Flowpaths in the Vadose Zone

The preceding analyses all treat the unsaturated zone as a homogeneous, porous medium. However, this is certainly not the case. In the root zone there are numerous large pores and cracks formed by such agents as plant roots, shrinkage cracks, and animal burrows. These **macropores** can form preferential pathways for the movement of water and solute, both vertically and horizontally through the root zone (Beven and Germann 1982). This situation can lead to “short-circuiting” of the infiltrating water as it moves through the macropores at a rate much greater than would be expected from the hydraulic conductivity of the soil matrix; see Figure 4.18(a).

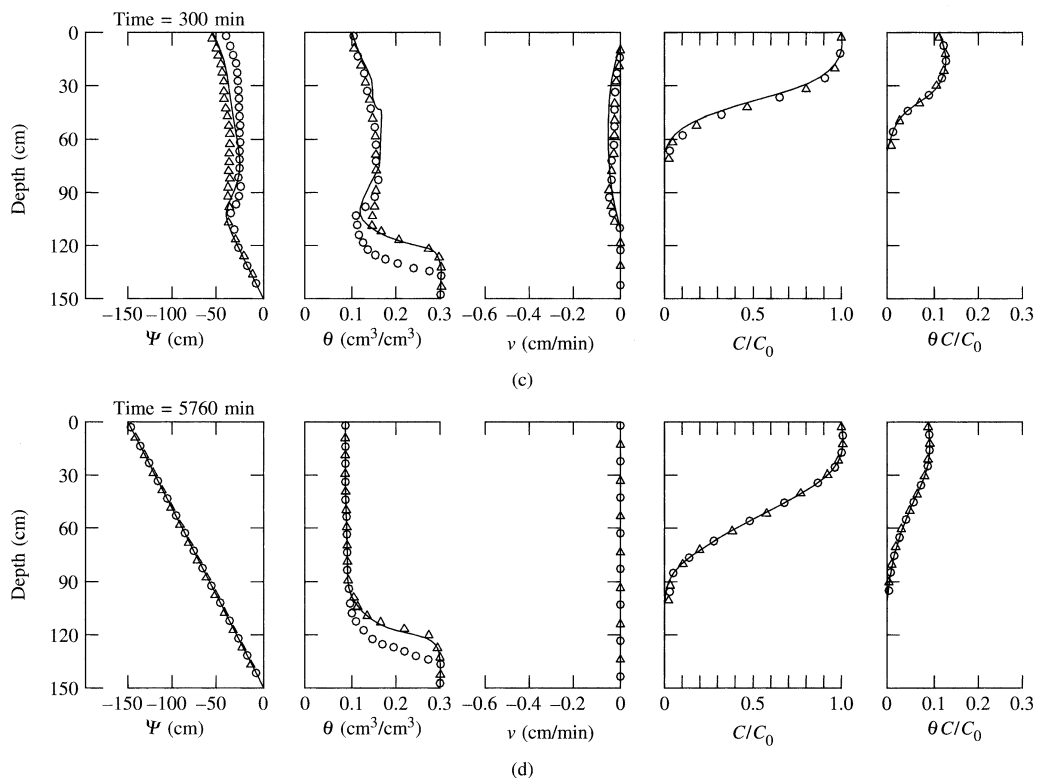
A second type of preferential flow is **fingering**, which occurs when a uniformly infiltrating solute front is split into downward-reaching “fingers” due to instability caused by pore-scale permeability variations. This is called wetting front instability, or Rayleigh-Taylor instability. Instability often occurs when an advancing wetting front reaches a boundary where a finer sediment overlies a coarser sediment, see Figure 4.18(b) (Hillel and Baker 1988).

A third type of preferential flow is **funneling** (Kung 1990b). Funneling occurs in the vadose zone below the root zone and is associated with stratified soil or sediment profiles. Sloping coarse-sand layers embedded in fine-sand layers can impede the downward infiltration of water. The sloping layer will collect the water like the sides of a funnel and direct the flow to the end of the layer, where it can again percolate vertically, but in a concentrated volume, as shown in Figure 4.18(c). Field studies using water containing dye placed in furrows indicate that the water is moving in the fine-sand layer above the discontinuity of the coarse-sand layer (Kung 1990a). These same dye studies

FIGURE 4.17 Model results of matric potential ψ , water content θ , pore-water velocity (v), relative solute concentration (C/C_0), and volumetric solute concentration ($\theta C/C_0$).



(Cont'd)

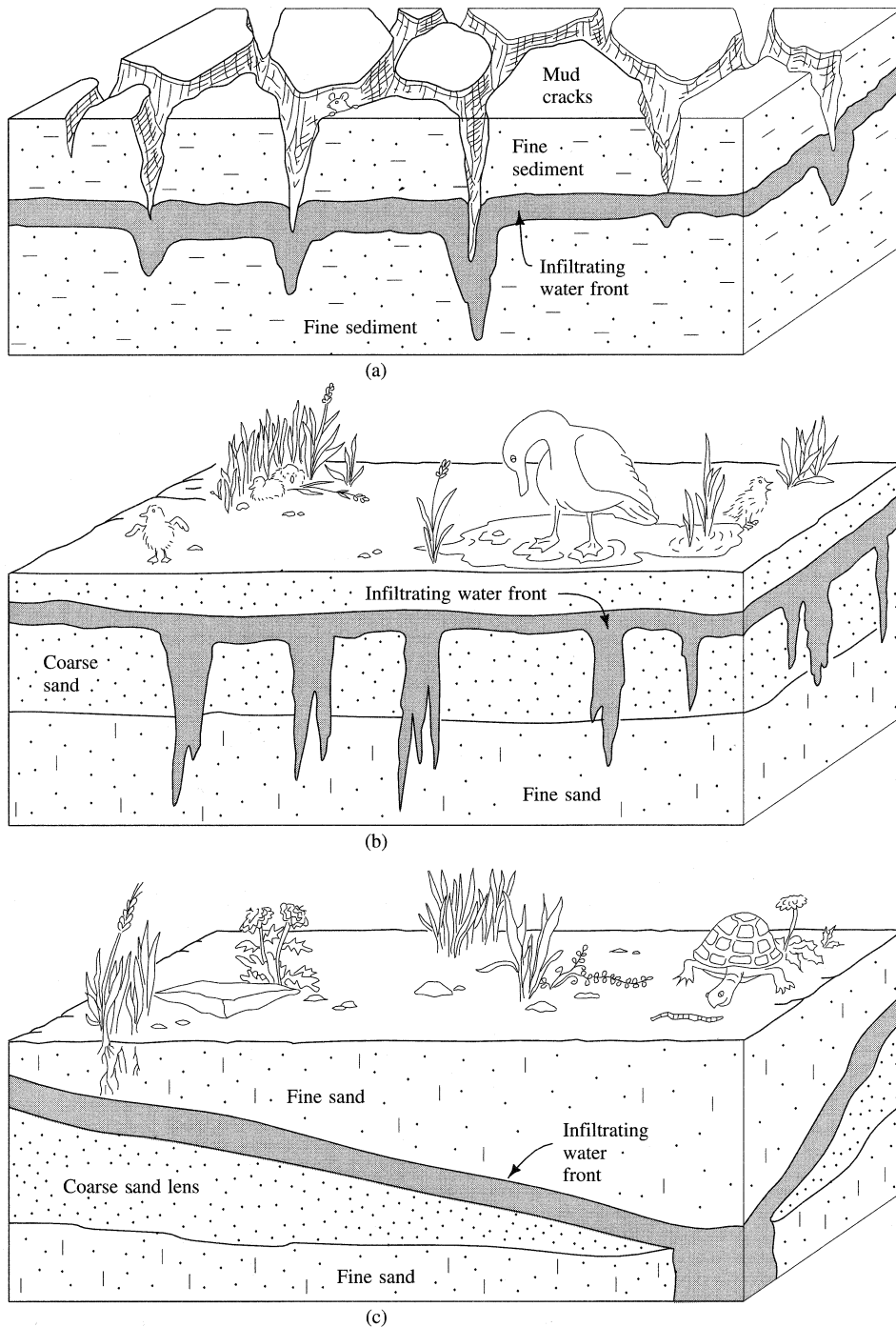
FIGURE 4.17 Cont'd

Source: Pickens and Gillham. 1980. Finite element analysis of solute transport under hysteretic unsaturated flow conditions. *Water Resources Research* 16:1071–1078. Copyright by the American Geophysical Union. Reproduced with permission.

Showed that because of funneling, the volume of the soil containing dye decreased with depth. The dyed soil region occupied about 50% of the soil volume at 1.5 to 2.0 m; from 3.0 to 3.5 m, it occupied only 10% of the soil volume, and by 5.6 to 6.6 m, it was found in about 1% of the soil volume. At this depth a single column of dyed soil was found, obviously formed by funneling of flow of dyed water from above (Kung 1990a).

These occurrences of preferential flow in particular and soil heterogeneity in general have disturbing implications for monitoring solute movement in the unsaturated zone. Some studies have recorded seemingly anomalous results, with deeper soil layers having greater concentrations of solute than more shallow layers (Kung 1990b). These anomalies can be explained by preferential flow patterns, with infiltrating solute being directed to certain regions of the vadose zone by short circuiting, fingering, and funneling. This suggests that a large number of sampling devices in the vadose zone might be needed if a reasonably accurate picture of the distribution of a contaminant is to be obtained. As contaminants reaching the water table may need to pass through the unsaturated zone, preferential flow paths in the unsaturated zone also have implications for groundwater monitoring. In the case of a contaminant that was evenly spread on

FIGURE 4.18 Preferential water movement in the vadose zone due to (a) short circuiting, (b) fingering, and (c) funneling.



the land surface—for example, an agricultural chemical—one would expect that there would be an evenly distributed solute load reaching the water table via the vadose zone. However, due to preferential flow paths the mass of solute may be concentrated in some locations, resulting in an uneven distribution in the shallow groundwater beneath the site. Monitoring wells beneath the site may show varying solute concentrations, depending upon how close they are to an up-gradient point of concentrated recharge.

■ 4.12 Vapor Phase Transport

It is recognized that volatile substances can change from a liquid phase to a gaseous phase, and that many of these compounds can also exist as dissolved species in water. The ability of gaseous compounds to transfer between several phases allows them many mechanisms and routes of movement unavailable to their nonvolatile counterparts. The migration of gaseous contaminants in unsaturated porous media is of concern for several reasons. In addition to the above ground hazards associated with venting gases, such as inhalation of harmful material and buildup of explosive gases in structures, there are many important considerations related to subsurface gaseous gas phase movement. Of particular importance is the ability of gaseous contaminants to migrate in directions which could be very different from that of liquid contaminants; the motion of gases is possible even in the opposite direction of an associated liquid phase. This has implications to the conceptualization of overall subsurface contaminant transport, to the representativeness of gaseous monitoring used to ascertain liquid pollutant movement, and to the complexity necessary in mathematical transport models.

Gases normally move from regions of high concentration or pressure to areas of low concentration or pressure. This means that gaseous movement can occur in a direction unrelated to, or even opposite to, nearby liquid flow. For example, in a vadose zone environment where rainwater and/or organic liquids could be fingering downward, immediately adjacent gases could be diffusing upward and venting at the ground surface. Another example would be gaseous diffusion horizontally above an underlying unconfined aquifer in which water flow is in some other direction. The ability of gases to move in ways contrary to liquid movement is an important distinction when considering the mobility of potential contaminants.

In the 19th century, Thomas Graham described the major mechanisms of vapor transport (Mason and Evans 1969). These basic categories still can be used to describe gaseous migration. These categories are: gaseous diffusion (also called Brownian movement), advection (also referred to as forced diffusion, laminar viscous flow, bulk flow, transpiration, and convection), and effusion (also called free molecule or Knudsen flow). These mechanisms are quite different physically and in their mathematical description, therefore modeling which considers vapor movement must make a clear distinction between the processes and identify which are dominant in any given site specific application.

4.12.1 Gaseous Diffusion

Diffusion is a process whereby elements in a single phase spatially equilibrate, and gaseous diffusion is particularly important as it is often 4 or 5 orders of magnitude faster than diffusion in liquids. This process arises from random molecular motions; each molecule is constantly undergoing collision with other molecules, and the result is constant

motion with many changes in direction and no preferred direction of motion. Although this motion is random, there is a net transfer of molecules of one compound from regions of high concentration to low concentration. The net transfer of molecules is predictable whereas the direction of any individual molecule at any moment is not. Gaseous diffusion is a spreading out or scattering of gases and may be divided into the categories of ordinary gaseous diffusion, particle diffusion (sorption), and thermal gaseous diffusion.

Ordinary gaseous diffusion is a process in which the components of any gas filled space will eventually become thoroughly mixed. Taylor and Ashcroft (1972) outline the rate potential of ordinary gaseous diffusion in the soil atmosphere, stating that no ordinary diffusion will take place if the density (concentration) of the diffusing substance is the same throughout a given region. Further, if the vapor density of the diffusing substance is different at different points, diffusion will take place from points of greater to lesser density, and will not cease until the density at all places is the same. Therefore it follows that ordinary gaseous diffusion of each gas component in the subsurface will occur whenever there is a difference in its concentration between (a) the soil and outer atmosphere, or (b) at points within the soil because of irregularities in the consumption or release of gases. The rate at which ordinary gaseous diffusion proceeds is governed, in part, by the magnitude of the concentration gradient at any point. In turn, the magnitude of the concentration gradient is dependent upon soil type, soil heterogeneity, and the amount of a vapor either generated by a source or lost by a sink. The interrelationships between these factors will govern the extent in which ordinary gaseous diffusion becomes a major mechanism for unsaturated zone vapor transport.

Ordinary gaseous diffusion is normally described by an equation written by Fick in 1855 after the principles described by Graham and in analogy with Fourier's Law for heat conduction. Fick's Law, as the equation has become known (see Chapter 2), when applied to gaseous diffusion in a porous medium, relates the diffusive flux to a concentration gradient over distance multiplied by an empirically derived coefficient called the effective diffusion coefficient. The magnitude of the effective diffusion coefficient is dependent on the properties of the porous media, (tortuosity, porosity, moisture content) and properties of the diffusing gas.

Fickian diffusion can be treated in a binary sense, that is, the diffusion of a gas (A) into another gas or mixture of gases (B). As gas A diffuses into gas B, B will diffuse into gas A equivalently, and in the opposite direction. Fick's second Law then, for transient state diffusion of one gas into another in one dimension is:

$$D_{AB} \frac{\partial^2 C}{\partial x^2} = \frac{\partial C}{\partial t} \quad (4.53)$$

where

C = the concentration of a gas, (mass/volume)

D_{AB} = the general diffusion coefficient, (length²/time)

x = distance (length), and

t = time

The general diffusion coefficient, D_{AB} , is an empirically-derived proportionality constant which relates the change in gaseous concentration with time to the divergence

of concentration with respect to distance. The above equation is written for diffusion of one gas into another, and does not account for effects of a porous medium. In most approaches to subsurface diffusion modeling, the general diffusion coefficient, D_{AB} , is modified to account for the influences of a porous media, and the general diffusion coefficient becomes what is called an effective diffusion coefficient, D' . For instance, Jury et al. (1983) estimated the effective diffusion coefficient by applying the Millington-Quirk tortuosity formula to diffusive flow to obtain the following relationship:

$$D' / D = \theta_D^{10/3} / (\theta_T^2) \quad (4.54)$$

where θ_D is the drained porosity (free pore space), and θ_T is the total porosity. There are many empirical formulae which can be used to estimate effective diffusion coefficient. These methods are based on a knowledge of the general diffusion coefficient, and normally this is determined by laboratory testing, or approximated by one of several different methods. For example, Slattery and Bird (1958), give one estimation method for non-polar compounds. Many researchers have described relationships between the general diffusion coefficient, D_{AB} , and the effective diffusion coefficient, D'_{AB} . A partial listing includes those by Hannon (1892), Buckingham (1904), Penman (1940), Blake and Page (1948), Taylor (1949), van Bavel (1951, 1952, and 1954), DeVries (1950, 1952), Marshall (1959), Millington (1959), Wessling (1962), Batterman et al. (1996), Scanlon et al. (2000), Molrup et al. (2005), Jassal (2005), Chau et al. (2005), and Cannavo et al (2006).

Particle diffusion refers to diffusion of ions to or from exchange sites on soil particles. Hellfereich (1962) states that the chemical potential for interactions between the gas molecules and a sorptive matrix depends on: (a) the generation of diffusion induced electrical forces, (b) the absorbent selectivity or preference for a particular gas, and (c) specific interactions such as Columbic forces, van der Waals forces, and hydrogen bonding.

The effects of sorption of components of a moving gas phase in a porous medium are not explicitly dealt with in the above equations. Obviously, two different sorbing gases which diffuse through the same porous medium would not exhibit the same relationship between effective and general diffusion coefficient. In order to develop an expression which relates gaseous diffusion to sorption, one can begin with Fick's second Law (Equation 4.53) and develop an equation which relates gaseous diffusion in air to gaseous diffusion in a three phase, including a sorbing porous medium. As Weeks et al. (1982) point out, the diffusion coefficient D is a constant analogous to hydraulic diffusivity (hydraulic conductivity divided by specific storage in flow through porous media) and thermal diffusivity (thermal conductivity divided by volumetric heat capacity). Therefore, the literature abounds with equations that can describe gaseous diffusion under a variety of boundary conditions (Carslaw and Jaeger, 1959; Crank, 1975). Many researchers have also explored the sorption and persistence of different gaseous contaminants onto soils of varying water content, organic content and mineralogy, for example, Houston and Kreamer (1989), Kim et al. (2001), Hamamoto et al. (2009), Provoost et al. (2011), and field gaseous tracer test observations have facilitated calculation of diffusion coefficients, tortuosity of porous media, and sorption, some by utilizing type-curve matching techniques on observed tracer breakthrough (Weeks et al. 1982; Kreamer et al. 1988; Kreamer 1988; Shcherbak and Robertson 2014).

Fick's second law can be generalized to describe gaseous diffusion into a partially saturated porous medium in one dimension (Weeks et al. 1982; Kreamer et al. 1988),

with an assumption of an immobile liquid phase that completely wets the solid phase and that rapid equilibrium occurs between the gas phase and the dissolved and sorbed concentration in the liquid and solid phases, as:

$$\tau \theta_D D \frac{\partial^2 C}{\partial x^2} = [\theta_D + \rho_w (\theta_T - \theta_D) K_w + \rho_s (1 - \theta_T) K_s] \frac{\partial C}{\partial t} + \omega \quad (4.55)$$

where:

τ = the tortuosity factor accounting for the added resistance to diffusion imposed by the structure of the porous medium (dimensionless),

θ_D and θ_T = the drained and total porosity respectively (dimensionless),

D = molecular diffusion of gas A into gas B under free air conditions (L^2/T),

ρ_w = density of water (M/L^3),

ρ_s = partial density of granular material making up solid matrix (i.e., grain density), (M/L^3),

C = concentration of the diffusing gas under consideration (M/L^3),

K_w = water-air distribution coefficient that describes the ratio of the concentration of the gas in solution to its concentration in the overlying air under equilibrium conditions, M/M of water/ M/L^3 of air, or $L^3/M, K_s = K_w K_D$ = gas-liquid-solid distribution coefficient that describes the ratio of the mass of the gas under consideration sorbed on the solid phase per unit mass of solid phase, M/M , to the concentration of the gas in the soil atmosphere, M/L^3 , (K_s therefore has units of L^3 gas/ M solid), and

K_D = solid-liquid distribution coefficient describing the ratio of the moles of solute under consideration sorbed on the solid phase per unit mass of solid to the concentration of the solute in the water (M/M solid $\div M/M$ water).

x = dimension in the direction of diffusion, L,

t = time, T, and

ω = a source or sink term.

In this treatment, the movement of the diffusing gas of interest through the liquid film prior to sorption on the solid phase is assumed to be essentially instantaneous with respect to the overall diffusion process. Houston and Kreamer (1989), Peterson et al. (1988), Steinberg et al. (1996) and others have shown for selected compounds that sorption decreases with increasing moisture content. This indicates that K_s is probably $\neq K_w K_D$ and that K_s should not be defined in terms of an equilibrium with the liquid phase, but as an equilibrium directly between the solid and gas phases as a function of moisture content. Equation 4.55 would then be rewritten:

$$\tau \theta_D D \frac{\partial^2 C}{\partial x^2} = [\theta_D + \rho_w (\theta_T - \theta_D) K_w + \rho_s (1 - \theta_T) K_{sf}] \frac{\partial C}{\partial t} + \omega \quad (4.56)$$

where K_{sf} is a gas-solid partitioning coefficient, which is the ratio of the moles of gas under consideration directly sorbed on the solid phase per unit mass of solid phase to the concentration of the gas in the soil atmosphere ($\text{L}^3 \text{ gas/M solid}$) at equilibrium as a function of moisture content.

K_w is often related to the reciprocal of the Henry's Law coefficient (Jury et al. 1983; Silka 1988). Both K_w (Thiboddeaux 1979) and K_{sf} (Kreamer et al. 1986) are temperature dependent, therefore isothermal conditions are often assumed in mathematical models. The assumption of rapid equilibrium is probably not bad for many compounds; for several compounds measured by Kreamer et al. (1988) virtually complete equilibrium was reached in one or two hours for a gas sorbing on a nonsaturated soil.

Rearrangement of Equation 4.56 yields:

$$\left[\frac{\tau \theta_D D}{\theta_D + \rho_w (\theta_T - \theta_D) K_w + \rho_s (1 - \theta_T) K_{sf}} \right] \frac{\partial^2 C}{\partial x^2} = \frac{\partial C}{\partial t} + \omega \quad (4.57)$$

In this form Fick's second law is generalized to describe gaseous diffusion into a partially saturated porous medium by replacing the diffusion coefficient D with an effective (apparent) diffusion coefficient D' :

$$D' \frac{\partial^2 C}{\partial x^2} = \frac{\partial C}{\partial t} \quad (4.58)$$

D' is a "lumped" parameter which has many subcomponents and is different for each different medium and diffusing gas. Therefore, in order to gain a better understanding of the physical significance of the subparameters of the effective diffusion coefficient, individual subparameters must be determined by other means. The denominator on the left-hand side of equation 4.57 can be considered a sorption term, referred to as the **sorption corrected porosity**.

Particle diffusion is significant when interactions between the exchange medium and diffusing gas are great. Often an equilibrium condition is attained, however, in which the contributions of gases to the particle site are matched by those returning to the gas phase. Particle diffusion, in such instances, makes insignificant contributions to the concentration gradient and, thus, has little influence on vapor densities.

Thermal gaseous diffusion occurs when a temperature gradient is established in a gaseous mixture and is particularly important in the presence of a heat generating subsurface waste, such as high-level nuclear material. The non-uniformity of temperature results in a concentration gradient as more dense molecules move down the temperature gradient while less dense molecules move in the direction of increasing temperature (Grew and Ibbs 1952). Thermal gradients in the vadose zone may be caused by heating of indoor facilities, radiant energy absorbed by surface pavement or structures, and geothermal sources, or by thermal remediation technologies (see Chapter 9). The greater the thermal gradient, the more effectively a gaseous mixture may be separated by this phenomena. Thermally induced diffusion is a slow process, however, and is not usually considered to contribute significantly to vapor transport in the absence of a heat generating waste.

4.12.2 Gaseous Advection

The advection of gases involves a transport process in which movement is in response to a pressure gradient. Unlike diffusion, advection occurs as bulk flow, i.e., any tendency that the mixture of gases has to migrate according to concentration gradient of its separate components is overwhelmed by its pressure response, and behaves as one gas. Whereas diffusion will produce varied movement of the individual component gases of a gaseous mixture, in advection, the entire gas mixture will move, retaining the same percentages of individual component gases as it is forced to regions of lower pressure.

Movement of gases in the unsaturated zone through advection is governed partly by the air permeability of the porous medium and partly by the pressure created by the gaseous source or sink. For example, a popular method for the cleanup of volatile compounds in the vadose zone utilizes extraction of soil vapors to induce gaseous advection and enhanced volatilization (see Chapter 9). As a general rule of thumb, the coefficient of permeability for air in the vadose zone usually is a minimum of approximately $1 \times 10^{-8}/\text{cm sec}$ (Bennedsen 1987) in order to utilize this soil vapor extraction (SVE) technique; otherwise gaseous advection would be too greatly inhibited to allow this method to be viable. In a more general sense, the subsurface pressure gradient can be affected by a number of other factors including: rising and falling water tables, barometric pressure changes, wind fluctuation, and rainfall percolation.

Analogous to the flow of water, laminar viscous flow of a fluid through a porous media is usually described by Darcy's Law. This empirical equation relates fluid flux to a pressure gradient over distance times a constant of proportionality called permeability which, in turn, is dependent on properties of the flowing fluid and the porous medium through which it flows. However, Klinkenberg (1941) pointed out that gases do not stick to the pore walls as required in Darcy's Law and that a phenomenon known as "slip" occurs. This gives rise to an apparent dependence of permeability on pressure, referred to commonly as the **Klinkenberg effect**, and often must be considered in mathematical descriptions of transient state advective flow.

If a heat generating source below the ground surface exists, thermal advection could become significant. Thermal advection is caused by a thermally induced pressure gradient. As temperature increases in unsaturated porous media, the resultant increase in molecular energies results in increased pressure exerted by the gaseous constituents. These heated gases then flow in an effort to reestablish pressure equilibrium. Kreamer (1988) observed an increase in rates of gaseous tracer movement when alluvial soils were heated at depth in simulation of buried, heat generating waste at the Nevada Test Site. Another important exception to the expected advection rates hinges on the idea that subsurface ventilation can be negligible "in the absence of any suitable air entry point at depth" (Currie 1971). It has been noted in regions of fractured hard rock with very deep water tables that holes drilled to great depths will seasonally advect gases and seemingly "breathe," with expulsion of gases from the ground normally in the winter months. This convection is likely related to the magnitude, frequency, continuity, and configuration of fractures, and the annual temperature variation. This factor obviously has important implications to waste repositories containing volatile compounds which are placed in deep, highly fractured media or Karst systems.

An analytical mathematical representation of advective flow of gases is normally extremely complex, because pressure driven movement is highly affected by

fluid compressibility. For equations of groundwater flow, water is usually assumed to be relatively incompressible, but this is not necessarily true for gases. Panton (1984) describes the relation of incompressible flow to **Mach number**, mathematically showing how low Mach numbers indicate incompressible flow. Mach numbers in nondimensional form contain variables which have been adjusted by the characteristic body length, which in porous media is related to pore size. Essentially, when all fluid velocities are small compared to the speed of sound, flow can be considered incompressible. In field situations, then, it is important to recognize how much density change accompanies a certain pressure change, and this can be facilitated by a determination of Mach number.

4.12.3 Effusion (Knudsen flow)

In porous media where pore spaces are extremely small, such as clays or competent rock devoid of significant, large secondary porosity, collisions between gas molecules can be ignored compared to collisions of molecule to the surrounding walls. If molecule-wall collisions dominate, the flux of molecules through any shape pore space is equal to the number of molecules entering the pore space times the probability that any one molecule will pass through and not be deflected back the way it entered. This forward flux is called effusion, free-molecule, or **Knudsen flow** and its mathematical description is different from diffusion or advection processes. Typically effusion can be a factor in fine grained material, yet is mostly ignored in models of contaminant migration.

4.12.4 Combinations of Vapor Transport Processes

The previously described vapor transport processes can and often do occur in combination. Effusion and advection in combination leads to the phenomenon, discovered experimentally in 1875 by Kundt and Warberg, known as “viscous slip.” Advection and diffusion processes occurring in concert were called “diffusive slip” when first discussed by Kramers and Kistemaker in 1943. A third combination, that of effusion and diffusion, was researched extensively in the early to mid-1940s in support of work on isotope separation. And, all three processes of diffusion, advection and effusion could be significant in a given field situation and could be described by yet another combination. This variability in types of transport processes points out the need to clearly understand gaseous migration in any field situation before accepting a mathematical representation of its migration in that situation.

4.12.5 Other Environmental Factors

Many other factors can affect gaseous transport in the unsaturated zone, including barometric effects, rising and falling water tables, evaporative effects, wind action, and the effect of rain water percolating downward through the unsaturated zone.

Buckingham (1904) and follow-up work by many scientists (including early work by Rommel 1922; Reist 1967; Weeks 1977) has indicated that barometric effects on soil gas transport are small under most conditions. Under conditions favorable to a large barometric effect, he showed gas velocities from diffusion to be 17 times greater than those created by large barometric fluctuations. Buckingham's work indicated that in a permeable soil column 3.05m (10 ft) deep, the calculated “rinsing” action of

atmospheric air penetrating into the soil would only be in the uppermost 3.05 to 5.59 mm (0.12 to 0.22 inch), dependent on the magnitude of the barometric change.

Regarding thermal convection it is difficult to estimate the significance of temperature effects on gas exchange in soils, unless there is a buried heating source. Rommel (1922) suggested that daily variations of temperature within a soil are responsible for less than 1/800 of the normal aeration. Temperature differences between soil and atmosphere were considered to be responsible for not more than 1/240 to 1/480 of the normal aeration. Thus it appears that temperature is a minor factor in soil aeration in the absence of buried heat-generating waste, proximal heated basements, or other temperature source or sink. However, the conditions which Reist (1967) noted might be significant for barometric pressure induced advection, (low porosity, high permeability) would concentrate the effect of any temperature related pressure difference into a few conduits, and therefore accentuate these differences and increase the possibility of flow. Work in fractured, welded tuff at the site of a potential nuclear waste repository in Nevada confirms this, particularly where there is a deep well drilled which can serve as a conduit between subterranean fractures and the atmosphere.

Convective movement in vadose zone gases can be set up by fluctuations in the elevation of the water table. In the case of an extremely shallow water table, the effect of fluctuations would be extremely pronounced. Proximity to actively pumping wells on variable schedules, or rivers of variable flow would be conditions were this sort of situation would be expected. For a mathematical representation which would account for changes in the water table, an additional convective term must be included in flow equations, along with a moving boundary condition and its associated mathematical complexity. For example, Weeks et al. (1982) add a convective term to equation 4.55 to account for water table fluctuations:

$$\tau \theta_D D \frac{\partial^2 C}{\partial x^2} - V \frac{\partial C}{\partial x} = [\theta_D + \rho_w (\theta_T - \theta_D) K_w + \rho_s (1 - \theta_T) K_s] \frac{\partial C}{\partial t} + \omega \quad (4.59)$$

where V is the velocity of water table decline and the other parameters are as previously defined. In this form, an assumption is made that the fluid is incompressible.

It is also possible that wind action could create pressure and suction in the uppermost soil and aid in exchange of soil-atmosphere gases. This gaseous penetration would be optimal in porous, coarse grained materials with high air permeability, no ground cover, compounded with conditions of high winds. However, Rommell (1922) concluded that wind action is not responsible for more than 1/1000 of the normal aeration of vegetated soils. Farrell et al. (1966) calculated that a wind speed of 24 km/hr (15 mph) could penetrate bare, mulched, coarse, soils up to only a few centimeters. Scotter et al. (1967) suggest that even if no mass transport occurs at the soil-air interface, wind induced pressure changes could produce some gas movement in the uppermost soil. Although it is unlikely that wind action would have any effect on the majority of subsurface gaseous movement, Reichmuth (1984) found that gasoline vapor, detected in a basement downgradient for an underground storage tank leak, worsened during period of high wind and low barometric pressure. He concluded that such conditions were optimal for maximum outgassing.

Percolating rainwater can affect a diffusing gas in several ways. Theoretically, tracer or contaminant gases could dissolve and be transported downward in the unsaturated

zone by percolating rainwater. Surface rainfall could also increase pressure on the gases in the vadose zone by air entrapment (Freeze and Cherry 1979). The latter occurs when an advancing wetting front traps air between itself and the water table. Lastly, the physical occlusion of pore space upon addition of moisture has a dramatic effect in reducing the transport of gases in the vadose zone. Heavy rain or snow cover could block normal venting of subsurface gases and exacerbate the thermal “chimney” effects of heated basements in winter. Rainfall can exchange soil and atmospheric gases (soil aeration) by the two processes of displacing soil gas and carrying dissolved gas in water. Rommel (1922) estimated that only 1/12 to 1/16 of normal soil aeration can be attributed to rainfall.

■ 4.13 Summary

The vadose zone extends from the land surface to the water table; moisture in the vadose zone is under tension. Soil particles can have charged surfaces, which can attract or repel anions and cations. Moisture moves through the vadose zone due to a potential that is the sum of the elevation potential and the matric potential. Matric potential is a function of the volumetric water content and depends upon whether the soil has previously undergone wetting or drying. The unsaturated hydraulic conductivity is also a function of the volumetric water content. The flux of moisture through the soil can be calculated from Darcy’s law or the Buckingham flux law. The nonsteady flow of soil moisture is described by the Richards’ equation. The nonsteady movement of soil vapor and soil moisture can also be described by a partial differential equation.

Solute movement through the vadose zone proceeds by both advection and diffusion. There is an advective-dispersive equation for solute transport in the vadose zone that accounts for retardation through sorption onto soil particles. Analytical solutions to this equation exist. Solute movement in the vadose zone is affected by regions of immobile water found in dead-end pores. It is also affected by an anion-exclusion zone when clays are present in the soil. Preferential pathways of solute movement may be present that create pathways for lateral movement of water in the vadose zone and concentrate infiltrating water into certain regions. Preferential pathways of water movement may make monitoring of the vadose zone and shallow water table difficult, and may change the rate at which percolating liquids travel vertically through the vadose zone.

Because vadose zone vapors move from high concentrations and pressure to low concentrations and pressure, contaminants in subsurface vapors can migrate in directions, magnitude, and speeds that are different from vadose zone liquid flow and underlying groundwater solutes. Gaseous movement can be affected by source strength and configuration, permeability, sorption, physical occlusion of pore space, and other environmental factors.

Chapter Notation

$A(z, t)$	Term defined by Equation 4.44	C^*	Solute phase bound to soil
$B(z, t)$	Term defined by Equation 4.45	C_i	Initial solute concentration in soil water
ρ_b	Bulk density of soil		
C	Solute concentration, or vapor concentration	C_{im}	Solute concentration in immobile water

C_m	Solute concentration in mobile water	v	Average linear soil moisture velocity
C_o	Solute concentration in injected water		(q/θ)
C_{calc}	Concentration of solute calculated in soil if the water in the anion exclusion zone is included	z	Elevation
D_v	Diffusion coefficient for water vapor	Z	Gravitational potential
D^*_s	Soil-diffusion coefficient, which is a function of θ	Z_o	Characteristic length or extent of the double layer
D	Gaseous diffusion coefficient	α	Van Genuchten soil parameter
D'	Effective gaseous diffusion coefficient	β	Mass transfer coefficient
D_s	Dispersion coefficient for soil moisture, which is a function of θ	ϵ	Dielectric constant
D_{sm}	Dispersion coefficient for mobile soil moisture	ζ	Empirical soil moisture dispersivity
e	Elementary charge of an ion	ζ_r	First-order rate coefficient
g	Acceleration of gravity	η	Consolidated first-order decay term
h	Pressure potential in units of length	η_l	First-order decay rate constant for liquid phase
J	Mass flux of solute	η_s	First-order decay rate constant for solid phase
K_B	Boltzman constant	θ	Volumetric water content
k	Intrinsic permeability	θ_s	Saturated pore volume at atmospheric pressure
$K(\theta)$	Unsaturated hydraulic conductivity, which is a function of θ	θ_r	Irreducible volumetric water content
$K_r(\theta)$	Relative permeability as a function of θ	θ_{ex}	Volume of excluded zone due to anion exclusion
K_d	Solid-liquid distribution coefficient	θ_m	Volumetric water content of mobile water
K_w	Air-water distribution coefficient	θ_{im}	Volumetric water content of immobile water
K_s	Gas-solid-liquid distribution coefficient	θ_T	Total Porosity
K_{sf}	Gas-solid distribution coefficient	θ_D	Air-filled porosity
m	Van Genuchten soil parameter	Λ	Brooks-Corey soil parameter
n	Van Genuchten soil parameter	μ_w	Dynamic viscosity of water
n_o	Concentration of ions in bulk solution	ξ	Consolidated zero order source term
P_c	Capillary pressure	ξ_l	Zero-order source term for liquid phase
q	Volumetric soil water flux (specific discharge)	ξ_s	Zero-order source term for solid phase
q_v	Vapor flux	ρ_v	Vapor concentration in vapor phase
u	Term defined by Equation 4.46	ρ_w	Density of water
R	Retardation factor	τ	Tortuosity factor of the porous medium
R_m	Retardation factor for mobile water	σ	Interfacial tension
R_{im}	Retardation factor for immobile water	γ	Various sources and sinks for solute
S	Slope	Φ_{EV}	Soil moisture potential in terms of energy per unit volume
S_p	Dimensionless slope	Φ_{EW}	Soil moisture potential in terms of energy per unit weight
S_w	Saturation ratio (θ/θ_s)	Φ_{EM}	Soil moisture potential in terms of energy per unit mass
T	Temperature in Kelvins	Ψ	Matric potential of soil
t	Time	ω	Source/ sink term
t_o	Time when pulse of injection of solute ceases		
V	Valence of ions in solution		

References

- Batterman, S., I. Padmanabham, and P. Milne. 1996. Effective gas-phase diffusion coefficients in soils at varying water content measured using a one-flow sorbent-based technique. *Environmental Science and Technology* 30:770–778.
- Bennedsen, M. B. 1987. Vacuum VOC's from soil. *Pollution Engineering* 19:66–69.
- Beven, K., and P. Germann. 1982. Macropores and water flow in soil. *Water Resources Research* 18:1311–1325.
- Blake, G. R., and J. B. Page. 1948. Direct measurement of gaseous diffusion in soils. *Soil Science Society of America Proceedings* 13:37–42.
- Boersma, L., et al. 1972. "Theoretical research." In *Soil Water*, eds. D. R. Nielsen, R. D. Jackson, J. W. Cary, and D. D. Evans, 21–63. Madison, WI: American Society of Agronomy, 175 pp.
- Bond, W. J., B. N. Gardiner, and D. E. Smiles. 1982. Constant flux adsorption of a tritiated calcium chloride solution by a clay soil with anion exclusion. *Soil Science Society of America Journal* 46:1133–1137.
- Bresler, E. 1973. Anion exclusion and coupling effects in nonsteady transport through unsaturated soils: 1. Theory. *Soil Science Society of America Proceedings* 37:663–669.
- Brooks, R. H., and A. T. Corey. 1966. Properties of porous media affecting fluid flow. *Proceedings, American Society of Civil Engineers, Irrigation and Drainage Division* 92:61–87.
- Buckingham, E. 1904. *Contribution to Our Knowledge of the Aeration of Soils*. Bulletin 25. Washington, DC: U.S. Department of Agriculture, Bureau of Soils, 52 pp.
- Buckingham, E. 1907. *Studies on the Movement of Soil Moisture*. Bulletin 38. Washington, DC: U.S. Department of Agriculture, Bureau of Soils, 61 pp.
- Cannava, P., F. Lafolie, B. Nicolardot, and P. Renault. 2006. Modeling seasonal variations in carbon dioxide and nitrous oxide in the vadose zone. *Vadose Zone Journal* 5:990–1004.
- Carsel, F. F., and R. S. Parrish. 1988. Developing joint probability distributions of soil water retention characteristics. *Water Resources Research* 24:755–769.
- Carslaw, H. S., and J. C. Jaeger. 1959. *Conduction of Heat in Solids*. New York: Oxford University Press, 510 pp.
- Chau, J. F., D. Or, and M. Sukop. 2005. Simulation of gaseous diffusion in partially saturated porous media under variable gravity with lattice Boltzmann methods. *Water Resources Research* 41:W08410.
- Coats, K. H., and B. D. Smith. 1964. Dead-end pore volume and dispersion in porous media. *Society of Petroleum Engineer Journal* 4:73–84.
- Constantz, J. 1982. Temperature dependence of unsaturated hydraulic conductivity of two soils. *Soil Science Society of America Journal* 46:466–470.
- Crank, J., 1975. *The Mathematics of Diffusion*. New York: Oxford University Press, 414 pp.
- Currie, J. A. 1971. Movement of gases in soil respiration. *SCI Monograph* 37:153–159.
- Dane, J. H., and A. Klute. 1977. Salt effects on the hydraulic properties of a swelling soil. *Soil Science Society of America Journal* 41:1043–1057.
- Davidson, J. M., D. R. Nielsen, and J. W. Biggar. 1966. The dependency of soil water uptake and release on the applied pressure increment. *Soil Science Society of America Proceedings* 30:298–304.
- Davis, D. D., R. Horton, J. L. Heitman, and T. Ren. 2009. Wettability and hysteresis effects on water sorption in relatively dry soil. *Soil Science Society of America Journal* 73:1947–1951.
- DeVries, D. A. 1950. Some remarks on gaseous diffusion in soils. *Transactions, 4th International Congress of Soil Science* 4:41–43.
- Farrell, D. A., E. L. Greacen, and C. G. Gurr. 1966. Vapor transfer in soil due to air turbulence. *Soil Science* 102:305–313.
- Fetter, C. W. 2001. *Applied Hydrogeology*, 4/E. Upper Saddle River, NJ: Prentice-Hall, 691 pp.
- Fick, A. 1855. On liquid diffusion. *Poggendorffs Annalen* 94:59.
- Freeze, R. A., and J. A. Cherry. 1979. *Groundwater*. Englewood, NJ: Prentice-Hall, 604 pp.
- Gillham, R. W., A. Klute, and D. F. Heermann. 1979. Measurement and numerical simulation of hysteretic flow in a heterogeneous porous medium. *Soil Science Society of America Journal* 43:1061–1067.

- Green, R. E., L. R. Ahuja, and S. K. Chong. 1986. "Hydraulic conductivity, diffusivity, and sorptivity of unsaturated soils: Field methods." In *Methods of Soil Analysis, 1. Physical and Mineralogical Methods, Second Edition*, ed. A. Klute. 1986. *Agronomy* 9:771–798.
- Grew, K. E., and T. L. Ibbs. 1952. *Thermal Diffusion in Gases*. Cambridge, UK: Cambridge University Press.
- Hamamoto, S., K. Seki, and T. Miyazaki. 2009. Effect of aggregate structure on VOC gas adsorption onto volcanic ash soil. *Journal of Hazardous Materials* 166:207–212.
- Hannen, F. 1892. Untersuchungen über den Einfluss der physikalischen Beschaffenheit des Bodens auf die Diffusion der Kohlensäure. *Forsh. Gebiete Agr.-Phys.* 15:6–25.
- Heinse, R and T. E. Link. 2013. Vadose zone processes: A compendium for teaching interdisciplinary modeling. *Journal of Contemporary Water Research & Education* 152:22–31.
- Helfferich, F. 1962. *Ion Exchange*. New York: McGraw-Hill, 624, pp.
- Hillel, D. 1980. *Fundamentals of Soil Physics*. New York: Academic Press, Inc., 413 pp.
- Hillel, D., and R. S. Baker. 1988. A descriptive theory of fingering during infiltration into layered soils. *Soil Science* 146:51–56.
- Houston, S. L., and D. K. Kremer. 1989. Effect of temperature on the potential for gaseous adsorption by partially saturated soils. *Proceedings of the Symposium on Engineering Geology and Geotechnical Engineering* 25:357–361.
- Ivanov, V. Y., S. Fatichi, G. D. Jenerette, J. F. Espeleta, P. A. Troch, and T. E. Huxman. 2010. Hysteresis of soil moisture spatial heterogeneity and the “homogenizing” effect of vegetation. *Water Resources Research* 46. DOI:10.1029/2009WR008611.
- Jackson, R. D. 1964. Water vapor diffusion in relatively dry soil: 1. Theoretical considerations and sorption experiments. *Soil Science Society of America Proceedings* 28:172–76.
- James, R. V., and J. Rubin. 1986. Transport of chloride ion in a water-unsaturated soil exhibiting anion exclusion. *Soil Science Society of America Journal* 50:1142–1150.
- Jassal, R., A. Black, M. Novak, K. Morgenstern, Z. Nesic, and D. Gaumont-Guay. 2005. Relationship between soil CO₂ concentrations and forest floor CO₂ effluxes. *Agricultural and Forest Meteorology* 130:176–192.
- Javandel, I., C. Doughty, and C. F. Tsang. 1984. *Groundwater Transport: Handbook of Mathematical Models*. Washington, DC: American Geophysical Union, 228 pp.
- Jury, W. A., W. F. Spencer, and W. J. Farmer. 1983. Behavior assessment model for trace organics in soils: I. model description. *Journal of Environmental Quality* 12:558–564.
- Kazimoglu, Y. K., J. R. McDougall, and I. C. Pyrah. 2005. Options for modeling hydraulic hysteresis. In *Unsaturated Soils*, eds. Mancuso and Tarantino. London: Taylor and Francis.
- Kim, H., M. D. Annable, and P. S. C. Rao. 2001. Gaseous transport of volatile organic chemicals in unsaturated porous media: Effect of water-partitioning and air/water interfacial adsorption. *Environmental Science and Technology* 35:4457–4462.
- Klinkenberg, L. J. 1941. "The permeability of porous media to liquids and gases." In *Drilling and Production Practice*, American Petroleum Institute Drilling Products Practices, 200–213.
- Klute, A., and C. Dirksen. 1986. "Hydraulic conductivity and diffusivity: Laboratory methods." In *Methods of Soil Analysis, 1. Physical and Mineralogical Methods, Second Edition*, ed. A. Klute. *Agronomy* 9(1):687–734.
- Kremer, D. K., S. L. Houston, and R. Marwig. 1986. Organic Hazardous Waste Project, Arizona State University Final Report to Reynolds Electrical and Engineering Company, #238-CUC-85, September 30.
- Kremer, D. K., E. P. Weeks, and G. M. Thompson. 1988. A Field Technique to Measure the Tortuosity and Sorption-Affected Porosity for Gaseous Diffusion of Materials in the Unsaturated Zone with Experimental Results from near Barnwell, South Carolina. *Water Resources Research* 24:331–341.
- Kremer, D. K. 1988. Monitoring Technology for Augered Shaft Waste Disposal—The Shallow Test Plot Experiments. Report for Reynolds Electrical and Engineering Company, Las Vegas, NV.
- . 1997. Determination of Pollutant Movement by Controlled Laboratory

- Experiments, SuDoc EP 1.89/2:600/S-97/004, U.S. Environmental Protection Agency Publication.
- Kung, K. J. S. 1990a. Preferential flow in a sandy vadose zone: 1. Field observation. *Geoderma* 46:51–58.
- . 1990b. Preferential flow in a sandy vadose zone: 2. Mechanism and implications. *Geoderma* 46:59–71.
- Marshall, T. J. 1959. The diffusion of gases through porous media. *Journal of Soil Science* 10:79–82.
- Mason, E. A., and R. B. Evans. 1969. Graham's laws: Simple demonstrations of gases in motion. Part I, Theory. *Journal of Chemical Education* 6:358–364.
- Millington, R. J. 1959. Gas diffusion in porous media. *Science* 130:100–102.
- Moldrup, P., T. Olesen, S. Yoshikawa, T. Komatsu, and D. E. Rolston. 2005. Predictive-descriptive models for gas and solute diffusion coefficients in variably saturated porous media coupled to pore-size distribution: I. Gas diffusivity in repacked soil. *Soil Science* 170:843–853.
- Nkedi-Kizza, P., J. W. Biggar, M. Th. van Genuchten, P. J. Wierenga, H. M. Selim, J. M. Davidson, and D. R. Nielsen. 1983. Modeling tritium and chloride-36 transport through an aggregated oxisol. *Water Resources Research* 19:691–700.
- Nielsen, D. R., M. Th. van Genuchten, and J. W. Biggar. 1986. Water flow and solute transport processes in the unsaturated zone. *Water Resources Research* 22:89S–108S.
- Panton, R. L. 1984. *Incompressible Flow*. New York: Wiley-Interscience, 780 pp.
- Penman, H. L. 1940. Gas and vapor movements in the soil: 1. The diffusion of vapors through porous solids. *Journal of Agriculture Science* 30:437–462.
- Peterson, M. S., L. W. Lion, and C. A. Shoemaker. 1988. Influence of vapor phase sorption and diffusion on the fate of trichloroethylene in an unsaturated aquifer system. *Environmental Science and Technology* 22:571–577.
- Pickens, J. F., and R. W. Gillham. 1980. Finite element analysis of solute transport under hysteretic unsaturated flow conditions. *Water Resources Research* 16:1071–1078.
- Provost, J., R. Ottoy, L. Reijnders, J. Bronders, I. Van Keer, F. Swartjes, D. Wilczek, and D. Poelmans. 2011. Henry's equilibrium partitioning between groundwater and soil air: Predictions versus observations. *Journal of Environmental Protection* 2:873–881.
- Richards, L. A. 1928. The usefulness of capillary potential to soil-moisture and plant investigators. *Journal of Agricultural Research* 37:719–742.
- . 1931. Capillary conduction of liquids through porous mediums. *Physics* 1:318–333.
- Reichmuth, D. R. 1984. *Subsurface Gasoline Migration Perpendicular to Ground Water Gradients—A Case Study*. Available from <https://info.ngwa.org/GWOL/pdf/850134610.PDF>
- Reist, P. C. 1967. The Disposal of Radioactive Krypton-85 in Porous Media, Ph.D. Thesis. Boston, MA: Harvard University.
- Rommell, L. G. 1922. Luftvaxlingen i marken som ekologisk faktor. Medd. Statens Skogsforsoksanstalt 19, no. 2.
- Scanlon, B. R., J. P. Nicot, and J. W. Massmann. 2000. Soil gas movement in unsaturated systems. In *Handbook of Soil Science*, ed. M. E. Sumner, p. A277–A319.
- Scotter, D. R., G. W. Thurtell, and P. A. C. Raata. 1967. Dispersion resulting from sinusoidal gas flow in porous materials. *Soil Science* 104:306–308.
- Shcherbak, I., and G. P. Robertson. 2014. Determining the diffusivity of nitrous oxide in soil using in situ tracers. *Soil Science Society of America Journal* 78:79–88.
- Silka, L. R. 1988. Simulation of vapor transport through the unsaturated zone. *Groundwater Monitoring Review* 8:115–124.
- Slattery, J. C., and R. B. Bird. 1958. Calculation of diffusion coefficient of dilute gases and of the self-diffusion coefficient of dense gases. *American Institute of Chemical Engineering Journal* 4:137–142.
- Sposito, G. 1986. The physics of soil water physics. *Water Resources Research* 22:83S–88S.
- Suarez, D. L. 1985. Chemical effects on infiltration. In *Proceedings National Resources Modeling Symposium*, ed. D. G. DeCoursey, 416–419. Washington, DC: U. S. Department of Agriculture, Agricultural Research Service.
- Suarez, D. L., J. D. Rhoades, R. Lavado, and C. M. Grieve. 1984. Effect of pH on

- saturated hydraulic conductivity and soil dispersion. *Soil Science Society of America Journal* 48:50–55.
- Taylor, S. A. 1949. Oxygen diffusion in porous media as a measure of soil aeration. *Soil Science Society of America Proceedings* 14:55–61.
- Taylor, A. T., and G. L. Ashcroft. 1972. *Physical Edaphology*. San Francisco: W. H. Freeman and Co.
- Thiboddeaux, L. J. 1979. *Chemodynamics: Environmental Movement of Chemicals in Air, Water and Soil*. New York: John Wiley and Sons, 501 pp.
- Tindall, J. A., J. R. Kunkel, and D. E. Anderson. 1999. *Unsaturated Zone Hydrology for Scientists and Engineers*. Upper Saddle River, NJ: Prentice Hall.
- University of California, Davis. 2015. Vadose Zone Modeling: Web-Links. Accessed October 2015 from http://groundwater.ucdavis.edu/Materials/Vadose_Zone_Modeling_Web-Links/
- van Bavel, C. H. M. 1951. A soil aeration theory based on diffusion. *Soil Science* 72:33–46.
- . 1952. Gaseous diffusion in porous media. *Soil Science* 73:91–104.
- . 1954. Simple diffusion well for measuring soil specific diffusion impedance and soil air composition. *Soil Science Society of America Proceedings* 18:229–234.
- Van Genuchten, M. Th. 1980. A closed-form equation for predicting the hydraulic conductivity of unsaturated soils. *Soil Science Society of America Journal* 44:892–898.
- . 1981. Analytical solutions for chemical transport with simultaneous adsorption, zero-order production, and first order decay. *Journal of Hydrology* 49:213–233.
- Van Genuchten, M. Th., J. M. Davidson, and P. J. Wierenga. 1974. An evaluation of kinetic and equilibrium equations for the prediction of pesticide movement in porous soils. *Soil Science Society of America Proceedings* 38:29–35.
- Van Genuchten, M. Th., F. Kaveh, W. B. Russell, and S. R. Yates. 1988. “Direct and indirect methods of estimating the hydraulic properties of unsaturated soils.” In *Land Qualities in Space and Time*, ed. J. Bouma and A. K. Bregt, 61–72. Wageningen, The Netherlands: International Society of Soil Science.
- Van Genuchten, M. Th., and P. J. Wierenga. 1976. Mass transfer studies in sorbing porous media, I, Analytical solutions. *Soil Science Society of America Journal* 40:473–480.
- Weeks, E. P. 1977. *Field Determination of Vertical Permeability to Air in the Unsaturated Zone*. U.S. Geological Survey Professional Paper 1051, 41 pp.
- Weeks, E. P., D. E. Earp, and G.M. Thompson. 1982. Use of atmospheric fluorocarbons F-11 and F-12 to determine the diffusion parameters of the unsaturated zone in the southern high-plains of Texas. *Water Resources Research* 18:1365–1378.
- Wessling, J. 1962. Some solutions of the steady-state diffusion of carbon dioxide through soils. *Netherlands Journal of Agricultural Science* 10:109–117.
- Wilson, L. G., L. G. Everett, and S. J. Cullen, eds. 1994. *Handbook of Vadose Zone Characterization & Monitoring*. Boca Raton, FL: CRC Press, 752 pp.
- Witkowska-Walczak, B. 2006. Hysteresis between wetting and drying processes as affected by soil aggregate size. *International Agrophysics* 20:359–365.

Problems

- 4.1** Using table 4.1, and equations 4.9 and 4.10, calculate the volumetric water content, θ , for silt at different metric potential values, ψ , ranging from 0 to -15,000 cm. Plot the resulting soil water retention curve.
- 4.2** Using table 4.1 and equations 4.9 and 4.10, calculate the volumetric water content, θ , as a function of the metric potential, ψ , for a soil texture assigned by your instructor. Plot the resulting soil water retention curve.

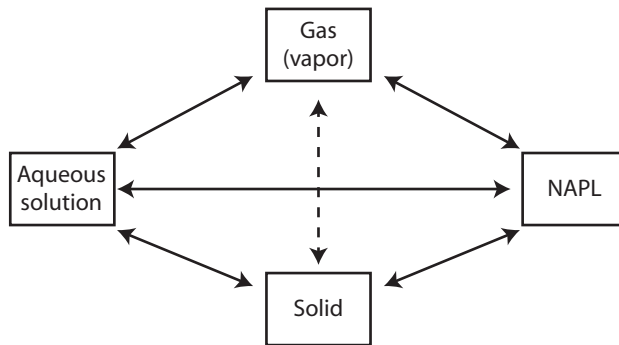
Multiphase Flow

■ 5.1 Introduction

The movement of liquids that are immiscible with water through the vadose zone as well as below the water table is an important facet of contaminant hydrogeology. Such liquids are often called **nonaqueous phase liquids**. They may have densities that are greater than water (dense nonaqueous phase liquids, or **DNAPLs**), densities that are less than water (light nonaqueous phase liquids, or **LNAPLs**), or mixtures with a combined density close to that of water (neutral non aqueous phase liquids, or **NNAPLs**). They may be partially soluble in water, so that a dissolved phase as well as a nonaqueous phase may be present (Schwille 1981; 1984; 1988; Newell et al. 1995). Two-phase flow may occur below the water table with water and a DNAPL (McWhorter and Sunada 1990; Huling and Weaver 1991). Three-phase flow may occur in the vadose zone with air, water, and an NAPL (Abriola and Pinder 1985a; 1985b; Mayer and Hassanzadeh 2005; Pinder and Gray 2008). In the vadose zone the NAPL may partition into the air as a vapor phase (Baehr 1987; Tillman and Weaver 2005). There may be multiple compounds in the nonaqueous phase, each with different properties (Corapcioglu et al. 1987; Pankow and Cherry 1996). Flow is dependent upon the densities, viscosities, and interfacial tensions of the liquids. In addition to dispersion and diffusion, compounds can undergo adsorption and chemical and biological degradation. These processes pose extremely complex hydrogeological challenges and sophisticated models have been developed, such as T2VOC (Falta et al. 1995), HSSM (U.S. EPA 1997), UTCHEM (Pope et al. 1999) or the NAPL Simulator (U.S. EPA 1997; 2010), to simulate NAPL transport and fate.

The basic theory of nonaqueous phase liquid transport has been worked out by petroleum reservoir engineers, who are concerned with the movement of petroleum through reservoirs that also contain water (e.g., Buckley and Leverett 1942). This theory has been extended to the vadose zone, since most nonaqueous phase liquid problems start with a spill or leak that creates a release above the water table. In addition, soil-moisture flow in the vadose zone may be viewed as a subset of multiphase flow (see Chapter 4).

Common LNAPLs include gasoline and diesel fuel, both of which are a mixture of many compounds. DNAPLs include the chlorinated hydrocarbons, such as tetrachloroethylene (PCE), trichloroethylene (TCE) and 1,1,1-trichlorethane (TCA), as well as coal tar, which again is a mixture of many compounds. NNAPLs are not discussed at

Figure 5.1 Partitioning processes in a multi-phase system.

length in the literature, but nonaqueous phase liquids with specific gravities close to 1 (near that of water) will often not clearly act as a LNAPL or DNAPL, particularly in the presence of changing water density due to temperature fluctuations or varying salt content. For example creosote has a specific gravity of approximately 1.07 and while it is slightly denser than water, in brine environments with denser water quickly approach NNAPL properties. Some industrial applications involve solutions of DNAPLs in mineral oils; the resulting solution is an LNAPL, even though the pure formulation of the compound of concern might be more dense than water. For example wood preservatives are sometimes formulated by dissolving pentachlorophenol in a carrier oil. Although pentachlorophenol has a specific gravity of 1.978, the commercial solution is less dense than water.

■ 5.2 Basic Concepts

5.2.1 Saturation Ratio

The **saturation ratio** of a fluid is the fraction of the total pore space filled with that liquid. The total of the saturation ratios for all the fluids present, including air, add up to 1.0. Saturation ratio can also be expressed as a percent saturation.

$$S_r = \frac{\text{Volume of NAPL}}{\text{Volume of Voids}} = \frac{\theta_{\text{NAPL}}}{n} = \frac{\text{Vol}_{\text{NAPL}}}{\text{Vol}_{\text{Total}} n}$$

The **residual saturation**, S_r , is the saturation at which NAPL becomes discontinuous and is immobilized by capillary forces and NAPL will not migrate due to convection or gravity (Mercer and Cohen 1990). The values of S_r vary from approximately 1% for gasoline in highly permeable media, such as coarse gravel and sand, to as much as 20% for heavy oil. Residual saturation values have also been reported to range from 10% to 50% of the total pore space (Huling and Weaver 1991). The magnitude of residual saturation is affected by hydraulic gradients and flow rates, pore-size distribution, wetting properties of the fluids and soil solids, interfacial tension, ratios of fluid viscosities and densities, gravity, buoyancy forces and others. Values for S_r for a number of

NAPL compounds and mixtures as function of soil types are provided in Mercer and Cohen (1990) or Brost and DeVaul (2000).

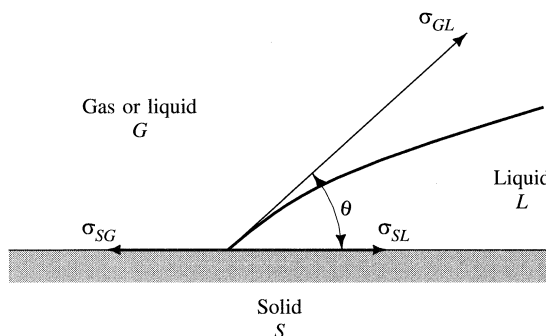
5.2.2 Interfacial Tension and Wettability

A liquid in contact with another substance, which can be a solid, an immiscible liquid, or gas, possesses interfacial energy. This energy is the result of the difference in the degree of attraction for the molecules of the substance at the liquid surface to each other compared with their degree of attraction for molecules of the other substance. This phenomenon is called **interfacial tension**. It is defined as the amount of work necessary to separate a unit area of one substance from another. Units are dynes per centimeter. The interfacial tension between substances i and j is designated as σ_{ij} .

Figure 5.2 shows the interfacial tension between two liquids, G and L , and a solid surface. The interface angle between the two liquids is indicated by θ . Equation 5.1 gives the relationship between θ and the interface tensions for the three interfaces: liquid G /solid, liquid L /solid, and liquid G /liquid L .

$$\cos \theta = \frac{\sigma_{SG} - \sigma_{SL}}{\sigma_{GL}} \quad (5.1)$$

Figure 5.2 Interfacial tensions between a solid surface, a wetting liquid phase, L , and a nonwetting gas or liquid phase, G .



By convention, θ is measured through the denser fluid. In general, one or the other of the fluids will preferentially spread over, or wet, the entire solid surface. If θ is less than 90° , then liquid L will preferentially wet the surface. If θ is more than 90° , then liquid G will preferentially wet the surface. That is, if we have two liquids competing for a surface, one dominates and coats the solid surface. In oil-water systems, water tends to preferentially wet the surface as many soils are hydrophilic. However, if the surface is dry and first becomes coated with oil, then the system is oil-wet, as the water does not come into contact with the surface. An automobile that has been waxed is an example of an oil-wet surface. Water will form beads and flow in rivulets rather than move uniformly over the surface, as it does for an unwaxed car.

Aquifers are naturally water-wet because they contain water before any NAPLs are discharged to them. The vadose zone may be either water-wet or oil-wet, depending

upon whether the soil is moist or dry when the oil is discharged. However, even soil in the vadose zone that appears to be dry will have water held to it by capillary pressures. At very low water content, water forms **pendular rings** around the grain contact points, with a thin film of water coating the rest of the grains. This water cannot flow, but it still coats the mineral grains, making the vadose zone water-wet.

5.2.3 Capillary Pressure

If two immiscible liquids are in contact, a curved surface will tend to develop at the interface. By measuring the pore pressure near the interface in each phase, one will find that the pressures are not the same. The difference is the **capillary pressure**.

In the vadose zone capillary pressure has a negative value. We can also refer to capillary pressure as a tension, in which case it would have a positive value. If P_w is the pressure of the wetting fluid and P_{nw} is the pressure of the nonwetting fluid, then P_c , the capillary pressure, is found from Equation 5.2.

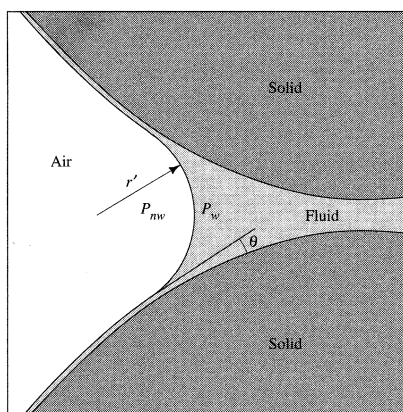
$$P_c = P_w - P_{nw} \quad (5.2)$$

Figure 5.2 shows the radius of curvature, r' , for a spherical air-water interface. Equation 5.3 gives the relationship between the capillary pressure, P_c , the interfacial tension, σ , and the radius of curvature.

$$P_c = -\frac{2\sigma}{r'} \quad (5.3)$$

Capillary pressure is directly proportional to the interfacial tension and inversely proportional to the radius of curvature. The radius of curvature is dependent upon the pore size and the amount of each fluid present. This means that the capillary pressure is a function of the properties of the two immiscible liquids present and is different for differing proportions of water and NAPL in the same porous media. Further, P_c is a property of the macroscopic geometry of the void spaces in the porous media, which cannot easily be described mathematically.

Figure 5.3 Radius of curvature for a spherical capillary interface.

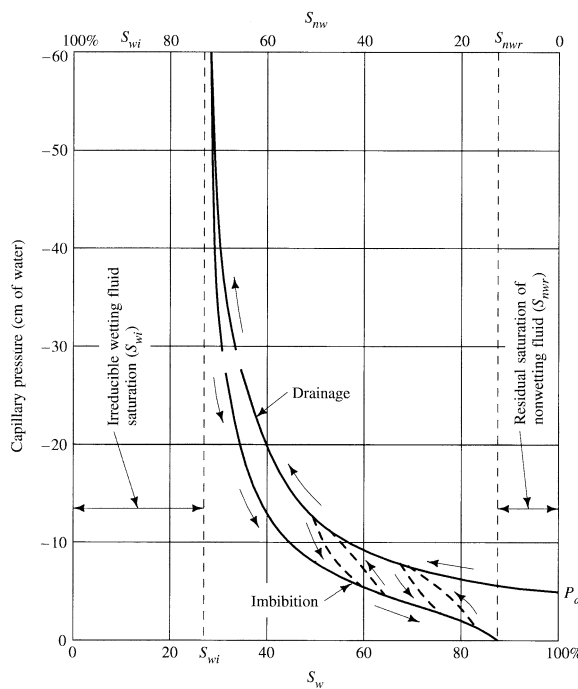


If we wish to know the capillary pressure in a real porous media, we must consider an analogous medium with known geometry. For example, we could consider the real porous media to be similar to a bundle of thin glass tubes of radius r . The capillary pressure in a thin tube, P_t , can be determined from Equation 5.4:

$$P_t = -\left(\frac{2\sigma}{r}\right)\cos\theta \quad (5.4)$$

For a given porous medium the relationship of the capillary pressure to the saturation ratio can be determined experimentally in the laboratory. Figure 5.4 shows capillary pressure curves. If the porous medium starts off saturated with the wetting fluid and the wetting fluid is slowly displaced by a nonwetting fluid, thus reducing the wetting-fluid saturation ratio, S_w , the result is a **drainage**, or **drying**, **curve**. As the wetting-fluid saturation ratio drops, the capillary pressure will become more negative. Eventually no more wetting fluid will be displaced by the nonwetting fluid, even with further decreases in capillary pressure. This saturation value is known as the **irreducible wetting-fluid saturation**, S_{wi} , also known as **residual wetting saturation**. Next, we will displace the nonwetting fluid by forcing the wetting fluid into the sample. The result is called an **imbibition**, or **wetting**, **curve**. Notice on Figure 5.4 that the imbibition curve does not follow the same pathway as the drainage curve. Recall that this phenomenon is called **hysteresis**. There is no unique relationship between capillary pressure and saturation ratio; the relationship depends upon which fluid is being

Figure 5.4 Capillary-pressure-wetting-fluid saturation curves for two-phase flow.

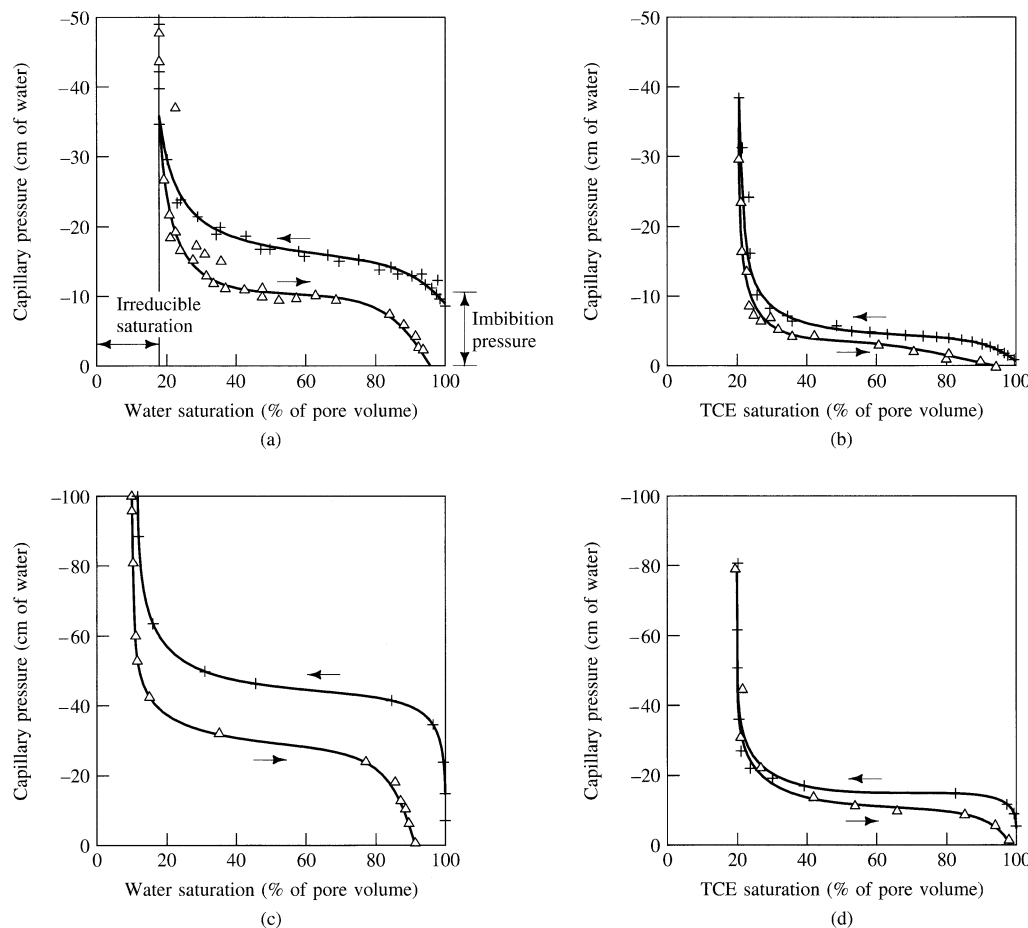


displaced. When the imbibition curve reaches zero capillary pressure, some of the nonwetting fluid will remain in the porous media. This saturation value is known as the **irreducible, or residual, nonwetting fluid saturation**, S_{nw} .

Notice that on Figure 5.4 the drainage curve starts off at a wetting fluid saturation ratio of 1.0 with a nonzero capillary pressure, P_d . This is the **threshold value**, also called the **displacement, imbibition, bubbling pressure, or air-entry value**. In order for the nonwetting fluid to start to displace the wetting fluid, this pressure must be exceeded.

Figure 5.5(a) shows an experimentally derived capillary-pressure curve for air and water in a medium sand. Figure 5.5(b) shows a capillary-pressure curve for air and TCE in the same medium sand. Figure 5.5(c) contains an air and water capillary-pressure curve for fine sand and Figure 5.5(d) shows an air and TCE curve for the

FIGURE 5.5 Experimentally derived capillary-pressure–wetting-fluid saturation curves for (a) air and water in medium sand, (b) air and trichloroethylene (TCE) in medium sand, (c) air and water in fine sand, and (d) trichloroethylene and air in fine sand.



same fine sand (Lin et al. 1982). These diagrams illustrate that the capillary-pressure relationships are unique for a given porous media and depend as well on the specific immiscible fluid.

5.2.4 Relative Permeability

During simultaneous flow of two immiscible fluids, part of the available pore space will be filled with one fluid and the remainder will be filled with the other fluid. Figure 5.6 shows possible fluid-saturation states for water and oil with differing ratios of each and for both water-wet and oil-wet circumstances.

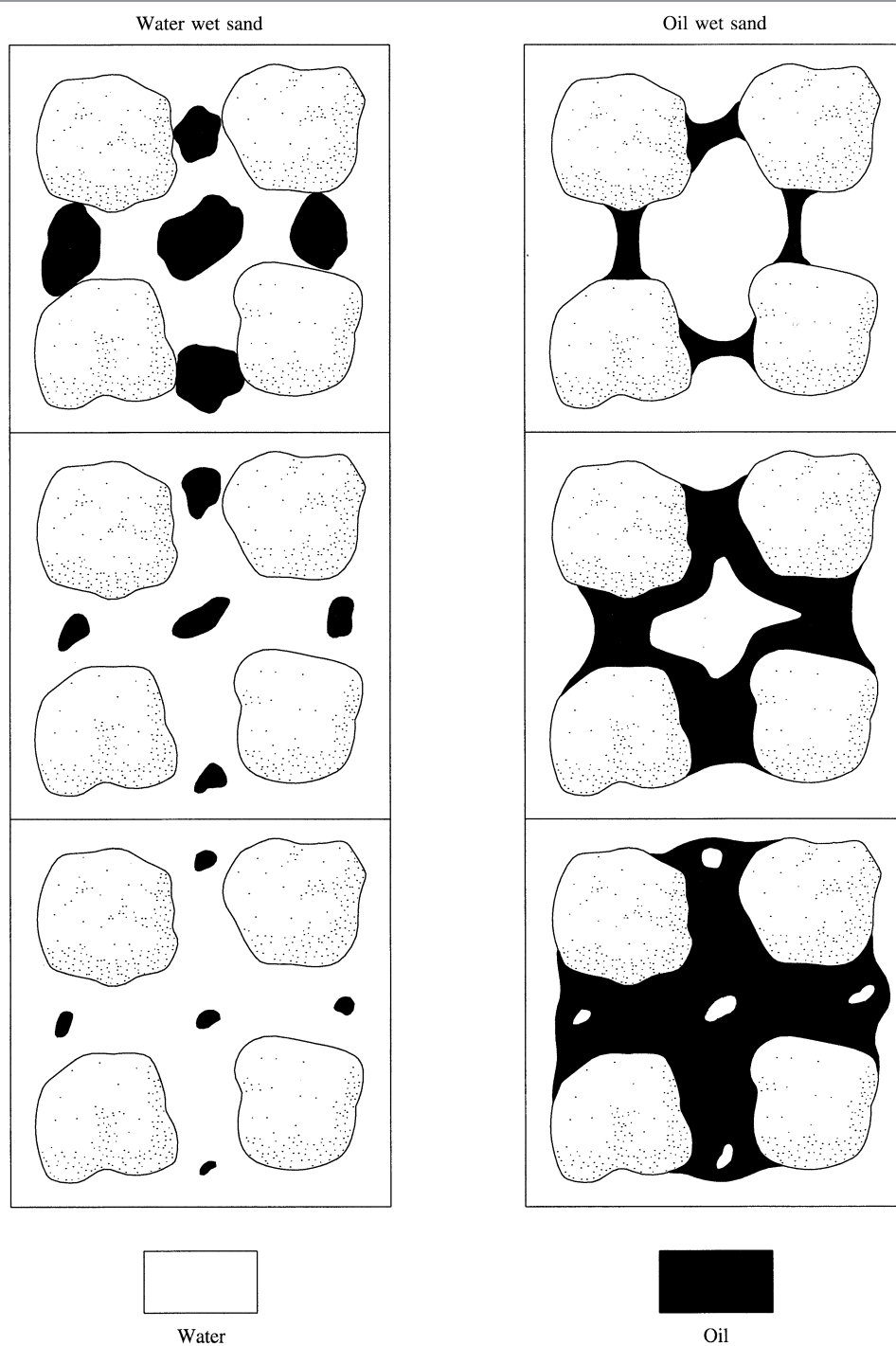
At residual saturation, NAPL is trapped in the pore space in isolated ganglia or blobs (Schnoor 1996). Besides being a function of the NAPL's fluid properties, the dissolution rate of entrapped, NAPL blobs is highly dependent on the range and size of the residual blobs (Powers et al. 1994), i.e., larger blobs dissolve less quickly than smaller ones. Also, blobs elongated in the direction of water flow are more easily mobilized than shorter ones (Allen, Cohen, and Kaplan 1989). The blobs can be bypassed by the groundwater or might snap-off into smaller blobs if the flow of the displacing water in the pore is sufficiently high (Pinder and Gray 2008). A standard method for estimating the transmissivity of LNAPL is described in ASTM E2856–13 (see references).

Because the NAPL and water must compete for space in which to flow, the cross-sectional area of the pore space available for each fluid is less than the total pore space. This leads to the concept of **relative permeability**. Relative permeability is the ratio of the intrinsic permeability for the fluid at a given saturation ratio to the total intrinsic permeability of the rock. A relative permeability exists for both the wetting and the nonwetting phase. Figure 5.7 shows typical two-phase relative-permeability curves for both wetting and nonwetting liquids.

The irreducible water saturation is the water content at which no additional water will flow. In Figure 5.7, water is the wetting fluid, and the irreducible water (wetting-fluid) saturation is shown on the left side. Thus water will not flow at all until the irreducible wetting-fluid saturation, S_{wr} , is exceeded. The nonwetting fluid will not begin to flow until the residual nonwetting-fluid saturation, S_{nwr} , is exceeded. This is shown on the right side of Figure 5.7. For a two-phase oil-water system, if the water content is less than the irreducible water saturation, oil can flow, but water will be held by capillary forces. Likewise, at an oil content less than the residual oil saturation, water can flow, but oil cannot, at least as a separate phase. Oil droplets dispersed in the water can still migrate.

Relative permeability is normally determined by laboratory tests of rock-core samples. There appears to be a hysteresis effect for relative permeability. This is not surprising, because such an effect exists for capillary pressure. Figure 5.8(a) shows experimentally derived relative-permeability curves in a fine sand for water in the presence of TCE (Lin et al. 1982). The left curve was measured in a core that initially had a high saturation ratio of TCE and then had varying amounts of water injected into it to increase the water-saturation ratio. The right curve was measured for a core that was saturated with water and then was injected with TCE. Note that the two curves have greatly different shapes and that the relative permeability for water can vary substantially, depending upon whether the particular water-saturation value was reached by water displacing TCE or TCE displacing water. Figure 5.8(b) shows experimentally

FIGURE 5.6 Different fluid saturation states for a porous media that contains water and oil.



derived relative-permeability curves for TCE in the presence of water for the same fine sand as Figure 5.8(a) (Lin et al. 1982). The two curves, representing water displacing TCE and TCE displacing water, are much closer than the curves for relative permeability of water. However, they are not exactly the same. Hysteresis is an added complexity to analytical treatment of multiphase flow. Parker and Lenhard (1987) and Lenhard

FIGURE 5.7 Typical relative permeability curves for a two-phase system.

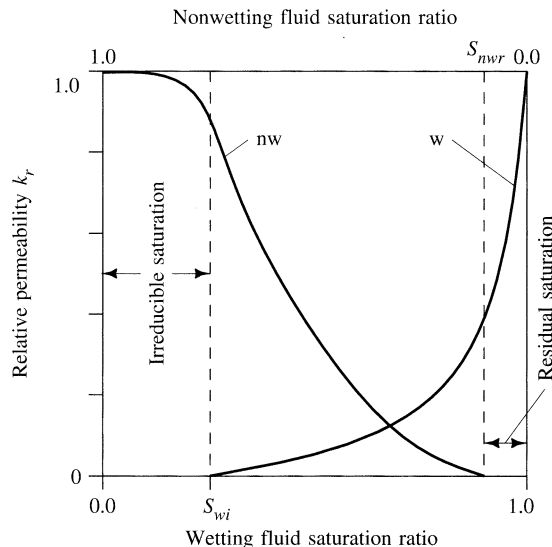
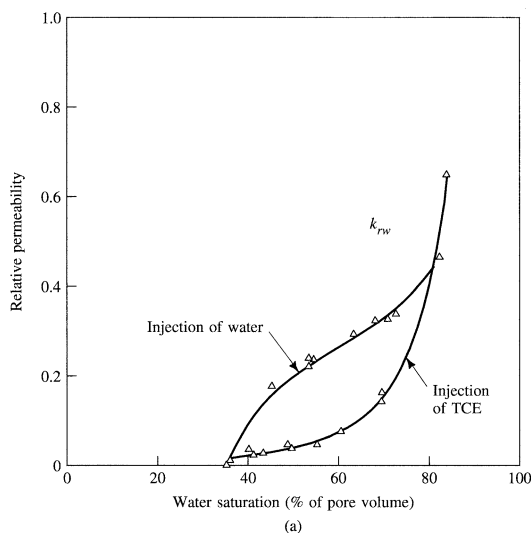
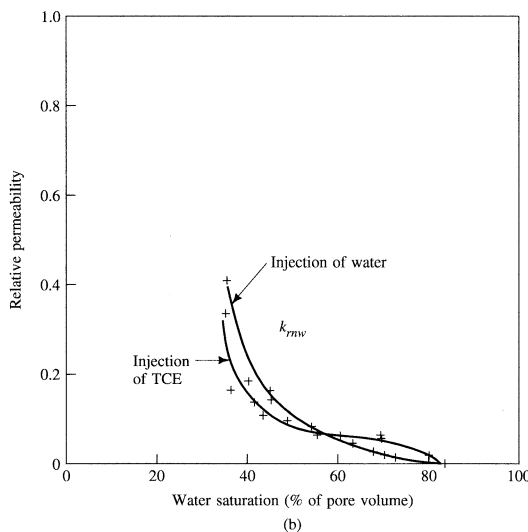


FIGURE 5.8(a) Experimentally derived relative permeability curves for water with respect to TCE.



Source: Lin et al. 1982.

FIGURE 5.8(b) Experimentally derived relative permeability curves for TCE with respect to water.

Source: Lin et al. 1982.

and Parker (1987a) have proposed models to describe the hysteretic relations of saturation-pressure ratios and permeability-saturation relations. Held and Celia (2000) suggest that the relative influence of snap-off and piston-type retractions during imbibition contribute significantly to hysteresis and concluded that hysteresis can essentially be eliminated from pore-scale network models using a specific choice of displacement rules for imbibition of the porous matrix.

Relative permeabilities of three-phase systems of air-water-nonaqueous phase liquids are more complex. A method of estimating these values from data developed for two-phase systems was devised by Stone (1973). First the relative permeability of water, k_{rw} , as a function of the saturation ratio for water, S_w , is obtained for a water-nonaqueous phase system. Next, the relative permeability of air, k_{ra} , as a function of the saturation ratio for air, S_a , is determined for an air-nonaqueous phase system. Finally, the relative permeability of the nonaqueous phase liquid, k_m , in the three-phase system is determined from Equation 5.5 (Faust 1985):

$$k_m = k_{rw}^* \left[\left(\frac{k_{rw}}{k_{rw}^*} + k_{rw} \right) \left(\frac{k_{ra}}{k_{rw}^*} + k_{ra} \right) - (k_{rw} + k_{ra}) \right] \quad (5.5)$$

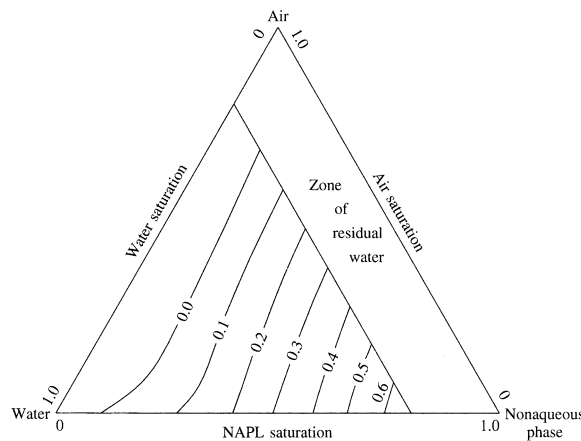
where

k_{rw}^* = the relative permeability of the nonaqueous phase at the residual saturation of water in a water-nonaqueous phase system

k_{rw} = the relative permeability of the nonaqueous phase system as a function of S_w

k_{ra} = the relative permeability of the nonaqueous phase in an air-nonaqueous phase system as a function of S_a .

FIGURE 5.9 Ternary diagram showing the relative permeability of the NAPL phase in an air-water-NAPL system as a function of phase saturation.



Source: Faust. 1985. Transport of immiscible fluids within and below the unsaturated zone: A numerical model. *Water Resources Research* 21:587–596. Copyright by the American Geophysical Union. Reproduced with permission.

Figure 5.9 is a ternary relative permeability diagram for the nonaqueous phase liquid in an air-water-nonaqueous phase system—i.e., the vadose zone—where the water is the wetting fluid (Faust 1985).

5.2.5 Darcy's Law For Two-Phase Flow

Darcy's law for the steady-state saturated flow of water in the presence of a nonaqueous phase liquid is given (Schwille 1984) as

$$Q_w = \frac{-k_{rw} k_i \rho_w}{\mu_w} A \frac{dh_w}{dl} \quad (5.6)$$

where

Q_w = volume of water flowing

k_{rw} = relative permeability of water in the presence of the nonwetting fluid

k_i = intrinsic permeability of the rock

ρ_w = density of the water

μ_w = dynamic viscosity of the water

A = cross-sectional area of flow

dh_w/dl = gradient of the head of the water

A similar expression for the nonwetting fluid is

$$Q_{nw} = \frac{-k_{rnw} k_i \rho_{nw}}{\mu_{nw}} A \frac{dh_{nw}}{dl} \quad (5.7)$$

5.2.6 Fluid Potential and Head

Hubbert (1953) defined fluid potential, Φ , as the amount of work needed to move a unit mass of fluid from some standard position and condition to a different position and condition. Position represents the potential energy of the fluid or elevation above the standard datum. The condition can be represented by the difference in pressure between the position under consideration and the standard pressure.

The fluid potential is thus defined as

$$\Phi = g(z - z_s) + (P - P_s)v_m \quad (5.8)$$

where

g = acceleration of gravity

z = elevation

z_s = standard elevation

P = pressure

P_s = standard pressure

v_m = volume per unit mass

Since volume per unit mass is the reciprocal of density, ρ , Equation 5.8 can be expressed as

$$\Phi = g(z - z_s) + \frac{P - P_s}{\rho} \quad (5.9)$$

If the standard pressure is taken as atmospheric and z is defined as elevation above a convenient datum, such as sea level, then Equation 5.9 becomes

$$\Phi = gz + \frac{P}{\rho} \quad (5.10)$$

If a pipe with an open bottom is inserted into an aquifer to a point at distance z above the datum, the fluid pressure at that location will cause the fluid in the aquifer to rise to a height h above the datum. The fluid pressure is equal to the weight of the fluid in the pipe per unit cross-sectional area:

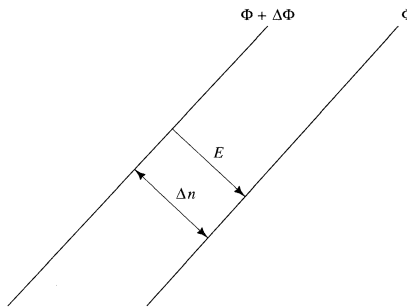
$$P = \rho g(h - z) \quad (5.11)$$

This can be substituted into Equation 5.10 to yield

$$\Phi = gz + \frac{\rho g(h - z)}{\rho} = gh \quad (5.12)$$

where h is the total head.

Fluid will flow from an area of higher fluid potential, $\Phi + \Delta\Phi$, to an area of lower fluid potential, Φ . The force per unit mass exerted on the fluid by its environment is a vector, \mathbf{E} . This force vector is perpendicular to the equipotential surfaces and in the direction of decreasing potential. It has a magnitude equal to the change in potential, $\Delta\Phi$, divided by the distance over which the change in potential is measured, Δn (Figure 5.10):

FIGURE 5.10 Relation between force field and potential gradient.

Source: Modified from M. K. Hubbert. 1953. *American Association of Petroleum Geologists Bulletin* 37:1954–2026.

$$\mathbf{E} = -\frac{\Delta \Phi}{\Delta n} \quad (5.13)$$

The force vector \mathbf{E} can be expressed several other ways:

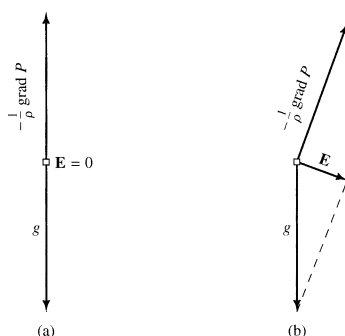
$$\mathbf{E} = -\text{grad } \Phi \quad (5.14)$$

$$\mathbf{E} = -g \text{ grad } h \quad (5.15)$$

$$\mathbf{E} = g - \frac{1}{\rho} \text{ grad } P \quad (5.16)$$

Equation 5.16 shows that at a point a unit mass of a fluid will be acted upon by a force \mathbf{E} , which is the vector sum of gravity and the negative gradient of the pressure divided by the fluid density. Figure 5.11 shows the vector components of the force vector \mathbf{E} for (a) the hydrostatic case where $\mathbf{E} = 0$ and (b) the hydrodynamic case where $\mathbf{E} \neq 0$.

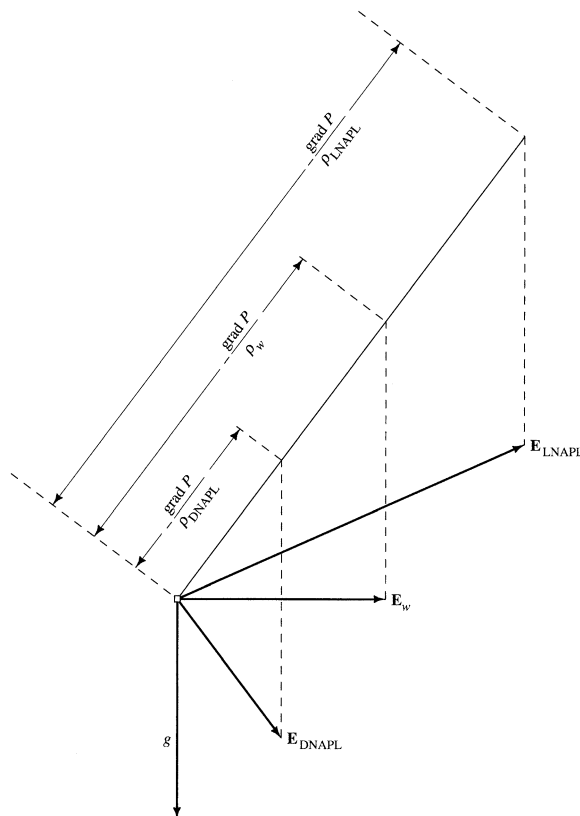
Equation 5.16 shows that the direction of the force vector is a function of the fluid density. Thus for the same point in the aquifer, different fluids will have different

FIGURE 5.11 Vector components of the force vector for (a) hydrostatic case and (b) hydrodynamic case.

Source: M. K. Hubbert (1953). *American Association of Petroleum Geologists Bulletin* 37:1954–2026.

force vectors and, hence, different flow directions in the same potential field. Consider Figure 5.12, which has a force vector for water, \mathbf{E}_w , a force vector for an **LNAPL**, \mathbf{E}_{LNAPL} , and a force vector for a **DNAPL**, \mathbf{E}_{DNAPL} . For convenience, the water is shown to be flowing horizontally; that is, the force vector \mathbf{E}_w is horizontal, although it could be going in any direction. Since the density of the LNAPL is less than the density of water, the vector $-\text{grad } P/\rho_{LNAPL}$ is longer than the vector $-\text{grad } P/\rho_w$ and the resulting vector \mathbf{E}_{LNAPL} is angled upward compared with \mathbf{E}_w . The vector \mathbf{E}_{DNAPL} is angled downward because the vector $-\text{grad } P/\rho_{DNAPL}$ is shorter than $-\text{grad } P/\rho_w$.

FIGURE 5.12 Force vectors for a DNAPL, water, and an LNAPL in the same potential field. The DNAPL sinks and the LNAPL rises with respect to the direction of groundwater flow.



Source: Modified from M. K. Hubbert (1953). *American Association of Petroleum Geologists Bulletin* 37:1954–2026.

This figure illustrates why a DNAPL will sink and an LNAPL will rise with respect to the direction of groundwater flow in the same potential field.

The fluid potential of a nonwetting fluid, either an LNAPL or a DNAPL, is given by

$$\Phi_{nw} = gz + \frac{P}{\rho_{nw}} \quad (5.17)$$

and the fluid potential for water is

$$\Phi_w = gz + \frac{P}{\rho_w} \quad (5.18)$$

If we solve Equation 5.18 for P and substitute it into 5.17, we obtain

$$\Phi_{nw} = \frac{\rho_w}{\rho_{nw}} \Phi_w - \frac{\rho_w - \rho_{nw}}{\rho_{nw}} gz \quad (5.19)$$

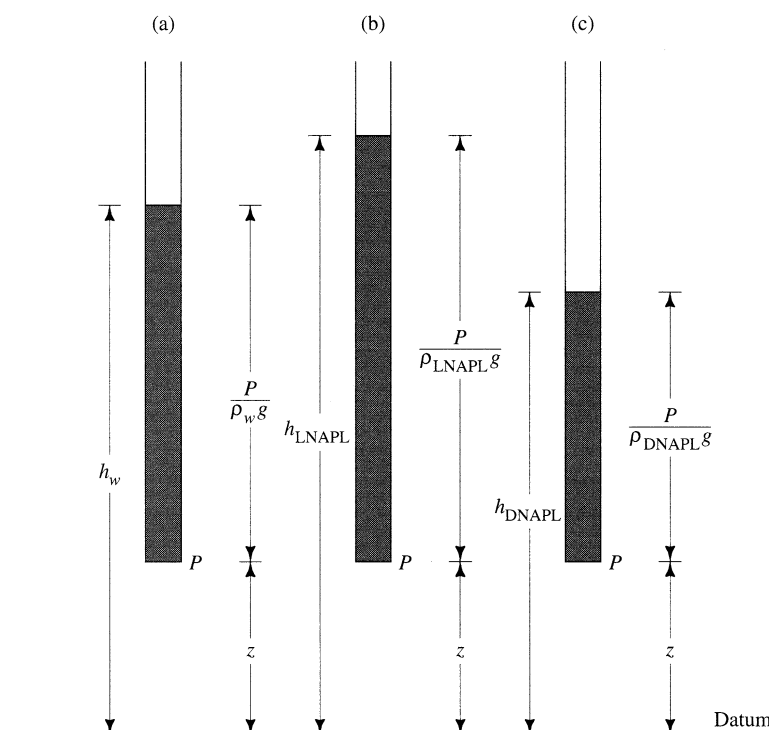
This expression relates the fluid potential of a nonwetting fluid to the fluid potential of water at the same location.

From Equation 5.12, $\Phi_{nw} = gh_{nw}$ and $\Phi_w = gh_w$, Equation 5.19 can be written as

$$h_{nw} = \frac{\rho_w}{\rho_{nw}} h_w - \frac{\rho_w - \rho_{nw}}{\rho_{nw}} z \quad (5.20)$$

In Equation 5.20, z is the elevation of the point in the aquifer, h_w is the height above the datum that water would stand in an open pipe terminating at the point, and h_{nw} is the height that a nonwetting fluid of density ρ_{nw} would stand. Figure 5.13 illustrates the relationships between h_w , h_{LNAPL} , and h_{DNAPL} . The fluid elevation in the pipe filled with

FIGURE 5.13 Total head, h , pressure head, $P/\rho g$, and elevation head, z , for open pipes filled with (a) water, (b) LNAPL, and (c) NAPL. All pipes have the same pressure at the open end.



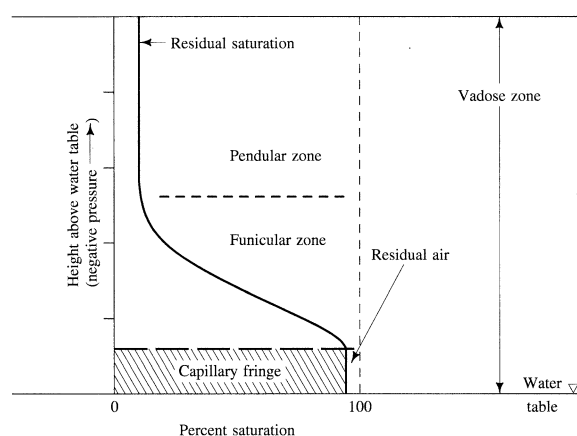
LNAPL will be higher than the pipe filled with water, whereas the fluid elevation of the pipe filled with DNAPL will be lower.

■ 5.3 Migration of Light Nonaqueous Phase Liquids (LNAPLs)

Light nonaqueous phase liquids are less dense than water. When spilled at the land surface, they migrate vertically in the vadose zone under the influence of gravity and capillary forces, just as water does. Unless the vadose zone is extremely dry, it will be water-wet, and the LNAPL will be the nonwetting phase.

Figure 5.14 shows the distribution of water in the vadose zone (Abdul 1988). Notice that at the top of the vadose zone the water is held at the irreducible water saturation. The water held here is called **pendular** water. Below that is a zone where the water content is above the irreducible saturation; this is sometimes called **funicular** water. When close to 100% water saturation is reached, we find the capillary fringe. The air-water relationship of the vadose zone behaves as a two-phase immiscible flow, so there is residual air saturation in the capillary zone. This is shown in Figure 5.14; however, we will ignore the residual air saturation in further analysis because it usually is a small value.

FIGURE 5.14 Vertical distribution of water in the vadose zone in the absence of nonaqueous phase liquids.



Source: A.S. Abdul. 1988. Migration of petroleum products through sandy hydrogeologic systems. *Groundwater Monitoring & Remediation* 8:73–81. Used with permission.

The capillary fringe is not a regular surface, such as the water table. The height of the capillary rise will be different in each vertical set of interconnected pores, depending upon the mean pore diameter of the set. Thus the capillary fringe has a ragged upper surface. However, for the sake of simplicity in diagrams of the capillary fringe, we will show it as a level surface. We can use the capillary tube model to estimate the

average height of the capillary fringe. Equation 5.4 can give us the capillary pressure, P_t , based on a mean pore radius, r . This is equal to the weight of the water in the capillary tube, which is found by multiplying the height of the water in the tube, h_c , by the specific weight of water, γ .

$$P_t = -h_c \gamma = -\left(\frac{2\sigma}{r}\right) \cos \theta \quad (5.21)$$

$$h_c = \left(\frac{2\sigma}{r\gamma}\right) \cos \theta \quad (5.22)$$

For pure water in a clean glass tube, θ can be taken as zero, so that $\cos \theta$ is 1.0. The value of σ for water in contact with glass at 20° C is 74 dyne/cm, or 74 g/s². The value of γ at 20° C is 0.98 g/cm³. Substitution of these values in Equation 5.22, with r in cm, results in:

$$h_c = \frac{0.15}{r} \text{ cm} \quad (5.23)$$

Table 5.1 shows the heights of the capillary fringe that were observed experimentally in various materials. The visual capillary height is the level where the water saturation ratio is close to 1.0. The capillary water in the funicular zone is above this height, although it is not visible.

Figure 5.14 shows the capillary fringe as extending to the height where the water-saturation ratio begins to decline. This height is based on the larger pores, in which the capillary rise would be least. For the smaller pores, the capillary rise would be greater, extend upward into what is labeled the funicular zone. Water in that zone is not moving downward but is being held in place by capillary forces. This illustrates the irregularity of the capillary fringe. We use the phrase **capillary zone** to mean the part of the capillary fringe where the water saturation ratio is at or close to 1.0.

TABLE 5.1 Visual capillary rise in unconsolidated materials (porosity of all samples is about 41%).

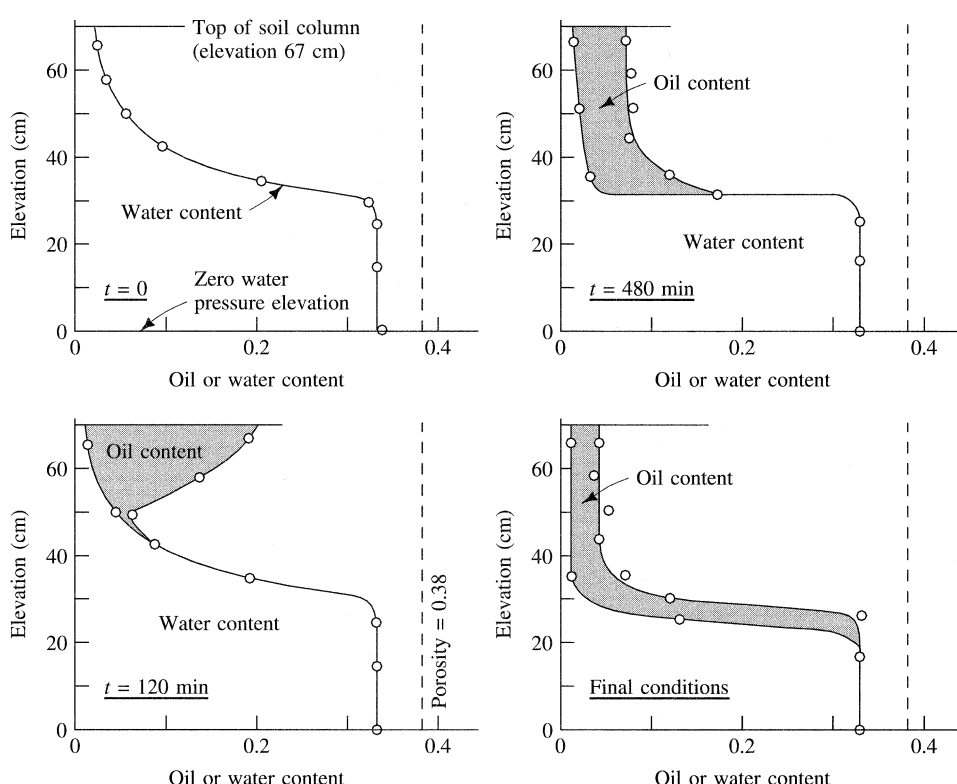
Material	Grain Size		Capillary Rise	
	(mm)	(inches)	(cm)	(inches)
Fine gravel	2–5	0.08–0.20	2.5	1.0
Very coarse sand	1–2	0.04–0.08	6.5	2.6
Coarse sand	0.5–1	0.02–0.04	13.5	5.3
Medium sand	0.2–0.5	0.008–0.02	24.6	9.7
Fine sand	0.1–0.2	0.004–0.008	42.8	16.9
Silt	0.05–0.1	0.002–0.004	105.5	41.5
Fine silt	0.02–0.05	$8 \cdot 10^{-4}$ – $2 \cdot 10^{-3}$	200+	>78.8

Source: Lohman (1972).

The LNAPL will travel vertically in the vadose zone. If a sufficient quantity is present so that the residual LNAPL saturation is exceeded, it will eventually reach the top of the capillary zone. However, much of the LNAPL may remain behind, trapped in the vadose zone. Eckberg and Sunada (1984) studied the distribution of oil in the vadose zone. Figure 5.15 shows the changes in the distribution of water and oil in a sand column into which a quantity of oil was added. Note that much of the oil remains throughout the thickness of the vadose zone as a residual oil.

In moving downward, an LNAPL may displace some of the capillary water in the vadose zone, causing it to move ahead of the advancing LNAPL front. Once the capillary zone is reached, LNAPL will begin to accumulate. Initially, the LNAPL will be under tension, just as the water in the vadose zone is under tension. As additional LNAPL accumulates above the capillary zone, an “oil table” will develop, with some LNAPL having a positive pore pressure. The capillary zone will become thinner, and mobile, or “free,” LNAPL will accumulate. Eventually, the capillary zone may disappear altogether and the oil table will rest directly on the water table. In the core of a

FIGURE 5.15 Changes in the vertical distribution of oil with time after a slug of oil is added to the top of a column of sand. Oil content and water content are expressed as a fraction of the total volume of the porous media.



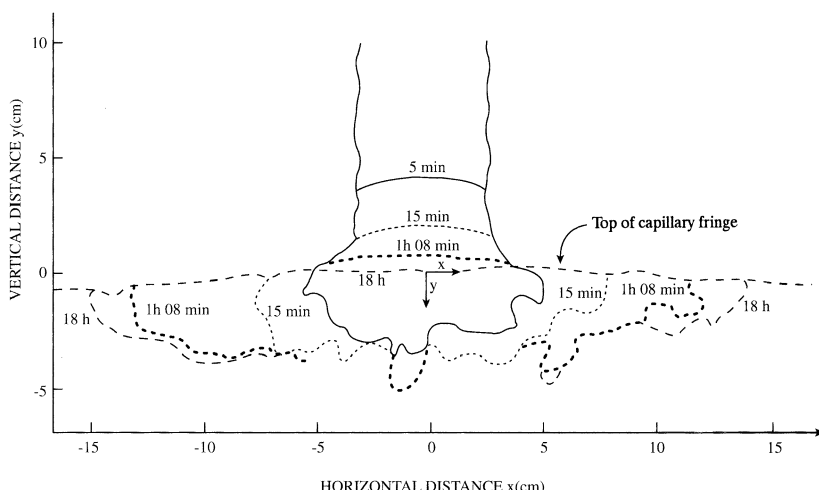
Source: D. K. Eckberg and D. K. Sunada. 1984. Nonsteady three-phase immiscible fluid distribution in porous media. *Water Resources Research* 20:1891–1897. Used with permission.

thick zone of mobile LNAPL, the water table may be depressed by the weight of the LNAPL.

Schroth and others (1995) examined the geometry of a LNAPL lens, which forms in a water-wetted porous media. Two different LNAPLs were released as a point source in an artificial aquifer. The LNAPLs traveled vertically through the vadose zone until they reached the top of the capillary fringe. They then spread out in the upper part of the capillary fringe until they eventually became stable. The LNAPL body had a convex lens-shaped bottom with the top even with the original position of the top of the capillary fringe. In homogeneous porous media the top of the LNAPL lens will be flat. The infiltrating LNAPL always completely penetrated the vadose zone, that is the lens top was always even with the top of the capillary fringe. The only LNAPL above the top of the capillary fringe was residual. Figure 5.16 shows the development of a LNAPL lens through time.

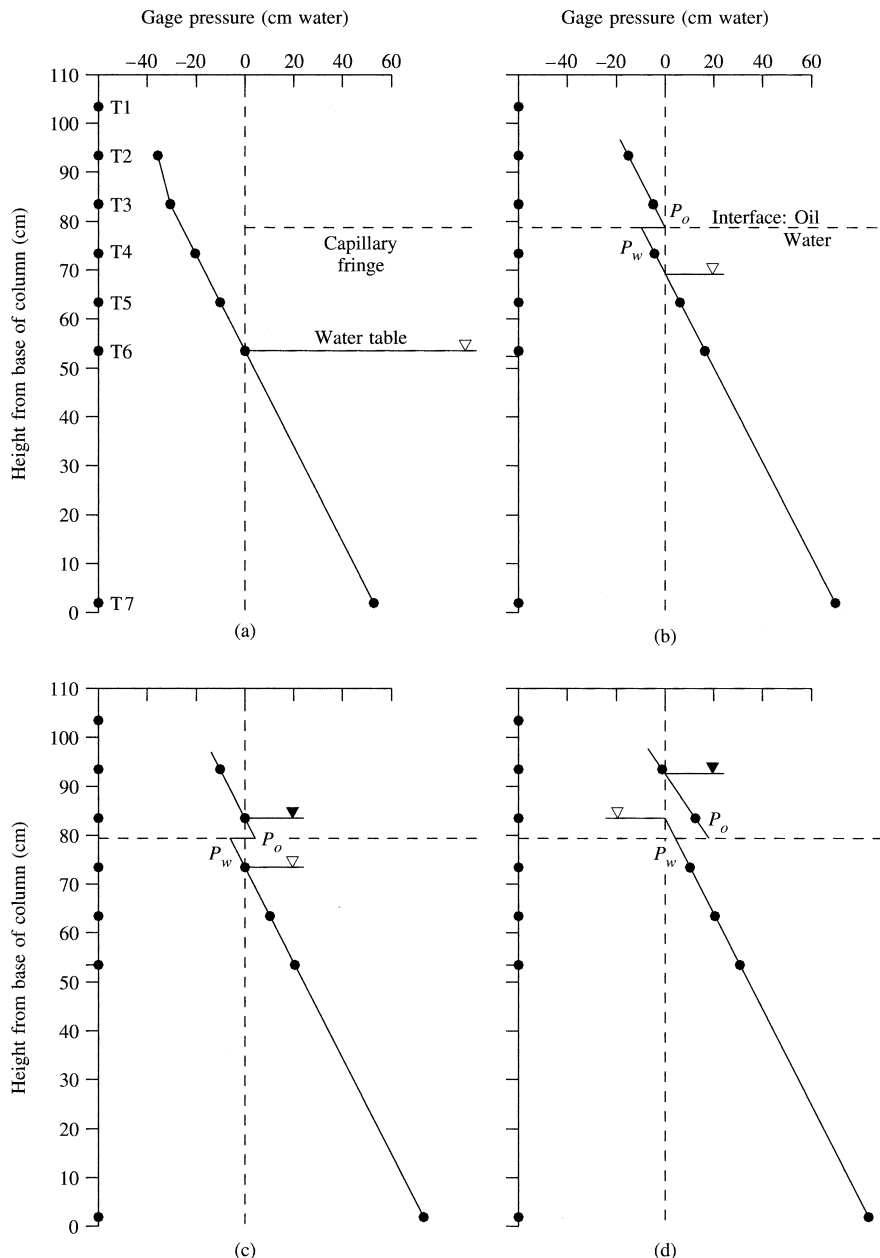
Abdul (1988) conducted an experiment to observe the development of an oil table. Vertical columns were packed with sand and partially filled with water. The columns had manometer/tensiometers installed at various heights to measure the pore-water pressure below the water table and tension above the water table. The elevation where the gauge pressure is zero is the water table. Figure 5.17(a) shows the distribution of pore pressures before any oil was added. Oil was then added to the top of the soil column, and the system was allowed to come into equilibrium. Figure 5.17(b) records the conditions after oil was added. The capillary fringe thinned, and the water table rose as the advancing oil displaced capillary water downward. Oil under tension accumulated above the capillary zone. Figure 5.17(c) shows that further addition of oil resulted in the formation of an oil table with positive pore pressure above the water capillary zone, which was still under tension. Eventually enough oil was added so the water capillary fringe disappeared and the oil table rested directly on the water table. An oil capillary fringe existed above the oil table (Figure 5.17(d)). It is important to note that a LNAPL lens or “pool” in the

FIGURE 5.16 Formation of an LNAPL lens on the tops of the capillary fringe as a function of time.

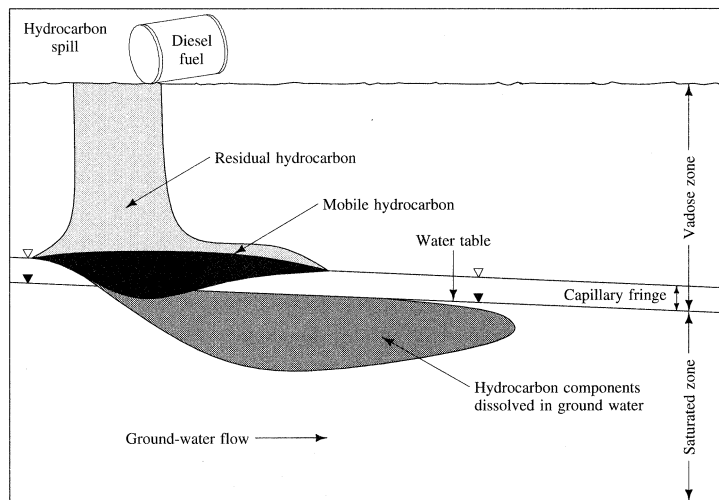


Source: Schroth et al. 1995. Geometry and position of light nonaqueous-phase liquid lenses in water-wetted porous media. *Journal of Contaminant Hydrogeology* 19:269–287, with kind permission of Elsevier Science-NL.

FIGURE 5.17 Hydrostatic pressure head/tension distribution in a sand column to which oil is being added to the top of the column. (a) Before the addition of the oil, (b) after addition of the oil showing the development of an oil fringe, (c) after addition of sufficient oil for an oil table to form, and (d) after sufficient mobile oil has accumulated to eliminate the water capillary fringe.



Source: A. S. Abdul. 1988. Migration of petroleum products through sandy hydrogeologic systems. *Groundwater Monitoring & Remediation* 8:73–81. Used with permission.

FIGURE 5.18 Subsurface distribution of an LNAPL spill.

capillary zone, and in some cases extending below the capillary zone into the water table, does not normally completely fill all pore space. Some isolated water globules are often trapped within the LNAPL pool, with water preferentially in the smaller spaces.

In general, the thickness and horizontal spreading of a LNAPL pool is controlled by the amount of LNAPL which reaches the capillary fringe, and the pore size of the geologic media near the capillary fringe and water table. As a lens of LNAPL spreads out on the capillary fringe, its outer edges are inhibited as they move outward by adjacent water in pore spaces. Fine grained material with smaller pore spaces will retain water with greater capillary force, therefore spreading NAPL will move more slowly and LNAPL lens will have to become thicker with more fluid pressure to supplant adjacent water in small pores. Conversely, LNAPL pools in gravels or coarse, clean sands with large pore spaces are less impeded by surrounding capillary water, and more easily spread out into broader, thinner lenses.

The mobile LNAPL can migrate in the vadose zone following the slope of the water table. Figure 5.18 shows the shape of a migrating spill of an LNAPL. Note that there is residual LNAPL in the unsaturated zone above the mobile LNAPL. In addition some of the LNAPL components can dissolve in the groundwater and move by diffusion and advection with the groundwater. For example, gasoline will release significant amounts of benzene, toluene, ethylbenzene, and xylene (BTEX) as soluble fractions. The resulting volume of contaminated groundwater is called a **plume**. The velocity by which the plume spreads is greater than that of the free LNAPL. Therefore, the plume will travel farther than the LNAPL during the same time.

■ 5.4 Capillary and Bond Numbers

Residual saturation of NAPL that is tightly held in the pore space represents a potential source for continued groundwater contamination. Immiscible displacement

(= mobilization) of residual NAPL becomes likely when the viscous and buoyancy forces dominate over the capillary forces. The potential of a NAPL to move freely can be estimated with the Capillary (N_C) and Bond (N_B) numbers. NAPL can be displaced if there is sufficient driving force to overcome the capillary pressure difference between the water and the NAPL. The criterion of **mobilization** can be expressed in terms of the ratio of viscous to capillary forces:

$$N_C = \frac{k_i \rho g \Delta H}{\sigma} = \frac{q \mu}{\sigma} \quad (5.24)$$

where k_i is the intrinsic permeability (L^2), ρ is the density of water (M L^{-3}), g is the acceleration of gravity (L T^{-2}), ΔH is the hydraulic gradient, σ is the interfacial tension between the immiscible liquid and water (dynes/cm). The parameter μ is the dynamic viscosity of water (N s cm^{-2}) and q is the Darcy velocity (L T^{-1}). The Capillary number is dimensionless. For low capillary numbers (approximately 10^{-5}), flow in porous media is dominated by capillary forces whereas for high capillary number the capillary forces are negligible compared to the viscous forces.

The effect of buoyancy forces on residual NAPL can be evaluated using the dimensionless Bond number:

$$N_B = \frac{k_i \Delta \rho g \square}{\sigma} \quad (5.25)$$

where $\Delta \rho$ is density difference between aqueous and NAPL phases. Under most environmental conditions, the magnitude of gravity and viscous forces are small relative to capillary forces, i.e., $N_C < 10^{-6}$ and $N_B < 5 \cdot 10^{-3}$. Under these circumstance, NAPL entrapment as residual is favored (Allen, Cohen, and Kaplan 1989).

The residual NAPL can be mobilized by increasing the hydraulic gradient and therefore the groundwater flow velocity and/or by reducing the interfacial tension between the residual NAPL and the aqueous phase. Increasing the groundwater flow velocity is limited by the hydraulic conductivity of porous materials. Allen, Cohen, and Kaplan (1989) provides an example: the result of laboratory experiments indicate that NAPL at residual saturation, or less, cannot be displaced from porous media under vertical flow conditions if the N_c is less than $2 \cdot 10^{-5}$. If gasoline is trapped in a homogenous sandy aquifer with $k_{\text{intr}} = 10^{-10} \text{ m}^2 (1.07 \cdot 10^{-8} \text{ ft}^2)$ equation 5.25 indicates that ΔH must be at least 0.24 to attain the critical value of N_c to initiate NAPL mobilization. For complete NAPL removal, N_c must be at least $1.5 \cdot 10^{-3}$, which can only be attained by a $\Delta H > 18$. This critical N_c value is a function of the porous medium and varies with particle size distribution. Hence, using just hydraulic mobilization, removal of residual NAPL can only, if at all, be achieved in very permeable strata, such as coarse sand or gravel. For this reason alone, it is considerably easier to reduce the interfacial tension between the NAPL and the aqueous phase, for example, by adding surface active compounds to the solution. The reduction of the interfacial tension increases N_c and N_b . This is the basis of some remediation technologies, such as surfactant enhanced mobilization of NAPL, which will be covered in greater detail in Chapter 9.

■ 5.5 Partitioning Interwell Tracer Tests

After NAPL has been detected at a contaminated site, it is often unknown how much NAPL was released during past site activities. *In situ* tracer tests have been developed to quantify the amount of NAPL in the subsurface in both saturated and unsaturated media and to describe the spatial distribution of the NAPL in the subsurface, often referred to as NAPL architecture or to determine how much NAPL was removed during site remediation. These tests are known as **partitioning interwell tracer tests** (PITT). First used in the petroleum industry, PITTs were later adopted for detecting NAPL contaminants in subsurface environments (Jin et al. 1995). Since then, many PITTs have been carried out to estimate the residual NAPL saturation under field conditions (e.g., Annable et al. 1998; Dwarakanath et al. 1999) or to determine the effectiveness of remediation efforts (e.g., Cain et al. 2000; Meinardus et al. 2002; Brooks et al. 2002; Divine et al. 2004) or to describe the NAPL architecture (e.g., Enfield et al. 2005). A number of well-documented PITTs have been described in the literature, including at Camp Lejeune, NC (Duke Engineering & Services 1999), Dover Air Force Base (Brooks et al. 2001), or Hill Air Force Base (Pope et al. 2000). Most PITT focused on DNAPL contamination and additional information about the application of PITTs for DNAPL site characterization is published by the U.S. EPA (2004).

The PITT approach is based on measuring the degree of retardation that a suite of tracer experience when coming in contact with NAPL. The partitioning of PITTs tracers between the aqueous phase and the NAPL can be defined as:

$$K_N = \frac{C_N}{C_W} \quad (5.26)$$

where K_N is the NAPL-water partitioning coefficient, C_N is the concentration of the tracer in the NAPL, and C_W is the tracer concentration in the aqueous phase. In a steady-state flow field, the degree of retardation of a partitioning tracer can be related to the saturation of entrapped NAPL, S_N (Annable et al. 1998)

$$R_N = 1 + \frac{K_N S_N}{(1 - S_N)} \quad (5.27)$$

where R_N is the retardation factor for the partitioning tracer. It is calculated directly from the first adjusted temporal moment ($M^1_{T,\text{adj}}$, see Chapter 3) of the tracer breakthrough curve (BTC) data

$$R_N = \frac{t_P}{t_{NP}} \quad (5.28)$$

where t_P and t_{NP} are the mean travel times of the partitioning and nonpartitioning conservative tracer, respectively. Typically, BTCs from field PITTs exhibit significant tailing, which is primarily caused by the hydraulics of the injection/extraction system. Truncation of this tail region due to early test termination can lead to moment estimation errors. Therefore, an exponential extrapolation method might be needed to model tracer BTC beyond test cutoff (Divine et al. 2004).

According to Mariner et al. (1999), Equation 5.27 can be modified to permit PITT investigations of the unsaturated zone:

$$R_N = 1 + \frac{HS_W + K_{NA}S_N}{(1 - S_W - S_N)} \quad (5.29)$$

where H is the air-water partitioning coefficient (Henry's coefficient), K_{NA} is the NAPL-air partitioning coefficient, and S_W is the fraction of water filled pore space. The denominator is equivalent to the fraction of air filled pore space.

Assuming local equilibrium during partitioning for the water-NAPL system, the S_N in the tracer swept volume in the saturated zone can be calculated (Jin et al. 1995):

$$S_N = 1 + \frac{R_N - 1}{R_N + K_N - 1} \quad (5.30)$$

Although single "push-pull" tests have been described (Istok et al. 2002), PITTs are typically conducted by injecting tracers in one well and extracting from one or more extraction wells. The total NAPL volume of the inter-well swept zone is:

$$V_N = \frac{S_N V_e}{1 - S_N} \quad (5.31)$$

where V_e is the effective pore volume for each injection/extraction well pair, which is equal to the extraction well pumping rate times the nonpartitioning tracer travel time ($V_e = Q t_{NP}$).

Theoretically, only one conservative tracer and one partitioning tracer are necessary to estimate S_N . However, a suite of multiple partitioning tracers is typically used in field applications, because the range of probable S_N values can be very large. If the tracer suite is chosen appropriately, it can provide redundancy while also increasing the likelihood that optimal tracer separation in terms of t_p will be observed for several tracers, regardless of the actual S_N . Jin et al. (1995) recommends a range of $1.2 < R_N < 4$ for tests in saturated porous media.

Alcohols are the most commonly used PITT tracers. The selection of appropriate partitioning tracers is a critical element of any PITT. Data from several field PITTs indicate that some partitioning tracers exhibit significant in-situ biodegradation, even during the typically short duration of the tests (e.g., Annable et al. 1998). Alcohol tracer, such as methylated and ethylated alcohols, are generally more recalcitrant than straight-chain alcohols, such as hexanol. In a field study at the Naval Amphibious Base Little Creek, VA, Divine et al. (2004) used a suite of alcohol tracers, including their K_{NW} values, shown in Table 5.2.

While alcohol compounds have been used as partitioning tracers for the majority of field PITTs, Divine et al. (2003) investigated the applicability of dissolved helium and neon partitioning tracer in the laboratory because these gases are nonbiodegradable, nontoxic, do not sorb to aquifer materials, and have low analytical detection limits. The author reported successful batch partitioning tests and column-scale PITTs using dissolved gas tracers. Gas tracers were later used with success at the Naval Amphibious Base Little Creek, VA (Divine et al. 2004).

Table 5.2 K_{NW} values for PITT alcohol tracers, including noble gases Helium and Neon.

Pre-PTT		Post-PTT	
Tracer	K_{NW}	Tracer	Effective K_{NW}
Bromide	0.0	Bromide	0.0
Helium	2.42 ^a	Neon	3.24 ^a
2-methyl-1-butanol	3.71 ^b	2-methyl-1-butanol	3.38 ^b
2-ethyl-1-butanol	13.4 ^b	4-methyl-2-pentanol	9.66 ^b
hexanol	18.6 ^d	2-ethyl-1-hexanol	131 ^a
2,4-dimethyl-3-pentanol	71.3 ^b	heptanol	163.1 ^c
heptanol	163.1 ^c		
2-ethyl-1-hexanol	202 ^a		

Sources: ^a Divine et al. 2003; ^b Dugan et al. 2003; ^c Young et al. 1999; ^d Wang et al. 1998.

Besides analyzing the first-order moments of tracer breakthrough curves, Datta-Gupta et al. (2002) described an inverse method for analyzing partitioning interwell tracer test data that relied on numerical modeling and an analytic sensitivity computation method yielding sensitivities of the partitioning tracer response to subsurface parameters, such as porosity, hydraulic conductivity, and NAPL saturation. Independent of the methodology of estimating S_N , the PITT method has distinct advantages over other NAPL saturation estimation methods. For instance, the PITT method provides a quantitative estimate of the errors involved in its estimation of NAPL saturation and volume (Dwarakanath et al. 1999). However, the analysis of data from a series of PITT underestimated S_N by 20% or more dependent on the tracer used in studies where initial DNAPL mass was well-known. The underestimation was believed to be the result of non-uniform distribution and hydraulic inaccessibility of the NAPL (Brooks et al. 2002). The degree of error increased with decreasing initial S_N values. Suthersan et al. (2014) suggests that inconclusive tracer tests in general suffer from an inadequate or incorrect conceptual site model, specifically as it relates to assumptions regarding groundwater flow directions and a lack of understanding of local-scale preferential flow pathways. Similarly, if the DNAPL is trapped in high-saturation area, such as pools, the contact between the PITT tracer and the NAPL might be limited and nonequilibrium partitioning conditions exist. Under those circumstances, Moreno-Barbero and Illangasekare (2006) recommend the use of an effective partitioning coefficient and the incorporation of nonequilibrium mass transfer kinetics in the PITT data analysis. This improved the DNAPL mass estimation by tracers in high-saturation zones. Overall, if carefully planned, conducted and analyzed, the PITT approach has given the contaminant hydrogeologist a valuable tool to describe the extent of the NAPL subsurface contamination.

■ 5.6 Volatilization of NAPLs

The residual NAPL material in the vadose zone can partition into the vapor phase as well as a soluble phase in capillary water. The degree of the partitioning will depend

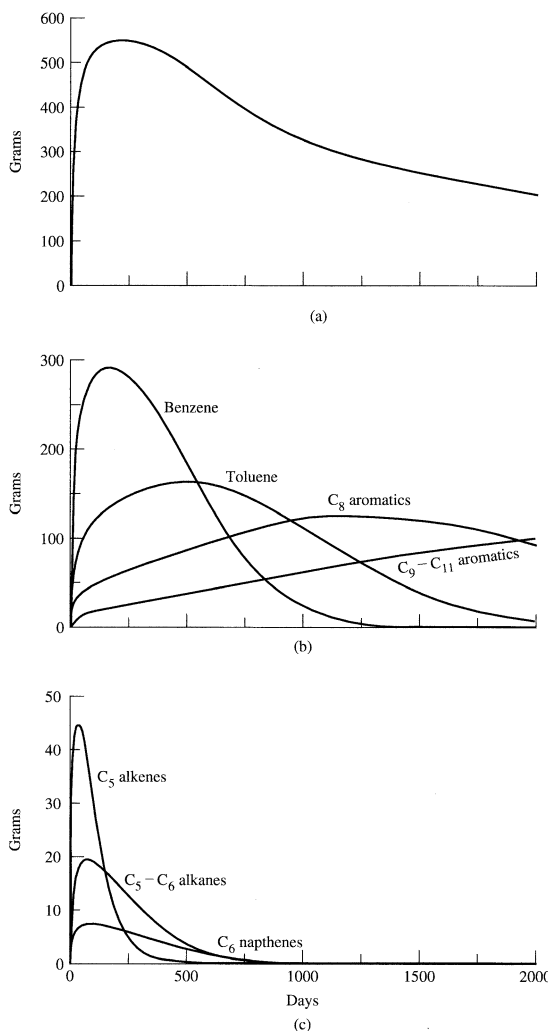
upon the relative volatility of the material and its solubility in water. Vapor phase transport of volatile NAPL solvents in the unsaturated zone is an important mechanism for the spread of contamination at NAPL spill sites and may be a significant process controlling the extent of groundwater contamination by volatile organic compounds (VOC). Several experimental studies were carried out to investigate transport of VOCs in porous soil media and its effects on groundwater contamination, including TCE vapor transport tests in the vadose zone at the Borden AFB site in Canada (Conant et al. 1996), or in a large-scale, artificial aquifer environment in Strasbourg, France (Jellali et al. 2003) A number of models for simulating vapor phase transport have been developed to predict the diffusive and density-driven spreading of vapors in the unsaturated zone (e.g., Conant et al. 1996; Jang and Aral 2007).

The basic concept behind the partitioning of volatile contaminants from the aqueous to the gas phase (and vice-versa) is **Henry's law**, which states there is a linear relationship between the vapor pressure of a solute above its aqueous solution and the concentration in solution. The proportionality constant between the two is called a **Henry's law constant**, which can be expressed in units of atmospheres/(moles/cubic meter water) (Section 7.2). The proportionality constant from Henry's law has also been expressed as a water-air partition coefficient. This is the ratio of the aqueous solubility of a substance, expressed in milligrams per liter at a given temperature to the saturated vapor concentration of the pure phase of the substance, also expressed in milligrams per liter (Baehr 1987).

Those compounds with low water-air partition coefficients, such as the alkanes, favor the vapor phase, whereas those with high water-air partition coefficients, such as benzene, favor the aqueous phase. Hydrocarbons such as gasoline are a mixture of approximately 200 different organic compounds; therefore, various water-air partition coefficients are needed to describe the behavior of the various constituent compounds. The volatilization and contaminant transport in the vapor phase can produce extensive lateral and vertical spreading of contamination beyond the original NAPL distribution (e.g., Seely et al. 1994; Conant et al. 1996; Johnson and Kueper 1996; Mendoza et al. 1996; Geller et al. 2000). Unlike dissolved or free-phase contaminants, the diffusive properties of the soil and contaminant vapors are also very important in controlling vapor phase transport (Baehr and Corapcioglu 1987; Mendoza and Frind 1990 see Chapter 4).

Baehr (1987) developed a model to describe the vapor phase and aqueous transport of residual hydrocarbons in the vadose zone. Figure 5.19 shows the partitioning of hydrocarbon mass from gasoline into vadose zone water as a function of time. This figure shows that the aromatic compounds, those based on the benzene ring, partition into water at a higher rate and for a longer time period than the nonaromatic compounds. This is to be expected, since the nonaromatic hydrocarbons studied, C₅ alkenes, C₅-C₆ alkanes, and C₆ naphthalenes, have much lower water-air partition coefficients, i.e. Henry's law constants than the aromatic constituents, benzene, toluene, ethylbenzene, xylene, etc. Table 5.3 gives water-air partition coefficients for selected gasoline constituents. The selective partitioning of benzene, toluene, ethylbenzene, and xylene (commonly known as BTEX) in the aqueous capillary phase helps to explain why these compounds are so diagnostic of a gasoline spill. They can reach the water table via infiltration of capillary water through a zone of residual

FIGURE 5.19 Mass of residual hydrocarbon in vadose zone partitioning into capillary water as a function of time, with (a) total hydrocarbons, (b) aromatic constituents, and (c) nonaromatic constituents.



Source: A. L. Baehr. 1987. Selective transport of hydrocarbons in the unsaturated zone due to aqueous and vapor phase partitioning. *Water Resources Research* 23:1926–1938. Used with permission.

gasoline, even if no gasoline itself reaches the water table. Figure 5.20 illustrates this phenomenon.

Each component of a non-aqueous phase product will vaporize into the soil atmosphere with a **vapor pressure** equal to the mole fraction of that component times its vapor pressure. This is a corollary to Raoult's law.

$$P_a = x_a P_a^n \quad (5.32)$$

where

P_a = the vapor pressure of a component of a NAPL mixture above the mixture

x_a = the mole fraction of the NAPL component

P_a^n = the vapor pressure of the NAPL component in pure-phase form

In the case of a pure NAPL, the vapor pressure in the soil atmosphere will be the published vapor pressure at the temperature of the NAPL in the soil. Montgomery (1996) is an excellent source of such values.

We can find the concentration of any vapor component from the ideal gas law, which is

$$PV = MRK^\circ / f_w \quad (5.33)$$

where

P = pressure

V = volume

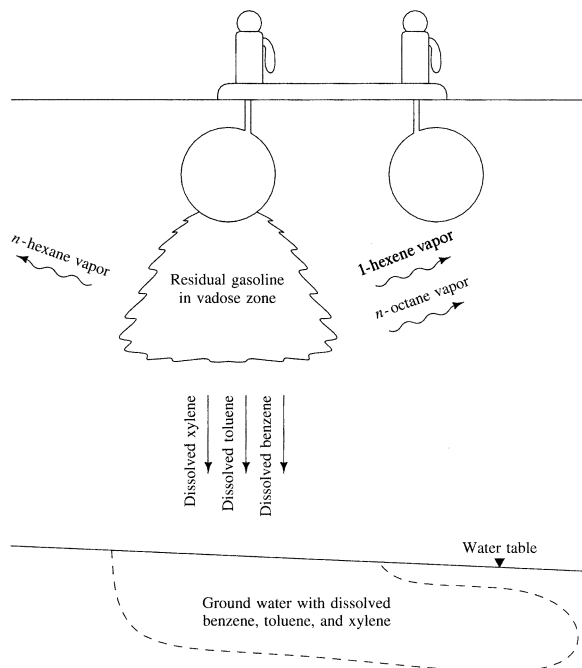
M = mass

R = the ideal gas constant (0.08206 atm-L/mol-K°)

K° = the temperature in Kelvin degrees

f_w = the formula weight

FIGURE 5.20 Process of groundwater being contaminated by gasoline constituents from residual gasoline in the vadose zone.



Since the concentration is mass/volume, and P can be found from Equation 5.32, Equation 5.33 becomes:

$$M/V = (x_a P_a^n f_w) / (RK^\circ) \quad (5.34)$$

where M/V is concentration.

TABLE 5.3 Water-air partition coefficients for selected gasoline constituents.

Compound	Formula	Molecular Weight	Water-Air Partition Coefficient
Aromatics			
Benzene	C ₆ H ₆	78	5.88
Toluene	C ₇ H ₈	92	3.85
o-Xylene	C ₈ H ₁₀	106	4.68
Ethylbenzene	C ₈ H ₁₀	106	3.80
Nonaromatics			
Cyclohexane	C ₆ H ₁₂	84	0.15
1-Hexene	C ₆ H ₁₂	84	0.067
n-Hexane	C ₆ H ₁₄	86	0.015
n-Octane	C ₈ H ₁₈	114	0.0079

EXAMPLE PROBLEM

Toluene is used in the manufacture of model airplane glue. A small amount is spilled when an above ground storage tank outside a glue factory is being filled from a tanker truck. A volume of 1.3 liters of toluene is spilled and soaks into a dry, sandy soil with a porosity of 0.33. If the vapors fill a volume of soil with a bulk volume of 2.5 cubic meters (a) what is the concentration of toluene in the soil atmosphere, (b) how much toluene remains in the soil as a LNAPL and (c) what is the concentration of toluene in the soil phase? Assume that no toluene is evaporated to the atmosphere. The soil is at a temperature of 20 degrees C (293 degrees K). The vapor pressure of toluene is 22 mm of mercury at 20 C°, and the formula weight is 92.14 g/mol.

Since one atmosphere of pressure is 760 mm of mercury, the vapor pressure of toluene is 22/760 or 0.029 atm.

(a) Substituting for the variables in Equation 5.26 we have:

$$M/V = (0.029 \text{ atm} \cdot 92.14 \text{ g/mol}) / (0.0821 \text{ atm-L/mol K}^\circ 293 \text{ K}^\circ)$$

$$M/V = 0.111 \text{ g/L (at } 20 \text{ C}^\circ\text{)}$$

(b) The volume of the pore space is the volume of the soil (2.5 cubic meters) times the porosity (0.33) or 0.825 cubic meters, which is 825 liters. The mass of toluene in the pore space is 0.111 g/L times 825 liters or 91.56 grams. The mass of the amount of toluene spilled is the volume (1.3 L) times the density (866.9 g/L) or 1126.97 grams. Thus, after volatilization into the pore space there would be 91.56 grams in the pore space as vapor and 1035.41 grams as a NAPL.

- (c) The solids in the soil have a volume of 1.675 cubic meters, which is the volume of the entire soil mass (2.5 cubic meters) less the volume of the voids (0.875 cubic meters). If the particle density of the soil is 2.65 g/cubic centimeter, then the soil has a mass of 4439 kilograms. The concentration of the NAPL in the soil is 1035.41 g/4439 kilogram or 0.233 g/kg. This can also be expressed as 233 mg/kg.
-

EXAMPLE PROBLEM

Gasoline contains many compounds including benzene, toluene, ethylbenzene and xylene (BTEX). These four compounds are much less volatile, i.e., have a lower vapor pressure than many of the other gasoline components. Gasoline spilled on the land surface may lose the most volatile components, concentrating the BTEX fraction. The following table contains an assumed concentration of each of the above after a loss of the most volatile fraction, the formula weights and vapor pressures at 25°C. Calculate the concentration of each in the soil atmosphere where weathered gasoline is present in the soil as a NAPL.

Compound	Percent in Weathered Gasoline	Formula Weight (g/mol)	Vapor Pressure (mm Hg)	Vapor Pressure (Atm)
Benzene	25	78.11	95	0.125
Toluene	45	92.14	28	0.037
Ethylbenzene	10	106.17	9.9	0.013
Xylenes	20	106.17	8.8	0.012

If we have one liter of weathered gasoline, and the density is 0.87 g/cm³, then we have 870 grams. The following table shows the calculation of the mole fraction of each component. We assumed that we had one liter only for purposes of calculating the mole fraction.

Compound	Percent of Total Mass	Grams (Percent times 870 g)	Moles (Grams divided by formula weight)	Mole Fraction (Moles divided by total number of moles)
Benzene	25	217.5	2.78	0.29
Toluene	45	391.5	4.25	0.45
Ethylbenzene	10	87	0.82	0.09
Xylenes	20	174	1.63	0.17

The concentration of each of the four compounds can be found from Equation 5.34.

Benzene

$$M/V = (0.29 \times 0.125 \text{ atm} \times 78.11 \text{ gm/mol}) / (0.0821 \text{ atm-L/mol K} \times 298 \text{ K})$$

$$M/V = 0.116 \text{ gm/L (at } 25^\circ\text{C})$$

Toluene

$$M/V = (0.45 \times 0.037 \text{ atm} \times 92.14 \text{ gm/mol}) / (0.0821 \text{ atm-L/mol K}^\circ \times 298 \text{ K}^\circ)$$

$$M/V = 0.063 \text{ gm/L (at } 25^\circ\text{C})$$

Ethylbenzene

$$M/V = (0.09 \times 0.013 \text{ atm} \times 106.17 \text{ gm/mol}) / (0.0821 \text{ atm-L/mol K}^\circ \times 298 \text{ K}^\circ)$$

$$M/V = 0.00508 \text{ gm/L (at } 25^\circ\text{C})$$

Xylenes

$$M/V = (0.17 \times 0.012 \text{ atm} \times 106.17 \text{ gm/mol}) / (0.0821 \text{ atm-L/mol K}^\circ \times 298 \text{ K}^\circ)$$

$$M/V = 0.00885 \text{ gm/L (at } 25^\circ\text{C})$$

The results indicate that even though Toluene's total mass percentage in the weathered gasoline was greater, Benzene is present in the soil atmosphere at higher concentration because of its greater vapor pressure.

■ 5.7 Vapor Density

The vapor density of most VOCs is greater than the density of air (Table 5.4). The vapor density is proportional to the molecular weight (f_w) of a compound (at boiling point):

$$\rho_{\text{vapor}} = \frac{P^a f_w}{RK^0} \quad (5.35)$$

The density of dry air is 1.2 grams per liter at 20°C . The average molecular weight of air is 29 g/mol. Based on these values, the vapor density of VOC can be calculated by comparing the weight of a vapor or gas compared to an equal volume of air (air = 1) (Table. 5.4).

All example compounds in Table 5.4 form vapors that are denser than air. As a result, those VOCs vapors tend to sink and accumulate deeper into the unsaturated zone. This phenomenon is known as **density driven transport** of vapors (Schwille 1988; Falta et al. 1989). Vapors from organic liquids that are suspended as residual in the unsaturated zone can migrate considerable distances through the aerated pore space and thus cause extensive contamination of the groundwater (Mendoza and Frind 1990; Jang and Aral 2007). The magnitude of the density driven vapor phase transport is dependent on the properties of the VOC and the porous medium. Neglecting density driven transport of vapors can underestimate the VOC distribution in the unsaturated and saturated zone.

The importance of density driven VOC transport in the vapor phase can be examined by introducing the gas phase retardation coefficient R_g (Falta et al. 1989).

TABLE 5.4 Molecular weights and vapor densities of select volatile organic compounds compared to air.

Compound	Molecular Weight (g/mol)	Vapor Density @ 25°C (g/liter)	(lb/ft ³)
Air	29	1	0.062
Trichloroethylene	131.5	4.5	0.281
Tetrachloroethylene	165.5	5.83	0.364
Dichloromethane	84.9	2.9	0.181
Gasoline	100–105	4.4	0.275

Source: <http://www.chemicalbook.com>

$$R_g = \frac{S_w}{HS_g} + \frac{\rho_b K_D}{HnS_g} \quad (5.36)$$

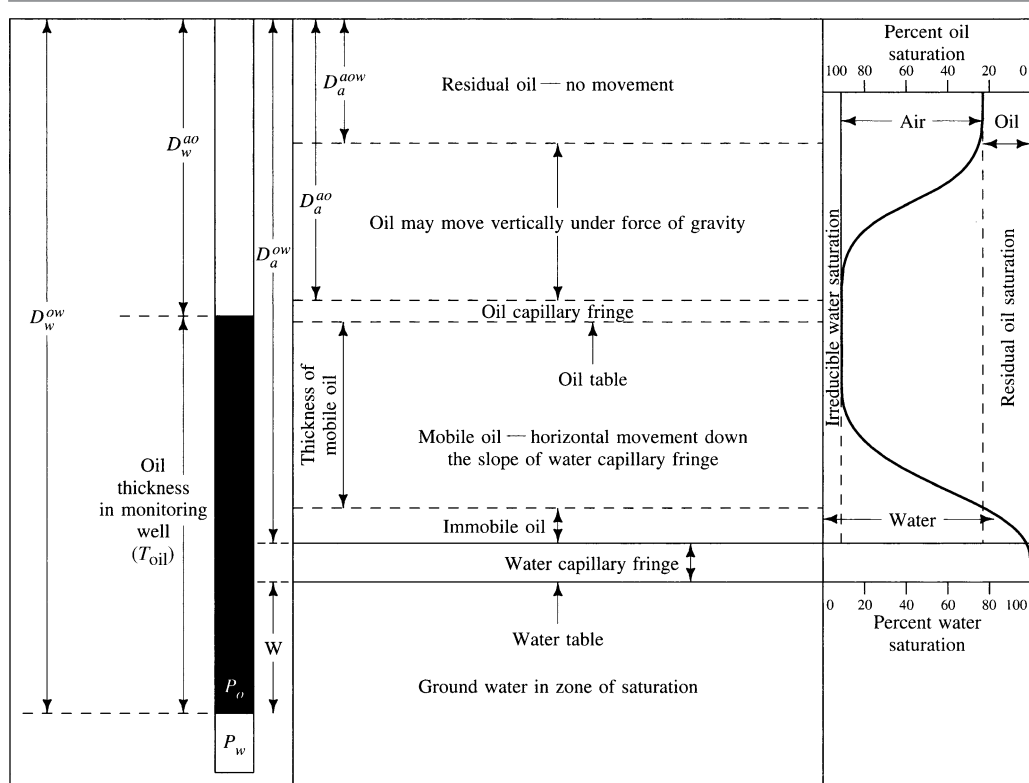
where H is the Henry's constant, ρ_b is the bulk density of the dry soil, K_D is the solid-water distribution coefficient. S_w and S_g are the fractions of pores occupied by water and gas, respectively. This definition of R_g is analogous to the standard water phase retardation coefficient, R (see Chapter 3). Essentially, R_g is equal to the ratio of the unretarded gas phase velocity to the actual VOC gas phase velocity retarded by the solid and aqueous phase partitioning. Falta et al. (1989) shows the estimated R_g values for a number of VOC. Most chlorinated aliphatic compounds, such as TCE or TCA, have comparably small R_g values ($R_g < 4$), which indicates that these VOCs are strongly affected by density driven transport processes. Conant et al. (1996) numerically simulated TCE vapor phase transport and found that variations in organic carbon content together with seasonal temperature variations exerted the greatest control on retardation of vapor migration, and to a lesser extent moisture content. In contrast to the saturated zone, diffusive transport processes proceed much faster in the gas phase and can contribute substantially to the overall mass transport, even over distances exceeding 100 meters (Jang and Aral 2007). Falta et al. (1989) concluded that the gas phase permeability of the unsaturated porous medium must be at least $1 \cdot 10^{-11} \text{ m}^2$ ($1.076 \cdot 10^{-9} \text{ ft}^2$) for density driven transport processes in the vapor phase to become important.

■ 5.8 Measurement of the Thickness of a Floating Product

The discovery of free gasoline, diesel, or other petroleum product flowing on top of the water table at or near gas stations or refineries in the 1980s was a major impetus for sparking research into contaminant fate and transport in the subsurface. While in most industrialized countries the worst of those NAPL sites have been investigated by now (e.g., Boving and Blue 2002; Essaid et al. 2011), it must be assumed that there are many undiscovered NAPL sites in countries where, so far, little or no attention has been paid to the systematic investigation of potential NAPL release sites. It is therefore likely that the discovery of free floating product will remain the starting point for many future site investigations and subsequent remediation projects.

The measurement of the amount of mobile LNAPL above the water table is not straightforward. Winegardner and Testa (2000) provide an overview about methods for the subsurface NAPL detection. Figure 5.21 shows the distribution of an LNAPL above the water table for the condition where a water capillary zone exists. This diagram shows that there is a zone of immobile LNAPL above the capillary zone where the LNAPL content is less than the residual LNAPL saturation. When the LNAPL content exceeds the residual LNAPL saturation and the sum of the water saturation and the LNAPL saturation is 100%, there will be positive pore pressures. In this zone LNAPL will be mobile and can flow laterally into a monitoring well. The screen zone of the monitoring well must thus extend above the top of the zone of free or mobile LNAPL. The water level in the monitoring well will initially be at the water table, which is below the level of the bottom of the mobile LNAPL zone. The LNAPL will flow down the monitoring well to the water table. The weight of the LNAPL will then depress the surface of the water in the monitoring well below that of the water table. As a result the thickness of LNAPL measured in a monitoring well is greater than the actual thickness of the mobile LNAPL in the vadose zone. This effect is greater for thin zones of free LNAPL, where the capillary zone may be much thicker, than for a thick

FIGURE 5.21 Comparison of distribution of mobile oil in an aquifer with the thickness of floating oil in a monitoring well for the case where a water capillary fringe exists below the zone of mobile oil.



zone of free LNAPL, where the capillary zone may be thin or missing. It is also greater in fine-grained materials, where the capillary fringe may be thicker.

The depth below the water table at which the LNAPL will reach equilibrium in a monitoring well can be calculated. At equilibrium, the pressure in the monitoring well on the LNAPL side of the interface is P_o , and the pressure on the water side of the interface is P_w . The two pressures must be equal:

$$P_o = P_w \quad (5.37)$$

P_o is equal to the density of the oil, ρ_o , times the thickness of the oil layer, T_{oil} .

$$P_o = \rho_o T_{oil} \quad (5.38)$$

P_w is equal to the density of the water, ρ_w , times the distance from the water table to the interface, W .

$$P_w = \rho_w W \quad (5.39)$$

Since $P_o = P_w$, then

$$\rho_o T_{oil} = \rho_w W \quad (5.40)$$

Solving for W yields

$$W = \left(\frac{\rho_o}{\rho_w} \right) T \quad (5.41)$$

The U.S. EPA published a guidance document regarding methods for evaluating the recoverability of free product (U.S. EPA 1996). In it, it compares seven methods for evaluating the volume of free product in the subsurface. Lundegard and Mudford (1998) estimated LNAPL volume from nonlinear regression analysis of LNAPL saturation profiles and van Genuchten equation parameters. Farr et al. (1990) and Lenhard and Parker (1990) developed two methods to estimate the volume of recoverable LNAPL in an aquifer based on the thickness of the LNAPL floating in a monitoring well. These methods are based on the capillary soil properties. One of the two methods is based on the determination of soil properties as reported by Brooks and Corey (1966). We will look at this method in some detail using the derivation of Farr et al. (1990).

T as shown in Figure 5.21 is the difference between the depth to the water-oil interface in the well, D_w^{ow} and the depth to the oil-air interface, D_a^{ao} . The values of the depth to the oil table in the aquifer, D_a^{ow} , and the depth to the top of the capillary fringe, D_a^{ao} , can be computed.

$$D_a^{ao} = D_w^{ao} - \frac{P_d^{ao}}{\rho_o g} \quad (5.42)$$

$$D_a^{ow} = D_w^{ow} - \frac{P_d^{ow}}{(\rho_w - \rho_o)g} \quad (5.43)$$

where

- P_d^{ao} = the Brooks-Corey air-organic displacement pressure
- P_d^{ow} = the Brooks-Corey organic-water displacement pressure
- g = the acceleration of gravity

Equation 5.43 may be rewritten as

$$D_a^{ow} = D_w^{ao} + T_{oil} - \frac{P_d^{ow}}{(\rho_w - \rho_o)g} \quad (5.44)$$

If any of the organic liquid exists at a positive pore pressure, then D_a^{ow} will be greater than D_w^{ao} and from Equation 5.43,

$$T_{oil} \geq \frac{P_d^{ow}}{(\rho_w - \rho_o)g} \quad (5.45)$$

If the organic liquid is all under tension in the capillary zone, then there will be no mobile organic layer and no organic liquid will collect in the monitoring well. Under these conditions, Equations 5.42 through 5.45 are not applicable. However, as soon as free organic liquid appears in the aquifer, it will collect to a depth of at least $P_d^{ow} / (\rho_w - \rho_o)g$.

The total volume of nonresidual organic liquid in the vadose zone is given by

$$V_o = n \left\{ \int_{D_a^{ow}}^{D_a^{ow}} (1 - S_w) dz - \int_{D_a^{ow}}^{D_a^{ao}} [1 - (S_w + S_o)] dz \right\} \quad (5.46)$$

where

- V_o = the volume of organic liquid per unit area
- n = the porosity
- S_w = the water-saturation ratio
- S_o = the organic liquid saturation ratio
- z = the vertical coordinate measured positively downward
- D_a^{ow} = a value determined from Equation 5.40
- D_a^{ao} = a value determined from Equation 5.39
- D_a^{ao} = the top of the zone where nonresidual oil occurs

Based on work by Lenhard and Parker (1987; 1988), the fluid-content relations are

$$S_o - S_{wi} = (1 - S_{wi}) \left(\frac{P_c^{ao}}{P_d^{ao}} \right)^{-\lambda} + S_{wi} \quad P_c^{ao} > P_d^{ao} \quad (5.47a)$$

$$S_o + S_w = 1 \quad P_c^{ao} < P_d^{ao} \quad (5.47b)$$

$$S_w = (1 - S_{wi}) \left(\frac{P_c^{ow}}{P_d^{ow}} \right)^{-\lambda} + S_{wi} \quad P_c^{ow} > P_d^{ow} \quad (5.48a)$$

$$S_w = 1 \quad P_c^{ow} < P_d^{ow} \quad (5.48b)$$

where

- S_{wi} = the irreducible water saturation
- λ = the Brooks-Corey pore-size distribution index

In addition,

$$P_c^{ao} = \rho_o g \left(D_w^{ao} - \left(P_d^{ao} / \rho_o g \right) - z \right) + P_d^{ao} \quad (5.49)$$

$$P_c^{ow} = g(\rho_w - \rho_o) \left[D_w^{ow} - \frac{P_d^{ow}}{(\rho_w - \rho_o)g} - z \right] + P_d^{ow} \quad (5.50)$$

Integration of Equation 5.46 for $D_w^{aow} > 0$, using Equations 5.47 through 5.50 yields the following. For λ not equal to 1,

$$V_o = \frac{\phi(1-S_{wi})D}{(1-\lambda)} \left[\lambda + (1-\lambda) \left(\frac{T_{oil}}{D} \right) - \left(\frac{T_{oil}}{D} \right)^{1-\lambda} \right] \quad (5.51a)$$

For λ equal to 1,

$$V_o = n(1-S_{wi}) \left[1 - D(1 + \ln T_{oil}) \right] \quad (5.51b)$$

where

$$D = \frac{P_d^{ow}}{(\rho_w - \rho_o)g} - \frac{P_d^{ao}}{\rho_o g}$$

$$T_{oil} = D_w^{ow} - D_w^{ow} \geq \frac{P_d^{ow}}{(\rho_w - \rho_o)g}$$

If organic liquid above the residual saturation exists all the way to the land surface, then D_a^{aow} does not exist. Under this condition integration of Equation 5.46 yields the following. For λ not equal to 1,

$$V_o = n(1-s_{wi}) \left\{ (T_{oil} - D) - \frac{P_d^{ao}}{\rho_o g(1-\lambda)} \left[1 - \left(\frac{\rho_o g D_w^{ao}}{P_d^{ao}} \right)^{1-\lambda} \right] \right\} \quad (5.52a)$$

$$+ \frac{P_d^{ow}}{(\rho_w - \rho_o)g(1-\lambda)} \left[1 - \left(\frac{(\rho_w - \rho_o)g D_w^{ow}}{P_d^{ow}} \right)^{1-\lambda} \right]$$

For λ equal to 1,

$$V_o = n(1-S_{wi}) \left[(T_{oil} - D) - \frac{P_d^{ow}}{(\rho_w - \rho_o)g} \ln D_w^{ow} + \frac{P_d^{ao}}{\rho_o g} \ln D_w^{ao} \right] \quad (5.52b)$$

The Brooks-Corey soil parameters can thus be used to estimate the volume of recoverable organic liquid in an aquifer based on the thickness of the organic liquid in the well, the measured depths in the well to the air-organic interface, and the organic water interface, along with the densities of the organic liquid and the water. One must measure the Brooks-Corey soil parameters and the densities in the lab. The weakness in the Brooks-Corey approach is that it may not be accurate for very small volumes of mobile organic liquid in the soil. From Equation 5.45 the thickness of organic liquid in the well is at least $P_d^{ow} / [(\rho_w - \rho_o)g]$, even for very small volumes of mobile LNAPL.

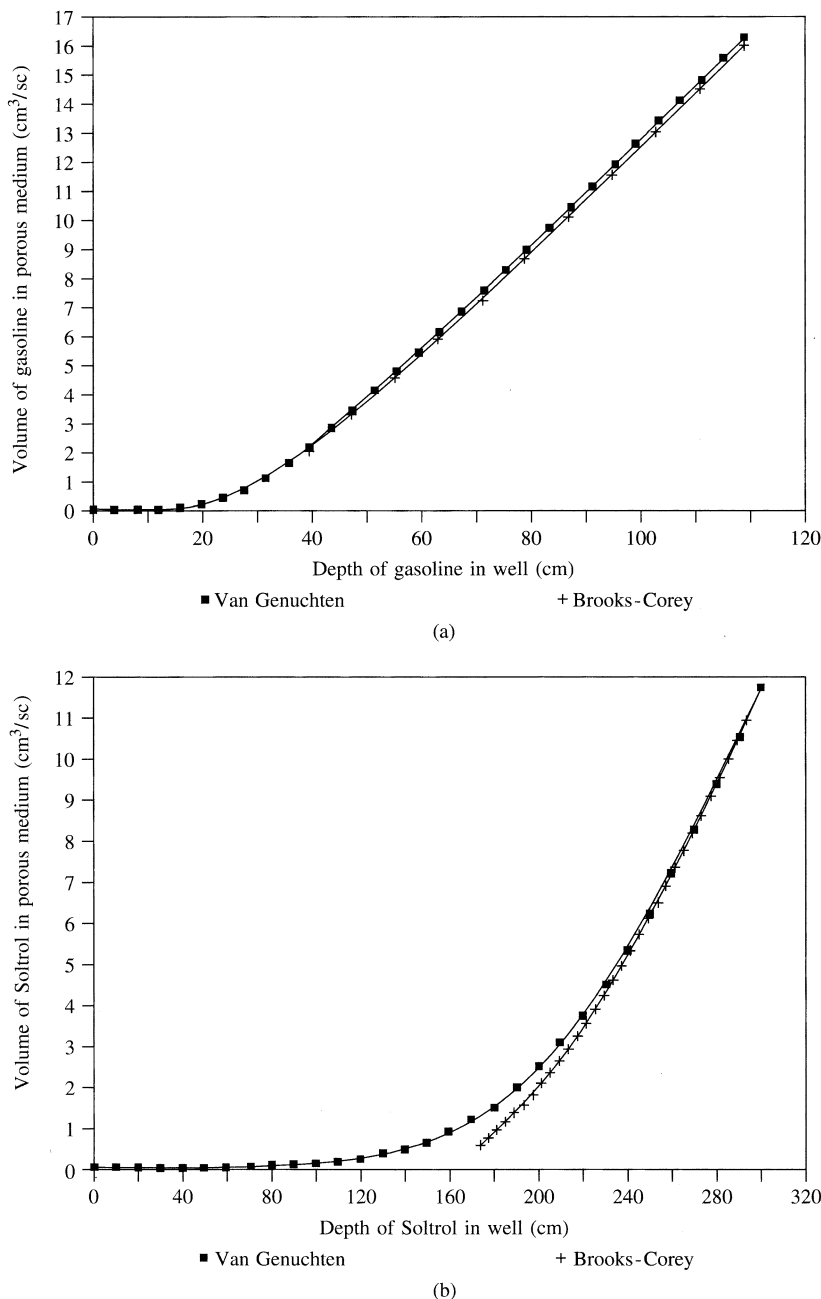
Farr et al. (1990) also presented an alternative method of analysis based on soil parameters developed by van Genuchten (1980). However, the equations based on the van Genuchten soil parameters are nonlinear and can't be solved analytically; they must be solved numerically. Thus this model is not as convenient as the one based on a Brooks-Corey soil. However, under certain conditions, such as thin layers of mobile organic liquid in the soil, the van Genuchten model may be more accurate than the Brooks-Corey model.

Figure 5.22(a) shows a graph of the volume of gasoline in a sandstone versus the measured thickness in a well computed by both the Brooks-Corey soil model and the van Genuchten soil model. Figure 5.22(b) shows the same thing for a different organic liquid, Soltrol (Farr et al. 1990). It can be seen that for gasoline in sandstone, the van Genuchten and Brooks-Corey models yield quite similar results. However, for Soltrol, they do not, because the Brooks-Corey model has a somewhat greater thickness of organic liquid in the well for very small volumes in the soil. Figure 5.23(a) shows the computed volume-thickness relationships, based on the van Genuchten soil model, for several LNAPLs in a sandstone. Figure 5.23(b) shows the computed volume-thickness relationships, again based on the van Genuchten soil model, for gasoline in a number of different porous media (Farr et al. 1990). These diagrams illustrate the fact that there is no simple, constant relationship between the volume of an LNAPL in a soil and the thickness as measured in a monitoring well. It is a function of the properties of both the soil and the organic liquid.

The above analyses assumed that the capillary pressure—saturation characteristic relations were independent of the prior wetting history of the soil. As was shown in Chapter 4, hysteresis does affect the soil characteristic curves.

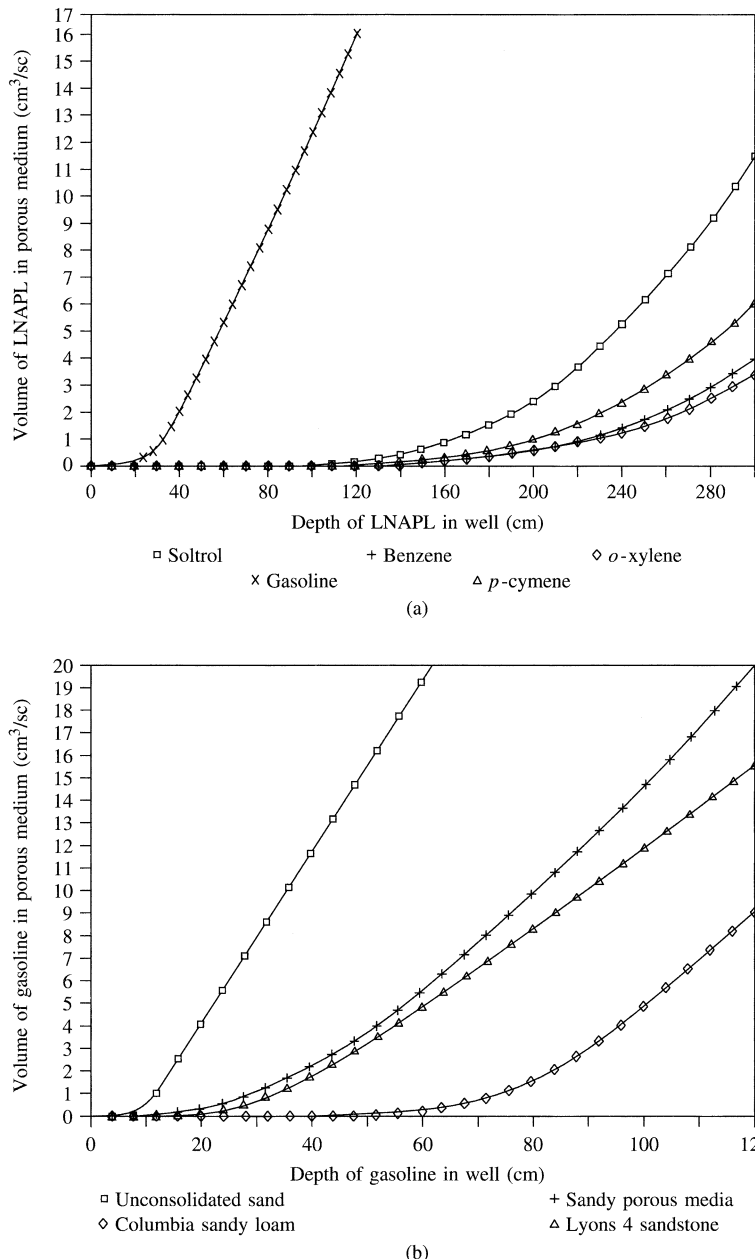
There is a tendency for the field hydrogeologist to conclude that if there is a layer of LNAPL found in a water table monitoring well, that mobile hydrocarbon must exist in the vicinity of the well. Indeed, the natural tendency is to assume that the greatest thickness of "mobile" LNAPL is in the area where the monitoring wells show the greatest thickness of product. However, both the Brooks-Corey and the van Genuchten capillary pressure models show that with equal amounts of LNAPL in the soil, a finer sediment will have a greater thickness of LNAPL in the monitoring well. If one puts a recovery well in the spot where the greatest thickness of product occurs in a monitoring well, that spot may be where the formation is finest and hence least permeable so that the opportunity to recover any LNAPL will be the least (Huntley et al. 1994a). Moreover, the thickness of the "mobile" layer as calculated by any equation cannot be multiplied by the soil porosity to find the volume of "mobile" oil. In the first place, even in the zone of "mobile oil" there is a certain amount of water trapped; in fact, the water content may even be greater than the oil content. As a result, the relative

FIGURE 5.22 Volume of recoverable LNAPL in a porous media as a function of the depth of product floating in a monitoring well as computed by the method of Farr et al. (1990) based on both van Genuchten and Brooks-Corey soils models for (a) gasoline and (b) Soltrol.



Source: A. M. Farr, R. J. Houghtalen, and D. B. McWhorter. 1990. Volume estimation of light nonaqueous phase liquids in porous media. *Groundwater* 28:48–56. Used with permission.

FIGURE 5.23 Volume of recoverable LNAPL in a porous media as a function of the depth of product floating in a monitoring well as computed by the method of Farr et al. (1990) based on a van Genuchten soil model (a) for various LNAPLs in a sandstone and (b) for gasoline in various porous media.



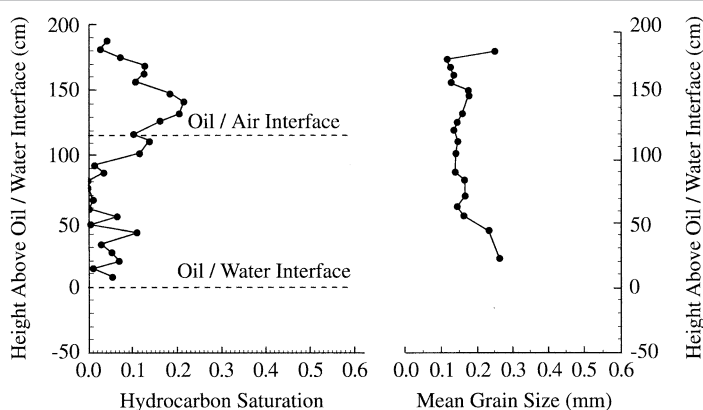
Source: A. M. Farr, R. J. Houghtalen, and D. B. McWhorter. 1990. Volume estimation of light nonaqueous phase liquids in porous media. *Groundwater* 28:48–56. Used with permission.

permeability for the LNAPL is much less than the permeability that would occur if the sediment were fully saturated with the LNAPL. The low relative permeability of the LNAPL means that it will not be possible to recover much of an LNAPL that has been spilled, especially in a fine-grained formation. Furthermore, there will be residual oil even after all “mobile oil” has been captured.

Huntley et al. (1994a) made a detailed study of the distribution of hydrocarbon in soil and groundwater in an area of fine-grained soils. There were five monitoring wells with floating hydrocarbon layers between zero and 1.5 m (~5 ft) thick. They made detailed measurements of the hydrocarbon saturation every six centimeter. They found that hydrocarbon saturation never exceeded 0.5, and was usually much less than that. (Hydrocarbon saturation of 1.0 would occur if the pores were filled only with hydrocarbon.) Figure 5.24 shows the hydrocarbon saturation and mean grain size of the sediment for a monitoring well, which had 116 cm (3.8 ft) of floating hydrocarbon. Note that the highest hydrocarbon saturation occurs above the oil/air interface and that some hydrocarbon saturation is present all the way down to the oil/water interface. They also found that the capillary pressure model of Lenhard and Parker (1990) and Farr et al. (1990) did a good job of predicting the range of saturation and volume of hydrocarbon that corresponded with the measured thickness of hydrocarbon in the monitoring wells.

Huntley et al. (1994b) examined the effect of grain size variability on the estimation of hydrocarbon volumes. They found that the measured soil characteristic curves varied widely across even a small site. The most accurate estimation of hydrocarbon volume occurred when a different soil characteristic curve was used for each borehole, even if the site were relatively small. The most accurate soil characteristic curves were obtained by a pressure plate apparatus (see Chapter 4 for a discussion of soil characteristic curves and the pressure plate apparatus.)

FIGURE 5.24 Vertical hydrocarbon saturation profile in a borehole and the grain size distributions of the fine-grained sandstone at each horizon where hydrocarbon saturation was tested. The oil/water interface location and the oil/air interfaces are from a monitoring well installed adjacent to the borehole location.



Source: D. Huntley, R. N. Hawk, and H. P. Corley. 1994a. Nonaqueous phase hydrocarbon in a fine-grained sandstone: 1. Comparison between measured and predicted saturations and mobility. *Groundwater* 32:626–634. Used with permission.

Ostendorf et al. (1993) used the Lenhard and Parker (1990) model to describe the amount of aviation gasoline retained in a medium sand. This was a coarser sediment than the Huntley et al. (1994a) study. They also found that the capillary pressure model accurately described the distribution of free and residual hydrocarbon.

■ 5.9 Effect of the Rise and Fall of the Water Table on the Distribution of LNAPLs

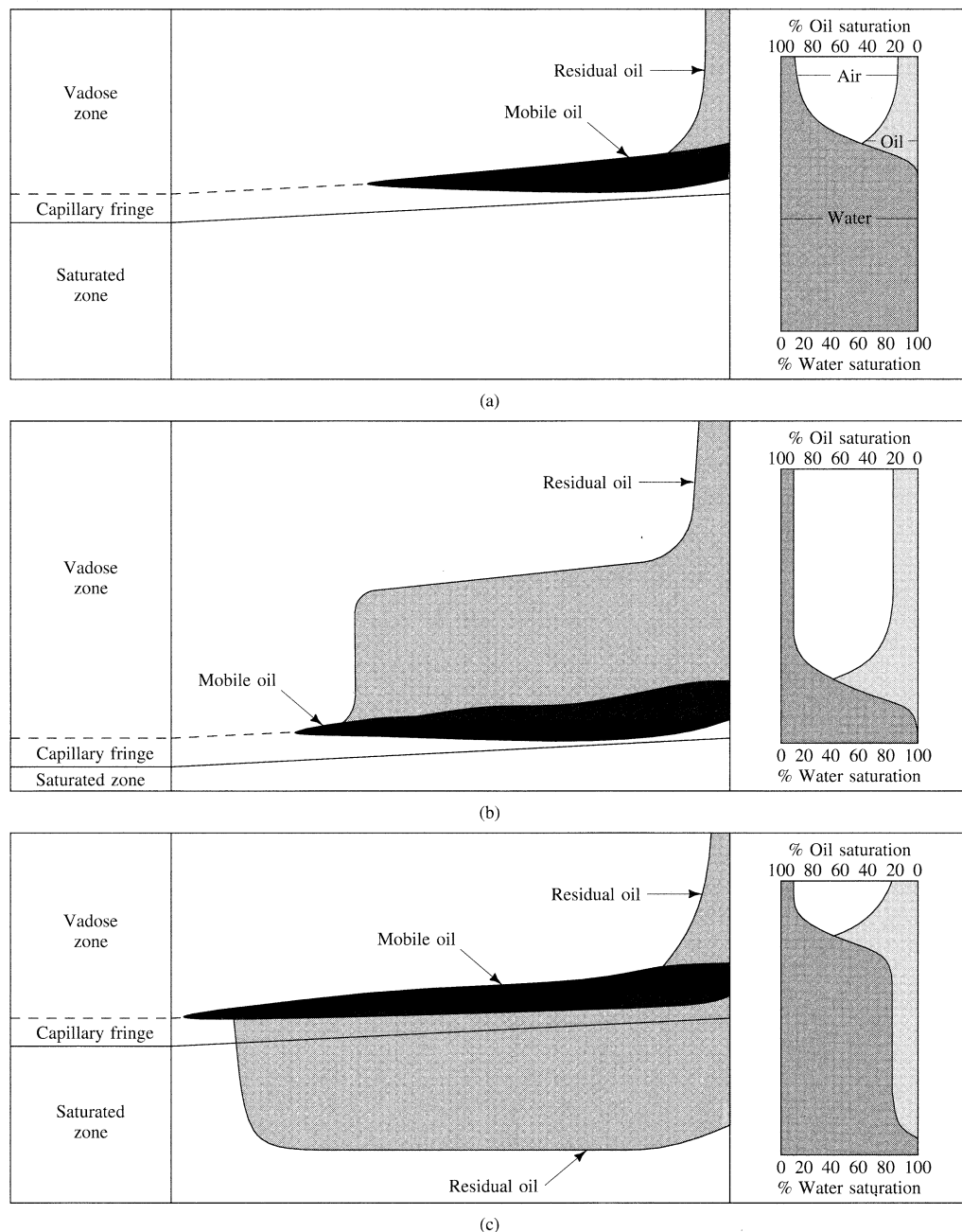
The flow of LNAPLs is complicated by the rise and fall of the water table with the seasons. Figure 5.25(a) shows a layer of oil floating on the surface of the capillary zone. As the water table falls, the layer of mobile oil also falls. Residual oil is left in the vadose zone above the oil table as it falls. This smearing of NAPL is illustrated in Figure 5.25(b). When the water table rises, the oil table also rises. However, as Figure 5.25(c) illustrates, residual oil is left behind in the saturated zone. If the water table rises faster than the oil table can rise, “pockets” of free oil might become left below the water table. The flow of water and hydrocarbons is controlled by Darcy’s law and depends upon the effects of density, viscosity, and relative permeability. Depending upon these factors, either the hydrocarbon or the water could have a greater velocity as the water table rises and falls.

Marinelli and Durnford (1996) noted four common observations that field hydrogeologists make at hydrocarbon spill sites and offered explanations for each that are related to the rise and fall of the water table.

1. *Monitoring wells may have no floating LNAPL even though there is considerable hydrocarbon in the adjacent soil.* This may occur due to entrapped hydrocarbon both above and below the water table due to fluctuations in the water table.
2. *The thickness of floating LNAPL in a monitoring well decreases when the water table rises.* Oil will be trapped in the soil as the water table rises and hence there is less mobile oil able to enter the well.
3. *LNAPL may suddenly appear or disappear in monitoring wells across the site.* A sudden increase in the water table may completely trap the hydrocarbon and result in a complete disappearance of floating LNAPL in monitoring wells. The Brooks-Corey model suggests that there is a minimum amount of mobile oil that must be present before any LNAPL will accumulate in a monitoring well. When the minimum amount is exceeded, LNAPL will suddenly appear in the well.
4. *If the water table drops to a point where it is lower than at any previous time, the floating LNAPL may disappear.* This may be due to the fact that the hydrocarbon may move slowly through the soil and does not drop at the same rate as the water table. Hence, the system is out of equilibrium and the mobile oil has simply not had enough time to reach a new equilibrium and enter the well.

Contaminant hydrogeologists in charge of remediating LNAPL sites have to be aware of the effect of fluctuating water tables on the amount of LNAPL in their observation wells. For example, an ill-designed treatment system can lower the water table by over-pumping. In that case LNAPL may reach deeper parts of a previously uncontaminated aquifer, resulting in artificially spreading the pollution problem and creating a “smear zone.” Not only will the recovery of free phase be more difficult if LNAPL is smeared over a larger volume of aquifer, but the aqueous phase concentration will

FIGURE 5.25 Effect of a falling and then rising water table on the distribution of mobile and residual phases of an LNAPL.



likely be much higher should the pumping stop for some time. This is because when the water table returns to its pre-pumping, natural elevation, groundwater comes into close contact with residual LNAPL trapped below the water table. The increased amount of isolated globules, with a much greater surface (contact) area between the oil and water phases, results in more effective dissolution of residual phase contaminants into the aqueous phase. Occasionally in cases of rising water tables with overlying LNAPL pools and with a very dry, hydrophilic vadose zone above, the rising LNAPL pool can be entirely bypassed by rising groundwater and be trapped below the water table. In porous media with large pores spaces and large volumes of LNAPL trapped below the water table, some buoyant LNAPL globules can join together forming elongated "stringers" which can move upward to regain the water table.

The mobility of LNAPL at the pore and plume scale is discussed in SAB (2006). In cleaning up LNAPL spills, the mobile LNAPL can be removed by passive treatment systems, such as skimming wells or trenches (Chapter 9). However, a considerable amount of LNAPL will be left as a residual on the soil. Volatile LNAPLs can be removed by a soil-vapor extraction system. However, nonvolatile products will remain behind in the soil. The amount depends upon the properties of the LNAPL and the texture of the soil and can be estimated with PITT (see Section 5.4). The oil retention capacity of soil is estimated to range from 5 L/m³ for gravel to 40 L/m³ for silty sand (Testa and Paczkowski 1989). Many hydrocarbons can be degraded by soil bacteria, especially if the soil is aerobic. Systems that diffuse air into the soil have been effective in bioremediation of hydrocarbon spills. This problem is addressed in Chapter 9.

Case Study

Jet fuel is a hydrocarbon that is similar to gasoline, but has fewer of the more volatile components. However, it does contain benzene, toluene, ethylbenzene and xylene (BTEX). Jet fuel is also less dense than water (LNAPL) and its components are sparingly soluble in water.

In 1974 about 314,000 L (83,000 gal) of jet fuel escaped from an above-ground storage tank at a tank farm in South Carolina (Vroblesky et al. 1995). The shallow geology consists of a zone of Pleistocene quartz sands with lenses of clay, which is about 10 m (33 ft) thick. This forms an unconfined aquifer; however, the clay lenses can form locally confined conditions. The shallow aquifer is underlain by a thick sequence of dense clay. The water table was about 3 m (10 ft) below grade. The seasonal fluctuation of the water table amounted to about 1.5 m (5.1 ft).

Shortly after the leak was repaired, a number of shallow well points were installed in the area of groundwater contamination. Initial rates of pumping were 2460 L/min (650 gal/min). The aquifer was pumped for two weeks and total of 78,569 L (20,750 gal) of product were recovered. However, because the product was floating on the water table, the well points were shallow and the pumping rate soon dropped off precipitously due to the drop in the water table induced by pumping and the resulting lack of available drawdown in the well points. After two weeks the pumping rate was only 113 to 189 L/min (30 to 50 gal/min) and as product recovery had drastically declined, pumping was stopped after only 25 percent of the last fuel was recovered.

Further product recovery efforts with deeper well points were not successful, with only small amounts of additional jet fuel recovered. However, a plume of the dissolved components of the jet fuel (BTEX) expanded into an adjacent residential area and contaminated private drinking water wells.

An in-depth study of the problem was initiated by the United States Geological Survey beginning in 1987. The USGS found that although the jet fuel was spilled above the water table, a considerable volume of product was trapped below some clay lenses, which were below the water table.

This occurred because during the initial recovery effort, the free-phase product followed the water table downward as the recovery wells were pumped. Fuel was able to pass through the clay layer via natural discontinuities. Further pumping from later recovery efforts, which were immediately followed by below-normal precipitation caused the water table to drop below the clay layer. When the water table later rose, the jet fuel, which was still floating on the water table, became stratigraphically trapped below the clay, and hence below the water table. Figure 5.26 shows a cross section through the area of the spill.

The clue that led to the realization that the product was trapped below the water table was the fact that total dissolved BTEX from a deeper monitoring well was higher than BTEX in a water-table monitoring well. This should not have been the case if the principal source of dissolved toluene was jet fuel floating on the water table.

■ 5.10 Migration of Dense Nonaqueous Phase Liquids (DNAPLs)

5.10.1 Relative Mobility

Dense nonaqueous phase liquids (DNAPLs) have a specific gravity greater than 1. They include a number of organic compounds that have one or more chlorine, bromine or fluorine atoms. Table 5.4 lists a number of chemicals that are denser than water.

In their pure phase these chemicals may have a different mobility in the porous matrix than in water. Recall that hydraulic conductivity is a function of the intrinsic permeability of the formation as well as properties of the liquid:

$$K = k_i \rho g / \mu \quad (5.53)$$

where

K = hydraulic conductivity

k_i = intrinsic permeability

ρ = fluid density

g = gravitational constant

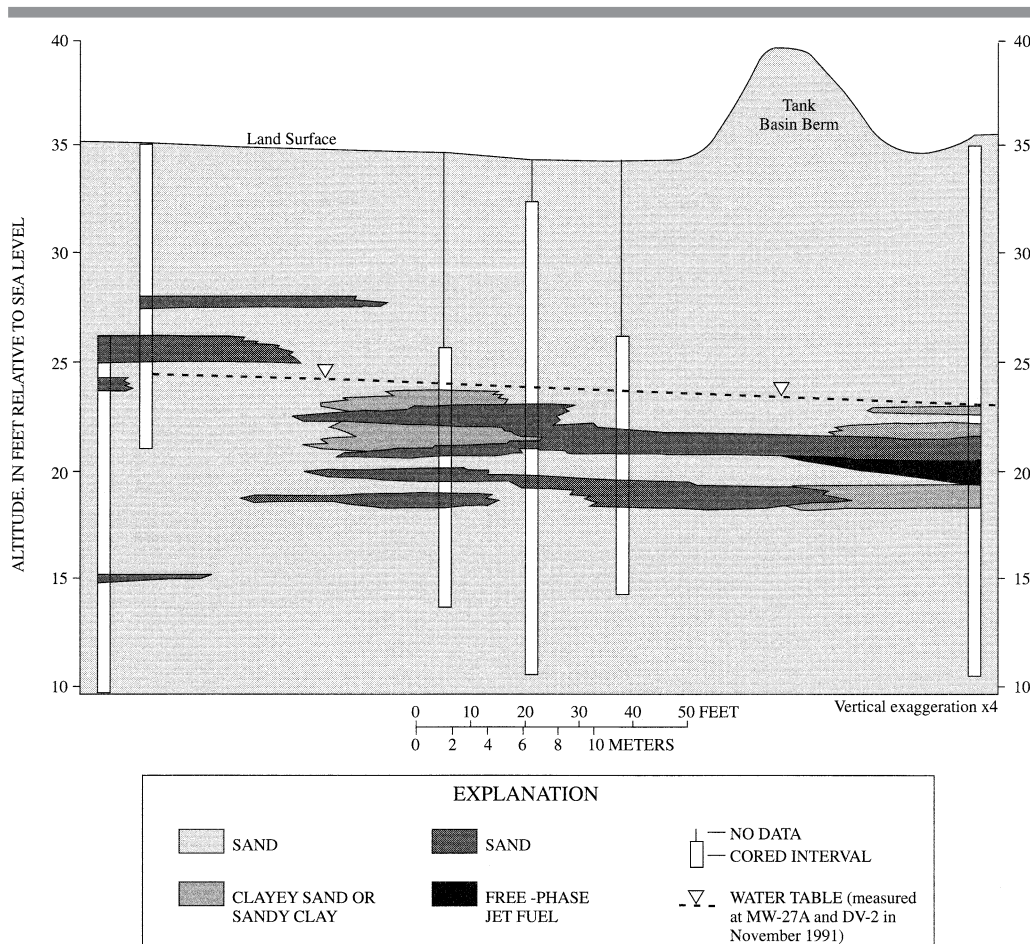
μ = fluid viscosity

The relative mobility of a nonaqueous phase liquid to water will be equal to the ratio of ρ/μ for the nonaqueous phase liquid to ρ/μ for water as the other factors are the same for both water and the nonaqueous phase liquid (Equation 5.53)

$$\text{Relative Mobility} = \frac{\left(\frac{\rho}{\mu}\right)_{\text{NAPL}}}{\left(\frac{\rho}{\mu}\right)_{\text{Water}}} \quad (5.54)$$

Many of the common chlorinated solvents are denser and less viscous than water and hence can form DNAPL with a greater relative mobility in the earth.

FIGURE 5.26 Hydrogeologic cross section beneath the location of an above ground tank from which jet fuel leaked. The free phase jet fuel is trapped beneath a clay layer due to the fall and subsequent rise of the water table.



Source: D. A. Vroblesky, J. F. Robertson, and L. C. Rhodes. 1995. Stratigraphic trapping of spilled jet fuel beneath the water table. *Groundwater Monitoring & Remediation* 15:177–183. Used with permission.

EXAMPLE PROBLEM

What is the relative mobility of trichloroethylene (TCE) to water? Consider the following properties of the two fluids:

	Density (g/cm ³)	Viscosity (lb/in ³)	Viscosity (Centipoise)
Water	0.997	0.0360	0.895
Trichloroethylene	1.465	0.0529	0.57

The ratio of ρ/μ for water is 1.114 and for TCE it is 2.57. The relative mobility of TCE is the ρ/μ ratio of TCE divided by the ρ/μ ratio of water or 2.57/1.114. Thus, for single phase flow, TCE is 2.31 times more mobile than water, all other things being the same.

5.10.2 Vadose Zone Migration

When spilled on the land surface or discharged to the subsurface, once the residual saturation value is exceeded DNAPLs move vertically in the vadose zone under the influence of gravity. Because it is the wetting liquid, water occupies the smaller pores and capillary channels in the vadose zone. The DNAPL migrates through the larger pore openings, which initially have water coating the mineral grains, with air filling the remainder of the pore. The DNAPL displaces the air, so the pore becomes filled with the small amount of water wetting the mineral surface and the DNAPL. The vadose zone permeability for the DNAPL can be greater than for water because the pores through which the DNAPL, as the nonwetting fluid, is migrating are larger than the pores through which the water, as the wetting fluid, resides. Downward DNAPL movement of large pore spaces, including through fractured rock can be inhibited by matrix diffusion, that is, if significant amounts of DNAPL are captured by surrounding rock thus reducing DNAPL's fluid pressure. If a downward moving DNAPL encounters a wet, fine layer such as a clay, the water held tightly in the pore space will form a capillary barrier, and the DNAPL will pool up above it and spread out horizontally. If the clay lens is limited in horizontal extent and "pinches out" DNAPL can move around it and continue downward. Alternatively, if the expanding DNAPL pool becomes thick enough, the DNAPL can build up enough fluid pressure to supplant water in the clay and continue downward through the clay, particularly if the clay contains fractures, microfractures, or discontinuities. Work by several authors including Reynolds, Pankow, Parker, Gillham and others have shown DNAPL movement through clay microfractures with aperture sizes as small as 15 μm . Aperture inclination and many other factors effect downward movement, but the geologic prevalence of horizontal capillary barriers often gives rise to a classic NAPL subsurface distribution of DNAPL in vertical or near vertical "fingers" coupled with horizontal or near horizontal "pools".

When the DNAPL reaches the capillary zone, where the pores are all filled with water, it must start to displace water in order to migrate downward. This displacement of water with DNAPL also occurs below the water table. Poulson and Kueper (1992) released tetrachlorethylene (PCE) into the vadose zone of a natural formation consisting of fine to medium grained quartz sand deposited as a prograding foreshore sequence associated with a glacial lake. The sands had horizontal bedding. The PCE was dyed so that it could be observed in the soil. After the release of PCE the formation was excavated and the resulting distribution of PCE was determined. It was found that the PCE did not immediately penetrate vertically but spread out horizontally due to fine-scale structure in the sand. The fine structure was the result of varying grain sizes in the sediment. Residual saturation was on the order of 0.5 to 1.5% PCE by bulk volume.

TABLE 5.5 DNAPL chemicals and compounds that are liquid at ambient temperatures (15 to 25°C).

	Density	
	(g/cm ³)	(lb/in ³)
Halogenated solvents with one carbon atom		
Methylene Chloride (Dichloromethane)	1.33	0.0480
Chloroform (Trichloromethane)	1.48	0.0535
Carbon tetrachloride (Tetrachloromethane)	1.59	0.0574
Dibromochloromethane	2.45	0.0885
Halogenated solvents with two carbon atoms		
1,1-Dichloroethane	1.18	0.0426
1,2-Dichloroethane	1.23	0.0444
1,1-Dichloroethylene	1.22	0.0441
1,2-Dichloroethylene (Cis- and trans- isomers)	1.26	0.0455
1,1,1-Trichloroethane	1.34	0.0484
1,1,2-Trichloroethane	1.43	0.0517
Trichloroethylene	1.46	0.0527
1,1,2,2-Tetrachloroethane	1.60	0.0578
Tetrachloroethylene (Perchloroethylene)	1.62	0.0585
Ethylene dibromide (1,2-Dibromoethane)	2.17	0.0784
Halogenated solvents with three carbon atoms		
1,2-Dibromo-3-chloropropane	2.05	0.0741
1,2-Dichloropropane	1.16	0.0419
Halogenated Aromatic Compounds		
1,2-Dichlorobenzene	1.30	0.0470
1,4-Dichlorobenzene	1.25	0.0452
Polychlorinated Biphenyls		
Aroclor 1016	1.33	0.0480
Aroclor 1221	1.15	0.0415
Aroclor 1232	1.24	0.0448
Aroclor 1242	1.39	0.0502
Aroclor 1248	1.41	0.0509
Aroclor 1254	1.51	0.0546
Nonhalogenated Chemicals		
Carbon Disulfide	1.26	0.0455

Mixtures

It is not uncommon to discover complex mixtures of NAPL contaminants at spill sites, such as coal tar, creosote, or asphalt. These mixtures contain many dense chemicals that are solids at ambient temperatures, such as the polynuclear aromatics. They also contain chemicals that are less dense than water but are liquid. If the proportion of the liquid chemicals is great enough, the mixture is a liquid. The exact density and consistency will depend upon the particular mix of chemicals present and, to some extent, the subsurface temperature.

5.10.3 Vertical Movement in the Saturated Zone

If water in the unsaturated zone is static, the DNAPL will continue to migrate downward under the force of gravity. In order to displace the water filling the pores, the DNAPL must have sufficient mass to overcome the capillary forces that hold the water in the pore. Vertical stringers of DNAPL can occupy vertically connected pores, also known as preferential flow pathways. When the vertical stringer has a sufficient height, its weight can displace the water in the pore. The critical height, h_o , can be determined from Robson's formula (Berg 1975):

$$h_o = \frac{2\sigma \cos \theta (1/r_t - 1/r_p)}{g(\rho_w - \rho_o)} \quad (5.55)$$

where

σ = interfacial tension between the two liquids

θ = wetting angle

r_t = pore-throat radius

r_p = pore radius

g = acceleration of gravity

ρ_w = density of water

ρ_o = density of the DNAPL

For a well-rounded, well-sorted sediment of diameter d with rhombohedral packing, the pore-throat radius, r_t and the pore radius, r_p , can be estimated from the following formulas:

$$r_p = 0.212d \quad (5.56)$$

$$r_t = 0.077d \quad (5.57)$$

The smaller the sediment diameter, the smaller both the pore-throat radius and pore radius. Equation 5.55 demonstrates that the value of h_o is inversely related to the pore diameter. For finer-grained materials, the DNAPL stringer must be longer than for coarser materials. Even thin, fine-grained layers could act as confining layers for a DNAPL.

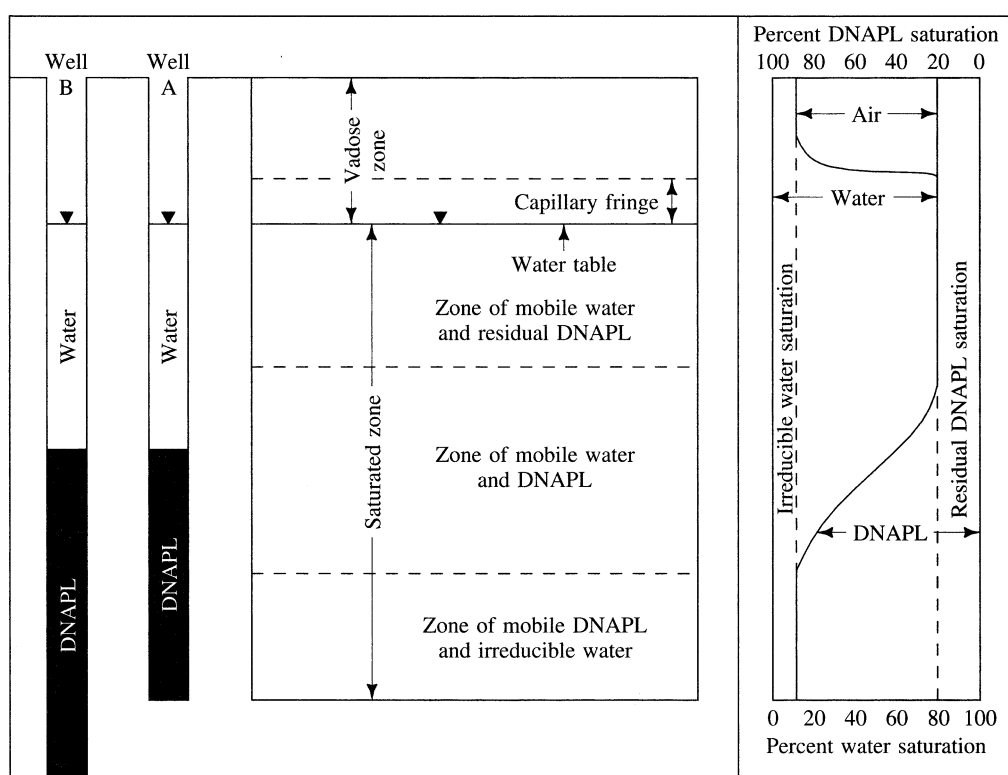
If sufficient amounts of the DNAPL are present to overcome the capillary pressure and expel water from pores, DNAPL will continue to migrate downward under the force of gravity until it reaches an aquitard layer, where the pore openings are so small that the DNAPL cannot overcome the capillary forces binding the water in the pores. A layer of DNAPL then accumulates on the surface of the aquitard. This zone also has irreducible water present. Fluid pumped from this zone is exclusively DNAPL. Above the layer of DNAPL and irreducible water, there is a zone with DNAPL and water content above the irreducible saturation. Fluid pumped from this level includes both DNAPL and water. From the top of this zone to the water table, the pores contain residual DNAPL and water. Fluid pumped from this zone is water. Since many DNAPLs are slightly to moderately soluble in water, water pumped from

any of these zones can also contain dissolved organics. Figure 5.27 shows the DNAPL zones described previously.

Monitoring wells to detect DNAPLs should be placed at the bottom of the aquifer, just at the top of the confining layer. There is a great danger that DNAPL might migrate deeper into parts of an aquifer system if a confining layer separating the aquifers is completely perforated and the area around the well has not been properly sealed. This seepage or hydraulic shortcircuiting has been reported in cases where compromised borehole seals, particularly at sites where wells were installed for remediation or monitoring purposes, act as conduits that transmit water and contaminants between aquifers separated by otherwise continuous and relatively impervious confining layers (U.S. EPA 1987; Lacombe et al. 1995; Santi et al. 2006; Mercer et al. 2007).

DNAPL from the zone of mobile DNAPL and irreducible water flows to the monitoring well, as will both water and DNAPL from the zone where both are mobile. The water and DNAPL from this zone will separate in the monitoring well, with the DNAPL sinking and the water rising. Well A in Figure 5.27 shows that the total depth of the DNAPL in the monitoring well is below the top of the zone where both water and DNAPL are present. The exact position depends upon the average DNAPL saturation

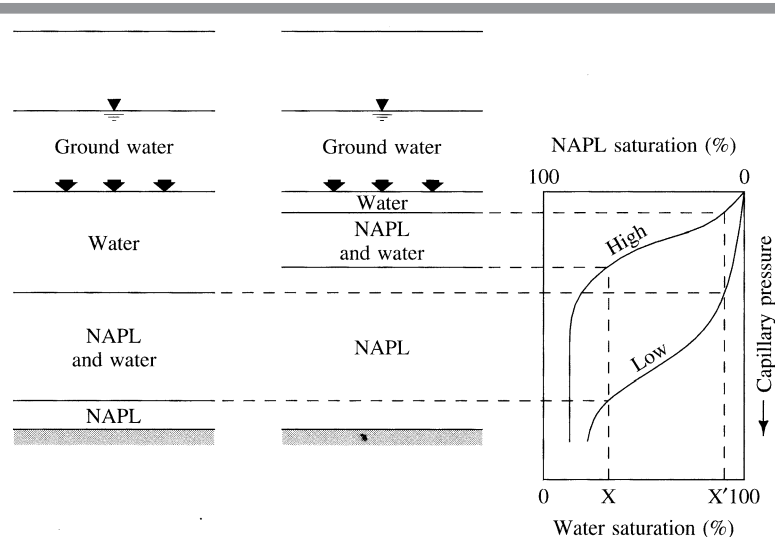
FIGURE 5.27 Zones of a DNAPL and the relationship of mobile DNAPL and nonmobile DNAPL to the DNAPL saturation; relationship of mobile DNAPL thickness to thickness of DNAPL is measured in a monitoring well.



in this zone. If a monitoring well extends below the top of the confining layer, a false thickness of the DNAPL will be measured, as it will fill the monitoring well below the level of the confining layer. Monitoring Well B in Figure 5.27 shows this circumstance.

The relative thickness of the various zones described here depends upon the grain-size distribution, which is reflected in the permeability of the saturated zone. A low permeability aquifer (small pores) will have a thin layer of DNAPL collect on the bottom, while a more permeable aquifer (large pores) will have a thicker zone of mobile NAPL on the bottom and a thinner zone where both DNAPL and water are mobile. Figure 5.28 illustrates this phenomenon (Villaume 1985).

FIGURE 5.28 Effect of high and low permeability (and porosity) on the distribution of mobile DNAPL at the bottom of an aquifer; the arrows indicate level of original injection of the DNAPL.



Source: J.F.Villaume. 1985. Investigations at sites contaminated with dense nonaqueous phase liquids (NAPLS). *Groundwater Monitoring & Remediation* 5:60–74. Used with permission.

5.10.4 Horizontal Movement in the Saturated Zone

If the DNAPL exists in a continuous phase, it will move below the water table according to the force vector E_{DNAPL} described in Equation 5.16. If the DNAPL is in the form of discontinuous stringers that are sinking in the aquifer, flowing groundwater will tend to displace the DNAPL stringers in the direction of flow. Just as the sinking DNAPL stringers displace water by overcoming the capillary pressure holding the water in a pore, the laterally moving water must overcome the capillary pressure of the DNAPL stringer to displace it sideways.

Villaume (1985) indicates that the lateral pressure gradient needed to displace a DNAPL sideways, grad P , is given by

$$\text{grad } P = \frac{2\sigma}{L_o \left(\frac{1}{r_t} - \frac{1}{r_p} \right)} \quad (5.58)$$

where

σ = interfacial tension

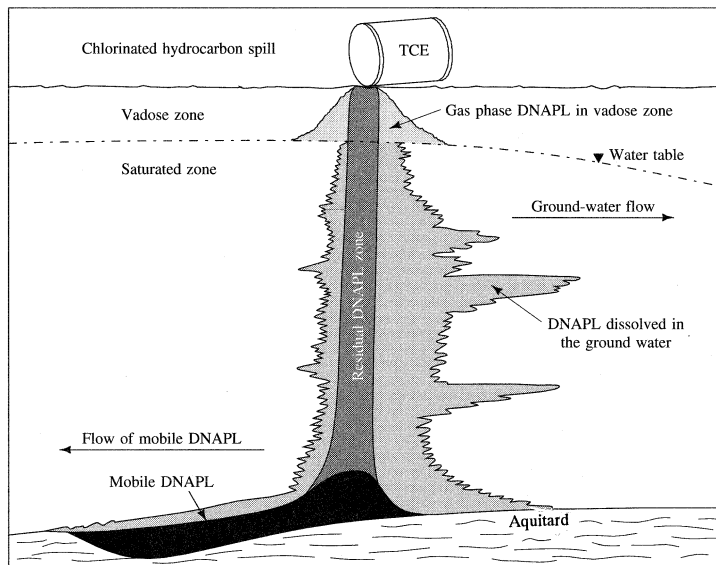
L_o = length of the continuous DNAPL phase in the direction of flow

r_t = pore-throat radius

r_p = pore radius

Once the percolating DNAPL reaches the aquitard layer, it can begin to move laterally, even in the absence of a hydraulic gradient on the water table. It migrates down the dip of the aquitard. DNAPLs can collect in low spots on the surface of an aquitard. It is possible for the DNAPL to migrate downdip, even if the hydraulic gradient and groundwater flow are in the opposite direction (Figure 5.29).

FIGURE 5.29 Distribution of a dense nonaqueous phase liquid in the vadose and saturated zone.



If a pocket of static DNAPL collects in a low spot on the surface of an aquitard and groundwater is flowing in the aquifer above the DNAPL, the interface between the flowing groundwater and the static DNAPL will be sloping. This angle can be found from (Hubbert 1953)

$$\tau_s = \frac{\rho_w}{\rho_w - \rho_{DNAPL}} dh/dl \quad (5.59)$$

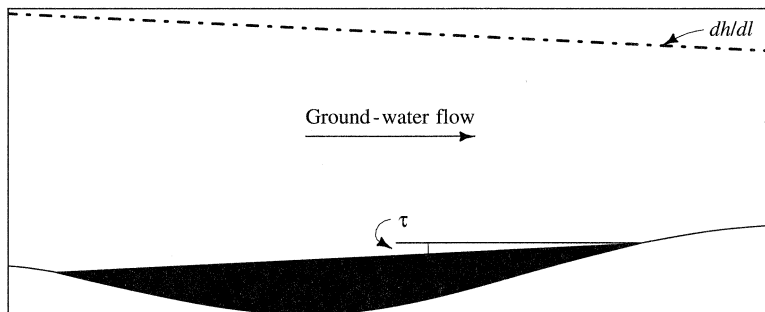
where τ_s is the angle of the interface and dh/dl is the slope of the water table (Figure 5.30). A negative value for τ_s means that the angle has a slope opposite to the direction of the water table.

Buckley and Leverett (1942) derived the following equation for the one-dimensional flow of two immiscible, incompressible fluids:

$$\frac{\partial}{\partial x} \left(G \frac{\partial S_w}{\partial x} \right) - q_t \frac{df}{dS_w} \frac{\partial S_w}{\partial x} = n \frac{\partial S_w}{\partial t} \quad (5.60)$$

$$f(S_w) = \left[1 + \frac{k_{nw}\mu_w}{k_w\mu_{nw}} \right]^{-1} \quad (5.61)$$

FIGURE 5.30 Sloping interface between a static layer of DNAPL and flowing groundwater.



where

q_t = total volume flux

S_w = relative saturation of the wetting phase

n = porosity

f = a function that depends upon the value of S_w and is defined as:

and G is a function that depends upon the value of S_w and is defined as

$$G(S_w) = -\frac{k_{nw}f}{\mu_{nw}} \frac{dP_c}{dS_w} \quad (5.62)$$

where

k_w = permeability to wetting fluid

k_{nw} = permeability to nonwetting fluid

μ_w = dynamic viscosity of wetting fluid

μ_{nw} = dynamic viscosity of nonwetting fluid

P_c = capillary pressure

The volume flux of the wetting phase, q_w , is given by

$$q_w = f q_t - G \frac{\partial S_w}{\partial x} \quad (5.63)$$

The volume flux of the nonwetting phase, q_{nw} , is given by

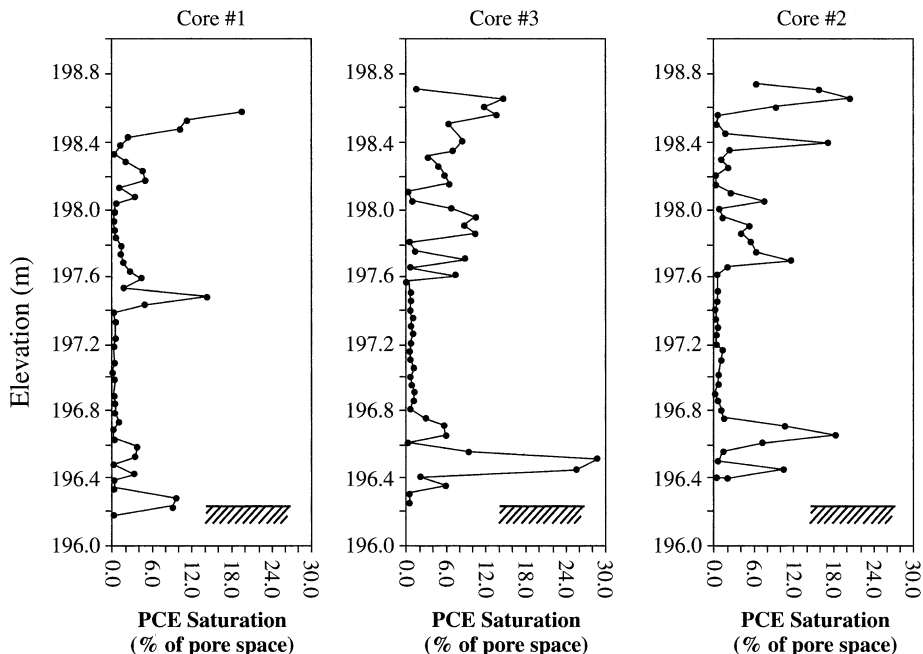
$$q_{nw} = q_t(1-f) + G \frac{\partial S_w}{\partial x} \quad (5.64)$$

Buckley and Leverett (1942) solved these equations by assuming that the force due to the rate at which the fluid is added at the boundary, q_t , is much greater than the capillary pressure force, P_c . Thus the second term in Equation 5.63 can be ignored. However, this may not be accurate. McWhorter and Sunada (1990) have developed an exact integral solution to this two-phase flow problem that accounts for both forces. They have solutions for either the displacement of the wetting fluid by the advance of a nonwetting fluid or the displacement of a nonwetting fluid by an invading wetting fluid. The former solution can be applied to the problem of the displacement of water in an aquifer by the lateral flow of a DNAPL.

Case Study

Kueper et al. (1993) and Brewster et al. (1995) both studied the distribution of tetrachloroethylene (PCE) below the water table after a controlled release into an unconfined, shallow

FIGURE 5.31 Distribution of PCE in the subsurface as a result of a controlled release below the water table. The cores are located one half to one m away from the spill location. Zones of high residual PCE represent layers of fine-grained sediments upon which the PCE spread laterally.



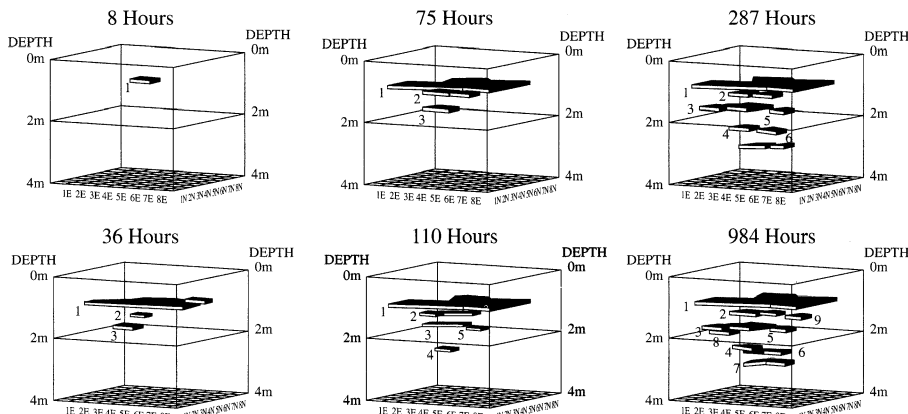
Source: B. H. Kueper et al. 1993. A field experiment to study the behavior of tetrachloroethylene below the water table: Spatial distribution of residual and pooled DNAPL. *Groundwater* 31:756–766. Used with permission.

fine to medium sand aquifer. Both experiments were conducted at Canadian Forces Base Borden near Alliston, Ontario, Canada. The aquifer was about 3.4 m thick (~11 ft) and was underlain by a 3 m (~10 ft) thick clay layer. In both experiments a portion of the aquifer was isolated by driving sheet piling into the underlying clay to form a hydraulically sealed cell. In the 1993 study the cell was 3 m by 3 m (10 ft by 10 ft) and in the 1995 study it was 9 m by 9 m (30 ft by 30 ft). In both experiments PCE was slowly released below the water table in a manner mimicking a leaking underground tank.

The PCE moved downward through the saturated zone in both experiments. However, microstratigraphy in the sand, which created horizontal discontinuities caused the PCE to spread laterally on the top of fine-grained layers. Figure 5.31 shows the PCE saturation in three cores taken from the 1993 study. The cores show that there are several layers where the PCE has been retained, but there is a zone from about elevation 197.6 to 196.8 where there was little PCE. All three cores were taken between 0.5 m (0.6 ft) and 1 m (1.2 ft) away from the point of PCE injection. The core elevations where PCE was present represent horizontal planes where PCE spread away from the point of injection while the places with no PCE represent horizons where PCE did not spread laterally.

The lateral spreading occurs where there is a fine-grained horizon, which creates a capillary pressure contrast to a coarser-grained layer. This spreading occurs irrespective of whether or not the DNAPL has penetrated the fine-grained layer. In both the 1993 study and the 1995 study the DNAPL migration was stopped by the walls of the cell. Figure 5.32 shows the growth of the pooled DNAPL during the 1995 study. These experiments demonstrate that even in a relatively uniform sandy aquifer there will be significant lateral spreading of DNAPL. However, they also showed that there can be surprising local variation in the rate of DNAPL movement. The 1993 cell and the 1995 cells were located only 10 m (33 ft) apart in the same apparently uniform sand aquifer. In the 1993 experiment PCE was released at a rate of 8 L/hr (0.035 gpm) while in 1995 the PCE release rate was 11 L/hr (0.048 gpm). In both cases the same injection head was

FIGURE 5.32 Three dimensional distribution of PCE pools in the subsurface as a result of a controlled release below the water table. PCE pool location was determined by geophysical methods. Pools of PCE are indicated for six times: 1) 8 hours, 2) 36 hours, 3) 75 hours, 4) 110 hours, 5) 287 hours and 6) 984 hours.

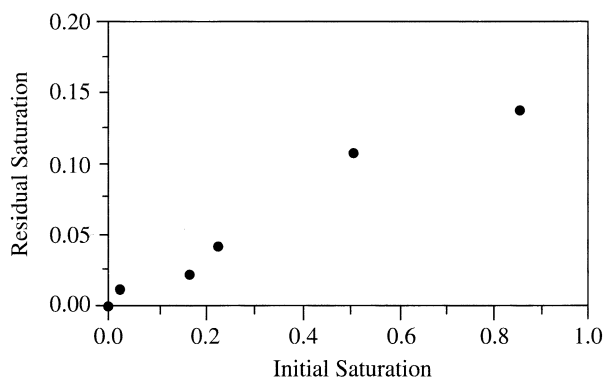


Source: Brewster et al. 1995. Observed migration of a controlled DNAPL release by geophysical methods. *Groundwater* 33:977–987. Used with permission.

used. In the 1995 study (9 m by 9 m cell) it only took 40 hours for PCE to first reach the clay layer at 3.4 m (11 ft) while it took 500 hours for PCE to travel the same distance in the 1993 experiment (3 m by 3 m cell). Apparently subtle changes in distribution of hydraulic properties in the same aquifer can have significant impacts on DNAPL migration rates.

Kueper et al. (1993) also studied DNAPL retention in the sandy soil from the experimental site. Figure 5.33 shows the residual PCE saturation as a function of the initial PCE saturation prior to draining. Residual saturation ranged up to 0.13 for a sample that had an initial saturation of 0.9.

FIGURE 5.33 Laboratory-determined relationship of residual saturation of PCE after drainage to initial saturation level for the Borden sand. When more pores are initially filled with PCE, i.e. higher initial saturation, then more PCE can be isolated in some of those pores when the PCE is drained.



Source: Brewster et al. 1995. Observed migration of a controlled DNAPL release by geophysical methods. *Groundwater* 33:977–987. Used with permission.

5.10.5 DNAPL Flow in Fracture Systems

A connected phase pool of a DNAPL may accumulate at the contact between a sedimentary aquifer and bedrock or clay. If the bedrock or clay is fractured, there is a potential for the DNAPL to enter the fracture. If the fracture is filled with water, the DNAPL must displace the water in order to enter the fracture. In order for this to occur, the capillary pressure of the DNAPL at the entrance to the fracture must be greater than the capillary pressure of the water in the fracture. If the fracture entrance has the shape of two parallel plates, the necessary entry pressure is (Kueper and McWhorter 1991):

$$P_E = 2\sigma \cos \theta / e \quad (5.65)$$

where

P_E = entry pressure into the fracture (Pascals)

σ = interfacial tension between DNAPL and water (N/m)

θ = contact angle between the DNAPL and water

e = fracture aperture (m)

In the case where the fracture opening is semicircular in shape, the entry pressure is given by (Kueper and McWhorter 1991):

$$P_E = 4 \sigma \cos \theta/e \quad (5.66)$$

These two equations bound the possible geometries of fracture openings. In both cases the wider the fracture aperture, the lower the entry pressure for a DNAPL. This means that DNAPLS will preferentially enter larger apertures

In the most conservative case, that is the lowest entry pressure, the height of a connected phase DNAPL pool, which is necessary to overcome the capillary pressure and initially enter a fracture is (Kueper and McWhorter 1991):

$$H_D = 2 \sigma / \Delta \rho g e \quad (5.67)$$

where

H_D = the height of the connected phase DNAPL pool (m)

$\Delta \rho$ = the density difference between the DNAPL and water (kg/m³)

g = the acceleration of gravity (m²/s)

Equation 5.66 determines the initial height that the connected phase pool of DNAPL must be to enter the fracture. It assumes that the capillary pressure of the top of the DNAPL pool is zero and that DNAPL is invading a water-wet fracture for the first time. This relationship is independent of the depth below the water table. It also assumes hydrostatic conditions, i.e., the water pressure outside the fracture is in hydrostatic equilibrium with the water in the fracture. For example, if there is a pool of DNAPL lying on top of a fractured clay aquitard, pumping of water from an aquifer beneath the aquitard could result in a drop in pressure within a fracture in the aquitard. This might induce the entry of the DNAPL into a fracture that under hydrostatic conditions it could not enter (Kueper and McWhorter 1991).

Once a DNAPL has invaded a fractured medium it will preferentially enter the larger fractures. There may be smaller fractures that it will not enter at all because the necessary entry pressures are greater than the capillary pressure of the DNAPL-water system. The DNAPL will migrate vertically under gravity, but will also migrate horizontally if the vertical fracture apertures become too small for the DNAPL to enter. (National Academy of Sciences, Engineering, and Medicine 2015).

Once a fracture has been invaded, there will be a continuous vertical phase represented by the DNAPL in the fracture and the remaining DNAPL in the pool. As the pool may have a much greater volume than the fracture, the fracture may be able to fill without too great a lowering of the height of the interconnected pool. This means that the DNAPL will now be able to enter a much smaller fracture than the original fracture at the top of the formation just below the interconnected pool. Eventually the DNAPL “finger” extending down the fracture will thin and break away from the overlying pool. This DNAPL will then become residual in the fracture as it no longer has a height great enough to displace water from the fracture. In the case of a vertical fracture with uneven aperture, the DNAPL will enter the fracture where the width is greatest and migrate downward as a “finger” following the wide spot in the fracture and avoiding the fracture where it is narrow.

Interconnected pools of DNAPL can also form in sloping fractures. In this case the DNAPL will be migrating down-dip in the fracture. The pool in the fracture will migrate until it can no longer overcome the capillary pressure and displace the water in the fracture. The difference between the residual DNAPL in the fracture and the pooled DNAPL in the fracture is that the residual is formed when a migrating finger thins and breaks off and while the pool is still continuous but is no longer able to migrate. The more steeply the fracture is dipping, the more deeply the DNAPL will be able to penetrate the fractured media. Downward hydraulic gradients across a fracture will increase the rate of DNAPL movement while upward hydraulic gradients will retard downward DNAPL movement.

The DNAPL will preferentially migrate through larger fractures and will only enter intersecting fractures if the capillary pressure can be overcome. Thus not all fractures in a fractured rock aquifer will contain DNAPL. Moreover, only the parts of the fracture with a larger aperture may hold DNAPL. The DNAPL will thus be distributed both horizontally and vertically according to the size, orientation and degree of connectivity of the fractures.

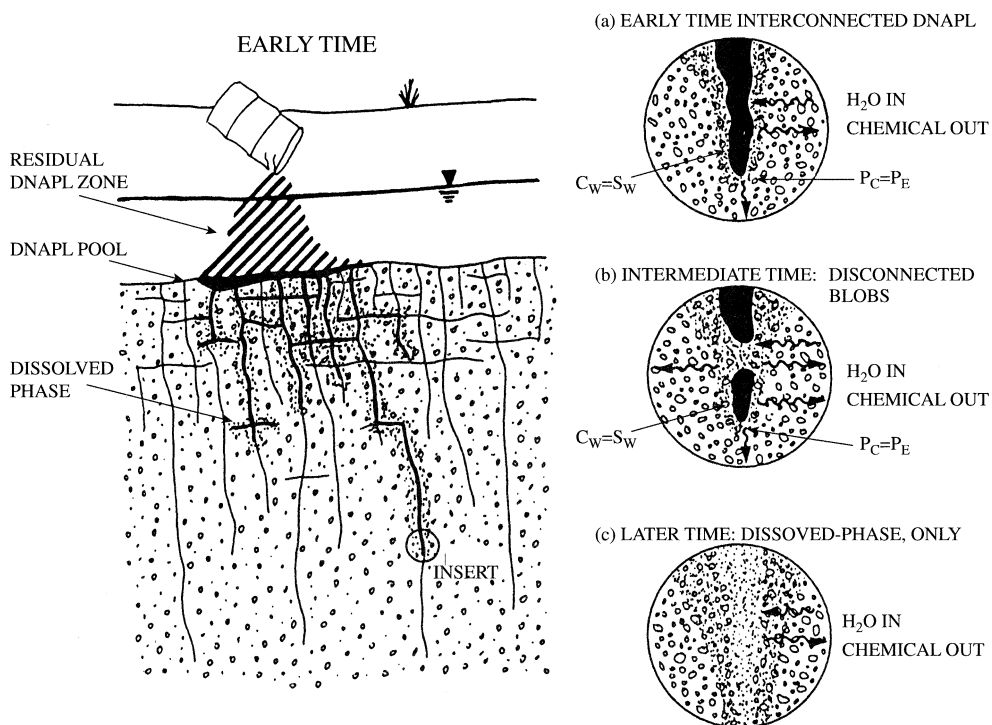
Once the DNAPL enters the fracture system, it can undergo molecular diffusion from the fracture into the groundwater in the pores of the rock or clay matrix (Parker et al. 1994). Clayey deposits can have matrix porosity of 30 to 60% for clays and 5 to 15% for fractured sedimentary rocks. The DNAPL will first spread through the fracture system, and then start to diffuse into the porous matrix. Figure 5.34 illustrates this process. First there are interconnected pools of DNAPL. Then some of the DNAPL diffuses as a dissolved phase into the porous matrix, leaving interconnected ganglia of DNAPL in the fractures. Finally, all of the DNAPL may disappear, leaving only the dissolved phase diffused into the fractures. Theoretical calculations suggest that the diffusive loss of DNAPL from fractures into the matrix of clay aquitards can be complete within a time frame of days to a few years (Parker et al. 1994). This would make the recovery of DNAPLs from the ground much more difficult as the liquid phase is no longer present and the total mass has diffused into a very low permeability unit.

5.10.6 Dissolution of DNAPL

A guidance document from the U.S. EPA suggests that if a chemical that can occur as a DNAPL is found dissolved in groundwater from monitoring wells in amounts of only 1% of the effective aqueous solubility there is a substantial probability that the DNAPL form is present in the subsurface (Newell and Ross, 1991). The opposite is not true; concentrations less than 1% of the effective aqueous solubility in groundwater does not mean that the nonaqueous phase is absent. Most of the time if a DNAPL is found in groundwater in dissolved form, it will be in concentrations that are much less than the effective aqueous solubility (Anderson et al. 1992). This is true even at sites where a pool of DNAPL is known to occur (e.g., Michalski et al. 1995).

In order for the DNAPL to dissolve, it must come into contact with flowing groundwater. The pools of DNAPL that form on the top of low permeability zones are relatively thin with flat tops (Anderson et al. 1992). This presents a very small cross-sectional area for the groundwater, which will be flowing parallel to the bedding planes. In addition, the rate of mass transfer of the chemical from the pure phase to the dissolved phase in groundwater is slow, indicating periods of 10s to 100s of years for pools containing

FIGURE 5.34 Conceptual model for DNAPL migrating into a fractured medium. (a) The initial step is of the DNAPL in invade a fracture with a layer of water between the DNAPL and the fractured geologic medium. DNAPL will dissolve into the water and the dissolved DNAPL can then diffuse into the water in the porous matrix. (b) As mass is lost from the DNAPL finger by diffusion into the porous matrix, the DNAPL finger thins and becomes discontinuous. (c) Eventually all of the DNAPL has dissolved and is present as a dissolved phase in water in the fracture as well as diffused into the porous matrix.



Source: B. L. Parker, R. W. Gillham, and J. A. Cherry. 1994. Diffusive disappearance of immiscible-phase organic liquids in fractured geologic media. *Groundwater* 32:805–820. Used with permission.

a few hundred to a few thousand of kg of chlorinated solvents to dissolve in flowing groundwater (Johnson and Pankow 1992). Moreover, many DNAPL pools contain a mixture of individual chemicals, so according to Raoult's Law the effective solubility of any one chemical is less than its individual solubility (Jackson and Mariner 1995).

In addition to the above factors that may limit the amount of a DNAPL that can dissolve in groundwater, the act of monitoring groundwater can reduce the concentration. If the DNAPL is concentrated in thin beds, and the groundwater flows parallel to those beds, dissolved DNAPL may occur in thin zones within the aquifer. Although the DNAPL will sink, groundwater containing the dissolved form of the DNAPL is not denser than the surrounding groundwater and hence doesn't sink. These thin zones of contamination are typically thinner than the screen length of a monitoring well. When the monitoring well is pumped to withdraw a water sample, uncontaminated water will enter as well as water from the contaminated zone. This dilutes the contaminated groundwater and results in a lower concentration of contamination. Further, dispersion

and dilution of the contamination can occur between the DNAPL pool and the monitoring well. If a recovery well is pumped in order to remove contaminated water from the aquifer, there will be a convergence of streamtubes carrying both contaminated and uncontaminated water. This will also reduce the contaminant concentration.

If the DNAPL is not spilled in sufficient amounts to overcome the residual saturation in the vadose zone, groundwater contamination by the dissolved phase can still occur. The residual DNAPL forms a source that, although not mobile, can slowly partition into both the vapor phase and the aqueous phase of the water infiltrating through the vadose zone. If the DNAPL is volatile, as many are, the vapor can diffuse through the vadose zone as well. The vapor phase can partition into the pore water so that the area of soil-water contamination can spread via the vapor phase.

■ 5.11 Monitoring for LNAPLs and DNAPLs

Special consideration must be given to the design of monitoring wells and the collection of groundwater samples to test for the presence of LNAPLs and DNAPLs (floaters and sinkers). Naturally, different types of wells are used for each separate phase.

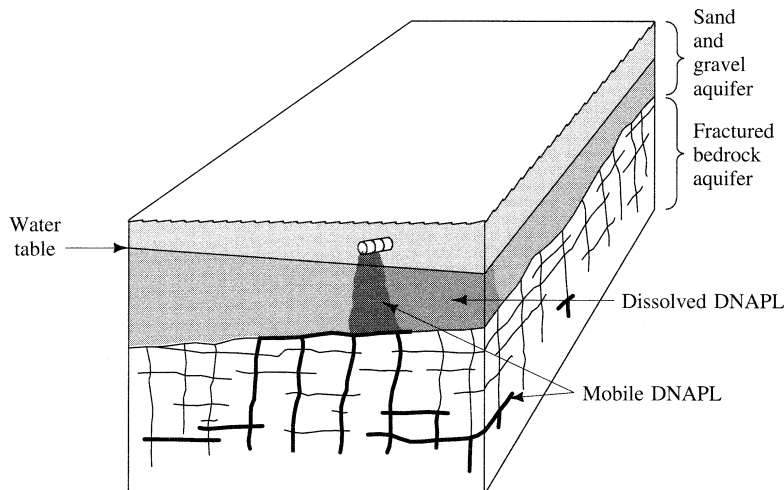
Because LNAPLs float on the capillary layer, a monitoring well for LNAPL detection should extend from above the capillary zone to below the water table. If an LNAPL is present, it will be floating at the surface of the liquid column in the monitoring well. Prior to any purging of the well, a top-loading bailer should be carefully lowered to just below the liquid surface so that the top layer of liquid drains into the bailer. If an LNAPL is present, the top-loading bailer should capture it. The LNAPL should be analyzed qualitatively. If there is a mixture of compounds present, it might be necessary to determine the proportion of each in the LNAPL. Special probes are available to measure the thickness of LNAPLs floating in a monitoring well.

To sample a DNAPL, a monitoring well should be constructed with a screen at the very bottom of the aquifer. It may be helpful to have a length of solid pipe as a sump at the bottom of the screen so that if even a thin layer of mobile DNAPL is present, it can collect in the sump in a sufficient thickness to sample. If a sump is used, the thickness of any measured product thickness must be reduced by the length of the sump. A bottom-loading bailer is used to collect the liquid from the bottom of the sump prior to any well purging. The bailer is slowly lowered all the way to the bottom of the monitoring well and then slowly raised. The collected sample should be placed into a glass jar to see if there is a dense layer on the bottom. In case the entire bailer is filled with a clear liquid, part of the contents should be placed in a jar partially filled with water to see if a separate phase forms.

If the chemical analysis of an aqueous water sample indicates that an organic compound is present in amounts greater than its published solubility value, the compound may be present as a nonaqueous phase that was emulsified in the sample collection process.

Monitoring for DNAPLs in areas of fractured bedrock geology is much more difficult than in sand aquifers. Figure 5.35 shows a buried barrel from which a DNAPL has leaked. The DNAPL moves vertically through the vadose zone and the saturated sand and gravel aquifer that overlies the fractured bedrock. Some of the DNAPL dissolves in the flowing groundwater and is transported by advection. When the DNAPL reaches the bedrock surface it flows downslope, in this case in a direction opposite to the flow

FIGURE 5.35 Movement of a DNAPL into a fractured bedrock aquifer that underlies a sand and gravel aquifer.

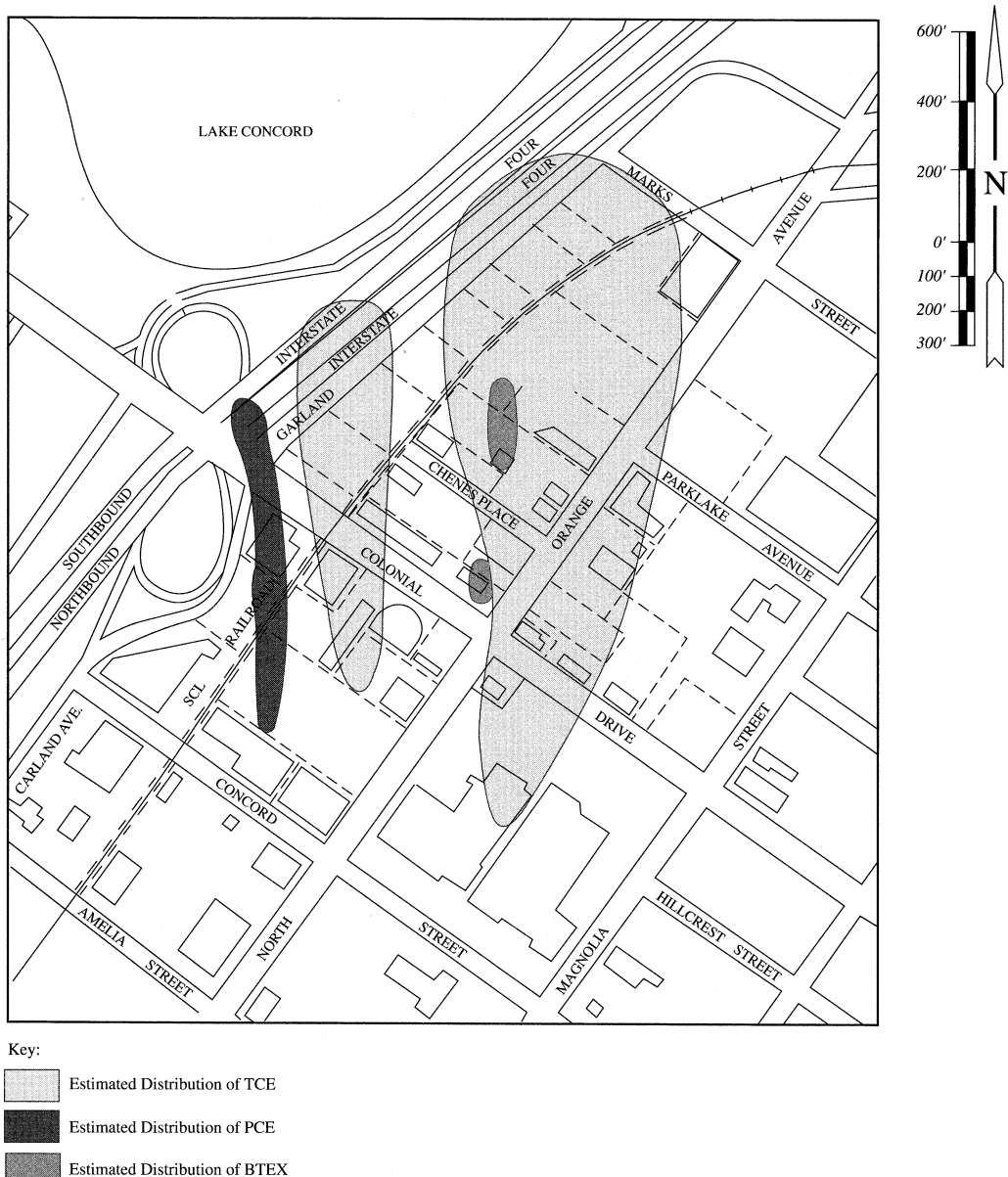


of groundwater. The DNAPL moves vertically into fractures in the bedrock below the pool that collects on the bedrock surface. The DNAPL can also migrate horizontally between vertical cracks. As a result, the DNAPL can spread in unexpected and unpredictable directions from the leaking barrel. Many bedrock monitoring wells would be needed even to find the portions of the DNAPL plume in the bedrock; it might be impossible to locate all of it (Mackay and Cherry 1989).

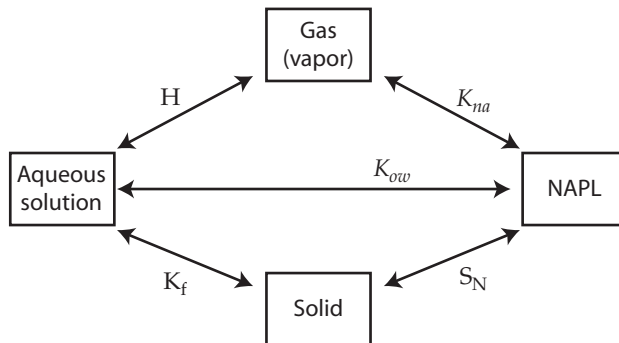
Groundwater monitoring for NAPLs and related dissolved compounds in urban areas is complicated due to the presence of buried utility lines, such as water mains, sewers, telephone lines and electrical cables. The trenches in which utility lines are placed are often backfilled with sand or gravel. This presents a potential preferential pathway for the movement of groundwater and LNAPLs due to the high hydraulic conductivity. Groundwater elevation data is typically interpreted to suggest that the groundwater flow direction is at right angles to the water table contours. However, both groundwater and LNAPLs can flow in the permeable backfill of a utility trench in a direction that is at an oblique angle to the water table contours, although flow must still be from areas of higher hydraulic head to areas of lower hydraulic head. In the vadose zone vapors of both LNAPLs and DNAPLs can move through the permeable backfill. Soil vapor studies conducted in urban areas might find soil vapor containing an organic chemical following a utility trench. This does not necessarily mean that LNAPL or DNAPL is at the location of the trench, although it might. It might only indicate that the vapor phase has moved along the trench.

A further complication in urban areas is that there may be several sources of contamination and several different intersecting and overlapping plumes of contamination. Figure 5.36 shows several plumes of groundwater contamination in the North Downtown Orlando, Florida area. There were three plumes of groundwater contaminated with chlorinated solvents, two from dry cleaning establishments and one from a newspaper printing plant. In addition there were two plumes of contamination of LNAPLs from

FIGURE 5.36 Multiple plumes of groundwater contamination in an urban area, North Downtown Orlando Florida. (Various sources.)



gasoline or diesel fuel. Since many separate properties were involved, and each was studied individually by different environmental consulting firms, it took a number of years for hydrogeologists from the Florida Department of Environmental Protection to accurately and completely understand the contamination picture in this area.

Figure 5.37 Partitioning processes in a multi-phase system—revisited.

■ 5.12 Summary

Many cases of groundwater contamination involve organic liquids that are either insoluble or only partially soluble in water. These liquids may be present both above and below the water table as separate nonaqueous phase liquids (NAPLs). A NAPL that is less dense than water (LNAPL) will float on the water table. A NAPL more dense than water (DNAPL) may sink into the aquifer.

Water and a NAPL may both be present in the ground. Depending upon their relative proportions, only the water or only the NAPL or both may be mobile. Depending upon the surface tension of the liquids, one will be a wetting fluid and one a nonwetting fluid. The term relative permeability refers to the permeability of the soil for one fluid in the presence of a given volumetric content of a second fluid. Darcy's law can be written in terms of the relative permeability for both a nonwetting and a wetting fluid.

In general, NAPL movement is affected by the mass of NAPL source, the NAPL and porous media properties, as well as by the groundwater system. The ease of NAPL spreading is determined by its aqueous solubility, interfacial tension and partition properties as well as is vapor pressure and density. Important porous medium properties include pore size distribution and soil structure and its permeability. Heterogeneities in the subsurface particularly influence the movement and distribution of NAPLs. The groundwater velocity and, in case of the vadose zone, the water content of the pore space are other important factors.

If a sufficient depth of an LNAPL collects on the surface of the capillary fringe, it can flow into a shallow monitoring well. The thickness of LNAPL measured in a monitoring well is greater than the thickness of the free LNAPL in the subsurface. If certain soil parameters are known, one can compute the thickness of the mobile LNAPL based on the thickness that accumulates in a monitoring well.

DNAPLs may have greater mobility in the earth than water due to their greater density/viscosity ratio. A DNAPL will sink vertically in the vadose zone, although it can spread laterally on the top of strata with small pore openings (fine-grained layers). The DNAPL will also sink below the water table, where it will spread out at the contact between coarse and fine-grained layers. DNAPLs can also flow through fractured media where they will preferentially flow through the fractures with larger apertures and may not even enter fractures with small apertures. DNAPL trapped in fractures may diffuse

into the groundwater in the pores of the rock or clay matrix. Pools of mobile DNAPL may form at the bottom of an aquifer. They will spread in the direction that the underlying aquitard is sloping. A monitoring well screened at the bottom of an aquifer may be used to detect the presence of a DNAPL. Alternatively, a partition interwell tracer test can assist in identifying the quantity and distribution of DNAPL in the subsurface.

Chapter Notation

A	Cross-sectional area of flow	H_D	Height of a connected phase pool
d	Porous media grain diameter	K	Hydraulic conductivity
dh_w/dl	Gradient of fluid potential for wetting fluid	K°	Temperature in degrees Kelvin
dh_{nw}/dl	Gradient of fluid potential for nonwetting fluid	k_i	Intrinsic permeability
C_N	Tracer concentration in the NAPL	k_r	Relative permeability
C_N	Tracer concentration in the aqueous phase	k_{rw}	Relative permeability of water
D	$\text{Argument} = (P_d^{ow}/(\rho_w - \rho_0)g) - (P_d^{ao} - \rho_0 g)$	k_{ra}	Relative permeability of air
D_a^{ao}	Depth in the aquifer to the top of the capillary fringe	k_m	Relative permeability of a nonaqueous phase liquid
D_a^{ow}	Depth in the aquifer to the top of the oil table	K_D	Solid-water distribution coefficient
D_a^{aow}	Depth in the aquifer to the top of the zone where nonresidual organic fluid occurs	K_{rmw}	Relative permeability of nonaqueous phase liquid at the residual saturation of water in a water-nonaqueous phase system
D_w^{ao}	Depth in a well to the air-organic interface	K_{rmw}	Relative permeability of the nonaqueous phase system as a function of S_w
D_w^{ow}	Depth in a well to the organic-water interface	K_{rma}	Relative permeability of the nonaqueous phase well in an air-nonaqueous phase system as a function of S_a
E	Force vector	K_n	NAPL-water partitioning coefficient
E_w	Force vector for water	L_o	Vertical length of a DNAPL stringer
E_{DNAPL}	Force vector for a DNAPL	M	Mass
E_{LNAPL}	Force vector for a LNAPL	N_c	Capillary number
e	Aperture of a fracture	N_B	Bond number
f_w	Formula weight	n	Porosity
f	A Buckley-Leverett function	P	Fluid pressure
G	A Buckley-Leverett function	P_a	Vapor pressure of a NAPL component
g	Acceleration of gravity	p_a^n	Vapor pressure of a NAPL in pure-phase form
$\text{grad } P$	lateral pressure gradient	P_d^{ao}	Brooks-Corey air-organic displacement pressure
h_c	Height of capillary rise in a tube	P_d^{ow}	Brooks-Corey organic-water displacement pressure
h_w	Head (potential) of wetting fluid	P_w	Pore pressure for a wetting fluid
h_{nw}	Head (potential) of nonwetting fluid	P_{nw}	Pore pressure for a nonwetting fluid
h_o	Critical height for a DNAPL stringer before it can displace water in the saturated zone	P_c	Capillary pressure
H	Henry constant		

p_d	Threshold or displacement pressure	t_{NP}	Non-partitioning tracer mean travel time
P_E	Entry pressure into a fracture	V	Volume
P_o	Pressure in an LNAPL at an LNAPL-water interface in a monitoring well	V_o	Volume of organic liquid per unit area
P_s	Reference pressure	V_e	Effective pore volume
P_t	Capillary pressure in a thin tube	V_N	Volume NAPL
P_w	Pressure in water at an LNAPL-water interface in a monitoring well	W	Depth from the water table to an organic fluid - water interface in a well
Q_w	Volume of wetting fluid flowing in a two-phase system	x_a	Mole fraction of a NAPL component
Q_{nw}	Volume of nonwetting fluid flowing in a two-phase system	z	Vertical coordinate measured positively downward
q_t	Total volume flux	z_s	Reference elevation
q_w	Volume flux of wetting fluid	$\Delta\rho$	Density difference between a DNAPL and water
q_{nw}	Volume flux of nonwetting fluid	θ	Interfacial angle between two non-wetting fluids
R	Ideal gas constant	θ_{NAPL}	NAPL saturation
R_N	Partitioning tracer retardation factor	σ_{ij}	Interfacial tension between substances i and j
r	Radius of a thin tube	γ	Specific weight
r'	Radius of curvature for an air-water interface	λ	Brooks-Corey pore-size distribution index
r_p	Pore radius	ρ	Density
r_t	Pore-throat radius	ρ_b	Bulk density
S_a	Saturation ratio for air	ρ_w	Density of water
S_e	Effective saturation	ρ_o	Density of an organic fluid
S_o	Organic liquid saturation ratio	ρ_{nw}	Density of a nonwetting fluid
S_r	Residual saturation	ρ_{DNAPL}	Density of a DNAPL
S_w	Wetting-fluid or water-saturation ratio	ρ_{LNAPL}	Density of a LNAPL
S_{wi}	Irreducible wetting-fluid saturation	μ_w	Dynamic viscosity of water
S_{nwr}	Residual nonwetting-fluid saturation	Φ	Fluid potential
S_g	Fractions of pore occupied by gas	Φ_w	Fluid potential for wetting fluid
S_w	Fractions of pore occupied by water	Φ_{nw}	Fluid potential for nonwetting fluid
T_{oil}	Thickness of oil in a monitoring well		
t_P	Partitioning tracer mean travel time		

References

- Abdul, A. S. 1988. Migration of petroleum products through sandy hydrogeologic systems. *Groundwater Monitoring & Remediation* 8:73–81.
- Abdul, A. S., S. F. Kau, and T. L. Gibson. 1989. Limitations of monitoring wells for the detection and quantification of petroleum products in soils and aquifers. *Groundwater Monitoring & Remediation* 9:90–99.
- Abriola, L. M., and G. F. Pinder. 1985a. A Multiphase approach to the modeling of porous media contamination by organic compounds: 1. Equation development. *Water Resources Research* 21:11–18.
- Abriola, L. M., and G. F. Pinder. 1985b. A Multiphase approach to the modeling of porous media contamination by organic compounds: 2. Numerical simulation. *Water Resources Research* 21:19–26.
- Allen, D., Y. Cohen, and I. R. Kaplan. 1989. *Intermedia pollutant transport: Modeling and field measurements*. New York: Plenum Press, 298 pp.

- Anderson, M. R., R. L. Johnson, and J. F. Pankow. 1992. Dissolution of dense chlorinated solvents into groundwater. *Groundwater* 30:250–256.
- Annable, M. D., P. S. C. Rao, K. Hatfield, W. Graham, A. L. Wood, and C. G. Enfield. 1998. Partitioning tracers for measuring residual NAPL: Field-scale test results. *Journal of Environmental Engineering* 124:498–503.
- ASTM E2856–13. 2013. *Standard Guide for Estimation of LNAPL Transmissivity*. ASTM International, West Conshohocken, PA. Accessed October 3, 2015 from <http://www.astm.org/Standards/E2856.htm>
- Baehr, A. L. 1987. Selective transport of hydrocarbons in the unsaturated zone due to aqueous and vapor phase partitioning. *Water Resources Research* 23:1926–1938.
- Baehr, A. L., and M. Y. Corapcioglu. 1987. A compositional multiphase model for groundwater contamination by petroleum products: 2. Numerical solution. *Water Resources Research* 23:201–213.
- Bear, J. 1972. *Dynamics of fluids in porous media*. New York: American Elsevier Publishing Company, 764 pp.
- Berg, R. R. 1975. Capillary pressures in stratigraphic traps. *Bulletin, American Association of Petroleum Geologists* 59:935–956.
- Boving, T. B., J. Blue. 2002. Long-term contaminant trends at the Picillo Farm Superfund Site in Rhode Island. *Remediation* 12:177–128.
- Brewster, M. L., A. P. Annable, J. P. Greenhouse, B. H. Kueper, G. R. Olhoeft, J. D. Redman, and K. A. Sander. 1995. Observed migration of a controlled DNAPL release by geophysical methods. *Groundwater* 33:977–987.
- Brooks, R. H., and A. T. Corey. 1966. Properties of porous media affecting fluid flow. *Proceedings, American Society of Civil Engineers, Irrigation and Drainage Division* 92:61–87.
- Brooks, M. C., M. D. Annable, M. D., S. C. Rao. 2001. Tracer techniques for DNAPL source delineation and in situ flushing techniques for enhanced source removal: Pilot scale demonstrations at the Dover National Test Site. NTIS: ADA410848, 293 pp.
- Brooks, M. C., M. D. Annable, P. S. C. Rao, K. Hatfield, J. W. Jawitz, and W. R. Wise. 2002. Controlled release, blind tests of DNAPL characterization using partitioning tracers. *Journal of Contaminant Hydrology* 59:187–210.
- Brost, E. J., and G. E. DeVaul. 2000. Non-aqueous phase liquid (NAPL) mobility limits in soil. *Soil and Groundwater Research Bulletin* 9: 1–9.
- Buckley, S. E., and M. C. Leverett. 1942. Mechanism of fluid displacement in sand. *Transactions, American Institute of Mining, Metallurgical, and Petroleum Engineering* 146:107–116.
- Cain, R. B., G. R. Johnson, J. E. McCray, W. J. Blanford, and M. L. Brusseau. 2000. Partitioning tracer tests for evaluating remediation performance. *Groundwater* 38:752–761.
- Conant, B. H., R. W. Gillham, and C. A. Mendoza. 1996. Vapor transport of trichloroethylene in the unsaturated zone: Field and numerical modeling investigations. *Water Resources Research* 32:9–22.
- Corapcioglu, Y. M., and A. L. Baehr. 1987. A compositional multiphase model for groundwater contamination by petroleum products: 1. Theoretical considerations. *Water Resources Research* 23:191–200.
- Datta-Gupta, A., S. Yoon, D. W. Vasco, and G. A. Pope. 2002. Inverse modeling of partitioning interwell tracer tests: A streamline approach. *Water Resources Research* 38:1079–1094.
- Divine, C. E., J. E. McCray, L. M. Wolf Martin, W. J. Blanford, D. J. Blitzer, M. Brusseau, and T. B. Boving. 2004. Partitioning tracer test as a remediation metric: Case study at Naval Amphibious Base Little Creek, Virginia Beach, Virginia. *Remediation* 14:7–31.
- Divine, C. E., W. E. Sanford, and J. E. McCray. 2003. Helium and neon groundwater tracers to measure residual DNAPL: Laboratory investigation. *Vadose Zone Journal* 2:382–388.
- Dugan, P. J., and J. E. McCray. 2003. Influence of a solubility-enhancing agent (cyclodextrin) on DNAPL-water partition coefficients, with implications for partitioning tracer tests. *Water Resources Research* 39:1.1–1.7.
- Duke Engineering & Services. 1999. *DNAPL Site Characterization Using a Partitioning Interwell Tracer Test at Site 88, Marine Corps Base Camp Lejeune, North Carolina*. Report to U.S. Department of the Navy, 131 pp.
- Dwarakanath, V., N. E. Deeds, and G. A. Pope. 1999. Analysis of partitioning interwell tracer tests. *Environmental Science and Technology* 33:3829–3836.
- Eckberg, D. K., and D. K. Sunada. 1984. Nonsteady three-phase immiscible fluid distribution in porous media. *Water Resources Research* 20:1891–1899.
- Enfield, C. G., L. Wood, F. P. Espinoza, M. C. Brooks, M. Annable, and P. S. C. Rao. 2005. Design of aquifer remediation systems: (1) Describing hydraulic structure and

- NAPL architecture using tracers. *Journal of Contaminant Hydrology* 81:125–147.
- Essaid, H. I., B. A. Bekins, W. N. Herkelrath, and G. N. Delin. 2011. Crude oil at the Bemidji site: 25 Years of monitoring, modeling, and understanding. *Groundwater* 49:706–726.
- Falta, R. W., I. Javandel, K. Pruess, and P. A. Witherspoon. 1989. Density-driven flow of gas in the unsaturated zone due to the evaporation of volatile organic compounds. *Water Resources Research* 25:2159–2169.
- Falta, R. W., K. Pruess, S. Finsterle, and A. Battistelli. 1995. *T2VOC User's Guide*. Berkeley, CA: Lawrence Berkeley Laboratory, 158 pp. Available from http://esd1.lbl.gov/files/research/projects/tough/documentation/T2VOC_Users_Guide.pdf
- Farr, A. M., R. J. Houghtalen, and D. B. McWhorter. 1990. Volume estimation of light nonaqueous phase liquids in porous media. *Groundwater* 28:48–56.
- Faust, C. R. 1985. Transport of immiscible fluids within and below the unsaturated zone: A numerical model. *Water Resources Research* 21:587–596.
- Geller, J. T., H.-Y. Holman, G. Su, M. E. Conrad, K. Pruess, and J. C. Hunter-Cevera. 2000. Flow dynamics and potential for biodegradation of organic contaminants in fractured rock vadose zones. *Journal of Contaminant Hydrology* 43:63–90.
- Hall, R. A., S. B. Blake, and S. C. Champlin, Jr. 1984. Determination of hydrocarbon thicknesses in sediments using borehole data. In *Proceedings of the Fourth National Symposium and Exposition on Aquifer Restoration and Ground Water Monitoring*. National Water Well Association, 300–310.
- Held, R. J., and M. A. Celia. 2001. Modeling support of functional relationships between capillary pressure, saturation, interfacial area and common lines. *Advances in Water Resources* 24:325–343.
- Hochmuth, D. P., and D. K. Sunada. 1985. Groundwater model of two phase immiscible flow in coarse material. *Groundwater* 23:617–626.
- Hubbert, M. K. 1953. Entrapment of petroleum under hydrodynamic conditions. *American Association of Petroleum Geologists Bulletin* 37:1954–2026.
- Huling, S. G., and J. W. Weaver. 1991. *Dense Nonaqueous Phase Liquids*. U.S. EPA Groundwater Issues, EPA/540/4-91-002.
- Huntley, D., R. N. Hawk, and H. P. Corley. 1994a. Nonaqueous phase hydrocarbon in a fine-grained sandstone: 1. Comparison between measured and predicted saturations and mobility. *Groundwater* 32:626–634.
- Huntley, D., J. W. Wallace, and R. N. Hawk. 1994b. Nonaqueous phase hydrocarbon in a fine-grained sandstone: 2. Effect of local sediment variability on the estimation of hydrocarbon values. *Groundwater* 32, no. 5:778–783.
- Istok, J. D., J. A. Field, M. H. Schroth, B. M. Davis, V. Dwarakanath. 2002. Single-well “push-pull” partitioning tracer test for NAPL detection in the subsurface. *Environmental Science and Technology* 36:2708–2716.
- Jackson, R. E., and P. E. Mariner. 1995. Estimating DNAPL composition and VOC dilution from extraction well data. *Groundwater* 33:407–414.
- Jang, W., and M. M. Aral. 2007. Density-driven transport of volatile organic compounds and its impact on contaminated groundwater plume evolution. *Transport in Porous Media* 67:353–374.
- Jellali, S., H. Benremita, P. Muntzer, O. Razakarisoa, and G. Schafer. 2003. A large-scale experiment on mass transfer of trichloroethylene from the unsaturated zone of a sandy aquifer to its interfaces. *Journal of Contaminant Hydrology* 60:31–53.
- Johnson, R. L., and J. F. Pankow. 1992. Dissolution of dense chlorinated solvents into Groundwater: 2. Some functions for pools of solvent. *Environmental Science and Technology* 26:896–901.
- Jin, M., M. Delshad, V. Dwarakanath, D. C. McKinney, G. A. Pope, K. Sepehrnoori, and C. E. Tilburg. 1995. Partitioning tracer test for detection, estimation, and remediation performance assessment of subsurface nonaqueous phase liquids, *Water Resources Research* 31:1201–1212.
- Kueper, B. H., and D. B. McWhorter. 1991. The behavior of dense, nonaqueous phase organic liquids in fractured clay and rock. *Groundwater* 29:716–728.
- Kueper, B. H., D. Redman, R. C. Starr, S. Reitsma, M. Mah. 1993. A field experiment to study the behavior of tetrachloroethylene below the water table: Spatial distribution of residual and pooled DNAPL. *Groundwater* 31:756–766.
- Lacombe, S., E. A. Sudicky, S. K. Frape, A. J. A. Unger. 1995. Influence of leaky boreholes on cross-formational groundwater flow and contaminant transport. *Water Resources Research* 31:1871–1882.

- Lenhard, R. J. 1992. Measuring and modeling of three phase saturation-pressure hysteresis. *Journal of Contaminant Hydrogeology* 9:243–269.
- Lenhard, R. J., and J. C. Parker. 1987a. A model for hysteretic constructive relations governing multiphase flow: 2. Permeability-saturation relations. *Water Resources Research* 23:2197–2206.
- . 1987b. Measurement and prediction of saturation pressure relationships in three-phase porous media systems. *Journal of Contaminant Hydrogeology* 1:407–424.
- . 1988. Experimental validation of the theory of extending two-phase saturation-pressure relations to three-fluid phase systems for monotonic drainage paths. *Water Resources Research* 24:373–80.
- . 1990. Estimation of free hydrocarbon volume from fluid levels in monitoring wells. *Groundwater* 28:57–67.
- Lin, C., G. F. Pinder, and E. F. Wood. 1982. *Water resources program report 83-WR-2*. Princeton, NJ: Princeton University.
- Lohman, S. W. 1972. *Ground Water Hydraulics*. U.S. Geological Survey Professional Paper 708, 70 pp.
- Lundegard, P. D., and B. S. Mudford. 1998. LNAPL volume valuation: Parameter estimation by nonlinear regression of saturation profiles. *Groundwater Monitoring & Remediation* 18:88–93.
- Mackay, D. M., and J. A. Cherry. 1989. Groundwater contamination: pump and treat remediation. *Environmental Science and Engineering* 23:630–637.
- Mariner, P. E., M. Jin, J. E. Studer, and G. A. Pope. 1999. The first vadose zone partitioning inter-well tracer test for nonaqueous phase liquid and water residual. *Environmental Science and Technology* 33:2825–2828.
- Mayer, A. S., and S. M. Hassanzadeh, eds. 2005. *Soil and Groundwater Contamination: Nonaqueous Phase Liquids*. Washington, DC: American Geophysical Union, 224 pp.
- Marinelli, F., and D. S. Durnford. 1996. LNAPL thickness in monitoring wells considering hysteresis and entrapment. *Groundwater* 34:405–414.
- McWhorter, D. B., and D. K. Sunada. 1990. Exact integral solutions for two-phase flow. *Water Resources Research* 26:399–413.
- Mendoza, C. A., and E. O. Frind. 1990. Advective-dispersive transport of dense organic vapors in the unsaturated zone 1. Model development. *Water Resources Research* 26:379–387.
- Mendoza, C. A., R. L. Johnson, and R. W. Gillham. 1996. Vapor migration in the vadose zone. In *Dense Chlorinated Solvents and other DNAPLs in Groundwater: History, Behavior and Remediation*, eds. J. F. Pankow, J. T. Geller, and J. A. Cherry. Portland, OR: Waterloo Press, pp. 179–201.
- Meinardus, H. W., V. Dwarakanath, J. Ewing, G. J. Hirasaki, R. E. Jackson, M. Jin, J. S. J. Ginn, J. T. Lonergan, C. A. Miller, and G. A. Pope. 2002. Performance assessment of NAPL remediation in heterogeneous alluvium. *Journal of Contaminant Hydrology* 54:173–193.
- Mercer, J. W., and R. M. Cohen. 1990. A review of immiscible fluids in the subsurface: Properties, models, characterization and remediation. *Journal of Contaminant Hydrology* 6:107–163.
- Mercer, J. M., J. Erickson, M. Slenska, and M. Brourman. 2007. Potential cross contamination due to drilling in source areas. *Groundwater Monitoring and Remediation* 3: 60–64.
- Michalski, A., M. N. Metlitz, and I. L. Whitman. 1995. A field study of enhanced recovery of DNAPL pooled below the water table. *Groundwater Monitoring & Remediation* 15:90–100.
- National Academy of Sciences, Engineering, and Medicine. 2015. *Characterization, Modeling, Monitoring, and Remediation of Fractured Rock*. Washington, DC: The National Academies Press.
- Newell, C., and R. R. Ross. 1991. *Estimating Potential for Occurrence of DNAPL at Superfund Sites*. Quick Reference Guide Sheet. U.S. Environmental Protection Agency. Publication 9355.4–07FS, Washington, DC.
- Newell, C. J., S. D. Acree, R. R. Ross, and S. G. Huling. 1995. Dense nonaqueous phase liquids. U.S. Environmental Protection Agency. Ground Water Issue. EPA/540/4-91-002.
- Ostendorf, D. W., R. J. Richards, and F. P. Beck. 1993. LNAPL retention in sandy soil. *Groundwater* 31:285–292.
- Pankow, J. F., and J. A. Cherry. 1996. *Dense Chlorinated Solvents and other DNAPLs in Groundwater*. Portland, OR: Waterloo Press, 525 pp.
- Parker, B. L., R. W. Gillham and J. A. Cherry. 1994. Diffusive disappearance of immiscible-phase organic liquids in fractured geologic media. *Groundwater* 32:805–820.
- Parker, J. C., and R. J. Lenhard. 1987. A model for hysteretic constructive relations governing multiphase flow: 2. Saturation-pressure relations. *Water Resources Research* 23:2187–2196.

- Pinder, G. F., and L. M. Abriola. 1986. On the simulation of nonaqueous phase organic compounds in the subsurface. *Water Resources Research* 22:109S–119S.
- Pinder, G. F., and W. G. Gray. 2008. *Essentials of Multiphase Flow and Transport in Porous Media*. Hoboken, NJ: Wiley and Sons, 258 pp.
- Pope, G. A., K. Sepehrnoori, M. M. Sharma, D. C. McKinney, G. E. Speitel, and R. E. Jackson. 1999. Three-dimensional NAPL fate and transport model. U.S. Environmental Protection Agency Document EPA/600/R-99/011, 344 pp.
- Pope, G. A., D. C. McKinney, A. D. Gupta, R. E. Jackson, and M. Jin. 2000. In-situ characterization of dense non-aqueous phase liquids using partitioning tracers. DOE/ER/14720, 219 pp.
- Poulson, M. M., and B. H. Kueper. 1992. A field experiment to study the behavior of tetrachloroethylene in unsaturated porous media. *Environmental Science and Technology* 26:889–895.
- Powers, S. E., L. M. Abriola, J. S. Dunkin, W. J. Weber, Jr. 1994. Development of phenomenological models for NAPL dissolution processes. *Journal of Contaminant Hydrology* 16:1–33.
- SAB—Science Advisory Board for Contaminated Sites in British Columbia. 2006. *Approaches and methods for evaluation of light non liquids*, 42 pp. Accessed October 3, 2015 from <http://www.sabcs.chem.uvic.ca>
- Santi, P. M., J. E. McCray, and J. L. Martens. 2006. Investigating cross-contamination of aquifers. *Hydrogeology Journal* 14:51–68.
- Schnoor, J. L. 1996. *Environmental Modeling. Fate and Transport of Pollutants in Water, Air, and Soil*. New York: John Wiley & Sons, 682 pp.
- Schroth, M. H., J. D. Istok, S. J. Ahearn and J. S. Selker. 1995. Geometry and position of light nonaqueous-phase liquid lenses in water-wetted porous media. *Journal of Contaminant Hydrogeology* 19:269–287.
- Schwille, F. 1981. Groundwater pollution in porous media by fluids immiscible with water. *The Science of the Total Environment* 21:173–85.
- . 1984. “Migration of organic fluids immiscible with water in the unsaturated zone.” In *Pollutants in porous media*, eds. B. Yaron, G. Dagen, and J. Goldshmid, 27–48. Berlin: Springer-Verlag.
- . 1988. *Dense chlorinated solvents in porous and fractured media*. Translated by J. F. Pankow. Chelsea, MI: Lewis Publishers, 146 pp.
- Seely, G. E., R. W. Falta, and J. R. Hunt. 1994. Buoyant advection of gases in unsaturated soil. *Journal of Environmental Engineering* 120:1230–1247.
- Stone, H. L. 1973. Estimation of three-phase relative permeability and residual oil data. *Journal of Canadian Petroleum Technology* 12:53–61.
- Suthersan, S., C. Divine, E. Cohen, and K. Heinze. 2014. Tracer testing: Recommended best practice for design and optimization of in situ remediation systems. *Groundwater Monitoring and Remediation* 34:33–40.
- Testa, S. M., and M. T. Paczkowski. 1989. Volume determination and recovery of free hydrocarbon. *Groundwater Monitoring & Remediation* 9:120–127.
- Tillman, F. D., and J. W. Weaver. 2005. *Review of Recent Research on Vapor Intrusion*. U.S. EPA Office of Research and Development, EPA/600/R-05/106. 47 pp.
- US EPA (Environmental Protection Agency). 1987. *Injection Well Mechanical Integrity*, EPA/625/9-87/007, Washington, DC.
- US EPA (Environmental Protection Agency). 1995. *The Hydrocarbon Spill Screening Model (HSSM)*, Volume 1: User's Guide. Publication No. EPA/600/R-94/039a.
- US EPA (Environmental Protection Agency). 1996. Methods for Evaluating Recoverability of Free Product. In *How To Effectively Recover Free Product At Leaking Underground Storage Tank Sites: A Guide For State Regulators*. Chapter 4. EPA 510-R-96-001. Accessed October 3, 2015 from <https://www.epa.gov/sites/production/files/2014-03/documents/fprg.pdf>
- US EPA (US Environmental Protection Agency). 1997. *NAPL: Simulator Documentation*. Publication NO. EPA/600/R-97/102. Document Revisions.
- US EPA (Environmental Protection Agency). 2004. Site characterization technologies for DNAPL investigations., EPA 542-R-04-017, 165 pp.
- US EPA (Environmental Protection Agency). 2010. *NAPL: Simulator Documentation*. Version 2. Accessed October 3, 2015 from <http://www2.epa.gov/water-research/non-aqueous-phase-liquid-napl-simulator>
- Van Genuchten, M. Th. 1980. A closed-form equation for predicting the hydraulic conductivity of

- unsaturated soils. *Soil Science Society of America Journal* 44:892–98.
- Villaume, J. F. 1985. Investigations at sites contaminated with dense nonaqueous phase liquids (NAPLS). *Groundwater Monitoring & Remediation* 5:60–74.
- Vroblesky, D. A., J. F. Robertson, and L. C. Rhodes. 1995. Stratigraphic trapping of spilled jet fuel beneath the water table. *Groundwater Monitoring & Remediation* 15:177–183.
- Wang, P., V. Searakanath, B. A. Rouse, G. A. Pope, and K. Sepehrnoori. 1998. Partition coefficients for alcohol tracers between nonaqueous-phase liquids and water from UNIFAC-solubility method. *Advances in Water Resources* 21:171–181.
- Winegardner, D. L., and S. M. Testa. 2000. *Restoration of Contaminated Aquifers: Petroleum Hydrocarbons and Organic Compounds, Second Edition*. Boca Raton, FL: CRC Press, 464 pp.
- Young, C. M., R. E. Jackson, M. Jin, J. T. Lonergan, P. E. Mainer, and G. A. Pope. 2001. Characterization of a TCE DNAPL zone in alluvium by partitioning tracers. *Groundwater Monitoring and Remediation* 19:84–94.

Problems

- 5.1** What is the relative mobility of carbon disulfide to water? The density of carbon disulfide is 1.26 gm/cm³ at 20°C and the viscosity in centipoise is 0.363 at 20°C.
- 5.2** What is the relative mobility of carbon tetrachloride to water? The density of carbon tetrachloride is 1.595 gm/cm³ at 20°C and the viscosity in centipoise is 0.969 at 20°C.
- 5.3** What is the relative mobility of benzene to water? The density of benzene is 0.878 gm/cm³ at 20°C and the viscosity in centipoise is 0.652 at 20°C.
- 5.4** What is the relative mobility of o-xylene to water? The density of o-xylene is 0.880 gm/cm³ at 20°C and the viscosity in centipoise is 0.810 at 20°C.
- 5.5** Trichloroethylene has the following properties:

Density 1.46 gm/cm³

Interfacial tension with water 34.5 dyne/cm

What is the height of a connected phase DNAPL pool of TCE necessary to enter a fracture that has an aperture of 0.032 cm?

- 5.6** Tetrachloroethylene has the following properties:

Density 1.62 gm/cm³

Interfacial tension with water 47.5 dyne/cm.

What is the height of a connected phase DNAPL pool of PCE necessary to enter a fracture that has an aperture of 0.032 cm?

Inorganic Chemicals in Groundwater

■ 6.1 Introduction

Groundwater is a solvent that is in contact with various earth materials. As a result, groundwater naturally contains dissolved cations and anions as well as some nonionic inorganic material, such as silica (SiO_2). Naturally occurring groundwater can contain dissolved solids that range in concentration from less than 100 mg/L to more than 500,000 mg/L (Hem 1985). The major ion constituents of natural water include calcium, magnesium, sodium, potassium, chloride, sulfate, and bicarbonate/carbonate. Dissolved gasses can include nitrogen, carbon dioxide, methane, oxygen, and hydrogen sulfide. There are a number of ions that can be naturally present in small amounts that can affect the water quality. In addition, inorganic ions that impact upon water quality can be released to the subsurface via human activity. For example, at least 18 inorganic elements can be used in pesticides (chromium, chlorine, fluorine, tin, arsenic, selenium, barium, cadmium, sulfur, phosphorus, mercury, zinc, lead, copper, thallium, bismuth, boron, and antimony), and many metals can be joined with carbon to form organometallic pesticides (Clarkson 2001).

We have already seen in Chapter 3 that ions can be removed from solution by ion exchange and sorption. In this chapter we will examine other chemical processes that act to remove inorganic ions from solution. We will also examine the chemical properties of a number of inorganic materials frequently found in groundwater. The geochemical zonation that can occur near landfills that have received municipal waste will be used to illustrate some basic principles.

■ 6.2 Units of Measurement and Concentration

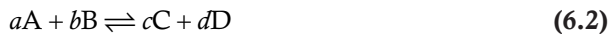
Chemical analyses are usually reported on the basis of weight of solute per volume of solvent. Common units are **milligrams per liter** (mg/L) and **micrograms per liter** (µg/L). Equivalent weight units are frequently used when the chemical behavior of a solute is being considered. The **equivalent weight** of an ion is the formula weight divided by the electrical charge. If the concentration of the ion in milligrams per liter is divided by the formula weight, the resulting concentration is expressed in terms of **milliequivalents per liter**. One **mole** of a substance is its formula weight in grams. A **1-molal** solution has 1 mole of solute in 1000 g of solvent. A **1-molar** (1-M) solution has 1 mole of solute in a liter of solution.

If a solution is dilute and there is no need to make density corrections, the molality can be determined from the concentration by the following equation:

$$\text{Molality} = \frac{\text{milligrams per liter} \times 10^{-3}}{\text{formula weight in grams}} \quad (6.1)$$

■ 6.3 Chemical Equilibrium and the Law of Mass Action

The law of mass action states that the rate of a chemical reaction will be proportional to the active masses of the participating substances (Hem 1985). If there are two substances, A and B, reacting to form two other substances, C and D, and if the process is reversible, then the reaction can be written as



The rate of the forward reaction, R_1 , is

$$R_1 = k'_1 [A]^a [B]^b \quad (6.3)$$

whereas the rate of the reverse reaction, R_2 , is

$$R_2 = k'_2 [C]^c [D]^d \quad (6.4)$$

where:

$[A]$ = active concentration of substance A

k'_1 = proportionality constant for the forward reaction

k'_2 = proportionality constant for the reverse

If the reaction progresses to a point where the forward reaction rate is equal to the reverse reaction rate, then

$$k'_1 [A]^a [B]^b = k'_2 [C]^c [D]^d \quad (6.5)$$

Equation 6.5 can be rearranged to yield the following expression:

$$\frac{[C]^c [D]^d}{[A]^a [B]^b} = \frac{k'_1}{k'_2} = K_{eq} \quad (6.6)$$

where K_{eq} is the equilibrium constant.

If two or more ions react to form a solid precipitate and the reaction is reversible, then it can be represented as



The equilibrium relationship of this reaction is:

$$K_{sp} = \frac{[A]^a [B]^b}{[AB]^c} \quad (6.8)$$

where K_{sp} is called a **solvability product**. The activity of the solid together with the water is defined as unity. Solubility products can be used to compute the concentration

of a solute in equilibrium with a solid phase, either via dissolution of the solid into an undersaturated solution or following precipitation of the solid from a saturated solution.

If one is dealing with a very dilute aqueous solution, then molal concentrations can be used to determine chemical equilibrium. However, for the general case, one must use **chemical activities** to employ the law of mass action.

The chemical activity of ion X , $[X]$, is equal to the molal concentration of X , m_x , times a factor known as an **activity coefficient**, γ_x :

$$[X] = m_x \gamma_x \quad (6.9)$$

The activity coefficient varies with the total amount of cations and anions in solution. The concentration and charge of the various ions in a solution determine its **ionic strength**. Ionic strength can be computed from the following formula:

$$I = \frac{1}{2} \sum m_i z_i^2 \quad (6.10)$$

where

I = ionic strength

m_i = molality of the i th ion

z_i = charge of the i th ion

Once the ionic strength is determined, the activity coefficient can be calculated using the Debye-Hückel equation:

$$-\log \gamma_i = \frac{Az_i^2 \sqrt{I}}{1 + a_i B \sqrt{I}} \quad (6.11)$$

where

γ_i = the activity coefficient for ionic species i

z_i = the charge on ionic species i

I = ionic strength of the solution

A = constant equal to 0.5085 at 25°C

B = constant equal to 0.3281 at 25°C

a_i = the effective diameter of the ion from Table 6.1

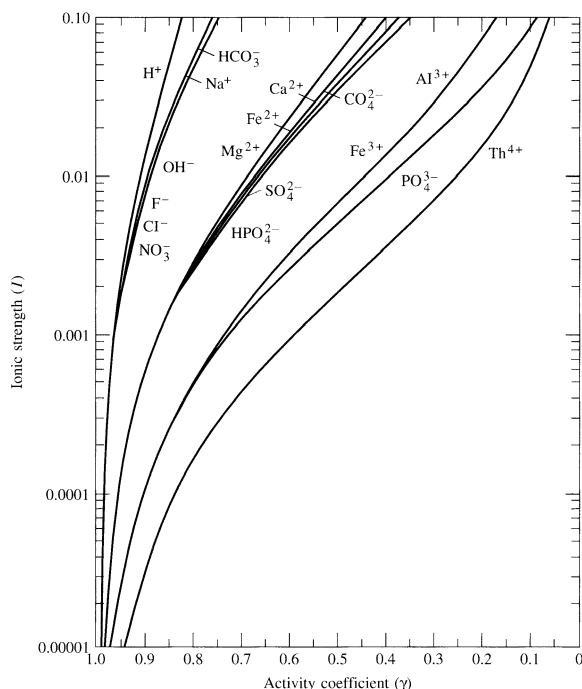
The Debye-Hückel equation can be used with solutions that have an ionic strength of 0.1 or less (approximately 5000 mg/L). Figure 6.1 is a graph showing the relationship of activity coefficient to ionic strength for specific ions; it was calculated using the Debye-Hückel equation. Specific curves are for ions with the same effective diameter and charge as listed in Table 6.1. Not all the ions to which a curve applies are listed on the figure. For example, the curve labeled Ca^{2+} and Fe^{2+} can also be used for Cu^{2+} , Zn^{2+} , Sn^{2+} , Mn^{2+} , Ni^{2+} , and Co^{2+} , because all these ions have the same effective diameter and charge.

Chemical equilibrium is a useful concept in studies of contaminant hydrogeology. Ionic contaminants discharged into groundwater may react with naturally occurring

TABLE 6.1 Values of the parameter a_i in the Debye-Hückel equation.

a_i	Ion
11	$\text{Th}^{4+}, \text{Sn}^{4+}$
9	$\text{Al}^{3+}, \text{Fe}^{3+}, \text{Cr}^{3+}, \text{H}^+$
8	$\text{Mg}^{2+}, \text{Be}^{2+}$
6	$\text{Ca}^{2+}, \text{Cu}^{2+}, \text{Zn}^{2+}, \text{Sn}^{2+}, \text{Mn}^{2+}, \text{Fe}^{2+}, \text{Ni}^{2+}, \text{Co}^{2+}, \text{Li}^+$
5	$\text{Fe}(\text{CN})_6^{4-}, \text{Sr}^{2+}, \text{Ba}^{2+}, \text{Cd}^{2+}, \text{Hg}^{2+}, \text{S}^{2-}, \text{Pb}^{2+}, \text{CO}_3^{2-}, \text{SO}_3^{2-}, \text{MoO}_4^{2-}$
4	$\text{PO}_4^{3-}, \text{Fe}(\text{CN})_6^{3-}, \text{Hg}_2^{2-}, \text{SO}_4^{2-}, \text{SeO}_4^{2-}, \text{CrO}_4^{3-}, \text{HPO}_4^{2-}, \text{Na}^+, \text{HCO}_3^-, \text{H}_2\text{PO}_4^-$
3	$\text{OH}^-, \text{F}^-, \text{CNS}^-, \text{CNO}^-, \text{HS}^-, \text{ClO}_4^-, \text{K}^+, \text{Cl}^-, \text{Br}^-, \text{I}^-, \text{CN}^-, \text{NO}_2^-, \text{NO}_3^-, \text{Rb}^+, \text{Cs}^+, \text{NH}_4^+, \text{Ag}^+$

Source: J. Kielland. 1937. Individual activity coefficients of ions in aqueous solutions. *American Chemical Society Journal* 59:1676–1678. Published by the American Chemical Society. Used with permission.

FIGURE 6.1 Relationship of activity coefficients of dissolved ions as a function of the ionic strength of a solution at 25°C.

Source: J. D. Hem. 1985. *Study and interpretation of the chemical characteristics of natural waters*. Water Supply Paper 2254, U.S. Geological Survey.

ions in the groundwater to form a precipitate or they may mobilize ions sorbed on solid surfaces. They may also undergo oxidation or reduction. Both these processes are reversible and can be described by chemical equilibrium. Many geochemical processes in groundwater are not readily reversible, such as weathering of silicate minerals. These reactions must be treated using kinetics. However, as this type of reaction is

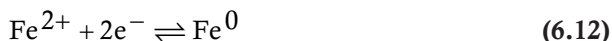
not of significant interest in contaminant hydrogeology, we do not typically consider kinetic models.

Table 6.2 contains the solubility products for a large number of minerals, including many that can be formed from trace metals that can be ground-water contaminants.

■ 6.4 Oxidation-Reduction Reactions

In some chemical reactions the participating elements change their valence state through the gain or loss of electron(s). If an electron is gained, there is a loss of positive valence called a reduction. A loss of negative valence is called an oxidation. Together, these are referred to as **oxidation-reduction**, or **redox**, reactions. In environmental systems they may be controlled by microorganisms that do not participate in the reaction but act as catalysts. The microbes occur as a biofilm on the surfaces of the aquifer materials. They obtain energy by oxidation of organic compounds or hydrogen or reduced inorganic forms of iron, nitrogen, and sulfur. Electron acceptors are necessary for these biologically mediated redox reactions to occur. Under aerobic conditions oxygen is the electron acceptor, whereas under anaerobic conditions nitrate, sulfate, and carbon dioxide are the electron acceptors (McCarty et al. 1984).

An example of a reduction is



In this example, ferrous iron is reduced to metallic iron by the addition of two electrons. This is a half-reaction, since the electrons must be supplied either by an electrical current or by a simultaneous reaction in which another element is oxidized and releases the requisite number of electrons. The standard electrical potential of a half-reaction is the voltage represented by the flow of electrons when the reaction is at equilibrium. Under standard conditions (25°C and 1 atm pressure) the standard potential is represented by the symbol E^0 . The potential is in volts, with a negative value representing reducing conditions and a positive value representing oxidizing conditions (Hem 1985). By convention, the standard potential for the reduction of H^+ to hydrogen gas is 0:



An example of oxidation occurs where ferrous iron loses an electron to form ferric iron:



Oxidation-reduction reactions involve elements that can occur in more than one valence state. In Equations 6.12 and 6.14, iron occurred in the metallic (0) as well as the +2 and +3 states. Metals can usually occur in the metallic state with a zero valence and at least one other valence state. Some elements that are environmentally important can occur in several different valence states. Table 6.3 lists several elements that occur in different valence states and examples of compounds and ions formed from those elements.

In order for oxidation or reduction to occur in a chemical reaction, one element must be reduced while a second element is being oxidized. For example, the complete equation for the oxidation of ferrous iron to ferric iron is

TABLE 6.2 Solubility products for selected minerals and compounds.

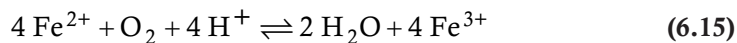
Compound	Solubility Product	Mineral Name
Chlorides		
CuCl	$10^{-6.7}$	
PbCl ₂	$10^{-4.8}$	
Hg ₂ Cl ₂	$10^{-17.9}$	
AgCl	$10^{-9.7}$	
Fluorides		
BaF ₂	$10^{-5.8}$	
CaF ₂	$10^{-10.4}$	Fluorite
MgF ₂	$10^{-8.2}$	Sellaite
PbF ₂	$10^{-7.5}$	
SrF ₂	$10^{-8.5}$	
Sulfates		
BaSO ₄	$10^{-10.0}$	Barite
CaSO ₄	$10^{-4.5}$	Anhydrite
CaSO ₄ ·2 H ₂ O	$10^{-4.6}$	Gypsum
PbSO ₄	$10^{-7.8}$	Anglesite
Ag ₂ SO ₄	$10^{-4.8}$	
SrSO ₄	$10^{-6.5}$	Celestite
Sulfides		
Cu ₂ S	$10^{-48.5}$	
CuS	$10^{-36.1}$	
FeS	$10^{-18.1}$	
PbS	$10^{-27.5}$	Galena
HgS	$10^{-53.3}$	Cinnebar
ZnS	$10^{-22.5}$	Wurtzite
ZnS	$10^{-24.7}$	Sphalerite
Carbonates		
BaCO ₃	$10^{-8.3}$	Witherite
CdCO ₃	$10^{-13.7}$	
CaCO ₃	$10^{-8.35}$	Calcite
CaCO ₃	$10^{-8.22}$	Aragonite
CoCO ₃	$10^{-10.0}$	
FeCO ₃	$10^{-10.7}$	Siderite
PbCO ₃	$10^{-13.1}$	
MgCO ₃	$10^{-7.5}$	Magnesite
MnCO ₃	$10^{-9.3}$	Rhodochrosite
Phosphates		
AlPO ₄ ·2 H ₂ O	$10^{-22.1}$	Variscite
CaHPO ₄ ·2 H ₂ O	$10^{-6.6}$	
Ca ₃ [PO ₄] ₂	$10^{-28.7}$	
Cu ₃ [PO ₄] ₂	$10^{-36.9}$	
FePO ₄	$10^{-21.6}$	
FePO ₄ ·2 H ₂ O	$10^{-26.4}$	

Source: K. B. Krauskopf, *Introduction to Geochemistry*, 2d ed. (New York: McGraw-Hill, 1979).

Source: K. B. Krauskopf. 1979. *Introduction to Geochemistry, Second Edition*. New York: McGraw-Hill.

TABLE 6.3 Selected elements that can exist in more than one oxidation state.

Element	Valence State	Examples
Carbon	+4	HCO_3^- , CO_3^{2-}
	0	C
	-4	CH_4
Chromium	+6	CrO_4^{2-} , $\text{Cr}_2\text{O}_7^{2-}$
	+3	Cr^{3+} , Cr(OH)_3
Copper	+1	CuCl
	+2	CuS
Mercury	+1	Hg_2Cl_2
	+2	HgS
Iron	+2	Fe^{2+} , FeS
	+3	Fe^{3+} , Fe(OH)_3
Nitrogen	+5	NO_3^-
	+3	NO_2^-
	0	N
	-3	NH_4^+ , NH_3
Oxygen	0	O
	-1	H_2O_2
Sulfur	-2	H_2O , O^{2-}
	+2	H_2S , S^{2-} , PbS
	+5	$\text{S}_2\text{O}_3^{2-}$
	+6	$\text{S}_2\text{O}_6^{2-}$
		SO_4^{2-}



This complete reaction is composed of two half-reactions:



An aqueous solution has an oxidation potential indicated by the symbol Eh. This can be calculated from the **Nernst equation**:

$$\text{Eh} = E^0 - \frac{RT}{nF} \ln \left[\frac{\text{products}}{\text{reactants}} \right] \quad (6.18)$$

where:

Eh = oxidation potential of the aqueous solution in volts

E^0 = standard potential of redox reaction in volts

R = gas constant, 0.00199 Kcal/(mole·K)

T = temperature in Kelvins

F = Faraday constant, 23.06 Kcal/V

n = number of electrons in half-reaction

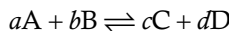
[] = activity of products and reactants

The standard potential for a reaction can be determined from the relationship

$$E^0 = \frac{-\Delta G_R^0}{nF} \quad (6.19)$$

where ΔG_R^0 in volts is the **free energy**, or **Gibbs free energy**, of the reaction.

The free energy of a reaction is the sum of the free energies of the products minus the sum of the free energies of the reactants. For the reaction



the free energy can be found from:

$$\Delta G_R^0 = c\Delta G_c^0 + d\Delta G_d^0 - a\Delta G_a^0 - b\Delta G_b^0 \quad (6.20)$$

Values of free energy for many elements, ions, and compounds are found in standard reference works. Table 6.4 contains values for a number of species.

The equilibrium constant for a reaction is related to the free energy of the reaction by

$$\Delta G_R^0 = -RT \ln K_{eq} \quad (6.21)$$

At standard temperature and pressure and with ΔG_R^0 in kilocalories, Equation 6.21 can be rewritten as

$$\log K_{eq} = \frac{-\Delta G_R^0}{1.364} \quad (6.22)$$

The oxidation potential of an aqueous solution can be measured using a redox or ORP electrode. If the value is positive, the solution is oxidizing, and if it is negative, the solution is reducing. Oxidation potential is measured in volts relative to the hydrogen electrode, which is at zero. Commercially available Eh meters are available that can be attached to a groundwater sampling pump. The groundwater sample is pumped under positive pressure into the flowthrough cell where the electrode is located. The water sample is never subjected to a vacuum, which could cause degassing. Moreover, it is not exposed to the atmosphere, where it can come into contact with atmospheric oxygen. This has simplified the accurate and precise measurement of Eh in groundwater. Eh is directly proportional to pE, which is defined as the logarithm of the electron concentration in a solution, and is an analogous measure of the **oxidation/reduction potential**, ORP.

■ 6.5 Relationship between pH and Eh

6.5.1 pH

Water undergoes a dissociation into two ionic species:



The equilibrium constant for this reaction is

$$K_{eq} = \frac{[H^+][OH^-]}{[H_2O]} \quad (6.24)$$

TABLE 6.4 Standard Gibbs free energy of formation for selected species.

Species	ΔG° kcal/mole	Species	ΔG° kcal/mole	Species	ΔG° kcal/mole
Arsenic		Manganese		Uranium	
$\text{As}_2\text{O}_5(\text{c})$	-187.0 ^a	$\text{MnO}_2(\text{c})$ (pyrolusite)	-111.18 ^b	$\text{UO}_2(\text{c})$ (uranite)	-246.61 ^c
$\text{As}_4\text{O}_6(\text{c})$	-275.46 ^a	Mn_2O_3 (bixbyite)	-210.6 ^b	$\text{UO}_2^+(\text{aq})$	-229.69 ^a
$\text{As}_2\text{S}_2(\text{c})$	-40.3 ^a	Mn_3O_4 (haussmannite)	-306.7 ^b	$\text{UO}_2^{2+}(\text{aq})$	-227.68 ^a
$\text{FeAsO}_4(\text{c})$	-185.13 ^a	$\text{Mn}(\text{OH})_2$ (amorphous)	-147.0 ^b	$(\text{UO}_2)_2[\text{OH}]_{2+}(\text{aq})$	-560.99 ^a
$\text{H}_3\text{AsO}_4(\text{aq})$	-183.1 ^a	$\text{MnCO}_3(\text{c})$ (rhodochrosite)	-195.2 ^b	$(\text{UO}_2)_3[\text{OH}]_5^+(\text{aq})$	-945.16 ^a
$\text{H}_2\text{AsO}_4^{-}(\text{aq})$	-180.04 ^a	$\text{Mn}^{2+}(\text{aq})$	-54.5 ^b	$(\text{UO}_2)_3[\text{OH}]_7^-$	-1037.5 ^a
$\text{HAsO}_4^{2-}(\text{aq})$	170.82 ^a	$\text{MnOH}^+(\text{aq})$	-96.8 ^b	$\text{UO}_2\text{CO}_3^0(\text{c})$	-367.07 ^a
$\text{AsO}_4^{3-}(\text{aq})$	-155.0 ^a	Molybdenum		$\text{UO}_2[\text{CO}_3]_2^{2-}(\text{aq})$	-503.2 ^a
$\text{HAsO}_2(\text{aq})$	-96.25 ^a	$\text{MoO}_3(\text{c})$	-159.66 ^b	$\text{UO}_2[\text{CO}_3]_3^{4-}(\text{aq})$	-635.69 ^a
$\text{AsO}_2^-(\text{aq})$	-83.66 ^a	$\text{MoO}_2(\text{c})$	-127.40 ^b	Miscellaneous species	
Chromium		$\text{FeMoO}_4(\text{c})$	-233 ^b	$\text{ZnFe}_2\text{O}_4(\text{c})$	-254.2 ^a
$\text{Cr}_2\text{O}_3(\text{c})$	-252.9 ^f	$\text{MoO}_4^{2-}(\text{aq})$	-199.9 ^b	$\text{CuFeO}_2(\text{c})$	-114.7 ^b
HCrO_4^-	-182.8 ^f	Silver		$\text{CuFe}_2\text{O}_4(\text{c})$	-205.26 ^b
$\text{Cr}_2\text{O}_7^{2-}(\text{aq})$	-311.0 ^f	$\text{Ag}_2\text{O}(\text{c})$	-2.68 ^b	$\text{NiFe}_2\text{O}_4(\text{c})$	-232.6 ^b
$\text{CrO}_4^{2-}(\text{aq})$	-173.96 ^f	$\text{AgCl}(\text{c})$	-26.24 ^b	$\text{H}_2\text{O}(\text{l})$	-56.687 ^a
Copper		$\text{Ag}_2\text{S}(\text{c})$	-9.72 ^b	$\text{OH}^-(\text{aq})$	-37.594 ^a
$\text{CuO}(\text{c})$	-31.0 ^b	$\text{Ag}_2\text{CO}_3(\text{c})$	-104.4 ^b	$\text{O}_2(\text{aq})$	-3.9 ^a
$\text{CuSO}_4 \cdot 3\text{Cu}(\text{OH})_2(\text{c})$ (brochantite)	-434.5 ^b	$\text{Ag}^+(\text{aq})$	18.43 ^b	$\text{HSO}_4^- (\text{aq})$	-180.69 ^a
$\text{Cu}_2\text{O}(\text{c})$	-34.9 ^b	$\text{AgOH}(\text{aq})$	-22.0 ^b	$\text{SO}_4^{2-}(\text{aq})$	-177.97 ^a
$\text{Cu}_2\text{S}(\text{c})$	-20.6 ^b	$\text{Ag}(\text{OH})_2^- (\text{aq})$	-62.2 ^b	$\text{H}_2\text{S}(\text{aq})$	-6.66 ^a
$\text{Cu}^{2+}(\text{aq})$	15.67 ^b	$\text{AgCl}(\text{aq})$	-17.4 ^b	$\text{HS}^- (\text{aq})$	2.88 ^a
$\text{CuSO}_4(\text{aq})$	-165.45 ^b	$\text{AgCl}_2^-(\text{aq})$	-51.5 ^b	$\text{S}^{2-}(\text{aq})$	20.5 ^a
$\text{HCuO}_2(\text{aq})$	-61.8 ^b	Vanadium		$\text{CO}_2(\text{g})$	-94.254 ^a
$\text{CuO}_2^{2-}(\text{aq})$	-43.9 ^b	H_4VO_4^+	-253.67 ^k	$\text{CO}_2(\text{aq})$	-92.26 ^a
$\text{Cu}^+(\text{aq})$	11.95 ^b	H_3VO_4^0	-249.2 ^k	$\text{H}_2\text{CO}_3(\text{aq})$	-148.94 ^a
Iron		H_2VO_4^-	-244 ^k	$\text{HCO}_3^- (\text{aq})$	-140.26 ^a
$\text{Fe(OH)}_3(\text{c})$ ppt.	-166.0 ^b	HVO_4^{2-}	-233.0 ⁱ	$\text{CO}_3^{2-}(\text{aq})$	-126.17 ^a
$\text{Fe(OH)}_2(\text{c})$ ppt.	-116.3 ^f	$\text{VO}_4^{3-}(\text{aq})$	-230.0 ⁱ	$\text{Cl}^-(\text{aq})$	-31.37 ^a
$\text{FeCO}_3(\text{c})$ (siderite)	-159.35 ^b	$\text{VO}^{2+}(\text{aq})$	-214.9 ^k	$\text{CH}_4(\text{g})$	-12.13 ^a
$\text{FeS}_2(\text{c})$ (pyrite)	-39.9 ^b	$\text{V}(\text{OH})_3^0(\text{aq})$	-106.7 ⁱ	$\text{CH}_4(\text{aq})$	-8.22 ^a
Fe_2O_3 (hematite)	-177.4 ^b	$\text{VOH}^{2+}(\text{aq})$	-212.9 ^k	$\text{H}^+(\text{aq})$	0.00
$\text{Fe}^{3+}(\text{aq})$	-1.1 ^b	$\text{V}(\text{OH})_2^+$	-111.41 ^k	$\text{Cl}^-(\text{aq})$	-31.38 ^c
$\text{FeOH}^{2+}(\text{aq})$	-54.83 ^b	VOOH^+	-163.2 ^k	$\text{PO}_4^{3-}(\text{aq})$	-243.5 ^a
$\text{Fe}(\text{OH})_2(\text{aq})$	-106.7 ^b	V^{3+}	-155.65 ^k	$\text{HPO}_4^{2-}(\text{aq})$	-260.34 ^a
$\text{Fe}^{2+}(\text{aq})$	-18.85 ^b	Uranium		$\text{H}_2\text{PO}_4^- (\text{aq})$	-270.14 ^k
$\text{FeOH}^+(\text{aq})$	-62.58 ^b	$\text{U}^{4+}(\text{aq})$	-126.44 ^e	$\text{H}_3\text{PO}_4^0(\text{c})$	-273.10 ^a
$\text{Fe}(\text{OH})_3^-(\text{aq})$	-147.0 ^b	$\text{UOH}^{3+}(\text{aq})$	-182.24 ^e	$\text{Na}^+(\text{aq})$	-62.59 ^c
$\text{Fe}(\text{OH})_4^-(\text{aq})$	-198.4 ^b	$\text{U}(\text{OH})_4^0(\text{c})$	-347.18 ^e	$\text{K}^+(\text{aq})$	-67.51 ^c
$\text{FeO}(\text{c})$	-60.03 ^b			$\text{NH}_4^+(\text{aq})$	-18.99 ^c
$\text{Fe}_2\text{S}(\text{c})$ (pyrite)	-38.3 ^b			$\text{Pb}^{2+}(\text{aq})$	-5.83 ^a
$\text{FeS}(\text{c})$	-24.22 ^b			$\text{O}_2(\text{g})$	0.00

c = solid

aq = aqueous solutions

g = gas

^a Wageman, D. D., W. H. Evans, V. B. Parker, I. Halow, S. M. Baily, and R. H. Schumm. 1968. *Selected values of chemical thermodynamic properties*. National Bureau of Standards Technical Note 270-3; 264 pp.

^b Wageman, D. D., W. H. Evans, V. B. Parker, I. Halow, S. M. Baily, and R. H. Schumm. 1969. *Selected values of chemical thermodynamic properties*. National Bureau of Standards Technical Note 270-4; 141 pp.

(Cont'd)

TABLE 6.4 Cont't

- ^c CODATA Task Group on Key Values for Thermodynamics. 1976. Recommended key values for thermodynamics 1975. *Journal of Chemical Thermodynamics* 8:603–5.
- ^d CODATA Task Group on Key Values for Thermodynamics. 1977. Recommended key values for thermodynamics 1976. *Journal of Chemical Thermodynamics* 9:705–6.
- ^e Giridhar J., and Donald Langmuir. 1991. Determination of E° for the $\text{UO}_2^{2+}/\text{U}^{4+}$ couple from measurement of the equilibrium: $\text{UO}_2^{2+} + \text{Cu(s)} + 4 \text{H}^+ = \text{U}^{4+} + \text{Cu}^{2+} + 2 \text{H}_2\text{O}$ at 25°C and some geochemical implications. *Radiochimica Acta* 54: 133–38.
- ^f *Handbook of Chemistry and Physics. Selected Values of Chemical Thermodynamic Properties*. Boca Raton, Fla.: CRC Press.
- ^g Robie, R. A., B. S. Hemingway, and J. R. Fisher. 1978. *Thermodynamic properties of minerals and related substances at 298.15 K and 1 bar (105 pascals) pressure and higher temperatures*. U.S. Geological Survey Bulletin 1452; 456 pp.
- ^h Feitknecht, Walter, and P.W. Schindler. 1963. Solubility constants of metal oxides, metal hydroxides and metal salts in aqueous solution. *Pure and applied Chemistry* 6: 130–57.
- ⁱ Baes, C. F., Jr., and R. E. Messmer. 1976. *The Hydrolysis of Cations*. New York: Wiley, 489 pp.
- ^j Wageman, D. D., W. H. Evans, V. B. Parker, I. Halow, S. M. Baily, and R. H. Schumm. 1968. *Selected values of chemical thermodynamic properties*. National Bureau of Standards Technical Note 270–5.
- ^k Langmuir, Donald. 1977. Uranium solution mineral equilibria at low temperatures. *Geochimica et Cosmochimica Acta* 42:547–69.

The value of this equilibrium constant depends upon the temperature, but at 25°C it is 1×10^{-14} . Water that is neutral has the same number of H^+ and OH^- ions. If there are more H^+ ions, water is acidic, and if there are more OH^- ions, it is basic.

The pH of an aqueous solution is a measure of the number of hydrogen ions or protons present. The definition of pH is the negative logarithm of the hydrogen ion activity. It ranges from 0 (most acidic) to 14 (most basic), and at 25°C a pH of 7 means that the solution is neutral. Because $[\text{H}_2\text{O}]$ is unity, from Equation 6.24 we have the relationship $[\text{H}^+][\text{OH}^-] = K_{eq} = 10^{-14}$. The pH of a solution is measured with a pH meter and an electrode. It should be measured in the field, preferably in a flowthrough cell so that dissolved gas isn't exchanged with the atmosphere prior to the measurement. The pH of a solution is especially sensitive to the amount of dissolved CO_2 .

6.5.2 Relationship of Eh and pH

We thus have two ways to characterize a solution. The pH describes the number of protons present and the Eh is related to the number of electrons. Eh and pH can be related through the Nernst equation for a reaction that contains water and H^+ ions. Such a reaction can be written (Robertson 1975)



where

- A = reactant
- B = product
- n = number of electrons released
- a = moles of reactant
- w = moles of water
- b = moles of product
- m = moles of hydrogen ions

The Nernst equation for Reaction 6.25 is

$$\text{Eh} = E^\circ - \frac{RT}{nF} \ln \frac{[A]^a [H_2O]^w}{[B]^b [H^+]^m} \quad (6.26)$$

The activity of water is unity. For a particular reaction, E° is given and R , T , and F are constants. The significant variables are the Eh and the activities of the reactant, the product, and the hydrogen-ion activity, which can be expressed as a pH. Equation 6.26 can be rearranged and expressed in base 10 logs as either

$$\text{Eh} = E^\circ - 2.303 \frac{RT}{nF} \log \frac{[A]^a}{[B]^b [H^+]^m} \quad (6.27)$$

or

$$\text{Eh} = E^\circ - 2.303 \frac{RT}{nF} \log \frac{[A]^a}{[B]^b} + 2.303 \frac{RTm}{nF} \log [H^+] \quad (6.28)$$

At 25°C and 1 atm of pressure, Equation 6.28 can be expressed as

$$\text{Eh} = E^\circ - \frac{0.0592}{n} \log \frac{[A]^a}{[B]^b} - 0.0592 \frac{m}{n} \text{pH} \quad (6.29)$$

6.5.3 Eh-pH Diagrams

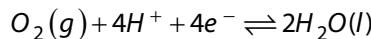
The Eh-pH relationship is particularly useful when applied in the form of an Eh-pH diagram, with Eh the ordinate and pH the abscissa. If a solution has several ions present that can react to form different products or occur in different valence states, the stable product or valence state at a given concentration of reactants will be a function of the pH and Eh of the solution.

Figure 6.2 is a basic Eh-pH diagram. The range of pH is 0 to 14. For Eh, it is convenient to specify a range of about +1.4 to -1.0 V. In certain regions of the Eh-pH field, water will be oxidized to O_2 , and in other regions water will be reduced to H_2 . We will calculate these regions as an example problem.

EXAMPLE PROBLEM

Calculate the stability field for water at standard conditions.

The oxidation of water is given by

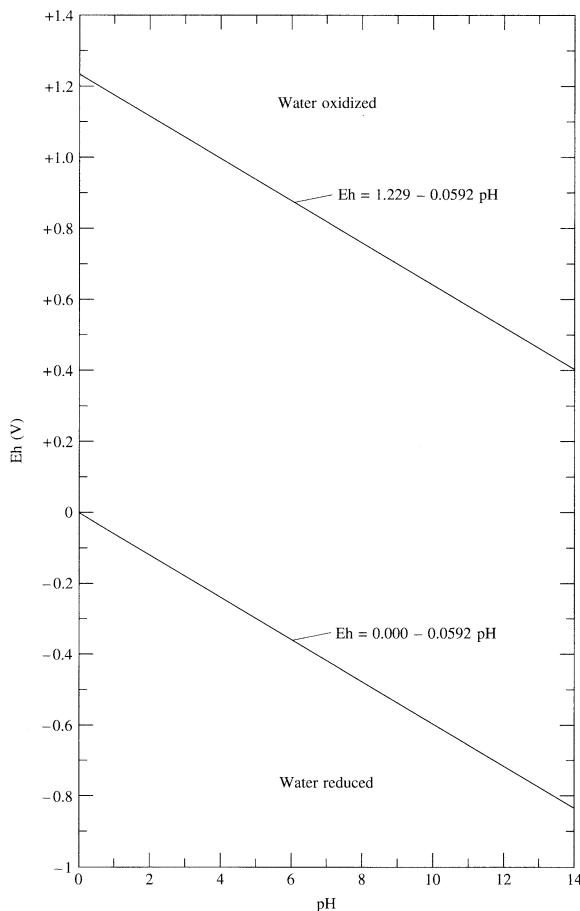


From Table 6.4,

$$\Delta G^\circ_{H_2O(l)} = -56.69 \text{ kcal}$$

$$\Delta G^\circ_{O_2(g)} = 0$$

$$\Delta G^\circ_{H^+} = 0$$

FIGURE 6.2 Eh-pH diagram showing the stability field for water.

From Equation 6.20,

$$\Delta G_R^0 = 2\Delta G_{H_2O(l)}^0 - \Delta G_{O_2(g)}^0 - 4\Delta G_{H^+}^0$$

$$\Delta G_R^0 = 2(-56.69) - 0 - 4(0) = -113.38 \text{ kcal}$$

The value of ΔG_R^0 in kilocalories is converted to a standard potential by use of Equation 6.19:

$$E^0 = \frac{-\Delta G_R^0}{nF} = \frac{-(-113.38)}{4 \cdot 23.06} = 1.229 \text{ V}$$

The Nernst equation (Equation 6.24) can be expressed as:

$$Eh = E^0 - \frac{RT}{nF} 2.303 \log \frac{[H_2O]}{[O_2][H^+]^4}$$

The activity of dissolved gaseous oxygen is expressed as a partial pressure, P_{O_2} . At standard conditions it has a value of 1 atm. The activity of water is unity. The Nernst equation thus reduces to

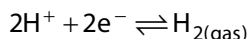
$$Eh = 1.229 - \frac{0.00199 \cdot 298}{4 \cdot 23.06} 2.303 \log [H^+]^{-4}$$

This expression can be reduced to

$$Eh_{(\text{Volts})} = 1.229 - 0.0592 \text{pH}$$

This equation defines the upper boundary of stability for water, above which oxidation would break apart the water molecule.

The reduction of hydrogen ions to form gaseous hydrogen is



From Table 6.4,

$$\Delta G_{H^+}^0 = 0$$

$$\Delta G_{H_2(\text{gas})}^0 = 0$$

The value of ΔG_R^0 for the formation of hydrogen gas is obviously zero. Therefore, the value of E^0 is also zero.

From the Nernst equation,

$$Eh = E^0 - \frac{0.00199 \cdot 298}{2 \cdot 23.06} 2.303 \log \frac{P_{H_2}}{[H^+]^2}$$

The value of P_{H_2} is 1 atm and the calculated value of E^0 is 0, hence the preceding expression can be reduced to

$$Eh_{(\text{volts})} = 0.000 - 0.0592 \text{pH}$$

This equation forms the lower boundary of the stability field for water. These boundaries are plotted in Figure 6.2.

6.5.4 Calculating Eh-pH Stability Fields

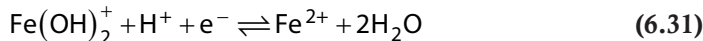
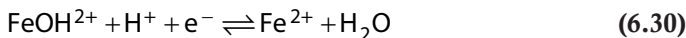
The stability fields within the Eh-pH diagram for various forms of an element can be computed using chemical thermodynamics. Basic sources of thermodynamic data include Bagman et al. (1968; 1969; 1971) and Robie et al. (1978).

Boundaries for an element between dissolved species that have different valence states are computed using the Nernst equation (Equation 6.27, 6.28, or 6.29). If both ions are at the same valence state, then the equation for chemical equilibrium is used. If one is calculating the boundary between a solid species and a dissolved form, the chemical activity of the solid species is 1. For some of the boundaries of solid species, it will be necessary to assume an activity for the dissolved species.

EXAMPLE PROBLEM

Calculate an Eh-pH diagram for iron in which the solid species are Fe(OH)_3 and FeO and the activity of dissolved iron is $56 \mu\text{g/L} (10^{-6} \text{ M})$.

Soluble forms of the ferrous ion and the ferric ion include Fe^{2+} , Fe^{3+} , FeOH^{2+} , and Fe(OH)_2^+ . Transformations between these ions are determined by redox equations:



The free energy and the standard potential for these reactions can be determined from Equations 6.20 and 6.19, respectively.

From Table 6.4 free energies are as follows.

$$\text{FeOH}^{2+} = -54.83 \text{ kcal/mol} \quad \text{FeO} = -60.03 \text{ kcal/mol}$$

$$\text{Fe(OH)}_2^+ = -106.7 \text{ kcal/mol} \quad \text{Fe(OH)}_3 = -166 \text{ kcal/mol}$$

$$\text{Fe}^{2+} = -18.85 \text{ kcal/mol} \quad \text{Fe(OH)}_4^- = -198.4 \text{ kcal/mol}$$

$$\text{Fe}^{3+} = -1.1 \text{ kcal/mol} \quad \text{H}^+ = 0$$

$$\text{H}_2\text{O} = -56.69 \text{ kcal/mol}$$

For Reaction 6.30 ($\text{FeOH}^{2+} + \text{H}^+ + \text{e}^- \rightleftharpoons \text{Fe}^{2+} + \text{H}_2\text{O}$):

$$\Delta G_R^0 = \left[\Delta G_{\text{H}_2\text{O}}^0 + \Delta G_{\text{Fe}^{2+}}^0 \right] - \left[\Delta G_{\text{FeOH}^{2+}}^0 + \Delta G_{\text{H}^+}^0 \right]$$

$$\Delta G_R^0 = -56.69 + (-18.85) - (-54.83) - 0$$

$$\Delta G_R^0 = -20.71 \text{ kcal/mol}$$

$$E^0 = \frac{-\Delta G_R^0}{nF} = \frac{-(-20.71)}{1 \cdot 23.06} \text{ V}$$

$$E^0 = +0.898 \text{ V}$$

For Reaction 6.31 ($\text{Fe(OH)}_2^+ + 2\text{H}^+ + \text{e}^- \rightleftharpoons \text{Fe}^{2+} + 2\text{H}_2\text{O}$):

$$\Delta G_R^0 = 2\Delta G_{\text{H}_2\text{O}}^0 + \Delta G_{\text{Fe}^{2+}}^0 - \Delta G_{\text{Fe(OH)}_2^+}^0 - 2\Delta G_{\text{H}^+}^0$$

$$\Delta G_R^0 = 2(-56.69) + (-18.85) - (-106.7) - 2(0)$$

$$\Delta G_R^0 = -25.53 \text{ kcal/mol}$$

$$E^0 = \frac{-\Delta G_R^0}{nF} = \frac{-(-25.53)}{1 \cdot 23.06} \text{ V}$$

$$E^0 = +1.107 \text{ V}$$

For Reaction 6.32 ($\text{Fe}^{3+} + e^- \rightleftharpoons \text{Fe}^{2+}$):

$$\begin{aligned}\Delta G_R^0 &= \Delta G_{\text{Fe}^{2+}}^0 - \Delta G_{\text{Fe}^{3+}}^0 \\ \Delta G_R^0 &= -18.85 - (-1.1) \\ \Delta G_R^0 &= -17.75 \\ E^0 &= \frac{-\Delta G_R^0}{nF} = \frac{-(-17.75)}{1 \cdot 23.06} V \\ E^0 &= +0.770 V\end{aligned}$$

The boundaries between the stability fields are determined from the Nernst equation. At the boundary between two fields, the activities of the iron species on the left of the reaction is equal to the activity of the iron species on the right of the equation—i.e., the two species are at equilibrium.

For Reaction 6.30 ($\text{FeOH}^{2+} + \text{H}^+ + e^- \rightleftharpoons \text{Fe}^{2+} + \text{H}_2\text{O}$):

$$\text{Eh} = E^0 - \frac{0.0592}{n} \log \frac{[\text{Fe}^{2+}]}{[\text{FeOH}^{2+}]} - 0.0592 \frac{m}{n} \text{pH}$$

Since $[\text{FeOH}^{2+}] = [\text{Fe}^{2+}]$, m (the number of hydrogen ions) = 1, n (the number of electrons) = 1, $E^0 = +0.898$ V, and $\log 1 = 0$:

$$\text{Eh}_{(\text{volts})} = 0.898 - 0.0592 \text{ pH} \quad (6.33)$$

For Reaction 6.31 ($(\text{Fe(OH})_2^+ + 2\text{H}^+ + e^- \rightleftharpoons \text{Fe}^{2+} + 2\text{H}_2\text{O}$):

$$\text{Eh} = E^0 - \frac{0.0592}{n} \log \frac{[\text{Fe}^{2+}]}{[(\text{Fe(OH})_2^+]^2]} - 0.0592 \frac{m}{n} \text{pH}$$

Since $[(\text{Fe(OH})_2^+)] = [\text{Fe}^{2+}]$, $m = 2$, $n = 1$, and $E^0 = +1.107$ V:

$$\text{Eh}_{(\text{volts})} = 1.107 - 0.1184 \text{ pH} \quad (6.34)$$

For Reaction 6.32 ($\text{Fe}^{3+} + e^- \rightleftharpoons \text{Fe}^{2+}$):

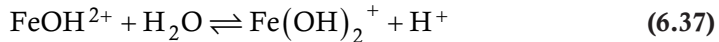
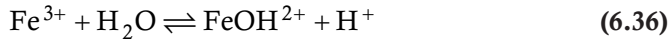
$$\text{Eh} = E^0 - \frac{0.0592}{n} \log \frac{[\text{Fe}^{2+}]}{[\text{Fe}^{3+}]} - 0.0592 \frac{m}{n} \text{pH}$$

This reaction is independent of pH because neither $[\text{H}^+]$ nor $[\text{OH}^-]$ appears in the reaction. Hence the value of m is 0. Because as $[\text{Fe}^{3+}] = [\text{Fe}^{2+}]$ and $\log 1 = 0$, Eh is a constant equal to E^0 , which is 0.770 V:

$$\text{Eh} = 0.770 \text{ V} \quad (6.35)$$

The boundary between two dissolved species that are at the same valence state can be determined from chemical equilibrium.

For iron there are two boundaries between dissolved ions of ferric iron. These boundaries are represented by these reactions:



For Reaction 6.36 ($\text{Fe}^{3+} + \text{H}_2\text{O} \rightleftharpoons \text{FeOH}^{2+} + \text{H}^+$), the equilibrium constant can be obtained from the free energy of the reaction. The first step is to find the free energy of the reaction using Equation 6.20.

$$\Delta G_R^0 = \Delta G_{\text{FeOH}^{2+}}^0 + \Delta G_{\text{H}^+}^0 - \Delta G_{\text{Fe}^{3+}}^0 - \Delta G_{\text{H}_2\text{O}}^0$$

$$\Delta G_R^0 = -54.83 + 0 - (-1.1) - (-56.69)$$

$$\Delta G_R^0 = +2.96 \text{ kcal/mol}$$

The next step is to determine the equilibrium constant using Equation 6.22.

$$\log k_{eq} = -\frac{\Delta G_R^0}{1.364} = -\frac{2.96}{1.364} = -2.17$$

$$K_{eq} = 10^{-2.17}$$

From Equation 6.6,

$$K_{eq} = \frac{[\text{FeOH}^{2+}][\text{H}^+]}{[\text{Fe}^{3+}][\text{H}_2\text{O}]} = 10^{-2.17}$$

Since $[\text{H}_2\text{O}] = 1$ and at the boundary $[\text{FeOH}^{2+}] = [\text{Fe}^{3+}]$,

$$[\text{H}^+] = 10^{-2.17} \quad (6.38)$$

This means that a vertical line at a pH of 2.17 separates these two stability fields.

For Reaction 6.37 ($\text{FeOH}^{2+} + \text{H}_2\text{O} \rightleftharpoons \text{Fe(OH)}_2^+ + \text{H}^+$), find the free energy of the reaction:

$$\Delta G_R^0 = \Delta G_{\text{Fe(OH)}_2^+}^0 + \Delta G_{\text{H}^+}^0 - \Delta G_{\text{FeOH}^{2+}}^0 - \Delta G_{\text{H}_2\text{O}}^0$$

$$\Delta G_R^0 = -106.7 + 0 - (-54.83) - (-56.69)$$

$$\Delta G_R^0 = +4.82 \text{ kcal/mol}$$

Next find the value of K_{eq} :

$$\log K_{eq} = \frac{-\Delta G_R^0}{1.364} = \frac{-4.82}{1.364} = -3.53$$

$$K_{eq} = 10^{-3.53}$$

Finally, from Equation 6.6,

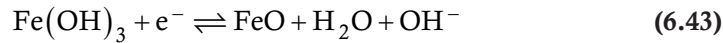
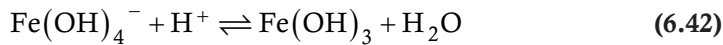
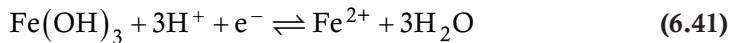
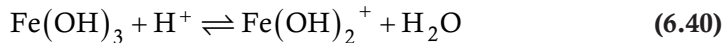
$$K_{eq} = \frac{[\text{Fe(OH)}^{2+}][\text{H}^+]}{[\text{FeOH}^{2+}][\text{H}_2\text{O}]} = 10^{-3.53}$$

Since $[\text{H}_2\text{O}] = 1$ and $[\text{Fe(OH)}^{2+}] = [\text{FeOH}^{2+}]$,

$$[\text{H}^+] = 10^{-3.53} \quad (6.39)$$

Lines that delineate the stability field for solids can be obtained by similar reasoning. Remember that the activity of a solid in equilibrium with dissolved species is 1. The location of the boundaries of solid species is a function of the amount of dissolved iron present.

In this situation there are two stable iron precipitates, Fe(OH)_3 and FeO . The reactions at the boundaries include



Reaction 6.40 $\text{Fe(OH)}_3 + \text{H}^+ \rightleftharpoons \text{Fe(OH)}_2^+ + \text{H}_2\text{O}$ is solved using an equilibrium approach:

$$\Delta G_R^0 = \Delta G_{\text{Fe(OH)}_2^+}^0 + \Delta G_{\text{H}_2\text{O}}^0 - \Delta G_{\text{Fe(OH)}_3}^0 - \Delta G_{\text{H}^+}^0$$

$$\Delta G_R^0 = -106.7 + (-56.69) - (-166) - 0 = 2.61$$

$$\log K_{eq} = -\frac{\Delta G_R^0}{1.364} = -\frac{2.61}{1.364} = -1.91$$

$$K_{eq} = 10^{-1.91}$$

$$K_{eq} = \frac{[\text{Fe(OH)}_2^+][\text{H}_2\text{O}]}{[\text{Fe(OH)}_3][\text{H}^+]} = 10^{-1.91}$$

Since $[Fe(OH)_3] = 1$ and $[H_2O] = 1$,

$$[H^+] = \frac{[Fe(OH)_2^+]}{10^{-1.91}}$$

Reaction 6.41 $Fe(OH)_3 + 3H^+ + e^- \rightleftharpoons Fe^{2+} + 3H_2O$ is solved using the Nernst equation:

$$\Delta G_R^0 = \Delta G_{Fe^{2+}}^0 + 3\Delta G_{H_2O}^0 - \Delta G_{Fe(OH)_3}^0 - 3\Delta G_{H^+}^0$$

$$\Delta G_R^0 = -18.85 + 3(-56.69) - (-166) - 0$$

$$\Delta G_R^0 = -22.95 \text{ kcal/mol}$$

$$E^0 = \frac{-\Delta G_R^0}{nF} = -\frac{(-22.95)}{1 \cdot 23.06} = +0.994 \text{ V}$$

$$Eh = E^0 - \frac{0.0592}{n} \log \frac{[Fe^{2+}]}{[Fe(OH)_3]} - 0.0592 \frac{m}{n} \text{ pH}$$

Since there are three hydrogen ions ($m = 3$) and one electron ($n = 1$) and $[Fe(OH)_3] = 1$, then

$$Eh_{(\text{Volts})} = 0.994 - 0.0592 \log [Fe^{2+}] - 0.178 \text{ pH} \quad (6.47)$$

Reaction 6.42 $(Fe(OH)_4^- + H^+ \rightleftharpoons Fe(OH)_3 + H_2O)$ is solved by using an equilibrium approach:

$$\Delta G_R^0 = \Delta G_{Fe(OH)_3}^0 + \Delta G_{H_2O}^0 - \Delta G_{Fe(OH)_4^-}^0 - \Delta G_{H^+}^0$$

$$\Delta G_R^0 = -166 - 56.69 - (-198.4) - 0$$

$$\Delta G_R^0 = -24.29$$

$$\log K_{eq} = -\frac{\Delta G_R^0}{1.364} = \frac{24.29}{1.364} = 17.8$$

$$K_{eq} = 10^{17.8}$$

$$K_{eq} = \frac{[Fe(OH)_3][H_2O]}{[Fe(OH)_4^-][H^+]} = 10^{17.8}$$

Since $[Fe(OH)_3] = 1$ and $[H_2O] = 1$,

$$[H^+] = \frac{10^{-17.8}}{[Fe(OH)_4^-]} \quad (6.48)$$

Equation 6.43 $(\text{Fe(OH)}_3 + e^- \rightleftharpoons \text{FeO} + \text{H}_2\text{O} + \text{OH}^-)$ is solved using the Nernst equation:

$$\Delta G^0_R = \Delta G^0_{\text{FeO}} + \Delta G^0_{\text{H}_2\text{O}} + \Delta G^0_{\text{OH}^-} - \Delta G^0_{\text{Fe(OH)}_3}$$

$$\Delta G^0_R = -60.03 + (-56.69) + (-37.59) - (-166)$$

$$\Delta G^0_R = +11.69$$

$$E^0 = \frac{-\Delta G^0_R}{nF} = \frac{-11.69}{1 \cdot 23.06} = -0.507 \text{ V}$$

$$\text{Eh} = E^0 - \frac{0.0592}{n} \log \frac{[\text{FeO}][\text{H}_2\text{O}][\text{OH}^-]}{[\text{Fe(OH)}_3]}$$

Since $[\text{Fe(OH)}_3] = 1$, $[\text{FeO}] = 1$, $[\text{H}_2\text{O}] = 1$, and $n = 1$,

$$\text{Eh} = -0.507 - 0.0592 \log [\text{OH}^-]$$

Because the diagram uses pH as a variable, $[\text{OH}^-]$ must be expressed in terms of pH. By definition, $[\text{OH}^-] = 10^{-14}/[\text{H}^+]$; therefore, $\log [\text{OH}^-] = \log 10^{-14} - \log [\text{H}^+]$, so that

$$\text{Eh} = -0.5.7 - 0.0592(\text{pH} - 14)$$

$$\text{Eh}_{(\text{volts})} = 0.322 - 0.0592 \text{ pH} \quad (6.49)$$

Reaction 6.44 $(\text{Fe(OH)}_4^- + 2\text{H}^+ + e^- \rightleftharpoons \text{FeO} + 3\text{H}_2\text{O})$ is solved using the Nernst equation:

$$\Delta G^0_R = \Delta G^0_{\text{FeO}} + 3\Delta G^0_{\text{H}_2\text{O}} - \Delta G^0_{\text{Fe(OH)}_4^-} - 2\Delta G^0_{\text{H}^+}$$

$$\Delta G^0_R = -60.03 + 3(-56.69) - (-198.4) - 0$$

$$\Delta G^0_R = -31.7 \text{ kcal/mol}$$

$$E^0 = \frac{-\Delta G^0_R}{nF} = \frac{-(-31.7)}{1 \cdot 23.06} = +1.375$$

$$\text{Eh} = E^0 - \frac{0.0592}{n} \log \frac{[\text{FeO}][\text{H}_2\text{O}]^3}{[\text{Fe(OH)}_4^-][\text{H}^+]^2}$$

Since $[\text{FeO}]$ and $[\text{H}_2\text{O}]$ are 1 and $n = 1$,

$$\text{Eh} = +1.375 - 0.0592 \log \frac{1}{[\text{Fe(OH)}_4^-][\text{H}^+]^2}$$

This can be expressed in terms of pH as

$$\begin{aligned}\text{Eh} &= 1.375 + 0.0592 \log \left[\text{Fe(OH)}_4^- + 2(0.0592) \log \left[\text{H}^+ \right] \right] \\ \text{Eh}_{(\text{volts})} &= 1.375 + 0.0592 \log \left[\text{Fe(OH)}_4^- \right] - 0.118 \text{pH} \quad (6.50)\end{aligned}$$

Reaction 6.45 ($\text{FeO} + 2\text{H}^+ \rightleftharpoons \text{Fe}^{2+} + \text{H}_2\text{O}$) is solved as an equilibrium reaction:

$$\Delta G^0_R = \Delta G^0_{\text{Fe}^{2+}} + \Delta G^0_{\text{H}_2\text{O}} - \Delta G^0_{\text{FeO}} - 2\Delta G^0_{\text{H}^+}$$

$$\Delta G^0_R = -18.85 + (-56.69) - (-60.03) - 2(0)$$

$$\Delta G^0_R = -15.51 \text{ kcal/mol}$$

$$\log k_{eq} = \frac{-\Delta G^0_R}{1.364} = 11.36$$

$$k_{eq} = 10^{11.36}$$

$$k_{eq} = \frac{[\text{Fe}^{2+}][\text{H}_2\text{O}]}{[\text{FeO}][\text{H}^+]^2}$$

Since $[\text{H}_2\text{O}]$ and $[\text{FeO}] = 1$,

$$\begin{aligned}[\text{H}^+]^2 &= \frac{[\text{Fe}^{2+}]}{10^{11.36}} \\ [\text{H}^+] &= \sqrt{\frac{[\text{Fe}^{2+}]}{10^{11.36}}} \quad (6.51)\end{aligned}$$

Several of the equations, including Equations 6.46, 6.47, 6.48, 6.50, and 6.51, depend upon the activity of the dissolved iron.

The following equations, which are independent of dissolved iron activity, have been derived.

Boundary	Equation Number	Equation
$\text{FeOH}^{2+} - \text{Fe}^{2+}$	6.31	$\text{Eh}_{(\text{volts})} = 0.898 - 0.0592\text{pH}$
$\text{Fe(OH)}_2^+ - \text{Fe}^{2+}$	6.32	$\text{Eh}_{(\text{volts})} = 1.107 - 0.118\text{pH}$
$\text{Fe}^{3+} - \text{Fe}^{2+}$	6.33	$\text{Eh}_{(\text{volts})} = 0.770$
$\text{Fe}^{3+} - \text{FeOH}^{2+}$	6.38	$\text{pH} = 2.17$
$\text{Fe(OH)}^{2+} - \text{Fe(OH)}_2^+$	6.39	$\text{pH} = 3.53$
$\text{Fe(OH)}_3 - \text{FeO}$	6.49	$\text{Eh}_{(\text{volts})} = 0.322 - 0.0592\text{pH}$

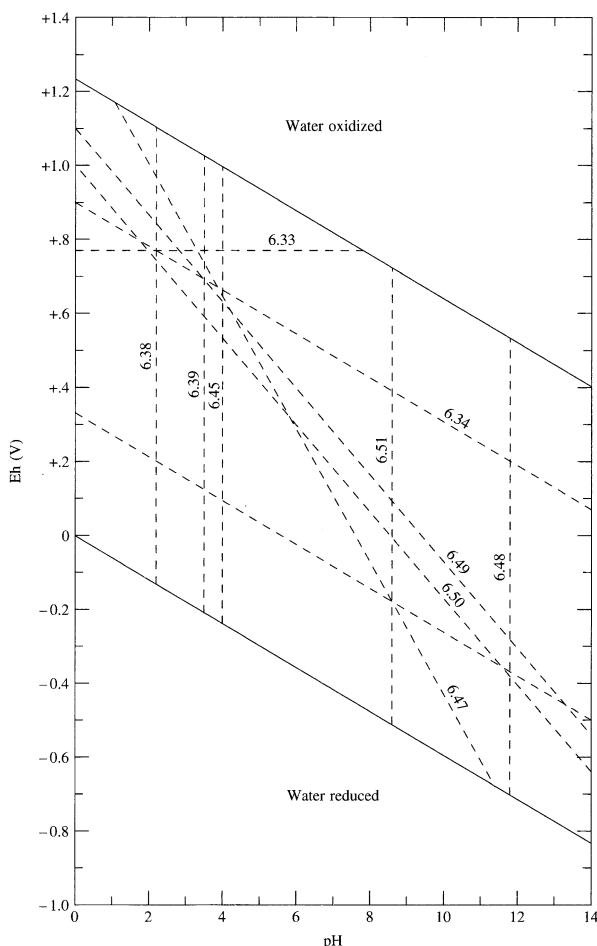
These equations need a dissolved iron activity, which is set at $10^{-6.00}$ mol:

Boundary	Equation	Equation Number	
			$[H^+] = [10^{-6}] / 10^{-1.91}$
$Fe(OH)_3 - Fe(OH)_2^+$	6.46		$= 10^{-4.09}$
			$pH = 4.09$
			$Eh_{(volts)} = 0.994 - 0.0592 \log[10^{-6}]$
$Fe(OH)_3 - Fe^{2+}$	6.47		-0.0178 pH
			$Eh_{(volts)} = 1.349 - 0.178 \text{ pH}$
			$[H^+] = 10^{-17/8} / [10^{-6}]$
$Fe(OH)_4 - Fe(OH)_3$	6.48		$= 10^{-11.8}$
			$pH = 11.8$
			$Eh_{(volts)} = 1.375 + 0.0592 \log [10^{-6}]$
$Fe(OH)_4 - FeO$	6.50		$= -0.118 \text{ pH}$
			$Eh_{(volts)} = 1.0202 - 0.118 \text{ pH}$
			$[H^+] = ([10^{-6}] / 10^{11.36})^{0.5}$
$FeO - Fe^{2+}$	6.51		$[H^+] = 10^{8.68}$
			$pH = 8.68$

Once the equations have been developed for the desired molar concentration of dissolved iron, the lines represented by the equations are plotted on an Eh-pH field. This has been done in Figure 6.3. The equation numbers are on the lines.

In order to finish the stability field diagram, we need to decide which segment of each line is needed. If we start with Fe^{3+} , it participates in two reactions, one characterized by Equation 6.33 and the other by Equation 6.38. Equation 6.33 is a horizontal line at 0.77 V and Equation 6.38 is a vertical line at $pH = 2.17$. These two lines define a corner at the upper left of the diagram in which Fe^{3+} can exist. Equation 6.38 divides the Fe^{3+} region from the $FeOH^{2+}$ region. This region is also bounded by Equations 6.31 and 6.39. The segments of these lines that intersect are used to define the $FeOH^{2+}$ region. In a similar manner of analysis, the line segments surrounding each of the stability fields are determined. The resulting Eh-pH diagram for the iron system is thus determined and is illustrated in Figure 6.4.

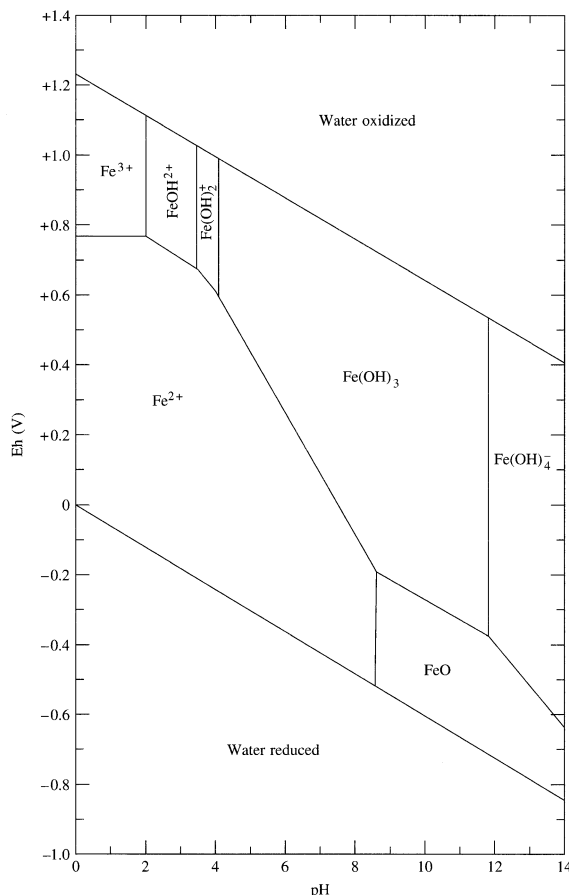
FIGURE 6.3 Equations for an Eh-pH diagram for dissolved iron with dissolved iron activity of 10^{-6} Mol under standard conditions. (Numbers adjacent to dotted lines refer to equations discussed in the text.)



The iron Eh-pH diagram of Figure 6.4 is for a system that contains only dissolved iron. If other elements are present, such as sulfur, then additional iron compounds are possible. Figure 6.5 shows an Eh-pH diagram for a system with an iron activity of $56 \mu\text{g/L}$ (10^{-6} mol), sulfur of 96 mg/L as SO_4^{2-} , and carbon dioxide of 61 mg/L as HCO_3^- . Solids in the shaded area are thermodynamically stable. Under the conditions specified in this diagram, iron carbonate (FeCO_3) saturation was not reached and none is recorded as a solid phase.

The area of the region in which iron is precipitated rather than dissolved is a function of the concentration of dissolved iron. The more dissolved iron that is present, the greater the size of the stability field for the precipitates. This is illustrated in Figure 6.6. In this diagram the sulfur is 96 mg/L as SO_4^{2-} and the carbonate is 61 mg/L as HCO_3^- . Dissolved iron ranges from $5.6 \mu\text{g/L}$ to 56 mg/L .

FIGURE 6.4 Final Eh-pH diagram for a dissolved iron system with dissolved iron at 10^{-6} moles under standard conditions.



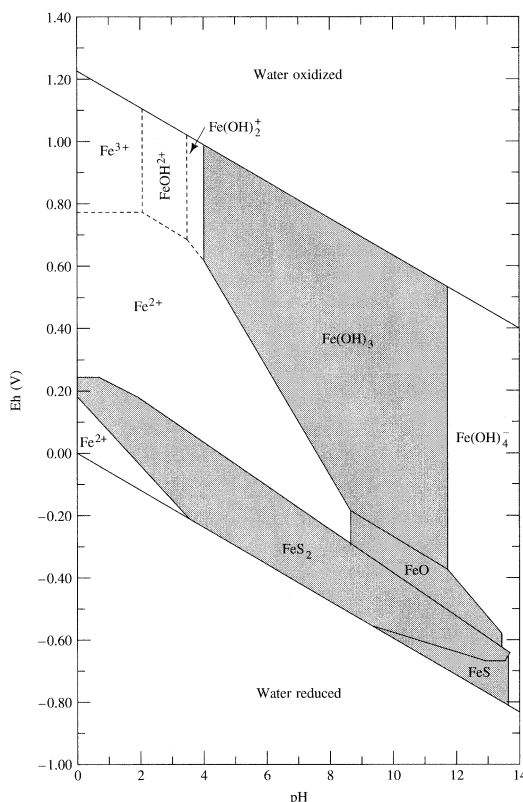
Eh-pH diagrams have been used in the ground-water literature to explain such phenomena as the solubility of ferric oxyhydroxides (Whittemore and Langmuir 1975), hexavalent chromium (Robertson 1975), manganese (Hem 1985), iron, copper, silver, chromium, manganese, vanadium, molybdenum, and arsenic (Hem 1977), uranium (Langmuir 1978), thorium (Langmuir and Herman 1980), and arsenic (Matisoff et al. 1982).

■ 6.6 Metal Complexes and Facilitated Particle Transport

6.6.1 Hydration of Cations

Although we consider that metallic ions exist in solution as an isolated ion, such as Cu^{2+} , in fact that is not the case. The Cu^{2+} ion is surrounded by polar water atoms that are chemically bound to the ion. Metallic ions, in general, have six water molecules

FIGURE 6.5 Eh-pH diagram showing fields of stability for dissolved iron under standard conditions. Activity of dissolved iron is 10^{-6} mol (56 µg/L), of sulfur species is 96 mg/L as SO_4^{2-} , and of carbon dioxide species is 61 mg/L as HCO_3^- .



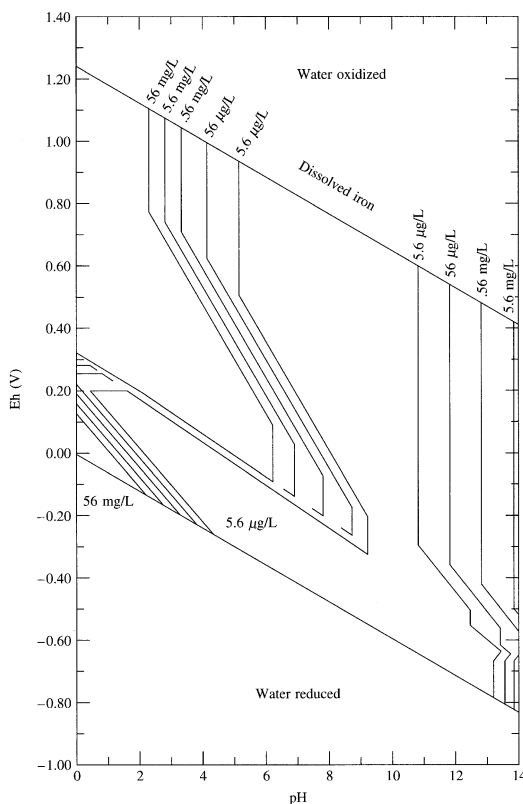
Source: J. D. Hem. 1985. *Study and interpretation of the chemical characteristics of natural waters*. Water Supply Paper 2254, U.S. Geological Survey.

surrounding them. The hydrated cupric ion is $\text{Cu}(\text{H}_2\text{O})_6^{2+}$. Even outside the shell of chemically bound water molecules, there is a region where the polar water molecules are ordered by the electrostatic charge of the metallic ion. Anions in close association with a metal cation are called **ligands**; together they form a coordination compound. Water is considered to be a **ligand** that is bound to the metal ion. If other ligands bind to the metal, they must replace some of the water molecules acting as ligands. The stability of a complex relative to cation or ligand exchange can be described by equilibrium constants for the reaction.

6.6.2 Complexation

The following inorganic anions act as simple ligands in natural waters: OH^- , CO_3^{2-} , SO_4^{2-} , Cl^- , Br^- , F^- , NO_3^- , SiO_3^{2-} , S^{2-} , S_2O_3^- , PO_4^{3-} , $\text{P}_2\text{O}_7^{4-}$, $\text{P}_3\text{O}_{10}^{5-}$, and CN^- . Ammonia (NH_3) is a polar molecule that can also act as a ligand. Ligands can bond either covalently or electrostatically with a metal to form a complex ion or compound. We have already

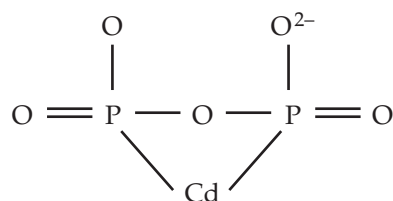
FIGURE 6.6 Equilibrium activity of dissolved iron as a function of Eh and pH under standard conditions, sulfur activity of 96 mg/L as SO_4^{2-} and activity of carbon dioxide of 61 mg/L as HCO_3^- .



Source: J. D. Hem. 1985. *Study and interpretation of the chemical characteristics of natural waters*. Water Supply Paper 2254, U.S. Geological Survey.

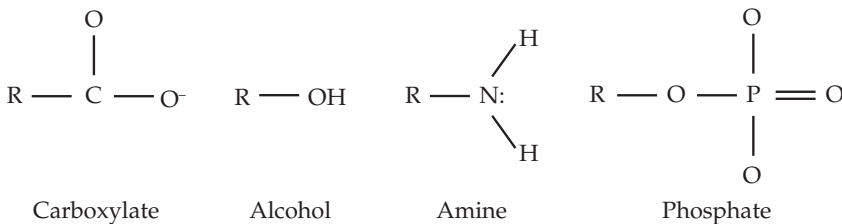
looked at the complex forms of the ferric ion and the hydroxyl ion. They form a series of complex ions: FeOH^{2+} , $\text{Fe}(\text{OH})_2^+$, $\text{Fe}(\text{OH})_3$ and $\text{Fe}(\text{OH})_4^-$. Complex formation is involved with chemical equilibrium of ionic compounds and oxidation-reduction reactions.

In the case of monovalent ions, there is only one site where the ligand bonds to the metal ion and the ligand is called monodentate (literally, “one tooth”). If the ligand has more than one site that can bond (polydentate), then it forms what is known as a **chelating agent**. For example, the pyrophosphate ion, $\text{P}_2\text{O}_7^{4-}$, can bond to a metal ion, such as cadmium, at two locations:



6.6.3 Organic Complexing Agents

Both natural waters and wastewaters contain a number of organic compounds that can act as chelating agents. In general, these organic compounds have a functional group that contains oxygen, nitrogen, phosphorous, or sulfur. If R symbolizes one or more carbon atoms with the appropriate number of hydrogens, then organic complexes can include functional groups such as



There are a number of organic complexing agents that occur in nature. They are associated with **humic substances** that form from the decomposition of vegetation. These are complex organic molecules with molecular weights ranging upward into the tens of thousands. If a humic substance is extracted with a strong base and then acidified, there are three products. The nonextractable organic material is called **humin**. Substances called **fulvic acids** remain in the acidic solution, and other substances called **humic acids** precipitate from the acidified extract. These represent classes of compounds that contain many different individual organic molecules. Humic and fulvic acids contain many functional groups that can chelate to metals. Metals may be kept in solution by chelation with soluble fulvic acids or they may bind to the insoluble humic substances by cation exchange (Manahan 1984).

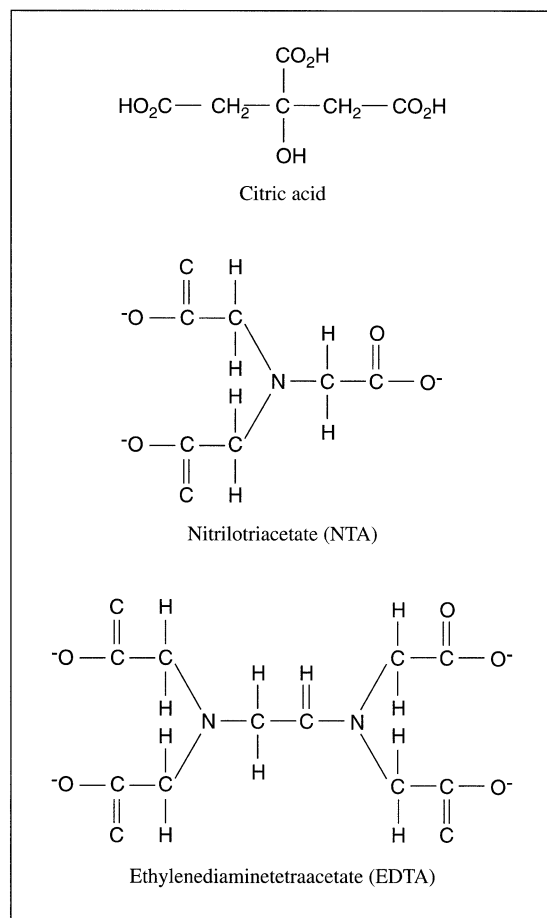
Synthetic organic complexing agents are used in a number of industrial processes. They can be used as cleaning compounds, as constituents of detergent, in metal plating baths, and in water conditioning. These compounds include sodium tripolyphosphate, sodium ethylenediaminetetraacetate (EDTA), citric acid, and sodium nitrilotriacetate (NTA). The structures of some of these compounds are given in Figure 6.7. Synthetic chelating agents may keep metals in solution under conditions where the unchelated metal would precipitate or undergo cation exchange.

EDTA in wastewater can vastly increase the mobility of associated metals in the subsurface. Monitoring wells near radioactive waste disposal trenches at the Oak Ridge (Tennessee) National Laboratory contained significant levels of sodium EDTA, which was used as a cleaning agent. The same wells also contained radioactive ⁶⁰Co, a metal that is normally not expected to migrate very far due to cation exchange. The ⁶⁰Co had been chelated by the EDTA and hence had greatly increased mobility in the subsurface (Means et al. 1978).

6.6.4 Facilitated Particle Transport

Many metals and other inorganic compounds have a great sorptive capacity and an affinity for particles suspended in water. Normally in subsurface environments this limits contaminant mobility in that most mobile particles and colloids are filtered out of flowing groundwater in porous media. However, particles suspended in groundwater

FIGURE 6.7 Structure of chelating agents including (a) citric acid, (b) nitrilotriacetate (NTA), and (c) ethylenediaminetetraacetate (EDTA).



can be mobilized in flow through fractured rock or karst rocks where groundwater moves through larger conduits and suspended particles are not filtered by the geologic medium. Contaminants sorbing on these particles, including many metals, essentially can “hitch a ride” on moving grains and colloids and this can increase the effective speed of contaminant movement through aquifers by orders of magnitude. This enhanced mobility is called **facilitated particle transport**.

Facilitated particle transport can pose problems in modeling contaminant movement and dispersion because of accelerated movement, and also impact the representativeness of groundwater sampling protocols. Many standard techniques for measuring metal concentrations in groundwater require samples to be filtered and acidified in the field. In conditions where groundwater contains contaminants sorbed on suspended particles and colloids, some practitioners collect both filtered and unfiltered samples for comparative chemical analysis.

■ 6.7 Chemistry of Nonmetallic Inorganic Contaminants

6.7.1 Fluoride

Fluoride occurs in water as the F^- ion. In natural waters the amount of fluoride present is generally less than 1.0 mg/L, although concentrations as great as 67 mg/L have been reported (Hem 1985). Fluoride is present in minerals such as fluorite (CaF_2) and apatite ($Ca_5(Cl,F,OH)(PO_4)_3$). Weathering of these minerals may release fluoride. It may be released as a contaminant from industrial processes utilizing hydrofluoric acid. Cryolite (Na_3AlF_6) is used as a flux in the electrolytic production of aluminum. The manufacture of phosphate fertilizer from phosphate-rich rock may also release fluoride. Effluent from a Florida fertilizer plant had fluoride ranging from 2810 to 5150 mg/L (Cross and Ross 1970).

Fluoride can form complexes in water with a number of cations, including aluminum, beryllium, and ferric iron (Hem 1985). Dissolved fluoride can react with calcium to form fluorite. The solubility product for fluorite is $10^{-10.4}$. Precipitation of fluorite can act as a control on the amount of dissolved fluoride in solution if dissolved calcium is present. Table 6.5 shows the equilibrium amount of dissolved fluoride calculated for various activities of calcium. Actual activities of fluoride are likely to be somewhat higher due to the effect of the ionic strength of the solution as well as the effect of any complexes that might form with the fluoride ion.

Fluoride can dissolve into groundwater from anthropogenic sources, but also from volcanic activity and other natural geologic sources through subsurface rock-water interaction. Magmatic fluorine is often in the form of hydrogen fluoride (HF) which is one of the most soluble gases in magmas, exsolving from molten rock only partially, and leaving large amounts of fluoride in cooled volcanic and plutonic rocks. High subsurface temperatures and acidic conditions enhance the dissolution of fluoride from these rocks into groundwater. Portions of the earth's large magmatic provinces, such as the Deccan flood basalts of India, the Siberian traps of central Asia, and the East African Rift Valley are endemic for fluorosis from consumption of high fluoride concentration in groundwater, as are smaller more isolated locales at the base of volcanoes (Brindha and Elango 2011; D'Alessandro 2006).

Corbett and Manner (1984) have reported on the distribution of fluoride in water from both unconsolidated and bedrock aquifers of northeastern Ohio. They found that 239 out of 255 wells had fluoride concentrations less than 1mg/L. However, 14 of

TABLE 6.5 Equilibrium fluoride concentrations as a function of calcium activity.

Calcium		Fluoride	
Activity (mol)	Concentration (mg/L)	Activity (mol)	Concentration (mg/L)
2×10^{-2}	800	4.48×10^{-5}	0.85
10^{-2}	400	6.31×10^{-5}	1.20
5×10^{-3}	200	8.92×10^{-5}	1.70
10^{-3}	40	2.00×10^{-4}	3.79
5×10^{-4}	20	2.82×10^{-4}	5.36
10^{-4}	4	6.31×10^{-4}	11.99

the wells had fluoride ranging from 1 to 5.9 mg/L. All these high-fluoride wells were associated with a specific bedrock formation. Such information is useful from a public health standpoint because there is a 2.0-mg/L drinking-water criteria for fluoride. Some fluoride is needed to build strong teeth in growing children; however, fluoride in excess of 2.0 mg/L will cause teeth to discolor. Chronic ingestion of high fluoride in drinking water can also produce a serious condition known as skeletal fluorosis, which can damage bones and joints.

6.7.2 Chlorine and Bromine

The halides chlorine and bromine have similar chemistry, although chlorine is far more abundant in nature than bromine. Even though the elements can exist in a number of oxidation states, the chloride and bromide ions (Cl^- , Br^-) are the only ones of significance in natural waters. These halides are widely distributed in rocks and soil, and can be naturally leached into groundwaters. The chloride ion occurs in natural waters in fairly low concentrations, usually less than 100 mg/L, unless the water is brackish or saline. Chloride is used by humans in many applications and can be added to the subsurface via industrial discharges, sewage, animal wastes, and road salting. Chlorine gas is used as a disinfectant for purification of water and is a strong oxidizing agent when dissolved in water. Commercial fertilizers can contain chloride as KCl . Chlorine and bromine are components of halogenated organic compounds used for industrial solvents and pesticides. These compounds have been released to the environment both intentionally through the use of pesticides and accidentally through spills and leaks. Recent increases in shale hydrocarbon development have produced large quantities of post-fracking brine waters (which flow back upwards to the surface after well development), as has brine production from dewatering associated with coal bed methane extraction (also called coal seam gas). These large quantities of brine have increasingly been disposed of through underground injection. Fracking flowback water with Cl^- concentrations as high as 151,000 mg/L have been reported (Haluszczak et al. 2013).

Chloride and bromide ions are not reactive. They don't participate in redox reactions, aren't sorbed onto mineral or organic surfaces, and don't form insoluble precipitates. Chloride is sometimes used as a tracer in groundwater studies because it is conservative. Distinctive ratios of Cl^- and Br^- and other elements in groundwater have been valuable in reconstruction groundwater's movement and origin, including determining mixing ratios of different source waters. These ions are highly mobile in the subsurface and are often eventually transported to closed basins or oceans. Additionally, concentrations of chlorine isotopes in groundwater have effectively been used for groundwater dating techniques, including bomb-pulse chlorine-36 put into atmosphere with nuclear weapons testing and falling with rainfall, infiltrating and percolating into groundwater (Challan 2016). These forensic groundwater analytical techniques aid in the tracking of groundwater pollution (see Chapter 8).

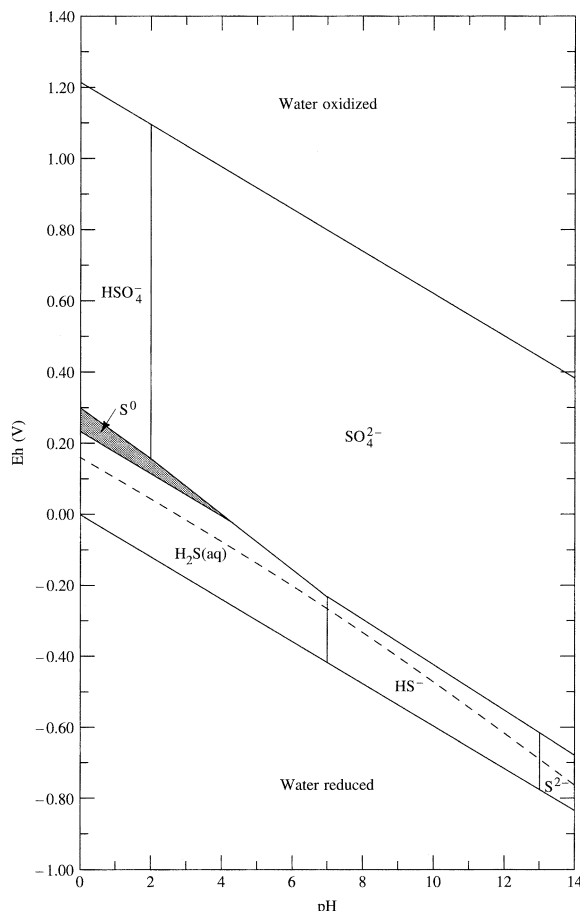
6.7.3 Sulfur

Sulfur is naturally released to the environment by the weathering of minerals containing the element. Rock containing pyrite can be oxidized to release sulfur, with microorganisms acting as a catalyst and mediating the oxidation. This is the source

of the acidic water that drains from many areas that have been mined. Sulfuric acid is widely used in industrial processes. Sulfur can be released to the environment by the processing of sulfide ores and by the burning of fossil fuels, all of which contain sulfur to some degree. Sulfur is also a component of many fertilizers and can leach into groundwater systems from agricultural sources.

Sulfur can exist in valence states ranging from S^{2-} to S^{+6} . Figure 6.8 is an Eh-pH diagram showing the stability of the two oxidized forms of sulfur, HSO_4^- and SO_4^{2-} , and the three reduced forms, S^{2-} , HS^- , and H_2S (aqueous). The field of stability for elemental sulfur is also shown. The total sulfur activity used in computing the diagram is 10^{-3} mol/L or 96 mg/L as SO_4^{2-} . If a greater total sulfur activity were used, the stability field for elemental sulfur would be larger. Although this is a very useful diagram

FIGURE 6.8 Eh-pH diagram for sulfur species at standard conditions with total dissolved sulfur activity of 96 mg/L.



Source: J. D. Hem. 1985. *Study and interpretation of the chemical characteristics of natural waters*. Water Supply Paper 2254, U.S. Geological Survey.

for understanding the equilibrium conditions for dissolved sulfur, the redox reactions can be slow if microbes are not mediating the reactions. Hence, it may take a long time for the system to reach equilibrium.

Gypsum (calcium sulfate) is quite soluble in water ($K_{eq} = 10^{-4.6}$) and, except for waters with extremely high sulfate, would not be a sink for sulfate. Strontium sulfate is sparingly soluble ($K_{eq} = 10^{-6.5}$), whereas barium sulfate is nearly insoluble ($K_{eq} = 10^{-10.0}$). However, strontium and barium are not found in much abundance in natural waters. Sulfate could act as a sink for strontium and barium. Sulfur isotopes can be used to distinguish pollutant sources in some cases.

6.7.4 Nitrogen

Nitrogen is another element that can occur in both oxidized and reduced forms as well as the elemental state. The common forms of inorganic nitrogen include nitrate, NO_3^- , nitrite, NO_2^- , nitrogen gas, N_2 , ammonium, NH_4^+ , and cyanide, CN^- . Nitrogen is also a major constituent of organic matter in the form of amino acids. The majority (78%) of the Earth's atmosphere is nitrogen gas. Atmospheric nitrogen can be "fixed", or converted to nitrate, by cyanobacteria in lakes and the ocean and by bacteria living on the roots of plants such as legumes and lichens. Atmospheric nitrogen can also be converted to oxidized and reduced forms via fertilizer production and by heating it to high temperatures in internal combustion engines, power plants, lightning discharges and forest fires. Rainwater contains dissolved nitrate and ammonia. Nitrogen is released to the subsurface from sewage, animal wastes, and fertilizers.

In soil and groundwater, oxidation and reduction of nitrogen species is accomplished by microorganisms. Under oxidizing conditions ammonia is converted to nitrite, which is converted to nitrate. Nitrite is a very reactive ion and is almost immediately converted to nitrate, so that little nitrite is normally found in the environment. Under reducing conditions nitrate is converted primarily to nitrogen gas, a process known as **denitrification**. Organic matter will decay to ammonia under reducing conditions. Septic tank effluent, for example, normally has high ammonia and very little nitrate. If the receiving groundwater is reducing, the nitrogen will stay in the ammonia form. If it is oxidizing, bacteria will convert the ammonia to nitrate (Feth 1966). Nitrate is chemically conservative, can be mobile in the subsurface environment, and understandably, high nitrate concentrations in drinking water are most often associated with privately owned wells. Since the 1940s, health concerns and regulatory standards for nitrogen in groundwater center on infant methemoglobinemia (commonly called the "blue baby" disease). The high gastric pH of infants and their great fluid intake relative to body weight contribute to their internal bacterial reduction of ingested nitrate to nitrite, and the generated nitrite inhibits the function of blood hemoglobin in the transfer of oxygen.

Nitrate contamination of groundwater has been documented in a number of areas (e.g., Hill 1982; Flipse et al. 1984; and Silver and Fielden 1980). Hill studied the distribution of nitrate in groundwater from a shallow unconsolidated sand aquifer. It was found that the groundwater beneath areas of forest or permanent pasture has less than 1.0 mg/L of nitrate as nitrogen. The groundwater beneath heavily fertilized potato fields typically contained in excess of 10 mg/L nitrate as nitrogen. Gray and Morgan-Jones (1980) found that the nitrate content of groundwater in a study area

increased over the past 40 years and that the use of fertilizers in this catchment area also increased over the same time period.

Nitrogen occurs as two isotopes, ^{14}N and ^{15}N . Of the two, ^{14}N is by far the most abundant in the atmosphere. The relative abundance of ^{15}N —that is, the $^{15}\text{N}/^{14}\text{N}$ ratio—in nitrate may be used to distinguish nitrate that comes from animal and human waste from nitrate that comes from mineral fertilizers (Flipse et al. 1984).

The $^{15}\text{N}/^{14}\text{N}$ ratio is usually expressed as a $\delta^{15}\text{N}$ value, which is defined as

$$\delta^{15}\text{N}(\text{\%}) = \frac{(^{15}\text{N}/^{14}\text{N})_{\text{sample}} - (^{15}\text{N}/^{14}\text{N})_{\text{standard}}}{(^{15}\text{N}/^{14}\text{N})_{\text{standard}}} \times 1000$$

where % stands for parts per thousand.

If the $\delta^{15}\text{N}$ is positive, then the nitrate of the sample has been enriched in ^{15}N with respect to the standard. For nitrogen, the standard is the atmospheric composition. Nitrate from animal and human waste typically has a $\delta^{15}\text{N}$ in excess of +10‰.

Flipse and Bonner (1985) found that mineral fertilizers used on Long Island had $\delta^{15}\text{N}$ values that averaged 0.2‰ at one site and -5.9‰ at another. However, the $\delta^{15}\text{N}$ of the groundwater beneath the sites that had been fertilized was about +6‰. This increase in $\delta^{15}\text{N}$ from the mineral fertilizer was attributed to fractionation that occurred during infiltration of the nitrogen. However, the resulting $\delta^{15}\text{N}$ was still clearly lower than that expected from animal and human waste.

6.7.5 Arsenic

Arsenic can occur in valence states of +5, +3, +1, 0 and -3. However, the important states of dissolved arsenic in water are the arsenate $\text{H}_n\text{AsO}_{4}^{3-n}$, with a valence state of +5, and the arsenite $\text{H}_n\text{AsO}_{3}^{2-n}$, with a valence state of +3. An Eh-pH diagram for arsenic that shows the fields of stability for the arsenates and arsenites is given in Figure 6.9. Dissolved arsenic species can be absorbed by ferric hydroxides. Arsenic (+5) is more strongly sorbed than arsenic (+3). Ferric hydroxides are stable over a wide Eh-pH range, so this fact limits the mobility of arsenic. However, conditions that reduce Fe^{3+} to Fe^{2+} and As^{5+} to As^{3+} increase the mobility of arsenic in the environment, because the precipitated ferric hydroxides become soluble ferrous hydroxides (Matisoff et al. 1982). In an oxidizing environment with a pH above 4.09, we will find colloidal ferric iron hydroxides, which will sorb arsenic and would thus expect to have little arsenic in solution. Under strongly reducing conditions, if both iron and hydrogen sulfide are present, arsenic sulfide coprecipitates with iron sulfide. Mildly reducing conditions that lack hydrogen sulfide present conditions under which one would expect to find the most mobile arsenic, as iron would be in the soluble ferrous state and arsenic would be in the arsenite form (Hounslow 1980).

Arsenic has been released to the environment through the burning of coal and the smelting of ores. In the past it was used in the formulation of insecticides and embalming corpses. Starting at the time of the Civil War in the United States (1860–1865), arsenic was an ingredient in a popular embalming fluid. As much as 3 lb of arsenic could have been used per corpse. The use of arsenic in embalming fluids was

banned by the federal government in 1910 because its use interfered with the investigation of suspected arsenic poisonings. However, graveyards from the Civil War and the late nineteenth century may be a source of arsenic contamination (Konefes 1990). It has some modern industrial uses. Groundwater has been found to have high (up to 96 µg/L) concentrations from natural sources in northeastern Ohio (Matisoff et al. 1982). Elevated arsenic (up to 5 mg/L) in groundwater in Nova Scotia, Canada, was reportedly due to the weathering of piles of mining waste that contained arsenopyrite (Grantham and Jones 1977). In the western United States high (>50 µg/L) concentrations of arsenic are common in groundwater. These are associated with areas of sedimentary rocks derived from volcanic areas, geothermal systems and gold and uranium mining districts. Irrigation in some areas has liberated arsenic to the extent that concentrations of up to 1 mg/L are found in shallow groundwater beneath irrigated fields (Welch, Lico, and Hughes 1988).

Naturally occurring arsenic in groundwater can also be a huge problem. In what one writer called “one of the largest mass poisonings in history,” thousands of tube wells were drilled in shallow aquifers contaminated with naturally-occurring arsenic in Bangladesh and India in the 1980s and 1990s before the problem was recognized (Brahic 2004). As a result, arsenic has posed risk to an estimated 57 million people in Bangladesh (Hossain 2006), and 100,000 are estimated to have been affected by high concentrations in shallow well water in the region (Brahic 2004). Annually, another 270,000 have been estimated to have had cancer related deaths, as long-term exposure to arsenic has been related to cancer of the kidneys, lungs, bladder and skin (Brahic 2004). The problem was unrecognized for many years, in part because a study by the British Geological Survey (BGS) and Britain’s National Environment Research Council (NERC) did not adequately test for arsenic in reconnaissance groundwater quality surveys which subsequently served as the basis for drawing up national water policies and the drilling of thousands of wells.

6.7.6 Selenium

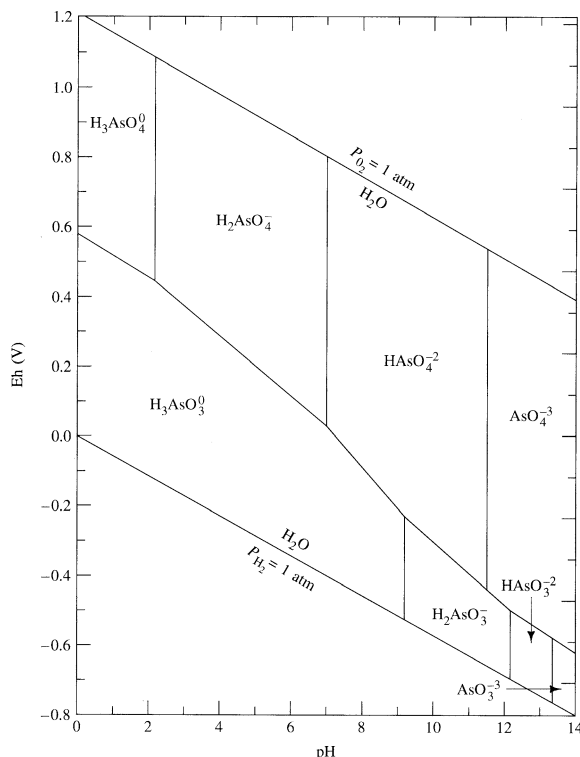
Selenium occurs in oxidizing solutions as selenite, SeO_3^{2-} , with a +4 valence and as selenate, SeO_4^{2-} , with a +6 valence. It can be reduced to the insoluble elemental form, Se^0 . It may also form a precipitate ferroselenite, FeSe_2 , under reducing conditions. Selenite may be sorbed onto amorphous ferric hydroxides. Selenium has a number of industrial uses, such as the manufacture of pigments, stainless steel, and rubber compounds. It is contained in phosphate fertilizers. Selenium has been known to concentrate in irrigation return water draining from land that has soil high in selenium, and can be present in waste liquids from metal smelting. It is naturally present in coal, particularly bituminous coal, and can be concentrated approximately 1,250 times in the burning process at coal-fired power plants (coal versus precipitator ash), and can be present in elevated concentrations in waste scrubber water, ash ponds or other liquid wastes which could leach and percolate into the subsurface.

In small concentrations selenium is an essential nutrient, but in large amounts it is harmful to humans, fish, and wildlife (Coefield 2009). High selenium in groundwater-dependent ecosystems can wipe out entire species and cause massive

wildlife and fish kills. High selenium has been problematic at many sites and from activities worldwide, including (Lemly 2002):

1. Nickel and silver mining in Torun, Poland.
2. Municipal landfill leachates in Stockholm, Sweden; Minnesota, U.S.A.; and in London, U.K.
3. Irrigation runoff in Chihuahua, Mexico; Utah, U.S.A.; and in Kesterson National Wildlife Refuge, California, U.S.A.
4. Coal combustion waste in Texas, Pennsylvania, Kentucky, North Carolina, U.S.A. and Alberta Canada.
5. Phosphate mining waste in Idaho, U.S.A.
6. Gold mining waste in Buenos Aires, Argentina; Quito, Ecuador; and Yukon, Canada.
7. Metal smelting waste in Ontario, Canada.
8. Oil-refinery waste in Louisiana, U.S.A.

FIGURE 6.9 Eh-pH diagram for arsenic species under standard conditions.



Source: A. H. Welch, M. S. Lico, and J. L. Hughes. 1988. Arsenic in ground water of the western United States. *Groundwater* 26:333–347. Used with permission.

6.7.7 Phosphorus

Phosphorus can occur in a number of valence states, but in natural water it is really significant only in the +5 state. Dissolved phosphorus in water occurs as phosphoric acid (H_3PO_4) and its dissociation products, the orthophosphate ions: $H_2PO_4^-$, HPO_4^{2-} and PO_4^{3-} . The proportion of each present in an aqueous solution is a function of pH. Dissolved phosphorus is readily sorbed onto soil and has a very low mobility in groundwater. In alkaline soils it can react with calcium carbonate to form a mineral precipitate, hydroxyapatite.



Phosphate is released to the environment from mineral fertilizers, animal wastes, sewage, and detergents.

■ 6.8 Chemistry of Metals

Metals are cations, and most have fairly limited mobility in soil and groundwater because of cation exchange or sorption on the surface of mineral grains. They can also form precipitates of varying solubility under specific Eh-pH conditions. Geologically, metal ores are typically in the form of sulfides, oxides, silicates, or “native” metals. Metals are mobile in groundwater if the Eh-pH range is such that soluble ions exist and the soil has a low cation-exchange capacity (Dowdy and Volk 1983). They can also be mobile if they are chelated or if they are attached to a mobile colloid. Conditions that promote mobility include an acidic, sandy soil with low organic and clay content. Discharge of a metal in an acidic solution would keep the metal soluble and promote mobility.

6.8.1 Beryllium

Beryllium occurs only in the +2 valence state. In natural waters we can have Be^{2+} , $Be(OH)^+$, $Be(OH)_2$ and $Be(OH)_3^-$. Beryllium oxide and hydroxide have low solubilities and can act as a control on beryllium concentration. At equilibrium with $Be(OH)_2$, the dissolved form would have an activity of about 100 $\mu\text{g/L}$ at a pH of 6 (Hem 1985). Nonetheless, beryllium can find its way into groundwater from industrial wastewater discharges or from natural weathering and dissolution of rocks, particularly igneous rock containing granites and pegmatites. Beryllium is used for making metal alloys for the aerospace industry, nuclear reactors, and is used in electrical equipment and microwave ovens.

6.8.2 Strontium

Strontium also occurs in the +2 valence state and has a chemistry similar to that of calcium. The solubility product for strontium sulfate, $SrSO_4$, is $10^{-6.4}$. This suggests that there might be an equilibrium control on strontium concentration if sulfate is present in the water. Strontium carbonate, $SrCO_3$, has a solubility product of 10^{-10} . In general, strontium is present in groundwaters in concentrations of less than 1 mg/L.

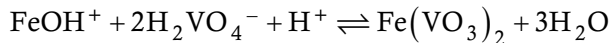
However, in tracing groundwater pathways and subsurface movement of potential contaminants, the isotopic ratio of $^{87}\text{Sr}/^{86}\text{Sr}$ can be a “powerful tool in distinguishing among solute sources,” as the ratio can reflect mineral interaction with groundwater, differences in initial water quality, recharge waters of varying evaporative concentrations or pCO_2 concentration, and differences in relative mobilities of different groundwaters (USGS 2015).

6.8.3 Barium

This alkaline earth element also has a valence of +2. Its distribution is controlled by the solubility of barite, BaSO_4 . Barite has a solubility product of 10^{-10} . If the activity of sulfate is 96 mg/L ($10^{-3} M$), then the activity of barium is $10^{-7} M$, or 0.014 mg/L. Barium is also found as witherite (BaCO_3), and other compounds, but is not found in the environment as a free element because of its high reactivity. Barium sulfate can be an additive to oil-well drilling fluid, medical waste, and because in its ionic form barium is soluble and toxic, it is a component of some rodenticides.

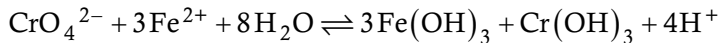
6.8.4 Vanadium

This transition metal has oxidation states of +3, +4, and +5. In aqueous solutions it forms 10 different oxides and hydroxides. Dissolved iron can react with vanadium to form an insoluble ferrous vanadate, which can act as a control on vanadium in natural water (Hem 1977).



6.8.5 Chromium

Chromium in natural waters occurs in a +3 and a +6 valence state. Stable ionic forms in aqueous systems include Cr^{3+} , CrOH^{2+} , Cr(OH)_2^+ , $\text{Cr}_2\text{O}_7^{2+}$ and CrO_4^{2-} . Chromous hydroxide, Cr(OH)_3 is a possible precipitate under reducing conditions. Figure 6.10 is an Eh-pH diagram for the stability field for chromous hydroxide. Under some conditions chromate might react with ferrous iron to produce a chromous hydroxide precipitate (Robertson 1975).

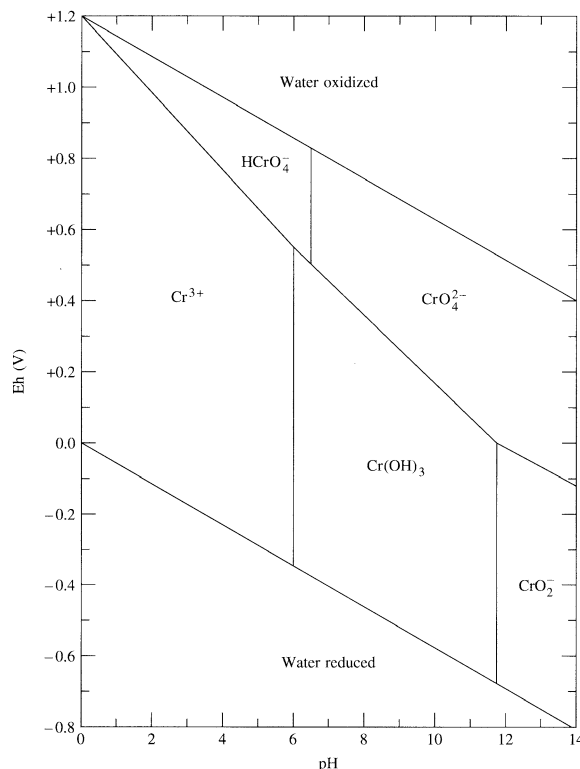


In general the hexavalent chromium in groundwater is soluble and mobile and trivalent chromium will be insoluble and immobile. Industrial discharges of hexavalent chromium are common from metal-plating industries. This material may be quite mobile in groundwater. A hexavalent chromium spill on Long Island, New York, U.S.A., traveled more than 900 m (≈ 3000 ft) from a waste-discharge pond to a stream (Perlmutter, Lieber, and Frauenthal 1963). Hexavalent chromium from a natural source has been found in groundwater in Paradise Valley, Arizona, U.S.A. (Robertson 1975), and the Blacksmith Institute reports that groundwater containing 6.2 mg/L Cr (VI) was found in Kanpur, India (the Indian government limit is 0.05 mg/L) from

tannery operations, potentially affecting 30,000 people. Popular attention was focused on groundwater pollution from hexavalent chromium in Hinkley, California, U.S.A., after it was dramatized in the 2000 film *Erin Brockovich*.

Chromium in groundwater is much more mobile in the aqueous Cr^{6+} phase than as Cr^{3+} . In a study of a three dimensional chromium plume in a glaciofluvial aquifer in Connecticut, Nikolaos et al. (1994) tested the sorbed chromium in the soil and the dissolved chromium in the groundwater. The mean soil concentration was 0.675 g/kg while 25 mg/L was dissolved in the groundwater. A mass balance calculation revealed that more than 99% of the mass of chromium was immobilized in the soil. This has important implications for groundwater remediation. The mobile chromium in the groundwater could be removed by pump and treat methods. However, if the geochemical equilibrium is upset and chromium is desorbed from the soil, then it would be very difficult to ever remove all of the chromium by pump and treat. As a part of a remedial investigation at a chromium spill site, one must determine how strongly the chromium is bound to the soil. Methods of extracting the dissolved portion without upsetting the equilibrium that binds the majority of the chromium to the soil must be developed.

FIGURE 6.10 Eh-pH diagram for chromium under standard conditions.



Source: Modified from F.N. Robertson. 1975. Hexavalent chromium in the ground water in Paradise Valley, Arizona. *Groundwater* 13:516–527. Used with permission.

Case History

Henderson (1994) investigated a chromium spill in the Trinity Sand aquifer near Odessa, Texas. He found that the mobile Cr⁶⁺ was being reduced to Cr³⁺ by ferrous iron (Fe²⁺) and organic carbon. The trivalent chromium is then sorbed onto the soil surfaces which are coated with solid iron oxyhydroxides. The soil contained up to 5 g/kg and 95 to 99 percent was in the trivalent state. Prior to the initiation of the study, the chromium plating operation had ceased operations, so that the source of hexavalent chromium ended. Over the course of the study, the plume of groundwater contaminated with Cr⁶⁺ stopped growing, and even began to shrink (Figure 6.11). The cause of this degradation is the reduction of the Cr⁶⁺ to Cr³⁺ which forms chromium hydroxide (CrOH₃) and its subsequent sorption onto the soil.

The calculated half life of the chromium was 2.5 years. The reduction in dissolved hexavalent chromium mass in the aquifer is illustrated in Figure 6.12. The shaded area represents observed conditions at four different sampling events. The curved line is a first order reduction with the 2.5 year half life.

With the transformation of dissolved to solid chromium as a function of time, the groundwater in the aquifer is undergoing natural remediation. Computer modeling of the plume resulted in a diminution of the dissolved Cr⁶⁺ below a 100 µg/L drinking water standard by no later than the year 2006 (Figure 6.13). Operation and maintenance at the site were still ongoing in 2017.

6.8.6 Cobalt

Cobalt occurs with valence states of +2 and +3. In the Eh and pH range of natural waters, only the +2 valence state is stable. It is thought that cobalt can coprecipitate or be absorbed by manganese and iron oxides. Cobalt carbonate has a solubility product of 10⁻¹⁰. At a pH of 8.0 with 100 mg/L of carbonate, the equilibrium solubility of cobalt is 6 µg/L (Hem, 1985). The solubility product of cobalt sulfide is very low, 10^{-21.3}. Virtually no cobalt would be in solution in a reducing environment. Radioactive cobalt is a waste product of certain defense activities (Means, Crerar, and Duguid 1978). Cobalt occurs in nature as smaltite (CoAs₂), and cobaltite (CoAsS). In the United States, stable cobalt has been identified at 426 of the 1,636 current or former National Priorities List (NPL) sites, whereas radioactive cobalt has been found at 13 sites (ATSDR 2015).

6.8.7 Nickel

This metal occurs in aqueous solutions in the +2 valence state. Nickel ores include a variety of minerals, consisting of nickel, antimony, sulfur, and arsenic: NiSb, NiAs₂, NiAsS, and NiSbS. Nickel carbonate is more soluble than cobalt carbonate ($K_{sp} = 10^{-6.9}$), whereas the sulfide has a similar solubility ($K_{sp} = 10^{-19.4}$). Nickel is widely used in industry.

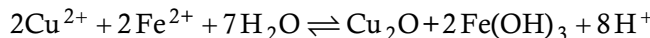
6.8.8 Molybdenum

Molybdenum occurs as the ore mineral molybdenite, MoS₂. The most common oxidation states are +4 and +6. Under oxidizing conditions the Mo⁶⁺ state dominates. Below pH 1.8 one finds H₂MoO₄ (aqueous). Between pH 1.8 and pH 5.3, HMoO₄⁻ occurs, whereas above pH 5.3 the molybdate ion, MoO₄²⁻, is stable. If ferrous iron is present, ferrous molybdate (FeMoO₄) presents a possible solubility control, since this has a solubility product of 10^{-10.45} at a pH range of 5.3 to 8.5 (Hem 1977). Molybdenum may also sorb

onto amorphous ferric hydroxide (Kaback and Runnels 1980). The solubility product of calcium molybdate, CaMoO_4 , is $10^{-8.7}$ (Hem 1985). Molybdenum is used as an alloy in steel and as an additive to lubricants. Waste sources include mining and smelting of ore.

6.8.9 Copper

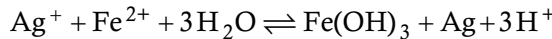
Copper occurs in either a +1 or a +2 valence state. Dissolved copper species in water include Cu^{2+} , HCuO_2^- , CuO_2^{2-} , and Cu^+ . Cupric copper and ferrous iron can undergo an oxidation-reduction:



Both cupric and cuprous sulfide have very low solubility products. Copper concentrations can be very high in acid mine drainage from metal mines, up to several hundred milligrams per liter. Copper can be leached from copper water-supply pipes and fixtures, especially by waters that have a pH of less than 7 (Hem 1985).

6.8.10 Silver

Silver, a rare element, is widely used in industry. It occurs in the +1 valence state. Silver chloride, AgCl , has a solubility product of $10^{-9.7}$, which limits the solubility of silver in waters with chloride ion. Silver can also be naturally reduced to the metallic state by ferrous iron:



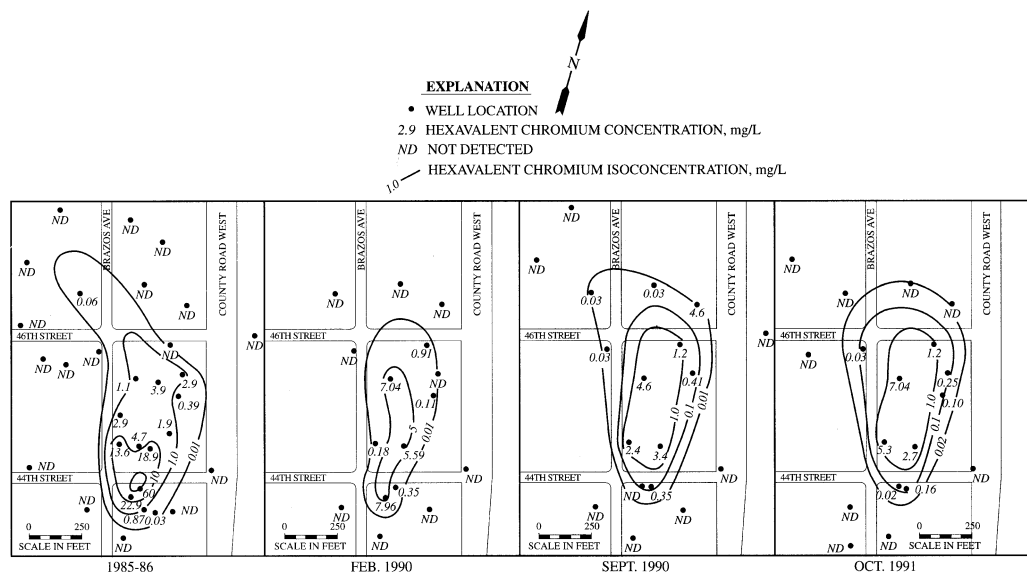
Silver sulfide has a low solubility. Thus, in water with chloride, iron, and sulfur present, stable solid forms of silver occur over the entire Eh-pH field (Hem 1977). As a result, there is very little soluble silver in natural waters.

6.8.11 Zinc

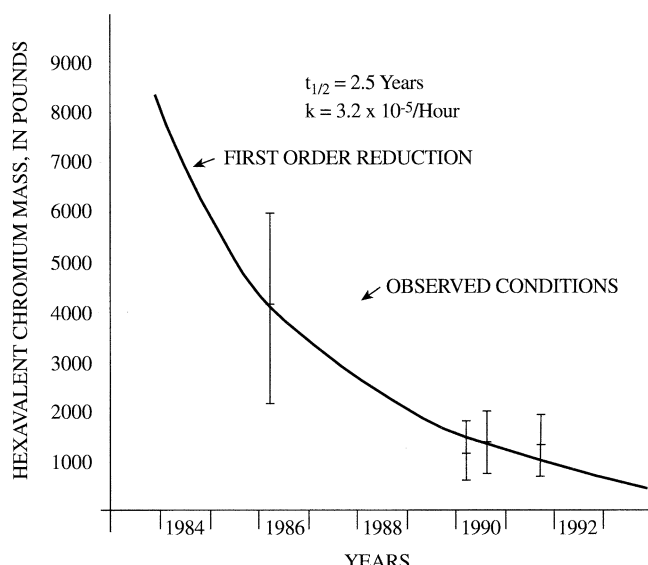
Zinc is a fairly common metal and is extensively used in metallurgy and as a pigment, zinc oxide, which is often worn on the noses of lifeguards and other people in the sun. It occurs in the +2 valence state. Zinc carbonate has a rather low equilibrium constant, 10^{-10} , which would limit the solubility at pH ranges where the carbonate ion predominates. In a pH range of 8 to 11 and with 610 mg/L of HCO_3^- , there should be less than 100 $\mu\text{g}/\text{L}$ of dissolved zinc (Hem 1985).

6.8.12 Cadmium

Cadmium has a very low maximum contaminant level (MCL) in drinking water, 4 $\mu\text{g}/\text{L}$, due to its toxicity. It exists in aqueous solution in the +2 valence state. Cadmium carbonate has a very low solubility product, $10^{-13.7}$. Although this could serve as a control on solubility under some conditions, cadmium can be mobile in the environment. On Long Island, New York, a metal-plating waste containing cadmium and chromium traveled about 3000 ft in a shallow aquifer (Perlmutter, Lieber, and Frauenthal 1963). Cadmium has been implicated in an outbreak of a disease in Japan resulting in a softening of the bones of the victims that resulted in extreme bone pain.

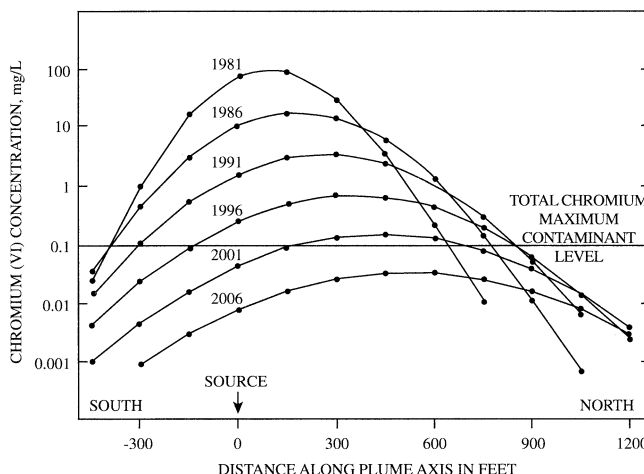
FIGURE 6.11 Shrinkage of the maximum extent of an observed plume of Cr⁶⁺ with time.

Source: T. Henderson. 1994. Geochemical reduction of hexavalent chromium in the Trinity Sand aquifer. *Groundwater* 32:477–486. Used with permission.

FIGURE 6.12 Reduction of the dissolved mass of Cr⁶⁺ with time.

Source: T. Henderson. 1994. Geochemical reduction of hexavalent chromium in the Trinity Sand aquifer. *Groundwater* 32:477–486. Used with permission.

FIGURE 6.13 Result of fate and transport modeling of concentration of Cr⁶⁺ along the axis of the plume.



Source: T. Henderson. 1994. Geochemical reduction of hexavalent chromium in the Trinity Sand aquifer. *Groundwater* 32:477–486. Used with permission.

The cadmium was traced to rice and soybeans grown in soil contaminated by airborne cadmium that came from a nearby lead-and zinc-smelting operation (Emmerson 1970).

6.8.13 Mercury

Mercury has the lowest MCL for any inorganic chemical, 2 µg/L. It is considered to be very toxic. It has been known to concentrate in the food chain, especially in fish. Several outbreaks of mercury poisoning have been confirmed in Japan. Local discharges of mercury from industrial processes into surface-water bodies resulted in high mercury levels in fish. Inhabitants of fishing villages ate fish up to three times a day. Mortality of those affected was about 40%, and the poisoning was passed to unborn babies by apparently healthy mothers (Waldbott 1973). Mercury occurs as a metal and in the valence states +1 and +2. Most of the inorganic mercury compounds have a low solubility. The solubility product of Hg₂Cl₂ is $10^{-17.9}$, and for HgS it is about 10^{-50} . Under most natural conditions there is little soluble inorganic mercury. However, methane-generating bacteria can convert metallic mercury to organic forms such as methyl mercury, HgCH₃⁺. The monomethyl mercury ion is soluble in water. Bacteria can also produce dimethyl mercury, Hg(CH₃)₂, which is volatile. Other organic forms of mercury, such as ethylmercuric chloride (C₂H₅HgCl), are manufactured and used as fungicides.

6.8.14 Lead

Lead occurs in aqueous solution as Pb²⁺ and in various hydroxides. Various lead compounds have solubility products that indicate that under the right Eh-pH conditions, lead solubility would be limited in natural waters: PbCl₂, $K_{sp} = 10^{-4.8}$; PbF₂, $K_{sp} = 10^{-7.5}$; PbSO₄, $K_{sp} = 10^{-7.8}$; PbCO₃, $K_{sp} = 10^{-13.1}$ and PbS, $K_{sp} = 10^{-27.5}$. Lead and the other metals are cations

that can be expected to undergo cation and exchange with clays. Hence, the mobility of lead in groundwater is limited. Lead is present in nature as a trace element. In two different studies soils in uncontaminated areas were reported to contain 17 µg of lead per gram of soil (µg Pb/g) (Nriagu 1972) and 29 µg Pb/g (Ure and Berrow 1972). However, there are a number of anthropogenic sources of lead, including mining and smelting, paint, use of sewage sludge as a soil conditioner, lead arsenate pesticides, and leaded gasoline. Urban areas especially have much higher levels of lead in the soil due primarily to paint flaking from buildings and burning of leaded gasoline (Davis 1990). A study of lead in soils near highways in the Minneapolis-St. Paul, USA, area revealed concentrations ranging from 128 to 700 µg Pb/g (Singer and Hanson 1969). A study in California, U.S.A. found that lead in soil decreased with distance from a freeway which ran through a rural area, with 118 µg Pb/g found 15 meters from the expressway and 85 µg Pb/g as much as 362 meters away (Page et al. 1971). Lead additives were used as anti-knock compounds in gasoline, but are now restricted or banned in many parts of the world.

Elevated lead is also found in soil around lead smelters. Davies (1990) estimates that in the immediate area of a well established lead smelter (1 to 3 km away), lead in soil is likely to be on the order of 1500 µg Pb/g. In a study conducted in southeastern Missouri, USA, the investigators were able to distinguish lead from automobile exhaust from lead from smelter activities on the basis of the ratio of stable lead isotopes, $^{206}\text{Pb}/^{204}\text{Pb}$ (Rabinowitz and Wetherill 1972). In that study they found lead in soil near smelters averaging 2600 µg Pb/g and near highways averaging 270 µg Pb/g.

In general urban soils have higher lead content than rural soils. In a major study of metals in urban soils in Great Britain a total of 4,126 lawns were tested, with a geometric mean lead content of 266 µg Pb/g and a range of thirteen to 14,100 µg Pb/g (Culbard et al. 1988). In London a total of 578 samples had a geometric mean lead content of 654 µg Pb/g.

Soluble lead is absorbed by soils, and its mobility is limited. The two most important factors in determining the amount of lead that will be sorbed by soil are the pH and the cation exchange capacity (CEC) of the soil (Zimdhahl and Skogerbe 1977). This relationship can be described by an equation, with the amount of lead sorbed per gram of soil represented by N^{*}:

$$N^* \text{ (mol/gm)} = 2.81 \times 10^{-6} \text{ CEC}_{(\text{meq}/100\text{g})} + 1.07 \times 10^{-5} \text{ pH} - 4.93 \times 10^{-5}$$

The above equation shows that with a pH greater than 4.61 the amount of lead sorbed by the soil increases and that below a pH of 4.61, it decreases. The cation exchange capacity of a soil is dependent upon the amount and type of clay in the soil and the amount of soil organic matter. Lead absorption is due to precipitation of the carbonate, fixation on organic matter, or sorption by hydrous oxides of iron and magnesium. Griffin and Shimp (1976) demonstrated that the sorption capacity of a clay for lead at a pH of 5.0 was much greater than at a pH of 4.0.

Because of the high affinity of soil for lead, the metal tends to accumulate in the upper few centimeters of soil. In a study of heavy metal mobility in soils near a zinc smelter, lead was found to be concentrated in the upper 10 cm of the soil (Scokart et al. 1983). This was due to the extremely low mobility of lead in soil. The reason that urban soils have such high lead levels is twofold. First, there are more

sources of lead. But more important is the fact that the lead in the soil is so immobile that it continues to accumulate. In a study of trace metals in virgin agricultural soil profiles in Canada, Wright and others (1955) found lead to be more concentrated in the upper part of the soil profile. The lead was assumed to come from the weathering process and was concentrated in the zone where leaching was the most prevalent. This is further evidence for the very low mobility of lead in the environment.

There is one potential pathway for lead migration. If lead is sorbed onto colloidal-sized metal hydroxides, and the hydroxide moves through an aquifer as a colloidal particle, then the lead would also move. This would show up as lead in total metals analysis, which is run on an unfiltered sample. The colloidal particles, which may impart turbidity to the sample, would be digested and any sorbed lead liberated in the analysis. Colloidal-sized lead particles could also migrate with groundwater and be detected with the total lead analysis.

6.8.15 Rare Earth Elements

Rare earth elements (REEs) are increasingly important materials for modern technologies and can be found in groundwater. Although REE concentrations in groundwater can be low, they are used in investigations as tracers to indicate water movement and source, and importantly have associated radioactive pollutants in REE mining waste. There are 17 REEs, but the name “rare” is misleading as some (e.g., cerium) can be relatively abundant in the earth’s crust. REE mining activity is rapidly expanding as are the economic uses of REEs. For example, REEs are used in cellular phones, laptop computer hard drives, automobile airbags and ABS brakes, medical magnetic resonance imaging (MRI), hybrid car batteries, wind turbine generators, plasma color televisions, satellite components, and communications equipment, to name a few applications. REEs have been shown to be useful in tracking and tracing groundwater (Johannesson et al. 1997; Kreamer et al. 1996; Johannesson 2006), and radioactive elements of uranium and thorium are commonly found in slurry tailing from REE mining.

■ 6.9 Radioactive Isotopes

6.9.1 Introduction

Certain isotopes of elements undergo spontaneous decay, resulting in the release of energy and energetic particles and consequent formation of different isotopes. Some of these radioactive isotopes are naturally occurring and others are created by the bombardment of the Earth by cosmic radiation. Humans have created nuclear isotopes through the detonation of nuclear weapons and the construction of nuclear reactors. Table 6.6 lists the sources of environmentally important isotopes.

Radionuclides emit ionizing radiation—alpha particles, beta particles, and gamma rays—when they decay. An alpha particle is a helium nucleus with atomic mass 4 and atomic number 2. A beta particle is either a negative electron or a positron (positive electron). Gamma radiation consists of electromagnetic radiation similar to X-rays but more energetic (i.e., it has a shorter wave length). Gamma radiation is more destructive to tissue than X-rays. The primary effect of these particles is to produce ions, hence the name ionizing radiation. Alpha particles do not penetrate very far into matter due

TABLE 6.6 Sources of environmentally important radioactive isotopes.

Source	Radionuclides
Naturally occurring	^{40}K , ^{222}Rn , ^{226}Ra , $^{230,232}\text{Th}$, $^{235,238}\text{U}$
Cosmic irradiation	^3H , ^7Be , ^{14}C , ^{22}Na
Nuclear weapons tests	^3H , ^{90}Sr , ^{137}Cs , $^{239,240}\text{Pu}$
Mining waste—uranium, phosphate, coal	^{222}Rn ^{226}Ra , $^{230,232}\text{Th}$, $^{235,238}\text{U}$
Industrial wastes—e.g., nuclear power plants, weapons manufacturing, research and medical waste	$^{59,63}\text{Ni}$, ^{60}Co , ^{90}Sr , $^{93,99}\text{Zr}$, ^{99}Tc , ^{107}Pd , ^{129}I , ^{137}Cs , ^{144}Ce , ^{151}Sm , $^{152,154}\text{Eu}$, ^{237}Np , $^{239,240,242}\text{Pu}$, $^{241,243}\text{Am}$

Source: G. W. Gee, D. Roi, and R. J. Serne. 1983. Mobility of radionuclides in soil. In D. W. Nelson et al. (ed.) *Chemical Mobility and Reactivity in Soil Systems*, 203. (Madison, WI: Soil Science Society of America Spec. Publ. 11, 1983).

to their large size, but they produce a lot of ions along their short path. Beta particles penetrate to a greater depth but produce fewer ions per unit path length.

Radionuclide concentrations can be reported in terms of their mass per volume concentration (e.g., milligrams per liter). However, they are more frequently reported in terms of a standard unit of radioactivity, the **curie** (Ci). A curie is 3.7×10^{10} disintegrations per second. In water we use the **picocurie** (pCi), which is 1×10^{-12} Ci, or 3.7×10^{-2} disintegrations per second. In the SI system the unit of radioactivity is the **becquerel** (Bq), which is 1 disintegration per second.

Radiation doses are measured in terms of **rads**, which are a measure of the absorption by the body of ionizing radiation of any type. A rad is equivalent to 100 ergs of energy from ionizing radiation absorbed per gram of soft tissue. In the SI system the unit of dose is a **gray** (Gy), which is equal to 100 rads.

The effect of ionizing radiation depends upon the type of particle and the body tissue with which it interacts. Therefore, the absolute measurement of dose must be converted to a **dose equivalent**. The unit of dose equivalent is the **rem**. Rads are converted to rems by multiplying by a factor that depends upon the type of ionizing radiation and its biological effect. For example, with gamma radiation the factor is 1 and a rad is equal to a rem. In the SI system the unit of dose equivalent is the **seivert** (Sv), and it is equal to a gray times the dose factor. A seivert is 100 rem.

6.9.2 Adsorption of Cationic Radionuclides

The cationic radionuclides may be subjected to ion exchange and other processes that sorb the radionuclide onto mineral or organic surfaces in the soil. The following transition metals and lanthanides have large distribution coefficients and hence low mobilities in waters that are in the neutral range: ^{60}Co , ^{59}Ni , ^{63}Ni , ^{65}Zn , ^{93}Zr , ^{107}Pd , ^{110}Ag , ^{114}Ce , ^{147}Pm , ^{151}Sm , ^{152}Eu , and ^{154}Eu . Many of them do not desorb significantly. The degree of sorption is strongly related to the pH of the solution. Insoluble metal hydroxides may also be formed. Technetium (Tc) solubility depends strongly upon the Eh of the solution, because under oxidizing conditions it forms the soluble pertechnetate ion (TcO_4^-) (Gee, Rai, and Serne 1983).

^{90}Sr , ^{137}CS , and ^{226}Ra undergo cation exchange in a fashion similar to other exchangeable cations, such as Ca^{2+} and Mg^{2+} . Thorium and lead also have high distribution coefficients and limited mobility in neutral to alkaline soil. Lead is sorbed on

hydrous oxides of iron, aluminum, and most likely manganese. Thorium hydroxides are of very limited solubility (Gee, Rai, and Serne 1983).

6.9.3 Uranium

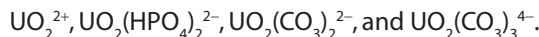
Uranium occurs primarily as ^{238}U , with ^{235}U being much more rare. One of the disintegration products of ^{238}U is ^{226}Ra . This decay series ends with ^{206}Pb , a stable isotope. ^{238}U can also degrade to ^{234}U . The $^{234}\text{U}/^{238}\text{U}$ ratio is useful in tracking and dating groundwater (see Chapter 8). ^{238}U has a very long half-life, 4.5×10^9 years, which indicates that it is not very radioactive. The ^{235}U isotope can decay to form ^{223}Ra .

The chemistry of dissolved uranium is somewhat complex (Giridher and Langmuir 1991; Langmuir 1978). It has three valence states, +4, +5, and +6. Uranium can undergo oxidation-reduction reactions such as oxidation from the +4 to the +6 state:



In a system with just uranium and water, stable species include (1) +4 valence: U^{4+} , UOH^{3+} , and (2) +6 valence: UO_2^{2+} , UO_2H^+ , $(\text{UO}_2)_3(\text{OH})_5^+$ and $(\text{UO}_2)_3(\text{OH})_7^-$. The stability fields for these ions and precipitates are shown in Figure 6.14 for an aqueous solution with a total uranium activity of 10^{-6} mol/L. The $\text{U}(6+)$ species has a tendency to form complexes with a wide variety of inorganic anions, including carbonate, hydroxide, phosphate, fluoride, and sulfate. This can be illustrated with an Eh-pH diagram of the same 10^{-6} mol/L solution of U but in contact with carbon dioxide at a partial pressure of 10^{-2} atm. This is represented by Figure 6.15. In Figure 6.14 the UO_2^{2+} formed a series of complexes with OH^- , starting with UO_2OH^+ , at a pH above about 5.2. With carbon present, as in Figure 6.15, UO_2^{2+} can form a series of carbonate complexes that replace the hydroxyl complexes.

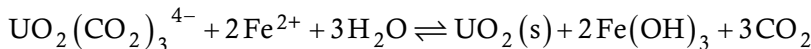
The soluble complexes of oxidized uranium depend upon the pH of the water. Most natural water contains fluoride, phosphorus, carbon dioxide, and sulfur. Figure 6.16 shows the distribution of uranyl complexes for a groundwater under standard conditions with $P_{\text{CO}_2} = 10^{-2.5}$ atm, $\text{F}^- = 0.3$ mg/L, $\text{Cl}^- = 10$ mg/L, $\text{SO}_4^{2-} = 100$ mg/L, and $\text{PO}_4^{3-} = 0.1$ mg/L. In different pH ranges the most prevalent stable species include



If reduced species of iron or sulfur are present, they could reduce $\text{U}(6+)$ to $\text{U}(4+)$ and precipitate the nearly insoluble mineral uranite, UO_2 . This reduction could occur by oxidation of HS^- to SO_4^{2-} :

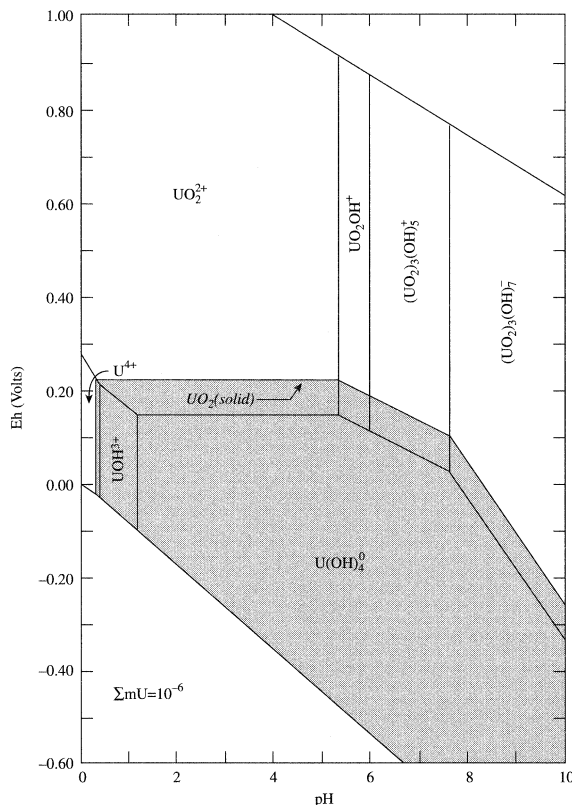


The same reduction could be accomplished by oxidation of ferrous iron to ferric hydroxide:



Because sulfur and iron are common in groundwater systems, under reducing conditions one could expect the formation of uranite, which would remove uranium from solution. Figures 6.14 and 6.15 show the stability field for uranite (UO_2). In the

FIGURE 6.14 Eh-pH diagram for dissolved species of uranium under standard conditions for the system U—O₂—H₂O with 10⁻⁶ mol/L U. The stability field for solid UO₂ (uranite) is shaded.



Source: J. Giridhar and D. Longmuir. 1991. Determination of E₀ for the UO₂₂₊/U₄₊ couple from measurement of the equilibrium: UO₂₂₊/U₄₊ + Cu(s) + 4H⁺ = U₄₊ + Cu₂₊ + 2H₂O at 25°C and some geochemical implications. *Radiochimica Acta* 54:133–138.

United States, the MCL for uranium in water is 30 µg/L, while the recommended limit is zero (see Chapter 1).

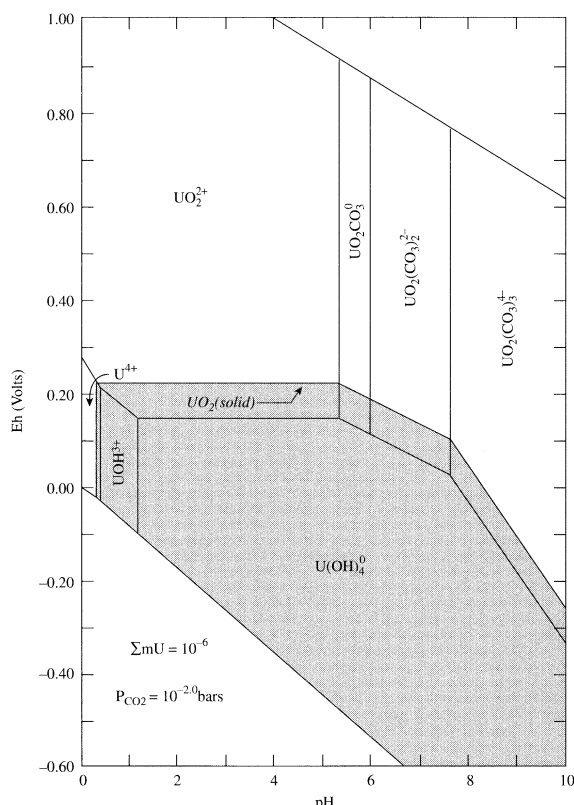
Geologically, uranium has been deposited in the earth's crust in several types of deposits, and different mining techniques in these ore bodies is very important to the long-term potential for contaminant migration. Australia has about 29% of the world's known recoverable uranium and the metal is mostly found in unconformity related complex orebodies and polymetallic iron oxide breccias. Kazakhstan is second with about 12% typically found in sedimentary rocks, followed by the Russian Federation at 9%, Canada at 8% (largely unconformity related), Niger at 7% (often sandstone deposits), Namibia and South Africa at 6% each, and Brazil at 5% (World Nuclear Association 2015). According to the World Nuclear Association about 41% of known uranium deposits occur in sandstones in either basal channel deposits (Russia and south Australia), tabular deposits (Niger, Czech Republic, and the Colorado Plateau in the U.S.A.), roll-front deposits (Kazakhstan and the U.S.A.), tectonic/ lithologic deposits (France and Gabon),

and mafic dykes or sills in Proterozoic sandstones (Canada and Australia). As alluded to in Chapter 1, in situ leaching (ISL) of uranium ore has often become the method of choice in sandstones for extracting uranium, particularly from roll-front deposits. ISL requires the injection of oxidizing lixivants and mobilizing chemicals into groundwater which are directed by the forced hydraulic gradients of injection and extraction wells to leach subsurface uranium. After ISL mining has been completed, chemical reductants are injected to sequester, immobilize, and stabilize any remaining dissolved uranium. Care must be exercised that post-mining groundwater quality audits and stabilization practices account for long-term effects and rebound of mobilized residuals in groundwater.

Case History

Uranium metal was refined from pitchblende ores at a former U.S. Department of Energy facility near Fernald, Ohio. As a result of this activity soluble-uranium ions are present in

FIGURE 6.15 Eh-pH diagram for dissolved species of uranium under standard conditions for the system $\text{U}-\text{CO}_2-\text{O}_2-\text{H}_2\text{O}$ with 10^{-6} mol/L U. The stability field for solid UO_2 (uranite) is shaded.



Source: J. Giridhar and D. Longmuir. 1991. Determination of E° for the $\text{UO}_2^{2+}/\text{U}^{4+}$ couple from measurement of the equilibrium: $\text{UO}_2^{2+}/\text{U}^{4+} + \text{Cu(s)} + 4\text{H}^+ = \text{U}^{4+} + \text{Cu}^{2+} + 2\text{H}_2\text{O}$ at 25°C and some geochemical implications. *Radiochimica Acta* 54:133–138.

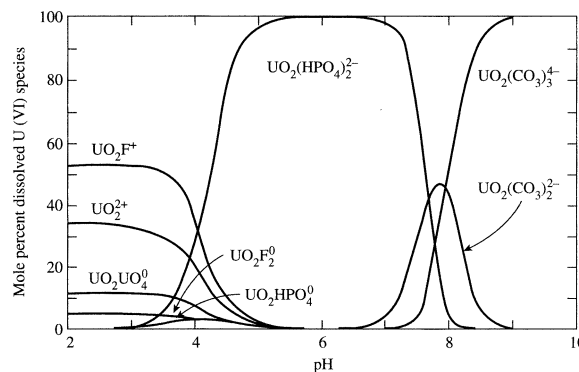
shallow glacial-drift materials beneath the facility as well as off-site (Sidle and Lee, 1996). The facility is located above a buried-bedrock valley in southwestern Ohio. The valley contains a glacial-outwash aquifer, with an average thickness of 61 m. This aquifer is overlain by a surficial-till deposit, which averages 9.1 m thick. The aquifer is unconfined and in the plant vicinity is recharged by leakage from an intermittent stream and several plant outfalls.

Groundwater flow is to the south, toward the Greater Miami River and the average linear groundwater velocity is 0.21 to 1.13 m/da. Horizontal-hydraulic conductivity was measured at values ranging from 36.6 m/da to 235.9 m/da. The aquifer is anisotropic, with a geometric mean K_h/K_v of 22.4.

Background dissolved U in the aquifer has a log-normal distribution with a mean value of 0.9 $\mu\text{g/L}$, and a maximum value of 3.1 $\mu\text{g/L}$. Groundwater containing dissolved U in excess of the background levels is found beneath and downgradient of the Fernald facility. The areas of the aquifer where the groundwater exceeds 20 $\mu\text{g/L}$ are outlined on Figure 6.17. In what is known as the "South Plume," the maximum-observed U concentration was 1573 $\mu\text{g/L}$, with a geometric mean of 35.1 $\mu\text{g/L}$. A cross section showing the vertical distribution of total U along the line A-A' from Figure 6.17 is shown on Figure 6.18.

The pH of the groundwater averaged 7.3 ± 0.7 and Eh ranged from +0.14 to +0.94 volts, indicating an oxidizing environment. Measured Eh-pH values from the site are shown as open circles on Figure 6.19. These fall in the range where UO_2^{2+} occurs. Because of high carbonate alkalinity at the site, carbonate complexes such as $\text{UO}_2(\text{CO}_3)_2^{2-}$ will form and enhance carbonate mobility. Calculated redox pairs for $\text{UO}_2^{2+}/\text{U}^{4+}$ are shown as solid circles on Figure 6.19 and fall in the UO_2CO_3^0 and $\text{UO}_2(\text{CO}_3)_2^{2-}$ fields.

FIGURE 6.16 Distribution of uranyl complexes as a function of pH for groundwater that contains 0.3 mg/L F^- , 10 mg/L Cl^- , 100 mg/L SO_4^{2-} , 0.1 mg/L PO_4^{2-} , and PcO_2 of $10^{-2.5}$ atm.



Source: D. Langmuir. 1978. Uranium solution-mineral equilibria at low temperatures with applications to sedimentary ore deposits. *Geochimica et Cosmochimica Acta* 42:547–570. Used with permission.

6.9.4 Thorium

Thorium is a naturally occurring element with a principal isotope of ^{232}Th , which has a half-life of 1.39×10^{10} years. Daughter products of thorium decay include ^{228}Ra and ^{224}Ra .

The chemistry of thorium is much simpler than that of uranium. Thorium occurs only in a +4 valence, so it does not undergo oxidation-reduction. Thorium oxide, ThO_2 ,

has a very low solubility. The primary thorium ore is monazite, which contains oxides of thorium, phosphorus, and the rare earths yttrium, lanthanum, and cerium.

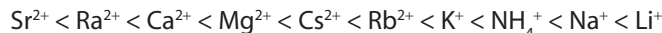
The mobility of thorium is greatly enhanced if ligands are present to form complexes. Figure 6.20 shows the inorganic thorium complexes that form as a function of the pH of the solution. The solution contains 0.3 mg/L F⁻, 10 mg/L Cl⁻, 100 mg/L SO₄²⁻ and 0.1 mg/L PO₄²⁻. It can be seen from this figure that the most abundant aqueous species in order of increasing pH are Th(SO₄)₂⁰, ThF₂²⁺, Th(HPO₄)₂⁰, Th(HPO₄)₃²⁻ and Th(OH)₄⁰. However, the mobility of thorium complexes formed by organic ligands such as EDTA and citric acid are much greater than those formed by inorganic ligands (Langmuir and Herman 1980).

Adsorption of dissolved thorium increases with increasing pH above pH 2. The sorption of thorium onto clays, oxides and soil organic matter is nearly total by a pH of 6.5. Strongly complexing organic ligands such as EDTA can retard sorption or even promote desorption (Langmuir and Herman 1980). Thorium in natural waters and soil should be nearly immobile due to the low solubility of the minerals and the strong tendency for dissolved forms to be sorbed only by clays, mineral oxides, and soil organic matter.

6.9.5 Radium

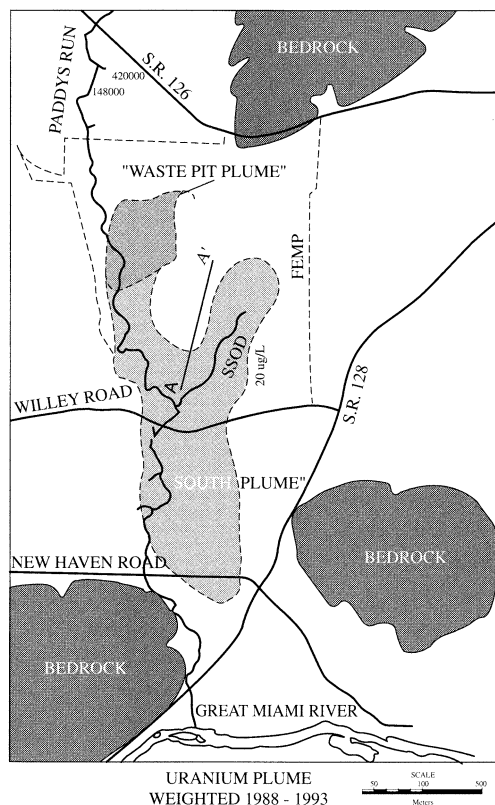
Radium occurs naturally in four isotopes: ²²³Ra, ²²⁶Ra and ²²⁸Ra. ²³²Th decays into both ²²⁸Ra and ²²⁴Ra, whereas ²³⁵U decays to ²²³Ra and ²³⁸U disintegrates to ²³⁵Th, which in turn decays to ²²⁶Ra. One isotope, ²²⁶Ra, has a much longer half-life than any of the others, 1599 years. Because of their short half-lives, the radium isotopes are strongly radioactive (Hem 1985).

Knowledge of the aqueous chemistry of radium is summarized in IAEA (2014). It is reportedly similar in chemical behavior to barium (Hem 1985) and calcium (Kathren 1984). It is more soluble than uranium or thorium and can be bioconcentrated by plants (Brazil nuts have an especially high radium content). Radium can be strongly exchanged in the cation exchange series. According to Kathren (1984), the cation exchange sequence for soils is



²²⁸Ra has a much shorter half-life, (5.8 yr) than ²²⁶Ra. However, its parent, ²³²Th, is more abundant in nature than ²³⁸U, the parent of ²²⁶Ra. As a result, both isotopes are found in groundwater. The U.S. EPA has proposed MCLs of 20 pCi/L for both ²²⁶Ra and ²²⁸Ra (Federal Register, July 18, 1991). Wells with high radium levels in groundwater have been discovered to be concentrated in two areas of the United States: the Piedmont and coastal plain of the Middle Atlantic states and the upper Northwestern states of Minnesota, Iowa, Illinois, Missouri, and Wisconsin (Hess et al. 1985). Table 6.7 summarizes the distribution of ²²⁶Ra and ²²⁸Ra in the Atlantic coastal plain and Piedmont region.

The radium content of groundwater is a function of the rock type of the aquifer. Igneous rocks, such as granites, contain the highest proportion of uranium and thorium, the parent isotopes of radium. Granitic rock aquifers and sands and sandstones derived from the weathering of granites have the potential to have high radium. Phosphate rock is also very high in uranium. Radium is not only a problem that is naturally occurring,

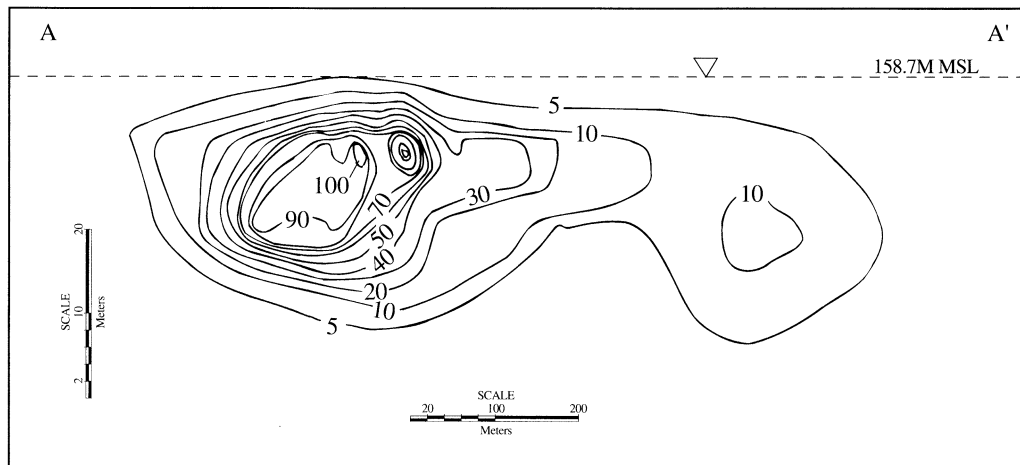
FIGURE 6.17 Composite plume of total dissolved uranium >0.20 µg/L for the period 1988 to 1993.

Source: W.C. Sidle and P.Y. Lee. 1996. Uranium contamination in the Great Miami Aquifer at the Fernald Environmental Management Project, Fernald Ohio. *Groundwater* 34:876–882. Used with permission.

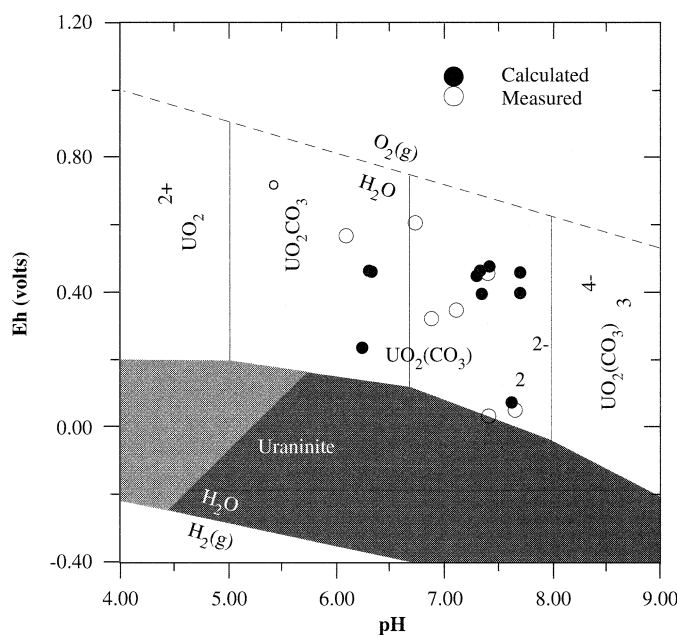
Table 6.7 Distribution of 226Ra and 228Ra by aquifer type in the Atlantic coastal plain and Piedmont provinces.

Aquifer Type	Number of Samples	Ra-228 (pCi/L)		Ra-226 (pCi/L)	
		Geometric Mean	Range	Geometric Mean	Range
Igneous (acidic)	42	1.39	0.0–22.6	1.8	0.0–15.9
Metamorphic	75	0.33	0.0–3.9	0.37	0.0–7.4
Sand	143	1.05	0.0–17.6	1.36	0.0–25.9
Arkose	92	2.16	0.0–13.5	2.19	0.0–23.0
Quartzose	50	0.27	0.0–17.6	0.55	0.0–25.9
Limestone	16	0.06	0.0–0.2	0.12	0.0–0.3

Source: C.T. Hess, J. Michel, T.R. Horton, H.M. Prichard, and W.A. Coniglio, "The occurrence of radioactivity in public water supplies in the United States," *Health Physics* 48 (1985):553–86.

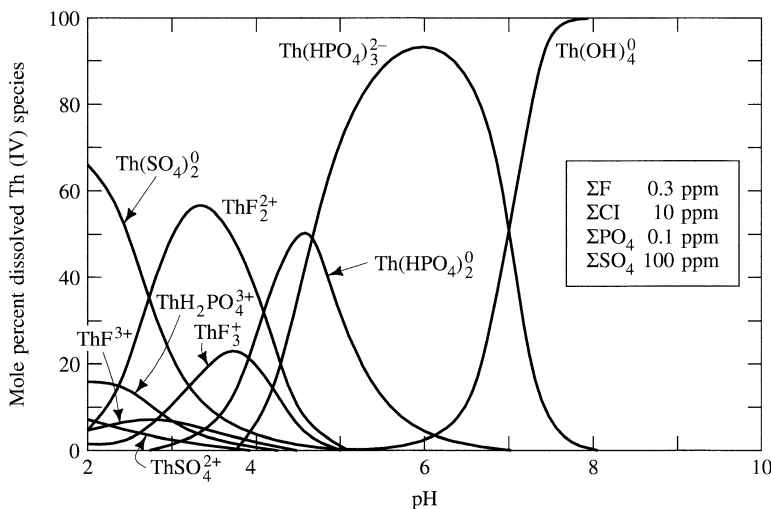
FIGURE 6.18 Longitudinal profile of total dissolved uranium along line A – A' from Figure 6.17.

Source: W. C. Sidle and P. Y. Lee. 1996. Uranium contamination in the Great Miami Aquifer at the Fernald Environmental Management Project, Fernald Ohio. *Groundwater* 34:876–882. Used with permission.

Figure 6.19 Measured and calculated redox potential for the $\text{UO}_2^{2+}/\text{U}^{4+}$ pair plotted on the $\Sigma\text{U} = 10^{-6}$ stability field.

Source: W. C. Sidle and P. Y. Lee. 1996. Uranium contamination in the Great Miami Aquifer at the Fernald Environmental Management Project, Fernald Ohio. *Groundwater* 34:876–882. Used with permission.

Figure 6.20 Distribution of thorium complexes as a function of pH under standard conditions for an aqueous solution containing 0.3 mg/L F⁻, 10 mg/L Cl⁻, 100 mg/L SO₄²⁻, and 0.1 mg/L PO₄³⁻.



Source: D. Langmuir and J. S. Herman. 1980. The mobility of thorium in natural waters at low temperatures. *Geochemica et Cosmochimica Acta* 44:1753–1766. Used with permission.

but there are localized areas of radium contamination from industrial operations. These are associated with uranium mill tailings as well as facilities where radioluminescent paints were prepared and used. For example, from World War I up until 1968 wrist watches with radium dials that glowed in the dark were sold in the United States.

6.9.6 Radon

There are several isotopes of radon, but ²²²Rn is the only one that is important environmentally. The other isotopes have half-lives of less than 1 min. The half-life of ²²²Rn is 3.8 days. ²²²Rn is produced by the decay of ²²⁶Ra, so that it is associated with rocks that are high in uranium. Radon can be associated with water that is low in dissolved ²²⁶Ra, because it comes primarily from the decay of the radium in the rock. Radon is a noble gas and does not undergo any chemical reactions, nor is it sorbed onto mineral matter. Radon is lost from water by diffusion into the atmosphere and by radioactive decay through a series of short-lived daughter products to ²¹⁰Pb, which has a half-life of 21.8 yr.

The EPA has proposed an MCL standard of 300 pCi/L for radon in drinking water (Federal Register, November 2, 1999). However, there is also a health concern for excessive radon accumulation in homes. Radon can enter homes through emanations from the soil as well as by diffusion from tap water with a high radon content.

Owners of private water systems are most at risk from radon in drinking water. Public water-supply systems normally have storage facilities to supply water during fires. The residence time for the water in these facilities allows the radon to both diffuse and decay. Private water systems rely upon wells and usually only have a very small storage facility used to maintain pressure.

Brutsaert et al. (1981) studied radon in groundwater in Maine. They found radon levels in private wells of up to 122,000 pCi/L. The average ^{222}Rn content of wells obtaining water from granites was 22,100 pCi/L, from sillimanite-grade metasedimentary rocks, it was 13,600 pCi/L, and from chlorite-grade metasedimentary rocks, it was 1100 pCi/L. The high radon values in the high-grade metamorphic terrains were believed to be due to metamorphic pegmatites and associated uranium mineralization.

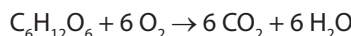
6.9.7 Tritium

Tritium, ^3H , is produced naturally by cosmic-ray bombardment of the atmosphere, by thermonuclear detonations and in nuclear reactors. As it is an isotope of hydrogen, it can form a water molecule or be incorporated into living tissue. Tritium has a half-life of 12.6 years. Much of the radiation at low-level radioactive waste sites is due to tritium (Kathren 1984). Low-level radioactive waste is disposed by shallow burial on land. If waste packages at low-level radioactive waste sites leak and if the landfill is not secure, tritium is likely to escape. Tritium migration via groundwater flow from low-level waste disposal has been detected at U.S. sites at the Savannah River facility, Los Alamos National Laboratory (Overcamp 1982), and the Sheffield, Illinois, commercial disposal site (Foster et al. 1984), and the Hanford, Washington, site (Levi 1992).

■ 6.10 Geochemical Zonation

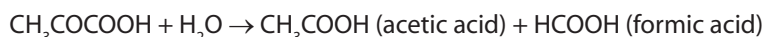
Landfills have proven to be a source of groundwater contamination in many different geologic terrains, climates, and hydrogeologic settings. **Landfill leachate** is the liquid that is the product of the liquid content of the waste, infiltrating precipitation, and groundwater if the waste is below the water table. These liquids mix with the waste and dissolve both inorganic and organic constituents. Leachate is a complex mixture of dissolved and colloidal organic matter and inorganic compounds and ions. Many of the chemical processes are controlled by microbial activity. In this section we will examine the geochemical zonation that occurs in groundwater affected by leachate from a landfill. This will serve to illustrate some of the reactions discussed in this chapter.

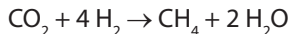
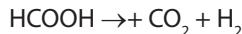
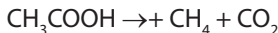
Organic matter is a major constituent of municipal landfills, where it is decomposed by bacteria and other microbes. The initial decomposition is under aerobic conditions. Once the oxygen in the landfill is consumed, anaerobic decomposition becomes prevalent. The complete aerobic decomposition of glucose, a sugar found in organic waste, yields carbon dioxide and water as products (Baedecker and Back 1979a):



The carbon dioxide thus produced forms carbonic acid in the leachate and can also escape from the waste as a gas.

Anaerobic decomposition produces a variety of organic acids as intermediate steps in the formation of methane. This process can be represented by the fermentation of glucose:





Any hydrogen gas produced is utilized by the methane-forming bacteria in their reduction of organic compounds. In addition, oxidized forms of nitrogen and sulfur compounds are also reduced to form NH_3 and H_2S (Baedecker and Back 1979b). The methane formed can escape from the landfill as a gas and can also dissolve in the leachate.

The pH of landfill leachate is generally in the range of 6.5 to 7.0. This is due to the buffering offered by the generation of large amounts of CO_2 , which dissociates to HCO_3^- , to a lesser extent the formation of NH_3 , which forms NH_4^+ in water, and the reduction of SO_4^{2-} to H_2S . As has been shown earlier in this chapter, the solubility of mineral species is a function of the Eh and pH of the environment. The Eh of landfill leachate is controlled by the reduction of organic compounds and oxidized forms of nitrogen, sulfur, iron, and manganese. When reduced leachate mixes with oxygenated groundwater, the Eh of the resulting solution can become more oxidizing.

Baedecker and Back (1979b) have compared the redox zonation of a landfill with that of marine sediments, a geochemical environment that has been extensively studied. The oxygenated water at the bottom of the sea represents an aerobic environment. The sediments at the bottom are anaerobic. In the transition from aerobic to anaerobic conditions, there is a sulfate-reducing zone, where decomposition of organic matter reduces sulfate to sulfide. Ferric iron will also be reduced to ferrous iron in this zone. Ferrous iron reacts with the hydrogen sulfide to form insoluble sulfide precipitates. The most reduced zone in marine sediments is an anaerobic carbonate-reducing zone that has become depleted in sulfur. In this zone we find the production of CH_4 and NH_4^+ .

In the study of leachate plumes at landfills, a three-part zonation has been found. The landfill itself represents an anaerobic zone. This anaerobic zone extends along the plume of leachate mixing with groundwater. In this zone we find the production of methane and ammonia as microorganisms decompose organic matter and obtain oxygen from the reduction of sulfate and nitrate. Reduction will liberate soluble ferrous iron. Manganese may also become soluble due to dissolution of native minerals. Ferrous sulfide may precipitate in this zone.

As the leachate mixes with oxygenated groundwater, it becomes less reducing and forms a transition zone. Most of the soluble organic matter has already been decomposed in this zone. In the transition zone there is coprecipitation of trace metals with iron and manganese hydroxides. Ahead of the transition zone, there is an aerobic zone, where the leading edge of the leachate has changed the native groundwater quality, but not enough to deplete the oxygen. The aerobic zone contains nitrate and sulfate at the background levels of the aquifer.

Baedecker and Back (1979a; 1979b) have defined the boundaries of these zones at a landfill on the basis of (1) dissolved oxygen content, (2) the ratio of reduced nitrogen to nitrate, (3) the presence of methane gas, and (4) the ratio of dissolved manganese to iron.

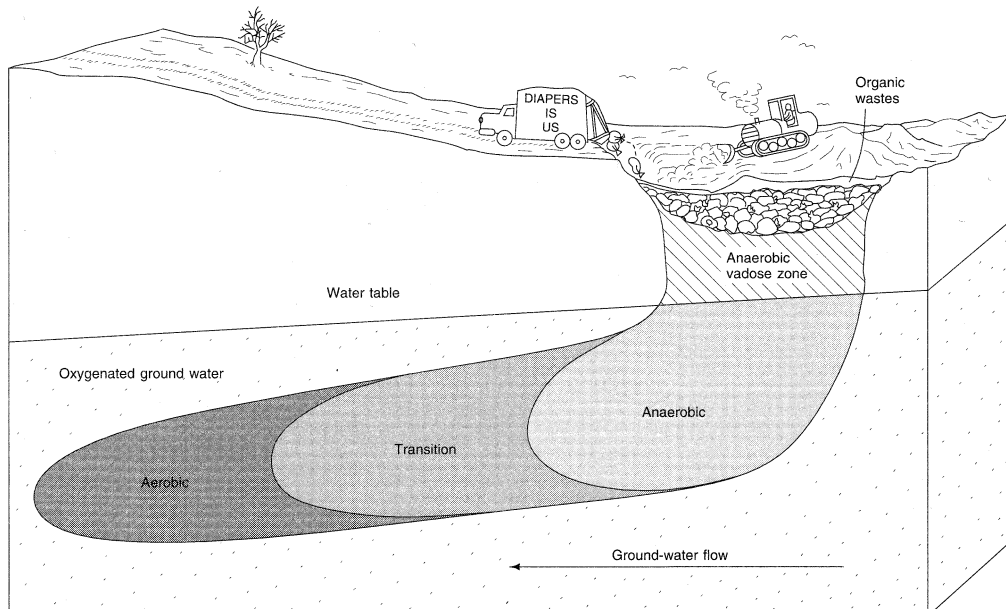
Total reduced nitrogen, the sum of organic nitrogen and ammonia, is measured by a test called Kjeldahl nitrogen (Kjl N). Baedecker and Back (1979a; 1979b) examined the ratio $\text{Kjl N}/\text{NO}_3^-$ and found that it was greatest in the anaerobic zone, where ammonia was present, decreased in the transition zone, and was quite low in the aerobic zone, where the nitrogen was primarily in the form of nitrate.

If there is limited sulfur present, there will be soluble iron and manganese in the anaerobic zone. As the iron traverses to the transition zone, it will begin to be oxidized and precipitate as ferric hydroxide. Manganese is soluble over a much larger Eh-pH range than iron and will remain in solution longer as the plume moves into oxygenated groundwater. Because iron is much more abundant than manganese, there will be a large ratio of dissolved iron to dissolved manganese in the anaerobic zone. This ratio will gradually decrease in the transition zone as the iron is preferentially precipitated. Eventually both dissolved iron and manganese will disappear as the aerated zone is reached.

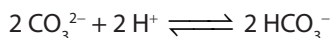
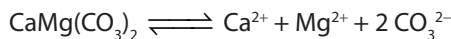
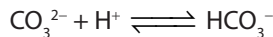
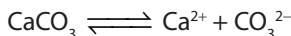
Methane gas and ammonia are found only in the anaerobic zone and dissolved oxygen is found only in the aerobic zone. Naturally, the preceding model of geochemical zonation is valid only for circumstances where the receiving groundwater contains dissolved oxygen. Figure 6.21 shows an idealized leachate plume and the geochemical zonation.

If landfill leachate is discharged into a carbonate rock aquifer, or an unconsolidated aquifer with large amounts of carbonate, reactions between the acids of the leachate and the carbonate can occur (Kehew and Passero 1990). Both organic acids

Figure 6.21 Geochemical zonation of the leachate plume from a landfill receiving organic waste.



produced by the reduction of organic compounds and carbonic acid from the production of carbon dioxide are present in leachate. It will react with the carbonate rock, releasing calcium and magnesium:



These reactions liberate calcium and magnesium, and the resulting leachate has a high hardness. The increase in bicarbonate buffers the leachate to nearly neutral and also promotes the precipitation of carbonate minerals such as siderite (FeCO_3).

■ 6.11 Summary

The inorganic chemistry of contaminated groundwater can be studied from the standpoint of chemical thermodynamics. The first step is to obtain a representative chemical analysis of the water. This should contain the major anions and cations: Ca^{2+} , Mg^{2+} , Na^+ , K^+ , HCO_3^- , Cl^- , PO_4^{3-} , SO_4^{2-} , NO_3^- , and F^- . In addition, pH and Eh should be measured in the field in a flowthrough cell so that the sample does not come into contact with the atmosphere. If the Eh is positive, dissolved oxygen should be measured; if it is negative, hydrogen sulfide and ammonia should be measured. These data should be obtained to aid in interpretation of species analyses for suspected inorganic contaminants.

Inorganic contaminants in groundwater can be removed by precipitation. The law of mass action can be used to study chemical equilibrium. Thermodynamically stable species may precipitate as the inorganic contaminant mixes with native groundwater. Many inorganic elements can exist in different valence states. The elements can participate in oxidation-reduction reactions. Some of the redox reactions are mediated by microorganisms. The Nernst equation relates the Eh and pH of an aqueous solution. The Nernst equation and chemical equilibrium can be used to construct Eh-pH diagrams, which show the fields of stability for various chemical spills.

Organic matter can be decomposed by microbes in a landfill. Under oxidizing conditions oxygen is the electron acceptor, whereas under reducing conditions the electron acceptor can be sulfate, nitrate, ferric iron, or carbon dioxide. Three redox zones have been identified in the leachate plumes at landfills: an anaerobic zone, where the waste is being decomposed, methane is being formed, and iron, sulfur, and nitrogen exist in reduced forms; a transition zone; and an anaerobic zone, with oxidizing conditions and oxidized forms of iron, sulfur, nitrogen, and carbon.

Chapter Notation

<i>A</i>	Constant equal to 0.5085 at 25°C	K_{eq}	Equilibrium constant
[A]	Activity of reactant A	K_{sp}	Solubility product
<i>a</i>	Moles of reactant	<i>m</i>	Moles of hydrogen ions
a_i	Effective diameter of an ion from (Table 6.1)	m_i	Molality of the <i>i</i> th ion
<i>B</i>	Constant equal to 0.3281 at 25°C	m_x	Molal concentration
[B]	Activity of product B	<i>n</i>	Number of electrons in half-reaction
<i>b</i>	Moles of product	<i>R</i>	Gas constant
Eh	Oxidation potential of the aqueous solution in volts	<i>T</i>	Temperature in Kelvins
E^0	Standard potential of redox reaction in volts	<i>w</i>	Moles of water
<i>F</i>	Faraday constant	Z_i	Charge on ionic species <i>i</i>
<i>I</i>	Ionic strength	G_R^0	Free energy of a reaction
		γ_i	Activity coefficient for ionic species <i>i</i>

References

- ATSDR. 2015. Toxic Substances Portal—Cobalt. *Agency for Toxic Substances and Disease Registry*. Accessed October 2015 from <http://www.atsdr.cdc.gov/PHS/PHS.asp?id=371&tid=64>
- Baedeker, M. J., and W. Back. 1979a. Hydrogeological processes and chemical reactions at a landfill. *Ground Water* 17:429–437.
- . 1979b. Modern marine sediments as a natural analog to the chemically stressed environment of a landfill. *Journal of Hydrology* 43:393–414.
- Brahic, C. 2004. Court clears geologists in Bangladesh arsenic case. *Science and Development Network*. Accessed October 2014 from <http://www.scidev.net/global/pollution/news/court-clears-geologists-in-bangladesh-arsenic-case.html>
- Brindha, K., and L. Elango. 2011. “Fluoride in groundwater: Causes, implications and mitigation measures.” In *Fluoride: Properties, Applications and Environmental Management*, ed. S. D. Monroy, 111–136. New York: Nova Science Publishers.
- Brutsaert, W. E., S. A. Norton, C. T. Hess, and J. S. Williams. 1981. Geologic and hydrologic factors controlling radon-222 in ground water in Maine. *Ground Water* 19:407–417.
- Challan, M. B. 2016. Application of chlorine-36 technique in determining the age of modern groundwater in the Al-Zulfi province, Saudi Arabia. *Isotopes in Environmental and Health Studies* 52:258–269.
- Clarkson, T. W. 2001. “Inorganic and organometal pesticides.” In *Handbook of Pesticide Toxicology*, ed. R. I. Krieger, 1357–1428. San Diego: Academic Press.
- Coefield, S. 2009. Selenium from power plants poses ecological risks, spurs EPA review. *Environmental Health News*. Accessed October 2015 from <http://www.environmentalhealthnews.org/ehs/news/selenium-from-power-plants>
- Corbett, R. G., and B. M. Manner. 1984. Fluoride in the ground water of Northeastern Ohio. *Ground Water* 22:13–17.
- Cross, F. L., and R. W. Ross. 1970. Fluoride uptake from gypsum ponds. *Fluoride* 3: 97–101.
- Culbard, E. B., I. Thornton, J. M. Watt, M. Wheatley, S. Moorcroft, and M. J. Thompson. 1988. *Journal of Environmental Quality* 17:226–234.
- D’Alessandro, W. 2006. Human fluorosis related to volcanic activity: A review. *Environmental Toxicology Transaction: Biomedicine and Health* 10:21–30.

- Davis, B. E. 1990. "Lead." In *Heavy Metals in Soils*, ed. B. J. Alloway, 177–196. New York: John Wiley & Sons.
- Dowdy, R. H., and V. V. Volk. 1983. "Movement of heavy metals in soil." In *Chemical Mobility and Reactivity in Soil Systems*, 229–239. Madison, WI: Soil Science Society of America.
- Emmerson, B. T. 1970. "Ouch-ouch" disease: The osteomalacia of cadmium nephropathy. *Annals of Internal Medicine* 73:854–855.
- Feth, J. H. 1966. Nitrogen compounds in natural water—a review. *Water Resources Research* 2: 41–58.
- Flipse, W. J., Jr., B. G. Katz, J. B. Lander, and R. Markel. 1984. Sources of nitrate in ground water in a seweried housing development, central Long Island, New York. *Ground Water* 22:418–425.
- Flipse, W. J., Jr., and F. T. Bonner. 1985. Nitrogen-isotope ratios of nitrate in ground water under fertilized fields, Long Island, New York. *Ground Water* 23:59–67.
- Foster, J. B., J. R. Erickson, and R. W. Healy. 1984. Hydrogeology of a low-level radioactive-waste disposal site near Sheffield, Illinois. U. S. Geological Survey, *Water Resources Investigations Report 83-4125*, 87 pp.
- Gee, G. W., D. Rai, and R. J. Serne. 1983. "Mobility of radionuclides in soil." In *Chemical Mobility and Reactivity in Soil Systems*, 203–227. Madison, WI: Soil Science Society of America.
- Giridhar, J., and D. Langmuir. 1991. Determination of E^0 for the $\text{UO}_2^{2+}/\text{U}^{4+}$ couple from measurement of the equilibrium: $\text{UO}_2^{2+}/\text{U}^{4+} + \text{Cu(s)} + 4\text{H}^+ = \text{U}^{4+} + \text{Cu}^{2+} + 2\text{H}_2\text{O}$ at 25°C and some geochemical implications. *Radiochimica Acta* 54:133–138.
- Grantham, D. A., and J. F. Jones. 1977. Arsenic contamination of water wells in Nova Scotia. *Journal American Water Works Association* 69:653–657.
- Gray, E. M., and M. Morgan-Jones. 1980. A comparative study of nitrate levels at three adjacent ground-water sources in a chalk catchment area west of London. *Ground Water* 18:159–167.
- Griffin, R. A., and N. F. Shimp. 1976. Effect of pH on exchange-adsorption or precipitation of lead from landfill leachates by clay minerals. *Environmental Science and Technology* 10:1256–1261.
- Haluszczak, L. O., A. W. Rose, and L. R. Kump. 2013. Geochemical evaluation of flowback brine from Marcellus gas wells in Pennsylvania, USA. *Applied Geochemistry* 28:55–61.
- Hem, J. D. 1977. Reactions of metal ions at surfaces of hydrous iron oxide. *Geochimica et Cosmochimica Acta* 41:527–538.
- . 1985. *Study and interpretation of the chemical characteristics of natural water*. U. S. Geological Survey Water Supply Paper 2254, 263 pp.
- Henderson, T. 1994. Geochemical reduction of hexavalent chromium in the Trinity Sand aquifer. *Ground Water* 32:477–486.
- Hess, C. T., J. Michel, T. R. Horton, H. M. Prichard, and W. A. Coniglio. 1985. The occurrence of radioactivity in public water supplies in the United States. *Health Physics* 48:553–586.
- Hill, A. R. 1982. Nitrate distribution in the ground water of the Alliston region of Ontario, Canada. *Ground Water* 20:696–702.
- Hossain, M. 2006. Arsenic-poisoning lawsuit rejected by Britain. Mail and Guardian, July 10, 2006. Accessed October 2014 from <http://mg.co.za/article/2006-07-10-arsenicpoisoning-lawsuit-rejected-by-britain>
- Hounslow, A. W. 1980. Ground-water geochemistry: Arsenic in landfills. *Ground Water* 18:331–333.
- IAEA. 2014. The environmental behaviour of radium: Revised edition. Tech. Report Series no. 476. International Atomic Energy Agency, Vienna. Accessed July 2017 from http://www-pub.iaea.org/MTCD/Publications/PDF/trs476_web.pdf
- Johannesson, K. H., K. J. Stetzenbach, V. F. Hodge, D. K. Kreamer, and X. Zhou. 1997. Delineation of ground-water flow systems in the southern Great Basin using aqueous rare earth element distributions. *Groundwater* 35:807–819.
- Johannesson, K. H. 2006. Rare Earth Elements in Groundwater Flow Systems, ed. Johannesson, 187–222. Netherlands: Springer.
- Kaback, D. S., and D. D. Runnels. 1980. Geochemistry of molybdenum in some stream sediments and waters. *Geochimica et Cosmochimica Acta* 44:447–456.
- Kathren, R. L. 1984. *Radioactivity in the environment*. Chur, Switzerland: Harwood Academic Publishers, 397 pp.
- Kehew, A. E., and R. N. Passero. 1990. pH and redox buffering mechanisms in a glacial drift aquifer contaminated by landfill leachate. *Ground Water* 28:728–737.

- Kielland, J. 1937. Individual activity coefficients of ions in aqueous solutions. *American Chemical Society Journal* 59:1676–1678.
- Konefes, J. 1990. Ground Water in the News. *Ground Water* 28:997.
- Kreamer, D. K., K. J. Stetzenbach, V. F. Hodge, K. Johannesson, and I. Rabinowitz. 1996. Trace element geochemistry in water from selected springs in Death Valley National Park, California. *Groundwater* 34:95–103.
- Langmuir, D. 1978. Uranium solution-mineral equilibria at low temperatures with applications to sedimentary ore deposits. *Geochimica et Cosmochimica Acta* 42:547–570.
- Langmuir, D., and J. S. Herman. 1980. The mobility of thorium in natural waters at low temperatures. *Geochimica et Cosmochimica Acta* 44:1753–1766.
- Lemly, A. D. 2002. *Selenium assessment in aquatic ecosystems: A guide for hazard evaluation and water quality criteria*. New York: Springer-Verlag.
- Levi, B. G. 1992. Hanford seeks short-and long-term solutions to its legacy of waste. *Physics Today* 45:17–21.
- Manahan, S. E. 1984. *Environmental chemistry, Fourth Edition*. Boston: PWS Publishers.
- Matisoff, G., G. J. Khoury, J. F. Hall, A. W. Varnes, and W. H. Strain. 1982. The nature and source of arsenic in Northeastern Ohio ground water. *Ground Water* 20:446–456.
- McCarty, P. L., B. E. Rittman, and E. J. Bouwer. 1984. “Microbiological Processes Affecting Chemical Transformations in Groundwater.” In *Groundwater pollution microbiology*, eds. G. Bitton and C. P. Gerba, 89–115. New York: John Wiley and Sons.
- Means, J. L., D. A. Crerar, and J. O. Duguid. 1978. Migration of radioactive wastes: Radionuclide mobilization by complexing agents. *Science* 200:1477–1481.
- Nikolaidis, N. P., G. A. Robbins, M. Scherer, B. McAninch, G. Binkhorst, J. Asikainen, and S. L. Suib. 1994. Vertical distribution and partitioning of chromium in a glaciofluvial aquifer. *Ground Water Monitoring Review* 14:150–159.
- Nriagu, J. O. 1972. “The Biogeochemistry of Lead in the Environment.” In *The Biogeochemistry of lead in the environment*, ed. J. O. Nriagu. Amsterdam: Elsevier/North Holland.
- Overcamp, T. J. 1982. “Low-level radioactive waste disposal by shallow land burial.” In *Handbook of environmental radiation*, ed. A. W. Kjement, Jr., 207–67. Boca Raton, FL: CRC Press.
- Page, A. L., T. J. Ganje, and M. S. Joshi. 1971. Lead quantities in plants, soil and air near some major highways in Southern California. *Hilgardia* 41:1–31.
- Perhnutter, N. M., M. Lieber, and H. L. Frauenthal. 1963. *Movement of waterborne cadmium and hexavalent chromium wastes in South Farmingdale, Nassau County, Long Island*. U. S. Geological Survey Professional Paper 475C, pp. C170–C184.
- Rabinowitz, M. B. and G. W. Wetherill. 1972. Identifying sources of lead contamination by stable isotope techniques. *Environmental Science and Technology* 8:705–709.
- Robertson, F. N. 1975. Hexavalent chromium in the ground water in Paradise Valley, Arizona. *Ground Water* 13:516–527.
- Robie, R. A., B. S. Hemingway, and J. R. Fisher. 1978. *Thermodynamic properties of minerals and related substances at 298.15 K and 1 bar(10⁵ pascals) pressure and at higher temperatures*. U.S. Geological Survey Bulletin 1452, 456 pp.
- Scokart, P. O., K. Meeus-Verdinne, and R. De Borger. 1983. Mobility of heavy metals in polluted soils near zinc smelters. *Water, Air, & Soil Pollution* 20:451–463.
- Sidle, W. C., and P. Y. Lee. 1996. Uranium contamination in the Great Miami Aquifer at the Fernald Environmental Management Project, Fernald Ohio. *Ground Water* 34:876–882.
- Silver, B. A., and J. R. Fielden. 1980. Distribution and probable source of nitrate in ground water of Paradise Valley, Arizona. *Ground Water* 18: 244–251.
- Singer, M. J., and L. Hanson. 1969. *Soil Science Society of America Proceedings* 33:152–153.
- USGS. 2015. United States Geological Survey—Resources on Isotopes. Accessed October 2015 from http://wwwrcamnl.wr.usgs.gov/isoig/period/sr_iig.html
- Ure, A. M., and M. L. Berrow. 1982. “The Elemental constituents of soils.” In *Environmental Chemistry Vol. 2*. London: Royal Society of Chemistry.
- Wagman, D. D., W. H. Evans, V. B. Parker, I. Halow, S. M. Bailey, and R. H. Schumm. 1968. *Selected values of chemical thermodynamic properties (tables)*

- for elements 1–34 in standard order of arrangement).* National Bureau of Standards Technical Note 270–3, 264 pp.
- . 1969. *Selected values of chemical thermodynamic properties (tables for elements 35–53 in standard order of arrangement).* National Bureau of Standards Technical Note 270–4, 141 pp.
- Wagman, D. D., W. H. Evans, V. B. Parker, I. Halow, S. M. Bailey, R. H. Schumm, and K. L. Churney. 1971. *Selected values of chemical thermodynamic properties (tables for elements 54–61 in standard order of arrangement).* National Bureau of Standards Technical Note 270–5, 41 pp.
- Waldbott, G. L. 1973. *Health Effects of Environmental Pollutants*, St. Louis, MO: C. V. Mosby Co., 316 pp.
- Welch, A. H., M. S. Lico, and J. L. Hughes. 1988. Arsenic in ground water of the western United States. *Groundwater* 26:333–347.
- Whittemore, D. O. and D. Langmuir. 1975. The solubility of ferric oxyhydroxides in natural waters. *Ground Water* 13:360–365.
- World Nuclear Association. 2015. Geology of uranium deposits. Accessed October 2015 from <http://www.world-nuclear.org/info/Nuclear-Fuel-Cycle/Uranium-Resources/Geology-of-Uranium-Deposits/>
- Wright, J. R., R. Levick, and H. J. Atkinson. 1955. Trace element distribution in virgin soil profiles representing four great soil groups. *Proceedings, Soil Science Society of America* 19:340–344.
- Zimndahl, R. L. and R. K. Skogerboe. 1977. Behavior of lead in soil. *Environmental Science and Technology* 11:1202–1207.

Problems

- 6.1** If CuCl is placed in water at 25°C, what will the equilibrium concentration of copper be?
- 6.2** If BaSO₄ is placed in water at 25°C, what will the equilibrium concentration of barium be?
- 6.3** If Hg₂Cl₂ is placed in water at 25°C, what will be equilibrium concentration of mercury be? What will the concentration of chloride be?
- 6.4** If Ag₂SO₄ is placed in water at 25°C, what will be equilibrium concentration of silver be? What will be concentration of sulfate be?
- 6.5** What is the ionic strength of a water with the following composition:

Potassium	24 mg/L	Sulfate	134 mg/L
Sodium	132 mg/L	Bicarbonate	330 mg/L
Calcium	8 mg/L	Chloride	21 mg/L
Magnesium	35 mg/L		
Iron	0.6 mg/L		

- 6.6** What is the ionic strength of a water with the following composition:

Potassium	24 mg/L	Sulfate	134 mg/L
Sodium	132 mg/L	Bicarbonate	330 mg/L
Calcium	23 mg/L	Chloride	22 mg/L
Magnesium	15 mg/L		
Iron	2 mg/L		

Organic Compounds in Groundwater

■ 7.1 Introduction

Organic compounds can occur in the ground either as pure compounds, a mixture of compounds, dissolved in water, vaporized in the gas phase, or sorbed to the porous matrix. In this chapter we will first examine the physical properties of organic compounds and the way that physical properties affect the behavior of organic chemicals in the subsurface. We will then learn the structure of common and emerging organic compounds, their nomenclature, and their possible sources in the subsurface. Finally, we will see how organic chemicals can undergo transformations by both chemical reactions and microbial degradation.

■ 7.2 Physical Properties of Organic Compounds

There are several important physical properties of organic compounds that help us to understand how they will behave. These compounds can exist as gases, liquids, and vapors. We can use the **melting points** and **boiling points** to evaluate if a particular compound will be a gas, liquid, or vapor at a certain temperature. If the specified temperature is below the melting point, the compound will be a solid. If the temperature falls between the melting point and the boiling point, the compound will be a liquid, and if the temperature is above the boiling point, the compound will be a gas. Boiling points are usually given at a pressure of 760 mm mercury (1 atm). Boiling points for a homologous series of compounds will increase with increasing molecular weight. (A **homologous series** is one with the same basic structure but increasing numbers of carbon atoms.)

The **specific gravity** of a substance (liquid or solid) is the ratio of the weight of a given volume of that substance to the weight of the same volume of water. The water weight is usually measured at 4°C, whereas the organic liquid weight may be measured at some other temperature, which is typically 20°C. If the specific gravity of the pure substance is less than 1.0, the substance will float on water, whereas if the specific gravity is greater than 1.0, the substance will sink in water.

Water solubility is an important property of organic substances. For a gas this must be measured at a given vapor pressure. For a liquid it is a function of the temperature of the water and the nature of the substance. Solubilities of organic materials can range from completely miscible with water to nearly insoluble. More soluble materials

have a greater potential mobility in the environment. Laboratory solubility is measured using distilled water, which may not have the same effect as natural waters. Also, a compound's solubility changes as a function of temperature, i.e., the higher the temperature, the greater the solubility of most solid compounds. It can be confusing when more than one solubility value is cited in the reference literature (e.g., Montgomery et al. 2007). Often, those solubility measurements refer to "room temperature"—an ill-defined term and quite variable from place to place.

The **octanol-water partition coefficient**, K_{ow} , is a measure of the degree to which an organic substance will preferentially dissolve in water or an organic solvent. The substance is mixed with equal amounts of two immiscible fluids, water and octanol (an eight-carbon chain alcohol). The coefficient is the ratio of the equilibrium concentration of the substance in octanol to the equilibrium concentration in water:

$$K_{ow} = \frac{C_{\text{octanol}}}{C_{\text{water}}} \quad (7.1)$$

This is usually given as a logarithm. The greater the value, the greater the tendency to dissolve in the organic liquid rather than the water. The greater the octanol water partition coefficient, the less mobile the compound tends to be in the environment.

Vapor pressure is a measure of the tendency of a substance to pass from a solid or a liquid to a vapor state. It is the pressure of the gas in equilibrium with the liquid or the solid at a given temperature. The greater the vapor pressure, the more volatile the substance.

The **vapor density** of a gas indicates if it will rise or sink in the atmosphere. If the gas is lighter than air, it will rise; if it is denser than air, it will sink. The vapor density, V_d , is related to the equilibrium vapor pressure, the gram molecular weight of the gas, and the temperature by Equation 7.2.

$$V_d = \frac{PM}{RT} \quad (7.2)$$

where

P = equilibrium vapor pressures in atm

M = gram molecular weight

R = gas constant ($0.082 \text{ L} \cdot \text{atm/mol/K}$)

T = temperature in K

Henry's law states that there is a linear relationship between the partial pressure of a gas above a liquid and the mole fraction of the gas dissolved in the liquid. It is given as Equation 7.3.

$$H_L = \frac{P_x}{C_x} \quad (7.3)$$

where

P_x = partial pressure of gas (atm at a given temperature)

C_x = equilibrium concentration of the gas in solution (mol/m^3 water)

H_L = Henry's law constant in $\text{atm}/(\text{mol/m}^3 \text{ water})$

Henry's law is valid if the gas is sparingly soluble, the gas phase is reasonably ideal, and the gas will not react with the solute. It can also be applied to organic compounds that are volatile liquids when they are dissolved in water. The greater the Henry's law constant, the greater the rate of volatilization. Although vapor pressure from pure phase and Henry's constant for dissolved phase are both measures of ability to volatilize into the gaseous phase, they are not analogous, i.e., a list of compounds from highest to lowest Henry's constant will not necessarily be in the same order as a list of the same compounds from highest to lowest vapor pressure.

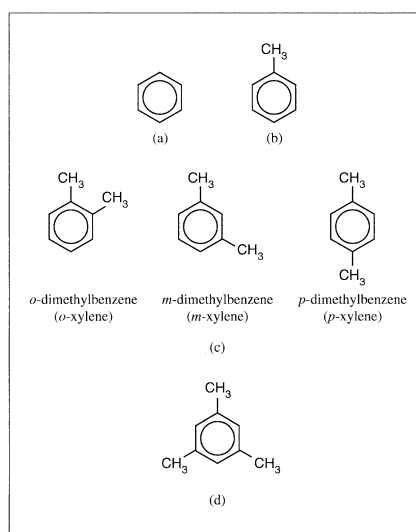
■ 7.3 Organic Structure and Nomenclature

7.3.1 Hydrocarbon Classes

Organic chemistry is based on the behavior of carbon atoms. The simplest organic compounds are **hydrocarbons**, which consist solely of carbon and hydrogen. Carbon has four bonding locations and can bond with such elements as oxygen, nitrogen, sulfur, phosphorus, chlorine, bromine, and fluorine as well as hydrogen. Carbon can form single, double, and triple bonds.

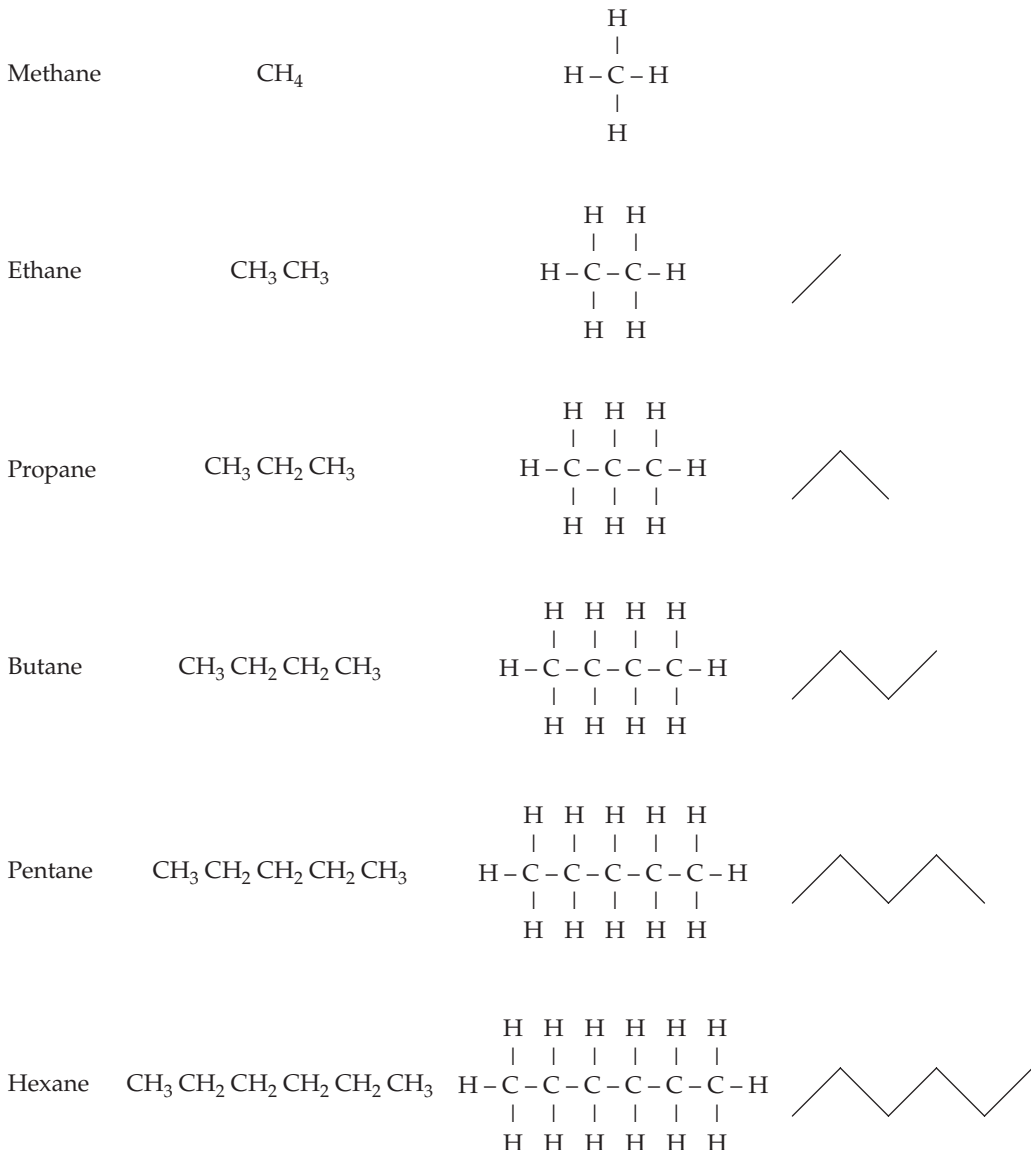
Hydrocarbons can be divided into two classes, **aromatic** hydrocarbons, which contain a **benzene** ring, and **aliphatic** hydrocarbons, which do not contain a benzene ring. The benzene ring contains six carbon atoms joined in a ring structure with alternating single and double bonds. The single and double bonds change positions on the ring so that they are considered to be equal. The six carbons occur in a single plane. A benzene ring is represented by the symbol in Figure 7.1(a).

FIGURE 7.1 Structure and nomenclature of the benzene ring. (a) Benzene ring; (b) methyl benzene (toluene); (c) o-dimethyl benzene, m-dimethyl benzene, and p-dimethyl benzene; (d) 1,3,5-trimethyl benzene.



Aliphatic hydrocarbons The carbons of aliphatic hydrocarbons with more than one carbon atom can be joined by single bonds (**alkanes**), double bonds (**alkenes**), or triple bonds (**alkynes**). If there is a combination of single and multiple bonds, the compound is classified on the basis of the multiple bond.

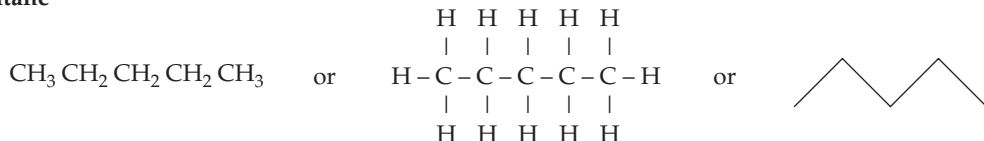
Alkanes Alkanes are also known as **saturated hydrocarbons**, or **paraffins**. The general formula is C_nH_{2n+2} . The first six straight-chain alkanes are as follows:



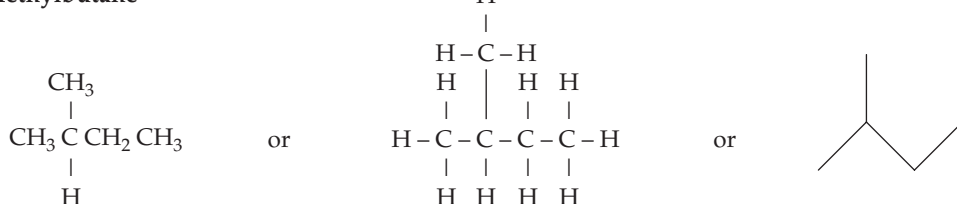
Organic compounds with the same formula may have different structural relationships. This is because alkanes can also have **branched chains**. These compounds

are **structural isomers**, and although they have the same formula, they are different compounds with different properties. For example the formula C₅H₁₂ represents three isomers:

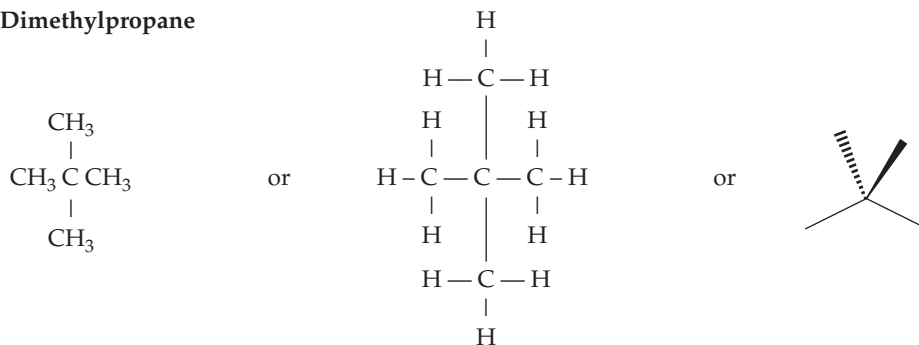
Pentane



2-Methylbutane



2,2-Dimethylpropane

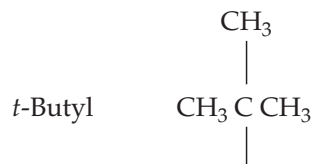


Note that there are several ways of illustrating the structural formula of a hydrocarbon. On the left is a condensed form, where only some of the bonds are shown, whereas in the middle all the bonds between atoms are shown. Another, even more condensed form of depicting organic compounds is the skeletal or line format (right) in which the hydrogen bonds are neglected and the bonds between the carbon atoms are depicted as lines. Other atoms, like chlorine, or functional groups, like –OH (phenolic) are added to the carbon skeleton as required. The line form is preferred in case the three-dimensional bonding geometry of a compound needs to be emphasized. In most cases we will use the condensed and line form or both.

These isomers have been named using the rules of the International Union of Pure and Applied Chemistry (IUPAC). For alkanes these rules are as follows:

1. The base name of the compound is the name of the longest straight-chain alkane that is present.

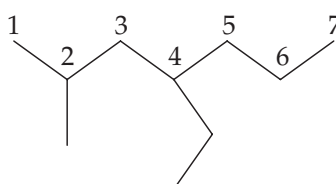
2. Any chain that branches from the straight chain or any functional group that is attached to the straight chain is named. Carbon chains are named as alkyl groups. The following are important alkyl groups:



Other functional groups include such things as chloride ions, indicated by the prefix chloro-.

3. The location of the functional group is indicated by numbering the carbon atoms in the longest straight chain, with the end carbon closest to the position of the first functional group being carbon 1.
4. For more than one of the same functional group, the prefixes *di-*, *tri-*, and *tetra-* are used.

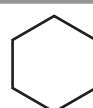
Consider the following branched-chain alkane:



The longest straight chain has seven carbons, so this is a heptane. The carbons are numbered starting with the end closest to an attached functional group. A methyl group is attached to the second carbon and an ethyl group is attached to the fourth carbon. The name of the compound is 2-methyl-4-ethylheptane.

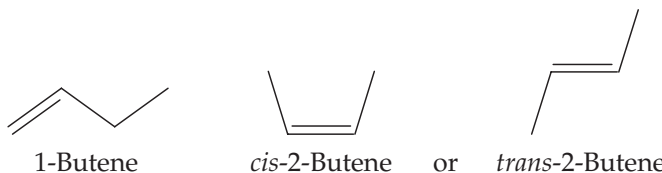
Alkanes can also have a cyclical structure—that is, the two ends of the carbon chain can be joined together. The shortest chain that can form a **cycloalkane** is propane. Cycloalkanes are also known as *cycloparaffins*, or *naphthenes*, and have a formula of C_nH_{2n} . Cyclopropane and other cyclic alkanes are shown in line form in Figure 7.2.

FIGURE 7.2 Structure of four cyclic alkanes (a) cyclopropane, (b) cyclobutane, (c) cyclopentane and (d) cyclohexane.

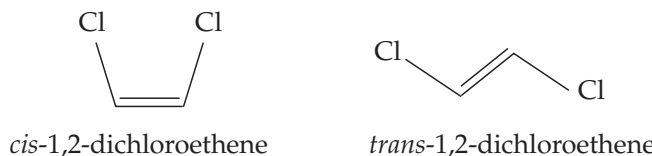


A word of caution, cyclohexane is often confused with benzene (Figure 7.1), but unlike benzene, it is not an aromatic hydrocarbon and its single bonded carbons do not exist in a single plane like benzene.

Alkenes Alkenes have a carbon-carbon double bond, with the general formula C_nH_{2n} . Alkenes are also known as **unsaturated hydrocarbons**, or **olefins**. They are named by finding the longest chain that contains the double bond. The base name ends in *-ene* (or *-ylene*) rather than *-ane*. The carbon atoms in the straight chain are numbered starting at the end nearest the double bond. The simplest alkene is ethene (ethylene); it has the formula $CH_2 = CH_2$. If the double bond can occur in more than one position, that position is indicated by a numerical prefix, which is the number of the first carbon atom containing the double bond. For example, butene can have the double bond in two positions:



If there are functional groups present, then their position is indicated by the carbon atom to which they are bonded. Note that 2-Butene has two different isomers referred to as *cis*- and *trans*-2-Butene, respectively. This illustrates that some alkenes can exist as **structural isomers** because of the double bond. Carbon molecules in alkanes can rotate around the single bonds so that a number of structural forms are equivalent. With double bonds, such rotation is not possible. An environmentally important compound with two structural isomers is 1,2-dichloroethene:



In addition to the formal names derived from the IUPAC system, many organic compounds have common names as well. Common names will be given as synonyms.

Alkynes are unsaturated hydrocarbons that have one or more carbon-carbon triple bonds. They have the general formula C_nH_{2n-2} . The simplest and most widely used alkyne is formally known as ethyne (C_2H_2), but more commonly called acetylene. It is used as a fuel and a precursor to other compounds, e.g., acrylates. Compared to alkanes and alkenes, the $C \equiv C$ bond of alkynes is the least stable, which explains why most of these compounds easily degrade and are of no great environmental concern.

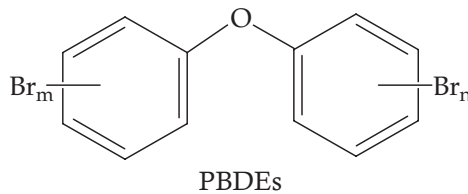
7.3.2 Aromatic Hydrocarbons

Aromatic hydrocarbons are based on the benzene ring. Figure 7.1(a) shows the line form of the benzene ring. Other molecules can be formed by joining functional groups to the benzene ring. Figure 7.1(b) shows methylbenzene, which has the common name toluene. If only one functional group is attached, then a position is not

specified, since all six carbon atoms are equivalent. If there are two functional groups attached, then there are three isomers. If the two functional groups are the same, they may be distinguished by the prefixes *ortho*- (*o*), *meta*- (*m*) and *para*- (*p*), as shown in Figure 7.1(c) for dimethylbenzene, which is commonly called xylene. A numbering system for the six carbon atoms may also be used, as illustrated in Figure 7.1(d) for 1,3,5-trimethylbenzene.

Two or more benzene rings may be joined together. The simplest **polycyclic aromatic hydrocarbon** (PAH) is naphthalene, which consists of two benzene rings. Three or more benzene rings can also join. The structure and some properties of a number of PAH compounds are shown in Figure 7.3. In these compounds the benzene rings share carbon atoms. PAHs are found in coal tar and creosote. They also form from the incomplete combustion of fossil fuels.

If the benzene ring is joined to another group, it may be named as a functional group, *phenyl*- . For example, Figure 7.4 shows the structure of biphenyl and diphenylmethane. If biphenyl is chlorinated, it yields a mixture of isomers containing 1 to 10 chloride ions. These compounds are called **polychlorinated biphenyls**, or **PCBs**, and always contain a mixture of isomers. They are quite resistant to chemical, thermal, or biological degradation and tend to persist in the environment. A group of structurally related compounds are polybrominated diphenyl ethers (PBDEs), which are used as **flame retardants** in many consumer products. The chemical structure shown below is that of two phenyl groups joined by an ether bond. The family of PBDEs consists of 209 congeners of which three (decabromodiphenyl ether, octabromodiphenyl ether, and pentabromodiphenyl ether) are the most widely manufactured and used.



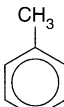
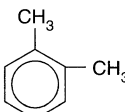
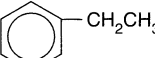
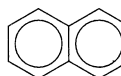
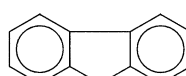
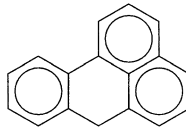
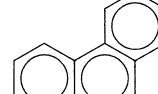
PBDEs enter the water, soil, and air during their manufacture and use. Because of their hydrophobicity and lipophilicity, they do not readily dissolve in water but bioaccumulate and sorb to aquifer and soil particles through which they can be transported in the environment. PBDEs are persistent in the environment and have been detected even in remote places, such as the Arctic (de Wit et al. 2010). In 2009, the Stockholm Convention for Persistent Organic Pollutants (POPs) listed penta-BDE and commercial octa-BDE as POP substances.

■ 7.4 Petroleum and Coal Tar

7.4.1 Petroleum Distillates

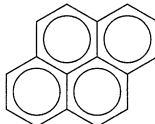
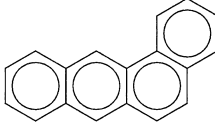
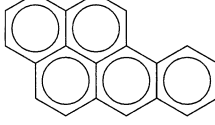
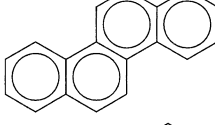
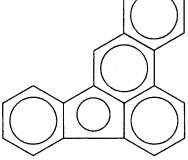
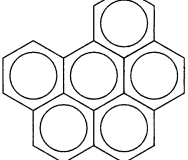
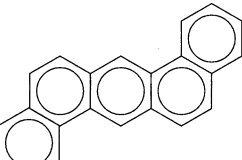
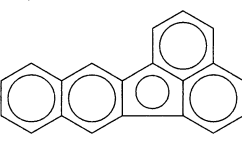
Crude oil consists of a mixture of hydrocarbons of varying molecular weight. The average composition of crude oil depends strongly on its place of origin (i.e., West Texas oil differs remarkably from oil produced in Venezuela). Also, the mode of production yield products of very different composition. That is, oil produced from

FIGURE 7.3 Structure and properties of some aromatic and polycyclic aromatic hydrocarbons.

Name	Structure	Molecular Weight	Solubility in Water	Soil-Water Partition Coefficient
Benzene		78.11	1780 mg/L	97
Toluene		92.1	500 mg/L	242
Xylene, ortho		106.17	170 mg/L	363
Ethyl benzene		106.17	150 mg/L	622
Naphthalene		128.16	31.7 mg/L	1,300
Acenaphthene		154.21	3.93 mg/L	2,580
Acenaphthylene		152.2	3.93 mg/L	3,814
Fluorene		166.2	1.98 mg/L	5,835
Fluoranthene		202	0.275 mg/L	19,000
Phenanthrene		178.23	1.29 mg/L	23,000
Anthracene		178.23	0.073 mg/L	26,000

(Cont'd)

FIGURE 7.3 Cont'd

Name	Structure	Molecular Weight	Solubility in Water	Soil-Water Partition Coefficient
Pyrene		202.26	0.135 mg/L	63,000
Benzo[<i>a</i>]anthracene		228	0.014 mg/L	125,719
Benzo[<i>a</i>]pyrene		252.3	0.0038 mg/L	282,185
Chrysene		228.2	0.006 mg/L	420,108
Benzo[<i>b</i>]fluoranthene		252	0.0012 mg/L	1,148,497
Benzo[<i>g,h,i</i>]perylene		276	0.00026 mg/L	1,488,389
Dibenz[<i>a,h</i>]anthracene		278.35	0.00249 mg/L	1,668,800
Benzo[<i>k</i>]fluoranthene		252	0.00055 mg/L	2,020,971

conventional oil reservoirs has a different chemical make-up than crude oil derived from tar sands or oil shales. On the average, crude oil contains about 82 to 87% carbon, 11 to 15% hydrogen, up to 8% sulfur, up to 1% nitrogen, and up to 0.5% oxygen (Speight 2005). A typical crude oil might consist of about 25% alkanes (paraffins), 50% cycloalkanes (naphthenes), 17% aromatics, including polycyclic aromatics, and 8% asphaltics, which are molecules of very high molecular weight with more than 40 carbon atoms. There have been more than 600 hydrocarbon compounds identified in petroleum (Hunt 1979).

Petroleum is separated into fractions by distillation (Gary and Handwerk 2001). The boiling point of hydrocarbons is correlated to the number of carbon atoms. For example, Table 7.1 lists several hydrocarbons with six carbon atoms and their boiling points. Although all have different structures, the boiling points are similar. In a homologous series, the boiling point of the hydrocarbon will rise with the number of carbon atoms. Table 7.2 shows the boiling points for some of the normal alkanes. Because of these two characteristics, during distillation petroleum is separated into the hydrocarbon fractions with similar numbers of carbon atoms according to Table 7.3.

Although the composition of each fraction is complex and is subject to a great deal of variation depending upon the crude oil and the refinery, the hydrocarbons in each fraction will have similar numbers of carbon atoms and boiling points. Gasoline, for example, typically contains more than 150 separate organic compounds, although as many as 1,000 compounds have been identified in some blends (Domask 1984; Mehlman 1990). Table 7.4 gives an analysis of two different brands of gasoline.

TABLE 7.1 Boiling points of several hydrocarbons with six carbon atoms.

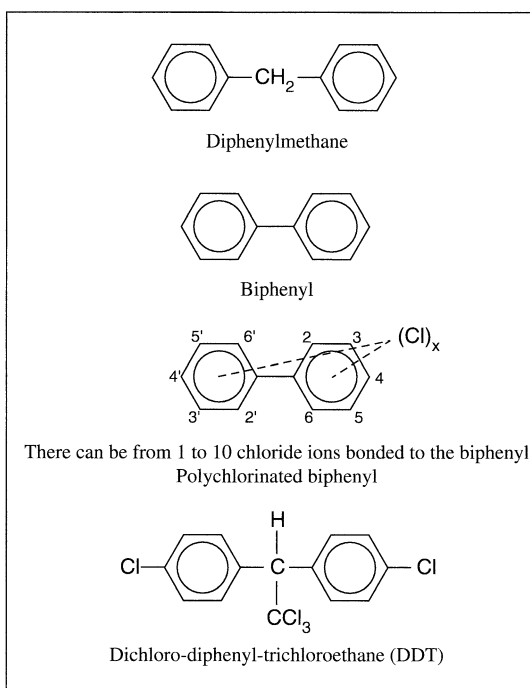
Hydrocarbon	Boiling Point (°C)
Benzene	80.1
Hexane	68.7
Cyclohexane	81.0
2-Methylpentane	60
Methylcyclopentane	72

TABLE 7.2 Boiling points of normal alkanes.

Alkane	Carbon Atoms	Boiling Point (°C)
Butane	4	0
Pentane	5	36
Hexane	6	69
Heptane	7	98
Octane	8	126
Nonane	9	151
Decane	10	174

TABLE 7.3 Hydrocarbon fractions separated by distillation.

Fraction	Range of C Atoms per Molecule	Boiling Point Range	Uses
Gas	1 to 4	20°C	Cooking, home heating, chemical feed stock
Gasoline	5 to 10	20–190°C	Fuel, benzene for chemical feed stock
Kerosene	11 to 13	190–260°C	Fuel, jet fuel
Diesel	14 to 18	260–360°C	Diesel fuel and fuel oil
Heavy gas and lubricating oils	19 to 40	360–530°C	Lubricating oil, greases, waxes
Residuum	>40	> 560°C	Asphalt

FIGURE 7.4 Structure of some phenyl compounds.

Gasoline will be formulated differently for winter versus summer and for high altitude versus sea-level use or to meet air pollution criteria in some markets (U.S. EPA 2010). Importantly, a number of additives and blending agents are, or have been, added to the hydrocarbon mixture to improve the performance and stability of gasoline. These compounds include anti-knock agents, anti-oxidants, metal deactivators, lead

TABLE 7.4 Chemical composition of 87 octane and 93 octane gasolines from Georgia, USA (weight % for compounds present at 0.50 wt % or greater).

87 Octane Cluster		93 Octane Cluster	
Toluene	10.3725	Toluene	14.2292
i-Pentane	6.4405	2,2,4-Trimethylpentane	8.4866
m-Xylene	4.3295	i-Pentane	6.108
n-Pentane	4.075	1,2,4-Trimethylbenzene	4.2254
2,2,4-Trimethylpentane	3.477		3.5538
2-Methylpentane	3.3808	Methyl-t-butylether	3.3262
Unidentified	3.2733	m-Xylene	3.246
1,2,4-Trimethylbenzene	2.814	1-Methyl-3-ethylbenzene	2.608
Ethyl-Tert-Butyl-Ethe and Methylcyclopropane	2.534	Unidentified	2.5376
2-Methylhexane	2.493	n-Pentane	2.2486
o-Xylene	2.3658	2-Methylhexane	2.2142
n-Hexane	2.3655	2-Methylpentane	2.1668
Ethylbenzene	2.236	o-Xylene	1.8414
3-Methylpentane	2.2058	Ethylbenzene	1.53
1-Methyl-3-ethylbenzene	2.0488	p-Xylene	1.5
p-Xylene	1.8975	1,3,5-Trimethylbenzene	1.346
3-Methylhexane	1.7058	2,3-Dimethylbutane	1.287
2,3,4-Trimethylpentane	1.6695	1-Methyl-4-ethylbenzene	1.2142
Benzene	1.4538	3-Methylhexane	1.1952
n-Heptane	1.3763	3-Methylpentane	1.1754
n-Butane	1.2463	2,4-Dimethylhexane	1.0838
2-Methylbutene-2	1.1935	2,2,5-Trimethylhexane	1.0666
2,3-Dimethylbutane	1.0755	2,4-Dimethylpentane	1.0514
Methylcyclohexane	0.9983	2,5-Dimethylhexane	1.032
1,3,5-Trimethylbenzene	0.9268	2,2-Dimethylbutane	1.001
1-Methyl-4-ethylbenzene	0.9265	n-Butane	0.9968
t-Pentene-2	0.8038	2,3-Dimethylhexane	0.9952
1-Methyl-2-ethylbenzene	0.7798	1,2,3-Trimethylbenzene	0.9942
3-Methylheptane	0.7228	1-Methyl-2-ethylbenzene	0.9716
1,2,3-Trimethylbenzene	0.7148	n-Hexane	0.903
2,4-Dimethylpentane	0.7038	Ethyl-Tert-Butyl-Ether and Methylcyclopropane	0.8538
n-Propylbenzene	0.701	n-Heptane	0.8476

(Cont'd)

TABLE 7.4 Cont'd

87 Octane Cluster		93 Octane Cluster	
1,2-Dimethyl-4-ethylbenzene	0.664	Benzene	0.822
n-Octane	0.6523	2-Methylbutene-2	0.8168
2-Methylheptane	0.6495	n-Propylbenzene	0.8078
Cyclohexane	0.6065	1,2-Dimethyl-4-ethylbenzene	0.678
2-Methylbutene-1	0.5715	1-Methyl-3-n-propylbenzene	0.6678
1-Methyl-3-n-propylbenzene	0.5595	t-Pentene-2	0.6048
2,4-Dimethylhexane	0.5475	1,3-Dimethyl-5-ethylbenzene	0.5464
2,3-Dihydroindene	0.5383	TAME	0.5064
2,3-Dimethylhexane	0.5208		
Methyl-t-butylether	0.5188		

Source: Weaver et al. 2005.

scavengers, anti-rust agents, anti-icing agents, upper-cylinder lubricants, detergents, and dyes (IARC 1989; U.S. EPA 2010). Many of those additives constitute less than 0.01% of the mixture (U.S. EPA 2003), but others are added at much higher concentrations, including compounds like ethanol or, until a few years ago, methyl-*tert*-butyl ether (MTBE). Until the end of 1995, tetraethyl lead was added to some gasolines in the U.S. as an antiknock compound, and was banned by the European Union in the late 1990s. Although leaded gasoline is being phased out worldwide, it was still available in parts of six countries in 2014, and its residuals in soils persist. Leaded gasoline could contain between 1 and 2% lead by weight. In order to prevent lead buildup in the engine parts lead scavengers were added to leaded gasolines. These included 1,2-dichloroethane and 1,2-dibromoethane (also known as ethylene dibromide or EDB). One important additive deals with adjusting the volatility (Reid vapor pressure) of gasoline between winter and summer months. For volatility, butane is added in winter to over 10% volume percent in cold climates, whereas in summer in warm climates it is adjusted down to about 2 percent to avoid vapor lock.

7.4.2 Coal Tar

When coal is heated in the absence of oxygen, volatile fractions of the coal are driven off and nearly pure carbon, known as coke, is left behind. From about 1850 to 1950 a gas was manufactured by this process for residential and commercial use. This manufactured gas has now been replaced by natural gas. However, coke is still made in byproduct coke ovens for use in blast furnaces during the manufacturing of steel.

When the gas from a coal gas manufacturing plant or a byproduct coke oven is cooled, liquid hydrocarbons separate out as oils and tars. These materials can be distilled into useful chemicals, such as benzene and toluene. In the latter part of the 19th Century chemists found ways of making both dyes and pharmaceuticals from coal tar. Among these products was the common aspirin. Coal tar was also distilled into

creosote, which was used as a wood preservative. A similar tar was produced from another manufactured gas process, the carbureted water gas process, which started with coke as a raw material and added liquid petroleum hydrocarbons which were thermally cracked to create light gasses.

Table 7.5 lists hydrocarbon compounds which are typically found in coal and carbureted water gas tars.

7.4.3 Groundwater contamination associated with petroleum products and coal tar

Serious cases of groundwater and soil contamination have been created by releases of gasoline, diesel fuel, coal tar, and carbureted water gas tar into the environment. Gasoline and diesel fuel contamination is associated with leaking underground storage tanks (LUST) at service stations, refineries, pipelines, terminals, and other localities. Coal and carbureted water gas tar contamination may be found at former manufactured gas plant sites, byproduct coke oven locations and tar refinery sites.

The water solubility of the hydrocarbons found in petroleum distillates and coal and carbureted water gas tars varies dramatically from compound to compound. As an example of this, see the solubility data listed on Figure 7.3. Benzene, toluene,

TABLE 7.5 Characteristic hydrocarbons found in coal tar.

Benzene
Toluene
Ethylbenzene
<i>m</i> -Xylene
<i>o</i> -Xylene
<i>p</i> -Xylene
Styrene
2,4,6-Trimethylbenzene
Naphthalene
1-Methylnaphthalene
2-Methylnaphthalene
Acenaphthylene
Acenaphthene
Fluorene
Phenanthrene
Anthracene
Fluoranthene
Pyrene
Benzo(a)anthracene
Chrysene
Benzo(b)fluoranthene
Benzo(k)fluoranthene
Benzo(a)pyrene
Indeno(1,2,3-cd)pyrene
Dibenz(a,h)anthracene
Benzo(g,h,i)perylene

ethylbenzene, and xylene all have aqueous solubility >100 mg per liter and are found in gasoline and to a lesser extent diesel fuel, coal tar, and carbureted water gas tar. However, all of these products will have the so-called **BTEX** (benzene, toluene, ethylbenzene, and xylene) contaminants associated with them. Coal tar and carbureted water gas tar will have a significant amount of naphthalene and methylnaphthalene, although usually less than BTEX. As the polynuclear aromatic compounds are much lower in solubility, they will be present in only very small amounts dissolved in water. However, the compounds that do not dissolve in water will be present in the soil. Thus coal tar sites often have high levels of a variety of polynuclear aromatics in the soil.

The additives found in gasoline can also appear as groundwater contaminants. In the past when leaded gasoline was used in the United States these included tetraethyl lead, ethylene dibromide, and 1,2-dichloroethane. When lead was phased out of gasoline in Europe and North America, other octane boosters were substituted, including MTBE and, since about 2000, ethanol.

FIGURE 7.5 Formulae of former and current gasoline oxygenate additives: (a) methyl *tert*-butyl ether (MTBE), (b) ethyl *tert*-butyl ether (ETBE), (c) *tert*-amyl methyl ether (TAME), and (d) ethanol.



Methyl *tert*-butyl ether (MTBE; chemical formula: $C_5H_{12}O$) has been added to U.S. gasoline at low concentrations since 1979. Starting in 1992, MTBE and other organic compounds that contain oxygen as part of their chemical structure, such as ethyl *tert*-butyl ether (ETBE) or *tert*-amyl methyl ether (TAME), have been used at higher concentrations (11 to 12.75%) in some gasoline to fulfill the oxygenate requirements of the 1990 U.S. Clean Air Act Amendments (Figure 7.4) (U.S. EPA 2010). In 1995, MTBE was the fourth most produced organic chemical in the United States (Johnson et al. 2000). Following the widespread use of MTBE and other oxygenates as a gasoline additive, between 5 and 10% of community drinking water supplies in high oxygenate use areas started to show at least detectable amounts of MTBE (U.S. EPA 1999). Major contributing factors to this pollution problem were the high water solubility of MTBE (>40 g/L), its recalcitrance to degradation, and very low sorption affinity to aquifer materials (Squillace et al. 1995). In result, MTBE is highly mobile, undergoing no to little retardation as it travels through a groundwater system. Therefore, MTBE essentially travels with about the same velocity as the flowing groundwater and typically becomes the lead component of a contaminant plume (Boving 2014). Because of these environmental concerns and in response to changing oxygenate requirements, MTBE and other oxygenates were phased out of fuels in the United States since 2003. Other countries used MTBE and other ether-based additives but primarily as octane enhancers rather than as oxygenates. If added as an octane-enhancer, much lower MTBE concentrations, typically 1 to 5%, were required relative to the 11 to 12.75% in oxygenated fuels (Dottridge et al. 2000).

Ethanol has now replaced MTBE as a major gasoline additive and is used to meet renewable fuel requirements in many countries. In 2014, more than 54 million cubic meters of ethanol were produced in the U.S., compared to less than a million in 1980 (Figure 7.6). The world's two largest ethanol producers are the United States and Brazil, which together accounted for 83.4% of the global production in 2014 (Renewable Fuel Association 2014). While less toxic than MTBE and other oxygenates, ethanol can make up a high volume percentage of the fuel. For instance, E85 is an ethanol fuel blend sold in the United States. Depending on the geographic area and climate, the blend can contain between 51% and 83% ethanol, with hydrocarbons making up the remainder (U.S. Department of Energy 2013). At these concentrations, ethanol may exert a cosolvent effect on hydrocarbons and enhance concentrations of benzene, toluene, ethylbenzene, and xylenes (BTEX) in groundwater (Capiro et al. 2007; Weaver et al. 2009). Simulations for gasoline containing about 10% ethanol (E10) show that benzene plumes are longer by 40 to 150% compared to gasoline without ethanol (Molson et al. 2002; Gomez et al. 2008). The presence of ethanol may possibly decrease the sorption-related retardation of these compounds. This can increase the length of BTEX plumes (Powers et al. 2001a). However, benzene plumes caused by the release of gasoline-ethanol blends may have shorter lifetimes than for gasoline alone because ethanol degradation might result in growth of benzene-degrading microbial populations (Gomez and Alvarez 2009; Rasa et al. 2013). Further, bench and near-field scale studies showed that highly concentrated fuel ethanol has a high affinity for vadose-zone pore water and can migrate through the capillary zone with minimal vertical dispersion (McDowell et al. 2003; McDowell and Powers 2003; Capiro et al. 2007). These properties, together with the increasingly widespread use of blended fuels, may increase the likelihood for ethanol releases during transport, storage, or mixing at blending terminals (Powers et al. 2001b).

FIGURE 7.6 Ethanol production in the United States of America in millions of cubic meter.

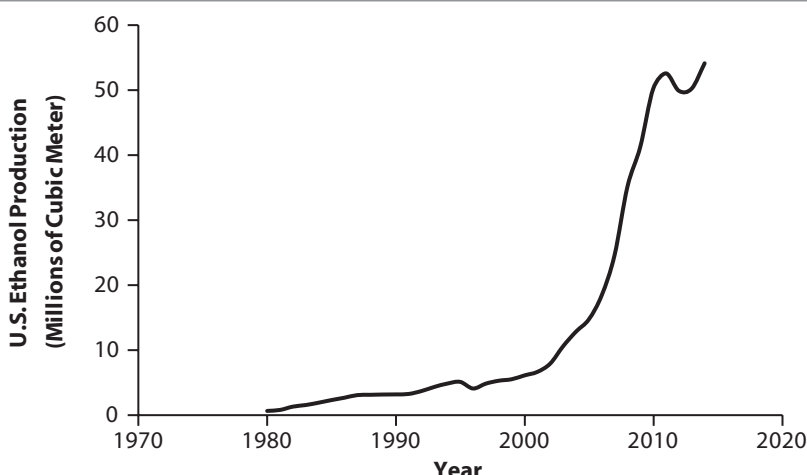


TABLE 7.6 Examples of functional groups, their chemical class, and formula.

Functional Group	Chemical Class	Formula	Structural Formula	Example
Aldehyde	Aldehyde	R-CHO		Ethanal
Azo compound	Azo	R-N ₂ -R'		Pigment Orange 5
Benzyl	Toluene derivative	R-CH ₂ C ₆ H ₅		1-Chlorotoluene
Carboxamide	Amide	R-CON-R ₂		Ethanamide
Carboxylic acid	Carboxyl	R-COOH		Ethanoic acid (Acetic acid)
Carboxylate	Carboxylate	R-COO ⁻		Sodium ethanoate (Sodium acetate)
Cyanate	Cyanates	R-OCN		Methyl isocyanate
Ether	Ether	R-O-R'		Ethoxyethane (Diethyl ether)
Ester	Ester	R-COO-R'		Ethyl propionate
Halo	Haloalkane	R-X (X= Cl, F, Br or I)		Methylchloride
Hydroxyl	Alcohol	R-OH		Ethanol

(Cont'd)

TABLE 7.6 Cont'd

Functional Group	Chemical Class	Formula	Structural Formula	Example
Isocyanates	Isocyanates	R-NCO		Methylene diphenyl diisocyanate (MDI)
Ketone	Ketone	R-CO-R'		Propanone (Aceton)
Nitrile	Nitrile	R-CN		Phenyl cyanide (Benzonitrile)
Nitro	Nitro compounds	R-NO ₂		2,4,6-Trinitrotoluene (TNT)
Peroxy	Peroxide	R-OO-R		Dibenzoyl peroxide
Phthalate	Phthalate	See right		Diisodecyl phthalate (DIDP)
Phenyl	Benzene derivative	R-C ₆ H ₅		Ethylbenzene
Pyridyl	Pyridine derivative	R-C ₅ H ₄ N		Nicotine
Sulfide	Sulfide	R-S-R'		Dimethyl sulfide
Sulphydryl	Thiol	R-SH		Ethyl mercaptans (Ethanethiol)
Sulfo	Sulfonic acid	R-SO ₃ H		Perfluorooctanesulfonic acid (PFOS)

Source: Modified from table available at https://en.wikibooks.org/wiki/Organic_Chemistry/Overview_of_Functional_Groups

■ 7.5 Functional Groups

The following section introduces the functional groups of the most relevant classes of environmental contaminants. Table 7.6 provides an overview of examples for functional groups as well as structural formulae and classes to which these contaminants belong.

7.5.1 Organic Halides

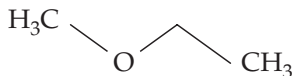
We have already seen that chlorine atoms can be substituted for hydrogen atoms at various places on organic molecules. This is also true for bromine and fluorine atoms. Such compounds are named by prefixing the name of the basic molecule with the term *chloro-*, *bromo-*, or *fluoro-* and specifying the number and position. Figure 7.7 shows the structure and uses of some **organic halides** that are sometimes found as groundwater contaminants. Table 7.7 gives the physical properties of methane, ethane, ethene, and their chlorinated forms. These were, and in some regions of the world still are, widely used organic compounds. Although now slowly replaced by chemicals of lesser environmental concern, these compounds are often found as contaminants in groundwater. Tetrachloroethene (perchloroethene or PCE), trichloroethene (TCE), and 1,1,1-trichloroethane (TCA) have a low flammability and a high vapor density, which make them very useful as solvents. They have been frequently used for degreasing metal parts and as the fluid in dry cleaning, but they are being increasingly replaced by less environmentally harmful substitutes. These chlorinated solvents are denser than water; if spilled on the ground in quantities great enough to overcome the residual saturation, the pure phase may migrate vertically downward through an aquifer. They are comparatively soluble (> 100 mg/L) in water and can migrate as a dissolved phase with flowing groundwater. Also, some chlorinated solvents require the addition of a stabilizer, which themselves can become a groundwater contamination problem later on. For example, the ether 1,4-dioxane (see Section 7.2.3) has been added to TCA to prevent degradation of the solvent during storage. It is therefore not uncommon to find those two compounds co-occurring at some spill sites.

7.5.2 Alcohols

An **alcohol** has one or more hydroxyl groups, $-OH$, substituted for hydrogen atoms on an aliphatic hydrocarbon. Alcohols are named by finding the longest hydrocarbon chain that includes the carbon atom to which the hydroxyl group is attached. That becomes the base name, to which suffix *-ol* is added. The position of the carbon atom to which the hydroxyl group is attached is indicated by a numerical prefix. If there are two hydroxyl groups, then the suffix *-diol* is used, and so forth. Figure 7.8 lists some common alcohols that may find their way to a hazardous waste site. Alcohols are miscible with water and hence have a potential for significant mobility in groundwater. However, many are also readily biodegraded.

7.5.3 Ethers

Ethers have an oxygen atom bonded between two carbon atoms. The common name is obtained from the names of the two hydrocarbons followed by the word ether. Methyl ethyl ether is:



Methyl ethyl ether

In the IUPAC system, the *methoxy* functional group is CH₃O⁻, so the preceding compound is also known as 1-methoxyethane.

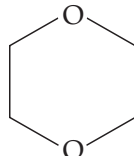
Two cyclical ethers have been found to be rather persistent contaminants in groundwater. Tetrahydrofuran is used in large quantities as a chemical intermediate and as a solvent for resins such as PVC, adhesives, and various coatings. It is miscible with water, is resistant to biodegradation, and has the following structure:



Tetrahydrofuran

1,4-Dioxane is also miscible with water and is extremely resistant to biodegradation. Because of its hydrophilicity and low affinity to soil organic matter (Log K_{ow} = -0.27, K_{oc} = 1.23) 1,4-dioxane is only weakly retarded by sorption processes. In addition, volatilization from water to air is negligible (Henry's Law constant K_H = 4.88 × 10⁻⁶ atm m³/mol) (Howard 1990; Zenker et al. 2003; DiGuiseppi & Whitesides 2007; Mohr et al. 2010). 1,4-dioxane is often found as a co-contaminant with chlorinated volatile organic compounds at solvent release sites, such as landfills, solvent recycling facilities, or fire training areas. Historically, soil and groundwater samples were not routinely analyzed for 1,4-dioxane and therefore the number of known 1,4-dioxane sites is still increasing (Eberle et al. 2015). At the Seymour Recycling Corporation Hazardous Waste Site in Indiana, more than 80 chemicals have been detected in the plume of contaminated groundwater. The compound that has traveled the greatest distance is 1,4-dioxane, with tetrahydrofuran being the second-most mobile compound. In the past, 1,4-dioxane was primarily used as a stabilizer in chlorinated solvents. Nearly 90% of the 1,4-dioxane produced in 1985 was used to stabilize 1,1,1-trichloroethane (1,1,1-TCA) (US EPA 1995). 1,4-dioxane was added to 1,1,1-TCA at concentrations between 2 to 8% by volume to prevent solvent degradation caused by reactions with metal surfaces (Mohr 2001; Mohr et al. 2010). The association of 1,4-dioxane with 1,1,1-TCA is well documented. However, its association with trichloroethylene (TCE) is a topic of debate (Mohr 2001; Zenker et al. 2003; Mohr et al. 2010; Eberle et al. 2015).

Note that 1,4-dioxane is not a dioxin, which is a class of compounds thought to be highly toxic. The structure of 1,4-dioxane is



1,4-dioxane

FIGURE 7.7 Common organic halides found in hazardous waste.

Name	Structure	Uses and Other Sources
Trichloromethane (chloroform)	$\begin{array}{c} \text{Cl} \\ \\ \text{Cl}-\text{C}-\text{Cl} \\ \\ \text{H} \end{array}$	Liquid used in manufacture of anesthetics, pharmaceuticals, fluorocarbon refrigerants and plastics. Used as solvent and insecticide. Formed from methane when chlorinating drinking water.
Vinyl chloride (chloroethylene)	$\begin{array}{cc} \text{H} & \text{H} \\ & \diagdown \\ \text{C} = \text{C} \\ & \diagup \\ \text{H} & \text{Cl} \end{array}$	Gas used in the manufacture of polyvinyl chloride. End product of microbial degradation of chlorinated ethanes.
Chloroethane	$\begin{array}{cc} \text{H} & \text{H} \\ & \\ \text{H}-\text{C} & -\text{C}-\text{Cl} \\ & \\ \text{H} & \text{H} \end{array}$	Liquid used to manufacture tetraethyl lead. Degradation product of chlorinated ethanes.
1,2-Dichloroethane	$\begin{array}{cc} \text{H} & \text{H} \\ & \\ \text{Cl}-\text{C} & -\text{C}-\text{Cl} \\ & \\ \text{H} & \text{H} \end{array}$	Liquid used to manufacture vinyl chloride. Degradation product of trichloroethane.
Trichloroethene (Trichloroethylene)	$\begin{array}{cc} \text{Cl} & \text{Cl} \\ & \diagdown \\ \text{C} = \text{C} \\ & \diagup \\ \text{Cl} & \text{H} \end{array}$	Solvent used in dry cleaning and metal degreasing. Organic synthesis. Defradation product of tetrachloroethene.
Tetrachloroethene (perchloroethene) (perchloroethylene)	$\begin{array}{cc} \text{Cl} & \text{Cl} \\ & \diagdown \\ \text{C} = \text{C} \\ & \diagup \\ \text{Cl} & \text{Cl} \end{array}$	Solvent used in dry cleaning and metal degreasing. Used to remove soot from industrial boilers. Used in manufacture of paint removers and printing inks.
1,2-Dibromo-3-chloropropane (DBCP)	$\begin{array}{ccccc} \text{Br} & \text{Br} & & \text{Cl} & \\ & & & & \\ \text{H}-\text{C} & -\text{C} & -\text{C}- & \text{H} & \\ & & & & \\ \text{H} & \text{H} & \text{H} & & \end{array}$	Soil fumigant to kill nematodes. Intermediate in organic synthesis.
o-Dichlorobenzene (1,2-dichlorobenzene)		Chemical intermediate. Solvent. Fumigant and insecticide. Used for industrial odor control. Found in sewage from odor control chemicals used in toilets.

TABLE 7.7 Common chlorinated alkanes and alkenes with their physical properties.

Alkanes	Synonym	Structure	Specific Gravity ^a	Melting Point ^a	Boiling Point ^a	Vapor Pressure ^a	Water Solubility ^a	Henry's Law Constant (M) X 10 ¹⁰ /M ^b
Methane	CH ₄			-97.7°C	-24°C	5.0 atm at 20°C	4,000 cu cm/L	0.00584 at 17.5°C
Methyl chloride	(Chloromethane) (Dichloromethane)	CH ₃ Cl CH ₂ Cl ₂		-97°C	40-52°C	349 mm at 20°C	20,000 mg/L at 20°C	0.00131 at 17.5°C
Methylene chloride	(Trichloromethane)	CHCl ₃	1.489 at 20°C	-64°C	62°C	160 mm at 20°C	8,000 mg/L at 20°C	0.00246 at 17.5°C
Chloroform	(Tetrachloromethane)	CCl ₄		-23°C	76.7°C	90 mm at 20°C	800 mg/L at 20°C	0.0211 at 17.5°C
Carbon tetrachloride								
Ethane	(Dimethyl) (Ethylchloride)	CH ₃ CH ₃ CH ₂ ClCH ₃		-172°C	-89°C	38.5 atm at 20°C	60.4 mg/L at 20°C	
Chloroethane			0.92 at 20°C	-138.3°C	12.4°C	1,000 mm at 20°C	5,740 mg/L at 20°C	0.00846 at 17.5°C
1,1-Dichloroethane			1.174 at 20°C	-97.4°C	57.3°C	180 mm at 20°C	5,500 mg/L at 20°C	0.00389 at 17.5°C
1,2-Dichloroethane	(Ethylenedichloride)	CH ₂ ClCH ₂ Cl	1.25 at 20°C	-35.4°C	83.5°C	61 mm at 20°C	8,690 mg/L at 20°C	
1,1,1-Trichloroethane	(Methylchloroform)	CCl ₃ CH ₃	1.35 at 20°C	-32°C	71/81°C	100 mm at 20°C	4,400 mg/L at 20°C	0.0120 at 17.5°C
1,1,2-Trichloroethane	(Vinylchloride)	CHCl ₂ CH ₂ Cl	1.44 at 20°C	-35°C	113.7°C	19 mm at 20°C	4,500 mg/L at 20°C	
1,1,2,2-Tetrachloroethane		CHCl ₂ CHCl ₂	1.60 at 20°C	-42.5°C	146.4°C	5 mm at 20°C	2,900 mg/L at 20°C	
1,2,2,2-Tetrachloroethane		CH ₂ ClCCl ₃	1.60		138°C			
Pentachloroethane		CCl ₃ CHCl ₂	1.67 at 25°C	-29°C	162°C	3.4 mm at 20°C		
Hexachloroethane	(Perchloroethane)	CCl ₃ CCl ₃	2.09 at 20°C	187.4°C	Ethenes		50 mg/L at 22°C	
Ethene	(Ethylene) (Chloroethene)	CH ₂ =CH ₂ CH ₂ =CHCl		-169°C	-104°C	> 40 atm at 20°C	131 mg/L at 20°C	
Vinyl chloride		CCl ₂ =CH ₂	1.218 at 20°C	-153°C	-13.9°C	2,660 mm at 25°C	1.1 mg/L at 25°C	0.0193 at 17.5°C
1,1-Dichloroethene		CHCl=CH ₂	1.28	-122.5°C	31.9°C	500 mm at 20°C		0.0191 at 17.5°C
cis-1,2-Dichloroethene		CHCl=CHCl		-81°C	60°C	200 mm at 25°C	800 mg/L at 20°C	0.00265 at 17.5°C
trans-1,2-Dichloroethene		CHCl=CHCl	1.26	-50°C	48°C	200 mm at 14°C	600 mg/L at 20°C	0.00660 at 17.5°C
Trichloroethene	[TCE]	CHCl=CCl ₂	1.46 at 20°C	-87°C	86.7°C	60 mm at 20°C	1,100 mg/L at 25°C	0.00032 at 17.5°C
Tetrachloroethene	(Perchloroethene)	CCl ₂ =CCl ₂	1.626 at 20°C	-22.7°C	12.4°C	14 mm at 20°C	150 mg/L at 25°C	0.0117 at 17.5°C

Sources:

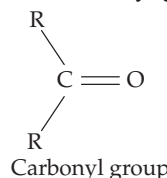
^a K. Verschueren. 1983. *Handbook of Environmental Data on Organic Chemicals*, Second Edition. New York: Van Nostrand Reinhold Company.^b J. M. Gossett. 1987. Measurement of Henry's law constants for C1 and C2 chlorinated hydrocarbons. "Environmental Science and Technology 21:202-208.

FIGURE 7.8 Alcohols found in hazardous waste.

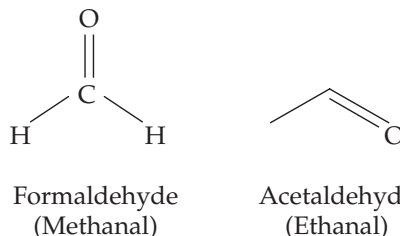
Name	Structure	Uses and Other Sources
Methanol (wood alcohol)	$\begin{array}{c} \text{H} \\ \\ \text{H}-\text{C}-\text{H} \\ \\ \text{OH} \end{array}$	Solvent. May be added to gasoline. Manufacture of formaldehyde and methyl halides.
Ethanol (grain alcohol) (ethyl alcohol)	$\begin{array}{cc} \text{H} & \text{H} \\ & \\ \text{H}-\text{C} & -\text{C}-\text{H} \\ & \\ \text{H} & \text{OH} \end{array}$	Preparation of distilled spirits. Solvent. Manufacture of acetaldehyde, acetic acid, ethyl ether, etc. Preparation of lacquers, perfumes, cosmetics, over-the-counter medicines. Degradation of ethyl acetate in excess of water.
Ethylene glycol (1,2-ethanediol)	$\begin{array}{ccc} \text{H} & \text{H} & \\ & & \\ \text{H}-\text{C} & -\text{C}-\text{H} & \\ & & \\ \text{OH} & \text{OH} & \end{array}$	Antifreeze (engine coolant) compound. Manufacture of polyester fiber and film. Deicing compound for airplanes at gate. Solvent base.
Propanol	$\begin{array}{ccc} \text{H} & \text{H} & \text{H} \\ & & \\ \text{H}-\text{C} & -\text{C}-\text{C}-\text{H} & \\ & & \\ \text{H} & \text{H} & \text{OH} \end{array}$	Released from fermentation of whisky and during sewage treatment and decomposition of organic matter. Solvent in printing, used in nail polish, brake fluid, lacquers, cleaners, polishes.
1,2-Propanediol (propylene glycol)	$\begin{array}{ccc} \text{H} & \text{H} & \text{H} \\ & & \\ \text{H}-\text{C} & -\text{C}-\text{C}-\text{H} & \\ & & \\ \text{H} & \text{OH} & \text{OH} \end{array}$	Solvent used in paints, inks, and coatings. Antifreeze formulations.
2-Methyl-2-butanol	$\begin{array}{ccccc} \text{H} & \text{CH}_3 & \text{H} & \text{H} & \\ & & & & \\ \text{H}-\text{C} & -\text{C}-\text{C}-\text{C}-\text{H} & & & \\ & & & & \\ \text{H} & \text{OH} & \text{H} & \text{H} & \end{array}$	Solvent.
<i>t</i> -Butanol (2-methyl-2-propanol)	$\begin{array}{ccccc} \text{H} & \text{CH}_3 & \text{H} & & \\ & & & & \\ \text{H}-\text{C} & -\text{C}-\text{C}-\text{H} & & & \\ & & & & \\ \text{H} & \text{OH} & \text{H} & & \end{array}$	Manufacture of flotation agents, flavors, and perfumes. Solvent. Paint removers. Octane booster in gasoline. Lacquer. Solvent for pharmaceuticals.
4-Methyl-2-pentanol	$\begin{array}{ccccc} \text{H} & \text{H} & \text{H} & \text{H} & \text{H} \\ & & & & \\ \text{H}-\text{C} & -\text{C}-\text{C}-\text{C}-\text{C}-\text{H} & & & \\ & & & & \\ \text{H} & \text{OH} & \text{H} & \text{CH}_3 & \text{H} \end{array}$	Solvent.

7.5.4 Aldehydes and Ketones

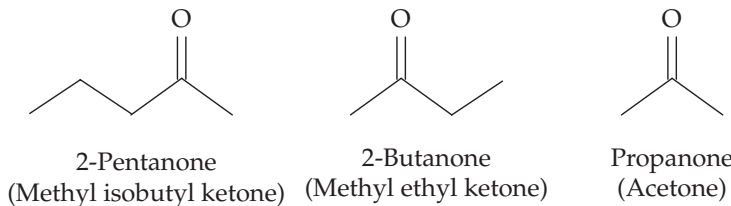
Aldehydes and ketones contain the **carbonyl group**, which has this structure:



An **aldehyde** has at least one hydrogen atom bonded to the carbon. The IUPAC name is obtained by finding the name of the hydrocarbon and adding the suffix *-al*. The two simplest aldehydes are methanal (formaldehyde) and ethanal (acetaldehyde):

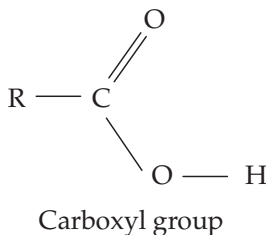


Ketones have the carbonyl group bonded to two hydrocarbons. They are named by indicating the name of the hydrocarbon and ending with the suffix *-one*. The simplest ketone is propanone, which is commonly known as acetone. Acetone is a widely used solvent, as are other ketones such as 2-butanone (methyl ethyl ketone), 4-methyl-2-pentanone (methyl isobutyl ketone) and 2-pentanone (methyl propyl ketone). Structures of some of these ketones include the following:

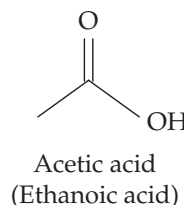


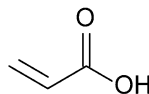
7.5.5 Carboxylic and Sulfonic Acids

Carboxylic acids have the **carboxyl group**, $-\text{COOH}$. They are named by taking the stem name and adding the suffix *-oic acid*. The structure of the functional group is



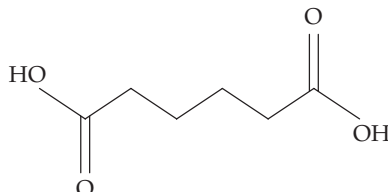
Acetic acid (ethanoic acid, shown in line format below) is a common industrial chemical, which is not thought to pose health threats. Another carboxylic acid that is widely used is 2-propenoic acid (acrylic acid). Large amounts are used during the manufacture of acrylic esters. Its structure is





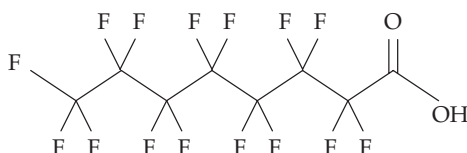
2-propenoic acid (Acrylic acid)

Another carboxylic acid used in large quantities for the manufacture of synthetic fibers, plasticizers, resins, and foams is adipic, or 1,6-hexanedioic acid, which has two carboxyl groups.



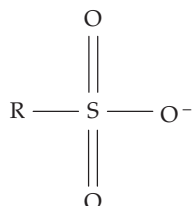
1,6-hexanedioic acid

Carboxylic acids are weak acids and do not strongly dissociate in water. The salts or esters (see next section) of carboxylic acids are called **carboxylates**. Many common soap or other surface active compounds (surfactants) are alkyl carboxylates that are characterized by a carboxyl group attached to a long chain of carbon-carbon bonds (alkyl group). Of particular interest to contaminant hydrogeologists are carboxylate-based fluorosurfactants, such as perfluorooctanoate (PFOA). This compound, including other perfluorinated compounds, such as Teflon® (polytetrafluoroethylene), have been widely used in oil and water repellants for clothing or food packing or in aqueous fire-fighting foams (AFFF) (Prevedouros et al. 2006; Paul et al. 2009; Filipovic et al. 2015). Because of their widespread use and recalcitrance, perfluorinated chemicals (PFCs) are ubiquitous in the environment and found around the world (e.g., Butt et al. 2010).



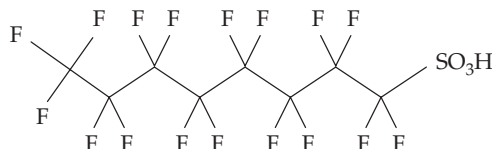
Perfluorooctanoate (PFOA)

If the carbon of the carboxyl group is replaced with a sulfur atom, the resulting acid is known as sulfonic acid. Its salts and esters (see next section) are **sulfonates**.



Sulfonate group

Like the carboxylates, compounds with a sulfonate moiety are important industrial chemicals. Examples include surfactants and perfluorooctane sulfonate (PFOS). PFOS was the key ingredient in popular fabric protector (Scotchgard®) and, together with PFOA, an ingredient in aqueous firefighting foam (AFFF). PFOS was added to the Stockholm Convention on Persistent Organic Pollutants in 2009.

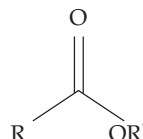


Perfluorooctane sulfonate (PFOS)

Compounds like PFOS and PFOA are also known as per- and polyfluoroalkyl substances (PFAS). Due to their strong fluorine-carbon bonds, PFASs are among the most stable organic compounds, i.e., they are largely resistant to hydrolysis, photolysis, and aerobic and anaerobic biodegradation. PFASs have been found in groundwater and soils (e.g., Moody & Field 1999; Moody et al. 2003; Schultz et al. 2004; Murakami et al. 2009; Chatwell 2012. The U.S. EPA and global health organizations have identified PFASs as toxic, persistent, and bioaccumulative (Lindstrom et al. 2011). In the United States, PFASs were produced in large quantities prior to a voluntary phase reduction in 2002 (Prevedouros et al. 2006; Paul et al. 2009). Although the manufacturing and use of PFASs has been restricted or banned in most nations, significant production and use continues in others (e.g., Lim et al. 2011; Xie et al. 2013).

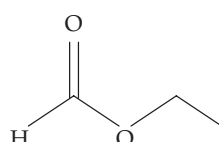
7.5.6 Esters

Esters are the result of the combination of a carboxylic acid with an alcohol. The functional group is:

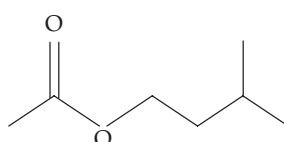


Ester group

where R represents the remainder of the carboxylic acid and R' is the alcohol. The ester is named by the name of the alcohol group followed by the name of the carboxylic acid group with the suffix *-ate*. Ethanol and formic acid join to create ethyl formate. Some esters have odors that are associated with many everyday substances. For example, ethyl formate smells like rum.



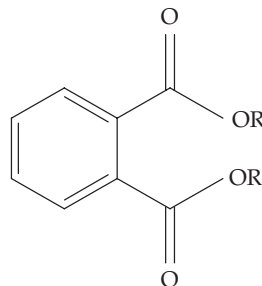
Ethyl formate



Isoamyl acetate

Esters that are used in industry for flavorings, in perfumes, and as solvents, especially for paints, include ethyl formate, pentyl acetate (*n*-amyl acetate), butyl acetate, ethyl acetate, isobutyl acetate, and 3-methylbutyl acetate (isoamyl acetate). Some esters are produced naturally, for example isoamyl acetate forms during the reaction of alcohol with organic acids and the acetyl coenzyme provided by the hops during the beer brewing process. This ester has a fruity banana aroma.

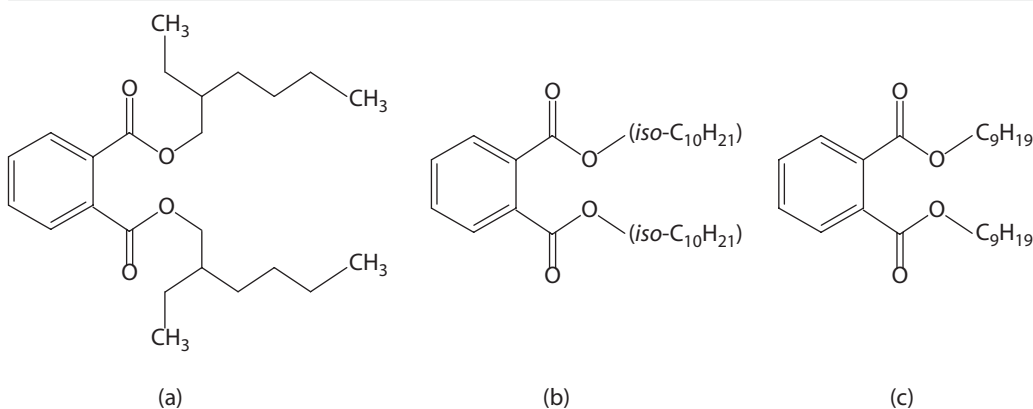
One class of esters that is very common in industrial products are phthalates. These compounds are esters of dicarboxylic acid (phthalic acid). They are used as plasticizers to improve the flexibility of various plastics. Others are used in many industrial, medical, and consumer products, including in building materials, flooring, food packing, or in personal care products. The base chemical structure of the phthalates is:



Phthalate group

Figure 7.9 shows the structural formulas for three widely used phthalates. Phthalates are often classified as **endocrine disruptors** of hormonally active agents because of their ability to interfere with the endocrine system in the body (US EPA 2007). Toxicological data is only available for a limited number of these compounds and their study remains an area of active research. For instance, the widely used compound di(2-ethylhexyl) phthalate (DEHP) is a colorless liquid with almost no odor.

FIGURE 7.9 Structure of some phthalates. (a) Di(2-ethylhexyl) phthalate (DEHP); (b) Diisodecyl phthalate (DIDP), and (c) Diisononyl phthalate (DINP).

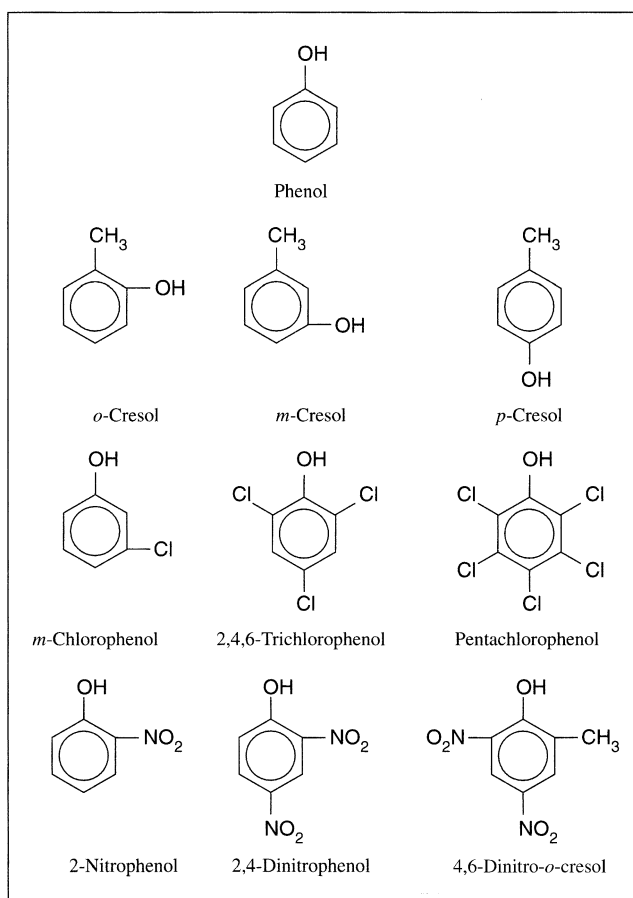


that is rapidly and almost completely absorbed via the oral and inhalation routes. A public health risk assessment study conducted in Australia (National Industrial Chemicals Notification and Assessment Scheme 2006) could not identify consistent associations between DEHP exposure and reproductive parameters either in adults or children. However, as a measure of precaution, the Australian government introduced a permanent ban on children's plastic products with more than 1% DEHP in 2011 (Australian Competition and Consumer Act 2010).

7.5.7 Phenols

Phenols are based on a hydroxyl radical bonded to a benzene ring. Phenol can occur naturally in groundwater, usually in low amounts associated with decomposing organic matter. Phenol is also a common groundwater contaminant, due to its use in many industrial processes. There are many phenol-based compounds used in industry that can occur in groundwater (Figure 7.10). Cresols have a methyl

FIGURE 7.10 Chemical structure of common phenolic compounds.



group attached to the benzene ring of toluene. They are used in industry and are also released during coal-tar refining. Chlorophenols have one or more chloride ions on the benzene ring of a phenol. Chlorophenol is a synthetic intermediate for the manufacture of dye and more highly chlorinated phenols. Trichlorophenol is used to preserve wood and leather and as a biocide and antimildew agent. Pentachlorophenol is used as a wood preservative. It is a solid and is usually dissolved in a carrier solvent, such as diesel fuel. Nitrophenols have a nitrate group bonded to the benzene ring of the phenol. Some phenols found in hazardous waste include phenol; *p*-chloro-*m*-cresol; 2-chlorophenol; 2,4-dichlorophenol; 2,4-dimethylphenol; 4,6-dinitro-*o*-cresol; 2,4-dinitrophenol; 2-nitrophenol; 4-nitrophenol; 2,4,6-trichlorophenol; and pentachlorophenol. The structure of some of these compounds is found in Figure 7.10.

7.5.8 Organic Compounds Containing Nitrogen

We have already seen that organic compounds can include nitrogen by attaching a nitrate ion to a carbon atom, for example Nitrophenols. Nitrotoluenes are also common industrial chemicals and include 2- and 4-nitrotoluene; 2,4-dinitrotoluene; and 2,4,6-trinitrotoluene (TNT). TNT is an explosive and, together with its degradation products, has been reported as a soil contaminant in areas of waste disposal from manufacture of munitions and explosives. In addition, military training sites or former war zones can be contaminated with unexploded ordnance (UXO; Table 7.8), where explosives in intact ammunition shells or bombs can eventually leach into the soil and groundwater. Surveys in Laos and Cambodia after the Vietnam War indicated that 10% to 30 % of bombs dropped on these countries failed to detonate (Lauritzen 2001). Exposure to explosives at high concentrations, such as among workers at ammunition plants, has caused blood disorders such as anemia and abnormal liver function, as well as allergic reactions to the skin and cataracts (ATSDR 1995). Each UXO compound, which often consists of mixtures of different compounds, has its own characteristic toxicity, water solubility, and propensity

TABLE 7.8 Common organic explosives and propellants found at sites contaminated with unexploded ordnance (UXO).

Common Organic UXO Compound	Abbreviation
2,4,6-Trinitrotoluene	TNT
Hexahydro-1,3,5-trinitro-1,3,5-triazine	RDX ("Research department explosive")
Octahydro-1,3,5,7-tetranitro-1,3,5,7-tetrazocine	HMX ("High-melting explosive")
Penetaerythritol tetranitrate	PETN
2 n-methyl-n,2,4,6-Tetranitroaniline	Tetryl
2,4-dinitrotoluene	2,4-DNT
Nitroglycerine	
Nitrocellulose	

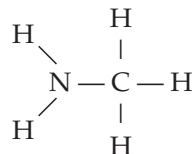
for sorption; and thus, differing potentials to impact surface water and groundwater quality. (SERDP 2004).

Especially after the end of the cold war, many military sites around the world have been closed or converted to other uses. This resulted in numerous studies of UXO contamination on military sites (Pichtel 2012). Probably the most extensively studied site contaminated with UXO, besides other contaminants, is Camp Edwards on the Massachusetts Military Reservation (MMR), which has been an active military site since 1911 (Clausen et al. 2004; WERC 2001). RDX, HMX, nitroglycerin, and several TNT breakdown products were detected in soil boring samples. The RDX concentrations as high as 9,300 µg/kg were detected about one meter below ground surface. Explosives detected in groundwater at that site included RDX, HMX, TNT, 2,4-DNT, 2-amino-4,6-dinitrotoluene (2A-DNT) and 4-amino-2,6-dinitrotoluene (4A-DNT). It is believed that the explosives and propellant contamination has migrated more than one kilometer down gradient (WERC 2001).

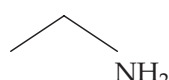
Besides organic UXO compounds, there are a number of other energetics or materials that might be present at sites contaminated with ammunition. One notable inorganic compound is **perchlorate** (ClO_4^-) that is used as an oxidizer in solid propellants for rockets, missiles, explosives, illumination rounds, and pyrotechnics. Perchlorate also has natural sources, such as evaporate deposits from which nitrate fertilizer is mined. However, none of those natural sources produce concentrations as high as those detected at some ammunition sites (Trumpolt et al. 2005). Perchlorates are typically very water soluble and once dissolved, perchlorate is extremely mobile, requiring decades to degrade. Before 1997, perchlorate could not be readily detected in groundwater at concentrations below 100 µg/L. Today, the detection limit is 4 µg/L or less. Because of the lower detection, many perchlorate contaminated sites have been identified (Motzer 2001).

Another inorganic compound that often is the popular topic of discussion is depleted uranium. This metal has been used as armor-piercing ammunition in recent conflicts. Compared to natural uranium, depleted uranium has the same chemo-toxicity, but its radiotoxicity is 60% lower. The major risk is depleted uranium dust, generated when projectiles hit hard targets. Currently, there is little evidence that depleted uranium poses a threat to soil and drinking water (Bleise et al. 2002), but with increased mining of uranium using *in situ* leaching techniques where a mobilizing and dissolving lixiviant is pumped underground, concern about groundwater concentrations and excursions of contaminated water are increasing.

Amines are organic compounds where the base molecule is ammonia and one or more of the hydrogen atoms is replaced by a nitrogen group. Some simple amines include the following:



Methylamine



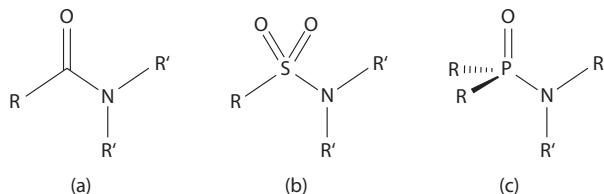
Ethyl amine



Dimethyl amine

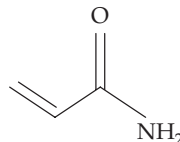
Amides have the following groups present (Figure 7.11):

FIGURE 7.11 Structures of three kinds of amides: an organic amide, a sulfonamide, and a phosphoramide.



Source: <https://commons.wikimedia.org/wiki/File:AmideTypes.png#/media/File:AmideTypes.png>

Acrylamide (2-propeneamide) is used in the synthesis of dyes and the manufacture of polymers, adhesives, and permanent-press fabrics. It has this structure:

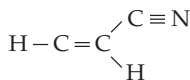


Acrylamide
(2-propeneamide)

Sulfonamides are synthetic antimicrobial agents that contain the sulfonamide group. Sulfonamide drugs were the first antibiotics to be used systemically in treatment of animals and humans and many thousands of molecules containing the sulfanilamide structure have been created since its discovery in 1932. Sulfonamides affect soil microorganisms and a dose-dependent effect of sulfadiazine on the soil microbial community and microbial biomass has been described (Hammesfahr et al. 2011). This class of potential soil and groundwater contaminants (Hruska and Franek 2012) is part of a class of compounds known as emerging contaminants (see Section 7.5.10).

The compound hexamethylphosphoramide (HMPA) is the most widely used phosphoramide. It is a colorless liquid and polar solvent used in the chemical synthesis. However, there are only a few instances where HMPA has caused groundwater pollution problems (e.g., Campos 1997).

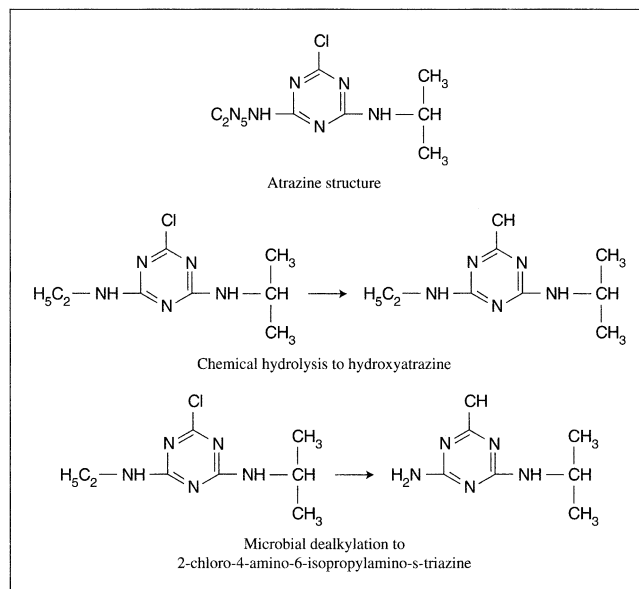
Nitriles have a cyanide group, in which there is a triple bond between a carbon atom and a nitrogen atom. An example of a nitrile is acrylonitrile (2-propenenitrile). This chemical is produced in very large amounts and is used in the manufacture of acrylic fibers, polyacrylonitrile plastics, ABS resins, and other products. It has this structure:



Acrylonitrile
(2-propenenitrile)

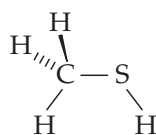
Atrazine, a complex molecule containing a six-sided ring structure with alternating carbon and nitrogen atoms, is a very widely used herbicide. It is used as a preemergent weed control on corn in the Midwestern United States and for weed control on sugar cane and pineapple fields in Hawaii. Its structure is given in Figure 7.12. Although atrazine is fairly quickly degraded in the environment by chemical and microbial processes it has been found in a number of wells in rural areas of Wisconsin, USA. During biodegradation the parent compound is transformed to other compounds, called **metabolites**. Two pathways by which the degradation of atrazine begins are shown in Figure 7.9. Biodegradation is discussed in detail later in this chapter.

FIGURE 7.12 Structure of atrazine and metabolic pathways leading to degradation.

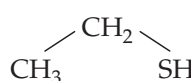


7.5.9 Organic Compounds Containing Sulfur and Phosphorus

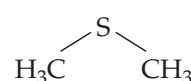
Organic compounds may also contain sulfur and phosphorus molecules. Sulfonates have already been introduced in Section 7.5.5. Organosulfur compounds tend to have offensive odors. Examples of simple organosulfur compounds include mercaptans, the active ingredients in the spray of a skunk, and a malodorous additive to natural gas to aid in recognition and detection of leaks.



Methyl mercaptan



Ethyl mercaptan



Dimethyl mercaptan

FIGURE 7.13 Structure and uses of organosulfur and organophosphorus pesticides.

Name	Structure	Use
Captan		Fungicide used on foliage
Disulfone		Systemic insecticide used on plants
Aldicarb		Systemic insecticide and nematicide
Endosulfan		Insecticide
Malathion		Insecticide
Parathion		Insecticide and acaricide
Glyphosate (Roundup)		Herbicide

Many pesticides include sulfur, phosphorus, or both in their composition. A prominent organophosphorus herbicide example is Glyphosate (N-(phosphonomethyl) glycine). Figure 7.13 gives the structure of some common organophosphorus and organosulfur pesticides. Most of these have been associated with groundwater contamination either in areas of their use or where they were manufactured.

7.5.10 Emerging Contaminants

Emerging contaminants is an umbrella term for chemicals that have recently been identified as a potential risk to the public health or the environment. The term “emerging” should not be interpreted as a compound that has not been previously released to the environment. It simply refers to the fact that these compounds could only recently be identified in environmental samples. That is, emerging contaminants do not fall under standard monitoring and regulatory programs but may be candidates for future regulation once more is known about their toxicity and health effects (Glassmeyer 2007). The number of emerging contaminants has been growing together with advances in analytical capabilities that permit scientists to identify and quantify compounds in the environment at levels as low as parts per trillion (ppt) or even parts per quadrillion (ppq) (Yamashita et al. 2004; Richardson and Ternes 2011; Trojanowicz and Koc 2013). Since many of these compounds have been detected only very recently, there is currently limited data available to determine their acute or long-term risk to humans and the environment. Common to most emerging contaminants is that they are proliferated around the world and can be detected in living tissue as well as all environmental compartments, including soil, groundwater, surface water, air, and the oceans (e.g., Loos et al. 2010; Lapworth et al. 2012; Lohman and Belkin 2014).

As illustrated in Table 7.9, emerging contaminants represent a diverse array of synthetic organic compounds, including pharmaceutical and personal care products (PPCP), “lifestyle” consumer products (e.g., caffeine or nicotine), industrial compounds, and engineered nanoparticles. Also included in this class of pollutants are “degradates,” i.e., metabolites and transformation products of the primary emerging contaminants. Figure 7.14 provides an overview of the frequency of detection of prominent emerging contaminants.

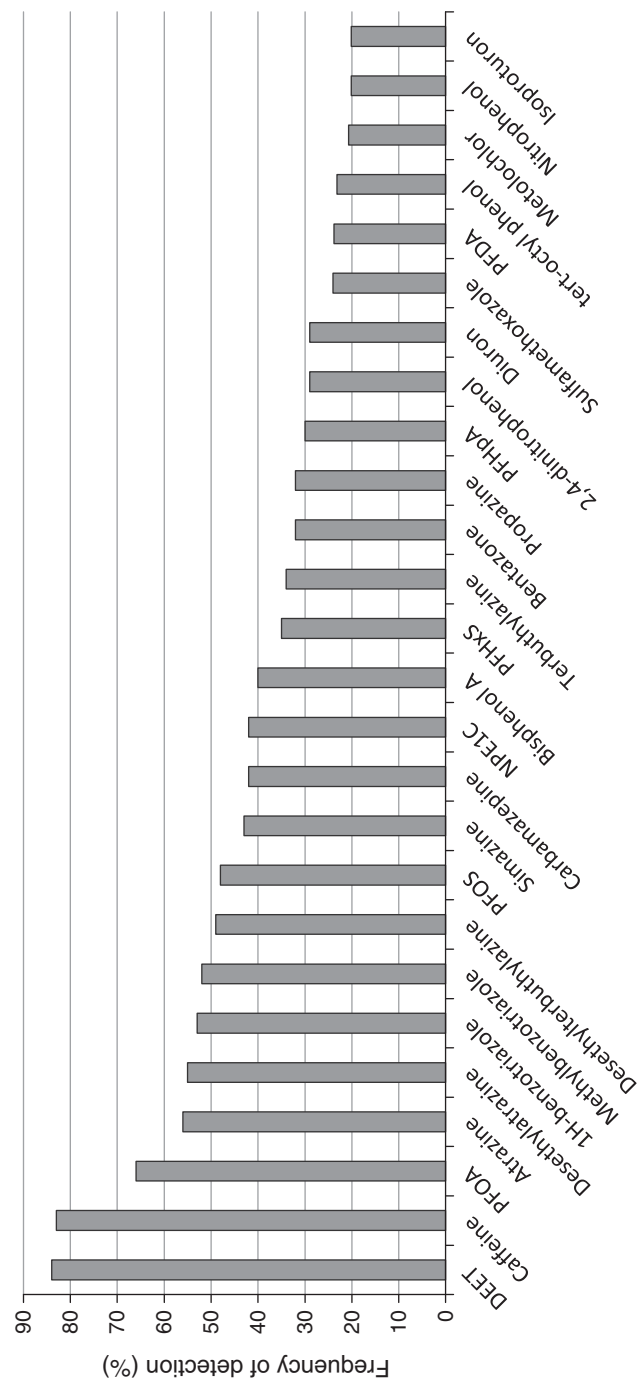
The contamination of groundwater resources by micro-organics is a growing concern and relatively poorly understood compared to other freshwater resources. Several potential pathways for spreading these compounds have been identified, including wastewater effluents from municipal treatment plants, septic tank effluent, and runoff from agricultural land (Figure 7.15). Lapworth et al. (2012) or Stuart et al. (2012) provide reviews of sources, fate, and occurrence and risk of emerging contaminants in groundwater.

Persistent organic pollutants (POP) is a term that refers to recalcitrant organic chemicals that resist degradation, bioaccumulate, have a known adverse toxicological effect, and have the potential for long-range environmental transport (Fiedler and Borja-Abrutto 2003; Harrad 2009). POP typically have a low aqueous solubility and volatility. Some emerging contaminants also fit the definition of POPs, for example PFOS and other flame retardants. There is no clear division between these terms except that POP emphasizes the longevity of contaminants in the environment. Which compounds are considered POPs is decided by the Stockholm Convention on Persistent Organic Pollutants, which in 1995 was formed by the United Nations Environment Programme (UNEP) to take action against POP. As of 2014, a total of 179 countries are parties to the Stockholm convention. Key elements of the Convention include measures to eliminate production and restrict the use of intentionally produced POPs, eliminate their unintentional production, and manage and dispose of POPs wastes in an environmentally sound manner. Since the listing of the first “dirty dozen” POPs in 2001, the number of POPs has grown to over 20 (Table 7.10).

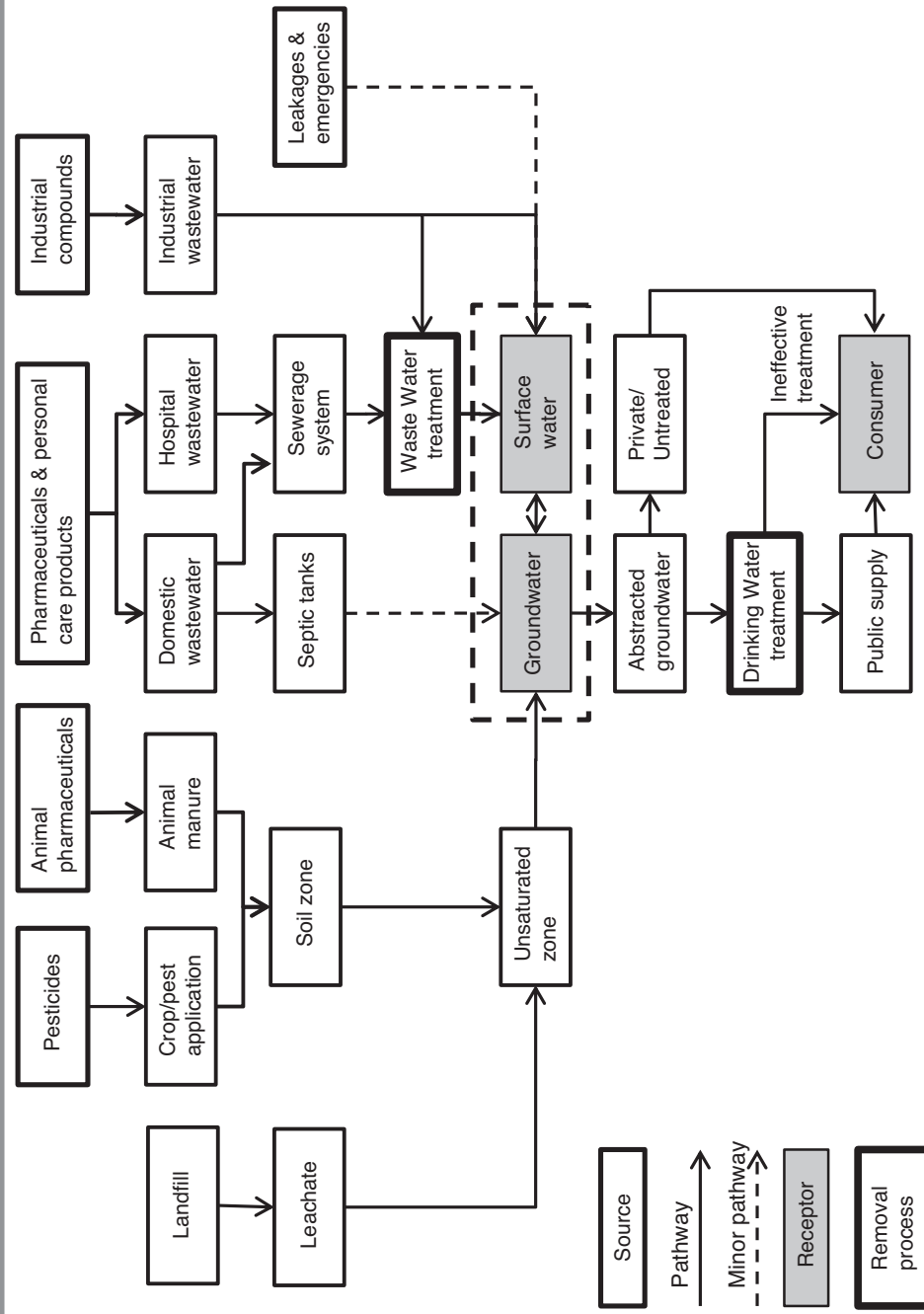
TABLE 7.9 Summary statistics for maximum concentrations (ng/L) found in groundwater for emerging contaminants and degradates that were detected in at least four separate studies, their major use and K_{ow} . n = number of studies. References to K_{ow} values are provided in source. DEET = *N,N*-diethyl-meta-toluamide, TCEP = Tris(2-Chloroethyl) phosphate.

Compound	Use	n	Lowest (ng/L)	Highest (ng/L)	Average (ng/L)	$\log K_{ow}$
<i>Pharmaceuticals</i>						
Carbamazepine	Antiepileptic	23	1.64	99,194	5312	1.51
Sulfamethoxazole	Antibiotic	15	5.7	1110	252	0.9
Ibuprofen	Anti-inflammatory	14	0.6	12,000	1491	2.48
Diclofenac	Anti-inflammatory	11	2.5	590	121	1.9
Clofibric acid ^{a,b}	Lipid regulator	8	4	7300	1113	2.88
Paracetamol ^d	Analgesic	8	15	120,000	15,142	0.46
Ketoprofen	Anti-inflammatory	6	3	2886	611	3.12
Triclosan	Antibiotic	6	7	2110	509	4.76
Iopamidol	X-ray contrast media	5	130	2400	760	-2.42
Lincomycin	Antibiotic	5	100	320	188	0.56
Propyphenazone	Analgesic	5	15	1250	553	2.02
Sulfamethazine	Veterinary medicine	5	120	616	298	0.28
Phenazone	Analgesic	4	25	3950	1503	2.32
Primidone	Barbiturate	4	110	12,000	3380	0.91
Salicylic acid (Aspirin)	Analgesic	4	43	1225	418	2.26
<i>Life-style compounds</i>						
Caffeine	Diuretic	14	13	110,000	9774	-0.07
Cotinine	Stimulant	4	60	400	173	0.07
<i>Hormones</i>						
Estrone	Estrogenic hormone	6	0.1	45	9	2.95
17b-Estradiol	Estrogenic hormone	4	0.79	120	31	3.86
<i>Industrials</i>						
DEET	Insect repellent	4	454	6500	2251	2
Bisphenol A	Plasticizer	9	470	9300	2527	3.18
Nonylphenol	Detergent	6	1500	84,000	23088	4.4
Galaxolide	Fragrance	5	6	23,000	4984	5.9
TCEP	Fire retardant	4	495	740	656	1.78

Source: Modified after Lapworth et al. 2012.

FIGURE 7.14 Frequency of detection and maximum detected concentrations of emerging contaminants in European groundwater.

Source: R. Loos et al. 2010. Pan-European survey on the occurrence of selected polar organic persistent pollutants in ground water. *Water Research* 44:4115–4126.

FIGURE 7.15 Sources (bold) and pathways for emerging contaminants to reach various receptors (grey).

Source: M. Stuart et al. 2012. Review of risk from potential emerging contaminants in UK groundwater. *Science of the Total Environment* 416:1–21. Used with Permission.

TABLE 7.10 Listing of POPs in the Stockholm Convention as of 2014.

POP Name	Prior Usages
Aldrin ^a	Insecticide
Chlordane ^a	Pesticide
Dieldrin ^a	Insecticide
Endrin ^a	Insecticide, rodenticide and piscicide
Heptachlor ^a	Insecticide
Hexachlorobenzene ^{a,c} (HCB)	Fungicide. Unintentional industrial by-products
Mirex ^a	Insecticide
Toxaphene ^a	Insecticide
Polychlorinated biphenyls ^{a,c} (PCB)	Dielectric and coolant fluids. Unintentional industrial byproducts
DDT ^b	Insecticide
Polychlorinated dibenzo-p-dioxins ^c ("dioxins") and polychlorinated dibenzofurans ^c	Unintentional industrial by-products. Incineration byproducts.
α -Hexachlorocyclohexane ^a	Byproduct of the production of the lindane
β -Hexachlorocyclohexane ^a	Byproduct of the production of the lindane
Chlordecone ^a	Insecticide
Hexabromobiphenyl ^a	Flame retardant
Hexabromodiphenyl ether ^a and heptabromodiphenyl ether ^a	Flame retardants
Lindane ^a (gamma-hexachlorocyclohexane)	Insecticide. Treatment for lice and scabies.
Pentachlorobenzene ^{a,c}	Intermediate in the manufacture of pesticides. Part of mixtures containing PCB.
Tetrabromodiphenyl ether ^a and pentabromodiphenyl ether ^a	Flame retardants
Perfluorooctanesulfonic acid ^b (PFOS), its salts and perfluorooctanesulfonyl fluoride ^b (PFOSF)	Flame retardants
Endosulfan ^a	Insecticide and acaricide
Hexabromocyclododecane ^a (HBCD)	Flame retardants

^a Production and use must be eliminated (Annex A)^b Production and use must be restricted (Annex B)^c Unintentional releases must be reduced (Annex C)

■ 7.6 Degradation of Organic Compounds

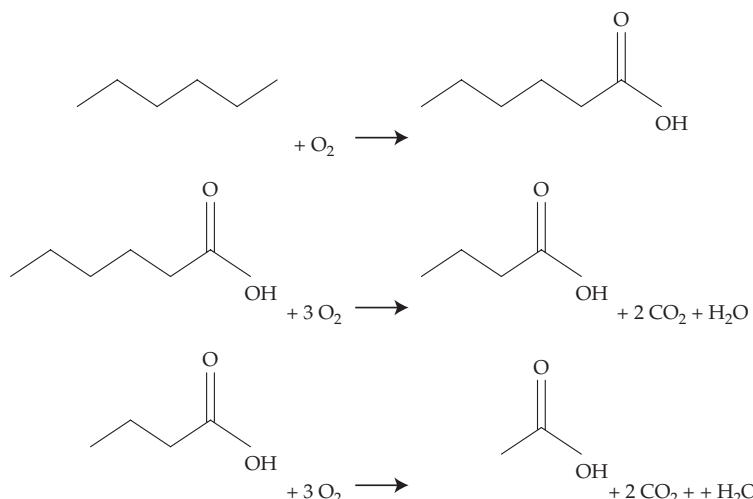
7.6.1 Introduction

It is well known that straight chain and aromatic hydrocarbons associated with petroleum products can undergo biological degradation (Barker et al. 1987; Wilson et al. 1986). Hydrogeologists first observed that halogenated organic solvents dissolved in groundwater undergo transformations under natural conditions with the compounds undergoing progressive dehalogenation (Roberts et al. 1982; Parsons et al. 1984; Cline and Viste 1985). Benzene, toluene, and xylene have also been observed to undergo degradation in aquifers (Chiang et al. 1989; Barker and Patrick 1985; Barker et al. 1987; Davis et al. 1994; Chapelle et al. 1996).

In this section we will examine the types of organic compounds that can undergo degradation, the means by which such degradation occurs, and the conditions under which it occurs. Degradation is defined as the process of an organic molecule becoming smaller by chemical or biological means. A molecule might have a halide ion replaced with a hydrogen ion, thus being transformed into a compound with a lower molecular weight. Carbon atoms can be broken off the molecule, leaving it with fewer atoms. The ultimate product of degradation of a hydrocarbon is methane or carbon dioxide and water.

7.6.2 Degradation of Hydrocarbons

Alkanes can be degraded under aerobic conditions by microbes (Manahan 1984). Bacteria that can do this include *Micrococcus*, *Pseudomonas*, *Mycobacterium*, and *Nocardia*. The first step in the process is the conversion of a terminal CH₃ group to a carboxyl group. The microbes then attack the second carbon of the newly formed carboxylic acid and remove a two-carbon fragment, forming carbon dioxide. The oxidation of n-hexane follows these steps:



Oxidation of n-hexane

The resulting acetic acid can easily be further degraded to carbon dioxide and water. Branched-chain hydrocarbons are more resistant to microbial degradation than normal alkanes, and generally short chains are more resistant than long chains.

Aromatic hydrocarbons can also be degraded under aerobic conditions. The first step in the cleavage of the ring is to replace two hydrogens on adjacent carbon atoms with hydroxyl groups. The benzene ring is then cleaved between these two rings to form a dicarboxylic acid. Figure 7.16(a) illustrates the ring-cleavage process, which requires molecular oxygen.

It is also possible for aromatic hydrocarbons to undergo anaerobic degradation (Evans 1977). The benzene ring can be degraded in the presence of nitrate by *Pseudomonas* sp. and *Moraxella* sp.* The benzene ring is first saturated to cyclohexane, then oxidized to a ketone, and finally cleaved by hydrolysis to form a carboxylic acid. Figure 7.16(b) shows the degradation of phenol, first to cyclohexanol, then an oxidation to cyclohexanone and then ring cleavage to form hexanoic acid. During this process the nitrate is reduced to nitrogen.

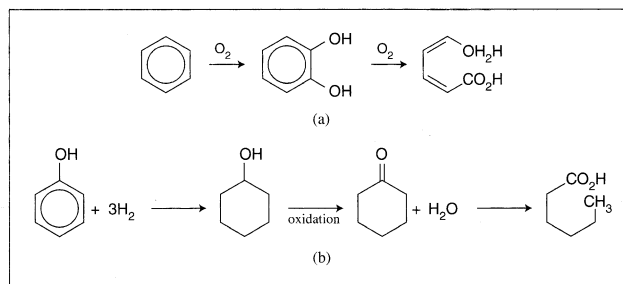
Major et al. (1988) made a study of biodegradation of benzene, toluene, *o*-xylene, and *m*-xylene in the laboratory using nitrate as the electron acceptor under denitrifying conditions. They found that degradation of all four compounds occurred and suggested that bioremediation using added nitrate to groundwater might be possible.

Polycyclic aromatic hydrocarbons (PAHs) are also biodegradable. Commonly studied PAH-degrading bacteria include *Pseudomonas aeruginosa*, *Pseudomonas fluorescens*, *Mycobacterium* sp., *Haemophilus* sp., *Rhodococcus* sp., *Paenibacillus* sp. (Johnsen et al. 2005; Haritash and Kaushik 2009). For instance, *Mycobacterium* sp. AP1 strain can utilize pyrene, fluoranthene, and phenanthrene as its sole source of carbon and energy (Vila et al. 2001; Lopez et al. 2006). The microbes themselves are initially found at sites where PAH compounds have been released to the soil. The *Mycobacterium* sp. bacterium was isolated from hydrocarbon-contaminated sediment samples from an oil field near Port Aransas, Texas (Heitkamp and Cerniglia 1988). Mueller et al. (1990) isolated a bacterium, *Pseudomonas paucimobilis*, that is capable of using fluoranthene as the sole source of carbon for energy and growth. This strain was discovered at a site where creosote, which is rich in PAH, had been discarded.

Peng et al. (2008) proposed catabolic pathways of PAH degradation by aerobic bacteria for several low- and high-molecular weight PAH compounds. Typically, low-molecular weight two- and three-ring PAHs, such as naphthalene or phenanthrene, are easier biodegradable than higher-molecular weight PAHs, including pyrene or benzo[a]pyrene. Low molecular PAHs are predominantly mineralized by Gram negative bacteria strains (mainly pseudomonads and related genera), while higher molecular PAHs are generally degraded by Gram-positive mycobacteria. Because PAHs are typically present in complex mixtures, such as creosote or coal tar, it is important to know that some bacteria, including *Mycobacterium* sp., are capable to simultaneously mineralize multiple PAHs (e.g. Heitkamp and Cerniglia 1989; Lopez et al. 2007).

*The designation *Pseudomonas* sp. means that the bacterium has been identified to the level of the genus *Pseudomonas*, but not to the species level.

FIGURE 7.16 Degradation of a benzene ring. (a) Aerobic degradation of benzene in the presence of oxygen. (b) Anaerobic degradation of phenol in the presence of nitrate.

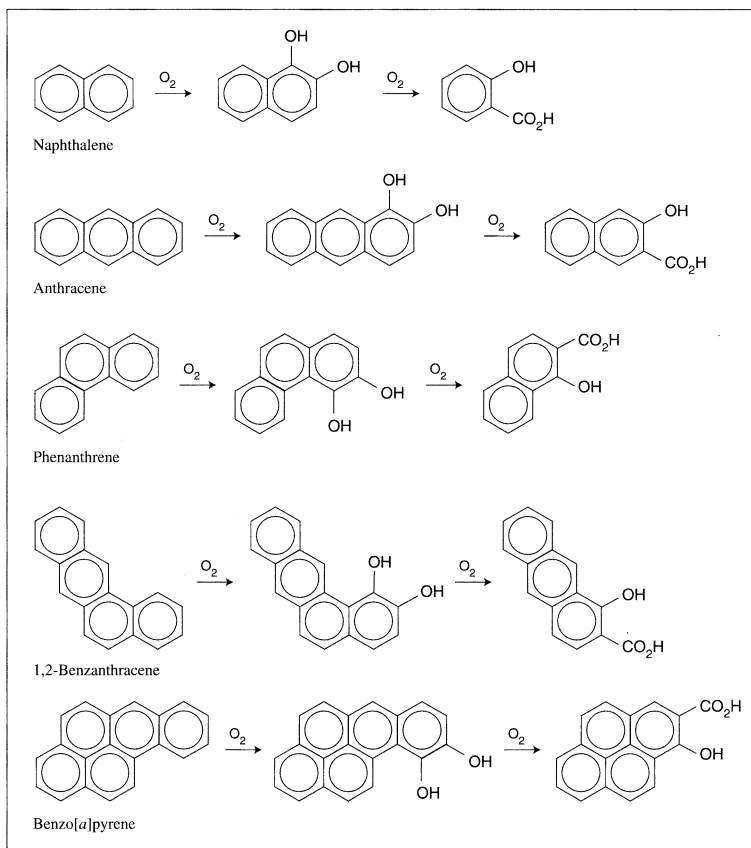


Some nonligninolytic and ligninolytic fungi are also capable of degrading PAH, including *Phanerochaete chrysosporium*, *Bjerkandera adusta*, and *Pleurotus ostreatus* (Peng et al. 2008; Haritash and Kaushik 2009). Bumpus (1989) demonstrated that under aerobic conditions in the laboratory the lignolytic fungus *Phanerochaete chrysosporium* degraded all the major PAHs in anthracene oil, which is a complex mixture of PAHs compounds obtained from the fractional distillation of coal oil. PAHs reported to be degraded by *Phanerochaete chrysosporium* include fluorene, phenanthrene, anthracene, carbazole, fluoranthene, pyrene, benzo [*a*] fluorene, 1-methylfluorene, and acenaphthalene.

The amount of PAH accessible to bacteria and other degraders is referred to as **bioavailability**. As rule of thumb, the PAH bioavailability decreases with increasing molecular mass. The microbial degradation of PAHs is therefore believed to be limited by the amounts dissolved in the water phase and bioavailability must be considered a dynamic process, determined by the rate of contaminant mass-transfer to microbial cells relative to their intrinsic catabolic activity (Johnsen et al. 2005).

The initial steps in PAH mineralization involves ring cleavage, as shown in Figure 7.17 for the PAH compounds naphthalene; phenanthrene; anthracene; 1,2-benzanthracene; and benzo [*a*] pyrene (Guerin and Jones 1988). Heitkamp et al. (1988) have identified some of the products of ring oxidation and ring fusion of pyrene, a four-ring PAH, that were produced by the bacterium *Mycobacterium* sp. in an oxygenated lab environment that had additional organic nutrients. The identified metabolites of pyrene are shown in Figure 7.18.

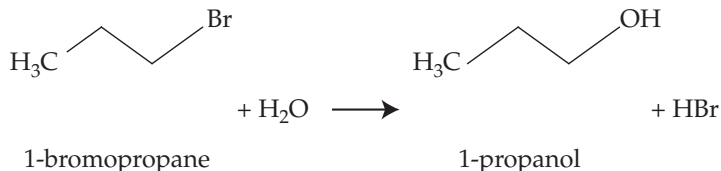
The previously cited studies were conducted under aerobic conditions. However, many sites with organic wastes have anaerobic conditions, because the soil bacteria consume oxygen in degrading the organic waste. Mihelcic and Luthy (1988) were the first to report the mineralization of acenaphthene and naphthalene in microcosm experiments under nitrate-reducing conditions. In microcosm studies by Meckenstock et al. (2004) it was demonstrated that anaerobic degradation of two-ring PAHs is also possible with ferric iron or sulfate as electron acceptors. Currently, it remains unclear if unsubstituted PAH can be metabolized under methanogenic conditions (Chang et al. 2006; Berdugo-Clavijo et al. 2012). Methanogenesis is a terminal electron accepting process for the degradation of organic compounds where other electron acceptors, like oxygen, nitrate, iron, or sulfate are depleted.

FIGURE 7.17 Cleavage of ring structure of some polycyclic aromatic hydrocarbons.

7.6.3 Degradation of Chlorinated Hydrocarbons

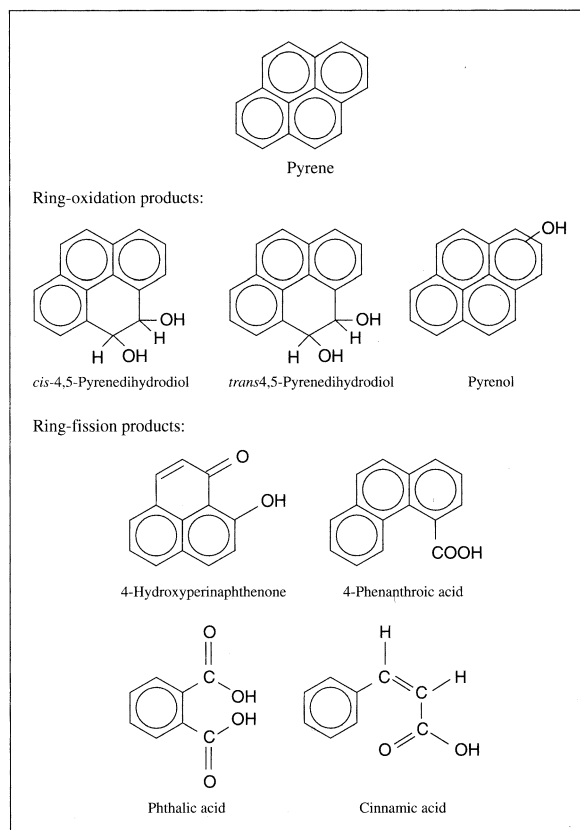
A large number of field and laboratory studies have demonstrated that many classes of chlorinated hydrocarbons can undergo either biotic or abiotic (chemical) degradation (Wiedemeier et al. 1999). Of those, the chlorinated ethanes, like 1,1,1-TCA, and ethenes, such as PCE or TCE, have been well studied because they are common groundwater contaminants. There are a number of reactions that can occur abiotically to break them into lower-molecular-weight compounds (e.g., Vogel et al. 1987; Rifai et al. 2001). Hydrolysis and dehydrohalogenation reactions are the most comprehensively studied abiotic attenuation mechanisms. Reductive dechlorination reactions include hydrogenolysis and dihaloelimination. Each of these transformation processes are introduced next.

Hydrolysis is a reaction where water reacts with the halogenated compound to substitute a hydroxyl group (OH^-) for a halogen (e.g., Cl^-), creating an alcohol. This can occur in water without either inorganic or biological catalysts, but the reaction rates are slow. The reaction is also called **substitution** reaction and can be illustrated with 1-bromopropane:



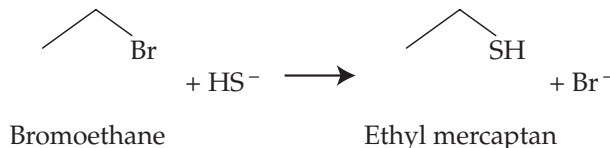
Hydrolysis reactions proceed most rapidly for monohalogenated compounds. Monohalogenated compounds have reaction half-lives of about one month. As the number of halogen ions increases, the half-life for reactions due to substitution increases rapidly into the range of years to hundreds of years. Also, higher molecular weight halogens are more susceptible to hydrolysis than lower molecular weight ones. The only major chlorinated solvent that can be transformed chemically in groundwater through hydrolysis is 1,1,1-trichloroethane. The TCA hydrolysis transformation product is acetic acid (McCarty 1996). Hydrolysis rates can generally be described using first-order kinetics (Rifai et al. 2001).

FIGURE 7.18 Structure of identified pyrene metabolites produced by *Mycobacterium* sp.

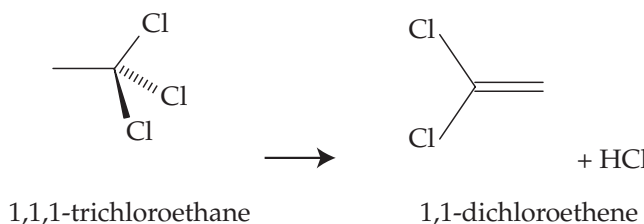


Source: Heitkamp et al. 1988.

Other groups can be substituted as well, such as the reaction with an HS^- radical under reducing (anaerobic) conditions to release a halogen ion and form a mercaptan:



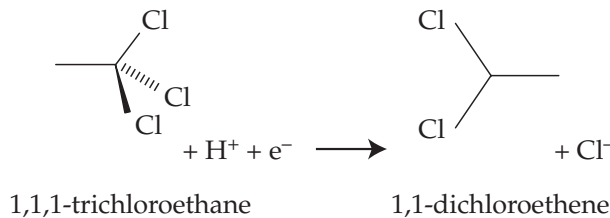
Dehydrohalogenation is a two-step reaction where an alkane loses a halide ion from one carbon atom and then a hydrogen ion from an adjacent carbon. The result is the formation of a double bond between the carbon atoms, thus creating an alkene. For example, dehydrohalogenation can transform 1,1,1-trichloroethane (1,1,1-TCA) to 1,1-dichloroethene (1,1-DCE):



Contrary to the patterns observed for hydrolysis, the rate of dehydrohalogenation increases with increasing numbers of halogen ions; hence compounds that undergo substitution most slowly undergo dehydrohalogenation most rapidly. Dehydrohalogenation rates may be approximated using pseudo-first-order kinetics.

Bromine ions are more rapidly removed than chlorine ions in these abiotic reactions. Burlinson et al. (1982) found that bromine is removed from dibromochloropropane six times faster than chlorine. A listing of half-lives for abiotic dehydrohalogenation and hydrolysis of some chlorinated solvents is presented in Butler and Barker (1996) or Rifai et al. (2001).

Reductions start with the removal of a halide ion by a reduced species, such as a reduced transition metal or a transition metal complex. The reduced species is thus oxidized. The alkyl radical thus formed can react with a H^+ ion, which substitutes for the departed halogen ion. This process is called **hydrogenolysis** or **reductive dechlorination** and can be illustrated with 1,1,1-trichloroethane being transformed to 1,1-dichloroethane (1,1-DCA):



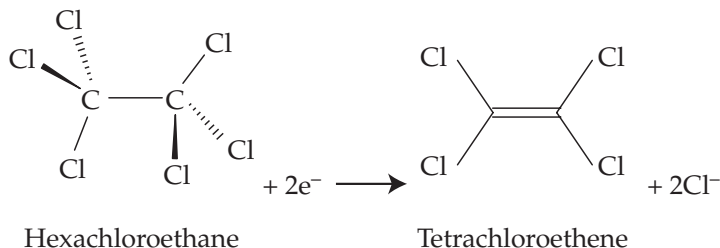
The reductive dechlorination process of many chlorinated organic compounds can be enhanced by granular or nano-particle zero-valent iron (ZVI) as and other metals.

This abiotic process involves the reduction of dissolved chlorinated compounds and the oxidation (corrosion) of iron (Fe^0):



The products of the dechlorination reaction that occur when a chlorinated compound comes in contact with iron are chloride (Cl^-), iron (Fe^{2+}), nonchlorinated (or less-chlorinated) hydrocarbons, and hydrogen. The rates of the dehalogenation process vary for the different halogenated contaminants (Gillham and O'Hannesin 1994). ZVI treatment of dissolved chlorinated contaminants is exploited in permeable reactive barriers (PRB), a remediation technology discussed in greater detail in Chapter 9.

Reductions can also occur if there are halides on adjacent carbon atoms. In this case the loss of a halogen from each carbon atom creates an alkene by formation of a double bond between the carbon atoms. This reduction is called **dihaloelimination** and can transform a chlorinated alkane into a chlorinated alkene. The process is illustrated by the transformation of hexachloroethane to tetrachloroethene:

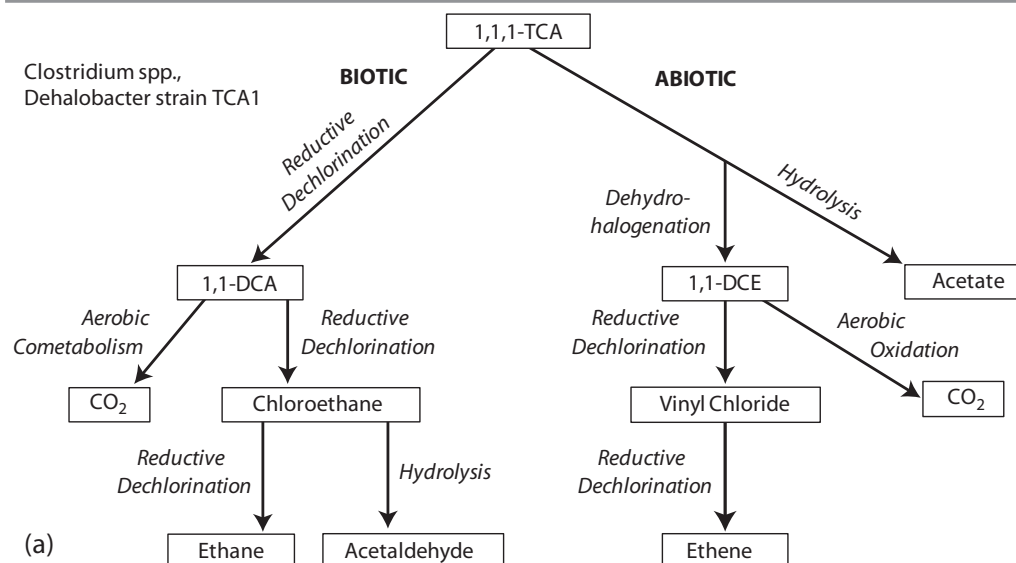


Dihaloelimination and hydrogenolysis reactions are thermodynamically possible under reducing conditions, but they often do not take place in the absence of biological activity (e.g., Butler and Barker 1996). It is therefore possible that some of these reactions are truly abiotic, while those that rely on microbial activity to produce reducing conditions or reactants are a form of cometabolism.

Figure 7.19 a and b illustrate pathways for the degradation of 1,1,1-TCA and PCE (tetrachloroethene) under abiotic and biotic conditions. While many of these reactions have been extensively studied and confirmed to occur in the field, alternative pathways exist. Identifying these pathways remains an area of active research.

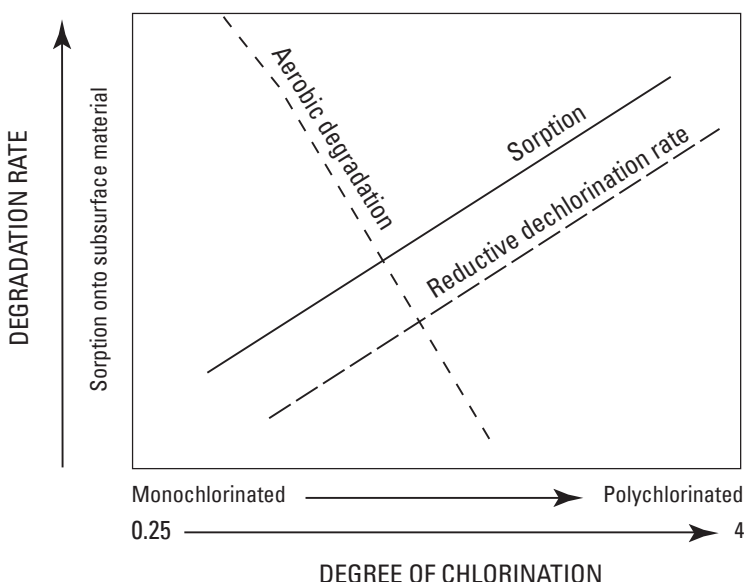
Figure 7.20 shows the relation between the degree of anaerobic reductive dechlorination (together with the degree of a compound's chlorination) to the anaerobic degradation rate and affinity of sorption to subsurface material. The figure illustrates that a chlorinated compound's chemistry as well as environmental conditions, such as the properties of the aquifer material, influence the type and rate of the transformation reactions. Besides those factors, other ones include pH, temperature, state of oxidation or reduction, microorganisms present, and types of other chemicals present. Reaction kinetics also play an important role in the determination of the abiotic and biotic fate of organic contaminants. Theoretically, the end products of the abiotic reactions are ethane and ethene, which should be amenable to further biodegradation. However,

FIGURE 7.19 Pathways for the abiotic and anaerobic degradation of (a) 1,1,1-trichloroethane 1,1,1-TCA and (b) tetrachloroethene PCE.



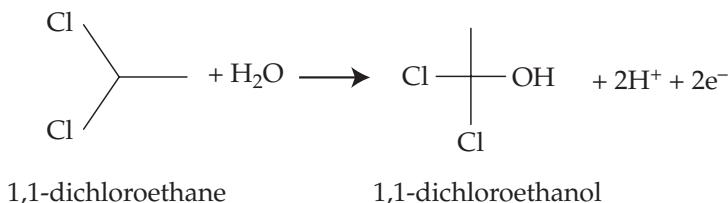
under field conditions such a favorable outcome might require many years to occur. Before it does, the contaminant might well flow from the point of origin to contaminate a large area of the aquifer system.

FIGURE 7.20 Relation between degree of chlorination and anaerobic reductive-dechlorination, aerobic degradation and sorption onto subsurface material. Degree of chlorination is number of chloride atoms divided by number of carbon atoms.

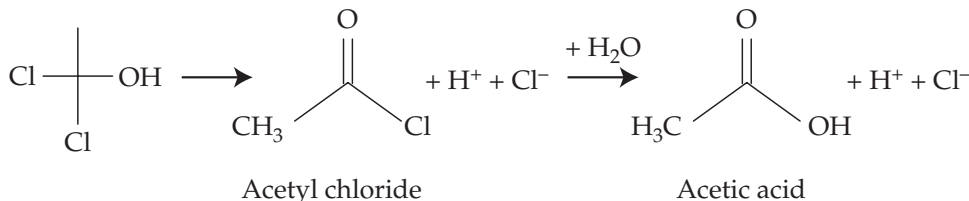


Source: Lawrence 2006.

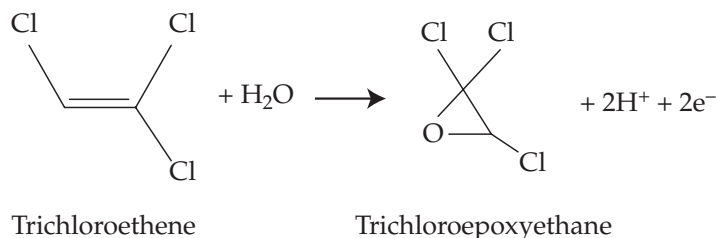
Oxidations are typically biologically mediated and require external electron donors or acceptors. In some cases polyhalogenated aliphatic compounds will act as electron acceptors and become reduced. In general, the oxidation potential decreases as the extent of halogenation increases. Oxidations include α -hydroxylation, which is the addition of an OH^- radical to an alkane in place of an H atom on a carbon that also contains a halogen ion. The result is the formation of a chlorinated alcohol. The α -hydroxylation of 1,1-dichloroethane at the C-1 position forms 1,1-dichloroethanol:



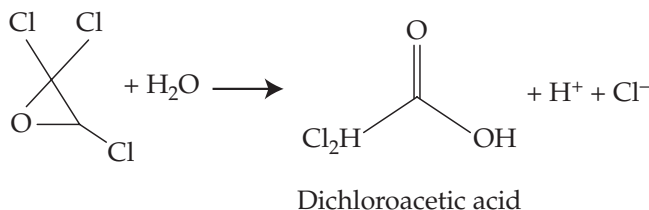
The halogenated alcohol can then undergo the further loss of hydrogen from the hydroxyl group and a halide to form acetyl chloride which then transforms into acetic acid by losing the last remaining halide.



Oxidation of a carbon-carbon double bond can result in the formation of an epoxy; the process is called **epoxidation**:



The epoxy is short-lived and under neutral pH conditions can be oxidized to a carboxylic acid:



Microbial transformations of halocarbons occur directly, i.e., the contaminant is the primary growth substrate for the microbial community or indirectly by a cometabolic process. If the halocarbon is the primary growth substrate, it can be used as either electron donor or acceptor. When used as an electron donor, the halocarbon is oxidized either under aerobic or anaerobic conditions. If the halocarbon is used as an electron acceptor, it is reduced and undergoes reductive dechlorination. This process is referred to as **halorespiration** when a halocarbon acts as an electron acceptor and a halogen atom on the molecule is replaced with a hydrogen atom. Hydrogen in the subsurface can be generated through a process called **fermentation**. It can occur when bacteria oxidize and reduce different portions of a single substrate. There are many organic substrates which can be fermented in the subsurface including alcohols, low-molecular-weight fatty acids (e.g., lactate), carbohydrates (e.g., sugars), vegetable oils, and plant debris (e.g., mulch) (Air Force Civil Engineer Center 2004). Table 7.11 shows examples of fermentation reactions yielding hydrogen.

When halocarbons, or other organic compounds, do not serve as the primary growth substrate, microorganism can still gain energy by cometabolizing these compounds via enzymes present in their metabolic pathway. **Cometabolism** reactions proceed under aerobic or anaerobic conditions and can be either oxidation or reduction reactions.

TABLE 7.11 Examples of Fermentation Half Reactions Using Organic Substrates as an Electron Donor to Yield Hydrogen.

Electron Donor	Electron-Donor (Oxidation) Reaction
Ethanol	$\text{C}_2\text{H}_6\text{O} + \text{H}_2\text{O} \rightarrow \text{C}_2\text{H}_3\text{O}_2^- + \text{H}^+ + 2\text{H}_2$ ethanol fermentation to acetate
Methanol	$\text{CH}_4\text{O} + 2\text{H}_2\text{O} \rightarrow \text{CO}_2 + \text{H}_2\text{O} + 3\text{H}_2$ methanol fermentation
Acetate	$\text{C}_2\text{H}_3\text{O}_2^- + 4\text{H}_2\text{O} \rightarrow 2\text{CO}_2 + 2\text{H}_2\text{O} + 4\text{H}_2$ acetate fermentation
Butyrate	$\text{C}_4\text{H}_7\text{O}_2^- + 2\text{H}_2\text{O} \rightarrow 2\text{C}_2\text{H}_3\text{O}_2^- + \text{H}^+ + 2\text{H}_2$ butyrate fermentation to acetate
Propionate	$\text{C}_3\text{H}_5\text{O}_2^- + 3\text{H}_2\text{O} \rightarrow \text{C}_2\text{H}_3\text{O}_2^- + \text{CO}_2 + \text{H}_2\text{O} + 3\text{H}_2$ propionate fermentation to acetate
Lactate	$\text{C}_3\text{H}_5\text{O}_3^- + 2\text{H}_2\text{O} \rightarrow \text{C}_2\text{H}_3\text{O}_2^- + \text{CO}_2 + \text{H}_2\text{O} + 2\text{H}_2$ lactate fermentation to acetate

Source: Naval Facilities Engineering Command 2004.

Rifai et al. (2001) point out that based on data from numerous field sites, cometabolic oxidation, unlike anaerobic, reductive cometabolism, processes are likely insignificant transformation process in plumes of chlorinated solvents.

7.6.4 Degradation of Organic Pesticides

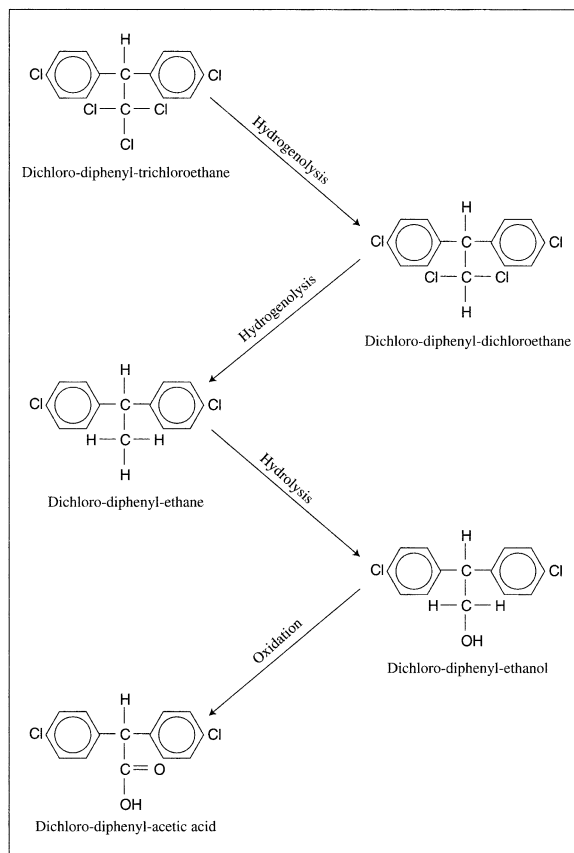
One of the first organic pesticides developed was DDT, or dichloro-diphenyl-trichloroethane. This proved to be a very effective agent against a wide variety of insects, and it was inexpensive. However it was found to be very resistant to degradation and hence persisted in the environment. Damage to nontargeted wildlife, especially birds, was reported, and the use of this compound was eventually banned in the United States. Although DDT does degrade, the first metabolite formed, dichloro-diphenyl dichloroethane (DDD), proved to be at least as toxic as DDT. DDD forms from DDT by the removal of a chlorine atom by hydrolysis. Figure 7.21 illustrates a metabolic pathway for the degradation of DDT.

Newer pesticides are formulated so that they will not persist in the environment. They have structures that will more readily undergo abiotic, or biologically mediated, degradation. Smith (1988) lists the following pathways by which herbicides are degraded. Naturally, the same reactions will apply to other pesticides.

Dealkylation: The biological removal of a methyl or other alkyl group from a nitrogen atom (see Figure 7.12)

Dealkoxylation: The biological removal of a methoxy (methyl ether) group from a nitrogen atom.

Decarboxylation: The biological or abiotic removal of one carbon and two oxygen atoms from a carboxyl group.

FIGURE 7.21 Metabolic pathway for the degradation of dichloro-diphenyl-trichloreoethane (DDT).

Dehalogenation: Biological replacement of a chlorine atom with a hydrogen atom. This is especially important in degradation of insecticides, many of which are chlorinated hydrocarbons.

Ether cleavage: The biological cleaving of an ether by breaking the bond between oxygen and carbon atoms.

Hydrolysis: The chemical or biological cleavage of molecules by the addition of water. The products usually include an alcohol or carboxylic acid.

Hydroxylation: The biological introduction of hydroxyl groups into either aliphatic or aromatic compounds.

Methylation: The biological addition of a methyl group to an alcohol or phenol to form a methyl ether.

Oxidation: Oxidation of an alcohol to an aldehyde, which can be further oxidized to a carboxylic acid, done by either chemical or biological processes. Epoxide formation is a major step in many oxidation processes.

Beta-oxidation: Biological removal of two carbon atoms from an alkane chain linked to an aromatic ring structure.

Reduction: Biological reduction of a nitrate group linked to a herbicide to form an amine group.

Ring cleavage: One of many processes by which microbes can break the structure of an aromatic ring.

7.6.5 Degradation of Gasoline Compounds

Most common gasoline compounds, such as BTEX, are generally more rapidly degraded than chlorinated solvents. This is because gasoline compounds are in a highly reduced state and the preferred terminal electron acceptor is oxygen, which is present in aerobic environments. Many aerobic microorganisms readily oxidize gasoline compounds while using them as primary substrates (Brown et al. 1996). The oxidation of BTEX compounds can proceed via several pathways as summarized by Lawrence (2006) and many others.

Under anaerobic conditions gasoline compounds are metabolized as electron donors. In some subsurface environments, their degradation can be limited by the availability of terminal electron acceptors, such as nitrate, sulfate, carbon dioxide, or iron (III). Lawrence (2006) points out that BTEX degradation rates decline in a sequence from mildly (nitrate reducing) reducing conditions to strongly reducing conditions (methanogenesis) in shallow aquifers.

Unlike the primary gasoline compounds, the former additives MTBE and other oxygenates are much more recalcitrant. MTBE is known to degrade under anaerobic conditions, but degradation rates are at least an order of magnitude slower than those of BTEX compounds (Lawrence 2006). The exact degradation pathways of MTBE and other oxygenates are still being studied. Under aerobic conditions, MTBE degradation appears to be even slower (Squillace et al. 1997) but under carefully controlled conditions, comparably rapid MTBE mineralization was observed (Wilson et al. 2005). Its recalcitrance to biodegradation together with its low affinity for sorption are two major reasons why MTBE groundwater plumes tend to be larger than those of other gasoline contaminants.

One important consideration in any mixture of organic compounds like fuels, oils, coal tars, creosotes, and other blends of chemicals is that each of the various compounds degrade, transform, volatilize, and dissolve at different rates. What this means is that not only do the fractions of the compounds in each mixture change with time, but the physical and chemical properties of the mixture change as well. As fractions of the mixture change in mass and distribution, the rates of change will alter. For example, fresh gasoline is fairly volatile but loses its 4, 5, and 6 carbon alkanes relatively rapidly, making aged petroleum spills less likely to contain volatiles and less amenable to vapor analysis or vapor extraction remedial strategies. The rate and nature of the changes are very specific to each site. The speed of groundwater flow could impact differential dissolution rates, as will the solubility and changing mole fractions of individual compounds with time. Similarly, biodegradation rates are different for individual components of a mixture.

■ 7.7 Field Studies of Biological Degradation of Organic Molecules

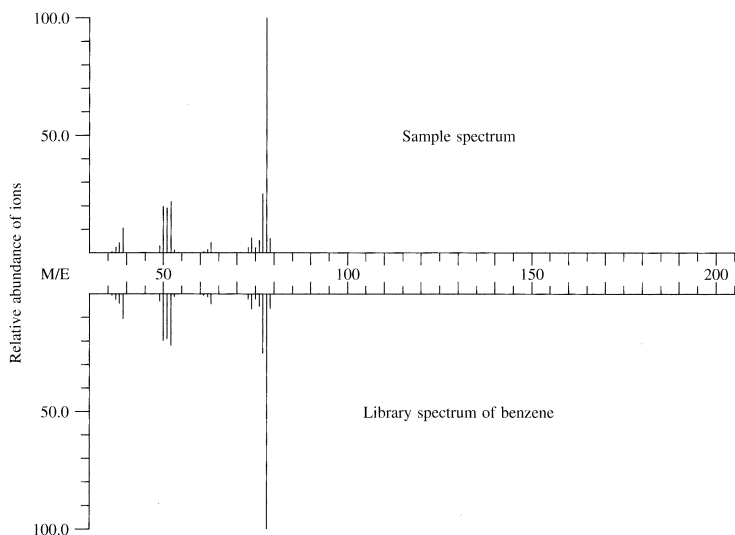
A vast body of information on biological and abiotic degradation of organic molecules has accumulated, based on laboratory studies using microcosms, the microbial equivalent of an aquarium. Under such carefully controlled conditions, the disappearance of a compound can be determined and the appearance of metabolites noted. Not surprisingly, it is far more difficult to undertake degradation field studies and interpret the results. At the most basic level, is a compound disappearing due to degradation, or is some other process such as volatilization, sorption, or dilution involved? Nonetheless, over the past two decades a number of well-documented field studies have contributed to our much better understanding of biodegradation processes of a variety of organic compounds in soil and groundwater. In Chapter 9 we will examine how enhanced biodegradation as well as managed natural attenuation (MNA) processes can be used as a means of remediating aquifers and soils contaminated with organic compounds.

■ 7.8 Analysis of Organic Compounds in Groundwater

There are a number of methods by which organic compounds dissolved in groundwater can be identified and quantified. In **gas chromatography** a mixture of volatile materials is transported by a carrier gas through a column packed with either an absorbing solid phase or an absorbing liquid phase that is coated on a solid material. The volatile component will partition between the carrier gas and the absorbing phase, and the length of time that it takes for the component to traverse the column will be characteristic. If there are several compounds in a mixture, the column will separate them and they will arrive at different times. A detector, such as a **photoionization detector** or a **flame-ionization detector**, located at the end of the column can determine the quantity and identity of each volatile component. It is important to understand that PID, FID, or other similar detectors, such as electron capture detector (ECD) or thermal conductivity (TCD), cannot necessarily be used to identify unknown compounds. For that reason, most laboratories rely on **mass spectrometry** in which a compound is ionized by an electrical discharge and the ions are then separated based on their charge-to-mass ratio. The output is a **mass spectrum**, which can be compared to the mass spectra of a large number of standard compounds stored in an electronic database called a mass-spectra library. The most commonly used laboratory method is gas chromatography combined with mass spectrometry, frequently known as **GC/MS**. In GC/MS the mass spectrometry is preceded by gas chromatography to separate the compounds. Figure 7.22 shows a library spectrum of benzene matched against the mass spectrum of a sample identified as benzene. A major disadvantage of GC/MS is that it cannot detect nonvolatile, polar, and thermally labile compounds. For these compounds, which include a large number of emerging contaminants, liquid chromatography–mass spectrometry (LC-MS) methods are being developed.

Another commonly used analytical technique for separating, identifying, and quantifying components of a mixture is **high-performance liquid chromatography** (HPLC). Instead of a carrier gas, HPLC relies on pumping a pressurized liquid solvent

FIGURE 7.22 Comparison of the mass spectrum of an unknown with the mass spectrum of benzene from the library of mass spectra.



Source: B. L. Roberts. 1985. In Pursuit of contaminant-free water. *Groundwater Monitoring & Remediation* 5:41–43.
Used with permission.

containing the sample mixture through a column filled with a solid adsorbent material. During their passage through the column, the compounds separate and are picked-up by a detector at the end of the system. The detector generates a signal proportional to the amount of component emerging from the column, hence allowing for quantitative analysis of the various components in a sample. Most commonly an ultraviolet-visible (UV-Vis) absorbance detector is used in HPLC.

The U.S. EPA has developed a series of standard methods for the analysis of chemical, physical, and biological components dissolved in water. These are known as the 600 series methods (40 CFR Part 136, *Federal Register*). Table 7.12 lists the 600 series and the target compounds. Method 601 for purgeable halocarbons, method 602 for purgeable aromatics and method 624 are gas-chromatograph methods using a purge-and-trap procedure to isolate volatile organics. Nitrogen is bubbled through a column of water containing the dissolved organics, so that the organics are purged from the water and carried with the gas. The organics are trapped on a solid sorbent. The sorbent is then heated, and the volatile organics are swept into a gas chromatograph for separation and then detected. Method 601 uses a halide-specific detector and method 602 specifies a photoionization detector. Method 624 is based on gas chromatograph/mass spectrometer (GC/MS) and is appropriate for the qualitative and quantitative confirmation of results for most of the parameters listed in method 601. The results are reported as volatile organics or purgeable organics.

Methods 603 through 612 are gas-chromatographic methods for substances other than purgeable hydrocarbons and aromatics. Method 613 is a GC/MS method for dioxin.

TABLE 7.12 Select U.S. EPA 600 series analytical methods for organic compounds promulgated under the authority of Section 304(h) of the Clean Water Act; also referred to as the "304(h)" or "Part 136" methods.

Method Number	Analytical Technique	Target Compounds
601	GC	Purgeable halocarbons
602	GC	Purgeable aromatics
603	GC	Acrolein and acrylonitrile
604	FIDGC	Phenols
605	HPLC	Benzidines
606	GC	Phthalate ester
607	GC	Nitrosamines
608	GC	Organochlorine pesticides and PCBs
609	GC	Nitroaromatics and isophorone
610	GC & HPLC	Polycyclic aromatic hydrocarbons
611	GC	Halooethers
612	GC	Chlorinated hydrocarbons
613	GC/MS	2,3,7,8-TCDD (dioxin)
624	GC/MS	Purgeable organics
625	GC/MS	Acid and base/neutral extractable organics

Key: GC = gas chromatography

FIDGC = flame ionization detector gas chromatography

HPLC = high-performance liquid chromatography

GC/MS = gas chromatography/mass spectrometry

Source: http://water.epa.gov/scitech/methods/cwa/methods_index.cfm

Many target compounds can be determined by either a GC or a GC/MS method. Method 624 is a GC/MS method for purgeable organic compounds that includes compounds also determined by GC methods 601, 602, 603, and 612. Method 625 is a GC/MS method for semi volatile organics that includes compounds also detected by GC methods 604, 606, 607, 609, 610, 611, and 612.

Because of the larger number of target compounds, methods 624 and 625 are usually specified for organic analysis of contaminated water. These are supplemented by method 608 for pesticides and polychlorinated biphenyls and method 613 for 2,3,7,8-TCDD (dioxin). If certain compounds are detected by method 625, they should then be confirmed with a GC method specific to that compound.

Not all the organic compounds are purged from the water by the nitrogen gas. These are the semi volatile compounds. Method 625 is for the analysis of extractable semi volatiles. The pH of a 1-L sample is adjusted so that it is greater than 11. The sample is then extracted with methylene chloride. This is known as the **base/neutral fraction**. The pH of the sample is then adjusted to less than 2. The sample is again extracted with methylene chloride to form the acid fraction. Each fraction is chemically dried to remove the water and concentrated by distillation to 1mL. The fractions are then analyzed separately by GC/MS.

The U.S. EPA has created a target compound list of organic chemicals for its contract laboratory program. The 126 compounds on this list are also known as **priority pollutant**

organic compounds. Laboratories are required to identify and quantify any compounds on this list through methods 608, 624, and 625. Table 7.13 presents the target compound list. The first 34 compounds are volatiles determined by method 624. Compounds 35 to 99 are semivolatiles determined through method 625. Pesticides and PCBs constitute compounds 100 to 126 and are detected through method 608.

There are a number of additional EPA methods for organic compounds. One example is **total petroleum hydrocarbons** by method 418.1. In this method a liter of sample is extracted with fluorocarbon 113 at a pH less than 2. Interfering compounds are then removed with a silica gel absorbent. An infrared analysis of the sample is made by direct comparison to a calibration curve made from prepared samples with a known concentration.

The EPA's "Test Methods for Evaluating Solid Waste, Physical/Chemical Methods," also known as SW-846, is a compendium of analytical and sampling methods for solid waste materials that have been approved for use in complying with the RCRA regulations. An example includes method 8260c "Volatile Organic Compounds By Gas Chromatography/Mass Spectrometry (GC/MS)," which is used to determine volatile organic compounds (VOC) in a variety of solid waste matrices. This method is applicable to nearly all types of samples, regardless of water content, including ground and surface water, soils, and sediments. Method 8095 "Explosives by Gas Chromatography" may be used to determine the concentrations of various explosives in water and soil using capillary column gas chromatography with an electron capture detector (GC/ECD). The compounds analyzed by this method are nitroaromatics, nitramines, and nitrate esters. (More information about SW-846 methods can be obtained from the U.S. EPA at <http://www.epa.gov/osw/hazard/testmethods/sw846/online/index.htm#table>).

Contaminants of emerging concern have only recently been detected in the environment and at this time, analytical methods are still being developed and tested. For instance, method 1694 is for determination of pharmaceuticals and personal care products (PPCPs) in multi-media environmental samples by high performance liquid chromatography combined with tandem mass spectrometry (HPLC/MS/MS). EPA Method 1698 is for determination of steroids and hormones in multi-media environmental samples by high resolution gas chromatography combined with high resolution mass spectrometry (HRGC/HRMS). Similarly, EPA Method 1614 is for determination of brominated diphenyl ether (BDE) congeners in water, soil, sediment, biosolids, tissue, and other sample matrices by HRGC/HRMS while method 1699 is for determination of selected organochlorine, organo-phosphorus, triazine, and pyrethroid pesticides by HRGC/HRMS. At this time, these methods have been peer reviewed and tested in a single lab. The contaminants in these methods are not currently regulated, nor have the methods been promulgated in 40 CFR Part 136. Analytical methods are constantly being upgraded. For instance, on August 7, 2017, the U.S. EPA updated its acceptable methods for analysis of physical, chemical, and biological components of water and wastewater under the Clean Water Act.

The analysis of water samples will frequently result in the analyst determining that a particular compound was not found. The answer that is reported, however, is not zero. It is instead reported as less than detection, with the **detection limit** given. The limit of detection is the lowest concentration level that can be determined to be

TABLE 7.13 Target compound list.

Number	Chemical Name	Number	Chemical Name	Number	Chemical Name
1	Chloromethane	43	<i>bis</i> (2-Chloroisopropyl) ether	85	<i>di</i> -Butyl phthalate
2	Bromomethane	44	4-Methylphenol	86	Fluoranthene
3	Vinyl chloride	45	<i>n</i> -Nitrosodi- <i>n</i> -Propylamine	87	Pyrene
4	Chloroethane	46	Hexachloroethane	88	<i>Butyl</i> benzyl phthalate
5	Methylene chloride	47	Nitrobenzene	89	3,3'-Dichlorobenzidine
6	Acetone	48	Isophorone	90	Benz[<i>a</i>]anthracene
7	Carbon disulfide	49	2-Nitrophenol	91	Chrysene
8	1,1-Dichloroethene	50	2,4-Dimethylphenol	92	<i>bis</i> [2-Ethylhexyl] phthalate
9	1,1,1-Dichloroethane	51	Benzzoic acid	93	<i>di</i> - <i>n</i> -Octyl phthalate
10	1,2-Dichloroethene	52	<i>bis</i> (2-Chloroethoxy) methane	94	Benz[<i>b</i>]fluoranthene
11	Chloroform	53	2,4-Dichlorophenol	95	Benz[<i>k</i>]fluoranthene
12	1,2-Dichloroethane	54	1,2,4-Trichlorobenzene	96	Benz[<i>a</i>]pyrene
13	2-Butanone	55	Naphthalene	97	Indeno [1,2,3- <i>c</i>]pyrene
14	1,1,1-Trichloroethane	56	4-Chloroaniline	98	Dibenz[<i>a</i> , <i>h</i>]anthracene
15	Carbon tetrachloride	57	Hexachlorobutadiene	99	Benz[<i>g</i> , <i>h</i>]perylene
16	Vinyl acetate	58	4-Chloro- <i>m</i> - cresol	100	BHC-alpha
17	Bromodichloromethane	59	2-Methylphthalene	101	BHC-beta
18	1,2-Dichloropropane	60	Hexachlorocyclopentadiene	102	BHC-gamma ([indane])
19	<i>cis</i> -1,3-Dichloropropene	61	2,4,6-Trichlorophenol	103	BHC-delta
20	Trichloroethene	62	2,4,5-Trichloropheno	104	Heptachlor
21	Chlor dibromomethane	63	2-Chloronaphthalene	105	Aldrin
22	1,1,2-Trichloroethane	64	2-Nitroaniline	106	Heptachlor epoxide
23	Benzene	65	Dimethyl phthalate	107	Endosulfan 1 (alpha)
24	<i>trans</i> - 1,3-Dichloropropene	66	Acenaphthylene	108	Dielein
25	Bromoform	67	2,6-Dinitrotoluene	109	4,4'-DDE
26	4-Methyl-2-pentanone	68	3-Nitroaniline	110	Endrin
27	2-Hexanone	69	Acenaphthene	111	Endosulfan 2 (beta)
28	Tetrachloroethene	70	2,4-Dinitrophenol	112	4,4'-DDD
29	Toluene	71	4-Nitropheno	113	Endosulfan sulfate
30	1,1,2,2-Tetrachloroethane	72	Dibenzo[furan]	114	DDT-P/P' (4,4'-DDT)
31	Chlorobenzene	73	2,4-Dinitrotoluene	115	Methoxychlor
32	Ethylbenzene	74	Diethyl phthalate	116	Endrin ketone
33	Styrene	75	4-Chlorophenyl phenyl ether	117	Chlordane, alpha
34	Xylene, total	76	Fluorene	118	Chlordane, beta
35	Phenol	77	4-Nitroaniline	119	Toxaphene
36	<i>bis</i> (2-Chloroethyl) ether	78	4,6-Dinitro-2-methylphenol	120	PCB-1016 (Aroclor 1016)
37	2-Chlorophenol	79	<i>NN</i> -Nitrosodiphenylamine	121	PCB-1221 (Aroclor 1221)
38	1,3-Dichlorobenzene	80	4-Bromophenyl phenyl ether	122	PCB-1232 (Aroclor 1232)
39	1,4-Dichlorobenzene	81	Hexachlorobenzene	123	PCB-1242 (Aroclor 1242)
40	Benzyl alcohol	82	Pentachlorophenol	124	PCB-1248 (Aroclor 1248)
41	1,2-Dichlorobenzene	83	Phenanthrene	125	PCB-1224 (Aroclor 1224)
42	2-Methylphenol	84	Anthracene	126	PCB-1260 (Aroclor 1260)

statistically different than a blank sample with 99% confidence (American Chemical Society 1983). A **method detection limit** is specified for each of the EPA 600 series analytical procedures. The **limit of quantification** is the level above which the quantitative results may be expressed with a specified degree of confidence. Values between the detection limit and the limit of quantification may be reported as **estimated values**.

Swallow, Shifrin, and Doherty (1988) point out some pitfalls in the analysis of organic compounds in groundwater. The GC/MS instruments are designed for automatic operation, with the mass spectra matched electronically to a library spectrum. This match may not be accurate. Swallow, Shifrin, and Doherty report one case where the same compound was reported as eight different compounds in 13 samples, even though the spectra were virtually identical. The only differences were small and could be attributed to background interferences. If an experienced analyst had not examined the spectra, the error would not have been found. Reference standards are run on a limited set of potential compounds, and the accuracy of matching is high with compounds that have been used as a reference. However, for many compounds for which a reference has not been run, the automated procedure may not get a good match between the sample spectrum and a library spectrum. If no match is found, then the sample will be reported as an unknown. However, this could be a significant pollutant at the site under investigation and very important, even though a library match could not be made. In that case reference standards of unusual compounds that might have been used in the area would need to be prepared to obtain additional spectra for the library.

The instruments are sensitive, and large concentrations of a compound may not be tolerated. **Sample dilution** may be necessary for samples where one or more compounds are in high concentration. These are reported as diluted samples. However, dilution raises the detection limits for all compounds. A sample may require dilution because of a high concentration of a more-or-less benign compound, and the resulting high detection limits may then mask the presence of an important compound. A 10:1 dilution will result in a 10-fold increase in the detection limit.

Quality assurance and quality control (QA/QC) are important parts of any analytical program for organic chemicals. A quality-assurance and quality-control program aims to determine the **accuracy**, or correctness, of the data as well as the **precision**, or repeatability, of the analyses.

Field and **method blanks** are used to detect if any organics are being inadvertently introduced during the sampling and analysis procedures. A field blank is a sample of very pure water that is run through the sampling equipment and then put into a bottle and returned to the lab for analysis. If all goes well, the field blank should not contain any organic compounds. Method blanks are also used to determine the purity of the solvents and reagents used in the analysis. Method blanks are samples of distilled water that are analyzed using the solvents and chemicals called for in the procedure.

If a field and/or method blank contains organic compounds, these compounds were introduced during the sampling or analytical procedures. Certain organic compounds that are used in laboratories are frequently detected in the method blanks. These compounds include acetone, methylene chloride, toluene, 2-butanone, di-*n*butyl phthalate, di-*n*-octyl phthalate, and *bis*(2-ethylhexyl) phthalate. If one of these compounds is present in a field or method blank, then the U.S. EPA's Laboratory Data Validation

Functional Guidelines specify that the detection limit for that compound be set at 10 times the greatest amount found in a blank. For all other organic compounds that might be found in a method or field blank, the detection limit is set at five times the greatest amount found in the blank.

Spiked samples have a known amount of an organic compound added to water and then run through the analytical process. If possible, uncontaminated groundwater from the site is used to prepare the spike. This becomes a standard solution; since the initial concentration is known, a **percent recovery** of the analyte can be determined. A perfect analysis will have a 100% recovery. The QA/QC specifications for the lab contract will determine an acceptable percent recovery for valid data. If too much or too little of the spiked compound is recovered, the reported data are not valid.

Duplicate samples are used to validate the precision of the analysis. The lab may take a sample from the field, split it into two or more aliquots, and analyze them to make a **lab duplicate**. The hydrogeologist may also collect a duplicate or triplicate sample in the field and submit it as a field duplicate. Most often field duplicates are submitted as blind duplicates so that the analyst doesn't know that a split sample was submitted. Standard procedures generally call for one split sample to be collected for every ten field samples.

■ 7.9 Fingerprinting Petroleum Distillates and Coal Tar

When one analyzes a NAPL, groundwater, or soil using the target compound list one obtains the concentrations of only those compounds on the list. A contract may also require the tentative identification of a few additional compounds. For instance, U.S. EPA methods 1614 and 418.1 target groups or fractions of chemical hydrocarbons; for example, measurement of total petroleum hydrocarbons (TPH) and EPA priority PAHs are determined. Also, EPA Methods, 1983, 1986, 1997, 1999 have been used as routine procedures for determination of volatile and semi volatile aromatic hydrocarbons presented in spilled oil and petroleum product samples. However, the data generated from these methods are generally insufficient to answer the fundamental questions raised in an oil spill investigation, such as type and source, weathering status of spilled oil, potential spillers (Wang and Fingas 2003) (see Chapter 8).

A screening analysis for hydrocarbons in soil may also be done using the total petroleum hydrocarbon test (TPH) (Zema et al. 1995). This is a gas chromatographic analysis that separates the organic compounds on the basis of their boiling point. All of the peaks that fall in a certain boiling point range are assumed to come from a petroleum hydrocarbon. Their mass is combined and the sum is assigned to the particular compound. Typically all of the peaks that would fall in the C_4 to C_{10} range are assumed to come from gasoline and all in the C_{10} to C_{24} peaks are assumed to come from diesel fuel. This approach has several problems. In the first place, it will include peaks that come from compounds that are not associated with refined petroleum compounds, such as chlorinated hydrocarbons and naturally occurring hydrocarbons. Moreover, gasoline and diesel fuel have a wide range of variability and there is overlap in their boiling range. As a result the TPH analysis is not particularly accurate and may even indicate the presence of gasoline or diesel fuel when none is there. In addition, there are numerous petroleum distillates that are neither gasoline nor diesel fuel that fall within these

two ranges. For example, the TPH test cannot distinguish between kerosene, diesel fuel, or fuel oil, all of which fall in the diesel fuel range. If TPH is used as a cleanup standard for petroleum contaminated soil undergoing bioremediation, the residuals in the soil after biodegradation may trigger a TPH response, even after all of the toxic compounds have been removed.

A much more exacting identification of hydrocarbons in soil and NAPLs can be made. One such method uses a gas chromatograph followed by a flame ionization detector (GC/FID) (Zema et al. 1995; Boehm et al. 1997). The GC/FID analysis creates a trace which shows peaks that elute from the gas chromatographic column as a function of time; the lower boiling point compounds will elute first. The GC/FID trace is like a fingerprint. It can be used to identify the particular petroleum distillate and also indicate if it is fresh or weathered.

Figure 7.23 shows GC/FID traces for unweathered gasoline. It can be seen that there is significant variation among different types of gasoline and gasoline sold in different seasons. Unweathered gasoline has peaks that in general elute between C_4 and C_{12} . Gasoline has a high concentration of monoaromatic hydrocarbons: benzene (C_6), toluene (C_7), ethylbenzene (C_8), xylene (C_8) and trimethylbenzene (C_9).

Figure 7.24 has GC/FID traces for unweathered middle distillates. The general range for the middle distillate fuel compounds is C_{10} to C_{24} . However, mineral spirits has a range of C_7 to C_{12} . The middle distillates do have components that elute in the gasoline range, including BTEX compounds. The middle distillates are primarily normal alkanes and naphthalenes, which are much less soluble than the BTEX compounds.

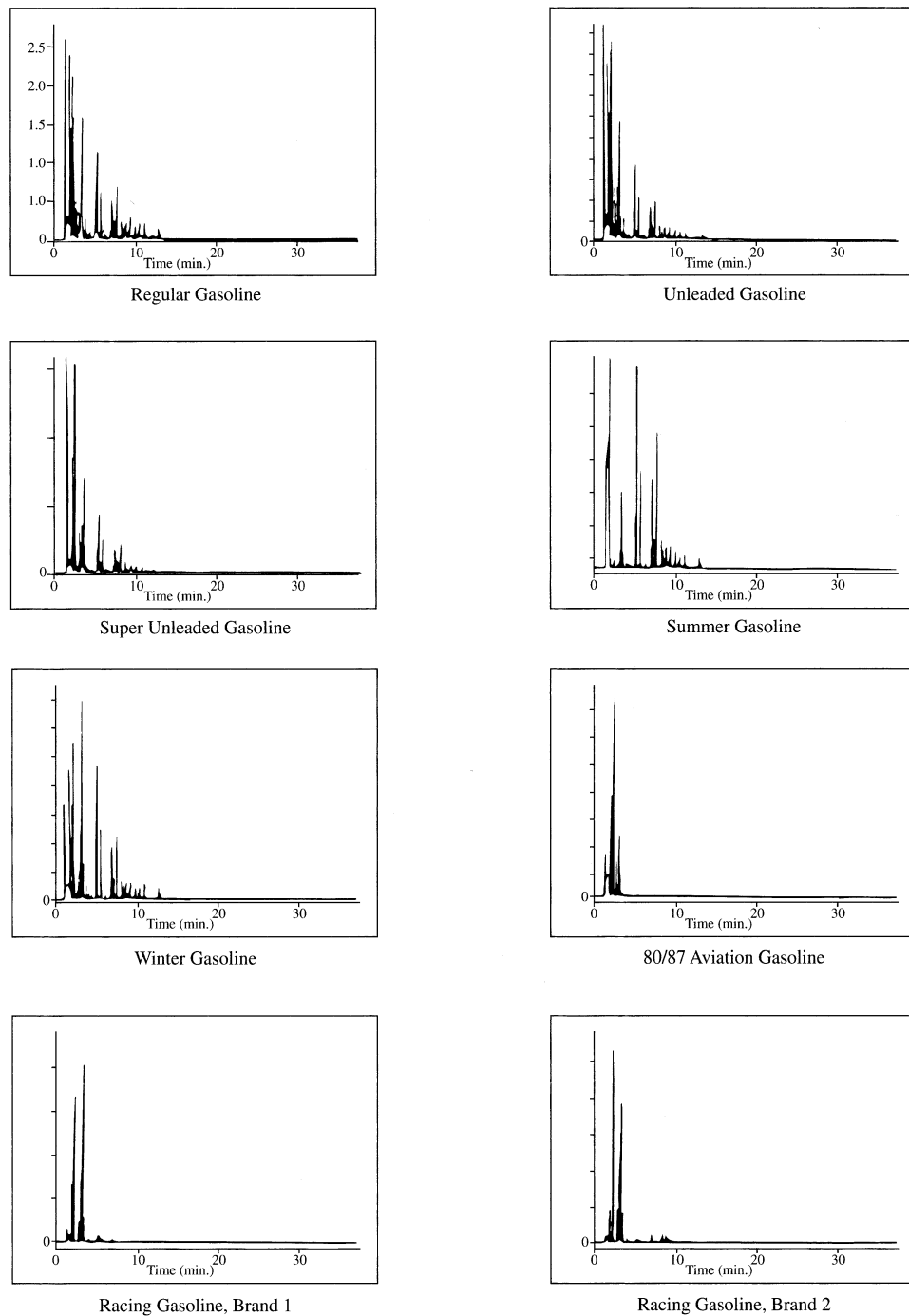
The late distillates are shown on Figure 7.25. These have most of their peaks greater than C_{24} . While they tend to have few compounds that are very soluble, they may contain polynuclear aromatic compounds.

Coal tar is shown on Figure 7.26. The compounds listed on Table 7.5 make up this chromatograph.

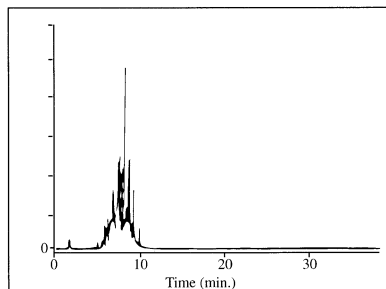
When petroleum hydrocarbons weather, they lose the more volatile compounds. The weathering may be due to volatilization or biodegradation. The result is a shift in the GC/FID trace to the higher molecular weight fraction of the distillate. This is illustrated in Figure 7.27.

The GC/FID traces in Figures 7.17 through 7.21 are for either a product sample or a soil sample. When these compounds dissolve in water, their fingerprint changes dramatically due to the differing solubilities of the various components of each product (Zemo et al. 1995). Table 7.14 lists the water solubility of selected gasoline components at 25°C. In order to know the water solubility of a compound in contact with a specific hydrocarbon, one would have to make a calculation using Raoult's Law. (Section 3.3.7) Most of the compounds in petroleum distillates have very low water solubilities. Gasoline will yield primarily BTEX, other benzenes (e.g., trimethylbenzene, methyethylbenzene, etc.), and naphthalenes. Diesel fuel will yield these same compounds plus phenanthrene and anthracene. Coal tar will have all of the above plus a few additional polynuclear aromatics, such as acenaphthene, acenaphthylene, and fluorene. Their dissolved phase GC/FID traces will be somewhat similar and difficult to interpret as to the parent product.

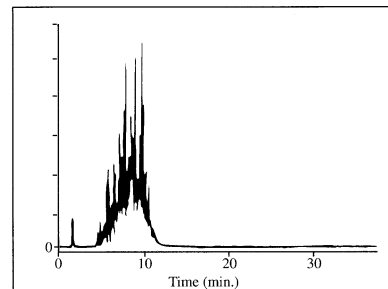
Advances in analytical methods have led to a number of different approaches to determine the parent compound of dissolved phase hydrocarbons (e.g., Stout et al. 2002).

FIGURE 7.23 GC/FID traces of unweathered gasoline.

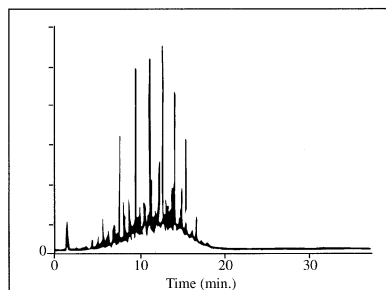
Source: J. E. Bruya, Friedman & Bruya, Inc., *Environmental Chemists*, Seattle WA. Used with permission.

FIGURE 7.24 GC/FID traces of unweathered middle distillate petroleum hydrocarbons.

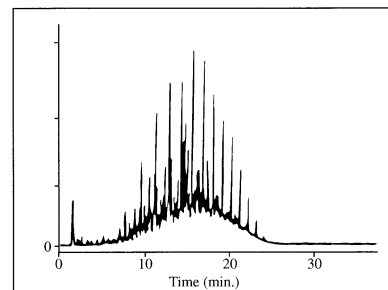
Stoddard Solvent



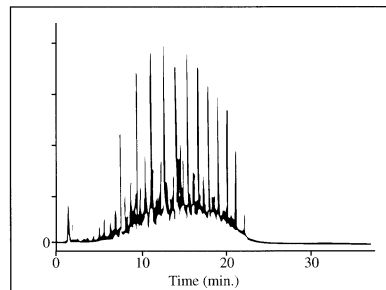
Mineral Spirits



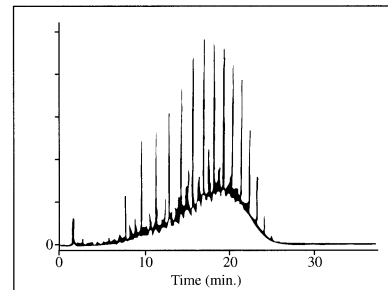
Kerosene



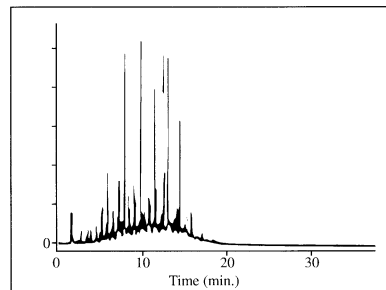
Fuel Oil



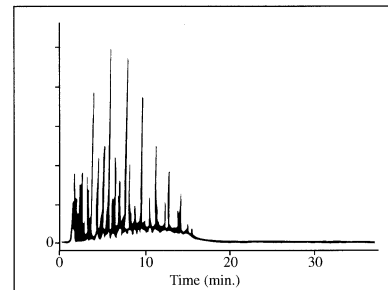
Diesel Fuel #1



Diesel Fuel #2

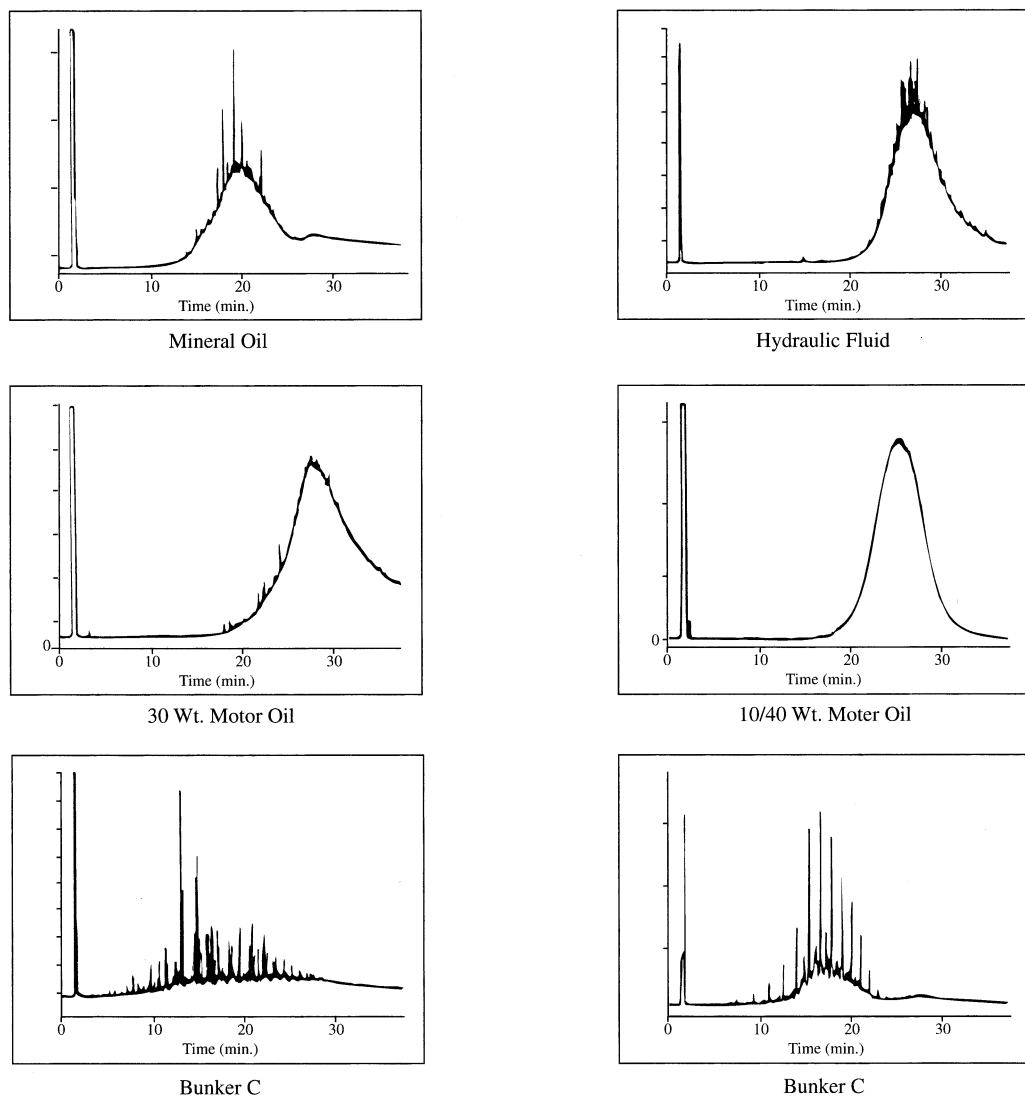


Jet A



JP-4

Source: J. E. Bruya, Friedman & Bruya, Inc., *Environmental Chemists*, Seattle WA. Used with permission.

FIGURE 7.25 GC/FID traces of late distillate petroleum hydrocarbons.

Source: J. E. Bruya, Friedman & Bruya, Inc., *Environmental Chemists*, Seattle WA. Used with permission.

One example is to perform a fingerprinting analysis of degradation-resistant PAH and biomarker compounds. PAH ratios can be useful for distinguishing petrogenic hydrocarbons—i.e., those compounds associated with petroleum—from pyrogenic hydrocarbons—i.e., compounds associated with the combustion of petroleum, wood, coal—including creosote and coal tar. By plotting PAH ratios, including anthracene / (anthracene+phenanthrene); fluoranthene / (fluoranthene+pyrene); benzo(a)anthracene / chrysene and fluoranthene / pyrene, it may be possible to distinguish between combustion and petroleum sources. The analysis of PAH ratios may require

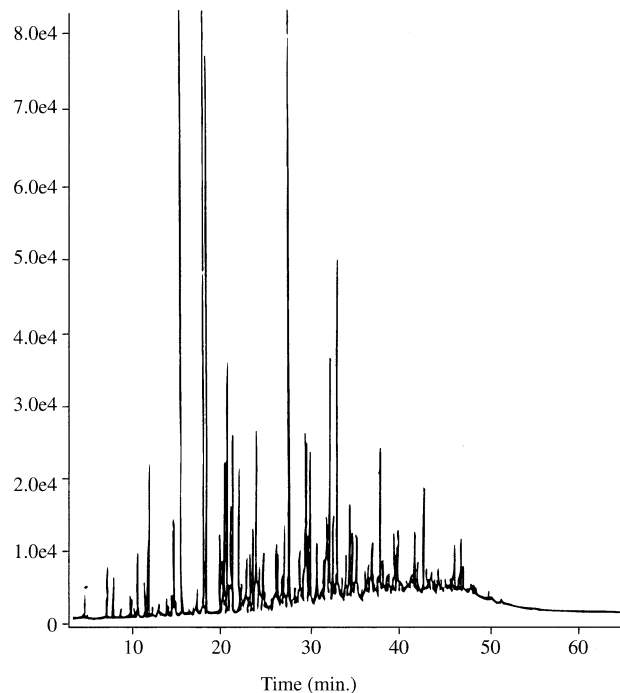
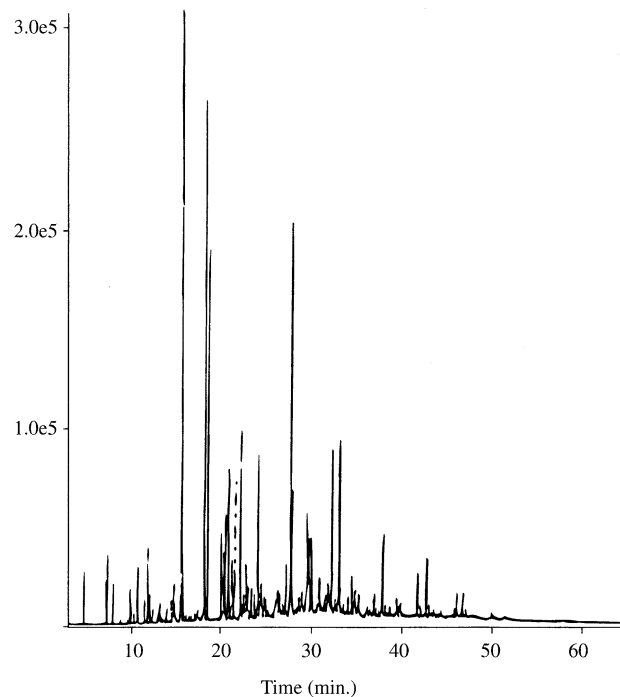
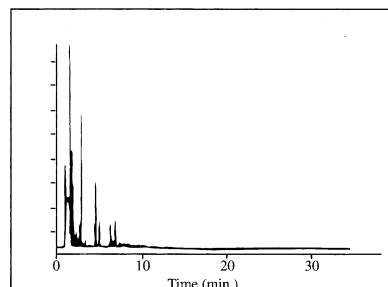
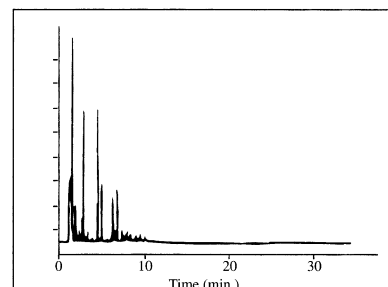
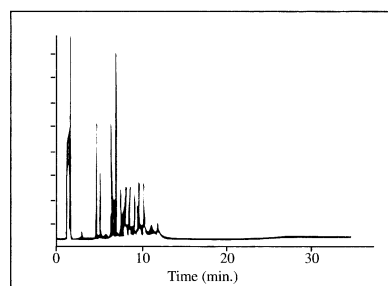
FIGURE 7.26 GC/FID trace of tar from two manufactured gas plants.

FIGURE 7.27 GC/FID traces showing the effects of weathering on gasoline and diesel fuel.

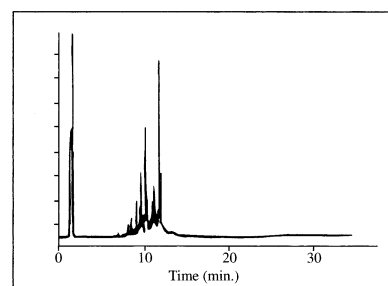
Unweathered Gasoline



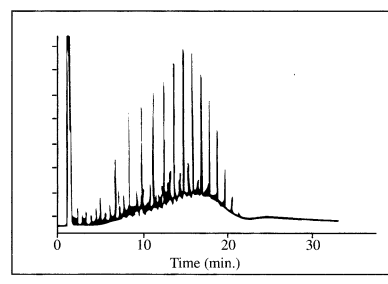
60% Evaporated Gasoline



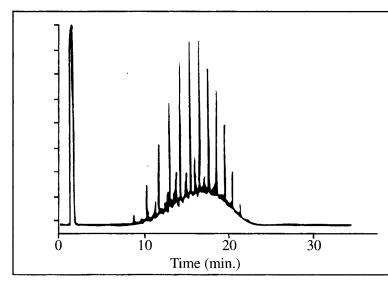
80% Evaporated Gasoline



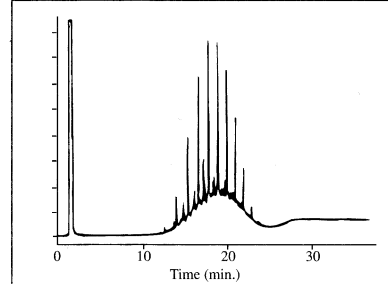
98% Evaporated Gasoline



Unweathered Diesel



20% Evaporated Diesel



50% Evaporated Diesel

Source: J. E. Bruya, Friedman & Bruya, Inc., Environmental Chemists, Seattle WA. Used with permission.

TABLE 7.14 Water solubility of selected hydrocarbons found in petroleum distillates and manufactured gas plant tars.

	Water solubility @ 25°C	Formula weight
Benzene	1780 mg/L	78.11
Toluene	500 mg/L	92.14
p-Xylene	200 mg/L	106.17
o-Xylene	170 mg/L	106.17
m-Xylene	170 mg/L	106.17
Ethylbenzene	150 mg/L	106.17
1,2,3-Trimethylbenzene	63 mg/L	120.19
1,2,4-Trimethylbenzene	57 mg/L	120.19
1,3,5-Trimethylbenzene	50 mg/L	120.19
Naphthalene	32 mg/L	128.18
2-Methylnaphthalene	25 mg/L	142.20
Acenaphthene	3.9 mg/L	154.21
Acenaphthylene	3.9 mg/L	152.20
Fluorene	2.0 mg/L	166.22
Phenanthrene	1.3 mg/L	178.24
Fluoranthene	0.26 mg/L	202.26
Pyrene	0.13 mg/L	202.26
Anthracene	0.075 mg/L	178.24

supplemental information that can be gained from a variety of biomarkers, such as tricyclic, tetracyclic and pentacyclic terpanes, and steranes. Biomarkers are derived from organisms involved in the oil formation process. These markers have been used in characterization of crude oils and oil fractions (e.g., Suneel et al. 2014).

Another fingerprinting approach relies on C₃-dibenzothiophenes, which represents a group of more than 20 individual isomers that are present at different relative abundances in oils. Their distributions provide information about the source carbon, depositional environment during the oil formation, the existence of any diagenetic sources that can be used to fingerprint the sample (Boehm et al. 1997). Another marker found in crude oil are naturally occurring pigments known as petroporphyrins. They are the product of the metabolism of chlorophyll by microorganisms and are usually complexed with metals, predominately nickel and vanadium. The chemical identity of petroporphyrins varies between sources, depending upon the biological conditions inherent to each site. This permits fingerprinting oil samples and link them to their geographic origin (Wang and Fingas 2003).

Finally, Hayes et al. (1990) used isotope ratio to investigate differences in the carbon isotope composition of individual saturated and aromatic hydrocarbons. This approach detects small isotopic differences between compounds such as alkylated aromatic isomers. Stable isotopes can also assist in elucidating the depositional environment, maturity, migration, and biodegradation of spilled oils. Philip (2002) provides an overview of the application of stable isotopes and radioisotopes in environmental forensics to classify crude oils, petroleum products, and tars. Forensics and tracing, tracking, dating, and fingerprinting techniques will be further discussed in the next chapter.

■ 7.10 Summary

There are a number of important physical properties of organic chemicals that influence their behavior. These include the melting point and boiling point, density, vapor pressure, vapor density, octanol-water partition coefficient, and Henry's law constant. Organic compounds are based on carbon, which may be bonded to hydrogen, halides, oxygen, nitrogen, phosphorus, and sulfur. The simplest organic compounds are hydrocarbons, which have only carbon and hydrogen. Carbon atoms have four bonding locations and may form single, double, and triple bonds with other carbon atoms. There is a formal system for naming organic compounds, although many compounds have common names that arose before the formal system was developed. Many organic compounds may be degraded by chemical and microbial means that reduce the molecular weight and complexity of the compounds. The end product of degradation of hydrocarbons is carbon dioxide or methane, depending upon the conditions under which degradation occurs. Organic compounds dissolved in water are most commonly analyzed by gas chromatography, mass spectrometry, or a combination of both.

Because of increasing analytical capabilities a number of emerging contaminants have been identified. Currently, little is known about their environmental fate and transport. Fingerprinting using such methods as GC/FID can be used to determine the origin of a NAPL product or a hydrocarbon in the soil and water.

References

- Air Force Civil Engineer Center. 2004. *Principles and Practices of Enhanced Anaerobic Bioremediation of Chlorinated Solvents*. Joint project of AFCEE and Naval Facilities Engineering Command Engineering Service Center, prepared by Parson Engineering, 138 pp.
- Australian Competition and Consumer Act. 2010. *Consumer Protection Notice No. 11 of 2011 - Permanent ban on children's products containing more than 1% diethylhexyl phthalate (DEHP) - F2011L00192*. Accessed October 5, 2015 from www.comlaw.gov.au/Details/F2011L00192
- Barker, J. F., and G. C. Patrick. 1985. Natural attenuation of aromatic hydrocarbons in a shallow sand aquifer. *Proceedings of the Conference on Petroleum Hydrocarbons and Organic Chemicals in Ground Water: Prevention, Detection and Restoration*, 160–177. Dublin, Ohio: National Water Well Association.
- Barker, J. F., G. C. Patrick, and D. Major. 1987. Natural attenuation of aromatic hydrocarbons in a shallow sand aquifer. *Ground Water Monitoring Review* 7:64–71.
- Bass, D. H., and B. Riley. 1995. Highly soluble MTBE responds to pumping. *International Ground Water Technology* 1:13–17.
- Berdugo-Clavijo, C., X. Dong, J. Soh, C. W. Sensen, and L. M. Gied. 2012. Methanogenic biodegradation of two-ringed polycyclic aromatic hydrocarbons. *FEMS Microbiology Ecology* 81:124–133.
- Bleise, A., P. R. Danesi, and W. Burkart. 2002. Properties, use and health effects of depleted uranium (DU): A general overview. *Journal of Environmental Radioactivity* 64:93–112.
- Brown, R. A., R. E. Hinchee, R. D. Norris, and J. T. Wilson. 1996. Bioremediation of petroleum hydrocarbons: A flexible, variable speed technology. *Bioremediation Journal* 6:95–108.
- Boehm, P. D., G. S. Douglas, W. A. Burns, P. J. Mankiewicz, D. S. Page, and E. A. Bence. 1997. Application of petroleum hydrocarbon chemical fingerprinting and allocation techniques after the Exxon Valdez oil spill. *Marine Pollution Bulletin* 38:599–613.
- Boving, T. B. 2014. Forensic analysis of MTBE contamination using basic hydrogeologic concepts. *Journal of Forensic Sciences* 59:967–973.
- Bumpus, J. A. 1989. Biodegradation of polycyclic aromatic hydrocarbons by *Phanerochaete chrysoporum*. *Applied and Environmental Microbiology* 55:154–158.

- Butler, B. J., and J. F. Barker. 1996. "Chemical and microbial transformations and degradation of chlorinated solvent compounds." In *Dense Chlorinated Solvents and other DNAPLs in Ground Water: History, Behavior, and Remediation*, eds. J. F. Pankow and J. A. Cherry. Waterloo, Canada: Waterloo Press, 522 pp.
- Butt, C. M., U. Berger, R. Bossi, and G. T. Tomy. 2010. Levels and trends of poly- and perfluorinated compounds in the arctic environment. *Science of the Total Environment* 408:2936–65.
- Campos, D. 1997. Field demonstration of UV.H₂O₂ on the treatment of groundwater contaminated with HMPA. In *Chemical Oxidation: Technology for the Nineties, Volume 6*, eds. W. W. Eckenfelder, A. R. Bowers, and J. A. Roth. Lancaster PA: Technomic Publishing Co., Inc., 297 pp.
- Cápiro, N. L., B. P. Stafford, W. G. Rixey, P. B. Bedient, and P. J. J. Alvarez. 2007. Fuel-grade ethanol transport and impacts to groundwater in a pilot-scale aquifer tank. *Water Research* 41:656–664.
- Chang, W., Y. Um, and T. R. Holoman. 2006. Polycyclic aromatic hydrocarbon (PAH) degradation coupled to methanogenesis. *Biotechnology Letters* 28:425–430.
- Chapelle, F. H., P. M. Bradley, D. R. Lovley, and D. A. Vroblesky. 1996. Measuring rates of biodegradation in a contaminated aquifer using field and laboratory methods. *Ground Water* 34:691–698.
- Chatwell, I. 2012. P21—Assessment, remediation and risk assessment of perfluorinated chemicals at 2 former fire training areas. *Reproductive Toxicology* 33:606.
- Chiang, C. Y., J. P. Salanitro, E. Y. Chai, J. D. Colhort, and C. L. Klein. 1989. Aerobic biodegradation of benzene, toluene, and xylene in a sandy aquifer-data analysis and computer modeling. *Ground Water* 27:823–34.
- Clausen, J., J. Robb, D. Curry, and N. Korte. 2004. A case study of contaminants on military ranges: Camp Edwards, Massachusetts, USA. *Environmental Pollution* 129:13–21.
- Cline, P. V., and D. R. Viste. 1985. Migration and degradation patterns of volatile organic compounds. *Waste Management & Research* 3:351–360.
- Davis, J. W., N. J. Klier, and C. L. Carpenter. 1994. Natural biological attenuation of benzene in ground water beneath a manufacturing facility. *Ground Water* 32:215–226.
- de Wit, C. A., D. Herzke, and K. Vorkamp. 2010. Brominated flame retardants in the Arctic environment—trends and new candidates. *Science of the Total Environment* 408:2885–918.
- DiGuiseppi, W. H., and C. Whitesides. 2007. Treatment options for remediation of 1,4-dioxane in groundwater. *Environmental Engineer: Applied Research and Practice* 2:1–7.
- Dottridge, J., P. Hardisty, A. Hart, and L. Zambellas. 2000. MTBE in groundwater in the UK and Europe. In *Ground Water: Prevention, detection, and remediation conference*. Anaheim, CA: National Groundwater Association. 321–331.
- Eberle, D., R. Ball, and T. B. Boving. 2015. Peroxone activated persulfate treatment of 1,4-dioxane in the presence of chlorinated solvent co-contaminants. *Chemosphere* 144:728–735.
- Ehrlich, G. G., D. F. Goerlitz, E. M. Godsy, and M. F. Hult. 1982. Degradation of phenolic contaminants in ground water by anaerobic bacteria: St. Louis Park, Minnesota. *Ground Water* 20:703–710.
- Evans, W. C. 1977. Biochemistry of the bacterial catabolism of aromatic compounds in anaerobic environments. *Nature* 270:17–22.
- Filipovic, M., A. Woldegiorgis, K. Norström, M. Bibi, M. Lindberg, and A. H. Österås. 2015. Historical usage of aqueous film forming foam: A case study of the widespread distribution of perfluoroalkyl acids from a military airport to groundwater, lakes, soils and fish. *Chemosphere* 129:39–45.
- Fiedler, H., and V. Borja-Aburto. 2003. *Persistent Organic Pollutants*. New York: Springer Science & Business Media, 443 pp.
- Gary, J. H., and G. E. Handwerk. 2001. *Petroleum Refining Technology and Economics, Fourth Edition*. New York: Marcel Dekker, Inc., 488 pp.
- Gillham, R. W., and S. F. O'Hannesin. 1994. Enhanced degradation of halogenated aliphatics by zero-valent iron. *Ground Water* 32:958–967.
- Glassmeyer, S. T. 2007. The cycle of emerging contaminants. *Water Resources Impact* 9:5–7.
- Gomez, D. E., and P. J. J. Alvarez. 2009. Modeling the natural attenuation of benzene in groundwater impacted by ethanol-blended fuels: Effect of ethanol content on the lifespan and maximum length of benzene plumes. *Water Resources Research* 45:W03409.
- Guerin, W. F., and G. E. Jones. 1988. Two-stage mineralization of phenanthrene by estuarine enrichment cultures. *Applied and Environmental Microbiology* 54:929–936.
- Hall, A. E. 1988. Transformations in soil. In *Environmental Chemistry of Herbicides*, Vol. 1, ed. R. Glover, 171–200. Boca Raton, FL: CRC Press.
- Hammesfahr U., R. Bierl, and S. Thiele-Bruhn. 2011. Combined effects of the antibiotic

- sulfadiazine and liquidmanure on the soil microbial-community structureand functions. *Journal of Plant Nutrition and Soil Science* 174:614–623.
- Harrad, S. 2009. *Persistent Organic Pollutants*. Chichester, UK: John Wiley & Sons, 288 pp.
- Haritash, A. K., and C. P. Kaushik. 2009. Biodegradation aspects of Polycyclic Aromatic Hydrocarbons (PAHs): A review. *Journal of Hazardous Materials* 169:1–15.
- Heitkamp, M. A., and C. E. Cerniglia. 1988. Mineralization of poly-cyclic aromatic hydrocarbons by a bacterium isolated from sediment below an oil field. *Applied and Environmental Microbiology* 54:1612–1614.
- Heitkamp, M. A., and C. E. Cerniglia. 1989. Polycyclic aromatic hydrocarbon degradation by a *Mycobacterium* sp. in a microcosm containing sediment and water from a pristine ecosystem. *Applied and Environmental Microbiology* 55:1968–1973.
- Heitkamp, M. A., J. P. Freeman, D. W. Miller, and C. Cerniglia. 1988. Pyrene degradation by a *Mycobacterium* sp.: Identification of ring oxidation and ring fission products. *Applied and Environmental Microbiology* 54:2556–2565.
- Howard, P. H. 1990. *Handbook of Environmental Fate and Exposure Data for Organic Chemicals, Volume II*. Chelsea, MI: Lewis Publishers, Inc.
- Hruska, K., and M. Franek. 2012. Sulfonamides in the environment: A review and a case report. *Veterinarni Medicina* 57:1–35.
- Hunt, J. M. 1979. *Petroleum Geochemistry and Geology*. New York: W. H. Freeman and Company.
- IRAC (International Agency for Research on Cancer). 1989. Mongraph on the evaluation of carcinogenic risk to humans. *Gasoline* 45:159–201.
- Johnson, R., J. F. Pankow, D. A. Bender, C. V. Price, and J. S. Zogorski. 2000. MTBE—To what extent will past releases contaminate community water supply wells? *Environmental Science & Technology* 34: 210A–217A
- Johnsen, A. R., L. Y. Wick, H. Harms. 2005. Principles of microbial PAH-degradation in soil. *Environmental Pollution* 133:71–84.
- Keith, L. H., W. Crummett, J. Deegan, Jr., R. A. Libby, J. K. Taylor, and G. Wentler. 1983. Principles of environmental analysis. *Analytical Chemistry* 55:2210–218.
- Klecka, G. M., J. W. Davis, D. R. Gray, and S. S. Madsen. 1990. Natural bioremediation of organic contaminants in ground water: Cliffs-Dow superfund site. *Ground Water* 28:534–543.
- Kreamer, D. K., and K. J. Stezenbach. 1990. Development of a standard, pure-compound base gasoline mixture for use as a reference in field and laboratory experiments. *Ground Water Monitoring Review* 10:135–145.
- Lapworth, D. J., N. Baran, M. E. Stuart, R. S. Ward. 2012. Emerging organic contaminants in groundwater: A review of sources, fate and occurrence. *Environmental Pollution* 163:287–303.
- Lauritzen, E. K. 2001. The challenge of demilitarisation and disposal of ammunition. *Military Technology* 25: 34–39.
- Lawrence, S. J. 2006. *Description, Properties, and Degradation of Selected Volatile Organic Compounds Detected in Ground Water—A Review of Selected Literature*. U.S. Geological Survey Open-File Report 2006–1338, 65 pp.
- Lim T. C., B. Wang, J. Huang, S. Deng, and G. Yu. 2011. Emission inventory for PFOS in China: Review of past methodologies and suggestions. *The Scientific World Journal* 11:1963–1980.
- Lindstrom, A. B., M. J. Strynar, and E. L. Libelo. 2011. Polyfluorinated compounds: Past, present, and future. *Environmental Science & Technology* 45:7954–7961.
- Lohmann, R., and I. M. Belkin. 2014. Organic pollutants and ocean fronts across the Atlantic Ocean: A review. *Progress in Oceanography* 128:172–184.
- Loos, R., G. Locoro, S. Comero, S. Contini, D. Schwesig, and F. Werres. 2010. Pan-European survey on the occurrence of selected polar organic persistent pollutants in ground water. *Water Research* 44:4115–126.
- Lopez, Z., J. Vila, C. Mingüillon, and M. Grifoll. 2006. Metabolism of fluoranthene by *Mycobacterium* sp. strain AP1. *Applied Microbiology and Biotechnology* 70:747–756.
- Lopez, Z., J. Vila, J. J. Ortega-Calvo, and M. Grifo. 2007. Simultaneous iododegradation of creosote-polycyclic aromatic hydrocarbons by a pyrene-degrading *Mycobacterium*. *Applied Microbiology and Biotechnology* 78:165–172.
- Major, D. W., C. I. Mayfield, and J. F. Barker. 1988. Biotransformation of benzene by denitrification in aquifer sand. *Ground Water* 26:8–14.
- Manahan, S. E. 1984. *Environmental Chemistry, Fourth Edition*. Boston: PWS Publishers, 612 pp.
- McCarty, P. L., M. Reinhard, and B. E. Rittman. 1981. Trace organics in groundwater. *Environmental Science and Technology* 15:40–51.

- McCarty, P. L. 1996. Symposium on Natural Attenuation of Chlorinated Organics in Ground Water, Dallas, TX, September 11–13, 1996, U.S. EPA, EPA/540/R-96/509, pp. 5–9.
- McDowell, C. J., and S. E. Powers. 2003. Mechanisms affecting the infiltration and distribution of ethanol-blended gasoline in the vadose zone. *Environ. Sci. Technol.*, 37, 1803–1810
- McDowell, C. J., T. Busheck, and S. E. Powers. 2003. Behavior of gasoline pools following a denatured ethanol spill. *Ground Water* 41:746–757
- Meckenstock, R. U., Safinowski, M., Griebler, C., 2004. Anaerobic degradation of polycyclic aromatic hydrocarbons. *FEMS Microbiology Ecology* 49:27–36
- Mihelcic, J. R., and R. G. Luthy. 1988. Microbial degradation of acenaphthene and naphthalene under denitrification conditions in soil-water systems. *Applied and Environmental Microbiology* 54:1188–1198.
- Mohr, T. 2001. 1,4-Dioxane and other Solvent Stabilizers. White Paper, 52 pp. Accessed June 23, 2015 from <http://www.valleywater.org/WorkArea/DownloadAsset.aspx?id=2686>
- Mohr, T. K. G., J. A. Stickney, and W. H. DiGuiseppe. 2010. *Environmental Investigation and Remediation: 1,4-Dioxane and other Solvent Stabilizers, First Edition*. Boca Raton, FL: CRC Press, 550 pp.
- Molson, J. W., J. F. Barker, E. O. Frind, and M. Schirmer. 2002. Modeling the impact of ethanol on the persistence of benzene in gasoline contaminated groundwater. *Water Resources Research* 38:4:1–4:12.
- Montgomery, J. M. 2007. *Groundwater Chemicals Desk Reference, Fourth Edition*. Boca Rotan, FL: CRC Press.
- Moody, C. A., and J. A. Field. 1999. Determination of perfluorocarboxylates in groundwater impacted by fire-fighting activity. *Environmental Science & Technology* 33:2800–2806.
- Moody, C. A., G. N. Heber, S. H. Strauss, and J. A. Field. 2003. Occurrence and persistence of perfluorooctanesulfonate and other perfluorinated surfactants in groundwater at a fire-training area at Wurtsmith Air Force Base, Michigan, USA. *Journal of Environmental Monitoring* 5:341–345.
- Motzer, W. E. 2001. Perchlorate: Problems, Detection, and Solutions. *Environmental Forensics* 2, no. 4:301–311.
- Mueller, J. G., P. J. Chapman, B. O. Blattmann, and P. H. Pritchard. 1990. Isolation and characterization of a fluorantheneutilizing strain of *Pseudomonas paucimobis*. *Applied and Environmental Microbiology* 56, no. 4:1079–1086.
- Murakami M., K. Kuroda, N. Sato, T. Fukushi, S. Takizawa, and H. Takada. 2009. Groundwater pollution by perfluorinated surfactants in Tokyo. *Environmental Science & Technology* 43, no. 10:3480–3486.
- Naval Facilities Engineering Command. 2004. *Principles and Practices of Enhanced Anaerobic Bioremediation of Chlorinated Solvents*. Technical Report TR-2250-ENV, 461 pp.
- National Industrial Chemicals Notification and Assessment Scheme (NICNAS). 2006. Existing chemical info sheets: Diethylhexyl phthalate. Accessed October 5, 2015 from <http://www.nicnas.gov.au/communications/publications/information-sheets/existing-chemical-info-sheets/diethylhexyl-phthalate-dehp-factsheet>
- Parsons, F., P. R. Wood, and J. DeMarco. 1984. Transformations of tetrachloroethene and trichloroethene in microcosms and groundwater. *Journal of American Water Works Association* 76, no. 2:56–59.
- Paul, A. G., K. C. Jones, and A. J. Sweetman. 2009. A first global production, emission, and environmental inventory for perfluoroctane sulfonate. *Environmental Science & Technology* 43, no. 2:386–392.
- Peng, R. H., X. Ai-Sheng, Y. Xue, X. Y. Fu, F. Gao, W. Zhao, Y. S.Tian, and Q. H. Yao. 2008. Microbial biodegradation of polyaromatic hydrocarbons. *FEMS Microbiology Reviews* 32:927–955
- Philp, R. P. 2002. "Application of stable isotopes and radioisotopes in environmental forensics." In *Introduction to Environmental Forensics*, eds. B. L. Murphy and R. D. Morrison, 99–136. London: Academic Press.
- Pichtel, J. 2012. Distribution and fate of military explosives and propellants in soil: A review. *Applied and Environmental Soil Science* 2012:Article ID 617236.
- Powers, S. E., D. Rice, B. Dooher, and P. J. J. Alvarez. 2001. Will ethanol-blended gasoline affect groundwater quality? *Environmental Science and Technology* 35: 24A–30A
- Prevedouros, K., I. T. Cousins, R. C. Buck, and S. H. Korzeniowski. 2006. Sources, fate and transport of perfluorocarboxylates. *Environmental Science and Technology* 40, no. 1:32–44.

- Rasa, E., B. A. Bekins, D. M. Mackay, N. R. de Sieyes, J. T. Wilson, K. P. Feris, I. A. Wood, and K. M. Scow. 2013. Impacts of an ethanol-blended fuel release on groundwater and fate of produced methane: Simulation of field observations. *Water Resources Research* 49:4907–4926.
- Renewable Fuel Association (RFA). 2015. World fuel ethanol production. Accessed from <http://www.ethanolrfa.org/pages/statistics#E>
- Richardson, S. D., and T. A. Ternes. 2011. Water analysis: Emerging contaminants and current issues. *Analytical Chemistry* 83:4614–4648.
- Rifai, H. S., C. J. Newell, and T. H. Wiedemeier. 2001. “Natural attenuation of chlorinated solvents in ground water.” In *Handbook of Solvents*, ed. G. Wypych, 1571–1611. New York: ChemTec Publishing, 1675 pp.
- Roberts, P. V., J. Schreiner, and G. D. Hopkins. 1982. Field study of organic water quality changes during groundwater recharge in the Palo Alto baylands. *Water Research* 16:1025–1035.
- Roberts, B. L. 1985. In Pursuit of contaminant-free water. *Groundwater Monitoring & Remediation* 5:41–43.
- Schultz, M. M., D. F. Barofsky, and J. A. Field. 2004. Quantitative determination of fluorotelomer sulfonates in groundwater by LC MS/MS. *Environmental Science and Technology* 38, no. 6:1828–1835.
- SERDP (Strategic Environmental Research and Development Program). 2004. *UXO Corrosion—Potential Contamination Source*. SERDP Project ER-1226. 195 pp.
- Smith, A. E. 1988. “Transformations in soil.” In *Environmental Chemistry of Herbicides*, ed. R. Grover, 171–200. Boca Raton, FL: CRC Press.
- Speight, J. G. 2005. *Environmental Analysis And Technology For The Refining Industry*. Hoboken, NJ: John Wiley & Sons, 416 pp.
- Squillace, P. J., J. S. Zogorski, W. G. Wilber, and C. V. Price. 1995. A preliminary assessment of the occurrence and possible sources of MTBE in ground water of the United States, 1993–94. U.S. Geological Survey Open-File Report 95-456.
- Squillace, P. J., J. F. Pankow, N. E. Korte, and J. S. Zorgorski. 1997. Review of the environmental behavior and fate of methyl tert-butyl ether. *Environmental Toxicology and Chemistry* 16:1836–1844.
- Stout, S. A., A. D. Uhler, K. J. McCarthy, S. Emsbo-Mattingly. 2002. “Chemical fingerprinting of hydrocarbons.” In *Introduction to Environmental Forensics*, eds. B. L. Murphy and R. D. Morrison, 137–260. London: Academic Press.
- Stuart, M., D. Lapworth, E. Crane, and A. Hart. 2012. Review of risk from potential emerging contaminants in UK groundwater. *Science of the Total Environment* 416:1–21.
- Suneel, V., P. Vethamony, B. G. Naik, K. Kumar, L. Sreenu, S. V. Samiksha, Y. Tai, and K. Sudheesh. 2014. Source investigation of the tar balls deposited along the Gujarat Coast, India, using chemical fingerprinting and transport modeling techniques. *Environmental Science and Technology* 48:11343–11351.
- Swallow, K. C., N. S. Shifrin, and P. J. Doherty. 1988. Hazardous organic compound analysis. *Environmental Science and Technology* 22:136–142.
- Trojanowicz, M., and M. Koc. 2013. Recent developments in methods for analysis of perfluorinated persistent pollutants. *Microchimica Acta* 180:957–971.
- Trumppolt, C. W., M. Crain, G. D. Cullison, S. J. P. Flanagan, L. Siegel, and S. Lathrop. 2005. Perchlorate: Sources, uses, and occurrences in the environment. *Remediation Journal* 16:65–89.
- U.S. Department of Energy. 2013. *Handbook For Handling, Storing, And Dispensing E85 And Other Ethanol-Gasoline Blends*. DOE/GO-102013-3861, 44 pp.
- U.S. EPA (Environmental Protection Agency). 1999. *Achieving Clean Air and Clean Water: The Report of the Blue Ribbon Panel on Oxygenates in Gasoline*.
- U.S. EPA, Office of Air and Radiation. EPA 420-R-99-021, 119 pp. Accessed October 4, 2015 from <https://www.epa.gov/caaac/achieving-clean-air-and-clean-water-report-blue-ribbon-panel-oxygenates-gasoline>
- U.S. EPA (Environmental Protection Agency). 2010. *Gasoline Composition Regulations Affecting LUST Sites*. EPA/600/R-10/001, 39 pp.
- U.S. EPA (Environmental Protection Agency). 2003. *Characteristics of Spilled Oils, Fuels, and Petroleum Products: 1. Composition and Properties of Selected Oils*. EPA/600/R-03/072, 286 pp.
- U.S. EPA (Environmental Protection Agency). 2007. Phthalates. TEACH chemical summary, 25 pp.
- Vila J., Z. Lopez, J. Sabate, C. Minguillon, A. M. Solanas, and M. Grifoll. 2001. Identification of a novel metabolite in the degradation of pyrene by *Mycobacterium* sp. strain AP1: Actions of the isolate on two- and three-ring polycyclic aromatic hydrocarbons. *Applied Environmental Microbiology* 67:5497–5505.

- Wang, Z., and M. F. Fingas. 2003. Development of oil hydrocarbon fingerprinting and identification techniques. *Marine Pollution Bulletin* 47:423–452.
- Weaver, J. W., L. Jordan, and D. B. Hall. 2005. *Predicted ground water, soil and soil gas impacts from US gasolines, 2004: First analysis of the autumnal data*. EPA/600/R-05/032.
- Weaver, J. W., S. A. Skaggs, D. L. Spidle, and G. C. Stone. 2009. Composition and behavior of fuel ethanol. Prepared for the U.S. Environmental Protection Agency, EPA/600/R-09/037, 69 pp.
- WERC (Water and Environmental Research Center) 2001. *MMR Explosive Remediation Technologies. Independent Technical Review*, 78 pp.
- Wiedemeier, T. H., H. S. Rifai, C. J. Newell, and J. T. Wilson. 1999. *Natural Attenuation of Fuels and Chlorinated Solvents in the Subsurface*. New York: John Wiley & Sons, Inc., 617 pp.
- Wilson, J. T., L. E. Leach, M. Henson, and J. N. Jones. 1986. *In situ* bioremediation as a ground water remediation technique. *Ground Water Monitoring Review* 6, no. 4:56–64.
- Wilson, J. T., P. M. Kaiser, and C. Adair. 2005. *Monitored Natural Attenuation of MTBE as a Risk Management Option at Leaking Underground Storage Tank Sites*. Washington, DC: U.S. Environmental Protection, EPA/600/R-04/179, 74 pp.
- Wisconsin Department of Natural Resources. 2014. Understanding Chlorinated Hydrocarbon Behavior in Groundwater: Investigation, Assessment and Limitations of Monitored Natural Attenuation. WISNR RR-699, October 2014, 101 pp.
- Xie, S., T. Wang, S. Liu, K. C. Jones, A. J. Sweetman, and Y. Lu. 2013. Industrial source identification and emission estimation of perfluorooctane sulfonate in China. *Environment International* 52:1–8.
- Yamashita N., K. Kannan, S. Taniyasu, Y. Horii, T. Okazawa, G. Petrick, and T. Gamo. 2004. Analysis of perfluorinated acids at parts-per-quadrillion levels in seawater using liquid chromatography-tandem mass spectrometry. *Environmental Science and Technology* 38:5522–5528
- Zemo, D. A., J. E. Bruya, and T. E. Graf. 1995. The application of petroleum hydrocarbon fingerprint characterization in site investigation and remediation. *Ground Water Monitoring and Remediation* 15, no. 2:147–156.
- Zenker, M. J., R. C. Borden, and M. A. Barlaz. 2003. Occurrence and treatment of 1,4-Dioxane in aqueous environments. *Environmental Engineering Science* 20:423–432.

Problems

Using the data in Table 7.14 and Equation 3.41, calculate the equilibrium concentrations of hydrocarbons with the following compositions in weight percent, dissolved in water: (Note: Analyses do not add up to 100% due to compounds not listed.)

7.1 Regular gasoline (Density = 0.86 gm/mL)

Benzene	1.7%
Toluene	5.5%
Ethyl benzene	1.2%
o-Xylene	2.4%
m-Xylene	2.2%
p-Xylene	2.6%
1,2,3-Trimethylbenzene	1.2%
1,2,4-Trimethylbenzene	3.8%
1,3,5-Trimethylbenzene	2.7%
Naphthalene	0.7%
Methylnaphthalene	0.9%

7.2 Premium gasoline (Density = 0.86 gm/mL)

Benzene	1.9%
Toluene	20.2%
Ethyl benzene	0.9%
<i>o</i> -Xylene	1.6%
<i>m</i> -Xylene	1.2%
<i>p</i> -Xylene	1.4%
1,2,3-Trimethylbenzene	1.3%
1,2,4-Trimethylbenzene	4.6%
1,3,5-Trimethylbenzene	3.4%
Naphthalene	0.5%
2-Methylnaphthalene	0.2%

7.3 Diesel fuel (density = 0.88 gm/ml)

Benzene Toluene	0.7%
Toluene	1.2%
Ethyl benzene	1.1%
<i>o</i> -Xylene	0.8%
<i>m</i> -Xylene	1.1%
<i>p</i> -Xylene	0.9%
1,2,3-Trimethylbenzene	1.3%
1,2,4-Trimethylbenzene	3.8%
1,3,5-Trimethylbenzene	1.7%
Naphthalene	1.8%
2-Methylnaphthalene	2.1%

7.4 Manufactured gas plant tar (Density = 1.10 gm/mL)

Benzene	0.62%
Toluene	0.60%
Ethyl benzene	0.9%
Xylene (Total)	1.1%
Naphthalene	32%
2-Methylnaphthalene	18%
Acenaphthene	4.3%
Fluorene	4.1%
Phenanthrene	11.1%
Pyrene	7.0%

Fluoranthene	4.1%
Anthracene	2.6%

- a. Make a “star plot” for the substance in problem 7.1.
- b. Make a “star plot” for the substance in problem 7.2.
- c. Make a “star plot” for the substance in problem 7.3.
- d. Make a “star plot” for the substance in problem 7.4.

Site Characterization—Groundwater and Soil Monitoring

■ 8.1 Introduction

Characterization of a potentially contaminated site involves field and laboratory analysis of subsurface properties, with a goal of building a conceptual model of contaminant source strength and configuration, and pollutant movement and transformation with time and space. This, in turn, is done to optimize monitoring strategies, and develop advantageous and cost effective remedial solutions.

The process of characterization begins with identifying the goals of characterization and remediation, and these goals can widely vary. Site characterization approaches will be quite different if the overall goal is to identify parties responsible for pollution, versus a goal of protecting public health, versus a goal of maintaining a vibrant groundwater dependent ecosystem. Further, a site can have several prioritized goals and not just one. Objectives are often linked, for example, one objective might be to minimize costs by requiring a thorough (and perhaps costly) site characterization in order to reduce potentially higher remediation costs by strategically targeting pollutants. There are many different site characterization methodologies including phased or progressive approaches and adaptive management techniques. At a site where very little is known about the nature and extent of subsurface contamination, often a first sampling step is collection and analysis for a broad range of potential contaminants, to be narrowed and focused based on the findings of those early surveys.

It must be emphasized that each site is unique and should not be addressed in a “one size fits all” or “we did it this way at the last site” boilerplate approach. Some of the seemingly smallest changes in geologic heterogeneities at different sites can radically alter subsurface fluid flow, and if unrecognized can cause inappropriate assumptions to be made and incorrect approaches to be followed. Likewise, site-specific physical, human-made features that protrude into or affect the subsurface (e.g., building footings, buried pipeline trenches backed-filled with gravel or other non-native material, groundwater pumping, surface irrigation or paving, application of chemicals at the ground surface, chronic and slow leaks versus massive leaks) all can alter how pollutants change their distribution, phase, form, and potential threat. An underlying note of caution is that the data that monitoring provides is not always representative of the complete hydrogeological picture

or demonstrates contaminant distribution. Not accounting for these unique properties at each site, or blindly assuming that selected monitoring data is broadly representative of actual field conditions, can cost huge sums in misspent money, useless monitoring, ineffective remediation, lost time, and misstated risks (Nielsen 2005).

There are some general perspectives and overall guiding principles regarding monitoring and site characterization that are helpful. They include the following:

1. Resources spent on proper and thorough site characterization typically save many times their investment in reduced remedial costs.
2. Incautious monitoring installation and practices can make the original environmental problem worse by allowing cross-contamination and short-circuiting of contaminant migration.
3. It is standard to have well-defined goals for characterization and remediation before embarking on site activities.
4. It is very helpful to calculate a good mass balance of contaminants early on, including an estimate (or range of estimates) in source mass, amount retained in vadose zone, amount reaching the water table, mass dissolving into water, mass volatilizing into the gaseous phase, amount sorbing onto soils, mass transforming and/or chemically or biologically degrading, and other sources and sinks of contaminant mass.
5. Typically assessment should begin with noninvasive methods (methods that do not appreciably disturb the subsurface at a site) in order to optimize subsequent invasive methods (such as monitoring well installation).
6. Employing an “outside-in” approach where possible is advantageous to reduce equipment contamination or to prevent contaminant spreading, (e.g., drilling monitoring wells first in areas suspected of low contamination rather than “hot spots,” or the practice of sampling wells deemed to be cleanest with low contamination first to reduce the possibility of cross contamination).
7. Phased approaches have benefits in allowing adjustment in monitoring strategies as more information is learned.
8. Consider early/interim remedial action as monitoring and monitoring plans are progressing (beyond just typical emergency response actions to immediate threats). Actions which are taken as monitoring plans are being completed can include: providing early source isolation, plume containment, and extraction of nonaqueous phase liquids to reduce their propensity to migrate.

There are a selection of noninvasive, or minimally invasive techniques available for initial groundwater surveys at potentially contaminated sites, and these procedures are often followed by groundwater and soil sampling. For groundwater sampling, the more invasive methods of installing monitoring wells and collecting groundwater samples have been developed with the specific intention of obtaining a representative sample of water from an aquifer (FDEP 2008; Hughes and Aarons 2014; Aller et al. 1991; NUDLC 2012; Arnold et al. 2009). These monitoring well methods minimize the potential for the introduction of contaminants into the ground through the process of installing a monitoring well. Wells and sampling devices can be constructed of materials that have a minimum tendency to leach materials into and sorb compounds from the water sample. Groundwater samples can be collected in such a manner that

dissolved gases are not lost or exchanged with the atmospheric gases. Soil samples can also be collected for classification and chemical analysis.

Various methods of collecting samples of soil water are also available, as are procedures for determining the location and nature of subsurface contamination. Soil gas sampling can be done to give an indication of areas where volatile organic compounds are contained in the soil or groundwater. Many other forensic approaches help with the determination of groundwater and contaminant travel times, source location and timing, contaminant transformations and phase changes, geological formations and structures, and potential risk.

Proper site characterization can transform understanding and advance the development of effective remedial strategies. Australian guidance defines the “sound science” associated with contaminated site characterization and development of robust site conceptual models as being based on “organized investigations and observations conducted by qualified personnel using documented methods and leading to verifiable results and conclusions” (NSW 2010).

■ 8.2 Noninvasive Measures

At the beginning of a site characterization program, noninvasive methods are employed to understand the site without excessive perturbation of the subsurface. Although monitoring wells are usually an essential part of characterizing groundwater contamination, their installation can trigger vertical migration of pollutants, depending on the method of installation. A site characterization process typically begins with definition of objectives and a review of site specifics and history. Records of facility operations and inventories are investigated, contaminant handling practices at the site are looked into, drains and drywells are located, surface features and drainage patterns are reviewed, buried pipelines are identified, past and present employees may be interviewed, pertinent climatic data checked, existing local wells pinpointed along with associated groundwater quality data, and applicable law and regulations reviewed. As part of this process, facility records and manifests are analyzed to understand the possible mass of contaminants handled historically at the site. Agency and utility files, and regional geologic and hydrogeologic information are evaluated. An integral part of these undertakings is an initial site water balance and contaminant mass balance. Most of these undertakings are office related and not carried out directly on-site.

Air photo interpretation, surface geophysics, and quick soil and surface water survey and screening techniques are minimally invasive field techniques. Soil gas surveys are particularly useful for volatile compounds, and there are other noninvasive and informative practices useful in initial site assessment.

8.2.1 Interpretation of Aerial Photography and Remote Sensing

A review of site surface features, both present-day and historical, are easily accessible with the advent of widely available air photo libraries, such as National Aeronautics and Space Administration (NASA) World Wind and Google Earth. Many things pertinent to site characterization can be observed from visible aerial photography. This includes past and present site structures, roads and access points, possible soil staining

or discoloration, the proximity of nearby creeks and streams, local wetlands and reservoirs and how these change with time, vegetative changes, urbanization, local erosion, industrial surface impoundments, and evaporation ponds. In tectonically active terrain, faults can sometimes be identified by observable surface lineaments. (Faults can be crucial to groundwater flow and contaminant movement in fractured terrain). Because of the replacement of film with digital imagery, the record of aerial photography has come to have a previously unrealized permanence. It should be noted that aerial photography displays a degree of radial distortion and without correction measurements of distance and topography are not accurate. Even so, aerial observation can provide better spatial resolution and geometric fidelity than many ground-based approaches.

The electromagnetic spectrum beyond visible light can also be quite helpful, as aerial photography provides broader spectral sensitivity than the human eye. Spectral bands or individual wavelengths can help identify many site activities. For example, near-infrared radiation (reflectance) can identify plant health, and thermal infrared (emitted spectra) can show heat sources on a property. Radar scanning can identify topographic expressions of subtle features like faults and folds often better than conventional satellite images. These radar techniques include Side-Looking Airborne Radar (SLAR) and LIDAR (a combination of the word “light” and “radar”) that can identify ground uplift or subsidence, and define geomorphologic features. There are also airborne geophysical techniques that are noninvasive and help define the geological surroundings of a site. Although traditionally used for geologic resource and mineral assessment, aeromagnetic, radiometric, and gravity surveys can add important information to an understanding of field geological influences on contaminant travel.

8.2.2 The Use of Surface Geophysical Techniques for Site Characterization

Noninvasive surface geophysical techniques can advance site characterization in many ways, although some techniques are expensive, and natural and human-made surface features can interfere with their efficacy. American Standard Testing Methods' ASTM D6429-(2011)e1 is a standard guide for selection of surface geophysical methods, and Olhoeft (1992) provides a Geophysical Advisor Expert System to facilitate field decisions on appropriate geophysical methods.

Electromagnetic Surveys (EM) One surface geophysical method is an electromagnetic survey that measures the magnetic susceptibility of earth materials and their variation. An electromagnetic (EM) induction sensor can detect subsurface electrical conductivity dissimilarities, and therefore is good for locating lateral changes or discontinuities in soil or rock, and fluid filled fracture zones. These heterogeneities can be extremely important in subsurface contaminant movement, particularly for non-aqueous phase liquids (NAPLs). EM techniques can directly detect: burial trenches or pits containing drums or bulk wastes, electrically conductive plumes (particularly useful in coastal saltwater intrusion and saline landfill plumes), plume movement using time-series measurements, and utility pipes/cables (which may transport contaminants through their trench backfill and/or interfere with other geophysical techniques). Electrical conductivity variation can also be an indicator of NAPL presence.

Airborne electromagnetic surveys can explore large swaths of land, helping to delineate factors directly pertinent to contaminant hydrogeology such as large faults, paleochannels and shear zones with appreciable groundwater and/or clay gouge, and dissimilarities in the electrical conductivity of groundwater bodies. Helicopter transient electromagnetic surveys (TEM) can examine subsurface properties down to 200m depth, and have been used to identify contaminated landfill sites, model pollution and coastal hydrogeology, and optimize management of mining tailings facilities (Silvestri et al. 2009; Pellerin et al. 2010; Kirkegaard et al. 2011; Christensen and Halkjaer 2014).

Direct Current Resistivity and Induced Polarization Another geophysical technique is a direct current resistivity survey that employs a constant electrical source using electrodes placed in the ground. The attenuation of voltage from between these electrodes (electrical resistance) allows calculation of depths to water tables or water-bearing horizons, freshwater/ saltwater interfaces, depth to bedrock, and stratigraphy at a site. Like EM techniques, direct current resistivity can identify electrically anomalous plumes and burial sites for bulk wastes and drums. Fencelines, pipelines, and other surface interferences can alter DC resistivity results. A related technique is induced polarization which measures the transient electrical response. This technique has been applied to locating subsurface NAPLs and tracking active or passive remediation, particularly for surfactants that might be injected for soil flushing cleanups (Personna et al. 2013; Magill 2009).

Time Domain Reflectometry Time Domain Reflectometry or TDR measures the relationship between the velocity that an electromagnetic wave moves through and between metal rods which are pushed into the ground, and the dielectric constant of the soil through which the wave propagates. This method has been used to estimate soil water content for many years, but many other applications for contaminated soil have been developed. For example, Olchawa and Kumor (2008) have used a soil's dielectric permittivity measured with TDR to measure the content of diesel oil in soil.

Magnetometry Magnetometry measures nonuniformities in the earth's magnetic field typically caused by buried tanks and drums made of ferrous material (iron and steel) and underground pipelines and utilities. Because many industrial sites have the potential to contain leaking tanks or pipes, these surveys can help locate problem areas. Even in the absence of leaking tanks and pipes, backfill surrounding underground tanks and pipes can be a conduit for some future pollutant flow and can be identified as a potential preferred pathway for fluid migration. Also, locating buried utility features is a critical step before drilling monitoring boreholes.

Seismic Surveys Reflective and refractive seismic techniques require an energy source such as a force striking the ground which generates low-amplitude waves through the earth to surface geophones that record the arrival of these waves. The time delay of wave arrival provides information that can help calculate subsurface stratigraphy, depths to both water table and bedrock, physical and elastic properties of subsurface formations, and lateral soil/rock discontinuities. Because pollution sources can either be pooled up above, or deflected by, subsurface layers, their identification is important in developing an accurate site conceptual model.

Ground Penetrating Radar (GPR) Ground penetrating radar (GPR) in optimal circumstances also can identify depth to water table and bedrock, stratigraphy, metallic and nonmetallic buried objects, and underground tunnels and cavities. It has limitations in clayey soils because of a lack of radar penetration.

8.2.3 Rapid Noninvasive Field Surveys and Screening

If a thousand soil samples are sent to the laboratory for contaminant analysis, and only one comes back as registering detectable concentration, time and money has been wasted in site characterization. There are rapid field methods for determining the extent of soil, water, and major well contamination that can help focus and direct characterization efforts and save resources. For example, surface water sampling and analysis surveys are normally simple and quick because of easy access, and are often a first measure taken at a site suspected of contamination. Certain surface waters, such as springs, gaining reaches of streams, and wetlands, often directly reflect changes in adjacent groundwater.

Unaided Methods Some survey methods are unaided, such as when soil staining is directly visible, or inferred from directly observable problems like noxious odors, stressed or dead vegetation, and impaired or dead animals. Test pits, holes for building footings, and trenches can be an easy way to observe large cross-sections of the shallow subsurface. Pits, holes, and trenches are often available at urban and industrial sites where buildings are being put in, old underground tanks are being exhumed, or underground pipelines and utilities are being established. These open holes and trenches can provide opportunities for visible identification of contamination because of large continuous exposure of the subsurface. Direct sampling of soil and any ponded water is simple with a limited risk of vertical contaminant migration. Test pits and trenches can delineate shallow stratigraphy, waste disposal areas, grossly contaminated sites, buried pipelines and underground storage tanks. Importantly, some of these site features potentially contain health hazards (e.g., toxic gases or potential trench wall collapse), and safety measures need to always be considered in these investigations.

Colorimetric Screening Techniques Classes of contaminants, like NAPLs, can be inexpensively and immediately detected by direct visual sightings in soil and water, but can be difficult when a NAPL or another pollutant of interest is clear or colorless, at low saturation, or distributed heterogeneously. NAPLs which cannot be visually detected can be quickly discovered by a number of other simple techniques. Many NAPLs like crude oil, coal tar, creosote, and other petroleum products naturally fluoresce when exposed to ultraviolet (UV) light. The inexpensive methodology of putting a soil sample in a transparent plastic bag and placing it under a “black” (UV) light is a cost effective way to screen soils for many sorts of NAPL contamination. Also for NAPLs there are hydrophobic dyes which, when put in transparent containers with soils and shaken, give indicator colors in the presence of NAPLs. In water, hydrophobic filters or hydrophobic materials can be used to detect NAPL, or centrifugation can more clearly separate a nonaqueous phase from water. A syringe needle can also be used to extract suspected globules in a surface water or groundwater sample, and the globule can be placed in a water column to observe whether it mixes, sinks, or floats. In wells, NAPL presence can be observed in a number of ways. A simple quick

method is dropping and retrieving a weighted string into a well and observing whether oil phases adhere to it. The weighted string should not be reused in another well to avoid cross-contamination. Hydrocarbon detection pastes (and water detection pastes for fuel storage tanks) can additionally help differentiate oils and water.

Immunological Surveys Another rapid field screening technique for water and soils are immunological surveys where polyclonal antibodies are mixed with soils and elicit a colorimetric response in the presence of certain pollutants. Polycyclic aromatic hydrocarbons (PAHs) have been shown to be detectable with about 5% false negatives and 5% false positives in one immunological survey (Knopp et al. 2000).

■ 8.3 Minimally Invasive Soil Monitoring

Monitoring techniques which have minor perturbation of field site geologic materials include soil vapor monitoring, soil water sampling, and phytoscreening. Although some of these techniques penetrate the subsurface, the disturbance is minor and at shallow depths.

8.3.1 Soil Vapor Monitoring—Introduction

Soil-gas monitoring can be valuable for several reasons. Volatile organic liquids in the subsurface can partition into a vapor phase in the vadose zone and therefore be identified with soil gas measurement. A volatile organic liquid source may be pure oil phase product either adhering to a mineral surface or forming a nonaqueous phase layer on top of the capillary zone. It may also be dissolved in soil water or groundwater. The major benefit of soil gas screening is that it can locate zones of contamination. Identified locations of undissolved product present in the vadose zone can be recognized as a potentially persistent reservoir for ongoing contamination of groundwater, and infiltrating precipitation could dissolve the product in these zones and carry it down to the water table in the aqueous phase. Soil-gas monitoring can also be used to help determine the location of spills and leaks, and the horizontal extent of a layer of a volatile, nonaqueous phase liquid, such as gasoline, floating on the water table. Vapors from the gasoline can partition into the vadose zone, so that if they are detected by soil-gas monitoring in an area where product spills or leaks are not likely, this is an indication that the product may be migrating into the area. Additionally, soil-gas monitoring has been used as a screening method to evaluate the extent of a plume of groundwater contaminated with volatile organic compounds. The soil gas above the plume may contain volatile organics if the plume is at the water table.

Contaminant vapors themselves can be problematic. They can intrude into buildings and homes, sometimes with adverse health and safety implications (USEPA 2002). The restoration of a site may involve soil remediation if organic compounds are detected in the vadose zone. Soil vapor monitoring has been incorporated into guidelines for site investigation for some countries, for example Denmark (Algreen et al. 2015a). Under many conditions soil gas monitoring can be done much more quickly and inexpensively than installing groundwater monitoring wells. Soil gas monitoring is a noninvasive technique with little subsurface disturbance which can be used to optimize follow-on invasive methods such as well installation (ITRC 2007).

8.3.2 Methods of Soil Gas Monitoring

There are at least four ways of monitoring the volatile compounds in the vadose zone: (1) direct sampling of soil, (2) surface flux chambers, (3) installation of a soil probe to withdraw soil gas for analysis (active sampling), and (4) installation of passive soil gas collectors (Davis et al. 2009). Indoor air samples from buildings can also be an indicator of surface vapor contamination.

Test borings can be installed and soil samples can be collected directly with a split-spoon sampler. The split spoon is opened and samples of soil can be collected with a small-diameter, thin-walled tube, such as a cork borer. For volatile organics, these samples are placed in a 40 mL VOA vial. Volatile organics can be measured in the headspace in the vial. The rate at which volatiles are lost during the sampling process is unknown, therefore the measured concentration will be less than the actual value.

Surface flux chambers, as the name implies, are used to determine the rate of upward vapor movement out of the ground, and into the atmosphere. Essentially, they are “lids” that are open at the bottom and pushed into the ground, allowing out-gassing vapors to accumulate beneath the lid. These entrapped, fugitive vapors are usually mixed with a small fan inside the flux chamber to allow average concentrations to be obtained. Sampling is conducted through a small monitoring port; either a syringe septum or valved attachment where gases can be withdrawn. It is important to note that misplacement of these flux chambers can lead to false negatives, and in heterogeneous or unevenly wet soils or in conditions where uneven subsurface biodegradation of contaminant vapors occurs, surface flux chambers may not distinguish actual out-gassing. Surface flux techniques are best-suited to attempts to quantify vapors of concern that are known to be moving out of the ground, not in situations aimed at demonstrating that surface emissions are low (NSW 2010).

In sand and other types of loose soil, a steel soil-probe pipe or direct-push device can be hydraulically driven into the vadose zone for dynamic soil gas monitoring. Active pumping of soil vapor involves driving a perforated steel pipe with a manifold that is connected to a vacuum pump. After ensuring that the annular space outside the pipe is adequately sealed, a vacuum is applied to the pipe and soil gas is drawn up it. Soil gas can be trapped in a container for later analysis, or it can be analyzed directly in the field by gas chromatography (Robbins et al. 1990a; 1990b). After some minutes of pumping for stabilization, a gas sample can either be collected using a Tedlar® bag, stainless steel ampule or similar container, or with a syringe placed into the vacuum line. The gas sample is either analyzed in the field or shipped to a laboratory where it is analyzed. Many commercial companies conduct these tests in many parts of the world. Active vapor sampling methods usually supply results in the form of mass of contaminant per volume of air. Soil gas from an actively pumping vacuum line on a probe can also be sorbed onto an activated carbon trap, which is then taken back to a laboratory for analysis (Wallingford et al. 1988).

Passive soil gas monitoring uses an *in situ* absorbent, which is placed in the vadose zone for a period of days to weeks. It is based on the principle of diffusion and measures the mass of contaminant that adsorbs to the adsorbent media in the buried location over a period of time. A shallow soil boring is made in the vadose zone and an activated-carbon, organic-carbon, or alternative sorbent vapor monitor is suspended in the boring. The top of the boring is sealed and the monitor left in place for days to weeks.

The boring is then unsealed; the vapor monitor is removed and sealed in a container for shipping to the lab, where it is analyzed (Kerfoot and Meyer 1986; NSW 2010).

Soil gas monitoring to find groundwater contamination plumes works best in areas where the vadose zone is comprised of dry, coarse-grained soils. The depth to water cannot be too deep, but at least 4.6 m (15 ft) is preferable. If the water table is too shallow, the concentration gradients are very steep, and a slight difference in depth of measurement may give a great difference in measured values (Marrin 1988). It is not possible to find an exact correlation between the soil gas concentration and contaminant concentration in the underlying groundwater. At best an order-of-magnitude correlation is possible (Thompson and Marrin 1987). Soil gas measurements are affected not only by the soil gas but also by the sampling technique and the soil-air permeability. After a rainfall, soil pores may be physically occluded by infiltrating rainwater and sampling may be impossible, particularly in finer soils. If there are several volatile organic compounds in the groundwater, they will partition into the vadose zone according to their individual Henry's law constants (Chapter 3). The organic compound with the greatest concentration in the soil gas may be the compound with the greatest Henry's law constant and not the one with the greatest concentration in the groundwater. Although care must be taken when interpreting the results of a soil gas survey, these surveys are valuable screening techniques and have significant qualitative value.

Samples of indoor air in buildings are important in identifying risks from explosive or toxic vapors, but at some sites they also show a general correlation between intrusive indoor air vapor concentrations and underlying groundwater volatile organic compound (VOC) plumes. These indoor air concentrations can vary greatly seasonally or with varying barometric pressure, but still can provide useful information which mirrors groundwater concentrations. Indoor air sampling uses a vacuum-filled ampule in which a valve is released and air is drawn in. Valve release can either be rapid for a single-time sample, or can have a slow timed release that collects an integrated sample with time.

8.3.3 Soil Water Sampling—Introduction

Contamination moving from the surface toward the water table passes through the vadose zone. Monitoring of soil-water quality in the vadose zone beneath hazardous-waste land-treatment systems is required under Subtitle C of the Resource Conservation and Recovery Act in the United States. States may also require vadose-zone monitoring beneath other types of hazardous-waste facilities.

In order to determine the chemical composition and quality of soil moisture in the vadose zone, a sample must be collected. Because the soil water in the vadose zone is under tension, it cannot flow into a well under gravity the way that groundwater flows into a well. Soil water must be collected with a suction lysimeter (Wilson 1990).

8.3.4 Suction Lysimeters

A **suction lysimeter** is a porous cup located on the end of a hollow tube. The tube can be PVC or even stainless steel. The porous cup can be ceramic, nylon, PTFE, or fritted stainless steel. Tubing connects the suction lysimeter with the surface.

A suction is applied to the hollow tube and held for a period of time. If the suction is greater (more negative) than the soil-moisture tension in the soil, a potential gradient

will develop from the soil to the porous cup. Soil-water will flow into the porous cup, from which it can then be directed through the tubing to the surface for collection. The flow of soil moisture can be slow, and it may be necessary to hold the vacuum overnight to supply a sufficient volume.

A vacuum lysimeter simply has a porous tip on the end of a hollow tube with a stopper that extends to the surface. The vacuum is applied to the lysimeter by means of a hand-vacuum pump attached to a small tube that extends down to the porous tip, and a sample is drawn to the surface when vacuum is applied (Figure 8.1). The practical depth of this type of sampler is about 1.8 m (6 ft) due to the awkwardness and cost of installing long tubes (Wilson 1990).

A pressure-vacuum lysimeter has a hollow tube that is about 5.08 cm (2 in.) in diameter and 0.3 m (1 ft) long. Two tubes run from the lysimeter to the surface (Figure 8.2). One of the tubes, the discharge line, extends to the bottom of the lysimeter and the other tube, the pressure-vacuum line, ends near the top. A vacuum is applied to the pressure vacuum line with a vacuum pump while the discharge line is shut off with a pinch clamp. The pressure-vacuum line is then sealed with a pinch clamp and the lysimeter is allowed to sit overnight so that the sample can be drawn into the cup. The pinch clamps are then removed. A hand-pressure pump is then attached to the pressure-vacuum line, and when pressure is applied, the water is forced up the discharge line to the surface. (A single pressure-vacuum hand pump can be used for this operation.) The maximum practical operational depth for the pressure vacuum pump is about 15 m (50 ft). At depths

FIGURE 8.1 Operation of a vacuum lysimeter.

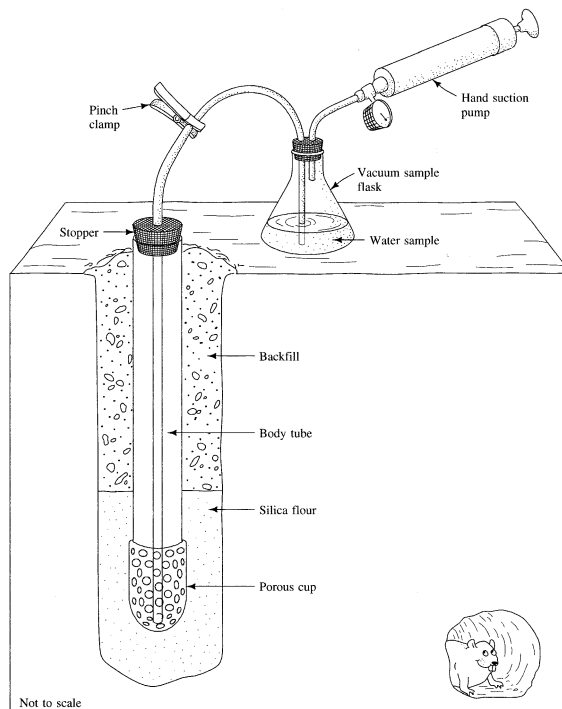
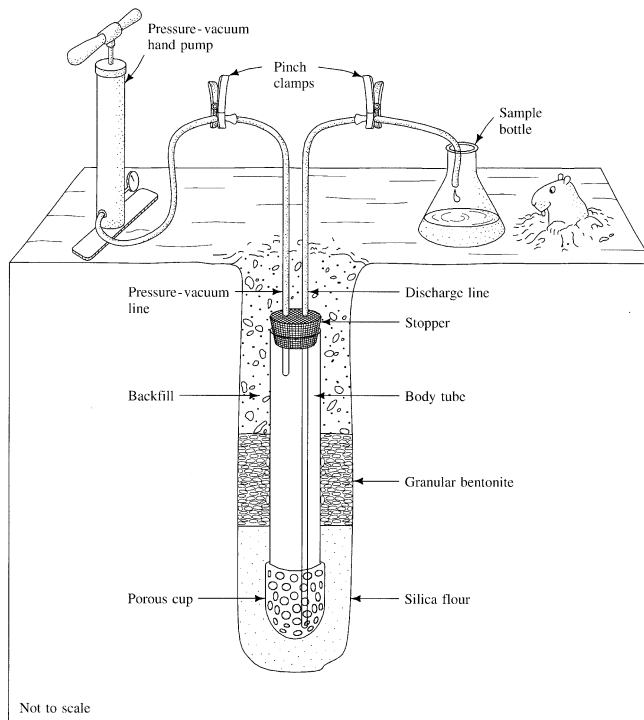


FIGURE 8.2 Operation of a pressure-vacuum lysimeter.

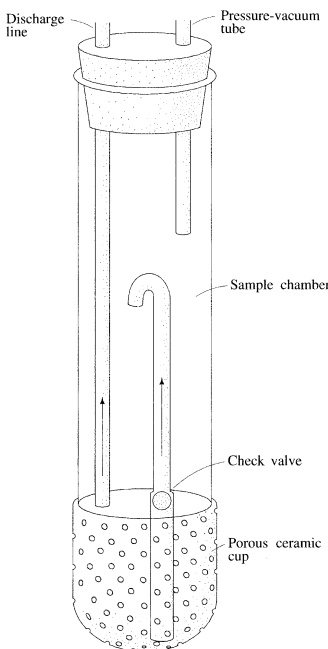
greater than this, the pressure needed to force the sample to the surface tends to drive it back out of the porous cup. This can be avoided by using a lysimeter with a check valve and an internal reservoir (Figure 8.3). When the vacuum is applied the water is drawn into the reservoir. When the pressure is then applied, the check valve prevents backflow into the porous cup and the sample must go to the surface.

8.3.5 Installation of Suction Lysimeters

In order for suction lysimeters to work properly, they must be carefully installed (Wilson 1991). Prior to use, new porous ceramic cups should be leached with a 10% hydrochloric acid solution for 24 hours to remove dust from manufacturing. They should then be thoroughly rinsed by passing distilled water through them. The lysimeter is then pressure tested before being installed by submerging it in water and applying a pressure of 207 kpa (30 lb/in.²) to test for leaks. No leaks should appear at any fittings, and air should bubble evenly through the porous cup.

The suction lysimeter is installed in an augered hole that has a greater diameter than the hollow tube. If the suction lysimeter is placed at a shallow depth, less than about 3 m (10 ft), then the access hole can typically be made by a hand auger. If it is greater than that depth, then a hollow-stem auger-drilling rig is needed to auger a hole.

The porous tip must be well bedded in slurry made of 200-mesh silica flour or native soil material that has been dried and screened to remove the fraction larger

FIGURE 8.3 Design of a pressure-vacuum lysimeter with a sample chamber and a check valve.

than coarse sand. There needs to be good hydraulic contact with the porous cup, the bedding material, and the native soil. Prior to installation the porous tip should be well hydrated by soaking in distilled water.

If a hollow-stem auger is being used, the augers should first be pulled back about 0.61 m (2 ft) to expose the native soil. A slurry made from silica flour and distilled water (0.45 kg (1 lb) of 200-mesh silica flour and 150 mL of distilled water) is put into the hole with a tremmie pipe to fill the hole with about 15.25 cm (6 in.) of slurry. The suction lysimeter is then lowered into the hole and centered. The tremmie pipe is then used carefully to place the slurry around the lysimeter up to an elevation of about 0.3 m (1 ft) above the top of the lysimeter. The unit should be held in place until the water drains from the slurry. The unit is then tested to see if it will hold a vacuum of 60 Kpa (0.6 bars). If it does, the augers are pulled back another 0.91 m (3 ft); then about 0.3 m (1 ft) of sieved native soil and 0.61 m (2 ft) of bentonite granules are added. The tremmie pipe is used to add distilled water to the bentonite to hydrate it. Finally, the augers are pulled and the borehole is backfilled with native soils that are tamped down to ensure compaction. Since a lot of distilled water was added to the soil during installation, the lysimeter needs to be purged until consistent water quality is obtained.

8.3.6 Phyto-screening

Phyto-screening is based on the ability of plants to translocate contaminants from their root zone to plant tissues above ground. Because the root zones of plants can be relatively large and their capture areas in the soil ill-defined, the method is somewhat

qualitative, but potentially useful, particularly in locales with shallow groundwater contamination at large sites. Trees can draw water from groundwater, the capillary fringe, and/or pore water in the vadose zone, and therefore phyto-screening can supplement and enhance soil gas screening techniques (Algreen et al. 2015a). Often tree coring or plant tissue harvesting is used as a collection and detection method for determining the location of subsurface pollutants. Coring and use of plant tissues has been used, with certain limitations, to locate chlorinated solvents (Vroblesky, Nietch, and Morris 1999; Orchard et al. 2000; Vroblesky et al. 2004; Sorek et al. 2008; Larsen et al. 2008; Limmer et al. 2011), BTEX compounds (Algreen et al. 2015b; Wilson et al. 2013) and heavy metals (Stefanov et al. 2012; Algreen et al. 2012; 2014).

■ 8.4 Invasive Methods - Monitoring Well Design

8.4.1 General Information

Monitoring wells are installed for a number of different purposes. During the installation of a monitoring well, a soil boring may be made or rock-core samples may be collected to determine the basic geology of the site. Prior to the design of a well, it is necessary to determine what its use will be. Some purposes of monitoring wells include:

- Measuring the elevation of the water table.
- Measuring a potentiometric water level within an aquifer, or at several depths in an aquifer.
- Collecting water samples for chemical analysis.
- Collecting samples of a nonaqueous phase liquid that are less dense than water.
- Collecting samples of a nonaqueous phase liquid that are more dense than water.
- Testing the permeability of an aquifer or aquiclude at discrete depths.
- Providing access for geophysical instruments.
- Collecting a sample of soil gas.

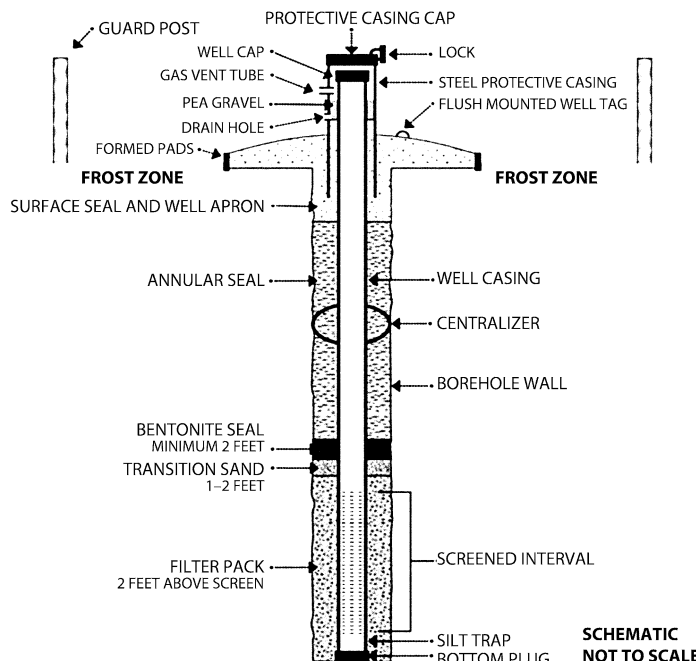
The use for which the well is intended will dictate the design. For example, if a well is to be used for the collection of water samples, the casing must be large enough to accommodate the water-sampling device. However, the diameter should not be much larger than the minimum size, because prior to the sampling of a well, stagnant water must be removed from the casing; the larger the diameter of the casing, the greater the volume of water that must be pumped and properly disposed. Some slightly more expensive characterization techniques can be well worth it for understanding a site. For example, high-resolution multilevel wells can produce orders of magnitude more data and understanding than single-screened wells. Figure 8.4 is a generalized schematic of a typical monitoring well. The following factors should be specified in the design of a monitoring well:

- Type of casing material.
- Diameter of the casing.
- If there will be a well screen, multiple screens, or an open borehole.
- If there is an open borehole, how deep the surface casing should be set. Cross connections between separate aquifers should be avoided.
- Length of casing.
- Depth of the well.
- Number of target sampling depths and screened intervals necessary in each well.
- Setting and length of the well screen(s).

- Diameter of well screen(s).
- Type of material for well screen(s).
- Slot opening of well screen.
- If an artificial filter pack (gravel pack) is necessary.
- Gradation of filter pack (gravel pack) material.
- Method of installation of well and screen.
- Material used to seal annular space between casing and borehole wall.
- Protective casing or well vault.

Monitoring network design is determined not only by intended well uses, but physical factors in the locale. Site specific influences of geography, practical consideration of surface conditions, and subsurface variability determine network monitoring design (Arnold et al. 2009). Geographical factors include natural and human-made topographic anomalies; natural and engineered surface drainage routes; areas of potential recharge and discharge such as wetlands; factors which influence the overall water balance such as weather and climatic variability; and anthropogenic features such as buildings, pavement, and pipelines. The practicalities of site accessibility and compatibility of monitoring wells with facility operations is often an important factor in well placement. Subsurface conditions also help dictate well network design. In general, more monitoring wells with closer intervals between wells, and multilevel sampling ability are required if there is complicated geology (e.g., discontinuous structures, tight folds, closely spaced

Figure 8.4 Typical monitoring well.



Source: E. Hughes and G. Aarons. 2014. *Well Design and Construction for Monitoring Groundwater at Contaminated Sites*. The California Environmental Protection Agency.

fractures, faults, solution channels), heterogeneous conditions (e.g., variable hydraulic conductivity, variable lithology), steep or variable hydraulic gradients, low dispersivity potential, high flow velocities, or if the aquifer is located near a recharge zone. Depths to water tables, confining layers, and bedrock surfaces are key in decisions about screen intervals and drilling depths. Lastly, the number and placement of wells often is based on prior application of noninvasive methods. These can include indirect methods (such as surface geophysics, soil gas where applicable, airborne remote sensing) or direct observation (such as existing wells, soil borings, test pits, and observation of local outcrops).

Common problems with groundwater monitoring systems include instances where wells are placed by regulatory mandate; where there is incomplete site data; when initial ideas on site (and regional) geology, hydrogeology, and water balance are not correct; and when incorrect assumptions are made regarding waste constituent migration. Difficulties also arise with improperly constructed wells, when they are not properly identified, or in cases when wells are not properly surveyed for location and elevation.

8.4.2 Monitoring Well Casing

All monitoring wells have a **casing**, whether they have a screen or terminate in an open borehole in bedrock. The casing is a piece of solid pipe that leads from the ground surface to the well screen or open borehole and is intended to keep both soil and water from entering the well other than through the screen or open borehole. Casing also prevents water from flowing from one aquifer horizon to another, provided the annular space outside the casing is properly sealed.

The diameter of the casing for a monitoring well is determined by the use for which the monitoring well is planned. If the only purpose of the monitoring well is to measure water levels, then a 2.54 cm (1 in.) inside-diameter casing is all that is needed. An electric probe to measure water level or a pressure transducer will fit inside the 2.54 cm (1 in.) casing. Figure 8.5 shows an electric probe being lowered into a 5.08 cm (2 in.) casing.

If a well is to be used to collect a groundwater sample, the diameter of the well needs to be such that standard well-sampling equipment can fit inside. The common standard for well-sampling equipment is a nominal 5.08 cm (2 in.) diameter. This can accommodate a wide variety of pumps that can withdraw water at rates of 0.03 to 0.13 or 0.19 L/s (0.5 to 2 or 3 gal./min). Specially designed borehole geophysical equipment can also fit inside a 5.08 cm diameter casing.

For some applications, monitoring wells may be intended for several functions such as measuring water levels, collecting water samples, pumping to remove contaminated water and perhaps floating nonaqueous phase liquids, and as a part of a vapor-extraction system. These wells sometimes have diameters larger than 5.08 cm (2 in.) to accommodate pumping equipment with a higher-flow capacity. The actual equipment to be used determines the casing diameter.

Casing diameter can also be influenced by the depth of the well. The deeper the well, the stronger the casing and screen must be to resist the lateral pressure at the final depth and the crushing force of the weight of the length of casing. Larger diameter casing can be made with thicker walls to have greater strength. It is easier to have a straight well with stronger casing. Straight wells are important in accommodating bailers and pumps.

The outside diameter of casing is standard; however, the inside diameter is a function of the wall thickness. Table 8.1 lists the wall thickness and inside diameter for

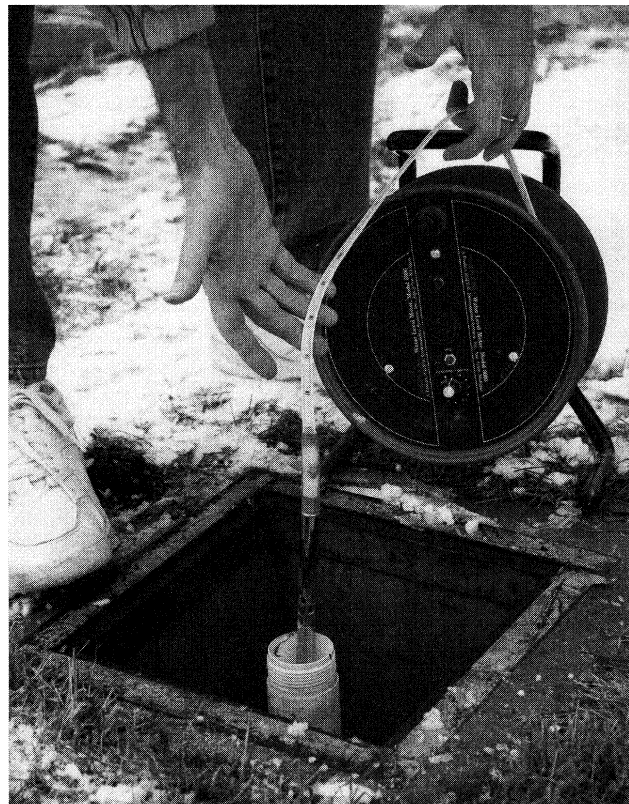
FIGURE 8.5 Electric probe used to measure water levels in monitoring wells.

Photo credit: Jim Labre.

TABLE 8.1 Dimensions of inside and outside diameters of well casings.

Pipe Size	Schedule 5			Schedule 10			Schedule 40			Schedule 80		
	Outside Diameter	Wall Thickness	Inside Diameter									
Nominal 2"	2.375"	0.065"	2.245"	0.109"	2.157"	0.154"	2.067"	0.218"	1.939"			
Nominal 3"	3.500"	0.083"	3.334"	0.120"	3.260"	0.216"	3.068"	0.300"	2.900"			
Nominal 4"	4.500"	0.083"	4.334"	0.120"	4.260"	0.237"	4.026"	0.337"	3.826"			
Nominal 5"	5.563"	0.109"	5.345"	0.134"	5.295"	0.258"	5.047"	0.375"	4.813"			
Nominal 6"	6.625"	0.109"	6.407"	0.134"	6.357"	0.280"	6.065"	0.432"	5.761"			

various schedules of casing. The sizes are listed in English units (inches) as many casings and screens were produced for decades in countries not yet on the metric system. Table 8.2 lists recommendations for selection of casing and screen material. Heavier-schedule casing is stronger because it has a thicker wall. The strength of a casing also depends upon the material from which it is constructed. A schedule 5 casing

TABLE 8.2 Recommendations for selection of casing and screen material.

Do Not Use:	Use:
1 PTFE if well depth exceeds 225–375 feet (68.6–14 meters)	PVC, ABS, SS
2 PVC or ABS if well depth exceeds 1200–2000 feet (366–610 meters)	SS
3 SS if pH < 7.0	PVC, ABS or PTFE
4 SS if D.O. > 2 ppm	PVC, ABS or PTFE
5 SS if H ₂ S > 1 ppm	PVC, ABS or PTFE
6 SS if TDS > 1000 ppm	PVC, ABS or PTFE
7 SS if CO ₂ > 50 ppm	PVC, ABS or PTFE
8 SS if Cl ⁻ > 500 ppm	PVC, ABS or PTFE
9 PVC if a neat PVC solvent/softening agent* is present or if the aqueous concentration of the PVC solvent/softening agent exceeds 0.25 times its solubility in water	SS, PTFE
10 Solvent-bonded joints for PVC casings	Threaded PVC casings
11 Welding stainless joints	Threaded SS casings
12 Any PVC well casing that is not NSF-ASTM approved—D-1785 and F-480	NSF-ASTM approved PVC well casings—D-1785 and F-480
13 Any stainless steel casing that is not ASTM approved—A312	ASTM approved SS 304 and SS 316 casings—A312
14 Any ABS well casing that is not ASTM approved	ASTM approved ABS casings—F-480

*Known PVC solvents/softening agents include:

Tetrahydrofuran, cyclohexane, methyl ethyl ketone, methyl isobutyl ketone, methylene chloride, trichloromethane, 1,1-dichloroethane, 1,1,1-trichloroethane, trichloroethylene, benzene, toluene, acetone, and tetrachloroethylene.

ABS Acrylonitrile butadiene styrene

D.O. Dissolved oxygen

ppm parts per million

PTFE Polytetrafluoroethylene

PVC Polyvinyl chloride

SS Stainless steel

TDS Total dissolved solids

Source: E. Hughes and G. Aarons. 2014. *Well Design and Construction for Monitoring Groundwater at Contaminated Sites*. The California Environmental Protection Agency.)

made of stainless steel is stronger than a schedule 40 casing made of polyvinyl chloride (PVC), yet leaves a greater inside diameter.

There are a number of materials used to make well casings and screens. These materials vary in chemical inertness, strength, durability, ease of handling, and cost. One must always consider the intended use of the monitoring well before selecting a material. What is the chemistry of the groundwater and associated contaminants?

Will any compounds present in the groundwater react with any of the possible casing materials? How deep will the well be? What are the strength requirements? Is the well intended for a short-term monitoring project or will it remain in service for many years?

Well casings are available in a variety of materials: fluoropolymers, such as PTFE, or polytetrafluoroethylene (Teflon® is the brand name of one manufacturer of PTFE), mild steel, galvanized steel, stainless steel, polyvinyl chloride (PVC), acrylonitrile butadiene styrene (ABS), fluorinated ethylene propylene (FEP), fiberglass-reinforced epoxy (FRE), polypropylene, and fiberglass-reinforced plastic (FRP). The ideal casing material is inexpensive, strong, not subjected to degradation in the environment, and will not affect water-quality samples by either leaching chemicals into or sorbing them from the groundwater (Ranney and Parker 1997). Mild or galvanized steel is often used for water-supply well casings but is not as frequently found in monitoring wells because it may react with the groundwater to leach metals from the casing (Barcelona et al. 1983). Polypropylene, FEP, and ABS are not widely available. Most monitoring wells are made of stainless steel or PVC, with PTFE being less common. PVC casing is the least expensive. Relative casing costs for other materials, compared with PVC, are mild steel = 1.1, polypropylene = 2.1, type 304 stainless steel = 6.9, type 316 stainless steel = 11.2, and PTFE = 20.7. Type 316 stainless steel is more resistant to corrosion than type 304 under reducing conditions (Aller et al. 1991).

Stainless steel has the greatest strength, followed by mild steel. Both are also resistant to heat, but they are heavier than the plastics and are, therefore, more difficult to install. The lower strength of the plastics is compensated for by using a heavier-schedule casing than necessary with steel. Most monitoring wells are shallow enough that schedule 40 or 80 PVC has sufficient strength. PTFE is more brittle and has less wear resistance than PVC or polypropylene and is hence less durable. PTFE also has a low tensile strength and high weight per unit length, which limits its use to shallow depths. Even there, PTFE casing tends to bow under its weight when installed in monitoring wells and may not be straight and plumb. Although its nonstick properties are good in frying pans, the neat cement grout used to seal the annular space between the casing and the borehole may not bond to the PTFE casing (Nielsen 1988). Table 8.3 gives comparative strengths of casing materials.

Groundwater monitoring wells can come into contact with pure organic compounds (LNAPLs and DNAPLs) as well as highly acidic and highly basic conditions. Ranney and Parker (1997) tested six different materials that are used or could be used as monitoring well casings in order to test their resistance to pure (neat) organic chemicals and acids and bases. (Stainless steel and galvanized steel are known to be unaffected by organic compounds but susceptible to corrosion by acids and bases.) They found that PTFE and FEP were unaffected by any of the 28 different organic chemicals in which they were immersed. The other four materials—PVC, ABS, FRE, and FRP—were affected to some degree by some, or in the case of ABS, all of the 28 chemicals. This study suggests that if contact with neat organic compounds is possible, PTFE, FEP, or stainless steel casings should be considered, although some PTFE materials are slightly porous, and are deformable and “ductile” under loading.

In the selection of casing material for groundwater monitoring wells, we must consider the potential chemical reactions between the casing material and the groundwater. Ideally, casing material should neither leach matter into water nor sorb

TABLE 8.3 Comparative strengths of casing materials. Note: 1 lb = 0.454 kg and 1 lb/in² = 0.07 kg/cm².

Material	Casing Tensile Strength (lb)		Casing Collapse Strength (lb/in ²)	
	2-inch diameter nominal	4-inch diameter nominal	2-inch diameter nominal	4-inch diameter nominal
Polyvinyl chloride (PVC)	7,500	22,000	307	158
PVC casing joint ^b	2,800	6,050	300	150
Stainless steel (SS) ^c	37,760	92,000	896	315
SS casing joint ^b	15,900	81,750	No data	No data
Polytetrafluoroethylene (PTFE)	3,800	No data	No data	No data
PTFE casing joints ^b	540	1,890	No data	No data
Epoxy fiberglass	22,600	56,500	330	250
Epoxy casing joints ^d	14,000	30,000	230	150
Acrylonitrile butadiene styrene (ABS)	8,830	22,000	No data	No data
ABS casing joints ^d	3,360	5,600	No data	No data

a Information provided by E.I. du Pont de Nemours & Company, Wilmington, DE.

b All joints are flush-threaded.

c Stainless steel casing materials are Schedule 5 with Schedule 40 joints; other casing materials (PVC, PTFE, epoxy, ABS) are Schedule 40.

d Joints are not flush-threaded, but are a special type that is thicker than Schedule 40.

Source: E. Hughes and G. Aarons. 2014. *Well Design and Construction for Monitoring Groundwater at Contaminated Sites*. The California Environmental Protection Agency.)

chemicals from water. Table 8.4 shows general recommendations for casing/ screen material selection.

Reynolds and Gillham (1985) studied the sorption from aqueous solution of five halogenated organic compounds by several polymer materials. The organic compounds used were 1,1,1-trichloroethane, 1,1,2,2-tetrachloroethane, hexachloroethane, perchloroethene, and bromoform. The materials tested were PVC, PTFE, nylon, polypropylene, polyethylene, and latex rubber. Nylon, polypropylene, polyethylene, and latex rubber rapidly absorbed all five compounds. PVC absorbed all the compounds but 1,1,1-trichloroethane, although the rate of absorption was low. PTFE absorbed all the compounds but bromoform; although the rate of adsorption of three of the four remaining compounds was low, PTFE absorbed 50% of the perchloroethylene in 8 hours.

Parker, Hewitt, and Jenkins (1990) evaluated the suitability of PVC, PTFE, stainless steel type 304 (SS 304), and stainless steel type 316 (SS 316) as casing material for monitoring metals in groundwater. They evaluated the interaction of four trace elements that are of concern in groundwater studies: arsenic, cadmium, chromium, and lead. The metals were tested at concentrations of 50 and 100 µg/L dissolved in groundwater. Figure 8.6 shows the results of this study. If the concentration relative to

TABLE 8.4 Recommendations regarding chemical interaction with well casings.

If Monitoring for:	Best Choices		Avoid If Possible
	1st Choice	2nd Choice	
Metals	PTFE	PVC	SS 304 and SS 316 ⁺
Organics	SS 304 and SS 316	PVC*	Galvanized Steel and PTFE**
Metals & Organics	None	PVC and PTFE	SS 304 and SS 316

+ Substantial concentrations of metals can be leached from SS if the contact time is 2 hours or longer.

* PVC is acceptable if free product is not present and concentrations are less than ~.25 solubility (Ohio 2008).

** Do not use PTFE for monitoring VOCs (see list on Table 1). PTFE tends to be more sorptive of organics than PVC. Hydrophobic organics ($\text{Log K}_{\text{ow}} > \sim 2$) are most readily sorbed.

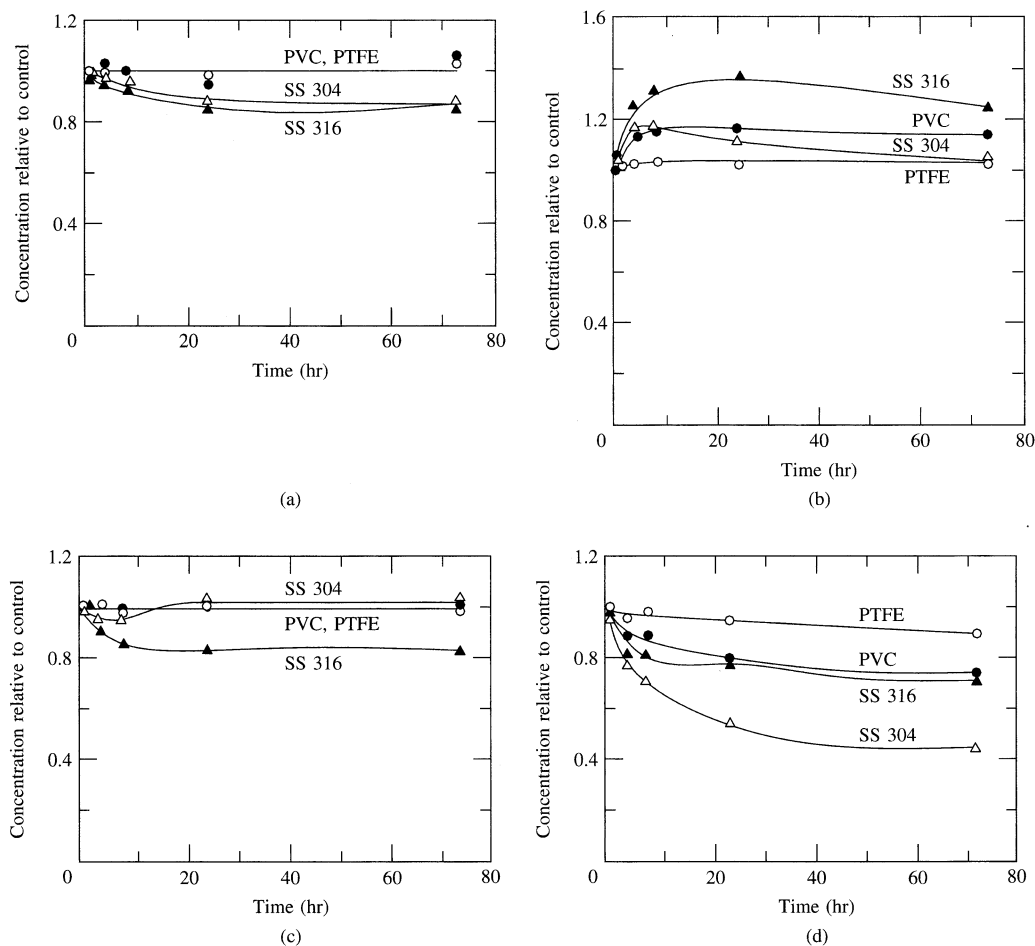
ABS	Acrylonitrile butadiene styrene
Kow	Octanol-water partition coefficient
PTFE	Polytetrafluoroethylene
PVC	Polyvinyl chloride
SS	Stainless steel
VOC	Volatile organic compound

Source: E. Hughes and G. Aarons. 2014. *Well Design and Construction for Monitoring Groundwater at Contaminated Sites*. The California Environmental Protection Agency.)

control remains at 1.0, there is no interaction; if it drops to less than 1.0, then the element is sorbing onto the casing material; and if it rises above 1.0, the element is being leached from the casing. The PTFE was the most inert with respect to the metals, and the PVC was much better than either SS 304 or SS 316.

The interaction of several organic compounds with the same well-casing materials was also studied by Parker, Hewitt, and Jenkins (1990). Ten organic compounds were tested, including chlorinated ethenes, chlorobenzenes, nitrobenzenes, and nitrotoluenes. The organic compounds used in this experiment were in the part per million range, which represents highly contaminated groundwater. None of the compounds were sorbed onto either type of stainless steel. Many of the compounds were sorbed by the plastic casings, with the PTFE sorbing at a greater rate than the PVC. The amount and rate of sorption varied by compound. Figure 8.7a shows the sorption of trichloroethene by the four casing types. While there was little sorption of dissolved organics by PVC in the part per million concentration range, we are often concerned about organic chemicals in groundwater in the part per billion concentration range. Parker and Ranney (1994) studied the sorption of nineteen organic compounds, including BTEX, PCE, TCE, 1,2-DCE, 1,1,1-TCA, 1,1,2,2-TCA, several chlorobenzenes and several explosive compounds at concentrations of 10 to 40 $\mu\text{g/L}$, by stainless steel, PVC and PTFE. The results were similar to those obtained by the research at the part per million range. Figure 8.7b shows the results of this research. A comparison with Figure 8.7a shows that absorption is independent of concentration. Clearly, stainless steel is the material of choice for monitoring organics, and PTFE is to be avoided. For a compromise material for monitoring both organics and inorganics, PVC is often used. It also has the appeal of having the lowest cost. PVC manufactured specifically

FIGURE 8.6 Sorption and leaching of a. arsenic, b. cadmium, c. chromium, and d. lead by well casings made from PVC, PTFE, type 304 stainless steel, and type 316 stainless steel.

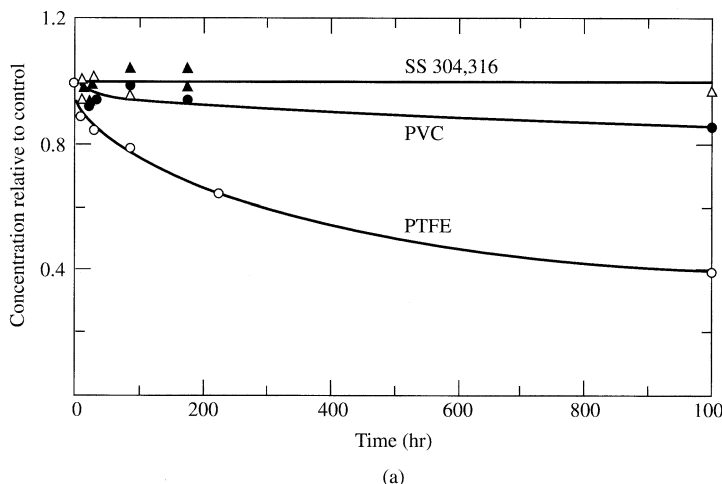


Source: L. V. Parker, A. D. Hewitt, and T. F. Jenkins. 1990. Influence of casing materials on trace-level chemicals in ground water. *Groundwater Monitoring & Remediation* 10:146–156. Used with permission.

for well casing should be used, and in the United States it should carry the designation *NSF wc*, which indicates that the casing conforms to National Sanitation Foundation Standard 14 for potable water supply (National Sanitation Foundation 1988).

However, PVC should be avoided if organic compounds are present in the ground as nonaqueous phase liquids. Likewise, PVC casing should also never be joined with solvent-glued joints. These solvents include compounds such as methylethylketone and tetrahydrofuran and they may leach into groundwater samples. Threaded joints that are machined directly onto the PVC are the preferred method of joining casing sections and casing to screen. Joints should be flush on the inside of the casing to prevent equipment being lowered into the casing from hanging up in a projecting joint inside

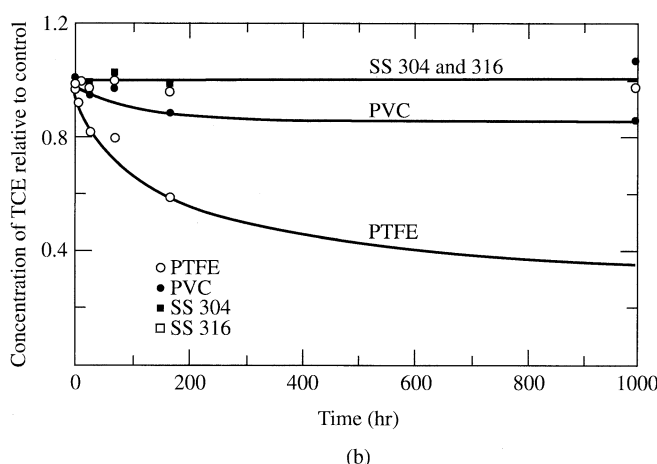
FIGURE 8.7a Sorption of trichloroethylene in the part per million range from groundwater by PVC, PTFE, type 304, and type 316 stainless steel well casings.



(a)

Source: L. V. Parker, A. D. Hewitt, and T. F. Jenkins. 1990. Influence of casing materials on trace-level chemicals in ground water. *Groundwater Monitoring & Remediation* 10:146–156. Used with permission.

FIGURE 8.7b Sorption of trichloroethylene in the part per billion range from by PVC, PTFE, type 304, and type 316 stainless steel well casings.



(b)

Source: L. V. Parker and T. A. Ranney. 1994. Effect of concentration on sorption of dissolved organics by PVC, PTFE and stainless steel well casings. *Groundwater Monitoring & Remediation* 14:139–149. Used with permission.

the well, or bridging and stoppage of grout or filter pack material in the annular space outside the well.

There are groundwater contaminants other than either metals or dissolved non-polar organic compounds. Many chemicals associated with agriculture are strongly

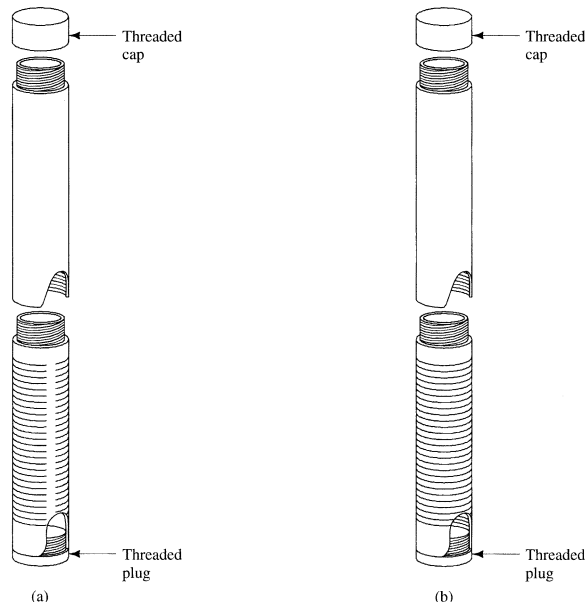
polar or ionic. Papiernik, Widmer and Spalding (1996) studied the impact of using various materials to sample agricultural contaminants, including nitrate-N, atrazine, diethylatrazine, diisopropylatrazine, cyanazine, alachlor, metolachlor and butachlor. They found that other than butachlor (which is not in common use in the United States) there was no significant difference in absorption of the target by either polytetrafluoroethylene (PTFE), rigid PVC, flexible PVC, stainless steel, high density polyethylene (HDPE), or low density polyethylene (LDPE). For any of the chemicals tested, other than butachlor, any of the materials could be used. The least expensive would be HDPE, LDPE, and rigid PVC.

8.4.3 Monitoring Well Screens

If the monitoring well terminates in an unconsolidated formation, a **screen** is necessary to allow the water to enter while keeping the sediment out. In most monitoring well applications, the well screen is the same diameter as the casing to which it is attached by a threaded coupling. Likewise, the well screen is normally made of the same material as the casing. The considerations that go into deciding the material to use for the casing also apply to the screen. In many cases multilevel sampling will provide crucial information and multiple, isolated screened intervals are necessary.

The screen or screens will have openings to permit the water to enter. Manufactured well screen should always be used rather than hand-cut slots or drilled holes in plastic pipe. The two common screens for monitoring wells are slotted pipe, which is available in PVC and PTFE, and continuous wire wrap, which is available in stainless steel. Figure 8.8 illustrates these two screen types.

FIGURE 8.8 Slotted (a) and continuous wire-wrapped (b) monitoring well screens.



The width of the slot or wire-wrap opening is precisely controlled during the manufacture of the screen; the screen is available in a variety of opening sizes, generally ranging from 0.02 to 0.635 cm (0.008 to 0.250 in.) A screen with an opening of 0.010 in. (0.0254 cm) is referred to as a 10-slot screen. Many manufacturers carry only a limited number of slot sizes in stock—for example, 10- and 20-slot. Since the casing and screen are typically ordered in advance of the well construction, the hydrogeologist usually has settled on a standard design prior to going on the job. Decisions on slot sizes are important in that too large a slot size without proper filter pack can allow sediment to enter the well during pumping. Conversely, a small slot size can inhibit nonaqueous phase liquids (NAPLs) from entering a well. NAPL must have enough thickness and fluid pressure to supplant water in small slots, overcoming capillary pressure. If well screen slots have small opening sizes, NAPL outside the well in a thin pool may not be able to enter through the screens.

8.4.4 Naturally Developed and Filter-Packed Wells

The casing and screen may be placed in the borehole and the native sediment allowed to cave around the screen. This is called a **naturally developed well** and is often used in sandy sediment with very limited amounts of silt and clay present, but is most realistic for wells with single screens. At least 90% of the sediment should be retained on a 10-slot screen before a naturally developed well is considered (Aller et al. 1991). When water is withdrawn from such a well, it may initially be cloudy due to suspended silt and clay, but the water should eventually clear as the fines near the screen are removed by a process called “well development.” In a naturally developed well the slot size is selected to allow some of the fine sediment to enter the well during development; this leaves only the coarser sediment outside the screen.

In designing a water well, it is very important that the well be hydraulically effective—i.e., there should be a minimal loss of energy as the water flows into the well. As mentioned, the selection of the slot opening for naturally developed water wells is very important and is based on a grain-size distribution curve of the sediment opposite the well screen. Monitoring wells are designed to retain much more of the natural formation than water wells because they are much more difficult to develop (Driscoll 1986). Monitoring wells are not usually designed with the precision necessary for a water-supply well. The well should be hydraulically efficient as well as being as clear of silt and clay as possible. If preliminary investigations indicate that the aquifer to be monitored has reasonably coarse sand or gravel and few fines, a standard slot size may be preselected for all the monitoring wells. Ten-slot screen is frequently used under these conditions.

If the formation is cohesive—that is, has a high clay content—or if it is sandy with a high silt content, it will be necessary to use an **artificial filter pack**. Filter packs have also been referred to as “sand packs” or “gravel packs.” Filter-pack material is typically medium to coarse sand that is predominately silica with no carbonates. It is mined and graded to have a specific grain-size distribution. Manufactured filter-pack material comes washed and bagged and is far preferable to native sand as artificial filter pack. The filter-pack material is placed in the borehole opposite the well screen. Its purpose is to stabilize the natural formation and keep it out of the screen. This will reduce the amount of silt and clay that enters the well when it is developed. There are also

dual-screen well intake systems (pre-packs) that have a small diameter screen within a larger, second larger diameter screen, and the space in between is filled with filter pack material. Dual screen intakes are sometimes used when there is a propensity for fine-grained material to enter the well. A major disadvantage of these systems is that the two screens can compound the inhibition of NAPLs to enter a well.

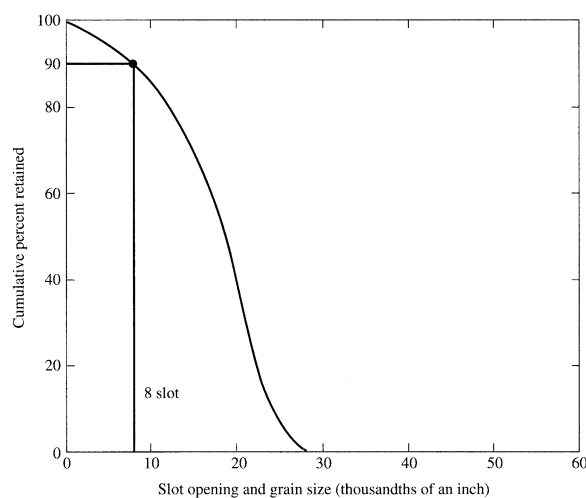
The grain size of the filter-pack material is based on the nature of the formation opposite the screen. If the formation is fine sand, then the grain-size distribution is determined. The filter pack material should have an average grain size that is twice the average grain size of the formation and have a uniformity coefficient (ratio of 40% retained size to 90% retained size) between 2 and 3 (Driscoll 1986). The screen-slot opening is then selected to retain 90% of the filter pack. The minimum practical slot size for monitoring well screens is 0.02 cm (0.008 in.) Figure 8.9 shows a grain-size distribution curve for a filter-pack material designed for an eight-slot screen. If the monitoring well is in silt or clay, all one can do is install an 8 slot screen and appropriate filter pack.

The filter-pack material should be approximately 5 to 7.5 cm (2 to 3 in.) thick. This means that a 5 cm (2 in.) diameter well screen should be installed in a borehole about 10 to 15 cm (6 to 8 in.) in diameter. The filter-pack material is normally extended 0.61 or 0.91 m (2 or 3 ft) above the top of the well screen to allow for settlement of the material during development.

8.4.5 Annular Seal

The **annular space** in the borehole above the filter pack must be sealed to prevent the movement of surface water downward to the filter pack. It may also be sealed to prevent vertical movement of groundwater from one zone to another or to isolate a discrete sampling zone. The seal should be made of a material that has a low permeability, bonds well to the natural formation and the casing, and expands after it has been

FIGURE 8.9 Grain-size distribution curve used to select an eight-slot screen for a monitoring well.



emplaced to ensure a tight seal. It should set up within a day or so and be durable and permanent.

Materials typically used for an annular seal are bentonite pellets, granular bentonite slurry, neat cement grout, bentonite-sand slurry, and neat cement grout with a powdered bentonite additive.

Neat cement grout is a mixture of 42.5 kg (94 lb) of type I Portland cement with about 19 to 23 L (5 to 6 gal.) of water. Granular bentonite slurry is a mixture of 13.6 kg (30 lb) of untreated bentonite powder mixed with 56.7 kg (125) lb of untreated bentonite granules with 378.5 L (100 gal) of water. Bentonite-cement grout is a mixture of 2.3 kg (5 lb) of untreated powdered bentonite with 42.5 kg (94 lb) of type I Portland cement and 32 L (8.5 gal.) of water. Bentonite-sand slurry is a mixture of 25 kg (55 lb) of untreated powdered bentonite with 378.5 L (100 gal.) of water and 10 to 25% sand by volume to make a slurry that weighs 9.6 kg/L (11 lb/gal.) All water used to make these slurries should be from a source that is fresh and known to be uncontaminated and free from floating oil.

Bentonite is a clay containing at least 85% sodium montmorillonite; it will swell to several times its original volume when thoroughly hydrated. This hydration takes place below the water table. However, bentonite has a high cation-exchange capacity and can affect the chemistry of water that comes into contact with it. Portland cement is used to make cement grout. When Portland cement cures, it is highly alkaline and can affect the pH of groundwater that comes into contact with it. Neat cement grout will shrink by at least 17% when it cures. The addition of bentonite to make a bentonite-cement grout significantly reduces the shrinkage problem. If neat cement grout or bentonite cement grout is used, the casing material should be either stainless steel or schedule 80 PVC due to the heat generated as the cement cures.

The materials available for an annular seal are not ideal. Although they can be used to make an impermeable seal, there is a chance they might affect groundwater quality in their immediate vicinity. This problem is mitigated if 0.61 m (2 ft) of fine sand is placed in the annular space above the filter-pack material or native sand opposite the screen. This keeps the annular seal material from coming into contact with the water entering the well screen.

Many hydrogeologists place a 0.61 m or 0.91 m (2 or 3 ft) layer of bentonite pellets above the fine sand if the pellets will be below the water table. The pellets will swell and keep the grout material from entering the filter-pack material. Clay pellets should not be used in the vadose zone due to lack of hydration and lack of swelling; a clay slurry should be used instead. If the top of the 0.61 m (2 ft) fine-sand seal is above the water table, then 0.61 m (2 ft) of granular bentonite may be placed prior to the addition of the annular seal.

8.4.6 Protective Casing

In order to provide physical protection for the investment in a costly monitoring well, as well as to protect from vandalism by individuals accidentally or intentionally putting foreign fluids and objects into a monitoring well, a locking protective steel casing or well vault is needed.

A protective casing extends several feet above the ground surface. It extends above the top of the monitoring well and has an inside diameter sufficiently large so that the

hydrogeologist can reach inside and unscrew a cap from the monitoring well. It is set into a surface cement seal. For monitoring wells installed in freezing climates, a drain hole at the bottom of the surface casing is desirable to prevent accumulation of moisture that could freeze in the annular space between the protective casing and the monitoring well. (One of the authors has seen a stainless-steel monitoring well casing pinched shut by water that accumulated in a protective casing without a drain hole and then froze!)

In some applications, it is not practical to have a monitoring well that extends above ground—for example, in the driveway at a gas station. There are small well vaults available that can be used for protection for monitoring wells. However, they should be in places that are not going to flood; otherwise floodwaters could enter the aquifer via the monitoring well. If a well vault is used in a gas station or similar location, it should be clearly marked and should be distinctive from the fillers for underground storage tanks so that an inattentive person does not try to fill it with gasoline! A locking well cap without a vent hole should also be used.

8.4.7 Screen Length and Setting

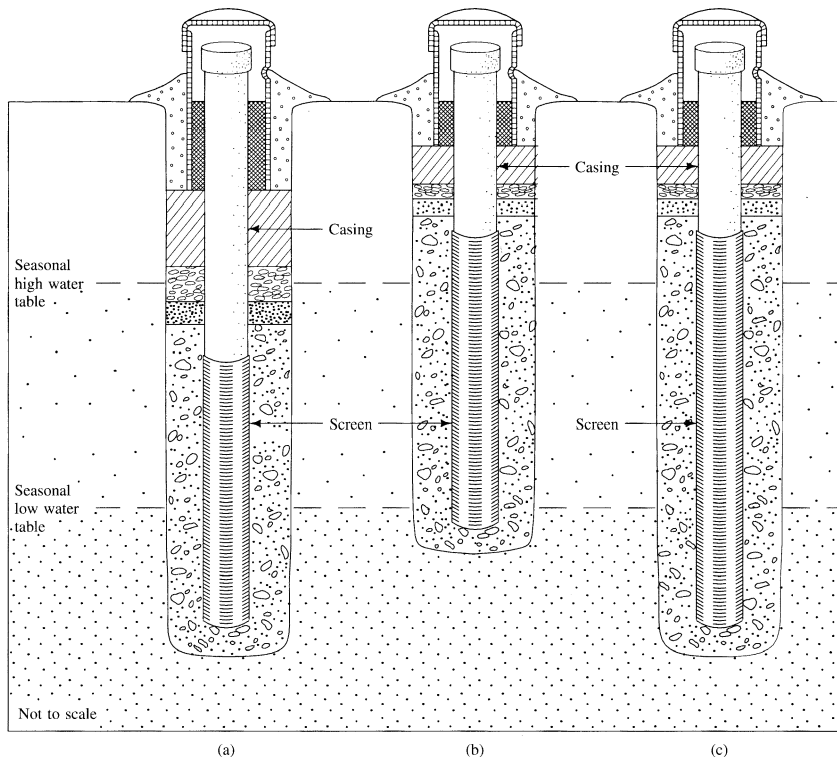
The hydrogeologist must decide on the length of the screen and the depth to which it will be set, based on the objectives of the monitoring program. Objectives could include monitoring the position of the water table, measuring the potentiometric head at some depth in the aquifer, collecting representative water samples from various depths in the aquifer, and detecting both light and dense nonaqueous phase liquids. Moreover, monitoring might be intended to detect the migration of groundwater containing contaminants into an aquifer or evaluating the effectiveness of removing contaminants from an aquifer. All might require different approaches.

To monitor the position of the water table or to detect the presence of LNAPLs, the screen must be set so that it intersects the water table. The screen must be long enough to intersect the water table over the range of annual fluctuation. In addition, the screen must be long enough so that when the water table is at its greatest depth below the land surface, there is enough of the screen remaining below the water table to contain sufficient water for a water sample. A water-table monitoring well will also be able to detect the presence of light nonaqueous phase liquids. In most applications the minimum length of the screen for a water table-monitoring well is 3 m (10 ft) with about 1.5 m (5 ft) above and 1.5 m (5 ft) below the water table. If the water table has more than 1.5 m (5 ft) of annual fluctuation, a longer well screen is needed. However, some governmental guidance specifies a maximum screen length of 3 m (10 ft) or less. Figure 8.10 shows examples of incorrect (a and b) and correct (c) placement of a multipurpose monitoring well intended to measure the position of the water table, detect floating nonaqueous phase liquids, and collect water samples from the upper part of the aquifer.

If the purpose of a monitoring well is to measure the potentiometric pressure at some depth in the aquifer, then the well is called a **piezometer**. A piezometer should have a relatively short screen length, 0.6 to 1.5 m (2 to 5 ft), so that the pressure that is recorded is representative of only a small vertical section of the aquifer. A piezometer can also be used to collect groundwater samples that are representative of a small vertical section of the aquifer.

Monitoring wells utilized to collect groundwater samples should be designed with respect to a specific groundwater monitoring goal. The concentration of groundwater

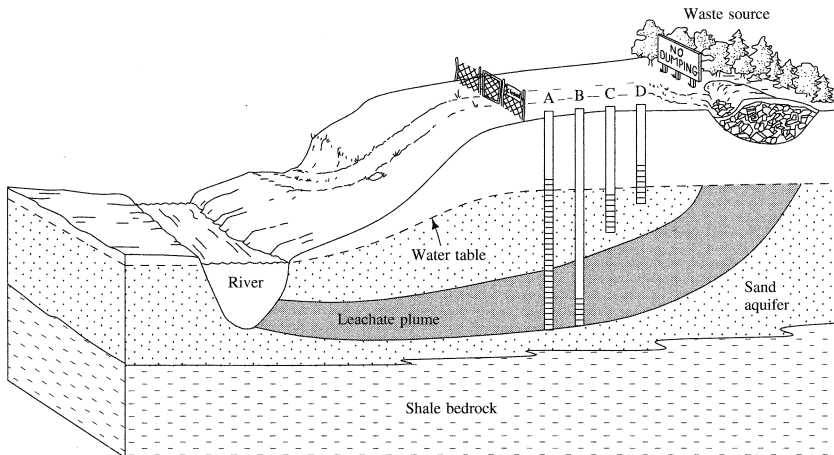
FIGURE 8.10 (a) Incorrect placement of water table-monitoring well screen. Seasonally high water table is above the top of the screen and floating, light nonaqueous phase liquids would be above the screen and not detected. (b) Incorrect placement of water table-monitoring well screen. Seasonally low water table is so far down in well that there is not enough water in well to collect a sample for chemical analysis. (The water table elevation could still be determined.) (c) Correct length and placement of water table-monitoring well screen.



contaminants can vary vertically. If a monitoring well has a long well screen, it has a greater probability of intersecting a plume of contamination. However, a water sample taken from such a well may draw water from both contaminated and uncontaminated parts of the aquifer, resulting in a reported concentration that is less than that of the groundwater in the plume. This is illustrated in Figure 8.11.

The collection of such unrepresentative water samples may have serious implications for the implementation of groundwater regulations. While monitoring groundwater in order to find the actual concentration of contaminants in a plume, it may be necessary to use several monitoring wells or piezometers screened at different depths at the same location (well cluster). Alternatively, several nested wells or piezometers can be placed in a single large borehole, each well with a screened interval and surrounding filter pack at a different depth, and with impermeable grout placed in the borehole between the screened intervals of the individual wells. These clustering and nested techniques can be expensive, not only due to the initial cost of the wells but also due to the costs of multiple chemical analyses for each round of sampling. However, such

FIGURE 8.11 Effect of monitoring well–screen length on water-quality sampling. Monitoring well A is fully screened through the thickness of the aquifer. It intersects the plume of leachate but the reported concentration will be less than the actual concentration as water is withdrawn from both contaminated and uncontaminated parts of the aquifer. Piezometer B is also screened to intersect the plume of leachate. The reported concentration will be representative of the leachate. Piezometer C and water-table monitoring well D don't intersect the plume, indicating that it is deep in the aquifer.



a configuration will yield the greatest amount of information about the hydraulic head as well as the water quality, and is typically a recommended regulatory approach for groundwater monitoring. Additionally, there are multilevel monitoring wells that allow discrete vertical sampling in a single borehole, along with measurement of other hydrogeologic properties such as hydraulic conductivity and fluid pressure (head). Multilevel sampling will be discussed further in Section 8.4.9.

If a monitoring well is intended to serve as a warning that a plume of contamination is escaping from a potential source, then it should be screened in the most permeable parts of the aquifer initially to intercept rapid excursions, with the understanding that measured concentrations may be diluted and not representative of the most contaminated parts of an aquifer. Groundwater, and contaminants that it may be carrying, not only preferentially travel through the most permeable material but travel faster there as well. Hence, the leading edge of a plume of contamination will follow the most permeable pathway.

If the plume of contaminated water is following a zone or direction of high hydraulic conductivity, it may flow in a direction that is not parallel to grad h . This may mean that the location of the plume is not exactly down-gradient from the source. (Likewise, as has been discussed in earlier chapters, nonaqueous phase liquids can pool up and deflect off low permeability geologic layers in down-dip directions totally inconsistent with the directions of groundwater flow).

On the other hand, long term monitoring can have different priorities. If an aquifer is contaminated and a monitoring well has been installed to monitor the progress of a remediation effort, the well should not be screened in the most permeable part of the aquifer. Many contaminants can become trapped in low permeability regions, and

can become sequestered for long periods of time. The eventual slow release of these trapped pollutants can cause a classically observed “rebound” in aqueous concentrations long after the high permeability zones appear to have been clean. In pump and treat systems, the water will preferentially travel through and flush out the more permeable zones. A well screened in a permeable zone may indicate that the aquifer is rapidly being cleaned, but in fact less permeable zones located nearby may still have high concentrations of contaminants that have yet to be removed. Therefore in contaminant investigations, monitoring low permeability zones is also typically carried out.

In general, the concentration of a solute obtained from a monitoring well will be less than the maximum concentration present in the aquifer. The well screen provides a vertically averaged value of the solute in the aquifer over the length of the screen. If the contaminant plume is thinner than the length of the screen, then the vertically averaged concentration of the solute that is obtained from a monitoring well will be less than the solute concentration in the plume as the monitoring well will be drawing in some uncontaminated water and diluting the contaminated water. Chiang, Raven, and Dawson (1995) found that if a monitoring well is purged continuously for 24 hours prior to sampling, it will draw in uncontaminated water from the aquifer below the well screen, and the concentration of solute in the well could be as much as an order of magnitude lower than the vertically averaged solute concentration in the aquifer.

8.4.8 Summary of Monitoring Design for Single Screened Wells

Figure 8.12 illustrates a comparison of the final design of a water-table observation well and a piezometer illustrating the design elements discussed in this section for single well screen designs.

8.4.9 Multiple-level Wells and Multilevel Devices for Groundwater Monitoring

Because many field studies have suggested that most contaminant plumes exhibit significant concentration changes over small vertical distances (Smith et al. 1987; Dumble et al. 2006; Biswas et al. 2014; USDOE 2015), multilevel monitoring wells (particularly high resolution techniques) often produce orders of magnitude more information and more accurate results than single, long-screened wells. Natural hydraulic gradients within long-screened wells can create vertical flow and cross-contamination within the well, and make definition of the vertical distribution of dissolved contaminants impossible (Reilly et al. 1989; Church and Granato 1996; Elci et al. 2001; Neilsen 2005; McMillan 2014). This message has not gotten through to all municipalities, industries, and regulators, however. The U.S. Nuclear Regulatory Commission (NRC), in its 2003 NUREG 1569 Guidance (pages 5-42 and 5-43) for in situ uranium leaching operations correctly states:

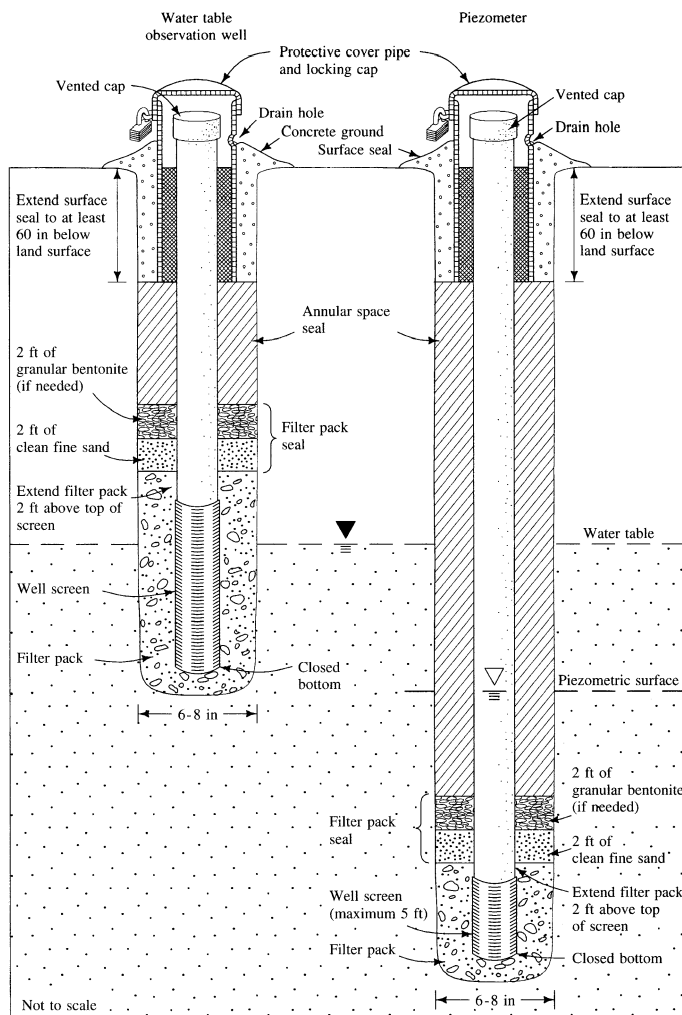
“Fully screened monitor wells sample the entire thickness of the aquifer. Therefore, excursions could not pass above or below the well screens. However, the concentration of the indicator parameters might be diluted and therefore may not provide timely warning that an excursion is occurring.

But then the NRC Guidance continues:

"Partially screened monitor wells only sample the zone of extraction within an aquifer. These wells might miss some excursions, but would suffer less from dilution effects than fully screened wells. For most situations the staff favors fully screened monitor wells."

In this document the U.S. Nuclear Regulatory Commission misrepresents multilevel sampling and does not recognize that high resolution multilevel monitoring: (1) is less likely to "miss" contaminant excursions than wells screened the entire aquifer

FIGURE 8.12 Construction details of a water-table observation well and piezometer.

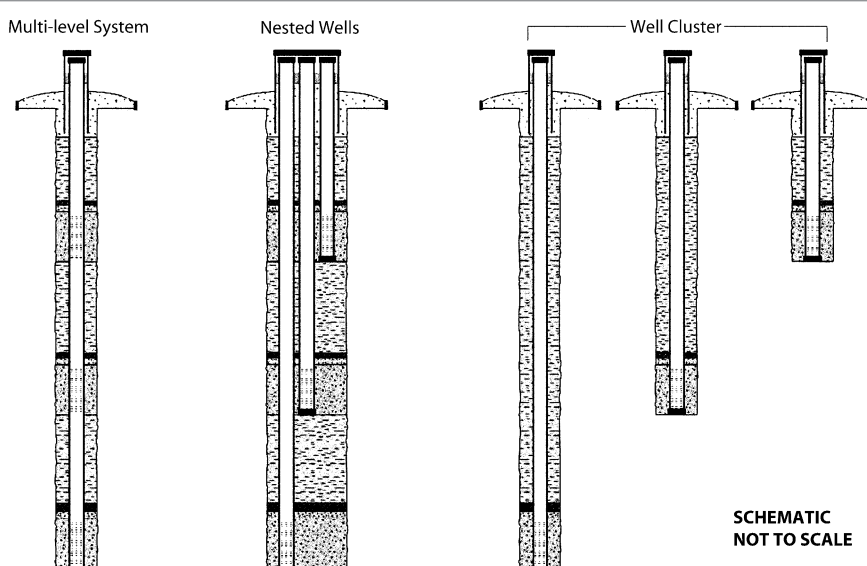


Source: Wisconsin Department of Natural Resources.

length, (2) has more possibility of accurately intercepting and quantifying excursions without bias, (3) reduces the possibility of contaminants migrating vertically within a monitoring well, (4) is many times more useful in post-mining remediation and site stabilization (both in directing cost-effective cleanup efforts and documenting their success), and (5) is much more protective of public health and ecological well-being.

Nested and Clustered Wells As mentioned in Section 8.4.7, to reduce dilution effects of long-screened wells and to preserve vertical sampling integrity, usually monitoring wells are installed in nested or clustered configurations (also called “multiple completions”), or with other types of multilevel sampling devices in a single borehole. Figure 8.13 illustrates multilevel sampling systems, nested wells, and well clusters. For nested wells, there is typically a single large borehole with several piezometers or wells placed in the same hole with screened intervals at different depths below the water table and with grout separating each different sampling depth. There has been some concern with the integrity of grout sealants in nested wells, and some criticism has been leveled at using these nested configurations. This is because of the difficulty in achieving effective and impermeable grout layers. These problems can be significant where the grout layers are thin because of many vertically close-spaced screen and grout intervals, or where there are many casing riser pipes in the nested well requiring grout to be placed effectively between the many pipes without void spaces developing. Clustered well groupings, on the other hand, sample different depths at the same locality by having several, closely spaced monitoring wells or piezometers with each in its own individual borehole. These individual wells typically can be placed within 1.5 m

FIGURE 8.13 Multilevel sampling systems, nested wells, and well clusters with above ground completion.



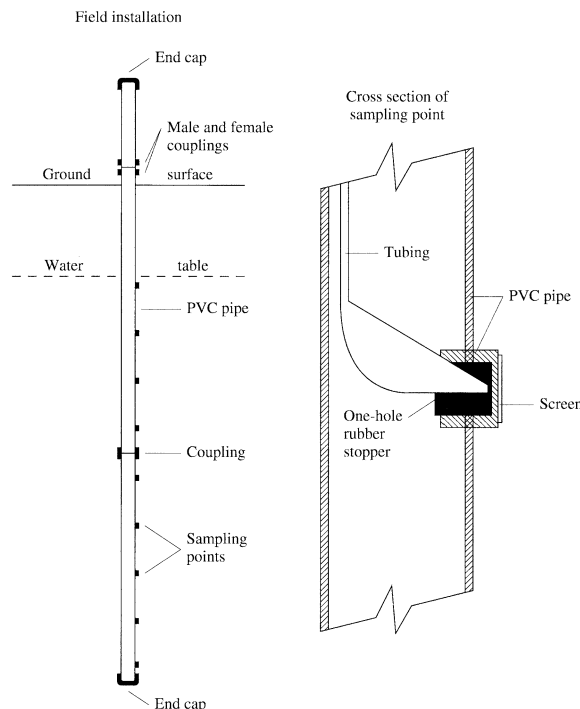
(5 ft) of each other. Under these circumstances it is possible to obtain an excellent seal to prevent vertical movement of water along the casing.

In nested wells, two or more monitoring wells or piezometers are placed in a large-diameter borehole with grout seal between screened intervals at different depths. For example, this could be done in an unconsolidated formation by (1) driving a 25.4 or 30.5 cm (10 or 12 in.) diameter casing with a cable tool rig to the depth of the bottom piezometer, (2) installing the deepest piezometer, (3) pulling back the casing and installing the filter pack and seal for the deepest piezometer, (4) pulling back the casing and grouting up to the level of the next piezometer, (5) allowing the grout to harden, (6) installing the next piezometer, (7) pulling back the casing and installing the filter pack and seal for the second piezometer, and (8) pulling back the casing and grouting up to the level of the third piezometer, etc.

Simple Manufactured Multilevel Samplers It is possible to install inexpensive multilevel sampling devices in a sandy aquifer. One early manufactured model of such a device consists of a rigid PVC tube, inside of which are multiple tubes of flexible tubing. Each tube leads from the surface and ends at a different depth. Each has a port into which a groundwater sample can be drawn. Sampling ports can be closely spaced vertically, so that very detailed vertical sampling can be accomplished. Water is withdrawn from the tubing by applying suction, so the water table had to be less than 7.6 m (25 ft) below the surface in these simple early multilevel sampling wells. These rudimentary methods include a variation by fastening a bundle of flexible tubes, each of a different length, to the outside of a rigid PVC pipe that acts as a spine. Several types of simple manufactured multilevel samplers have been developed (Pickens et al. 1978; Cherry and Johnson 1982; Ronen et al. 1986).

Barker et al. (1987) evaluated the bias in samples that can be introduced by the use of multilevel piezometers constructed out of flexible tubing. Leaching of plastics from the plastic tubing is one problem. Another problem is the sorbing of organics by the tubing. Both these problems can be minimized by using Teflon® tubing and thoroughly purging the tube prior to sampling, although Teflon® is porous and can have some minimal memory effect. Many types of flexible tubing can actually transmit organics from groundwater through the tubing wall to the sample water in the tubing. This is especially true for polyethylene tubing. Samples drawn from below an organic plume may indicate contamination, when in fact the organics are being transmitted across the plastic tubing from adjacent contaminated groundwater. This can apparently occur even with Teflon® tubing. For this reason, multilevel piezometers, designed so that the flexible tubing is exposed to groundwater, may not be appropriate for monitoring plumes of organic contaminants. If the flexible tubing is contained within a casing, such as in Figure 8.14, this should not be an issue because the tubing doesn't come into contact with the groundwater.

A simple multilevel sampler can be installed by using a hollow-stem auger. The device is constructed at the surface and lowered to the desired depth through the augers. It is not possible to develop the sampling ports, so this device is best suited for clean, sandy sediment. No filter pack or grout is used in this very simple construction. The augers are withdrawn and the native sand is allowed to slump around it. One disadvantage of this device is that it is usually not possible to measure water levels with it.

FIGURE 8.14 Multilevel groundwater sampling device for use in sandy soil.

Source: J.F. Pickens et al. 1981. A multilevel device for ground-water sampling. *Groundwater Monitoring & Remediation* 1:48–51. Used with permission.

Another more innovative type of device is the multilevel sampling using multi-channel tubing. In this system called Continuous Multichannel Tubing (CMT®), high density polyethylene (HDPE) tubing is pre-formed with seven internally partitioned, vertical channels across the interior diameter of a larger, outside HDPE cylindrical tube. The “honeycombed” design has six outer pie-shaped vertical tubes and a central hexagonal tube. Each of the pie-shaped channels can have sampling ports drilled at a target depth. This single large tube with continuous internal partitions does not require bundles of tubes and can be constructed with an external stainless steel casing/screen combination for strength (Einarson and Cherry 2002).

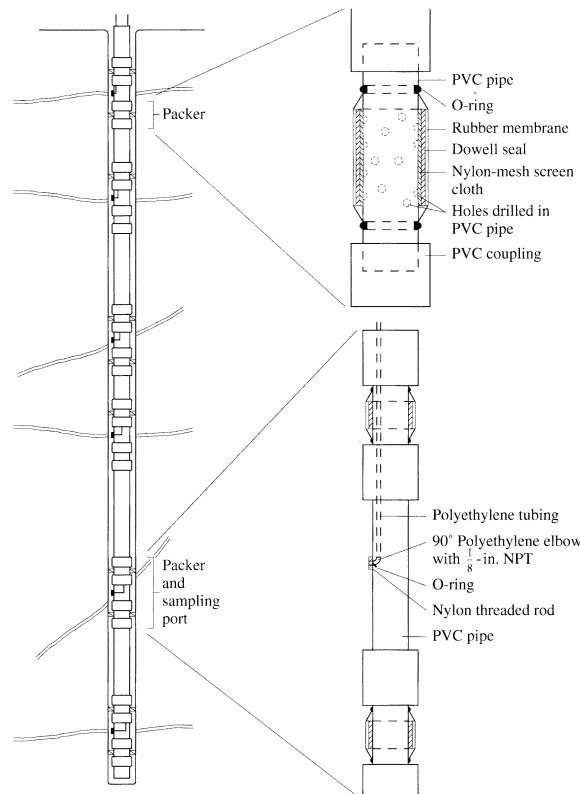
Multiport Vertical Sampling There are many sophisticated multilevel sampler systems for a single borehole with multiple, vertically displaced ports that can be remotely accessed to allow sampling at different depths. One multiple depth well of this kind is the Westbay® system. In this type of well there are multiple ports at different depths and an individual sampler probe inside the casing can attach and seal to any port. Then the sampler and port valves (that are operable from the surface) can be opened and a sample taken. After the valves are closed, the sample container can be retrieved to the surface, and either decanted to other containers, or directly transported to the laboratory, maintaining formation pressure along with water quality analysis. While

generally expensive, these multilevel wells have advantages of allowing fewer wells and subsurface disturbance at each site, collection of fluid samples without repeated purging, prevention of vertical flow within the borehole, less possibility of cross contamination with discrete depth sampling, and options for automated sampling at any number of multiple depths in a single well.

Flexible Liner Systems Another type of multilevel sampling practice employs the flexible liner system (developed by FLUTe™) and represents a significant advancement over a simple multilevel system. Similar to the simple system above, it has a series of internal tubes inside a liner which allow sampling and pressure measurement at selected intervals down hole in uncased wells. In hard rock consolidated systems, downhole television logging in uncased boreholes can identify exact locations of fractures (and other depths of interest) and tubing can be customized to sample those depths. In this system, a flexible polyurethane-coated, nylon fabric liner is emplaced with eversion (turning inside out) from a shipping reel. The liner is pressurized (pneumatically or hydraulically), inflated, and extends downward from internal pressure head. The liner deploys from the ground surface downward, creating a sealing pressure that prevents vertical flow outside the liner, and has tubing (usually made of polyvinylidene fluoride—PVDF) inside the liner from ground surface to vertically displaced subsurface ports. The system is versatile in that the inflating liner can be placed in boreholes that change direction due to directional drilling, and can move in varying diameter boreholes, such as narrow, shallow surface casing to wider uncased sections below, or narrowing or telescoping boreholes. Interestingly, this system can be modified to measure discrete depths of nonaqueous phase liquids (NAPLs) by use of a hydrophobic “ribbon” sampler. In this application, a porous, continuous, hydrophobic sleeve, that is impregnated with a powdered oil dye (Sudan IV), is deployed concurrently on the outside of the flexible liner. The hydrophobic material readily “wicks” NAPLs and when retrieved identifies depths of NAPL contamination. The hydrophobic sleeve is replaceable for additional deployments on the same flexible liner (Riha et al. 2000; USEPA 2004).

Packer Systems A type of multilevel sampler optimal in bedrock boreholes involves straddle packers, which when inflated isolate a section of a borehole for hydrological testing and sampling. In this design (Figure 8.15) packers are located above and below each sampling port; when they are inflated, they seal off that part of the borehole and are particularly effective in segregating individual fractures or groups of fractures for analysis in uncased boreholes. Packers can also be used within well casing in less consolidated material. Packers can be permanently installed, or they can be removed and reused if desired. Though designs vary, the inside of a typical single packer is a perforated pipe forming the inner packer body, covered with a porous plastic sleeve and an expansion sleeve. External to that is a gum rubber inner sheath, often enveloped in woven Kevlar® and encased in a durable gum rubber outer sheath, with the assembly secured on either end with stainless steel clamps. One type is the Solinst® Waterloo System with includes multi-purge manifold well heads and dedicated sampling pumping and transducers.

Interesting specialized variants of packer systems have been constructed for specialized applications. Packers have been used in small, bedrock boreholes in conjunction with seals created by injecting grout into a flexible cylindrical impervious fabric liner. These liners have a diameter slightly larger than the borehole, ensure that the

FIGURE 8.15 Multilevel groundwater sampling device for use in fractured rock aquifers.

Source: J. A. Cherry and P. E. Johnson. 1982. A multilevel device for monitoring in fractured rock. *Groundwater Monitoring & Remediation* 2:41–44 Used with permission.

entire borehole above a screened interval is sealed, and prevent grout from entering fractures and altering groundwater chemistry (Parker et al. 2015; Pierce et al. 2015).

■ 8.5 Installation of Monitoring Wells

8.5.1 Decontamination Procedures

Because the purpose of drilling a monitoring well is to collect a sample of water and analyze it for very small concentrations of chemicals, it is highly desirable not to introduce any chemicals into the aquifer as a part of the well-drilling and installation procedure. The process of cleaning the equipment and supplies that will be used is called **decontamination**.

When materials are manufactured, they may become coated with substances such as grease and oil. Therefore, unless the manufacturer specifically guarantees that the article has been decontaminated and has shipped it in a well-sealed wrapper, it should be decontaminated. Equipment that has been used at a contaminated site should be

assumed to be contaminated and should be decontaminated before it is used at another site. Even at the same site, if a drill rig or a bailer is used at different wells, decontamination is required to prevent cross contamination (contamination from one area being introduced into a clean area) that could occur.

There is wide variability in required and recommended decontamination procedures in the United States between the USEPA and the various states (Mickam et al. 1989). The hydrogeologist must consult with the appropriate regulatory authority to determine if a specific decontamination procedure is required. In the absence of a specific requirement, the following generic procedure should adequately clean equipment and supplies. In some cases not all the steps are required. For cleaning large equipment such as a drilling rig, a specific area must be set aside and a decontamination pad must be constructed to capture all the fluids used in the process. If the rig is contaminated, wash water from it may also become contaminated. Be careful that any solvents used aren't accidentally released to the environment. Small tools such as bailers and Shelby tubes can be cleaned in buckets set on a polyethylene sheet. Sampling pumps can be cleaned by running various wash solutions through them, as well as washing the exterior.

The following steps are used to clean drilling and soil sampling equipment including drill rig, augers, drill rod, tools, sampling tubes, etc.:

1. Use a wire brush or similar equipment to remove all dried sediment and thick accumulations of grease.
2. Wash the equipment with a soft brush and water with phosphate-free detergent.
3. In extreme conditions organic residues can be removed by washing the equipment with an organic solvent such as methanol or propanol. Don't use solvents such as trichloroethene that might be expected to be found at a hazardous waste site.
4. Clean and rinse the equipment with potable water.
5. Rinse the equipment with deionized water.

Steam cleaning with a pressure sprayer can be used in step 4 for equipment that can withstand the heat and force of the spray. After equipment has been decontaminated, it should not be placed on the ground. It can be wrapped in clean paper or aluminum foil or set on polyethylene sheets.

Sampling equipment should also be decontaminated between uses. If the equipment has not come into contact with nonaqueous-phase liquids, rinsing with potable water and washing thoroughly with phosphate-free detergent, including scrubbing the inside of tubes with a bottle brush, followed by a potable-water wash and then a deionized-water rinse, should suffice. If the equipment has come into contact with nonaqueous-phase organic liquids, then an initial solvent wash may be necessary.

The cost of decontamination of sampling equipment and the uncertainty introduced by solvent washing has led many hydrogeologists to specify dedicated sampling equipment in each well. Disposable bailers are also available that are less expensive than the cost of labor involved in cleaning reusable bailers.

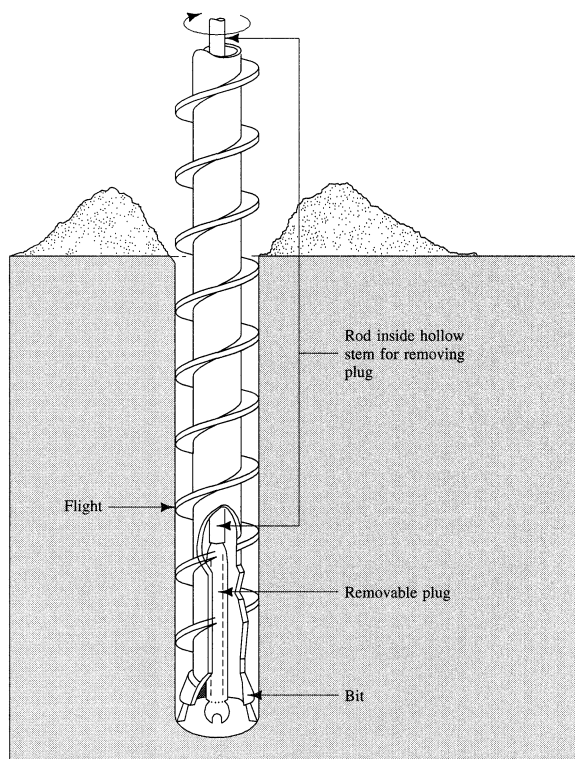
8.5.2 Methods of Drilling

There are a number of methods of drilling that are appropriate for installation of monitoring wells. When working in shallow unconsolidated formations, hollow-stem

augers are commonly used. If a well is to be drilled deeper than about 30.5 m (100 ft) or into bedrock, a rotary drilling method may be appropriate. Cable-tool drilling is an excellent way of installing monitoring wells in both unconsolidated and consolidated formations, but it is slow and may be expensive. Hollow-stem augers with a bit that contains carbide teeth can also be used in weak, indurated rock. Newer techniques include sonic drilling and directional drilling.

Hollow-Stem Augers Hackett (1987; 1988) presents an authoritative discussion of all aspects of drilling with hollow-stem augers. A hollow-stem auger looks a little like a large, untapered screw (Figure 8.16). The auger flights are constructed around a hollow pipe. A drilling rig rotates the augers and a bit on the end of the auger loosens the sediment, which is then brought up to the surface by the rotating auger flights. The cuttings accumulate at the surface and must be shoveled away from the augers. Figure 8.17 pictures an auger-drilling rig. The auger is advanced into the ground as it is rotated. A plug on the end of a rod inserted through the hollow-stem may be screwed into the bit to seal the end of the opening and prevent sediment from coming up inside the hollow-stem. Alternatively, a nonretrievable plug can be placed in the end of the

FIGURE 8.16 Hollow-stem auger drill rod and bit.



Source: M. L. Scalf et al. 1981. *Manual of Ground Water Sampling Procedures*. National Water Well Association. Used with permission.

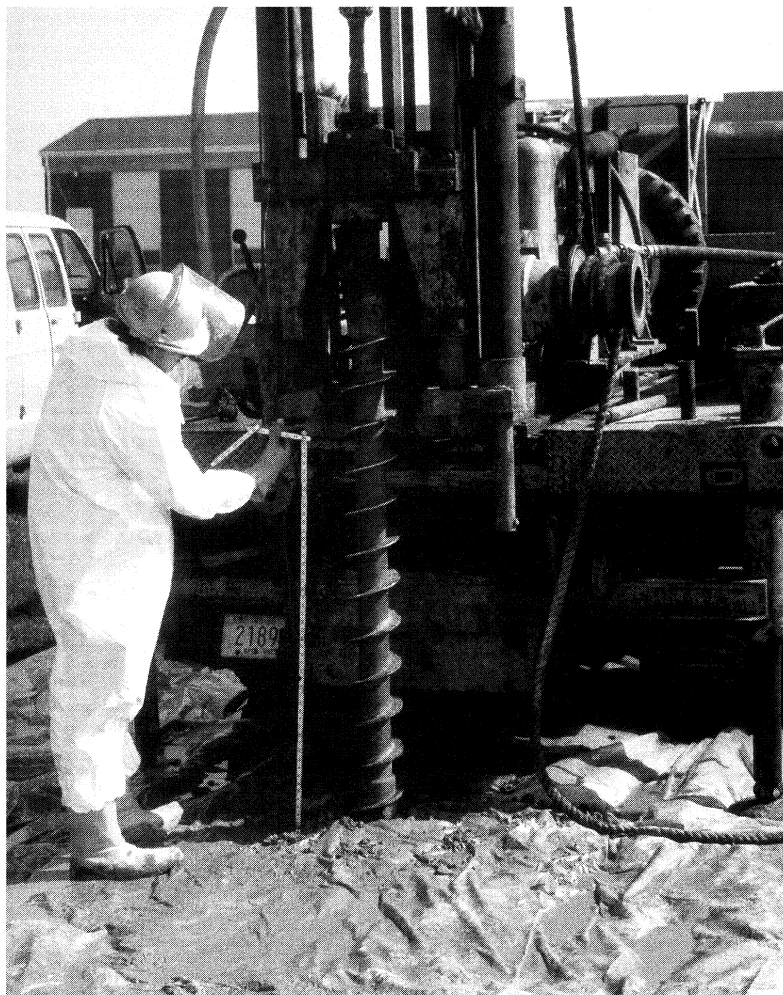
FIGURE 8.17 Hollow-stem auger drilling rig.

Photo credit: C.W. Fetter.

bit. This plug is knocked out of the end of the augers when the final depth is reached and it is no longer needed. However knock-out plugs preclude the collection of soil and water samples during drilling.

One advantage of drilling with hollow-stem augers is that drilling fluids and mud are normally not required. Circulation of drilling fluids has the potential to spread contaminants throughout the borehole. Drilling mud is a viscous liquid needed in mud-rotary drilling that can line the borehole and partially seal it. However, when drilling in formations with cohesive layers, the auger bit may smear clay from the cohesive layers so that it mixes with sand and gravel layers at the perimeter of the borehole. Auger drilling typically can advance about 15.3 to 30.5 m (50 to 100 ft) per day if samples are

being taken. Occasionally, downward progress can cease if a large cobble or boulder is encountered (called auger refusal).

Augers usually come in lengths of 1.5 m (5 ft). One flight is advanced into the ground and then the drill stem is disconnected and another flight is attached to the augers in the ground. At this time samples of the formation ahead of the auger bit may be taken. The plug on the end of the bit must be removed before sampling can occur. The maximum depth at which hollow-stem auger drilling can normally be used is 45.8 m (150 ft) (Hackett 1987); as a practical matter, it rarely exceeds 30.5 m (100 ft).

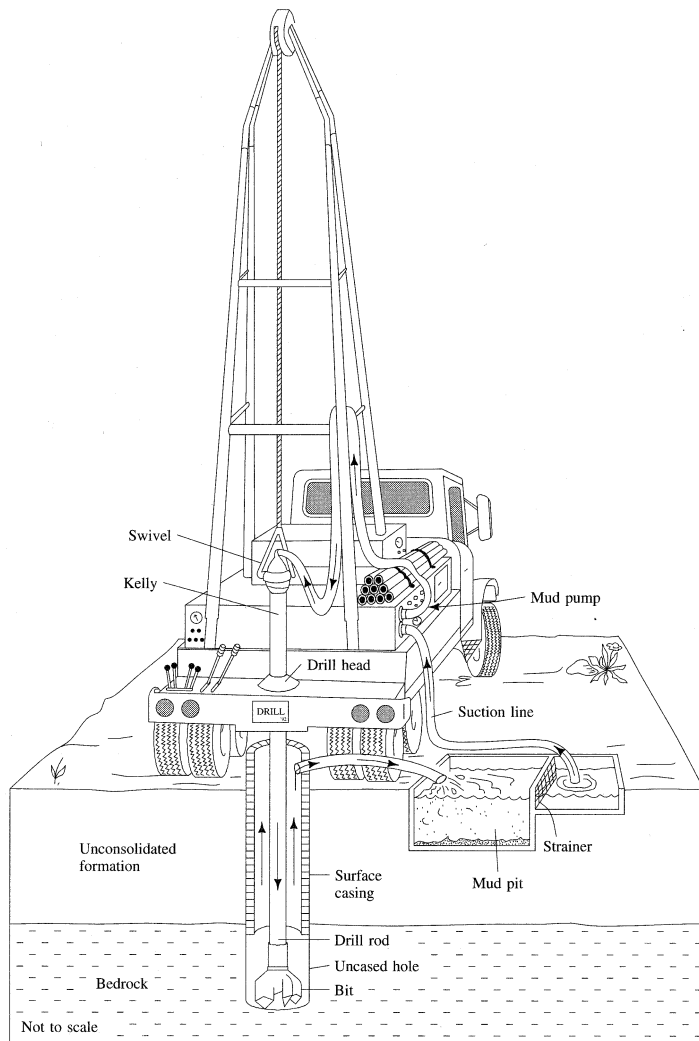
Some loosely consolidated sands, called heaving sands, can enter into the borehole when the plug is being removed. This problem can be avoided by keeping the hollow stem filled with potable water when the plug is removed. The potable water should not contain any contaminants that might be found in the groundwater. If no formation sampling is planned, then a knock-out plug can be used to prevent the introduction of heaving sands into the hollow-stem during drilling. The knock-out plug can be removed after the final depth is reached by pushing down with the well casing if it is stainless steel; otherwise it will be necessary to use a rod prior to the time that the well is installed.

Hollow-stem auger drilling can also be used to sample water quality at various depths during drilling. At a selected horizon the plug at the end of the hollow stem is removed. A well point on the end of a rod is lowered to the bottom of the augers and then is driven ahead of the bit by hammering or hydraulic pressure. The well point is developed by pumping until clear water is obtained. A sample of groundwater at that depth is then obtained. It is best if potable water is not used in the borehole during this procedure, because it could interfere with the groundwater quality. If there is heaving sand inside the augers, the well point can be driven through it. Alternatively, a slotted hollow-stem auger can be used (sometimes called a screened hollow-stem auger or Keck auger) which allows water to flow into the stem.

Keeley and Boateng (1987) suggested a modification of the hollow-stem auger drilling technique, in which a temporary casing that is larger in diameter than the auger bit is employed. The auger is advanced several feet and then the temporary casing is driven to the depth of the auger bit by repeatedly dropping a heavy weight on the top of the casing. The advantage of this modification is that it prevents mixing of soil horizons as the augers rotate.

Mud-Rotary Drilling Mud-rotary drilling can be used in both unconsolidated and consolidated formations. It is fairly rapid, up to 30.5 m (100 ft)/day, and can be used to depths far in excess of most that might be required for groundwater-contamination studies. A heavy drilling fluid, made by mixing various additives to water, is circulated in the borehole by pumping it down the inside of hollow drill rods. The mud rises back to the surface in the annular space between the borehole wall and the drill pipe. The rising mud carries with it the drill cuttings, which settle out in a mud tank at the surface. Figure 8.18 shows the circulation pattern for mud-rotary drilling. Alternately, reverse circulation is often used where drilling fluid goes down the annular space and returns upward through the drill pipe (opposite of Figure 8.18). This method, discussed below, can allow greater upward velocities and larger, heavier cuttings can be retrieved.

One advantage of mud-rotary drilling is that the borehole will remain open after the string of drill pipe and the bit are removed. This means that a complete suite of geophysical logs can be run on the hole, which is kept open by the weight of the mud

FIGURE 8.18 Circulation of drilling fluid in mud-rotary drilling.

inside it. However, the fluid in the drilling mud can penetrate the native formations and alter the groundwater geochemistry. The coating of drilling mud on the borehole walls may be difficult to remove. This can impede the hydraulic connection between the well and the formation. Bentonite-based drilling muds may remove metals from the groundwater and affect the chemistry. Certain additives to drilling mud can also be problematic from a water quality standpoint. Because of the potential problems with drilling mud, rotary drilling may not be as suitable for groundwater contamination studies as hollow-stem augers. However, under many hydrogeologic conditions it is the only drilling method that is practical. Good well development to remove the residual drilling mud in the screen zone is very important.

Air-Rotary Drilling If the monitoring well is to be installed in bedrock, then air-rotary drilling may be considered. First a surface casing needs to be installed through any unconsolidated material. Typically this is done by using mud-rotary drilling. The surface casing is large enough that the air-rotary bit can fit inside of it.

The fluid used in air rotary is compressed air, which is blown down the inside of the drill pipe. The air then blows the cuttings back up the annular space, where they accumulate around the borehole. When the water table is encountered, the air may blow groundwater out of the borehole as well. If this occurs, it is possible to determine when the water table is encountered and the relative yield of the well. However, the air may also force the water back into the formation. Air-rotary drilling using a down-hole percussion bit can drill up to 18 m (60 ft)/hr. Samples are collected as chips, which are brought to the surface with the return flow of air and water.

Air-rotary drilling is fast and can go to depths of a thousand feet or more. Because air is the drilling fluid, contamination problems are minimized. However, the drillers may want to add a foaming agent to the air (air/polymer mix) as it goes down the hole. The foam helps to float the chips to the surface, but it consists of organic chemicals such as isopropyl alcohol, ethyl alcohol, and alcohol ether sulfate, and its use should be avoided. The air compressors have air filters, which need to be in good working condition; otherwise, lubricating oil and other contaminants may be introduced into the borehole with the compressed air. Percussion hammers used for air-rotary drilling may also need lubricants.

Air-rotary drilling may introduce volatile organic compounds into the atmosphere as well as blowing contaminated dust out of the borehole.

Reverse-Rotary Drilling In reverse-rotary drilling the circulating drilling fluid drains down the annular space and then is pulled up the center of the drill stem by a suction pump located on the drill rig. Because the drilling fluid rises with a much greater velocity in reverse-rotary than in mud-rotary drilling, a much less viscous drilling fluid is used. In many cases clear water mixed with the drill cuttings is all that is necessary. This gives the reverse-rotary method an advantage over mud-rotary drilling, since it is much easier to develop the well because there is no mud wall on the borehole to break down. However, reverse-rotary drilling is more expensive than the mud-rotary method, and the minimum borehole diameter is 30.5 cm (12 in.)

Cable-Tool Drilling Cable-tool drilling is one of the oldest drilling methods and has been used widely for the installation of water wells. Although the drilling equipment is less expensive than for some other methods, the drilling is slow and overall costs may be expensive due to high labor costs.

In cable-tool drilling a heavy bit is located at the end of a tool string hanging from a cable. The drill rig repeatedly lifts and drops the hammer, which breaks up consolidated rock or loosens unconsolidated sediment. A steel casing is driven into the formation behind the bit. When the bottom of the casing fills with broken rock and sediment, the tool string and bit are removed, and a bottom-loading bailer is used to remove the accumulated cuttings. Below the water table, the groundwater and cuttings make a slurry. Above the water table, water must be added to make a slurry so that the bailer can be used. Drive casing is needed only until bedrock is reached. In most bedrock formations the hole will stay open without drive casing. Figure 8.20 shows the tools used for cable-tool drilling.

Advantages of cable-tool drilling include the fact that no drilling fluids are used and that nothing is circulated through the well. Both factors serve to limit contamination problems. It is easy to collect representative samples of the formation during bailing of the casing. Well points can be driven ahead of the casing in unconsolidated formations for the collection of water quality samples. Cable-tool drilling can be used to depths in excess of 305 m (1000 ft). This method however can be extremely slow for deep boreholes, as the tool string and bit must be removed from progressively deeper depths to allow insertion of a bailer for the removal of cuttings, the bailer must then be removed from depth, and the tool string and bit reinserted. As depths increase the time required for this process compounds.

Sonic (Vibratory) Drilling Sonic drilling uses high frequency mechanical oscillation with rotary motion to fluidize subsurface material. As soils and formation materials experience liquefaction, temporary porosity reduction and inertial effects reduce friction on the drill string and drill. The destroyed shear strength of the subsurface formations allows rapid downward advancement in most instances. Advantages include a minimal amount of formation disturbance, reduction of drill spoils and waste compared to other methods, the method can produce continuous cores, sonic does not require circulating drilling fluids, and it can be converted to air or mud rotary or cable tool percussion techniques. Its disadvantages are that the technique is not as readily available as other techniques and is generally more expensive initially.

Other Types of Drilling Other types of drilling include percussion rotary air blast (RAB), air core drilling, and diamond core drilling. RAB combines rotary fluid circulation with the percussive impacts of a pneumatic, reciprocating, piston-driven "hammer" to pulverize rock. This is an effective way to advance drilling downhole in consolidated rock and mixed consolidated/unconsolidated terrain. Like most rotary fluid circulation techniques, circulation can be lost if a large cavity is encountered such as caverns in karst areas, lava tubes in volcanic regions, or human-made features such as subsurface mine shafts. Air core drilling cannot penetrate consolidated rock as well as RAB; it normally is used on weathered regolith or other unconsolidated material. The air core method utilizes hardened steel or tungsten blades to cut into the ground, and collects a more representative sample of solid material compared to RAB. Diamond core drilling is a very slow method used in hard, consolidated rock. It produces a rock core that can be inspected. Often fracture patterns, fracture orientation and aperture size can be determined from these cores. Diamond coring for short intervals can also be used on smaller consolidated formations encountered while drilling with other methods.

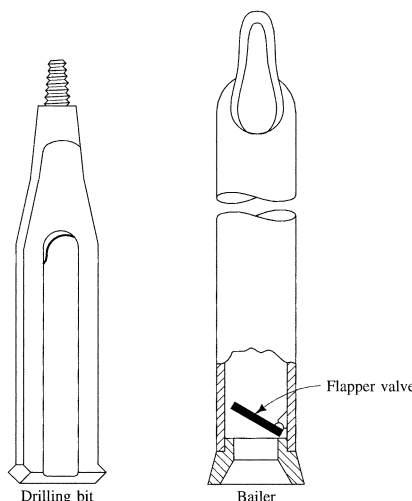
When drilling in areas with muddy or spongy soils, it may be necessary to build temporary roads, e.g., laying down a layer of crushed rocks to permit the heavy drilling equipment to reach the drilling locations without getting stuck (Figure 8.19). Alternatively, portable coring drilling machines, originally designed for mineral exploration, can be used to advantage to install hard rock monitoring wells in sites that are hard to access, in remote locations and wilderness sites, and in eco-sensitive areas. Drills, such as the Shaw Portable Core Drill and the Winkie Drill can produce small diameter holes amenable to fractured rock monitoring (Parker et al. 2015).

FIGURE 8.19 When drilling in difficult-to-access areas or where soggy soils prevent heavy drill equipment to reach the site, a portable drill rig can be used. Shown here is the installation of an 8-inch bedrock well with a portable air-rotary drill rig in a rice field in Goa, India. The drill rig is powered by pneumatic pressure provided by a truck-mounted compressor which is safely stationed on hard ground approximately 100 m (300 ft) away.



Photo credit: T.B. Boving.

Directional Drilling Directional drilling involves the placement of nonvertical boreholes. Most of the above drilling methods are able to be used in slant drilling (excepting cable tool), where in the simplest application, the mast or drill rig tower is tilted and drilling proceeds at an angle. This modification allows great horizontal access under structures such as buildings, landfills and highly contaminated areas. Drilling through a subsurface NAPL pool, for example, can be avoided in some cases. Traditional drilling methods can be difficult to control in slant drilling because of unwanted deflection, as in slant auger drilling. As slant auger drilling proceeds, cuttings which fall on the bottom side of the hole can eventually force the bit upward into a more horizontal line.

FIGURE 8.20 Tools used for cable-tool drilling.

Controlling wellbore trajectory has become more of a refined technology in recent years. Most modern directional drilling begins in a vertical direction until a desired kick off point where the well inclination is changed using drilling motors and rotary steerable systems. While the use of directional drilling is much more common in oil and gas development, its applications to contaminant hydrogeology are plentiful, particularly where surface or near-surface features or contaminant hotspots must be avoided, but geologic, hydrogeologic, and contaminant information from greater depths directly under these areas is needed.

8.5.3 Drilling in Contaminated Soil

When drilling at a contaminated site, the cuttings that are brought to the surface may be contaminated. Drilling personnel should wear appropriate protective clothing and, if necessary, use breathing apparatus. A large, heavy sheet of plastic should be placed in the work area, and the drill bit should be advanced through a hole in the center of the plastic sheet.

The cuttings augered to the surface can be collected from the plastic sheet and put into containers for proper disposal.

8.5.4 Sample Collection of Solid Material During Drilling

Samples of unconsolidated materials and rock are needed to delineate the geology of a site. They are collected by drilling **boring**s. Borings may be made just for sample collection, or they may be made as a part of the process of installing a monitoring well. Borings may be made by any of the methods of drilling discussed in Section 8.5.

During the drilling process, earth materials are brought to the surface. During the augering process, soil and sediment ride up the augers; in the mud-rotary process, earth materials come up mixed with the mud; in air-rotary drilling there is a slurry of rock and

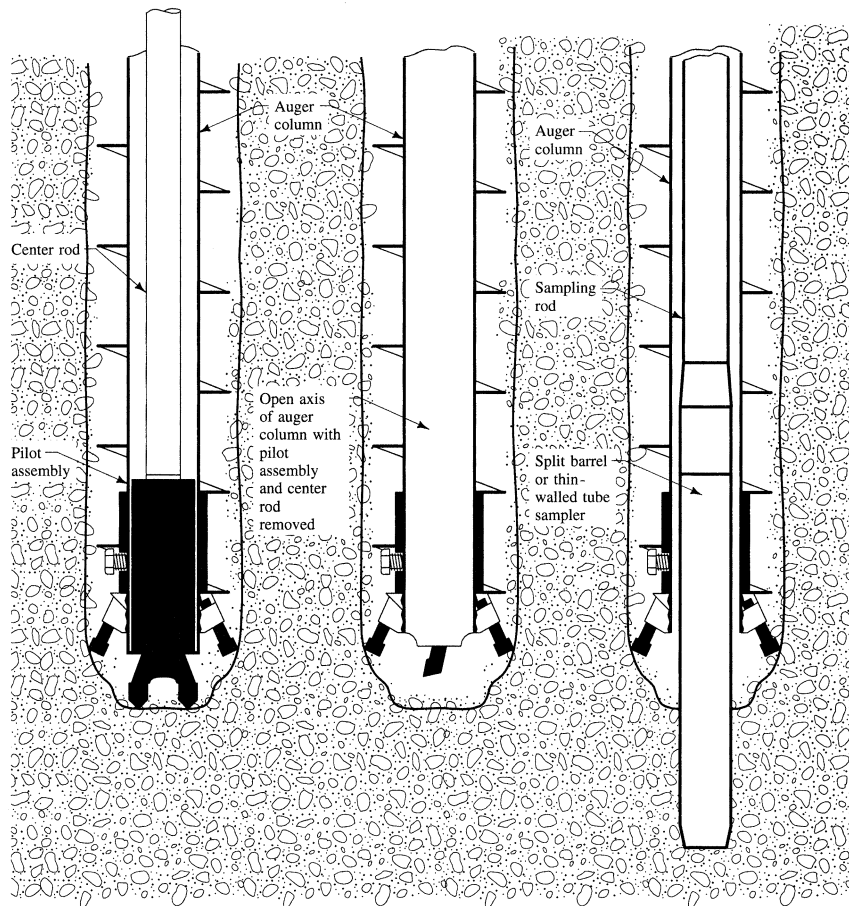
water brought to the surface by air pressure; and cuttings are brought to the surface with a bailer in cable-tool drilling. In all cases the samples are disturbed, some (such as the samples on the augers) more than others. In addition, it may be difficult to tell the exact depth represented by the sample. Fine layering of sedimentary materials cannot be distinguished in such samples. An imprecise model of the geology can be constructed from these samples, but for more details, undisturbed samples should be collected.

A **core sample** is collected for consolidated material by obtaining a **rock-core sample** with a special drilling bit studded with industrial diamonds as mentioned above, or for unconsolidated material with special sampling tubes that are driven into the unconsolidated formations. Interpretation of hard rock cores in consolidated, fractured media suspected of contamination has become quite advanced in the last few decades and can include field geologic core analysis, and laboratory analysis (Parker et al. 2012). The initial field analysis involves determination of the number of fractures, fracture orientation and aperture size, and fracture porosity measurement. This analysis can also observe any occluding chemical precipitates filling (or “healing”) the fractures. The orientation of fractures from several core holes can be analyzed to give a three-dimensional view of fractures at a site. Combined with downhole geophysics and tomographic methods, field data can give considerable insight into a fractured rock media and the potential for contaminant movement.

Laboratory measurement of bedrock cores can quantify contaminants in the core, simulate degradation microcosms, and provide core physical, mineralogical, and microbial measurements to determine contaminant phase and mass distribution. Typically, most groundwater flow in fractured consolidated rock occurs through interconnected networks of fractures and secondary porosities, surrounded by low permeability blocks of rock. In adjacent blocks with porosity greater than 1% however, particularly in sedimentary rocks, an appreciable mass of a contaminant can move into the rock matrix. This matrix diffusion in low-permeability blocks or effectively reduces the mass flux in the surrounding fractures (Parker et al. 1997; Parker et al. 2010; Kennel 2008).

Great care must be exercised in the interpretation of rock cores or unconsolidated borings, particularly in the measurement of subsurface contamination or characterization of stratigraphy based on just a few samples. The absence of contamination in a core could be the result of preferential flow (also called “funneling,” “fingering,” wetting front instabilities, or Rayleigh Taylor instabilities), allowing contamination to completely bypass a boring but still be present in massive amounts. Likewise, unwarranted extrapolation of meager stratigraphic data, particularly assuming continuous layers of unvarying properties, is a common problem particularly in situations where incomplete site characterization goes unchallenged. There are two main types of sampling tubes for unconsolidated samples. Both types of tubes can be used with hollow-stem augering and mud-rotary drilling if the drill rod and bit have a provision for a sample tube to be extended through them into the formation ahead of the bit. Figure 8.21 shows the sequence for the extension of a sampler through the end of the bit of a hollow-stem auger. The sampler is driven or pushed into undisturbed formation ahead of the bit. In cable-tool drilling the drill bit is removed from the borehole and the sampler is lowered on a rod or cable.

A **Shelby tube** is a thin-walled tube that can be screwed to the end of a rod, lowered to the bottom of the drilled hole, and pressed into cohesive sediments by using hydraulic pressure reacting against the weight of the drill rig. These samples are said

FIGURE 8.21 Sequential steps for the collection of a core sample through a hollow-stem auger.

Source: G. Hackett. 1987. Drilling and constructing monitoring wells with hollow-stem augers part 1:Drilling considerations. *Groundwater Monitoring & Remediation* 7:51–62. Used with permission.

to be *undisturbed*, although they are in fact minimally disturbed. The precise method of collecting a Shelby tube sample is described in method ASTM D1587 (American Society for Testing and Materials 1983). The sample can be extruded from the Shelby tube in the lab and trimmed into a permeameter for a permeability test. Details of the microstratigraphy can be examined as well. Shelby tube sampling does not work with noncohesive sediments.

A **split-spoon sampler** can be used for the collection of samples of both cohesive and noncohesive sediments. The split-spoon sampler consists of a split tube with thicker walls than a Shelby tube. The two halves are placed together and joined by screwing a circular drive shoe on the bottom and a head assembly on the top. The assembled split-spoon sampler is screwed to a rod and lowered to the bottom of the drill hole. A pipe-like weight of 63.5 kg (140 lb) is placed on the top of the rod.

The weight is repeatedly raised and dropped a distance of 76 cm (30 in.) in order to drive the split-spoon sampler into the formation. The number of blows necessary to drive the sampler every 15cm (6 in.) is recorded as the sampler is driven 46 cm (18 in.) into the formation. The more dense the formation, the greater the number of blows needed to drive it 15 cm (6 in.). The process is described by ASTM 1586 (American Society for Testing and Materials 1984).

After the split-spoon sampler is driven 46 cm (18 in.), or after refusal, it is brought to the surface and opened. Frequently, less than 46 cm (18 in.) of sediment have been collected. Fine, noncohesive sediment such as sand may fall out of the sampler as it is being retrieved. Sediment greater in diameter than one-third of the diameter of the sampler may not enter it at all. A pebble may lodge in the barrel and not allow any other sediment to enter. Sediments may compact in the sampler so that a full 18-inch sample may actually occupy less than 46 cm (18 in.) of the core barrel. The hydrogeologist examining the split-spoon sample must use his or her judgment in making a log based on the split-spoon samples. Figure 8.22 is a photograph of a split-spoon sample.

FIGURE 8.22 Hydrogeologist describing a split-spoon sample.



Photo credit: C. W. Fetter.

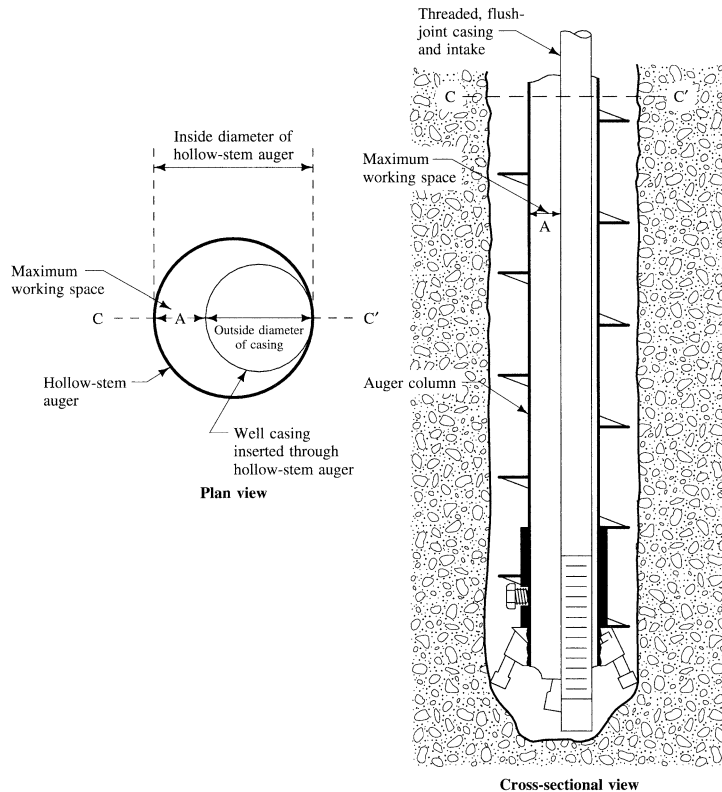
A standard for core samples is to collect one 46 cm (18 in.) sample every 1.5 m (5 ft). This frequency of sampling is suitable for relatively homogeneous formations. However, if the microstratigraphy of the formations is important—for example, if there are permeable sand seams in a clay formation—then continuous-core samples should be collected. Continuous cores are made by advancing the drill bit to the full depth that was sampled by a split spoon and then immediately taking another core sample of the fresh formation ahead of the previous core. Continuous-core samples can also be collected in cohesive soils by using a special core barrel that collects a 1.5 m (5 ft) long sample inside a hollow-stem auger as the auger is being advanced. If a sequence consisting of a 3-inch split spoon followed by a 6.35 cm (2.5 in.) split spoon followed by a 5 cm (2 in.) split spoon is used, 1.37 to 1.5 m (4.5 to 5 ft) of continuous sample core can be collected before the augers need to be advanced.

In consolidated formation a rock-core sample is collected by use of a core barrel with a diamond-studded bit. The rotating bit grinds up rock in an annular pattern, leaving an undisturbed center of rock that enters the core barrel. There is a core lifter just behind the bit to keep the core from falling out of the core barrel when the drill rods and bit are retrieved from the borehole. For shallow soil sampling, some coring and auger soil sampling devices can be operated by hand. Helical or post-hole augers gather a disturbed, near-surface sample and are superior to coring devices in rocky soils. Soil cores can be taken by hand from the ground surface with specialized coring devices that can allow sampling for VOCs and other potential contaminants. Cores are typically extruded after sampling and readied for transport or analysis. Decontamination techniques for coring equipment between samples is required to prevent cross-contamination.

8.5.5 Installation of Monitoring Wells

Following the collection of samples during the installation of borings, a monitoring well can be installed in the borehole. Boreholes drilled with mud should stay open with the drill rod removed. Hollow-stem augers are generally left in the ground and the well is installed through them, as is drive casing in cable-tool drilling. There must be a sufficient working opening inside the casing or augers. For a 5 cm (2 in.) nominal monitoring well, this means a minimum 10.8 cm (4.25 in.) opening is needed. The casing can be offset within the auger to give the largest working opening (Figure 8.23) although care must be taken to keep the well casing and screen as centrally located as possible. With a 10.8 cm (4.25 in.) inside diameter auger and a 5 cm (2 in.) nominal casing, this creates a 4.76 cm (1.875 in.) working opening.

The first step in the installation of a monitoring well is to screw the well screen to the casing and then lower the assembly through the inside of the augers or temporary casing. Prior to installation the casing and screen should be thoroughly decontaminated. The casing and screen may be wrapped in white butcher paper after it has been decontaminated and then kept wrapped until just before it is lowered into the augers. Figure 8.24 shows a 6.1 m (20 ft) casing and screen being lowered by hand. Longer casings need to be lowered on a cable using the drilling rig. In boreholes not drilled by hollow-stem augering, it is generally important to have centralizers (mechanical collars-type devices) attached to the casing/ screen combination to keep them from contacting the wellbore walls (Nielsen 2005).

FIGURE 8.23 Casing offset inside hollow-stem auger to give greatest working opening.

Source: G. Hackett. 1988. Drilling and constructing monitoring wells with hollow-stem augers part 2: Monitoring well installation. *Groundwater Monitoring & Remediation* 8:60–68. Used with permission.

Once the casing and screen have been lowered into the well, the filter-pack material needs to be placed. The volume of filter-pack material necessary to fill the annular space between the screen and casing and the borehole wall from the bottom of the borehole to a point 0.6 m (2 ft) above the top of the screen should be computed. At least this much material must be on hand before starting the filter-pack installation. A weighted measuring tape is lowered into the working opening between the casing and the hollow-stem auger and the total depth of the borehole is measured and recorded.

If the formation is cohesive and can stand open for a short while, the augers are withdrawn 0.3 or 0.6 m (1 or 2 ft) from the bottom. Filter-pack material is then poured into the working opening, and the annular space is filled to the level of the auger bit. Care should be taken that the filter-pack sand doesn't fill the space between the casing and the augers, because it can lock the casing and hollow-stem augers together. The weighted tape is used to determine the position of the top of the filter pack. The augers are then withdrawn another 0.3 to 0.6 m (1 to 2 ft), and the process is repeated until the entire filter pack is placed. Figure 8.25 illustrates what is known as the free-fall method of filter-pack emplacement.

FIGURE 8.24 Lowering well screen and casing into hollow-stem augers. Note the white wrapping paper around the decontaminated casing.

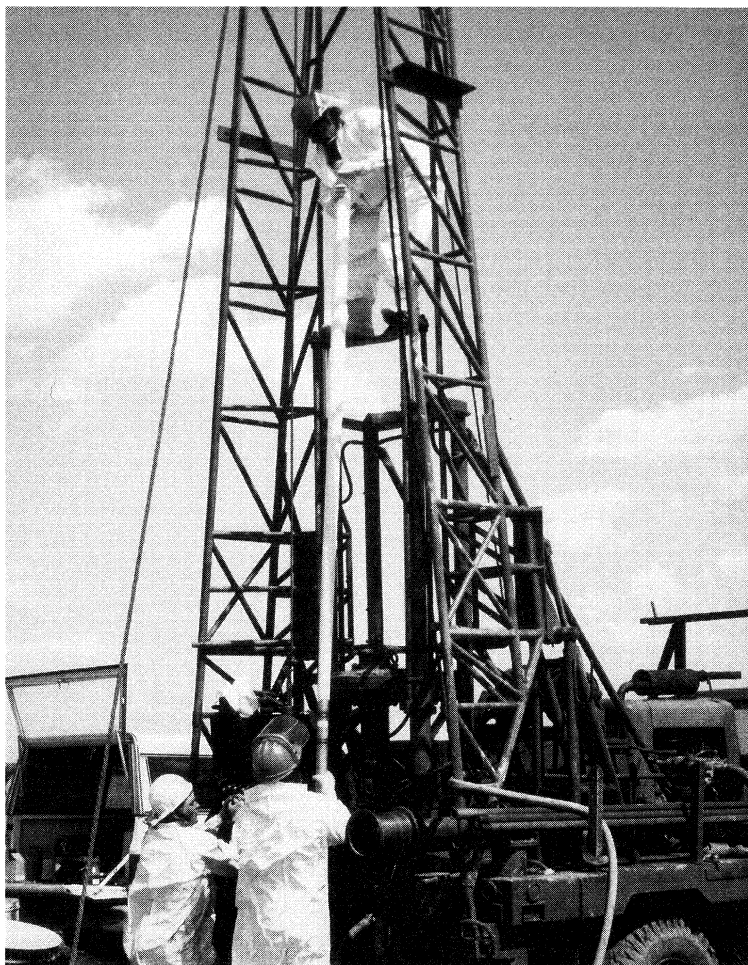
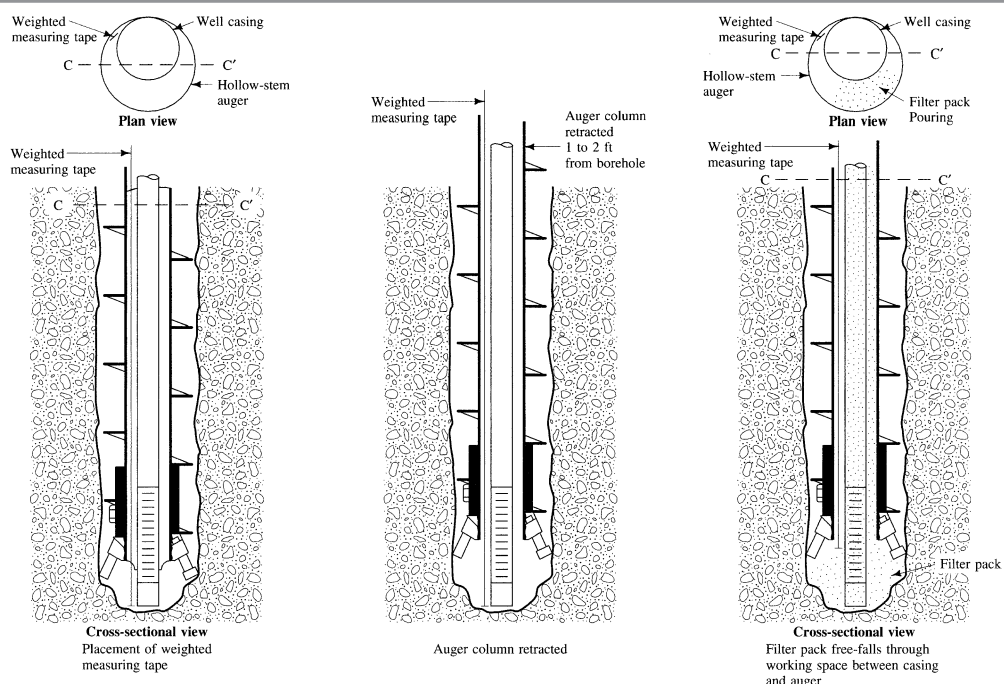


Photo credit: C.W. Fetter.

When filter-pack material drops through a water column, it may separate according to size. It may also bridge the space between the casing and the auger and create a void below. To avoid these problems, a **tremmie pipe** should be used wherever possible (Figure 8.26). A tremmie pipe is a pipe that extends from the surface and through which the filter-pack sand may be poured. After the augers are withdrawn a few feet, the annular space is filled with sand being poured down the tremmie pipe. The tremmie pipe is raised as the level of sand rises. The tremmie pipe can be used to tamp down the sand, and the weighted tape is used to measure the position of the top of the filter pack.

If the formation is noncohesive, it will collapse as the augers are withdrawn. Under these conditions, the withdrawal of the augers and the addition of the filterpack

FIGURE 8.25 Free-fall method of filter-pack emplacement with a hollow-stem auger. The method also works with drive casing.

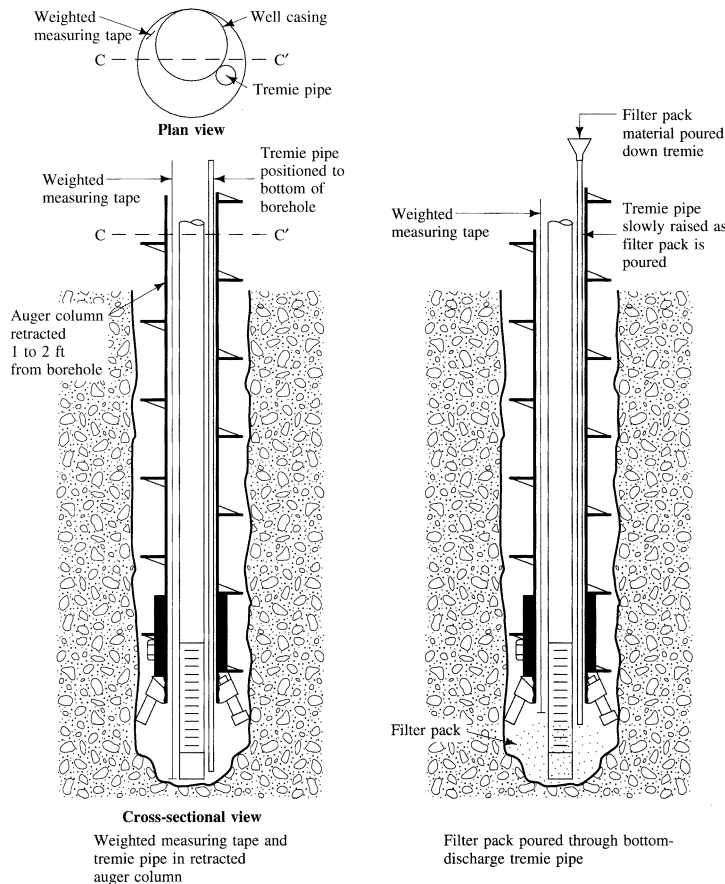


Source: G. Hackett. 1988. Drilling and constructing monitoring wells with hollow-stem augers part 2: Monitoring well installation. *Groundwater Monitoring & Remediation* 8:60–68. Used with permission.

material must occur simultaneously (Hackett 1988). A cable must be attached to the top of the auger string so that the working opening is accessible at all times. The hollow stem of the augers is filled with clean water, and a positive hydraulic head is thus maintained throughout the operation. The augers are very slowly withdrawn, and at the same time filter-pack material is added so that the top of the filter pack is within an inch or so of the bottom of the augers. This requires precise coordination of the rate of addition of filter-pack sand and the rate of withdrawal of the augers.

The final depth of the top of the filter pack is confirmed by measurement with the weighted tape. It should be 0.6 m (2 ft) above the top of the screen. The augers are then withdrawn another 0.6 m (2 ft) and 0.6 m (2 ft) of pure bentonite clay is placed by free fall through the working space. If the area is below the water table, bentonite pellets are used; if the area is above the water table, granular bentonite or slurry is used (see 8.4.5). Pellets should be dropped a few at a time so that they aren't caught in the working space as they start to swell by hydration. The weighted tape is used to confirm the final thickness of the bentonite layer after enough time has elapsed to allow the bentonite to hydrate. Bentonite pellets should not be used as grout in the vadose zone, as hydration is extremely slow even if water is poured through the pellets.

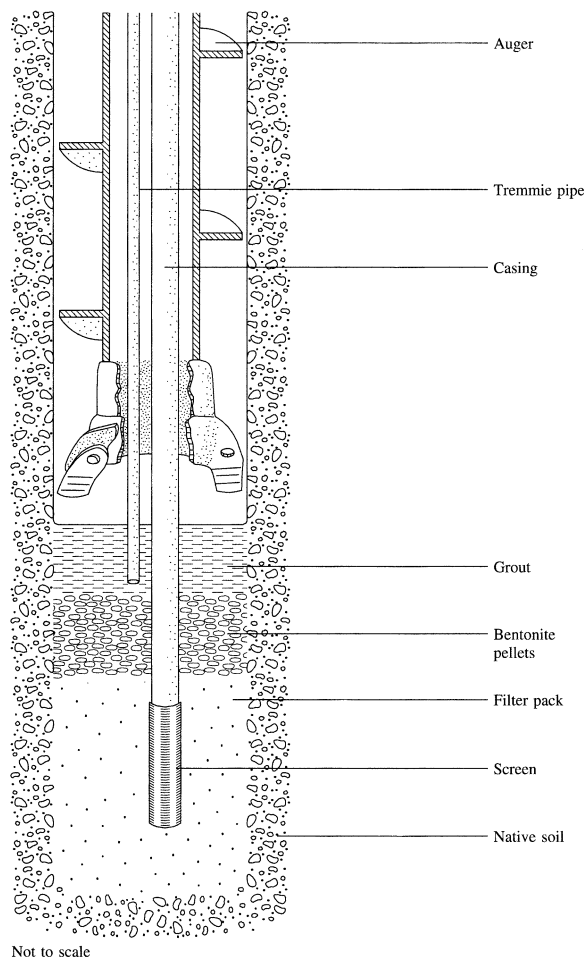
Placement of the annular seal should take place by use of a tremmie pipe. The tremmie pipe should be lowered to the top of the bentonite seal. The augers are

FIGURE 8.26 Use of a tremmie pipe for emplacement of filter-pack material.

Source: G. Hackett. 1988. Drilling and constructing monitoring wells with hollow-stem augers part 2: Monitoring well installation. *Groundwater Monitoring & Remediation* 8:60–68. Used with permission.

withdrawn 0.6 m (2 ft) or so and the annular space is filled from the bottom with grout, which is either pumped down the tremmie pipe or is fed by gravity (Figure 8.27). The weighted tape is used to confirm the position of the top of the grout. The augers are then repeatedly withdrawn and grout is emplaced until it is brought close to the surface. The tremmie pipe can be left at the bottom until the grout is brought to the surface, or it can be raised as the augers are withdrawn. For slumping sediments, the grout must be emplaced simultaneously and at the same rate as the augers are withdrawn.

The final step is the installation of a locking protective cap. Bentonite-cement can be brought all the way to the surface. If bentonite grout or bentonite-sand grout is used, the final few feet filling the annular space must be neat cement or bentonite-cement grout. A slight mounding of the surface grout will prevent the pooling of water at the surface next to the well. The locking protective casing can be pushed into the cement grout when

FIGURE 8.27 Use of a tremmie pipe for emplacement of grout above the bentonite pellets.

it is still soft. If the grout settles overnight, its level should be brought to the surface with additional material. A stronger surface seal can be obtained if the top 0.61 m (2 ft) of the annular space is filled with concrete, as opposed to bentonite-cement grout.

8.5.6 Monitoring Well Development

Once a monitoring well is constructed, it is necessary that it undergo development. This is a process of removing fine sand, silt, and clay from the aquifer around the well screen. If drilling mud was used, then vigorous development may be needed to break down the mud pack on the borehole wall. Development is needed to create a well that ideally will not pump silt and clay when it is sampled. It also may create a zone around the well screen that is more permeable than the native soil and that stabilizes the native soil so that the fine sediments do not enter the filter pack.

Aller et al. (1991) made the following observations about monitoring well development:

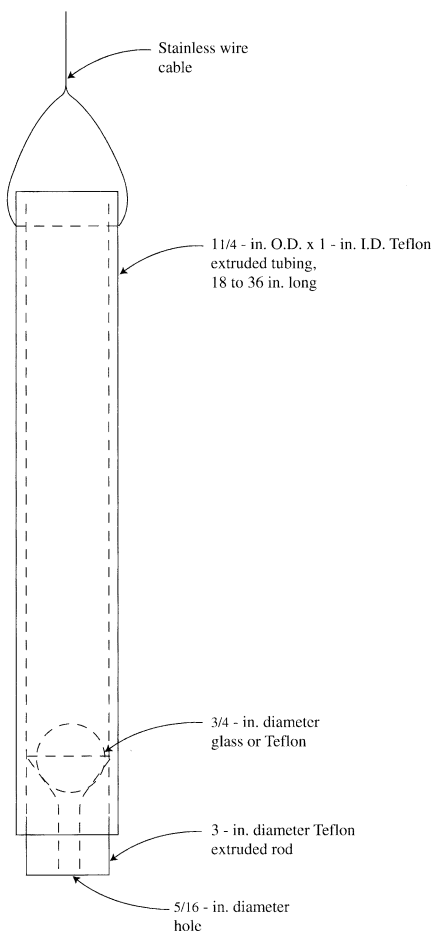
1. Using compressed air for well development may alter native water chemistry, crack the casing, or blow the bottom cap off the screen.
2. Adding water to the well for flushing the well or surging can alter the groundwater chemistry, at a minimum by dilution.
3. Breaking down a mud wall left in the borehole from mud-rotary drilling is very difficult.
4. Developing a well when the screen is in a clean, homogeneous, high-permeability aquifer is relatively easy.
5. Developing a well when the screen is in a fine-grained, stratified, low-permeability formation is difficult.
6. Developing a large-diameter well is easier than developing a small-diameter well.
7. Shallow monitoring wells are easier to develop than deeper monitoring wells.
8. Monitoring wells that can be bailed dry tend to be turbid because of the steep hydraulic gradients that are developed.
9. In the final analysis, many monitoring wells cannot be developed to the point where a nonturbid, groundwater sample can be collected. This is especially true if the formation does not yield very much water, so that extensive development is not possible.

If the borehole is drilled into a stable, consolidated formation, especially if mud is used during the drilling, it may be advantageous to flush the borehole with potable, fresh water to wash out as much of the mud as possible prior to installation of the well and filter pack. This will greatly cut the time needed for well development. In some cases it will not be permissible to add water to the borehole, since this might alter the groundwater chemistry.

There are three procedures used for monitoring well development: bailing, surge block surging, and pumping/overpumping/backwashing. These may be used alone or in combination.

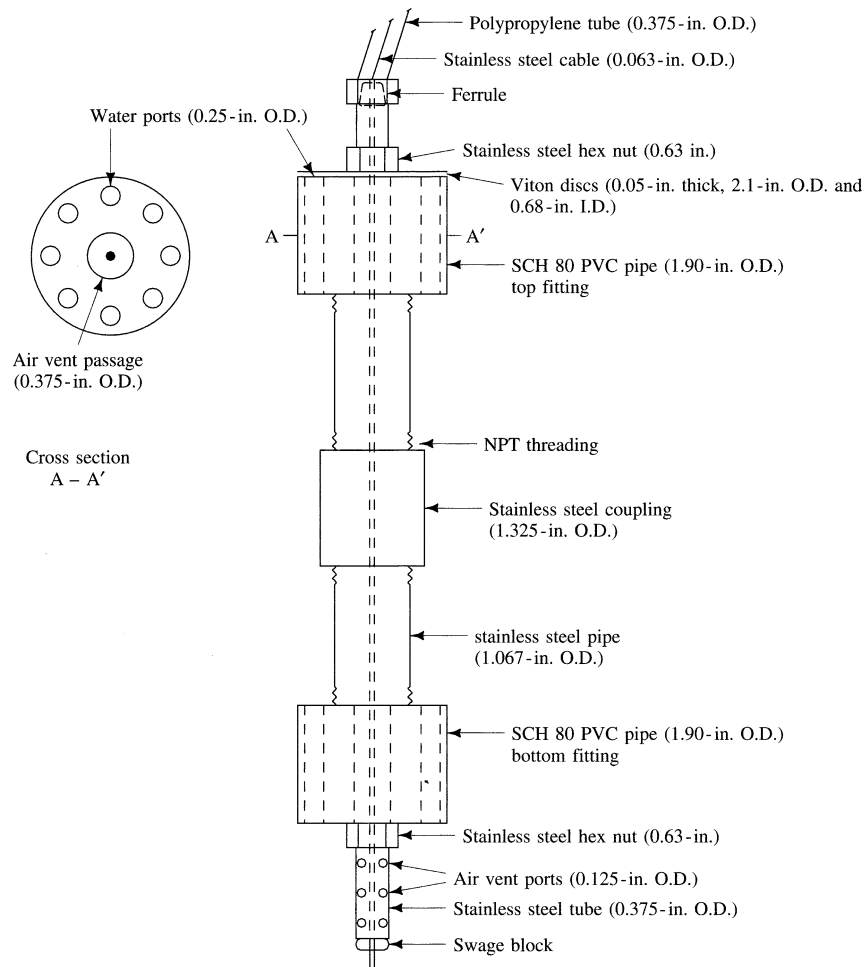
A **bailer** for a monitoring well is a section of pipe that is open on the top end and has a foot valve on the bottom end. It is attached to a line so that it can be lowered into the well. Water fills it from the bottom; then when it is raised by the line, the foot valve closes and the water inside is trapped. Figure 8.28 is a diagram of a bailer.

When developing a well by bailing, the bailer should be allowed to freefall to the water surface. When it strikes the water, a pressure wave results, which pushes water from the well screen out into the formation. After the bailer is filled with water, it is withdrawn and water from the formation enters the screen. This back-and-forth motion of water through the filter pack loosens fine sediment so that it can be drawn into the well and removed by the bailer. The bailer should be allowed to sink to the screen area so that the water that fills it contains the fine sediment that is brought into the well from the filter pack. The bailer can also be raised and lowered when it is submerged to force water to move back and forth through the screen area. Bailing can take some hours to develop a monitoring well effectively; this can translate into significant labor cost. Bailing for development can be undertaken by hand or by using a cable attached to a

FIGURE 8.28 Diagram of a bottom-loading bailer.

power-operated drum on a drill rig or truck. Some well-development outfits have an arm that can go up and down like a walking beam to create a surging action. Care should be taken so that the surging action is not vigorous enough to collapse the well screen.

A **surge block** is a device that fits inside the well with a flexible gasket that is close in size to the inside diameter of the well. Figure 8.29 shows the design of a surge block for small-diameter monitoring wells. It is attached to a rod that is raised and lowered with a stroke of about 0.9 m (3 ft). Most of the water is moved up or down by the action of the surge block, although some fraction of the water bypasses the surge block. The surging is initiated with the surge block at the top of the well screen, and the block is gradually lowered until the entire screened area has been surged. Every so often the surge block is removed and the well bailed to remove the sediment that has been brought into the well. If too much sediment accumulates above the surge block, it can bind between the surge block and the casing wall and lock up the surge block. To avoid this, the surge block

FIGURE 8.29 Design of a specialized surge block for monitoring wells.

Source: R. Schalla and R.W. Landick. 1986. A new valved and air-vented surge plunger for developing small-diameter monitor wells. *Groundwater Monitoring & Remediation* 6:77–80. Used with permission.

must be removed and the well bailed frequently. Surging begins with a gentle action; as development progresses it becomes more vigorous, with a more rapid plunging action. Again, too vigorous a surging action might cause the screen to collapse.

Pumping the well can aid in development. A number of different types of pumps are suitable. However, some pumps might be damaged by the sediment that must necessarily be removed during development. The ideal pump for development is capable of a wide range of flow velocities and does not have a valve that prevents backflow. The pump intake should be in the screen zone so that it will immediately pick up sediment that is brought into the well. The pump is started at a low velocity and is shut off every so often. When it is shut down, the water in the pump column between the water

surface and the pump will flow back into the well and out into the filter pack. When the pump is started again, this water will be drawn into the well and will loosen fine sediment in the filter pack. With time, the rate at which the well is pumped is increased so that the water velocity through the filter pack into the screen is increased. Eventually, the well will be overpumped—that is, pumped at a rate that is greater than the flow into the well through the well screen. There will be a rapid decrease in the water level in the well during overpumping, and it cannot be sustained for very long. Eventually the water from the well should clear. Monitoring wells should be periodically redeveloped.

8.5.7 Record Keeping During Monitoring Well Construction

Many localities have detailed record-keeping requirements for monitoring well construction. Even when detailed records aren't required by statute, they should be kept as a matter of sound professional practice. Figure 8.30 shows a one-page form that can be used to record important information on monitoring well construction. Many firms have their own forms, and many states, provinces, and regions have a required form. The form should be filled out in the field as the information is collected.

Records should also be kept of well development, including the date that it occurred, the method used, the water level at the start of development, the water level at the end of development, the time spent developing the well, and the volume of water removed. The thickness of sediment on the bottom of the well can be determined by measuring the depth to the bottom of the well with a weighted tape. This measured distance is subtracted from the measured length of the well casing and screen that was installed. The difference between the two dimensions is the thickness of sediment inside the well. This thickness should be measured and recorded both before and after development. If possible, sediment should be removed with a bottom-loading bailer.

8.5.8 Monitoring Well and Borehole Abandonment

Sometimes difficulties are encountered during the construction of a monitoring well that prevent its completion. Monitoring wells may be installed for a specific time period, after which they must be removed. Test borings may be made with no intention of using the borehole for construction of a monitoring well. In all such cases, proper abandonment of the well should be undertaken. Many countries and regions have specific well-abandonment codes. In the absence of specific requirements, monitoring wells and boreholes should be abandoned in such a manner that surface water cannot drain into the aquifer. Otherwise a direct connection for contaminated water from the surface to the aquifer can result. Nor should contaminated water or fluids be allowed to move vertically within the borehole to contaminate other depths.

If a casing and screen have been installed, they should be removed if possible. This can be accomplished by pulling if the annular seal has not been filled with a cement-type grout. If a plastic casing breaks while being pulled, it can be removed by drilling it out with hollow-stem augers. Following the removal of the casing, a tremmie pipe should be used to fill the resulting borehole from the bottom with an appropriate material, such as neat cement or bentonite grout. The grout is placed while the augers are being pulled out of the hole. Material removed from a monitoring well may be contaminated and should be properly disposed of.

FIGURE 8.30 Form for recording information about construction details of a monitoring well.

Facility/Project Name _____	Date Well Installed _____/_____/_____ m m d d y y
Section Location ____ 1/4 of ____ 1/4 of Section _____. T _____ R _____	Well Installed By: (Person's Name and Firm) _____
<p>Protective pipe, top elevation _____ ft MSL</p> <p>Well casing, top elevation _____ ft MSL</p> <p>Land surface elevation _____ ft MSL</p> <p>Surface seal, bottom _____ ft MSL or _____ ft</p> <p>USCS classification of soil near screen:</p> <ul style="list-style-type: none"> <input type="checkbox"/> GP <input type="checkbox"/> GM <input type="checkbox"/> GC <input type="checkbox"/> GW <input type="checkbox"/> SW <input type="checkbox"/> SP <input type="checkbox"/> SM <input type="checkbox"/> SC <input type="checkbox"/> ML <input type="checkbox"/> MH <input type="checkbox"/> CL <input type="checkbox"/> CH <input type="checkbox"/> Bedrock <p>Sieve analysis attached? <input type="checkbox"/> Yes <input type="checkbox"/> No</p> <p>Drilling method used:</p> <ul style="list-style-type: none"> <input type="checkbox"/> Rotary <input type="checkbox"/> Hollow Stem Auger <input type="checkbox"/> Other _____ <p>Drilling fluid used: Water <input type="checkbox"/> 02 Air <input type="checkbox"/> Drilling Mud <input type="checkbox"/> 03 None <input type="checkbox"/></p> <p>Drilling additives used? <input type="checkbox"/> Yes <input type="checkbox"/> No</p> <p>Describe _____</p> <p>Source of water (attach analysis): _____</p>	
<p>1. Cap and lock? <input type="checkbox"/> Yes <input type="checkbox"/> No</p> <p>2. Protective</p> <ul style="list-style-type: none"> a. Inside diameter: _____ in. b. Length: _____ ft c. Material: Steel <input type="checkbox"/> Other _____ <p>d. Additional protection? <input type="checkbox"/> Yes <input type="checkbox"/> No If yes, describe: _____</p> <p>3. Surface seal: Bentonite <input type="checkbox"/> Concrete <input type="checkbox"/> Other <input type="checkbox"/></p> <p>4. Material between well casing and protective pipe: Bentonite <input type="checkbox"/> Annular space seal <input type="checkbox"/> Other <input type="checkbox"/></p> <p>5. Annular space seal: Granular Bentonite <input type="checkbox"/> ____ Lbs/gal mud weight . . . Bentonite-sand slurry <input type="checkbox"/> ____ Lbs/gal mud weight Bentonite slurry <input type="checkbox"/> ____ % Bentonite Bentonite-cement grout <input type="checkbox"/> ____ ft³ volume added for any of the above</p> <p>How installed: Tremie <input type="checkbox"/> Tremie pumped <input type="checkbox"/> Gravity <input type="checkbox"/></p> <p>6. Bentonite seal: Bentonite granules <input type="checkbox"/> ____ 1/4 in. <input type="checkbox"/> 3/8 in. <input type="checkbox"/> 1/2 in. Bentonite pellets <input type="checkbox"/> Other <input type="checkbox"/></p> <p>7. Fine sand material: Manufacturer, product name and mesh size _____ Volume added _____ ft³</p> <p>8. Filter pack material: Manufacturer, product name and mesh size _____</p> <p>9. Well casing: Flush threaded PVC schedule 40 <input type="checkbox"/> Flush threaded PVC schedule 80 <input type="checkbox"/> Other <input type="checkbox"/></p> <p>10. Screen material: _____</p> <p>Screen type:</p> <ul style="list-style-type: none"> Factory cut <input type="checkbox"/> Continuous slot <input type="checkbox"/> Other <input type="checkbox"/> <p>Manufacturer _____ 0.____ in. Slot size: _____ ft Slotted length: _____ ft</p> <p>11. Backfill material (below filter pack): None <input type="checkbox"/> Other <input type="checkbox"/></p>	

Source: Modified from Wisconsin Department of Natural Resources.

If the casing and screen have been grouted into place, it may not be possible to remove them. If this is the case, several approaches can be used. The casing could be cut off below grade; then the screen and casing must be filled from the bottom using a

tremmie pipe and an appropriate material such as neat cement or bentonite grout. If the casing is in poor condition it can be ripped or perforated with casing rippers allowing grout to be injected into the annular space. Alternatively, casing can be gun-perforated using either a device that fires steel projectiles through the casing and into the formation, or a jet type perforator that uses small shaped explosive charges to burn holes through the casing and allow grout injection (Aller et al. 1991).

Boreholes in sediments can be filled with grout or native soils mixed with bentonite. Boreholes into bedrock should be grouted with a cement-type grout.

■ 8.6 Well Sampling

8.6.1 Introduction

After a monitoring well has been designed, installed, and developed, the next step is to collect a water sample. The water sample should be representative of the water in the formation; that is, the sampling techniques should collect water from the aquifer and not from water that has been standing in the well casing or screen. In addition, the sampling device should provide a sample that has not been altered by the sampling process and should not cause cross contamination.

8.6.2 Fluid Level and Pressure Measurement

Several devices are available for the downhole measurement of water levels, pore pressures and NAPL layers in wells or piezometers. Historically, steel tape was used to measure water levels in wells. Chalk would be applied to the tape at the expected water level depth, and then retrieved to the surface. The depth to water would be indicated on depth markings on the tape at the point where the chalk had been washed away by the water. Another historical method to measure hydraulic head is a “bubble tube” which is a pipe or tube sent downhole with a known air pressure to depths below land surface and below the water table or piezometric surface. The tube continues to bubble until it reaches a depth where the water pressure is equal to the air pressure within the tube and the depth below water surface can be calculated. This method is not used in situation where volatilization of contaminants is possible or LNAPLs are suspected in the wells.

Water levels are now often determined by electrical probes with depth demarcations which are lowered in a well or piezometer until a peeping sound indicates that the water level has been reached. For more exacting and quantitative NAPL determinations in wells, depth-discrete and transparent bailers can be sent downhole, or interface probes can be used. An interface probe is a modified electrical water level probe which has an ability to give separate acoustic and visual signals for water and NAPL in the fluid column (Mercer and Cohen 1990; Cohen and Mercer 1993). Unlike the bailer, however, interface probes cannot retrieve a NAPL sample for analysis, but only measure the vertical thickness of NAPL in a well.

Long term water level measurements are now often made with a recording transducer which measures temporal pressure changes in a well at a specified depth, which correlates to overlying water levels. Vibrating wire piezometers are useful in measuring well water levels and pore pressures for geotechnical applications.

8.6.3 Well Purging

Water that has been standing in the well has been in contact with atmospheric gases and the well casing and screen. This contact can affect the water chemistry. Oxygen can diffuse into the water and dissolved gases can volatilize or oxidize. Trace elements may be leached from the well casing. Organics may be sorbed by the well casing. In order to be sure that the water being drawn into the sampling device comes from the aquifer, the well must be purged of standing water prior to sampling. The goal of purging is to remove all the water that has been standing in the well. The volume of water that must be removed to accomplish that goal depends upon the method of purging and formation permeability.

The first step in well purging is to measure the depth of water in the well, the total well depth, and the inside diameter of the well casing. These measurements are used to compute the volume of water standing in the casing. If a well is purged by a method that withdraws water from the top of the water column, then theoretically only one well volume needs to be withdrawn. For example, purging with a bailer that is lowered slowly into the well to a depth no greater than the length of the bailer will remove water only from the top of the column. If a pump is used to purge the well, the pump intake should be as close as possible to the top of the water column. Although one well volume would theoretically remove all the standing water, good practice suggests that at least three well volumes should be removed to be sure that the standing water in the casing and screen is totally removed. This also removes water from the filter-pack area. If a well is bailed dry, or nearly so, it is not necessary to attempt to remove multiple-well volumes. As soon as the well has recovered enough to contain sufficient sample volume, the sample can be collected.

If the pump intake is lowered to the level of the screen in the well during purging, then most of the water will come from the screen area, and an area of stagnant water will develop in the water column above the pump intake. Under such conditions up to five well volumes need to be pumped to remove all of the stagnant water in the well (Gibb et al. 1981). Keeley and Boateng (1987) advocate a staged technique when purging with a pump. The pump intake is lowered to just below the water surface at the beginning of the purging process and then is gradually lowered through the water column until it is at the screen zone, when purging is complete. Purging three well volumes with this technique should be adequate.

Electrical conductivity and pH can be monitored during the well-development procedure. If they vary widely during the well-purging process, this may mean that water from different sources is being withdrawn. If these values do not stabilize, this does not necessarily mean that the stagnant water has not been withdrawn from the well. There may be instrument drift, or the water quality in the aquifer may be changing as water from different parts of the aquifer is being withdrawn. If possible, the well should be purged until it is not turbid.

The water being purged from the monitoring well may be contaminated. If so, it must be properly disposed of in a treatment facility. For this reason, purging techniques that limit the amount of water withdrawn are desirable.

8.6.4 Well-Sampling Devices

There are a large number of sampling devices available for monitoring wells. They operate under different physical principles and designs and have different applications.

Most are available in a variety of materials. The following is a partial list of available devices (Nielsen and Yeates 1985; Pohlmann and Hess 1988):

1. *Open bailer*: This device is a rigid tube with an open top and either a closed bottom or a check valve on the bottom. It is attached to a line and is lowered and raised by hand. It withdraws the sample from the top of the water column.
2. *Point-source bailer*: This device has a check valve on both the top and bottom and can be lowered on a line to a given depth below the surface, where the valves can be closed by a cable. It can collect grab samples from any depth in the water column. Some bailers are intentionally disposable to prevent cross-contamination from multiple sampling, and some are transparent or translucent allowing visual identification of colored NAPLs or other compounds in the bailer.
3. *Syringe sampler*: A medical syringe, or similar device, is attached to a length of tubing and is lowered to a selected depth in the water column. A suction is applied to the tubing and the syringe, which was lowered in the “empty” position. The syringe fills as the water comes into the needle because of the vacuum being developed by the suction on the tubing.
4. *Gear-drive pump*: This device is similar to a traditional submersible electrical pump. There is a miniature electrical motor attached to the pump, which rotates a set of gears to drive the sample up the discharge line via positive displacement. A continuous flow of water under positive pressure is developed.
5. *Bladder pump*: This sampler has a rigid tube containing an internal flexible bladder. There are check valves on either end of the rigid tube. When the bladder is deflated, water enters the lower end of the tube through the check valve. When the tube is full, the bladder is inflated with an inert gas pumped down from the surface. The bottom check valve closes, the top check valve opens, and the water sample flows up the discharge line. When the bladder deflates, the water in the discharge line can’t drain back into the rigid tube because of the check valve. The water is under positive pressure at all times and doesn’t come into contact with the gas.
6. *Helical-rotor pump*: This pump has a submersible electrical motor. It rotates a helical rotor-stator, which drives water up the discharge line under positive pressure.
7. *Gas-drive piston pump*: A piston that pumps the water is driven up and down by gas pressure from the surface. The gas does not contact the sample.
8. *Submersible centrifugal pump*: A submersible electrical motor drives an impeller in the pump, which creates a pressure and forces the water up a discharge line.
9. *Peristaltic pump*: Unlike the others, this is a pump located at the land surface. It is a self-priming vacuum pump that can draw a water sample up tubing under suction. Loss of volatile compounds and dissolved gases may occur due to the vacuum developed.
10. *Gas-lift pump*: A constant stream of gas or air is used to force the water up a discharge tube. The water comes into contact with the gas or air and oxidation and loss of volatiles can occur.
11. *Gas-driven pump*: An inert gas is used to alternately pressurize and depressurize a sample chamber. The sample chamber has check valves to create a one-way flow

of water up a discharge line. This is similar to a bladder pump except that there is no bladder, so the gas comes into contact with the water sample.

12. *Passive samplers:* Consist of an organic phase, such as a plastic film or polymer, which accumulates contaminants from the aqueous phase or (soil) air. Passive samplers are useful for sampling the water column as well as interstitial water (ITRC 2005; USEPA 2012).

Figure 8.31 is a matrix of sampling devices and the suitable applications for collection of groundwater samples.

Pearsall and Eckhardt (1987), Yeskis et al. (1988), and Tai, Turner, and Garcia (1991) evaluated the efficacy of a number of different sampling devices in collecting representative samples of volatile organic compounds in groundwater. The first two studies were performed by withdrawing water from monitoring wells with different devices and comparing the results. The authors had no controls—that is, they did not know the actual concentration of the contaminants in the aquifer.

Yeskis et al. (1988) tested a bailer, a bladder pump, a piston pump, a submersible electric impeller pump, and a submersible electric helical stator-rotor pump. They found very little variation in the results except for the bailer. The bailer samples were in general less than half of the values obtained by the other devices. Pearsall and Eckhardt (1987) evaluated two 5 cm (2 in.) submersible helical stator-rotor pumps made of different materials, a 4-inch submersible electrical water-well pump, a cast-iron centrifugal suction pump, a peristaltic pump, and a bailer. The submersible pumps all gave similar results; the peristaltic and centrifugal suction pumps gave somewhat lower results. Silicon and PVC tubing appeared to give lower results than Teflon® tubing when used with the same pump. The bailer gave variable results, depending upon the concentration.

Tai, Turner, and Garcia (1991) built a 30.5 m (100 ft) tall, 12.7 cm (5 in.)-diameter, stainless-steel, vertical standpipe with sampling ports at various depths. They were able to use a sampling device to collect a sample from the standpipe, at the same time drawing a control sample from that depth through a sample port. They tested a Teflon® point-source bailer, a manual-driven piston pump, a motor-driven piston pump, a submersible helical-rotor pump, a peristaltic pump, and a bladder pump. Teflon® tubing was used to convey samples to the surface from the pumps. Because they had control samples, they were able to calculate a percent recovery for each sampling device. Table 8.5 shows the percent recovery for each sampling device at different depths. Examination of this table shows that the submersible pump, the peristaltic pump, and the bladder pump all had excellent recoveries, ranging from 98.5 to 100.5%. The other three devices were not as accurate, with the bailer having the lowest recovery.

The low recovery using the bailer was probably due to agitation of the sample as it was being transferred from the bailer to a 40 mL sample bottle for volatile organic analysis. Although it is a simple piece of equipment, an experienced operator is needed for correct use of a bailer.

On the basis of available research (Parker 1994) the piston pump, the bladder pump, and the electrical submersible helical-rotor pump appear to be the best devices for the collection of water samples containing volatile organic compounds. Peristaltic pumps are also suitable for metals and semivolatile organics if used with a rheostat to

FIGURE 8.31 Matrix showing applications of a number of groundwater sampling devices.

		Ground Water Parameters														
		Inorganic					Organic					Radioactive		Biol.		
Device	Approximate Maximum Sample Depth	Minimum Well Diameter	Sample Delivery Rate or Volume	EC	pH	Redox	Major Ions	Trace Metals	Nitrate	Dissolved Fluoride Gases	Non-volatile	Volatile	TOC	TOX	Gross Alpha & Beta	California Bacteria
Grab	Open boiler	no limit	1 in.	Variable	•	•	•	•	•	•	•	•	•	•	•	•
	Point-source boiler	no limit	1 in.	Variable	•	•	•	•	•	•	•	•	•	•	•	•
	Syringe sampler	no limit	1 1/2 in.	0.01–0.2 ml	•	•	•	•	•	•	•	•	•	•	•	•
	Gear-drive	200 ft	2 in.	0–0.5 g/min	•	•	•	•	•	•	•	•	•	•	•	•
(submersible)	Bladder pump	400 ft	1 1/2 in.	0–2 g/min	•	•	•	•	•	•	•	•	•	•	•	•
	Helical rotor	160 ft	2 in.	0–1.2 g/min	•	•	•	•	•	•	•	•	•	•	•	•
	Piston pump (gas-drive)	500 ft	1 1/2 in.	0–0.5 g/min	•	•	•	•	•	•	•	•	•	•	•	•
	Centrifugal	variable	3 in.	variable	•	•	•	•	•	•	•	•	•	•	•	•
Gas-contact	Peristaltic	26 ft	1/2 in.	0.01–0.3 g/min	•	•	•	•	•	•	•	•	•	•	•	•
	Gas-lift	variable	1 in.	variable	•	•	•	•	•	•	•	•	•	•	•	•
	Gas-drive	150 ft	1 in.	0.2 g/min	•	•	•	•	•	•	•	•	•	•	•	•

Source: K. F. Pohlmann and J. W. Hess. 1988. Generalized ground water sampling device matrix. *Groundwater Monitoring & Remediation* 8:82–84. Used with permission.

TABLE 8.5 Percent recovery of sampling devices compared with control samples.

Sampler	Water Depth					
	17.5 ft		54 ft		92 ft	
	Low ^a Conc.	High ^b Conc.	Low ^a Conc.	High ^b Conc.	Low ^a Conc.	High ^b Conc.
Submersible pump	97.8	99.7	99.5	98.5	100.1	100.1
Peristaltic pump	97.7	98.7	98.7	98.5	97.7	100.0
Bladder pump		101.5		100.5		99.9
Teflon bailer	93.9	96.3	92.4	93.9	92.7	91.4
Manual-driven piston pump	102.2	—	102.5	101.1	102.3	103.5
Motor-driven piston pump	97.4	96.8	99.8	98.4	100.9	100.7

Source: Tai et al. 1991.

create a low pumping rate. A bailer is acceptable if used properly with a minimum of agitation so as not to create splashing in the well and loss of volatiles. Bailers should have a bottom-emptying device. Such a bailer should be able to recover 90% of the volatile organics in the water.

Parker and Ranney (1996) examined the effect on using various rigid and flexible tubing used in water sampling devices on trace-level dissolved-organic compounds present in groundwater. They found that fluorinated ethylene propylene (FEP), FEP-lined polypropylene and polyvinylidene fluoride (PVDF) were the least absorptive of the rigid tubing. In addition, they do not leach constituents into water. Of these, PVDF is the least expensive. Where a flexible tubing is necessary, such as the head of a peristaltic pump, fluoroelastomer tubing and a copolymer of vinylidene fluoride and hexafluoropropylene were much less sorptive than the other flexible tubing. They also leached the fewest constituents into the water. The copolymer is less expensive than the fluoroelastomer.

Wherever possible, dedicated sampling equipment should be used in each well. This prevents the possibility of cross contamination between wells. It also eliminates the cost of decontaminating the equipment between wells and the possibility of interference from solvents used for decontamination. Inexpensive disposable bailers are available and may be an acceptable sampling device for many studies where the cost of dedicated sampling equipment in each well is not justified.

8.6.5 Methods of Collecting a Groundwater Sample Without Drilling a Well

The installation of a monitoring well is a costly proposition, generally in the range of \$5,000 to over \$15,000 USD for shallow wells in unconsolidated materials. Moreover, the process can be disruptive to the property owner and can damage lawns and crops. At some sites there may be limited knowledge about the direction of groundwater movement and the existence and location of contaminated groundwater. The hydrogeologist may find it desirable to perform some type of screening investigation prior to the installation of permanent monitoring wells. During the screening the

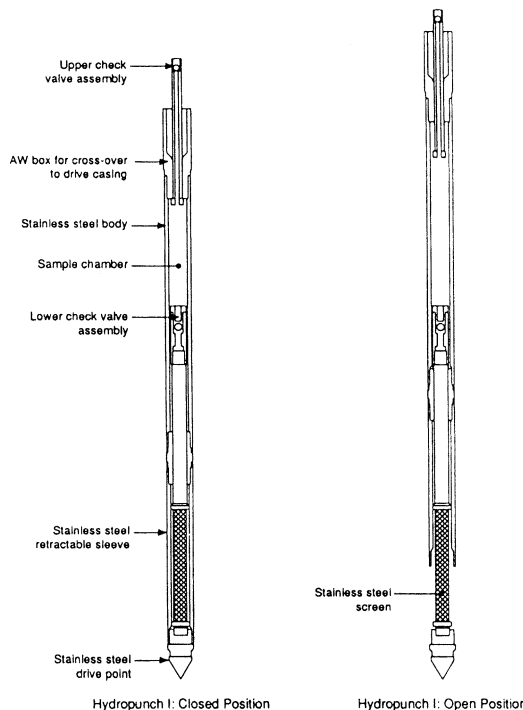
hydrogeologist may try to find the location and depth of groundwater contamination. There are devices that one can use to collect a groundwater sample without installing a monitoring well. These devices, as well as a standard sandpoint piezometer, can be used during the installation of a test boring.

These methods all allow the collection of discrete samples in a vertical profile which gives one the ability to construct a vertical-concentration profile similar to that of a multilevel sampler. However, they have a drawback in that the samples cannot be replicated at a future date because the sampler is withdrawn after use.

The HydroPunch™ is one such device, a direct-push sampler, that can be used to collect a groundwater sample from a discrete depth in the earth (Edge and Cordry 1989). It consists of a pointed sampling probe that is attached to a hollow drill rod. The rod is pushed into the earth by the hydraulic ram of a drilling machine or cone penetrometer rig, or is driven into the earth by the dropping of a weight using a drilling machine. Such a device will obviously only work in unconsolidated materials. Moreover, HydroPunch I™ cannot be used in very coarse sediment. As a general rule, if a 2-inch split-spoon sampler cannot be driven into the earth, then the HydroPunch I™ will most likely be damaged if an attempt is made to drive it. A sturdier HydroPunch II™ has been made which can be used with cone penetrometers or in conjunction with drill rigs. When the probe has been advanced to the target depth, the drive pipe is retracted about 1.5 ft (0.5 m). This raises a shield on the probe which exposes a stainless steel well screen that is 10 in. (25 cm) long. The probe has to be pushed at least five feet below the water table to completely fill the sampler. Hydrostatic pressure in the aquifer forces water to flow into the screen where it will rise into the probe until it reaches equilibrium with the hydrostatic pressure in the aquifer. Figure 8.32 illustrates the HydroPunch™ in both the closed and open positions. The screen openings in the HydroPunch™ are relatively large, and although water will enter relatively rapidly, the sample may be turbid. A check valve in the probe prevents water from draining back out of the screen and the entire assembly is withdrawn from the ground in order to retrieve the groundwater sample.

The BAT Enviroprobe™ is another type of discrete depth sampler (Mines et al. 1993). It is manufactured by Hogentogler & Co. Inc. of Columbia, Maryland. It is also pushed or driven into the earth to the desired depth by a drilling or cone penetrometer rig. When the drive pipe to which the probe is attached is pulled back about 1 ft. (0.3 m), a stainless steel sleeve is moved upward which exposes a 4-inch (10 cm) long screen. Figure 8.33 shows the BAT Enviroprobe™ in both a closed and an open position. There is a septum on the top of the screen which prevents groundwater from rising higher than the screen. The sample is collected by lowering a device with a double-ended hypodermic needle with an evacuated glass vial, which also contains a septum. The hypodermic needle penetrates both septa, and the water can move from the screen zone into the evacuated vial. The vial containing the groundwater sample is then withdrawn. Should this not contain sufficient sample volume, additional vials can be lowered through the riser pipe.

In the case of both the HydroPunch™ and the BAT Enviroprobe™, the water entering the screen is formation water and there is no need to either develop the well or purge it prior to sampling. This reduces the cost as the sample collection is quicker and also there is no contaminated purge and development water to dispose. Zemo et al. (1995) field-tested both the HydroPunch™ and BAT Enviroprobe™ and found that there was no statistically significant difference in trichloroethylene concentration found in

FIGURE 8.32 Closed and open position of the HydroPunch™ probe.

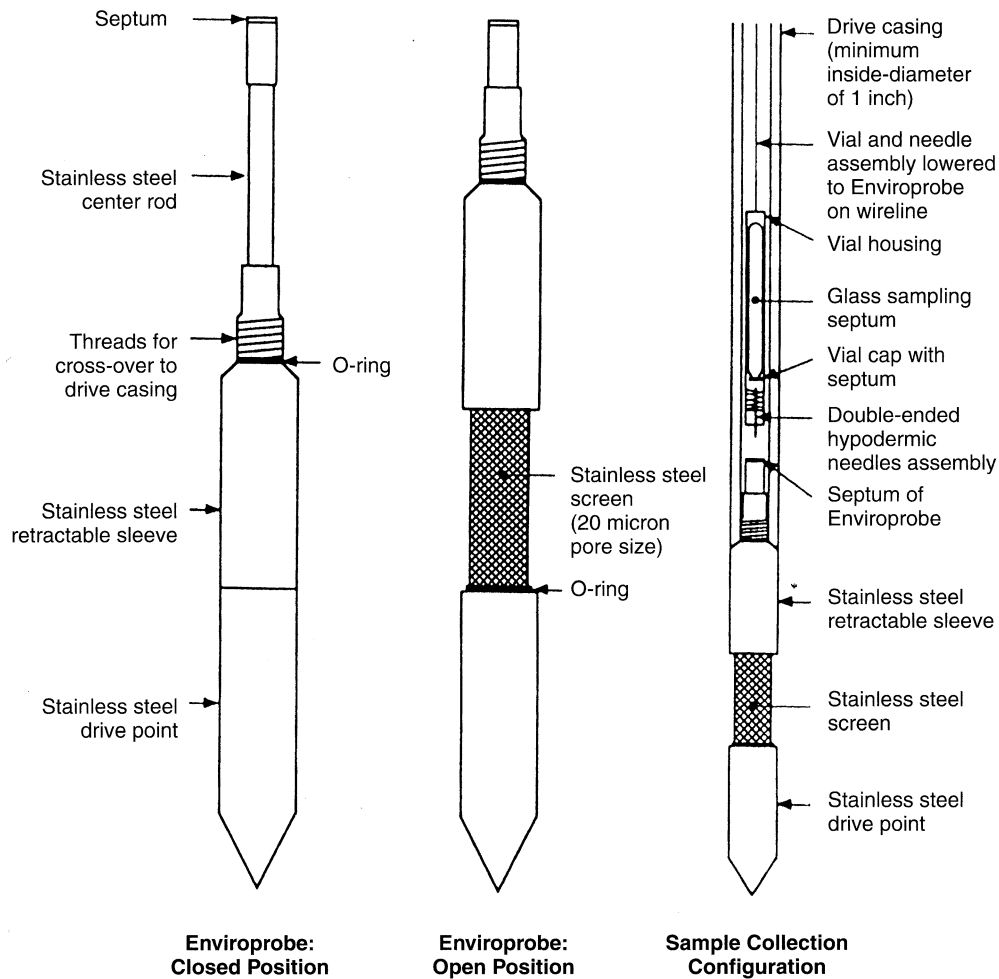
Source: Zemo et al. 1995. Field comparison of analytical results from discrete-depth ground water samplers. *Ground Water Monitoring & Remediation* 15:133–141. Used with permission.

groundwater samples collected from either probe. However, they did find that there was a difference in chlorobenzene concentration. They were unable to determine why such a difference should exist.

If the unconsolidated material is too coarse for the sampling probes to be pushed very far into the earth, then they can be used with a hollow-stem auger drilling rig. The drilling rig is used to install a test boring. At selected depths, either probe can be advanced within the augers and ahead of the drill bit to collect a groundwater sample. This approach has the distinct advantage of gathering stratigraphic data along with water-quality data. In the absence of a specific sampling probe, a standard 2-foot long sandpoint piezometer can be driven ahead of the drill bit to collect a water sample. In this case a bailer is used to collect the groundwater sample. After the water sample has been collected, the device is withdrawn from the borehole and the augers advanced.

8.6.6 Low-Flow Purging of Monitoring Wells

An important advance in contaminant hydrogeology field methods is the development of micropurging or low-flow purging techniques (Puls and Paul 1995). The purging techniques presented in section 8.6.3 are designed to remove all of the stagnant water in both the screen and the casing above the screen. The micropurging technique withdraws

FIGURE 8.33 Closed and open position of the BAT Enviroprobe™ probe.

Source: Zemo et al. 1995. Field comparison of analytical results from discrete-depth ground water samplers. *Ground Water Monitoring & Remediation* 15:133–141. Used with permission.

water directly from the screen zone at a rate that is less than the recharge rate from the aquifer into the screen. The stagnant water in the casing does not mix with the fresh water entering the screen (Powell and Puls 1993). This purging rate is less than 1 L per minute; a suggested rate is only 100 mL/min. At this rate there is minimal drawdown in the pumping well and the water chemistry of the purged water tends to reach a constant value within one-half of a casing volume (Barcelona, Wehrmann, and Varljen 1994).

Micropurging is accomplished by using either a dedicated bladder or submersible pump with the intake set in the center of a well screen or a peristaltic pump with the end of the sample tubing set in the screen zone (Kearl et al. 1994). If a dedicated pump is not used, the pump should be placed in the well at least 24-hours prior to the time that the sample is collected. The purge rate should be about 100 mL/min, although

somewhat higher rates could be used for very permeable formations. Two volumes of water contained in the pump and the tubing should be removed prior to collecting the sample. This will be much less than the volume of water in only one well casing. Samples do not need to be field filtered.

One of the problems that arises when sampling groundwater for metals occurs when the water sample is turbid. The turbidity is due to suspended mineral grains. These particles may contain sorbed metals. Some U.S. EPA programs and some U.S. state agencies prohibit the filtration of samples used for metal analysis as it is known that metals can travel in the groundwater with colloids (Puls and Powell 1992). However, turbidity in a sample can be caused by the process of lowering sampling instruments into the monitoring well (Kearl, Korte, and Cronk 1992) or by high screen-entrance velocities developed when significant drawdown occurs during purging. Micropurging techniques utilizing dedicated sampling equipment in each well will provide a sample with the least amount of artificially introduced turbidity. This will provide the best sample for use in determining total metals.

Kearl et al. (1994) compared samples collected by micropurging with samples collected by traditional purge and sample techniques. For most inorganic analytes and all organic analytes, there was no statistically significant difference between the two methods.

In addition to the ability to collect a nonturbid sample, there are other advantages of the micropurging technique. In some monitoring wells located in low permeability formations, traditional purging may withdraw most or all of the water from the well. This means that one must wait for a day or more for the well to recover enough water to yield a sample. This means that the sampled water was still stagnant for a period of time before being withdrawn. With a micropurging technique, a very low pumping rate could draw fresh formation water into the screen zone without much lowering of the water level in the casing.

There are two variable costs associated with groundwater sampling: personnel time and the expense of disposing of the contaminated purge water (Schilling 1995). With dedicated pumping equipment, the time for micropurging is generally less than that needed for traditional purge and sampling, hence the cost will be lower. The amount of contaminated water which must be disposed is much less in micropurging, hence the cost will be less.

While the impact of turbidity in a groundwater sample can have a significant effect on the concentration of metals in the sample, the same is not true for at least some chlorinated solvents. Paul and Puls (1997) examined the impact of sample turbidity on the concentration of trichloroethylene, cis-1,2-dichlorethylene and vinyl chloride. In both field and laboratory samples they found that solids entrained in the sample had no significant impact on the measured concentration of any of the three compounds. On this basis they concluded that turbidity in the sample does not appear to be of significance when sampling for VOC analysis. They did note that if the turbidity was the result of sample agitation that factor might result in loss of volatiles.

8.6.7 Sampling Frequency

Groundwater sampling is carried out commensurate with efforts to understand the nature and extent of groundwater contamination, predict future movement, ensure that harmful excursions of pollutants do not occur, facilitate remediation, and other goals

pertinent to site characterization. Many regulatory agencies specify and sometimes codify periodic time frames for sampling of monitoring well arrays, such as monthly, quarterly, or annual sampling. These periodic samplings have the benefits of allowing practitioners to predict many costs in advance, and look for long-term trends in water quality. From a regulatory standpoint this makes sense, although natural events that can alter water quality are not always periodic. For example, in karst systems great changes in subsurface water quality can occur during pulse flow events, and perhaps in many cases the best monitoring strategies for cave systems include sampling immediately before, during, and after intense rainfall and infiltration. Regulatory monitoring requirements are sometimes wrongly viewed as the maximum effort necessary to understand and deal effectively with groundwater contamination, particularly if monitoring costs are to be minimized. In reality, although standardized monitoring intervals make regulatory expectations clear, a one-size-fits-all sampling frequency is not always the best way to understand subsurface contamination at a particular site. Long-term costs are typically reduced with a clear understanding of contaminant distribution and movement, and sometimes this necessitates more frequent, strategic sampling before remedial action and site closure is attempted.

■ 8.7 Other Site Characterization Methods and Groundwater Contamination Forensics

8.7.1 Introduction

Site characterization is much more than just identifying groundwater pollutants and measuring their occurrence in the subsurface. A challenge is that many well-defined characterization goals and objectives require a deep understanding of a site's geology, an understanding of groundwater travel times, knowledge of the chemical characteristics of potential contaminants, and awareness of logistical and safety concerns, just to name a few necessities. These complex objectives are often resolved by geologic testing, detailed environmental chemistry analysis, and environmental forensics.

There are many wide-ranging applications of site characterization techniques and groundwater forensics that support a robust understanding of source water protection, the potential for contaminant movement and transformation, groundwater vulnerability, and the integrity of aquitards or barriers which are relied upon to isolate waste. Numerous monitoring and characterization techniques have been, and continue to be developed, adding to the arsenal of methodologies to characterize subsurface contamination, and many of these methods rely on probes to be driven into the subsurface, measurements to be taken from boreholes, or samples to be taken from wells. In some cases contamination can be suspected based on field conditions. Field observations for NAPLs illustrate this point. For example, if DNAPL chemical concentrations in groundwater increase with depth in a pattern inconsistent with advective groundwater flow, or increase counter to a hydraulic gradient, there is support for the possibility of DNAPL being spread in its free phase. Other indicators of free-phase NAPL include situations where the aqueous concentration of NAPL compounds in groundwater is greater than 1% of the pure phase (for a single NAPL compound) or effective solubility limit (for NAPL mixtures). Note that the opposite is not true; concentrations

below 1% may or may not be associated with free-phase NAPL. In soils where NAPL concentrations are greater than 10,000mg/kg (1% of soil mass) free phase can be suspected. Other qualitative signs of free-phase NAPL include erratic concentrations of NAPL chemicals in groundwater, soil, and soil gas; rebound of elevated dissolved NAPL concentrations after a pumping system is turned off; the presence of DNAPL chemicals in groundwater that is older than potential release dates; and observed deterioration of pumps and well components.

Quantitative methods can often be used as evidence in legal proceedings and the field of environmental forensics is based on efforts to distinguish pollutant sources (Morrison and Murphy 2006). Environmental forensics is defined by Hester and Harrison (2008) as “a combination of analytical and environmental chemistry, which is useful in the court room context. It therefore involves field analytical studies and both data interpretation and modeling connected with the attribution of pollution events to their causes.” There are a vast number of techniques to determine the source and pathways of groundwater contamination that fall into the realm of forensic hydrogeology.

8.7.2 Borehole Geophysics and Downhole Techniques

Many geophysical techniques originally developed for oil and gas exploration are often used in drilled boreholes to define subsurface geology and hydrogeology, directly identify pollutants, and/or understand the potential movement and distribution of contamination. Downhole logging approaches will “ground truth” surface geophysical techniques and results can be directly compared to borehole cuttings or core samples. Like borehole cuttings and core, downhole geophysics provides vertically continuous data, but geophysical methods sample a greater subsurface volume with relatively little bias. As more boreholes are logged at a site and cross-borehole techniques are used, 3-dimensional imaging techniques (tomography) can assist visualization of contaminants and subsurface geological structures, faults, and formations (Obiadi et al. 2012). Downhole surveys have assumed great importance in contaminant site surveys because the specific site characteristics and heterogeneities in porous media and fractured rock can profoundly influence the distribution and the potential for remediation for a host of contaminants. Borehole geophysics can provide information directly applicable to site characterization, including delineation of hydrogeologic properties, subsurface water quality, and determination of a well’s construction, status, and condition.

Physical, Visual, and Acoustic Borehole Geophysics Several techniques can measure the physical, visual, or acoustic properties of boreholes. One of the most straightforward downhole techniques is television (TV) logging where a color optical image is made of the borehole walls. This is particularly effective in identifying and characterizing fractures in hard rock materials, but can also identify lithology, water level, cascading water from perched zones (which could transmit contamination vertically), well construction failure, and water quality indicators such as suspended particles, gases, and chemical precipitates. TV logging can be viewed real-time and/or be stored and archived, and cameras and focal lengths can be adjusted to view either straight downhole, angled, or side-looking for inspection of borehole walls. An extension of TV logging is acoustic-television logging which records a photographic, digital image of the acoustic reflectivity of the borehole, oriented magnetically. These televiwer logs

are used in water or mud-filled open holes, and can identify geologic contacts between different strata, and fault location, strike, and dip. Televewers use a rotating transducer which can transmit and receive many samples per revolution and have azimuthal information from magnetometers on the device. This acoustic or sonic logging can help determine the porosity of a rock, aid in identification of lithology, facilitate estimation of secondary porosity and fracturing, and help assess rock permeability. Seismic logging, which transmits sound at lower frequencies, can be extended to cross-borehole tomography where images of seismic velocity between boreholes is generated, and geologic and hydrologic properties between the boreholes can be better understood.

Another type of physical downhole measurement is a caliper log which measures the varying diameter of an uncased borehole. Variable borehole diameter can indicate the potential for material to fracture or slough away from the walls and into a borehole, and therefore be a sign of media which may transport contamination. Alternatively, hydrogeologically transmissive zones can be directly identified with flowmeter monitoring. Vertical flowmeter testing in a single hole involves moving a flow measuring device up and down a hole during pumping or during nonpumping times, pinpointing zones of high and low groundwater transmissivity. Single-hole flow metering can also measure the rate and direction of vertical flow which can cause pollutants to migrate, and show relative vertical hydraulic gradients. In cross-hole flowmeter profiling, a flowmeter is placed in one hole while water is added or withdrawn from another borehole at a constant rate, allowing calculation of transmissivities, head differences, or storage coefficient between the boreholes. Packer systems (see section 8.4.9) can further isolate individual fractures and/or test hydrologic properties at individual depths between holes. Impeller flowmeters (rotameters, spinners) are most commonly used for these measurements, but have less resolution than heat-pulse or electromagnetic flowmeters. Vertical measurement of water temperature in a borehole can also be useful. These temperature measurements can define hydrostratigraphic layers, vertical flow, and water-bearing zones. Vertical borehole flow is implied by temperature gradients that are inconsistent with the regional geothermal gradient which is typically about 2.5°C per 100 m (1°F per 70 ft.). Distributed temperature sensing (DTS) has been used in boreholes to delineate hydrostratigraphic heterogeneities by synoptically profiling temperature distribution changes from thermal dilution tests. These tests do not disturb the fluid column (Leaf, Hart, and Bahr 2012).

Gamma and Neutron Logging Other borehole logging techniques are useful in site characterization. Downhole gamma logging records the amount of natural gamma radiation emitted by a formation in the vicinity of a borehole. Specific sources of gamma emission are potassium-40 (^{40}K) and daughter products of uranium and thorium decay series which are common in clays and shale. This is because these geologic materials contain weathered products from potassium feldspar and mica, and are apt to concentrate uranium and thorium. Importantly, clay and shale typically have low permeability and are barriers to contaminant flow. Another technique, neutron logging, measures the amount of water in any particular vertical section of borehole. Energetic or “fast” neutrons are sent out into the formation surrounding the borehole usually from an Americium Beryllium (Am-Be) or Plutonium Beryllium (Pu-Be) source, and these neutrons are slowed down by collision with hydrogen ions associated with water. The returning “slow” neutrons are measured by a detector and indicate water bearing strata in the vadose zone, and water-filled porosity below the water table.

Electrical Techniques in Borehole Geophysics Several borehole electrical techniques are available for site characterization. These include single point resistance logs, normal-resistivity logs, spontaneous-potential logs, electromagnetic induction logs, and fluid-resistivity logs. Single point resistance logs measure the electrical resistance between selected points in the borehole and an electrical ground on the surface, and are useful for understanding lithology, water quality and the amount of fracturing in hard rocks. Interpretation involves identifying zones of increasing resistance associated with small diameter boreholes, whereas lower resistance is related to saline water, large borehole diameter, and highly fractured media. Normal-resistivity logs record the resistance to electrical flow immediately outside an open, uncased borehole, and interpretation generally is similar to that of single point resistance measurement. Normal-resistivity logs typically involve deployment of a string of vertically displaced electrodes in a single hole.

Electromagnetic-induction (EM) logs also measure electrical conductivity or resistivity immediately outside a borehole and are excellent for indicating porosity, permeability, clay content, and total dissolved solids in fluids. Further, EM and other electrical techniques are proficient in identifying landfill leachate and saline water intrusion. EM borelog techniques are designed to optimize readings outside the borehole and minimize influence of the borehole and borehole fluids. Conversely, fluid-resistivity logs are geared toward examining borehole fluids, particularly the dissolved salt and solid concentrations.

Other Borehole Geophysical Techniques One versatile monitoring procedure for organic compounds is laser induced fluorescence (LIF) that uses laser light to excite fluorescent molecules in petroleum products. The excitation is specific for PAH compounds, but nearly all petroleum products contain some PAHs. LIF field measurements utilize a direct push logging arrangement which allows vadose zone and aquifer material to be examined at depth below ground surface. Further, LIF can distinguish different NAPLs in the subsurface using the intensity of the fluorescence in the media, its spectral signature, and the lag time between the laser pulse and emission of fluorescence. The laser light is transmitted down and uphole by two separate fiber optic threads, and the signal is processed and analyzed in real time.

Fiber optic chemical sensors (FOCS) are a variant of LIF and have been developed using a sensor for analysis of soil, air, or water that records changes in light absorbance, reflectance, fluorescence, and light polarization of the medium. Unlike LIF which just uses fiber optics to transport light down and uphole, FOCS uses the fiber optic cable as an integral part of the sensor. Specifically, part of the fiber optic cladding is removed from the cable in the sensor and replaced with a chemically selective layer that, when placed in the sample media, reacts with a specific analyte of interest. Raman spectroscopy is used to identify specific metals and organic chemicals. The detection limits are typically in the ppm range for VOCs.

8.7.3 Water Quality Indicators of Groundwater Provenance and Movement—Tracers

Beyond sampling water for contaminant concentrations and conducting geophysical surveys for defining subsurface geology, there are many other methodologies and water-quality indicators pertinent to site characterization. The chemical mixtures in measured contaminants and certain characteristic compounds (or “tracers”) can be

key indicators of pollutant source, travel pathways, and transformation. Tracer techniques for groundwater can be divided into water quality surrogates that are either (1) chemicals added to aquifer systems or to potential contaminants in regions where subterranean flow is expected to be rapid, or (2) “environmental tracers” which are groundwater quality changes which have occurred over longer periods of time in groundwater. The former includes dyes and chemicals intentionally added to track movement and flow, and the latter refers to “natural or anthropogenic compounds or isotopes that are widely distributed in the near-surface environment of the Earth, such that variations in their abundances can be used to determine pathways and timescales of environmental processes” (Cook and Böhlke 2000).

Payne et al. (2008) and Suthersan et al. (2014) present guidance for tracer selection, tracer test design, and data interpretation. An optimal groundwater tracer is highly detectable, mimics either groundwater or pollutant movement, is chemically stable for a desired length of time, has little background concentration in the groundwater being investigated, is not sorbed or filtered by the geologic media, and does not have adverse health or ecological effects (Davis et al. 1980). Conservative compounds that are not sorbed or retarded in their flow are particularly useful and these include chloride, bromide, iodide, nitrate, sulfate, and boron. These compounds can reflect groundwater origins with less ambiguity than other dissolved species, because they are often present in groundwater and some, like boron, are relatively unaffected by evaporation or chemical reactions (Barth 1998; Bassett et al., 1995; Vengosh 1998).

Dyes and Injected Tracers, Artificially Introduced Tracers In many fast-flowing (e.g., karst, carbonate rock, and caves) groundwater systems, tracer dyes can be released to track direction and travel times of flow. Optimal systems typically transmit water and pollutants quickly, which is advantageous because a long waiting time for the re-emergence of injected tracers is not favorable. Tracers can be artificially injected into wells, sinkholes, caverns, and disappearing streams in karst terrain. Popular tracer dyes include fluorescent dyes such as fluorescein which was developed over 145 years ago, pyranine, lissamine FF, photine CU, amino G acid (7-amino 1,3 napthalene disulphonic acid), optical brighteners, and a variety of rhodamine dyes. A downside of some of these dyes is that some have negative health effects. Dyes can be used either qualitatively by visual observation, or collected with adsorbing devices to quantitatively measure flow. A simple adsorption apparatus involves placement of a charcoal packet along expected pathway of subterranean flow. More sensitive devices include filter fluorometers and spectrofluorometers which can determine specific fluorescent wavelengths, quantify flow more accurately, and distinguish background fluorescence and other interferences. In addition to the tracing of natural waters, dyes can help determine pipeline leaks. Nonpolar fuel dyes can be added to demarcate different fuel types and are required in some countries. This can help distinguish the individual impacts of multiple fuel leaks of similar types, but from different sources.

Things other than dyes can be injected as tracers of groundwater flow. A common tracer for groundwater is chloride (Cl^-) which is a component of common table salt. Care must be used when using ionic tracers so that the concentration of salts added to groundwater does not change its density and subsequently impact natural groundwater flow. A more unusual tracer that has been used in cave systems is a signal emitting float which has a delayed explosion. The seismic signals emitted from these generated

impulses can help locate subsurface passages. Other tracers that have been used with varying degrees of success include silicic acid, boric acid, phosphoric acid, acetic acid, alcohols including ethanol, sugars (sucrose, maltose, dextrose, glucose), and glycerol (Davis et al. 1985). Each of these tracers has disadvantages: acid can react with aquifer material, sugars decompose rapidly, and alcohols tend to be absorbed onto organic material (which can actually be used to advantage by measuring partitioning into suspected organic contaminants).

Tracers developed for contaminant hydrogeology include a class of compounds called partitioning tracers. These newer methods involve circulating a suite of tracer compounds, not just a single tracer, in the subsurface to measure how some tracers are slowed by contaminant mass, particularly a mass of nonaqueous phase liquids. Partitioning tracers measure groundwater flow and the mass of a stagnant immiscible liquid pollutant blocking groundwater's path by observing the differential tracer retardation. The underlying principles of this tracer method have been discussed in Chapter 3.

Scientific developments include the study of colloidal tracers and smaller, nanoparticle tracers. These colloidal tracers have included yeasts, bacteriophages (viruses), fluorescent latex microspheres, bacteria (living and dead), spores (*Lycopodium* and vegetative spores), and other nanoparticles (Davis et al. 1980; McKay et al. 2000; Zhang et al. 2015). Solid tracers are larger than dissolved aqueous tracers and have the negative possibility of being sieved or filtered through porous media and small-aperture fractured media. Larger particle tracers do, however, have the positive quality of not being absorbed in the rock matrix. Occasionally, solid tracers have been observed to move faster than average groundwater velocity—this has been explained by the notion that larger particles move through larger pore spaces or fracture apertures where groundwater velocities are higher than average (Zhao 2015).

Gases can be used as tracers of vapor migration, and of liquid migration by injection and dissolution of gases into groundwater. Inert radioactive tracer gases have been considered, such as xenon (^{133}Xe) and radon (^{222}Rn), particularly in identifying groundwater/surface water interaction, but health concerns and a short half-life for radon are inhibitory (Xie et al. 2016). Noble gases of helium, neon, argon, krypton, and xenon are other potential tracers as their natural background in the environment is low. Chlorofluorocarbons (CFCs or Freon® compounds), also have low environmental background and have been used for both groundwater and gaseous tracer experiments (Thompson et al. 1974, Weeks et al. 1982; Kreamer et al. 1990).

Environmental Tracers Environmental tracers which show water-quality patterns and changes do not have to be injected by site investigators, and are directly relevant to understanding a contaminated site. Some of these tracer signals arise due to natural fluctuations in local, regional, or global conditions, while others reflect anthropogenic influences and activities. Some take advantage of short term changes. For example, diurnal temperature fluctuations can be used to define gaining and losing reaches of streams. Probes placed in bottom sediments of streams that show daily temperature variation can be associated with losing reaches as water, affected by daily conditions, infiltrates. Conversely, steady temperatures in stream bottom sediments can be indicative of a gaining groundwater contribution to a stream through the sediments, as most groundwater is typically more constant in temperature. Other tracer signals arise from longer-term changes in climate, recharge differences, or substances that humans

introduced into the environment decades ago. Compounds and isotopes that have leaked into the atmosphere from human activities (e.g., chlorofluorocarbons from refrigerants, radionuclides from testing of nuclear weapons) return through rainfall to the vadose zone and groundwater, and allow dating of groundwater age, whereas pharmaceuticals, personal care products, and specific compounds in some foods (e.g., caffeine) are not readily removed by sewage treatment and become tracers of wastewater release into the environment.

The source of a pollutant strongly influences its chemical makeup, and chemical differences from dissimilar sources can be used to trace and track environmental contamination. Biogenic gaseous mixtures containing methane are typically “dry” which means a higher concentration of methane and light hydrocarbons, whereas thermogenic gases and those from pipelines have less light 2 to 4 carbon compounds (C2s to C4s) and are “wet” with a higher concentration of 5 carbon (C5) and higher molecular weight compounds. Landfill gases are often approximately half methane and half carbon dioxide with an absence of oxygen. Natural gas derived from dewatering of coal layers, an extraction process whose retrieved product is called “coal seam gas” or “coal bed methane,” is typically higher in methane than natural gas extracted from other sources and is therefore sometimes called “sweet gas.” Crude oil and coal from different regions of the world have different chemical constituents which can be tracked, for example differences in the amount of sulfur compounds designates different quality of crude oil. The petroleum industry has noted that uptake of sulfur into plants is possible. Because different isotopes of sulfur can fractionate in different ways, the transport and fate of sulfur bearing compounds can be further tracked. Also, natural gas in pipelines in municipal and urban settings typically has noxious smelling mercaptan added so that leaks of this normally odorless gas are readily noticeable and are often reported. The added gases which allow leak detection and tracking sometimes have descriptive names like Cadaverine and Putrescine.

Human sewage and animal waste have a host of associated compounds and microbes which can be used to track their contamination in groundwater systems. Bacterial indicators, like *Escherichia coli* (*E.coli*) are useful, but often can be filtered out in porous media, whereas bacteriophages and human viruses are smaller and can travel farther. When microbes occur in groundwater they can indicate source by phenotype, genotype, and speciation (some microbes are more associated with human waste and others with ruminant species). Some genera and species of bacteria studied as indicators differentiating human from other mammalian waste include: *E.coli*, relative amounts of fecal streptococci and fecal staphylococci, *Bacteroides* spp., *Rhodococcus coprophilus* (animal herbivores), *Clostridium perfringens*, *Bifidobacterium adolescentis* (human), and *Bifidobacterium thermophilum* (animal). Other tracers of human and animal waste include: sterols, steroid estrogens (found in human sewage outfall), fatty acids and lipids, surfactants and detergents, caffeine (human ingestion and sewage outfall), triclosan (an antibacterial and antifungal agent found in hand soaps, body washes, toothpastes, and some cosmetics—sewage outfall), and sewage/septic tank related nonylphenol ethoxylate metabolites (Swartz et al. 2006).

Ionized substances have been used both as artificially injected tracers and measured as natural environmental tracers indicating source. There are a large number of ions which can be tracked and traced, and these substances do not decompose with

time. Historically, those chemical species with high concentrations, easy detection, and low sorption have been the most popular. This includes negatively charged anion species which are repelled by negatively charged clay surfaces and therefore resist sorption. Traditional tracer ions include Cl^- , Br^- , Li^+ , NO_3^- , NH_4^+ , SO_4^{2-} , Mg^{++} , K^+ , B , and I^- . Of these, Cl^- and Br^- are the most popular. Organic anions have been used as tracers, including benzoate. Metal complexes with chelating agents have been used to track groundwater flow, balancing the need for a detectable tracer with the potentially negative health effects of mobilizing a heavy metal pollutant (Davis et al. 1980). With the advent of Inductively Coupled Plasma Mass Spectrometers (ICP-MS) investigations of naturally occurring trace elements to identifying groundwater pathways increased (Stetzenbach et al. 1994; Kreamer et al. 1996; Johannessen et al. 1997).

Importantly, CFCs have also been used for dating recharge from precipitation, because the first wide use Freon® refrigerants began after 1930, and subsequently increasing amounts of gaseous CFCs leaked into the atmosphere and mixed with precipitation, eventually infiltrating the ground surface and recharging groundwater. CFCs were also used as aerosol spray can propellants, but because they contribute to ozone layer depletion in the atmosphere, their use has been phased out under the Montreal Protocol. CFCs are greenhouse gases with an approximate residence time in the atmosphere of 65 to 130 years and their abundance or absence in groundwater is an indicator of groundwater age. The ratio of CFCs to SF_6 (sulfur hexafluoride) has a groundwater dating age range of about 1 to 40 years.

8.7.4 Water Quality Indicators of Groundwater Provenance and Movement—Groundwater Composition, Compound Ratios, Daughter Products, Degradation Indicators, and Other Indicator Compounds

A considerable number of methods to track, trace, and date groundwater contamination rely on looking at the changing composition of pollutant compounds, associated chemicals, and differences in the chemical nature of multiple sources. Identifying and utilizing compositional differences is a powerful tool in understanding groundwater and contaminant flow.

Inorganic Indicators One of the simplest ways to distinguish different sources and transformation of contaminants is by analyzing groundwater chemical quality and compound ratios. Significant analytical chemistry advancements have been, and continue to be, made since major anions and cations were first measured in groundwater, but these ions, and the ratios between these ions (particularly the more mobile anions) continues to be a source of groundwater definition. Piper, Stiff, and Maucha diagrams visually portray the major ionic components of water quality and can indicate groundwater provenance. Ratios of ions can also be used to distinguish waters. For example, a common anion comparison used to trace groundwater has been the Cl^-/Br^- ratio. Davis et al. (1998) report on many of the uses and applications of this ratio, including determining the origin and evolution of salt water and brines, and studying salt in potable groundwater. Factors which can affect this ratio include distance from the ocean, dry lake beds, or other sources of salt, including pollution (Davis et al. 2004; Alcala

and Custodio 2008). These ratios have been used to track septic tank pollution in the United States (Katz et al. 2011). Other useful ratios are total inorganic carbon to total organic carbon ratios, and carbon to nitrogen ratios.

Mining operations for various metals often can have more than one metallic species that can enter groundwater, or mobilizing agents and additives associated with the particular extraction method and target metal. These other species and additives can often be used to track the influence of mining operations on groundwater systems. Several metals, metalloids, and nonmetals can often be found together in metal extraction and mining (e.g., it is possible to observe combinations of uranium, copper, arsenic, gold, silver, vanadium, sulfur, thorium, lead, zinc, or others from some precious metal operations). Other types of mining undertakings have other potential tracers released into the environment. *In situ* leach mining typically uses an injected lixiviant to dissolve and mobilize extractable metals, and these lixiviants can be used as one indicator of potential contaminant migration, with the cautionary note that while a rapidly moving lixiviant can give early warning of potentially slower-moving contamination, the disappearance of the lixiviant does not necessarily indicate the disappearance of the spectrum of potential groundwater contaminants at a mining site. Metals can also be used as surrogate tracers for energetic compounds, that is propellants, explosives, and pyrotechnics (PEP) compounds. For propellants and some fuels particularly linked with the rocket fuel oxidizer perchlorate, Cr⁺³, Cr⁺⁶, Cu⁺², and Zn have been evaluated as surrogates. Surrogate compounds in fireworks and flares include Na, K, Ba, Cu⁺³, Sb, Sr, Al, As, and Cr⁺⁵ (Motzer 2001).

Organic Indicators Organic compounds, particularly mixtures of organic chemicals, have a wide range of sources, additives, and degradation products which can be tracked in groundwater (Chapter 7). The differing rates of degradation of the compounds in subsurface organic mixtures produce changes in the ratios of those compounds and of generated daughter compounds. Many organic mixtures have unique source compositions and all eventually weather and transform with time. Hydrocarbon fuels in particular have different compositions, depending on fuel type and additives. These differences serve as distinguishing features when several different fuels have leaked or have been spilled. Fuels and oils normally consist of mixtures of hundreds of compounds, and different fuel types have different dominant ranges in the number of their carbon atoms. Crude oil has compounds that range from having one or two carbon atoms (C1 and C2) to compounds with close to sixty (C60). Crude is fractionally distilled to establish different types of hydrocarbon products, and different additives are put in for these varied purposes. Gasoline for cars (petrol) and small airplanes (aviation gas or AV-gas) typically have light hydrocarbons predominantly ranging from the 4 carbon compounds (C4) to about the 11 or 12 carbon range (C11 to C12). Kerosene is a heavier fuel with approximately the C8 to C17 compounds, diesel fuels are roughly in the C8 to C24 range, the jet fuel JP-4 is about C5 to C14, and JP-8 and Jet-A approximately C8 to C18. Stoddard solvent, which was used in the past as a dry cleaning fluid, has a typical petroleum distillate fractions of C7 to C12, heavy fuel oils are generally between C8 and C50, bunker fuel used in ships are approximately C10 to C26, and lubricating oils are even heavier with carbon numbers around the C14 to C50 range. Other residuum from crude distillation often have more than 20 carbon atoms in their constituent compounds, with waxes ranging approximately from C20 to

C50 and asphalts and pitch going from C24 to C56. These fundamental compositional differences can be used to identify sources and pathways of contamination.

Fuel additives can also be tracked in the subsurface as well during site characterization activities. Some additives have been used for a time and then been phased out of usage or supplanted by another additive, giving a discrete time range for possible past release. Additives for gasoline include: butanes which add volatility (Reid vapor pressure) for cold climates, tetraethyl lead as an anti-knock component (beginning in the 1920s, phased out in the United States starting in the 1970s), ethylene dibromide (scavenger for antiknock lead), dyes, oxidation inhibitors, metal deactivators, corrosion inhibitors, anti-icing compounds, detergents, methylcyclopentadienyl managanese tricarbonyl or MMT (antiknock), demulsifiers, deposit control additives, oxygenates, and deposit and evaporation control such as the Underwriter's Laboratories (UL) additives which are for fuel storage. The oxygenates in particular, include ethanol and methyl-tert-butyl ether (MTBE) which have significant aqueous solubility. MTBE has had reduced usage in the United States because of its propensity to pollute groundwater. Because the commercial usage of MTBE has a known time frame, as a tracer it can help estimate the age of fuel releases, but is less effective in differentiating gasoline plumes because of its ubiquitous use.

Biological and chemical transformation of compounds is another potent means of understanding the movement, age, pathway, and source of contamination. For example, when MTBE degrades, the carbon isotope ratio of atomic weights $^{13}\text{C}/^{12}\text{C}$ (expressed as $\delta^{13}\text{C}$) preferentially becomes heavier, because the bacteria assimilate the petroleum ^{12}C isotope more quickly, which enriches the remaining MTBE in the heavier ^{13}C isotope.

The weathering of compounds gives clearer definition to contaminant age and fate, and generally petroleum products lose the very lightest and most volatile compounds (C4 through C6) with time by volatilization, as well as losing some of the heaviest compounds with long chains of carbons which are cleaved in the degradation process (Senn and Johnson 1987). Distinctions can be made in the unequal degradation and transformation rates of paired organic compounds or groups of compounds with gas chromatography. For example, benzene/toluene ratios, pristine/phytane ratios, or comparisons of the overall ensemble of fresh fuel compounds versus weathered fuel compounds are often indicators of transformation along a transport pathway. Comparing ratios of EPH (Extractable Petroleum Hydrocarbons) to PAH (Poly Aromatic Hydrocarbons) is often a useful first step in assessing fuel spills or releases. At sites where the EPH/PAH ratio is low or near even, there is a prevalence of heavier petroleum hydrocarbons and/or weathered fuel oils (e.g., this is characteristic of coal ash and old fuel oil sites). High EPH to PAH ratios can indicate gasoline, jet fuels, or fresher, more recent releases of fuel oils. Some chemical fingerprinting of petroleum involves biological markers (biomarkers), which are complex molecules originally from living organisms. Each source of crude oil can have a unique assemblage of biomarkers due to the geologic conditions in which it was formed, and these oil biomarkers contain the isoprene compounds, terpenoids, and isoprenoids which can be used to differentiate between sources (Wang et al. 2006). Some researchers have used stable isotopic ratios (carbon isotope microbial fractionation) and noble gases ($4\text{He}/40\text{Ar}$ vs. $4\text{He}/20\text{Ne}$) to identify fugitive gas leaks into drinking wells overlying oil shale plays (Osborne et al. 2011; Jackson et al. 2013;

Darrah et al. 2013). Recently, examining methane in concert with noble gases in stream beds has been used to identify thermogenic methane fluxes from groundwater overlying regions of shale gas development (Heilweil et al. 2015). Methane isotopes as well as dissolved organic carbon and tritium have been used to evaluate connectivity between aquifers and underlying coal seam gas operations (Iverach et al. 2015).

Quantifying the uptake of nutrient compounds during biodegradation and the resultant production of daughter products and residuals are ways to monitor the rates of transformation of organics. Petroleum degradation is normally an aerobic process which uses oxygen and produces carbon dioxide; by monitoring the extent of change in these compounds one can calculate the rate of biodegradation and, importantly, determine whether the plume is moving faster than the rate of natural or augmented pollutant attenuation.

Harmful compounds can have additives or impurities which are not only good tracers in the environment, but they can be pollutants in their own right. Chlorinated solvents have several stabilizers. For trichloroethene (TCE), 1,4 dioxane is an important stabilizer used to facilitate transport and storage in aluminum containers. It is itself considered a solvent with negative health effects. The ratios of the chlorine-35 to chlorine-37 can be another way to fingerprint chlorinated solvents. Another example of mixtures and impurities is polychlorinated biphenyls (PCBs) which are never a pure, single compound, but mixtures of PCBs by the nature of their manufacture. PCBs can also have co-contaminants of polychlorinated dibenzofurans and polychlorinated naphthalenes. The nature of the mixtures can be a good source of differentiation, and the disparity in the degradation rates of contaminants, additives, impurities, and inert compounds can indicate age and source.

Historically, pesticides were mixed with some hydrocarbon fuels to apply them to crops. Many of these pesticides have comingled substances (some inert) and trace substances (e.g., dioxins and furans) which can help fingerprint their spatial distribution at a site. Like PCBs above, the source and age of pesticide releases can be established by comparing the ratio of inert and degrading compounds.

8.7.5 Water Quality Indicators of Groundwater Provenance and Movement—Isotopic Identification of Pollution Sources and Groundwater Pathways

The measurement and evaluation of stable, radioactive, and radiogenic isotopes has played an important role in hydrologic and geologic investigations, and are equally consequential in the characterization of contaminated sites. Because physical, chemical, or biological transformation of a contaminant can alter the compound's original isotopic ratios (fractionation), transformation processes can often be distinguished from contaminant dilution (which typically does not alter these ratios). The mathematics of Rayleigh distillation to quantify isotopic fractionation accompanying phase changes and chemical reactions are well known, and make available numerical estimates of the magnitude of isotopic change. The analytical detection of isotopes in groundwater and vapors is rapidly advancing, with the required sample volumes becoming smaller, and analyses becoming faster, less expensive, and routine. From older methods like scintillation counting of radioisotopes which required large volumes of water, through

isotope ratio mass spectrometry advances, to new analytic techniques such as Laser Isotope Ratio Infrared Spectrometry IRIS, which can be portable and field deployable, the analytical chemistry underpinnings of contaminant surveys has increased the ability of the contaminant hydrogeologist to assess a site and its properties. Accelerator mass spectrometry (AMS) can sometimes separate atomic isobars (for example nitrogen-14 from carbon-14) and makes possible the detection of many isotopes, including many that are long-lived. AMS has been applied to the analysis of many isotopes including ^{36}Cl , ^{10}Be , ^{14}C , ^3H , ^{129}I , ^{26}Al , ^{236}U , ^{240}Pu , and ^{210}Pb .

Applications of isotope hydrology to challenges of groundwater movement and source are numerous, diverse, and are used worldwide. Isotope hydrology has been used to ascertain renewable and nonrenewable, deep groundwater in Syria (Al-Charideh and Kattaa 2016), the origin of groundwater in the Negev Desert (Vengosh et al. 2007), preferential flow along faults in Germany (Gumm et al. 2016), altered spring flow quality in Grand Canyon National Park in the United States (Ingraham, Zukosky, and Kremer 2001), assessment of fluid inclusions at the proposed nuclear waste repository at Yucca Mountain, Nevada, as evidence of a hypogene paleohydrogeological event (Dublyansky and Spötl, 2010), baseline measurement and assessment of methane concentrations of a well in Alberta, Canada (Humez et al. 2016), and has been employed for countless other assessments at locales around the globe.

Tracing Groundwater and Pollution with Isotopes More than fifty years ago, paleoclimatologists and environmental geochemists began using the stable isotopes of hydrogen and oxygen to track meteoric water movement on the environment (Craig 1961; Dansgaard 1964). An equation showing the average relationship between these isotopes was established (the global meteoric water line) and variations due to temperature, seasonality, precipitation and recharge altitude, latitudinal relationships, and paleo-effects were key in understanding global water movement, including groundwater source and pathway. Because surface waste impoundments (ponds, pits, and lagoons) have the potential to partially evaporate water, then have the remaining surface water leak into the subsurface, isotopic fractionation during evaporation of water is particularly important to contaminant site characterization studies. Evaporated water has a lighter isotopic composition, enriching the remaining liquid with heavier isotopes which can often be tracked into the subsurface, distinguished from background groundwater isotopic signatures, and used to establish mixing ratios of leaked, contaminated water to natural background groundwater signatures. For very old groundwater, past climatic change can be observed and contribute to studies of aquifer isolation and aquitard or aquiclude integrity. Aquitard integrity and the origin of pore water has been investigated in Canada for mining operations and potential nuclear waste storage by comparing Pleistocene age versus modern stable isotope ratios, below and above thick aquitards (Hendry et al. 2013; Hendry et al. 2015). The stable isotopes of water are hydrogen and deuterium, and oxygen-16 and oxygen-18.

The stable isotopes of nitrogen (nitrogen 14 and 15) in concert with those of oxygen have been used to discern anthropogenic sources of nitrate, nitrite, and ammonium in groundwater. These contaminant sources can include septic tank effluent or wastewater, animal manure, and mineral fertilizers, and can often be distinguished by isotopic ratios. Because there is some overlap and ambiguity between isotopic composition in

wastewater and animal manure, and denitrification processes in the subsurface can result in fractionation after nitrate release, additional indicators can be used to help tell different sources apart. Distinguishing co-contaminants from agriculture can include herbicides, pesticides, and major ions and trace elements from soil amendments. From wastewater, co-contaminants can include pharmaceutical compounds, residuals from personal care products, caffeine, and artificial sweeteners. Some animal feeds contain unique inorganic additives as well. Relatively conservative stable isotopes of boron (10 and 11) have also been used to make a distinction between wastewater and animal manure (Eppich et al. 2012). In China, stable isotopes of hydrogen, and oxygen and sulfur have been used to delineate the sources of anthropogenic nitrate and sulfate groundwater pollution (Li et al. 2006). Sulfate isotopic values indicated much of the pollution came from recharge of air pollutants from the combustion of coal, with some contribution of sulfur additives in fertilizer.

Mining residuals and mineral waste products can be distinguished by isotopic analysis. In uranium oxides, stable isotopes of oxygen can help distinguish anthropogenic mining activities from natural background as can activity ratios of uranium-234 to uranium-238. $^{234}\text{U}/^{238}\text{U}$ ratios are close to 1, (secular equilibrium) near uranium mining outfall, whereas naturally occurring uranium background in groundwater often has a higher ratio, particularly in old groundwater. Conversion of ^{238}U to ^{234}U can further be examined by its concurrent production of alpha particles, ^4He . Another isotope, uranium-236 is dominantly anthropogenic, is found in spent nuclear fuels and some reprocessed uranium, and can therefore help trace nuclear waste leaks. Plutonium (Pu) is also of human manufacture, and while trace amounts can be found in nature (parts per trillion in groundwater) larger concentrations of this fissile material indicate contaminant excursion. A potential nuclear waste product and tracer is technetium-99 which is the most significant long-lived fission product of uranium.

Other mining and industrial by-products, including metals and salts, can be characterized with isotopic analysis, sometimes in conjunction with other approaches. For example, stable isotopic analysis of chromium species in groundwater can give a picture of the natural reduction of mobile and harmful Cr(VI) to less problematic Cr(III). It can also characterize the extent and rate of Cr reduction during remedial activities. Another industrially produced compound which has been found in groundwater, and is an endocrine disruptor in humans, is perchlorate. Perchlorate has some naturally occurring salts, but is mostly generated by industrial processes especially for the production of rocket fuel oxidizers. Tracking the compound in the environment has included measurement of the oxygen and chlorine isotopes of perchlorate itself as well as other isotopic ratios and attendant compounds. Other useful isotopic analyses for perchlorate tracking are stable isotopes of strontium, nitrogen, and tritium, and isotopic ratios of $^{37}\text{Cl}/^{35}\text{Cl}$, $^{87}\text{Sr}/^{86}\text{Sr}$, and $^{16}\text{O}/^{17}\text{O}$. Some of perchlorate's additional surrogates in groundwater that can assist in source identification and age dating include: nitrates, sodium, chlorides, strontium, phosphate, metals, and nitroglycerins (Morrison and Murphy 2006). These methods can help determine whether perchlorate in the environment is natural or synthetic.

Isotopes and Groundwater Dating Isotopes are also used for characterizing the fate and transport of organic compounds. Processes affecting dense chlorinated solvents

and other volatile organic compounds can be evaluated using chlorine isotopes which are fractionated during biodegradation, but are unaffected by dilution and dispersion. MTBE biodegradation can be analyzed with isotopic analysis, the difference between production methane from natural, shallow biodegradation versus leaks from pipelines or production wells can be ascertained. When a compound such as trichloroethene is discovered at a site, compound specific isotopic analysis can help determine whether it is a daughter product of previously spilled tetrachloroethene, or a leak in and of itself.

Site characterization involves understanding groundwater flow and travel times. Isotopic techniques are pivotal in age dating of groundwater, and there are different approaches depending on groundwater's suspected residence times. Relatively young groundwater is often dated by using radionuclides released into the atmosphere during past nuclear weapons testing. For example, tritium (^3H), with a half-life of 12.4 years, with its decay product ^3He , provides a useful tracer of recently recharged groundwater. When calculating groundwater age from tritium, adjustments to $^3\text{H}/^3\text{He}$ ratios must be made if there is terrigenic helium in the groundwater from the earth's mantle or crust. Tritium to helium-3 ratios are most effective at dating groundwater 0.5 to approximately 40 years old. Another dating technique for modern groundwater 10 years old or younger uses krypton-85, which is produced by nuclear reprocessing and has a similar half-life to tritium, and comparable dating range as well. Nuclear bomb-pulse chlorine-36 is also used to date young groundwater recharged after the 1950s, but in lower, natural concentrations in deep systems can also be used to evaluate submodern groundwater that is 50,000 to a million years old. Methods for dating submodern groundwater (>1,000 years since recharge) include radiocarbon dating (carbon-14). The amount of ^{14}C (half-life 5,730 years) in groundwater can indicate when it was last in contact with the atmosphere, but care must be taken to account for uncertainties due to potential groundwater interaction with carbon from other sources, such as the "dead" carbon in limestones and other carbonate rocks which has no ^{14}C . In optimal conditions ^{14}C can be used to date groundwater about 1,000 to 40,000 years old and can sometimes be used in concert with argon-39 (half-life 269 years). Silicon-32 has the beneficial aspect for groundwater dating of having a half-life of 140 years which allows it to fill a gap between tritium and carbon-14 dating, but its loss and interaction with solid phase silica in an aquifer and analytical difficulties have limited its use. Uranium isotopic ratios are also a useful groundwater dating tool. $^{234}\text{U}/^{238}\text{U}$ ratios (called uranium isotope disequilibrium) typically increase with groundwater age and can be used to give approximate ages from 10,000 to one million years old. Some isotopes with long half-lives have the potential to date very old groundwater with applications for understanding the isolation of deep contaminant burial, nuclear storage, or deep waste injection. These include iodine-129 (half-life 15.7×10^6 years), krypton-81 (half-life 2.29×10^5 years), and Xeon-139 (half-life 2.165×10^{21} years).

8.7.6 Water Quality Indicators of Groundwater Condition— Microbial testing and Genome Sequencing

Studying subsurface microbiology at contaminated waste sites allows groundwater professionals to calculate the rate of natural attenuation of pollutants, the efficacy of amendments added to groundwater to enhance contaminant breakdown, and the

impact of toxic spills that might sterilize the subsurface. It allows tracking of sewage releases or spills of other animal contaminated waste, particularly in geologic systems with little ability for porous media to filter waste, such as karst systems. Shifts in subsurface biota can also change redox conditions, which in turn can either mobilize or sequester metal species and other compounds. These microbially mediated changes can be crucial in the evaluation of a contaminated site.

Traditional methods for culturing indigenous subsurface bacteria originated with inappropriate growth media from health studies and human and animal hosts, and early tests to determine the microbial underworld revealed few active microbes below ground surface. As growth media and culturing processes became more sophisticated, however, a huge number of both active and quiescent microbes were shown to exist in groundwater and subsurface aquifer material. In soils and root zones near the surface, groundwater teems with bacterial life with numbers as high as millions of bacteria per gram of soil. With depth these numbers drop off, but bacteria can be quite abundant even at great depth. Protozoa, fungi, algae, and viruses can also be significantly present in groundwater environments. Because few nutrients are typically available in aquifer material, and physical filtering often can occur, most naturally occurring subsurface microbes are slow-growing and few are normally associated with animals or pathogenicity. Indigenous subsurface bacteria can have the beneficial quality of being able to break down and transform toxic and carcinogenic waste. Some pollutants like hydrocarbon fuels are rapidly broken down, while others like solvents and many pesticides are recalcitrant to degradation and are longer-lived in the subsurface.

These microbiological agents of contaminant change and transformation can be monitored directly, or can have key constituents monitored (e.g., lipids or DNA) to access changing conditions (Dojka et al. 1998; David et al. 2014). Alteration of microbial flora can be linked with subsurface environments which undergo stress. Stresses on microbiotic communities can be caused by naturally occurring contaminants, or with anthropogenic contamination including deleterious spills that reduce the number of indigenous microbes in the subsurface (Rahm et al. 2006). Changes in subsurface microorganisms can also be an indicator of the consequence and impact of nutrient amendments added at a site to induce biodegradation. For example, enhanced *in situ* bioremediation for chlorinated solvents (Chapter 9) could take the form of biostimulation with added electron donors, and/or bioaugmentation with addition of microbial consortia containing dechlorinating bacteria such as *Dehalococcoides* and *Dehalobacter*. Both biostimulation and bioaugmentation produce detectable changes in microbial diversity, function, and taxonomic composition (Giddings, Jennings, and Gossett 2010).

The science of genome sequencing has grown by leaps and bounds, making DNA analysis of contaminant sites rapid and inexpensive. Just a few years ago, Sanger techniques allowed only a few hundred base pairs to be able to be analyzed over a week's time; now millions can be distinguished in the same time period at low cost. After identification, by merging taxa into functional groups (e.g., methanogens, sulfate reducing bacteria, denitrifiers) the function of these communities can be better understood. Considering *in situ* cleanup scenarios, microbial community structure can be correlated to remediation performance and practices can be adjusted (e.g., addition of oxidizers, pH buffers, electron donors, bioaugmentation cultures, etc.).

■ 8.8 Summary

Site characterization involves goal setting and outcome definition, use of noninvasive techniques, followed by strategic application of invasive methods of investigation. In order to collect data for groundwater contamination studies, it is usually necessary to install monitoring wells. Such wells can permit one to measure water levels, collect water samples for analysis, and detect the presence of nonaqueous phase liquids.

Monitoring-well design considers the type and diameter of casing and screen, the material from which the casing and screen is constructed, and whether the well will have an artificial-filter pack or be naturally developed. The annular space between the casing and the borehole must be properly sealed, and the well needs a protective covering. Monitoring wells may be installed by hollow-stem auger drilling, mud-rotary drilling, air-rotary drilling, reverse-rotary drilling, and cable-tool drilling. The equipment used for monitoring-well installation and the material used for the well must be properly decontaminated. Once installed, the well needs to be developed to remove fine material from the area outside the well screen. Water-table wells are installed to monitor the water table and piezometers are used to monitor formations below the water table. Frequently, a water-table well and several piezometers are installed at the same location to form a nest of wells to sample the formations at different depths. Multilevel monitoring devices may be used to collect samples from very closely-spaced vertical intervals.

There are a number of sampling devices that have been developed to withdraw water samples from monitoring wells. These include bailers, bladder pumps, stator-rotor pumps, piston pumps, and peristaltic pumps. The ability of these devices to collect an unbiased sample varies with the design, technique used, and material from which they are constructed. Prior to sampling a well, it is necessary to purge it to remove stagnant water from the casing. Micropurging techniques result in a water quality sample that is as free of turbidity as possible and at a lower cost than traditional purge and sample techniques due to a shorter time to collect the sample and reduced costs for disposal of contaminated purge water. Soil water must be collected through the use of a suction lysimeter. These are installed in boreholes above the water table. Soil gas vapor can be sampled through active probes that withdraw soil gas samples for analysis or passive devices that sorb soil gas onto activated charcoal devices. Monitoring soil gas can indicate areas where the soil has been contaminated and requires remediation. It can also be used to delineate areas where shallow groundwater is contaminated by volatile organic compounds and where there is a layer of a volatile, nonaqueous phase liquid floating on the top of the capillary zone. Phyto-screening, surface geophysics, and aerial photographic interpretation are other noninvasive or low impact characterization techniques that are appropriate at many sites.

There are a host of chemical and microbial analysis technologies that assist interpretation of the source, movement, and transformation of subsurface contaminants. Differences in source chemistry, generation of daughter compounds, and comparison of compound ratios lend themselves naturally to environmental forensic investigations. Chemical compound transformation, the utilization and uptake of nutrient compounds, varying chemical compound ratios, and changes in subsurface microbial communities all can be indicators of bioremediation and compound attenuation. Geophysics, groundwater dating, and borehole core analysis can define the geologic provenance and flow constraints which affect pollutants.

References

- Alcala, F. J., and E. Custodio. 2008. Using the Cl/Br ratio as a tracer to identify the origin of salinity in aquifers in Spain and Portugal. *Journal of Hydrology* 359:189–207.
- Al-Charideh, A., and B. Kattaa. 2016. Isotope hydrology of deep groundwater in Syria: renewable and non-renewable groundwater and paleoclimate impact. *Hydrogeology Journal* 24:79–98.
- Algreen, M., S. Trapp, P. R. Jensen, and M. M. Broholm. 2015a. Tree coring as a complement to soil gas screening to locate PCE and TCE source zones and hot spots. *Groundwater Monitoring & Remediation* 35:57–66.
- Algreen, M., M. Kalisza, M. Stalder, E. Martac, J. Krupaneka, S. Trapp, and S. Bartkee. 2015b. Using pre-screening methods for an effective and reliable site characterization at megasites. *Environmental Science and Pollution Research* 22: 14673–14686.
- Algreen, M., S. Trapp, and A. Rein. 2014. Phytoscreening and phytoextraction of heavy metals at Danish polluted sites using willow and poplar trees. *Environmental Science and Pollution Research* 21:8992–9001.
- Algreen, M., A. Rein, C. N. Legind, C. E. Amundsen, U. G. Karlson, and S. Trapp. 2012. Test of tree core sampling for screening of toxic elements in soils from a Norwegian site. *International Journal of Phytoremediation* 14:305–319.
- Aller, Linda, T. W. Bennett, G. Hackett, R. J. Petty, J. H. Lehr, Helen Sedoris, D. M. Nielsen, and J. E. Denne. 1991. *Handbook of Suggested Practices for the Design and Installation of Ground-Water Monitoring Wells*. U.S. Environmental Protection Agency, EPA/600/4-89/034. NTIS #PB90- 159807, 221 p.
- American Society for Testing and Materials. 1983. Standard practice for thin-wall tube sampling of soils: D1587. 1986 Annual Book of American Society for Testing and Materials Standards. Philadelphia, Penn., pp. 305–307.
- American Society for Testing and Materials. 1984. Standard method for penetration test and split barrel sampling of soils: D1586. 1986 Annual Book of American Society for Testing and Materials Standards. Philadelphia, PA. pp. 298–303.
- Arnold, L. R., J. L. Flynn, and S. S. Paschke. 2009. *Design and Installation of a Groundwater Monitoring-Well Network in the High Plains Aquifer, Colorado*. U.S. Geological Survey Data Series 456, 47 p.
- Barcelona, M. J., J. P. Gibb, and R. A. Miller. 1983. *A Guide to the Selection of Materials of Monitoring Well Construction and Ground-Water Sampling*. Illinois State Water Survey, Contract Report 327, 78 pp.
- Barcelona, M. J., H. A. Wehrmann, and M. D. Varljen. 1994. Reproducible well-purging procedures and VOC stabilization criteria for ground-water sampling. *Ground Water* 32:12–22.
- Barker, J. F., G. C. Patrick, L. Lemon, and G. M. Travis. 1987. Some biases in sampling multilevel piezometers for volatile organics. *Groundwater Monitoring & Remediation* 7:48–54.
- Barth, S. 1998. Application of boron isotopes for tracing sources of anthropogenic contamination in groundwater. *Water Research* 32:685–690.
- Bassett, R. L., P. M. Buszka, G. R. Davidson, and D. Chong-Diaz. 1995. Identification of groundwater solute sources using boron isotopic composition. *Environmental Science and Technology* 29:2915–2922.
- Biswas, A., H. Neidhardt, A. K. Kundu, and H. Dipti. 2014. Spatial, vertical and temporal variation of arsenic in shallow aquifers of the Bengal Basin: Controlling geochemical processes. *Chemical Geology* 387:157–169.
- Cherry, J. A., and P. E. Johnson. 1982. A multi-level device for monitoring in fractured rock. *Groundwater Monitoring & Remediation* 2:41–44.
- Chiang, C., G. Raven, and C. Dawson. 1995. The relationship between monitoring well and aquifer solute concentrations. *Ground Water* 33:718–726.
- Christensen, N. B., and M. Halkjaer. 2014. Mapping pollution and coastal hydrogeology with helicopterborne transient electromagnetic measurements. *Exploration Geophysics* 45:243–254.
- Church, P. E., and G. E. Granato. 1996. Bias in groundwater data caused by well-bore flow in long-screen wells. *Groundwater* 34:262–273.
- Cohen, R. M., and J. W. Mercer. 1993. *DNAPL Site Evaluation*. Boca Raton, FL: CRC Press, 342 pp.
- Cook, P. G., and J. K. Böhlke. 2000. “Determining Timescales for Groundwater Flow and Solute Transport.” In *Environmental Tracers in Subsurface Hydrology*, eds. P. G. Cook and A. L. Herczeg, 1–30. Springer: New York.
- Craig, H. B. 1961. Isotopic variations in meteoric waters. *Science* 133:1702–1703.

- Dansgaard, W. 1964. Stable isotopes in precipitation. *Tellus* 16:4436–468.
- Darrah, T. H., A. Vengosh, R. B. Jackson, N. A. Warner, and R. J. Poreda. 2014. Noble gases identify the mechanisms of fugitive gas contamination in drinking-water wells overlying the Marcellus and Barnett Shales. *Proceedings of the National Academy of Sciences* 111:14076–14081.
- David, M. M., S. Cecillon, B. M. Warne, E. Prestat, J. K. Jansson, and T. M. Vogel. 2014. Microbial ecology of chlorinated solvent biodegradation. *Environmental Microbiology* 17:4835–4850.
- Davis, G. B., J. Wright, and B. M. Patterson. 2009. Field Assessment of Vapours, CRC CARE Technical Report no. 13, CRC for Contamination Assessment and Remediation of the Environment, Adelaide. Accessed November 2015 from www.crcare.com/publications/downloads/CRC-CARE-Tech-Report-13.pdf
- Davis, S. N., G. M. Thompson, H. M. Bentley, and G. Stiles. 1980. Ground-water tracers: A short review. *Ground Water* 18:14–23.
- Davis, S. N., D. O. Whittemore, J. Fabryka-Martin. 1998. Uses of chloride/bromide ratios in studies of potable water. *Ground Water* 36:338–350.
- Davis, S. N., J. Fabryka-Martin, L. E. Wolfsberg. 2004. Variations of bromide in potable ground water in the United States. *Ground Water* 42:902–909.
- Dojka, M. A., P. Hugenholtz, S. K. Haack, and N. R. Pace. 1998. Microbial diversity in a hydrocarbon and chlorinated solvent contaminated aquifer undergoing intrinsic bioremediation. *Applied and Environmental Microbiology* 64:3869–3877.
- Driscoll, F. G. 1986. *Ground Water and Wells*. St. Paul, MN: Johnson Division, 1089 pp.
- Dublyansky, Y., and C. Spötl. 2010. Evidence for a hypogene paleohydrogeological event at the prospective nuclear waste disposal site Yucca Mountain, Nevada, USA, revealed by the isotope composition of fluid-inclusion water. *Earth and Planetary Science Letters* 289:583–594.
- Dumble, P., M. Fuller, P. Beck, and P. Sojka. 2006. Assessing contaminant migration pathways and vertical gradients in a low-permeability aquifer using multilevel borehole systems. *Land Contamination & Reclamation* 14: 699–711.
- Edge, R. W., and K. Cordry. 1989. The Hydropunch: An in situ sampling tool for collecting ground water from unconsolidated sediments. *Groundwater Monitoring & Remediation* 9:177–183.
- Einarson, M. D., and J. A. Cherry. 2002. A new multilevel groundwater system using multi-channel tubing. *Ground Water Monitoring and Remediation* 22:52–65.
- Elci, A., F. Molz, and W. R. Waldrop. 2001. Implications of observed and simulated ambient flow in monitoring wells. *Ground Water* 39:853–862.
- Eppich, G. R., M. J. Singleton, S. K. Roberts, J. B. Wimpenny, E. Derubeis, J. E. Moran, B. K. Esser, and Q. Yin. 2012. *Source determination of anthropogenic NO₃ in groundwater by analysis of δ 15N, δ 18O, and δ 11B: A case study from San Diego County, California, LLNL-ABS-551872, LLNL-PRES-559675*. Fresno, CA: Groundwater Resources Association of California.
- FDEP. 2008. *Monitoring Well Design and Construction Guidance Manual*. Florida Department of Environmental Protection Bureau of Water Facilities Regulation 2008. Accessed October 2015 from <https://www.dep.state.fl.us/water/groundwater/docs/monitoring-well-manual-formatted-final.pdf>
- Folkes, D., W. Wertz, J. Kurtz, and T. Kuehster. 2009. Observed spatial and temporal distributions of CVOCs at Colorado and New York vapor intrusion sites. *Ground Water Monitoring & Remediation* 29:70–80.
- Gibb, J. P., R. M. Schuller, and R. A. Griffin. 1981. *Procedures for the Collection of Representative Water Quality Data from Monitoring Wells*. Illinois State Geological Survey and Illinois State Water Survey Cooperative Report 7, 61 p.
- Giddings, C. G. S., L. K. Jennings, and J. M. Gossett. 2010. Microcosm assessment of DNA probe applied to aerobic degradation of cis-1,2 Dichlorethane by Poaromonas sp. strain JS666. *Ground Water Monitoring & Remediation* 30:97–105.
- Gilbert, R. O., and R. R. Kinnison. 1981. Statistical methods of estimating the mean and variance from radionuclide data sets containing negative, unreported or less than values. *Health Physics* 40:377–390.
- Gumm, L. P., V. F. Bense, P. F. Dennis, K. M. Hiscock, N. Cremer, and S. Simon. 2016. Dissolved noble gases and stable isotopes as tracers of preferential fluid flow along faults in the Lower Rhine Embayment, Germany. *Hydrogeology Journal* 24:99–108.

- Hackett, G. 1987. Drilling and constructing monitoring wells with hollow-stem augers—Part I: Drilling considerations. *Groundwater Monitoring & Remediation* 7:51–62.
- Hackett, G. 1988. Drilling and constructing monitoring wells with hollow-stem augers—Part II: Monitoring well installation. *Groundwater Monitoring & Remediation* 8:60–68.
- Heilweil, V. M., P. L. Grieve, S. A. Hynek, S. L. Brantley, D. K. Salomon, and D. W. Risser. 2015. Stream measurements locate thermogenic methane fluxes in groundwater discharge in an area of shale-gas development. *Environmental Science & Technology* 49:4057–4065.
- Hendry, M. J., S. L. Barbour, K. Novakowski, and L. I. Wassenaar. 2013. Paleohydrogeology of the Cretaceous sediments of the Williston Basin using stable isotopes of water. *Water Resources Research* 49:4580–4592.
- Hendry, M. J., D. K. Solomon, M. Person, L. I. Wassenaar, W. P. Gardner, I. D. Clark, K. U. Mayer, T. Kumimaru, K. Nakata, and T. Hasegawa. 2015. Can argillaceous formations isolate nuclear waste? Insights from isotopic, noble gas, and geochemical profiles. *Geofluids* 15:381–386.
- Hester, R. E., and R. M. Harrison. 2008. *Environmental Forensics*. Cambridge, England: Royal Society of Chemistry Publishing.
- Hughes, E., and G. Aarons. 2014. *Well Design and Construction for Monitoring Groundwater at Contaminated Sites*. The California Environmental Protection Agency. Accessed October 2014 from https://www.dtsc.ca.gov/PublicationsForms/upload/Well_Design_Constr_for_Monitoring_GWContam_Sites1.pdf
- Humez, P., B. Mayer, M. Nightingale, J. Ing, V. Becker, D. Jones, and V. Lam. 2016. An 8-year record of gas geochemistry and isotopic composition of methane during baseline sampling at a groundwater observation well in Alberta (Canada). *Hydrogeology Journal* 24:109–122.
- Ingraham, N., K. Zukosky, and D.K. Kremer. 2001. The application of stable isotopes to identify problems in large-scale water transfer in Grand Canyon National Park. *Environmental Science and Technology* 35:1299–1302.
- ITRC. 2005. “Technology overview of passive sampler technologies. DSP-4.” Interstate Technology & Regulatory Council, Authoring Team.
- ITRC. 2007. “Vapour intrusion pathway: A practical guideline, Technical Regulatory Guidance.” Interstate Technology & Regulatory Council, Vapour Intrusion Team. Accessed November 2015 from www.itrcweb.org/guidancedocument.asp?TID=49
- Iverach, C. P., D. I. Cendon, S. I. Hankin, D. Lowry, R. E. Fisher, J. L. France, E. G. Nisbet, A. Baker, and B. F. J. Kelly. 2015. Assessing connectivity between an overlying aquifer and a coal seam gas resource using methane isotopes, dissolved organic carbon and tritium. *Scientific Reports* 5:DOI: 10.1038/srep15996.
- Jackson, R. B., A. Vengosh, T. Darrah, N. R. Warner, A. Down, R. J. Poreda, S. G. Osborn, K. Zhao, and J. D. Karr. 2013. Increased stray gas abundance in a subset of drinking water wells near Marcellus shale gas extraction. *Proceedings of the National Academy of Sciences USA* 110:11250–11255.
- Johannesson, K. H., K. J. Stetzenbach, V. F. Hodge, D. K. Kremer, and X. Zhou. 1997. Delineation of groundwater flow systems in the southern Great Basin using aqueous rare earth element distributions. *Ground Water* 35:807–819.
- Katz, B. G., S. M. Eberts, and L. J. Kauffman. 2011. Using Cl/Br ratios and other indicators to assess potential impacts on groundwater quality from septic systems: A review and examples from principal aquifers in the United States. *Journal of Hydrology* 397:151–166.
- Kearl, P. M., N. E. Korte, and T. A. Cronk. 1992. Suggested modifications to ground water sampling procedures based on observations from the colloidal borescope. *Groundwater Monitoring & Remediation* 12:155–161.
- Kearl, P. M., N. E. Korte, M. Stites, and J. Baker. 1994. Field comparison of micropurging vs. traditional ground water sampling. *Ground Water Monitoring and Remediation* 14:183–190.
- Keeley, J. F., and K. Boateng. 1987. Monitoring well installation, purging and sampling techniques—Part I: Conceptualizations. *Ground Water* 23:300–313.
- Kenkel, J. R. 2008. *Advances in Rock Core VOC Analyses for High Resolution Characterization of Chlorinated Solvent Contamination in a Dolostone Aquifer*. Master's thesis, Department of Earth & Environmental Sciences, University of Waterloo, Waterloo, ON.
- Kerfoot, H. B., and C. L. Meyer. 1986. The use of industrial hygiene samplers for soil-gas surveying. *Groundwater Monitoring & Remediation* 6:88–93.

- Kirkegaard, C., T. O. Sonnenborg, E. Auken, and F. Jorgensen. 2011. Salinity distribution in heterogeneous coastal aquifers mapped by airborne electromagnetics. *Vadose Zone Journal* 10:125–135.
- Knopp, D., M. Seifert, V. Väänänen, and R. Niessner. 2000. Determination of polycyclic aromatic hydrocarbons in contaminated water and soil samples by immunological and chromatographic methods. *Environmental Science & Technology* 34:2035–2204.
- Kreamer, D. K., V. F. Hodge, I. Rabinowitz, K. H. Johannesson, and K. J. Stetzenbach. 1996. Trace elements geochemistry in waters from selected springs in Death Valley National Park, California. *Ground Water* 34:95–103.
- Kreamer, D. K., E. P. Weeks, and G. M. Thompson. 1988. A field technique to measure the tortuosity and sorption-affected porosity for gaseous diffusion of materials in the unsaturated zone with experimental results from near Barnwell, South Carolina. *Water Resources Research* 24:331–341.
- Larsen, M., J. Burken, J. Machackova, U. G. Karlson, and S. Trapp. 2008. Using tree core samples to monitor natural attenuation and plume distribution after a PCE spill. *Environmental Science & Technology* 42:1711–1717.
- Leaf, A. T., D. J. Hart, and J. M. Bahr. 2012. Active thermal tracer tests for improved hydrostratigraphic characterization. *Ground Water* 50:726–735.
- Li, X., H. Masuda, M. Kusakabe, E. Yanagisawa, and H. Zeng. 2006. Degradation of groundwater quality due to anthropogenic sulfur and nitrogen contamination in the Sichuan Basin, China. *Geochemical Journal* 40:309–332.
- Limmer, M. A., J. C. Balouet, F. Karg, D. A. Vroblesky, and J. G. Burken. 2011. Phyto-screening for chlorinated solvents using rapid in vitro SPME sampling: Application to urban plume in Verl, Germany. *Environmental Science & Technology* 45:8276–8282.
- Magill, M. 2009. *Geoelectrical Response of Surfactant Solutions in a quartzitic sand analog aquifer*. Master's thesis. Department of Geosciences, University of Nevada, Las Vegas. 177p.
- Marrin, D. L. 1988. Soil-gas sampling and misinterpretation. *Groundwater Monitoring & Remediation* 8:51–54.
- McKay, L. D., W. E. Sanford, and J. M. Strong. 2000. Field-scale migration of colloidal tracers in a fractured shale saprolite. *Ground Water* 38:139–147.
- McMillan, L. A., M. O. Rivett, J. H. Tellam, P. Dumble, and H. Sharp. 2014. Influence of vertical flows in wells on groundwater sampling. *Journal of Contaminant Hydrology* 169:50–61.
- Mercer, J. W., and R. M. Cohen. 1990. A review of immiscible fluids in the subsurface: properties, models, characterization and remediation. *Journal of Contaminant Hydrology* 6:107–163.
- Mickam, J. T., R. Bellandi, and E. C. Tiffet, Jr. 1989. Equipment decontamination procedures for ground water and vadose zone monitoring programs: Status and prospects. *Groundwater Monitoring & Remediation* 9:100–121.
- Mines, B. S., J. L. Davidson, D. Bloomquist, and T. B. Stauffer. 1993. Sampling of VOCs with BAT ground water sampling system. *Ground Water Monitoring and Remediation* 13:115–120.
- Motzer, W. E. 2001. Perchlorate: Problems, detection, and solutions. *Environmental Forensics* 2:301–311.
- Morrison, R. D., and B. L. Murphy. 2006. *Environmental Forensics*. Burlington, MA: Academic Press, 576 p.
- National Sanitation Foundation. 1988. *National Sanitation Foundation Standard 14*. Ann Arbor, MI, 65 p.
- Nielsen, D. M. 1988. Much ado about nothing: The monitoring well construction materials controversy. *Groundwater Monitoring & Remediation* 8:4–5.
- Nielsen, D. M. 2005. *Practical Handbook of Environmental Site Characterization and Ground-Water Monitoring*, 2nd ed. Boca Raton, FL: CRC Press.
- Nielsen, D. M., and G. L. Yeates. 1985. A comparison of sampling mechanisms available for small-diameter ground-water monitoring wells. *Groundwater Monitoring & Remediation* 5:83–99.
- NSW. 2010. *Vapour Intrusion: Technical Practice Note*. Sydney, Australia: Department of Environment, Climate Change and Water. Accessed November 2015 from <http://www.epa.nsw.gov.au/resources/clm/10774vapourintr.pdf>
- NUDLC. 2012. *Minimum Construction Requirements for Water Bores in Australia*, 3rd ed. National Uniform Drillers Licensing Committee.
- Obiadi, I. I., A. G. Onwuemesi, O. L. Anike, C. M. Obiadi, N. E. Ajaegwu, E. K. Anakwuba, E. O. Akpunonu, and E. O. Ezim. 2012.

- Imaging subsurface fracture characteristics using 2D electrical resistivity tomography. *International Research Journal of Engineering Science, Technology and Innovation* 1:103–110. Available online at <http://www.interesjournals.org/IRJESTI>
- Olchawa, A., and M. Kumor. 2008. Time Domain Reflectometry (TDR)—measuring dielectric constant of polluted soil to estimate diesel oil content. *Archives of Hydro-Engineering and Environmental Mechanics* 55:55–62.
- Olhoeft, G. R. 1992. *Geophysics advisor expert system version 2.0*. U.S. Geological Survey Open-File Report 92-526-A. Accessed October 2015 from <http://pubs.er.usgs.gov/publication/ofr92526A?currow=466>
- Orchard, B. J., W. J. Doucette, and J. K. Chard, B. Bugbee. 2000. Uptake of trichloroethylene by hybrid poplar trees grown hydroponically in flow-through plant growth chambers. *Environmental Toxicology and Chemistry* 19:895–903.
- Osborn, S. G., A. Vengosh, N. R. Warner, and R. B. Jackson. 2011. Methane contamination of drinking water accompanying gas-well drilling and hydraulic fracturing. *Proceedings of the National Academy of Sciences USA* 108:8172–8176.
- Papiernik, T. D., S. K. Widmer, and R. F. Spalding. 1996. Effect of various materials in multilevel samplers on monitoring commonly occurring agrichemicals in ground water. *Groundwater Monitoring & Remediation* 16:80–84.
- Parker, B. L., D. B. McWhorter, and J. A. Cherry. 1997. Diffusive loss of non-aqueous phase organic solvents from idealized fracture networks in geologic media. *Ground Water* 35:1077–1088.
- Parker, B. L., S. W. Chapman, and J. A. Cherry. 2010. Plume persistence in fractured sedimentary rock after source zone removal. *Ground Water* 48:1–5.
- Parker, B. L., J. A. Cherry, and S. W. Chapman. 2012. Discrete fracture network approach for studying contamination in fractured rock. *AQUA mundi Am*06052:101–116.
- Parker, B. L., A. A. Pierce, M. Einarson, R. Ingleton, T. Gorecki, M. O. Bower, and E. VanderVelde. 2015. Versatile completions for bedrock vadose zone VOC gas sampling. Paper presented at the International Association of Hydrogeologists, Canadian National Chapter Conference, October 27–30, 2015, Waterloo, Canada.
- Parker, L. V. 1994. The effects of ground-water sampling devices on water quality: A literature review. *Ground Water Monitoring and Remediation* 14:130–141.
- Parker, L. V. 1996. Sampling trace-level organics with polymeric tubings. U. S. Army Corps of Engineers. Cold Regions Research and Engineering Laboratory. Special Report 96–3.
- Parker, L. V., A. D. Hewitt, and T. F. Jenkins. 1990. Influence of casing materials on trace-level chemicals in ground water. *Groundwater Monitoring & Remediation* 10:146–156.
- Parker, L. V., and T. A. Ranney. 1994. Effect of concentration on sorption of dissolved organics by PVC, PTFE and stainless steel well casings. *Groundwater Monitoring & Remediation* 14:139–149.
- Parker, L. V., and T. A. Ranney. 1997. Sampling trace-level organics with polymeric tubings: Part I, static studies. *Ground Water Monitoring & Remediation* 17:115–124.
- Paul, C. J., and R. W. Puls. 1997. Impact of turbidity on TCE and degradation products in ground water. *Ground Water Monitoring and Remediation* 17:128–133.
- Payne, F. C., J. A. Quinnan, and S. T. Potter. 2008. *Remediation Hydraulics*. Boca Raton, FL: CRC Press.
- Pearsall, K., and D. A. V. Eckhart. 1987. Effects of selected sampling equipment and procedures on the concentrations of trichloroethylene and related compounds in ground water samples. *Groundwater Monitoring & Remediation* 7:64–73.
- Pellerin, L., L. P. Beard, and W. Mandell. 2010. Mapping structures that control contaminant migration using helicopter transient electromagnetic data. *Journal of Environmental and Engineering Geophysics* 15:65–75.
- Personna, Y. R., L. Slater, D. Ntarlagiannis, D. Werkema, and Z. Szabo. 2013. Electrical signatures of ethanol-liquid mixtures: Implications for monitoring biofuels migration in the subsurface. *Journal of Contaminant Hydrology* 144:99–107.
- Pickens, J. F., J. A. Cherry, G. E. Grisak, W. F. Merritt, and B. A. Risto. 1978. A multilevel device for groundwater sampling and piezometric monitoring. *Ground Water* 16:322–327.
- Pickens, J. F., J. A. Cherry, R. M. Coupland, G. E. Grisak, W. F. Merritt, B. A. Risto. 1981. A multilevel device for ground-water sampling. *Groundwater Monitoring & Remediation* 1:48–51.

- Pierce, A. A., B. L. Parker, J. A. Cherry, S. Chapman, C. Kennedy, and R. Ingleton. 2015. Bedrock groundwater monitoring created using portable drills for remote and ecosensitive areas. Paper presented at the International Association of Hydrogeologists, Canadian National Chapter Conference, October 27–30, 2015, Waterloo, Canada.
- Pohlmann, K. F., and J. W. Hess. 1988. Generalized groundwater sampling-device matrix. *Groundwater Monitoring & Remediation* 8:82–84.
- Powell, R. M. and R. W. Puls. 1993. Passive sampling of ground-water monitoring wells without purging: multilevel well chemistry and tracer disappearance. *Journal of Contaminant Hydrogeology* 12:51–77.
- Puls, R. W. and C. J. Paul. 1995. Low-flow purging and sampling of ground-water monitoring wells with dedicated systems. *Ground Water Monitoring and Remediation* 15, no. 1:116–123.
- Puls, R. W. and R. M. Powell. 1992. Acquisition of representative ground-water quality samples for metals. *Groundwater Monitoring & Remediation* 12:167–176.
- Rahm, B. G., S. Chauhan, V. F. Holmes, T. W. Macbeth, K. S. Sorenson, and L. Alvarez-Cohen. 2006. Molecular characterization of microbial populations at two sites with differing reductive dechlorination abilities. *Biodegradation* 17:523–534.
- Ranney, T. A. and L. V. Parker. 1997. Comparison of fiberglass and other polymeric well casings. Part I: Susceptibility to degradation by chemicals. *Ground Water Monitoring and Remediation* 17, no. 1:97–103.
- Reilly, T. E., O. L. Franke, and G. D. Bennett. 1989. Bias in groundwater samples caused by wellbore flow. ASCE. *Journal of Hydraulic Engineering* 115:270–276.
- Reynolds, G. W., and R. W. Gillham. 1985. "Absorption of halogenated organic compounds by polymer materials commonly used in ground-water monitors." In *Proceedings of the Second Canadian/ American Conference on Hydrogeology*, 125–32. Banff, Alberta, Canada: National Water Well Association.
- Riha, B., J. Rossabi, C. Eddy-Dilek, D. Jackson, and C. Keller. 2000. DNAPL Characterization Using the Ribbon NAPL Sampler: Methods and Results. Accessed October 2015 from <http://sti.srs.gov/fulltext/ms2000182/ms2000182.html>
- Robbins, G. A., B. G. Deyo, M. R. Temple, J. D. Stuart, and M. J. Lacy. 1990. Soil-gas surveying for subsurface gasoline contamination using total organic vapor detection instruments—Part 1: Theory and laboratory experimentation. *Groundwater Monitoring & Remediation* 10:122–131.
- Robbins, G. A., B. G. Deyo, M. R. Temple, J. D. Stuart, and M. J. Lacy. 1990. Soil-gas surveying for subsurface gasoline contamination using total organic vapor detection instruments—Part 2: Field experimentation. *Groundwater Monitoring & Remediation* 10:110–117.
- Ronen, D., M. Magaritz, and I. Levy. 1986. A multi-level Sampler for the study of detailed hydrochemical profiles in groundwater. *Water Resources Research* 20: 311–315.
- Schalla, R., and R. W. Landick. 1986. A new valved and airvented surge plunger for developing small-diameter monitor wells. *Groundwater Monitoring & Remediation* 6:77–80.
- Schilling, K. E. 1995. Low-flow purging reduces management of contaminated groundwater. *Environmental Protection* 6, no. 12:24–26.
- Senn, R. B., and M. S. Johnson. 1987. Interpretation of gas chromatographic data in subsurface hydrocarbon investigations. *Groundwater Monitoring and Remediation* 7:58–63.
- Silvestri, S., A. Viezzoli, A. Edsen, E. Auken, and M. Giada. 2009. L'uso del telerilevamento satellitare e da elicottero per l'identificazione di discariche abusive e siti contaminati. Sardinia 2009 Proceedings of the International Waste Working Group. Accessed December 2015 from <https://www.tuhh.de/iue/iwwg/publications/conference-proceedings/sardinia-2009.html>
- Smith, R. L., R. W. Harvey, J. H. Duff, and D. R. LeBlanc. 1987. *Importance of close-interval vertical sampling in delineating chemical and microbiological gradients in ground-water studies*. USGS Open File Report 87-109, B33–B35 pp.
- Sorek, A., N. Atzman, O. Dahan, Z. Gerstl, L. Kushisin, Y. Laor, U. Mingelgrin, A. Nasser, D. Ronen, L. Tsechansky, N. Weisbrod, and E. R. Gruber. 2008. "Phytoscreening": The use of trees for discovering subsurface contamination by VOCs. *Environmental Science & Technology* 42, no. 2:536–542.
- Stefanov, D., K. Georgieva, K. Ananieva, S. Doncheva, I. Mitova, and N. Dinev. 2012. Rapid screening of soil contamination by using tomato plants as bioindicators. A pulse amplitude modulation fluorescence study. *Comptes rendus de l'Académie bulgare des sciences* 65, no. 10:1461–1466.

- Stetzenbach, K. J., M. Amano, D. K. Kremer, and V. F. Hodge. 1994. Testing the limits of ICP-MS: Determination of trace elements in ground water at the parts-per-trillion level. *Ground Water* 32:976–985.
- Suthersan, S., C. Divine, E. Cohen, and K. Heinze. 2014. Advances in in situ remediation. Tracer Testing: Recommended best practice for design and optimization of in situ remediation systems. *Ground Water Monitoring and Remediation* 34:33–40.
- Swartz, C. H., S. Reddy, M. J. Benotti, H. Yin, L. B. Barber, B. J. Brownawell, and R. A. Rudel. 2006. Steroid estrogens, nonylphenol ethoxylate metabolites, and other wastewater contaminants in groundwater affected by a residential septic system on Cape Cod, MA. *Environmental Science & Technology* 40:4894–4902.
- Tai, D. Y., K. S. Turner, and L. A. Garcia. 1991. The use of a standpipe to evaluate ground water samplers. *Groundwater Monitoring & Remediation* 11:125–132.
- Thompson, G., and D. Marrin. 1987. Soil gas contaminant investigations: A dynamic approach. *Groundwater Monitoring & Remediation* 7:88–93.
- Thompson, G. M., and J. M. Hayes. 1979. Trichlorofluoromethane in groundwater—A possible tracer and indicator of groundwater age. *Water Resources Research* 15:546–554.
- USDOE. 2015. “Applied Studies and Technology: The Third Dimension—Variation in Groundwater Aquifers.” U.S. Department of Energy, Office of Legacy Management, October 12, 2015. Accessed November 2015 from <http://energy.gov/lm/articles/applied-studies-and-technology-third-dimension-variation-groundwater-aquifers>
- USEPA. 2002. “OSWER Draft Guidance for Evaluating the Vapour Intrusion to Indoor Air Pathway from Groundwater and Soils (subsurface vapour intrusion guidance).” November, EPA530-D-02-004, Office of Solid Waste and Emergency Response, US Environmental Protection Agency. Accessed November 2015 from www.epa.gov/osw/hazard/correctiveaction/eis/vapor/complete.pdf
- USEPA. 2004. “Site Characterization Technologies for DNAPL Investigations.” U.S. Environmental Protection Agency, Office of Solid Waste and Emergency Response (5102G), EPA 542-R-04-017, 105 pp. Accessed October 2015 from <https://clu-in.org/download/char/542r04017.pdf>
- USEPA. 2012. “Guidelines for Using Passive Samplers to Monitor Organic Contaminants at Superfund Sediment Sites.” OSWER Directive 9200.1-110 FS, December 2012, 32 p. U.S. Environmental Protection Agency, Office of Solid Waste and Emergency Response.
- Vengosh, A. 1998. The isotopic composition of anthropogenic boron and its potential impact on the environment. *Biological Trace Element Research* 66:145–151.
- Vengosh, A., S. Hening, J. Ganor, B. Mayer, C. E. Weyhenmeyer, T. D. Bullen, and A. Paytan. 2007. New isotopic evidence for the origin of groundwater from the Nubian Sandstone Aquifer in the Negev, Israel. *Applied Geochemistry* 22:1052–1073.
- Vroblesky, D. A., C. T. Nietch, and J. T. Morris. 1999. Chlorinated ethenes from groundwater in tree trunks. *Environmental Science and Technology* 33:510–515.
- Vroblesky, D. A., B. D. Clinton, J. M. Vose, C. C. Casey, G. J. Harvey, and P. M. Bradley. 2004. Ground water chlorinated Ethenes in tree trunks: Case studies, influeunce of recharge, and potential degradation mechanism. *Ground Water Monitoring and Remediation* 24:124–138.
- Wallingford, E. D., F. A. DiGiano, and C. T. Miller. 1988. Evaluation of a carbon absorption method for sampling gasoline vapors in the subsurface. *Groundwater Monitoring & Remediation* 8:85–92.
- Wang, Z., M. Fingas, C. Yang, and J. H. Christensen. 2006. “Crude Oil and Refined Product Fingerprinting: Principles.” In *Environmental Forensics*, eds. R. D. Morrison and B. L. Murphy, 409–461. Burlington, MA: Academic Press.
- Weeks, E. P., D. E. Earp, G. M. Thompson. 1982. Use of atmospheric fluorocarbons F-11 and F-12 to determine the diffusion parameters of the unsaturated zone in the southern high plains of Texas. *Water Resources Research* 18:1365–1378.
- Wilson, L. G. 1990. “Methods for sampling fluids in the vadose zone.” In *Groundwater and Vadose Zone Monitoring*, eds. D. M. Nielsen and A. I. Johnson, 7–24. Philadelphia, PA: American Society for Testing and Materials.
- Wilson, L. G. 1991. Characterization and Modeling of the Vadose Zone. Lecture Notes. University of Arizona.
- Wilson, J., R. Bartz, M. Limmer, and B. Burken. 2013. Plants as bio-indicators of subsurface conditions: Impact of groundwater level on Btex concentrations in trees. *International Journal of Phytoremediation* 5, no. 3:257–267.

- Xie, Y., P. G. Cook, M. Shanafield, C. T. Simmons, and C. Zheng. 2016. Uncertainty of natural tracer methods for quantifying river-aquifer interaction in a large river. *Journal of Hydrology* 535:135–147.
- Yeskis, D., K. Chiu, S. Meyers, J. Weiss., and T. Bloom. 1988. “A field study of various sampling devices and their effect on volatile organic compounds.” Proceedings, Second National Outdoor Action Conference on Aquifer Restoration, Groundwater Monitoring and Geophysical Methods, 471–479. Dublin, OH: National Water Well Association.
- Zemo, D. A., T. A. Delfino, J. A. Gallinatti, V. A. Baker, and L. R. Hilpert. 1995. Field comparison of results from discrete-depth groundwater samplers. *Ground Water Monitoring and Remediation* 15:133–141.
- Zhang, W., X. Tang, N. Weisbrod, P. Zhao, and B. J. Reid. 2015. A coupled field study of subsurface fracture flow and colloid transport. *Journal of Hydrology* 524:476–488
- Zhao, Y. 2015. The use of nanoparticles to assess subsurface flow heterogeneity. Ph.D. Dissertation. Cornell University.

Problem

- 8.1** A basic initial mass balance of a contaminant at a site can be instructive in directing monitoring and remediation.

Let’s assume a hypothetical site where there has been a 20,000 L spill of gasoline (petrol) on land surface with a water table 5 m below ground surface. The soil is a homogeneous, medium sand with a retention capacity of 30 L/m³ and the fuel spill spreads out onto the land surface in a circular pool with 6 m diameter. Assuming no volatilization, no dissolution of the fuel into water, no biodegradation, and no preferential flow paths (that is, no wetting front instabilities or funneling) as the leak moves directly downward in a cylindrical shape:

- a. How much fuel will be trapped in the vadose zone?
- b. How much fuel will reach the vicinity of the water table?
- c. What would be the next steps in refining your mass balance at the site to understand the distribution of contamination?

Site Remediation

■ 9.1 Introduction

Since the early 1980s groundwater scientists and engineers have developed a number of techniques for both containing and remediating soil and groundwater contamination. In the United States this has been driven by federal legislation including the Resource and Conservation and Recovery Act (RCRA) and the Comprehensive Environmental Response, Compensation and Liability Act (CERCLA). The Hazardous and Solid Waste Amendments of RCRA address the storage of liquids in underground tanks. Individual states have also passed environmental regulations that may be triggered when property is sold. Regulations associated with these laws dictate when it is necessary to evaluate if a site is contaminated, and if it is, what must be done to remediate the contaminated soil and groundwater. Even in the absence of a specific regulatory requirement, many potential property buyers will require the seller to demonstrate that a property is not contaminated. This may take the form of a Phase I Environmental Study, which involves a detailed review of the historical uses of the property and a review of state records to determine if there is a likelihood of a potentially contaminating activity in the past. This may be followed by a Phase II Environmental Study, where several soil borings are drilled and one or more groundwater monitoring wells are installed. These investigations are for the protection of the buyer and the financing institution because if the property is found to be contaminated after purchase, the new owner would be responsible for some or all of the cleanup costs (Phase III).

In general, remediation of a site must address two issues. If there is an ongoing source of contamination, control of the source will be necessary. There is no point in remediating the environment if new contamination is being released to the soil or groundwater. Examples of sources include landfills, mine tailings piles, leaking underground storage tanks, pipelines, septic tanks, and sewer lines. In addition to primary sources, such as those listed above, there can be secondary sources of contamination due to contaminants which have already been released to the environment. These secondary sources include nonaqueous phase liquids (NAPLS) which may be trapped in the vadose zone, floating on the water table or trapped below the water table. Once the primary source has been removed or isolated, then secondary sources must be identified and isolated. Only after that has occurred is treatment of contaminated soil and groundwater effective.

The final goal of a remediation program for contaminated soils and groundwater is generally subject to approval of a state or federal regulatory agency. In almost all

cases it will be impossible to completely remove all contamination so that the site returns to a pristine condition. After all, many contaminated sites have been the locus of industrial activities for decades; indeed, some sites in the eastern United States or in Europe have been used by one industry or another for centuries. In the United States of America, state agencies or the U.S. Environmental Protection Agency may have numerical standards for the soil and groundwater that must be met after site remediation. Similarly, in the European Union, the European Environment Agency (EEA) works together with national agencies on defining what are “good” and “poor” quality water bodies (Water Framework Directive 2000/60/EC of the European Parliament and of the Council). Many other countries have modeled their environmental standards on EPA or European regulations. These standards are generally based on anticipated future land use. Soil remediation standards for future residential land use will be more stringent than those for industrial use. Groundwater standards may be based on drinking water Maximum Contaminant Levels (MCLs).

The application of very stringent standards may result in the expenditure of large amounts of money to reduce extremely small or even nonexistent risks (Viscusi and Hamilton 1996). As much as everyone would like to live in a pristine environment, it simply is not practicable in the post-industrial world. There are limited funds available for environmental cleanup; we should expend those funds in a manner that is most effective in terms of reducing real risks. This has led to the concept of risk based corrective actions (RBCA). Rather than cleaning up all sites to a set standard, a risk assessment of the site is made, and risks to specific receptors are addressed. For example, if the groundwater is saline and not used as a drinking-water source, it may not be really necessary to remove a chlorinated solvent to the drinking-water standard.

Contaminant hydrogeologists in collaboration with engineers, chemists, biologists, modelers, and many other experts have developed some very powerful methods of removing contamination from soil and groundwater. However, these methods are not capable of totally removing all contamination. A zero contamination strategy is not possible, even if we were willing to commit unlimited funds.

In this chapter we will examine a number of source zone and groundwater plume remedial techniques, some proven and some experimental. Table 1 provides an overview of some of the most common technologies and their applicability and development status. There are a few textbooks (e.g., Suthersan et al. 2017) and a number of public domain resources that can guide us in the discussion of these remediation technologies. For instance, the Interstate Technology and Regulatory Council (ITRC) makes available documents ranging from technical overviews and case studies of innovative remediation technologies to technical and regulatory guidance documents for applying cleanup technologies (www.itrcweb.org/guidance). Similarly, the Federal Remediation Technologies Roundtable (FRTR) provides access to a remediation technology screening matrix for screening potentially applicable technologies for a remediation project, including a long list of technology descriptions (www.frtr.gov/scrntools.htm). The National Academies of Sciences, Engineering, and Medicine—National Research Council (NRC) publishes periodic reports on the state-of-the-art in the remediation of contaminated sites (<http://www.nap.edu/topic>). The Strategic Environmental Research and Development Program (SERDP) is an environmental science and technology program, planned and executed by the U.S. Department

TABLE 9.1 Common and innovative contaminant remediation technologies.

Technology	Application	Development Status
Pump-and-Treat (P&T)	(Source Zone) / Plume / Containment	Established
Physical Containment	Source Zone / Plume	Established
Solidification/Stabilization	Source Zone	Established
Soil Vapor Extraction / Air Sparging	Unsaturated Zone; Source Zone / Plume	Established
Bioremediation and Monitored Natural Attenuation (MNA)	Source Zone / Plume	Innovative / Established
Permeable Reactive Barrier	Source Zone / Plume	Innovative / Established
Chemically Enhanced Flushing	Source Zone	Established
Thermal Treatment	Source Zone / Unsaturated Zone	Innovative / Established
In Situ Oxidation	Source Zone / Plume	Innovative / Established
Phytoremediation	Plume / Unsaturated Zone / Containment	Innovative / Established

Note: The boundary between what is a conventional and innovative technology is fluid.

Source: Modified after NRC 2013.

of Defense (DOD), Department of Energy, and the EPA and others. Together with another U.S. DOD program, the Environmental Security Technology Certification Program (ESTCP), these programs support the development and demonstration of the latest remediation technologies. They also provide access to documents describing innovative, cost-effective, and sustainable environmental cleanup solutions, including for the treatment of DNAPL source zones or groundwater plumes (www.serdp-estcp.org). Funded by the European Union, the EUGRIS (European Groundwater and Contaminated Land Remediation Information System) is an openly available information platform for contaminated land and groundwater information (www.eugris.info/index.asp). While there are many more resources available to students as well as practitioners, one of the largest depositories of information about contaminated site characterization and remediation technologies is maintained by the U.S. EPA (www.clu-in.org). Currently, the website includes information on several hundred field-scale remediation technology demonstration projects.

■ 9.2 Source-Control Measures

9.2.1 Solid Waste

Solid waste may have been buried in an unsecure landfill, placed in an open excavation or old quarry, or simply spread on the land surface. If contaminants continue to be leached from these sources by infiltrating precipitation, or even groundwater if the solid wastes have been buried below the water table, then a source-control measure

is necessary before groundwater remediation is attempted. If the source continues to leach contaminants, then groundwater remediation may be futile.

Source-control measures include physical removal of the waste and transportation to a secure landfill or incinerator, construction of impermeable covers or low-permeability caps to eliminate or minimize infiltration of precipitation, and construction of physical barriers around the waste source.

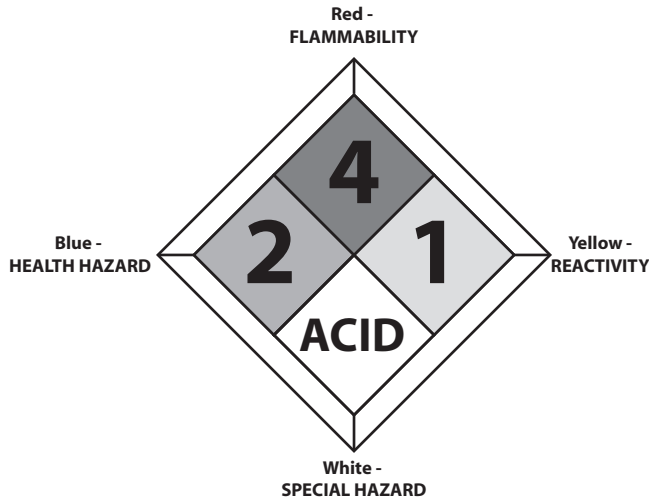
9.2.2 Removal and Disposal

If the source is removed, then wastes can no longer migrate from it. Solid waste that has been spread on the land surface can easily be removed by conventional earthmoving equipment. Waste that has been buried in a landfill can also be exhumed and transported to a secure landfill. A hazardous-waste landfill was operated near Wilsonville, Illinois, USA, from 1976 to 1981. Hazardous wastes, including liquids, were buried in drums that were placed in 26 trenches, each approximately 3.3 m to 6.5 m (10 to 20 ft) deep, 15 to 30 m (50 to 100 ft) wide, and 53 m to 122 m (175 to 400 ft) long. In 1981, it was found that hazardous wastes had migrated up to 16.7 m (50 ft) from the trenches over a 3-year period, a rate 100 to 1000 times greater than predicted prior to construction of the landfill. Following a court order, the site owner exhumed and removed all the drums and transported them to a more secure landfill. The process took 4 years and many millions of dollars (Herzog et al. 1989).

Excavation and removal of hazardous materials must be done in a manner that protects the health and safety of workers and the public. The materials may be hazardous if one comes into contact with them, they give off toxic or dangerous vapors, or if ingestion of these materials would be harmful. The risk of moving material as opposed to leaving it in place must always be evaluated prior to a removal action.

Furthermore, the final disposition must be environmentally sound. In at least one case, spent solvents were moved from an abandoned hazardous-waste site to a solvent-recycling facility. The latter facility eventually went bankrupt and became a hazardous-waste site itself. Under CERCLA, the courts have found that the generator of hazardous wastes is responsible for their cleanup and disposal costs if the disposal-site operator becomes bankrupt. In this case, the generator had to pay twice for the disposal of wastes. This policy is known as “cradle-to-grave” and is designed to ensure that hazardous waste is controlled from the time it is generated until its ultimate disposal. The EPA defines hazardous waste as “waste with properties that make it dangerous or potentially harmful to human health or the environment” (U.S. EPA 2016). In regulatory terms, an RCRA hazardous waste falls into two categories: (1) waste specifically listed by EPA and (2) characteristic waste which exhibits one or more of the following: ignitability, corrosivity, reactivity, or toxicity. These four waste characteristics are communicated in many different ways, including Material Safety Data Sheets (MSDS) or by hazard labels. For instance, the NFPA 704 chemical hazard label standard uses a diamond-shaped diagram of symbols and numbers to indicate the degree of hazard associated with a particular chemical or material (Figure 9.1). You probably have seen this or similar signs posted in laboratories or other places where potentially hazardous materials are being stored. In any given state, the EPA or the state hazardous waste regulatory agency enforces hazardous waste laws and most universities have hazardous waste offices to ensure compliance with those laws.

FIGURE 9.1 The NFPA 704 chemical hazard label. Each quadrant is labeled with its respective color and hazard.



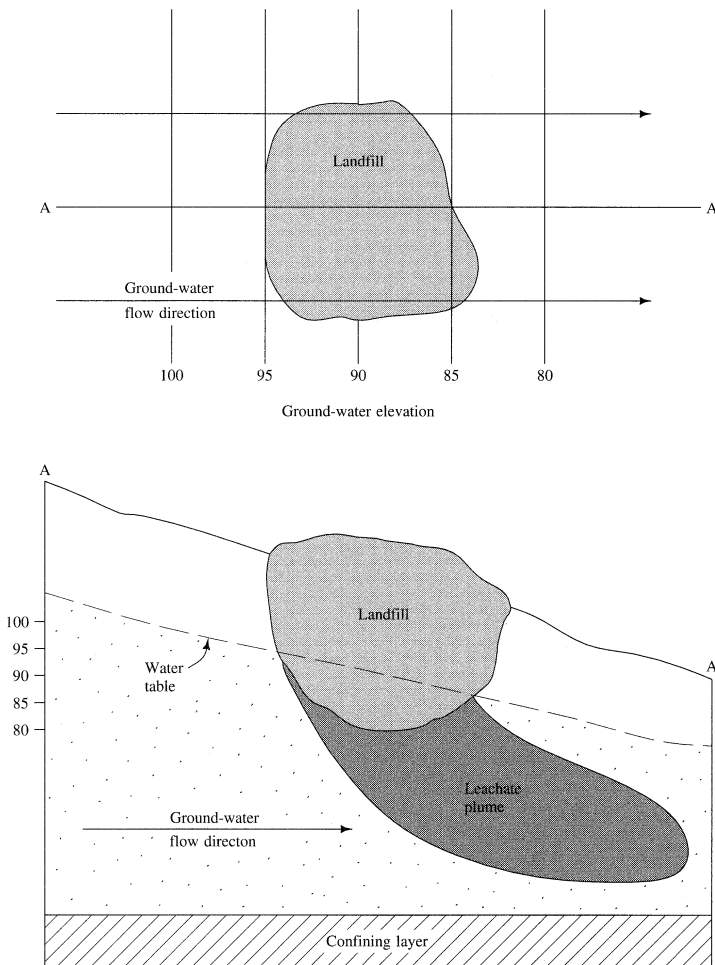
Soil contaminated with organic compounds may be remediated by excavation and incineration. This is a technique that has been proposed for highly refractory organic compounds, such as PCBs and some pesticides. The organic matter of the soil is incinerated while a supplemental fuel is burned in the incinerator. Incineration converts the waste into ash, flue gas, and heat. While the heat can be utilized for beneficial purposes, there is concern about toxic compounds that might accumulate in the ash and gaseous emissions of the incinerator plant. The appropriate disposal of the ash and the filtration of the flue gas add significant cost to the waste incineration and make this process expensive. Compounds with a high BTU (heat) value, such as hydrocarbons, can also be incinerated. This is less costly, since supplemental fuel is not needed. However, permits are needed for incineration, and these may be difficult to obtain from state and local authorities.

9.2.3 Containment

If the waste cannot economically or technically be excavated, then it may be possible to contain it. If the waste is below the water table, flowing groundwater can pass through it and create leachate as illustrated in Figure 9.2a. Such buried waste can be surrounded by a **groundwater cutoff wall**. The purpose of the groundwater cutoff wall is to divert groundwater flow from passing through the waste so that it cannot form leachate (Lynch et al. 1984; Need and Costello 1984). The cutoff wall needs to be deep enough to key into an impermeable layer so that groundwater cannot pass under the wall, which is referred to as encapsulation. Note that the term encapsulation is not only used to describe the isolation of an area of waste, but is used also to describe the different measure of surrounding an individual container with impermeable material.

There are several ways that cutoff walls can be used (U.S. EPA 1998). The wall can extend all around the waste (Figure 9.2b). If this is done, the groundwater will flow around the wall and be diverted from the waste. The water table will rise on the upgradient

FIGURE 9.2a Top view and cross section of a landfill that was constructed with an excavation that extends below the water table. Groundwater can flow through the waste and create leachate.

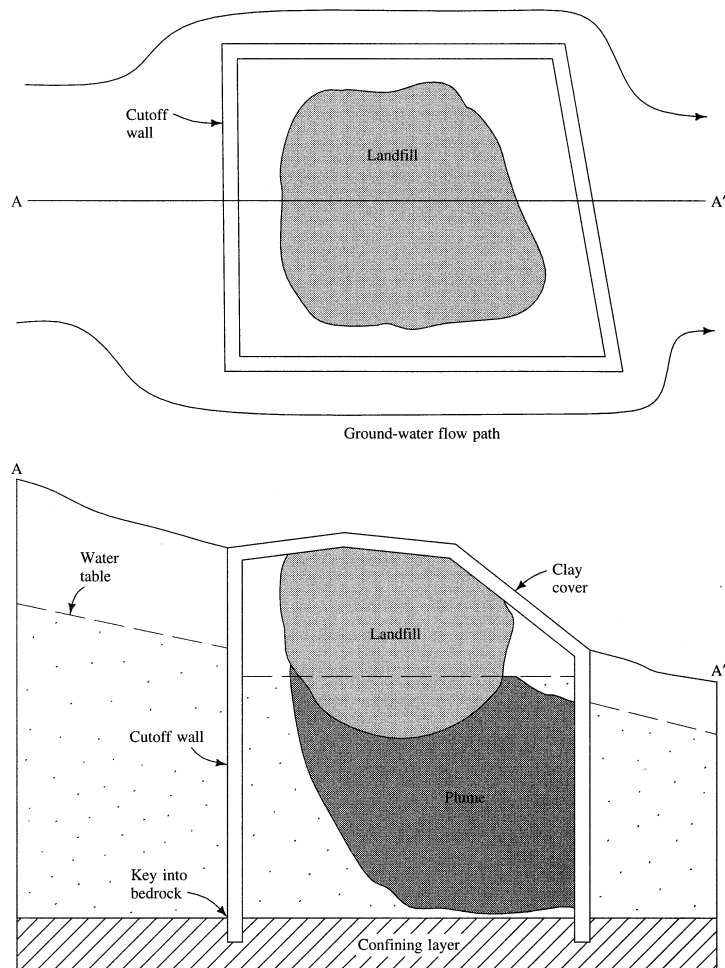


wall and fall on the downgradient wall. If there is no recharge or flow through the cutoff walls, the water table within the cutoff walls will be flat. However, there is generally leakage through the cover or cutoff walls, so some extraction wells will be needed for added hydraulic control within the cutoff walls to prevent build-up of water within walls.

If the cutoff walls are extended far enough to surround both the waste body and the plume of contamination, then remediation may proceed without worry that it will spread further. One of the problems that have arisen with the remediation of groundwater is that the plume may spread rapidly, whereas legal action to assess blame for the plume proceeds through the courts with glacial speed. If a cutoff wall is installed as an emergency action, then the plume can wait until the courts have spoken.

Cutoff walls have also been used to stop the spread of a contaminant plume. At the Rocky Mountain Arsenal near Denver, Colorado, USA, a cutoff wall was constructed

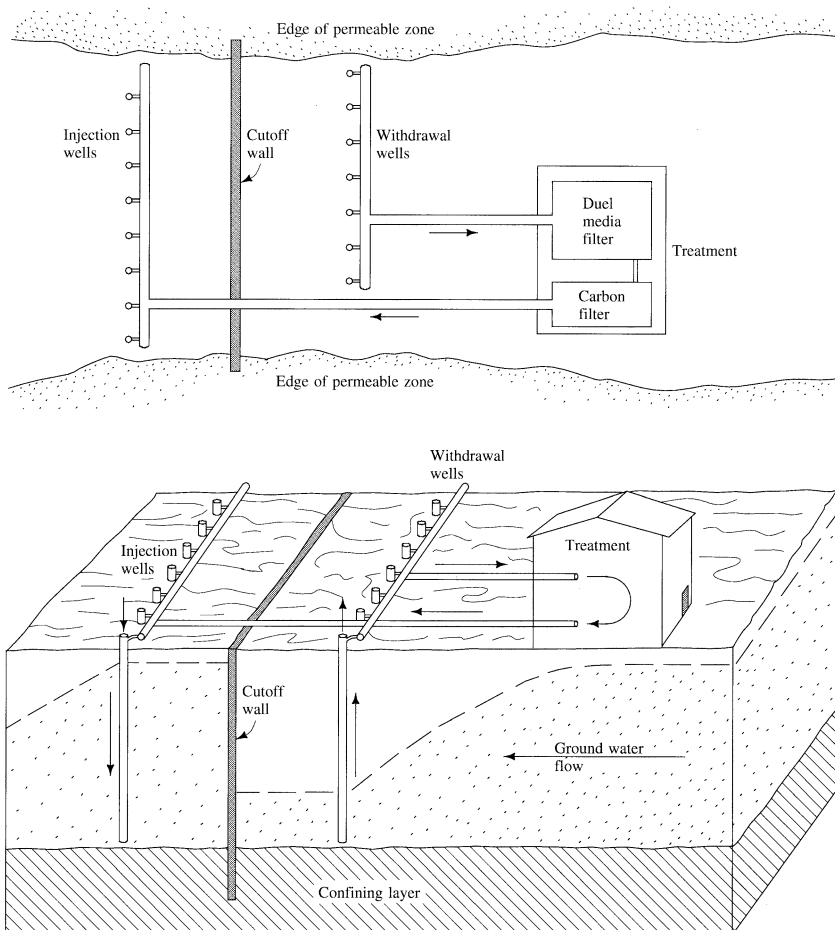
FIGURE 9.2b Top and side view of a cutoff wall that completely surrounds the landfill in (a), opposite page. Cutoff wall is keyed into underlying low-permeability formation.



across a bedrock valley containing higher-permeability, unconsolidated deposits that acted as a pathway for a contaminant plume. The contaminated water is pumped from the upgradient side of the cutoff wall, treated to remove the contamination, and injected into the aquifer on the downgradient side of the cutoff wall (U.S. EPA 1998). This system is illustrated in Figure 9.3.

A number of different types of materials have been suggested for use in cutoff walls (Pearlman 1999). Most are constructed of soil-bentonite slurries, but concrete and concrete/polymer mixtures are also used particularly in regions of topographic relief. A trench is excavated with an excavator or backhoe. The trench is held open by a slurry of bentonite and water. The slurry acts in the same manner as the drilling mud that holds open a borehole. The bentonite slurry penetrates into the more permeable formations and forms a low-permeability filter cake. As the working end of the trench

FIGURE 9.3 Cutoff wall used with extraction and injection wells at the Rocky Mountain Arsenal, Denver, Colorado, to isolate and treat a plume of contaminated groundwater.



is built around the site, the opposite end of the trench is back-filled with a soil-bentonite slurry. The soil-bentonite slurry has a very low permeability and minimizes the movement of most groundwater through it. The trench is typically 1 m (2 to 3 ft) wide and can be up to 18.3 m (60 ft) deep if excavated with a backhoe or up to 36.5 m (120 ft) deep if dug with a clamshell shovel (Need and Costello 1984). While expensive, technology to install cutoff walls as deep as 122 m (400 ft) is available (Valkenburg 1991). Preconstruction design studies are needed to determine if the waste that is to be contained is compatible with the bentonite-soil slurry.

A grout curtain may also be constructed as a cutoff barrier. Grout is injected into the earth through a borehole. The grout is liquid when injected but eventually hardens into an impermeable material. This approach was used to contain radioactive water at the Fukushima nuclear power plant disaster site in Japan, according to the company in charge for the site remediation (www.tepco.co.jp). Other construction methods include

steel-sheet piling, bored pile walls and, as temporary solution, artificial ground freezing. The selection of a cut-off barrier construction method will depend on the desired depth of wall, ground conditions, and geometry of wall.

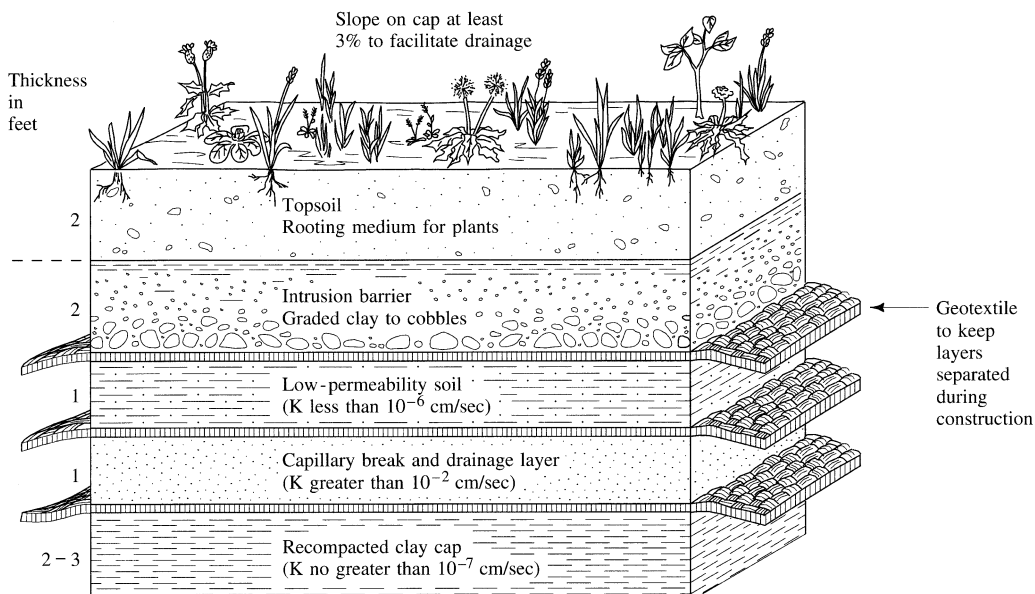
If contaminated material can be immobilized or its solubility reduced through a chemical reaction, this process is called stabilization. Similarly, if the contaminated material can be encapsulated to form a solid and to restrict its migration by decreasing the surface area exposed to leaching, that process is referred to as solidification. **Solidification/Stabilization** is an established technology that has been used for decades to address a variety of *in situ* and *ex situ* solid and liquid wastes. Typically, the contaminated material is treated with an inorganic or organic binder, such as cement, fly ash, lime, soluble silicates or asphalt, epoxide, polyesters, and polyethylene (U.S. EPA 2000).

In most cases it will also be necessary to construct a cover over the waste material to prevent the infiltration of precipitation. If the waste material is above the water table, a cover without a slurry wall might be all that is needed. For a waste material buried below the water table, a low-permeability cover is needed in association with a slurry wall. In the absence of a cover, the infiltrating water will fill the area within the slurry wall like a bathtub.

Covers may be constructed of native soils, synthetic membranes, or a combination of both. Covers are typically sloped in order to promote runoff of precipitation. It may even be necessary to bring in fill material to create the necessary elevation at the center of the cover to form the needed slope.

A multilayer cover constructed of natural materials might have the following elements, starting from the surface (Figure 9.4): (1) 0.6 m (2 ft) of topsoil as a rooting medium for vegetation with shallow roots, such as grass or crown vetch, which is

FIGURE 9.4 Typical design of a multilayer cap for a landfill that is constructed of natural soil materials.



needed to prevent erosion; (2) a 0.6 m (2 ft) thick compacted layer of cobbles mixed with clay to stop burrowing animals from breaching the cap; (3) a 0.3 m (1 ft) thick low-permeability zone to separate the cobble layer from the next-lower zone; (4) a 0.3 m (1 ft) thick layer of very permeable sand, which acts as a capillary break to the movement of soil moisture and provides for lateral drainage of any infiltrating precipitation; and (5) a bottom layer that consists of 0.6 to 1 m (2 to 3 ft) of recompacted clay with a maximum permeability less than 10^{-7} cm/sec (8.5×10^3 ft/d) to act as a final barrier to groundwater recharge. Geotextile fabric would be needed between several of the layers to keep the materials from mixing during construction and to distribute the stresses evenly. Figure 9.4 shows the details of this design. Erosion of the soil and penetration of the cover by tree roots are the main concerns for the long-term integrity of this design.

Synthetic geomembranes can also be used in cover designs as low-permeability layers. One advantage of using native soil materials is that their long-term performance is assured, whereas the long-term behavior of plastic membranes, and those made of other materials has not been tested for all types of soil, climatic, and contaminant mixture scenarios. However, for many applications, plastic membrane covers are suitable. They can easily be installed so that monitoring and extraction wells extend through the cap.

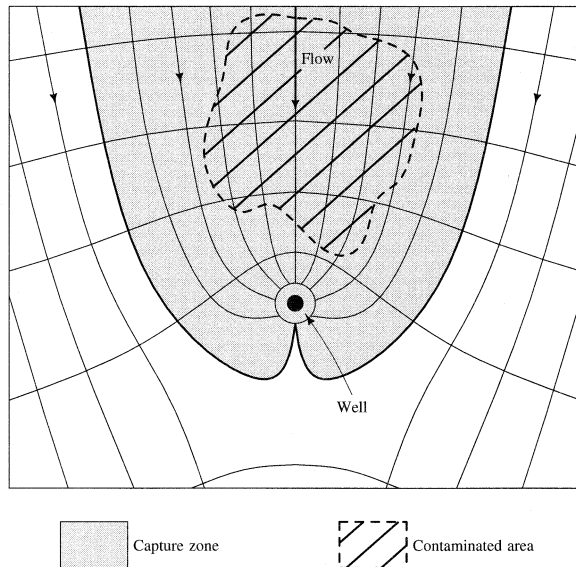
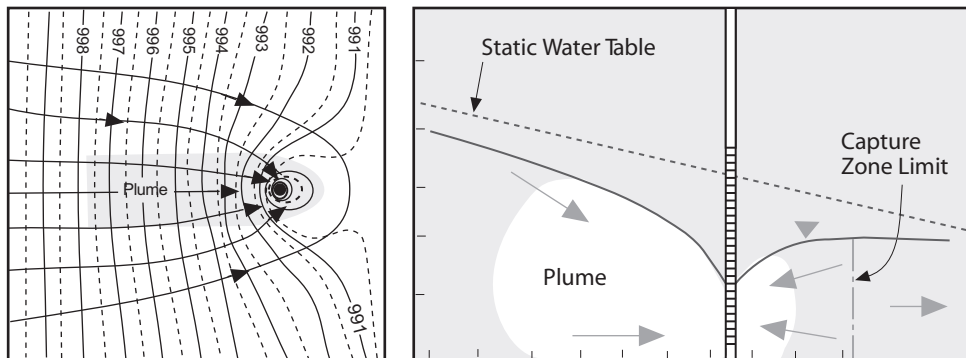
Infiltration of precipitation into the ground can also be reduced by paving the surface with a material such as asphalt. However, an asphalt seal is more permeable than a multilayer cover and would require extensive maintenance to seal cracks that form. Diversion ditches and drains might be used to prevent surface runoff from entering an area where it can infiltrate into the soil and come into contact with buried waste material.

There are alternative cover designs that are increasingly being used for waste disposal sites and hazardous waste landfills. For instance, the evapotranspiration (ET) cover system relies on the properties of one or more vegetated soil layers to store water until it is either transpired through vegetation or evaporated from the soil surface (e.g., Hauser et al. 2001). Compared to conventional land fill covers, ET cover systems are less costly to construct. However, ET cover systems are mostly limited to areas that have arid or semi-arid climates, such as the southwestern United States (U.S. EPA 2003; 2011).

9.2.4 Hydrodynamic Isolation

Hydraulic controls can also be used to isolate a zone where the groundwater has been contaminated. An extraction well positioned at the leading edge of a contaminant plume can be used to stabilize the position of the plume or contain it (Figure 9.5). The plume-stabilization well will pump contaminated water, which may require treatment before disposal. It will prevent the encroachment of the plume of contamination to uncontaminated parts of the aquifer. With the contamination thus isolated, work on source control and other remediation measures can progress at the most expedient pace.

The downgradient limit of the capture zone is called the stagnation point. Figure 9.6 shows a water table profile along the y-axis. It can be seen that the stagnation point forms a groundwater divide between flow toward the well and flow in the regional direction. The stagnation point and the capture zone are also shown for an LNAPL spill in Figure 9.7. Note that there is a maximum quantity of water that can be pumped from a single extraction well. If the plume is wider than the capture zone developed by the maximum pumping rate, then multiple extraction wells are needed. One concern with multiple extraction wells is that their capture zones must overlap,

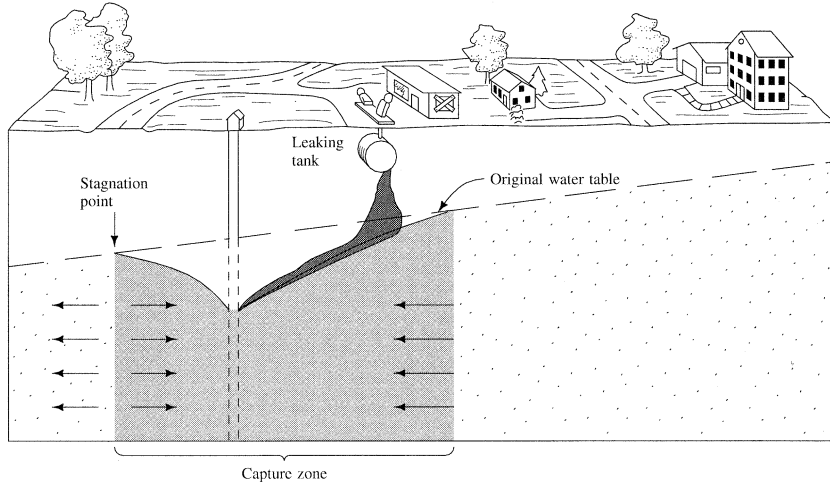
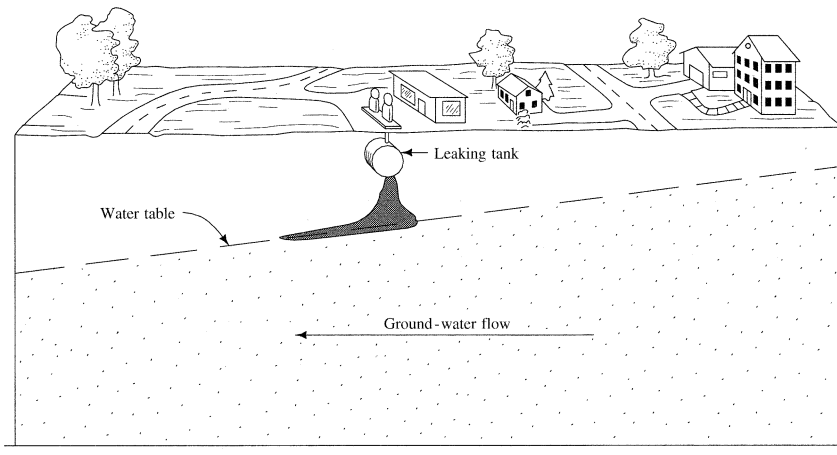
FIGURE 9.5 Plume-stabilization well used to isolate plume of contaminated groundwater.**FIGURE 9.6** Example of plume stabilization by a well which is used to hydraulically contain a plume of contaminated groundwater. Shown are plan view and cross sections.

Source: After Cohen et al. 1993; as cited in U.S. EPA 1995, Report EPA/625/R-95/005.

or groundwater flow can pass between them. These considerations illustrate why contaminant hydrogeologists regularly rely on groundwater models as an important aide in designing remediation systems.

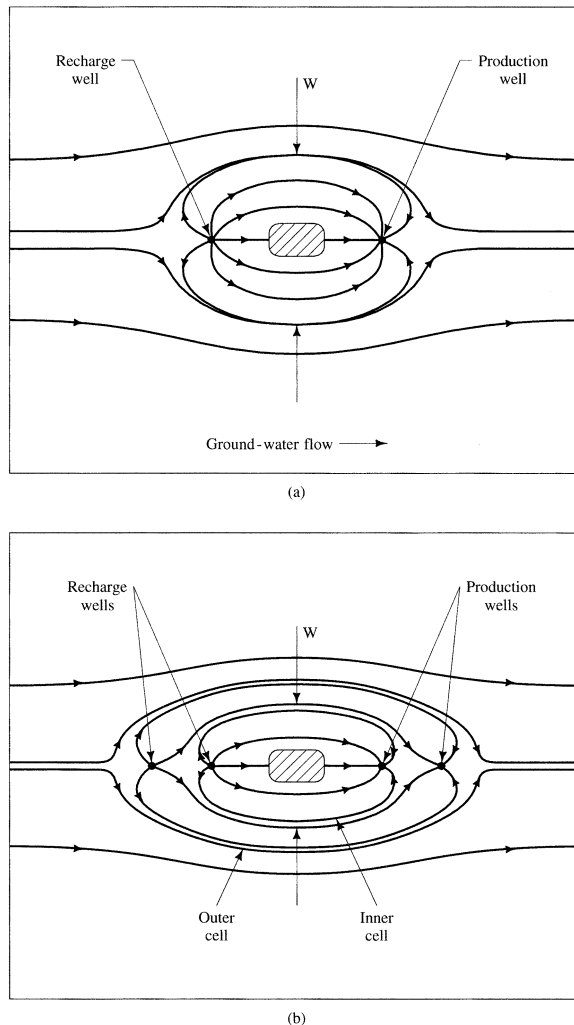
Wilson (1984) described the use of a pair of injection and withdrawal wells to create a hydraulic isolation zone around a plume of gasoline contamination. The withdrawal well draws contaminated water to it; the water is then reinjected into the ground upgradient of the position of the plume (Figure 9.8a). The withdrawn water may be treated prior to injection, or nutrients can be added to promote bioremediation. In addition, treatment systems may need periodic maintenance necessitating a shutdown.

FIGURE 9.7 Cross section along the x axis showing the cone of depression for a single extraction well superimposed on the regional water table.



With a reinjection system the untreated water can still be injected and the downgradient plume-stabilization well can be kept pumping. Otherwise, if the plume-stabilization well is shut down, the plume might be able to spread beyond its hydraulic boundary. Care must be exercised to minimize smearing of LNAPLs by reducing rigorous pumping that results in great fluctuations of the water table. Wilson (1984) also described a double-cell hydraulic containment system with two pairs of injection and production wells, as shown in Figure 9.8b. This system provides further isolation of the plume and also creates a smaller inner cell so that the production well that is pumping contamination will pump a smaller volume of water, which will lower treatment costs. With two injection and pumping wells, there is a possibility of shutting down one well periodically for maintenance and still having the system operational.

FIGURE 9.8 Plan view of (a) single-cell and (b) double-cell hydraulic containment of contaminated groundwater.



Source: J. L. Wilson. 1984. Proceedings of the Fourth National Symposium and Exposition on Aquifer Restoration and Ground Water Monitoring, 65–70. National Water Well Association. Used with permission.

■ 9.3 Pump-and-Treat Systems

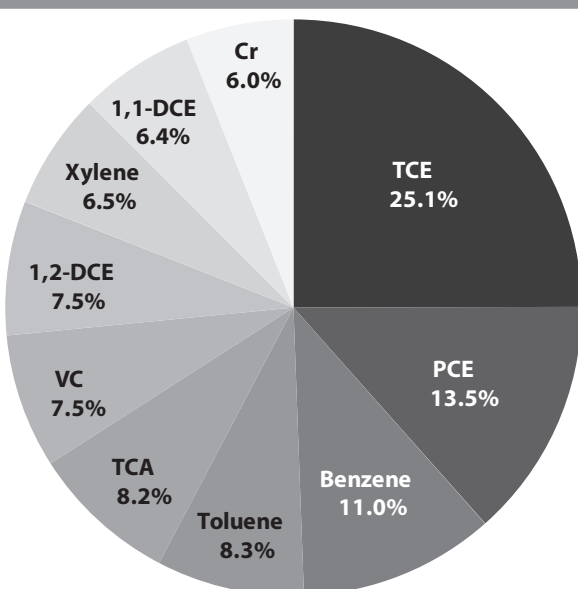
9.3.1 Overview

For a long time, almost all groundwater remediation was based on extraction wells or drains that were usually accompanied by treatment of the extracted water before discharge (Mackay and Cherry 1989). The extraction of groundwater that contains dissolved inorganic and organic chemicals removes the contaminants from the subsurface

so that the contaminated groundwater can be treated at the surface. This remediation approach is known as Pump-and-Treat (P&T). The advantage of the P&T method is that conventional methods of wastewater treatment can be employed. Pump-and-treat was the sole remedy at 56% (485 of 877 sites) of National Priority List (NPL) sites in the United States between fiscal years 1982 and 2005, representing the most common groundwater remedial action during that period (U.S. EPA 2007). Figure 9.9 provides an overview of the 10 most frequently treated contaminants using P&T technology. P&T systems also are frequently used to treat metals and metalloids, including chromium (U.S. EPA 2007). There are, however, a number of disadvantages that limit the usefulness of this technology to emergency responses, plume containment in combination with source-control measures, or treatment of highly water soluble compounds. Since the early 1990s many highly efficient groundwater treatment technologies have been devised and tested so that contaminated site managers now have alternatives to the P&T technologies. Not surprisingly, by 2011 only 22% of groundwater remedies at NPL sites were P&T based (U.S. EPA 2013).

Depending on the efficacy of treatment and regulatory requirements, the treated water can be discharged to a receiving water body, passed to a publicly owned wastewater treatment plant for further treatment and dilution, or reinjected into the ground. Often the disposal of the treated wastewater requires state and local permits or regulatory approval. Discharge to a publicly owned wastewater-treatment plant may require local permits for industrial discharge and there might be pretreatment standards. Water

FIGURE 9.9 Contaminants treated most commonly by pump-and-treat systems: trichloroethene (TCE); tetrachloroethene (PCE); 1,1,1-trichloroethane (TCA); 1,2-dichloroethene (1,2-DCE); 1,1-dichloroethene (1,1-DCE), vinyl chloride (VC), and chromium (Cr).



Source: U.S. EPA 2007.

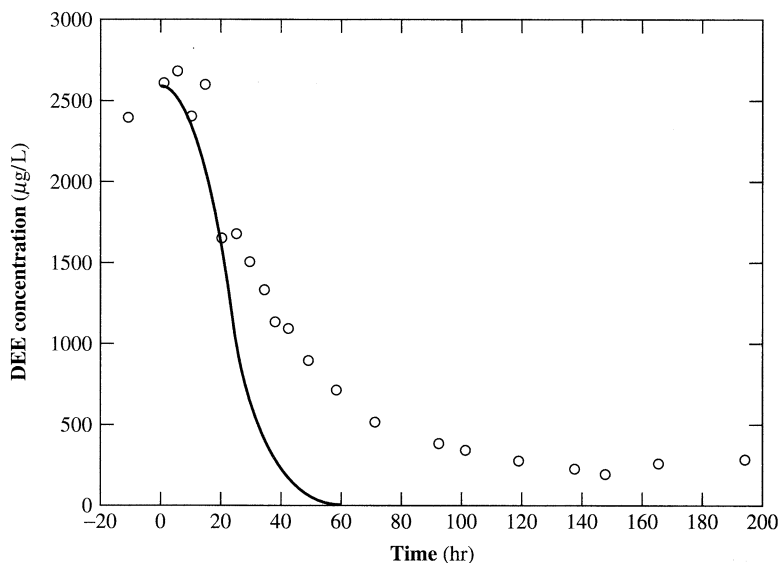
discharged to a surface-water body in the United States requires state permits, including a National Pollutant Discharge Elimination System (NPDES) permit. Many states, provinces, and regions require a permit to inject water into the ground and there may be concentration limits specified as a part of the permit. If there are NAPLs present, the situation is much more complex than if all contaminants are in a dissolved form. As long as an NAPL is present, it will partition between the NAPL phase and the dissolved phase. Thus, as contaminated water is withdrawn from the aquifer for treatment, the clean water that is drawn into the aquifer eventually becomes contaminated with pollutants partitioning from the remaining NAPL. If some of the NAPL is mobile, it may be captured by pumping. LNAPLs that are floating on the water table are relatively easy to locate and remove if the LNAPL has not been smeared vertically. However, DNAPLs that sink to the bottom of the aquifer are very difficult even to locate, much less recover (Mackay and Cherry 1989; Freeze and Cherry 1989). Because considerable amounts of residual NAPL will remain even if the mobile NAPL is removed, a great many years may be required for pump-and-treat systems to remove all the residual NAPL by partitioning into the recoverable dissolved phase. In the case of contamination by DNAPLs especially in fractured rock aquifers, it may be very difficult or impossible to remediate a contaminated aquifer (Mackay and Cherry 1989; Freeze and Cherry 1989; National Academies of Sciences, Engineering, and Medicine 2015).

If the dissolved phase sorbs onto the mineral matter of the soil, that phase may desorb as the contaminated water is flushed from the pores. The greater the distribution coefficient, the more slowly the sorbed phase will be released and the longer it will take to remediate the aquifer. The kinetics of desorption dictate that many pore volumes of uncontaminated water might be needed to remove completely the sorbed phase of both organic and inorganic contaminants. Whiffin and Bahr (1984) noted that the observed rate at which organic compounds desorbed from an aquifer was slower than the rate predicted by transport equations that assumed equilibrium conditions between the sorbed phase and the dissolved phase (Figure 9.10). The advection-dispersion equation results were initially fairly accurate; however, when the concentration dropped to about half the initial concentration, the actual rate of removal was slower than the predicted rate.

The discrepancy between the Whiffin and Bahr (1984) model and the observations in the field are related to contaminant residence time in the subsurface and diffusion transport processes. Hence, in heterogeneous media, some contaminants can be sequestered for long periods of time, despite active pumping. Contaminants that have been in the ground for a long period of time have been able to diffuse into the less permeable zones of porous media aquifers or into the bedrock matrix of fractured rock aquifers. Pump-and-treat systems are inefficient in removing these contaminants, because the majority of the water being removed by pumping will come from the most permeable zones of the aquifer. In alternating layers of sand and clay, the contaminated water will penetrate the fine clay, which has very limited permeability, from the highly permeable sands over time. Some of the contamination will remain in the dissolved phase, some will partition onto the surface of the clay lens and associated soil organic carbon and some will diffuse into the clay lens. The fine sediment will have a larger surface area per unit volume of the aquifer than the coarse sediment and thus will sorb more contamination.

These mass transport limitations have been illustrated by Mackay and Cherry (1989) (Figure 9.11). Figure 9.11a shows contamination residing in homogenous aquifer

FIGURE 9.10 Measured desorption values for diethyl ether for water pumped from a purge well (open circles) versus calculated desorption curve based on advection-dispersion equation (solid line).



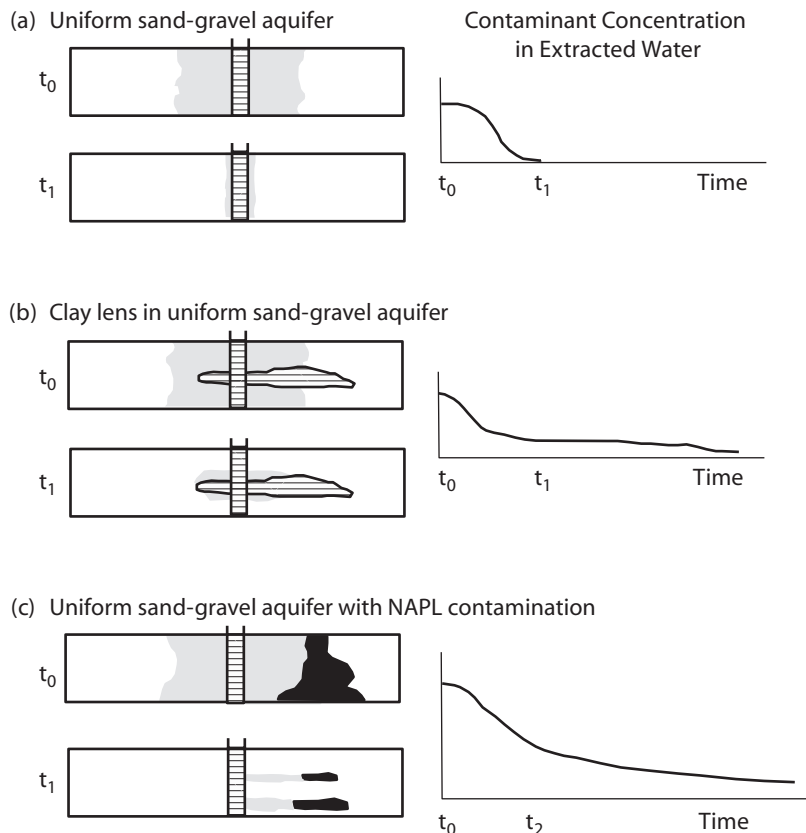
Source: R. B. Whiffin and J. M. Bahr. 1984. Proceedings of the Fourth National Symposium and Exposition on Aquifer Restoration and Ground Water Monitoring, 75–81. National Water Well Association. Used with permission.

composed of uniform sand. During the time interval t_0 to t_1 , the contamination is effectively flushed out. However, if the porous media is heterogeneous and the aquifer consists of sand with an interbedded clay lens, the concentration in the effluent from the extraction well is still elevated at t_1 (Figure 9.11b). Water removed by pumping will come primarily from the sandy material. The contaminated water in the pores of sand will be fairly quickly removed; perhaps only a few pore volumes of water will need to be flushed through to accomplish this. Contaminants sorbed onto the sand grains will be removed by partitioning into the clean water that then occupies the pores in the coarse sand layers.

Meanwhile, the contaminated water occupying the pores of the clay lens will be flushed from this layer very slowly. It will take the movement of many pore volumes of water through the sand to flush just a few pore volumes of water through the much less permeable clay layer. Hence, it will take much longer to remove the contaminants that are desorbing from the fine sediments after the contaminated pore water is removed from the sand.

There will be an initial rapid decline in the concentration of contaminants in the water being removed by a pump-and-treat system. This decline represents the removal of the contaminated water contained in the larger pores of the aquifer. Initially, when the larger pores in the sandy material are being flushed, the drop in concentration will be rapid. Flushing the much smaller pores in the clay will take much more time and, the rate at which the concentration declines will decrease. The concentration will eventually approach somewhat constant value, which represents a steady state condition where the rate at which the contaminants are being removed by the pump-and-treat

FIGURE 9.11 Hypothetical examples of contaminant removal during pump-and-treat treatment. Gray areas indicate sorbed and dissolved contaminants (uniform initial distribution). Lined shapes indicate clay lens. Black areas indicate NAPL.

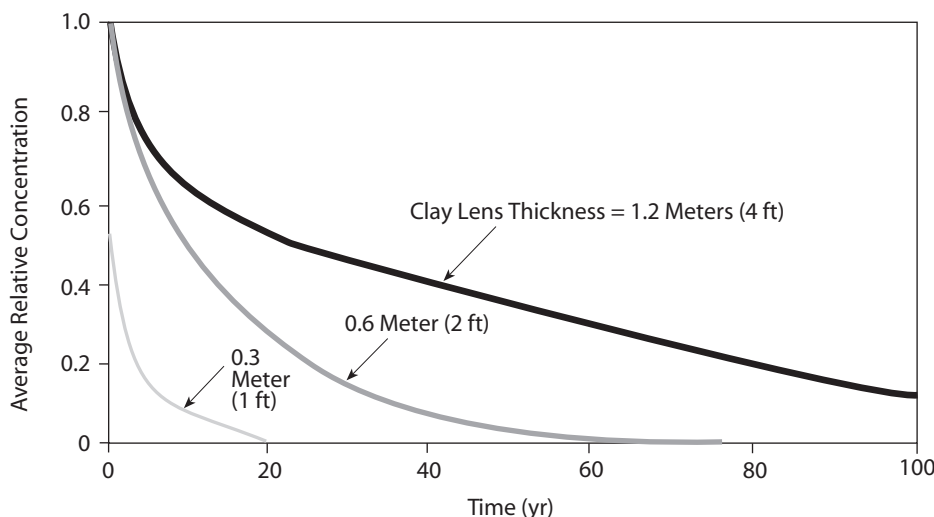


Source: Modified after Mackay and Cherry 1989.

system is equal to the rate at which they are being released into the groundwater by diffusion desorption and/or partitioning from residual NAPLs (Figure 9.11c). The resulting long period of slow release of contaminants to the groundwater is called the **tailing** phase of the remediation.

During the tailing phase in the remediation process contaminant mass is still being removed from the aquifer, but the groundwater is not becoming any cleaner. The concentration at which this occurs may be higher than the cleanup goals for the remediation. It may take many years of pumping at this stage to reduce the amount of sorbed contaminants and/or the residual NAPLs sufficiently for the groundwater quality to improve to a point where it meets cleanup goals. Figure 9.12 depicts how the slow, diffusion-controlled release of contamination from material of low hydraulic permeability (clay) can determine the length of the remediation period. For instance, it would take about 10 years to reduce the TCE concentration by 90% if the clay lens is 0.3 m (1 ft) thick. The time increases to almost 40 years for a lens 0.6 m (2 ft) thick and to over

FIGURE 9.12 The effect of matrix diffusion on the average relative trichloroethene (TCE) concentrations in clay lenses of varying thickness as a function of time.



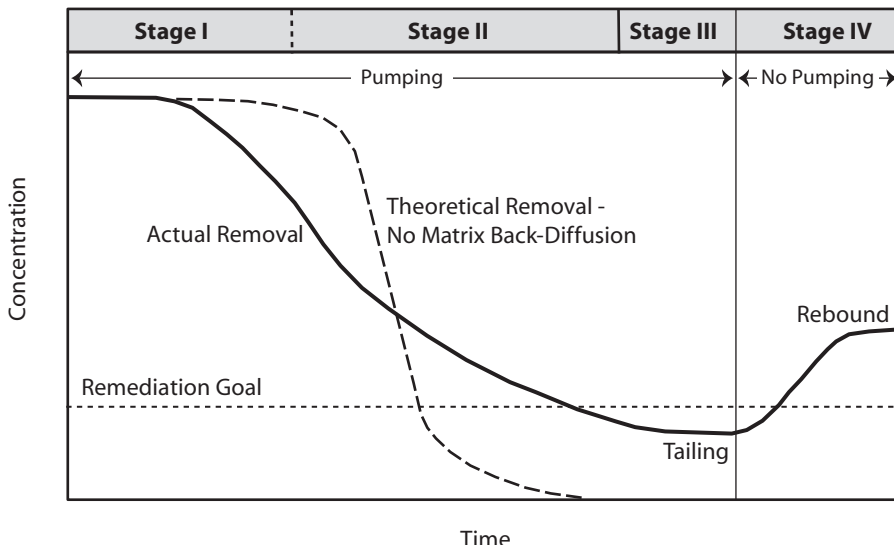
Source: U.S. EPA 1996.

100 years for a lens 1.2 m (4 ft) in thickness. These simulations show that it may take decades or longer to significantly lower the contaminant concentration in clay lenses.

A study of pump-and-treat cleanup at 16 sites in the United States where the groundwater was contaminated with organics revealed that if the initial concentration of contamination was high ($>1000 \mu\text{g/L}$), pumping could achieve reductions of contaminant concentrations of 90 to 99% before leveling occurred. At sites where the initial concentration was less than $1000 \mu\text{g/L}$, leveling occurred before a 90% reduction was accomplished (Doty and Travis 1991). Moreover, if remediation is halted before the sorbed phase is completely removed, the dissolved concentration will eventually **rebound** and rise above the level detected at the end of the remedial period as additional material desorbs to come to equilibrium with the dissolved phase. Typically, the rebound of the dissolved contaminant concentration is quick, i.e., can occur within a few days after the pumping ceased.

The effects of rebound and tailing on the progress of P&T treatment are illustrated in Figure 9.13. It must be noted that these effects are not solely limited to P&T systems, but also affect other, more innovative groundwater treatment technologies that rely on chemically-enhanced flushing processes to remove contamination from low-permeability material.

Figure 9.13 illustrates the multiple stages in remediation of a contaminated aquifer or soil. Early during the treatment (Stage I), there is rapid removal of contaminant mass and concentrations drop quickly. Stage I transitions into Stage II which represents the diffusion-controlled period as the concentration graph attains an asymptotic shape. During the tailing stage (Stage III), the rate of mass removal slows because the site geology controls the rate at which the remaining contamination is released. The impact of matrix diffusion is illustrated by the dashed line curve, which shows the theoretical removal expected in

FIGURE 9.13 Stages in the remediation of a contaminated aquifer or soil.

Source: Modified after U.S. EPA 1996.

the absence of diffusion from low-permeability domains into higher permeable zones. Remediation efforts continue until a pre-determined clean up goal has been reached. In some cases, that remediation goal may be higher than the pollutant specific standard, like the maximum contaminant level (MCL) defined by the U.S. EPA. When at one point the pumping stops, it is likely that the slow, diffusion-controlled release of contaminants from low-permeability domains results in an increase in the dissolved phase concentration. This is Stage IV, the rebound stage. Should the rebound result in groundwater concentrations higher than the cleanup standard, remediation must continue. Under these circumstances, it may be necessary to periodically turn on the pump(s) until the residual concentration drops beneath the remediation goal again. Such a treatment scheme is known as **pulsed pumping** (U.S. EPA 1996). Another option is to vary the pumping rates or turn injection wells into extraction wells and vice-versa. This **adaptive pumping** approach limits the development of stagnation zones, which are parts of the aquifer that are not, or only minimally, flushed if the extraction/injection scheme was static.

Figure 9.13 illustrates an aquifer where the contaminant is in the dissolved phase or is sorbed onto soil particles. If there is an undissolved phase (DNAPL) present, then the release of contaminant into the flushing water will be controlled by the solubility of the DNAPL. More soluble DNAPLs, such as trichloroethylene, which has a solubility of 1100 mg/L, will become dissolved much more rapidly than low-solubility NAPLs, such as coal tar or creosote. However, as the DNAPL will tend to form pools on the top of low-permeability layers, the flushing liquid will only come in contact with the top of the DNAPL pool and little dissolution will actually occur (Johnson and Pankow 1992). As a result, pump-and-treat will be inefficient for mass removal in the case of DNAPLs. In spite of this inefficiency pumping still is viable as a means of plume containment.

Pump-and-treat methods have been shown to be effective in removing a large amount of more soluble contaminant mass from the aquifer during the initial phase of pumping. They are also useful in halting the spread of a plume of contamination, i.e., plume containment. However, if the contaminant concentration in the aquifer is still above the cleanup goal once a pump-and-treat project reaches the stage where the contaminant release is diffusion controlled, decades of additional pumping might be required before the aquifer is “clean.” This does not mean that the pump-and-treat approach failed, it only means that it was an unrealistic expectation to attain complete remediation of an aquifer with pump-and-treat as the only remedy. The shortcomings of conventional pump-and-treat schemes have led to the development of many innovative remediation technologies, which will be discussed in greater detail later in this chapter.

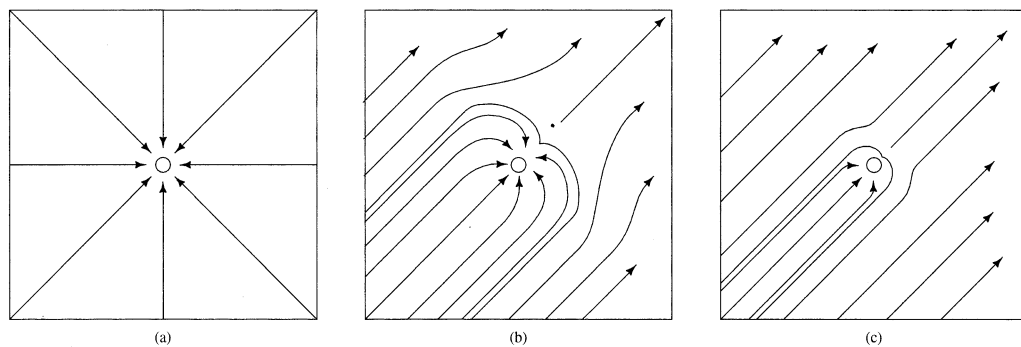
9.3.2 Capture Zones

In order to capture a plume of contaminated water, it is necessary to have one or more pumping wells located downgradient of the source area. Each well will have what is known as a **capture zone**, which is the area contributing flow to that particular well.

If the water table is flat, there is no regional flow. The capture zone of a well is radially symmetrical, centered on the well and extending as far as the edge of the cone of depression (see Figure 9.14a). If there is a slope to the water table, the groundwater flows and the capture zone are asymmetrical, with the greatest extent in the upgradient direction (Figure 9.14b). As the groundwater velocity increases, the width of the capture zone decreases for a given pumping rate (see Figure 9.14c).

The shape of the capture zone is a function of the average linear groundwater velocity, the quantity of the water being pumped from the aquifer, and the distribution of hydraulic conductivity. The upgradient extent of the capture zone depends upon the length of time over which the pumping occurs. The Wellhead Protection Area (WHPA) program was developed by the U.S. EPA that may be used to delineate capture zone. It is a semi-analytical groundwater flow simulation program that can account for multiple pumping and injection wells and delineates the area contributing flow to those wells.

FIGURE 9.14 (a) Flow lines toward a well in an aquifer with no water table gradient; (b) flow lines toward a well and the capture zone with uniform flow to the upper right of the figure; (c) flow lines toward a well and the capture zone with uniform flow to the upper right at a rate 10 times the rate of (b).



WHPA is applicable to homogeneous aquifers exhibiting two-dimensional, steady groundwater flow in an areal plane and appropriate for evaluating multiple aquifer types (i.e., confined, leaky-confined, and unconfined) (U.S. EPA 1993).

If the hydrogeology is not homogeneous or if more complex geologic or contaminant transport problems have to be accounted for, there are a number of sophisticated models available today. For instance, FLOWPATH II is a 2-D finite difference, steady-state groundwater flow model for calculation of wellhead protection zones, hydraulic heads, groundwater velocities, time related path lines, capture zones, water balances, and steady state drawdown distributions. Another model is PATH3D, which can help delineating contaminant capture zones or wellhead protection zones or can be used to evaluate the effectiveness of groundwater remedial scenarios under complex hydrogeological conditions. There are a number of other noteworthy programs and the Integrated Groundwater Modeling Center (IGWMC) at the Colorado School of Mines in Golden, CO, USA, provides reviews and links to many of those models.

9.3.3 Computation of Capture Zones

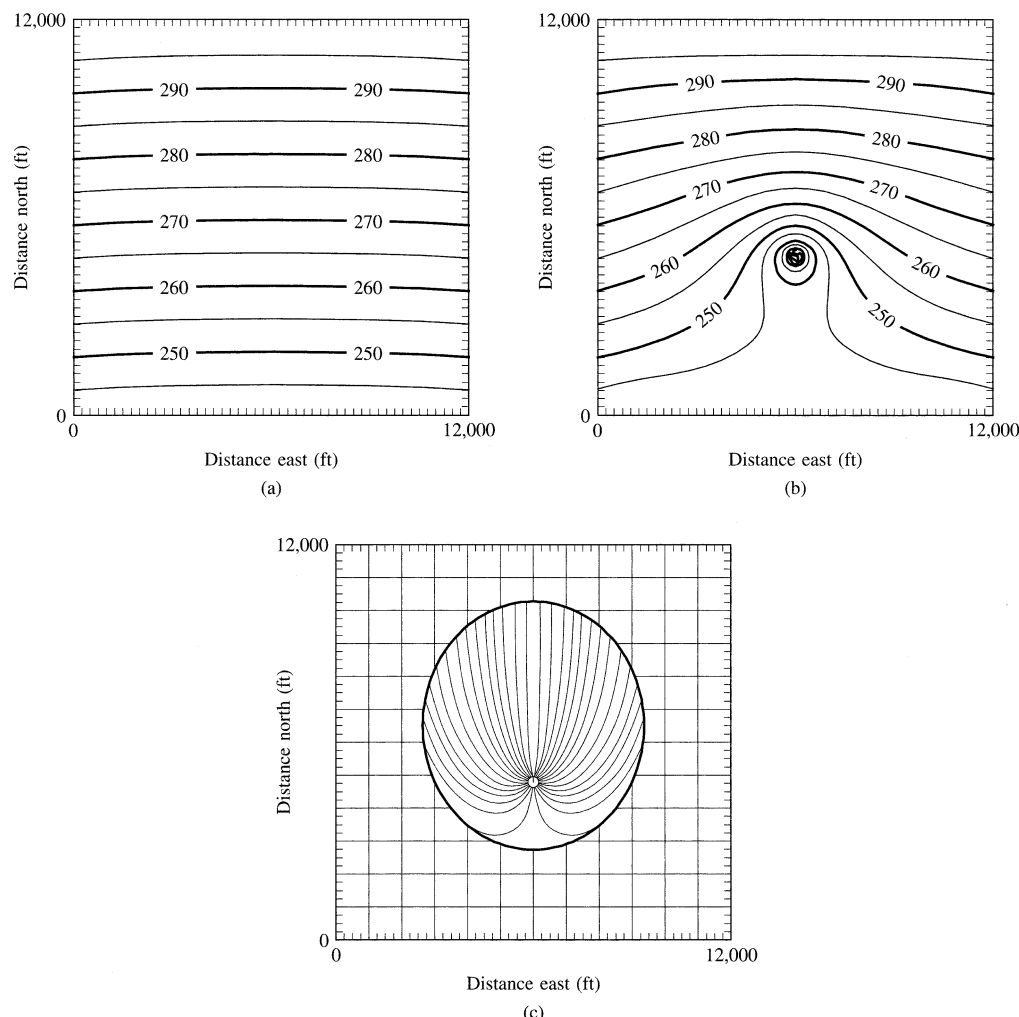
The effect of aquifer heterogeneity was illustrated by Shafer (1987). Figure 9.15a shows the initial hydraulic head for a homogeneous, isotropic, unconfined aquifer. The hydraulic-head distribution after 20 years of pumping from a single well is shown in Figure 9.15b. During this time period, the cone of depression has not spread all the way to the upgradient end of the diagram. The extent of the capture zone is shown superimposed on the model grid in Figure 9.15c. Figure 9.16a shows the distribution of hydraulic conductivity in nonhomogeneous aquifer with the same initial head distribution as the one in Figure 9.15a. In contrast to the homogenous system, the hydraulic head distribution in the nonhomogeneous aquifer with one well pumping is not symmetric and the shape of the 20-year capture zone is irregular (Figures 9.16b and c). The nonsymmetric, irregularly shaped capture zone reflects the heterogeneous distribution of the hydraulic conductivity in the nonhomogeneous aquifer. This example illustrates that ignoring aquifer heterogeneity can lead to incomplete capture of a contaminant plume.

9.3.4 Optimizing Withdrawal-Injection Systems

The rate at which groundwater restoration can be accomplished by pump-and-treat systems depends in part on how many pore volumes of water can be withdrawn from the contaminated zone. If the entire plume falls within the capture zone of one or more withdrawal wells, then we know that the plume will not spread and eventually maximum feasible restoration will occur. However, by increasing the rate (number of pore volumes of water per year) at which contaminated water is pumped, the restoration time can be decreased. For optimal conditions we also want to minimize the volume of contaminated water that is pumped, because that also must be treated.

Satkin and Bedient (1988) used a contaminant-transport model to investigate the use of various pumping and injection patterns to remediate a plume of contamination. They examined the effectiveness of seven different well patterns for various combinations of hydraulic gradient, maximum drawdown, and aquifer dispersivity. The patterns are shown on Figure 9.17.

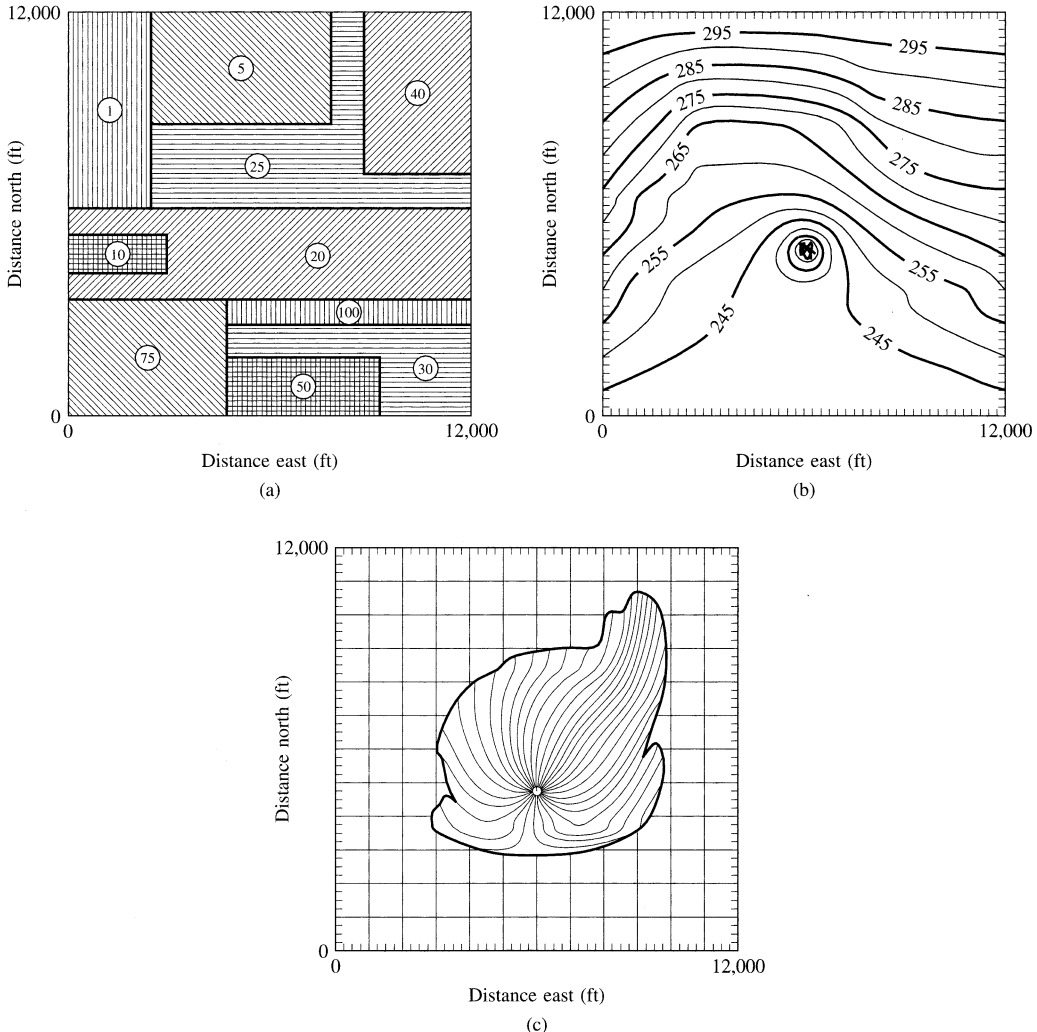
FIGURE 9.15 (a) Hydraulic head distribution with no wells pumping. (b) Hydraulic head distribution in a homogeneous, isotropic aquifer with one well pumping. (c) Shape of the 20-year capture zone based on hydraulic head distribution of Figure 9.15b.



Source: J. M. Shafer. 1987. Reverse pathline calculation of time-related capture zones in nonuniform flow. *Groundwater* 25:283–289. Used with permission.

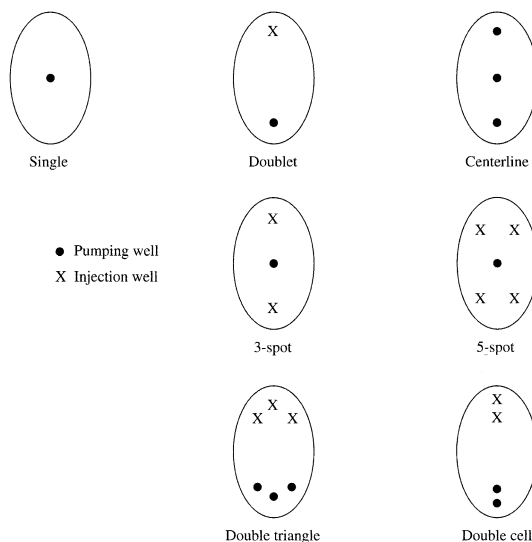
If a single pumping well is used, it must be placed so that the capture zone encompasses the plume. The closer the well can be to the center of mass of the contaminant, the faster the contamination can be removed. If the plume can be captured by a single withdrawal well, then multiple pumping wells aligned along the axis of the plume will increase the rate of cleanup over a single well by pumping a greater volume of water. The use of pumping wells without injection wells may create a problem if there isn't a receiving body of water in which to dispose of treated groundwater.

FIGURE 9.16 (a) Distribution of hydraulic conductivity in nonhomogeneous aquifer with the initial head distribution of Figure 9.15a. (b) Hydraulic head distribution in the nonhomogeneous aquifer with one well pumping. (c) Shape of the 20-year capture zone based on hydraulic head distribution of Figure 9.16b.



Source: J. M. Shafer. 1987. Reverse pathline calculation of time-related capture zones in nonuniform flow. *Groundwater* 25:283–289. Used with permission.

If injection wells are used in combination with withdrawal wells, cleanup time can be reduced, because steeper hydraulic gradients can be created. These steeper gradients will produce more water flowing to the withdrawal well(s) than occurs if extraction wells alone are used. We have already seen how a system of a downgradient withdrawal well in conjunction with an upgradient injection well can be used to create a circulation cell

FIGURE 9.17 Possible patterns for extraction and extraction-injection well systems.

Source: R. L. Satkin and P. B. Bedient. 1988. Effectiveness of various aquifer restoration schemes under variable hydrogeologic conditions. *Groundwater* 26:488–498. Used with permission.

to isolate the plume. This is called a doublet on Figure 9.17. Other injection-withdrawal combinations tested included the double cell and double triangle, which are variations of the doublet. Two patterns tested were based on one extraction well and multiple injection wells: the three-spot and the five-spot. When injection wells are used in conjunction with extraction wells, the treated water is disposed via reinjection. However, groundwater injection wells are prone to clogging and may need periodic maintenance (Fetter 1994). Additionally, states, provinces, or regions may have water-quality standards for any water that is reinjected; many locales require a permit for injection wells.

Satkin and Bedient (1988) found that the best well pattern for cleanup was highly site-specific. They also found that even with the same well pattern, variation in the placement of the wells yielded different cleanup times. When the hydraulic gradient is low, the doublet, double cell, and three-spot patterns were very effective. Under conditions of high hydraulic gradient, the centerline was most effective. In this pattern the downgradient injection well, which must be located beyond the leading edge of the plume, creates a hydraulic barrier to further migration of the plume. The five-spot pattern was not found to be very effective under any conditions.

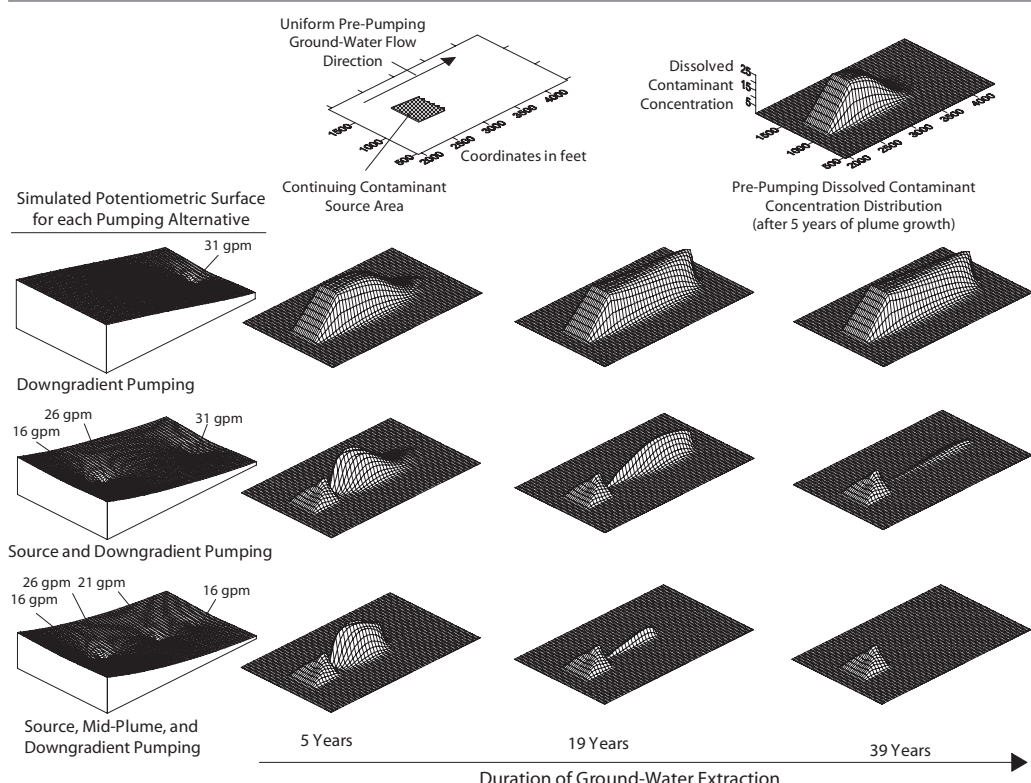
9.3.5 Permanent Plume Stabilization

Decades of experience with pump-and-treat technology showed that in most cases it is not feasible or even technically possible to fully remediate a badly contaminated aquifer by pump-and-treat technology. This is especially true if the source cannot be located and removed, for example, if there are nonbiodegradable residual DNAPLs present in a fractured rock aquifer. For such aquifers the only feasible technology might

be permanent plume stabilization. One or more plume stabilization wells would be installed and just enough water pumped to capture the plume. The volume of water pumped could be less than that needed for a full site remediation since there is no need to maximize the number of pore volumes drawn through the aquifer. The pumped water could either be treated and discharged into a surface water body or reinjected upgradient to recirculate through the aquifer. This arrangement would be necessary in perpetuity.

In a U.S. EPA document (Cohen et al. 1997) titled "Design Guidelines for Conventional Pump-and-Treat Systems," a conceptual modeling analysis is presented for three alternative pumping strategies of which only one resulted in permanent plume stabilization. The model is based on FTWORK (Faust et al. 1993) and is for an idealized site with a uniform medium, linear equilibrium sorption, a single non-degrading contaminant, and a continuing release. Figure 9.18 shows three different pumping scenarios (1) downgradient pumping, (2) source control with downgradient pumping, and (3) source control with mid-plume and downgradient pumping. The first case illustrates that at this hypothetical site pumping from a single downgradient

Figure 9.18 Simulation of three pump-and-treat alternatives for an idealized site (with uniform media, linear equilibrium sorption, and a single non-degrading contaminant) showing dissolved contaminant concentrations with time of pumping.

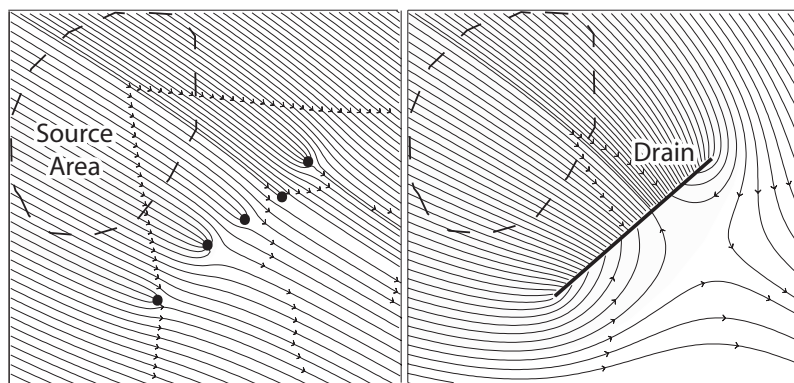


Source: Modified after Cohen et al. 1997.

well is insufficient to prevent the plume from growing. Pumping at the source zone and downgradient improved the situation but some contaminated groundwater still escaped downgradient. Only the installation of a mid-gradient well prevented the escape of contaminated groundwater. The modeling results underline the importance of source control pumping and the establishment of sufficiently large downgradient capture zones to prevent continued offsite migration of contaminated groundwater.

A different approach to plume containment is to construct a **French drain** perpendicular to the direction of the plume migration. Such a drain system is typically constructed by excavating a ditch to the maximum depth of the plume and back filling it with gravel or other highly permeable material. Embedded at the base of the trench is a horizontal perforated pipe that connects to a vertical well. Contaminated water intercepted by the trench is collected by the pipe and then pumped to the surface for further treatment. As shown in Figure 9.19, a French drain may provide more effective plume containment than a series of extraction wells (Cohen et al. 1997). These drain systems are limited to comparably shallow plumes in unconsolidated material because digging deep trenches ($>>30$ m or >100 ft) is typically cost prohibitive and often not feasible, particularly if the sediment is unstable and prone to caving. Constructing French drains in bedrock is generally possible, but typically too expensive.

Figure 9.19 Compared to a line of conventional pump-and-treat wells (left), a plume emanating from an up gradient source zone can be effectively intercepted by a trench drain constructed perpendicular to the main axis of groundwater flow (right).



Source: Cohen et al. 1997.

■ 9.4 Treatment of Extracted Groundwater

9.4.1 Overview

It is often necessary to withdraw water during site remediation projects and that water must be treated *ex situ* according to the type of contamination. Different types of treatment are needed for water contaminated with heavy metals or that is contaminated by dissolved organic compounds. Similarly, the treatment approach will be different for compounds that are volatile versus those that are not, or those pollutants that can be chemically or physically destroyed or converted into non-toxic compounds versus

those that cannot. Most of the treatment techniques that are used were developed for wastewater and have been adapted to contaminated groundwater. Generally, there are two types of treatment approaches (1) separation and (2) destruction technologies. Examples for the former include adsorption to granular activated carbon (GAC), or air stripping. Destruction technologies include, for instance, UV oxidation and other advanced oxidation processes or biological treatment methods. These and other *ex situ* treatment technologies for contaminated groundwater are described in detail on the Federal Remediation Technologies Roundtable (FRTR) or EUGRIS websites and other online information depositories introduced in Section 9.1. Some of these treatment technologies require the contaminated matrix, soil or groundwater, to be transported to the treatment facility; others can be easily set up on the contaminated site. The treatment methods for contaminated soil and sediment are not covered in this chapter.

The design of a treatment system must be cost effective. To this end the designer must consider the trade-off between capital costs and operating costs. Extraction systems can be designed by the hydrogeologist to withdraw the maximum volume of water in the shortest period of time. This yields the fastest, but not necessarily the most cost-effective cleanup of the aquifer. The size of the treatment plant is dictated by the maximum rate by which water will be pumped for treatment. The capital costs for the treatment plant include the treatment vessels, pumps, piping, and tanks. The greater the flow rate at which contaminated water is pumped through the treatment system, the larger these items must be and the greater the initial capital costs.

Operating costs include the electricity to run the plant, the cost of chemicals, the labor to operate the plant, and the cost of repairs. Some of the operating costs will be continuous no matter how long the project lasts (e.g., the cost of chemicals used to treat the water). If the same total volume of water is treated, the same amount of chemicals will be needed, no matter how long or short the treatment period. Other costs, such as labor, depend primarily upon the length of time of the operation. If the total volume of contaminated water is treated over a very short period of time, there will be high initial capital costs for the large-capacity plant and low operating costs because of the short time period. If the same volume of water is pumped over a longer period of time, the capital costs will be lower, since a smaller treatment plant is needed, but the operating costs will be higher. The smallest treatment plant possible is that needed to treat the quantity of water generated by the minimum pumping rate, which is just high enough to capture the plume. There will be some optimum treatment rate that minimizes the combined capital and operating costs.

9.4.2 Treatment of Inorganic Contaminants

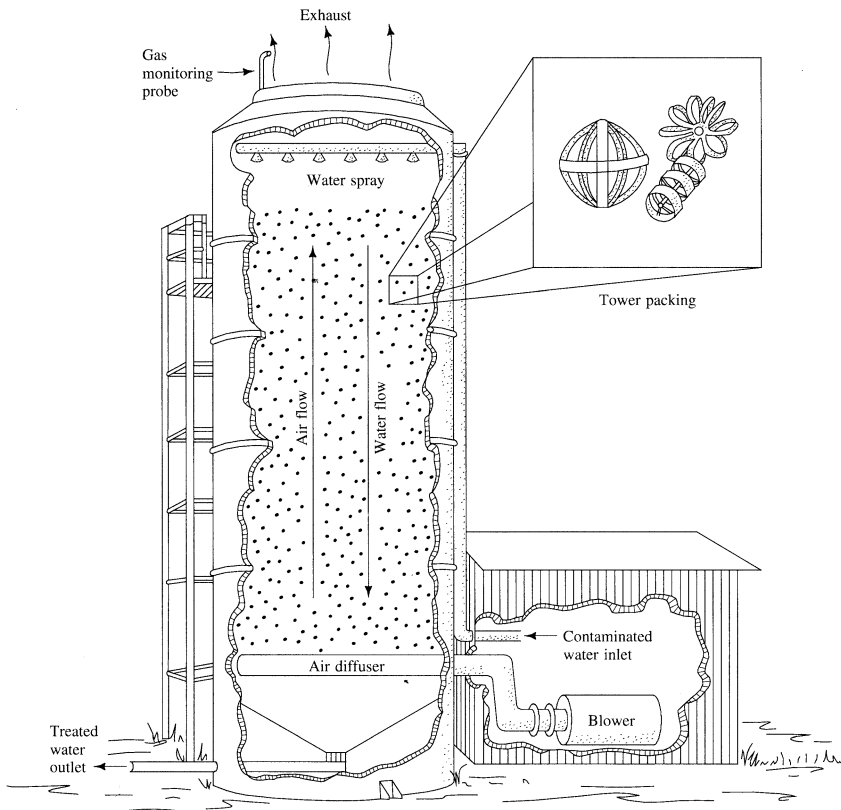
The majority of inorganic contamination needing treatment consists of metals, which can be removed by precipitation or adsorption. Often the treatment involves mixing of reactive agent(s) into the extracted contaminated water. Many metal hydroxides precipitate at a specific alkaline pH value. For these metals, adjustment of pH by adding lime can cause precipitation of the metal hydroxide, which is removed via a clarifier followed by filtration. Ferrous iron can be removed by aeration to create ferric iron, which will precipitate at a slightly alkaline pH. Hexavalent chromium must first be reduced to the trivalent state by lowering the pH to 3 and then adding a reducing agent such as sulfur dioxide. The trivalent chromium can then be precipitated as a

hydroxide by raising the pH above the neutral value. Arsenic can be coprecipitated with iron by adding dissolved iron at a pH of 5 to 6 and then raising the pH with lime to between 8 and 9. Arsenic also adsorbs to activated alumina.

Inorganic compounds can be removed by ion exchange. This process uses a resin to adsorb and retain anionic or cationic contaminants from groundwater. In place of the toxic ions, the resin releases benign anions or cations, such as chloride and calcium. When the resin becomes saturated after all of the resin's functional groups have been occupied, it needs to be recharged before reuse, or possibly disposed and replaced. This treatment approach is used commonly for nitrate, which cannot be removed by precipitation. Ion exchange has also been used for removing radiogenic isotopes, like uranium (Botha, Bester, and Hardwick 2009). Inorganic contaminants can also be removed by reverse osmosis and electro dialysis. In reverse osmosis, water is pressured to flow through a semi-porous membrane. While the water molecule passes through the membrane, many molecules and ions cannot and are retained on the membrane surface. In case of electro dialysis, flow through a membrane is induced by an electric potential and because the membranes are cation- or anion-selective, either positive ions or negative ions will flow through and can be exchanged for benign ions. This method has been used to remove radium, uranium, arsenic, nitrate, perchlorate, and hardness from drinking water (U.S. EPA 2015) or to remove cooper, chromium and arsenic from chromated copper arsenate (CCA) treated timber waste water (Ribeiro, Mateus, and Ottosen 2000).

9.4.3 Treatment of Dissolved Organic Contaminants

Many of the organic contaminants found in groundwater are volatile. They can be stripped from the water by exposing the water to a flow of air. This is accomplished in an air-stripping tower (Figure 9.20). The tower is a tall cylinder filled with an inert packing material, typically made of polypropylene. The packing material is designed to have a very high porosity and a large total surface area. The contaminated water is sprayed into the top of the tower onto the packing material. A blower attached to the bottom of the tower forces air up the tower at the same time that the water, which was broken up into droplets by the spray nozzles, trickles down the packing material. The volatile organic chemicals vaporize from the water into the air and are expelled out of the top of the tower. Care must be taken that emissions from the air-stripping tower do not create an air-pollution problem. For this reason, the exhaust from the air stripper is typically treated by sorption onto activated carbon or a thermal treatment unit, as can be the case for gasoline type vapors. For typical air stripping towers 4.6 to 6 m (15 to 20 ft) in height and containing conventional packing, removal efficiencies of VOC are around 99%. The removal efficiencies can be improved by adding a second air stripper in series with the first, heating the contaminated water, or changing the configuration of packing material (FTRC 2015). A potential problem with air stripping is biological fouling, which describes the buildup of biofilms growing on the inside of the air stripping tower. If not attended to, biofouling can lead to decreasing treatment and eventually clogging of the system. Another common problem with air strippers is precipitation of iron or other minerals. Typically, if the treated groundwater contains more than 5 mg/liter iron or its hardness is greater than 800 mg/liter (FRTR 2015), it becomes likely that mineral precipitates will build up inside the stripper tower. Mechanical filters, such as sand beds, might be needed to filter the precipitated iron from the wastewater stream.

FIGURE 9.20 Design of an air-stripping tower.

and to greatly reduce the risk of declining treatment effectiveness of the system. These and other air stripping system design considerations are covered by Kuo (2014).

A number of organic compounds have low volatility and, hence, a low removal rate in an air-stripping tower. For example, the former gasoline additive MTBE has a Henry's Law constant 0.0224 at 20°C whereas that of benzene is about 10 times greater (0.228). This indicates that MTBE is much more difficult to remove by air stripping than benzene. Many of these low volatility compounds can be sorbed onto granular activated carbon (GAC). The contaminated water is pumped through a reaction vessel filled with GAC. These compounds partition onto the carbon and are hence removed from the water. The ability of the carbon to remove organics is eventually exhausted, and it must be replaced. Spent activated carbon can be regenerated by heating to drive off the sorbed organics.

Other methods for treating dissolved organic matter include the many biological methods that have been developed for wastewater treatment. A few organics, such as 1,4-dioxane, are resistant to air stripping, carbon absorption, or biological treatment and prove to be very difficult to remove from contaminated groundwater. However, Kiker et al. (2010) tested four *ex situ* advanced oxidation processes, i.e., Fenton's Reagent, hydrogen peroxide with ultraviolet (UV) light, hydrogen peroxide with ozone,

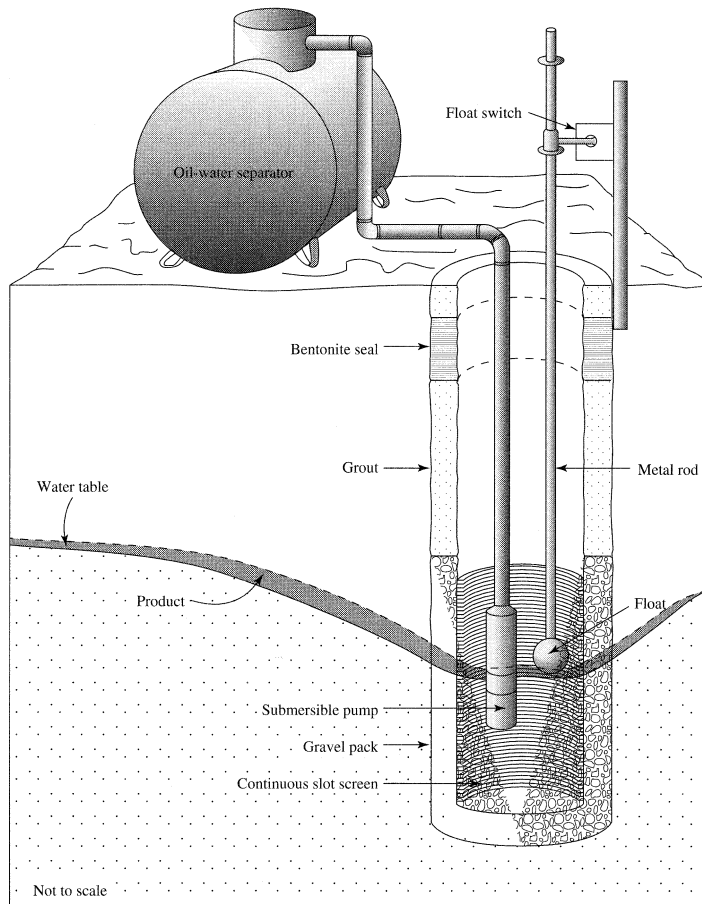
and catalyzed persulfate. Based on their studies, they found that *ex situ* application of Fenton's Reagent was successfully destroying 1,4-dioxane and TCE co-contaminants and converting them into carbon dioxide, water, and chloride ion.

■ 9.5 Recovery of Nonaqueous Phase Liquids

If a mobile layer of a light nonaqueous phase liquid (LNAPL) has accumulated on the water table or the top of the capillary zone, it will flow in the direction in which the water table is sloping. The floating product can be recovered by depressing the water table with extraction wells or trenches. The product then flows to the well or trench, where it can be captured.

Figure 9.21 shows a simple **LNAPL skimming** well. The well has a continuously slotted screen, which extends from above the top of the floating product to below the planned drawdown of the water table. A single pump is positioned so that it can pump both water and skim the LNAPL. The pump is activated by a float switch set so that the pumping level is maintained close to the pump intake so that both water and LNAPL will be withdrawn. If a floating skimmer pump is used, the switch is not needed. Such a system is relatively inexpensive and easy to operate. However, there are two potential problems with such a treatment system. First, by lowering the water table during pumping, the LNAPL can penetrate deeper into previously uncontaminated parts of the aquifer (smearing). Second, the pump may emulsify the water and oil, so that an oil-water separator is needed to recover the product (Blake and Lewis 1982). In addition, soluble organics may be introduced into the water during the mixing process. If this occurs, then the water may also need treatment. However, the water may already contain soluble organics from the floating-product layer, so water treatment would already be required.

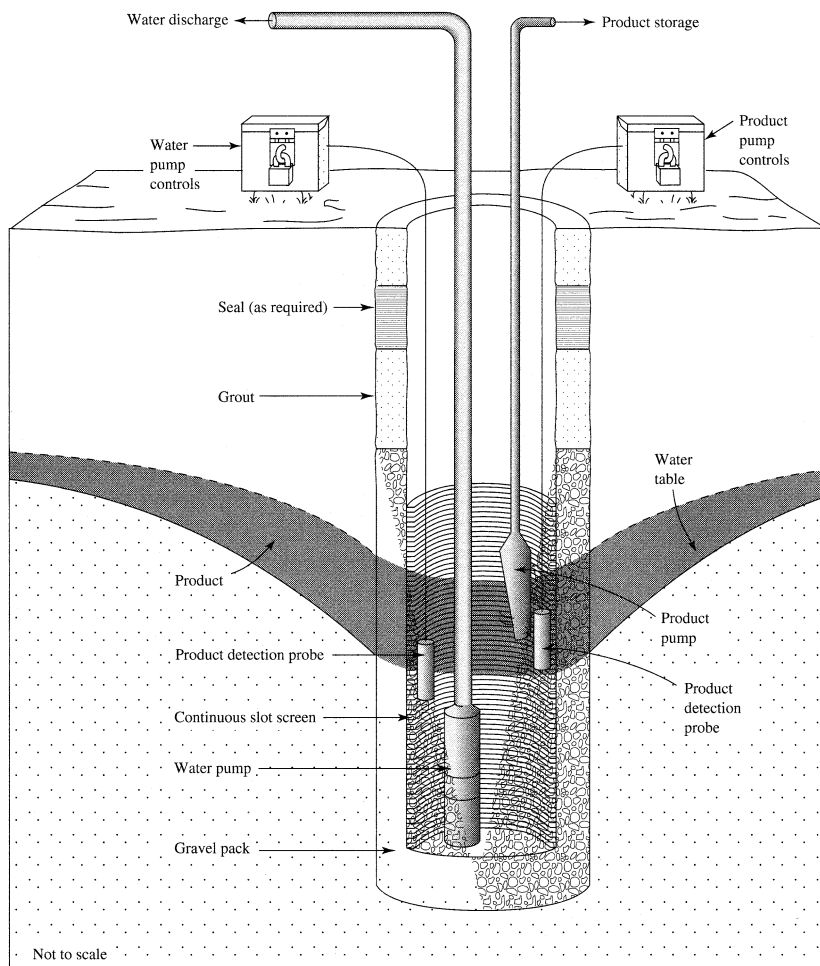
While the risk of LNAPL smearing remains, the use of a two-pump liquid extraction system avoids the problem of the oil-water emulsion forming. A water pump is used to depress the water table. This is set some distance below the pumping-water level. A product-recovery pump set at the pumping level of the water table recovers the product in a condition allowing it to be sent directly to storage for later disposal. Two-pump systems can be installed in a single well (Figure 9.22). The casing and screen must have a large-enough diameter to hold both pumps and some float switches. A continuous-slot screen that extends from a point above the LNAPL layer to well below the water-pumping level is used. The water pump is set near the bottom of the well. A product-detection probe is located just above the water pump. If the product level drops to that depth, it is detected, and a signal is sent to shut down the water pump so that product is not drawn into the water pump. This isolates the water discharge so that it doesn't become contaminated with product. The product pump is located at the planned pumping level and has a switch activated by a product-detection probe to turn it on and off. An alternative to a dedicated LNAPL pump is a belt skimmer, which consist of a hydrophobic belt that is partially immersed into the LNAPL layer. While the belt is moving slowly through the NAPL, the free product adheres to the belt and is lifted to the surface where it can be scraped off and collected before the belt descents back into the subsurface. Because such a **belt skimmer** requires more space than most wells can afford, such systems are usually installed in LNAPL interception trenches. The advantage of this and the dual-pump extraction system is that the water

FIGURE 9.21 Single-pump system for recovery of light nonaqueous phase liquid.

Source: S. B. Blake and R. W. Lewis. 1982. Proceedings of the Second National Symposium on Aquifer Restoration and Ground Water Monitoring, pp. 69–76. Used with permission.

and LNAPL are not mixed in large measure. In general, LNAPL recovery works for all LNAPL types; however, lower-viscosity LNAPL (0.5–1.5 cP), such as gasoline or kerosene is much more recoverable than high-viscosity LNAPL (>6 cP) (ITRC 2009a). The recovered LNAPL can often be refined or mixed with cleaner product for use, so some cost recovery is possible.

Another LNAPL extraction approach is **multiphase extraction** technology in which one or two pumps are employed to create a vacuum in the soil surrounding the well and to pump contaminated groundwater. The advantage of this more complex treatment system is that it simultaneously removes LNAPL, contaminated groundwater, and vapors. If a vacuum is applied to the unsaturated soil surrounding the multiphase extraction well and the soil is pneumatically connected to the atmosphere, additional oxygen is drawn into the pore space. The extra oxygen can enhance the

FIGURE 9.22 Double-pump, single-well system for recovery of light nonaqueous phase liquid.

Source: S. B. Blake and R. W. Lewis. 1982. Proceedings of the Second National Symposium on Aquifer Restoration and Ground Water Monitoring, pp. 69–76. Used with permission.

aerobic biodegradation of organic compounds and thus help to speed up the remediation process. Such a treatment system is known as **bioslurping**.

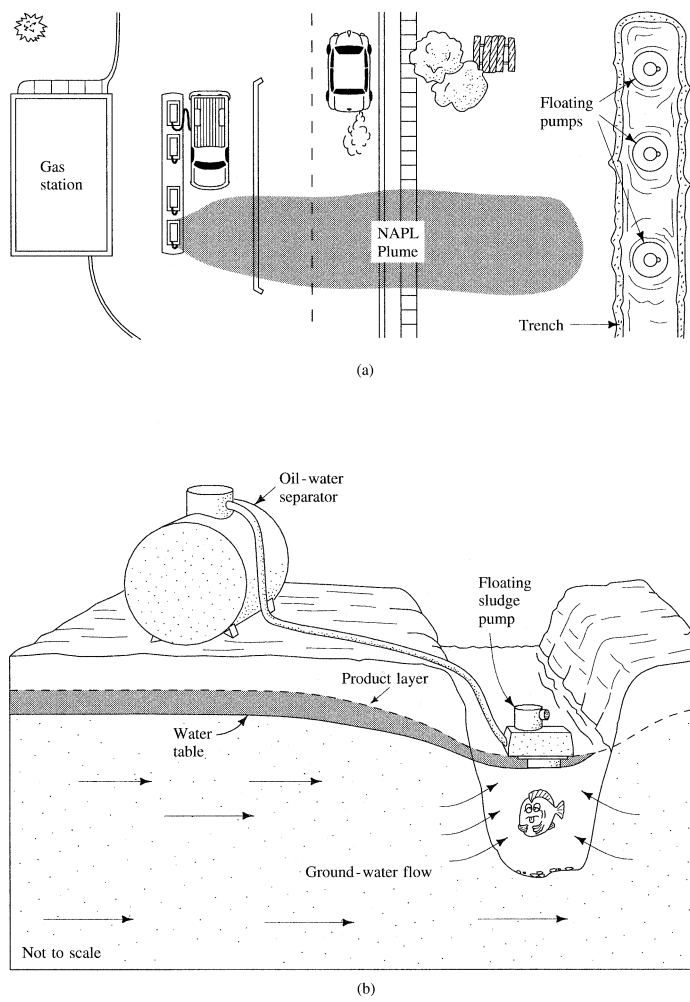
If wells already exist that are not suitable to hold two pumps—for example, their diameters are too small or the screen does not intercept the water table—then two pumps in two wells can be used. The deeper well, with a screen set below the water table, can be used as the extraction well to depress the water table. A second well for the product pump is constructed so that the screen extends from above the top of the product layer to below the pumping level. Product-detection probes are used to turn the pumps on and off.

Care needs to be taken when the product-recovery wells are first installed to be sure the pumps are set at the proper elevation and pumping rate. It will take several days of

adjustment to determine the stable pumping level and the proper setting of the product-recovery pump. These systems can be set up to operate automatically and need only periodic checking to determine that the pumps and controls are still operating properly.

Skimming trenches can also be used to recover floating product. The trench is excavated to a depth below the water table and extends beyond the limits of the product plume. If possible, the trench should be downgradient from the plume so that a minimal amount of water needs to be withdrawn from the trench to capture the plume, as shown in Figure 9.23a. Drawdown in the trench needs to be great enough to reverse the groundwater gradient on the downgradient side of the trench so that the floating product cannot flow out. A floating single or dual-pump system utilizing a skimmer

FIGURE 9.23 (a) Location of an interceptor trench used to capture a floating plume of a light nonaqueous phase liquid. (b) Cross section of trench and floating pump to capture the floating product and depress the water table.



pump or a belt skimmer can be used to lower the water table and remove the product. The mixture of product and water is sent to an oil-water separator (Figure 9.23b).

Floating product can also be captured by buried drains. A trench is excavated below the lowest expected position of the water table at a location downgradient of the floating plume. Six inches of coarse stone is placed at the bottom of the trench and then a perforated plastic pipe is laid on the stone. The plastic material of the pipe must be compatible with the product to be recovered. The pipe drains into a sump, from which product and groundwater are pumped for treatment. The fluid level in the sump is kept low enough that the water table falls to the elevation of the pipe, causing the product layer to drain into the pipe. This type of system can be installed in urban areas where an open trench would present a safety hazard. It can also be used with gasoline, which can present an explosion hazard. If gasoline is being recovered, explosion-proof pumps and motors must be used.

■ 9.6 Removal of Leaking Underground Storage Tanks

Underground storage tanks (UST) have been used for many types of products, particularly petroleum distillates. USTs are therefore common on industrial sites, gas stations, and even private homes, where heating oil is often stored in buried tanks. In 2011, there were approximately 590,000 federally-regulated, active USTs at approximately 212,000 sites across the United States (U.S. EPA 2012a). It must be noted that in some jurisdictions, like the United States, a UST may not necessarily have to be buried entirely but is considered an “underground” storage tank if at least 10% of its combined volume is buried beneath the surface (Resource Conservation and Recovery Act, 42 U.S.C. § 6901-6992k). While the number of gas stations in Europe, the United States, and many other developed countries is decreasing, in parts of the developing world, thousands of new gas stations are being built. For instance, in India the number of petrol stations has jumped from roughly 18,000 to over 43,000 in the three years prior to 2012 (Indian Express 2012). India now has more than three times as many petrol stations than Germany (14,209 in 2015) (ADAC 2015). Around the world, USTs have been in use for many decades and many of older tanks have exceed their design life time. For instance, the U.S. EPA documented 501,000 releases from UST (U.S. EPA 2012a). It is therefore not surprising that tanks spring leaks, resulting in large numbers of new soil and groundwater pollution problems globally.

A typical UST system consists of the tank, fittings, and piping to add product to the tank as well as to remove it. Particularly at gas stations, it is not uncommon to have two or more underground storage tanks located closely together in what is sometimes referred to as a tank field. Those tanks can be large, e.g., 100 m³ (26,417 gal) and are frequently refilled, sometimes daily at very busy gas stations. Leaks can develop in the tank or in the associated fittings and pipes. USTs storing volatile liquids have an off-gas exhaust. At gas stations, the fuel distribution terminates in the dispensing systems (pumps), which add other possible sources of leakage or accidental spills. Old-style single wall steel tanks can corrode to the point where holes develop. This is referred to as pitting. Tank hull corrosion can be reduced by burying a sacrificial anode near the UST, which will corrode first and inhibit tank corrosion. Further, pipe fittings may not have been properly tightened when installed. Ruptures may develop due to settling, and

the tank may simply overflow if it is overfilled. Leaky tanks are generally identified by means of a “tightness” test performed by a qualified contractor. At many gas stations in the United States, Europe, and Australia, the old single wall steel tanks have been replaced by double-walled tanks, sometimes fabricated from corrosion resistant material, such as carbon fiber or a combination of steel and aluminum. These modern tanks are outfitted with overfill protection, leak detection, and anti-corrosion systems which largely reduced, but not entirely eliminated, the number of leaking UST incidences.

The remedy for an underground tank that is known or suspected of leaking is to remove it. In most jurisdictions, the removal of a leaking underground storage tank (LUST) is highly regulated. In the United States, for example, the Resource Conservation and Recovery Act, 42 U.S.C. § 6901 et seq. addresses LUSTs and the U.S. Environmental Protection Agency together with other state and local agencies offer resources and tools to help implement these regulations (e.g., EPA Office of Underground Storage Tanks; www.epa.gov/oust/index.htm). The removal process is performed by a contractor, but the process should be monitored by an environmental professional. Figure 9.24 shows a leaking underground storage tank being removed. This tank is still leaking, because the product was not removed before the tank was lifted from the excavation. This is an example of how not to “yank a tank.”

FIGURE 9.24 Removal of a leaking underground storage tank. Note the product pouring from holes in the tank!

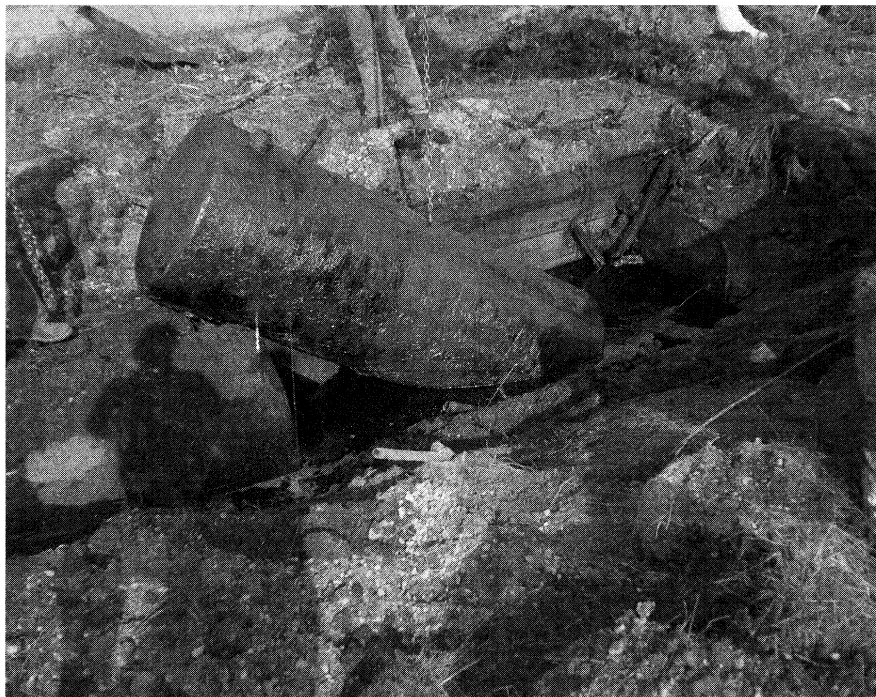


Photo credit: Kenneth Hawk.

A UST removal operation is typically preceded by a detailed site investigation during which soil and, if present, groundwater samples are collected at locations known as potential problem areas, i.e., at or near the UST or the distribution pumps. In the United States, this initial site investigation is called a Phase I environmental site assessment (ESA). It typically addresses both the subsurface as well as physical structures on the property that could potentially be a source of soil and groundwater contamination, e.g., waste oil storage areas. An ESA should also investigate if potential contamination sources exist beyond the property line because in some instances soil and groundwater pollutants might have migrated from an adjacent property. Many countries have detailed rules governing initial site assessment activities. In the United States, standards for the Phase I ESA have been established by the *American Society for Testing and Materials* (ASTM). The most current version of these standards (ASTM E1527-13) was approved by the U.S. EPA in 2013 as sufficient under the Comprehensive Environmental Response, Compensation, and Liability Act (“CERCLA”) 78 Fed. Reg. 79,319.

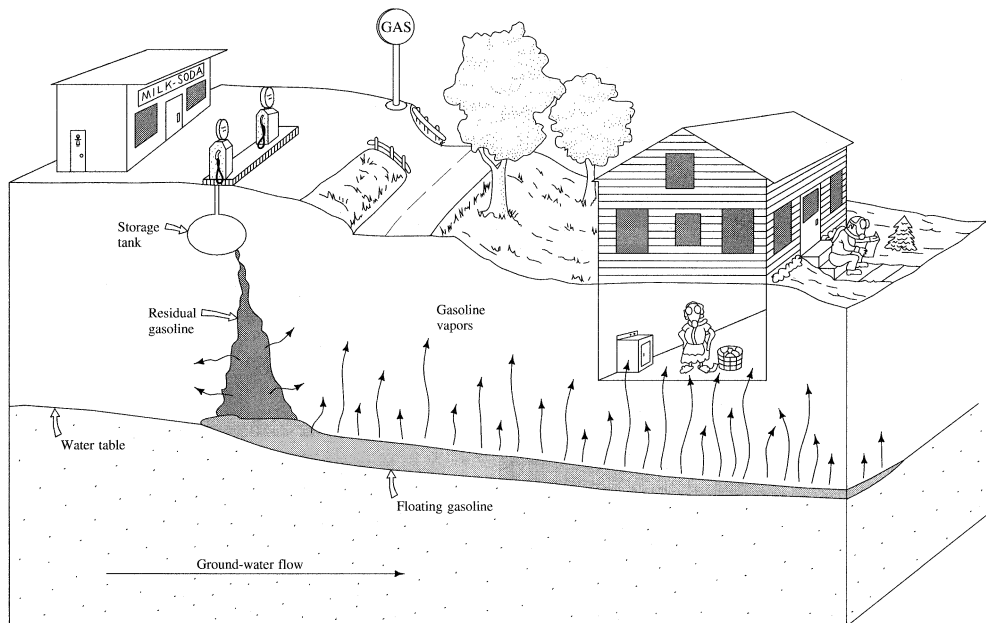
If the tank held an LNAPL, then a floating-product layer might have formed. If the tank held a DNAPL, then the DNAPL may have sunk into underlying aquifers. In either case, the investigations differ substantially for sites with LNAPL contamination than for those with DNAPL contamination, because the NAPLs behave differently in the subsurface. While a properly conducted site investigation should discover soil and groundwater contamination problems, sometimes contaminants “hide” below tanks or the foundations of nearby buildings. The experienced supervising environmental professional therefore expects the unexpected and has planned for unforeseen complications.

■ 9.7 Soil Vapor Extraction (SVE)

Volatile organic compounds (VOCs) that are released on the ground surface or in the ground above the water table will leave residual materials in the vadose zone. This residual material can be in the form of residuals of pure phase product trapped in pore throats of coarse-grained soil by capillary forces, or pure phase material which has been absorbed into the matrix of fine-grained soil where it occupies most of the pore space. The volatile organic material will partition between the pure phase and the vapor phase, occupying the pores in the vadose zone. Both LNAPLs and DNAPLs can be trapped in the vadose zone in this manner.

LNAPLs floating on the surface of the capillary zone can also partition so that the vadose zone above the LNAPL lens will have vapors present. As a LNAPL lens moves, additional parts of the vadose zone can become contaminated with VOC vapors. Even if the LNAPL is not moving, VOC vapors can migrate through the vadose zone (Figure 9.25).

The presence of VOCs in the vadose zone can be determined by collecting a soil sample and having it analyzed. Care must be taken to prevent the loss of VOCs from the sample. It is common practice to composite several soil samples into a single sample in order to reduce the cost of laboratory testing. However, the process of compositing may result in significant loss of volatile materials, especially on a hot day. An often better way to trace VOC vapors in the vadose zone is by soil vapor sampling techniques described in the previous chapter. Collecting soil gas samples by these methods is limited to sites with sufficiently permeable vadose zone material and a water table which is not near the surface.

FIGURE 9.25 Release of organic vapors in vadose zone from residual saturation and floating product.

Soils contaminated with VOCs can be remediated with **soil vapor extraction** (SVE), also known as “soil venting,” “vacuum extraction,” or “vapor extraction systems” (VES). This process is analogous to pump-and-treat for groundwater except that air is the medium that is moved through the area of contamination in the vadose zone. The contaminant partitions into the moving air and is removed. As with water moving through an aquifer, the air will preferentially flow through the more permeable materials and bypass the low-permeability zones. The result is the multi-stage process illustrated by Figure 9.13. Initially there will be a large mass removal. In fact the mass removal will be much faster than with water since one can move many more pore volumes of air than water through a given mass of the earth in the same amount of time (Nyer and Schafer 1994). However, eventually vapor extraction will reach the asymptotic part of the removal curve of Figure 9.13 as diffusion of vapor from the fine-grained zones into the coarse zones where the air is moving becomes the rate-limiting factor. The process can be advanced somewhat by using heated air, especially in the winter when the outside air is cold.

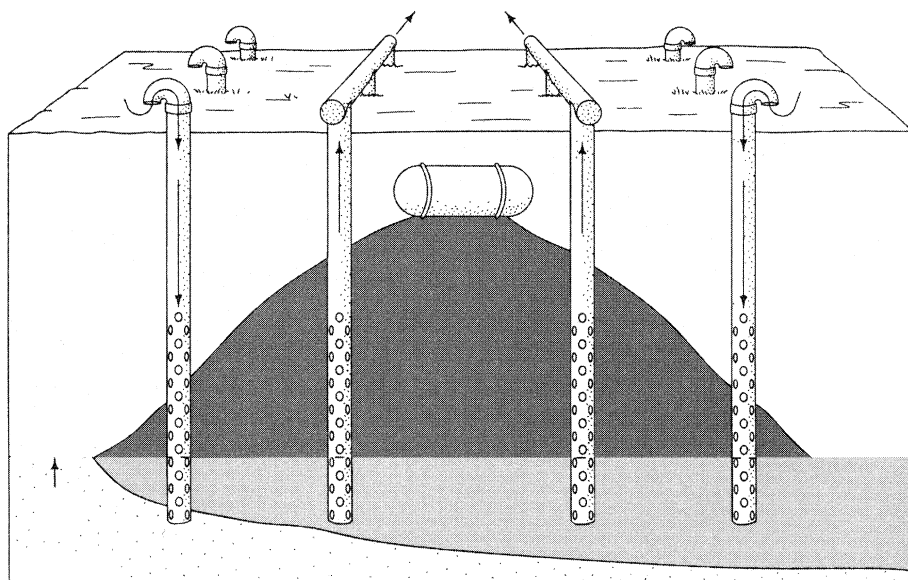
Removing the residual NAPL in the vadose zone not only remediates the soil, but it aids in the remediation of the groundwater. The residual NAPL in the vadose zone is an ongoing source for groundwater contamination as it becomes dissolved by infiltrating precipitation that recharges the water table.

Soil vapor extraction can also be used to remediate floating layers of highly volatile hydrocarbons. Rather than the LNAPL being removed in liquid form, it can be removed as a vapor through the SVE wells (U.S. ACE 2003). If the water table is depressed by pumping, the uppermost part of the aquifer will become part of the vadose zone. LNAPLs floating on the top of the capillary fringe will also drop and

leave residual material in the newly formed part of the vadose zone. Since soil vapor extraction is more efficient than pump-and-treat in removing contamination, the smear zone between the original position of the water table and the new position of the water table can be remediated more efficiently if the SVE system is designed to move air through that part of the earth. For this reason, it is good design practice to extend the SVE system a little below the water table. This will take advantage of both seasonal declines in the water table and declines caused by pumping.

Soil vapor extraction systems can be constructed using wells in the vadose zone that are designed in much the same way as groundwater wells. Wells would be used in areas where the depth to the water table is 3 m (10 ft) or more deep. The wells contain a slotted-plastic well screen. The wells will not be developed the way that water wells are, so the well screen is set in coarse gravel backfill for greatest air flow. The upper 1.5 m (5 ft) or so of the well is solid plastic casing set in cement grout. It is important to seal the annular space so that the well does not just pull atmospheric air down the outside of the casing (short-circuiting). A SVE well is designed to withdraw vapor from the vadose zone in a circular area around the well. Air-vent wells can be used in conjunction with the SVE wells, to direct flow and allow easy air entry to the subsurface. In order to extract the vapors, fresh air must be circulated through the pores containing the VOC. The air-vent wells provide a pathway of least resistance to ensure that air will circulate through the entire volume of the soil that is being remediated (Figure 9.26). Air-vent wells are constructed in the same way as SVE wells, but instead of being connected to a suction header, the upper end is open and capped with an inverted-U trap to keep out rain. If air-vent wells are not used, the SVE wells must be pumped at varying rates to make sure permanent stagnation zones between wells do not develop.

FIGURE 9.26 Soil vapor extraction system consisting of vapor extraction wells and air-vent wells.

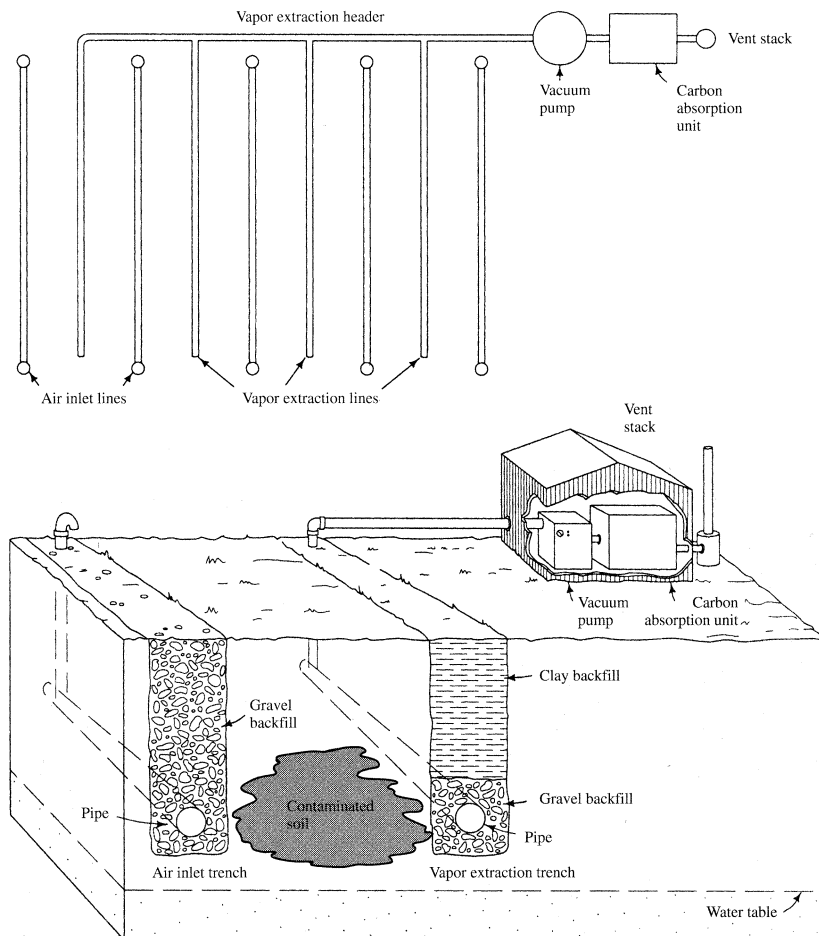


If the water table is shallow, SVE wells are not effective. In this case, soil vapor extraction trenches can be used. The trenches are excavated through the vadose zone to just above the seasonally high water table. A layer of gravel is put down and then a perforated plastic pipe is laid in the trench and covered with gravel. The rest of the trench is backfilled with low-permeability material to prevent short-circuiting of the vadose zone by atmospheric air circulating through the backfill material. If a low-permeability cap is to be constructed over the SVE system, then some type of venting system using air-inlet trenches or wells may be needed to allow air to sweep through the vadose zone in order to flush out the vapors and allow the residual organic compounds sorbed onto the soil to partition into the air. Even if a cap is not placed over the SVE system, the air-inlet trenches or wells will help to circulate air through the entire depth of the contaminated soil. Air inlet wells can be closed and opened to change the pattern of subsurface air flow patterns during SEV to see if greater contaminant mass withdrawal can occur. Changing patterns of air infiltrating from the ground surface can also be temporarily achieved by soaking the surface with water and physically occluding the soil pore space, producing more horizontal and less vertical flow. Figure 9.27 shows a vapor extraction system with air-inlet trenches. Air trenches or wells alternate with SVE trenches or wells. Such a system can be designed so that a given trench could be used as either an air-inlet trench or an SVE trench. This maximizes the operational utility of the system.

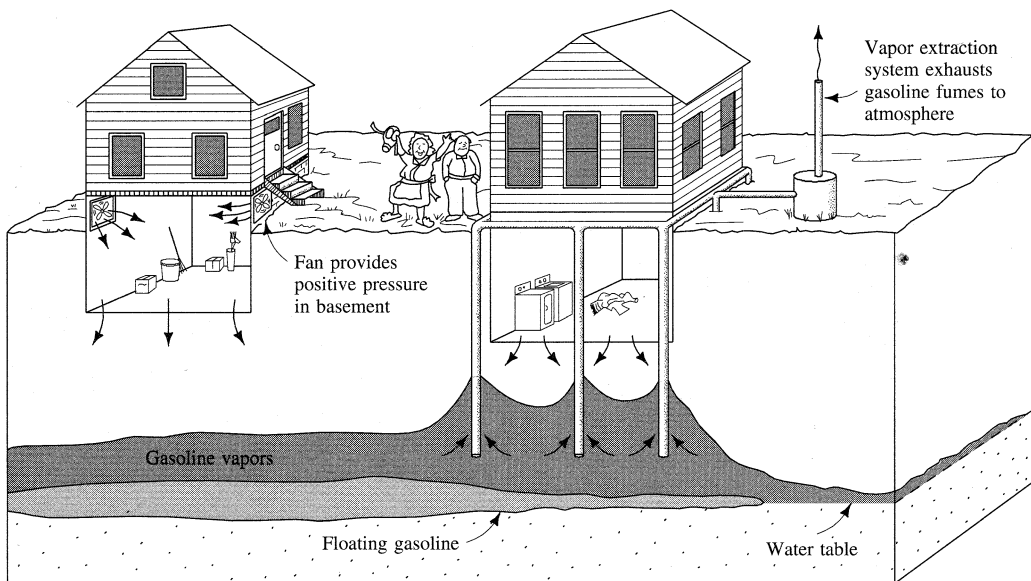
Whether SVE wells or trenches are used, a vacuum system is needed to apply suction to the wells or pipes. A suction header is attached to each extraction pipe or well and extended to a vacuum pump. The exhausted air with the vapors is passed through activated-carbon filters to remove the vapor if an air-pollution problem would result from the discharge of the vapors to the atmosphere, but not before a monitoring point on the outlet line (often a septum for a syringe port, or a valve where vapor can be diverted to collection in a Tedlar® bag or evacuated metal canister for analysis). Such monitoring points are essential to measure concentrations of contaminants in exhaust vapor and calculate mass removal with time.

There are general limitations to the SVE approach. First, the permeability of the soil material must be sufficiently high to permit gas flow through the treatment zone. The reach of each well is defined as the radius of influence (ROI) which can be estimated using computational models (e.g., Sawyer and Kamakoti 1998). Heterogeneous soils with layers of less permeable, fine-grained strata, such as silt or clay, are more difficult, if not impossible, to treat because of mass transfer limitations associated with the fine-grained materials or the development of preferential pathways circumventing those low-permeability areas. Also, high soil moisture content of the soil can limit the gas flow. Soil moisture can be controlled by capping the treatment area to prevent infiltration of precipitation from the surface. However, during the SVE treatment soil moisture is removed together with VOC vapors. The resulting drying of the soil can result in soil compaction and possibly settlement movements that can damage nearby buildings. There are a number of guidance documents available to aide in the design of SVE systems and to assess their performance (e.g., U.S. EPA 2001; U.S. ACE 2002).

Vapors can migrate through the soil and accumulate in basements, where they can reach toxic levels or pose a threat of fire or explosion in case of many hydrocarbons. This situation is referred to as a **vapor intrusion** problem. Careful consideration of vapor intrusion into buildings is warranted at all sites where vapor forming chemicals are

FIGURE 9.27 Soil vapor extraction system consisting of trenches installed under a clay cap.

present in the soil or groundwater (NRC 2013). To this end, the U.S. EPA has published a number of guidance documents to illustrate how subsurface conditions and building-specific characteristics determine the distribution of vapor forming chemicals in the subsurface, how the indoor air concentrations relate to a source concentration, and how to mitigate the vapor intrusion problem (e.g., U.S. EPA 2012b; 2015b; 2015c). Vapor control measures may be needed to protect the health of humans living or working in the affected structures. Such measures can be accomplished by installing wells in the vadose zone and pumping air and vapors from them (Figure 9.28). This will keep the vapors from migrating into the basement. Another remedy is to place a fan so that it blows air into a basement. This pressurizes the basement and may keep the vapors out. The positive-pressure technique may be most useful to mitigate the build-up of radiogenic radon gas in basements but it is not recommended for preventing vapor intrusions related to organic VOC. Also, this approach cannot be used in climates where the outside air in the winter is below freezing; otherwise the cold air will freeze the pipes in the basement.

FIGURE 9.28 Control of organic vapors in the vadose zone.

Source: Modified from M. J. O'Conner, J. G. Agar, and R. D. King. 1984. Proceedings of Conference on Petroleum Hydrocarbons and Organic Chemicals in Ground Water: Prevention, Detection and Restoration. National Ground Water Association.

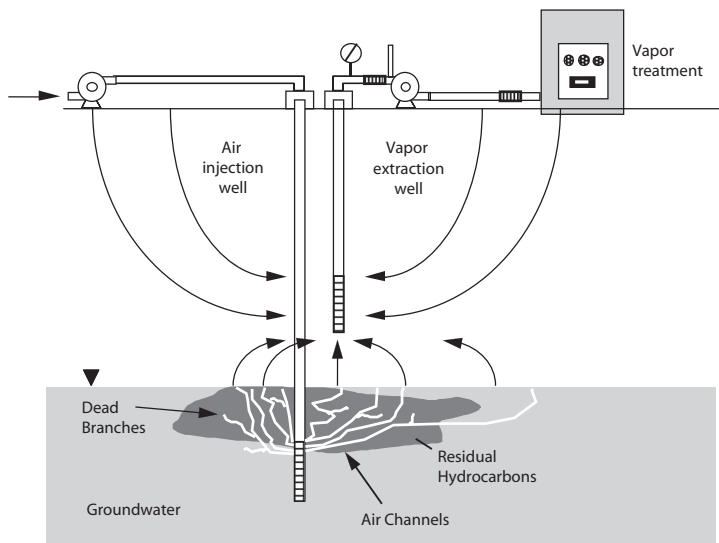
■ 9.8 Air Sparging and Bioslurping

As we have seen in the previous section, air is a much more efficient medium for removing volatile organic contaminants than water because we can move air through the ground more rapidly than water. The next two techniques utilize this principle to effect soil and groundwater contamination.

In air sparging an air injection well is installed below the water table. The air is injected into the aquifer through a well point that is located below the zone of groundwater contamination. The idea is that the air bubbles will rise through the contaminated zone and strip the VOCs that are present. The air bubbles will then rise to the vadose zone where a vapor extraction system will remove the volatile vapors (Figure 9.29). Ideally, they will rise in a zone shaped like an inverted cone, with the well point at the tip of the cone. The air should not rise along the well casing, thus bypassing the zones of contamination. This means that the well point should be well sealed so that air cannot follow the casing to the surface. The amount of air that is injected is small and small-diameter well points, less than one inch in diameter, are sufficient. These can be driven using flush-jointed steel pipe in many geologic environments.

As with all other methods, it has been found that the air bubbles will follow the most permeable pathways (Nyer and Suthersan 1993). This means that the air will follow preferential pathways and not be evenly distributed, which can lead to the development of “dead zone,” i.e., area not reached by the air flow. This brings us back to the

FIGURE 9.29 Schematic diagram of a simplistic *in situ* air sparging system combined with soil vapor extraction.



Source: Leeson et al. 2002.

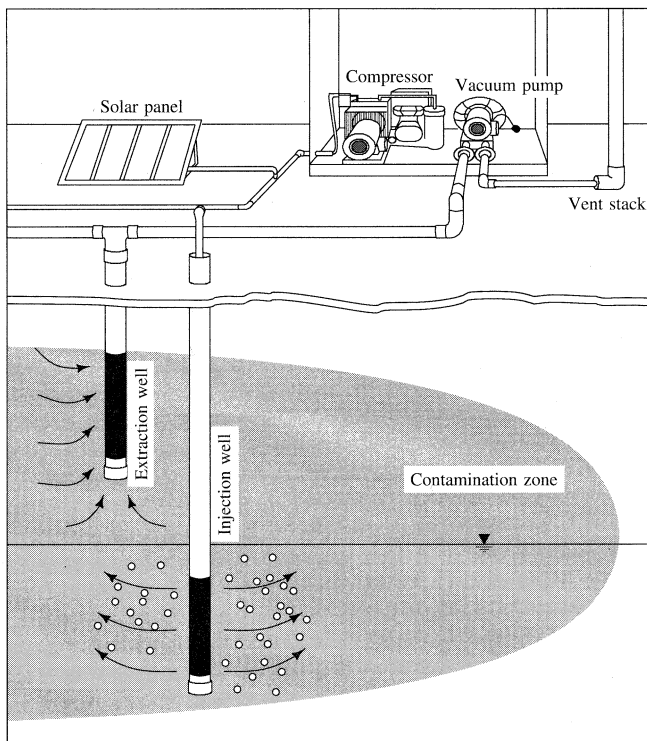
stages illustrated in Figure 9.13 where there will be a high initial rate of mass removal, but eventually diffusion will become dominant and the rate of removal will fall to some small number. Besides the preferential pathway and dead-zone problem, air sparging should not be considered at sites where LNAPL is present (unless it is part of a “treatment train” of successive remedial actions and follows LNAPL recovery/skimming). This is because air sparging can cause upwelling of the groundwater table which may displace free product to migrate away from the original source zone. Similarly, if the flow of the air injected into the subsurface by the air sparging system cannot be adequately controlled, there is a risk that contaminated vapors migrate away from the well. This can result in vapor intrusion problems in the basements of nearby buildings. Finally, this technique cannot be used for the treatment of confined aquifers because the injected air would be trapped underground or emerge by short-circuiting through monitoring wells.

A variation of the air sparging approach is biosparging, which is a frequently used term referring to air sparging systems operated without an SVE component (Leeson et al. 2002).

■ 9.9 Combination Methods

Ardito and Billings (1990) described a hybrid method called the subsurface volatilization and ventilation system. The system consists of a number of well nests. Each nest consists of an air-injection well, which is screened below the water table, and a vapor extraction well, which is screened in the vadose zone (Figure 9.30).

This approach combines physical removal of hydrocarbons with bioremediation. The SVE wells remove the volatile fraction of residual NAPL. The air sparged into the

FIGURE 9.30 Subsurface volatilization and ventilation system.

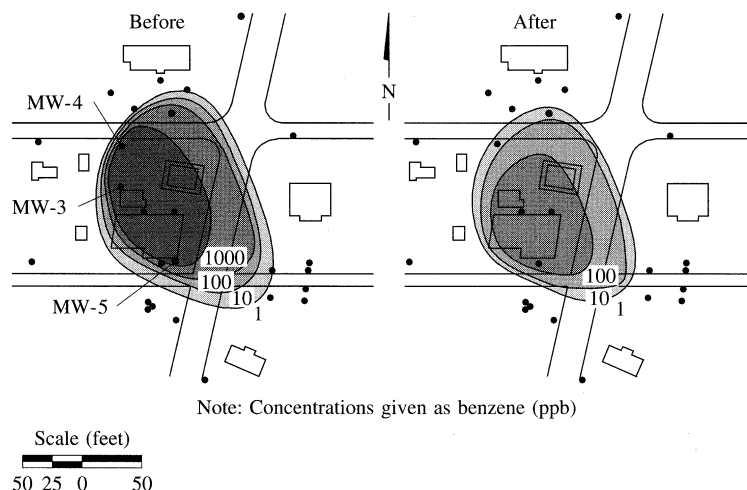
Source: C. P. Ardito and J. E. Billings. 1990. *Proceedings of Petroleum Hydrocarbons and Organic Chemicals in Ground Water: Prevention, Detection and Restoration*, pp 281–96. © 1990 National Ground Water Association. Used with permission.

groundwater removes some of the dissolved organics by air stripping. The oxygen added to the groundwater promotes biological activity to degrade organics below the water table. Nutrients can also be introduced by batch addition to further bioremediation. Ardito and Billings (1990) reported the use of this system to treat a site where 40,000 gal of leaded gasoline leaked from an underground storage tank. A pump-and-treat system at the site was operated for 3 yrs but had operational problems due to clogging of the injection well. A subsurface volatilization and ventilation system was installed and in 6 mo. caused a significant reduction in the extent and concentration of benzene, toluene, ethylbenzene, and xylene. Figure 9.31 shows the extent of the plume, in milligrams per liter of benzene, before and after the 6-month period. The reduction in benzene, toluene, xylene, and ethylbenzene in three monitoring wells is shown in Figure 9.32.

This system is particularly attractive for remediation of a plume that contains compounds such as chlorinated solvents, which are not as biodegradable as hydrocarbons. The air sparging provides an *in situ* air-stripping system, with the stripped material being captured by the SVE wells.

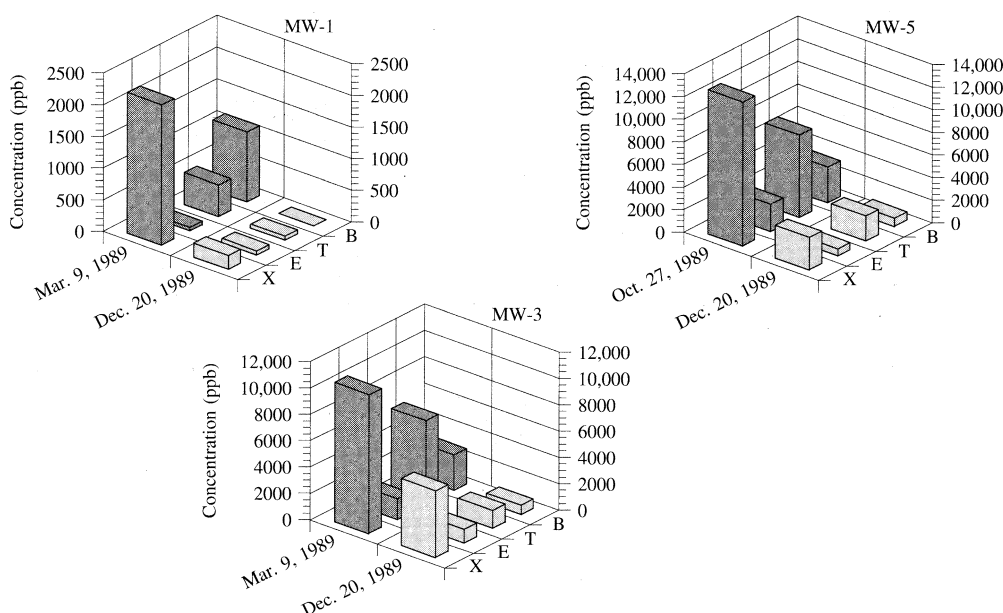
Soil vapor extraction wells can be combined with product-recovery wells to provide remediation of both a floating NAPL and a residual product in the vadose zone. This is

FIGURE 9.31 Extent of plume of benzene at a gasoline spill before and after treatment by subsurface volatilization and ventilation system.



Source: C. P. Ardito and J. E. Billings. 1990. *Proceedings of Petroleum Hydrocarbons and Organic Chemicals in Ground Water: Prevention, Detection and Restoration*, 281–96. National Ground Water Association. Used with permission.

FIGURE 9.32 Reduction in benzene, ethylbenzene, xylene, and toluene measured in monitoring wells after 6 mo. of operation of subsurface volatilization and ventilation system.



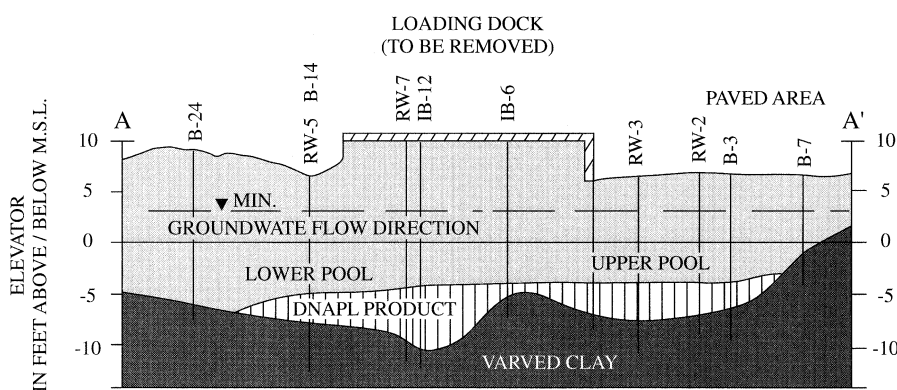
Source: C. P. Ardito and J. E. Billings. 1990. *Proceedings of Petroleum Hydrocarbons and Organic Chemicals in Ground Water: Prevention, Detection and Restoration*, 281–96. National Ground Water Association. Used with permission.

especially useful for volatile NAPLs such as gasoline. The product-recovery well has a well screen that extends up through much of the vadose zone. A single skimming pump is used; it pumps enough water to create a cone of depression. The product in the area of influence of the cone of depression flows into the product-recovery well, where it is also pumped by the skimming pump. If gasoline is being recovered, an explosion-proof pump is needed. Similarly, vapors moving through PVC piping can build up an unwanted static charge that can ignite explosive vapors. Vacuum is applied to the well when the skimming pump is operating. The vacuum extracts the vapors from the vadose zone. Many times such systems are installed under pavement areas at service stations. The pavement prevents short circuiting of the air flow so that it sweeps from outside the paved area and across the area where the soil is contaminated. The water and product are pumped to a separator, where the product is recovered and sent to storage. The water is then directed either to an air-stripping tower or, if only a few gallons per minute are being pumped, to a diffuser, which strips the volatile compounds from the water. A diffuser is a tank, which water enters at one end. There are a series of baffles in the tank that are each progressively lower, so the water cascades over each baffle as it flows toward the outlet. The volatiles are stripped as the water becomes turbulent going over the baffles. The volatiles are collected in a hood over the tank and exhausted with a blower to a stack. The exhausts from the vacuum-extraction pump and from the diffuser or air stripper are combined for dispersion through a stack. Regulations vary worldwide on permissibility of venting to the atmosphere and the conditions for air quality of those venting gases.

Case Study: Recovery of DNAPL pooled below the water table.

Discharge of solvents through a settling chamber next to an industrial facility in New Jersey, USA, resulted in the formation of a subsurface pool of DNAPL consisting of a mixture of 1,1,1-trichloroethane and carbon tetrachloride (Michalski et al. 1995). The site has 3 to 5 m (10 to 15 ft) of fine sand overlying varved clay. The bottom of the settling chamber was only

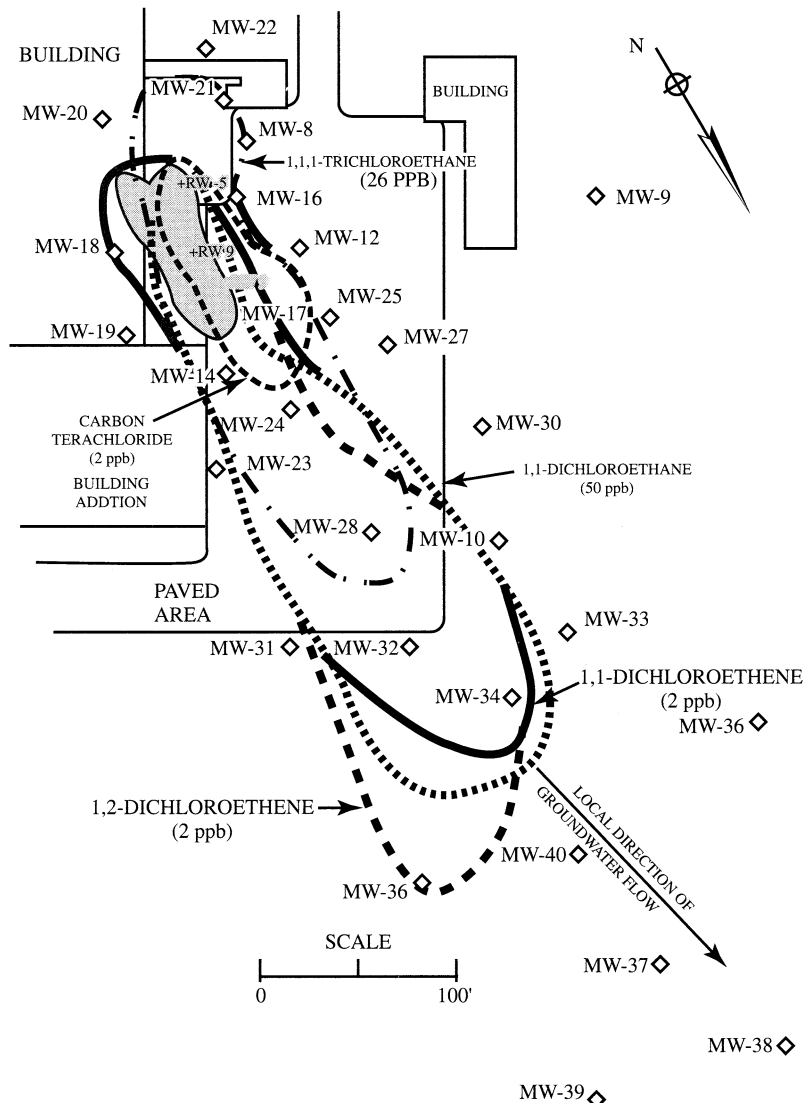
FIGURE 9.33 Cross section through a pool of DNAPL trapped in depressions on the surface of a varved clay.



Source: A. Michalski, M. N. Metlitz, and I. L. Whitman. 1995. A field study of enhanced recovery of DNAPL pooled below the water table. *Ground Water Monitoring and Remediation* 15:90–100. Used with permission.

about 0.6 m (2 ft) above the varved clay. The DNAPL flowed down the clay surface to accumulate in a pool. The initial pool overflowed into an adjacent low area and two pools were eventually formed (Figure 9.33). The shape of the clay surface controlled the movement and final location of the DNAPL. The DNAPL pool covered an area of ~255 m² (2750 ft²) and

FIGURE 9.34 Extent of DNAPL pool (shaded area) and dissolved chlorinated VOC plume.



Source: A. Michalski, M. N. Metlitz, and I. L. Whitman. 1995. A field study of enhanced recovery of DNAPL pooled below the water table. *Ground Water Monitoring and Remediation* 15:90–100. Used with permission.

was up to 0.9 m (3 ft) feet thick. The porosity of the sand which contained the DNAPL pool was 0.31 and the DNAPL was at a saturation ratio of 0.53. The volume of product was 14,200 Liter (3760 gal). A plume of dissolved constituents extended downgradient from the DNAPL pool (Figure 9.34). Dissolved constituents included 1,1,1-TCA and daughter products, 1,1-DCA, 1,2-DCA, and 1,1-DCE as well as carbon tetrachloride.

The primary recovery of the DNAPL was accomplished by the use of nine wells. The wells had a sump set into the clay so that any DNAPL could drain down into the sump. After 24 months of pumping 13,230 liter (3,495 gal) of DNAPL was recovered, with the majority recovered in the first six months. The recovery of the DNAPL was a surprisingly high 93–94% due to the favorable geology and the detailed knowledge of the site gained by the installation of numerous test borings and wells.

■ 9.10 Bioremediation

9.10.1 Introduction

In the preceding sections we have seen that physical removal of contaminants from soil and groundwater is limited by several factors (MacDonald and Kavanagh 1994):

- The physical heterogeneity of earth materials results in air or water flushing media moving primarily through the most permeable parts of the earth.
- Contaminants will diffuse into regions of the earth which are inaccessible and then slowly diffuse back into the more permeable zones.
- Contaminants will sorb onto solid surfaces and then slowly desorb.
- DNAPLs pools may be present as well as globules of DNAPLs which cannot be flushed from the aquifer by flowing water.

All of the above factors lead to Stage II (Figure 9.13) of the remedial process where physical removal of the contaminant is no longer effective. However, bioremediation can effectively renovate soil and groundwater containing small amounts of dissolved organic molecules, even those trapped in low-permeability zones and those clinging to soil particles.

The subsurface is populated with microbes, which in the near-surface have a fairly consistent population density with depth. This subsurface includes not only the soil-moisture zone, but also the rest of the vadose zone and underlying aquifers. The majority of subsurface microbes are growing on a substrate, i.e., a soil particle. Low levels of microbes in groundwater do not mean low levels of microbes in the ground. The majority of subsurface microbes are bacteria, but fungi, viruses, and protozoa are also found. The most important group of contaminant degrading bacteria is known as chemo-heterotrophic bacteria, which are organisms that obtain energy by the oxidation of electron donors.

Microorganisms produce enzymes. These natural catalysts aid in the metabolism (degradation) of many organic compounds, forming CO₂, methane (CH₄), water, and mineral salts. Such a complete degradation is called mineralization. Occasionally the (catabolic) enzymes participating in the degradation may transform contaminants to metabolites. This process is referred to as transformation. Strongly persistent substances are incorporated into the humic substance matrix mostly by means of radically acting enzyme reactions; this is designated as humification (ICSS 2006). Microbes from soil that has been contaminated with various synthetic organic compounds have

been found capable of degrading these compounds. In some cases microbes from uncontaminated soil have been unable to degrade the same compounds. However, other compounds can readily be degraded by microbes from uncontaminated soil. In some cases it is necessary for microflora to become acclimated to contamination before they can begin to metabolize it. The length of time that this acclimatization may take is highly site specific.

The environmental factors in the subsurface that affect the rate that microbes can metabolize organic contaminants include the pH and Eh, temperature, moisture, carbon substrate, amount of nutrients present (nitrogen, potassium, and phosphorous) and amount of electron acceptors (oxygen, ferric iron, nitrate, sulfate, and carbon dioxide). Some microbes can grow in either an aerobic or an anaerobic environment, while others only thrive in either aerobic or anaerobic conditions. However, many sites have a sufficiently varied microbial population to affect at least some degree of natural or intrinsic biodegradation processes.

9.10.2 Monitored Natural Attenuation

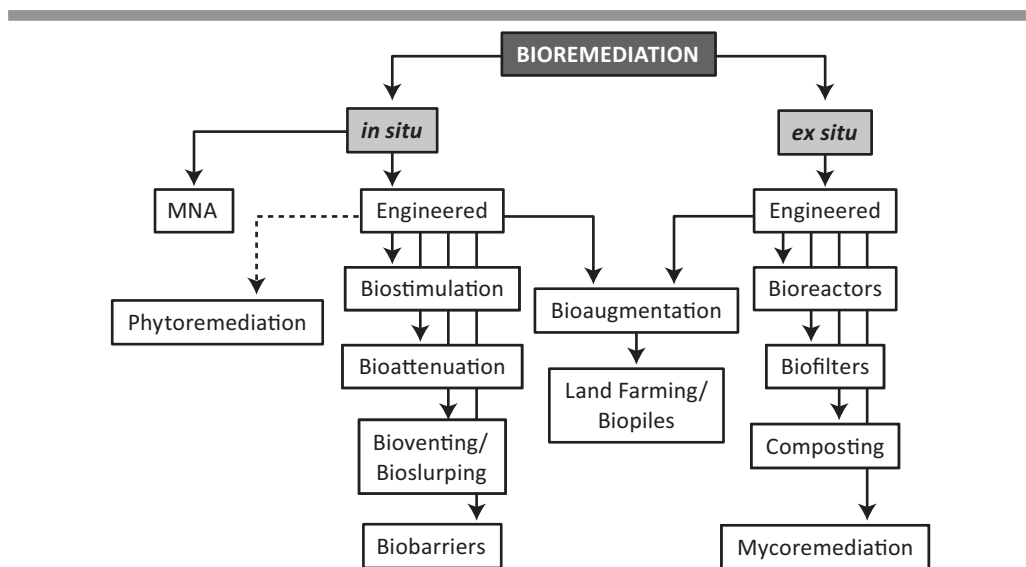
Natural attenuation refers to intrinsic processes that degrade predominantly organic contaminants to benign by-products. These processes include some combination of sorption, volatilization, dilution, and dispersion coupled with biodegradation. Natural attenuation may be biological, abiotic, or biogenic, i.e., where bacteria are required to create the necessary abiotic reagent(s) (NRC 2013). Bioattenuation can occur under either aerobic conditions where oxygen is the electron acceptor, or anaerobic decomposition where nitrate, ferrous iron, sulfate, or carbon dioxide is the electron acceptor. The geochemistry of biodegradation has been discussed in section 7.6.

While initially discredited by some as a “do-nothing” approach, it is now recognized that an effective remedial strategy can be based on natural attenuation if these processes are monitored very closely to ensure that attenuation continues over time and that contaminants are not migrating off-site. In recognition of the extensive monitoring requirements, this treatment approach has become known as **Monitored Natural Attenuation** (MNA) (Figure 9.35).

Over the last decades, MNA has been effectively used for treating many petroleum hydrocarbons, particularly BTEX and PAH (e.g., Sarkar et al. 2005; Neuhauser et al. 2009). Other compounds, including chlorinated contaminants (e.g., Wiedemeier et al. 1999) and oxygenates (e.g., API 2007) as well as inorganic compounds (e.g., perchlorate; Coates and Achenbach 2004) have also been successfully targeted by MNA. This treatment approach is often implemented after more aggressive treatments, such as chemically-enhanced flushing or *in situ* oxidation technologies leave residual contamination in place or if other techniques are cost prohibitive. In many countries, MNA is now a well-established remedial approach (Ruegner et al. 2006; NRC 2013). MNA is often used in combination with pump-and-treat. These two treatment approaches, either alone or in combination, were used as groundwater remedy at 82% of 164 Superfund facilities between 2005 and 2008 (NCR 2013).

MNA is most widely used for treating petroleum hydrocarbons plumes. Under natural conditions the capacity of a given subsurface environment to attenuate these compounds depends upon the naturally occurring concentrations of electron acceptors.

FIGURE 9.35 Bioremediation technologies for *in situ* or *ex situ* treatment of contaminated soil and groundwater. MNA: monitored natural attenuation.



Source: Modified after Mrozik and Piotrowska-Seget 2010.

Wiedemeier and others (1995) has given the following approximate stoichiometric values for calculating the assimilative capacity of a subsurface environment for BTEX:

- One mg of dissolved oxygen can be used by microbes to degrade approximately 0.32 mg of BTEX.
- One mg of nitrate can be used by microbes to degrade approximately 0.21 mg of BTEX.
- One mg of sulfate can be used by microbes to degrade approximately 0.21 mg of BTEX.
- Approximately one mg of BTEX will be degraded for every 21.8 mg of ferrous iron produced by the reduction of ferric iron.
- Approximately one mg of BTEX will be degraded for every 0.78 mg of methane produced by the reduction of carbon dioxide.

There is considerable evidence that under natural conditions many incidents of soil and groundwater contamination with BTEX compounds have reached a steady-state condition so that the plume is no longer spreading. Rice and others (1995) examined the database of leaking underground fuel tank sites in California. They found that only 0.5% of the documented underground releases of petroleum fuels had impacted water wells. In most cases the plume of petroleum contaminated groundwater did not extend more than 60 m (200 feet); the conclusion was that this was due to natural biodegradation. Of course, in highly permeable materials hydrocarbon plumes can travel a greater distance.

At many gas stations and other petroleum hydrocarbon LUST sites, MNA might be the most cost effective treatment technology. If there is a leaking fuel tank, once the

leak has been fixed, and if no groundwater contamination has occurred, the site may be closed and left to the natural soil microbes. MNA of BTEX contaminated groundwater may be particularly attractive if the concentration of dissolved BTEX is low and there is no LNAPL present, if the groundwater velocity is low, and if there are no downgradient water supply wells that could be threatened by the plume.

9.10.3 Enhanced Bioremediation

While monitored natural attenuation (MNA) is a predominantly passive treatment approach, enhanced *in situ* bioremediation relies on actively modifying subsurface conditions to optimize the growth conditions of contaminant-degrading microorganisms. Enhanced bioremediation activities typically involve biostimulation and/or bioaugmentation (Tyagi, da Fonseca, and de Carvalho 2011). As shown in Figure 9.35, bioremediation also covers biosparging and bioslurping methods as well as mycoremediation and bioactive permeable barriers (see Section 9.11). Mycoremediation is a form of bioremediation that uses conditioned native fungi and fungal mycelium applied mostly *ex situ* to soils to remove and degrade contaminants (Thomas et al. 2009). Another technology referred to in Figure 9.35 is phytoremediation. Although it relies on living plants and in part involves consortia of naturally occurring microorganisms to attenuate or sequester contaminants in soil and groundwater, phytoremediation is generally considered a stand-alone treatment approach separate from bioremediation (see Section 9.15).

Biostimulation refers to the delivery of electron acceptors (e.g., oxygen for aerobic metabolism), electron donors (e.g., hydrogen for reductive dehalogenation), or suitable precursors that are utilized by organisms to support the biochemical transformation of the target contaminant (NCR 2013). Varied combinations of injection and pumping systems are sometimes used to promote subsurface mixing, and new studies are investigating the creation of *in situ* engineered chaotic advection by altering time-dependent Darcy flows in porous media (Trefry et al. 2012; Cho et al. 2014). **Bioaugmentation** is the practice of amending specialized microbial strains, which can potentially include genetically modified indigenous or allochthonous strains, at sites where the native microbial populations are insufficient or incapable of transforming the contaminant. Mrozik and Piotrowska-Seget (2010) reviewed the *in situ* bioaugmentation of soils polluted with aromatic hydrocarbons. This approach has also been used for the *ex situ* treatment of heavy metal contaminated dredging material (Belochini et al. 2009) and radionuclides (e.g., Natural and Accelerated Bioremediation Research 2003) or combatting oil spills (e.g., Nikolopoulou et al. 2013). There are number of commercial bioaugmentation and biostimulation products available, but all require site specific evaluation procedures before implementation. In general, negative factors influencing the bioaugmentation processes include predation and competition for nutrients by autochthonous microorganisms, extreme pH, adverse temperature and moisture conditions, or loss of microbial viability during and after inoculation (Tyagi, da Fonseca, and de Carvalho 2011).

The earliest use of enhanced bioremediation in the United States was in remediating groundwater contaminated with high-octane gasoline (Jamison et al. 1975). The process that was used was patented by Raymond (1974). Nutrients in the form of inorganic nitrogen and phosphorus were added via injection wells and air was supplied to the aquifer by bubbling (sparging) it into the water standing in the injection wells. After the addition of the nutrients, the number of bacteria in groundwater increased by a

factor of 1000. Ten months after the addition of the nutrients, gasoline could no longer be detected in the groundwater. As mentioned in the previous chapter, powerful, new advances in microbial genome sequencing allow changes in the subsurface to be monitored relatively inexpensively as remediation proceed. These sequencing techniques allow practitioners to characterize the subsurface microbial community before, during and after the addition of electron donor amendments and/or biostimulants such as emulsified vegetable oil, lactate, polylactate, or zero valent iron. Likewise, bioaugmentation for solvents by addition of dechlorinating bacterial consortiums containing *Dehalococcoides*, *Dehalobacter*, *Geobacter*, and other microbes can be monitored with time, to determine their efficacy and follow any changes in the subsurface biocommunity.

Initially *in situ* enhanced bioremediation was considered a plume treatment technology only, but field studies have proven that it is also effective for treating DNAPL source zones under anaerobic conditions via enhanced reductive dechlorination (ITRC 2008). The DNAPL source zone treatment is a two stage process: first, the microbes enhance the dissolution and/or desorption of nonaqueous- and/or sorbed-phase contaminant mass and, second, make it bioavailable for degradation to nontoxic end products.

Prior to the start of an enhanced biodegradation process, the nutrient requirements of the native-soil bacteria are determined with a laboratory investigation. Microcosms of soil from the site are assembled and the contaminant is added. As much as possible, the microcosm should resemble the site conditions. If the groundwater is to be remediated the soil should be saturated with groundwater from the site. Soil remediation should be evaluated in unsaturated microcosms. Various microcosms are dosed with different amounts of nutrients, and the rates at which the contaminant disappears in the various microcosms are determined.

Enhanced bioremediation of NAPL source zones was long considered not feasible, particularly in case of DNAPL sites. However, the activity of *in situ* microorganisms can enhance the dissolution rates of NAPL contaminants during treatment and thereby reduce groundwater concentrations after treatment (e.g., Stroo et al. 2012). Therefore, *in situ* enhanced bioremediation can potentially be coupled with more aggressive remediation approaches, such as the source zone treatments discussed in the following sections. Such a combined remedy approach can achieve a “polishing” or “treatment train” approach for treating residual contamination and low-permeability zones (e.g., NRC 2013).

Aerobic Bioremediation Enhanced *in situ* bioremediation under aerobic bioremediation proceeds in the presence of sufficient oxygen, nutrients and microorganisms and ultimately results in the conversion of organic contaminants into carbon dioxide, water and microbial cell mass. Oxygen serves as the electron acceptor (= oxidizing agent) and the organic contaminant is the carbon source. While primarily used for degrading petroleum hydrocarbons, such as fuels or oils, aerobic processes can also alter the ionic form of metals, such as arsenic, into a non-bioavailable form or re-speciation into less toxic form (Valls and de Lorenzo 2002).

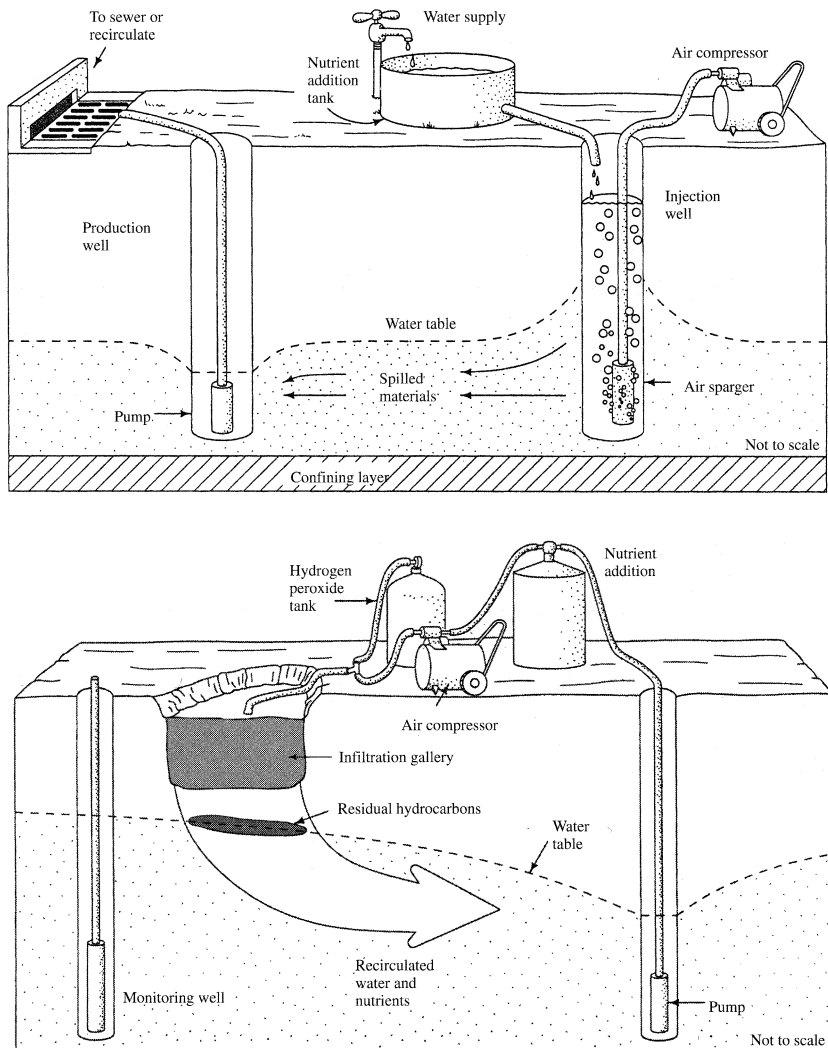
An important factor that determines the success of *in situ* enhanced bioremediation schemes is the nature of the geologic medium. It has to be permeable enough to allow for the introduction of oxygen and nutrients and not too heterogeneous to prevent the effective distribution of these amendments in the subsurface. The *in situ* biodegradation project will fail if the nutrients cannot reach the zone of contamination.

Oxygen can be added to groundwater by sparging either air or pure oxygen. Hydrogen peroxide can be used as an efficient way of adding oxygen to water, but it can be toxic to some microbes and hence does not have universal application and can lack persistence in the subsurface (Raymond et al. 1986; Yaniga 1982). In addition, hydrogen peroxide can be expensive. Air-vent wells and SVE wells can be used to supply oxygen to the vadose zone if biostimulating nutrients or microbes have been added by injection or infiltrating water.

In many instances the shallow subsurface has sufficient nutrient material so that the only ingredient lacking for successful bioremediation is oxygen. Above the water table, oxygen is added through soil vapor extraction. If the soil is dry, humid air can be vented into it to add moisture. The native soil microbes will degrade the VOCs at the same time that they are being removed by volatilization. This will result in a lower final concentration in the soil than soil vapor extraction alone. Likewise, with bioventing and bioslurping, the movement of air through the vadose zone will provide oxygen to the native soil bacteria so that bioremediation also occurs along with the physical removal of the VOCS.

Sparging of air, oxygen or hydrogen peroxide into a well as a means of supplying oxygen to groundwater can be an expensive process due to the equipment needed and the personnel time involved. Alternatively, solid metal peroxide material can be placed in wells either in the core of a BTEX plume or immediately downgradient of the plume. For example, a solid calcium oxy-hydroxide based material is called Oxygen Release Compound™ (ORC Advanced®). ORC can be placed in a filter tube with sand and lowered into a well. The ORC will hydrate and react with the sand to form a type of concrete. Oxygen will be slowly released from the concrete and diffuse into the water flowing through the well (Chapman et al. 1997; Bianchi-Mosquera et al. 1994). This technique is most useful where the levels of dissolved BTEX are not too high and where there is little dissolved iron (Bordon et al. 1997). The oxygen release rate may be too low for high BTEX concentrations and dissolved iron in the groundwater will tend to precipitate in the well containing the ORC which can reduce the flow of water through the treatment well. However, the use of ORC or other amendments does enhance natural bioremediation by adding supplemental oxygen.

Anaerobic Bioremediation Biodegradation of an organic substrate depletes the aquifer of dissolved oxygen and other terminal electron acceptors (e.g., nitrate or sulfate), and lowers the oxidation-reduction potential (ORP) of groundwater, thereby stimulating conditions conducive to anaerobic degradation processes. After the dissolved oxygen is consumed, anaerobic microorganisms may use native electron acceptors (as available) in the following order of preference: nitrate, manganese and ferric iron oxyhydroxides, sulfate, and finally carbon dioxide (Parsons Corporation 2004). Under anaerobic conditions (less than 0.1 to 0.5 mg/L dissolved oxygen), the organic contaminants will be ultimately metabolized to methane, limited amounts of carbon dioxide, and trace amounts of hydrogen gas. Under sulfate-reduction conditions, sulfate is converted to sulfide or elemental sulfur, and under nitrate-reduction conditions, dinitrogen gas is ultimately produced (FTRC 2015). Anaerobic conditions are conducive to the *in situ* biodegradation of chlorinated organic compounds, such as chloroethenes, chloroethanes, and chloromethane. Other common groundwater contaminants that can be degraded under anaerobic conditions include explosives, chlorinated aromatic hydrocarbons (e.g., chlorobenzenes) as well as inorganic compounds, such as perchlorate, hexavalent chromium or nitrate.

FIGURE 9.36 Enhanced *in situ* aerobic bioremediation.

Source: Lee et al. 1988.

As was shown in Section 7.6, chlorinated organic compounds can be broken down by several mechanisms. The most rapid is direct reductive dechlorination in which the chlorinated compound acts as an electron acceptor so that a chloride atom is removed and replaced with a hydrogen atom. The microbes that accomplish reductive dechlorination operate under anaerobic conditions and need a source of carbon. This process results in the reduction of the more chlorinated compounds, i.e., perchloroethane (PCA), perchloroethylene (PCE), 1,1,1-trichloroethane (TCA), trichloroethylene (TCE), and the production of less chlorinated compounds, i.e., cis-1,2-dichloroethylene (cis-1,2-DCE), 1,1-dichloroethane (1,1-DCA) 1,2-dichloroethane (1,2-DCA),

v vinyl chloride (VC), and chloroethane (CA). The vinyl chloride and chloroethane are not readily degraded under anaerobic conditions, but can be quickly oxidized to ethylene, ethane or ethanol in aerobic environments.

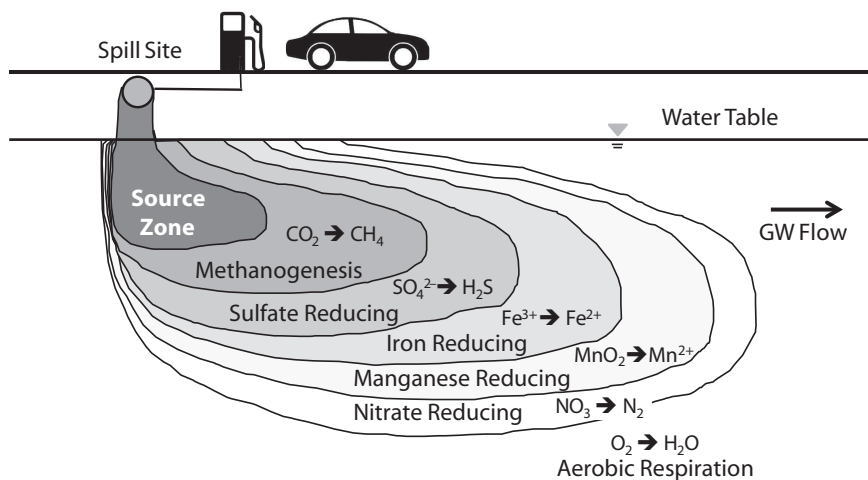
As a general rule, the highest rates and greatest extent of anaerobic dechlorination occurs under more reducing, i.e., sulfate-reducing and methanogenic conditions. Similarly, higher chlorinated compounds typically degrade under less reducing conditions than their less chlorinated counterparts. For example, the anaerobic dechlorination of PCE to TCE proceeds much quicker than the degradation of TCE to DCE. When DCE eventually degrades to vinyl chloride, the degradation rates are so slow that vinyl chloride concentrations are building up. This is of concern to the site manager because vinyl chloride is even more toxic than its parent compounds, although its volatility allows it to transform into the gaseous phase.

Autochthonous electron acceptors compete with anaerobic dechlorination of chlorinated hydrocarbons, and anaerobic reductive dechlorination will only occur under the suitable geochemical conditions. An organic substrate can be added to the subsurface to provide sufficient organic carbon to overcome native electron acceptor demand and be fermented to produce hydrogen for anaerobic dechlorination. One way to stimulate the biological reductive dechlorination of chlorinated compounds and to manipulate the redox conditions of the aquifer is to deliver hydrogen to the treatment zone by injecting soluble nontoxic organic materials. The substrates most commonly added for enhanced anaerobic bioremediation include lactate, molasses, Hydrogen Release Compound (HRC®), and emulsified vegetable oils. Other less frequently used substrates include ethanol, methanol, benzoate, butyrate, high-fructose corn syrup (HFCS), whey, bark mulch and compost, chitin, and gaseous hydrogen. The selected organic substrate should be suitable for the biogeochemical and hydrodynamic character of the aquifer to be treated (Naval Facilities Engineering Command 2004). For instance, microbial populations can tolerate a wide range of pH. But, a pH close to neutral (6 to 8) is the most conducive to the growth and proliferation of healthy and diverse microbial populations necessary for anaerobic dechlorination.

The amount of organic carbon substrates present in the treatment zone is considered the most important factor driving the anaerobic dechlorination because organic carbon determines the geochemical characteristics within a chlorinated contaminant plume. Three different types of anaerobic degradation environments with different biodegradation potential have been defined (e.g., Wiedemeier et al. 1996; Parsons 2004). In a Type 1 environment, the organic carbon concentration is relatively high and dissolved oxygen concentrations are very low (< 0.5 mg/L). Often, Type 1 conditions characterize the core of a plume. Type 1 conditions are most conducive for the degradation of higher chlorinated compounds, such as PCE or 1,1,1-TCA which are quickly broken down to daughter products. Type 2 environments are characterized by relatively moderate organic carbon concentrations and mildly anaerobic conditions. The prevailing redox reactions include nitrate, iron and manganese. Type 2 conditions are typical for the more peripheral parts of a contaminant plume. Under these conditions, the highly chlorinated VOCs act as the electron acceptor for microbes consuming the soil organic carbon and daughter products are also rapidly formed. However, compared to Type 1 environments, degradation rates are slower and daughter products, such as cis-1,2-DCE or vinyl chloride, tend to accumulate in a Type 2 environment. If sampling of the

Type 2 environment indicates that the amount of organic carbon is a limiting factor to further degrade higher chlorinated contaminants, the injection of organic substrate can turn the treatment area into a Type 1 environment that is more conducive for degrading these compounds. If more than 1.0 mg/L of dissolved oxygen is present, then reductive dehalogenation of the chlorinated VOCs does not occur. Under the well-oxygenated conditions, low organic carbon concentrations of a Type 3 environment, lesser chlorinated compounds, such as vinyl chloride or chloroethane can be destroyed. But higher chlorinated compounds will not biodegrade under these conditions. The Type 3 environment often characterizes the largest, longest part of a groundwater plume. The most favorable type of chlorinated VOC plume is one where there is an anaerobic zone where reductive dehalogenation is breaking down the highly chlorinated VOCs followed by an aerobic zone where the vinyl chloride and chloroethane can be consumed (Figure 9.37).

FIGURE 9.37 Redox zones of a typical contaminant plume.



Source: Modified after Parsons Corporation 2004.

Abiotic and cometabolic degradation pathways can also be used to degrade chlorinated hydrocarbons in a plume. An abiotic degradation reaction is not associated with biological activity, i.e., a chlorinated contaminant is degraded by a reactive compound. In cometabolism bacteria will consume both an organic substrate and a chlorinated VOC while using oxygen as an electron acceptor. The following case study illustrates this pathway.

Case Study: Enhanced Biodegradation of Chlorinated Ethenes

Chlorinated ethenes are among the more common ground-water contaminants due to their widespread use as solvents. In Section 7.6.3 methods of degradation of this class of compounds were discussed. A field experiment was conducted at the Moffett Naval Air Station, Mountain View, California, USA, to see if biostimulation could be used to enhance their *in situ* degradation (Roberts, Hopkins, Mackay, and Semprini 1990; Semprini, Roberts, Hopkins, and McCarty 1990; Semprini, Hopkins, Roberts, Grbic-Galic, and McCarty 1991).

An uncontaminated, confined sand aquifer that was 1.5 m (5 ft) thick was instrumented with a line of injection and extraction wells located 6 m apart. The direction of ground-water flow from the injection to the extraction wells was parallel to the regional hydraulic gradient. Intermediate sampling wells were placed at distances of 1, 2.2, and 4 m (3 to 12 ft) from the injection wells. Depending upon the injection and withdrawal rates, travel times from the injection wells to the withdrawal wells were from 20 to 42 hr. When oxygenated water was injected into the aquifer prior to the biostimulation experiments, the oxygen was transported to the extraction wells with little loss.

The compounds that were selected for study were vinyl chloride (VC), *trans*-1,2-dichloroethene (t-DCE), *cis*-1,2-Dichloroethene (c-DCE), and trichloroethene (TCE). When these were injected prior to biostimulation, they were retarded in the rank order of TCE > t-DCE > c-DCE > VC. It was found that with a long period of injection prior to biostimulation, the sorption capacity of the aquifer could be saturated with respect to TCE, t-DCE, and c-DCE. After 1000 hr. of injection, the concentration of these compounds in the monitoring well located 1 m (~3 ft) from the injection well was found to be 90 to 95% of the injected concentration.

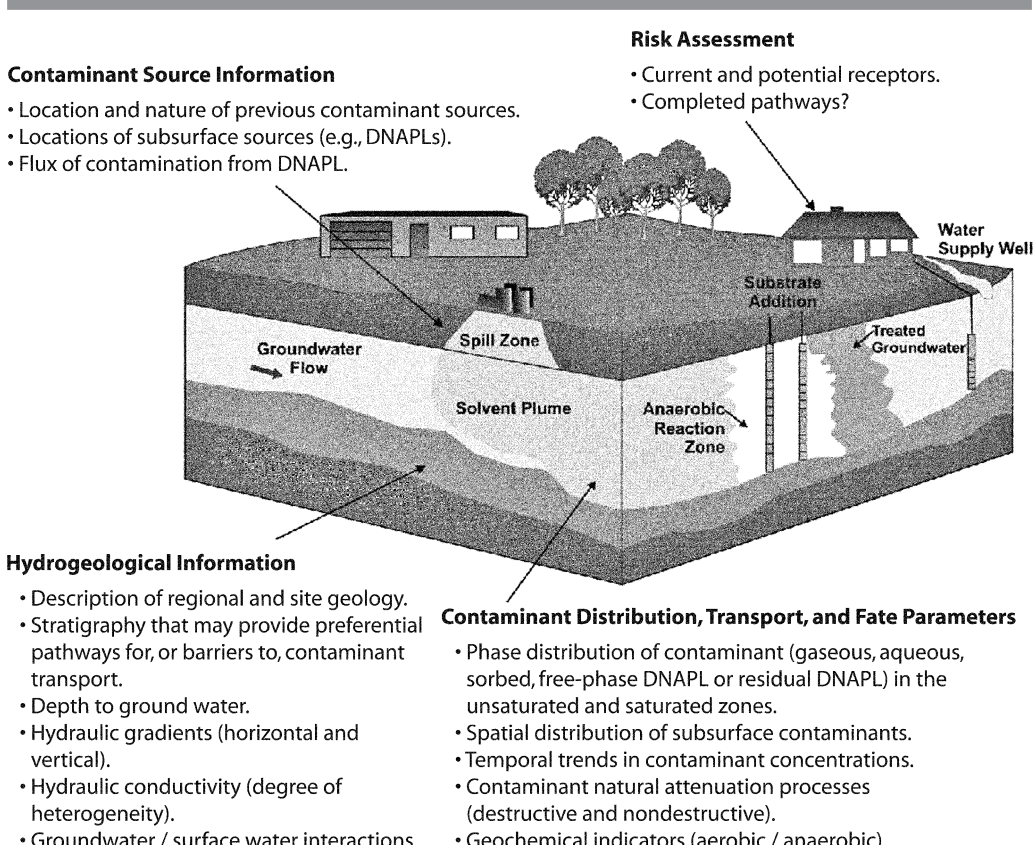
After the aquifer reached steady-state concentrations of the organic halides, it was biostimulated by injecting alternating pulses of dissolved oxygen and methane, along with continuous injection of the organic halides. The methane acted as the primary substrate (electron donor) for the growth of indigenous methane-utilizing bacteria, while the oxygen was the electron acceptor. The organic halides were degraded by cometabolism, a process by which the methanotropic bacteria that are utilizing the methane produce enzymes that are able to degrade the chlorinated ethenes. During the biostimulation experiments, decreases in concentration of both methane and the organic halides were observed. Within 2 m (6 ft) of travel through the aquifer, VC was reduced by 90 to 95%, t-DCE by 80 to 90%, c-DCE by 45 to 55%, and TCE by 20 to 30%. Residence times in the aquifer were only 1 to 2 days for this amount of biodegradation. It took about three weeks for the biostimulation experiment to reach these steady-state rates of reduction. An intermediate degradation product, *trans*-dichloroethene epoxide, was detected. When the injection of methane was halted, the concentration of the epoxide quickly decreased and the concentration of the halogenated ethenes slowly increased. However, when the rate of methane addition was increased beyond a certain concentration, it was shown to reduce the rate of transformation of VC and tDCE. Thus, while methane was necessary for stimulating *in situ* aerobic biotransformation, there appears to be an optimal concentration beyond which it inhibits the process.

■ 9.11 Conceptual Site Models

The bioremediation approach serves as an example for the complexity of the biochemical and hydrogeologic interactions and their dependency on aquifer characteristics and the physical/chemical properties of the contaminant(s). Failure to understand these conditions can determine the success or failure of site cleanup activities. Therefore, the development of a conceptual model of the site is an essential part of the site remediation process. Such a model is referred to as a conceptual site model (CSM). A CSM develops during the course of a site investigation. Elements of a CSM include at minimum a conceptualization of the processes that determine contaminant releases, contaminant migration, and the relationship between contaminant sources and receptors. The CSM is used to integrate all site information and data and to determine whether data gaps exist and whether additional information needs to be collected at the site. The model is used furthermore to facilitate the selection of remedial

alternatives and to evaluate the effectiveness of remedial actions in reducing the exposure of environmental receptors to contaminants (ASTM 2014). The CSM should be maintained and refined as new information and data is collected from the initial assessment through site closeout. Different types of CSM are common, including text documents and pictorial and graphical depictions of current and future site conditions. Parsons Corporation (2004) provides an example of the elements of a graphical CSM (Figure 9.38). Typical CSM information needs and other elements of a CSM for sites contaminated with unexploded ordnance and/or other hazardous, toxic, and radioactive waste is provided by the U.S. Army Corp of Engineers (2012).

FIGURE 9.38 Elements of a Conceptual Site Model.



Source: Parsons Corporation 2004.

■ 9.12 Permeable Reactive Barriers

A permeable reactive barrier (PRB) is a subsurface emplacement of reactive materials through which a dissolved contaminant plume must move as it flows, typically under natural gradient conditions. Treated water exits on the other side of the PRB. This *in*

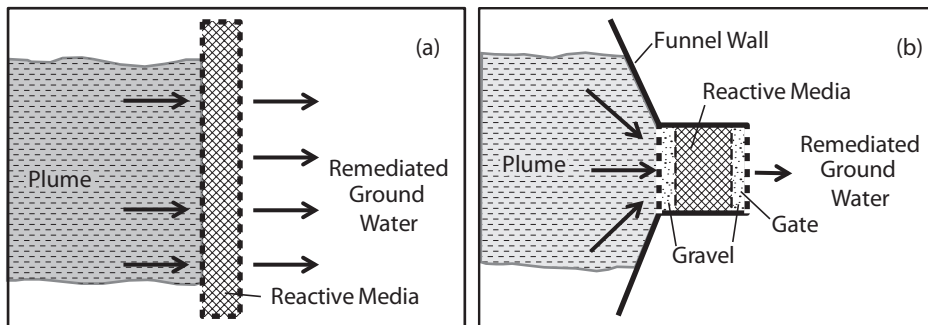
situ method for remediating dissolved-phase contaminants in groundwater combines a passive chemical or biological treatment zone with subsurface fluid flow management (U.S. EPA 2015d). The purpose of a PRB is to intercept a contaminant plume and prevent it from migrating to downgradient receptors, such as drinking water wells.

The concept of placing reactive materials in the path of a plume was developed based on observations by Reynolds et al. (1990). The authors noticed that at their field site concentration of dissolved chlorinated compounds were systematically lower in wells with galvanized iron casing compared to wells constructed from non-metallic pipe material. Laboratory experiments showed that metallic or zero valent iron (ZVI) reacted with the chlorinated compounds and degraded them to non-toxic products, such as ethane and ethane (Gillham and O'Hannesin 1994). The first field trial of a PRB was carried out by Gillham and O'Hannesin on the Canadian Air Force Base Borden, Ontario in 1991. A trench of up to 6 m (20 ft) in length and 2.5 m (8 ft) deep was excavated and backfilled with a mix of 22% of granular iron from a local foundry and 78% coarse sand. The total volume of the reactive matrix was 20 m³. The groundwater flow velocity in the unconfined sandy aquifer at the site was 9 cm/day (0.3 ft/day). The groundwater concentration of TCE was 258 mg/L and 68 mg/L for PCE. After installation, approximately 90% of the TCE and 86% of the PCE were removed within this proto-type PRB system, with no measurable decrease in performance over the first five year duration of the test. All degradation intermediates, including *cis*-1,2-DCE, were degraded within the reactive barrier. Changes in water chemistry indicated that calcium carbonate was precipitating within the reactive material. However, the clogging caused by the precipitates was inconsequential for the performance of the system within the five year study period. The authors concluded that full removal would have been achieved by increasing the amount of ZVE (O'Hannesin and Gillham 1998). Since these early trials, more than 200 reactive barriers have been installed and PRB technology is now an accepted practice for groundwater remediation, particularly for the treatment of dissolved chlorinated VOC plumes (ITRC 2011).

In situ PRB systems are typically constructed by digging a continuous trench perpendicular to the flow direction of a groundwater plume (Figure 9.39). After excavation, the trench is backfilled with a mix of reactive material and coarse sand and gravel, which provides the mix with a hydraulic permeability and porosity that is greater than the surrounding natural sediments. The length and depth of the PRB is determined by the dimensions of the groundwater plume, i.e., the trench must be large enough to capture the entire plume in both horizontal and vertical direction. If possible, the trench is anchored in a less permeable stratum, such as a clay layer, to prevent the plume from diving under the treatment system. In some cases, funnel-and-gate PRB systems have been installed in which an impermeable barrier blocks the advancing plume and redirects (funnels) the flow of contaminated groundwater through an opening (gate) in the wall and into a PRB system (ITRC 2005a). A funnel-and-gate system is depicted in Figure 9.39. The length of PRB systems is limited by site conditions and typically ranges from a few meters to a few hundred meters. The depth, however, is limited by the equipment available to excavate the trench. Trenches excavated with conventional equipment, such as back hoes or chain trencher, are comparably shallow (10 to 15 m or 33 to ~50 ft). Depths of 20 m (66 ft) or more can be achieved by caisson installation or cofferdam/sheet pile methods. Alternatively, the reactive material can be mixed *in situ*

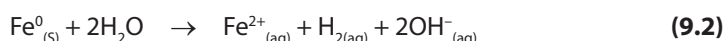
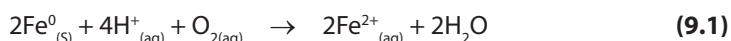
into the treatment zone or slurries of reactive materials can be directly injected into the subsurface. The cost of constructing the trench and backfilling it with reactive material is the major cost driver of this remediation technology.

FIGURE 9.39 Permeable reactive barrier (PRB) designs (map view). (a) Continuous trench and (b) Funnel-and-gate systems.

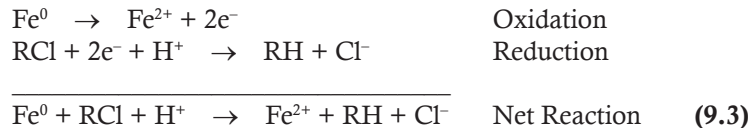


The thickness of the PRB wall is a critical design parameter. It depends on hydrogeologic factors, (such as groundwater flow velocities and flow directions which may change over the seasons), the strength and chemical make-up of the source zone including which contaminants are present and how much mass of dissolved contaminant must be treated, and the reactivity of the PRB material, including the geochemical conditions that can influence the reactive material, such as the pH of the groundwater. The reactivity of the material inside a PRB can be quantified in terms of a reaction rate constant or the half-life time of the contaminant coming in contact with the reactive material. Because some contaminants, including PCE and TCE, undergo sequential degradation, which involves the production of toxic intermediates, such as vinyl chloride, reaction rates for each compounds need to be taken into consideration. If the flow-through thickness and contaminant residence time inside the PRB is underestimated, still-contaminated water will emerge on the downgradient side of the wall. It is therefore not surprising that extensive laboratory and field tests are required to ensure the field performance of a PRB system. A lot of practical information about the proper installation of PRB systems has been accumulated over the past two decades and many PRB installations manuals and guidance documents are available on the internet, including Gavaskar et al. (2000) and ITRC (2011).

Zero-valent iron based PRBs are most commonly used for the *in situ* treatment of chlorinated aliphatic VOC, such as PCE and TCE. The reactions involved in the degradation of chlorinated VOC by metallic iron (Fe^0) within a PRB are abiotic in nature. Zero valent iron is a mild reductant and can react with dissolved oxygen (Eqn. 9.1) and to some extent with water (Eqn. 9.2):



These two equations illustrate the corrosion (=oxidation) of iron when coming in contact with oxygen or water. The two electrons released during the oxidation of iron can be readily accepted by chlorinated hydrocarbons, which are degraded via reductive dehalogenation, as shown in Equation 9.3



The products of the reductive dechlorination reaction are chloride (Cl^-), ferrous iron (Fe^{2+}), less chlorinated hydrocarbons, and hydrogen. Dechlorination of chloroethenes and chloroethanes is complete with ethene and ethane as the final carbon-containing compounds, respectively (Orth and Gillham 1996; Fennelly and Roberts 1998). The corrosion of the iron can generate large amounts of iron oxides and (oxy)hydroxide precipitates, which may eventually decrease the porosity and permeability of the reactive material within the PRB; particularly at the upgradient side of the barrier. However, these iron precipitates can convert to magnetite, which does not passivate the reactive surface of the iron. Also, field experiences from many PRB sites indicate that the loss of permeability due to precipitation is a relatively slow process that takes decades to cause significant changes in the hydraulic performance of the system. If installed properly, it is therefore likely that the dechlorination reaction is sustainable for many years of PRB operation (EPA 1998).

The degradation of chlorinated hydrocarbons by ZVI is a stepwise process during which intermediates are produced, such as *cis*-1,2-dichloroethene, vinyl chloride or chloroacetylene in cases where the parent compound is TCE or PCE. The degradation reactions are typically described using pseudo first-order kinetics with respect to the halogenated hydrocarbon, with the rate constant relatively insensitive to the initial hydrocarbon concentration (IRTC 2011).

$$C = C_0 e^{-k' t}$$

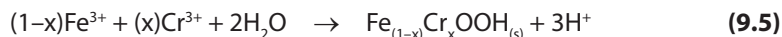
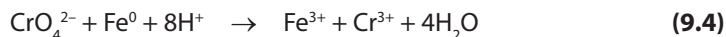
or:

$$\ln\left(\frac{C}{C_0}\right) = -k' t$$

where C_0 and C are the concentrations of the chlorinated compound of the influent and at time t , respectively. The pseudo-first order rate constant is k' , which equals the first order rate constant, k , when the concentration of the iron remains constant. Dehalogenation rates vary for the different halogenated contaminants. The primary determinant of degradation rate is the iron surface area, i.e., the surface area of iron per unit volume of pore water. For this reason, some PRB designs are based on nanoscale iron particles, which have larger surface areas and higher surface reactivity compared to conventional granular iron. Nanoscale iron particles range in size from approximately 10 to 100 nm and have a high iron content (>99.5% Fe) (Zhang 2003).

The reaction rates can be enhanced further by coating the iron particles with metallic catalyst, such as palladium (Li and Farrel 2000). One advantage of nanoscale iron particles is that slurries of these particles can be injected directly into the treatment zone. This approach alleviates the need of excavating a trench and back-filling it with mixes of ZVI and highly permeable sand/gravel materials.

Dissolved chlorinated compounds were the first groundwater contaminants treated by *in situ* PRB systems using metallic iron as the reactive material. Since then, the list of ZVI treatable compounds has rapidly expanded and now includes many other organic and inorganic contaminants (Table 9.2). For instance, metallic iron can **transform** explosives, such as TNT (Johnson and Tratnyek 2008), and pesticides, e.g., Lindane (U.S. EPA 2002) or can **immobilize** inorganic ions, such as arsenic (VI) and chromium (VI). Particularly metals that occur as anions exhibit a high degree of mobility because anions do not readily sorbed to the predominantly negatively-charged aquifer materials. For example, chromium (VI) is usually speciated as chromate, CrO_4^{2-} , which is a known carcinogen. The anion is comparably soluble under typical near-neutral pH and only slightly negative Eh conditions in typical aquifers. However, when reduced to trivalent Cr(III), relatively non-toxic and little soluble precipitates are formed. The immobilization of Cr(VI) by iron is a two-step process: first, Cr(VI) is reduced to Cr(III) (Eqn. 9.4). Subsequently, the Cr(III) precipitates as Fe(III) oxyhydroxide (Eqn. 9.5) (U.S. EPA 1998):



The mechanisms of Cr(VI) reduction by Fe(0) and their effects on the pH and Eh conditions of the system have been described by Powell et al. (1995) and Powell and Puls (1997). At some sites, Cr(VI) occurs together with other contaminants, such as TCE. Research has shown that it is possible to simultaneously treat both chromium and TCE with ZVI (U.S. EPA 1998).

While ZVI remains the most widely used reactive material used in PRB systems, an increasing number of new reactive materials and variations of the PRB based treatment approach are being developed and tested. These advances are greatly expanding the number of treatable groundwater contaminants. They also make it possible to apply this technology to hydrogeologic environments other than the unconsolidated aquifers for which PRB was initially developed. For example, a fractured bedrock aquifer comprised of shale and siltstone is contaminated with PCE at a manufacturing plant in northern New Jersey, USA (U.S. EPA 2011b). The main source area is located in shallow bedrock to a depth of approximately 13 m (42.5 ft) below ground surface, with some contamination in deeper parts of the aquifer. The lateral extent of the PCE plume is approximately 25 m (80 ft) by 37 m (120 ft). The plume was approximately 1.2 km (4,000 ft) in length prior to treatment. A pump-and-treat system and later, an enhanced bioremediation system were installed for containment of the PCE plume. After observing some reduction of contaminant flux, a nanoscale zero-valent iron injection was proposed as a more aggressive strategy. Before the injection of the nanoscale particles into the bedrock, the hydraulic communication within the fracture network was improved by hydrofracturing. This technology involves applying

TABLE 9.2 Common environmental contaminants that can be transformed by ZVI, including bimetallic and nanoscale iron particles.

Chlorinated methanes	Chlorinated ethenes/ethanes	Chlorinated benzenes	Trihalomethanes
Carbon tetrachloride (CCl_4)	Tetrachloroethene (C_2Cl_4)	Hexachlorobenzene (C_6Cl_6)	Bromoform (CHBr_3)
Chloroform (CHCl_3)	Trichloroethene (C_2HCl_3)	Pentachlorobenzene (C_6HCl_5)	Dibromochloromethane (CHBr_2Cl)
Dichloromethane (CH_2Cl_2)	cis-Dichloroethene ($\text{C}_2\text{H}_2\text{Cl}_2$)	Tetrachlorobenzenes ($\text{C}_6\text{H}_2\text{Cl}_4$)	Dichlorobromomethane (CHBrCl_2)
Chloromethane (CH_3Cl)	trans-Dichloroethene ($\text{C}_2\text{H}_2\text{Cl}_2$)	Trichlorobenzenes ($\text{C}_6\text{H}_3\text{Cl}_3$)	
	1,1-Dichloroethene ($\text{C}_2\text{H}_2\text{Cl}_2$)	Dichlorobenzenes ($\text{C}_6\text{H}_4\text{Cl}_2$)	
	Vinyl chloride ($\text{C}_2\text{H}_3\text{Cl}$)	Chlorobenzene ($\text{C}_6\text{H}_5\text{Cl}$)	
	1,1,1-trichloroethane ($\text{C}_2\text{H}_3\text{Cl}_3$)		
	1,1,2-trichloroethane ($\text{C}_2\text{H}_3\text{Cl}_3$)		
	1,1,2-dichloroethane ($\text{C}_2\text{H}_4\text{Cl}_2$)		
Other polychlorinated hydrocarbons	Pesticides	Organic dyes	Other organic contaminants
Dioxins	DDT ($\text{C}_{14}\text{H}_9\text{Cl}_2$)	Orange II ($\text{C}_{16}\text{H}_{11}\text{N}_2\text{NaO}_4\text{S}$)	TNT ($\text{C}_7\text{H}_5\text{N}_3\text{O}_6$)
Pentachlorophenol ($\text{C}_6\text{HCl}_5\text{O}$)	Lindane ($\text{C}_6\text{H}_6\text{Cl}_6$)	Chrysoidine ($\text{C}_{12}\text{H}_{13}\text{ClN}_4$)	RDX ($\text{C}_3\text{H}_6\text{N}_6\text{O}_6$)
PCBs		Tropaneolin O ($\text{C}_{12}\text{H}_9\text{N}_2\text{NaO}_5\text{S}$)	N-nitrosodimethylamine (NDMA) ($\text{C}_4\text{H}_{10}\text{N}_{20}$)
Heavy metal ions		Acid Orange	Acid Red Arsenic (AsO_3^{4-})
Mercury (Hg^{2+})		Inorganic ions	
Nickel (Ni^{2+})		Perchlorate (ClO_4^{-})	
Silver (Ag^+)		Nitrate (NO_3^-)	
Cadmium (Cd^{2+})		Dichromate ($\text{Cr}_2\text{O}_7^{2-}$)	
		Selenium (SeIV)	
		Arsenic (AsVII)	

Source: Modified after Zhang 2003 and U.S. EPA 1998.

high hydrostatic pressures to the well wall until the solid bedrock fractures. The newly opened fractures permit enhanced injection and farther reach of the nanoparticle slurry into the bedrock. Following hydrofracturing, approximately 800 pounds of nanoscale iron particles was delivered through four injection wells. Performance monitoring of the ZVI injection indicated significant impacts on source area geochemistry, including increased pH levels (~9) and low ORP values (-500 mV). Although it is likely that the iron particles did not reach all contaminated areas of the bedrock aquifer, it appears that amount of injected iron was sufficient to control both the primary PCE source and any back diffusion from the shale and siltstone matrix.

Innovative reactive materials for PRB include surfactant-modified zeolites, metal hydroxides or carbonates, organoclays, peat moss, mulch, compost and agricultural waste products (Thiruvenkatachari et al. 2008). Zeolites are clay minerals that have an elevated permeability (for a clay) and a high capacity for cation exchange. When coated with non-ionic surfactants, the surface of the zeolites becomes more hydrophobic, which makes it attractive to non-polar organic compounds. When modified with cationic surfactants, the zeolite surface has a positive charge and hence a greater affinity for anions, such as dissolved chromate (Bowman 2003; Misaelides 2011). Surfactant modified zeolites retain some of their cation ion exchange capacity. Peat moss has an affinity for both heavy metal ions, such as nickel or uranium and anions, e.g., chromate. Compounds like mulch or agricultural waste products used in PRBs are intended to be long-term sources of organic carbon or, in case of compost, serve as a source of nutrients (IRTC 2011). For instance, Lu et al. (2008) investigated the performance of pilot-scale permeable reactive barrier filled with plant mulch that was installed at Altus Air Force Base in Oklahoma, USA in 2002. The barrier was 139 m long (~450 ft), 7 m deep (~2 m), and 0.5 m (1.6 ft) wide and was constructed to treat trichloroethylene (TCE) contamination in groundwater emanating from a landfill. Data from over four years' monitoring indicated that the PRB stimulated TCE degradation to cis-DCE and vinyl chloride. Ongoing biodegradation reactions were corroborated by the detection of TCE degrading bacteria DNA (*Dehalococcoides*) and the detection of vinyl chloride within and downgradient of the PRB.

Systems like the one described by Lu et al. (2008) are also called **biowalls** or **bio barriers**. These *in situ* biowalls use solid low-cost organic materials, such as mulch or compost, to stimulate anaerobic degradation of chlorinated solvents, energetic (e.g., perchlorate) and explosive compounds (e.g., TNT, anions (nitrate and sulfate), and heavy metals (e.g., chromium and cadmium). Biowall materials can be amendment with, for example, emulsified vegetable oil, to stimulate both biotic and abiotic degradation processes. This permits to optimize biowall performance based on the type of contaminant(s) present and the desired degradation pathway(s) to be stimulated (Air Force Center for Engineering and the Environment 2008). Typically, biowalls stimulate anaerobic degradation processes, including reductive dechlorination and biotic anaerobic oxidation, and therefore are most often used for treating dissolved chlorinated compounds like PCE and TCE and their degradation products (DCE isomers and vinyl chloride). According to the ITRC (2011), an advantage of biological PRB systems over purely abiotic systems, such a ZVI, is that the treatment processes may extend downgradient of the constructed treatment zone due to migration of soluble organic carbon, enabling the effects of anaerobic degradation beyond the biowall. In addition,

the biowall system can be amended with specific bacteria (bioaugmentation) to target one or multiple contaminants and accelerate their degradation. A drawback is that the longevity of biowalls is anticipated to be shorter than that of ZVI walls and replenishment of organic substrate may be required.

The geochemistry of the solution inside a PRB system and downgradient can be adjusted by materials to buffer pH (e.g., limestone gravel) or to adjust the redox potential and further stimulate abiotic biogeochemical transformation processes (e.g., addition of reactive iron sulfite minerals, such as pyrite or mackinawite). The redox conditions in the treatment zone can also be manipulated by injecting sodium dithionite solution. The dithionite reduces ferric iron (Fe III) that is naturally present in the aquifer material to ferrous iron (Fe II). The presence of Fe(II) in the treatment zone can reduce, for example, soluble Cr(VI) to Cr(III) precipitates (Naftz et al. 2002). Also, the injection of oxidants, like hydrogen peroxide (H_2O_2) or potassium permanganate ($KMnO_4$) into the PRB can create strongly oxidizing conditions that are suitable for the *in situ* chemical oxidation and destruction of many organic contaminants, including BETX and other petroleum hydrocarbons (Thiruvenkatachari et al. 2008). Finally, sorbing barriers systems have been developed which use granular activated carbon or ion exchange materials. However, these systems have a limited live time and need to be replacement when the capacity of the sorbent is exhausted.

There now are a great variety of the reactive materials and amendments that permit tailoring the PRB treatment to specific contaminants, including ones that cannot be treated with the original ZVI approach, e.g., BTEX compounds. Barriers of different chemistries may also be placed sequentially which further increases the treatment options for contaminated site managers. It is likely that future research into PRB system will further enhance the applicability of this remediation approach.

■ 9.13 Chemically-Enhanced *In Situ* Flushing

Some chemicals, such as surface active agents (surfactants), complexing agents (cyclodextrins) or cosolvents (alcohols), can increase the solubility of otherwise slightly soluble hydrophobic organic contaminants, such as petroleum hydrocarbons or chlorinated solvents. In case of some metals or ionic organic contaminants, a similar solubility enhancing effect can be achieved by injecting acidic, basic, or reducing solutions. When injected into the aquifer and flushed through the contaminated source zone, these solubility enhancing agents increase the aqueous phase concentration of the contaminants, sometimes by orders of magnitude. After its passage through the treatment zone, the flushing solution is extracted and treated at the surface. Therefore, in its most basic form, chemically-enhanced flushing technology can be considered an enhancement of pump-and-treat in which water is the flushing solution. Compared to P&T, chemically-enhanced flushing is a much more aggressive and relatively rapid treatment approach with treatment durations often an order or two magnitudes shorter than P&T (ITRC 2009a).

In situ flushing is considered a mature remediation technology. The chemically-enhanced flushing approach is used predominantly to remediate source zones, particularly residual NAPL compounds. It is less well suited for the treatment of dissolved plumes or contaminants residing in the unsaturated zone. Flushing is most efficient in relatively homogeneous and permeable (hydraulic conductivity $>10^{-3}$ cm/sec) soil

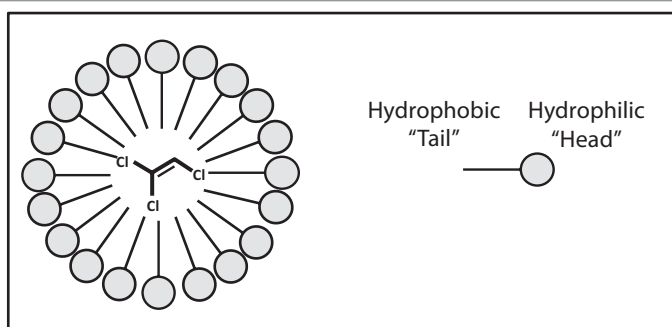
(Naval Facilities Engineering Command 2002). Heterogeneous aquifer conditions, including fractured bedrock aquifers, typically stand in the way of effectively flooding the treatment zone because lower permeable zones may be by-passed. Chemically-enhanced flushing is sometimes used in combination with other *in situ* remediation technologies, such as bioremediation or *in situ* oxidation (e.g., Dugan et al. 2010). Although their effect on the solubility of contaminants is similar, there are major differences between surfactant, cosolvent, or complexing agents. The following sections provide a brief overview of these agents. One disadvantage is that field applications typically have limited areal extent. For further readings, there have been a great number of papers, books, and manuals written about these flushing agents (e.g., Keuper et al. 1997; Lowe et al. 1999; Ward et al. 2000; Boving and Brusseau 2000; Naval Facilities Engineering Command 2002; 2003; ITRC 2003; Pennel et al. 2014).

9.13.1 Surfactant Enhanced *In Situ* Flushing

Surfactants are amphiphilic organic molecules that have both hydrophobic and hydrophilic moieties. When dissolved in water, surfactant molecules tend to cluster together and form **micelles** (Figure 9.40). These micelles aggregate when a specific threshold, known as critical micellar concentration (CMC), is exceeded. In water, the hydrophilic “heads” of the dissolved surfactant molecules point towards the aqueous phase, assuring that surfactants are highly water soluble. The hydrophobic “tails” of the surfactant molecule project inside the micelle. The “heads” and “tails” of surfactant molecules are typically separated by hydrocarbon chains. The non-polar core of these micelles attracts equally non-polar compounds, like TCE or other chlorinated solvents. This partitioning of hydrophobic contaminants into the micelle structure is the basis of the surfactant enhanced flushing technology, which is also referred to as Surfactant Enhanced Aquifer Remediation (SEAR). The enhancement of contaminant solubility is directly proportional to the concentration of the surfactant above the CMC.

Surfactants also reduce the interfacial tension between the aqueous and NAPL phases. At very low interfacial tensions, larger globules of NAPL spontaneously break

FIGURE 9.40 Surfactants are amphiphilic compounds; they have both hydrophobic and hydrophilic moieties. Above the critical micelle concentration, surfactant molecules aggregate into micelles. Hydrophobic contaminants (TCE shown here) can partition into the hydrophobic interior of the micelle.



up into tiny droplets of about 5 to 50 nm in radius. At that point, the system consists of water, NAPL droplets and surfactants and is called a **microemulsion**. The reduction in interfacial tension and formation of microemulsions can be exploited to **mobilize** NAPL. Relative to surfactant enhanced solubilization, NAPL mobilization can remove more contaminant mass in less time. But, in case of DNAPL, there is greater risk of uncontrolled downward movement, as DNAPL is being physically displaced by the surfactant solution. When injecting surfactant solution with the primary purpose of inducing mobilization, it is therefore necessary to prevent vertical DNAPL migration. This can either be achieved by having competent bedrock or a capillary barrier underlying the treatment zone or by manipulating the density the DNAPL, for example, by co-injection of cosolvents. Because of the risk of vertical displacement, mobilization flooding should only be considered when there is a high degree of certainty that the flushing solution can be recovered. In general, a surfactant flushing system can be tailored to remove contaminants either primarily by solubilization or primarily by mobilization (Pope 2015). Under appropriate site conditions, removal rates as high as 98.5% of the original DNAPL mass have been reported (Londergan et al. 1997). A number of very well documented field tests have demonstrated that *in situ* flushing can achieve these high removal percentages in months, and sometimes even days (EPA 2000).

Surfactants are produced at industrial scales and are one of the most widely used chemicals. Many different kinds of surfactants have been developed for a large number of applications, including detergents, fire-fighting agents (see Chap. 5) or pharmaceuticals and cosmetics. Depending on the charge of their polar heads, surfactant can be non-ionic., cationic or anionic. For most remediation applications, non-ionic or anionic surfactants are preferred because they do not sorb as strongly to the charged surfaces of natural minerals (i.e., clays) as cationic surfactants. Also, they are generally less toxic than cationic surfactants.

Case Study: Hill Air Force Base, Utah.

The Hill Air Force Base is located near Ogden, Utah, USA. The test site was used continuously from 1967 until 1975 for base-wide disposal of spent degreasing fluids and other solvents. At the site, DNAPL pooled within the topographic lows of a clay aquitard approximately 15 to 17 m (50 to 56 ft) below ground surface. The DNAPL was composed of approximately 70% TCE, 10% PCE, 5% TCA with other minor volatile organic constituents. In addition, there was a significant oil and grease fraction entrained in the DNAPL. The groundwater contaminants included PCE, TCE, TCA, DCE and trace heavy metals. The depth to groundwater was 8.3 m (27 ft). The unconfined aquifer consists of alluvial sands and gravel. The deposits are highly heterogeneous and are underlain by a thick uniform and continuous clay layer. The effective porosity of the aquifer is 20% and its hydraulic conductivity is 6×10^{-3} to 5×10^{-2} cm/sec (17 ft/day to 146 ft/day).

Prior to the surfactant flooding, a DNAPL source-recovery system was installed. Partitioning interwell tracer tests (PITT) were conducted pre- and post- surfactant flooding to characterize the DNAPL distribution and to demonstrate the removal efficiency of the surfactant treatment. The flushing solution injected into the treatment zone consisted of 8% an anionic surfactant (Aerosol MA-801) and 4% isopropyl alcohol. About 0.7% of sodium chloride was added to adjust the ionic strength of the mixture. The solution decreased the interfacial tension between the surfactant solution and the DNAPL to 0.02 dynes/cm. About 2.4 pore volumes of the flushing solution were injected during a 3 day period, followed by 5.5 days

of pumping clean water through the systems. The water flooding following the surfactant injection was designed to drive the flushing solution toward the extraction wells and flush out the surfactant/contaminant solution from the subsurface. The test results indicate that 1290 liters (340 gal) or 98% of the residual DNAPL was removed during the entire technology demonstration (Lonergan et al. 2001; Meinardus et al. 2002; IRTC 2003).

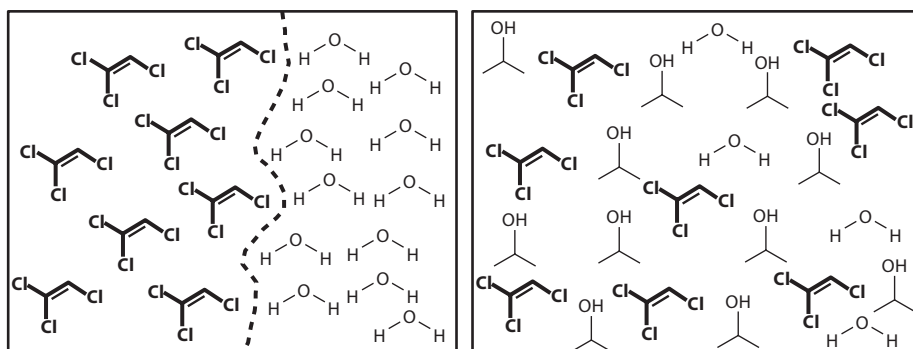
9.13.2 Cosolvent Enhanced *In Situ* Flushing

Cosolvents are chemicals that dissolve in both water and NAPL and reduce the polarity of the aqueous phase, thereby increasing the aqueous concentration of sparingly soluble organic compounds. This is illustrated in Figure 9.41. Unlike surfactants, cosolvents do not form separate phases but “true” solutions in which the solute particles are of molecular dimensions and invisible. Common cosolvents are alcohols, such as ethanol or isopropanol. The cosolvent enhanced *in situ* flushing method is similar to SEAR, i.e., a cosolvent solution is injected into the treatment zone to increase NAPL solubilization and mobility. The dissolved phase and mobilized NAPL is then recovered via one or more extraction wells.

The amount of alcohol cosolvent available for interaction determines the physical properties of the NAPL in the mixtures. Alcohol contents exceeding 75% are typical for cosolvent flooding of contaminated aquifers (IRTC 2003). When such high concentrations of alcohol are used, the alcohol may partition into both the NAPL and aqueous phases, which can result in the reduction of the NAPL-water interfacial tension, optimize the fluid density and viscosity, and allow complete miscibility. This can result in the mobilization of the NAPL (U.S. EPA 2000).

Cosolvents are sometimes co-injected with surfactants, which provides the flushing solution with the desired viscosity and interfacial tension properties. The presence of cosolvents can also improve the surfactant solubility in solution and density of the NAPL. Depending upon the initial density of the NAPL and the proportions of alcohol and water in the solution, the NAPL/cosolvent phase may be more or less dense than water (U.S. EPA 2006). The partitioning of alcohol into the NAPL can be used to control the vertical movement of mobilized NAPL in the aquifer.

FIGURE 9.41 When in contact with water, TCE builds a separate non-aqueous phase (left). The addition of a cosolvent (iso-propanol in this example) facilitates the dissolution of TCE, creating a “true” solution.



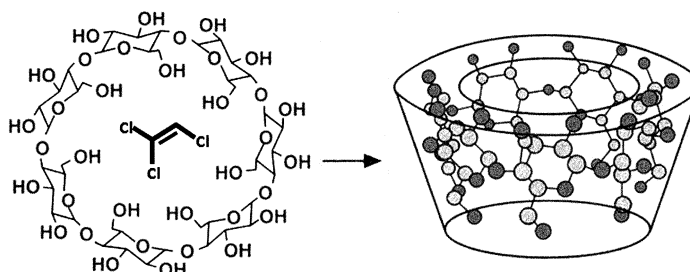
Case Study: Sages Dry Cleaner site in Jacksonville, FL

The unconfined aquifer at the former Sages Dry Cleaner site in Jacksonville, FL, USA, was contaminated with DNAPL. The main contaminant was PCE (21,300 µg/kg), but TCE and DCE isomers were present as well. The aquifer at the site consists of fine-grained sand to a depth of 16 to 20 m (~50 to 66.5 ft) below ground surface (bgs). A discontinuous clay layer approximately 0.15 m (0.5 feet) thick was encountered at a depth of approximately 12 m (40 ft). The depth to groundwater was 2.4 m (~8 ft). The hydraulic conductivity was 3.6×10^{-3} cm/sec (10.35 ft/day) and the hydraulic gradient was 0.002 m/m. *In situ* cosolvent enhanced flushing was selected for treating the DNAPL source zone. In 1998 was a pilot test was conducted during which 34,000 liter (~9,000 gal) of a 95% ethanol / 5% water mix was injected into three wells. Six recovery wells were pumped for 8 days and approximately 43 liters (~11 gal) of PCE was removed from the test zone. The removal effectiveness was 62 % in this pilot scale study (Jawitz et al., 2000; IRTC 2003).

9.13.3 Complexing Agent Enhanced *In Situ* Flushing

Cyclodextrins are a class of non-toxic cyclic sugars produced commercially from corn-starch. The glucose-based cyclodextrin molecule forms a toroidal ("lamp shade") structure that has a hydrophobic cavity within which low polarity organic compounds of appropriate shape and size can form clathrates, or inclusion complexes (Figure 9.42). Cyclodextrins are widely used in pharmaceuticals, food processing, and cosmetic applications because the interior of the molecule can deliver drugs to receptors or slowly release flavoring/fragrance compounds. The hydrophilic exterior of the molecule makes cyclodextrin very water-soluble. For most low polar contaminants, such as PAH or TCE, the hydrophobic interior of the cyclodextrin molecule is thermodynamically more attractive than being dissolved in water. Together, these two properties result in the formation of water soluble cyclodextrin-contaminant complexes that significantly increase the apparent solubility of many sparingly soluble organic compounds. Cyclodextrins also promote desorption of organic contaminants from the soil matrix (Brusseau et al. 1994; Ko et al. 1999). Enhanced solubilization and desorption are the basis for cyclodextrin use in soil and groundwater remediation (Boving and

FIGURE 9.42 The glucose-based β -cyclodextrin molecule forms a toroidal ("lamp shade") structure that has a hydrophobic cavity within which low polarity organic compounds of appropriate shape and size, such as TCE in this example, can form inclusion complexes.



Source: Boving and McCray 2000.

McCray 2000; McCray, Boving, and Brusseau 2000). In addition, Wang et al. (1998) and Ishiwata and Kamiya (1999) and other researchers reported that the presence of cyclodextrin enhanced the biodegradation of a PAH and pesticide compounds. These findings indicate that cyclodextrins can possibly be used simultaneously for bioremediation as well as for enhanced solubilization purposes.

For site remediation purposes, the most commonly used cyclodextrin variety is hydroxypropyl- β -cyclodextrin (HPCD). In general, the solubility enhancement of low polarity organic compounds by cyclodextrin is analogous to that of surfactants except that, on stoichiometric basis, cyclodextrin forms 1:1 molecular inclusion complexes with contaminants rather than requiring a minimum concentration, i.e., the surfactant critical micelle concentration. In addition, the exterior of the cyclodextrin molecule can be chemically modified to further increase its water-solubility or to add ligand-forming functional groups, such as the carboxyl group. Cyclodextrins with such coordinate bonds, such as carboxyl-methyl- β -cyclodextrin (CMCD) can chelate heavy metals and can possibly be used of treating metal contaminated sites (Brusseau et al. 1997). Most cyclodextrins do not partition substantially to NAPL phases (McCray and Brusseau 1998) and, compared to common anionic surfactant flushing agents and cosolvents, do not appreciably reduce the interfacial tension to cause mobilization of NAPL (Boving and McCray 2000).

The concept of using cyclodextrin as an agent for chemically-enhanced solubilization was introduced by Wang and Brusseau (1993) and Brusseau et al. (1994). Since then, CD flushing has been successfully used to treat NAPL source zones contaminated with chlorinated solvents and other compounds. For instance, McCray et al. (1999) used at a 10-wt% solutions of HPCD during a field-scale pilot scale test at the Hill Air Force Base, Utah, USA. The HPCD solution increased the aqueous concentrations of all the target contaminants by 100 to more than 20,000 times as compared to concentrations obtained during a water flush conducted immediately before the cyclodextrin flood. Additional cyclodextrin technology demonstrations have been carried out on the Naval Amphibious Base Little Creek, VA (Boving et al. 2004) and on Dover Air Force Base, DE (Tick et al. 2003; see case study).

Other complexing or chelating agents considered for *in situ* flushing include dissolved organic matter, DOM (Johnson and Amy 1995; Yang et al. 2001) or ethylenediaminetetraacetate, EDTA (Francis and Dodge 1998).

Case Study: Dover National Test Site (DNTS) at Dover Air Force Base

A test site was created in an uncontaminated part of Dover Air Force Base, Delaware, USA, to investigate innovative remediation technologies for the cleanup or containment of chlorinated-solvent-contaminated groundwater (McCray et al. 2011). One technology tested was cyclodextrin enhanced flushing of NAPL. Prior to the test, a sufficiently large volume of PCE was emplaced to mimic NAPL contamination at other field sites. The volume of the released PCE was only known to the test site managers, but not to the researchers.

The test aquifer consisted of medium to fine sands with interbedded gravels, silts, and clays lenses. Depth to groundwater in the unconfined aquifer varied between 4.5 and 9 m (~15 to 30 ft), and the saturated thickness varied between 4 and 7 m (13 to 23 ft). At about 9 to 12 m (30 to 39 ft) from the surface, the aquifer is underlain by a silty-clay aquitard with thickness varying between 5.5 and 8.5 m (18 to 26 ft). The average horizontal hydraulic conductivities ranged between 2.8×10^{-3} and 1.2×10^{-2} cm/s (~8 to 34 ft/d) and porosities

ranged from 17% to 28%. The test site was completely enclosed with interlocking, sealed sheet pilings. The sheet piles were driven into the clay aquitard to depths of approximately 14 m (46 ft) bgs. The pore volume of the treatment zone was 12.0 m³ (424 ft³). The residual NAPL saturation before the test was 0.57%.

A 7-pore volume, 15 wt% cyclodextrin solution was injected into the test cell and it increased the aqueous concentration of PCE in the extraction-well effluent 21.7 times the concentrations measured during the previous water flush (Tick et al. 2003). The cyclodextrin flushing experiment removed 33 L (8.7 gal) of 68.6 L (18 gal) PCE from the subsurface. This is equivalent to 48% of the NAPL mass initially released to the test site.

■ 9.14 *In Situ* Thermal Treatment (ISTT)

In situ thermal treatment (ISTT) technologies involve raising the temperature within the treatment zone to enhance the removal of NAPL components either through vapor pressure increase, which enhances recovery by vapor extraction or through viscosity reduction and decrease in interfacial tension which, in turn, increases contaminant mobility and enhances recovery by liquid pumping. In some settings, thermal treatment may also accelerate a contaminant's *in situ* destruction of select compounds through hydrolysis and pyrolysis. Also, ISTT has been shown to have a potentially beneficial effect on microbial degradation rates. Some ISTT technologies, like radio frequency heating, result in internal steam generation that helps drive contaminants from lower permeability regions (U.S. EPA 2004; Triplett Kingston, Dahlen, and Johnson 2010; Johnson et al. 2010; U.S. EPA 2014a). In addition to liquid phase recovery wells, ISTT systems are typically combined with soil vapor extraction (SVE) and a vapor cap above the treatment zone to control and collect the gases produced during the treatment process. These gasses are extracted via vacuum wells and cleaned up in an *ex situ* treatment unit.

Thermal treatment technologies were originally developed for enhanced oil recovery applications. The *in situ* heating concept was later adopted to address sites contaminated with higher molecular weight, semi volatile organic compounds (SVOC), such as PCB, coal and tar PAH from former manufactured gas plants, or creosote and pentachlorophenol (PCP) at wood treating facilities. Thermal methods are particularly useful for treatment of NAPLs, including chlorinated volatile organic compounds, such as TCE and PCE. ISTT can be used in a variety of hydrogeologic settings, including in low-permeability strata, such as silt and clay, in fractured rock aquifers or in deeper parts of the subsurface (> 30 m or >100 ft), which are not readily accessible by other *in situ* treatment technologies. Also, ISTT has been used to treat contamination beneath operating industrial and residential structures. Thermal treatment methods can be applied to the saturated and unsaturated zone. However, this form of *in situ* treatment is limited to sites where groundwater flow velocity does not exceed 30 cm/day (1 ft/day). At greater flow velocities, groundwater can transfer away the heat from the treatment zone, which decreases treatment efficiencies and increases cost (EPA 2014a).

Several technologies have been developed to raise the temperature of the treatment zone. These methods differ primarily by the method of energy delivery, which may include electrical resistance heating, radio frequency heating, thermal conduction, or injection of hot water, hot air, or steam. Technologies like electrical resistance heating and steam injection are limited by the boiling temperature of water.

Much higher temperatures can be achieved by conductive heating (USACE 2006). Table 9.3 provides an overview of common ISTT.

If a site is contaminated with high concentrations of combustible compounds, such as coal tar NAPL, it may be possible to ignite them *in situ* and destroy those

TABLE 9.3 Common *in situ* thermal treatment (ISTT) technologies.

ISTT Technology	Description
Electrical Resistance Heating	Arrays of electrodes are installed around a central neutral electrode to create a concentrated flow of current toward the treatment zone. The flow of current creates heat as the soil acts as an electrical resistor. Resistance to flow in the soils generates temperatures of 100°C to 120 °C. This results in the generation of steam and mobilization of contaminants. This treatment approach is best suited for sites contaminated with NAPL and/or VOC. Hydration may be required for soils in the unsaturated zone.
Three-phase heating	
Six-phase soil heating	
Thermal Conductive Heating	Radiant heat is transferred to the treatment zone via conduction from steel heater wells or heater blankets that cover the ground surface. Heater wells typically operate at 750°C to 800°C. These temperatures are high enough to accomplish pyrolysis, if required. While applicable to NAPL and VOC, this remediation approach primarily targets SVOC.
Steam Enhanced Extraction	Injection of steam heats the soil and groundwater and enhances the release of contaminants from the soil matrix by decreasing viscosity and accelerating volatilization. The steam front drives a bank of contamination toward a system of multi-phase extraction wells, where vapor, groundwater, and displaced fluids, including NAPL, are recovered. This treatment approach is best suited for sites contaminated with NAPL and/or VOC.
Hot Air / Hot Water Injection	Similar in principle to steam enhanced extraction except that heat is transferred into the treatment zone by hot air or hot water. In case of hot water injection, the treatment temperature is limited to about 100°C, while higher temperatures can be achieved by hot air injection. These two technologies can be applied together with <i>in situ</i> soil mixing with large diameter augers.
Radio Frequency Heating	Two rows of vertical ground electrodes on the outside of the treatment zone receive high frequency electromagnetic energy radiating away from a third row midway between the border rows. The electromagnetic energy causes movement of the “polar” water molecules, and this vibration creates mechanical heat. When energy is applied to the electrode array, heating begins at the top center and proceeds vertically downward and laterally outward through the soil volume. The technique can heat soils to over 300°C.
Vitrification	A high voltage electric current applied to a graphite electrode array generates temperatures of 1,600 to 2,000°C. Another approach uses plasma arc technology. At these extreme temperatures contaminated soil melts and organic materials are either destroyed or vaporize. Upon cooling, the melt solidifies into a chemically stable, leach-resistant, glass and crystalline material similar to obsidian or basalt rock. Radionuclides, heavy metals and other nonvolatile compounds are retained within the vitrified matrix.

compounds by self-sustaining smoldering processes (Switzer et al. 2009; Pironi et al. 2009). This approach is commercialized as self-sustaining treatment for active remediation (STAR) technology.

ISTT field applications are growing in number, partially because clean up goals can be achieved quickly, often within days or weeks. ESTCP (2010) provides a critical evaluation of 182 ISTT applications conducted between 1988 and 2007. Of those 182 applications, 87 used electrical resistance heating, 46 steam-based heating, 26 conductive heating, and 23 other heating technology applications. Measured in terms of reducing contaminant concentration and mass flux from the treatment zone, improvements ranged from less than 10 to over 1000 times. Overall, the electrical resistance heating and thermal conductive heating variants of ISTT are less affected by heterogeneous and low-permeability lithologies (EPA 2014a), which is why *in situ* thermal technology performance appears less hindered by the geologic stratification and mass-transfer resistances that limit other *in situ* remediation technologies (Triplett Kingston, Dahlen, and Johnson 2010).

■ 9.15 *In situ* Chemical Oxidation (ISCO)

In situ chemical oxidation (ISCO) refers to a groundwater remediation technology that relies on the chemical oxidation of a wide variety of dissolved contaminants by strong oxidants, such as permanganate (MnO_4^-), hydrogen peroxide (H_2O_2), ozone (O_3), catalyzed hydrogen peroxide (Fenton oxidation), persulfate ($S_2O_8^{2-}$), perozone (H_2O_2 and O_3), or percarbonate. The reactive species and other properties of common oxidants are summarized in Table 9.4. Relative to each other, ozone and persulfate are stronger oxidants than permanganate and hydrogen peroxide. Fenton's reagent produces a variety of oxidizing species of different strengths.

An ISCO treatment system is similar to *in situ* enhanced flushing systems, except that generally no extraction well(s) is required. A solution of the oxidant in water is prepared on the site and then injected into the subsurface. Vertical injection wells and direct push probes are the most common delivery methods. As the oxidant solution moves through the treatment zone it comes into contact with the contaminant and degrades it into benign compounds, including carbon dioxide and water. The oxidant concentration and the amount of oxidant mass injected into the treatment zone must be determined beforehand based on the initial soil and groundwater contaminant concentrations. Also, natural organic matter (NOM) or reduced minerals, carbonate, and other free radical scavengers in the subsurface can reduce the amount of oxidant available to degrade the target compounds. Thus, the amount of ISCO reagent that can be potentially wasted on oxidant consuming compounds must be included into the oxidant dose calculations. This **natural oxidant demand** is an important ISCO design parameter and failure to consider it will influence the treatment performance and cost of the ISCO system. However, there is little advantage in an “over injection of oxidant” approach because there is the potential to enhance the release and migration of the target contaminants, generate excessive heat, and form undesired by-products, including precipitates (NRC 2005b; IRTC 2005; Siegrist et al. 2011).

Oxidizing agents like sodium or potassium permanganate, persulfate and percarbonate are solids, whereas hydrogen peroxide is a liquid and ozone is a gas. Because

TABLE 9.4 Common oxidants and their most important oxidant reactions, including persistence and electrode potentials of the reactive species involved. Reduction potential is negative.

Oxidant	Reactive Species	Reactions	Persistence ⁺	Electrode Potential (Eh)
Permanganate	Permanganate ion (MnO_4^-)	$MnO_4^- + 4H^+ + 3e^- \rightarrow MnO_{2(solid)} + 2H_2O$ ($3.5 < pH < 12$)	>3 months	1.7 V
Hydrogen peroxide	Hydrogen peroxide (H_2O_2)	$H_2O_2 + 2H^+ + 2e^- \rightarrow 2H_2O$	min.-hrs	1.8 V
Ozone	Ozone (O_3)	$O_3 + 2H^+ + 2e^- \rightarrow O_2 + 2H_2O$	min.-hrs	2.1 V
Fenton's (catalyzed hydrogen peroxide)	Hydroxyl radical ($\cdot OH$)	$2O_3 + 3H_2O \rightarrow 4O_2 + 2\cdot OH + 2H_2O$ $Fe^{2+} + H_2O_2 \rightarrow Fe^{3+} + \cdot OH + OH^-$ (initiation rxn)		2.8 V
	Hydroxyl radical ($\cdot OH$)	$2\cdot OH + 2H^+ + 2e^- \rightarrow 2H_2O$		2.8
	Perhydroxyl radical ($\cdot OH_2$)	$\cdot OH_2 + 2H^+ + 2e^- \rightarrow 2H_2O$		1.7
	Superoxide radical ($\cdot O_2$)	$\cdot O_2 + 4H^+ + 3e^- \rightarrow 2H_2O$		-2.4 V
	Hydroperoxide anion (HO_2^-)	$HO_2^- + H_2O + 2e^- \rightarrow 3OH^-$		-0.9 V
Persulfate ($S_2O_8^{2-}$)	Persulfate ($S_2O_8^{2-}$)	$S_2O_8^{2-} + 2e^- \rightarrow 2\cdot SO_4^{2-}$ (initiation rxn)	hrs-weeks	2.1 V
	Sulfate radical ($\cdot SO_4^-$)	$\cdot SO_4^- + e^- \rightarrow SO_4^{2-}$		2.6 V
Activated Persulfate ($S_2O_8^{2-}$)		$S_2O_8^{2-} + Heat^* \rightarrow 2\cdot SO_4^-$ (initiation rxn)	min-weeks	2.1 V
	Sulfate radical ($\cdot SO_4^-$)	$2\cdot SO_4^- + 2H_2O \rightarrow 2HSO_4^- + 2\cdot OH$		2.6 V
	Hydroxyl radical ($\cdot OH$)	$2\cdot OH + 2H^+ + 2e^- \rightarrow 2H_2O$		2.8 V

⁺ Literature values and estimates.

* Other persulfate activators: Fe^{2+} , elevated pH >10.5 and peroxyoxone (H_2O_2 and O_3).

Source: Huling and Pivetz (2006); ITRC 2005b.

ozone is inherently unstable, it must be produced at the site immediately before injection into subsurface. Permanganate salts might be delivered to the site in form of an aqueous solution. Most oxidants are hazardous chemicals that must be handled properly by trained field personnel.

ISCO treatment is applicable to variety of contaminants; however, chlorinated solvents are by far the most commonly treated ones. In an analysis of ISCO field applications and performance data, Krembs et al. (2010) found that of 223 sites analyzed, 70% treated chloroethenes and 8% chloroethanes. Other commonly treated contaminants include chlorobenzenes, BTEX and other petroleum hydrocarbons, incl. PAH and gasoline additives (MTBE). About 54% of sites contained NAPL. In general, fuel-related compounds, particularly MTBE, can be treated more effectively relative to chlorinated compounds. However, a number of organic compounds (e.g., PCB or perfluorinated flame retardants) are resistant or even impossible to treat with currently existing ISCO methods. Therefore, the development of advanced oxidation processes is an area of ongoing research.

ISCO is a comparably aggressive contaminant mass-reduction technology and primarily applied to NAPL source zones and groundwater plumes with high dissolved contaminant concentrations. ISCO has been implemented at sites with varied subsurface conditions, ranging from unconsolidated permeable and homogeneous materials to fractured bedrock environments. Generally, ISCO is a relative rapid treatment process that can achieve treatment goals within weeks or months. However, a comparably small percentage of ISCO treatments met pre-defined remediation goals, such as maximum contaminant levels (MCL) (Krembs et al. 2010). This may signify that remediation practitioners overestimated the performance of ISCO or underestimated the impact of site conditions on this technology.

Of the ISCO projects reviewed by Krembs et al. (2010), 89% combined the use of ISCO with other *in situ* remediation technologies. For instance, ISCO has been coupled with surfactants/cosolvents enhanced DNAPL removal, either in sequence or simultaneously (Dugan et al. 2010). Similarly, Eberle et al. (2017) reports on a pilot-scale field project where activated persulfate oxidant was used in combination with cyclodextrin, an enhanced solubilization agent discussed in Section 9.12. The advantage of combining the two treatment approaches is that the enhanced solubilization agent increases the mass of contaminant in solution and thereby makes it available for destruction by the oxidizing agent. This *in situ* “treatment train” approach, when performed as designed, can eliminate the need for extracting and *ex situ* treatment of contaminated liquids. Also, there is ample field site evidence that microbial populations are not permanently reduced by ISCO. In fact, it appears that microbial populations even flourish after ISCO treatment, which permits coupling ISCO with enhanced bioremediation or monitored natural attenuation (MNA) technologies (NRC 2005).

■ 9.16 Phytoremediation

Phytoremediation is a set of technologies that rely on plants and their associated microorganisms to sequester, extract, or degrade toxic compounds in groundwater, soils, sediment and surface water. Because it is a natural process, phytoremediation can be an effective remediation method for a variety of sites and contaminants,

including metals, radioactive materials, pesticides, explosives, chlorinated compounds and petroleum hydrocarbons. Phytoremediation has also been tested for the control of high salt content (salinity) in soils. Based on the primary removal mechanism, six phytoremediation technologies have been developed, including phytosequestration, rhizodegradation, phytohydraulics, phytoextraction, phytodegradation, and phytovolatilization. These technologies are described in Table 9.5. The mechanisms used most commonly for containing the lateral movement of contaminated groundwater include phytosequestration, phytohydraulics (tree hydraulic barrier and riparian buffer) and phytoextraction. For groundwater remediation, rhizodegradation, phytoextraction, phytodegradation, and phytovolatilization are used (ITRC 2009b; Lee 2013).

TABLE 9.5 Summary of phytoremediation mechanisms.

Mechanism	Description	Cleanup Goal
Phytosequestration	The ability of plants to sequester certain contaminants in the rhizosphere through exudation of phytochemicals and on the root through transport proteins and cellular processes	Containment
Rhizodegradation	Exuded phytochemicals can enhance microbial biodegradation of contaminants in the rhizosphere	Remediation by destruction
Phytohydraulics	The ability of plants to capture and evaporate water off the plant and take up and transpire water through the plant	Containment by controlling hydrology
Phytoextraction	The ability of plants to take up contaminants into the plant with the transpiration stream	Remediation by removal of plants
Phytodegradation	The ability of plants to take up and break down contaminants in the transpiration stream through internal enzymatic activity and photosynthetic oxidation/reduction	Remediation by destruction
Phytovolatilization	The ability of plants to take up, translocate, and subsequently transpire volatile contaminants in the transpiration stream	Remediation by removal through plants

Source: ITRC 2009b.

The phytoremediation approach works best where groundwater and soil contaminant concentrations are low because high concentrations may limit plant growth and may take long time to clean up. Phytoremediation is especially well suited for sites where the contamination is spread out over a large area and/or present at shallow depths. While the root system of some plants can reach more than 10 m (>30 ft) below ground surface, the maximum practical depth of the phytoremediation approach is approximately 8 m (26 feet) bgs. A general rule of thumb is that tree roots will not penetrate deeper than 1.8 m (5 feet) into the saturated zone (ITRC 2009b). In temperate climates, phytoremediation is limited by the length of the growing season. During winter when plants are dormant, water consumption and contaminant uptake essentially stops. Degradation by microbes and the rhizosphere effect continue but

at a reduced rate. A large number of plants have been evaluated for potential use in phytoremediation applications. The selection of one or more plant species is based on factors such as ability to extract or degrade the contaminants of concern, adaptation to local climates, high biomass, depth root structure, compatibility with soils, growth rate, ease of planting and maintenance, and ability to take up large quantities of water through the roots (U.S. EPA 2012c). Recent developments in transgenic plant research may lead to a greater selection of plant varieties or the treatment of contaminants currently not possible (Lee 2013). The duration of the treatment generally depends on the type and initial contaminant concentration, its distribution within the treatment zone, plant selection and their growth rate, hydrogeologic and climatologic conditions, and other site characteristics.

Phytoremediation has become an alternative to other, more aggressive cleanup technologies because of relatively low capital costs and the inherently aesthetic nature of planted sites. However, this treatment technology is not a “Do something quick and cheap in the field and then walk away” approach. Like any remediation system, phytoremediation requires significant operation, maintenance, and monitoring for several years after planting. For instance, plants may require irrigation, fertilization, weed and pest control or replanting (ITRC 2009).

■ 9.17 Summary

There is great interest in developing effective and efficient methods of remediating contaminated soils and groundwater in order to meet the mandates of public concern and federal legislation such as RCRA and CERCLA in the United States.

In order to have a successful remediation, it is necessary to first isolate or remove the source of the contamination. Sources can include hazardous wastes spread on the land or improperly buried in the earth, leaking landfills, leaking underground storage tanks, or soils that have become contaminated by accidental spills and leaks. If it is not possible to remove sources, they can be isolated by physical barriers, such as slurry walls and impermeable covers or by hydrodynamic barriers created by pumping and injection wells.

While not very effective, contaminated groundwater can be pumped from the ground and treated. Pump-and-treat technologies can be effectively used to hydraulically control plumes. Before initiating a pump-and-treat program, any mobile NAPL present should be removed. Floating NAPLs can be removed by multi-phase extraction pumps located in wells. Residual NAPL and contaminants sorbed onto mineral surfaces and soil organic carbon will slowly partition into the clean groundwater that replaces the contaminated groundwater removed by pumping. This will greatly prolong the period of time that it takes to remediate the aquifer. If all the residual contamination is not removed from the aquifer, the concentration of contaminants will increase after the termination of a pump-and-treat operation. It may be impossible to remediate sites contaminated with DNAPLs by conventional pump-and-treat methods. Such aquifers might require permanent plume-stabilization wells to prevent the spread of the plume, or need to be remediated with more advanced technologies.

Water that is extracted from the aquifer can be treated to remove both organic and inorganic contaminants. Methods of treatment of dissolved organics include

air stripping and carbon absorption. Underground tanks that are leaking should be removed and replaced. Soil and groundwater remediation is frequently necessary after a leaking tank has been removed.

Vadose zone soil contaminated by residual volatile organic compounds (VOC) can be remediated by soilvapor extraction systems. Air, containing organic vapors, is drawn from the soil pores via SVE wells in the vadose zone and replaced with fresh air. Some methods exist that combine pumping water for treatment with soil vapor extraction to treat contaminated soil and groundwater simultaneously.

Soil and groundwater contaminated by organic compounds may be amenable to bioremediation by both aerobic and anaerobic microbes. Electron acceptors and/or donor may be added to the soil or aquifer to encourage microbial activity. *In situ* bioremediation and related monitored natural attenuation (MNA) processes have the advantage of treating the contaminants dissolved in soil and groundwater at the same time as residual contaminants in the soil.

Permeable Reactive Barriers (PRB) are linear structures placed in the path of an advancing groundwater plume. Reactive materials inside the PRB, such as metallic iron, interact with the dissolved contaminants and degrade or immobilize them. PRBs are passive treatment systems because no pumping is required.

Chemically-enhanced *in situ* flushing technology relies on chemicals that enhance the solubility and, in some case, mobility of NAPL compounds in the subsurface. The primary objective of this remediation technology is to remove the maximum amount of contaminant with a minimum amount of chemicals and in minimal time while maintaining hydraulic control over the injected chemicals and contaminant. This approach requires injection and extraction wells with above ground treatment of the extracted liquids.

During thermal *in situ* treatment, heat is delivered to the treatment zone to volatize, displace, or destroy amendable contaminants in the subsurface. Convection and conduction heat sources have been tested and found effective for remediating a variety of contaminants, including some that are not treatable with other methods. However, high temperature necessary to destroy those compounds can also affect the soil properties. Thermal treatment is typically combined with SVE systems to capture volatilized compounds. New approaches include subsurface controlled, contaminant burning, or smoldering techniques.

In situ oxidation relies on strong oxidants that, when injected into the treatment zone, degrade organic contaminants. This aggressive remediation approach typically does not require the extraction of contaminated liquids from the subsurface and is applicable to a large number of organic compounds.

Phytoremediation takes advantage of green plants and their ability to take up, transform or volatilize a number of metal and organic contaminants. While limited to relatively low soil and groundwater contaminant concentrations, and typically requiring many growing seasons to achieve clean up goals, phytoremediation is a green technology.

While great advances have been made in the field of remediation over the past decades, many contaminants and site-settings, particularly fractured bedrock aquifers, remain difficult or impossible to treat with current methods. Hence, this topic will remain an area of active research for many years.

Chapter Notation

<i>B</i>	Uniform thickness of a confined aquifer	<i>d</i>	Distance between extraction wells
<i>Bgs</i>	Below ground surface	<i>k</i>	Pseudo-first order rate constant
<i>C</i>	Concentration	<i>x</i>	Distance along the <i>x</i> axis
<i>Co</i>	Initial concentration	<i>y</i>	Distance along the <i>y</i> axis
<i>U</i>	Regional specific discharge (Darcy velocity)	$h_0 - h$	Drawdown
<i>Q</i>	Pumping rate of plume-capture well	<i>T</i>	Aquifer transmissivity
		<i>S</i>	Aquifer storativity
		<i>R</i>	Radius of a pumping well
		<i>t</i>	Time since pumping began

References

- ADAC. 2015. Entwicklung der Tankstellenanzahl seit 1965 in Deutschland. Accessed September 3, 2015 from <https://www.adac.de/infotestrat/tankens-kraftstoffe-und-antrieb/probleme-tankstelle/anzahl-tankstellen-markenverteilung/default.aspx>
- Air Force Center for Engineering and the Environment (AFCEE). 2008. Technical Protocol for Enhanced Anaerobic Bioremediation Using Permeable Mulch Biowalls and Bioreactors. Available from <https://clu-in.org/download/techfocus/prb/Final-Biowall-Protocol-05-08.pdf>
- American Petroleum Institute (API). 2007. API 2007. Technical Protocol for Evaluating the Natural Attenuation of MTBE. API Publication 4761. 186 pp.
- Standard Practice for Environmental Site Assessments: Phase I Environmental Site Assessment Process. Accessed September 13, 2015 at <http://www.astm.org/Standards/E1527.htm>
- ASTM. 2014. ASTM E1689—95 Standard Guide for Developing Conceptual Site Models for Contaminated Sites. Available from <http://www.astm.org/Standards/E1689.htm>
- Ardito, C. P., and J. F. Billings. 1990. "Alternative remediation strategies: The subsurface volatilization and ventilation system." In *Proceedings of Petroleum Hydrocarbons and Organic Chemicals in Ground Water: Prevention, Detection and Restoration*, 281–96. Dublin, Ohio: National Water Well Association.
- Bainchi-Mosquera, G. C., R. M. Allen-King, and D. M. Mackay. 1994. Enhancing degradation of dissolved benzene and toluene using a solid oxygen-releasing compound. *Ground Water Monitoring and Remediation* 14:120–128.
- Belochini, F., A. Dell'Anno, L. DeProris, S. Ubaldini, F. Cerrone, and R. Danovaro. 2009. Auto- and heterotrophic acidophilic bacteria enhance the bioremediation efficiency of sediments contaminated by heavy metals. *Chemosphere* 74:1321–1326.
- Blake, S. B., and R. W. Lewis. 1982. "Underground oil recovery." *Proceedings of the Second National Symposium on Aquifer Restoration and Ground Water Monitoring* 69–76. Dublin, OH: National Water Well Association.
- Borden, R. C., R. T. Goin, and C.-M. Kao. 1997. Control of BTEX migration using a biologically enhanced permeable barrier. *Ground Water Monitoring and Review* 17:70–80.
- Botha, M., L. Bester, and E. Hardwick. 2009. Removal of uranium from mine water using ion exchange at Driefontein Mine. In *Abstracts of the International Mine Water Conference 19th–23rd October 2009*, Pretoria, South Africa.
- Bowman, R. S. 2003. Applications of surfactant-modified zeolites to environmental remediation. *Microporous and Mesoporous Materials* 61:43–56.
- Boving, T. B., and J. E. McCray. 2000. Cyclodextrin-enhanced remediation of organic and metal contaminants in porous media and groundwater. *Remediation Journal* 10:59–83.
- Boving, T. B., and M. L. Brusseau. 2000. Solubilization and removal of residual trichloroethene from porous media: Comparison of several solubilization agents. *Journal of Contaminant Hydrology* 42:51–67.
- Boving, T. B., J. E. McCray, W. J. Blanford, and M. L. Brusseau. 2004. "Cyclodextrin enhanced remediation at NAB Little Creek, Virginia Beach, VA: Cost and performance assessment."

- Report to Environmental Security Technology Certification Program, ESTCP, Arlington, VA. Accessed September 26, 2015 from http://www.clu-in.org/download/contaminantfocus/dnapl/Treatment_Technologies/CyclodextrinC&P.pdf
- Brusseau, M. L., X. Wang, and Q. Hu. 1994. Enhanced transport of low-polarity organic compounds through soil by cyclodextrin. *Environmental Science and Technology* 28:952–956.
- Brusseau, M. L., X. Wang, and W. Wang. 1997. Simultaneous elution of heavy metals and organic compounds from soil by cyclodextrin. *Environmental Science and Technology* 31:1087–1092.
- Chapman S. W., B. T. Byerley, D. J. A. Smith, and D. M. Mackay. 1997. A pilot test of passive oxygen release for enhancement of in situ bioremediation of BTEX-contaminated ground water. *Ground Water Monitoring and Remediation* 17:93–105.
- Cho, M. S., M. G. Trefry, N. R. Thomson, D. R. Lester, G. Metcalfe, and K. Regenauer-Lieb. 2014. “Field trials of subsurface chaotic advection: stirred reactive reservoirs.” 19th Australasian Fluid Mechanics Conference Melbourne, Australia 8–11 December 2014.
- Coates, J. D., and L. A. Achenbach. 2004. Microbial perchlorate reduction: Rocket-fueled metabolism. *Nature Reviews Microbiology* 2:569–580.
- Cohen, R. M., J. W. Mercer, and J. Matthews. 1993. *DNAPL Site Evaluation*. Boca Raton, FL: CRC Press.
- Cohen, R. M., J. W. Mercer, R. M. Greenwald, and M. S. Beljin. 1997. *Design Guidelines for Conventional Pump-and-Treat Systems*. Washington, DC: U.S. EPA. Available from https://clu-in.org/download/contaminantfocus/dnapl/Treatment_Technologies/pmpreat.pdf
- Cookson, J. T., Jr., and J. E. Leszczynski. 1990. “Restoration of a contaminated drinking water aquifer.” *Proceedings of the Fourth National Outdoor Action Conference on Aquifer Restoration, Ground Water Monitoring and Geophysical Methods*, 669–681. Dublin, OH: National Water Well Association.
- Czarnecki, R. C. 1989. “Hot mix asphalt technology and the cleaning of contaminated soils.” *Petroleum Contaminated Soils, Volume 2*, eds. E. J. Calabrese and P. T. Kostecki, 267–278. Chelsea, MI: Lewis Publishers.
- Doty, C. B., and C. C. Davis. 1991. *The effectiveness of groundwater pumping as a restoration technology*.
- Oak Ridge National Laboratory Report ORNL/TM-11866.
- Dugan, P. J., R. L. Siegrist, and M. L. Crimi. 2010. Coupling surfactants/cosolvents with oxidants for enhanced DNAPL removal: A review. *Remediation Journal* 20:27–49.
- Eberle, D. E. H., R. G. Ball, and T. B. Boving. 2017. Solubility-Enhanced in situ Chemical Oxidation of VOC Contaminated Soil and Groundwater: A Pilot-Scale Field Test (Submitted).
- Eklund, K. 1989. “Incorporation of contaminated soils into bituminous concrete.” In *Petroleum Contaminated Soils, Volume I*, eds. E. J. Calabrese and P. T. Kostecki, 191–200. Chelsea, MI: Lewis Publishers.
- Faust, C. R., P. N. Sims, C. N. Spalding, P. F. Andersen, B. H. Lester, M. G. Shupe, and A. Harrover. 1993. FTWORK: Groundwater flow and solute transport in three dimensions. Sterling, VA: GeoTrans, Inc.
- Fennelly, J. P., and A. L. Roberts. 1998. Reaction of 1,1,1-trichloroethane with zero-valent metals and bimetallic reductants. *Environmental Science and Technology* 32:1980–1988.
- Fetter, C. W. 1994. *Applied Hydrology, Third Edition*. Upper Saddle River, NJ: Prentice Hall, Inc.
- Freeze, R. A., and J. A. Cherry. 1989. What has gone wrong. *Ground Water* 27:458–04.
- Francis, A. J., and C. J. Dodge. 1998. Remediation of soils and wastes contaminated with uranium and toxic metals. *Environmental Science and Technology* 32:3993–3998.
- FTRC. 2015. “Air Stripping.” Remediation Technologies Screening Matrix and Reference Guide, Vers. 4.0. Accessed September 1, 2015 from <http://www.frtr.gov/matrix2/section4/4-46.html>.
- FTRC. 2015b. “Enhanced Bioremediation.” Remediation Technologies Screening Matrix and Reference Guide, Vers. 4.0. Accessed September 9, 2015 from <http://www.frtr.gov/matrix2/section4/4-2.html>
- Gavaskar, A., N. Gupta, and B. Sass, R. Janosy, and J. Hicks. 2000. Design Guidance for Application of Permeable Reactive Barriers for Groundwater Remediation. Columbus, OH: Strategic Environmental Research and Development Program (SERDP).
- Gillham, R. W., and S. F. O’Hannesian. 1994. Enhanced degradation of halogenated aliphatics by zero-valent iron. *Ground Water* 32:958–967.

- Hauser, V. L., B. L. Weand, and M. D. Gill. 2001. Natural covers for landfills and buried waste. *Journal Environmental Engineering* 9:768–775.
- Herzog, B. L., R. A. Griffin, C. J. Stohr, L. R. Follmer, W. J. Morse, and W. J. Su. 1989. Investigation of failure mechanisms and migration of organic chemicals at Wilsonville, Illinois. *Ground Water Monitoring Review* 9:82–88.
- Huling, S. G., and B. E. Pivetz. 2006. *Engineering issue: In situ chemical oxidation*. United States Environmental Protection Agency—Engineering Issue.
- Indian Express. 2012. Govt bars oil PSUs from setting up self-funded petrol pumps. New Delhi, December 06, 2012. Accessed Sept 2, 2015 from <http://archive.indianexpress.com/news/govt-bars-oil-psus-from-setting-up-selffunded-petrol-pumps/1041360/>
- Interstate Technology & Regulatory Council. 2003. Technical and Regulatory Guidance for Surfactant/Cosolvent Flushing of DNAPL Source Zones. DNAPLs-3. Washington, DC: Interstate Technology & Regulatory Council, DNAPLs Team. Accessed September 22, 2015 from <http://www.itrcweb.org>
- Interstate Technology & Regulatory Council. 2005a. Permeable Reactive Barriers: Lessons Learned/New Directions. PRB-4. Washington, DC: Interstate Technology & Regulatory Council, Permeable Reactive Barriers Team. Accessed September 23, 2015 from www.itrcweb.org
- Interstate Technology & Regulatory Council. 2005b. *Technical and Regulatory Guidance for In Situ Chemical Oxidation of Contaminated Soil and Groundwater, Second Edition*, 172 pp. ISCO-2. Washington, DC: Interstate Technology & Regulatory Council. Accessed September 27, 2015 from <http://www.itrcweb.org>.
- Interstate Technology & Regulatory Council. 2008. In Situ Bioremediation of Chlorinated Ethene: DNAPL Source Zones. BioDNAPL-3. Washington, DC: Interstate Technology & Regulatory Council, Bioremediation of DNAPLs Team. Available online at www.itrcweb.org
- Interstate Technology & Regulatory Council. 2009a. Evaluating LNAPL Remedial Technologies for Achieving Project Goals. Washington, DC: Interstate Technology & Regulatory Council, LNAPLs Team, 157 pp. Accessed September 23, 2015 from www.itrcweb.org
- Interstate Technology & Regulatory Council. 2009b. Phytotechnology Technical and Regulatory Guidance and Decision Trees, Revised. Washington, DC: Interstate Technology & Regulatory Council, Phytotechnologies Team. Accessed September 27, 2015 from <http://www.itrcweb.org/Guidance/GetDocument?documentID=64>
- Interstate Technology & Regulatory Council. 2011. Permeable Reactive Barrier: Technology Update. PRB-5. Washington, DC: Interstate Technology & Regulatory Council, PRB: Technology Update Team. Accessed September 23, 2015 from <http://www.itrcweb.org/GuidanceDocuments/PRB-5-1.pdf>
- Ishiwata, S., and M. Kamiya. 1999. Cyclodextrin inclusion: Catalytic effects on the degradation of organophosphorus pesticides in neutral aqueous solution. *Chemosphere* 39:1595–1600.
- Jamison, V. W., R. L. Raymond, and J. O. Hudson. 1975. Biodegradation of high octane gasoline in ground water. *Developments in Industrial Microbiology* 16:305 ff.
- Johnson, R. L. and J. F. Pankow. 1992. Dissolution of dense chlorinated solvents in groundwater. 2. Source functions for pools of solvent. *Environmental Science and Technology* 26:896–901.
- Johnson, W. P., and G. L. Amy. 1995. Facilitated transport and enhanced desorption of polycyclic aromatic hydrocarbons by natural organic matter in aquifer sediments. *Environmental Science and Technology* 29(3):807–817.
- Johnson, R. L., and P. Tratnyek. 2008. Remediation of Explosives in Groundwater Using a Zero-Valent Iron Permeable Reactive Barrier. Final report, ESTCP Project ER-0223.
- Johnson, P. C., P. Dahlen, J. Triplett Kingston, E. Foote, and S. Williams. 2010. Critical Evaluation of State-of-the-Art In Situ Thermal Treatment Technologies for DNAPL Source Zone Treatment ESTCP Project ER-0314. 1272 pp. Accessed September 27, 2015 from <https://clu-in.org/download/techfocus/thermal/Thermal-ER-0314-FR.pdf>
- Kiker, J. H., J. B. Connolly, W. A. Murray, S. C. Pearson, S. E. Reed, and R. J. Tess. 2010. Ex-Situ wellhead treatment of 1,4-dioxane using Fenton's reagent. *Proceedings of the Annual International Conference on Soils, Sediments, Water and Energy* 15: 210–226. Accessed September 30, 2015 from <http://scholarworks.umass.edu/soilsproceedings/vol15/iss1/18>
- Ko, S-O, M. A. Schlautman, and E. R. Carraway. 1999. Partitioning of hydrophobic organic

- compounds to hydroxypropyl- β -cyclodextrin: Experimental studies and model predictions for surfactant-enhanced remediation applications. *Environmental Science and Technology* 33(16):2765–2770.
- Kostecki, P. T., E. J. Calabrese, and E. J. Fleischer. 1989. Asphalt batching of petroleum-contaminated soils as a viable remedial option." In *Petroleum Contaminated Soils, Volume 1*, eds. E. J. Calabrese and P. T. Kostecki, 175–90. Chelsea, MI: Lewis Publishers.
- Kueper, B., M. Pitts, K. Wyatt, T. Simpkin, and T. Sale. 1997. Technology Practices Manual for Surfactants and Cosolvents (TR-97-2). Advanced Applied Technology Demonstration Facility Program, Rice University. Accessed September 22, 2015 from <https://clu-in.org/PRODUCTS/AATDF/Toc.htm>
- Kuo, J. 2014. *Practical Design Calculations for Groundwater and Soil Remediation, Second Edition*. Boca Raton, FL: CRC Press.
- Lee, M. D., J. M. Thomas, R. C. Borden, P. B. Bedient, C. H. Ward, and J. T. Wilson. 1988. Bioremediation of aquifers contaminated with organic compounds. *Critical Reviews in Environmental Control* 18:29–89.
- Lee, J. H. 2013. An overview of phytoremediation as a potentially promising technology for environmental pollution control. Review Paper. *Biotechnology and Bioprocess Engineering* 18:431–439.
- Leeson, A., P. C. Johnson, R. L. Johnson, C. M. Vogel, R. E. Hinchee, M. Marley, T. Peargin, C. L. Bruce, I. L. Amerson, C. T. Coonfare, R. D. Gillespie, and D. B. McWhorter. 2002. Air sparging design paradigm. Accessed September 22, 2015 from <https://clu-in.org>
- Li, T., and J. Farrell. 2000. Reductive dechlorination of trichloroethene and carbon tetrachloride using iron and palladized-iron cathodes. *Environmental Science & Technology* 34:173–179.
- Lonergan, J. T., H. W. Meinardus, P. E. Mariner, R. E. Jackson, C. L. Brown, V. Dwarakanath, G. A. Pope, J. Ginn, and S. Taffinder. 2001. DNAPL removal from a heterogeneous alluvial aquifer by surfactant-enhanced aquifer remediation. *Ground Water Monitoring & Remediation* 21: 57–67.
- Lowe, D. L., L. O. Carrol, and C. H. Ward. 1999. *Surfactants and Cosolvents for NAPL Remediation. A Technology Practices Manual*. Boca Raton, FL: CRC Press.
- Lu X., J. T. Wilson, H. Shen, B. M. Henry, and D. H. Campbell. 2008. Remediation of TCE-contaminated groundwater by a permeable reactive barrier filled with plant mulch (Biowall). *Journal of Environmental Science and Health, Part A* 43:24–35.
- Lynch, E. R., S. W. Anagnos, G.A. Swenson, and R. K. Goldman. 1984. Design and evaluation of in-place containment structures utilizing ground-water cutoff walls. *Proceedings of the Fourth National Symposium and Exposition on Aquifer Restoration and Ground Water Monitoring*, 1–7. Dublin, OH: National Water Well Association.
- Lynch, J., and B. R. Genes. 1989. "Land treatment of petroleum contaminated soils." In *Petroleum Contaminated Soils, Volume 1*, eds. E. J. Calabrese and P. T. Kostecki, 163–74. Chelsea, MI: Lewis Publishers.
- MacDonald, J. A., and M. C. Kavanaugh. 1994. Restoring contaminated ground water: An achievable goal? *Environmental Science and Technology* 28:363A–368A.
- Mackay, D. M., and J. A. Cherry. 1989. Groundwater contamination: pump and treat remediation. *Environmental Science and Technology* 23:630–636.
- McCray, J. E., and M. L. Brusseau. 1998. Cyclodextrin-enhanced in situ flushing of multiple-component immiscible organic liquid contamination at the field scale: Mass removal effectiveness. *Environmental Science and Technology* 32:1285–1293.
- McCray, J. E., K. Bryan, R. Cain, G. Johnson, B. Blanford, and M. Brusseau. 1999. "Field test of cyclodextrin for enhanced in-situ flushing of immiscible organic liquids: Comparison to water flushing." In *Innovative Subsurface Remediation: Field Testing of Physical, Chemical, and Characterization Technologies*, eds. M. Brusseau, D. Sabatini, J. Gierke, M. Annable. New York: Oxford University Press.
- McCray, J. E., T. B. Boving, and M. L. Brusseau. 2000. Enhanced dissolution of hydrophobic organic compounds with implications for aquifer remediation. *Ground Water Monitoring and Remediation* 20:94–103.
- McCray J. E., G. R. Tick, J. W. Jawitz, J. S. Gierke, M. L. Brusseau, R. W. Falta, R. C. Knox, D. A. Sabatini, M. D. Annable, J. H. Harwell, and A. L. Wood. 2011. Remediation of NAPL source zones: Lessons learned from field studies at hill and dover AFB. *Ground Water* 49:727–744.

- Accessed September 27, 2015 from <http://digitalcommons.unl.edu/usepapapers/89>
- Meinardus, H. W., V. Dwarakanath, J. E. Ewing, G. J. Hirasaki, R. E. Jackson, M. Jin, J. S. Ginn, J. T. Lonergan, C. A. Miller, G. A. Pope. 2002. Performance assessment of NAPL remediation in heterogeneous alluvium. *Journal of Contaminant Hydrology* 54:173–193.
- Michalski, A., M. N. Metlitz, and I. L. Whitman. 1995. A field study of enhanced recovery of DNAPL pooled below the water table. *Ground Water Monitoring and Remediation* 15:90–100.
- Misaclides, P. 2011. Application of natural zeolites in environmental remediation: A short review. *Microporous and Mesoporous Materials* 144:15–18.
- Mrozik, A., and Z. Piotrowska-Seget. 2010. Bioaugmentation as a strategy for cleaning up of soils contaminated with aromatic compounds. *Microbiological Research* 165:363–375.
- Naftz, D., S. J. Morrison, C. C. Fuller, and J. A. Davis. 2002. *Handbook of Groundwater Remediation using Permeable Reactive Barriers: Applications to Radionuclides, Trace Metals, and Nutrients*. San Diego, CA: Academic Press.
- National Research Council (NRC). 2013. *Alternatives for Managing the Nation's Complex Contaminated Groundwater Sites*. Washington, DC: National Academies Press.
- National Academies of Sciences, Engineering, and Medicine. 2015. *Characterization, Modeling, Monitoring, and Remediation of Fractured Rock*. Washington, DC: The National Academies Press. Accessed October 5, 2015 from <http://www.nap.edu/21742>
- Natural and Accelerated Bioremediation Research (NABIR). 2003. *Bioremediation of Metals and Radionuclides... What it is and How it Works, Second Edition*. Prepared for the Natural and Accelerated Bioremediation Research Program, Office of Biological and Environmental Research, Office of Science, U.S. Department of Energy. Available from https://www.researchgate.net/publication/233784020_Bioremediation_of_Metals_and_Radionuclides_What_It_Is_and_How_It_Works_2nd_Edition
- Naval Facilities Engineering Command (NAVFAC). 2002. Surfactant-Enhanced Aquifer Re-mediation (SEAR) Design Manual, NFESC Technical Report TR-2206-ENV, 110 pp. Accessed September 22, 2015 from https://clu-in.org/download/contaminantfocus/dnapl/Treatment_Technologies/SEAR_Design.pdf
- Naval Facilities Engineering Command (NAVFAC). 2003. Surfactant-Enhanced Aquifer Re-mediation (SEAR) Implementation Manual, NFESC Technical Report TR-2219-ENV, 54 pp. Accessed September 22, 2015 from <https://clu-in.org/download/techdrct/td-tr-2219-sear.pdf>
- Need, E. A., and M. J. Costello. 1984. "Hydrogeologic aspects of slurry wall isolation systems in areas of high downward gradients." *Proceedings of the Fourth National Symposium and Exposition on Aquifer Restoration and Ground Water Monitoring* 18–26. Dublin, Ohio: National Water Well Association.
- Neuhauer, E. F., J. A. Ripp, N. A. Azoolina, E. L. Madsen, D. M. Mauro, and T. Taylor. 2009. Monitored natural attenuation of manufactured gas plant tar mono- and polycyclic aromatic hydrocarbons in ground water: A 14-year field study. *Ground Water Monitoring and Remediation* 29:66–76.
- Nikolopoulou, M., N. Pasadakis, and N. Kalogerakis. 2013. Evaluation of autochthonous bioaugmentation and biostimulation during microcosm-simulated oil spills. *Marine Pollution Bulletin* 72:165–173.
- Nyer, E. K., and D. C. Schafer. 1994. There are no in situ methods. *Ground Water Monitoring and Remediation* 14:120–123.
- Nyer, E. K., and S. S. Suthersan. 1993. Air sparging: Savior of ground water remediation of just blowing bubbles in the bath tub. *Ground Water Monitoring and Remediation* 13:87–91.
- O'Hannesin, S. F., and R. W. Gillham. 1998. Long-term performance of an in situ "iron wall" for remediation of VOCs. *Ground Water* 36:164–170.
- Orth, W. S., and R. W. Gillham. 1996. Dechlorination of trichloroethene in aqueous solution using Fe0. *Environmental Science and Technology* 30:66–71.
- Parsons Corporation. 2004. *Principles and Practices of Enhanced Anaerobic Bioremediation of Chlorinated Solvents*. Available from https://frtr.gov/cost-performance/pdf/remediation/principles_and_practices_bioremediation.pdf
- Pearlman, L. 1999. Subsurface Containment and Monitoring Systems: Barriers and Beyond (Overview Report). Accessed September 23, 2015 from <https://clu-in.org/download/studypapers/pearlman.pdf>
- Pennell, K. D., N. L. Capiro, and D. I. Walker. 2014. "Surfactant and cosolvents flushing." In

- Chlorinated Solvent Source Zone Remediation*, eds. B. H. Kueper, H. F. Stroo, C. M. Vogel, and C. H. Ward. New York: Springer-Verlag.
- Pironi, P., C. Switzer, G. Rein, J. I. Gerhard, and J. L. Torero. 2009. Small-scale forward smouldering experiments for remediation of coal tar in inert media. *Proceedings of the Combustion Institute* 32:1957–1964.
- Pope, G. A. 2015. “Surfactant enhanced aquifer remediation.” Center for Petroleum and Geosystems Engineering. Available from http://www.cpgc.utexas.edu/?q=RsP_SEAR
- Powell, R. M., R. W. Puls, S. K. Hightower, and D. A. Sabatini. 1995. Coupled iron corrosion and chromate reduction: Mechanisms for subsurface remediation. *Environmental Science and Technology* 29:1913–1922.
- Powell, R. M., and R. W. Puls. 1997. Permeable Reactive Subsurface Barriers for the Interception and Remediation of Chlorinated Hydrocarbon and Chromium (VI) Plumes in Ground Water. U.S. EPA Remedial Technology Fact Sheet. EPA/600/F-97/008.
- Raymond, R. L. 1974. Reclamation of Hydrocarbon Contaminated Ground Water. U.S. Patent 3,846,290.
- Raymond, R. L., R. A. Brown, R. D. Norris, and E.T. O’Neill. 1986. Stimulation of Biooxidation Processes in Subterranean Formations. U.S. Patent 4,588,506, May 13, 1986.
- Reynolds, G. W., J. T. Hoff, and R. W. Gillham. 1990. Sampling bias caused by materials used to monitor halocarbons in groundwater. *Environmental Science and Technology* 24:135–142.
- Rice, D. W., R. D. Grose, J. C. Michaelson, B. P. Dooher, D. H. Mac-Queen, S. J. Cullen, W. E. Kasterberg, L. G. Everett and M. A. Marino. 1995. *California Leaking Underground Fuel Tank (LUFT) Historical Analysis*. Lawrence Livermore National Laboratory UCRL-AR-122207.
- Ribeiro, A. B., E. P. Mateus, and L. M. Ottosen. 2000. Electrodialytic removal of Cu, Cr, and As from chromated copperarsenate-treated timber Waste. *Environmental Science and Technology* 34: 784–788.
- Roberts, P. V., G. D. Hopkins, D. M. Mackay, and L. Semprini. 1990. A field evaluation of in-situ biodegradation of chlorinated ethenes: Part 1, methodology and field site characterization. *Ground Water* 28:591–604.
- Ruegner, H., M. Finkel, A. Kaschl, and M. Bittens. 2006. Application of monitored natural attenuation in contaminated land management—A review and recommended approach for Europe. *Environmental Science Policy* 9:568–576.
- Sarkar, D., M. Ferguson, R. Datta, and S. Brinbaum. 2005. Bioremediation of petroleum hydrocarbons in contaminated soils: Comparison of bio-solids addition, carbon supplementation, and monitored natural attenuation. *Environmental Pollution* 136:187–195.
- Satkin, R. L., and P. B. Bedient. 1988. Effectiveness of various aquifer restoration schemes under variable hydrogeologic conditions. *Ground Water* 26:488–498.
- Sawyer, C. S., and M. Kamakoti. 1998. Optimal flow rates and well locations for soil vapor extraction design. *Journal of Contaminant Hydrology* 32:63–76.
- Semprini, L., P. V. Roberts, G. D. Hopkins, and P. L. McCarty. 1990. A field evaluation of in-situ biodegradation of chlorinated ethenes: Part 2, results of biostimulation and bio-transformation experiments. *Ground Water* 28:715–727.
- Semprini, L., G. D. Hopkins, P. V. Roberts, D. Grbic-Galic, and P. L. McCarty. 1991. A field evaluation of in-situ biodegradation of chlorinated ethenes: Part 3, studies of competitive competition. *Ground Water* 29:239–250.
- Shafer, J. M. 1987. Reverse pathline calculation of time-related capture zones in nonuniform flow. *Ground Water* 25:283–89.
- Siegrist, R. L., M. Crimi, and T. J. Simpkin. 2011. *In Situ Chemical Oxidation for Groundwater Remediation Series: SERDP ESTCP Environmental Remediation Technology, Volume 3*. New York: Springer-Verlag.
- Stroo, H. F., A. Leeson, J. A. Marqusee, P. C. Johnson, C. H. Ward, M. C. Kavanaugh, T. C. Sale, C. J. Newell, K. D. Pennell, C. A. Lebron, and M. Unger. 2012. Chlorinated ethene source remediation: Lessons learned. *Environmental Science and Technology* 46:6438–6447.
- Suthersan S. S., J. Horst, M. Schnobrich, N. Wlety and J. McDonough. 2017. *Remediation Engineering—Design Concepts, Second Edition*. Boca Raton, FL: CRC Press.
- Switzer, C., J. I. Gerhard, P. Pironi, G. Rein, and J. L. Torero. 2009. Self-sustaining smouldering combustion: A novel remediation process for non-aqueous phase liquids in porous media. *Environmental Science and Technology* 43:5871–5877.

- Thiruvenkatachari, R., S. Vigneswaran, and R. Naidu. 2008. Permeable reactive barrier for groundwater remediation. *Journal of Industrial and Engineering Chemistry* 14:145–156.
- Thomas, S. A., L. M. Aston, D. L. Woodruffand, and V. I. Cullinan. 2009. *Field Demonstrations of Mycoremediation for Removal of Fecal Coliform Bacteria and Nutrients in the Dungeness Watershed, Washington*. Oak Ridge, TN: U.S. Department of Energy.
- Thomsen, K. O., M. A. Chaudhry, K. Dovantzis, and R. R. Riesing. 1989. Ground water remediation using an extraction, treatment and recharge system. *Ground Water Monitoring Review* 9:92–99.
- Tick, G. R., F. Lourenso, A. L. Wood, and M. L. Brusseau. 2003. Pilot-scale demonstration of cyclodextrin as a solubility enhancement agent for remediation of a tetrachloroethene contaminated aquifer. *Environmental Science and Technology* 37:5829–5834.
- Trefry, M. G., D. R. Lester, G. Metcalfe, A. Ord, and K. Regenauer-Lieb. 2012. Toward enhanced subsurface intervention methods using chaotic advection. *Journal of Contaminant Hydrology* 127:15–29.
- Tripplett Kingston, J. L., P. R. Dahlen, and P. C. Johnson. 2010. State-of-the-practice review of in situ thermal technologies. *Groundwater Monitoring Remediation* 30:64–72.
- Tyagi, M., M. R. da Fonseca, and C. C. C. R. de Carvalho. 2011. Bioaugmentation and biostimulation strategies to improve the effectiveness of bioremediation processes. *Review Paper. Biodegradation* 22:231–241.
- U.S. Army Corps of Engineers (U.S. ACE). 2002. *Engineering and Design: Soil Vapor Extraction and Bioventing*. EM 1110-1-4001. Available from http://www.publications.usace.army.mil/Portals/76/Publications/EngineerManuals/EM_1110-1-4001.pdf
- U.S. Army Corps of Engineers (U.S. ACE). 2006. *Unified facilities criteria (UFC) Design: In situ thermal remediation*. Publication FC 3-280-05. Available from https://clu-in.org/download/contaminantfocus/dnapl/Treatment_Technologies/USACE-In_Situ_Thermal_Design.pdf
- U.S. Army Corps of Engineers (U.S. ACE). 2012. *Conceptual site models*. Report EM 200-1-12. Available from <http://www.publications.usace.army.mil/Portals/76/>
- Publications/EngineerManuals/EM_200-1-12.pdf?ver=2013-09-04-073011-260
- U.S. EPA. 1993. *Wellhead Protection Area Model User's Guide: Implementation of Hydraulic Head Computation and Display into the WHPA Code*. Accessed September 3, 2015 from <http://www2.epa.gov/water-research/wellhead-protection-area-whpamodel>
- U.S. EPA. 1996. *Pump-and-Treat Ground-Water Remediation: A Guide for Decision Makers and Practitioners*. EPA/625/R-95/005. Available from https://cfpub.epa.gov/si/si_public_record_Report.cfm?dirEntryId=22618&CFID=76006783&CFTOKEN=22484979
- U.S. EPA. 1998. *Evaluation of Subsurface Engineered Barriers at Waste Sites*. EPA 542-R-98-005. Available from <https://www.epa.gov/remediatech/evaluation-subsurface-engineered-barriers-waste-sites-volumes-1-and-2>
- U.S. EPA. 2000. *Solidification/Stabilization use at Superfund Sites*. EPA-542-R-00-010. Available from <https://www.epa.gov/sites/production/files/2015-08/documents/solidification-stabilization-sf-sites.pdf>
- U.S. EPA. 2001. *Development of Recommendations and Methods to Support Assessment of Soil Venting Performance and Closure*. EPA/600/R-01/070.
- U.S. EPA. 2002. *Field Applications of In Situ Remediation Technologies: Permeable Reactive Barriers*. Accessed September 20, 2015 from https://clu-in.org/download/rtdf/fieldapp_prb.pdf
- U.S. EPA. 2003. *Evapotranspiration Landfill Cover Systems Fact Sheet*. EPA 542-F-03-015.
- U.S. EPA. 2004. *In Situ Thermal Treatment of Chlorinated Solvents: Fundamentals and Field Applications*. EPA 542/R-04/010. Accessed September 29, 2015 from https://www.epa.gov/sites/production/files/2015-04/documents/istt_cs_epa542r04010.pdf
- U.S. EPA. 2006. *In Situ Treatment Technologies for Contaminated Soil*. (Engineering forum issue paper). EPA 542/F-06/013. 35 pp. Accessed September 29, 2015 from https://www.epa.gov/sites/production/files/2015-04/documents/tsp_issue_paper_542f06013.pdf
- U.S. EPA. 2007. *Treatment Technologies for Site Cleanup: Annual Status Report (Twelfth Edition)*. EPA-542-R-07-012. Available from https://www.epa.gov/sites/production/files/2015-08/documents/asr12_full_document.pdf

- U.S. EPA. 2011. *Fact Sheet on Evapotranspiration Cover Systems for Waste Containment*. EPA 542-F-11-001. Available from https://www.epa.gov/sites/production/files/2015-04/documents/fs_evap_covers_epa542f11001.pdf
- U.S. EPA. 2011b. *Fractured Bedrock Project Profiles*. Accessed September 30, 2015 from <https://clu-in.org/products/fracrock/sitedt1.cfm?mid=415>
- U.S. EPA. 2012a. *FY 2011 Annual Report on The Underground Storage Tank Program*. EPA 510-R-12-001. Accessed September 3 2015 from https://www.epa.gov/sites/production/files/2014-02/documents/fy11_annual_ust_report_3-12.pdf
- U.S. EPA. 2012b. *Conceptual Model Scenarios for the Vapor Intrusion Pathway*. EPA-530-R-10-003. Accessed September 30, 2015 from <http://www.epa.gov/oswer/vaporintrusion/documents/vi-cms-v11final-2-24-2012.pdf>
- U.S. EPA. 2012c. *Using Phytoremediation to Clean Up Sites*. Accessed September 30, 2015 from <http://www.epa.gov/superfund/accomp/news/phyto.htm>
- U.S. EPA. 2013. *Superfund Remedy Report, 14th Edition*. EPA 542-R-13-016. Accessed Sept. 11, 2015 from www.epa.gov/superfund
- U.S. EPA. 2014a. *Engineering Issue Paper: In Situ Thermal Treatment Technologies. Lessons learned*. Accessed September 27, 2015 from https://clu-in.org/download/techfocus/thermal/istt_ll_issue_paper.pdf
- U.S. EPA. 2014b. *Thermal Treatment: In Situ. An Overview*. Accessed September 27, 2015 from http://clu-in.org/techfocus/default.focus/sec/thermal_treatment:_in_situ/cat/overview/
- U.S. EPA. 2015. *Radionuclides in Drinking Water*. Accessed September 30, 2015 from http://cfpub.epa.gov/safewater/radionuclides/radio-nuclides.cfm?action=Rad_Electrodialysis
- U.S. EPA. 2015b. *Technical Guide for Addressing Petroleum Vapor Intrusion At Leaking Underground Storage Tank Sites*. EPA 510-R-15-001. 129 pp. Accessed September 7, 2015 from <http://www.epa.gov/oswer/vaporintrusion/documents/OSWER-Vapor-Intrusion-Technical-Guide-Final.pdf>
- U.S. EPA. 2015c. *Technical Guide for Assessing and Mitigating the Vapor Intrusion Pathway from Subsurface Vapor Sources to Indoor Air*. OSWER Publication 9200.2-154. Available from <http://www.epa.gov/oswer/vaporintrusion/documents/PVI-Guide-Final.pdf>
- U.S. EPA. 2015d. *Permeable Reactive Barriers, Permeable Treatment Zones, and Application of Zero-Valent Iron*. Accessed September 9, 2015 from https://clu-in.org/techfocus/default.focus/sec/Permeable_Reactive_Barriers%2C_Permeable_Treatment_Zones%2C_and_Application_of_Zero-Valent_Iron/cat/Overview/
- U.S. EPA. 2016. *Learn the Basics of Hazardous Waste*. Accessed from <https://www.epa.gov/hw/learn-basics-hazardous-waste>
- Valkenburg, N. 1991. Vice President, Geraghty and Miller, Inc. Personal communication.
- Valls, M., and V. de Lorenzo. 2002. Exploiting the genetic and biochemical capacities of bacteria for the remediation of heavy metal pollution. Review Paper. *FEMS Microbiology Reviews* 26:327–338.
- Viscusi, W. K., and J. T. Hamilton. 1996. Cleaning up superfund. *The Public Interest* 124:52–60.
- Wang, X., and M. L. Brusseau. 1993. Solubilization of some low-polarity organic compounds by hydroxypropyl- β -cyclodextrin. *Environmental Science and Technology* 27:2821–2825.
- Wang, J. M., E. M. Marlowe, R. Miller-Maier, and M. L. Brusseau. 1998. Cyclodextrin-enhanced biodegradation of phenanthrene. *Environmental Science and Technology* 32:1907–1912.
- Ward, C. H., S. Fiorenza, C. A. Miller, and C. L. Oubre. 2000. *NAPL Removal: Surfactants, Foams and Microemulsion*. Boca Raton, FL: CRC Press.
- Whiffin, R. B., and J. M. Bahr. 1984. “Assessment of purge well effectiveness for aquifer decontamination.” *Proceedings of the Fourth National Symposium and Exposition on Aquifer Restoration and Ground Water Monitoring* 75–81. Dublin, OH: National Water Well Association.
- Wiedemeier, T. H., J. T. Wilson, D. H. Kampbell, R. N. Miller, and J. E. Hansen. 1995. *Technical protocol for implementing intrinsic bioremediation with long term monitoring for natural attenuation of fuel contamination dissolved in ground water*. San Antonio, TX: U.S. Air Force Center for Environmental Excellence.
- Wiedemeier, T. H., M. A. Swanson, D. E. Moutoux, J. T. Wilson, D. H. Kampbell, J. E. Hansen, and P. Haas. 1996. Overview of the Technical Protocol for Natural Attenuation of Chlorinated Aliphatic Hydrocarbons in Groundwater under Development for the U.S. Air Force Center for Environmental Excellence. Symposium on

- Natural Attenuation of Chlorinated Solvents. 35–59. Washington, DC: USEPA.
- Wiedemeier, T. H., H. S. Rifai, C. J. Newell, and J. T. Wilson. 1999. *Natural Attenuation of Fuels and Chlorinated Solvents in the Subsurface*. New York: John Wiley and Sons.
- Wilson, J. L. 1984. “Double-cell hydraulic containment of pollutant plumes.” *Proceedings of the Fourth National Symposium and Exposition on Aquifer Restoration and Ground Water Monitoring*, 65–70. Dublin, Ohio: National Water Well Association.
- Yaniga, P. M. 1982. Alternatives in decontamination for hydrocarbons-contaminated aquifers. *Proceedings of the Second National Symposium on Aquifer Restoration and Ground Water Monitoring*, 47–57. Dublin, OH: National Water Well Association.
- Yang, Y., D. Ratte, B. F. Smets, J. J. Pignatello, and D. Grasso. 2001. Mobilization of soil organic matter by complexing agents and implications for polycyclic aromatic hydrocarbon desorption. *Chemosphere* 43:1013–1021.
- Zhang, W. X. 2003. Nanoscale iron particles for environmental remediation: An overview. *Journal Nanoparticle Research* 5:323–332.
- Boving, T. B., C. W. Fetter, and D. K. Kremer. 2017. “Site remediation.” Chapter 9 in *Contaminant Hydrogeology, Third Edition*, Fetter et al., 543–628. Long Grove, IL: Waveland Press.

Appendix A

Error Function Values

VALUES OF THE ERROR FUNCTION, $\text{erf}(x)$, AND THE COMPLEMENTARY ERROR FUNCTION, $\text{erfc}(x)$, FOR POSITIVE VALUES OF x

x	$\text{erf}(x)$	$\text{erfc}(x)$	x	$\text{erf}(x)$	$\text{erfc}(x)$
0	0	1.0	1.1	0.880205	0.119795
0.05	0.056372	0.943628	1.2	0.910314	0.089686
0.1	0.112463	0.887537	1.3	0.934008	0.065992
0.15	0.167996	0.832004	1.4	0.952285	0.047715
0.2	0.222703	0.777297	1.5	0.966105	0.033895
0.25	0.276326	0.723674	1.6	0.976348	0.023652
0.3	0.328627	0.671373	1.7	0.983790	0.016210
0.35	0.379382	0.620618	1.8	0.989091	0.010909
0.4	0.428392	0.571608	1.9	0.992790	0.007210
0.45	0.475482	0.524518	2.0	0.995322	0.004678
0.5	0.520500	0.479500	2.1	0.997021	0.002979
0.55	0.563323	0.436677	2.2	0.998137	0.001863
0.6	0.603856	0.396144	2.3	0.998857	0.001143
0.65	0.642029	0.357971	2.4	0.999311	0.000689
0.7	0.677801	0.322199	2.5	0.999593	0.000407
0.75	0.711156	0.288844	2.6	0.999764	0.000236
0.8	0.742101	0.257899	2.7	0.999866	0.000134
0.85	0.770668	0.229332	2.8	0.999925	0.000075
0.9	0.796908	0.203092	2.9	0.999959	0.000041
0.95	0.820891	0.179109	3.0	0.999978	0.000022
1.0	0.842701	0.157299			

Appendix B

Bessel Functions

MODIFIED BESSEL FUNCTIONS OF THE SECOND KIND AND ZERO ORDER, $K_0(x)$

x	$K_0(x)$	x	$K_0(x)$	x	$K_0(x)$
0.010	4.721	0.040	3.336	0.070	2.780
0.011	4.626	0.041	3.312	0.071	2.766
0.012	4.539	0.042	3.288	0.072	2.752
0.013	4.459	0.043	3.264	0.073	2.738
0.014	4.385	0.044	3.241	0.074	2.725
0.015	4.316	0.045	3.219	0.075	2.711
0.016	4.251	0.046	3.197	0.076	2.698
0.017	4.191	0.047	3.176	0.077	2.685
0.018	4.134	0.048	3.155	0.078	2.673
0.019	4.080	0.049	3.134	0.079	2.660
0.020	4.028	0.050	3.114	0.080	2.647
0.021	3.980	0.051	3.094	0.081	2.635
0.022	3.933	0.052	3.075	0.082	2.623
0.023	3.889	0.053	3.056	0.083	2.611
0.024	3.846	0.054	3.038	0.084	2.599
0.025	3.806	0.055	3.019	0.085	2.587
0.026	3.766	0.056	3.001	0.086	2.576
0.027	3.729	0.057	2.984	0.087	2.564
0.028	3.692	0.058	2.967	0.088	2.553
0.029	3.657	0.059	2.950	0.089	2.542
0.030	3.623	0.060	2.933	0.090	2.531
0.031	3.591	0.061	2.916	0.091	2.520
0.032	3.559	0.062	2.900	0.092	2.509
0.033	3.528	0.063	2.884	0.093	2.499
0.034	3.499	0.064	2.869	0.094	2.488
0.035	3.470	0.065	2.853	0.095	2.478
0.036	3.442	0.066	2.838	0.096	2.467
0.037	3.414	0.067	2.823	0.097	2.457
0.038	3.388	0.068	2.809	0.098	2.447
0.039	3.362	0.069	2.794	0.099	2.437

Source: Adapted from M. S. Hantush, "Analysis of Data From Pumping Tests in Leaky Aquifers," *Transactions, American Geophysical Union* 37 (1956):702—14.

MODIFIED BESSEL FUNCTIONS OF THE SECOND KIND AND ZERO ORDER, $K_0(x)$

x	$K_0(x)$	x	$K_0(x)$	x	$K_0(x)$
0.10	2.427	0.60	0.777	1.0	0.421
0.11	2.333	0.61	0.765	1.1	0.366
0.12	2.248	0.62	0.752	1.2	0.318
0.13	2.169	0.63	0.740	1.3	0.278
0.14	2.097	0.64	0.728	1.4	0.244
0.15	2.030	0.65	0.716	1.5	0.214
0.16	1.967	0.66	0.704	1.6	0.188
0.17	1.909	0.67	0.693	1.7	0.165
0.18	1.854	0.68	0.682	1.8	0.146
0.19	1.802	0.69	0.671	1.9	0.129
0.20	1.753	0.70	0.660	2.0	0.114
0.21	1.706	0.71	0.650	2.1	0.101
0.22	1.662	0.72	0.640	2.2	0.0893
0.23	1.620	0.73	0.630	2.3	0.0791
0.24	1.580	0.74	0.620	2.4	0.0702
0.25	1.541	0.75	0.611	2.5	0.0623
0.26	1.505	0.76	0.601	2.6	0.0554
0.27	1.470	0.77	0.592	2.7	0.0493
0.28	1.436	0.78	0.583	2.8	0.0438
0.29	1.404	0.79	0.574	2.9	0.0390
0.30	1.372	0.80	0.565	3.0	0.0347
0.31	1.342	0.81	0.557	3.1	0.0310
0.32	1.314	0.82	0.548	3.2	0.0276
0.33	1.286	0.83	0.540	3.3	0.0246
0.34	1.259	0.84	0.532	3.4	0.0220
0.35	1.233	0.85	0.524	3.5	0.0196
0.36	1.207	0.86	0.516	3.6	0.0175
0.37	1.183	0.87	0.509	3.7	0.0156
0.38	1.160	0.88	0.501	3.8	0.0140
0.39	1.137	0.89	0.494	3.9	0.0125
0.40	1.114	0.90	0.487	4.0	0.0112
0.41	1.093	0.91	0.480	4.1	0.0100
0.42	1.072	0.92	0.473	4.2	0.0089
0.43	1.052	0.93	0.466	4.3	0.0080
0.44	1.032	0.94	0.459	4.4	0.0071
0.45	1.013	0.95	0.452	4.5	0.0064
0.46	0.994	0.96	0.446	4.6	0.0057
0.47	0.976	0.97	0.440	4.7	0.0051
0.48	0.958	0.98	0.433	4.8	0.0046
0.49	0.941	0.99	0.427	4.9	0.0041
0.50	0.924			5.0	0.0037
0.51	0.908				
0.52	0.892				
0.53	0.877				
0.54	0.861				
0.55	0.847				
0.56	0.832				
0.57	0.818				
0.58	0.804				
0.59	0.791				

MODIFIED BESSEL FUNCTIONS OF THE SECOND KIND AND ZERO ORDER, $K_0(x)$

x	$K_0(x)$	x	$K_0(x)$
5.0	3.69×10^{-3}	7.6	2.24×10^{-4}
5.1	3.31×10^{-3}	7.7	2.01×10^{-4}
5.2	3.00×10^{-3}	7.8	1.81×10^{-4}
5.3	2.66×10^{-3}	7.9	1.63×10^{-4}
5.4	2.39×10^{-3}	8.0	1.46×10^{-4}
5.5	2.14×10^{-3}	8.1	1.32×10^{-4}
5.6	1.92×10^{-3}	8.2	1.18×10^{-4}
5.7	1.72×10^{-3}	8.3	1.07×10^{-4}
5.8	1.54×10^{-3}	8.4	9.59×10^{-5}
5.9	1.39×10^{-3}	8.5	8.63×10^{-5}
6.0	1.24×10^{-3}	8.6	7.76×10^{-5}
6.1	1.12×10^{-3}	8.7	6.98×10^{-5}
6.2	1.00×10^{-3}	8.8	6.28×10^{-5}
6.3	9.00×10^{-4}	8.9	5.65×10^{-5}
6.4	8.08×10^{-4}	9.0	5.09×10^{-5}
6.5	7.26×10^{-4}	9.1	4.58×10^{-5}
6.6	6.52×10^{-4}	9.2	4.12×10^{-5}
6.7	5.86×10^{-4}	9.3	3.71×10^{-5}
6.8	5.26×10^{-4}	9.4	3.34×10^{-5}
6.9	4.73×10^{-4}	9.5	3.01×10^{-5}
7.0	4.25×10^{-4}	9.6	2.71×10^{-5}
7.1	3.82×10^{-4}	9.7	2.44×10^{-5}
7.2	3.43×10^{-4}	9.8	2.19×10^{-5}
7.3	3.08×10^{-4}	9.9	1.97×10^{-5}
7.4	2.77×10^{-4}	10.0	1.78×10^{-5}
7.5	2.49×10^{-4}		

Appendix C

$W(t_D, B)$ Values

VALUES OF THE FUNCTION $W(t, B)$ FOR VARIOUS VALUES OF t_D

$t_D \backslash B$	0.002	0.004	0.006	0.008	0.01	0.02	0.04	0.06	0.08
0	12.7	11.3	10.5	9.89	9.44	8.06	6.67	5.87	5.29
0.000002	12.1	11.2	10.5	9.89	9.44	8.06	6.67	5.87	5.29
0.000004	11.6	11.1	10.4	9.88	9.44	8.06	6.67	5.87	5.29
0.000006	11.3	10.9	10.4	9.87	9.44	8.06	6.67	.87	5.29
0.000008	11.0	10.7	10.3	9.84	9.43	8.06	6.67	5.87	5.29
0.00001	10.8	10.6	10.2	9.80	9.42	8.06	6.67	5.87	5.29
0.00002	10.2	10.1	9.84	9.58	9.30	8.06	6.67	5.87	5.29
0.00004	9.52	9.45	9.34	9.19	9.01	8.03	6.67	5.87	5.29
0.00006	9.13	9.08	9.00	8.89	8.77	7.98	6.67	5.87	5.29
0.00008	8.84	8.81	8.75	8.67	8.57	7.91	6.67	5.87	5.29
0.0001	8.62	8.59	8.55	8.48	8.40	7.84	6.67	5.87	5.29
0.0002	7.94	7.92	7.90	7.86	7.82	7.50	6.62	5.86	5.29
0.0004	7.24	7.24	7.22	7.21	7.19	7.01	6.45	5.83	5.29
0.0006	6.84	6.84	6.83	6.82	6.80	6.68	6.27	5.77	5.27
0.0008	6.55	6.55	6.54	6.53	6.52	6.43	6.11	5.69	5.25
0.001	6.33	6.33	6.32	6.32	6.31	6.23	5.97	5.61	5.21
0.002	5.64	5.64	5.63	5.63	5.63	5.59	5.45	5.24	4.98
0.004	4.95	4.95	4.95	4.94	4.94	4.92	4.85	4.74	4.59
0.006	4.54	4.54	4.54	4.54	4.54	4.53	4.48	4.41	4.30
0.008	4.26	4.26	4.26	4.26	4.26	4.25	4.21	4.15	4.08
0.01	4.04	4.04	4.04	4.04	4.04	4.03	4.00	3.95	3.89
0.02	3.35	3.35	3.35	3.35	3.35	3.35	3.34	3.31	3.28
0.04	2.68	2.68	2.68	2.68	2.68	2.68	2.67	2.66	2.65
0.06	2.30	2.30	2.30	2.30	2.30	2.29	2.29	2.28	2.27
0.08	2.03	2.03	2.03	2.03	2.03	2.03	2.02	2.02	2.01
0.1	1.82	1.82	1.82	1.82	1.82	1.82	1.82	1.82	1.81
0.2	1.22	1.22	1.22	1.22	1.22	1.22	1.22	1.22	1.22
0.4	0.702	0.702	0.702	0.702	0.702	0.702	0.702	0.702	0.701
0.6	0.454	0.454	0.454	0.454	0.454	0.454	0.454	0.454	0.454
0.8	0.311	0.311	0.311	0.311	0.311	0.311	0.311	0.310	0.310
1	0.219	0.219	0.219	0.219	0.219	0.219	0.219	0.219	0.219
2	0.049	0.049	0.049	0.049	0.049	0.049	0.049	0.049	0.049
4	0.0038	0.0038	0.0038	0.0038	0.0038	0.0038	0.0038	0.0038	0.0038
6	0.0004	0.0004	0.0004	0.0004	0.0004	0.0004	0.0004	0.0004	0.0004
8	0	0	0	0	0	0	0	0	0

Source: After M. S. Hantush, "Analysis of data from Pumping Tests in Leaky Aquifers," *Transactions, American Geophysical Union*, 37 (1956):702—14.

W(t_d , B) Values

$t_d \backslash B$	B	0.1	0.2	0.4	0.6	0.8	1	2	4	6	8
0	4.85	3.51	2.23	1.55	1.13	0.842	0.228	0.0223	0.0025	0.0003	
0.000002	4.85	3.51	2.23	1.55	1.13	0.842	0.228	0.0223	0.0025	0.0003	
0.000004	4.85	3.51	2.23	1.55	1.13	0.842	0.228	0.0223	0.0025	0.0003	
0.000006	4.85	3.51	2.23	1.55	1.13	0.842	0.228	0.0223	0.0025	0.0003	
0.000008	4.85	3.51	2.23	1.55	1.13	0.842	0.228	0.0223	0.0025	0.0003	
0.00001	4.85	3.51	2.23	1.55	1.13	0.842	0.228	0.0223	0.0025	0.0003	
0.00002	4.85	3.51	2.23	1.55	1.13	0.842	0.228	0.0223	0.0025	0.0003	
0.00004	4.85	3.51	2.23	1.55	1.13	0.842	0.228	0.0223	0.0025	0.0003	
0.00006	4.85	3.51	2.23	1.55	1.13	0.842	0.228	0.0223	0.0025	0.0003	
0.00008	4.85	3.51	2.23	1.55	1.13	0.842	0.228	0.0223	0.0025	0.0003	
0.0001	4.85	3.51	2.23	1.55	1.13	0.842	0.228	0.0223	0.0025	0.0003	
0.0002	4.85	3.51	2.23	1.55	1.13	0.842	0.228	0.0223	0.0025	0.0003	
0.0004	4.85	3.51	2.23	1.55	1.13	0.842	0.228	0.0223	0.0025	0.0003	
0.0006	4.85	3.51	2.23	1.55	1.13	0.842	0.228	0.0223	0.0025	0.0003	
0.0008	4.85	3.51	2.23	1.55	1.13	0.842	0.228	0.0223	0.0025	0.0003	
0.001	4.85	3.51	2.23	1.55	1.13	0.842	0.228	0.0223	0.0025	0.0003	
0.002	4.85	3.51	2.23	1.55	1.13	0.842	0.228	0.0223	0.0025	0.0003	
0.004	4.85	3.51	2.23	1.55	1.13	0.842	0.228	0.0223	0.0025	0.0003	
0.006	4.85	3.51	2.23	1.55	1.13	0.842	0.228	0.0223	0.0025	0.0003	
0.008	4.85	3.51	2.23	1.55	1.13	0.842	0.228	0.0223	0.0025	0.0003	
0.01	4.83	3.51	2.23	1.55	1.13	0.842	0.228	0.0223	0.0025	0.0003	
0.02	4.71	3.50	2.23	1.55	1.13	0.842	0.228	0.0223	0.0025	0.0003	
0.04	4.42	3.48	2.23	1.55	1.13	0.842	0.228	0.0223	0.0025	0.0003	
0.06	4.18	3.43	2.23	1.55	1.13	0.842	0.228	0.0223	0.0025	0.0003	
0.08	3.98	3.36	2.23	1.55	1.13	0.842	0.228	0.0223	0.0025	0.0003	
0.1	3.81	3.29	2.23	1.55	1.13	0.842	0.228	0.0223	0.0025	0.0003	
0.2	3.24	2.95	2.18	1.55	1.13	0.842	0.228	0.0223	0.0025	0.0003	
0.4	2.63	2.48	2.02	1.52	1.13	0.842	0.228	0.0223	0.0025	0.0003	
0.6	2.26	2.17	1.85	1.46	1.11	0.839	0.228	0.0223	0.0025	0.0003	
0.08	2.00	1.94	1.69	1.39	1.08	0.832	0.228	0.0223	0.0025	0.0003	
0.1	1.80	1.75	1.56	1.31	1.05	0.819	0.228	0.0223	0.0025	0.0003	
0.2	1.22	1.19	1.11	0.996	0.857	0.715	0.227	0.0223	0.0025	0.0003	
0.4	0.700	0.693	0.665	0.621	0.565	0.502	0.210	0.0223	0.0025	0.0003	
0.6	0.453	0.450	0.436	0.415	0.387	0.354	0.177	0.0222	0.0025	0.0003	
0.8	0.310	0.308	0.301	0.289	0.273	0.254	0.144	0.0218	0.0025	0.0003	
1	0.219	0.218	0.213	0.206	0.197	0.185	0.114	0.0207	0.0025	0.0003	
2	0.049	0.049	0.048	0.047	0.046	0.044	0.034	0.011	0.0021	0.0003	
4	0.0038	0.0038	0.0038	0.0037	0.0037	0.0036	0.0031	0.0016	0.0006	0.0002	
6	0.0004	0.0004	0.0004	0.0004	0.0004	0.0004	0.0003	0.0002	0.0001	0	
8	0	0	0	0	0	0	0	0	0	0	

Appendix D

Exponential Integral

Values of the exponential integral, $Ei(x)$

$$Ei(x) = \int_{-\infty}^x \frac{e^\nu}{\nu} d\nu$$

x	$Ei(x)$	x	$Ei(x)$	x	$Ei(x)$	x	$Ei(x)$
0.0	$-\infty$	3.0	9.93383	6.0	85.9898	9.0	1,037.88
0.1	-1.62281	3.1	10.6263	6.1	93.0020	9.1	1,132.04
0.2	-0.82176	3.2	11.3673	6.2	100.626	9.2	1,234.96
0.3	-0.30267	3.3	12.1610	6.3	108.916	9.3	1,347.48
0.4	0.10477	3.4	13.0121	6.4	117.935	9.4	1,470.51
0.5	0.45422	3.5	13.9254	6.5	127.747	9.5	1,605.03
0.6	0.76988	3.6	14.9063	6.6	138.426	9.6	1,752.14
0.7	1.06491	3.7	15.9606	6.7	150.050	9.7	1,913.05
0.8	1.34740	3.8	17.0948	6.8	162.707	9.8	2,089.05
0.9	1.62281	3.9	18.3157	6.9	176.491	9.9	2,281.58
1.0	1.89512	4.0	19.6309	7.0	191.505	10.0	2,492.23
1.1	2.16738	4.1	21.0485	7.1	207.863	10.5	3,883.74
1.2	2.44209	4.2	22.5774	7.2	225.688	11.0	6,071.41
1.3	2.72140	4.3	24.2274	7.3	245.116	11.5	9,518.20
1.4	3.00721	4.4	26.0090	7.4	266.296	12.0	14,959.5
1.5	3.30128	4.5	27.9337	7.5	289.388	12.5	23,565.1
1.6	3.60532	4.6	30.0141	7.6	314.572	13.0	37,197.7
1.7	3.92096	4.7	32.2639	7.7	342.040	13.5	58,827.0
1.8	4.24987	4.8	34.6979	7.8	372.006	14.0	93,193.0
1.9	4.59371	4.9	37.3325	7.9	404.701	14.5	147,866
2.0	4.95423	5.0	40.1853	8.0	440.380	15.0	234,955
2.1	5.33324	5.1	43.2757	8.1	479.322		
2.2	5.73261	5.2	46.6249	8.2	521.831		
2.3	6.15438	5.3	50.2557	8.3	568.242		
2.4	6.60067	5.4	54.1935	8.4	618.919		
2.5	7.07377	5.5	58.4655	8.5	674.264		
2.6	7.57611	5.6	63.1018	8.6	734.714		
2.7	8.11035	5.7	68.1350	8.7	800.749		
2.8	8.67930	5.8	73.6008	8.8	872.895		
2.9	9.28602	5.9	79.5382	8.9	951.728		

Appendix E

Unit Abbreviations

Length (L)		Radiation	
m	meter	Ci	curie
cm	centimeter	pCi	picocurie
mm	millimeter	Bq	becquerel
μm	micrometer (micron)	Gy	gray
in.	inch	rad	radiation dose
ft	foot	rem	roentgen equivalent man
mi	mile	Sv	sievert
Mass (M)		Volume (M^3)	
kg	kilogram	L	liter
g	gram	mL	milliliter
mg	milligram	gal	gallon
μg	microgram	m^3	cubic meters
Time (T)		Pressure ($ML^{-1}T^{-2}$)	
sec	second	atm	atmosphere
min	minute	N/m^2	newtons per square meter
hr	hour	Pa	pascal
da	day		
mo	month		
yr	year		
Weight (ML/T^2)		Temperature and Heat	
lb	pound	$^\circ\text{C}$	degrees Celsius
		K	kelvin
		Btu	British thermal unit
Acceleration (LT^{-2})		Area (M^2)	
mi/hr/sec	miles per hour per second	ha	hectares
m/sec^2	meters per second per second	m^2	square meters
Discharge (L^3T^{-1})		Molecular Weight	
gal/min	gallons per minute	mol	mole
		M	molar
Concentration (ML^{-3})		Velocity (LT^{-1})	
mg/L	milligrams per liter	cm/sec	centimeters per second
$\mu\text{g/L}$	micrograms per liter	ft/hr	feet per hour
		ft/da	feet per day
		mi/hr	miles per hour

Index

- Abiotic degradation, 422
Above-ground storage tanks, 33
Absorption, 134
Accuracy, 433
Acetaldehyde, 400
Acetic acid, 400, 424
Acetyl chloride, 424
Acrylamide, 407
Acrylonitrile, 407
Activity coefficient, 318
Adjusted first temporal moment, 71
Adsorption, 134
Advection, mass transport, 61–63
Advection-dispersion equation, 187, 557, 558
analytical solutions
 boundary and initial conditions, 76–77
 concentration, one-dimensional step change, 77–78
 solution methods, 75–76
third-type boundary condition, 82
derivation of, 66–68
Advection-dispersion transient storage (ADTS) model, 122, 123
Advective transport, 61
Aerial photography, 452–453
Aerobic biodegradation, 172
Aerobic biofilm reactor, 174
Aerobic degradation, 423
Aggregates, 199
Air-entry, 252
Air sparging, 583–584
Air stripping, 570, 571
Air-vent wells, 580
Air-water-nonaqueous phase liquids, 256
Airborne electromagnetic surveys, 454
Alcohol, 270, 271, 395, 399, 609
Aldehyde, 393, 399–400
Aliphatic hydrocarbons, 378, 379
Alkanes, 379–381, 415
 boiling points, 386
 chlorinated, 398
Alkenes, 182, 379, 398
Alkynes, 379, 382
Alpha particle, 358
Amides, 407
Amines, 406
Ammonia, 339, 346, 370
Anaerobic decomposition, 368
Anaerobic degradation, 422
Anaerobic reductive-dechlorination, 423
Anisotropic, 47
Annular space, 474–475
Apparent longitudinal dispersivity, 107–109
Aqueous firefighting foam (AFFF), 401
Aquifer organic carbon, 154, 155
Aquifers, 249
Aromatic hydrocarbons, 4–5, 378, 382–385, 416
Arsenic, 43, 347–348, 470
Artificial filter pack, 473
Asbestos fibers, 177
Atmospheric pollutants, percolation of, 37
Atrazine, 36, 408
Attachment/detachment theory, colloid, 179–186
Autocorrelation function, 106
Autocovariance, 106
Average linear velocity, 61
Azo compound, 393
Bailer, 504
Barium, 351
Barometric effects, 239
Base/neutral fraction, 430
Bedrock cores, 495
Belt skimmer, 572
Bentonite, 475
 cement, 502
 pellets, 503
Benzene, 429
Benzene ring, 378
 degradation, 416, 417
Benzene, toluene, ethylbenzene and xylene (BTEX), 272, 276, 289–290, 391, 427, 591
Benzyl, 393
Beryllium, 350
Beta particle, 358
Beta-oxidation, 427
Bi-continuum transport models, 152
Bilinear adsorption model, 151
Bimetallic and nanoscale iron, 604
Bio barriers, 605
BIO1D model, 174, 175
Bioaugmentation, 533, 592
Bioavailability, 417
Biodegradation, 171–176, 408
Biofilm, 171
Biogenic cell materials, 177
Bioslurping, 574, 583–584
Biostimulation, 533, 592
Biowalls, 605
Bladder pump, 511
Boiling points, 376
Bond numbers, 267–268
Borden landfill plume, 112–113
Borehole abandonment, 507–509
Borehole geophysics, 520–522
Borings, 494
Boundary conditions, 76–77
Branched chains, 379
Breakthrough curve (BTC), 71–73, 269
Bromine, 344, 420
Bromoethane, 420

- 1-Bromopropane, 419
 Brooks-Corey soil parameters, 283, 284
 Brunauer, Emmett, and Teller (BET) sorption, 142–143
 Bubble tube, 509
 Bubbling pressure, 205, 252
 Buckingham flux law, 218–219
 Bulk water, 152
 Buoyancy forces, 268
 Butane, 379
 2-Butanone, 400
 Butoxymethylbenzene, 14
- Cadmium, 354, 356, 470
 Calcium, 343
 Capillary condensation, 143
 Capillary fringe, 198, 265
 Capillary numbers, 267–268
 Capillary potential, 204
 Capillary pressure, 204, 207, 250–253
 Capture zone, 263
 computation of, 563, 564
 pump-and-treat systems, 562–563
 Carbon capture and storage (CCS), 27
 Carbon sequestration, 27
 Carbon tetrachloride plumes, 184, 185
 Carbonyl group, 399
 Carboxamide, 393
 Carboxyl group, 400
 Carboxylate, 393, 401
 Carboxylic acid, 393, 400–402
 Carboxyl-methyl-*b*-cyclodextrin (CMCD), 611
 Cation
 exchange, 134, 202
 hydration of, 338–339
 Cationic radionuclides, adsorption of, 359–360
 Caution, 158
 Center of mass, 90
 Cesspools, 24–26
 Chelating agent, 340
 Chemical activities, 318
 Chemical equilibrium, 168, 317–320
 Chemical kinetics, 168–169
 Chemical reactions, classification of, 134
 Chemically-enhanced *in situ* flushing, 606–607
- complexing agent enhanced *in situ* flushing, 610–612
 cosolvent enhanced *in situ* flushing, 609–610
 surfactant enhanced *in situ* flushing, 607–609
- Chemisorption, 134
 Chimney effects, 241
 Chloride, 59, 81, 225–227, 523
 plume, 115, 119, 184
 Chlorinated ethenes, 597–598
 Chlorinated hydrocarbons, 247
 degradation, 418–425
 Chlorine, 24, 344
 Chlorite, 200
 Chlorophenols, 405
 Chromatographic effect, 182
 Chromium, 351–353, 355–356, 470, 603
 Cis-1,2-dichloroethylene (cis-1,2-DCE), 596
 Citric acid, 342
 Classical hydrogeology, 198
 Clay particles, 200
 Clean bed filtration theory (CFT), 179
 Clustered wells, 481–482
 Coal seam gas, 38
 Coal tar, 389–390
 distillation, 43
 fingerprinting, 434–440
 groundwater contamination, 390–392
 Cobalt, 353
 Coke, 389
 Colloids, 176
 colloidal-sized lead particles, 358
 iron oxide, 177
 tracers, 524
 transport, 176–186
 soil, 200
- Cometabolism, 424
 Commercial computer model, 144
 Comprehensive Environmental Response, Compensation and Liability Act (CERCLA), 17, 22, 41, 543, 546
 Conceptual site models (CSM), 598–599
 Conservative solute, 67
 Conservative tracer, 75
 Construction excavation, 39
 Containment, 547–552
- Contaminant remediation technologies, 545
 Contaminant-transport model, 563
 Continuous Multichannel Tubing (CMT®), 483
 Continuous wire-wrapped screens, 472
 Copolymer, 514
 Copper, 354
 Core sample, 495
 Correlation length, 106
 Cosolvency effect, 165
 Cradle-to-grave, 546
 Creosote, 166–167
 Cresols, 404–405
 Critical micellar concentration (CMC), 607
 Crude oil, 383, 441, 527
 Curie, 359
 Curve, 251
 Cutoff walls, 548–550
 Cyanate, 393
 Cyclobutane, 181
 Cyclodextrins, 610–611
 Cyclohexane, 181
 Cyclopentane, 181
 Cyclopropane, 181
- Darcy flux, 46
 Darcy's law, 46–47, 121, 238, 257, 287
 Dead zone, 583
 Dealkoxylation, 425
 Dealkylation, 425
 Debye-Hückel equation, 318, 319
 Decarboxylation, 425
 Decontamination procedures, 485–486
 Dehalogenation, 426
 Dehydrohalogenation reactions, 418, 420
 Denitrification, 346
 Dense nonaqueous phase liquids (DNAPLs), 247, 248, 260, 297
 dissolution, 303–305
 horizontal movement, 296–301
 saturated zone, 296–297
 monitoring, 30–308
 recovery of, 587–589
 relative mobility, 290–292
 vadose zone migration, 292–293

- vertical movement, saturated zone, 294–296
- Density driven transport, 277
- Derivatives, 44–46
- Destruction technologies, 559
- Detection limit, 16, 431
- Deterministic model, 103, 109–117
- C₃-Dibenzothiophenes, 441
- Dicarboxylic acid, 403
- Dichloroacetic acid, 424
- Dichloro-diphenyltrichloroethane (DDT), 425, 426
- Di(2-ethylhexyl) phthalate (DEHP), 403
- Diesel fuel, 440
- Diffusion, 56, 59
- coefficients, 57, 234–235
 - vs. dispersion, 68–70
- Diffusion-controlled rate law, 152
- Diffusive slip, 239
- Diffusive transport processes, 149
- Dihaloelimination, 421
- 1,4-Dioxane, 396, 529, 571
- Discharge substances, 24–28
- Diisooctyl phthalate (DIDP), 403
- Diisopropylmethylphosphonate (DIMP), 32
- Dimethyl mercaptan, 408
- 2,2-Dimethylpropane, 380
- Direct current resistivity, 454
- Dispersion
- diffusion *vs.*, 68–70
 - scale effect of, 98–103
- Dispersivity
- laboratory tests, 93–96
 - quantifying dispersivity, in field, 96–97
 - single-well tracer test, 97–98
- Displacement, 252
- Dissolved gasses, 316
- Dissolved organic contaminants, 570–572
- Dissolved solids, 61
- Distillation, 386, 387
- Distributed temperature sensing (DTS), 521
- Distribution coefficient, 135
- Dithionate reduces ferric iron, 606
- Divergence, 49
- Dose equivalent, 359
- Double-cell hydraulic containment, 555
- Double-pump system, 574
- Dover National Test Site (DNTS), 611–612
- Downhole techniques, 520–522
- Drainage, 251
- Drilling
- contaminated soil, 494
 - method, 486–487
 - air core drilling, 492
 - air-rotary drilling, 491
 - cable-tool drilling, 491–492
 - diamond core drilling, 492
 - directional drilling, 493–494
 - hollow-stem augers, 487–489
 - mud-rotary drilling, 489–490
 - RAB, 492
 - reverse-rotary drilling, 491
 - sonic drilling, 492
 - solid material during, sample collection, 494–498
- Drinking water, 17, 23–25
- boreholes and dug wells, 1, 2
 - risk and, 17, 23–25
 - source of, 1
 - standards and health goals, 16–22
- Dry wells, 38–39
- Drying curve, 210, 251
- Dual-pump system, 575
- Dyes tracers, 523
- Dynamic dispersivity, 64
- Effective diffusion coefficient, 58, 235
- Effective porosity, 61
- Effusion, 239
- Electric probe, 465, 509
- Electrical resistance heating, 612
- Electromagnetic-induction logs, 522
- Electromagnetic (EM) surveys, 453–454
- Electromagnetic spectrum, 453
- Electrostatic attraction, 200
- Electrostatic double layer, 200–202
- Elements, 322
- Emerging contaminants, 410–414
- Endocrine disruptors, 403
- Ensemble mean concentration, 106
- Environmental forensics, 520
- Environmental Protection Agency (EPA), 17, 22, 28, 40, 280, 545, 546, 582
- Environmental tracers, 523–526
- Epoxidation, 424
- Equilibrium distribution coefficients, 178
- Equilibrium surface reactions, solutes
- BET sorption, 142–143
 - equilibrium retardation, effect of, 144–148
- Freundlich sorption isotherm, 138–140
- Langmuir sorption isotherm, 140–142
- linear sorption isotherm, 135–138
- PDM sorption isotherm, 143–144
- Equipotential lines, 116
- Equivalent weight, 316
- Ergodic hypothesis, 105
- Error function, 60
- Esters, 393, 402–404
- Estimated values, 433
- Estimation Programs Interface (EPISuite™), 164
- Ethane, 379
- Ethanol, 391, 392, 528
- Ether, 393, 395–396
- cleavage, 426
- Ethyl formate, 402
- Ethyl mercaptan, 408, 420
- Ethyl *tert*-butyl ether (ETBE), 391
- Ethylene dibromide (EDB), 389
- Ethylenediaminetetraacetate (EDTA), 341, 342
- European Groundwater and Contaminated Land Remediation Information System (EUGRIS), 545
- Evapotranspiration (ET) cover system, 552
- Exploration borings, 38
- Extracted groundwater, treatment, 568–569
- dissolved organic contaminants, 570–572
 - inorganic contaminants, 569–570
- Extraction systems, 559

- Extraction-injection well systems, 566
- Fabric protector, 401
- Farm animal wastes, 36
- Federal Clean Water Act, 40
- Federal Remediation Technologies Roundtable (FRTR), 544, 559
- Fermentation, 424
- half reactions, 425
- Ferric hydroxides, 347
- Ferrous iron, 320
- Fertilizer application, 36
- Fiber optic chemical sensors (FOCS), 522
- Fick's law, 103, 149
- Fick's first law, 56–57
 - Fick's second law, 57, 235
- Fickian diffusion, 234
- Field bank, 433
- Field scale, 107–109
- Filter-packed wells, 473–474
- Filtration theory, 179
- Fingering, 230, 232
- Fingerprinting petroleum distillates and coal tar, 434–440
- Finite difference method (FDM), 109–110
- Finite element method (FEM), 109–110
- Finite volume method (FVM), 110
- Finite-difference grid, 111
- Finite-difference solute-transport model, 112
- First derivative of distance, 44
- First normalized moment, 71
- First order, 169
- First-type boundary condition, 77–78
- Fixed concentration, 76
- Fixed gradient, 76
- Fixedstep function, 77
- Flame ionization detector (FID), 428, 435
- Flame retardants, 383
- Flexible liner system, 484
- Floating product, thickness measurement, 278–287
- Flow equation, derivation of, 49–51
- Flowmeter, 521
- FLOWPATH II, 563
- Fluid potential, 258–262
- Fluid-content relations, 281–282
- Fluoride, 343–344
- Fluorinated ethylene propylene (FEP), 514
- Fluoropolymers, 467
- Forced hydraulic gradient tests, 97
- Formaldehyde, 400
- Fourier's Law, 234
- Fourth central moment, 71
- Fracking fluids, 38
- Fracture systems, 118, 301–303
- Fractured media, transport in, 117–123
- Free energy, 323
- Free-fall method, 501
- French drain, 568
- Freundlich sorption isotherm, 138–140, 145, 146
- FTWORK, 567
- Fuel additives, 528
- Fulvic acids, 341
- Functional groups, 393–395
- alcohol, 395, 399
 - aldehydes and ketones, 399–400
 - carboxylic and sulfonic acids, 400–402
 - emerging contaminants, 410–414
 - esters, 402–404
 - ethers, 395–396
 - organic compounds containing nitrogen, 405–408
 - organic compounds containing sulfur and phosphorus, 408–409
 - phenols, 404–405
- Funicular water, 262
- Funnel-and-gate PRB systems, 600, 601
- Funneling, 230, 232
- Gamma logging, 521
- Gamma radiation, 358
- Gas chromatograph/mass spectrometer (GC/MS), 428, 429
- Gas phase permeability, 278
- Gas tracer, 270, 271
- Gas-drive piston pump, 511
- Gas-driven pump, 511–512
- Gaseous advection, 238–239
- Gaseous diffusion, 233–237
- Gas-lift pump, 511
- Gasoline, 274, 276, 284, 387, 389, 391
- Gasoline compounds, degradation, 427
- Gaussian distribution, 65, 90
- Gear-drive pump, 511
- Gelhar graph, 99
- Genome sequencing, 532–533
- Geochemical zonation, 368–371
- Geotextile fabric, 552
- Gibbs free energy, 323, 324
- Gibbsite, 200
- Glyphosate, 409
- Goethite, 200
- Granular activated carbon (GAC), 571
- Gravel packs, 473
- Graveyards, 33
- Gray, 359
- Ground penetrating radar (GPR), 455
- Groundwater, 1
- contaminants, types of, 3–16
- Gypsum, 346
- Half-reaction, 320–323
- Halogenated alcohol, 423
- Halorespiration, 424
- Helical-rotor pump, 511
- Helicopter transient
- electromagnetic surveys, 454
- Henry's law, 237, 272, 377, 378
- Heterogeneity, stochastic descriptions of, 104–106
- Hexamethylphosphoramide (HMPA), 407
- Hexane, 379
- 1,6-Hexanedioic acid, 401
- Hexavalent chromium, 351, 563
- High density polyethylene (HDPE) tubing, 483
- High resolution multilevel monitoring, 480–481
- High-level radioactive wastes, 34
- High-performance liquid chromatography (HPLC), 428–429
- High-resolution multilevel wells, 462
- Hollow-stem auger, 461, 487–489, 496, 499–501
- Home water softeners, 37
- Homogeneous medium, 68

- Homologous series, 376
 Honeycombed design, 483
 Horizontal movement, saturated zone, 296–301
 Hot spots, 451
 Humic acids, 341
 Humic substances, 341
 Humin, 341
 Humus, 200
 Hydraulic conductivity, 46, 51–52, 100–102
 scalar, vector and tensor properties, 47–49
 soil, salinity effects, 202–203
 Hydraulic head conductivity, 47–49
 Hydrocarbon, 272, 289–290
 anaerobic decomposition of, 171
 boiling points, 386
 coal tar, 390
 classes, 378–382
 degradation, 415–419
 fractions, distillation, 387
 saturation profile, 286
 in vadose zone partitioning, 273
 Hydrodynamic dispersion coefficient, 65
 Hydrogen, stable isotopes of, 531
 Hydrogen fluoride (HF), 343
 Hydrogen gas, 369
 Hydrogenolysis, 420
 Hydrolysis, 418, 419, 426
 Hydrophobic compound sorption, solutes, 153–154
 estimating K_{oc} from K_{ow} data, 155–156
 K_{oc} from K_{ow} data, 155–156
 molecular structure, K_{oc} from, 161–163
 multiple solute effects, 165–168
 QSPR, 163–165
 soil/aquifer organic carbon, partitioning onto, 154, 155
 solubility data, estimating K_{oc} from, 156–161
 Hydrophobic effect, 153
 HydroPunch™, 515, 516
 Hydrostatic pressure, 266
 Hydroxyl, 393
 Hydroxylation, 423, 426
 Hydroxypropyl- β -cyclodextrin (HPCD), 611
 HYDRUS-1D, 153
 Hygiene sandstone, 218
 Hysteresis, 210–211, 216, 251, 255
 Ill-designed treatment system, 287
 Illite, 200
 Imbibition, 251, 252
 Immobilize inorganic ions, 603
 Immunological surveys, 456
 Impoundments, 31–32
 Inorganic contaminants, treatment, 569–570
In situ air sparging system, 583, 584
In situ chemical oxidation (ISCO), 614–616
In situ leaching (ISL), 32–33, 362, 406, 527
In situ PRB systems, 600
In situ thermal treatment (ISTT) technologies, 612–614
 Indoor air in buildings, 457
 Induced polarization, 454
 Inert radioactive tracer gases, 524
 Infiltration galleries, 38–39
 Initial conditions, 76–77
 Injected tracers, 523
 Injection wells, 26–27
 Inner product, 48
 Inorganic indicators, 526–527
 Insufficiently fast reactions, 134
 Integral scale, 106
 Interfacial tension, 249–250
 International Agency for Research on Cancer (IARC), 23
 International Union of Pure and Applied Chemistry (IUPAC), 380–381
 Interstate Technology and Regulatory Council (ITRC), 544
 Invasive methods, site characterization
 annular space, 474–475
 multiple-level wells and multilevel devices, 479–485
 naturally developed and filter-packed wells, 473–474
 protective casing, 475–476
 screen length and setting, 476–479
 single screened wells, monitoring design, 479
 Ionic strength, 318
 I-region model, 225
 Irreducible fluid saturation, 252
 Irreducible water saturation, 253
 Irreducible wetting-fluid saturation, 251
 Irreversible first-order kinetic sorption model, 149
 Irrigation, 35
 Isoamyl acetate, 402, 403
 Isocyanates, 394
 Isomers, 380
 Isotherm, 135
 Isotopes and groundwater dating, 531–532
 tracing groundwater and pollution with, 530–531
 Isotope ratio infrared spectrometry (IRIS), 530
 Isotropic, 47
 Jet fuel, 289
 Kaolinite, 200
 Karst systems, 238
 Ketone, 394, 399–400
 Kinetic sorption model, 135, 148–153
 Kjeldahl nitrogen (KjN), 370
 Klinkenberg effect, 238
 Knudsen flow, 239
 Kurtosis, 74
 Lab duplicate, 434
 Lag, 106
 Lagrangian approach, 72
 Land application, 27–28
 Landfills, 28
 Longitudinal dispersion, 63, 64, 99, 100, 124
 Laser induced fluorescence (LIF), 522
 Le Bas method, 164
 Leachate, 28–30, 368–370
 Lead, 359–360, 470
 Leaking underground storage tank (LUST), removal of, 576–578, 591
 Leaky well function, 86
 Ligand, 339

- Light nonaqueous phase liquids (LNAPLs), 247, 248, 260, 262–267, 572, 573
 measurement, 279, 280
 migration, 262–267
 monitoring, 305–308
 site remediation, 572–576
 skimming well, 572
 volume of, 285
 water table, distribution of, 287–290
- Ligninolytic fungi, 417
- Limit of quantification, 433
- Limonite, 200
- Linear Langmuir two-surface sorption isotherm, 147
- Linear-sorption isotherm model, 135–138, 137, 147
- Liquid hazardous wastes, 33
- Liquid mass transport, 220–221
- Liquid radioactive cesium, 170–171
- Liquid wastes, 26
- Local mechanical dispersion, 103
- Long term water level measurements, 509
- Low water-air partition coefficients, 272
- Low-level radioactive wastes, 34
- Lumped parameter, 237
- Mach number, 239
- Macrodispersion, 99, 124
- Macropores, 229
- Magmatic fluorine, 343
- Magnetometry, 454
- Managed natural attenuation (MNA) processes, 428
- Mass action law, 317–320
- Mass conservation law, 49
- Mass per volume unit, 156
- Mass spectrometry, 428
- Mass spectrum, 428, 429
- Mass transport, 56
 advection, 61–63
 advection-dispersion equation (*see* advection-dispersion equation)
 apparent longitudinal dispersivity and field scale, regression analysis, 107–109
 concentration gradients, 56–61
 determine dispersivity values
- laboratory tests, 93–96
 quantifying dispersivity, in field, 96–97
 single-well tracer test, 97–98
- deterministic models, 109–117
 diffusion *vs.* dispersion, 68–70
 equilibrium models, 221–224
 in fractured media, 117–123
 nonequilibrium models of, 224–225
- scale effect of dispersion, 98–103
- stochastic models of, 103–104
 heterogeneity, stochastic descriptions, 104–106
 stochastic approach, 106–107
- transverse dispersion, effects of, 92
- Material Safety Data Sheets (MSDS), 546
- Material stockpiles, 33
- Material transport and transfer, 35
- Matrix potential, 204, 241
- Maximum contaminant level (MCL), 17
- Maximum contaminant level goals (MCLGs), 17
- Mechanical dispersion, 63–65
- Mechanical filters, 570–571
- Melting points, 376
- Mercury, 356
- Metabolites, 408
- Metal hydroxide, 569
- Metal complexes
 complexation, 339–340
 and facilitated particle transport, 341–342
- Methane gas, 370, 379
- Methanogenesis, 417
- Method blanks, 433
- Method detection limit, 433
 1-Methoxyethane, 396
 2-Methylbutane, 380
 Methyl ethyl ether, 396
 Methyl mercaptan, 408
 Methylation, 426
 Methyl-*tert*-butyl ether (MTBE), 389, 391, 427, 528
- Micelles, 607
- Michaelis-Menten function, 171
- Microbial testing, 532–533
- Microbial transformations, 424
- Microemulsion, 608
- Micrograms per liter, 316
- Micro-organics, 410
- Micropurging, 517, 518, 534
- Milliequivalents per liter, 316
- Milligrams per liter, 316
- Millington-Quirk tortuosity formula, 235
- Mineral fertilizers, 347
 solubility products, 321
- Mine drainage, 37–38
- Mine wastes, 32–33
- Minimally invasive soil monitoring, 456
 installation, suction lysimeters, 460–461
 methods, soil gas monitoring, 457–458
 phyto-screening, 461–462
 soil water sampling, 458
 suction lysimeter, 458–460
- Mobile oil, 283, 286
- Mobilization, 268
- Mobilize NAPL, 608
- MODFLOW program, 110
- Moisture, 199
- Molarity, 156
- Mole, 156, 316
- Mole fraction, 156
- Molecular diffusion, 56, 121
- Molecular topology, 161
- Molybdenum, 353–354
- Moment analysis, 70–75
- Monitored natural attenuation (MNA), 590–592
- Monitoring network design, 463
- Monitoring well, 38, 534
 casing
 chemical interaction with, 469
 electric probe, 464, 465
 inside and outside diameters, dimensions, 464–465
 materials, 467, 472
 selection, recommendations for, 466
 sorption and leaching, 468–470
 stainless steel, 467
 trichloroethylene, sorption of, 469, 471
- factors, 462–463

- installation, 498–503
and borehole
abandonment, 507–509
construction, record
keeping during, 507
decontamination
procedures, 485–486
development, 503–507
solid material, sample
collection, 494–498
problems with groundwater
monitoring systems, 464
purposes of, 462
screens, 472–473
typical, 462–463
Monod function, 171, 172
Monodentate, 340
Montmorillonite, 200
MT3DMS, 153
Multi-continuum model, 118
Multilayer cap, 551
Multilevel devices, 479–485
Multiphase extraction
technology, 573
Multiphase flow
floating product, thickness
measurement, 278–287
fluid potential and head,
258–262
interfacial tension and
wettability, 249–250
Multi-phase system, 248, 308
Multiple-level wells, 479–485
Multiport vertical sampling,
483–484
Municipal landfills, 28
Mycobacterium sp., 416, 417, 419

Nanoscale iron particles, 603
National Pollutant Discharge
Elimination System
(NPDES), 557
Natural attenuation, 590–592
Natural gas, 43
production, 37–38
Natural gradient tests, 96
Natural oxidant demand, 614
Naturally developed wells,
473–474
Near-field scale, 118
Near-infrared radiation, 453
Nernst equation, 322, 328, 334,
371
Nested wells, 481–482
Neutron logging, 521

NFPA 704 chemical hazard
label, 546, 547
Nickel, 353
Nitrate, 346
Nitrile, 394, 407
Nitrilotriacetate (NTA), 342
Nitrogen, 346–347, 530
Nitrophenols, 405
Nitrotoluenes, 405
Nonaqueous phase liquid
(NAPL), 165, 166, 247, 253,
308, 453, 543, 572–576
sorption, 148–153
Nonhomogeneous aquifer, 565
Noninvasive measurement, 452
aerial photography and
remote sensing,
interpretation, 452–453
rapid noninvasive field
surveys and screening,
455–456
surface geophysical
techniques, 453–455
Nonligninolytic fungi, 417
Nonlinear Langmuir sorption
isotherm, 142
Nonlinear sorption isotherms,
136
Nonwetting fluid saturation, 252
Nonwetting phase, 299
Not In My Back Yard (NIMBY)
syndrome, 28
Nuclear bomb-pulse chlorine-36,
532
Numerical mathematical model,
109

Octanol-water partition
coefficient, 154, 377
Oil
production, 37–38
table, 264, 265
wastes, 27
One-dimensional advection-
dispersion equation, 133
Open bailer, 511
Open dumps, 30
Open incineration sites, 34
Organic complexing agents, 341
Organic compounds
degradation, 415
chlorinated hydrocarbons,
418–425
gasoline compounds,
427
hydrocarbons, 415–419
organic pesticides,
425–427
organic molecules, field
studies of biological
degradation, 428
organic structure and
nomenclature
aromatic hydrocarbons,
382–383
hydrocarbon classes,
378–382
petroleum distillates, 383,
386–389
physical properties, 376–378
Organic compounds containing
sulfur and phosphorus,
408–409
Organic halides, 395, 397
Organic indicators, 527–529
Organic liquid, 281
Organic matter, 368, 371
Organic pesticides, degradation,
425–427
Organic solutes, 187
Organochlorides, 35
Organophosphorus herbicide, 409
Organophosphorus pesticides,
409
Organosulfur, 409
Oxidation, 423, 426
Oxidation potential, 323
Oxidation-reduction potential
(ORP), 323, 594
Oxidation-reduction reactions,
320–323
Oxidizing agents, 616
Oxygen, 510, 531, 594
Oxygen Release Compound™,
594

Packer systems, 484–485
Paraffins, 379
Parsimonious model, 109
Partial derivatives, 46
Partial differential equations
(PDEs), 109
Particle diffusion, 235, 237
Partitioning, 134, 308
Partitioning interwell tracer tests
(PITTs), 269–271
Passive samplers, 512
Passive treatment systems, 289
PATH3D model, 563
Peat moss, 605

- Peclet number, 68–70, 80
 Pendular rings, 250
 Pendular water, 262
 Pentachlorophenol, 405
 Pentane, 379, 380
 2-Pentanone, 400
 Percent recovery, 434
 Perchlorate, 406
 Perfluorooctane sulfonate (PFOS), 401
 Perfluorooctanoate (PFOA), 401
 Peristaltic pump, 511, 512, 514
 Permanent plume stabilization, 566–568
 Permeable reactive barrier (PRB), 599–606, 619
 Persistent organic pollutants (POP), 410, 414
 Pesticide applications, 35
 Pesticides, 31, 36
 Petroleum, 383, 386–389
 groundwater contamination, 390–392
 degradation, 529
 fingerprinting, 434–440
 Petroporphyrins, 441
 pH
 Eh vs., 325–326
 inorganic chemicals, 323–325
Phanerochaete chrysosporium, 417
 Pharmaceuticals and personal care products (PPCPs), 431
 Phase I environmental site assessment, 578
 Phenols, 404–405
 Phenyl compounds, 387, 394
 Phosphorus, 36, 147, 350
 Photoionization detector, 428
 Phthalate, 394, 403
 Phytoremediation, 616–618
 Phyto-screening, 461–462
 Picocurie, 359
 Piezometer, 476, 480
 Pilot-scale field project, 616
 Pipelines, 35
 Plug flow, 62
 Plume, 267
 Plume-stabilization well, 552–554
 Plutonium (Pu), 531
 Point-source bailer, 511
 Polanyi-Dubinin-Manes (PDM) sorption isotherm, 143–144
 Polar organic compounds, 163
 Polybrominated diphenyl ethers (PBDEs), 383
 Polychlorinated biphenyls (PCBs), 383, 529
 Polycyclic aromatic hydrocarbons (PAHs), 383–385, 416–418, 438, 456
 Polypropylene and polyvinylidene fluoride (PVDF), 514
 Polytetrafluoroethylene (PTFE), 467
 Polyvinyl chloride (PVC), 468, 470
 Porosity, 101
 Power law relationship, 108
 Power plants, 31
 Preceding model, 225
 Precision, 433
 Preferential flowpaths, 229–233
 Preferential pathways, 241
 Pressure-vacuum lysimeter, 459–461
 Priority pollutant organic compounds, 430–431
 Probability density function (PDF), 105
 Production wells, 38
 Product-recovery well, 587
 Propane, 379
 1-Propanol, 419
 Propanone, 400
 2-Propeneamide, 407
 2-Propenoic acid, 401
 Protective casing, 475–476
Pseudomonas paucimobilis, 416
 Pulsed pumping, 561
 Pump-and-Treat (P&T) system, 603
 adaptive pumping, 561
 contaminant
 removal, hypothetical examples, 559
 concentration of, 558
 treatment, 556
 discrepancy, 557
 groundwater, extraction of, 555–556
 mass transport limitations, 557–558
 NAPL, 557
 optimizing withdrawal-injection systems, 563–566
 permanent plume
 stabilization, 566–568
 pulsed pumping, 561
 rebound, 560
 remediation process, 559, 560
 tailing phase, 559
 treatment and regulatory requirements, 556
 Push-pull tests, 270
 Pyrene, 419
 Pyrite, 344
 Quality assurance and quality control (QA/QC), 433
 Quantitative structure-property relationships (QSPR), 163–165
 Radar techniques, 453
 Radioactive decay, 170
 Radioactive isotopes, 358–359
 cationic radionuclides, adsorption of, 359–360
 radium, 364, 367
 radon, 367–368
 thorium, 363–364
 Radioactive-waste-disposal sites, 34
 Radionuclides, 3
 Radionuclides emit ionizing radiation, 358
 Radium, 364, 367
 Radius of influence (ROI), 581
 Radon, 367–368
 Rads, 359
 Rainfall, 241
 Rainwater infiltrating, 36
 Random walk model, 121
 Raoult's law, 165, 273, 304
 Rapid noninvasive field surveys, 455–456
 Rare earth elements (REEs), 358
 Rayleigh-Taylor instability, 230
 Rebound, 560
 Redox reactions, 320–323
 Redox zones, 597
 Reduction, 420, 421, 427
 Reductive dechlorination reactions, 418, 420
 Regression analysis, 107–109
 Relative permeability, 253–257
 Rem, 359
 Remote sensing, 452–453
 Representative elementary volume (REV), 49–51, 66
 Residential disposal, 30–31
 Residual fluid saturation, 252
 Residual oil, 287
 Residual saturation, 248
 Residual wetting saturation, 251

- Resource and Conservation and Recovery Act (RCRA), 27, 28, 30, 31, 34, 543
- Retardation, 133
- Retardation factor, 136
- Return flow, 35
- Reversible linear kinetic sorption model, 149
- Reversible nonlinear kinetic sorption model, 151
- Richards' equation, 219–220, 241
- Ring cleavage, 427
- Risk based corrective actions (RBCA), 544
- Robson's formula, 294
- Rock-core sample, 495, 498
- Rotary air blast (RAB), 492
- Safe Drinking Water Act, 2
- Sample dilution, 433
- Sand packs, 473
- Sanger techniques, 533
- Saturated hydrocarbons, 379
- Saturated zone
- horizontal movement, 296–301
 - vertical movement, 294–296
- Saturation ratio, 248–249
- Scalar, 47
- Scale effect of dispersion, 98–103
- Screens, monitoring well, 472–473
- Second central moment, 71
- Second temporal moment, 73
- Secondary utilization, 172
- Second-type boundary condition, 78–80
- Seismic surveys, 454
- Seivert, 359
- Selenium, 348–349
- Self-supplied systems, 2
- Separation, 106
- Septic tank, 24–27
- effluent, 346
- Sesquioxides, 200
- Sewers, 35
- Shallow soil boring, 457
- Shelby tube, 495–496
- Short circuiting, 229, 231, 232
- Silicon-32, 532
- Silver, 354
- Simple manufactured multilevel samplers, 482–483
- Single-cell containment, 555
- Single-pump system, 573, 574
- Single screened wells, monitoring design, 479
- Single-well tracer test, 97–98
- Single withdrawal well, 564
- Site remediation
- bioremediation, 589–590
 - enhanced bioremediation, 592–598
 - MNA, 590–592
 - combination methods, 584–589
 - CSM, 598–599
 - ISCO, 614–616
 - ISTT, 612–614
 - phytoremediation, 616–618
 - PRB, 599–606
 - SVE, 578–583
 - USTs, 576–578
- Size-exclusion effect, 177
- Skewness, 73
- Skimming trenches, 575
- Sloping coarse-sand layers, 230
- Slug injection, 88–91
- Smear zone, 287
- Sodium adsorption ratio (SAR), 202–203
- Soil vapor extraction (SVE), 289, 578–583, 585
- Solid tracers, 524
- Solid waste, 545–546
- Solidification, 551
- Soltrol, 284
- Solubility products, 321
- Solute(s), 133–134
- biodegradation, 171–176
 - chemical reactions, classification of, 134
 - colloidal transport, 176–186
 - nonequilibrium sorption models, 148–153
 - radioactive decay, 170
 - relative movement of, 228–229
 - sorption processes, 134–135
- Solute-transport model, borden landfill, 116, 117
- Sorbing barriers systems, 606
- Sorption corrected porosity, 237
- Sorption processes, 134–135
- Sound science, 452
- Source-control measurement, site remediation
- containment, 547–552
- hydrodynamic isolation, 552–555
- removal and disposal, 546–547
- solid waste, 545–546
- Spatial moment technique, 70
- Specific discharge, 46
- Specific gravity, 376
- Spiked samples, 434
- Spills, 35
- Split-spoon sampler, 457, 496–497
- Stability fields, Eh-pH diagram, 328–338
- Stabilization, 551
- Stable isotopes, 441
- Stagnant film concept, 149
- Stainless steel, 467
- Steam injection, 612
- Stochastic hydrology, 104–106
- Stochastic models, 103–104
- heterogeneity, stochastic descriptions, 104–106
 - stochastic approach, 106–107
- Straining theory, 179–186
- Strategic Environmental Research and Development Program (SERDP), 544
- Strontium, 350–351
- Strontium sulfate, 346
- Structural isomers, 380
- Submersible centrifugal pump, 511
- Substitution, 418
- Subsurface distribution, 267
- Subsurface volatilization, 585, 586
- Suction lysimeter, 458–460
- installation, 460–461
- Sufficiently fast reactions, 134
- Sulfate isotopic values, 531
- Sulfide, 394
- Sulfonamides, 407
- Sulfonates, 401
- Sulfonic acid, 400–402
- Sulfur, 344–346, 531
- Superfund Amendments and Reauthorization Act (SARA), 41
- Superfund program, 40
- Surface flux chambers, 457
- Surface geophysical techniques, 453–455
- Surface impoundments, 31–32

646 Index

- Surge block, 505, 506
Synthetic chelating agents, 341
Synthetic geomembranes, 552
Syringe sampler, 511
- Tailing phase, 559
Target compound, 432
Technetium (Tc) solubility, 356–359
Television (TV) logging, 520–521
Tensiometer, 213, 215
Tension plate assembly, 212, 213
Tensors, 47
Tert-amyl methyl ether (TAME), 391
Test borings, 457
Tetachloroethylene plumes, 184
Tetrachloroethylene, 292, 422
Tetrachloroethene, 421
Tetrachloroethylene (PCE), 299–301
Tetrahydrofuran, 396
Thermal advection, 238
Thermal gaseous diffusion, 237
Thermal treatment technologies, 612–614
Third central moment, 71
Third-type boundary condition, 82
Thorium, 359, 363–364
Three-phase flow, 247
Three-phase systems
 relative permeabilities, 256
 two-phase flow, Darcy's law for, 257
Threshold value, 252
Time domain reflectometry (TDR), 454
Toluene, 166, 275
Tortuosity, 58
Total dissolved solids (TDS), 31
Total petroleum hydrocarbons, 431
Total reduced nitrogen, 370
Toxic Substances Control Act (TCSA), 34
Tracers, 522–526
Tracer test, 70, 72
Transform explosives, 603
- Transformation, 589
Transport, reactive and
 nonreactive solutes, 180–186
Transverse dispersion, 64, 92, 124
Tremmie pipe, 500, 502, 503
Triazine, 36
Trichloroepoxyethane, 424
1, 1, 1-Trichloroethane (TCA), 167–168, 422
Trichloroethene (TCE), 162, 167–168, 174, 252, 253, 291, 469, 471, 529, 560
Trichlorophenol, 405
2,4,6-Trinitrotoluene (TNT), 405, 406
Tritium, 368, 532
Two-phase systems, 256, 257
Two-region/bi-continuum transport models, 152, 225
Two-Site non-equilibrium sorption models, 151
Type-I sites, 151
Type-II sites, 151
- Underground Injection Control Program of the Safe Drinking Water Act, 26–27
Underground storage tanks (UST), 33–34
 removal, 576–578
Unexploded ordnance (UXO), 405
Uniform two-dimensional flow field, 83–87
 continuous injection into
Unsaturated hydraulic conductivity, 214–218
Uranium, 360–363, 365, 366, 406
Uranium oxides, 531
Urban runoff, 37
- Vacuum lysimeter, 459
Vadose/water-unsaturated zone, 198
van Genuchten soil model, 208, 209, 283–285
Vanadium, 351
Vapor density, 277–278, 377
- Vapor extraction systems (VES).
 See Soil vapor extraction
Vapor intrusion, 581
Vapor phase transport, 233
 combinations, 239
 effusion, 239
 environmental factors, 239–241
 gaseous advection, 238–239
 gaseous diffusion, 233–237
Vapor pressure, 273, 377
Variable flux, 76
Ventilation system, 585, 586
Vertical flowmeter testing, 521
Vertical movement, saturated zone, 294–296
Viscous slip, 239
Volatile organic compounds (VOC), 272, 277, 431, 578
Volatilization, multiphase flow, 271–277
Volumetric water, 216
- Water-air partition coefficients, 275
Water solubility, 376
Water-table observation well, 480
Well purging, 510
Well sampling
 devices, 510–514
 fluid level and pressure measurement, 509
 monitoring wells, low-flow purging, 516–518
 sampling frequency, 518–519
Wellhead Protection Area (WHPA) program, 562
Wettability, 249–250
Wetting curve, 210, 251
Wetting front instability, 230
Wetting phase, 298
Withdrawal-injection systems, 563–566
- Zero order, 169
Zero valent iron (ZVI), 600–604
Zeroth absolute moment, 71
Zinc, 354

About the Authors

Dr. Thomas (“Tom”) Boving, Ph.D., is a Professor of Environmental Hydrogeology at the University of Rhode Island (URI) in Kingston, USA. He is appointed to both the Department of Civil and Environmental Engineering and the Department of Geosciences. His Diploma in Geology is from the University of Tübingen, Germany, and he received his Ph.D. in Hydrology and Water Resources Management from the University of Arizona, Tucson, USA. He worked as an Environmental Hydrogeologist in Germany for several years. His areas of research include innovative remediation technologies, water treatment solutions for developing countries, and stormwater quality studies. Outside the United States, Dr. Boving conducts his research in Africa and Asia. Dr. Boving is also the Director of *Water:E²S²*, which is a URI consortium of experts addressing global water issues from the engineering, economic, science, and social perspective.

Dr. David K. Kreamer is a Professor of Geoscience, a Graduate Faculty member in Civil and Environmental Engineering, and past Director of the interdisciplinary Water Resources Management Graduate Program at the University of Nevada, Las Vegas. Dave serves as Vice President for Science and Program for the International Association of Hydrogeologists, is past Director of the National Groundwater Association’s Division of Scientists and Engineers, and is a past President of the Universities Council on Water Resources. Dave’s research includes environmental contamination, spring vulnerability and sustainability, and clean water and energy supply. He has authored over 65 professional publications, and has given over 150 invited lectures, seminars and workshops in recent years for groups including the U.S. EPA, U.S. BLM, the National Ground Water Association, and has presented short courses for over half the States and Commonwealths in the United States. He has also given presentations at over 50 universities, and has been an invited speaker in Europe, Asia, the Caribbean, Australia and the Pacific island nations, South America, Africa, and the Middle East. Dave has served as a professional consultant and expert witness in legal proceedings concerning groundwater, testified before the U.S. Congress on groundwater pollution challenges, and has been an external peer reviewer for numerous groups and projects including nuclear waste storage at Yucca Mountain, Nevada, USA.

"Thomas Boving and David Kreamer are to be congratulated for updating C.W. Fetter's decade-old gem and giving us all a state-of-the art treatment of a field more important than ever."

—Michael E. Campana, Professor of Hydrogeology, Oregon State University, and Technical Director, AWRA

Third Edition

Contaminant Hydrogeology

Tremendous progress has been made in the field of remediation technologies since the second edition of *Contaminant Hydrogeology* was published two decades ago, and its content is more important than ever. Recognizing the extensive advancement and research taking place around the world, the authors have embraced and worked from a larger global perspective. Boving and Kreamer incorporate environmental innovation in studying and treating groundwater/soil contamination and the transport of those contaminants while building on Fetter's original foundational work.

Thoroughly updated, expanded, and reorganized, the new edition presents a wealth of new material, including new discussions of emerging and potential contaminant sources and their characteristics like deep well injection, fracking fluids, and in situ leach mining. New sections cover BET and Polanyi adsorption potential theory, vapor transport theory, the introduction of the Capillary and Bond Numbers, the partitioning interwell tracer testing technique for investigating NAPL sites, aerial photographic interpretation, geophysics, immunological surveys, high resolution vertical sampling, flexible liner systems, groundwater tracers, and much more.

Contaminant Hydrogeology is intended as a textbook in upper level courses in mass transport and contaminant hydrogeology, and remains a valuable resource for professionals in both the public and private sectors.

Waveland Press, Inc.
waveland.com

ISBN 13: 978-1-4786-3279-5
ISBN 10: 1-4786-3279-8



9 781478 632795



9 0000